INTERNATIONAL SYMPOSIUM

Print: ISSN 2344 - 4118
CD-ROM: ISSN 2344 - 4126
Online: ISSN 2537 – 3773
ISSN-L 2344 – 4118

ISB-INMA TEH

AGRICULTURAL AND MECHANICAL ENGINEERING

Bucharest
09 – 11 October 2025

ISB-INMA-TEH

AGRICULTURAL AND MECHANICAL ENGINEERING

Bucharest
2025

ORGANIZING COMMITTEE

- Prof. Ph.D. Eng. **Sorin-Ştefan BIRIŞ** - Politehnica Bucharest (RO)
- Tech. **Marian CHIRIŢESCU** - INMA Bucharest (RO)
- Assoc. Prof. Ph.D. Eng. **Gabriel CONSTANTIN** - Politehnica Bucharest (RO)
- Eng. **Mihai CONSTANTINESCU** – INMA Bucharest (RO)
- Prof. Ph.D. Eng. **Andrei CRĂIFĂLEANU** - Politehnica Bucharest (RO)
- Prof. Ph.D. Eng. **Cristina-Ileana COVALIU-MIERLĂ** - Politehnica Bucharest (RO)
- PhD. Eng. **Cătălin DUMITRESCU** – INOE 2000 IHP (RO)
- Lect. Ph.D. Eng. **Mihaela DUŢU** - P.U. Bucharest (RO)
- PhD. Eng. **Iuliana GĂGEANU** - INMA Bucharest (RO)
- Lect. Ph.D. Eng. **George Cătălin ION** - P.U. Bucharest (RO)
- Prof. Ph.D. Eng. **Edmond MAICAN** - Politehnica Bucharest (RO)
- Ph.D. Eng. **Mihai MATACHE** - INMA Bucharest (RO)
- Prof. Ph.D. Eng. **Gabriel NEGREANU** - Politehnica Bucharest (RO)
- Prof. Ph.D. Eng. **Gigel PARASCHIV** - Politehnica Bucharest (RO)
- Prof. **Daniela RADU** - INMA Bucharest (RO)
- Lect. Ph.D. Eng. **Mădălina ŞTEFAN** - Politehnica Bucharest (RO)
- PhD. Stud. Eng. **Ana-Maria TĂBĂRAŞU** - INMA Bucharest (RO)
- Assoc. Prof. PhD. Eng. **Nicoleta UNGUREANU** - Politehnica Bucharest (RO)
- Ph.D. Eng. **Valentin VLĂDUŢ** - INMA Bucharest (RO)

SECRETARY

- Tech. Tania Țicu - INMA Bucharest (RO);
- Eng. Tăbărașu Ana-Maria - INMA Bucharest (RO);
- Tech. Marian CHIRIŢESCU - INMA Bucharest (RO)

SUPPORT AND TRANSLATION

- Prof. Daniela-Cristina RADU - INMA Bucharest (RO);
- PhD. Eng. Iuliana GĂGEANU - INMA Bucharest (RO)
- Assoc. Prof. PhD. Eng. Nicoleta UNGUREANU - Politehnica Bucharest (RO)

PROGRAMME COMMITTEE

- Assoc. Prof. Ph.D. Eng. **Atanas ATANASOV** - University of Rouse (BG)
- Prof. Ph.D. **Mihaela BEGEA** – Politehnica Bucharest (RO)
- Assoc. Prof. Ph.D. Eng. **Nastasia BELC** - IBA Bucharest (RO)
- Prof. Ph.D. Eng. **Sorin-Ştefan BIRIŞ** - Politehnica Bucharest (RO)
- Assoc.Prof.Ph.D. Eng. **Sorin BORUZ** - University of Craiova (RO)
- Assoc.Prof. Ph.D. Eng. **Sorin BUNGESCU** – USAMVB Timișoara (RO)
- Assoc. Prof. Ph.D. Eng. Petru **Marian CÂRLESCU** - USAMV Iaşi (RO)
- Ph.D. Eng. **Luminița CATANĂ** - IBA Bucharest (RO)
- Ph.D. Eng. **Valerian CEREMPEI** – Technical University of Moldova (MD)
- Prof. Ph.D. Eng. **Leonardi CHERUBINO** – Universita degli Studi di Catana (IT)
- Prof. Ph.D. Eng. **Sorin CÎMPEANU** - USAMV Bucharest (RO)
- Prof. Ph.D. Eng. **Lucian-Ionel CIOCA**, Lucian Blaga University of Sibiu (RO)
- Prof. **Laura Clarizia**, University of Naples Federico II (IT)
- Ph.D. Eng. **Mihnea COSTOIU** - Politehnica Bucharest (RO)
- Prof. Ph.D. Eng. **Cristina-Ileana COVALIU-MIERLĂ** - Politehnica Bucharest (RO)
- Prof. Ph.D. Eng. **Andrei CRAIFĂLEANU** - Politehnica Bucharest (RO)
- Prof. Ph.D. Eng. **György DEÁK** – NIRDEP Bucharest (RO)
- Ph.D. Eng. **Mihaela-Monica DINU** – ICDPP Bucharest (RO).
- Prof. **Vasyl DMYTRIV** - Lviv Polytechnic National University (UA)
- Prof. Ph.D. Eng. **Ilie DUMITRU** - University of Craiova (RO)
- Ph.D. Eng. **Adam EKIELSKI** - Warsaw University of Life Sciences (PL)
- Prof. Ph.D. Eng. **Can ERTEKIN** - Akdeniz University, Antalya (TR)
- Prof. Ph.D.Eng. **Inacio Maria dal FABRO** – Campinas State University (BR)
- Assoc. Prof. Ph.D. Eng. **Lucian FECHETE** - Technical University Cluj Napoca (RO)
- Assoc. Prof. Ph.D. Eng. **Mariana FERDEŞ** - Politehnica Bucharest (RO)
- Prof. Ph.D. Eng. **Nicolae FILIP** - Technical University Cluj Napoca (RO)
- Prof. Ph.D. Eng. **Liviu Gaceu** - Transilvania" University of Brașov (RO)
- Ph.D. Eng. **Iuliana GĂGEANU** – INMA Bucharest (RO)
- Ph.D. Stud. Eng. **Gabriel GHEORGHE** - INMA Bucharest (RO)
- Assoc. Prof. Ph.D. Eng. **Marius GHEREŞ** - Technical University Cluj Napoca (RO)
- Prof. Ph.D. Eng. **Omar GONZÁLEZ** - Central University "Marta Abreu" de las Villas, (CU)
- Prof. Ph.D. Eng. **Marian GRIGORE** – Universitatea Tehnică a Moldovei (MD)
- Prof. **Francisco de Paula Martin Jimenez**, University of Malaga (ES)
- Assoc. Prof. Ph.D. Eng. **Önder KABAŞ** - Akdeniz University, Antalya (TR)
- Assoc. Prof. Ph.D. Eng. **Imre KISS** - P.U. Timișoara (RO)
- Assoc. Prof. Ph.D. **Igor KOVAČEV** - Zagreb University (HR)
- Lect. Ph.D. Eng. **Daniel LATEŞ** – U.M.P.S.T of Tîrgu Mureş (RO)
- Prof. **María Cruz LÓPEZ ESCALANTE**, University of Malaga (ES)
- Prof. Ph.D. Eng. **Edmond MAICAN** - Politehnica Bucharest (RO)
- Ph.D. Eng. **Eugen MARIN** - INMA Bucharest (RO)
- Ph.D. Eng. **Gabriela MATACHE** – INOE 2000 IHP (RO)
- Ph.D. Eng. **Mihai MATACHE** - INMA Bucharest (RO)
- Assoc. Prof. Ph.D. Eng. **Gheorghe MATEI** - University of Craiova (RO)
- Prof. Ph.D. Eng. **Florentina MUNTEANU** – "Aurel Vlaicu" University of Arad (RO)
- Prof. Ph.D. Eng. **Nikolai MIHAILOV** - University of Rouse (BG)
- Ph.D. Eng. **Vasile MOCANU** - ICDP Brașov (RO)
- Ph.D. Eng. **Florin NENCIU** - INMA Bucharest (RO)
- Prof. Ph.D. Eng. **Vasile PADUREANU** – "Transilvania" University of Brașov (RO)
- Prof. Ph.D. Eng. **Mirela PANAINTE-LEHĂUŞ** – V. Alecsandri University of Bacău (RO)
- Prof. Ph.D. Eng. **Gigel PARASCHIV** - Politehnica Bucharest (RO)
- Assoc. Prof. Ph.D. Eng. **Elena POP** - Politehnica Bucharest (RO)
- Prof. Ph.D. Eng. **Tudor PRISECARU** - Politehnica Bucharest (RO)
- Ph.D. Eng. **Elena Cristina RADA** – Insubria University (IT)
- Prof. Ph.D. Eng. **Marco RAGAZZI** - University of Trento (IT)
- Prof. Ph.D. Eng. **Răzvan-George RÎPEANU** – UPB Ploiești (RO)
- Prof. Ph.D. Eng. **Radu ROŞCA** – USAMV Iași (RO)
- Prof. Ph.D. Eng. **Carmen RUSĂNESCU** - Politehnica Bucharest (RO)
- Prof. Ph.D. Eng. **Ion SĂRĂCIN** - University of Craiova (RO)
- Assoc. Prof. Ph.D. Eng. **Lazar SAVIN** - University of Novi Sad (SR)
- Assoc. Prof. Ph.D. Eng. **Kemal SELVİ** - Ondokuz Mayıs Üniversity (TR)
- Ph.D. Eng. **Cristian SORICĂ** - INMA Bucharest (RO)
- Ph.D. Eng. **Dorin Ioan SUMEDREA** – INCDBH Stefanesti-Arges (RO)
- Prof. Ph.D. Eng. **Răzvan Ionuț TEODORESCU** - USAMV Bucharest (RO)
- Prof. Ph.D. Eng. **Vincenzo TORRETTA** - Insubria University (IT)
- Prof. Ph.D. Eng. **Ion ŢENU** - USAMV Iași (RO)
- Ph.D. Eng. **Valentin VLĂDUŢ** - INMA Bucharest (RO)
- Ph.D. Eng. **Iulian VOICEA** - INMA Bucharest (RO)
- Prof. Ph.D. Eng. **Gheorghe VOICU** - Politehnica Bucharest (RO)
- Ph.D. Eng. **Roxana ZAHARIA** – ICDPP Bucharest (RO)
- Ph.D. Eng. **Tomasz ŻELAZIŃSKI** - Warsaw University of Life Sciences (PL)

HONORARY COMMITTEE

- Ph.D. Eng. Aurel BADIU- ASAS of Romania (RO);
- Prof. Ph.D. Eng. Ioan Jelev- ASAS of Romania (RO);
- Prof. PhD. Eugen RUSU – Romanian Academy (RO);
- Ph.D. Eng. Ovidiu BADEA - Romanian Academy (RO);
- Ph.D. Eng. Ion PIRNĂ - ASAS of Romania (RO);
- Ph.D. Eng. Mihai NICOLESCU - ASAS of Romania (RO)
- Ph.D. Eng. Vergil GÂNGU - ASAS of Romania (RO)

ISB-INMA-TEH' 2025

NATIONAL INSTITUTE FOR RESEARCH - DEVELOPMENT OF MACHINES AND INSTALLATIONS DESIGNED FOR AGRICULTURE AND FOOD INDUSTRY
- INMA Bucharest
6 Ion Ionescu de la Brad Blvd., sector 1, Bucharest

BIOTECHNICAL SYSTEMS ENGINEERING
- ISB Bucharest
290 Splaiul Independenţei Str., sector 6, Bucharest

Print: ISSN 2344 - 4118
CD-ROM: ISSN 2344 - 4126
Online: ISSN 2537 - 3773
ISSN-L 2344 – 4118
Indexed in CAB DIRECT, http://www.cabdirect.org/ , **Google Scholar**

Disclaimer/Publisher's Note: The statements, opinions and data contained in all publications are solely those of the individual author(s) and contributor(s) and not of INMA / ISB and the editor(s). INMA and the editor(s) disclaim responsibility for any injury to people or property resulting from any ideas, methods, instructions or products referred to in the content.

CONTENTS

No.	Article Title & Authors	page
1.	CLIMATE CHANGE MITIGATION BY BIOLOGICAL CARBON SEQUESTRATION OF MAIZE HYBRIDES *UBLAŽAVANJE KLIMATSKIH PROMJENA BIOLOŠKOM SEKVESTRACIJOM UGLJIKA RAZLIČITIH HIBRIDA KUKURUZA* Darija BILANDŽIJA, Marija GALIĆ, Grubor MATEJA, Tajana KRIČKA, Bilandžija NIKOLA	16
2.	ROBOTIC SYSTEMS FOR HARVESTING THE INFLORESCENCES OF MEDICINAL PLANT SPECIES - A REVIEW *SISTEME ROBOTIZATE DESTINATE RECOLTĂRII INFLORESCENȚELOR UNOR SPECII DE PLANTE MEDICINALE - A REVIEW* Adriana MUSCALU, Cătălina TUDORA, Dragoș ANGHELACHE, Dorin CÎRSTEA, Margareta NAIE	22
3.	THE EU DIGITAL PRODUCT PASSPORT DPP AS A KEY INNOVATION IN PRODUCT DESIGN AND MANUFACTURING PROCESSES *PAŞAPORTUL UE DE PRODUS DIGITAL DPP CA O INOVAȚIE CHEIE ÎN PROIECTAREA PRODUSELOR ȘI PROCESELE DE FABRICAȚIE* Carmen BRĂCACESCU, Oana Diana CRISTEA, Raluca-Veronica BRĂCACESCU, Lorena-Diana POPA	32
4.	RESEARCH ON THE INFLUENCE OF RAW WOOL QUALITY ON THE PARAMETERS FOR OBTAINING HYDROLYSATE BY THE ALKALINE METHOD *CERCETARI PRIVIND INFLUENTA CALITAȚII LÂNII BRUTE ASUPRA PARAMETRILOR DE OBȚINERE A HIDROLIZATULUI PRIN METODA ALCALINĂ* Elena Mihaela NAGY, Teodor Gabriel FODOREAN, Evelin-Anda LAZA, Marius GHERES	42
5.	EFFICACY AND SELECTIVITY OF IMAZAMOX AND PENDIMETHALIN BASED HERBICIDE IN WEED CONTROL IN SOYBEAN CROPS *EFICACITATEA ȘI SELECTIVITATEA AMESTECULUI DE IMAZAMOX ȘI PENDIMETHALIN ÎN CONTROLUL BURUIENILOR DIN CULTURILE DE SOIA* Marga GRĂDILĂ, Daniel JALOBĂ, Valentin Marius CIONTU, Raluca Monica CRISTEA, Mihaela ŞERBAN, Victor PETCU, Nicolae-Valentin VLĂDUȚ, Cătălina TUDORA	48
6.	SAFFLOWER CULTIVATION: CHALLENGES AND PERSPECTIVES *CULTURA DE ȘOFRĂNEL: PROVOCĂRI ȘI PERSPECTIVE* Cătălina TUDORA, Adriana MUSCALU, Marga GRĂDILĂ, Oana MÎRZAN, Florentina GATEA	56
7.	AERODYNAMIC RESPONSE OF PEPPER SEEDS TO VARYING MOISTURE LEVELS: A BASIS FOR OPTIMIZING PNEUMATIC HANDLING AND SEED DISPERSAL *BIBER TOHUMLARININ DEĞIŞEN NEM SEVIYELERINE AERODINAMIK TEPKISI: PNÖMATIK TAŞIMA VE TOHUM DAĞITIMINI OPTIMIZE ETMEK İÇIN BIR TEMEL* Onder KABAS, K.Cagatay SELVI	62
8.	CONSIDERATIONS REGARDING THE USE OF MODERN EQUIPMENT FOR THE EFFICIENT UTILISATION OF PERMANENT PASTURES *CONSIDERAȚII PRIVIND UTILIZAREA ECHIPAMENTELOR MODERNE PENTRU VALORIFICAREA EFICIENTĂ A PĂȘUNILOR PERMANENTE* Remus Marius OPRESCU, Dan CUJBESCU, Iulian VOICEA, Cătălin PERSU, Radu RĂDOI	70
9.	BLACK SOLDIER FLY LARVAE (HERMETIA ILLUCENS): FROM SUSTAINABLE ANIMAL FEED TO EMERGING HUMAN FOOD SOURCE *LARVELE DE MUSCĂ SOLDAT NEGRU (HERMETIA ILLUCENS): DE LA FURAJ SUSTENABIL PENTRU ANIMALE LA SURSĂ ALIMENTARĂ EMERGENTĂ PENTRU OAMENI* Nicoleta UNGUREANU, Nicolae-Valentin VLĂDUȚ, Sorin-Ștefan BIRIȘ, Mariana IONESCU, Neluș-Evelin GHEORGHIȚĂ, Valeria-Elena VLĂDUȚ, Oana-Elena MILEA, Ștefan DUMITRU	80
10.	BLACK SOLDIER FLY (HERMETIA ILLUCENS) FOR SUSTAINABLE ORGANIC WASTE MANAGEMENT: LIFECYCLE, SUBSTRATES, AND BIOCONVERSION PARAMETERS *MUSCA SOLDAT NEGRU (HERMETIA ILLUCENS) ÎN MANAGEMENTUL SUSTENABIL AL DEȘEURILOR ORGANICE: CICLUL DE VIAȚĂ, SUBSTRATURI ȘI PARAMETRII BIOCONVERSIEI* Nicoleta UNGUREANU, Nicolae-Valentin VLĂDUȚ, Sorin-Ștefan BIRIȘ, Mariana IONESCU, Neluș-Evelin GHEORGHIȚĂ, Mirela-Nicoleta DINCĂ	98
11.	THE EFFECTS OF PRUNING SHEAR DESIGN ON HAND FORCES DURING HAZELNUT SUCKERS CUTTING *FINDIK SÜRGÜNLERININ KESIMI SIRASINDA BUDAMA MAKASI TASARIMININ EL KUVVETLERI ÜZERINDEKI ETKILERI* Kemal Çağatay SELVI, Mehmet Ali ERDOĞAN, Ehsan Fartash NAEIMI	114
12.	APPLICATION OF UAV MULTISPECTRAL IMAGERY FOR VINEYARD MANAGEMENT THROUGH VEGETATION STATUS ASSESSMENT *APLICAREA IMAGINILOR UAV MULTISPECTRALE PENTRU MANAGEMENTUL VITICOL PRIN EVALUAREA STĂRII DE VEGETAȚIE* Dan CUJBESCU, Cătălin PERSU, Mihai MATACHE, Iuliana GĂGEANU, Iulian VOICEA	122

No.	Article Title & Authors	page
13.	**ASPECTS REGARDING THE REMEDIATION OF SOILS POLLUTED WITH POLYCYCLIC AROMATIC HYDROCARBONS THROUGH OZONATION** ***ASPECTE PRIVIND REMEDIEREA SOLURILOR POLUATE CU HIDROCARBURI AROMATICE POLICICLICE PRIN OZONARE*** Carmen-Otilia RUSĂNESCU, Gigel PARASCHIV, Irina Aura ISTRATE, Gabriel Alexandru CONSTANTIN, SORIN-Ştefan BIRIŞ, Gheorghe VOICU, Andrei-Marian RUSĂNESCU, Maria GHEORGHE, Anca Ștefania MAXIM	132
14.	**BIOREMEDIATION OF SOILS CONTAMINATED WITH HYDROCARBONS USING MICROBIAL CONSORTIA** ***BIOREMEDIEREA SOLURILOR CONTAMINATE CU HIDROCARBURI UTILIZÂND CONSORȚII MICROBIENE*** Mirela-Nicoleta DINCĂ, Mariana FERDEȘ, Irina - Aura ISTRATE, Gabriel - Alexandru CONSTANTIN, Gigel PARASCHIV, Mariana IONESCU, Bianca - Ștefania ZĂBAVĂ, Gabriel MUȘUROI, Georgiana MOICEANU, Carmen-Otilia RUSĂNESCU	140
15.	**ENGINEERING MEASURES FOR SOIL EROSION CONTROL: A MECHANISM-BASED SYNTHESIS** ***CONSIDERAȚII PRIVIND PRINCIPALELE METODE UTILIZATE ÎN CONTROLUL EROZIUNII SOLULUI*** Roxana Patricia IONAȘCU, Remus Marius OPRESCU, Dan CUJBESCU, Iulian VOICEA	148
16.	**THE STAGE OF POSSIBILITY OF SIMPLIFICATION AND MODERNIZATION OF HYDRAULIC SYSTEM CONTROLS FOR COMBINE HARVESTERS** ***STADIUL POSIBILITĂȚII DE SIMPLIFICARE ȘI MODERNIZARE A COMENZILOR SISTEMULUI HIDRAULIC AL COMBINELOR DE RECOLTAT*** Stefano-Andrea MANTOVANI, Vasilica STEFAN, Radu CIUPERCA, Lucretia POPA, Ana ZAICA, Dragos DUMITRU, Alin HARABAGIU, Melania CISMARU, Catalin DUMITRESCU	156
17.	**ASSESSMENT OF AIRBORNE POLLUTION IN INDUSTRIAL CITIES OF THE DNIPROPETROVSK REGION AND PROSPECTS FOR THE CREATION OF GREEN PROTECTIVE BELTS** ***ОЦІНКА ЗАБРУДНЕННЯ ПОВІТРЯ В ПРОМИСЛОВИХ МІСТАХ ДНІПРОПЕТРОВСЬКОЇ ОБЛАСТІ ТА ПЕРСПЕКТИВИ СТВОРЕННЯ ЗЕЛЕНИХ ЗАХИСНИХ СМУГ*** Mykola KHARYTONOV, Nadia MARTYNOVA, Liubov MATUSHEVYCH, Svitlana SYTNYK	166
18.	**POTENTIAL AND PERSPECTIVES OF ORCHARD LIGNOCELLULOSIC BIOMASS AS A SOURCE OF RENEWABLE ENERGY IN THE REPUBLIC OF MOLDOVA** ***POTENȚIALUL ȘI PERSPECTIVELE BIOMASEI LIGNOCELULOZICE POMICOLE CA SURSĂ DE ENERGIE REGENERABILĂ ÎN REPUBLICA MOLDOVA*** Grigore MARIAN, Alexandru BANARI, Andrei GUDÎMA, Boris NAZAR, Leonid MALAI, Nicolae DARADUDA, Andrei PAVLENCO, Teodor MARIAN	172
19.	**METHODS OF OBTAINING BIOCHAR** ***METODE DE OBȚINERE A BIOCHARULUI*** Nicoleta-Alexandra VANGHELE, Nicolae - Valentin VLĂDUȚ, Andreea MATACHE, Augustina PRUTEANU, Florin NENCIU, Laurențiu VLĂDUȚOIU, Ana-Maria TĂBĂRAȘU, Dragoș ANGHELACHE, Alexandru IONESCU, Elena-Melania CISMARU, Cristian RADU	182
20.	**EVALUATION OF NETTLE PARTS FOR FUNCTIONAL FOODS, BASED ON A NOVEL ANTIOXIDANT-DIETARY ELEMENT INDEX (ADEI)** ***EVALUAREA PĂRȚILOR DE URZICĂ PENTRU ALIMENTE FUNCȚIONALE, PE BAZA UNUI INDICE NOU DE ANTIOXIDANȚI ȘI ELEMENTE NUTRITIVE*** Patricia-Cristina TARKANYI, Nicolae-Valentin VLADUȚ, Mihaela LĂCĂTUȘ, Laura RĂDULESCU, Liana Maria ALDA, Georgeta Sofia POPESCU, Ioan Ladislau CABA, Despina Maria BORDEAN	192
21.	**CFD-BASED INVESTIGATION OF A COUNTER-ROTATING VERTICAL AXIS WIND TURBINE FOR LOW-WIND AGRICULTURAL ENVIRONMENTS** ***INVESTIGAȚIE NUMERICĂ BAZATĂ PE CFD A UNEI CONFIGURAȚII CONTRAROTATIVE DE TURBINE EOLIENE CU AX VERTICAL PENTRU MEDII AGRICOLE CU VÂNT REDUS*** Adrian PANDELE, Bogdan Ovidiu DURAN, Dragos Mihail PREDA, Robert BILA, Elena VILCU, Andrei VULPE, Gheorghe VOICU	198
22.	**CHICKPEA PRODUCTIVITY UNDER BIOTIC AND ABIOTIC STRESSES: CURRENT STATUS AND PERSPECTIVES** ***PRODUCTIVITATEA NĂUTULUI ÎN CONDIȚII DE STRES BIOTIC ȘI ABIOTIC: SITUAȚIA ACTUALĂ ȘI PERSPECTIVE*** Costin MIRCEA, Florin NENCIU, Alexandru IONESCU, Iulian DUMITRU, Raluca-Adriana ZOTA	212
23.	**TECHNOLOGIES IN THE DEHYDRATION OF BERRIES: A REVIEW** ***TEHNOLOGII ÎN DESHIDRATAREA FRUCTELOR DE PĂDURE*** Mariana IONESCU, Gabriel-Alexandru CONSTANTIN, Sorin-Ștefan BIRIȘ, Neluș-Evelin GHEORGHIȚĂ, Mirela-Nicoleta DINCĂ, Elena-Mădălina ȘTEFAN, Nicoleta UNGUREANU, Bianca-Ștefania ZĂBAVĂ	222
24.	**DESIGN AND SIMULATION OF A RANDOM FOREST-BASED CONTROL ALGORITHM FOR GREENHOUSE MANAGEMENT** ***PROIECTAREA ȘI SIMULAREA UNUI ALGORITM DE CONTROL BAZAT PE RANDOM FOREST PENTRU MANAGEMENTUL SERELOR*** Mihai-Gabriel MATACHE, Robert CRISTEA, Dragoș-Ioan SĂCĂLEANU, Cristina-Mihaela DOBRE	232

No.	Article Title & Authors	page
25.	**SUSTAINABLE SOUND ABSORBING COMPOSITE STRUCTURES BASED ON ECO-FRIENDLY MATERIALS FOR ROAD NOISE REDUCTION** ***STRUCTURI COMPOZITE FONOABSORBANTE SUSTENABILE PE BAZĂ DE MATERIALE ECOLOGICE PENTRU REDUCEREA ZGOMOTULUI RUTIER*** Jazmina SCORTEA, Sorina ZLATOIANU, Ovidiu VASILE	240
26.	**VALORIZATION OF RENEWABLE RESOURCES FOR THE PRODUCTION OF BIOPLASTICS IN A CIRCULAR ECONOMY** ***VALORIFICAREA SURSELOR REGENERABILE PENTRU PRODUCEREA BIOPLASTICELOR ÎNTR-O ECONOMIE CIRCULARĂ*** Ana-Maria TĂBĂRAȘU, Iuliana GĂGEANU, Dragoș-Nicolae ANGHELACHE, Alin-Teofil ONCESCU, Doru-Relu ANTON, Nicoleta-Alexandra VANGHELE, Melania-Elena CISMARU, Alexandru CIOACLĂ, Alexandru IONESCU, Cristian RADU	250
27.	**CURRENT STATE OF RESEARCH ON THE INFLUENCE OF VIBRATIONS ON THE HUMAN BODY OF VEHICLE OPERATORS** ***STADIUL ACTUAL AL CERCETĂRILOR PRIVIND INFLUENȚA VIBRAȚIILOR ASUPRA ORGANISMULUI UMAN AL CONDUCĂTORULUI AUTO*** Teofil-Alin ONCESCU, Nicolae-Valentin VLADUT, Iuliana GAGEANU, Ioan Catalin PERSU, Gabriel-Mihai MATACHE, Oana Elena MILEA, Ana-Maria TABARASU, Lavinia Madalina MICU	258
28.	**THE INFLUENCE OF STORAGE CONDITIONS ON THE QUALITY OF CANNED MEAT** ***INFLUENȚA CONDIȚIILOR DE DEPOZITARE ASUPRA CALITĂȚII CONSERVELOR DE CARNE*** Andreea Ioana BADIU, Sorin-Ștefan BIRIȘ, Florentina BRATOSIN, Alexandru Ionuț CÎRÎC, Mihaela BEGEA	270
29.	**STUDY ON OPTIMIZING THE PERFORMANCE OF ROW CROP SEEDERS** ***STUDIU PRIVIND OPTIMIZAREA PERFORMANȚELOR SEMĂNĂTORILOR DE PLANTE PRĂȘITOARE*** Eugen MARIN, Nicolae-Valentin VLĂDUȚ, Mihai-Gabriel MATACHE, Dan-Iulian CUJBESCU, Mario CRISTEA, Alexandru IONESCU	276
30.	**VIBRATORY CULTIVATORS FOR SUSTAINABLE AGRICULTURE: A REVIEW OF DESIGN, PERFORMANCE, AND SMART TECHNOLOGIES** ***CULTIVATOARELE VIBRATOARE ÎN AGRICULTURA SUSTENABILĂ: ANALIZĂ A PROIECTĂRII, PERFORMANȚEI ȘI TEHNOLOGIILOR INTELIGENTE*** Neluș-Evelin GHEORGHIȚĂ, Sorin-Ștefan BIRIȘ, Raluca-Adriana ZOTA, Mariana IONESCU, Daria-Ioana SICARU, Dragoș ANGHELACHE	288
31.	**REMEDIATION METHODS OF CONTAMINATED SOILS - REVIEW** ***METODE DE REMEDIERE A SOLURILOR CONTAMINATE - REVIEW*** Mariana Gabriela MUNTEANU, Irina Aura ISTRATE, Gheorghe VOICU, Georgiana MOICEANU, Elena Mădălina ȘTEFAN, Mihai Sabin MAGUREAN, Gabriel GHEORGHE	296
32.	**STUDY OF JERK FOR A ROBOTIC ARM** ***STUDIUL DERIVATEI ACCELERAȚIEI PENTRU UN BRAȚ ROBOTIC*** Florinel LUPU, Andrei CRAIFALEANU, Sorin NEGROIU	306
33.	**THE IMPORTANCE OF PNEUMATIC DEDUSTING SYSTEMS IN CEREAL MILLS** ***IMPORTANȚA SISTEMELOR PNEUMATICE DE DESPRĂFUIRE ÎN MORILE DE CEREALE*** Liliana-Caliopi ISCRU, Daniel-Mirel DUMITRESCU, Gheorghe VOICU	312
34.	**TESTING METHODOLOGY FOR A MIXED INTELLIGENT CROP BIRD SCARING SYSTEM** ***METODOLOGIE DE TESTARE PENTRU UN SISTEM INTELIGENT MIXT DE SPERIAT PĂSĂRILE DIN CULTURI*** Augustina PRUTEANU, Mihai MATACHE, Alexandru IONESCU, Dorin Andrei CÎRSTEA, Dorin Robert CRISTEA, Simona-Florina ISTICIOAIA	318
35.	**EVALUATION OF THE NUTRITIONAL COMPOSITION OF HEMP-BASED DIETARY SUPPLEMENTS AND FUTURE TRENDS** ***EVALUAREA COMPOZIȚIEI NUTRIȚIONALE A SUPLIMENTELOR ALIMENTARE PE BAZĂ DE CÂNEPĂ ȘI TENDINȚELE VIITOARE*** Andreea MATACHE, Nicoleta Alexandra VANGHELE, Florin NENCIU, Augustina Mirabela PRUTEANU, Tatiana ONISEI, Alexandra LEONTE, Lorena-Diana POPA	326
36.	**STUDIES AND RESEARCH ON THE TECHNOLOGICAL PROCESS OF REMOVING SOLID PARTICLES FROM WASTEWATER OF A RECIRCULATING AQUACULTURE FISH FARMING SYSTEM, BY USING TECHNICAL MECHANICAL FILTRATION EQUIPMENT** ***STUDII ȘI CERCETĂRI ASUPRA PROCESULUI TEHNOLOGIC DE ÎNDEPĂRTARE AL PARTICULELOR SOLIDE DIN APĂ REZIDUALĂ A UNUI SISTEM ACVACOL RECIRCULANT DE CREȘTERE A PEȘTILOR, PRIN UTILIZAREA UNUI ECHIPAMENT TEHNIC DE FILTRARE MECANICĂ*** Evelin-Anda LAZA, Dragoș Vasile NICA, Ioan Ladislau CABA, Ana-Cristina VASILE, Aurelian GRUIN	334

No.	Article Title & Authors	page
37.	**INTEGRATED MECHANICAL AND METABOLIC ENGINEERING STRATEGIES FOR HIGH-CELL-DENSITY CULTIVATION OF SACCHAROMYCES CEREVISIAE IN STIRRED-TANK BIOREACTORS: A CRITICAL REVIEW** ***STRATEGII INGINEREȘTI MECANICE ȘI METABOLICE INTEGRATE PENTRU CULTIVAREA LA DENSITATE RIDICATĂ A SACCHAROMYCES CEREVISIAE ÎN BIOREACTOARE CU AGITARE MECANICĂ: O ANALIZĂ CRITICĂ*** Elena-Valeria VLĂDUȚ, Sorin-Ștefan BIRIȘ, Mariana FERDEȘ, Adrian IOSIF, Alina-Daiana IONESCU, Raluca Adriana ZOTA	338
38.	**GIS TECHNOLOGY AND ITS APPLICATIONS IN ENVIRONMENTAL ENGINEERING** ***TEHNOLOGIA GIS ȘI APLICAȚIILE ACESTEIA ÎN INGINERIA MEDIULUI*** Bianca-Ștefania ZĂBAVĂ, Gheorghe VOICU, Mirela - Nicoleta DINCĂ, Gigel PARASCHIV, Mariana IONESCU, Georgiana MOICEANU, Mariana FERDEȘ	346
39.	**STONE PAPER AS A SUSTAINABLE ALTERNATIVE: APPLICATIONS, CHALLENGES AND OPPORTUNITIES** ***STONE PAPER CA ALTERNATIVĂ SUSTENABILĂ: APLICAȚII, PROVOCĂRI ȘI OPORTUNITĂȚI*** Andreea-Nicoleta BURCEA, Daniel ȘIPU, Cristina-Ileana COVALIU-MIERLĂ	352
40.	**ADSORPTION EFFICIENCY OF COOPER FROM WASTEWATER BY USE SOME ALTERNATIVE ADSORBENT MATERIALS** ***EFICIENȚA DE ADSORBȚIE A CUPRULUI DIN APE UZATE PRIN UTILIZAREA UNOR MATERIALE ADSORBANTE ALTERNATIVE*** Cristina-Ileana COVALIU-MIERLĂ, Maria RÂPĂ, Sorin IONESCU	358
41.	**EXPERIMENTAL STUDY ON THE DYNAMIC BEHAVIOR OF THE 3SLP SPRINGBOARD IN RUNNING TESTS** ***STUDIU EXPERIMENTAL PRIVIND COMPORTAMENTUL DINAMIC AL TRAMBULINEI 3SLP ÎN TESTELE DE ALERGARE*** Daniel-Mirel DUMITRESCU, Gheorghe VOICU, Nicolaie ORĂȘANU, Liliana-Caliopi ISCRU, Gabriel-Alexandru CONSTANTIN, Adrian IOSIF	362
42.	**KINEMATIC ANALYSIS OF A DISINFECTION SPIDER ROBOT** ***ANALIZA CINEMATICĂ A UNUI ROBOT PĂIANJEN DE DEZINFECȚIE*** Sorin NEGROIU, Andrei CRAIFALEANU, Florinel LUPU	370
43.	**DEEP LEARNING–POWERED APP FOR EARLY DETECTION OF TOMATO AND PEPPER LEAF DISEASES** ***APLICAȚIE BAZATĂ PE DEEP LEARNING PENTRU DETECTAREA TIMPURIE A BOLILOR FRUNZELOR DE ROȘII ȘI ARDEI*** Robert-Dorin CRISTEA, Ionel Lucian DUMITRESCU, Alexandru-Cristian CIOACLA, Dorin-Andrei CÎRSTEA	380
44.	**MODERN METHODS FOR PROCESSING FERMENTED DAIRY PRODUCTS** ***METODE MODERNE DE PROCESARE A PRODUSELOR LACTATE FERMENTATE*** Florentina BRATOSIN, Sorin-Ștefan BIRIȘ, Andreea-Ioana BADIU, Alexandru Ionuț CÎRÎC, Mihaela BEGEA	388
45.	**EXTRUSION FABRICATION OF SHEEP-WOOL REINFORCED PLA/PBAT/PA BIOCOMPOSITES FOR AGRICULTURE 4.0/5.0 APPLICATIONS** ***FABRICAREA PRIN EXTRUDARE A BIOCOMPOZITELOR DIN PLA/PBAT/PA RANFORSATE CU LÂNĂ DE OAIE PENTRU APLICAȚII ÎN AGRICULTURA 4.0/5.0*** Teodor Gabriel FODOREAN, Elena Mihaela NAGY, Dragos-Vasile NICA, Eveline Anda LAZA, Ioan KABA, Valentin VLADUT, Teodor VINTILA	396
46.	**EFFECT OF FRUITS POWDERS ADDITION ON WHEAT FLOUR DOUGH RHEOLOGICAL PROPERTIES - REVIEW** ***INFLUENȚA ADAOSULUI PUDREI DE FRUCTE ASUPRA PROPRIETĂȚILOR REOLOGICE ALE ALUATULUI DIN FĂINĂ DE GRÂU - REVIEW*** Elena-Mădălina ȘTEFAN, Aura-Irina ISTRATE, Gabriel-Alexandru CONSTANTIN, Mariana-Gabriela MUNTEANU, Gheorghe VOICU, Gabriel MUȘUROI, Alina-Daiana IONESCU, Elena-Melania CISMARU	402
47.	**OBTAINING FORTIFIED WINES WITH GRAPE POMACE BIOCOMPOUNDS OBTAINED BY MAE EXTRACTION METHOD** ***OBȚINEREA VINURILOR FORTIFIATE CU BIOCOMPUȘI DIN TESCOVINĂ OBȚINUȚI PRIN METODA DE EXTRACȚIE MAE*** Petronela Anca ONACHE, Irina Elisabeta GEANĂ, Corina Teodora CIUCURE, Iulia Cristina CIOBANU, Victoria ARTEM, Georgiana CÎRSTEA, Alina FLOREA, Dorin Ioan SUMEDREA, Mircea NEGRUTA	418
48.	**IMPLEMENTATION OF A MICROHYDROPOWER SYSTEM FOR SUSTAINABLE AERATION OF FISH PONDS** ***REALIZAREA UNUI SISTEM MICROHIDROENERGETIC PENTRU AERAREA SUSTENABILĂ A BAZINELOR PISCICOLE*** Marinela MATEESCU, Dragoș MANEA, Eugen MARIN, Dragoș- Nicolae DUMITRU, Elena-Melania CISMARU, Ioan PAVEL	432
49.	**PERFORMANCE EVALUATION OF THE EXPERIMENTAL PLANER-GRADER MODEL FOR PERMANENT GRASSLAND MAINTENANCE** ***EVALUAREA PERFORMANȚELOR MODELULUI EXPERIMENTAL DE RINDEA-GREDER PENTRU ÎNTREȚINEREA PAJIȘTILOR PERMANENTE*** Eugen MARIN, Vasile MOCANU, Tudor-Adrian ENE, Dragoș MANEA, Mihai-Gabriel MATACHE, Laurențiu-Constantin VLĂDUȚOIU, Alexandru IONESCU	438
50.	**SIMPLIFIED MODELING OF ACOUSTIC ATTENUATION FOR SOUND BARRIERS** ***MODELAREA SIMPLIFICATĂ A ATENUĂRII ACUSTICE PENTRU BARIERE SONICE*** Ana-Maria GROSU, Ovidiu VASILE	446

No.	Article Title & Authors	page
51.	**ULTRASONIC ASSESSMENT OF MECHANICAL PROPERTIES IN ISOTROPIC AND ORTHOTROPIC MATERIALS** ***EVALUAREA ULTRASONICĂ A PROPRIETĂȚILOR MECANICE ALE MATERIALELOR IZOTROPE ȘI ORTOTROPE*** Andreea-Denisa GRIGUȚA, Mihai Valentin PREDOI, Cristian-Cătălin PETRE, Laura-Mariana BARBU, Gheorghe FLOROIU	452
52.	**PM10 AND PM2.5 PARTICLE POLLUTION IN TARGOVISTE CITY, DAMBOVITA COUNTY** ***POLUAREA CU PARTICULE PM10 ŞI PM2,5 ÎN ORAŞUL TÂRGOVIŞTE, JUDEŢUL DÂMBOVIŢA*** Florina Roxana DUMITRU, Lucica BARBEŞ, Daniel Emil Constantin DUNEA	462
53.	**OPTIMIZING PROCESSES IN AGRICULTURE AND THE FOOD INDUSTRY** ***OPTIMIZAREA PROCESELOR ÎN AGRICULTURĂ ȘI INDUSTRIA ALIMENTARĂ*** Gabriel NAE, Florin NENCIU, Andreea MATACHE, Nicoleta VANGHELE, Diana-Lorena POPA, Floarea SERBANCEA, Cristian SERBANCEA	466
54.	**EXTENSIVE GREEN ROOFS FOR SMART BUILDINGS** ***ACOPERIȘURI VERZI EXTENSIVE PENTRU CLADIRI SMART*** Dragos Mihail PREDA, Adrian PANDELE, Bogdan Ovidiu DURAN, Elena VILCU, Andrei Vulpe, Gheorghe VOICU	476
55.	**COMPARATIVE STUDY ON SOIL TYPES AND AGRICULTURAL POTENTIAL IN THE MAIN REGIONS OF ROMANIA** ***STUDIU COMPARATIV ASUPRA TIPURILOR DE SOL ȘI POTENȚIALULUI AGRICOL ÎN PRINCIPALELE REGIUNI ALE ROMÂNIEI*** Iuliana GĂGEANU, Ana-Maria TĂBĂRAȘU, Teofil-Alin ONCESCU, Lorena-Diana POPA	482
56.	**MINERAL COMPOSITION AND AROMA QUALITY IN BAY LAUREL (LAURUS NOBILIS) LEAVES** ***COMPOZIȚIA MINERALĂ ȘI CALITATEA AROMEI FRUNZELOR DE DAFIN (LAURUS NOBILIS)*** Petruta ANDREI, Corina Dana MISCA, Aurica Breica BOROZAN, Ioan Ladislau CABA, Diana MOIGRADEAN, Despina - Maria BORDEAN	488
57.	**CAPITALIZING ON CLIMATE-IMPACTED AGRICULTURAL AREAS WITH *CHAENOMELES* FRUIT SHRUBS** ***VALORIFICAREA SUPRAFEȚELOR AGRICOLE AFECTATE DE SCHIMBĂRILE CLIMATICE CU ARBUȘTI FRUCTIFERI CHAENOMELES*** Tamara Elena MIHOCIU, Denisa Eglantina DUȚĂ, Luminița CATANĂ, Gabriela Daniela CRIVEANU-STAMATIE, Monica CATANĂ, Iulia GRIGORE	494
58.	**DESIGN OPTIMIZATION OF CUTTING BLADES FOR MOWING EQUIPMENT THROUGH COMPARATIVE STUDY USING SOLIDWORKS SIMULATION** ***OPTIMIZAREA CONSTRUCTIVĂ A CUȚITELOR PENTRU ECHIPAMENTE DE COSIT PRIN STUDIU COMPARATIV UTILIZÂND SOLIDWORKS SIMULATION*** Alin-Nicolae HARABAGIU, Vasilica ȘTEFAN, Lucreția POPA, Dragoș-Nicolae DUMITRU, Elena-Melania CISMARU, Dragoș MANEA, Polifron CHIRITA	504
59.	**BIOCHAR IN SUSTAINABLE AGRICULTURE: EFFECTIVE APPLICATION STRATEGIES FOR SOIL IMPROVEMENT AND PRODUCTIVITY INCREASE- REVIEW** ***BIOCHARUL ÎN AGRICULTURA DURABILĂ: STRATEGII EFICIENTE DE APLICARE PENTRU ÎMBUNĂTĂȚIREA SOLULUI ȘI CREȘTEREA PRODUCTIVITĂȚII - REVIEW*** Iulian DUMITRU, Laurențiu VLĂDUȚOIU, Florin NENCIU, Valentin VLĂDUȚ, Alexandru IONESCU, Oana-Elena MILEA, Gabriel NAE, Costin MIRCEA, Iulian VOICEA, Andreea-Iulia GRIGORE, Adriana BORȘ	512
60.	**ANALYSIS OF INTERNATIONAL STANDARDS THAT CERTIFAY THE PRODUCTS QUALITY OF PYROLYSIS PROCESS- REVIEW** ***ANALIZA STANDARDELOR INTERNAȚIONALE CARE CERTIFICA CALITATEA PRODUSELOR OBȚINUTE DIN PROCESUL DE PIROLIZĂ*** Alexandra-Liana VIȘAN, Vasilica ȘTEFAN, Alin HARABAGIU, Radu CIUPERCĂ, Ana ZAICA	522
61.	**CREATING A DATABASE FOR ARTIFICIAL INTELLIGENCE TRAINING/** ***CREAREA UNEI BAZE DE DATE CU SCOPUL ANTRENARII INTELIGENCEI ARTIFICIALE*** Dorin-Andrei CÎRSTEA, Robert-Dorin CRISTEA, Mihai Gabriel MATACHE	532
62.	**ENHANCING SOIL SAMPLING ACCURACY THROUGH IOT INTEGRATION** ***ÎMBUNĂTĂȚIREA PRECIZIEI EȘANTIONĂRII SOLULUI PRIN INTEGRAREA IOT*** Alexandru-Cristian CIOACLA, Iuliana GAGEANU, Robert Dorin CRISTIEA, Mario CRISTEA, Dorin-Andrei CÎRSTEA, Roxana-Georgiana AMARGHIOALEI	538

CLIMATE CHANGE MITIGATION BY BIOLOGICAL CARBON SEQUESTRATION OF DIFFERENT MAIZE HYBRIDES

/

UBLAŽAVANJE KLIMATSKIH PROMJENA BIOLOŠKOM SEKVESTRACIJOM UGLJIKA RAZLIČITIH HIBRIDA KUKURUZA

Darija BILANDŽIJA*[1)], Marija GALIĆ[1)], Grubor MATEJA[2)], Tajana KRIČKA[2)], Bilandžija NIKOLA[2)]

[1)] University of Zagreb Faculty of Agriculture, Division of Agroecology / Croatia;

[2)] University of Zagreb Faculty of Agriculture, Division of Agricultural Engineering and Technology / Croatia.

**E-mail: dbilandzija@agr.hr; mcacic@agr.hr; mgrubor@agr.hr; tkricka@agr.hr; nbilandzija@agr.hr*

Keywords: *maize hybrides, biomass C content, C allocation, above-ground biomass, below-ground biomass, Croatia*

ABSTRACT

The year 2024 is the warmest year since records began and the first calendar year in which the global average temperature exceeded 1.5°C above pre-industrial levels. Therefore, methods to reduce greenhouse gas emissions and increase their sinks are being intensively investigated. The aim of this research is to determine the potential of different maize hybrids to mitigate climate change through biological carbon sequestration. In this research, biomass yield and biomass carbon content are determined for four different maize hybrids grown in continental Croatia during the 2021 harvest. The investigations showed that the carbon content in the root, stubble, stalk, cob, husk and grain of the different maize hybrids on average amounted 1.21 t ha-1, 0.4 t ha-1, 5.42 t ha-1, 0.91 t ha-1, 0.47 t ha-1 and 4.33 t ha-1, respectively. There is no statistically significant difference between the studied hybrids in the carbon content in cob and grain, while statistically significant differences were found for the carbon content in root, stubble, stem and husk. The results of the study suggest that by selecting maize hybrids that sequester more carbon and through good biomass management, more atmospheric carbon can be removed from the atmosphere and soil fertility can be increased.

SAŽETAK

Najtoplija godina od kada postoje mjerenja i prva godina kada je globalna prosječna temperatura zraka bila iznad 1.5°C viša u odnosu na predindustrijsko razdoblje je 2024. Stoga, metode smanjenja emisija i povećanja ponora stakleničkih plinova se sve više istražuju. Cilj ovoga rada je utvrditi za različite hibride kukuruza njihov potencijal ublažavanja klimatskih promjena putem biološke sekvestracije ugljika. Prinos biomase i sadržaj ugljika u biomasi, su utvrđeni za četiri različita hibrida kukuruza uzgojena u kontinentalnoj Hrvatskoj tijekom žetve 2021. godine. Sadržaj ugljika u korijenu, strništu, stabljici, klipu, oklasku i zrnu različitih hibrida kukuruza u prosjeku redom iznosi 1,21 t ha^{-1}, 0,4 t ha^{-1}, 5,42 t ha^{-1}, 0,91 t ha^{-1}, 0,47 t ha^{-1} i 4,33 t ha^{-1}. Nisu utvrđene statistički značajne razlike između istraživanih hibrida kukuruza za sadržaj ugljika u klipu i zrnu, dok su statistički značajne razlike utvrđene za sadržaj ugljika u korijenu, strništu, stabljici i oklasku. Rezultati pokazuju da odabirom hibrida kukuruza koji vežu više ugljika i dobrim gospodarenjem biomasom se može ukloniti više ugljika iz atmosfere i povećati plodnost tla.

INTRODUCTION

Periodic climate change, global warming and cooling, are natural climatological cycles of climate variability in the Earth's atmosphere that change at different intervals. Since the industrial revolution, however, climate change has been dominated by human influences that exceed the limits of natural variability *(Karl and Trenberth, 2003).* According to the IPCC (2001) report on climate change, the concentration of carbon dioxide (CO_2) has increased by 31%, of methane (CH_4) by 151% and of nitrous oxide (N_2O) by 17% since the beginning of the industrial revolution up to the year 2000. It was predicted that if anthropogenic greenhouse gas emissions continue to be emitted the atmosphere at this rate, it will be possible that the predicted, previously unrecorded increase in average air temperature of 1.1 to 5.8 °C will be reached by the end of the century *(Tokgöz, 2010).* Unfortunatelly, the 2024 is confirmed by the Copernicus Climate Change Service (2025) to be the warmest year on record globally, and the first calendar year that the average global temperature exceeded 1.5°C above its pre-industrial level. Therefore, methods to reduce

greenhouse gass emissions and increase their sinks are being intensively investigated. The most important greenhouse gas is considered to be CO_2, which in Croatia has the largest contribution with 71.7 % to the total GHGs emission in 2022 excluding LULUCF sector (NIR 2024, 2025).

Carbon circulates in relatively short periods between the atmosphere, the biosphere and the pedosphere. Biological carbon sequestration represents the uptake of atmospheric CO2 in the process of photosynthesis and storage in plant biomass. In agriculture, depending on how the agricultural biomass is managed, some of the biomass is incorporated into the soil after harvesting, storing atmospheric carbon in the soil pool. This not only helps to reduce atmospheric CO_2 levels, but also improves soil health, leading to higher yields, nutrient levels and other agroecological benefits. The storage of atmospheric carbon in the plant/soil pools is complex and depends on many factors, such as crop type and its variety, biomass management, agrotechnical measures, etc. Different crops and their varieties with their morphological and physiological predispositions have a direct effect on carbon sequestration and C input into the plant/soil pool.

Therefore, the aim of this study is to determine the carbon content and its distribution within the plant parts of old and new Croatian maize hybrids.

MATERIALS AND METHODS

Location

A study was conducted during the 2021 growing season at experimental field near Osijek city, continental Croatia (φ = 45°31′56.47″ N, λ = 18°44′16.07″ E; 90 m a.s.l). The size of each experimental plot of the individual maize hybrids was 150 m2 (15 m x 10 m) in three replicates (Figure 1).

Fig. 1 - Experimental field in continental Croatia

Climate

According to Bilandžija and Martinčić (2021), the average air temperature at experimental field during the vegetation season is 18.6 °C and the annual average is 11.7 °C (Table 1).

The average seasonal air temperature of spring is 12.1 °C, of summer 21.7 °C, of fall 11.6 °C and of winter 1.5 °C.

Table 1

Average air temperature (°C) at experimental field during period 1991. – 2018.

	spring	summer	autumn	winter	vegetation	annual
1991. – 2018.						
av	12,1	21,7	11,6	1,5	18,6	11, 7
sd	1,0	1,0	1,0	1,6	0,9	0,8
max	13,7	23,8	13,6	5,0	20,1	12,9
min	10,4	20,1	9,6	-1,5	17,2	10,2

** spring (3.-5.month), summer (6.-8. month), autumn (9.-11. month), winter (12.-2. month), vegetation season (4.-9. month), annual (1-12 month), av – average, sd - standard deviation, max – maximum, min – minimum. (source: Bilandžija and Martinčić, 2021)*

The average precipitation amount of the period 1991–2018 during the growing season is 390 mm and annualy 707 mm with the highest recorded precipitation amount in June (80.7 mm) *(Bilandžija and Martinčić, 2021)* (Table 2).

Table 2

Average precipitation amount (mm) at experimental field during period 1991. – 2018.

	spring	summer	autumn	winter	vegetation	annual
1991. – 2018.						
av	167	207	196	142	390	707
sd	55	91	70	60	149	161
c_v	0,33	0,44	0,36	0,43	0,38	0,23
P_{max}	282	519	318	295	699	1038
P_{min}	35	78	45	1	155	317

** spring (3.-5.month), summer (6.-8. month), autumn (9.-11. month), winter (12.-2. month), vegetation season (4.-9. month), annual (1-12 month), av – average, sd - standard deviation, cv - variation coefficient, P_{max} – maximum, P_{min} – minimum. (source: Bilandžija and Martinčić, 2021)*

Soil properties

The soil at the experimental site has a silty-loam texture with a content of 2.33% sand, 56% silt, and 41.67% clay. The water holding capacity is 37.7%, air holding capacity is 10.2%, soil porosity is 47.8%, and bulk density is 1.39 g cm−3. The soil pHKCl is 7.24, and the soil contains 2.3% humus, 0.11% total nitrogen, 1.25% total carbon, 0.06% total sulfur, 17.9 mg of P_2O_5, and 15.5 mg of K_2O per 100 g of soil.

Maize hybrides

The experiment includes 4 different maize hybrids (Zea mays L.) bred by the Agricultural Institute Osijek. Two new hybrids Rudolfov 60 and Kulak and two old hybrids OSSK 515 and OSSK 596 were studied. Maize hybrides properties are presented in table 3 and more on maize hybrides can be found in cataloque of Agricultural Institute Osijek *(AIO, 2020)*.

Table 3

Properties of maize hybrides

	RUDOLFOV	KULAK	OS 596	OS 515
Purpose	dry grain production, ear harvesting, silage production		ear harvesting, silage production	silage production
Kernel type	dent-type kernel			
Number of rows of kernels	16 – 18		14 – 16	16 – 18
Recommended plant density	68 000 – 71 000 germinable seeds/ha	71 000 – 75 000 germinable seeds/ha	65 000 – 68 000 germinable seeds/ha	68 000 – 71 000 germinable seeds/ha
Sowing distance	20 – 21 cm apart	19 – 20 cm apart	21 – 22 cm apart	20 – 21 cm apart

Source: Agricultural Institute Osijek (2020)

Biomass sampling

Sampling of the below-ground (root) and above-ground (stubble, stalk, cob, husk and grain) plant parts of the maize hybrids was carried out in three replicates. The biomass was sampled by destructive method from 1 m^2 of the experimental plot (Figure 2).

Fig. 2 - Field biomass sampling

After field sampling of biomass at the experimental field, the samples were delivered on the same day to the Faculty of Agriculture University of Zagreb where the below-ground biomass was cleaned of soil particles and the above-ground biomass was fragmented (Figure 3) and weighed.

After weighing, subsamples were taken from each plant part of the maize and prepared for the laboratory determination of the carbon content in the biomass.

Fig. 3 - Fragmentation of above-ground biomass

Determination of carbon content in biomass

Total carbon content in above- and belowground biomass was determined simultaneously bye dry combustion method. Biomass samples were dried in an oven *(Nueve, FN 120, Ankara , Turkey)* at 105 °C to a constant weight, weighed (Sartorius CP 64; d = 0.1 mg, Göttingen, Germany), and analyzed using the Vario Macro CHNS analyzer (Elementar, Langenselbold, Germany). Total biomass carbon content was determined according to the HRN ISO 10694 2004 protocol. To obtain carbon yields in t/ha, the dry matter yield of each biomass fraction is multiplied by the carbon concentrations of each fraction.

Statistical analysis

The statistical analysis was performed with the statistical software SAS 9.*1 (SAS Inst. Inc., 2002–2004, Cary, NC, USA)*. The variability between the investigated maize hybrides was analyzed by analysis of variance (ANOVA) and, if necessary, tested with the Fisher post-hoc t-test. The significance threshold for all analyzes was 5%. The quality management system (QM) complies with good laboratory practice and includes internal and external quality controls (QC).

RESULTS AND DISCUSSION

The average carbon contents of all maize hybrides studied are 1.21 t ha^{-1} for root, 0.4 t ha^{-1} for stubble, 5.42 t ha^{-1} for stalk, 0.91 t ha^{-1} for cob, 0.47 t ha^{-1} for husk and 4.33 t ha^{-1} for grain. The descriptive statistic for carbon content average values of all maize hybrids by the individual plant parts of the biomass are presented in Table 4.

Table 4

Average carbon content of all maize hybrides (t ha^{-1}) in individual plant parts

	Root		Stubble		Stalk		Cob		Husk		Grain	
	av	sd	av	sd	av	sd	av	sd	avr	sd	av	sd
average	1.21	0.33	0.4	0.06	5.42	1.17	0,91	0,1	0,47	0,12	4,33	0,53
min	0.85		0.31		3.88		0.75		0.28		3.61	
max	1.81		0.5		7.85		1.06		0.77		5.41	

*av – average, sd - standard deviation, max – maximum, min – minimum

Figure 4 presents carbon content in individual plant parts for each maize hybrid studied. The The dry matter yield of roots ranges from 2.57 to 4.43 t ha^{-1} and percentage of carbon in roots between 34.8 to 38.19 % depending on maize hybride. The carbon content in the roots ranges from 0.94 to 1.65 t ha^{-1}. The statistical analyses determined that the carbon content in the root (Figure 4a) of the Rudolfov hybrid is significantly higher than that of the other hybrids studied.

The Kulak hybrid contains a statistically significantly higher amount of carbon in the roots compared to the OS 596 and OS 515 hybrids, and significantly lower compared to Rudolfov. There is no statistically significant difference in the carbon content in the roots between the OS 596 and OS 515 hybrids.

The dry matter yield of stubble ranges from 0.97 to 1.33 t ha^{-1} and percentage of carbon in stubble between 34.28 to 38.19 % depending on maize hybride. The carbon content in the stubble ranges from 0.36 to 0.46 t ha^{-1}. The carbon content in the stubble (Figure 4b) differs significantly only between the Rudolfov

hybrid and OS 596, which has the highest amount of stored carbon in the stubble, while no significant difference was found between the other hybrids studied. The dry matter yield of stalk ranges from 10.40 to 14.40 t ha^{-1} and percentage of carbon between 45.34 to 48.03 % depending on maize hybride. The carbon content in the stalk (Figure 4c) ranges from 4.71 to 6.92 t ha^{-1}. The carbon content in the stalk of the Rudolfov hybrid is significantly higher than that of the other maize hybrids studied, between which no statistically significant difference was found. The dry matter yield of cob ranges from 1.74 to 2.00 t ha-1 and percentage of carbon between 48.44 to 50.38 % depending on maize hybride. The carbon content in the cob ranges from 0.88 to 0.97 t ha^{-1} (Figure 4d). No statistically significant difference in the amount of carbon in the cob was found between the maize hybrids studied. The dry matter yield of husk ranges from 0.77 to 1.23 t ha^{-1} and percentage of carbon between 44.50 to 48.82 % depending on maize hybride The carbon content in the husk ranges from 0.36 to 0.60 t ha^{-1}.

The carbon content in the husk of the Rudolfov hybrid is significantly higher than that of the Kulak hybrid, but no statistically significant difference was found between the other hybrids studied (Figure 4e). The dry matter yield of grain ranges from 9.92 to 11.28 t ha^{-1} and percentage of carbon between 40.01 to 41.72 % depending on maize hybride. The carbon content in the grain (Figure 4f) varies between 4.10 and 4.71 t ha^{-1}, and no statistically significant difference in the carbon content of the grain was found between the studied hybrids.

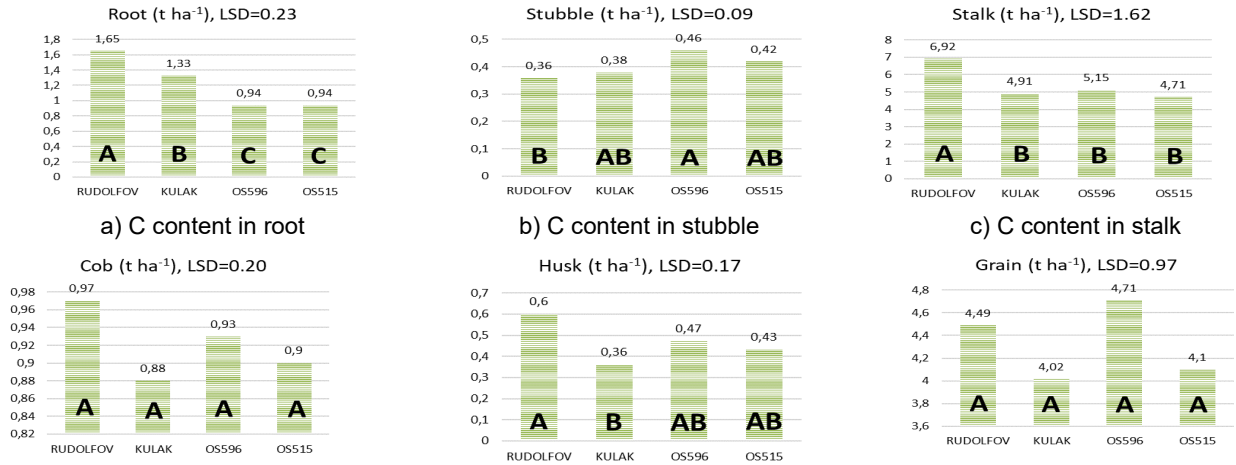

a) C content in root b) C content in stubble c) C content in stalk

d) C content in cob e) C content in husk f) C content in grain

Fig. 4 - Carbon content in: a) root, b) stubble, c) stalk, d) cob, e) husk and f) grain for each maize hybrid studied

By the literature review it was found that the Amos and Walters (2006) determined 0.64 t ha^{-1} of carbon in maize roots, which is almost half of the values determined in this study, and 0.29 t ha^{-1} in stubble, which is slightly lower than the value determined in this study. In the study conducted by Zhao et al. (2018), rhizodeposition was added to the belowground plant biomass, and the total value obtained was 3.00 t C ha^{-1}. Jans et al. (2010) found 0.40 t ha^{-1} of carbon in belowground biomass and 7.50 t ha^{-1} in the total aboveground biomass, which is lower than the values obtained in this study. Wang et al. (2022) determined the mass of carbon in the dry matter of the husk to be in the range of 0.48 to 0.65 t ha-1 , which is consistent with the valeus obtained in this study. According to Zhao et al. (2018), the husk contains 10 % of the carbon content in the stalk, which roughly corresponds to the values determined. Since the results from the literature review differ somewhat from the values obtained in this study, it can be attributed to the different morphology of the studied hybrids as well as the cultivation conditions.

Considering percentage of carbon content in the individual plant parts, Grignani et al. (2007) determied percentage of carbon content in root, stalk and husk of 40.0%, 45.0% and 47.0%, respectively. The obtained percentages correlate with the average values of the carbon content in the dry matter of same plant parts determined in this study, whose values on average amounts 36.6%, 46.6% and 46.4%, respectively.

CONCLUSION

The following conclusions can be drawn from this investigation:

1) no statistically significant difference between different hybrides in carbon content of:
   - cob (overall average value is 0.92 t C ha^{-1}),

- grain (total average value is 4.33 t C ha^{-1})

2) statistically significant difference between different hybrides in carbon content of:
   - root (Rudolfov and Kulak differ from OS 596 and OS 515; overall average value is 1.21 t C ha-1),
   - stubble (Rudolfov differ from OS 596, Rudolfov and OS 596 do not differ from Kulak and OS 515; overall average value is 0.40 t C ha-1),
   - stalk (Rudolfov differ from other hybrides; overall average value is 5.42 t C ha-1),
   - husk (Rudolfov differ from Kulaka, Rudolfov and Kulak do not differ from OS 596 and OS, 515; overall average value is 0.47 t C ha-1)

The study implicates that with selection of maize hybrides that sequestrate more carbon, as well with good biomass management more atmospheric carbon can be removed from the atmosphere and soil fertility can be increased

ACKNOWLEDGEMENT

This research was funded by European union from Operational Program Competitiveness and cohesion of European Regional Development Fund via project via project “Production of food, biocomposites and biofuels from cereals in the circular bioeconomy” (grant number KK.05.1.1.02.0016)

REFERENCES

[1] AIO-Agricultural Institute Osijek (2020) Katalog Poljoprivrednog instituta Osijek: Proljeće 2020 - KUKURUZ | SOJA | SUNCOKRET LUCERNA | JARI JEČAM, Poljoprivredni institut Osijek | 2020. url: https://www.poljinos.hr/wp-content/uploads/2022/04/Poljinos-katalog-proljece-2020.pdf (10.9.2024.)

[2] Amos, B., i Walters, D. T. (2006). Maize Root Biomass and Net Rhizodeposited Carbon. Soil Science Society of America Journal, 70(5), 1489–1503.

[3] Bilandžija, D., i Martinčić, S. (2021). Agroclimatic conditions of the Osijek area during referent (1961–1990) and recent (1991–2018) climate periods. Hrvatski meteorološki časopis, 54/55(54/55), 55–64.

[4] Copernicus Climate Change Service (C3S) and World Meteorological Organization (WMO), 2025: European State of the Climate 2024, climate.copernicus.eu/ESOTC/2024, doi.org/10.24381/14j9-s541

[5] Grignani, C., Zavattaro, L., Sacco, D., i Monaco, S. (2007). Production, nitrogen and carbon balance of maize-based forage systems. European Journal of Agronomy, 26(4), 442–453.

[6] HRN ISO 10694 2004; Kakvoća tla—Određivanje organskoga i ukupnog ugljika suhim spaljivanjem (elementarna analiza). (ISO 10694:1995).

[7] IPCC (2001). International panel on climate change 2001. https://www.ipcc.ch/site/assets/uploads/2018/05/SYR_TAR_full_report.pdf (1.9.2024.)

[8] Jans, W. W. P., Jacobs, C. M. J., Kruijt, B., Elbers, J. A., Barendse, S., i Moors, E. J. (2010). Carbon exchange of a maize (Zea mays L.) crop: Influence of phenology. Agriculture, Ecosystems and Environment, 139(3), 316–324.

[9] Karl, T. R., i Trenberth, K. E. (2003). Modern Global Climate Change. Science, 302(5651), 1719–1723.

[10] NIR 2024 - National Inventory Report 2024 (Croatian greenhouse gas inventory for the period 1990 - 2022). https://www.haop.hr/sites/default/files/uploads/dokumenti/012_klima/dostava_podataka/Izvjesca/Croatian%20NIR%202024.pdf

[11] Tokgöz, N. (2010). Numerical Analysis of Worldwide CO 2 Emissions and Effects on Atmospheric Warming in Turkey. Energy Sources, Part A: Recovery, Utilization, and Environmental Effects, 32(8), 769–783.

[12] Wang, Z., Chen, J., Zhang, J., Tan, X., Ali Raza, M., Ma, J., Zhu, Y., Yang, F., i Yang, W. (2022). Assessing canopy nitrogen and carbon content in maize by canopy spectral reflectance and uninformative variable elimination. Crop Journal, 10(5), 1224–1238.

[13] Zhao, H., Shar, A. G., Li, S., Chen, Y., Shi, J., Zhang, X., i Tian, X. (2018). Effect of straw return mode on soil aggregation and aggregate carbon content in an annual maize-wheat double cropping system. Soil and Tillage Research, 175, 178–186.

ROBOTIC SYSTEMS FOR HARVESTING THE INFLORESCENCES OF MEDICINAL PLANT SPECIES - A REVIEW

/

SISTEME ROBOTIZATE DESTINATE RECOLTĂRII INFLORESCENȚELOR UNOR SPECII DE PLANTE MEDICINALE - A REVIEW

Adriana MUSCALU*[1)], Cătălina TUDORA[1)], Dragoș ANGHELACHE[1)], Dorin CÎRSTEA[1)], Margareta NAIE[2)]

[1)] National Institute of Research - Development for Machines and Installations Designed to Agriculture and Food Industry - INMA Bucharest / Romania;

[2)] Agricultural Research and Development Station Secuieni, Neamt County / Romania.

*Tel: 0726 234 242; *E-mail: amuscalis@yahoo.*

Keywords: *medicinal plants; harvesting; inflorescences; robotic systems.*

ABSTRACT

The use of medicinal plants and their derived products in the therapy of many diseases is common, with phytotherapy experiencing a strong revival in recent years. For certain species, only the inflorescences are harvested, due to their high content of bioactive compounds beneficial to human health. Although used since ancient times for their therapeutic properties as well as their sensory and nutritional characteristics, consumers continue to show interest in them. Moreover, the inflorescences of medicinal plants are sought after for the development and improvement of modern cosmetic products. Their manual harvesting requires a high labor input, which is difficult to achieve and sustain financially today. Due to specific technological requirements, the mechanized harvesting of inflorescences remains a challenge for researchers in the field, with numerous studies being conducted for its development and optimization. Technical progress requires the use of automated methods in the harvesting process. This paper provides a brief review of current research regarding the introduction of robotic systems for harvesting the inflorescences of certain medicinal plant species.

REZUMAT

Utilizarea plantelor medicinale și a produselor derivate în terapia multor boli, este frecventă, fitoterapia cunoscând un puternic reviriment in ultimii ani. De la anumite specii, se recoltează doar inflorescențele, datorită conținutului ridicat de compuși bioactivi, benefici pentru sănătatea umană. Deși utilizate din cele mai vechi timpuri, datorită proprietăților terapeutice, dar și a caracteristicilor senzoriale și nutriționale, consumatorii manifestă interes pentru ele. De asemenea, inflorescențele plantelor medicinale sunt căutate pentru dezvoltarea și îmbunătățirea produselor cosmetice moderne. Recoltarea lor manuală necesită un consum mare de forță de muncă, dificil de realizat și de susținut financiar astăzi. Datorită tehnologiilor specifice, recoltarea mecanizată a inflorescențelor rămâne o provocare pentru cercetătorii din domeniu, efectuându-se numeroase studii pentru dezvoltarea și optimizarea ei. Progresul tehnic impune utilizarea metodelor automatizate în procesul de recoltare. In aceasta lucrare se prezintă o scurtă sinteză a cercetărilor actuale privind introducerea sistemelor robotizate pentru recoltarea inflorescențelor anumitor specii de plante medicinale.

INTRODUCTION

For thousands of years, medicinal plants have represented a valuable resource for healing as well as for preserving the cultural characteristics of different ethnic groups *(Niazi et al., 2024; Fitzgerald et al., 2020)*. The phytotherapeutic action of medicinal plants refers to their beneficial effects on the health of the human or even animal body. Thus, flowers, leaves, stems, roots, fruits, or seeds of these species are used directly or in the form of preparations to prevent, treat, or cure various disorders *(Maldonata 2021*; *Jamshidi-Kia et al., 2018)*. Most useful parts of medicinal plants represent a rich source of biologically active substances, namely chemical compounds referred to as active principles.

The presence of some of these compounds influences the specific effects of these plants on the physiology of living organisms, particularly on human metabolism, which are enhanced through their synergistic action, leading to direct or indirect therapeutic effects *(Donkor et al., 2023; Jamshidi-Kia et al., 2018; Grigore et al. 2016)*. The value of medicinal plants is given by the natural bioactive compounds used in both traditional and modern medical practices *(Hosseinzadeh et al. 2015)*. Medicinal plants are harvested

during the period when the accumulation of active principles in their useful parts is at its maximum. The timing and method of performing this operation are essential for the quality of the plant material and, implicitly, for the pharmacodynamic action of these species *(Hazrati, S., Mousavi, Z., Nicola, S. 2024, Rao, K.S.; Haran, R.H.; Rajpoot, V.S. 2022)*.

The harvesting of inflorescences is a specific operation in the cultivation technologies of certain medicinal plant species, and its mechanized harvesting remains a constant challenge for specialists. This operation is common for chamomile (*Matricaria recutita* L.), marigold (*Calendula officinalis* L.), French marigold (*Tagetes patula* L.), and chrysanthemum (*Chrysanthemum indicum* L.), all belonging to the Asteraceae family. Inflorescence harvesting systems have been studied mainly for chamomile, later being applied to the other species mentioned above. Thus, they have been classified into comb-type systems with linear or rotary motion, with or without additional cutting, as well as rotor-type harvesters, characterized as a "virtual comb," equipped with pin drums and brush pairs *(Veselinov et al, 2014; Brabandt et al., 2011*; *Martinov et al., 2007)*. Numerous studies on mechanized harvesting systems for medicinal plant inflorescences have reported results regarding the working performance of various harvesting devices, including those designed for small areas, characteristics of the quality of harvested plant material, economic efficiency, etc. *(Mohamed et al., 2020; Radwan et al., 2015; Ivanović et al., 2014; Detlef et al., 2014)*. Medicinal and aromatic plants are part of the category of non-traditional food crops, being characterized by a higher market value compared to staple crops *(Taddei Dalla Torre et al. 2024)*.

In general, the harvesting of medicinal plant inflorescences represents an economic challenge for farmers, who must either have access to mechanized technical systems dedicated to this operation or to qualified labor. In the last 10 years, numerous studies have been carried out for the implementation of robotic technology for this purpose. Deep learning (DL) has been used as a tool to improve performance in computer vision and object detection. In addition, some mechanical systems have been optimized, being electrically operated and equipped with intelligent lifting (e.g., LiDAR-type) and control systems *(Liu et al., 2024; Zhou et al., 2019; Kamilaris et al., 2018)*.

This paper presents a brief synthesis of research results regarding the implementation of innovative intelligent systems in the automated harvesting process of chamomile (*Matricaria chamomilla*) inflorescences and certain edible plant species. For the latter, the focus has been on developing an artificial intelligence (AI)-based vision framework to support robotic harvesting, adaptable across different species and varieties.

MATERIALS AND METHODS

The development of a robotic system for chamomile inflorescence harvesting requires going through certain step-by-step stages (Fig. 1). These include: *Programming* - creating the detection model for the inflorescences; *Design stage* - integrating the mechanical elements of the system; and *Evaluation* - real-time assessment of the system *(Nasr et al., 2024)*.

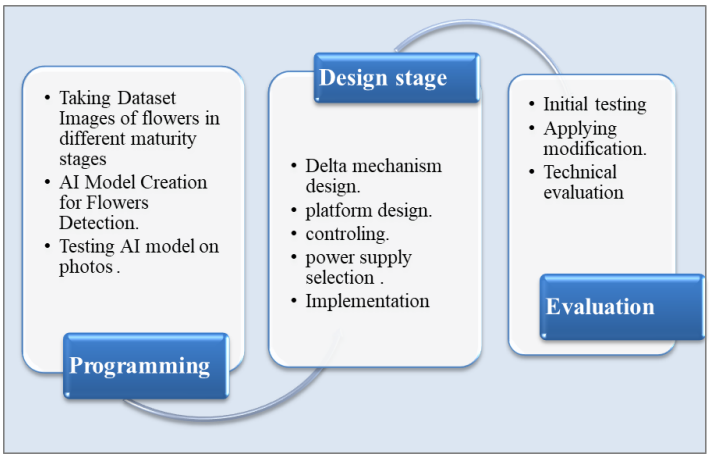

Fig. 1 - Stages in the development of a robotic system for chamomile inflorescence harvesting
(Nasr et al., 2024)

Within the *Programming* stage, in order to enable subsequent cutting, the classification of mature chamomile inflorescences was carried out using extended robotic tools. The detection model was created from a dataset of images of chamomile flowers at different phenological development stages, taken under

natural conditions. This model is compared with the data stream. A camera captures images of the flowers, and then, using an object detection algorithm to locate them instantly, the classification and filtering of mature chamomile flowers are performed.

The algorithm returns their coordinates, which are transmitted to an integrated system equipped with a microcontroller that controls the cutting and collecting mechanisms. For flower detection, using the TensorFlow machine learning system, the YOLO (v4) algorithm was combined with a deep convolutional neural network (CNN), developing a common interface *(Nasr et al., 2024)*. TensorFlow enables the implementation of machine learning models to be faster, more flexible, and more accessible for developers, assisting in data acquisition, prediction delivery, and refinement of future results. It is designed to run efficiently on various hardware components, being optimized for GPU (Graphics Processing Unit), but it can also operate with CPU (Central Processing Unit) *(Nur, 2022)*.

In the *Design* stage, the prototype of the Chamomile Flower Harvesting Robot – CFHR (Fig. 2) was developed, consisting of mechanical parts represented by the chassis, the delta robot mechanism, and the cutting mechanism, along with the control system *(Nasr et al., 2024)*.

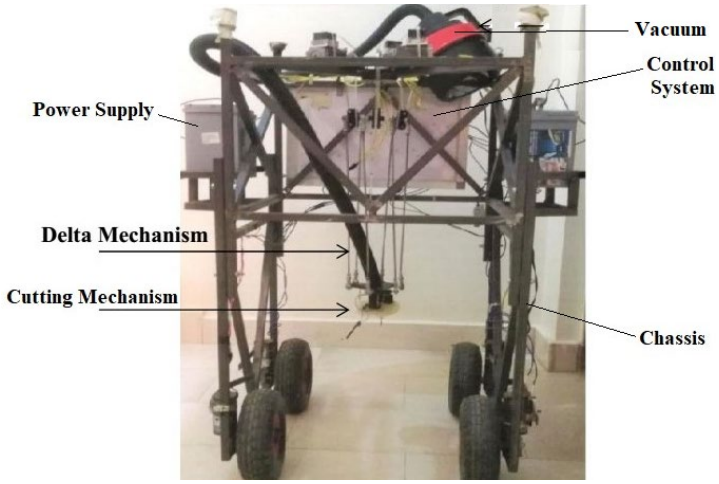

Fig. 2 - Chamomile Flower Harvesting Robot – CFHR

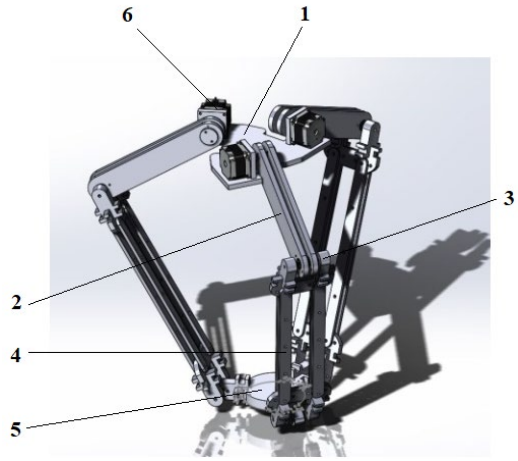

Fig. 3 - The delta robot mechanism

(adapted after *Nasr et al., 2024)*

The chassis (Fig. 2) is made of steel profiles (20×20×2), having a square shape of 0.6×0.6 m (L×W), with adjustable height up to 1.2 m. It is equipped with four durable rubber wheels, each with a diameter of 250 mm, driven by a 24 V DC motor. The delta robot mechanism (Figs. 2, 3) has the role of raising and lowering the cutting mechanism, being composed of: (1) Fixed base; (2) Input link; (3) Revolute joint; (4) Forearm; (5) Travelling plate; (6) Actuator. For this mechanism, the workspace was determined using numerical methods *(Nasr et al., 2024)*.

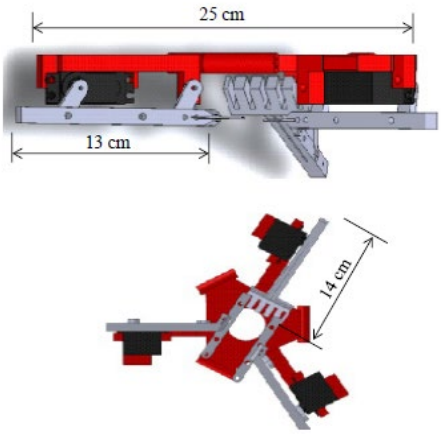

Fig. 4 - The cutting mechanism
(Nasr et al., 2024)

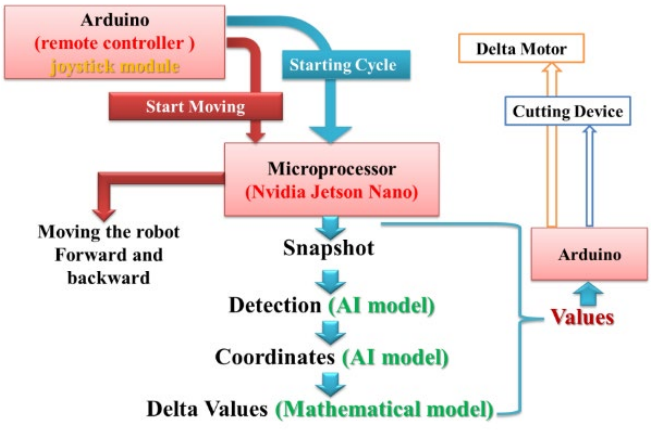

Fig. 5 - Control system diagram
(Nasr et al., 2024)

The cutting mechanism (Fig. 4) consists of a linear comb for flower fixation, complemented by a pair of cutting blades. Their role is to cut the flower stem after an appropriate time interval to ensure optimal harvesting results. Flowers with a petiole length of up to 50 mm are accepted, as first-quality flowers have petioles shorter than 10 mm, second-quality flowers have petioles of 10-30 mm, and third-quality flowers have petioles of 30-50 mm. The mechanism is actuated by three servomotors.

The control system (Fig. 5) consists of automation, monitoring, and control components. Its role is to visually detect chamomile flowers suitable for harvesting and to automatically command the mechanical elements to perform this operation. Thus, it includes: Raspberry Pi Camera Module, Nvidia Jetson Nano controller, Arduino UNO, stepper motors, DC motors, motor drivers, power supply, and battery.

To test and evaluate the robot's performance criteria, an experiment was conducted using 20 pots, each containing one chamomile plant (5 rows × 4 pots), simulating a spacing of 30 × 30 cm between plants in the field. The soil in the pots had a medium texture, with irrigation and fertilization carried out according to the recommended doses for chamomile cultivation. Under Egyptian conditions, the height of the cultivated chamomile plants ranged between 70 and 80 cm, with the average height considered to be 77 cm. At the peak flowering stage, each plant had between 15 and 25 flowers, distributed as shown in Figure 6 *(Nasr et al., 2024)*.

Fig. 6 - Flower distribution as percentage along plant stem
(Nasr et al., 2024).

With regard to the automated harvesting of certain edible plants, the study was carried out in a commercial greenhouse, focusing on several species important for the company's production. These were: French marigolds (*Tagetes patula* cv. Texana), snapdragon (*Antirrhinum majus*, cv. Leo), pansy and horned pansy (*Viola* × *wittrockiana* cv. Carneval and *Viola cornuta* cv. Sorbet, respectively), selected due to the distinct characteristics of their flowers as well as the morphology of the plants (Fig. 7). They were cultivated on benches with a height of 70 cm, a width of 110 cm, and a length of approximately 50 m. This method is commonly used in floriculture, providing favorable conditions for robotic harvesting *(Taddei Dalla Torre et al., 2024)*.
(*cv – cultivar)

a) French marigold (Texana) b) Snapdragon (Leo) c) Pansy (Carneval) d) Horned Pansy

Fig. 7 - Flower species considered in the experiments
(*Taddei Dalla Torre et al. 2024*)

For the estimation of the position and picking point, the flowers of the plants were examined: snapdragon flowers had an average diameter of 28 mm, marigolds 36 mm, while pansies reached up to 60 mm (both varieties being considered together).

Taking into account the cultivation method described above, a transport cart made of aluminum profiles with four wheels was built (Fig. 8). Its dimensions (width 120 cm, height 175 cm, track width 80 cm)

allow it to “straddle” the cultivation benches and move easily, with data (image) acquisition performed from the vertical position (Fig. 9) relative to the plants *(Taddei Dalla Torre et al., 2024)*.

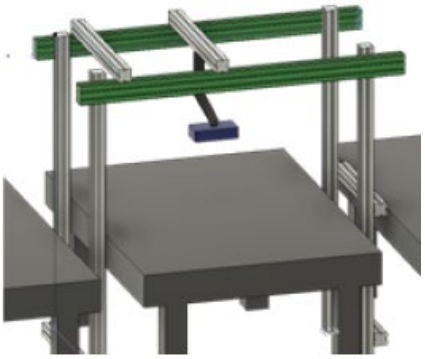

Fig. 8 - Straddle cart
(Taddei Dalla Torre et al. 2024)

Fig. 9 - Dates acquisition in greenhouse
(Taddei Dalla Torre et al. 2024)

Stereo RGB-D cameras were used: Zed 2 (field of view up to 120°, two 4 MP sensors of 2.1 mm in a native 16:9 format) and Zed 2i (field of view 81°, two 4 mm sensors with additional polarized filters). These generate a depth point cloud, associating a depth measurement with each captured pixel. The point cloud is derived using Neural Stereo Depth Sensing technology, with the cart being equipped with a Jetson TX2 module (a complete system-on-module developed by Nvidia, running AI models at the “edge,” i.e., configuring operations in real time). Using the combination of a Python GUI and Stereolab’s Python programming interface, Jetson TX2 can compute images and point clouds of the crop. Two data collection campaigns were conducted (on July 22 and November 17, 2023) for French marigold and snapdragon. For pansies, data were collected only in the last campaign. For model development and validation, the FloraDet dataset included 134 images containing a total of 2,443 flowers (Tab. 1). The Roboflow online annotation tool was used for manual labeling. According to the commercial quality standard, an edible flower is considered ripe and ready for picking when it has reached 70-80% of its full opening. Therefore, only flowers meeting this criterion were annotated *(Taddei Dalla Torre et al., 2024)*.

Table 1

Structure of the FloraDet dataset
(Taddei Dalla Torre et al., 2024)

	Items	French marigold	Snapdragon	Pansy
July	Images	25	13	-
	Flowers	854	762	-
November	Images	21	11	64
	Flowers	401	51	375

By merging images from two distinct sources (ImageNet and Kaggle), an additional dataset D0 was created for preliminary testing and fine-tuning of the AI model. Thus, dataset D0 included flower species different from those in FloraDet and was further enriched with images of pansy flowers, due to their variability as well as their underrepresentation in the initial dataset.

Figure 10 shows the operational workflow composed of three individual modules: *Flower Detection*, *Pose Estimation*, and *Plucking Point Estimation (Taddei Dalla Torre et al., 2024)*.

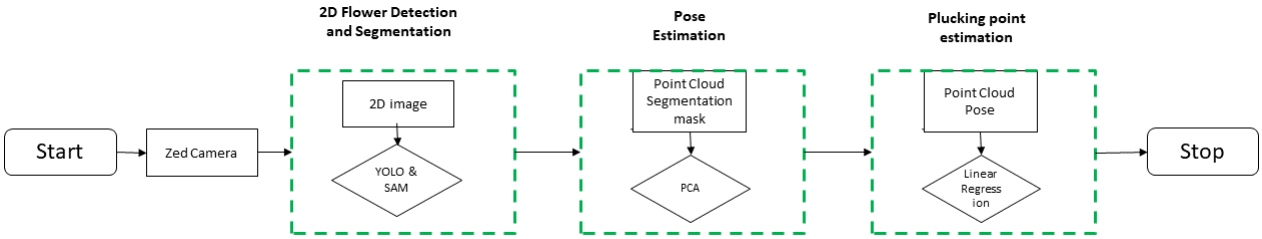

Fig. 10 - Operational workflow
(*Taddei Dalla Torre et al. 2024*)

In the first module, *Flower Detection*, an image together with the bounding boxes predicted by YOLO is fed into SAM (Software Asset Management), generating a binary mask as output, which effectively separates the pixels corresponding to flowers from other objects *(Taddei Dalla Torre et al., 2024)*.

In the next module, *Pose Estimation*, the flowers in the input image are segmented by SAM, with the generated binary mask used for each flower of interest to extract a point cloud. Once the point cloud is extracted, the PCA algorithm is applied to identify the vector components describing its distribution. The pose of the flower is then determined from the PCA (Principal Component Analysis) axes (Fig. 11) *(Taddei Dalla Torre et al., 2024)*.

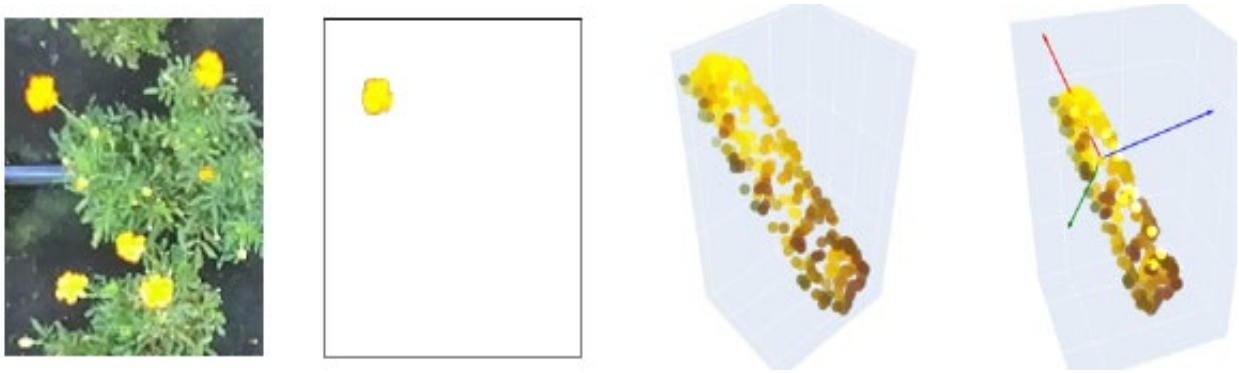

Fig. 11 - Flower pose estimation

From left to right: input image, single flower cutout trough SAM, derived isolated point cloud in the 3D space, and PCA-based point cloud analysis

(*Taddei Dalla Torre et al. 2024*)

At the end of the operational workflow, the visual framework includes a module designed to estimate the optimal picking point of the flower. An attempt was made to identify this picking point, located just below the calyx, but this was not achieved due to occlusion caused by the flower itself or by surrounding leaves. In the case of flowers, 3D matching cannot be applied due to their complex and variable morphology, the method being applicable only to denser objects with well-defined shapes.

Figure 12a shows the previously calculated flower position vectors together with the extension of the vertical component aligned with the optimal picking point. To estimate this, an attempt was made to define a numerical relationship between d - the flower diameter (Fig. 12b) and h - the distance from the flower apex to the picking point (Fig. 12c).

For this purpose, 300 flowers from the three species of interest were measured, from the same rows where the images were captured *(Taddei Dalla Torre et al., 2024)*.

a) Marigold flower featuring pose vectors and the plucking point (side view)

b) Marigold flower, showcasing its circumference and diameter **d** (top view)

c) Marigold flower, highlighting height and plucking point **h** (side view)

Fig. 12 - The side and top view of a marigold flower

(Taddei Dalla Torre et al. 2024).

RESULTS

The technological performance of the chamomile harvesting robot was analyzed by evaluating several parameters throughout a harvesting cycle carried out in three stages. Table 1 provides a synthesis of the results obtained.

Table 2

Synthesis of results

(adapted from *Nasr. et al., 2024).*

Parameter		Collection times			
		1st	2nd	3rd	Average
Harvesting time for one plant [s]		13	22	28	21
Total harvesting time for a row of pots [s]		52.15	88.20	112.20	84.18
Flower number for one plant		4	7	9	6
Total harvesting time for experimental pots [min]		10.35	13.95	17.35	13.88
Harvesting success ratio for CFHR during harvesting season [%]		75.0	85.70	89.7	83,47
Visual selection evaluating parameters for CFHR	Accuracy [%]	72,4	59,5	53,9	61,93
	Detection precision rate [%]	75,0	50,0	49,7	58,23

Figure 13 shows the quality of chamomile flowers harvested by CFHR during the three collection periods. The results obtained were compared with those from manual harvesting under the same conditions.

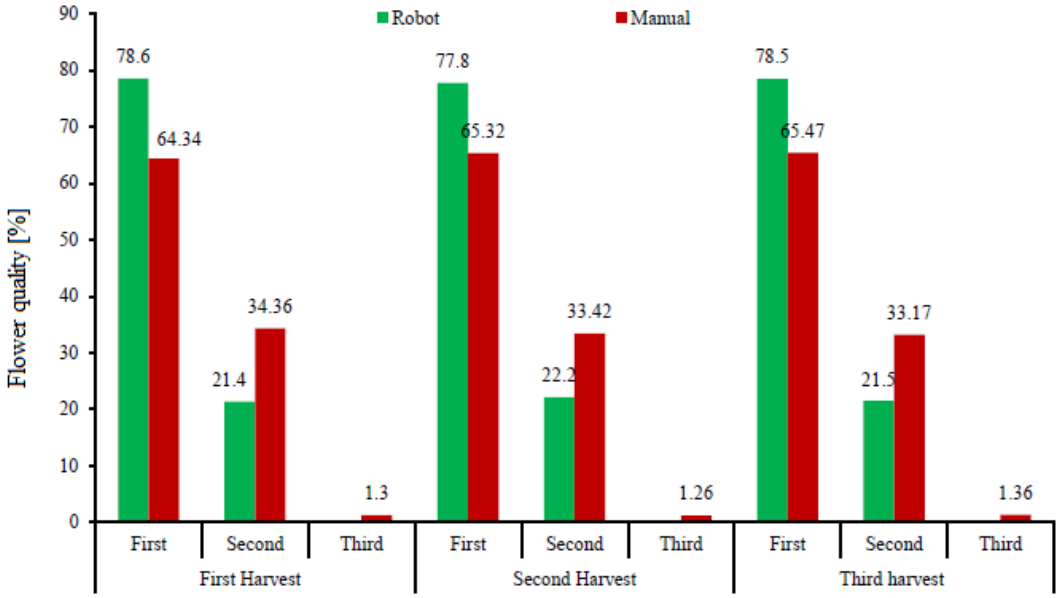

Fig. 13 - Quality of chamomile flowers harvested with CFHR and manually

(Nasr et al., 2024).

With regard to the automated harvesting of edible plants, the relevant results corresponding to each module of the operational workflow are presented. Detection was the only aspect subjected to training and evaluation. The models were obtained after two fine-tuning processes, with the respective datasets split into 75% for training, 15% for testing, and the remaining 10% for validation.

The optimal models were selected based on the period during which, on the validation set, the model achieved the highest performance.

The low value of 0.045 for the object detection error on the validation set demonstrated the effectiveness of the model in accurately identifying and locating flowers at the harvesting stage (Fig. 14) for marigold and snapdragon.

In the case of pansies, the model results were not relevant due to the limited amount of data as well as the natural variability within the species, which in this case included two distinct cultivars *(Taddei Dalla Torre et al., 2024)*.

Fig. 14 - Cropped images from FLOLO model detection results (Mar=Marigold; Snap=Snapdragon representing flowers ready for harvesting)
(*Taddei Dalla Torre et al. 2024*).

With regard to determining the position of the flowers to be harvested, after applying the PCA algorithm, the vector component was calculated for each corresponding point cloud, following their isolation by the binary segmentation mask. In some cases, the segmentation masks may include separate polygons for the same bounding box of the prompts, since each bounding box contains a single flower. Therefore, it was necessary to eliminate some of these polygons. For this purpose, the center of each polygon was extracted, and only the mask with the centroid closest to the center of the bounding box was selected. This mask was then used to filter the pixels in the 3D point cloud that were not identified as detected flowers *(Taddei Dalla Torre et al., 2024)*. With regard to the estimation of the harvesting point position, for each species it was considered that a potential relationship between **d** and **h** could be evaluated through linear regression. Eighty percent of the measurements were used to investigate the relationship, while the remaining 20% were used for testing. Table 3 presents the corresponding equations for the linear regression and the respective upper boundary for each flower type. To mitigate possible flower damage, the estimation module used a translated line corresponding to the upper limit of the 85% confidence interval to determine **h** as a function of **d** *(Taddei Dalla Torre et al., 2024)*.

Table 3

Equations for the linear regression and the respective upper boundary for each of the different flower types
(*Taddei Dalla Torre et al. 2024*)

	Pansy	Snapdragon	Marigold
Linear Regression	$h_v = 0.36d_v + 26.33$	$h_s = 0.38d_s + 5.33$	$h_m = 0.66d_m + 7.10$
Upper boundary	$h_v = 0.36d_v + 43.20$	$h_s = 0.38d_s + 34.57$	$h_m = 0.66d_m + 37.91$

The flower diameter **d** was calculated by estimating the smallest convex polygon enclosing the points, taking into account the binary mask. The flower's central point is located among the upper points of the 3D cloud and is defined as the point within the polygon situated at the maximum distance from the polygon boundary. The distance **h** was calculated using the equations presented above. Once the flower position was determined, the central point was translated downward along the main vertical vector by the calculated distance **h**. This point represents the estimated optimal picking point and is marked with a red square in Figure 15 *(Taddei Dalla Torre et al., 2024)*.

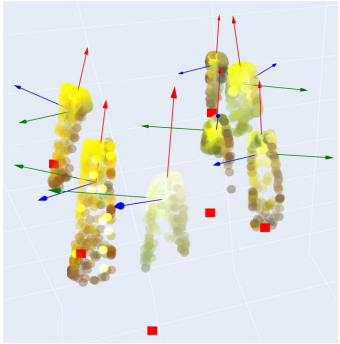

Marigold

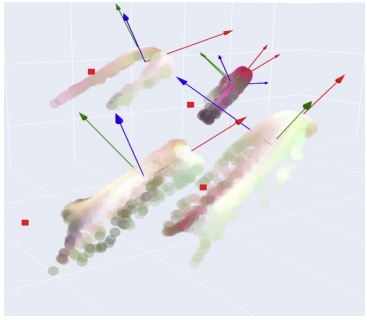

Snapdragon

Fig. 15 - Isolated point clouds of marigold and snapdragon flowers and the respective vector components (red, green and blue vectors) and estimated picking point (red squares)
(*Taddei Dalla Torre et al. 2024*).

Table 5 presents the average time (s) required for processing the validation images with a variable number of flowers for two species of interest. The averages are calculated based on the analysis of 10 images for each species, including a total of 457 marigold flowers and 975 snapdragon flowers *(Taddei Dalla Torre et al., 2024)*.

Table 4

Average processing inference time (s) for each step of the AI framework on an NVIDIA GeForce RTX 3090

(*Taddei Dalla Torre et al. 2024*)

	Detection	Localization			Estimation		Total Time	Time per Flower
	YOLO	SAM	Clean Masks	Isolate 3D Poins	Pose (PCA)	Picking Points		
Marigold	0.285	4.37	0.08	42.36	1.44	1.48	48.35	1.064
Snap dragon	0.293	4.36	0.165	89.90	5.76	5.87	95.99	0.98

The processing times obtained in this study (1.064 s for marigold and 0.98 s for snapdragon) are comparable to the values reported in the literature by *Li et al. (2023)*. These results demonstrate that the tested procedure can be implemented in the field, with the total time required for processing a single flower representing the key indicator for this perspective.

CONCLUSIONS

For the performance indicators, the results obtained for the chamomile harvesting robot demonstrate the viability of the proposed solution. Considering that these were obtained at the experimental stage, further research and development are necessary. In the chamomile harvesting process, future work should focus on increasing the success rate, productivity, accuracy, and efficient use of working time.

With regard to the robotic harvesting of edible flowers, the study evaluated the viability of an artificial intelligence (AI)-based vision framework, as well as its performance across different species. By adjusting the workflow, the general framework could also be applied to the validation stages of field inferences. Ensuring the effectiveness and reliability of the framework in real agricultural environments will require rigorous testing and validation through extensive further research. The detection, position estimation, and picking point estimation capabilities of the framework represent a premise for robotic harvesting, with implications for increasing efficiency for growers.

The robotic harvesting of medicinal and edible plant inflorescences could represent a socio-economically sustainable alternative to manual harvesting.

ACKNOWLEDGEMENT

This paper was supported: by Ministry of Education and Research one funding source the NUCLEU Program, Contract 9N/01.01.2023, Project PN 23 04 02 05 "Innovative technology for the superior use of inflorescences and seeds of medicinal plants".

REFERENCES

[1] Brabandt, H., Ehlert D. (2011). Chamomile harvesters: a review. *Industrial Crops and Products* 34 (1): 818–824. https://doi.org/10.1016/j.indcrop.2011.03.017

[2] Detlef, E., Beier, K. (2014). Development of picking devices for Chamomile harvesters. *Journal of Applied Research on Medicinal and Aromatic Plants* 1, 73–80

[3] Donkor, M. N., Donkor, A. M., Mosobil, R. (2023) Combination therapy: synergism among three plant extracts against selected pathogens. *BMC Res Notes* 16, 83. https://doi.org/10.1186/s13104-023-06354-7

[4] Fitzgerald, M., Heinrich, M., Booker, A. (2020) Medicinal Plant Analysis: A historical and regional discussion of emergent complex techniques. *Frontiers in Pharmacology* 10:1480, 1-14. doi: 10.3389/fphar.2019.01480

[5] Grigore, A., Pirvu, L., Bubueanu, C., Colceru-Mihul, S., Ionita, C. & Ionita, L. (2016). Medicinal plant crops-important source of high value-added products. In *Scientific Papers. Series A. Agronomy LIX*: 298-307. https://agronomyjournal.usamv.ro/index.php/scientific-papers/past-issues?id=636

[6] Hazrati, S., Mousavi, Z., Nicola, S. (2024) Harvest time optimization for medicinal and aromatic plant secondary metabolites. *Plant Physiology and Biochemistry*, 12, https://doi.org/10.1016/j.plaphy.2024.108735

[7] Ivanović, S., Pajić, M., Marković, T. (2014). Economic effectiveness of mechanized harvesting of Chamomile, *Economics of Agriculture*, 61(2), 319-330, https://doi.org/10.5937/ekoPolj1402319I

[8] Jamshidi-Kia F., Lorigooini, Z., & Amini-Khoei H., (2018) Medicinal plants: past history and future perspective. *Journal Herbmed Pharmacology* 7(1):1-7. doi: 10.15171/jhp.2018.01

[9] Kamilaris, A., Prenafeta-Boldú F., X. (2018). Deep learning in agriculture: A survey. *Computers and Electronics in Agriculture*, 147: 70-90. https://doi.org/10.1016/j.compag.2018.02.016

[10] Li, Y., Wu, S., He, L., Tong, J., Zhao, R., Jia, J., Chen, J. & Wu, C. (2023) Development and field evaluation of a robotic harvesting system for plucking high-quality tea, Elsevier - *Computers and Electronics in Agriculture* 206, 107659, 1-11, https://doi.org/10.1016/j.compag.2023.107659

[11] Liu, Y., Li, T., Wang, G., Sun, W., Yang, S. & Gao, S. (2024) Design and test of an intelligent lifting electric marigold picker, (This work is licensed under a Creative Commons Attribution 4.0 International License.) Research Square, https://doi.org/10.21203/rs.3.rs-4941338/v1 (accesed Feb 11 2025)

[12] Maldonata J. J. M., (2021). Chapter 7 - Medicinal plants and their traditional uses in different locations. *Phytomedicine 2021*, 207-223. https://doi.org/10.1016/B978-0-12-824109-7.00014-5

[13] Martinov, M., Konstantinovic, M. (2007). Harvesting. Medicinal and aromatic crops. *Harvesting, drying, and processing (Öztekin S, Martinov M, Eds.).* The Haworth Press Inc., NY (USA), 56-84.

[14] Mohamed, T. H., Mosa, S. E., Hamad, T. O. (2020). Development a machine for picking Calendula inflorescences to suit the small holding farmers. *Misr Journal of Agriculture Engineering,* 37(3), 263-284, DOI:10.21608/mjae.2020.103158

[15] Nasr, G., E., M., Ibrahim, M., M., Tayel, M., Y. & Salama, D., S. (2024) Innovative robot for chamomile flower harvesting as a new approach based on visual selection, *AgricEngInt: CIGR Journal*, 26 (4), 261-275, https://cigrjournal.org/index.php/Ejounral/article/view/9221

[16] Niazi P., Monib, A. W., (2024) The role of plants in traditional and modern medicine. *Journal of Pharmacognosy and Phytochemistry* 13(2): 643-647. DOI: https://doi.org/10.22271/phyto.2024.v13.i2d.14905

[17] Nur, H. (2022) Research on Tensor Flow with a system for large-scale machine learning. *Research Gate 2022* [Online] Available from: https://www.researchgate.net/publication/363937209_Research on_Tensor_Flow_with_a_system_for_large-scale_machine_learning [accessed Aug 21 2025]

[18] Radwan, H. A., Mohamed, T. H., Elashhab, A. O. (2015). Design a machine for picking Chamomile to suit the small holding. *Egyptian Journal of Agriculture Research*, (3(5) (B), 405-425

[19] Rao, K.S.; Haran, R.H.; Rajpoot, V.S. (2022) Value Addition: A Novel Strategy for Quality Enhancement of Medicinal and Aromatic Plants. *Journal of Applied Research on Medicinal and Aromatic Plants*, *31*, https://doi.org/10.1016/j.jarmap.2022.100415

[20] Taddei Dalla Torre, F., Melgani, F., Pertot, I. & Furlanello, C. (2024) Artificial Intelligence vision methods for robotic harvesting of edible flowers. *Plants 2024*, 13, 3197, 1-16, https://doi.org/10.3390/plants13223197

[21] Veselinov, B., Adamovic, D., Martinov, M., Viskovic, M., Golub, M., & Bojic, S. (2014). Mechanized harvesting and primary processing of Calendula officinalis L. inflorescences. *Spanish Journal of Agricultural Research*, 12(2), 329-337. https://doi.org/10.5424/sjar/2014122-4876

[22] Zhou, X., Wang, D., Krähenbühl, P. (2019). Center Net: objects as points. *In Proceedings of the IEEE Conference on Computer Vision and Pattern Recognition,* pp. 16-20. Long Beach, CA, USA, 15-20th June 2019. https://doi.org/10.48550/arXiv.1904.07850

THE EU DIGITAL PRODUCT PASSPORT DPP AS A KEY INNOVATION IN PRODUCT DESIGN AND MANUFACTURING PROCESSES

/

PAŞAPORTUL UE DE PRODUS DIGITAL DPP CA O INOVAȚIE CHEIE ÎN PROIECTAREA PRODUSELOR ȘI PROCESELE DE FABRICAȚIE

Carmen BRĂCACESCU*[1)], Oana Diana CRISTEA[1)], Raluca-Veronica BRĂCACESCU [2)], Lorena-Diana POPA[3)]

[1)] National Institute of Research - Development for Machines and Installations Designed to Agriculture and Food Industry - INMA Bucharest / Romania;

[2)] National University of Science and Technology Politehnica Bucharest (UNSTPB) / Romania;

[3)] Agricultural Research and Development Station Secuieni, Neamt County / Romania.

**Tel: 0770 513 926; *E-mail: carmenbraca@yahoo.com*

Keywords: *digital product passport, data requirements,* product transparency and sustainability

ABSTRACT

Sustainability and circularity are quickly becoming a key strategic priority for organizations, brands and even consumers. Digital Product Passports (DPPs) are designed to collect and share data about a product and its supply chain across the entire value chain. As Digital Product Passports impact and involve multiple stakeholders from across value-chains and sectors – the benefits and value are far reaching. From organizations, to consumers, to policy makers and recyclers – digital passports provide benefits for all. This paper presents what is known about digital product passports, such as who needs to comply, what data needs to be included in a DPP, how to implement a DPP system, and its importance and benefits.

REZUMAT

Sustenabilitatea și circularitatea devin rapid o prioritate strategică cheie pentru organizații, mărci și chiar consumatori. Pașapoartele pentru produse digitale (DPP) sunt concepute pentru a colecta și a partaja date despre un produs și lanțul său de aprovizionare de-a lungul întregului lanț valoric. Pe măsură ce pașapoartele pentru produse digitale au impact și implică mai multe părți interesate din toate lanțurile valorice și sectoare, beneficiile și valoarea sunt de mare anvergură. De la organizații, la consumatori, la factorii de decizie și reciclatori – pașapoartele digitale oferă beneficii pentru toți. Această lucrare prezintă ceea ce se știe despre pașapoartele pentru produse digitale, cum ar fi cine trebuie să se conformeze, ce date trebuie incluse într-un DPP, cum se implementează un sistem DPP și importanța și beneficiile acestuia.

INTRODUCTION

The reason that digital technologies should be able to facilitate circularity in the economy is that circular as opposed to linear production, consumption and disposal will require far more communication and exchange of data and information between the various links in the life cycle of products. Here's why the European Union *(European Commisson, 2022; EURACTIV, 2021)* has the initiative of establishing a Digital Product Passport (DPP).

A Digital Product Passport (DPP) is a digital record that provides comprehensive information about a product and its entire value chain, including everything from the origin of the product, materials used, environmental impact, and disposal recommendations *(King et al, 2023).*

DPPs' main purpose is to close the gap between the transparency demanded by consumers, investors, and other stakeholders and the current lack of reliable data on product journeys *(Baumgartner, 2023).*

The Digital Product Passport DPP will include essential details such as a unique product identifier, compliance documentation and information on substances of concern. It will also provide user manuals, safety instructions, and guidance on product disposal. By offering a detailed digital record of a product's lifecycle, the DPP will enhance supply chain management, ensure regulatory compliance, and help companies identify and mitigate risks related to authenticity and environmental impact *(Berger et al, 2023).*

DPPs enable all stakeholders, including consumers, to gain a deeper understanding of the materials used in products and their associated environmental impacts […].

On the other hand, Digital Product Passports DPP are a mandatory component of the Ecodesign for Sustainable Products Regulation *(ESPR, 2022)* and one of the key actions under the Circular Economy Action Plan *(CEAP, 2022).* Under the ESPR, all regulated products — including textiles, construction materials, industrial and electric vehicle batteries, and at least one additional key value chain identified in the Circular Economy Action Plan, such as consumer electronics, packaging, or food — will be required to implement DPPs.

This means that once Ecodesign for Sustainable Products Regulation *(ESPR, 2022)* is formally adopted, sustainable products will be the new benchmark for smart business.

DPP are also not a stand-alone idea; they are part of a broader framework that includes elements of traceability, chain of custody, supply chain collaboration, and data-sharing requirements, all of which are integral to a range of other regulations. These all, form part of the European Union's Digital Transition and Data Spaces plans designed to harmonize and standardize access to data *(European Commission, 2020).*

Blockchain technology provides a clear and verifiable record of product and travel information, making it easier for consumers to make informed choices based on the origin, sustainability, and authenticity of a product, improving transparency *(Damvakeraki, 2024).*

As Digital Product Passports impact and involve multiple stakeholders from across value-chains and sectors – the benefits and value are far reaching. Digital passports provide benefits for all interested parties, from organizations, to consumers, to policy makers and recyclers.

By pursuing early compliance and adopting voluntary certifications, companies can capture a larger market share. As traceability becomes a basic requirement for material procurement, developing robust product traceability and supply chain impact-tracking methods will position businesses as leaders *(Neligan et al., 2023; Sudusinghe and Seuring, 2022).*

This paper presents what is known about digital product passports, such as who needs to comply, what data needs to be included in a DPP, how to implement a DPP system, and its importance and benefits.

MATERIALS AND METHODS

Digital Product Passport DPP's implementation

The Digital Product Passport DPP's implementation aligns closely with open data principles by making detailed product information publicly available *(Henten et al, 2025).* This approach will not only improve product visibility and sustainability practices but also facilitate better data sharing and collaboration across the industry. Open data's role in this context highlights the importance of accessible, standardised information in driving transparency and accountability *(Gieß and Möller, 2025; Jensen et al, 2023).*

A DPP is a tool aimed at enhancing transparency about a product's environmental impact by offering relevant and comprehensive information about its lifecycle (see figure 1).

Similar to traditional passports, each product has a unique identity that's linked to one source with information about just that specific product.

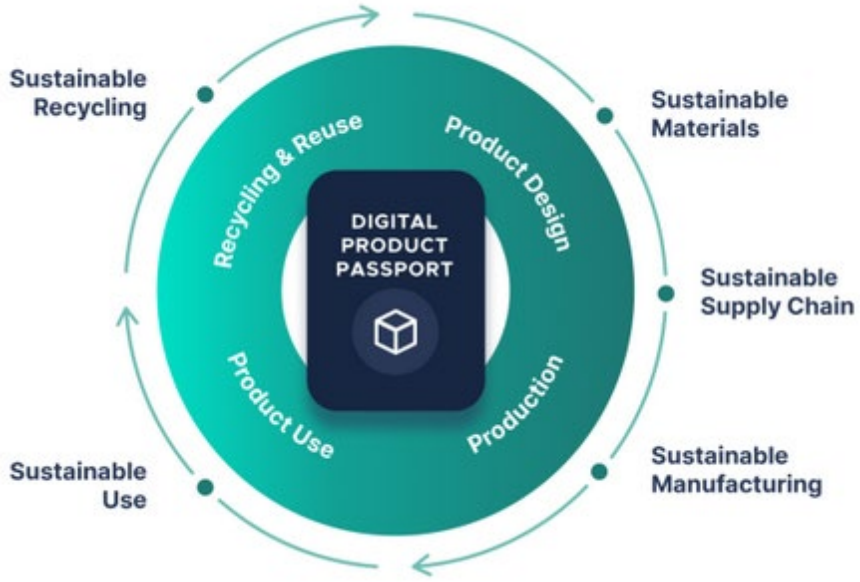

Fig. 1 - Dimensions of Digital Product Passport (DPP)

A DPP will soon be required for a range of products. Products with a high environmental impact and potential for improvement (textiles, furniture, chemicals, batteries, consumer electronics, electronic devices and construction products) will be prioritized.

The implementation of digital product passports in these value chains is designed to support:

- **Sustainable product production**: boosting material and energy efficiency, extending product lifetimes, and optimizing product use.
- **Businesses to create more value through circular business models**: improved access to data with digital product passports, more businesses can implement service and repair-based business models.
- **Consumers to make more informed purchasing decisions:** providing them with accurate information on the true impact of their buying behaviours.
- **Compliance with legal obligations:** product complies with standards and provide auditors with information to evaluate and verify.

According to the *(EU ESPR, 2022),* the first batch of products that need to have DPPs include: iron and steel, aluminum, textiles (garments and footwear particularly), furniture, tyres, detergents, paints, lubricants, chemicals, energy-related products with ecodesign requirements, information and communication technology products and other electronics *(Schuberth et al, 2024).*

Starting with 19 April 2025, manufacturers, importers, distributors, and retailers of these products must make their DPPs accessible. More categories will be known in the upcoming years, as the Commission is set to regularly update the list of products having to comply with the Regulation.

The textiles, construction, electronic waste, plastics, chemicals, and automotive sectors are all experiencing significant pressure and initiatives to adopt more sustainable business practices. Legislation is being developed to create connections across these various product categories, reflecting the growing emphasis on digitization, interconnected data sets, and the assessment of environmental impacts throughout product life cycles *(Panza et al, 2023; Saliger et al., 2024; Veenstra et al, 2025).*

Data requirements for digital product passports

Data requirements for DPP have been defined by the Ecodesign for Sustainable Products Regulation *(ESPR, 2022),* but implementation calls for the whole supply chain to cooperate and define the crucial information that could prevent a product from going to waste.

While DPP solutions can be adapted to a number of different use cases and can include various features and functionality, the ESPR outlines a number of key Digital Product Passport requirements for compliance that can be categorized into three key categories *(Framling et.al, 2007),* which include general requirements, access requirements and data requirements (see figure 2).

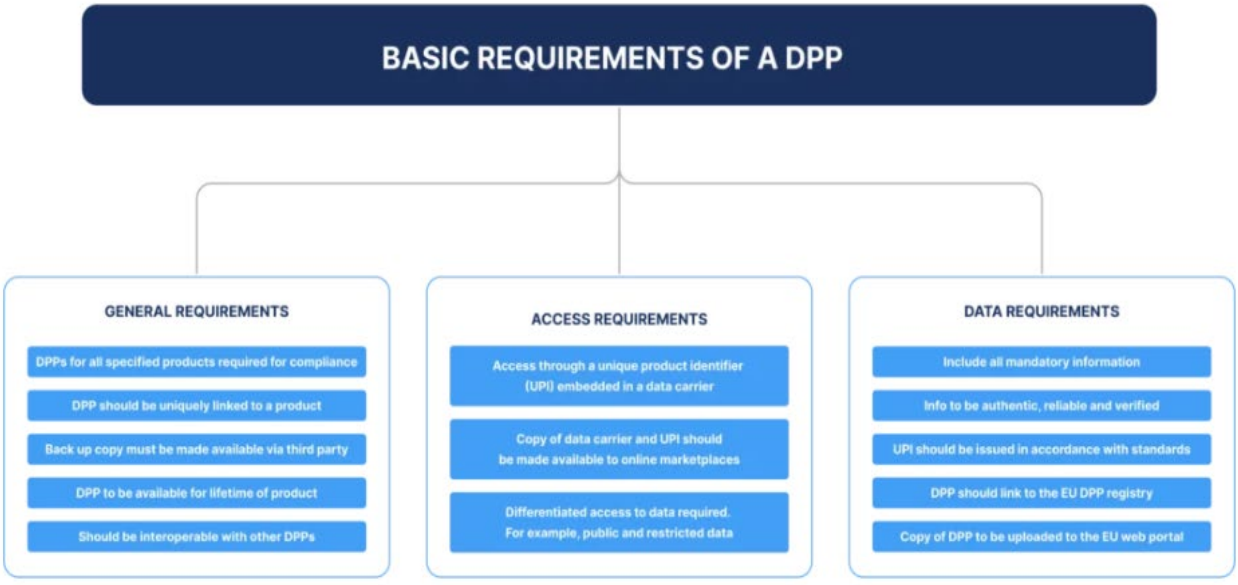

Fig. 2 - Overview of the basic requirements of a Digital Product Passport according to the ESPR.

General DPP requirements include:

- Passport should exist and be in compliance with essential requirements
- A DPP should be uniquely linked to a product.
- A back up copy must be made available via third party product passport service provider.
- The passport must remain available for at least expected lifetime of product.
- A DPP must be fully interoperable with other digital product passports.

The data requirements for DPP are:

- **Unique Product Identifier.** Each DPP links to a unique product ID via a data carrier (e.g., barcode, QR code) placed on the product, its packaging, or in accompanying documentation.
- **Compliance with Global Standards.** The DPP follows *(ISO, 2015)* standards to ensure consistency, quality, and global interoperability.
- **Structured, Machine-Readable Data.** All information in the DPP is structured, machine-readable, and based on open standards, making it searchable and compatible with digital systems.
- **Comprehensive Product Information.** The DPP contains key details about the product model, batch, or individual item, enhancing transparency across the supply chain.
- **Controlled Access to Information** Access to DPP information is regulated per Article 10, with specific access levels for each product group as set by Article 4 *(ESPR, 2022).*

Implementing a data transfer infrastructure for DPPs

Once a framework is defined for the information to be included in DPP, traceability software can be used to standardize data sets coming from existing ERP systems. The required unique product identifiers can use existing technologies such as barcodes, QR codes, Radio-frequency identification (RFID) tags, or similar, for digital product passport data submission. In the end, this process can be almost entirely automated.

In most cases, the main gap for companies lies in establishing the infrastructure for an open, standard, interoperable format for the DPP data – one that is also machine-readable, structured, and searchable, as outlined in the essential requirements of Article 9 of *(ESPR, 2022).*

The rapidly developing of blockchain and decentralized systems will be able to meet these requirements and provide key product information to the parties who value it most. These technological advances also mitigate the past criticism that decentralized blockchains have high operating costs and energy consumption. New blockchain technology developments will allow vast amounts of secure data transfer.

Protecting proprietary information by blockchain technology

When creating digital product passports, ensuring data security is essential for the protection of trade secrets. Different industries will require tailored approaches to data storage and encryption to address security challenges. Data storage can either be centralized or decentralized; but given the significance of the data being shared, a centralized system with a private party in control of data storage and integrity could be a less secure scalable solution for DPP infrastructure (. In some instances, a decentralized system provides the most effective means of data interoperability *(Damvakeraki and Vlachos, 20240).*

Decentralization also means the owner of the product is also the owner of the digital record, preventing reliance on a centralized system where data could be vulnerable to tampering. This approach complements the EU Data Strategy *(EURACTIV, 2021),* which encourages the use of high-value, publicly accessible data to generate value for companies, governments, and consumers. Circularize 's product traceability system is customizable, enabling businesses to opt for a public, decentralized blockchain for enhanced transparency and security if needed.

Blockchain technology acts as the perfect foundation on which to build a DPP solution for several reasons such as:

- **Data Security:** A consensus approach to validating data, underpinned by the most robust encryption system virtually eliminates data tampering and fraud. Decentralized technology also removes single points of failure securing data like never before.

- **Immutability:** As an immutable digital ledger, blockchains offer an extremely high level of trust in the data they contain. Consensus-based data validation guarantees that the information held is accurate and hasn't been changed or tampered with by malicious parties.
- **Transparency:** All blockchain transactions are provable, traceable and searchable on-chain, providing complete transparency for all ecosystem stakeholders in relation to the data stored within DPP.
- **Efficiency:** Data is processed, exchanged and validated quickly with blockchain.
- **Decentralization:** Blockchains are decentralized, censorship-resistant, and less vulnerable than legacy technologies that rely on centralized servers.

The key advantages of using blockchain for digital product passports, therefore, include improved transparency, less fraud, improved compliance, sustainability, supply chain efficiency, and consumer empowerment.

Marketing, sales and customer success teams can all utilize the digital passport application as a means of offering new services or features that are otherwise unavailable.

Essential Steps to Prepare for DPP Compliance

Efficient management of product data requires a Product Information Management (PIM) system, which serves as the backbone for ensuring consistent and transparent product information across all channels - a critical factor in meeting DPP requirements and building customer trust.

Fig. 3 - Key information in a Digital Product Passport

To prepare for Digital Product Passport (DPP) compliance, businesses need to first understand the regulations and their specific scope, then conduct a thorough product audit, and finally develop and implement a comprehensive data management strategy, including establishing traceability. This includes gathering product data, creating unique identifiers, and ensuring data security and interoperability (Navarro et al.,2022; Zhang and Seuring, 2024).

When taking a more holistic view of Digital Product Passports in terms of their current and potential utility – there are multiple different data categories that can be collected (see figure 4).

Fig. 4 - An example of the data sets that DPP can include

As previously mentioned, Digital Product Passports as a technology is still early and use-cases continue to grow – directly tied to the type of data being collected. Ultimately, DPP provide multiple parties including manufacturers, consumers, re-sellers and recycling entities with a full audit-trail of events and transactions that have occurred through a product's life.

For now, the key focus is on the sustainability, repairability and recyclability of a product that all ties into the broader circularity of the actual product. But as more businesses dive into the technology and understand its potential, DPP use-cases and opportunities will continue to scale.

Data Carrier

Data carriers refer to the mechanism that enables end-users to access the Digital Product Passport tied to a particular product. At present, EU guidelines suggest that organizations will have the freedom to decide what data carriers they utilize for any single, batch or type of product. Data carrier types suitable for DPPs include:

- **QR Code:** Already commonly utilized across several different industries and verticals for a multitude of purposes – the QR code could be considered the current go-to data carrier. Also famed for its durability and flexibility, QR codes are also widely accessible due to their easy connectivity with a smart device.
- **Barcode:** A similar option to the QR code carrier type, but offering less flexibility in terms of data held and utility due to its general purpose being to store product basic data and not for example, act as a conduit between a user and a webpage (that could contain the associated DPP).
- **NFC:** Already used for contactless payments, Near Field Communication (NFC) are similar to QR codes in that they are accessible by the majority of modern days smart devices, although they do carry additional cost as they are essentially standalone hardware devices (stickers with embedded antenna and microchip). A large advantage non-fungible token (NFT) tags have over QR & barcodes is their ability to be installed 'inside' a product and not necessarily on the 'outside' that offers further security benefits.

Data Sharing

Given the broad number of stakeholders and entities that participate in any given value chain, along with the varied demands and usage of data – a DPP solution will require a flexible approach to data sharing and accessibility.

Current proposals will categorize data stored within the DPP between private or public – whilst permissions to access, modify or update data will be defined by the European Commission. Although specific delegated acts to formalize DPPs for each target industry are still under development, the Commission has ensured that data security and privacy is at the heart of DPP design.

RESULTS

The benefits of implementing Digital Product Passports are:

- **Enhanced transparency**: DPPs provide companies with detailed information about their products' origin, materials, and environmental impact. This enhances global visibility for a company's brand and towards its customers.

- **Improved supply chain management**: The passports offer a comprehensive digital record that spans a product's entire value chain. This enhanced visibility enables companies to optimize processes to reduce environmental impact and ensure a more sustainable and efficient supply chain.

- **Regulatory compliance**: The DPP ensures that companies can easily adhere to environmental standards and regulations, fostering a commitment to responsible and sustainable business practices.

- **Identifies risks**: The DPP spots potential and actual risks by collecting clear information, real-time monitoring, and collaborative data sharing. It helps companies catch problems with authenticity, compliance, and environmental impact, taking a proactive approach to minimize risk.

- **Builds trust**: By providing transparent and verifiable information on a product's origin, authenticity, and compliance with relevant standards, the passports will help companies to build trust among customers, investors, and other important stakeholders.

The benefits to Businesses and Organizations are:

- **New Business Models:** The push towards a circular economy with more focus on product longevity provides a plethora of new business opportunities (such as product-as-a-service) that can be utilized to unlock additional revenue streams and growth drivers for companies. Digital passports can be seen as an additional channel that marketing, sales and business operations can tap to provide new services and an enriched customer experience.

- **Increase Consumer Trust:** By recording events across the full lifecycle of products from manufacturing all the way to recyclability or disposal – businesses can offer consumers a fully transparent view into the authenticity and state of the product they are purchasing.

- **Validate Green Claims**: Greenwashing is becoming a serious issue that is tainting the reputation of companies who are making legitimate claims. Through a digital passport, the sustainability attributes and claims are fully validated and secured on an immutable blockchain network.

- **Consumer Protection**: By ensuring that the raw materials and manufacturing processes abide by pre-set standards, businesses can protect their customers from illegitimate, dangerous and sub-par raw materials and end-products.

- **Ensure Compliance:** Through digital passports as a single and shared source of truth, the required data can be more easily tracked and accessed, leading to businesses being able to track their compliance with initiatives in real-time.

- **Quality Control:** The verifiable product data collected at each production stage by DPPs can allow businesses to improve their quality control measures.

- **Promote Sustainable Manufacturing:** From the provenance of sustainable raw materials used to providing operational data for improved oversight of the manufacturing process, DPPs

promote circularity and sustainability in manufacturing and can help minimize the negative impacts of production.

The benefits to Consumers and End-Users are:

- **Buyer Confidence:** Digital passports enable consumers to make more informed purchase choices related to the sustainability performance of the brands they buy from**.**

- **Maximized Product Value:** Similar to the above, consumers can rest assured that their products are legitimate – enabling them to avoid faulty or forged goods.

- **Identify Greenwashing:** Digital passports are a perfect tool to enable consumers to identify greenwashing and validate a company's claim in relation to their green initiatives. Though the immutability and transparency provided by blockchain, consumers can identify whether they are being purposely misled.

- **Recognize Carbon Footprint:** Many consumers who are seeking more sustainable responsibility from their chosen brands are looking to improve their own performance and reduce their carbon footprint. Depending on the type of product, accurate data on energy consumption and environmental impact can be gathered from an associated digital passport, which could also include additional blockchain-enabled services. Blockchain and digital passports opens new doors for encouraging positive action from consumers in joining the pledge to champion circularity.

- **Selecting Quality Products:** For customers, being able to compare the quality of two similar products side by side can make their purchase decision easier. Organizations can demonstrate that their products meet the highest quality standards by including certifications and warranties within their DPP, which the customer can easily access in a transparent and verifiable manner.

The benefits to Policy Makers and Governing Bodies are:

- **Verify Compliance:** DPP's provide a unified basis for tracking the sustainability performance of business entities and organizations, providing a mechanism for policy makers to benchmark KPI's and take necessary action if required.

- **Drive Sustainability:** Under a digital passport system, greenwashing and false claims are significantly reduced, giving policy makers the best chance of meeting their key sustainability, resource optimization and circularity goals.

CONCLUSIONS

- The Digital Product Passport represents a significant advance in product transparency and sustainability. As the EU moves towards full adoption of this regulation, it will foster a more open and responsible marketplace.

- By integrating open data principles, the DPP will enhance both the visibility and integrity of product information, benefiting companies, consumers, and the environment alike.

- Going through the process of DPP implementation will also enable manufacturers to gain a clearer view of their material flows and process efficiencies, paving the way for impactful improvements.

- By addressing and mapping out sustainability roads through the entire product lifecycle, emphasising the importance of transparency, supply chain traceability and accountability, the ESPR fosters a culture of sustainability and brings the EU one step closer to the goals of the European Green Deal.

REFERENCES

[1] Baumgartner, R. J. (2023). Confidentiality-preserving data exchange to enable sustainable product management via digital product passports—A conceptualization. Procedia CIRP, 116, 354–359. https://doi.org/10.1016/j.procir.2023.02.060

[2] Berger, K., Rusch, M., Pohlmann, A., Popowicz, M., Geiger, B. C., Gursch, H., Schöggl, J.-P., & Ducuing, C., & Reich, R. H. (2023). Data governance: Digital product passports as a case study. *Competition and Regulation in Network Industries*, 24(1), 3–23.

[3] Damvakeraki T., Vlachos I. (2024) Digital Product Passport: A Blockchain-based Perspective DOI:10.13140/RG.2.2.36103.41125

[4] Främling, K., Harrison, M., Brusey, J. and Petrow, J. (2007). Requirements on unique identifiers for managing product lifecycle information: Comparison of alternative approaches. *International Journal of Computer Integrated Manufacturing*, Vol. X, No. X, Month

[5] Gieß, A., Möller, F. (2025) Exploring the value ecosystem of digital product passports, *Journal of Industrial Ecology* ;29:561–573. DOI: 10.1111/jiec.13621

[6] Henten, A. Morten F. and Tadayoni, R. (2025). Digital Product Passport standardization – factors, actors and institutions. Available at SSRN: https://ssrn.com/abstract=5138036. doi: 10.20944/preprints202504.1765.v1

[7] Henten, A., Falch, M., Tadayoni, R. (2025) Digital Product Passport—EU Sustainability and Circularity Regulation

[8] Jensen, S. F., Kristensen, J. H., Adamsen, S., Christensen, A., & Waehrens, B. V. (2023). Digital product passports for a circular economy: Data needs for product life cycle decision-making. *Sustainable Production and Consumption*, 37, 242–255. https://doi.org/10.1016/j.spc.2023.02.021

[9] King, M. R., Timms, P. D., & Mountney, S. (2023). A proposed universal definition of a Digital Product Passport Ecosystem (DPPE): Worldviews, discrete capabilities, stakeholder requirements and concerns. *Journal of Cleaner Production*, 384, 135538. https://doi.org/10.1016/j.jclepro.2022.135538

[10] Navarro, L., Esteban, J.C., Miralles, M.F. and Griso, D.F., 2022. Digital transformation of the circular economy: Digital product passports for transparency, verifiability, accountability. *Manuscript submitted for publication.*: A systematic literature review, International Journal of Production Economics ,245, 1–19.

[11] Neligan, A., Schleicher, C., Engels, B., & Kroke, T. (2023). Digital product passport as enabler for the circular economy: Relevance and practicability for companies. IW Report. https://circulareconomy.europa.eu/platform/sites/default/files/2024-02/IW-Report_2023-Digitaler-Produktpass-englisch.pdf

[12] Panza, L., Bruno, G. and Lombardi, F., 2023. Integrating absolute sustainability and social

[13] sustainability in the digital product passport to promote industry 5.0. *Sustainability*, 15(16), p.12552

[14] Saliger A., Malisa V., Schellander M., Grafinger M. (2024). Development and Implementation of a Digital Safety Passport in Compliance with EU Machinery Regulation, Conference: *MTSM2024* - Mechanical Technologies and Structural Materials

[15] Schuberth, J., Ebert, T., Schlegel, M-C, Rödig, L., Jepsen, D., Memelink, R. and Hauschke, F. (2024). The Front-Runner Approach—Facilitating Progressive Product Policy by Using Information from EU Product Databases, *Energies* 2024,17, 504. https://doi.org/10.3390/en17020504

[16] Sudusinghe, J.I. and Seuring, S. (2022). Supply chain collaboration and sustainability performance in circular economy

[17] Veenstra, A., Rukanova, B., Tan, Y. (2025). Final report digital product passports and EU regulation, UPT, DOI:10.13140/RG.2.2.26888.94722

[18] Zhang, A., & Seuring, S. (2024). Digital product passport for sustainable and circular supply chain management: A structured review of use cases. *International Journal of Logistics Research and Applications*, 27(12), 2513–2540. https://doi.org/10.1080/13675567.2024.2374256

[19] *** European Commission. (2022). *Circular economy action plan* CEAP. https://ec.europa.eu/environment/strategy/circular-economy-action-plan_en

[20] *** European Commission. (2022). *Proposal for Ecodesign for Sustainable Products Regulation ESPR*. https://ec.europa.eu/environment/publications/proposal-ecodesign-sustainable-products-regulation_en

[21] *** EURACTIV (2021). *EU plans 'digital product passport' to boost circular economy*. https://www.euractiv.com/section/circular-economy/news/eu-plans-digital-product-passport-to-boost-circular-economy/.
[22] *** European Commission. (2022). *Ecodesign for Sustainable Products Regulation (ESPR)*
[23] https://commission.europa.eu/energy-climate-change-environment/standards-tools-and-labels/products-labelling-rules-and-requirements/ecodesign-sustainable-products-regulation_en
[24] *** European Commission. (2020). Sustainable Products Initiative - Initiative details - European Union https://ec.europa.eu/info/law/better-regulation/have-your-say/initiatives/12567-Sustainable-products-initiative_en
[25] *** International Organization for Standardization. (2015). *Information technology — Automatic identification and data capture techniques — Unique identification Part 2: Registration procedures* (ISO/IEC 15459-2:2015)
[26] *** European Union (2024). *EU's Digital Product Passport: Advancing transparency and sustainability*. https://data.europa.eu/en/news-events/news/eus-digital-product-passport-advancing-transparency-and-sustainability.

RESEARCH ON THE INFLUENCE OF RAW WOOL QUALITY ON THE PARAMETERS FOR OBTAINING HYDROLYSATE BY THE ALKALINE METHOD

/

CERCETARI PRIVIND INFLUENTA CALITAȚII LÂNII BRUTE ASUPRA PARAMETRILOR DE OBȚINERE A HIDROLIZATULUI PRIN METODA ALCALINĂ

Elena Mihaela NAGY*[1)], Teodor Gabriel FODOREAN[1)], Evelin-Anda LAZA[1)], Marius GHERES[2)]

[1)] National Institute of Research - Development for Machines and Installations Designed for Agriculture and Food Industry - INMA Bucharest / Romania;

[2)] Technical University of Cluj-Napoca, Faculty of Automotive Engineering, Mechatronics and Mechanics, Cluj-Napoca, Cluj County / Romania.

**Tel: 0748 165 302; *E-mail: nagy_m2002@yahoo.co.uk*

***Keywords**: wool waste, hydrolysate, alkaline, fertilizer*

ABSTRACT

Wool waste or unsaleable wool is a growing resource in Europe, which, due to the low biodegradability of keratin, can be a source of long-term environmental pollution. At the same time, the chemical composition of wool, especially keratin, is a protein compatible with cell growth and has a high sulphur content, which is important in the formation of proteins, enzymes, vitamins and chlorophyll in plants. A simple method for solubilising keratin from wool is alkaline hydrolysis. In this regard, our research has investigated the influence of wool waste quality on the parameters of the alkaline hydrolysis process (temperature, processing time) and on some physical properties of the hydrolysate obtained (degree of decomposition, undegraded residues).

REZUMAT

Deseurile de lana sau lana nevandabilă reprezinta o resursa in crestere la nivel european, care datorita gradului redus de biodegradare a keratinei poate constituii o sursa de poluare pe termen lung a mediului. Totodata compozitia chimica a lanaii, in special keratina reprezinta o proteina cu compatibilitate pentru cresterea celulara si cu un continut ridicat de sulf-element important in formarea proteinelor, enzimelor, vitaminelor si clorofilei in plante. O metoda simpla pentru solubilizarea keratinei din lana o reprezinta si hidroliza alcalina. In acest sens cercetarile au urmarit influenta calitatii deseurilor de lana asupra parametrilor procesului de hidroliza alcalina (temperatura, durata de procesare, si asupra unor proprietati fizice a hidrolizatului obtinut (grad de descompunere, resturi nedegradate).

INTRODUCTION

The global sheep population stands at approximately 1.27 billion head, with a production of approximately 1.9 million metric tons of wool (*IWTO, 2022*). At EU level, it is estimated that there are approximately 85 million sheep in various production systems (*Theodoridis et al. 2021*), with an annual wool production exceeding 200,000 tons, classified into several groups (*Petek and Marinšek Logar 2021*). In 2024, Romania was ranked in second place with a total of 11.87 million sheep (*https://www.stiripesurse.ro/romania-urca-in-topul-european-cu-peste-11-milioane-de-oi-si-capre-locul-2-in-ue-dupa-spania_3685104.html*).

Approximately 60% of wool is used in the production of woolen clothing (*Woods, 2012*), which has continued to experience a decline in demand, leading to the elimination of large volumes of low-quality wool (*Ossai et al., 2022*). Cheap, low-quality wool is mainly considered a by-product (*Chereji and Munteanu 2022*).

Due to the economic situation, raw wool production is an economic burden for sheep farmers in many EU countries, although wool is a biological resource rich in protein (95%–98% of wool weight) that is available in large quantities and at affordable prices.

Wool waste significantly affects the biological properties of soil (*Lal et al. 2020*). β-glucosidase activity, which plays a crucial role in the decomposition of cellulose and the cycling of carbon within the soil, has been shown to increase with sheep wool treatments (*Çetin Karaca et al. 2023*).

Wool is a rich source of important nutrients, containing high quantities of N, S and C, which are necessary for plant growth (*McNeil et al., 2007*). Greasy raw wool is composed of protein 'keratin' with an abundance of carbon (C 50%), nitrogen (N 16- 17%) and sulphur (S 3-4%), which play an essential role in plant nutrition (*Von Bergen et al., 1963*).

Keratin is a group of insoluble, filamentous proteins, with high-sulfur content forming the bulk of epidermal appendages such as wool, claws, horns, beaks, and feathers (*Wang et al., 2016*). Keratin extracted from wool is a biopolymer with excellent properties that synthetic polymers cannot achieve (*Cardamone, 2010*).

Wool keratin has a distinct three dimensional structure and contains approximately 95% protein, 0.5% minerals, 5% lipids (*Aluigi, A., et al.2014*). Due to its low cost, biophysical stability in physiological environments, and biodegradability, previous studies focused on keratin production for biomaterials, agriculture and textile applications (*Shavandi et al., 2016; Goyal et al., 2022; Zoccola et al., 2015*). Keratin can be extracted using strong acid, alkali, high concentration of salt solutions or expensive enzymes.

Recent methods use ionic liquids for keratin extraction from wool, feathers and hair with improved yield (*Ji et al., 2016).* As compared to other reported research (*Gaidau, C et al. 2019*) we have used KOH as hydrolysis agent for its nutritional potential for plant growth.

This paper presents the method of obtaining alkaline hydrolysate from raw wool at different stages of preparation, studying if and how the hydrolysis process may be influenced by the condition of the wool.

MATERIALS AND METHODS

The raw wool was purchased from local farmers, potassium hydroxide (KOH), NH3(25% solution), Na_2CO_3 and citric acid were purchased from Silver Chemicals and the detergent was purchased from local shop.

We prepared three hydrolysate samples: sample UW- hydrolyzate from raw, unwashed wool; sample W-hydrolyzate from raw, washed wool and sample WD- hydrolysate from raw, washed, and degreased wool.

Wool washing, degreasing and hydrolysis

For sample W the raw wool was washed with tap water, mixed manually, in three one-hour sessions, until the water remained clean.

For sample WD the raw wool was washed and degreased in water in ratio 1:10 with 1% NH_3, 1% Na_2CO_3 and 1% detergent by manually stirred for three hours at 35°C.

For both samples W and WD the wool was dried in the sun in the open air. Large impurities such as straw, pieces of wood, soil, burrs, etc. were manually separated from all wool samples (Fig.1).

The alkaline hydrolysis was made in a solution containing water in ratio 1:5 and 8%KOH at room temperature for 24 hours, followed by boiling at 100°C for 1 hour, followed by filtration. The pH of the hydrolysate was adjusted by adding citric acid.

a) b) c)

Fig. 1 - a) Raw wool; b) large impurities from raw wool; c) washed wool

The obtained keratin hydrolysates were physically analyzed for remain impurities and dry matter. Impurities obtained after filtration were measured with a Partner precision electronic balance.

The measurable parameter determined was the dry matter content determined by heating a quantity of hydrolysate to 70°C until the liquid evaporated completely and the dry matter was measured with a Partner precision electronic balance.

RESULTS

Three keratin hydrolysates were obtained using raw wool in various stages of cleaning and degreasing, following the technological steps presented above.

The chemical action of the alkaline medium manifests itself on the wool keratin by releasing electro-valences, breaking the cystine bridge, and hydrolyzing peptide bonds under the influence of the pH value of the reaction environment, working time, and temperature *(Ifrim, 1979).*

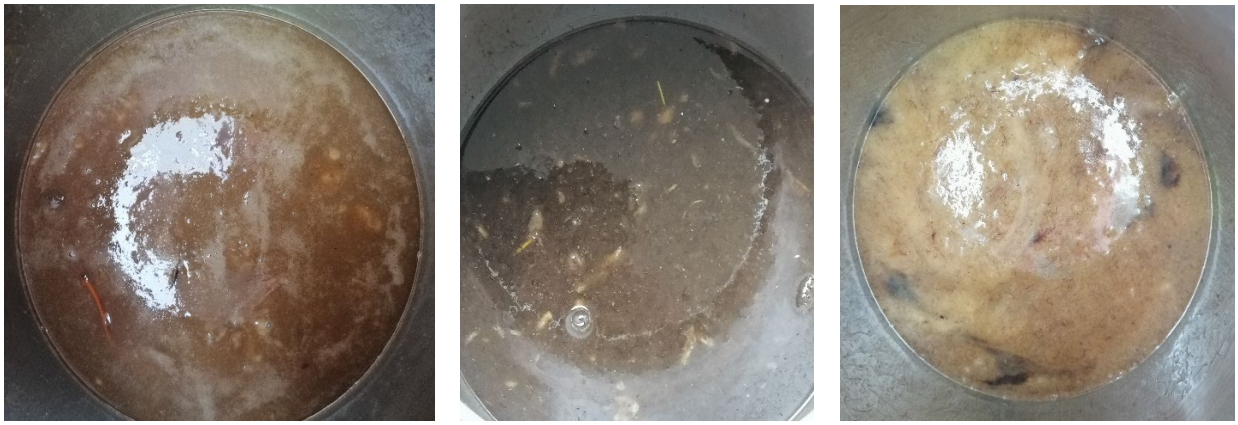

Sample UW **Sample W** **Sample WD**

Fig. 2 - Mixture of wool with 8% KOH solution after 24 h

Table 1

Values for hydrolysed mass, impurities, and citric acid for pH adjustment

Sample	Hydrolysed mass, g	Dry Impurities g	Citric acid for pH 6.5-7 g / %
Sample UW	785	1.15	43 / 5.2%
Sample W	970	1.05	44 / 4.3%
Sample WD	980	0.49	54.7 / 5.3%

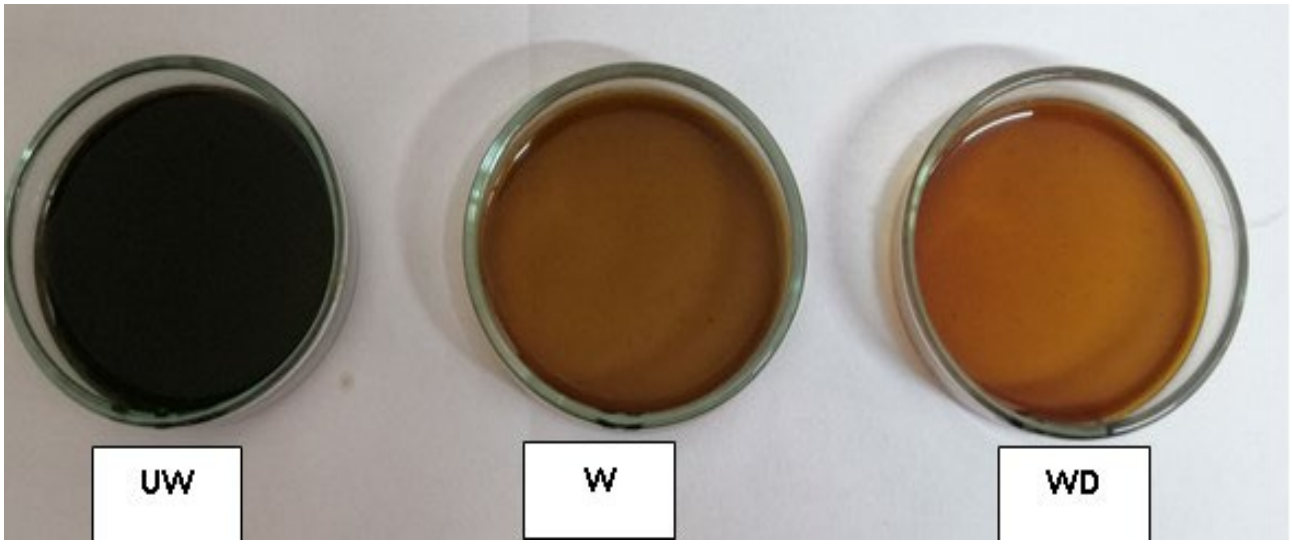

Fig. 3 - Appearance of the hydrolysate samples obtained

Analyzing the data in Table 1, we can see that the hydrolysate sample UW, obtained from unwashed wool, as expected, has the highest impurity content after hydrolysis.

The hydrolysate sample obtained from washed and degreased wool, WD, has a much lower impurity content, approximately half that of the other two samples.

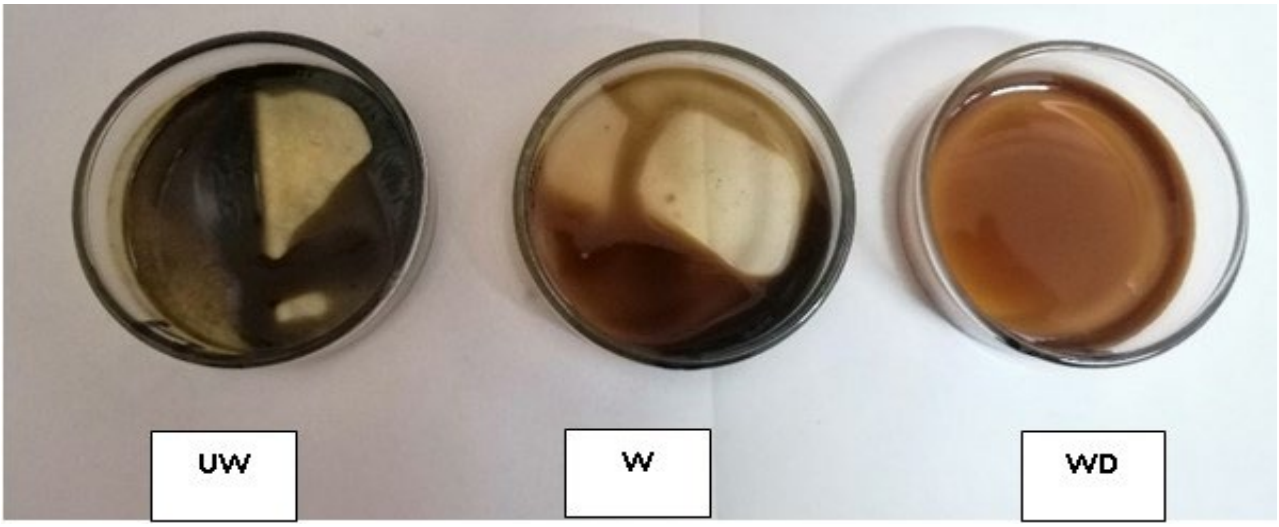

Fig. 4 - Dry matter resulting from drying the samples

Table 2

Values obtained for dry matter

Sample	Liquid phase			Dry phase	
	Vessel weight, g	Liquid weight, g	Total weight, g	Total weight, g	Dry matter, g
Sample UW	14.14	3	17.14	15.37	1.23
Sample W	14.25	3.1	17.35	15.24	0.99
Sample WD	14.74	3	17.74	15.50	0.76

The data in Table 2 confirm the results in Table 1, namely that the WD sample has the lowest dry matter content, which correlates with the lowest impurity content. This is due to the washing and degreasing process, which removes and breaks down most of the impurities in the raw wool.

CONCLUSIONS

The production of keratin hydrolysates from wool by-products is an environmentally friendly option for creating new value-added products in the category of bio-stimulants and organic fertilizers.

The results of the research showed that complete solubilization of wool can be achieved by alkaline hydrolysis with potassium hydroxide, with a concentration of 8% for raw wool in various stages of cleaning/degreasing.

It has been observed that the hydrolysate obtained from wool that has been washed and degreased beforehand in water in ratio 1:10 with 1% NH_3, 1% Na_2CO_3 and 1% detergent has the lowest content of impurities obtained after filtration - approx. 42% compared to the impurity content in the hydrolysate obtained from unwashed raw wool, and also the lowest dry matter content - approx. 60% compared to the hydrolysate obtained from unwashed raw wool.

The data obtained in this research refer only to the physical characteristics of the hydrolysate obtained from raw wool and prove that, at first glance, hydrolysate can also be obtained from unwashed raw wool using the same technology, which would lead to savings in wool washing and degreasing costs.

As a continuation of this research, the chemical characteristics of the three types of hydrolysates should be studied to verify whether the cleanliness of the wool influences the composition and chemical characteristics of the hydrolysates intended for use in agriculture.

ACKNOWLEDGEMENT

This work was supported by a grant of the Romanian Ministry of Education and Research, through the project "Research on the use of wool waste to obtain organic fertilizers for agriculture in order to improve soil properties and reduce environmental pollution" – PN 23 04 02 02– Ctr. 9N/01.01.2023.

REFERENCES

[1] Aluigi, A., Tonetti, C., Rombaldoni, F., Puglia, D., Fortunati, E., Armentano, I., Santulli, C., Torre, L., Kenny, J.M., (2014) Keratins extracted from Merino wool and Brown Alpaca fibres as potential fillers for PLLA-based biocomposites, *J Mater Sci*, 49, 18, 6257–6269, https://doi.org/10.1007/s10853 014-8350-9.

[2] Cardamone,J.M. (2010), Investigating the microstructure of keratin extracted from wool: Peptide sequence (MALDI-TOF/TOF) and protein conformation (FTIR), *Journal of Molecular Structure*, 969, 97–105, https://doi.org/10.1016/j.molstruc.2010.01.048.

[3] Çetin Karaca U, Chalabee OAH, Saba M (2023) The effect of sheep wool fertilizer on some biochemical properties of a clay loam soil. *Commun Soil Sci Plant Anal* 54:48–61. https://doi.org/10.1080/00103624.2022.2109662

[4] Chereji B-D, Munteanu F-D (2022) the Impact of sheep waste wool on the environment. Sci Pap E-l *Reclam Earth Obs Surv Environ Eng* 11:458–463

[5] Gaidau, C., Epure, D.G., Enascuta, C.E., Carsote, C., Proietti, N., Chen, W., Gu, H., (2019), Wool keratin total solubilisation for recovery and reintegration-an ecological approach, *J Clean Prod*, 236, 117586, https://doi. org/10.1016/j.jclepro.2019.07.061.

[6] Gambelli D, Solfanelli F, Orsini S, Zanoli R (2021) Measuring the economic performance of small ruminant farms using balanced scorecard and importance-performance analysis: a european case study. *Sustain.* https://doi.org/10.3390/su13063321

[7] Govi, M., Ciavatta, C., Sitti, L. and Gessa, C. (1998). Influence of organic fertilisers on soil organic matter: a laboratory study. In: *16th World Congress of Soil Science*, http://natres.psu.ac.th/Link/SoilCongress/bdd/symp40/ 974-r.pdf, accessed on 08.05.2017

[8] Goyal, S., Dotter, M., Diestelhorst, E., Storck, J. L., Ehrmann, A., & Mahltig, B. (2022). Extraction of keratin from wool and its use as biopolymer in film formation and in electrospinning for composite material processing. *Journal of Engineered Fibers and Fabrics*, 17. https://doi.org/10.1177/15589250221090499

[9] Ifrim, S. (1979), *Chimia Lânii*, Editura Tehnica, Bucharest.

[10] Ji, Y., Chen, J., Lv, J., Li, Z., (2014), Extraction of keratin with ionic liquids from poultry feather, *Separation and Purification Technology*,132, 577–583,https://doi.org/10.1016/j.seppur.2014.05.049.

[11] Lal B, Sharma SC, Meena RL, Sarkar S, Sahoo A, Balai RC, Gautam P, Meena BP (2020) Utilization of byproducts of sheep farming as organic fertilizer for improving soil health and productivity of barley forage. *J Environ Manage*. https://doi.org/10.1016/j.jenvm an.2020.110765

[12] McNeil, S.J., Sunderland, M.R. and Zaitseva, L.I. (2007) Closed-loop wool carpet recycling. *Resources, Conservation and Recycling* 51: 220-224.

[13] Ossai, I. C., Shahul Hamid, F., & Hassan, A. (2022). Valorisation of keratinous wastes: A sustainable approach towards a circular economy. *Waste Management*, 151, 81–104. https://doi.org/10.1016/j.wasman.2022.07.021

[14] Petek B, Marinšek Logar R (2021) Management of waste sheep wool as valuable organic substrate in European Union countries. *J Mater Cycles Waste Manag* 23:44–54. https://doi.org/10.1007/ s10163-020-01121-3

[15] Shavandi, A., Silva, T. H., Bekhit, A. A., & Bekhit, A. E. A. (2017). Keratin: dissolution, extraction and biomedical application. *Biomaterials Science*, 5(9), 1699–1735. https://doi. org/10.1039/c7bm00411g

[16] Theodoridis A, Vouraki S, Morin E, Rupérez LR, Davis C, Arsenos G (2021) Efficiency analysis as a tool for revealing best practices and innovations: the case of the sheep meat sector in Europe. *Animals.* https://doi.org/10.3390/ani11113242

[17] Von Bergen, W. 1963. *Wool Handbook* Vol. 1, 3 ed., John rd Wiley and Sons, New York, London

[18] Wang,B., Yang, W., Mckittrick, J., Meyers M.A., (2016), Keratin: Structure, mechanical properties, occurrence in biological organisms, and efforts at bioinspiration, *Progress in Materials Science*, 76, 229–318, https://doi.org/10.1016/j.pmatsci.2015.06.001

[19] Woods, A. (2012). Global view of the apparel market. WOOL422/522 Wool marketing and clip preparation. *The Australian Wool Education Trust licensee for educational activities*. Retrieved from https://www.woolwise.com/wp-content/uploads/2017/07/ WOOL-422-522-12-T-16.pdf

[20] Zoccola, M., Montarsolo, A., Mossotti, R., Patrucco, A., & Tonin, C. (2015). Green hydrolysis as an emerging technology to turn wool waste into organic nitrogen fertilizer. *Waste and Biomass Valorization*, 6(5), 891–897. https://doi.org/10.1007/s12649-015-939 3-0

[21] ****www.stiripesurse.ro/romania-urca-in-topul-european-cu-peste-11-milioane-de-oi-si-capre-locul-2-in-ue-dupa-spania_3685104.html*

EFFICACY AND SELECTIVITY OF IMAZAMOX AND PENDIMETHALIN BASED HERBICIDE IN WEED CONTROL IN SOYBEAN CROPS

/

EFICACITATEA ȘI SELECTIVITATEA AMESTECULUI DE IMAZAMOX ȘI PENDIMETHALIN ÎN CONTROLUL BURUIENILOR DIN CULTURILE DE SOIA

Marga GRĂDILĂ*[1)], Daniel JALOBĂ[1)], Valentin Marius CIONTU[1)], Raluca Monica CRISTEA[1)], Mihaela ŞERBAN[2)], Victor PETCU[2)], Nicolae-Valentin VLĂDUȚ[3)], Cătălina TUDORA[3)]

[1)] Research - Development Institute for Plant Protection - ICDPP Bucharest / Romania;

[2)] National Agricultural Research and Development Institute Fundulea, 915200 Fundulea, Călăraşi County / Romania;

[3)] National Institute of Research - Development for Machines and Installations Designed to Agriculture and Food Industry - INMA Bucharest / Romania.

*Tel: 0724 925 155; *E-mail:marga_gradila@yahoo.com*

***Keywords**: imazamox, pendimethalin, soybean, weeds, control, efficacy*

ABSTRACT

The research was conducted in 2021, in Călărași County, in 3 experimental plots seeded with soybean and aimed to evaluate the selectivity and efficacy of the herbicide based on imazamox and pendimethalin for weed control. The experiments were placed in randomized blocks, in 4 repetitions with a plot area of 100 m^2. Weed density was assessed as number of plants/m^2 and as percentage of ground cover. Efficacy was evaluated at 14, 28 and 40 days after treatments application, being compared to the untreated control, according to the EWRS scale. Statistical data calculation was performed using the ARM-9 software (P= .05, Student-Newman-Keuls). The floristic composition of the experimental plots has been diverse, as annual species prevailed. The following species were recorded: Abutilon theophrasti, Amaranthus retroflexus, Ambrosia artemisiifolia, Cannabis ruderalis, Chenopodium album, Galium aparine, Fumaria officinalis, Hibiscus trionum, Papaver rhoeas, Polygonum spp.*, Solanum nigrum, Sonchus* spp.*, Viola arvensis and Xanthium* spp*. of dicotyledonous class and among the monocotyledonous were Setaria* spp.*, Echinochloa crus-galli and Poa annua. The treatments were applied in pre-emergence after sowing until BBCH 05 (radicle emerged from seed) at doses of 2.2, 3.4 and 4.5 l/ha. The herbicide based on Imazamox and Pendimethalin provided good efficacy in controlling annual weeds in soybean crops whereas the best results being obtained at higher doses of 4.5 l//ha. At doses of 2.2 l/ha and 3.4 l/ha, the species of Setaria, Echinochloa, Galium, Solanum, Xanthium, Sonchus, Polygonum are not controlled or are insufficiently controlled. No phytotoxicity phenomena were recorded in experimental plots.*

REZUMAT

Cercetările au fost efectuate în anul 2021, în județul Călărași în 3 loturi experimentale cultivate cu soia și au avut ca scop evaluarea selectivității și eficacității erbicidului pe bază de imazamox și pendimethalin în controlul buruienilor. Experiențele au fost amplasate în blocuri randomizate, în 4 repetiții cu suprafața parcelei de 100 m^2. Densitatea buruienilor a fost evaluată ca număr de plante/m^2 și ca procent de acoperire a solului. Eficacitatea a fost evaluată la 14, 28 și 40 de zile de la aplicarea tratamentelor, comparativ cu martorul netratat, conform scalei EWRS. Calculul statistic al rezultatelor s-a efectuat cu ajutorul software-ului ARM-9 (P= .05, Student-Newman-Keuls). Compoziția floristică a loturilor experimentale a fost diversă, dominante fiind speciile anuale. Au fost prezente următoarele specii: Abutilon theophrasti, Amaranthus retroflexus, Ambrosia artemisiifolia, Cannabis ruderalis, Chenopodium album, Galium aparine, Fumaria officinalis, Hibiscus trionum, Papaver rhoeas, Polygonum spp.*, Solanum nigrum, Sonchus* spp.*, Viola arvensis și Xanthium spp. din clasa dicotiledonate iar dintre monocotiledonate Setaria spp., Echinochloa crus-galli și Poa annua.Tratamentele au fost aplicate în premergență după semănat până la BBCH 05 (până când radicula a ieșit din sămânță) la doze de 2,2, 3,4 și 4,5 l/ha. Erbicidul pe baza de Imazamox și Pendimethalin a avut o eficacitate bună în controlul buruienilor anuale din culturile de soia, cele mai bune rezultate obținându-se la doza de 4,5 l/ha. La dozele de 2,2 l/ha și 3,4 l/ha speciile de mohor, iarba barboasă, turiță, zărnă, cornuți, susai, hrișcă nu sunt controlate sau sunt controlate insuficient. Nu s-au înregistrat fenomene de fitotoxicitate în loturile experimentale.*

INTRODUCTION

Weed control is an essential link in soybean crop technology (*Glycine max* (L.) Merril) as yield loss due to weed infestation could be between 40 și 90%, depending on type of weed, soil, seasons and weed infestation intensities (*Gogoi et al., 1991; Kachroo et al., 2003; Berca, 1996 and 2004; Sodangi et al., 2006 and 2007; Nainwal et al., 2010; Caverzan et al., 2019; Zain et al., 2020*).

Soybean plants have a particularly sensitivity to weeds, from the first days after emergence until harvest time, thus damage caused by weeds is significant, resulting in increased production costs. Once infested by weeds, especially in the early stages of growth, soybean crops cannot recover and cannot ensure best yields, even if the weeds are subsequently controlled (*Rusu et al., 2014*).

The more abundant and earlier the degree of weed infestation, the more obvious the contribution to yield decrease (*Thurlow and Buchanan, 1972; Coble et al., 1981; Baysinger and Sims, 1991; Begonia et al., 1991; Fellows and Roeth, 1992; Van-Acker et al., 1993; Senthil et al., 2009; Yadav et al., 2017*). Therefore, one of the most important aspects of soybean crop technology is weed management (*Lamptey et al., 2015; Jannink et al., 2000*).

In agricultural practice, various control methods are used collectively to effectively manage weed infestations in soybeans: preventive, cultural, mechanical, biological and chemical (*Datta et al., 2017; Song et al., 2020; Tehulie et al., 2021*). Herbicide application is the most common method for weed control in soybean crops due to its efficiency, velocity and low cost compared to other control methods.

The lack of labor force during the peak weed infestation period, the difficulty of performing mechanical hoeing due to rain, and high costs raise problems for effective weed control in soybean crops. Weed management through herbicide application remains the only applicable alternative in these situations. Herbicide treatments applied to the soil during seedbed tillage or immediately after sowing, supplemented with treatments during the growing season, can ensure weed-free soybean crops until harvest.

Taking account that soybean crop is subject to fierce competition by weeds, especially in the early stages of growth, early herbicide control is a necessity for this crop in order to achieve adequate yields and to manage weed resistance (*Kalpana and Velayutham 2004; Parmar et al., 2016; Oliveira et al., 2017; Nunes et al., 2018; Coradin et al., 2019)*. In almost all situations, the best results in weed control in soybean crop are fullfilled with combination herbicides (mixtures).

Under these circumstances, this paper provides data on efficacy of the herbicide based on imazamox and pendimethalin applied in pre-emergence to control of annual weeds in soybean crops.

MATERIAL AND METHOD

Field experiments were conducted during 2021, in 3 experimental lots cultivated with soybeans in Călărași county. The soybean crops assessed were cultivated by private farmers according to their own technologies. Agrophytotechnical data regarding experimental plots (location, soil, previous crop, plant stage BBCH, phytosanitary treatments) are written in Table 1.

Table 1

Agrophytotechnical data regarding soybean experimental plots

Location	Pelinu	Tămădău Mare	Borcea
GPS coordinates	44°27'43" N, 27°01'46" E	44°28'14" N, 26°34'23" E	44°17'791" N; 27°47'24" E
Soil	Cernoziom cambic		
Previous crop	Maize	Winter wheat	Winter barley
Variety	Procera 1020	Dakota	Ovidiu
Sowing date	07.05.2021	04.05.2021	05.05.2021
Density	55 000 pl/ha	60 000 pl/ha	60 000 pl/ha
Emergence date	21.05.20201	18.05.2021	25.05.2021
Fungicides/Insecticides	Pictor: 0.5l/ha-20.06.2021 Ercole:10 kg/ha-25.04.2021	Ridomil gold MZ: 2.5 kg/ha - 11.06.2021 Trika Expert: 12 kg/ha - 22.04.2021	Pictor -0.5l/ha 2 treatments:14.06.2021; 28.06.2021 Ortus 5 SC: 0.5 l/ha; 30.05.2021 Nissorun 10 WP:0.4 kg/ha; 14.06.2021
Treatment date	10.05.2021	11.05.2021	8.05.2021
BBCH (Growth stage)	BBCH 01*	BBCH 03**	BBCH 05***

*Beginning of seed imbibition **Seed imbibition complete ***Radicle emerged from seed

The experiments were placed in randomized blocks, in 4 repetitions, with a plot area of 100 m^2 each. A nontreated control was included for comparison. Imazamox (16.7 g/l) and Pendimethalin (250 g/l) based herbicide, formulated as CE (Emulsifiable Concentrate), was applied preemergence at doses of 2.2, 3.4 and 4.5 l/ha. Observations were focused on the determination of weed species found in the experimental fields, weed density and control effectiveness. Weeds density was assessed as percentage of soil coverage and in number of plants per square meter. Determination of segetal flora was performed on one square meter using a metric frame.

The number of weeds per square meter was determined by weed mapping with a metric frame of 1 m^2 side in 4 repetitions on the diagonal of the plot. The percentage of weed cover was assessed visually, according to species, density and phenological aspects of each weed (emerging, budding, flowering, fruiting, ripening, seed dispersal, height, etc.). The herbicide efficacy was recorded at the 14, 28 and 40 days after treatments according EWRS (European Weed Research Society) and the effectiveness was calculated in % control compared to untreated samples.

Crop phytotoxicity was assessed visually on a rating scale from 0% to 100% (0 - no injury to soybean plants and 100 - complete drying of the plants). Statistical data calculation was performed using ARM-9 software (P = .05, Student-Newman-Keuls).

RESULTS

The experimental field taken into study was infested by various annual weed species, consisting of both dicot and monocot weeds**.** Major weed flora found in the experimental field was grouped into broad leaved and grass weeds. Thus, at Pelinu, the following weed species were encountered: *Setaria* spp., *Echinochloa crus-galli*, *Galium aparine*, *Amaranthus retroflexus*, *Chenopodium album*, *Polygonum aviculare*, *Solanum nigrum* and *Abutilon theophrasti* (Table 2). The species *P. persicaria*, *Hibiscus trionum*, *Sonchus arvensis*, *Cannabis ruderalis*, and *Sorghum halepense* were also encountered, but did not raise any control problems, due to their density of <5 plants/m^2.

Annual monocotyledons (*Setaria* and *Echinochloa*) were dominant, with a weed infestation rate of 40.5% in the control sample 40 days after treatment application. Infestation with dicotyledonous species was more homogenous, with the presence of *G. aparine* (cleavers) being notable.

Under these infestation conditions, at 40 days after the application of the treatments, Imazamox and Pendimethalin based herbicide had a good efficacy in controlling annual weeds, with the best results being obtained in the Pelinu experimental plot, obviously at higher doses of 3.4 and 4.5 l/ha (Table 2).

Table 2

The efficacy of Imazamox and Pendimethalin in soybean after 40 days of treatment (Pelinu 2021)

Experimental sample	Dose l/ha	Efficacy (% control compared to untreated check)							
		SETSS	ECHCG	GALAP	AMARE	CHEAL	POLAV	SOLNI	ABUTH
% of soil coverage at untreated		22.5%	18.0%	15.5%	11.2%	14.2%	8.7%	7.7%	7.2%
Untreated		0.0b	0.0c	0.0c	0.00d	0.00d	0.0d	0.00d	0.00c
Imazamox and Pendimethalin based herbicide	2.2	52.5a	35.0b	50.0c	50.0c	50.0c	41.2c	37.5c	53.7b
	3.4	61.2a	55.0a	82.5b	82.5b	82.5b	71.2b	62.5b	72.5ab
	4.5	75.0a	68.7a	100.0a	100.0a	100.0a	90.0a	90.0a	88.7a
LSD P =.05		21.66	15.89	29.93	15.48	15.48	17.53	20.56	19.50
Standard Deviation		13.54	9.93	18.71	9.68	9.68	10.96	12.85	12.19

For *Setaria* species, we determined a weed infestation rate >22% in the control, monitoring four species of foxtail: *S. viridis*, *S. glauca*, *S. verticilata*, and *S. faberi*. The efficacy for controlling *Setaria* species was 52% at a dose of 2.2 l/ha, 61% at a dose of 3.4 l/ha, respectively 75% at a dose of 4.5 l/ha.

For barnyard grass, the efficacy did not exceed 68.7% at the maximum dose tested. For annual dicotyledonous species, the efficacy was quite good, being lower for common knotgrass, black nightshade, and velvetleaf, especially at lower doses.

The lowest efficacy in the experimental plot at Pelinu was recorded at a dose of 2.2 l/ha, being 35.0% for *Echinochloa*, 37.5% for *Solanum*, and 43.2% for *Polygonum*, with efficacy for the other species being approximately 50%.

The following species were encountered in the experimental field at Tămădău Mare: *Polygonum convolvulus* (synonym *Fallopia convolvulus*), *C. album*, *Xanthium* species, *Viola arvensis*, *Ambrosia artemisiifolia*, *Hibiscus trionum* of the dicotyledonous class, and *Poa annua* of the monocotyledonous class. Other species with a density of <5 plants/m^2 were also found: *A. retroflexus*, *Cirsium arvense*, *S. halepense*, *Convolvulus arvensis* and *E. crus-galli*. The dominant species was *P. convolvulus*, with a weed infestation rate >40% at 40 days after treatment application in the control plot (Table 3). Black bindweed is an annual flowering plant of the *Polygonaceae* family, with rapid growth, native to Europe, Asia and North Africa, and an invasive species in North America. It coils itself around crop plants and can block harvesting equipment.

The ideal temperature for seeds to germinate is 5 °C, but they can germinate at temperatures as high as 30 °C. Four to five weeks after emergence, the stems of climbing buckwheat begin to wrap around surrounding plants. During this time, the stems grow about 1-2 cm per day, and the roots branch out more and more. Two to three weeks after emergence, climbing buckwheat is very sensitive to herbicides, which is the optimal period for applying treatments. The flowering period occurs in stages from June to September, so that this weed may produce up to 200 seeds per plant.

Table 3

The efficacy of Imazamox and Pendimethalin in soybean after 40 days of treatment (Tămădău Mare 2021)

Experimental sample	Dose l/ha	Efficacy (% control compared to untreated check)							
		POLCO	CHEAL	XANSS	VIOAR	AMBEL	HIBTR	GALAP	POAAN
% of soil coverage at untreated		40.5%	20.0%	12.0%	6.7%	8.5%	8.2%	11.2%	12.5%
Untreated		0.0 c	0.0 c	0.0 c	0.00 d	0.00 b	0.0 c	0.00 c	0.00 c
Imazamox and Pendimethalin based herbicide	2.2	23.7 b	57.5 b	40.0 c	50.0 c	60.0 a	66.2 b	51.2 b	48.7 b
	3.4	47.5 a	80.0 a	67.5 b	82.5 b	73.7 a	92.5 a	68.7 b	60.0 ab
	4.5	55.0 a	88.7 a	83.7 a	100.0 a	85.0 a	100.0 a	90.0 a	78.7 a
LSD P =.05		18.29	14.61	22.47	15.48	21.16	12.38	19.86	19.27
Standard Deviation		11.43	9.13	14.05	9.68	13.72	7.73	12.41	12.04

Under these weed infestation conditions, 40 days after treatment application, the Imazamox and Pendimethalin-based herbicide showed good efficacy in controlling annual weeds in the experimental plot at Tămădău Mare, except for the black-bindweed species, for which the efficacy at 42 days was only 23.7% at a dose of 2.2 l/ha, 47.5% at a dose of 3.4 l/ha, and 55% at a dose of 4.5 l/ha, since this weed prevailed in the experimental field.

At the maximum dose tested, the mixture of iamzamox and pendimethalin had good efficacy in controlling annual weeds: 83.7% for *Xanthium* species, 85% for *Ambrosia*, 90% for *Galium* and 100% for *Viola* and *Hibiscus*. Adequate control was also recorded for the species *P. annua*, with an efficacy of 48.7% at a dose of 2.2 l/ha, 60% at a dose of 3.4 l/ha and 78.7% at a dose of 4.5 l/ha.

In the experimental field in Borcea, the following dicotyledons were encountered: *P. persicaria, G. aparine, C. album, Fumaria officinalis, Papaver rhoeas, C. ruderalis*, *Sonchus* species and among the monocotyledons, the species *E. crus-galli* (Table 4). Annual dicotyledons predominated with a weed infestation rate of approximately 76%, 40 days after treatment application in the control sample.

Table 4

The efficacy of Imazamox and Pendimethalin in soybean after 40 days of treatment (Borcea, 2021)

Experimental sample	Dose l/ha	Efficacy (% control compared to untreated check)							
		POLPE	GALAP	CHEAL	FUMOF	PAPRH	CNIRU	SONSS	ECHCG
% of soil coverage at untreated		20.5%	12.7%	10.7%	5.5%	11.2%	8.7%	7.2%	18.2%
Untreated		0.0 c	0.0 c	0.0 d	0.00 b	0.00 c	0.0 c	0.00 c	0.00 c
Imazamox and Pendimethalin based herbicide	2.2	50.0 b	35.0 b	62.5 c	60.0 a	52.5 b	37.5 c	23.7 b	32.5 b
	3.4	66.2 a	55.0 a	90.0 a	73.7 a	73.7 ab	62.5 b	47.5 a	51.2 a
	4.5	77.5 a	68.7 a	100.0 a	85.0 a	90.0 a	76.2 a	55.0 a	61.2 a
LSD P =.05		13.34	15.89	9.33	21.16	22.78	16.66	18.28	15.71
Standard Deviation		8.34	9.93	5.83	13.72	14.24	10.41	11.43	9.82

Forty days after application, the imazamox and pendimethalin based herbicide showed good efficacy in controlling annual weeds in the experimental plot in Borcea, providing effective control of *Chenopodium*, *Fumaria* and *Papaver*, and satisfactory control of *P. persicaria* and *C. ruderalis*.

The lowest efficacy was recorded for *Sonchus* species, being 23.7% at a dose of 2.2 l/ha, 47.5% at a dose of 3.4 l/ha, and 55% at a dose of 4.5 l/ha. Weeds from the *Polygonaceae* family showed differences in sensitivity, as *Polygonum convolvulus* biotypes proved to be much more resistant to the action of Imazamox and Pendimethalin-based herbicides than P. persicaria and *P. aviculare*.

For the control of cockspurgrass, the efficacy was 32.5% at a dose of 2.2 l/ha, 51.2% at a dose of 3.4 l/ha, and 61.2% at a dose of 4.5 l/ha, with results similar to those obtained at Pelinu. The mixture of imazamox and pendimethalin proved to be very effective for controlling *Chenopodium album*, which was found in all experimental plots.

Imazamox [3-pyridinecarboxylic acid, 2-[4,5-dihydro-4-methyl-4-(1-methylethyl)-5-oxo-1H-imidazol-2-yl]-5-(methoxymethyl] - is an active substance of the chemical group of imidazolinones that is easily absorbed and taken up by the roots and leaves of weeds. Imazamox acts by inhibiting the enzyme acetohydroxyacid synthase (AHAS).

This inhibition disrupts protein synthesis and subsequently stops cell growth and division due to the lack of proteins necessary for growth, ensuring weeds demise. The chemical is absorbed through the foliage and translocated through both the xylem and phloem. Imazamox also has long residual activity, ensuring reliable protection against a new wave of weeds (*Brady et al., 1998*; *Shaner and O'Connor, 1991*; *Tan et al., 2005*; *Senseman, 2007*).

Pendimethaline [N – (I ethylpropoly) – 3,4 dimethyl – 2,6– benzamine] is an organic herbicide of the dinitroaniline class used to control annual monocotyledonous and some annual dicotyledonous weeds. It inhibits both cell division and its elongation in the root meristem.

Weed development is directly stopped as a result of absorption through the coleoptile/hypocotyl growth tips. Weeds die immediately after germination or emergence, being excluded early from competition (*Cork and Krueger, 1992*; *Smith, 2004*; *Oyeleke, 2011*; *Zain et al., 2020*; *Onwuchekwa, 2023*).

The combination of the two active substances enlarged the spectrum of weeds controlled, ensured higher levels of control, and highlighted the importance of using herbicides with different modes of action, preventing the development of resistance (*Vidal et al., 2016*).

Overall, imazamox and pendimethalin based herbicides provided good protection for soybean crops against annual weeds, with results varying depending on the cultivation technologies applied by farmers, the spectrum and intensity of weed infestation and soil and climate conditions. In general, the action of the two active substances on dicotyledons was better.

Regarding the occurring of resistance, we observed that although the *G. aparine* species was present in all experimental plots, the populations in the Borcea plot proved to be the most sensitive to the action of the two active substances.

This species is a problematic weed that has become increasingly difficult to control by herbicides, being resistant to the herbicide 2.4-D+MCPA. Several populations of *G. aparine* have shown cross-resistance to ALS-inhibiting herbicides. Some populations have been found to have developed multiple resistance to both auxin and ALS herbicides (*Nosratti and Muhammadyari, 2019*; *Papapanagiotou et al., 2019*; *Babaei and Moradi, 2025*).

Furthermore, following observations and evaluations, we once again noted the influence of the previous crop on the weed species noted in the crop. Thus, in the experimental plots at Tămădău Mare and Borcea, where the previous crops were cereals, the soybean crops were infested by some weed species characteristic of these crops: *Galium, Fumaria and Papaver.* Instead, in Pelinu, where the previous crop was corn, there were weed species that are usually found in hoeing crops: *Amaranthus, Solanum, Setaria*, etc. No phytotoxicity was recorded in experimental plots *(OEPP/EPPO Standards Bulletin, 2014).*

No yellowing, browning, deformation of plants, stunting or deficiency of soybean growth and development was observed.

Aspects from experimental field are presented in Figure 1.

Fig. 1 - Aspects from experimental field

CONCLUSIONS

Floral composition of experimental plots was diverse depending on the previous crop and the growing technology applied by the farmers, the annual weed species were found dominant.

The herbicide based on imazamox and pendimethalin, applied pre-emergence, demonstrated high efficacy in controlling annual weeds across all three experimental locations (Pelinu, Tămădău Mare, Borcea).

Timing is critical – the herbicide must be applied immediately after sowing but before crop and weed emergence to prevent early competition.

Crop rotation plays an important role, as the previous crop influences the weed flora; for example, cereal crops favor the presence of *Fumaria*, *Papaver*, and *Galium* species.

The herbicide's efficacy was dose-dependent, with the best results observed at the highest tested dose (4.5 l/ha), effectively controlling problematic species such as *C. album*, *A. retroflexus*, and *G. aparine*.

Weeds from the Polygonaceae family (e.g., *P. convolvulus*) exhibited higher tolerance to treatment, especially when dominant in the field.

Integrating chemical control with cultural and mechanical methods, where possible, can enhance the effectiveness and sustainability of weed management system

ACKNOWLEDGEMENT

This research work was carried out with the financial support of the Ministry of Agriculture and Rural Development Romania, in the frame of the national project ADER 1.4.1 (contract 141/19.07.2023) coordinated by the Agricultural Research and Development Station Turda in which the Research - Development Institute for Plant Protection, Bucharest is a partner (P1).

REFERENCES

[1] Babaei, S., Moradi, M. (2025). Evaluation of the resistance *of Galium aparine* to common herbicides in wheat fields of Western and Southwestern Iran. *Journal of Applied Research in Plant Protection, 13*(4), 373-385.

[2] Baysinger, J. A., Sims, B. D. (1991). Giant ragweed (*Ambrosia trifida*) interference in soybeans (*Glycine* max). *Weed Sci. 39*: 358–362.

[3] Berca, M. (1996). Combaterea buruienilor din culturile agricole. *Ed. Fermierul Român, București*, 178.

[4] Berca, M. (2004). Weed Integrated Management. *Ceres Publishing House*, 534.

[5] Brady, T. M., Cross, B., Doehner, R. F., Finn, J., Ladner, D. L. (1998). The discovery of imazamox, a new broad-spectrum imidazolinone herbicide. *In: Baker DR, American Chemical Society (eds) Synthesis and chemistry of agrochemicals V. ACS Symposium Series*, *NewJersey*, 30–37.

[6] Begonia, G. B., Aldrich, R. J., Salisbury, C. D. (1991). Soybean yield and yield components as influenced by canopy heights and duration of competition of velvetleaf (*Abutilon theophrasti* Medik.). *Weed Res. 31*: 117–124.

[7] Caverzan, A., Piasecki, C., Chavarria, G., Stewart Jr, C. N., Vargas, L. (2019). Defenses against ROS in crops and weeds: the effects of interference and herbicides. *International journal of molecular sciences*, *20*(5), 1086.

[8] Coble, H. D., Williams, F. M., Ritter, R. L. (1981). Common ragweed (*Ambrosia artemisiifolia*) interference in soybeans (*Glycine max*). *Weed Sci. 29:* 339–342.

[9] Coradin, J., Braz, G. B. P., Machado, F. G., Silva, A. G., Sousa, J. D. (2019). Herbicidas aplicados em pré-emergência para o controle de milho voluntário e capim-amargoso. *Revista Científica Rural*, *21*(3), 51-64.

[10] Cork, D. J., Krueger, J.P. (1992). Pesticide. *Biodegradation in Encyclopedia of Microbiology (Lederberg, J-ed), 3*: 357-36.
[11] Datta, A., Ullah, H., Tursun, N., Pornprom, T., Knezevic, S. Z., Chauhan, B. S. (2017). Managing weeds using crop competition in soybean [*Glycine max* (L.) Merr.]. *Crop protection, 95*, 60-68.
[12] Fellows, G. M., Roeth, F. W. (1992). Shattercane (*Sorghum bicolor*) interference in soybean (*Glycine max*). *Weed Sci. 40*: 68–73.
[13] Gogoi, A. K., Kalita, H., Pathak, A. K. (1991). Integrated weed management in soybean [*Glycine max* (L.) Merrill]. *Indian J. Agron. 36(3)*, 453-454.
[14] Jannink, J. K., Orf, J. H., Jordan, N. R., Shaw, R. G. (2000). Index selection for weed suppressive ability in soyabean, *Crop Science. 40(4)*, 1087-1094.
[15] Kachroo, D., Dixit, A. K., Bali, A. S. (2003). Weed management in oilseed crop - a review. *J. Res. SKUAST – Jammu, 2(1):*1-12.
[16] Lamptey, S., Yeboah, S., Sakodie, K., Berdjour, A. (2015). Growth and yield response of soybean under different weeding regimes. *Asian J. Agric. Food Sci., 3*, 153-163.
[17] Nainwal, R. C., Saxena, S. C., Singh, V. P. (2010). Effect of pre-and post-emergence herbicides on weed infestation and productivity of soybean. *Indian Journal of Weed Science, 42(1&2),* 17-20.
[18] Nosratti, I., Muhammadyari, A. (2019). First report of multiple resistance in *Galium aparine* to ALS-inhibiting and auxin analog herbicides in Kermanshah, Iran. *Planta Daninha, 37,* e019187358.
[19] Nunes, A. L., Lorenset, J. Gubiani, J. E., Santos, F. M. (2018). A Multy-Year Study Reveals the Importance of Residual Herbicides on Weed Control in Glyphosate-Resistant Soybean. *Planta Daninha*, *36*, 018176135.
[20] Kalpana, R., Velayutham, A. (2004). Effect of herbicides on weed control and yield of soybean. *Indian Journal of Weed Science, 36(1&2)*, 138-140.
[21] OEPP/EPPO Standards Bulletin 2014, PP1/135 (4) Phytotoxicity assessment. *Efficacy evaluation of plant protection products. Evaluation biologique des produits phytosanitaires, vol. 44, no. 3,* 265-273.
[22] Oliveira, M. C., Feist, D., Eskelsen, S., Scott, J. E., Knezevic, S. Z. (2017). Weed control in soybean with preemergence-and postemergence-applied herbicides. *Crop, Forage & Turfgrass Management*, *3*(1), 1-7.
[23] Onwuchekwa, H. C. B., Coe, R., Ogtrop, F. V., Roche, R., Tan, D. K. (2023). Efficacy of pendimethalin rates on barnyard grass (*Echinochloa crus-galli* (L.) Beauv) and their effect on photosynthetic performance in rice. *Agronomy, 13(2)*, 582.
[24] Oyeleke, S. B., Oyewole, O. A., Dagunduro, J. N. (2011). Effect of herbicide (pendimethalin) on soil microbial population. *J. Sci. Food Agric.*, 1, 40-43.
[25] Papapanagiotou, A. P., Damalas, C. A., Bosmali, I., Madesis, P., Menexes, G. C., Eleftherohorinos, I. G. (2019). *Galium spurium* and *G. aparine* resistance to ALS-inhibiting herbicides in northern Greece. *Planta Daninha*, *37*, e019207288.
[26] Parmar, P. S., Jain, N., Kumar, D., Solanki, R. (2016). Efficacy of different herbicides for weed control in soybean. *Indian Journal of Weed Science 48:* 453-454.
[27] Peer, F. A., Hassan, B., Lone, B. A., Qayoom, S., Ahmad, L., Khanday, B. A., Singh, G. (2013). Effect of weed control methods on yield and yield attributes of soybean. *African Journal of Agricultural Research, 8(48)*, 6135-6141.
[28] Rusu, T., Chetan, C., Bogdan, I., Chetan, F., Ignea, M., Duda, B., Bunea, G. (2014). Researches regarding weed control in soybean crop. *Bulletin UASVM, 71(1),* 50-54.
[29] Senseman, S. A. (2007). Herbicide Handbook 9th. *Ed. Lawrence, KS: Weed Science Society of America. Pp, 82*, 243-246.
[30] Senthil, A., Chinnusamy, C., Prabu, K. G., Prabhakaran, N. K. (2009). Identification of threshold level of horse purslane (*Trianthema portulacastrum*) in irrigated cowpea (*Vigna unguiculata*). *Indian J. Crop Sci. 4*: 141-143.
[31] Smith, M. A. K. (2004). Pendimethalin phytotoxicity and seedling weed control in Indian spinach (*Basella alba* L.). *Crop Prot., 23,* 201-204.
[32] Shaner, D. L., O'Connor, S. L. (1991). The imidazolinone herbicides. *In: Duke SO (ed) Herbicide resistant crops. CRC Press, Boca Raton,* 289.
[33] Sodangi, I. A., Gworgwor, N. A., Joshua, S. D. (2006). Effects of weed interference and inter-row spacing on productivity of soyabean (*Glycine Max* (L) Merril). *In Maiduguri, Nigeria. Nigerian Journal of Weed Science. 19*: 33-40.

[34] Sodangi, I. A., Gworgwor, N. A., Joshua, S. D. (2007). Effects of weed interference on narrow row soybean in a semi-arid environment. *Production Agriculture and Technology 3(2):* 117-123.

[35] Song, J. S., Chung, J. H., Lee, K. J., Kwon, J., Kim, J. W., Im, J. H., Kim, D. S. (2020). Herbicide-based weed management for soybean production in the Far Eastern region of Russia. *Agronomy, 10(11),* 1823.

[36] Tan, S., Evans, R. R., Dahmer, M. L., Singh, B. K., Shaner, D. L. (2005). Imidazolinone-tolerant crops: history, current status and future. *Pest Manage. Sci. 61*:246-257.

[37] Tehulie, N. S., Misgan, T., Awoke, T. (2021). Review on weeds and weed controlling methods in soybean (*Glycine max* L.). *Journal of Current Research in Food Science, 2(1),* 01-06.

[38] Thurlow, D. L., Buchanan, G. A. (1972). Competition of sicklepod with soybeans. *Weed Sci. 20*: 379-384.

[39] Van-Acker, R. C., Swanton, C. J., Weise S. F. (1993). The critical period for weed control in soybean (*Glycine m*ax). *Weed Sci. 41:* 194-200.

[40] Vidal, R. A., de Queiroz, A. R. S., Trezzi, M. M., & Kruse, N. D. (2016). AssociaÃ § Ã£ o de glyphosate com outros agroquÃmicos: sÃntese do conhecimento. Revista Brasileira de Herbicidas, 15(1), 39-47.

[41] Yadav, R., Bhullar, M. S., Kaur, S., Kaur, T., Jhala, A. J. (2017). Weed control in conventional soybean with pendimethalin followed by imazethapyr+imazamox/quizalofop-p-ethyl. *Canadian Journal of Plant Science*, *97*(4), 654-664.

[42] Zain, S., Dafaallah, A., Zaroug, M. (2020). Efficacy and selectivity of pendimethalin for weed control in soybean (*Glycine max* (L.) Merr.), Gezirastate, Sudan. *Agricultural Science and Practice, 7(1),* 59-68.

SAFFLOWER CULTIVATION: CHALLENGES AND PERSPECTIVES
/
CULTURA DE ȘOFRĂNEL: PROVOCĂRI ȘI PERSPECTIVE

Cătălina TUDORA*[1)], Adriana MUSCALU[1)], Marga GRĂDILĂ[2)], Oana MÎRZAN[3)], Florentina GATEA[4)]
[1)] Testing Department, National Institute of Research-Development for Machines and Installations Designed for Agriculture and Food Industry - INMA Bucharest, 6 Ion Ionescu de la Brad Blvd, District 1, 013813, Bucharest / Romania;
[2)] Research - Development Institute for Plant Protection - ICDPP, Bucharest / Romania;
[3)] Agricultural Research and Development Station Secuieni, Neamt County / Romania;
[4)] National Institute for Biological Sciences, 296, Splaiul Independentei, 060031 Bucharest / Romania.
**Tel: 0726 274 958; *E-mail: cmc_tudora@yahoo.com*

Keywords: *Safflower, cultivation technology, challenges, perspectives.*

ABSTRACT
Safflower (Carthamus tinctorius L., fam. Asteraceae) is cultivated due to its high adaptability to arid regions with low rainfall. Compared to other oilseed crops (rapeseed, sunflower, soybean, etc.), it shows good tolerance to cold, which makes it suitable for cultivation in various climatic zones. Safflower is mainly grown for its seeds, from which high-quality vegetable oil is extracted, and for its flower petals, which are used as a substitute for Saffron. This paper aims to present the main challenges as well as the perspectives for this crop. The challenges include aspects such as limited knowledge related to this plant, the cultivation technology adapted to different regions, and several economic issues. The perspectives for this valuable crop consider its multifunctional uses, the high added value represented by the nutritious oil and petals, and its applications in various industries (food, cosmetics, textiles, etc.).

REZUMAT
Șofrănelul (Carthamus tinctorius L., fam. Asteraceae), este cultivat datorită adaptabilității sale ridicate la regiunile aride, cu precipitații scăzute. În comparație cu alte culturi de oleaginoase (rapiță, floarea-soarelui, soia, etc.) are o rezistență bună la frig, ceea ce îl face potrivit pentru cultivare în diverse zone climatice. Cultura de Șofrănel este predominantă pentru semințe, din care se obține un ulei vegetal de calitate și pentru petalele florilor, care sunt utilizate ca înlocuitor al Șofranului. Lucrarea își propune prezentarea principalelor provocări dar și perspectivele pentru această cultură. Provocările includ aspecte privind: cunoștințele limitate legate de această plantă, tehnologia de cultură adaptată diferitelor regiuni, dar și o serie de aspecte economice. Perspectivele acestei culturi valoroase țin cont de: utilizarea multifuncțională a acesteia, valoarea adăugată ridicată reprezentată de uleiul nutritiv și de petale, de utilizările sale în diferite industrii (alimentară, cosmetică, textilă, etc.).

INTRODUCTION

Safflower (*Carthamus tinctorius* L., fam. *Asteraceae*) is an annual herbaceous plant, native to India, cultivated for its achenes, rich in oil (37 - 42%). The cultivation of this plant is underutilized, however, it has gained attention due to its ability to grow under high temperatures, drought, and salinity conditions, as well as its potential to produce high-quality oil. Salinity and drought have negative effects by disrupting the ionic and osmotic balance of plant cells.

The stress signal is perceived by membranes and then transduced into the cell to activate stress-responsive genes (*Hussain, M. I. et al, 2016*). The plant is adaptable to various conditions and can be cultivated in semi-arid areas where other crops fail, which makes it even more attractive for cultivation in the context of water scarcity and the challenges related to global warming (*Erbas and Mutlucan, 2023*).

The plant grows alongside wheat and barley in temperate regions, but it develops slowly during periods with short and cold days, while being tolerant to low temperatures (up to frost), with resistance varying among species varieties. Safflower is a long-day plant, requiring a photoperiod of 14 hours. It is intolerant to shade and weed infestation, with good tolerance to salts similar to cotton, but lower than that of barley. It develops well on loamy soils with high water-holding capacity, although heavy sandy soils are also suitable for safflower. It can be successfully introduced in crop rotation immediately after rice, as the soil remains saturated in depth with water resulting from rice irrigation. Safflower is recommended for cultivation in areas where the average annual precipitation is below 430 mm (*Askın and Erbas, 2020*). Regarding

moisture, in the early growth stages safflower is tolerant to high humidity and frequent rainfall. However, after flowering, a period of persistent rain and fog may facilitate infection with *Botrytis* (no resistant varieties are available). Excessive humidity can also facilitate the occurrence of alternaria leaf spot. Safflower grows optimally in regions with rainy and warm springs, followed by long, dry summers. Strong winds do not damage the yield, as the seeds are very resistant to shattering.

Safflower is generally able to withstand temperatures of -4 °C, although some lines tolerate field conditions as low as -7 °C. Experimentally, seeds buried at 10 cm depth resisted a two-week freezing period at -24 °C. During summer, temperatures of 43 °C do not pose problems for safflower, even under prolonged drought conditions. However, young plants, just at the beginning of vegetation, are sensitive to sudden temperature fluctuations, and subzero temperatures affect them. Increased humidity is required at this stage, when plants are also highly sensitive to weed competition.

The plant presents a series of economic benefits: due to its high content of oleic acid and linoleic acid, safflower oil is considered to be of high quality. The oil cakes obtained after oil extraction have a high protein content and are used in animal feed. The oil extracted from safflower seeds has a growing market demand, due to its applications in the food, pharmaceutical, and cosmetic industries, being an oil with high added value.

The flowers are used for obtaining food colorants or in the pharmaceutical industry, as the petals are rich in chalcone-type pigments (yellow and red), with applications in the food, textile, cosmetic, and pharmaceutical industries. Therefore, the plant is of particular interest as an alternative source that could ensure the production of food colorants. Recent studies (*Savcenco A., 2024*) have shown that there are problems in the use of synthetic colorants, and their consumption negatively affects the health status of the population, raising concerns regarding food safety.

The disadvantage of using synthetic colorants lies in their toxicological properties, since being synthetically produced, many of them contain residues of toxic elements (Pb, As, Cu, Cd, Se, U, Hg) or organic compounds (solvents, aromatic hydrocarbons, etc.).

In our country, the plant is included among the species with a “large biodiversity portfolio,” but it remains underutilized for commercial cultivation. Safflower offers a viable agricultural alternative to sunflower cultivation, being well adapted to growth on marginal lands. Its tolerance to water availability differentiates safflower from other oilseed species (such as sunflower and especially rapeseed), which require a constant water supply (*Ivan and Tudora, 2014; Nasiyev et al., 2022*).

Although the crop is less demanding in terms of soil quality and performs well on poorer soils and in humid areas, the plant is still not cultivated and valorized to the same extent as sunflower. Since this species is naturally well adapted to dry and warm conditions, it can be cultivated in the southern and south-eastern regions of the country. It is worth mentioning that within the “*biodiversity heritage*” of Romania, the “*wild relative*” of cultivated safflower, *Carthamus lanatus* L., can be found in spontaneous flora. Safflower is a crop with agricultural and economic potential, but it requires careful consideration of the challenges and appropriate management in order to fully exploit its perspectives, especially in the context of climate change and the continuously increasing demand for natural products.

To maximize the benefits of this crop, a strategic approach is needed, taking into account local conditions and new cultivation technologies, with the aim of improving disease resistance, adaptation to climatic conditions, and crop yield. Despite the fact that safflower could become a valuable plant for the country’s agriculture and economy, domestic studies on the chemical composition of different parts of the plant and on processing methods into commercial products have not yet been carried out.

MATERIALS AND METHODS

Under the climatic conditions of our country, safflower is sown early in spring, at the beginning of march, after completing soil preparation works (plowing, harrowing, and leveling). For sowing, the soil should be moist (down to a depth of 10 cm), with a minimum temperature of 4 °C. Any seed drill for small grains can be used for sowing, and if necessary, the seeds may be mixed with sand or sawdust to ensure homogeneous distribution in the field, after which they are incorporated into the soil at a depth of 2.5 - 5 cm.

The seeding rate is 23 kg/ha (with a density of 6 - 7 plants/m²) under non-irrigated conditions, and between 23 - 27 kg/ha (with a density of up to 10 plants/m²) under irrigation systems. Fertilization requirements depend on the soil. When cultivated on poor soils or under irrigated conditions, it is advisable to apply nitrogen fertilizers (urea 135 kg/ha). Crop maintenance consists of harrowing, carried out across the rows immediately after plant emergence. The safflower crop is parasitized by many weeds (*Orobanche* sp.,

Striga sp., etc.); among viral diseases, it is attacked by *Chilli mosaic* virus and *Cucumber mosaic* virus, while among bacterial diseases, by *Pseudomonas solanacearum*. In our country, *Zamfirescu, N., et al.* describe safflower rust, caused by the fungus *Puccinia carthami*, as a frequent disease, manifesting at different stages of plant development. The disease appears on leaves in the form of small brown-silver pustules. These begin to dry out, and the plants cease growing. Control measures include rational crop rotations, destruction of infected plants, and deep plowing. Among insects, the darkling beetle (*Opatrum sabulosum*) attacks safflower crops. This coleopteran appears in spring, feeding on the edges of cotyledons and later damaging the stems. In crop rotation, safflower can be introduced after barley or rice, as well as after other cereals. When sown immediately after rice, in addition to nitrogen fertilizers it is advisable to apply phosphorus fertilizers (19 - 34 kg/ha), placed near the seeds rather than broadcast, since phosphorus has low mobility in the soil. Crop rotation is mandatory, as the risk of disease occurrence is high.

According to some authors (*Baltensperger, D., et al., 2002*), it is also recommended to implement a fallow period on the same plot immediately after safflower cultivation, since it is considered that due to the plant residue left on the field after harvest and the high extraction capacity of the root system, the soil may become depleted. Other researchers (*Zamfirescu, N., et al., 1958*) do not mention such a negative impact of safflower cultivation on subsequent crops grown on the same plot. It is recommended that safflower should not alternate on the same plot with mustard, sunflower, or beans, due to the increased risk of *Sclerotinia* sp. occurrence. Safflower reaches maturity 110 - 150 days after sowing, and harvesting is carried out when the leaves are dry. An advantage of this crop is that it does not shatter its seeds, nor are they eaten by birds. These are two of the reasons why *Bîlteanu, Gh., et al., 1991*, recommended its cultivation in Romania.

Harvesting is done mechanically with a combine; the cylinder speed should be set at 550 rpm, and the forward speed should be 25% faster than the ground speed. For storage, the maximum allowable moisture content in silos is 8%. The oil percentage for a premium seed stock is at least 34 - 36%. No foreign matter is accepted. Yields range from 800 to 4000 kg/ha.

RESULTS

At the global level, the cultivated area of safflower in 2023 (Fig. 1) was 910,848 ha (*FAOSTAT, 2023*), with an estimated global production of 723,874.9 t (*FAOSTAT, 2023*). The global production of safflower oil in 2022 was 75,060.94 t (Fig. 2).

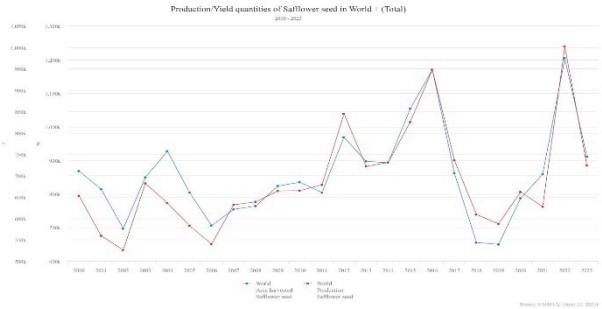

Fig. 1 - Production and yield of safflower seed worldwide (2000-2023)

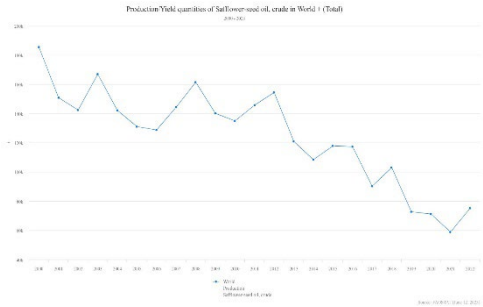

Fig. 2 - Production and yield of crude safflower seed oil worldwide (2000-2023)

With regard to safflower seed and oil production, distributed across the world regions, these are presented in Figures 3 and 4.

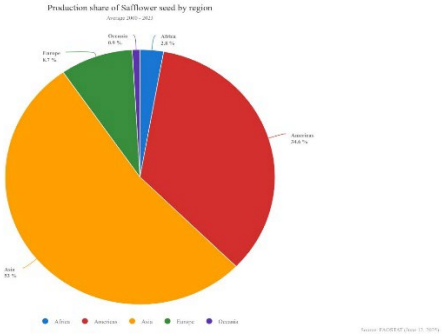

Fig. 3 - Regional production share of safflower seed *(FAOSTAT, 2023)*

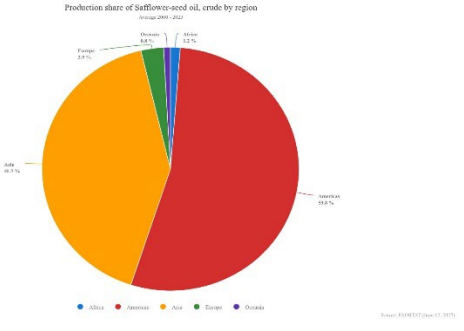

Fig. 4 - Regional production share of crude safflower seed oil (2000-2023)

According to FAO data, the regional distribution of total seed production (Fig. 3) was as follows: Asia with 363,635.2 t, representing 53% of total seed production; America with 237,281.4 t (34.6%); Europe with 59,785.48 t (8.7%); Africa with 19,287.02 t (2.8%); and Oceania with 6,018.27 t (0.9%).

Similarly, the situation regarding safflower oil production by region (Fig. 4) is as follows: America with 66,931.29 t, representing 53.8% of total oil production, followed by Asia with 51,404.15 t (41.3%); Europe with 3,561.96 t (2.9%); Africa with 1,512.99 t (1.2%); and Oceania with 1,049.66 t (0.8%).

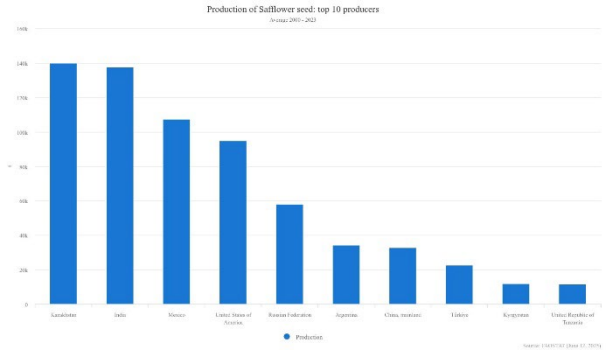

Fig. 5 - Top 10 safflower seed producers *(FAOSTAT, 2023)*

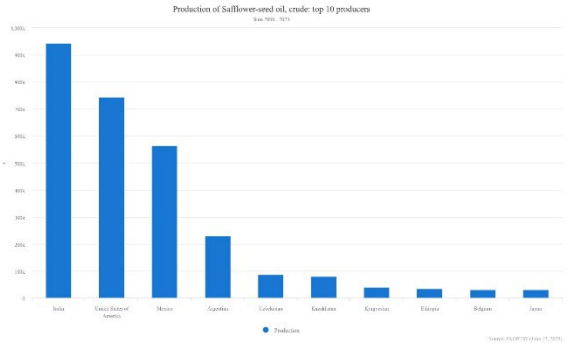

Fig. 6 - Top 10 crude safflower seed oil producers (2000-2023)

The ranking of the top 10 safflower seed-producing countries is presented in Figure 5 and is as follows: Kazakhstan with a seed production of 140,000.8 t, followed by India with 137,735.5 t, and Mexico with 107,476.4 t. The ranking is completed by the USA (95,088.75 t), Russia (58,058.82 t), Argentina (34,270.42 t), China (32,724.74 t), and Turkey (22,625.13 t). In Turkey, according to the study conducted by *Akgun, M.,and Soylemez, E.* in *2022*, it is projected that in the following five years (2022–2026), the cultivated areas of safflower as well as the annual seed quantities will decrease, on average by 515 t, while producer prices will increase by 20% per year.

Nevertheless, production yield is expected to increase by 2.5% by the end of the five-year period. As possible solutions to prevent the decrease of safflower cultivated areas and to increase production, the authors recommend providing purchase guarantees for producers, supporting entrepreneurs, and conducting studies on modern cultivation practices, marketing, and promotion.

At the global level, the top 10 safflower oil-producing countries (Fig. 6) are: India with 41,043.48 t, followed by the USA with 32,353.91 t, and Mexico with 24,556.33 t. The ranking of safflower oil-producing countries is completed by Argentina (10,021.05 t), Kyrgyzstan (4,918.91 t), Japan (3,912.5 t), Uzbekistan (3,754.57 t), Kazakhstan (3,504.09 t), Ethiopia (1,506.68 t), and Belgium (1,368.48 t). General market estimates, according to market reports (e.g., Market Research Future, IMARC), show that the global safflower oil market is valued at over USD 300 million, with an estimated annual growth rate of between 5-7%. Demand is concentrated in the USA, India, China, and EU countries (Germany, France, the Netherlands). The price is variable on international markets and depends on quality, origin, and processing methods.

The Situation in Romania - The interest in drought-resistant crops in the context of climate change brings safflower into the focus of both European and Romanian farmers. The crop is still relatively little known and not widely used, which provides an advantage. Romania has favorable soil and climatic conditions for safflower cultivation (continental, drought-prone zone). In the country, safflower is cultivated on small areas, mainly in plains and hilly regions where climatic conditions are favorable. Precise data on cultivated areas and annual production are not centralized at the national level, but interest in this crop has increased due to demand from the food, cosmetic, and pharmaceutical industries. In Romania, the price of dried flowers may vary between 100 and 200 lei/kg, depending on quality and demand.

Development Perspectives - In Romania, there is a growing interest in crop diversification and in harnessing the economic potential of safflower. Support from authorities and agricultural organizations can stimulate the development of this crop, contributing to increased farmers' incomes and to the promotion of a sustainable agricultural model.

The market potential of safflower ("false saffron") is increasing globally, due to its multiple applications in industries such as food, cosmetics, alternative medicine, and biofuels. There is also an export potential toward Western European markets, where the demand for natural ingredients is higher. However, at the national level, there are several *challenges* related to:

- a still undeveloped local market, requiring the promotion and education of both consumers and processors;
- the lack of seed processing infrastructure for oil extraction in Romania;
- difficult access to external markets without certifications (e.g., BIO, Fair Trade).

The challenges include cultivation for oil, natural colorant, and medicinal properties, as well as drought resistance, resistance to diseases and pests, competition with other crops, and adaptation to various climatic conditions. The perspectives are based on its nutritious oil and its diverse uses in the food and cosmetic industries.

The *challenges* faced by safflower cultivation include:

Climate and soil – The plant is drought-tolerant, but this may affect yield in certain regions, particularly during prolonged drought periods. It requires a warm and dry climate, but is sensitive in the germination stage. Soil quality (it prefers well-drained soils) significantly influences yield. Although drought-tolerant, safflower can be sensitive to extreme temperatures, and the selection of suitable varieties for different climatic zones may be difficult. Competition with other crops – Safflower may compete with other crops, especially in areas with low-quality soils, requiring proper soil and weed management.

Pesticide-related concerns (susceptibility to diseases and pests) – Safflower is vulnerable to various diseases and pests (mold, fusarium, rust, aphids, etc.), which can lead to yield losses and additional costs for treatments, with a negative environmental impact. Cultivation technology – There is a need for technologies adapted to temperate zones, and to maximize crop yield it is necessary to apply appropriate cultivation techniques (irrigation during critical periods, fertilization, etc.), as well as the use of specialized seed drills and harvesting equipment.

The harvesting process can be more complex and labor-intensive compared to other crops, and in some case it is carried out manually. Another challenge is the lack of certified, high-quality seeds available on the market. Economic aspect – Production costs may be higher in the case of safflower cultivation, and the selling price of products can fluctuate. Harvesting costs are also higher compared to other oilseed crops, while the marketing network remains underdeveloped, especially in Eastern Europe. The fluctuating market price of safflower oil may be volatile due to international supply and demand, and profitability can be affected by price fluctuations. Promotion and development of short supply chains are required.

Limited knowledge related to this plant – There is a lack of research and in-depth studies (investments in agricultural research), insufficient support through agricultural policies, and limited development of processing and value chains, while farmers are not familiar with the advantages and cultivation practices.

The *perspectives* for this valuable plant are as follows:

Sustainability and durability – The crop is drought-resistant, making it ideal for sustainable agriculture, representing a viable alternative to sunflower cultivation in areas affected by climate change.

Integration into organic agriculture – The plant can be cultivated in organic farming systems, without the intensive use of pesticides and chemical fertilizers, which attracts consumers concerned with health and the environment. It requires less water compared to other crops, being suitable for semi-arid regions. Moreover, it can be included in diverse crop rotations, improving soil fertility.

Economic potential of this crop – The global demand for natural and organic products is increasing, creating opportunities for the development of niche products (cold-pressed oil, natural colorants, dietary supplements). From safflower flowers, products based on natural colorants (carthamin) or dietary supplements can be obtained, which may provide farmers with additional income. High added value – The growing demand for safflower oil, considered healthier than other vegetable oils due to its high content of unsaturated fatty acids, rich in linoleic acid (Omega-6) and conjugated linoleic acid (CLA), contributes to its use in various food products (margarine, cooking oils, dietary supplements, etc.).

It is also used in the cosmetic industry, where oil extracted from safflower seeds is an ingredient in creams, lotions, and other cosmetic products (skin and hair care), due to its moisturizing, emollient, and antioxidant properties.

Competition with other crops – In some regions, farmers may choose to cultivate traditional, more profitable plants (sunflower, soybean), which can reduce the land available for safflower cultivation.

Establishment of crops for obtaining a natural colorant – From safflower flowers, a natural colorant (carthamin) is obtained, used in the food and textile industries as an alternative to synthetic colorants.

Medicinal properties – Safflower flowers have vasodilatory, antioxidant, anti-inflammatory, and anti-aggregating properties, being used in the treatment of cardiovascular diseases, hypertension, and rheumatic pain.

Uses in the textile industry – Safflower oil can be used in the production of certain types of varnishes and paints, as well as in the textile industry.

Feed and biomass – Residues can be used in animal feed or for the production of biofuels.

Price fluctuations on external markets – Safflower cultivation depends heavily on external markets (especially for oil), and global price fluctuations or a decrease in demand may endanger the profitability of the crop.

Supply chain issues – Although demand is increasing, in some regions there may be a lack of infrastructure necessary for the processing and distribution of safflower oil, which can lead to economic losses.

CONCLUSIONS

Safflower cultivation can represent a profitable and environmentally friendly opportunity, considering its advantages under drought conditions and the increasing demand for derived products obtained from this plant. However, in order to harness this potential, farmers must take into account the risks related to diseases, pests, and market instability. The implementation of modern agricultural practices and the use of appropriate technologies can contribute to the long-term success of this crop.

ACKNOWLEDGEMENT

This work was supported by the NUCLEU Programme, carried out with the support of ANCSI, **Contr. 9N/01.01.2023**, **Project PN 23 04 02 05** - "***Innovative technology for the superior utilization of inflorescences and seeds of medicinal plants***".

REFERENCES

[1] Akgun, M., Soylemez, E. (2022). Determining the Future Trends of Safflower Plant in Türkiye. *International Journal of Agriculture, Environment and Food Sciences*, 6 (1), 50-57. https://doi.org/10.31015/jaefs.2022.1.8

[2] Askın, E., Erbas, S. (2020). Superior lines for agro-technological traits in Safflower (*Carthamus tinctorius L.*). *Turkish Journal of Field Crops*, 25(1), 50-56. https://doi.org/10.17557/tjfc.737511

[3] Baltensperger, D., Frickel, G., Lyon, D., Krall, J., Nightingale, T. (2002). Safflower management and adaptation for the high plains. Reprinted from: *Trends in new crops and new uses*. J. Janick, J., Whipkey, A. (eds.). ASHS Press, Alexandria, VA.

[4] Bîlteanu, Gh., Salontai, Al., Vasilică, C., Bîrnaure, V., Borcean, I. (1991). *Phytotechnics*. Didactic and Pedagogical Publishing House, Bucharest.

[5] Erbas, S., Mutlucan, M. (2023). Investigation of flower yield and quality in different color Safflower Genotypes. *Agronomy*, 13(4), 956-977. https://doi.org/10.3390/agronomy13040956

[6] Hussain, M. I., Lyra, D. A., Farooq, M., Nikoloudakis, N., Khalid N. (2016). Salt and drought stresses in safflower: a review. *Agronomy for Sustainable Development,* 36 (4). https://doi.org/10.1007/s13593-015-0344-8

[7] Ivan, Gh., Tudora, C. (2014). Evaluation of Safflower culture (Carthamus tinctorius) as a forage alternative for Sunflower culture (Helianthus annuus) in the arid areas of Southern Romania. *Annals of the University of Craiova - Agriculture, Montanology, Cadastre Series*, XLIV, pp. 127-132.

[8] Nasiyev, B., Bushnev, A., Zhanatalapov, N., Bekkaliyev, A., Zhylkybay, A., Vassilina, T., Shibaikin, V., Tuktarov, R. (2022). Initiation of safflower sowings in the organic farming system of Western Kazakhstan. *OCL*, 29 (21). https://doi.org/10.1051/ocl/2022015

[9] Savcenco, A. (2024). Extraction and Use of Natural Colorants from Safflower *(Carthamus tinctorius L.)* Petals in Food Product Technology – PhD Thesis. Technical University of Moldova, Chișinău.

[10] Zamfirescu, N., Velican, V., Saulescu, N., Valuta, Gh., Cantir, F. (1957) - Phytotechnics. State Agro-Silvic Publishing House.

[11] *** "Production yearbook", Food and Agriculture Organization of the United Nations (FAOSTAT 2023). World Production of Safflower. Available online: http://www.fao.org/faostat/en/#data/QC (accessed on June 2025).

AERODYNAMIC RESPONSE OF PEPPER SEEDS TO VARYING MOISTURE LEVELS: A BASIS FOR OPTIMIZING PNEUMATIC HANDLING AND SEED DISPERSAL

/

BIBER TOHUMLARININ DEĞIŞEN NEM SEVIYELERINE AERODINAMIK TEPKISI: PNÖMATIK TAŞIMA VE TOHUM DAĞITIMINI OPTIMIZE ETMEK İÇIN BIR TEMEL

Onder KABAS*[1)], K.Cagatay SELVI[2)]

[1)] Department of Machine, Technical Science Vocational School, Akdeniz University, 07070 Antalya / Turkey;

[2)] Department of Agriculture Machinery and Technologies Engineering, Faculty of Agriculture, Ondokuz Mayıs University, 55139 Samsun / Turkey.

*Tel: +90 242 3106700; *E-mail: okabas@akdeniz.edu.tr*

Keywords: *terminal velocity, drag coefficient, lift force, projection area*

ABSTRACT

This study investigates the effect of moisture content on the aerodynamic properties of pepper (Capsicum spp.) seeds to improve seed processing and transportation efficiency in agricultural operations. The experiments were conducted at four different moisture levels (5.4%, 8.6%, 12.1%, and 15.4%) and analyzed using a data set consisting of 100 pepper seeds in terms of drag coefficient, terminal velocity, lift coefficient, Reynolds number, projected area, mass, bulk density, and shape factor. The measurements of aerodynamic properties were carried out under controlled conditions and the data were evaluated by one-way ANOVA and Duncan test to evaluate the differences among moisture levels. The results revealed that moisture significantly affected the mass, bulk density, drag coefficient and final velocity, while higher moisture increased the mass and density, decreased the drag coefficient and increased the terminal velocity, probably due to changing surface roughness and water absorption. In contrast, lift coefficient, Reynolds number, surface area and shape factor remained constant, indicating consistent seed geometry and airflow properties. These findings highlight the critical role of moisture in regulating the physical and aerodynamic behavior of the seed, providing insights to optimize seed processing, storage, and pneumatic separation processes. By explaining moisture-driven changes, this study supports the development of specialized seed technologies that increase agricultural productivity and sustainability under diverse climatic conditions.

ÖZET

Bu çalışmada, tarımsal işlemlerde tohum işleme ve taşıma verimliliğini artırmak amacıyla, nem içeriğinin biber (Capsicum spp.) tohumlarının aerodinamik özellikleri üzerindeki etkisi araştırılmıştır. Deneyler dört farklı nem seviyesinde (%5,4, %8,6, %12,1 ve %15,4) yürütülmüş ve 100 biber tohumundan oluşan bir veri seti kullanılarak; sürükleme katsayısı, terminal hız, kaldırma katsayısı, Reynolds sayısı, yansıtılmış alan, kütle, yığın yoğunluğu ve şekil faktörü açısından analiz gerçekleştirilmiştir. Aerodinamik özelliklerin ölçümleri kontrollü koşullar altında yapılmış ve veriler, nem seviyeleri arasındaki farklılıkları değerlendirmek amacıyla tek yönlü ANOVA ve Duncan testi ile analiz edilmiştir. Sonuçlar; nemin kütle, yığın yoğunluğu, sürükleme katsayısı ve terminal hızı anlamlı düzeyde etkilediğini, daha yüksek nemin kütle ve yoğunluğu artırırken, sürükleme katsayısını azalttığını ve muhtemelen yüzey pürüzlülüğü ile su emilimindeki değişikliklerden dolayı terminal hızı artırdığını ortaya koymuştur. Buna karşılık; kaldırma katsayısı, Reynolds sayısı, yüzey alanı ve şekil faktörü sabit kalmış, bu da tohum geometrisi ve hava akışı özelliklerinin tutarlılığını göstermiştir. Elde edilen bulgular, tohumun fiziksel ve aerodinamik davranışını düzenlemede nemin kritik rolünü vurgulamakta; tohum işleme, depolama ve pnömatik ayırma süreçlerini optimize etmek için önemli içgörüler sunmaktadır. Bu çalışma, nem kaynaklı değişiklikleri açıklayarak, farklı iklim koşullarında tarımsal üretkenlik ve sürdürülebilirliği artırmaya yönelik özel tohum teknolojilerinin geliştirilmesine katkı sağlamaktadır.

INTRODUCTION

The assessment of the physical and engineering attributes of agricultural crops is of paramount significance for the optimization of design parameters pertaining to agricultural machinery and equipment utilized in the processes of production, handling, and storage. Consequently, it is imperative to establish a comprehensive database encompassing the aerodynamic and mechanical characteristics of such products,

as these attributes are crucial in the design and development of specialized machines and their operational functionalities, including sorting, separating, and cleaning *(Kabas and Özmerzi, 2018).*

The understanding of aerodynamic behavior such as the parameters of drag force, terminal velocity, drag coefficient, and Reynolds number is crucial for operations related to the movement of air, such as pneumatic conveying, separation, cleaning, harvesting, and the drying of agricultural commodities.

The terminal velocity at the top of which particles are suspended due to a stationary vertical airflow can be measured through several testing methods. These methods consist of the free-fall, air tunnel, and elutriation techniques *(Mohsenin, N.N. 1980; Grift, T.E. et al, 1997).*

The terminal velocity of grains can be calculated from both the empirical laboratory studies and the theoretical formulas. Various ways have been devised to estimate the theoretical terminal velocity of grains *(Gorial and O'Callaghan, 1990; Song and Litchfield, 1991).* When pneumatically conveying and separating different particles in an air stream, the particle behavior is significantly affected by their aerodynamics.

During relative motion between air and materials, the aerodynamic forces acting vary in accordance with the different particles. In a vertical air stream, particle separation is achievable if only a range of particle sizes is there such that the lighter materials are carried along with the air stream and the heavy ones fall off.

When an air stream is the technology used for separating a product like lentil seed from its related matters, for example straw and chaff, it is required to have the idea about the aerodynamic characteristics of all the particles involved.

This will determine the suitable air velocities for the efficient separation of the grain from the foreign materials. As a result, the terminal velocity of the particles has been adopted as a key aerodynamic characteristic for materials during pneumatic conveying and separation from foreign materials *(Mohsenin, N.N. 1980).*

Researchers have previously conducted various studies to determine the aerodynamic properties of different cereals and seeds. *Abubakar, A.J. et al. (2019)* developed a measuring device to determine the terminal velocities of rice, sorghum and bean grains; the values of 6.95 ± 0.37 m/s, 4.71 ± 0.24 m/s and 10.98 ± 0.27 m/s were obtained, respectively.

It is known that moisture content directly and positively affects grain terminal velocity; this has also been observed in crambe *(Cardoso Neto, S.R. et al, 2020)* and cereal sorghum *(Rodrigues, G.B. et al, 2019).* However, there is limited information on this subject for quinoa.

Badr and Eissa (2018) determined the terminal velocity of quinoa grains at only 11.6% moisture content and reported high variability in sphericity, geometric diameter and surface area values. *Ibrahim, M.M. et al. (2023)* stated that no significant change was observed in the physical properties of palm pollen grains in the 4–7% moisture range, but aerodynamic properties, especially the Reynolds number ranging from 0.29–0.42 and the average terminal speed of 0.6 m/s, made significant contributions to increasing the efficiency of pollination machines. *Caetano, J.M. et al. (2022) examined* the aerodynamic properties of two quinoa varieties in the 12.1–19.5% moisture range; they determined that the terminal speed varied between 2.57–3.26 m/s, the drag coefficient varied between 1.42–2.77, and the moisture content positively affected the Reynolds number.

The aim of this study is to investigate the physical and aerodynamic properties of bell pepper seeds in detail depending on different moisture contents (5.4%, 8.6%, 12.1% and 15.4%). In this context, the drag coefficient, terminal velocity, lift coefficient, Reynolds number, surface area, mass, bulk density and shape factor of the seeds were determined, the effect of moisture content on these parameters was evaluated and the usability of the obtained data in the design and optimization of agricultural mechanization systems was revealed.

MATERIALS AND METHODS

The experiments were carried out in the laboratories of Akdeniz University Technical Sciences Vocational School. The bell pepper seeds used in the study were obtained from "Balo" type bell peppers grown in producer greenhouses in the Antalya region. 100 seeds were randomly selected from these peppers and numbered to prevent repetition of measurements (Figure 1).

After the seeds were obtained, they were stored in plastic bags at 5 ± 1 °C for seven days until the beginning of the experiment in order to preserve their original characteristics. In addition, the seed samples were manually cleaned using a sieve to remove foreign substances and then mixed to obtain a homogeneous structure.

Fig. 1 - "Balo" bell pepper seeds

The dry mass was obtained by the preparation of the samples before the addition of the water content suggested *(Vilche, C. et al, 2003).* The quantity of water added to the samples using a manual spray and calculated based on the initial moisture content.

The samples returned to the plastic bags and were kept under 4 ± 1 °C for eight days to achieve moisture equilibrium, *according to Caetano, J.M. et al. (2022).* The moisture contents established for this study were: 5.4%, 8.6%, 12.1% and 15.4% %d.b. The drying method was used to measure the moisture content of the grains, which was done for 24 hours at 105 °C in a hot air oven. In accordance with the guidelines of Seed Analysis, this process was carried out three times *(Jimoh, K.A. et al., 2023*).

The ratio of a single grain mass to its volume was used to calculate the bulk density (ρ_p, kg m^{-3}). Grain volume was computed as the product of grain thickness and surface area, as suggested by *Mohsenin, N.N. (1980), Kabas, O. et al. (2007) and Singh, S.K. et al, (2021).* A digital calliper with a resolution of 0.01 mm was used to measure the length, width and thickness of the grain.

Each sample had four replications and consisted of 100 randomly selected grains for each moisture content value. The grains were weighed on a digital scale with a precision of 0.001 g prior to the measurements of dimensions. The weight was divided by the number of grains to determine the unitary grain mass indirectly.

The projection area (A_p) of the pepper seeds was determined using ImageJ (NIH, USA) software. Digital images of the seeds placed on the surface taken from a vertical angle were analysed. Scale reference was used for calibration, and the projection area (mm^2) was automatically calculated by determining the seed contours with the thresholding method *(Ermiş, S. et al, 2025).*

A radial fan powered by a 1.5 kW electric motor was used to create the air flow. The air generated by this fan is transmitted to the pressure chamber with dimensions of 600 x 600 x 400 mm through a 200 mm diameter channel. To examine the movement of the material in the air, a transparent test channel with a diameter of 80 mm was placed in the air outlet channel and experiments were carried out using the air channel equipped with a grid that homogenizes the air flow (Figure 2).

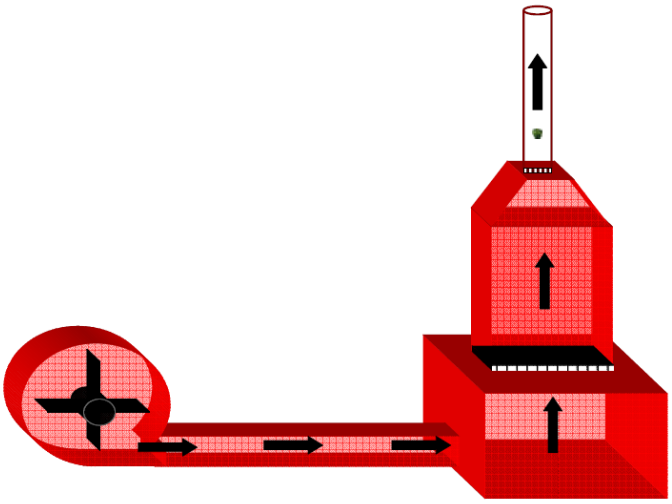

Fig. 2 - Layout of the equipment used to determine experimentally terminal velocity of pepper seeds

For the terminal velocity determination, a randomly selected pepper seed sample was placed in the center of the grid. The air flow was gradually increased until the product began to float. When the lowest rotational motion of the grains was obtained, the air velocity was measured using a digital anemometer centered at the top of the column.

The friction coefficient was calculated using the following equation, which was obtained using the terminal speed equation of *Mohsenin, N.N. (1980) and Kabas and Ozmerzi (2018).*

$$C=(2.m.g.(\rho_p-\rho_f)) / (V.\rho_p.\rho_f.A_p) \quad (1)$$

where: C is the drag coefficient (dimensionless), m is the grain mass (kg), g is the gravity acceleration (9.81 m s^{-2}), ρp is the grain density (kg m^{-3}), ρf is the air density (1.293 kg m^{-3}), V is the terminal velocity (m s^{-1}), and A_p is the grain projected area, normal to its movement in relation to the fluid (m^2). The Reynolds number was calculated using the following equation, which also includes the terminal velocity *(Mohsenin, N.N. 1980; Gojiya, D. et al., 2023).*

$$R_e=(V.D_g.\rho_f) / \mu \quad (2)$$

where: R_e is the Reynolds number (dimensionless), ρ_f is the air density (1.293 kg m^{-3}), V is the terminal velocity (m s^{-1}), D_g is the grain average geometric diameter (m), and μ is the air viscosity ($1.816.10^{-5}$ N s m^{-2}, by 20°C).

The lift coefficient was determined in a wind tunnel at 25°C with airflow velocities of 2–5 m s^{-1} *(Shaha and Pachapuri 2015).*

$$Cl=F_L / (1/2\ \rho_f.V^2.A_p) \quad (3)$$

The lift force (F_L) was calculated indirectly using the relationship F_L=m.g.sinθ where m is the seed mass (measured gravimetrically), g is gravitational acceleration (9.81 m s^{-2}), and θ is the angle of seed orientation relative to airflow, determined from high-resolution digital images (12 MP, 0.1 mm/pixel) captured during suspension in the wind tunnel. Air density (ρ_p) was set at 1.293 kg m^{-3}, airflow velocity (V) was controlled, and the seed's projected surface area (A_p) perpendicular to airflow was measured using ImageJ software.

To assess seed geometry, shape factors (SF) was calculated using the following method and equations (Kaliniewicz, Z. et al. 2022). Seeds were photographed using a high-resolution digital camera (12 MP, 0.1 mm/pixel) against a calibrated grid.

$$SF=d_e/d_{max} \quad (4)$$

The equivalent spherical diameter (d_e) was determined to represent the diameter of a sphere with the same volume as the seed, providing a standardized measure of seed size for aerodynamic comparisons.

$$d_e=\sqrt[3]{(6V/\pi)} \quad (5)$$

Images were processed with ImageJ software to measure the maximum diameter (d_{max}), defined as the longest linear dimension across the seed's surface. The equivalent spherical diameter (d_e) was determined to represent the diameter of a sphere with the same volume as the seed, providing a standardized measure of seed size for aerodynamic comparisons. Seed volume (V) was estimated by dividing the gravimetrically measured seed mass (m) by the bulk density (ρ_b), both obtained from direct measurements (mass via precision balance, ±0.01 mg; density via volumetric displacement).

All data obtained were statistically analysed using variance analysis (ANOVA) to examine differences between groups. Duncan's multiple comparison test was used to determine text.

RESULTS

Table 1 shows the mean values and standard deviations of the aerodynamic properties of pepper seeds at four different moisture levels (5.4%, 8.6%, 12.1%, 15.4%).text.

Table 1

Summary statistics: Mean and standard deviation by moisture level

Parameters	5.4%		8.6%,		12.1%		15.4%	
	Mean	Std	Mean	Std	Mean	Std	Mean	Std
Drag Coefficient	0.475	0.021	0.445	0.020	0.415	0.019	0.387	0.018
Terminal Velocity (m	2.50	0.09	2.63	0.09	2.74	0.08	2.83	0.08
Lift Coefficient	0.278	0.005	0.279	0.005	0.281	0.005	0.283	0.005
Reynolds Number	996.35	10.21	991.47	10.19	1000.24	10.31	1014.60	10.42
Surface Area (mm²)	10.23	0.25	10.05	0.24	10.29	0.25	10.15	0.24
Mass (mg)	4.56	0.13	4.86	0.14	5.37	0.15	5.87	0.16
Bulk Density (kg m-	1216.38	25.08	1260.77	26.11	1356.65	27.23	1444.75	28.06
Shape Factor	0.863	0.008	0.860	0.008	0.855	0.008	0.858	0.008

As given in Table 1, with higher humidity there is an increase in mean values for Mass (from 4.56 mg to 5.87 mg) and mean values for Density (from 1216.38 kg m^{-3} to 1444.75 kg m^{-3}). This reflects water absorption, and the standard deviations show moderate variability (0.13–0.16 mg for Mass, 25.08 – 28.6 kg m^3 for density). While drag coefficient decreases with moisture content terminal velocity increases. Lift coefficient and shape factor show low variability (S.D 0.005–0.008), indicating stability.

Table 2 shows the F and p values obtained from the one-way ANOVA test testing significant differences among humidity levels for each parameter.

Table 2

Analysis of variance (ANOVA) on the effects of different moisture contents on pepper seed aerodynamic properties

Parameters	F-Statistic	P-Value
Drag Coefficient	56.78	<0.05
Terminal Velocity (m	53.24	<0.05
Lift Coefficient	0.12	>0.05
Reynolds Number	1.45	>0.05
Surface Area (mm²)	1.67	>0.05
Mass (mg)	302.45	<0.05
Bulk Density (kg m^{-3})	298.67	<0.05
Shape Factor	0.34	>0.05

One-way ANOVA was conducted with 100 observations per level (total N = 400, df_between = 3, df_within = 396) to assess whether the means of each aerodynamic parameter were significantly different across four moisture levels (5.4%, 8.6%, 12.1% 15.4%). The ANOVA for the drag coefficient (Cd) yielded an F-value of 56.78 with a p-value less than 0.05, indicating significant differences in the drag coefficient across moisture levels. This suggests that moisture content affects air resistance during fall by changing the surface properties of the seed. Similarly, terminal velocity (m/s) showed a significant result with an F-value of 53.24 ($p < 0.05$), indicating that the speed at which seeds reach terminal fall velocity varies with moisture, probably due to changes in mass or shape. In contrast, the lift coefficient (Cl) had an F-value of 0.12 ($p > 0.05$), indicating no significant difference, indicating that the buoyancy forces acting on the seeds remained constant regardless of moisture content.

The Reynolds number also did not show a significant change ($F = 1.45$, $p > 0.05$), meaning that the airflow characteristics around the seeds were not significantly affected by moisture depending on the speed and seed size. The surface area (mm²) had an F-value of 1.67 ($p > 0.05$), confirming that the surface area of the seeds remained constant across moisture levels, probably because physical expansion due to water absorption was minimal. The mass (mg) exhibited a highly significant difference ($F = 302.45$, $p < 0.05$), reflecting a strong effect of moisture on seed weight, consistent with water absorption increasing mass. The density (kg m^{-3}) also showed a similarly significant change ($F = 298.67$, $p < 0.05$), indicating that moisture increased the density of the seed, possibly filling the internal structures with water. Finally, the F value of the

shape factor was 0.34 ($p > 0.05$), indicating that there was no significant difference in seed shape between moisture levels, as shape is determined primarily by genetic factors rather than moisture. The results of this ANOVA test indicate that moisture significantly affected drag, terminal velocity, mass, and density, while lift coefficient, reynolds number, surface area, and shape were relatively unaffected, indicating that certain aerodynamic and physical properties were affected by moisture content.

Table 3 presents the groupings obtained from Duncan's multiple comparison test in detail; the different letters used in this table (A, B, C, D) clearly show that there are statistically significant differences between the moisture content levels examined. These groupings visually and quantitatively express the extent to which the variables measured at specific humidity levels differ from each other.

Table 3

Duncan test for aerodynamic properties of pepper seeds with different moisture contents

Parameters	5.4%	8.6%,	12.1%	15.4%
Drag Coefficient	A	B	C	D
Terminal Velocity (m	D	C	B	A
Lift Coefficient	A	A	A	A
Reynolds Number	A	A	A	A
Surface Area (mm²)	A	A	A	A
Mass (mg)	D	C	B	A
Bulk Density (kg m^{-3})	D	C	B	A
Shape Factor	A	A	A	A

The parameters with ANOVA test results ($p < 0.05$: drag coefficient, terminal velocity, mass, density) were determined to have significantly different moisture levels by applying Duncan's multiple range test, while the parameters that were not significant were assigned to the same group (A) due to no difference.

The average values for drag coefficient were found to be 0.475, 0.445, 0.415 and 0.387 at 5.4%, 8.6%, 12.1% and 15.4% moisture levels, respectively. Duncan's test grouped them as A, B, C and D, respectively, and showed that each moisture level formed a separate group, with the friction coefficient decreasing as moisture increased.

This suggests that wetter seeds may have smoother surfaces and reduce air resistance. The mean values of terminal velocity (m/s) were measured as 2.50, 2.63, 2.74 and 2.83 at 5.4%, 8.6%, 12.1% and 15.4% moisture levels respectively and were grouped as A, B, C and D respectively.

This confirms that terminal velocity increased with higher moisture content which is due to the relative decrease in drag force with decreasing surface roughness despite the increase in seed mass and density. The mass and density of seeds also increased with moisture content. Both parameters were grouped as A, B, C and D according to increasing moisture content.

These results showed a clear trend that mass increased with moisture due to water absorption while density also increased significantly with moisture and the internal structure of the seed was filled with water.

As a result of the test, lift coefficient, Reynolds number, surface area and shape factor were all placed in Group A for the parameters that were not significant, indicating that there was no significant difference between them and that these properties remained consistent across humidity levels. Duncan test results emphasize that humidity significantly changes mass and density, each humidity level forms different groups, while drag and terminal velocity decrease with increasing humidity, reflecting aerodynamic changes.

The ANOVA test results show that moisture content significantly affects the drag coefficient, terminal velocity (m s^{-1}), mass (mg) and density (kg m^{-3}) values with high f statistics and p values less than 0.05, while lift coefficient (Cl), Reynolds number, surface area (mm²) and shape factor show no significant difference ($p > 0.05$).

The Duncan test results showed that different moisture levels produced statistically significant differences in the aerodynamic and physical properties. The increase in moisture content caused significant increases in seed mass and bulk density, while it caused a decrease in drag coefficient and an increase in terminal velocity.

These changes are thought to be related to the fact that moisture changes the porosity structure of the seed, surface roughness and hence liquid-particle interactions. These findings indicate that moisture levels play an important role in seed aerodynamic and physical properties and have important consequences for seed transportation and processing.

CONCLUSIONS

This study presents a comprehensive analysis of the aerodynamic behavior of pepper seeds under changing moisture conditions, providing critical insights into how water content regulates key physical and functional properties. The findings show that increasing seed moisture content leads to significant increases in bulk and bulk density, accompanied by a decrease in friction coefficient and an increase in terminal velocity. In contrast, parameters such as lift, estimated surface area, shape factor, and airflow pattern were not significantly affected by moisture change.

These results highlight the complex yet systematic effect of moisture on seed structure and performance. Water absorption appears to alter internal and surface properties such as porosity and roughness, which in turn alter seed-air interactions. This nuanced relationship suggests that moisture is not merely a passive factor but a determinant of seed mechanics, particularly in contexts involving pneumatic conveying, mechanical sorting, and air-assisted planting systems.

From an applied perspective, the implications are significant. Higher moisture content may necessitate recalibration of pneumatic systems to reduce clogging and ensure consistent seed flow. Additionally, the observed increase in terminal velocity may affect seed dispersal dynamics, particularly in wind-dispersed species, potentially affecting ecological dispersal and establishment rates.

Given the increasing variability in climate conditions and the prevalence of moisture fluctuations in many agricultural regions, these findings advocate for moisture-adaptive seed processing and storage protocols. Incorporating moisture-responsive parameters into the design of agricultural machinery and processing systems may increase operational efficiency, reduce seed loss, and improve crop establishment under a variety of environmental conditions.

In conclusion, this study highlights the importance of integrating seed moisture dynamics into both experimental design and technological applications in seed science. Recognizing seeds as moisture-responsive systems rather than static materials opens new avenues for innovation in precision agriculture, postharvest processing, and climate-resilient farming practices.

ACKNOWLEDGEMENT

We are very grateful to the Akdeniz University Technical Sciences Vocational School and Department of Agriculture Machinery and Technologies Engineering, Faculty of Agriculture, Ondokuz Mayıs University for their cooperation and effort in supporting the experiments.

REFERENCES

[1] Abubakar, A. J., Iya, S. A., Kabri, H. U., & Abdulrafeeu, M. A. (2019). Development of a terminal velocity measuring device for grains. *Nigeria Journal of Engineering Science and Technology Research, 5*(1), 76–83.

[2] Badr, M. M., & Eissa, A. S. (2018). Some physical, mechanical and aerodynamic properties of quinoa seeds (Chenopodium quinoa Wild). *Misr Journal of Agricultural Engineering, 35*(4), 1365–1382. https://doi.org/10.21608/mjae.2018.95306

[3] Caetano, J. M., Devilla, I. A., de Carvalho Melo, P., Sérvulo, A. C. O., & Ferreira, R. B. (2022). Aerodynamic properties of two quinoa (Chenopodium quinoa Willd.) cultivars. *Revista Brasileira de Ciências Agrárias, 17*(1), 1–8.

[4] Cardoso Neto, S. R., Resende, O., Costa, L. M., Oliveira, D. E. C., Rodrigues, G. B., & Quequeto, W. D. (2020). Velocidade terminal dos frutos e sementes de crambe em função do teor de água. *Research, Society and Development, 9*(3), e152932592. https://doi.org/10.33448/rsd-v9i3.2592

[5] Ermiş, S., Ercan, U., Kabaş, A., Kabaş, Ö., & Moiceanu, G. (2025). Machine learning-based morphological classification and diversity analysis of ornamental pumpkin seeds. *Foods, 14*(9), 1498.

[6] Gojiya, D., Barad, A., Gohil, V., Dabhi, M., Dhamsaniya, N., Naliapara, V., & Sapariya, P. (2023). Quantification of design associated engineering properties of sesame (Sesamum indicum L.) seed varieties as a function of moisture content. *Journal of the American Oil Chemists' Society, 100*(8), 663–678.

[7] Gorial, B. Y., & O'Callaghan, J. R. (1990). Aerodynamic properties of grain/straw materials. *Journal of Agricultural Engineering Research, 46*, 275–290.

[8] Grift, T. E., Walker, J. T., & Hofstee, J. W. (1997). Aerodynamic properties of individual fertilizer particles. *Transactions of the ASAE, 40*, 13–20.

[9] Ibrahim, M. M., Ghonimy, M., & Abd El Rahman, E. (2023). Physical and aerodynamic properties of date palm pollen grains. *Acta Agriculturae Slovenica, 119*(4), 1–11.
[10] Jimoh, K. A., Hashim, N., Shamsudin, R., Man, H. C., Jahari, M., & Onwude, D. I. (2023). Recent advances in the drying process of grains. *Food Engineering Reviews, 15*(3), 548–576.
[11] Kabas, O., Yilmaz, E., Ozmerzi, A., & Akinci, I. (2007). Some physical and nutritional properties of cowpea seed (Vigna sinensis L.). *Journal of Food Engineering, 79*(4), 1405–1409.
[12] Kabaş, Ö., & Özmerzi, A. (2018). Determination of some aerodynamic properties of "Balo" bell pepper for pneumatic sorting. In *Proceedings of the International Symposium ISB-INMA TEH' 2018, Agricultural and Mechanical Engineering* (pp. 97–100). Bucharest, Romania.
[13] Kaliniewicz, Z., Choszcz, D., & Lipiński, A. (2022). Determination of seed volume based on selected seed dimensions. *Applied Sciences, 12*(18), 9198.
[14] Mohsenin, N. N. (1980). *Physical properties of plant and animal materials*. Gordon and Breach Science Publishers.
[15] Rodrigues, G. B., Resende, O., Oliveira, D. E. C. de, & Sousa, K. A. (2019). Propriedades físicas das sementes de sorgo granífero. *Revista Engenharia na Agricultura, 27*(6), 490–497. https://doi.org/10.13083/reveng.v27i6.969
[16] Shaha, S. N., & Pachapuri, M. S. A. (2015). NACA 2415-finding lift coefficient using CFD, theoretical and Javafoil. *International Journal of Research in Engineering and Technology, 4*(7), 444–449.
[17] Singh, S. K., Kautkar, S., & Patil, A. (2021). Impact of engineering properties of grass seeds in developing post-harvest operations and machineries. *Environment Conservation Journal, 22*(3), 395–399.
[18] Song, H., & Litchfield, J. B. (1991). Predicting method of terminal velocity for grains. *Transactions of the ASAE, 34*(1), 225–231.
Vilche, C., Gely, M., & Santalla, E. (2003). Physical properties of quinoa seeds. *Biosystems Engineering, 86*(1), 59–65. https://doi.org/10.1016/S1537-5110(03)00114-4

CONSIDERATIONS REGARDING THE USE OF MODERN EQUIPMENT FOR THE EFFICIENT UTILISATION OF PERMANENT PASTURES

/

CONSIDERAȚII PRIVIND UTILIZAREA ECHIPAMENTELOR MODERNE PENTRU VALORIFICAREA EFICIENTĂ A PĂȘUNILOR PERMANENTE

Remus Marius OPRESCU*[1)], Dan CUJBESCU[1)], Iulian VOICEA[1)], Cătălin PERSU[1)], Radu RĂDOI[2)]

[1)] National Institute of Research - Development for Machines and Installations Designed to Agriculture and Food Industry - INMA Bucharest / Romania;

[2)] INOE 2000 - IHP / Romania.

**E-mail: oprescu.remusmarius@gmail.com; *Tel: 0766 580 791*

Keywords: *permanent pastures, pasture-based agriculture, agricultural equipment, maintenance.*

ABSTRACT

Permanent pastures represent an essential resource for animal feed and therefore contribute directly to the sustainability of livestock farms. Proper maintenance of these resources requires the use of modern equipment adapted to the pedo-climatic conditions and to the vegetation type. Pastures provide a range of ecosystem services, including regulation and storage of water flows, nutrient cycling and carbon sequestration. Grazing is the most important factor shaping and stabilising pasture biodiversity. Opportunities for exploiting pastures lie in the nutritional and health-promoting qualities of milk and dairy products, particularly milk from cows fed on pasture. The beneficial effects of grazing on animal health and welfare are not negligible. Available organisational innovations can help improve the management of livestock grazing and, above all, lead to a better understanding of the impact of grazing on the environment and climate change. This paper presents modern equipment used in pasture management operations as well as its impact on productivity and biodiversity conservation.

REZUMAT

Pășunile permanente reprezintă o resursă esențială pentru hrana animalelor, contribuind la sustenabilitatea fermelor zootehnice. Întreținerea corespunzătoare a acestora presupune utilizarea unor echipamente moderne adaptate condițiilor pedoclimatice și tipului de vegetație. Pășunile oferă servicii ecosistemice, inclusiv reglarea și stocarea fluxurilor de apă, ciclul nutrienților și sechestrarea carbonului. Pășunatul este cel mai important factor care modelează și stabilizează biodiversitatea pășunilor. Câteva oportunități pentru hrănirea pășunilor sunt calitățile nutritive și benefice pentru sănătate ale laptelui și produselor lactate, în special ale laptelui provenit de la vacile hrănite pe pășuni. Efectele benefice ale hrănirii pe pășuni asupra sănătății și bunăstării animalelor nu sunt nesemnificative. Inovațiile organizaționale disponibile pot ajuta la o mai bună gestionare a pășunatului animalelor și, mai presus de toate, la o mai bună înțelegere a impactului procesului de pășunat asupra mediului și a schimbărilor climatice. Lucrarea prezintă echipamente moderne utilizate în lucrările de administrare a pășunilor, precum și impactul acestora asupra productivității și conservării biodiversității.

INTRODUCTION

Permanent grasslands, including pastures, are characterised by a diverse species composition resulting from interspecific competition modified by human activity. The most important factors are the habitat conditions and the method and intensity of agricultural use, which determine the type of sward and its natural values. One of the characteristics of grasslands of high natural value is their richness in species. However, maintaining this richness is not a priority on farms focused on intensive animal production. In such farms the main goal is to obtain large quantities of valuable forage, so the sward composition is generally poor in species, dominated by selected grasses with a proportion of legumes and only a few herb species. Many of these herbs are considered weeds from a production standpoint and indicate degradation. By contrast, high species diversity is favoured by extensive grazing and limited use of sward management practices (*Wróbel et al., 2023*).

One of the most important factors shaping and stabilising valuable communities in permanent grasslands is sustainable grazing, which is sometimes used as a protective treatment to arrest secondary

succession. Grazing has a beneficial effect on floristic composition and sward structure, contributing to the maintenance of an open pastoral landscape and the conservation of species-rich habitats. The vegetation structure of pastures is the result of processes and environmental factors determined by the grazing animals—namely their dietary requirements and preferences and the intensity of grazing.

Moderate trampling by grazing animals leads to localised damage and the formation of bare patches where seeds can germinate; it also allows light to reach the lower parts of the sward, promoting the development of light-loving species. Furthermore, animals transport plant diaspores, facilitating their reproduction and spread, and their excreta supply nutrients locally, creating numerous micro-habitats (*Wróbel et al., 2023, Musagaliev & Shodiev, 2023*).

Grazing has been practised since the beginnings of agriculture. According to the Food and Agriculture Organization, around 60 % of the world's grasslands (slightly less than half of the Earth's land area) are occupied by grazing systems. Such systems provide about 9 % of global beef production and roughly 30 % of the world's sheep and goat meat.

For about one hundred million people in arid areas, and probably a similar number elsewhere, livestock grazing is the only possible livelihood. Pasture-based dairy systems are found mainly in temperate regions, where grass is the cheapest feed used in milk production (*De Haan et al., 1997*). Grazing can also be used in dairy-cow feeding systems elsewhere in Europe, but its importance is lower.

It is estimated that 98 % of dairy farms in Ireland and 92 % of those in Britain operate pasture-based systems, compared with only 20 % in the Czech Republic, less than 10 % in Greece and virtually none in Bulgaria. Even herds with access to pasture are usually housed during winter and the calving period (*Wilkinson et al., 2020; Van den Pol-van Dasselaar et al., 2020; Crump et al., 2019*).

In general, pasture grass is a higher-quality feed for milk production than grass silage (*Kennedy et al., 2005; Hurtado-Uria et al., 2013; Ruelle et al., 2018*). In the temperate regions of Europe, grass growth is highly variable—differing from year to year, between seasons and between regions. It depends on many factors: pasture management, sward renewal practices, the level of fertilisation, the evolution of weather conditions (e.g., precipitation, temperature, solar radiation) and soil type. The nutritional value of the sward also varies with season, growth stage and regrowth age.

The quality of pasture grass can be optimised through rational grazing and pasture management. For example, rotation length, pre-grazing biomass and sward height before and after grazing can affect grass quality and availability. A leaf-rich sward in spring has a high nutritional value, whereas a sward in the reproductive stage in summer contains more fibre and is less digestible. The nutritional value of the sward also depends on its botanical composition; swards with a significant proportion of legumes often have a higher nutritional value than swards composed only of grasses (*Wims et al., 2010; Ganche et al., 2013; McDonald et al., 1998; Egan et al., 2018*).

Properly managed pastures provide grazing animals with high-quality forages containing energy, protein, macro- and micro-elements and vitamins. Alongside valuable grasses and legumes, the sward contains dicotyledonous forbs.

These forbs contain biologically active substances—tannins, flavonoids, saponins, pectins, terpenes, alkaloids, phenols and essential oils—that have positive effects on the digestive system and the health of cattle (antioxidant and antiparasitic effects, improved immunity) and improve the quality of beef and dairy products (*Riberio Filho et al., 2003; Peyraud & Delagarde, 2013; MacAdam & Villalba, 2015; Distel et al., 2020; Niderkorn & Jayanegara, 2021; Kaur et al., 2021*).

Despite the importance of grazing, current trends in European livestock husbandry are reducing the popularity of pasture-based feeding for dairy cows. The reasons vary, owing mainly to the different farming systems typical of each region. In Central Europe, dairy farmers are under pressure to maximise milk output. Consequently, dairy cows are often not grazed but are kept indoors throughout their lives and fed mainly on silage and concentrates (*Wilkinson et al., 2020; Van den Pol-van Dasselaar et al., 2020; Läpple & Sirr, 2019*).

Grazing requires more time and labour than keeping cattle indoors or in loose housing. It also involves costs for purchasing and installing fences and for delimiting paddocks. Electric fences and wire mesh structures may also disrupt the natural landscape and prevent the migration of wild species (*Langworthy et al., 2021*).

Agriculture is significantly influenced by climate change and is at the same time a driver of climate change through the release of greenhouse gases into the atmosphere. Reducing agriculture's carbon

footprint is therefore essential to mitigate climate change. Agriculture and forestry can also remove CO_2 from the *atmosphere. Grasslands play a significant role in climate change because of their large carbon stocks and fluxes (Bai & Cotrufo, 2022; Rasche et al., 2023*).

Demand for animal-based protein products is predicted to increase by more than 70 % in the coming decades, as wealth increases in developing countries. Consequently, this could lead to an 80 % increase in greenhouse-gas emissions from agriculture if not mitigated. Pasture-based agriculture has an important role in increasing food production in an environmentally sustainable manner.

Over recent decades there has been a 30 % reduction in European grassland use owing to increased production efficiency and the controllability of feed in confinement systems, where animals are fed indoors. In contrast, pasture-based systems in suitable climates have the potential to be more economically and environmentally sustainable than confinement systems (*Van den Pol-van Dasselaar et al., 2020; Hennessy et al., 2015; Barthram et al., 2005; Klootwijk et al., 2019; Nakagami, 2016*).

Nevertheless, they are hindered by reduced feed controllability due to the spatial and temporal heterogeneity of pastures: the amount of available herbage can vary between 15 % and 60 % owing to selective grazing, dung patches and seasonal changes in sward morphology, making accurate measurement and allocation for grazing difficult (*Herrero et al., 2015; Henchion et al., 2017; Tilman & Clark, 2014; Huyghe et al., 2014; Hennessy et al., 2020).*

To maintain the productive capacity of these ecosystems, proper management is required, involving both agronomic measures and specialised agricultural equipment. Inadequate maintenance leads to pasture degradation, reduced biodiversity and the emergence of invasive species.

This paper presents an overview of modern equipment used in permanent pasture management and discusses how such technologies can enhance productivity while preserving biodiversity.

MATERIALS AND METHODS

Precision technology enables efficient pasture management. Using GPS, drones and vegetation sensors makes it possible to monitor pasture condition, apply fertilisers variably and intervene rapidly in problem areas. Such approaches reduce costs and improve sustainability.

Developing accurate grass-measurement technologies is vitally important for ensuring the future sustainability of pasture-based animal production systems. There is potential to increase grassland production sustainably by measuring herbage quantity and quality more precisely. One of the main obstacles—sward heterogeneity—is discussed together with optimal sampling techniques to address it.

With respect to grass quality, there are no established farm-level methods that farmers can use to estimate the quality of grass on their own pastures.

Existing methods for qualitative analysis are usually laboratory-based and involve time-consuming pre-processing such as grinding and oven drying, which may take several days. Important quality parameters for grazing systems include dry matter, digestible dry matter, metabolizable energy, digestible organic matter, crude protein and water-soluble carbohydrates.

Precision agriculture technologies offer significant potential to improve the availability and accuracy of grassland-measurement information. Precision agriculture focuses on acquiring precise field data at spatial and temporal scales that capture variability and allow targeted management responses, aiming to increase economic returns and reduce environmental impact.

Adoption of precision technologies has been relatively slow in grassland farming compared with arable farming, partly because pastures are more diverse in terms of spatial variation in soil and sward characteristics and because grass species change rapidly over time.

In the present context, ground-based sensing refers to non-spectral sensors that interact with the sward at or near ground level. Mobile ground-based sensing using electrodes was employed by Vogel and colleagues to investigate relationships between soil pH, moisture content and spatial variation in herbage mass on grazed German pastures.

Their study used a tractor-mounted Veris mobile sensor platform (Fig. 1) for rapid soil analysis; apparent soil electrical conductivity was measured to predict soil moisture.

Fig. 1 - Mobile Veris sensor platform mounted on a tractor for on-the-go soil analysis on pastures
(*Vogel, et al., 2019*)

The use of a sensor to measure sward height directly by means of ultrasound was investigated on mixed-species German swards by Reddersen et al., 2014. They found that it predicted herbage mass with reasonable accuracy (R^2 = 0.73–0.76, RMSECV = 0.88–1.17 t DM ha^{-1}). Moreover, combining ultrasonic sward-height data with remote-sensing data in a multi-sensor approach (leaf area index and hyperspectral sensors) increased prediction accuracy by 30 %. An earlier study by Fricke et al. investigated combining ultrasonic height sensing with GPS on a vehicle for real-time, on-the-go measurement and rapid mapping of pasture yield, as illustrated in Figure 2a.

That study highlighted several limitations of ultrasonic measurement, including poor accuracy caused by the wide ultrasonic response area and low responsiveness to changes in sward geometry and heterogeneity. Nevertheless, it emphasised the potential of combining networks of low-cost ultrasonic sensors, which could be mounted on tractors or mowers, to generate inexpensive herbage-mass predictions with minimal effort. Safari et al. compared mobile ultrasonic sensing and spectral detection (Figure 2b) with static detection, reporting lower prediction accuracy for mobile measurements owing to positional errors caused by soil-profile variation. Moeckel et al. obtained poor results (R^2 = 0.36–0.74, SE = 675–1,118 kg DM ha^{-1}) when predicting herbage mass using ultrasound on mixed-species pastures and reported large errors on mature swards owing to patches of rejected grass remaining after grazing.

Their study further explored the potential of combining spectral data from spectrometers and satellites with ultrasound and found that using both visible and near-infrared spectral data improved herbage-mass prediction (R^2 = 0.66–0.88, SE = 485–866 kg DM ha^{-1}). A similar ultrasound system, which could be mounted on an agricultural vehicle travelling at 20 km h^{-1}, achieved prediction accuracies of R^2 = 0.75 and SE = 270–350 kg ha^{-1} on New Zealand pastures. Ultrasonic sensing is relatively fast, inexpensive and easy to implement, with potential for mobile applications; conversely, it has accuracy limitations arising from the large variation in signal responses to sward heterogeneity.

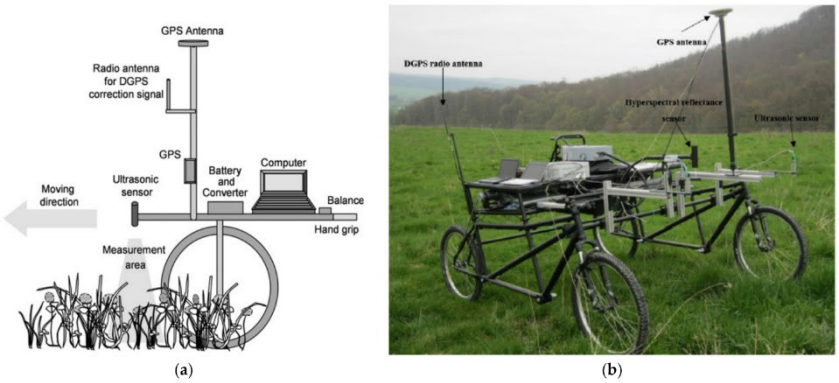

Fig. 2 (a) - Diagram of the on-the-go grass-measurement system presented in *(Fricke et al.)*
(b) Image of a similar system
(Safari et al., 2016)

Ground-based sensing can enable grass measurement by autonomous ground vehicles (AGVs) working remotely at close proximity to the soil surface. Research on AGVs for precision agriculture applications has focused mainly on arable farming. A more recent adaptation of the C-DAX platform is a

proposed pasture robot currently under development in New Zealand (*Manderson & Hunt, 2013; Safari et al., 2016; Murphy et al., 2021*).

The concept combines an AGV with the C-DAX system: the robot is designed to navigate autonomously from a central charging station to a paddock and to traverse the pasture according to a pre-programmed sampling strategy, eliminating manual labour. An entire 2 ha paddock could be sampled for mapping in five hours, or a representative area could be sampled for basic pasture management in less than thirty minutes.

The potential to mount soil-sampling and herbage-quality sensors on this system is also being considered. Gobor et al. proposed a similar robotic system for use on German pastures. Their concept incorporates a mulching unit on the robotic platform (Fig. 3) so that rejected pasture areas identified by a sward-height sensor can be mulched to encourage regeneration of high-quality swards; areas with low herbage mass could be reseeded using a seeder mounted on the robot. Sampling-protocol design is a significant consideration when using AGVs for pasture measurement.

Designing optimal AGV sampling protocols should adhere to best practices for pasture sampling, yet labour and measurement time do not impose the same constraints when using AGVs. Compared with unmanned-aerial-vehicle (UAV) remote sensing, AGV systems have disadvantages—slower data collection, sward damage caused by vehicle tracks and higher cost—but these may be offset by higher resolution and reduced climatic noise (*Safari et al., 2016; Moeckel et al., 2017*).

Fig. 3 - Concept of the robotic pasture system proposed by *Gobor et al. 2015*, incorporating a mulcher and a seeder

Remote sensing refers to detection techniques operating more than two metres above ground level. This category includes methodologies using drones, manned aircraft and satellites. In the past decade, research on remote sensing methods for predicting grass yield and quality has increased. Remote sensing can cover large sampling areas with minimal labour.

Various remote-sensing technologies can be mounted on drones flying at low altitude to obtain high-resolution spectral data. Rueda-Ayala et al. found poor correlations ($R^2 < 0.6$) between RGB wavelength data and herbage mass on Norwegian PRG-dominated pastures, and reported difficulties in measurement accuracy due to environmental factors such as wind speed, sunlight and cloud cover. However, they observed that UAV-based detection was less variable than ground-based data.

Askari et al. showed that red and green wavelength bands were important for predicting crude protein content through UAV detection on Irish PRG pastures. Capolupo et al. demonstrated that hyperspectral drones could predict sward height ($R^2 = 0.70–0.86$, RMSE = 2.13–2.29 cm), herbage mass ($R^2 = 0.36–0.83$, RMSE = 2.95–3.81 kg DM per plot) and crude protein ($R^2 = 0.56–0.76$, RMSE = 11.73–12.28 g kg^{-1} DM) on plots in controlled German studies.

Multispectral sensors (MS) emit light in discrete spectral bands and at broader resolutions than hyperspectral sensors and have been used more frequently in UAV research for pasture analysis. A major advantage of MS devices is that they are usually cheaper than hyperspectral instruments.

Pullanagari et al. reported reasonable accuracy ($R^2 = 0.60–0.68$; RMSE = 0.65–5.27 %) for crude protein, metabolizable energy and organic matter digestibility on PRG-dominated pastures in New Zealand over two grazing seasons, using a proximal MS sensor covering 16 discrete wavelengths (460–1680 nm).

An important drawback identified was that many MS sensors depend on natural light to illuminate the sward, so low light intensity can cause sampling problems. Askari et al. obtained good prediction results for herbage mass (R^2 = 0.78, RMSE = 215 kg DM ha^{-1}) and crude protein (R^2 = 0.77, RMSE = 13.6 g kg DM^{-1}) using UAV-borne MS sensing (Fig. 4) on Irish PRG pastures across two grazing seasons.

Togeiro de Alckmin et al. reported that MS sensing (R^2 = 0.79, RMSE = 405.8 kg DM ha^{-1}) had a smaller error (by 116 kg DM ha^{-1}) than rising-plate meters for predicting herbage mass when an optimal selection of vegetation indices was used. Oliveira et al. showed that combining hyperspectral detection with 3-D imaging outperformed MS measurements on Finnish swards, accurately predicting herbage mass (relative prediction error of 14.6 %), digestibility (1.9 %) and nitrogen content (13.6 %).

(a) (b)

Fig. 4 - (a) UAV equipped with a multispectral sensor; (b) example of a UAV survey from *Askari et al., 2019*

RESULTS

Recent developments in robotics and artificial intelligence are transforming agricultural practices. Results from the literature show that advanced technologies such as automation, service robots and AI-assisted systems address labour shortages, improve efficiency and enhance product quality.

Agriculture is indispensable to humanity: people rely on it to produce food, so there must be continuous supply and production to meet the needs of a growing population. Owing to the shortage and ageing of the rural workforce in recent years, agricultural production must depend on mechanisation to improve efficiency.

To enhance labour productivity and reduce costs, however, automation and technologisation represent the inevitable path of agricultural development beyond mechanisation (*Belanche et al., 2020; Wirtz et al., 2018; Genesys, 2019*).

The world is moving towards the fourth industrial revolution, and technologies such as the Internet of Things, artificial intelligence and cloud computing are becoming mainstream. Image processing plays a very important role in industrial production: it can visualise the anatomical structure of products, check and evaluate their advantages and disadvantages in real time and reduce unnecessary losses. Consequently, operators need to avoid the errors inherent in traditional manual judgement and to accelerate the harvesting of agricultural products.

Through deep learning and advances in image-recognition technology, high-tech innovative agriculture can be developed from traditional agriculture to solve problems such as labour shortages and limited research and development, thereby improving productivity and the international competitiveness of agricultural products.

Advanced robotics, artificial intelligence and machine-learning technologies enable providers to offer their services with increased productivity, effectiveness and efficiency. Service robots and artificial intelligence promise to increase productivity and reduce costs, leading to substantial growth in service-robot sales. Developed countries are currently affected by an ageing population and declining birth rates, causing a continuous decline in the workforce and a serious lack of labour productivity. How to bridge this labour-demand gap is a challenge many countries are eager to solve.

The rise of robotics has been felt across all industries. High-tech robots, coupled with artificial intelligence and machine learning, can deliver greater productivity and better product quality and steadily increase service efficiency, thereby improving customer satisfaction. A survey of business leaders in the United States showed that 24 % of companies were already using artificial intelligence and 60 % expected to use it by 2022. Sales of service robots continue to grow by more than 30 % per year, and the International

Federation of Robotics predicts that over the next decade the range of professional and personal uses for service robots will expand further and permeate various industries to support production and service activities.

Artificial intelligence specifically refers to machines that exhibit aspects of human intelligence. Initially conceived as a way to combine perception, reasoning and learning, AI development has focused increasingly on algorithms, while robotics has addressed mechanical operation. From a service-management perspective, the value of AI derives not from its virtual or unseen use but from its ability to interact socially with customers.

With the rapid development of AI, intelligent robots have been widely adopted in fields such as agricultural management and water-resource management. In the past, machine operators were separated from machinery for safety reasons, but Industry 4.0 aims to support future factories and reduce operator fatigue: robots are integrated into assembly lines to work with humans, producing high-quality goods and completing tasks more efficiently and satisfactorily.

Fig. 5 - Finished product of the automatic robotic lawn mower
(*Liao et al., 2021*)

Companies such as Honda and Husqvarna have recently launched a range of robotic lawn mowers priced between USD 1,000 and USD 2,500. At present, such mowers are more popular in Europe; sales in the United States are not as strong. Some mowers from the Swedish company Husqvarna cost USD 5,100 per unit and can handle steep slopes (45°) and adverse weather. With GPS-assisted navigation and Automower Connect, the mowers can be controlled from anywhere.

Robotic mowers from iRobot can memorise positions and automatically generate a digital map of the area to be mown; they can also be programmed to mow regularly and to control the cutting height. Users of the Honda mowers can mow without pushing and benefit from anti-theft alerts; these units cost USD 2,500. Robotic lawn mowers are diverse and offer different functions, allowing consumers to select a model to suit their needs

CONCLUSIONS

Efficient management of permanent pastures is impossible without modern equipment adapted to specific needs. Correct application of agricultural technologies leads to increased productivity and ecosystem conservation. In the context of climate change and environmental-protection requirements, smart mechanisation and precision agriculture will become central to the sustainable exploitation of pastures.

Recent advances in robotics and artificial intelligence provide promising solutions for labour shortages in agriculture and enhance precision in pasture management, paving the way for technologically driven pastoral systems. Integrating autonomous ground vehicles, remote sensing and AI-driven decision support will enable farmers to monitor forage quantity and quality more accurately, leading to sustainable and resilient livestock production.

ACKNOWLEDGEMENT

This research was supported by the Ministry of Agriculture and Rural Development – Romania - MADR through the Sectoral Project ADER 20.1.2. "Enhanced Utilization of Agricultural Land Subject to

Erosion through the Conservation of Water and Soil Resources under Climate Change Conditions", Ctr. 27.07.2023.

REFERENCES

[1] Askari, M. S., McCarthy, T., Magee, A., & Murphy, D. J. (2019). Assessment of grass quality in different soil management scenarios using remote sensing techniques. *Remote Sensing*, *11*, 1835.

[2] Bai, Y., & Cotrufo, M. F. (2022). Carbon sequestration in grassland soils: Current understanding, challenges and solutions. *Science*, *377*, 603–608.

[3] Barthram, G. T., Duff, E. I., Elston, D. A., Griffiths, J. H., Common, T. G., & Marriott, C. A. (2005). Frequency distributions of sward height under sheep grazing. *Grass and Forage Science*, *60*, 4–16.

[4] Belanche, D., Casaló, L. V., Flavián, C., & Schepers, J. (2020). Service robot implementation: A theoretical framework and research agenda. *Service Industries Journal*, *40*, 203–225.

[5] Capolupo, A., Kooistra, L., Berendonk, C., Boccia, L., & Suomalainen, J. (2015). Estimation of grassland plant traits from drone-acquired hyperspectral images: A comparison of statistical approaches. *ISPRS International Journal of Geo-Information*, *4*, 2792–2820.

[6] Chen, Y. S., Tsao, H. H., Chen, S. W., Liu, C. Y., & Yeh, L. C. (2018). An integrated study on the recognition system of the mature fruit. *Electronic Commerce Studies*, *16*, 233–258.

[7] Crump, A., Jenkins, K., Bethell, E. J., Ferris, C. P., & Arnott, G. (2019). Pasture access affects behavioural indicators of dairy cow welfare. *Animals*, *9*, 902.

[8] De Haan, C., Steinfeld, H., & Blackburn, H. (1997). *Animals and the environment: Finding a balance*. Directorate-General for Development of the European Commission, Development Policy, Sustainable Development and Natural Resources.

[9] Distel, R. A., Arroquy, J. I., Lagrange, S., & Villalba, J. J. (2020). Designing diverse agricultural pastures for improving ruminant production systems. *Frontiers in Sustainable Food Systems*, *4*, 596869.

[10] Egan, M., Galvin, N., & Hennessy, D. (2018). Incorporating white clover (Trifolium repens L.) into perennial ryegrass (Lolium perenne L.) receiving variable levels of nitrogen fertilizer: Effects on milk and herbage production. *Journal of Dairy Science*, *101*, 3412–3427.

[11] Fricke, T., Richter, F., & Wachendorf, M. (2011). Evaluation of forage mass on pasture by measuring sward height using an ultrasonic sensor. *Computers and Electronics in Agriculture*, *79*, 142–152.

[12] Ganche, E., Delaby, L., O'Donovan, M., Boland, T. M., Galvin, N., & Kennedy, E. (2013). Post-grazing sward heights imposed during the first 10 weeks of lactation: Influence on early and total lactation production of dairy cows and spring and annual sward characteristics. *Livestock Science*, *157*, 299–311.

[13] Genesys. (2019). *U.S. Employers Expect Growth of Artificial Intelligence in the Workplace but Not Major Job Reductions.* https://www.prnewswire.com/news-releases/us-employers-expect-growth-of-artificial-intelligence-in-the-workplace-but-not-major-job-reductions-300901926.html

[14] Gobor, Z., Cariou, C., Seiferth, B., Thurner, S., Feucker, W., Tessier, C., Tekin, B., & Berducat, M. (2015). Advanced pasture management through innovative robotic pasture maintenance. In *Proceedings of the IROS Workshop Agri-Food Robot*, Hamburg, Germany, 2 October 2015; Kootstra, G., Edan, Y., & Henten, E. v. B. M. (Eds.), HAL: Lyon, France.

[15] Henchion, M., Hayes, M., Mullen, A., Fenelon, M., & Tiwari, B. (2017). Future protein demand and supply: Strategies and factors influencing a sustainable balance. *Foods*, *6*, 53.

[16] Hennessy, D., Delaby, L., van den Pol-van Dasselaar, A., & Shalloo, L. (2020). Advancing grazing in dairy production systems in Europe. *Sustainability*, *12*, 2443.

[17] Hennessy, D., Delaby, L., Van den Pol-van Dasselaar, A., & Shalloo, L. (2015). Opportunities and constraints for grazing in high milk-yield systems. In *Proceedings of the 18th Symposium European Grassland Federation*, Wageningen, The Netherlands, 15–17 June 2015; Van den Pol-van Dasselaar, A., Aarts, H. F. M., De Vliegher, A., Elgersma, A., Reheul, D., Reijneveld, J. A., Verloop, J., & Hopkins, A. (Eds.), Wageningen Academic Publishers: Wageningen, The Netherlands, pp. 151–162.

[18] Herrero, M., Wirsenius, S., Henderson, B., Rigolot, C., Thornton, P., Havlík, P., De Boer, I., & Gerber, P. J. (2015). Livestock and the environment: What have we learned in the last decade? *Annual Review of Environment and Resources*, *40*, 177–202.

[19] Hurtado-Uria, C., Hennessy, D., Shalloo, L., O'Connor, D., & Delaby, L. (2013). Relationships between weather data and grass growth over time in southern Ireland. *Irish Geography*, *46*, 175–201.

[20] Huyghe, C., De Vliegher, A., Van Gils, B., & Peeters, A. (2014). *Grasslands and Herbivore Production in Europe and the Effects of Common Policies.* Éditions Quae: Versailles, France.
[21] Kennedy, E., O'Donovan, M., Murphy, J.-P., Delaby, L., & O'Mara, F. (2005). Effects of grass swards and concentrate-based feeding systems for spring-calving dairy cows in early spring on performance during lactation. *Grass and Forage Science*, *60*, 310–318.
[22] Kaur, A. P., Bhardwaj, S., Dhanjal, D. S., Nepovimova, E., Cruz-Martins, N., Kuca, K., Chopra, C., Singh, R., Kumar, H., Sen, F., et al. (2021). Plant prebiotics and their role in ameliorating diseases. *Biomolecules*, *11*, 440.
[23] Klootwijk, C. W., Holshof, G., de Boer, I. J., Van den Pol-Van Dasselaar, A., Engel, B., & Van Middelaar, C. E. (2019). Correcting the fresh grass allocation for patches refused due to excreta in intensive grazing systems for dairy cows. *Journal of Dairy Science*, *102*, 10451–10459.
[24] Langworthy, A. D., Verdon, M., Freeman, M. J., Corkrey, R., Hills, J. L., & Rawnsley, R. P. (2021). Virtual fencing technology for intensive grazing of lactating dairy cows. I: Technology efficacy and pasture use. *Journal of Dairy Science*, *104*, 7071–7083.
[25] Läpple, D., & Sirr, G. (2019). Milk production intensification and quota removal: A comparative study of production in Ireland and the Netherlands. *EuroChoices*, *18*, 26–32.
[26] Liao, J. C., Chen, S. H., Zhuang, Z. Y., Wu, B. W., & Chen, Y. J. (2021). Designing and manufacturing of automatic robotic lawn mower. *Processes*, *9*(2), 358.
[27] MacAdam, J. W., & Villalba, J. J. (2015). Beneficial effects of temperate forage legumes containing condensed tannins. *Agriculture*, *5*, 475–491.
[28] Manderson, A., & Hunt, C. (2013). Introducing the Agri-Rover: An autonomous moving sensing rover for science and agriculture. In *Proceedings of the 26th Annual Farmed Landscapes Research Center Workshop*, Palmerston North, New Zealand, 12–14 February 2013; Currie, L., & Christensen, C. L. (Eds.), Massey University: Palmerston North, New Zealand.
[29] McDonald, P., Edwards, R. A., Greenhalgh, J. F. D., & Morgan, C. A. (1998). Grass and forage crops. In *Animal Nutrition* (5th ed.). Longman Group Ltd.: New York, NY, USA. Chapter 18.
[30] Moeckel, T., Safari, H., Reddersen, B., Fricke, T., & Wachendorf, M. (2017). Fusion of ultrasonic and spectral sensor data to improve biomass estimation in heterogeneously structured grassland swards. *Remote Sensing*, *9*, 98.
[31] Murphy, D. J., Murphy, M. D., O'Brien, B., & O'Donovan, M. (2021). A review of precision technologies for optimising pasture measurement on Irish grassland. *Agriculture*, *11*(7), 600.
[32] Musagaliev, A. J., & Shodiev, B. T. (2023). Issues of efficient usage of pastures in the development of the cattle farming network. *Uttar Pradesh Journal of Zoology*, *44*(1), 81–87.
[33] Nakagami, K. (2016). A method for approximate estimation of on-farm grass mass using two assessments per paddock. *Grass and Forage Science*, *71*, 490–496.
[34] Niderkorn, V., & Jayanegara, A. (2021). Opportunities offered by plant bioactive compounds for improving silage quality, animal health and product quality for sustainable ruminant production: An analysis. *Agronomy*, *11*, 86.
[35] Oliveira, R. A., Näsi, R., Niemeläinen, O., Nyholm, L., Alhonoja, K., Kaivosoja, J., Jauhiainen, L., Viljanen, N., Nezami, S., Markelin, L., et al. (2020). Machine-learning estimators for the quantity and quality of sward used for silage production using spectrometry and drone-based photogrammetry imaging. *Remote Sensing of Environment*, *246*, 111830.
[36] Peyraud, J. L., & Delagarde, R. (2013). Managing variations in nutrient intake of dairy cows during grazing. *Animal*, *7*, 57–67.
[37] Pullanagari, R. R., Yule, I. J., Tuohy, M. P., Hedley, M. J., Dynes, R. A., & King, W. M. (2012). Proximal detection of seasonal variability in nutritive value of pastures using multispectral radiometry. *Grass and Forage Science*, *68*, 110–119.
[38] Rasche, L., Schneider, U. A., & Steinhauser, J. (2023). A stakeholders' pathway towards a future land use and food system in Germany. *Sustainability Science*, *18*, 441–455.
[39] Reddersen, B., Fricke, T., & Wachendorf, M. (2014). A multi-sensor approach for predicting biomass in extensively managed grasslands. *Computers and Electronics in Agriculture*, *109*, 247–260.
[40] Riberio Filho, H. M. N., Delagarde, R., & Peyraud, J. L. (2003). Including white clover in strip-grazed perennial ryegrass swards: Grass intake and milk production of dairy cows at different sward regrowth ages. *Animal Science*, *77*, 499–510.

[41] Rueda-Ayala, V., Peña, J., Höglind, M., Bengochea-Guevara, J., & Andújar, D. (2019). Comparing UAV-based technologies and RGB-D reconstruction methods for monitoring plant height and biomass on Ley grass sensors. *Sensors*, *19*, 535.

[42] Ruelle, E., Delaby, L., & Hennessy, D. (2018). Development of the Moorepark St Gilles (MoSt GG) grass growth model: A predictive model for grass growth in pasture-based systems. *European Journal of Agronomy*, *99*, 81–90.

[43] Safari, H., Fricke, T., Reddersen, B., Möckel, T., & Wachendorf, M. (2016). Comparing mobile and stationary biomass assessment in heterogeneous grasslands using a multi-sensor system. *Journal of Sensors and Sensor Systems*, *5*, 301–312.

[44] Tilman, D., & Clark, M. (2014). Global diets link environmental sustainability and human health. *Nature*, *515*, 518–522.

[45] Van den Pol-van Dasselaar, A., Hennessy, D., & Isselstein, J. (2020). Grazing dairy cows in Europe—An in-depth analysis based on the perception of pasture experts. *Sustainability*, *12*, 1098.

[46] Vogel, S., Gebbers, R., Oertel, M., & Kramer, E. (2019). Evaluating soil causes of biomass variability in grasslands using remote sensing and proximal detection. *Sensors*, *19*, 4593.

[47] Wilkinson, J. M., Lee, M. R. F., Rivero, M. J., & Chamberlain, A. T. (2020). Some challenges and opportunities for grazing dairy cows on temperate pastures. *Grass and Forage Science*, *75*, 1–17.

[48] Wims, C. M., Deighton, M. H., Lewis, E., O'Loughlin, B., Delaby, L., Boland, T. M., & O'Donovan, M. (2010). Effect of pre-grazing herbage mass on methane production, dry matter intake and milk production of dairy cows grazing mid-season pasture. *Journal of Dairy Science*, *93*, 4976–4985.

[49] Wirtz, J., Patterson, P. G., Kunz, W. H., Gruber, T., Lu, V. N., Paluch, S., & Martins, A. (2018). Brave new world: Service robots in the frontline. *Journal of Service Management*, *29*, 907–931.

[50] Wróbel, B., Zielewicz, W., & Staniak, M. (2023). Challenges of pasture feeding systems—Opportunities and constraints. *Agriculture*, *13*(5), 974.

[51] *****International Federation of Robotics. (2018). *World Robotics Report 2018. Press Conference Summary, Tokyo*. https://ifr.org/free-downloads/

BLACK SOLDIER FLY LARVAE (*HERMETIA ILLUCENS*): FROM SUSTAINABLE ANIMAL FEED TO EMERGING HUMAN FOOD SOURCE

/

LARVELE DE MUSCĂ SOLDAT NEGRU (HERMETIA ILLUCENS): DE LA FURAJ SUSTENABIL PENTRU ANIMALE LA SURSĂ ALIMENTARĂ EMERGENTĂ PENTRU OAMENI

Nicoleta UNGUREANU[1)], Nicolae-Valentin VLĂDUȚ[*2)], Sorin-Ștefan BIRIȘ[1)], Mariana IONESCU[1)], Neluș-Evelin GHEORGHIȚĂ[1)], Valeria-Elena VLĂDUȚ[1)], Oana-Elena MILEA[1,2)], Ștefan DUMITRU[1, 2)]

[1)] National University of Science and Technology Politehnica Bucharest / Romania;

[2)] National Institute of Research - Development for Machines and Installations Designed for Agriculture and Food Industry - INMA Bucharest / Romania.

**E-mail: valentin_vladut@yahoo.com*

Keywords: black soldier fly (BSF); insect larvae; alternative protein source; aquaculture feed; livestock feed; pet food; human food

ABSTRACT

The black soldier fly (BSF, Hermetia illucens) has emerged as a promising agent for circular bioeconomy models, addressing critical challenges related to organic waste management and protein supply. This paper explores the biological, nutritional, and functional attributes of BSF larvae that support their use in feed and food systems. The larvae demonstrate exceptional bioconversion efficiency, transforming a wide range of organic residues into high-value biomass rich in proteins, lipids, and micronutrients. Particular attention is given to their application in aquaculture, poultry, swine, and pet nutrition, where they enhance growth, immunity, and sustainability. BSF-derived products also show potential as alternative protein sources for human consumption, offering high nutritional value and low environmental impact. However, safety concerns, regulatory hurdles, and cultural perceptions continue to limit widespread adoption. The paper also reviews recent scientific findings, industrial applications, and legal frameworks governing BSF larvae use in the EU and globally. Overall, BSF larvae represents a sustainable and multifunctional protein source with expanding applications in both feed and food industries, provided that safety, processing standards, and consumer acceptance are adequately addressed.

REZUMAT

Musca soldat negru (BSF, Hermetia illucens) este tot mai recunoscută ca soluție sustenabilă în bioeconomia circulară, contribuind atât la valorificarea deșeurilor organice, cât și la diversificarea surselor de proteine. Lucrarea analizează caracteristicile biologice și nutriționale ale larvelor de BSF, care permit utilizarea acestora în sistemele de furajare și alimentație. Larvele prezintă o eficiență ridicată de conversie, transformând diverse resturi organice în biomasă bogată în proteine, lipide și micronutrienți. Aplicațiile lor în acvacultură, avicultură, creșterea porcinelor și hrana animalelor de companie sunt bine documentate, evidențiind beneficii privind creșterea, imunitatea și sustenabilitatea. Produsele derivate din BSF sunt tot mai explorate ca surse proteice pentru consumul uman, având valoare nutrițională ridicată și impact ecologic redus. Totuși, adoptarea largă este limitată de provocări legate de siguranță, reglementări stricte și bariere culturale. Lucrarea sintetizează și rezultatele recente, aplicațiile industriale și cadrul legislativ aplicabil la nivel european și global. În ansamblu, larvele de BSF reprezintă o sursă sustenabilă și multifuncțională de proteine, cu utilizări în creștere, atât în industria furajelor, cât și în alimentație, cu condiția respectării standardelor de siguranță și a acceptabilității consumatorilor.

INTRODUCTION

The growing global demand for sustainable food systems and alternative protein sources is intensifying due to the convergence of multiple crises: rapid population growth, climate change, depletion of agricultural resources, and unsustainable waste generation.

According to the United Nations, the world population is projected to exceed 9.7 billion by 2050, placing unprecedented pressure on land, water, and energy resources. This situation underscores the urgent

need for innovative food production strategies that are both ecologically sound and economically viable. Conventional meat production is no longer considered a sustainable source of protein (*Miron et al., 2023a*).

At the same time, the volume of organic waste, including food scraps, agricultural by-products, and animal manure, continues to grow, leading to significant greenhouse gas (GHG) emissions and environmental degradation when inadequately managed.

In this context, the black soldier fly (BSF, *Hermetia illucens*) has emerged as a promising solution within circular bioeconomy models. Its larvae can convert a wide variety of organic residues into high-value biomass, including protein-rich material suitable for use as animal feed and, increasingly, as a potential human food source. The valorization of BSF larvae addresses two critical challenges: improving organic waste management and diversifying protein supply chains in a sustainable manner.

Globally, insects are increasingly recognized as high-efficiency bio-converters and sustainable protein sources due to their low environmental footprint and ability to thrive on organic waste streams. Compared to conventional livestock, insect farming requires significantly less water, land, and feed, while producing far lower GHG emissions (*Seyedalmoosavi et al., 2022*).

Consequently, insects are being explored as viable alternatives for both feed and food applications in circular and resilient food systems. Insect farming has been proposed as a sustainable protein production strategy in response to multiple challenges: limited natural resources, climate change, supply chain disruptions, and competition between food, feed, and biofuel production (*Muscat et al., 2020*).

The production of edible insects as a protein source is considered two to five times more environmentally efficient compared to conventional animal-based protein sources (*Cruz et al., 2023*).

Table 1 presents a comparative assessment of energy use and environmental impacts associated with alternative protein sources.

Table 1

Energy and environmental impacts of the alternative protein sources

(EPRS, 2024)

Type of protein	Source	Comparison with conventional protein sources			
		Energy	**Land use**	**Water use**	**GHG emissions**
Insects	Black soldier fly	Higher to much higher than soy protein, depending on animal diet	Similar to feed formulations	Significantly higher than feed formulations	Similar to feed formulations
	Mealworm	Slightly higher than dairy and chicken; lower than beef	Significantly lower than beef; similar to chicken and feed formulations	Higher than beef and significantly higher than chicken and feed formulations	Significantly lower than beef; slightly lower than poultry; similar to feed formulations
Algae	Sugar kelp (*Saccharina latissima*)	Higher to much higher than soy protein	Lower to significantly lower than all conventional proteins	Much lower than conventional proteins	Higher than soy protein; lower than dairy and chicken; significantly lower than beef
	Spirulina or *Chlorella*	Lower to higher than beef, depending on the production process	Lower to significantly lower than all conventional proteins	Much lower than all conventional proteins	Significantly higher than soybean; higher than dairy and chicken; significantly lower than beef
Microbial fermentation	Mycoprotein (*Fusarium venetatum*)	Lower, similar to or higher than meat and soy protein	Lower than chicken; significantly lower than beef	Significantly lower to higher than meat	Lower than chicken; significantly lower than beef
	Dairy alternative	Lower, similar to or higher than dairy	Significantly lower than dairy	Lower, similar to or higher than dairy	Lower to significantly lower than dairy

Cultured meat	Cultured chicken	Higher to much higher than conventional chicken	Similar to or lower than chicken	Higher or similar to chicken depending on method	Higher than chicken
	Cultured beef	Slightly lower to much higher (up to 3 times higher) than beef	Significantly lower than beef	Significantly lower than beef	Lower to much lower than beef

To produce 1 kg of BSF larvae, only 1.5 kg of feed is required, an efficiency far superior to that of other livestock. For comparison, poultry requires 2.5 kg of feed, pigs 5 kg, and cattle up to 10 kg to achieve the same weight gain (*FAO, 2013*). This demonstrates the exceptional feed conversion efficiency of BSF larvae.

Figure 1 compares the amounts of water, land, and feed required to produce 100 kg of protein from various sources, emphasizing the resource efficiency of insect farming over conventional protein production.

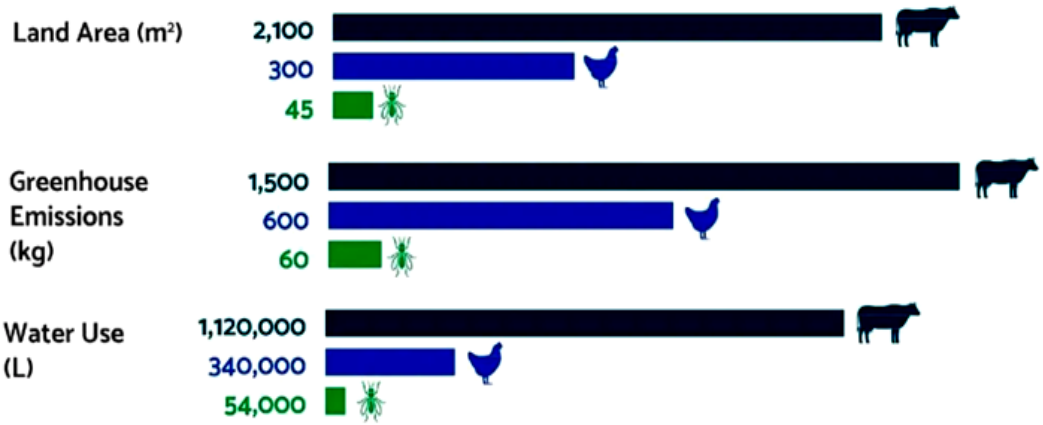

Fig. 1 - Resource inputs for insect protein production: a comparative analysis with beef and poultry (*https://hexafly.com/*)

To date, large-scale applications of BSF larvae have primarily focused on animal nutrition, particularly in aquaculture, poultry, and pet food sectors. However, advances in insect processing technologies, coupled with growing consumer interest in sustainable and functional foods, have created new opportunities for incorporating BSF-derived products into human diets (*Gahukar, 2011*). This potential is especially relevant in regions with limited agricultural resources or high levels of food insecurity, where insect-based proteins offer a scalable, nutrient-dense solution for enhancing food system resilience.

While the biological efficiency of BSF larvae in organic waste conversion is well documented, the next critical step is to understand how the resulting biomass can be safely and effectively integrated into feed and food chains. However, the adoption of insect-derived products is still limited by regulatory uncertainty and cultural resistance in many parts of the world.

A clear understanding of safety, consumer acceptability, and legal frameworks is essential to facilitate the global integration of insect-based proteins.

This review explores the dual role of BSF larvae as both animal feed and an emerging human food source. The analysis will examine the nutritional composition and safety aspects of BSF-derived products, current industrial applications, regulatory and cultural considerations, and the broader implications for food security and sustainable development.

By synthesizing existing scientific evidence and the regulatory landscape, this paper aims to support the integration of BSF-based proteins into future food systems.

BLACK SOLDIER FLY: BIOCONVERSION AND BIOLOGICAL PROFILE

Hermetia illucens is a dipteran insect of tropical origin, currently recognized as one of the most efficient bioconversion agents for organic waste streams. Its development includes five stages: egg, larva, prepupa, pupa and adult.

BSF larvae demonstrates resilience to challenging environmental conditions, including periods of drought, limited oxygen availability, and temporary food scarcity. However, optimal conditions for adult BSF mating and oviposition occur within a temperature range of 27–37 °C, with ambient humidity levels of 40–60% and relative humidity between 60–70% (*Jalil et al., 2021*).

Under controlled rearing conditions, the complete life cycle can be completed within 35–45 days, with the larval stage lasting around two weeks and representing the most metabolically active phase (*Chia, 2019*). During this phase, the larvae exhibit voracious feeding behavior and can degrade a wide range of organic substrates, including agricultural by-products, household food waste, and animal manure.

This results not only in a substantial reduction in waste volume and environmental pollutants, but also in the accumulation of valuable larval biomass. Both acidic (pH 2, 4, and 6) and alkaline (pH 8 and 10) environments support relatively high survival rates of BSF larvae. However, the pH range of 6 to 10 has been identified as significantly more favorable for optimal larval development and increased biomass accumulation compared to the more acidic range of pH 2 to 4 (*Meneguz et al., 2018; Pang et al., 2020*).

This enhanced performance is attributed to the alkalization of the substrate induced by larval metabolic activity, which promotes protease enzyme activation. The resulting increase in proteolytic activity facilitates greater protein availability, thereby supporting improved larval growth and weight gain.

At the final stage of development, larvae can reach lengths of up to 27 mm, widths approaching 6 mm, and a weight near 220 mg (*Makkar et al., 2014*). During the prepupal phase, the last stage before metamorphosis, they clear their digestive tracts and depart from their feeding environment to find a dry, protected site suitable for pupation.

This instinctive behavior, termed “self-harvesting,” has greatly simplified larval collection by removing the need for manual harvesting efforts previously required in farming operations. At this point, the larvae have attained their largest physical dimensions and possess a protein content between 35–45%, and approximately 35% lipids. They usually complete their transformation into adults within about two weeks. The lipids reserved in their body is converted into energy for adults’ mating and continuous life cycle (*Amrul et al., 2022*).

Compared to other insects used for organic waste management, BSF larvae offer multiple advantages: a rapid growth cycle, high feed conversion rate (<2), resilience to many pathogens, and adaptability to large-scale production systems.

Moreover, BSF do not act as vectors for human diseases and do not require feeding during the adult stage, which simplifies management in industrial environments. Their ability to thrive on low-value substrates, combined with compatibility with vertical farming systems, makes them particularly attractive for decentralized waste treatment models and sustainable biomass production.

BSF rearing can be implemented in fully enclosed, automated facilities that minimize contamination risks and ensure high levels of biosecurity. Furthermore, integrated insect farming within closed-loop systems allows for precise control over environmental conditions, substrate inputs, and waste outputs.

These modular and scalable designs support flexible industrial deployment in both centralized and decentralized contexts. Their tolerance to a wide range of environmental factors further reinforces their suitability for diverse operational settings. The by-product of the process, frass, is rich in nutrients and can be valorized as an organic fertilizer, contributing to the circularity of the system.

Although a higher moisture content in organic waste enhances larval growth rates, levels exceeding 80% significantly hinder the separation of frass from the black soldier fly larvae biomass through sieving techniques (*Cheng et al., 2017*).

This biological efficiency and operational flexibility have stimulated increasing interest in the downstream applications of BSF larvae, both as animal feed and, more recently, as potential ingredients for human food. Before their use as feed or food, BSF larvae are harvested at the prepupal stage and must undergo post-harvest processing to ensure product safety and quality.

This refinement includes steps such as killing (commonly by blanching in boiling water), cleaning, sterilization, and fractionation to separate proteins and lipids as needed. To ensure shelf stability, the final products should contain less than 10% moisture and fat (*Amrul et al., 2022*). Moisture reduction is typically achieved through sun drying or controlled drying methods, while oil pressing is employed to reduce lipid content.

These processing steps are essential to produce safe, stable, and hygienic larvae-based products suitable for various applications.

COMPOSITION OF BSF LARVAE

The nutritional profile of *Hermetia illucens* larvae is a key factor driving their increasing relevance in sustainable food and feed systems. It is important to note that the primary nutritional components of BSF larvae, specifically proteins and lipids, exhibit significant variability depending on the substrates used for their rearing (*Suryati et al., 2023*).

Dried BSF larvae typically contain between 35% and 45% crude protein and 15% to 35% lipids, with variations depending on the larvae's developmental stage and the substrate on which they are reared (*Macwan et al., 2023; Muslykhah et al., 2024*). The protein fraction is rich in essential amino acids such as lysine, methionine, and threonine, providing a high-quality protein source for animal nutrition.

In addition to protein, BSF larvae contain antimicrobial peptides, the biopolymer chitin and its derivative chitosan, as well as various fatty acids (*Macwan et al., 2023; Muslykhah et al., 2024*). The average ash content of BSF larvae is approximately 82.4 g/kg, ranging from 27 g/kg to 132 g/kg, which is higher than that of conventional soybean meal (71.9 g/kg) but lower than fishmeal (171.5 g/kg). The crude fiber content averages 95.4 g/kg, with a range between 41 g/kg and 213 g/kg, exceeding the crude fiber found in soybean meal (74.3 g/kg) and being substantially greater than that of fishmeal (2.6 g/kg). The average chitin content is 61.7 g/kg, varying between 38.7 g/kg and 72.1 g/kg (*Lu et al., 2022*).

BSF larvae oil consists mainly of triglycerides and phospholipids, with relative proportions influenced by diet and rearing conditions (*Tognocchi et al., 2024*). It typically contains less than 0.5% free fatty acids and is rich in saturated fatty acids, particularly lauric, palmitic, myristic, and stearic acids, alongside monounsaturated fatty acids synthesized by the larvae (*Muangrat and Pannasai, 2024*).

Lauric acid is associated with immunomodulatory effects, including anti-inflammatory, antimicrobial, and antioxidant properties, making it valuable in skin treatments, medicines, and cosmetics. While total fat content depends on the larvae's diet, the fatty acid profile remains relatively stable under consistent rearing conditions (*Quigley et al., 2025*). Beyond their high protein and lipid content, BSF larvae are rich in essential micronutrients and bioactive compounds, enhancing their value as sustainable, nutrient-dense feed ingredients (*Cruz et al., 2023*). Notably, they provide elevated levels of calcium (Ca), phosphorus (P), zinc (Zn), and iron (Fe), with a calcium-to-phosphorus ratio particularly well-suited to the dietary requirements of monogastric animals such as poultry and aquaculture species.

When compared to conventional protein sources like fishmeal, soybean meal, and meat by-products, BSF larvae biomass offers competitive or superior nutritional qualities. Although fishmeal contains a slightly higher protein content, BSF larvae provide advantages in fat quality, especially due to their lauric acid content, as well as sustainability and independence from overexploited marine resources. In contrast to soy protein, BSF larvae deliver a more balanced amino acid profile and circumvent environmental issues related to land-use change and deforestation.

Table 2

Comparative nutritional profile of BSF larvae and other protein sources (per 100g dry matter)

(*Authors' own elaboration*)

Parameter	BSF Larvae	Fishmeal	Chicken meat	Soy protein
Protein (%)	35–45	60–72	27–30	36
Lipid (%)	15–35	8–12	14	18
Lauric acid	High (up to 50% of total fat)	Absent	Low	None
Calcium (mg)	150–250	50–80	10–15	200
Phosphorus (mg)	180–240	1,200–1,500	200	550
Zinc (mg)	5–8	2–4	1.5	3
Iron (mg)	5–10	2–4	1	9
Essential amino acids	Complete set	Complete set	Complete set	Low in methionine
Sustainability	High – waste-based	Medium – marine stock depletion	Medium – land use	Low – deforestation risk

The chemical composition of BSF larvae is strongly influenced by rearing conditions such as substrate type and quality, temperature, moisture, light exposure, and larval density. Protein content generally increases when larvae are fed substrates rich in nitrogen, whereas lipid content varies with carbohydrate availability (*Tognocchi et al., 2024*). Environmental factors also affect developmental rates and nutrient accumulation; for example, suboptimal temperatures can slow development but reduce biomass yield and nutrient density (*Muangrat and Pannasai, 2024*).

Understanding and optimizing these parameters is essential to tailor BSF larvae production to specific nutritional goals, whether for animal feed or future food-grade applications. The values presented in Table 2 are indicative and may vary depending on raw material origin, processing methods, and analytical techniques. BSF larvae are distinguished by their high lauric acid content, which is absent in conventional protein sources.

Although fishmeal offers a higher protein concentration, its sustainability is increasingly challenged due to pressure on marine ecosystems. Soy protein lacks certain essential amino acids, particularly methionine, and its production is associated with deforestation risks. BSF larvae production, based on organic waste streams, offers a circular and environmentally sustainable alternative.

BSF LARVAE AS FEED: USE, BENEFITS, AND REGULATIONS

Although more than 2,000 insect species are considered edible and traditionally consumed by humans across 113 countries, not including the western nations (*Tao and Li, 2018*), only a limited number have been extensively studied for their potential use as feed in livestock and aquaculture systems. Among the most researched species are the yellow mealworm (*Tenebrio molitor* L., Coleoptera: Tenebrionidae), the black soldier fly (*Hermetia illucens* L., Diptera: Stratiomyidae), and the house fly (*Musca domestica* L., Diptera: Muscidae) (*Meneguz et al., 2018*).

Over the past 30 years, the black soldier fly has gained significant attention as a sustainable and nutritious alternative protein source in animal feed formulations. The protein meal, oils, and other by-products derived from BSF larvae processing represent valuable ingredients for animal feed. BSF larvae are considered safe for animal consumption as they are free from pests and do not bioaccumulate mycotoxins or pesticides (*Raksasat et al., 2020*).

While historically there has been some social hesitation regarding the use of insects in animal feed, this stigma has substantially diminished recently due to increased awareness of their sustainability and safety, leading to growing acceptance within livestock and aquaculture industries.

The inclusion of BSF larvae in animal feed offers multiple benefits, including reducing the risk of diseases transmitted by animals, enhancing overall health and growth performance of livestock, and significantly lowering the costs associated with animal production (*Nyamuhirwa et al., 2025*).

Dry edible insects provide between 50% and 80% of the protein required for animal nutrition. The primary target species for BSF larvae use include poultry, swine, beef, and aquaculture. Numerous studies have demonstrated both nutritional and functional benefits of BSF larvae in these diets. BSF larvae offer a balanced amino acid profile, high-quality lipids, especially antimicrobial lauric acid, and bioactive compounds that support animal health, growth performance, and immune function.

The oil extracted from BSF larvae represents a potentially more sustainable alternative to palm and coconut oils, which are commonly used in calf milk replacers worldwide (*Quigley et al., 2025*). The sustainability of palm and coconut oils is increasingly debated, particularly in the European Union, due to serious concerns including deforestation, biodiversity loss, destruction of rainforest habitats for endangered species, land clearing by fire, and displacement of local communities in palm-growing regions (*Oosterveer, 2020*).

In aquaculture, BSF larvae protein has been successfully incorporated into diets for species such as species such as tilapia, freshwater prawns, catfish, shrimp, and other omnivorous fish. Studies have demonstrated that BSF larvae meal plays a multifaceted role in supporting the health and performance of culturable aquatic species.

BSF larvae meal has been shown to regulate survival and growth rates, enhance both specific and non-specific immune responses, and improve disease resistance against a range of pathogens. In addition, it contributes to the modulation of intestinal microbiota, promoting a more balanced and functional gut environment. Several investigations have also reported that dietary inclusion of BSF larvae meal can improve the expression of genes related to growth and immunity, further underlining its potential as a functional feed ingredient in aquaculture systems (*Bruni et al., 2020; Mohan et al., 2022*).

In swine and poultry nutrition, BSF larvae-based feeds contribute to improved gut health and nutrient absorption. BSF larvae is a valuable feed component for pigs because of its high fat content and protein composition, including a well-balanced amino acid profile tailored to swine nutritional requirements (*Oh et al., 2024*).

Inclusion of BSF larvae in pig diets has not been shown to adversely affect growth performance, feed intake, nutrient digestibility, or intestinal morphology. In some cases, positive effects have been observed, such as improved growth rates, enhanced feed conversion ratios, and beneficial shifts in caecal microbiota composition (*Biasato et al., 2020*; *Yu et al., 2020*). Furthermore, pigs demonstrate a strong preference for live BSF larvae, exhibiting high motivation to interact with and consume them compared to other feed or enrichment options (*Ipema et al., 2021*).

Feeding trials have shown that BSF larvae can partially or fully replace traditional protein sources such as soybean and maize meals without compromising growth rates or feed conversion ratios. Soybean-based feeds can be entirely substituted with BSF larvae meal and fats in diets of high-performing laying hens (*Xin et al., 2024*). BSFL supplementation (50%) or total replacement of soybean cake in the diets of laying hens had no impact on hen health or performance and little to no effect on the eggs themselves (*Maurer et al., 2016*). BSF larvae oil represents a sustainable and nutrient-dense alternative in poultry and broiler chicken diets, contributing to enhanced meat quality, improved blood profiles, and beneficial impacts on muscle metabolism (*Somparn et al., 2024; Srikha et al., 2024*). However, due to nutritional variations among larvae derived from different sources, the quality of the insect material must be carefully evaluated before use (*Heuel et al., 2021*).

The use of BSF larvae as feed for ruminants has shown limited success, primarily due to their high chitin and fat content, which negatively affect ruminal fermentation and nutrient digestibility (*Jayanegara et al., 2017*). However, studies have shown that BSF-derived fat can be successfully incorporated into the diets of dairy cows, resulting in improved milk yield and quality, likely due to enhanced digestive efficiency and strengthened immune function (*Nekrasov et al., 2022*). Beyond livestock and aquaculture, BSF larvae are increasingly used in pet food formulations for companion animals such as dogs and cats.

The insect-derived proteins are hypoallergenic and easily digestible, making them suitable for animals with sensitivities to conventional protein sources. Additionally, the presence of lauric acid and other beneficial lipids supports digestive health and may have antimicrobial effects (*Freel et al., 2021; Li et al., 2024*). Dried whole black soldier fly larvae have been shown to support gestation, lactation, and growth in cats when included in their diet (*Banks et al., 2025*). Products containing BSF larvae protein include dry kibble, treats, and nutritional supplements, with growing market acceptance driven by environmental sustainability and functional benefits. BSF larvae can also be processed into soft gel capsules for cats, dogs, rabbits and other pets, offering a convenient and palatable source of high-quality proteins and essential fatty acids, including omega-3, omega-6, and omega-9, which support skin and coat health, immune function, and overall well-being.

BSF larvae oil

Whole dried BSF larvae

BSF larvae fish food

BSF larvae gel capsules

Dried mealworms from BSF larvae

Dried BSF larvae for chicken

BSF proteic bar for dogs

Dog food with BSF larvae

Fig. 2 - Various BSF larvae-derived products for animal feed

The regulatory framework in the European Union regarding insect-derived proteins has evolved progressively over recent years. Initially, Regulation (EU) 2017/893 authorized the use of processed animal proteins (PAPs) derived from insects exclusively in aquaculture feeds, marking the first significant step toward integrating insect proteins into animal nutrition.

Subsequently, this authorization was expanded by Regulation (EU) 2021/1372 to include poultry and swine feeds, reflecting growing confidence in the safety and efficacy of BSF larvae products for these livestock species. Despite these approvals, the regulations impose stringent conditions to ensure feed safety.

A crucial requirement is the strict prohibition of substrates containing catering waste or materials of animal origin for larval rearing, as these pose risks related to transmissible spongiform encephalopathies and other contaminants.

Consequently, BSF larvae must be reared exclusively on substrates derived from plant-based or non-animal organic waste streams, such as vegetable residues, manure-free food processing by-products, or agricultural waste.

These measures collectively aim to safeguard animal health while promoting sustainable and safe use of insect-derived proteins within the European Union feed industry.

Under European Union's regulations, insects may only be reared on substrates of vegetable origin or on specifically authorized materials of animal origin, such as fishmeal and hydrolyzed proteins derived from non-ruminants. Furthermore, substrates must exclude manure, catering waste, and other prohibited waste materials (*Lähteenmäki-Uutela et al., 2021*).

In some regions, however, regulations governing the safety of substrates used for insect rearing may not be as stringent as those enforced by the European Union. According to experts, the primary obstacle preventing the global development of the insect production sector is the stringent regulatory framework imposed by the European Union (*Van Huis & Gasco, 2023*).

Compliance with Regulation (EC) No 183/2005 on feed hygiene and Regulation (EC) No 767/2009 on the marketing and use of feed ensures traceability and quality control throughout the production chain. Additionally, insect producers must follow Good Manufacturing Practices (GMP) and Hazard Analysis and Critical Control Points (HACCP) principles to minimize contamination risks.

Adherence to these legislative frameworks is essential for commercial BSF larvae producers to guarantee product safety, regulatory approval, and market acceptance within the European Union. It is important to note that, initially, insect proteins were not universally authorized for all farmed animal species but only for specific uses; the authorization process and conditions vary depending on the target animal species and feed category.

BSF LARVAE AS FOOD FOR HUMANS: POTENTIAL AND CHALLENGES

Black soldier fly larvae contain approximately 42–45 g of crude protein per 100 g of dry matter (*Miron et al., 2019*), including all essential amino acids required in the human diet (*Montevecchi et al., 2021*). Therefore, BSF larvae represents a promising and nutritionally complete protein and lipids source for applications in the food industry (*Smetana et al., 2016; Miron et al., 2023a*).

To harness these nutritional benefits, BSF larvae can be processed through specific extraction steps to obtain protein and lipid-rich ingredients suitable for food applications (Figure 3).

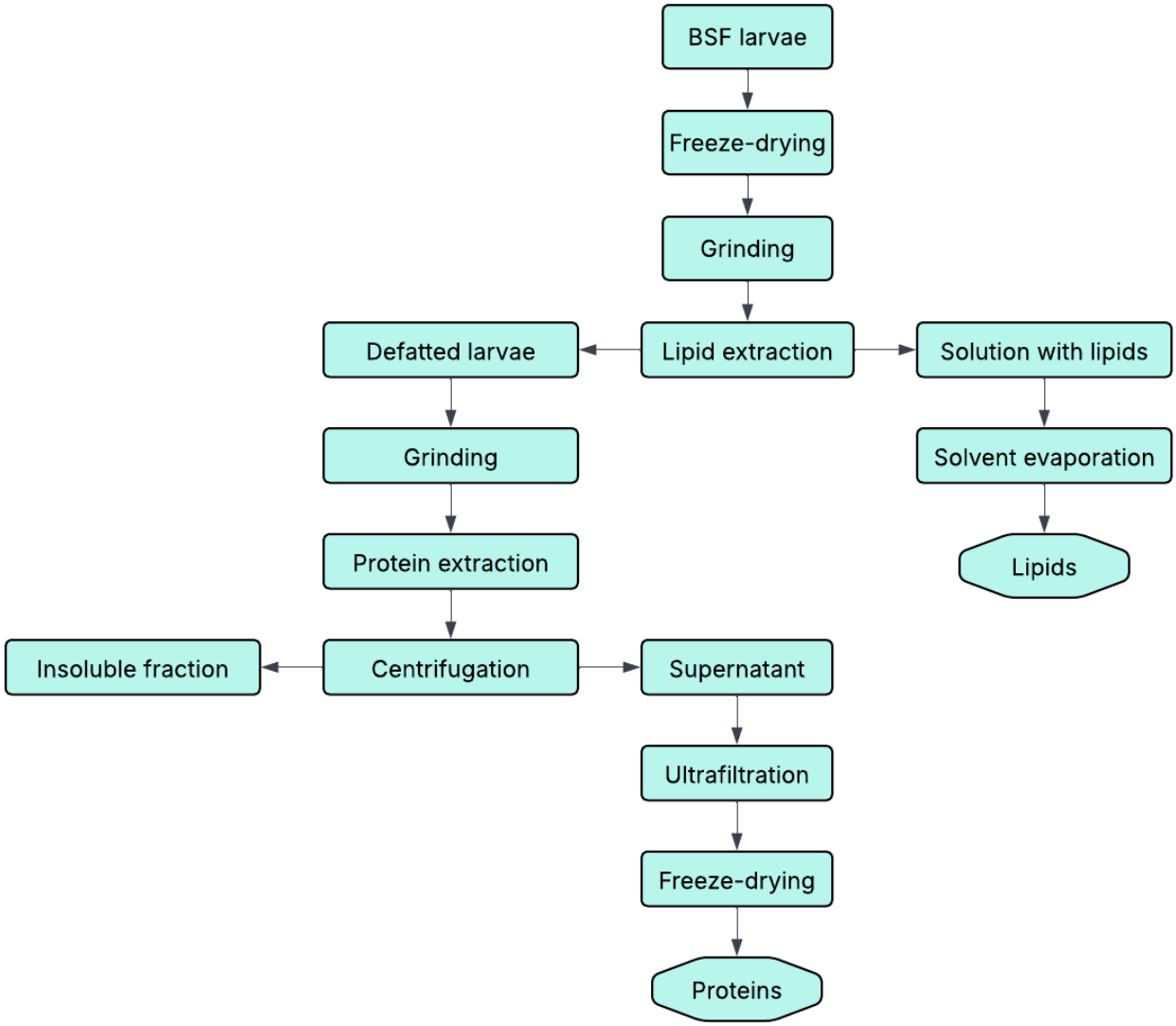

Fig. 3 - Flow diagram of protein and lipid extraction from black soldier fly larvae
(adapted from Miron et al., 2023a, under the terms of under the CC BY-NC-ND 4.0 license)

Several BSF larvae-derived products for human consumption have been developed or proposed, including dried snacks, protein powders, oils, and fermented forms, as well as their incorporation into familiar foods such as pasta, biscuits, protein bars, sausages, or protein-enriched flours used in baking and meal fortification. Insects have even been proposed as a viable protein source for space missions.

Researchers in China, Japan, and the United States are actively exploring the potential of insects as sustainable nutrition options for astronauts during space travel and aboard space stations (*FAO, 2013*).

BSF protein bar | BSF larvae oil | BSF larvae snacks (Life Origin) | Roasted BSF larvae

Fig. 4 - BSF-larvae derived products for human consumption

The commercial production and availability of farmed insects have experienced the most rapid expansion in South-East Asia, particularly through the development of cricket farming, which began in Thailand and has subsequently spread to neighboring countries such as Laos and Cambodia. Despite this

growth, national food consumption data in Thailand do not specifically categorize edible insects, although several insect species are included in national food composition tables across South-East Asia and select African countries (*EFSA, 2015*). Among the edible insect species gaining attention, BSF larvae are increasingly consumed in certain Asian countries, notably Vietnam and Thailand, where entomophagy is culturally embedded and traditionally practiced. BSF larvae are typically prepared through washing and boiling or roasting and are either consumed whole or incorporated into composite dishes such as soups, stir-fries, and snacks.

In addition to these methods, sun-drying and deep-frying are employed in some regions to enhance shelf life and flavor. In addition to direct consumption, BSF larvae are also processed into fermented products or ground into pastes used to fortify sauces and condiments with added nutritional value.

In Thailand, for example, BSF larvae are sometimes transformed into protein-rich powders, which are incorporated into noodles, rice-based products, or used as seasoning. Larval oil, extracted via mechanical pressing or solvent-based techniques, is utilized in culinary applications or as a dietary supplement, owing to its high lauric acid concentration and associated antimicrobial benefits. In Malaysia, BSF larvae are consumed raw alongside tapai, a traditional fermented beverage, with the larvae being collected from the fermented tapioca used in its production (*Wang and Shelomi, 2017*).

Although not yet widely adopted, these practices underscore a growing consumer interest in sustainable and nutrient-dense protein alternatives. BSF larvae appeal both through their rich nutritional profile, high in protein, lipids, and micronutrients such as calcium, iron, and zinc, and through their pleasant umami flavor and crunchy texture when roasted or fried.

Despite cultural familiarity with entomophagy in many Asian societies, BSF larvae remain less commonly consumed than more traditional edible insects such as crickets or silkworm pupae. However, interest in BSF is increasing due to its efficiency in organic waste conversion and superior nutrient profile, particularly in areas where food security and sustainability are pressing concerns.

As a result, BSF is gradually being incorporated into local food systems, both in rural settings and through urban initiatives promoting alternative proteins. Some small-scale food enterprises and agricultural cooperatives have started developing BSF-based food products aimed at school meals or nutritional programs, especially in regions affected by undernutrition.

Although crickets are widely consumed in many Asian and African countries, where entomophagy is culturally accepted and long practiced, in the European Union and other Western regions, the idea of farming and eating insects is still met with skepticism.

Nevertheless, interest is slowly growing. In Europe, several cricket farms have emerged in countries such as the Netherlands, Belgium, and Finland, focusing on the production of cricket powder and snacks for human consumption. At the same time, in highly developed countries such as Canada and the USA, several organic-certified farms have been established to raise crickets for food, offering products like roasted crickets, cricket powder, and frozen crickets.

These developments indicate a growing acceptance and commercialization of edible insects in both traditional and non-traditional regions, paving the way for exploring other insect species such as the BSF for both feed and food purposes.

A few innovative start-ups have emerged in Europe, attempting to introduce BSF-based foods through rebranding strategies that emphasize their nutritional and ecological advantages.

One of the key barriers to acceptance in Western cultures is the strong sense of disgust and the persistence of social taboos associated with eating insects, mainly because insects have never played a substantial role in Western food culture (*FAO, 2013; Bessa et al., 2020*). However, this perception may slowly shift due to increased awareness of the environmental benefits of insect farming, as well as rising concerns about food security and the ecological impact of conventional livestock production.

The presence of BSF larvae in pet food and animal feed, already authorized in the European Union, has contributed indirectly to increasing familiarity with the species. This growing exposure, particularly through pets, may help reduce the psychological distance between humans and insect-based products, potentially enhancing future acceptability.

Consumers are generally more willing to accept insect-based foods when insects are incorporated in processed or invisible forms, rather than presented whole (*Bußler et al., 2016; House, 2016*). Using water-soluble insect proteins in food formulations is a particularly effective strategy, as it helps reduce the visibility of the insect origin and may ease the psychological barriers related to entomophagy.

Beyond consumer perception, these soluble proteins have demonstrated valuable techno-functional properties, such as foaming and gelation, making them suitable as food additives (*Laroche et al., 2019; Dharani et al., 2025*). One promising application of insect-derived proteins is in the development of meat analogues, which are designed to replicate the sensory and, in some cases, chemical attributes of traditional meat (*Joshi & Kumar, 2015*).

These products typically include ingredients like soy protein, wheat gluten, mushrooms, legumes, algal proteins (*Jones, 2016*), and increasingly, insect proteins (*Azzollini et al., 2019*), often combined with fats and flavorings to mimic the taste and texture of meat or seafood (*Kyriakopoulou et al., 2019*).

From a legal standpoint, the consumption of BSF larvae in the European Union falls under the scope of Regulation (EU) 2015/2283 on Novel Foods, adopted in November 2015, which governs the authorization of food products without a significant history of consumption within the European Union before 1997 (*de Boer and Bast, 2018; Lähteenmäki-Uutela et al., 2021*).

The European Food Safety Authority's 2016 guidance document further elaborates on the criteria necessary for novel food approval, encompassing data on composition, production methods, toxicological and allergenic potential, and anticipated levels of human exposure (*EFSA, 2016*).

In addition to the Novel Food Regulation, several other legislative frameworks are applicable. Regulation (EC) No 852/2004 on the hygiene of foodstuffs outlines general food safety requirements, including the implementation of HACCP principles and adherence to good manufacturing practices.

Furthermore, Regulation (EU) 2017/893, although focused on the use of insects in animal feed, sets a useful precedent for the safe use of BSF larvae as a biological resource (*Lähteenmäki-Uutela et al., 2021*).

Currently, *Hermetia illucens* larvae are not included on the list of approved edible insects under the European Union's Novel Foods Regulation and therefore remain subject to the novel food authorization process for human consumption (*Miron et al., 2023b*).

While insect-based products such as *Tenebrio molitor*, *Locusta migratoria*, *Acheta domesticus*, and *Alphitobius diaperinus* have been granted authorization under the Novel Food Regulation, BSF larvae remain under evaluation, and no positive scientific opinion from EFSA has been issued to date regarding their suitability for human diets.

Consequently, the use of BSF larvae continues to be legally restricted to non-food applications, including animal feed, pet food, and fertilizers, where they are subject to strict safety, hygiene, and traceability standards.

Within the European Union, several farms and companies in countries such as France, the Netherlands, and others are already producing and marketing BSF larvae-based products intended for human consumption. These activities currently operate under specific national regulations and are subject to local food safety standards, as a unified European Union wide approval for BSF larvae as food has not yet been granted.

Despite their rich nutritional profile, several health risks associated with the consumption of BSF larvae have been reported in scientific literature. Documented adverse effects include gastrointestinal discomfort (e.g., nausea, cramps, diarrhea), often linked to microbial contamination or inadequate processing techniques.

Another important concern is the allergenic potential, particularly among individuals sensitized to crustaceans or dust mites, due to shared allergens such as tropomyosin and arginine kinase. Moreover, if larvae are reared on poorly controlled substrates, there is a risk of bioaccumulation of heavy metals or contamination with pathogens such as *Salmonella* or *Listeria monocytogenes*.

The safety of direct human consumption of BSF larvae was evaluated by examining microbial, heavy metal, and allergenic hazards. The findings indicated that blanching effectively reduced both *Escherichia coli* counts and the total viable microbial load by approximately 3 log units.

No *Salmonella* or *Listeria* species were detected. Heavy metal residues were detected but remained below established legal thresholds. However, cross-reactive allergens such as tropomyosin and arginine kinase were identified, although their clinical relevance remains to be clarified.

These results underscore the importance of proper decontamination methods, such as blanching, and highlight the influence of rearing substrates on safety outcomes (*Bessa et al., 2021*). A recent study investigated the microbiological quality of BSF larvae intended for human consumption, analyzing the effects of different rearing substrates, including those permitted by European Union regulations (cereals, fruits, vegetables) and others not permitted (e.g., co-products, nearing shelf-life or meat-based substrates).

The results highlight that substrate choice significantly influences microbial load and safety outcomes, emphasizing the need for strict monitoring and judicious selection of larval feed sources to mitigate health risks (*Brulé et al., 2024*).

To address these concerns, European Union regulations require the implementation of rigorous safety protocols, including validated thermal processing methods, full traceability of production chains, and comprehensive toxicological assessments. In practice, safe and standardized processing steps typically include blanching, drying, grinding into powder, oil extraction, and hygienic packaging. Given the allergenic potential and the novelty of insect-based foods, it is essential that products containing BSF larvae are accompanied by clear labeling and transparent consumer information to ensure safe and informed consumption.

Overall, while BSF larvae hold considerable promise as a sustainable and nutrient-dense food source, their widespread adoption for human consumption remains contingent on successfully addressing regulatory, health-related, cultural, and technological challenges.

INDUSTRIAL BSF FARMING AND COMMERCIAL PROSPECTS

In recent years, industrial-scale insect farming has grown significantly, driven by increasing demand for sustainable protein sources in both animal feed and human food sectors. In European insect production systems, species such as *Hermetia illucens* are typically reared in enclosed, controlled environments, such as boxes or cages, where key parameters like temperature, humidity, substrate composition, and water availability are precisely regulated.

When larvae represent the target harvest stage, they are grown directly on organic substrates that also serve as the medium for frass (insect waste) excretion. Egg deposition onto the substrate can occur through natural oviposition by adult flies or be facilitated manually or mechanically. Harvesting the larvae generally requires active separation from the substrate.

Furthermore, in the pre-pupal stage, BSFL naturally migrate away from the feeding substrate in search of a dry, elevated area, a behavior known as “self-harvesting”, which eliminates the need for manual collection and simplifies the harvesting process (*Wang and Shelomi, 2017*).

In small-scale or traditional farms, this is often done manually through sieving. In contrast, industrial-scale facilities employ automated systems specifically designed to optimize the efficiency of larval separation. In less industrialized systems, insects are typically deprived of feed for several hours or days before harvest to allow for gut emptying, a depuration step intended to improve hygiene. However, this procedure is not always practiced in industrial settings, where larvae usually undergo extensive post-harvest processing that may eliminate the need for prior intestinal clearance (*EFSA, 2015*).

Companies specializing in BSF larvae production have diversified their operational models, targeting various applications such as aquaculture, pet food, livestock feed, and, increasingly, human consumption. While leading producers are primarily based in Europe and North America, emerging markets are also showing increased interest and investment. Leading industrial producers such as Hexafly (Ireland),

Protix (Netherlands), InnovaFeed (France), and Agronutris (France) have established themselves as pioneers in large-scale BSF larvae production, emphasizing traceability, biosecurity, and sustainability throughout their operations.

- Hexafly (Ireland) is a company specialized in the industrial-scale cultivation of Hermetia illucens through vertical farming systems. The company applies circular economy principles by converting organic waste streams into high-value insect-derived products, including a protein-rich meal, insect oil, and an organic frass-based biofertilizer. Its production process is designed to operate with minimal land, water, and energy inputs, while maintaining high levels of efficiency and environmental sustainability. The resulting protein and oil are primarily targeted toward both human food and animal nutrition sectors, including aquaculture, pet food, and livestock feed, whereas the frass is utilized in agriculture as a natural soil enhancer with biostimulant properties. Through technological innovation and a zero-waste approach, Hexafly demonstrates the potential of insect bioconversion as a scalable solution to global challenges in food security, resource efficiency, and sustainable agriculture (*https://hexafly.com/).*

- Protix (Netherlands) operates across the entire value chain of Hermetia illucens production, from rearing larvae on carefully selected organic waste streams to processing them into high-quality

insect-based products. In its fully integrated facility, the company transforms up to 250,000 tonnes of food waste per year into valuable outputs, including up to 70,000 tonnes of live larvae equivalent. These are further processed into protein-rich meals, insect oils, fresh larvae mass, and organic fertilizers. Protix primarily supplies these ingredients to the aquaculture, pet food, and livestock feed industries, while also exploring innovative applications such as fermented insect products to improve digestibility and functionality, as well as the potential for use in human food (https://protix.com/).

- InnovaFeed (France) specializes in the industrial-scale production of Hermetia illucens larvae. Their vertically integrated operations encompass breeding, rearing, and processing larvae into high-quality insect-based products. These products include Hilucia™ Protein and Hilucia™ Oil, which are primarily utilized in aquaculture, pet food, and livestock feed sectors. Additionally, Innovafeed produces Hilucia™ Frass, a 100% natural organic fertilizer derived from insect droppings, contributing to sustainable agriculture practices. The company employs a unique industrial symbiosis model, optimizing resource efficiency and minimizing environmental impact. Innovafeed's commitment to sustainability and innovation positions them as a key player in the insect-based nutrition industry (https://innovafeed.com/en/).

- Agronutris (France) is a biotechnology company specializing in the large-scale breeding and processing of insects, particularly the black soldier fly (Hermetia illucens), mealworm (Tenebrio molitor), and cricket (Gryllodes sigillatus). Their vertically integrated operations encompass the entire value chain, from insect breeding and bioconversion of organic by-products to the production of high-quality insect-based ingredients. These include protein-rich insect meal and oils, which are primarily utilized in aquaculture, pet food, and livestock feed sectors. Additionally, Agronutris produces organic fertilizers from insect frass, contributing to sustainable agriculture practices. The company employs a circular economy model, transforming agro-industrial co-products and bio-residues into valuable nutritional ingredients, thereby reducing environmental impact and promoting resource efficiency. Their commitment to sustainability and innovation positions them as a key player in the insect-based nutrition industry. *(https://www.agronutris.com/en/).*

Together, these companies illustrate the commercial viability of BSF LARVAE farming and processing, offering a range of products, from live larvae and dried meals to specialized functional ingredients that contribute substantially to circular economy initiatives and help reduce dependence on conventional protein sources.

In the European Union, the sector continues to grow rapidly, supported by ongoing innovation, favorable policy trends, and a rising demand for alternative proteins. Countries such as France and the Netherlands are at the forefront of industrial insect farming, benefiting from strong regulatory frameworks and public-private partnerships. Romania also shows potential for development, particularly due to local interest and the availability of agri-food waste as a substrate for insect rearing.

However, the absence of specific national regulations and dedicated investment incentives remains a limiting factor for large-scale deployment. With increasing awareness of environmental sustainability, resource efficiency, and food security, BSF farming is well positioned to become a strategic sector within the emerging bioeconomy. Its potential contributions span circular agriculture, waste valorization, and innovation in both food and feed production.

CONCLUSIONS AND FUTURE DIRECTIONS

Black soldier fly (*Hermetia illucens*) larvae represent one of the most promising sustainable protein sources for both animal feed and human food applications. Their exceptional ability to convert a wide range of organic waste streams into high-quality biomass rich in protein, lipids, and micronutrients makes them ideal candidates for integration into circular bioeconomy models.

In animal nutrition, particularly in aquaculture, poultry, and swine sectors, BSF larvae have demonstrated positive effects on growth performance, feed efficiency, and immune function, while also contributing to reduced environmental impact and feed costs.

Beyond feed, BSF-derived products are increasingly explored as alternative protein sources for human consumption due to their complete amino acid profile, high lauric acid content, and techno-functional properties.

They offer opportunities for innovation in functional foods, protein supplements, and meat analogues, especially in regions facing food security challenges or resource constraints. However, despite their nutritional potential, several barriers still limit their broader adoption, particularly in Western markets. Regulatory constraints, allergenic concerns, and consumer skepticism, often rooted in cultural perceptions, remain significant hurdles.

To facilitate the mainstream use of BSF larvae in food systems, future developments should prioritize the implementation of rigorous safety protocols, standardized processing methods, and transparent labeling practices. Further research is also needed to assess long-term health risks, including allergenicity and bioaccumulation, and to provide clear scientific evidence supporting their safety.

Public education campaigns and rebranding strategies that highlight the ecological and nutritional benefits of insect-derived products can play a key role in shifting consumer attitudes.

With coordinated efforts in legislation, industry, and research, BSF larvae can contribute meaningfully to building more sustainable, resilient, and resource-efficient food systems.

REFERENCES

[1] Amrul, N. F., Kabir Ahmad, I., Ahmad Basri, N. E., Suja, F., Abdul Jalil, N. A., & Azman, N. A. (2022). A review of organic waste treatment using black soldier fly *(Hermetia illucens). Sustainability*, 14(8), 4565. https://doi.org/10.3390/su14084565.

[2] Azzollini, D., Wibisaphira, T., Lakemond, C. M. M., & Fogliano, V. (2019). Toward the design of insect-based meat analogue: the role of calcium and temperature in coagulation behavior of *Alphitobius diaperinus* proteins. LWT-Food Science & Technology, 100, 75–82. https://doi.org/10.1016/j.lwt.2018.10.037.

[3] Banks, I. J., Adams, D., Belgrave, J. R., Lewis, E. A., & Koutsos, E. A. (2025). Dried whole black soldier fly larvae consumption supports gestation, lactation, and growth in cats. *Animals,* 15(8), 1078. https://doi.org/10.3390/ani15081078.

[4] Bessa, L. W., Pieterse, E., Marais, J., & Hoffman, L. C. (2020). Why for feed and not for human consumption? The black soldier fly larvae. *Comprehensive Reviews in Food Science and Food Safety, 19,* 2747–2763. https://doi.org/10.1111/1541-4337.12609.

[5] Bessa, L. W., Pieterse, E., Marais, J., Dhanani, K., & Hoffman, L. C. (2021). Food safety of consuming black soldier fly (*Hermetia illucens)* larvae: microbial, heavy metal and cross-reactive allergen risks. *Foods,* 10(8), 1934. https://doi.org/10.3390/foods10081934.

[6] Biasato, I., Ferrocino, I., Colombino, E., Gai, F., Schiavone, A., Cocolin, L., Vincenti, V., Capucchio, M. T., & Gasco, L. (2020). Effects of dietary *Hermetia illucens* meal inclusion on cecal microbiota and small intestinal mucin dynamics and infiltration with immune cells of weaned piglets. *Journal of Animal Science and Biotechnology*, 11, 64. https://doi.org/10.1186/s40104-020-00466-x.

[7] de Boer, A., & Bast, A. (2018). Demanding safe foods – Safety testing under the novel food regulation (2015/2283). *Trends in Food Science & Technology*, 72, 125–133. https://doi.org/10.1016/j.tifs.2017.12.013.

[8] Brulé, L., Misery, B., Baudouin, G., Yan, X., Guidou, C., Trespeuch, C., Foltyn, C., Anthoine, V., Moriceau, N., Federighi, M., & Boué, G. (2024). Evaluation of the microbial quality of *Hermetia illucens* larvae for animal feed and human consumption: study of different type of rearing substrates. *Foods*, 13(10), 1587. https://doi.org/10.3390/foods13101587.

[9] Bruni, L., Randazzo, B., Cardinaletti, G., Zarantoniello, M., Mina, F., Secci, G., Tulli, F., Olivotto, I., & Parisi, G. (2020). Dietary inclusion of full-fat *Hermetia illucens* prepupae meal in practical diets for rainbow trout (*Oncorhynchus mykiss):* lipid metabolism and fillet quality investigations. *Aquaculture*, 529, 735678. https://doi.org/10.1016/j.aquaculture.2020.735678.

[10] Bußler, S., Rumpold, B. A., Jander., E., Rawel, H. M., & Schlüter, O. K. (2016). Recovery and techno-functionality of flours and proteins from two edible insect species: *mealworm (Tenebrio molitor) and black soldier fly (Hermetia illucens)* larvae. *Helyion*, e00218. http://dx.doi.org/10.1016/j.heliyon.2016.e00218.

[11] Cheng, J. Y. K., Chiu, S. L. H., & Lo, I. M. C. (2017). Effects of moisture content of food waste on residue separation, larval growth and larval survival in black soldier fly bioconversion. *Waste Management*, 67, 315–323. https://doi.org/10.1016/j.wasman.2017.05.046.

[12] Chia, S. Y. (2019). *Black soldier fly larvae as a sustainable animal feed ingredient in Kenya* [PhD thesis, Wageningen University, Wageningen, the Netherlands]. DOI: 10.18174/502357. https://research.wur.nl/en/publications/black-soldier-fly-larvae-as-a-sustainable-animal-feed ingredient-

[13] Cruz, V. A., Ferreira, N. J., Cornelio-Santiago, H. P., Santos, G. M. T., & Oliveira, A. L. (2023). Oil extraction from black soldier fly *(Hermetia illucens* L.*)* larvae meal by dynamic and intermittent processes of supercritical CO2 - global yield, oil characterization, and solvent consumption. *The Journal of Supercritical Fluids*, 195, 105861. https://doi.org/10.1016/j.supflu.2023.105861.

[14] Dharani, N., Shriranjani, K., Saranya, R., Raghu, R., Gnanamangai, B. M., Prabha, K., & Shanmugam, P. (2025). Commercialising potential of protein powder extracted from black soldier fly larvae. *IOP Conference Series: Earth and Environmental Science*, 1519, 012010. DOI: 10.1088/1755-1315/1519/1/012010.

[15] Freel, T. A., McComb, A., & Koutsos, E. A. (2021). Digestibility and safety of dry black soldier fly larvae meal and black soldier fly larvae oil in dogs. *Journal of Animal Science*, 99(3). DOI: 10.1093/jas/skab047.

[16] Gahukar, R. T. (2011). Entomophagy and human food security. *International Journal of Tropical Insect Science*, 31(3), 129–144. DOI: 10.1017/S1742758411000257.

[17] Heuel, M., Sandrock, C., Leiber, F., Mathys, A., Gold, M., Zurbrugg, C., Gangnat, I. D. M., Kreuzer, M., & Terranova, M. (2021). Black soldier fly larvae meal and fat can completely replace soybean cake and oil in diets for laying hens. *Poultry Science*, 100, 101034. https://doi.org/10.1016/j.psj.2021.101034.

[18] House, J. (2016). Consumer acceptance of insect-based foods in The Netherlands: Academic and commercial implications. *Appetite*, 107, 47–58. https://doi.org/ 10.1016/j.appet.2016.07.023.

[19] Ipema, A. F., Gerrits, W. J. J., Bokkers, E. A. M., Kemp, B., & Bolhuis, J. E. (2021). Live black soldier fly larvae *(Hermetia illucens)* provisioning is a promising environmental enrichment for pigs as indicated by feed- and enrichment-preference tests. *Applied Animal Behaviour Science*, 244, 105481. https://doi.org/10.1016/j.applanim.2021.105481.

[20] Jalil, N. A. A., Abdullah, S. H., Ahmad, I. K., Basri, N. E. A., & Mohamed, Z. S. (2021). Decomposition of food waste from protein and carbohydrate sources by black soldier fly larvae, *Hermetia illucens* L. *Journal of Environmental Biology*, 42(3), 756–761. DOI: 10.22438/jeb/42/3(SI)/JEB-04.

[21] Jayanegara, A., Novandri, B., Yantina, N., & Ridla, M. (2017). Use of black soldier fly larvae *(Hermetia illucens)* to substitute soybean meal in ruminant diet: An in vitro rumen fermentation study. *Veterinary World*, 10(12), 1439–1446. https://doi.org/10.14202/vetworld.2017.1439-1446.

[22] Jones, O. G. (2016). Recent advances in the functionality of non-animal-sourced proteins contributing to their use in meat analogs. *Current Opinion in Food Science*, 7, 7–13. https://doi.org/10.1016/j.cofs.2015.08.002.

[23] Joshi, V., & Kumar, S. (2015). Meat analogues: Plant based alternatives to meat products - a review. *International Journal of Food and Fermentation Technology*, 5, 107–119. https://doi.org/10.5958/2277-9396.2016.00001.5.

[24] Kyriakopoulou, K., Dekkers, B., & van der Goot, A. J. (2019). Chapter 6 - plant-based meat analogues. In *Sustainable meat production and processing*, 103–126. Academic Press. https://doi.org/10.1016/B9780-12-814874-7.00006-7.

[25] Lähteenmäki-Uutela, A., Marimuthu, S. B., & Meijer, N. (2021). Regulations on insects as food and feed: a global comparison. *Journal of Insects as Food and Feed*, 7, 849–856. doi:10.3920/JIFF2020.0066.

[26] Laroche, M., Perreault, V., Marciniak, A., Gravel, A., Chamberland, J., & Doyen, A. (2019). Comparison of conventional and sustainable lipid extraction methods for the production of oil and protein isolate from edible insect meal. Foods, 8(11), 572. https://doi.org/10.3390/foods8110572.

[27] Li, Y., Liu, M., Wei, Y., Li, L., Ma, D., Weng, Y., Wang, H., & Xu, X. (2024). Influence of a mixture of protein hydrolysate from black soldier fly larvae and schizochytrium on palatability, plasma biochemistry, and antioxidative and anti-inflammatory capacity in cat diets. *Animals*, 14(5), 751. https://doi.org/10.3390/ani14050751.

[28] Lu, S., Taethaisong, N., Meethip, W., Surakhunthod, J., Sinpru, B., Sroichak, T., Archa, P., Thongpea, S., Paengkoum, S., Purba, R. A. P., & Paengkoum, P. (2022). Nutritional composition of black soldier fly larvae *(Hermetia illucens* L.*)* and its potential uses as alternative protein sources in animal diets: a review. *Insects*, 13(9), 831. https://doi.org/10.3390/insects13090831.

[29] Macwan, S., de Souza, T. S. P., Dunshea, F. R., DiGiacomo, K., & Suleria, H. A. R. (2023). Black soldier fly larvae *(Hermetica illucens)* as a sustainable source of nutritive and bioactive compounds, and their consumption challenges. *Animal Production Science*, 64, AN23192. https://doi.org/10.1071/AN23192.

[30] Makkar, H. P. S., Tran, G., Heuzé, V., & Ankers, P. (2014). State-of-the-art on use of insects as animal feed. *Animal Feed Science and Technology*, 197, 1–33. https://doi.org/10.1016/j.anifeedsci.2014.07.008.

[31] Maurer, V., Holinger, M., Amsler, Z., Früh, B., Wohlfahrt, J., Stamer, A., & Leiber, F. (2016). Replacement of soybean cake by *Hermetia illucens* meal in diets for layers. *Journal of Insects for Food and Feed*, 2(2), 83–90. https://doi.org/10.3920/JIFF2015.0071.

[32] Meneguz, M., Gasco, L., & Tomberlin, J. K. (2018). Impact of pH and feeding system on black soldier fly (*Hermetia illucens*, L.; Diptera: Stratiomyidae) larval development. *PLoS ONE*, 13, 1–15. https://doi.org/10.1371/journal.pone.0202591.

[33] Miron, L. T., Postma, R. P., Bosch, G., & Eppink, M. H. M. (2019). Preliminary evaluation of aqueous protein extraction from black soldier fly larvae (*Hermetia illucens* L.). *Industrial Biotechnology*, 15, 365–369. https://doi.org/10.1089/ind.2019.0017.

[34] Miron, L., Montevecchi, G., Macavei, L. I., Maistrello, L., Antonelli A., & Thomas, M. (2023a). Effect of black soldier fly larvae protein on the texture of meat analogues. *LWT - Food Science and Technology*, 181, 114745. https://doi.org/10.1016/j.lwt.2023.114745.

[35] Miron, L., Montevecchi, G., Broggeman, G., Macavei, L. I., Maistrello, L., Antonelli A., & Thomas, M. (2023b). Functional properties and essential amino acid composition of proteins extracted from black soldier fly larvae reared on canteen leftovers. *Innovative Food Science and Emerging Technologies*, 87, 103407. https://doi.org/10.1016/j.ifset.2023.103407.

[36] Mohan, K., Rajan, D. K., Muralisankar, T., Ganesan, A. R., Sathishkumar, P., & Revathi, N. (2022). Use of black soldier fly (*Hermetia illucens* L.) larvae meal in aquafeeds for a sustainable aquaculture industry: A review of past and future needs. *Aquaculture*, 553, 738095. https://doi.org/10.1016/j.aquaculture.2022.738095.

[37] Montevecchi, G., Licciardello, F., Masino, F., Miron, L. T., & Antonelli, A. (2021). Fortification of wheat flour with black soldier fly prepupae. Evaluation of technological and nutritional parameters of the intermediate doughs and final baked products. *Innovative Food Science & Emerging Technologies*, 69, 102666. https://doi.org/10.1016/j.ifset.2021.102666.

[38] Muangrat, R., & Pannasai, S. (2024). Exploring the potential of black soldier fly larvae oil: supercritical CO2 extraction, physicochemical analysis, antioxidant properties, shelf life, and keratinocyte growth inhibition. *Journal of Agriculture and Food Research*, 15, 101008. https://doi.org/10.1016/j.jafr.2024.101008.

[39] Muscat, A., de Olde, E. M., de Boer, I. J. M., & Ripoll-Bosch, R. (2020). The battle for biomass: a systematic review of food-feed-fuel competition. *Global Food Security*, 25, 100330. https://doi.org/10.1016/j.gfs.2019.100330.

[40] Muslykhah, U., Phupaboon, S., Suriyapha, C., Matra, M., & Wanapat, M. (2024). Encapsulation of protein-based bioactive from black soldier fly for ruminant feeding. *Journal of Agriculture and Food Research,* 18, 101325. https://doi.org/10.1016/j.jafr.2024.101325.

[41] Nekrasov, R. V., Ivanov, G. A., Chabaev, M. G., Zelenchenkova, A. A., Bogolyubova, N. V., Nikanova, D. A., Sermyagin, A. A., Bibikov, S. O., & Shapovalov, S. O. (2022). Effect of black soldier fly (*Hermetia illucens* L.) fat on health and productivity performance of dairy cows. *Animals*, 12(16), 2118. https://doi.org/10.3390/ani12162118.

[42] Nyamuhirwa, D. M., Feleke, S., Dontsop Nguezet, P. M., Sissoko, D., Moussa, B., Kouakou, A. G., Zakari, S., Abdoulaye, T., & Manyong, V. (2025). Perspectives on the adoption of black-soldier fly larvae for animal feed among livestock farmers in Sub-Saharan Africa. *Frontiers in Environmental Economics*, 4, 1519767. DOI: 10.3389/frevc.2025.1519767.

[43] Oh, J., Kim, H., Park, K., & Kim, B. G. (2024). Drying methods for black soldier fly (*Hermetia illucens*) Larvae as a feed ingredient for pigs affect in vitro nutrient disappearance. *Agriculture,* 14(10), 1792. https://doi.org/10.3390/agriculture14101792.

[44] Oosterveer, P. J. M. (2020). Sustainability of palm oil and its acceptance in the EU. *Journal of Oil Palm Research*, 32, 365–376. https://doi.org/ 10.21894/jopr.2020.0039.

[45] Pang, W., Hou, D., Chen, J., Nawar, E. E., Li, Z., Hu, R., Tomberlin, J. K., Yu, Z., Li, Q., & Wang, S. (2020). Reducing greenhouse gas emissions and enhancing carbon and nitrogen conversion in food wastes by the black soldier fly. *Journal of Environmental Management*, 260, 110066. https://doi.org/10.1016/j.jenvman.2020.110066.

[46] Quigley, J. D., Zontini, A., Schroeder, G. F., Roman-Garcia, Y., Houbiers, L., & Bach, A. (2025). Nutritional value of black soldier fly larvae oil in calf milk replacers. *Journal of Dairy Science*, 108(3), 2481–2488. https://doi.org/10.3168/jds.2024-25666.

[47] Raksasat, R., Lim, J. W., Kiatkittipong, W., Kiatkittipong, K., Ho, Y. C., Lam, M. K., Font-Palma, C., Zaid, H. F. M., & Cheng, C. K. (2020). A review of organic waste enrichment for inducing palatability of black soldier fly larvae: wastes to valuable resources. *Environmental Pollution*, 267, 1–17. https://doi.org/10.1016/j.envpol.2020.115488.

[48] Schiavone, A., Cullere, M., & De Marco, M. (2017). Partial or total replacement of soybean oil by black soldier fly larvae (Hermetia illucens L.) fat in broiler diets: effect on growth performances, feed-choice, blood traits. *Italian Journal of Animal Science*, 16(1), 93–100. DOI: 10.1080/1828051X.2016.1249968.

[49] Seyedalmoosavi, M. M., Mielenz, M., Veldkamp, T., Daş, G., & Metges, C. C. (2022). Growth efficiency, intestinal biology, and nutrient utilization and requirements of black soldier fly (*Hermetia illucens*) larvae compared to monogastric livestock species: a review. *Journal of Animal Science and Biotechnology*, 13, 31. https://doi.org/10.1186/s40104-022-00682-7.

[50] Smetana, S., Palanisamy, M., Mathys, A., & Heinz, V. (2016). Sustainability of insect use for feed and food: Life Cycle Assessment perspective. *Journal of Cleaner Production*, 137, 741–751. https://doi.org/10.1016/j.jclepro.2016.07.148.

[51] Somparn, N., Pootthachaya, P., Puangsap, W., Pintaphrom, N., Srikha, T., Tengjaroenkul, B., Cherdthong, A., & Wongtangtintharn, S. (2024). Evaluation of black soldier fly larvae oil as a feed ingredient for broiler chickens: effects on performance, carcass traits, meat characteristics, and blood parameters. *Frontiers in Animal Science*, 5, 1496763. DOI: 10.3389/fanim.2024.1496763.

[52] Srikha, T., Pootthachaya, P., Puangsap, W., Pintaphrom, N., Somparn, N., Boonkum, W., Cherdthong, A., Tengjaroenkul, B., & Wongtangtintharn, S. (2024). Effects of black soldier fly larvae oil on growth performance, blood biochemical parameters, carcass quality, and metabolomics profile of breast muscle of Thai native chickens. *Animals*, 14(21), 3098. https://doi.org/10.3390/ani14213098.

[53] Suryati, T., Julaeha, E., Farabi, K., Ambarsari, H., & Hidayat, A. T. (2023). Lauric acid from the black soldier fly (*Hermetia illucens*) and its potential applications. *Sustainability*, 15(13), 10383. https://doi.org/10.3390/su151310383.

[54] Tao, J., & Li, Y. O. (2018). Edible insects as a means to address global malnutrition and food insecurity issues. *Food Quality and Safety*, 2, 17–26. DOI: 10.1093/fqsafe/fyy001.

[55] Tognocchi, M., Abenaim, L., Adamaki-Sotiraki, C., Athanassiou, G. C., Rumbos, I. C., Mele, M., Conti, B., & Conte, G. (2024). Effect of different diet composition on the fat profile of two different black soldier fly larvae populations. *Animal,* 18, 101205. https://doi.org/10.1016/j.animal.2024.101205.

[56] Van Huis, A., & Gasco, L. (2023). Insects as feed for livestock production. *Science*, 379(6628), 138–139. DOI: 10.1126/science.adc9165.

[57] Wang, Y.-S., & Shelomi, M. (2017). Review of black soldier fly (*Hermetia illucens*) as animal feed and human food. *Foods*, 6(10), 91. https://doi.org/10.3390/foods6100091.

[58] Xin, Y., Xu, M., Chen, L., Wang, G., Lu, W., Liu, Z., Shang, R., Li, Y., Wang, Z., Sun, H., & Li, L. (2024). Effects of different defatting methods of black soldier fly (*Hermetia illucens)* larvae meal on the metabolic energy and nutrient digestibility in young laying hens. *Animals,* 14(17), 2521. https://doi.org/10.3390/ani14172521.

[59] Yu, M., Li, Z., Chen, W., Rong, T., Wang, G., Wang, F., & Ma, X. (2020). Evaluation of full-fat Hermetia illucens larvae meal as a fishmeal replacement for weanling piglets: effects on the growth performance, apparent nutrient digestibility, blood parameters and gut morphology. *Animal Feed Science and Technology*, 264, 114431. https://doi.org/10.1016/j.anifeedsci.2020.114431.

[60] *** European Food Safety Authority – EFSA. (2015). Scientific opinion on a risk profile related to production and consumption of insects as food and feed. *EFSA Journal*, 13(10), 4257. DOI: 10.2903/j.efsa.2015.4257.

[61] *** European Food Safety Authority – EFSA. (2016). Guidance on the preparation and presentation of an application for authorisation of a novel food in the context of Regulation (EU) 2015/2283. *EFSA Journal, 14*(11), 4594. DOI: 10.2903/j.efsa.2016.4594.

[62] *** European Parliamentary Research Service – EPRS. (2024). Alternative protein sources for food and feed. Scientific Foresight Unit (STOA) PE 757.806 – April 2024. Brussels, Belgium.
[63] *** Food and Agriculture Organization of the United Nations - FAO. (2013). *Edible insects: future prospects for food and feed security*. FAO Forestry Paper 171. Rome, Italy.
[64] *** Agronutris. https://www.agronutris.com/en/.
[65] *** Hexalfy. https://hexafly.com/.
[66] *** InnovaFeed. https://innovafeed.com/en/.
[67] *** Protix. https://protix.com/.

BLACK SOLDIER FLY (*HERMETIA ILLUCENS*) FOR SUSTAINABLE ORGANIC WASTE MANAGEMENT: LIFECYCLE, SUBSTRATES, AND BIOCONVERSION PARAMETERS

/

MUSCA SOLDAT NEGRU (HERMETIA ILLUCENS) ÎN MANAGEMENTUL SUSTENABIL AL DEȘEURILOR ORGANICE: CICLUL DE VIAȚĂ, SUBSTRATURI ȘI PARAMETRII BIOCONVERSIEI

Nicoleta UNGUREANU[1)], Nicolae-Valentin VLĂDUȚ*[2)], Sorin-Ștefan BIRIȘ[1)], Mariana IONESCU[1)], Neluș-Evelin GHEORGHIȚĂ[1)], Mirela-Nicoleta DINCĂ[1)]

[1)] National University of Science and Technology Politehnica Bucharest / Romania;

[2)] National Institute of Research-Development for Machines and Installations Designed for Agriculture and Food Industry - INMA Bucharest / Romania.

**E-mail: valentin_vladut@yahoo.com*

Keywords: black soldier fly (BSF); insect-based organic waste treatment; food waste; municipal solid waste; sludge; agricultural residues; animal manure; bioconversion efficiency

ABSTRACT

The rapid increase in the volume of organic waste generated by households, agriculture, the food industry, and wastewater treatment facilities pose a significant challenge from both environmental and economic perspectives. Traditional waste management methods such as landfilling, composting, or anaerobic digestion are often limited by inefficiency, slow processing times, or environmental constraints. In recent years, the Black Soldier Fly (BSF, Hermetia illucens) has emerged as a highly promising species for sustainable bioconversion of various organic waste streams. This review analyzes the biological characteristics and life cycle stages of BSF larvae that enable their efficient use in waste valorization. Emphasis is placed on the types of organic substrates that can be processed and the key environmental and operational parameters influencing larval development and conversion efficiency. Critical aspects such as substrate composition, moisture, pH, larval density, and processing temperature are explored in relation to their impact on bioconversion rates. Furthermore, the environmental and economic implications of using BSF in waste management are examined, along with current challenges and future research directions. This synthesis aims to provide a solid knowledge base for optimizing large-scale bioconversion systems using BSF.

REZUMAT

Creșterea accelerată a volumului deșeurilor organice generate de gospodării, agricultură, industria alimentară și stațiile de epurare a apelor uzate reprezintă o provocare majoră atât din perspectiva mediului, cât și din cea economică. Metodele tradiționale de gestionare a deșeurilor, precum depozitarea în gropi, compostarea sau digestia anaerobă, sunt adesea limitate de eficiență scăzută, timpi mari de procesare sau restricții de mediu. În ultimii ani, musca soldat negru (BSF, Hermetia illucens) a devenit o specie extrem de promițătoare pentru bioconversia sustenabilă a diferitelor fluxuri de deșeuri organice. Această lucrare analizează caracteristicile biologice și etapele ciclului de viață ale larvelor BSF, care permit utilizarea lor eficientă în valorificarea deșeurilor. Se pune accent pe tipurile de substraturi organice care pot fi procesate și pe principalii parametri de mediu și operare care influențează dezvoltarea larvelor și eficiența conversiei. Aspecte critice precum compoziția substratului, umiditatea, pH-ul, densitatea larvară și temperatura de procesare sunt analizate în raport cu impactul lor asupra randamentului bioconversiei. De asemenea, sunt abordate implicațiile de mediu și economice ale utilizării BSF în gestionarea deșeurilor, precum și provocările actuale și direcțiile viitoare de cercetare. Această sinteză oferă o bază solidă de cunoștințe pentru optimizarea sistemelor de bioconversie la scară largă cu ajutorul BSF.

INTRODUCTION

The global generation of organic waste has reached alarming levels, posing severe environmental, economic, and social challenges. According to the most recent estimates, approximately 1.05 billion tonnes of food were wasted globally in 2022 across households, retail, and food service sectors, equivalent to 19% of all food available to consumers, or about 132 kg/person/year. Households alone were responsible for 631

million tonnes, accounting for 60% of consumer-level food waste (*UNEP, 2024a*). Similar trends have been observed in the European Union. In 2021, 58 million tonnes of food waste were recorded, of which 54% originated from households, followed by 21% from the food and beverage manufacturing sector, 9% from primary production, 9% from food services, and 7% from retail (*Statista, 2024*).

Food waste contributes to 8–10% of global greenhouse gas (GHG) emissions, almost five times the emissions from the aviation sector, and uses nearly 30% of all agricultural land (*UNCC, 2024*). The issue also aligns with SDG 12.3, which calls for halving global per capita food waste at the retail and consumer levels by 2030, and for reducing food losses along production and supply chains.

Beyond food waste, the broader organic fraction of municipal solid waste (MSW), which includes yard trimmings, paper, and other biodegradable materials, remains a major concern. MSW generation reached 2.3 billion tonnes in 2023 and, if current trends continue, is projected to rise to 3.8 billion tonnes by 2050 (*UNEP, 2024b*).

In certain urban contexts, organic waste may account for up to 70% of total MSW. When poorly managed, this fraction becomes a potent source of CH_4, a GHG over 20 times more powerful than CO_2 over a 100-year timeframe.

Other major organic residues, such as animal manure, agricultural by-products, and sewage sludge, also represent substantial sources of pollution and environmental concern, yet offer untapped opportunities for valorization through insect-based bioconversion.

These figures highlight the unsustainability of current waste management systems and reinforce the urgency of transitioning to circular, resource-efficient solutions.

In this context, bioconversion using the black soldier fly (BSF, *Hermetia illucens* (L.), Diptera: Stratiomyidae) has attracted increasing interest. BSF larvae are capable of rapidly converting various organic residues (e.g., organic fraction of municipal solid waste, food waste, manure, agricultural by-products, and sewage sludge) into protein-rich biomass, valuable lipids, and a processing residue, also called frass (*Adebayo et al., 2021; Kim et al., 2021; Mahmood et al., 2021*).

These transformations occur with relatively low environmental impacts, offering a viable path toward integrated waste valorization and nutrient recovery.

Additionally, BSF bioconversion presents significant advantages in land and water use efficiency compared to conventional livestock production and can be integrated into decentralized waste management strategies, particularly in urban or peri-urban environments, where insects offer high conversion efficiency and generate fewer greenhouse gas emissions than traditional livestock (*Mertenat et al., 2019*).

Their nutritional profile makes insects a promising option for both human food and animal feed (*van Huis and Tomberlin, 2017*). For insects to serve as effective recyclers within sustainable food systems, their production should adhere to the core principles of circular livestock farming. In this context, insects intended for human consumption should be reared exclusively on organic substrates that are unsuitable for direct human use, such as food industry by-products, unavoidable food waste, and crop residues.

Conversely, insects destined for animal feed should be raised on organic materials that are not fit for consumption by either humans or conventional livestock and aquaculture species (*Parodi et al., 2021*). This approach ensures food safety while unlocking the potential of insects as a sustainable protein source in human diets.

While bioconversion using BSF larvae offers significant promise, several restrictions and risks must be addressed. Contaminants such as heavy metals, personal care products, halogenated organic compounds, pesticides, and pharmaceutical residues, usually found in biowaste (*Brisolara and Bourgeois, 2019*), may accumulate in larvae or frass, potentially limiting their use in feed or fertilizer applications.

Pathogenic microorganisms in certain waste streams pose health risks, so effective pathogen control measures are needed during and after the bioconversion process. Regulatory constraints on the collection, processing, and utilization of organic waste and insect-derived products vary widely across regions, impacting scalability and market acceptance.

Additionally, public concerns about safety and insect rearing on waste require clear communication and strict standards for wider acceptance.

The aim of this review is to synthesize recent research on BSF-based bioconversion systems. We focus on the insect's biological characteristics, optimal rearing parameters, substrate types and conversion efficiencies, as well as the environmental, economic, and regulatory implications of scaling such systems.

By consolidating insights from multiple studies, we assess the potential and limitations of BSF bioconversion and explore how this emerging biotechnology can support the transition to circular

bioeconomy and contribute meaningfully to the achievement of global sustainability targets by 2030 and beyond.

BLACK SOLDIER FLY BIOLOGY AND LIFECYCLE

Characteristics of *Hermetia illucens*

The black soldier fly (*Hermetia illucens*) is a non-pest, non-vector dipteran species. Although it was first reported in Europe in 1926, it is native to the neotropical regions of the Americas (*Gladun, 2019; Siddiqui et al., 2022*). Its presence across the Palearctic region, including Southeastern Europe, the Middle East, Austria, Belgium, and the United Kingdom, is largely due to intentional introductions aimed at controlling housefly populations in agricultural settings such as farms and stables (*Demetriou et al., 2022*).

Its subsequent spread throughout Europe is likely facilitated by both natural dispersal (e.g., wind currents) and anthropogenic factors (e.g., human-mediated transport).

Today, BSF is a cosmopolitan species and has garnered global attention as a model organism for organic waste bioconversion, owing to its remarkable biological resilience, ecological adaptability, and economic potential.

Adult BSFs have a dark coloration and a wasp-like appearance. Lacking functional mouthparts, they do not feed during the adult stage, which eliminates the risk of disease transmission through regurgitation (*Siddiqui et al., 2022*). Their sole purpose in this stage is reproduction, which makes them well-suited for indoor or controlled rearing environments. Females typically lay eggs in dry crevices near decomposing organic matter.

The larval stage, which lasts about 14–18 days, is the most important for bioconversion. During this stage, BSF larvae are voracious consumers, capable of efficiently processing a wide variety of organic substrates. Under optimal conditions, they can reduce organic waste mass by 50–75%, while accumulating high levels of protein (up to 42%) rich in essential amino acids, lipids (up to 35%) (*Wang and Shelomi, 2017*), calcium (8%), phosphorus (1–2%), sodium (0.1–0.3%), and magnesium (0.4–1%) (*Chia et al., 2019*), depending on the feedstock. Once mature, the larvae enter the prepupal stage and seek dry environments for pupation.

BSF is highly tolerant of a broad range of environmental conditions. Its resilience, high feed conversion efficiency, and rapid development make it especially suitable for industrial-scale rearing systems. In addition to its bioconversion role, BSF also contributes ecologically by accelerating the decomposition of organic waste and suppressing populations of nuisance insects such as the common housefly through competitive exclusion.

These combined biological traits, alongside its environmental and economic benefits, position BSF as a key species in sustainable waste management and circular bioeconomy strategies.

Life cycle stages relevant for bioconversion

In natural environments, black soldier flies deposit their eggs in or near moist organic matter, providing newly hatched larvae with immediate access to a nutrient-rich substrate. After mating, females oviposit clusters of approximately 500–900 eggs per reproductive event.

Shortly after having oviposited, the female dies. BSF eggs are oval-shaped, approximately 1 mm in length, and have a yellowish-cream color that gradually darkens as they near hatching (*Raihan et al., 2023*). Eggs typically hatch within 3 to 4 days depending on environmental factors such as temperature and humidity (*Chia, 2019*).

Upon hatching, larvae begin intensive feeding on a broad range of organic substrates, including food waste, agricultural residues, and manure. The larval stage, lasting approximately 14–18 days under optimal conditions, is the most metabolically active and critical phase for bioconversion. During this period, larvae exhibit remarkable feed conversion efficiency, rapidly consuming organic matter and transforming it into valuable biomass.

Through bio-catalytic digestion, larvae convert complex organic substrates into high-value proteins and lipids, with lipids accounting for roughly 30% of their body mass. These lipid reserves are crucial for the non-feeding adult stage (*Nguyen et al., 2015*).

The larval development proceeds through six instars, each marked by specific physiological changes and increasing biomass. In adverse conditions, such as nutrient scarcity or unsuitable environmental factors, the larval stage can be extended up to six months, allowing the insect to survive until favorable conditions

return. Upon reaching full maturity, larvae enter the prepupal stage, characterized by cessation of feeding and cuticle darkening.

They actively migrate away from the feeding substrate to locate a dry and secure environment for pupation. The pupal stage, a non-feeding metamorphic phase lasting 1 to 2 weeks, transforms the larvae into an adult fly. Environmental variables including temperature, humidity, and light exposure influence the duration of this stage.

Adult black soldier flies have a brief lifespan of 5 to 8 days. Devoid of functional mouthparts and digestive organs, adults do not feed and rely entirely on energy reserves accumulated during larval development.

Their primary biological roles are reproduction, mating and oviposition, after which the cycle begins again. This non-feeding adult stage also limits disease transmission risks, making BSF suitable for controlled rearing environments focused on larval biomass production.

Understanding each stage of the BSF life cycle is essential for optimizing rearing strategies, maximizing biomass yield, and ensuring the efficiency and safety of bioconversion systems.

Figure 1 illustrates the complete life cycle of *Hermetia illucens*, from egg through larval, prepupal, and pupal stages to the adult fly.

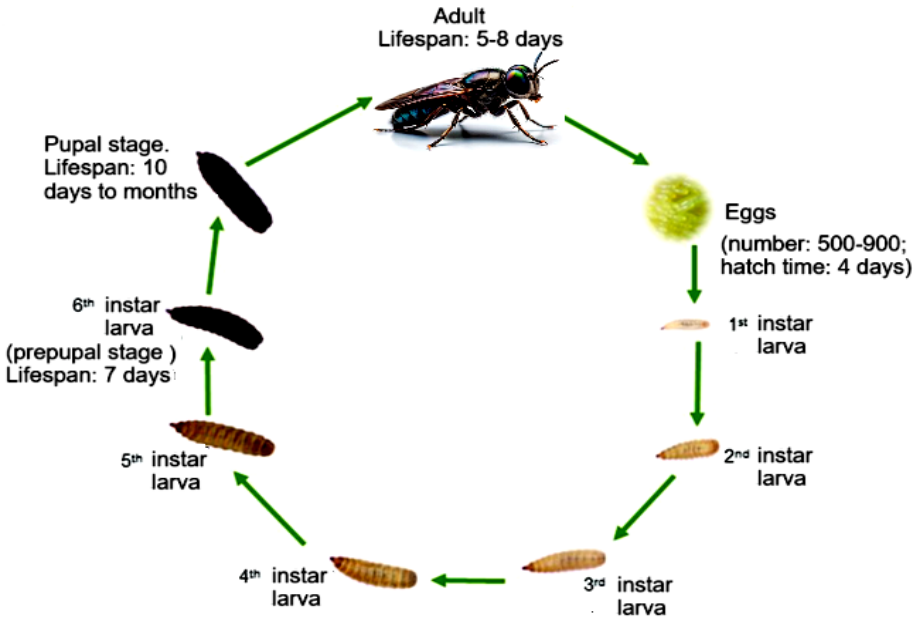

Fig. 1 - The complete life cycle of *Hermetia illucens*

(adapted from Chia, 2019, under the terms of the Creative Commons Attribution License (CC BY 4.0))

Figure 2 shows the development of larvae which were reared on chicken feed together with the corresponding mean body weight (BW) (wet weight) of at least 100 larvae; the body weight development corresponds to an 8083 fold increase from day 1 to day 18 (maximum body weight at day 18); each division of the scaling from day 1 to day 18 represents 1 mm; at day 31 the division of the scaling represents 10 mm (*Seyedalmoosavi et al., 2022*).

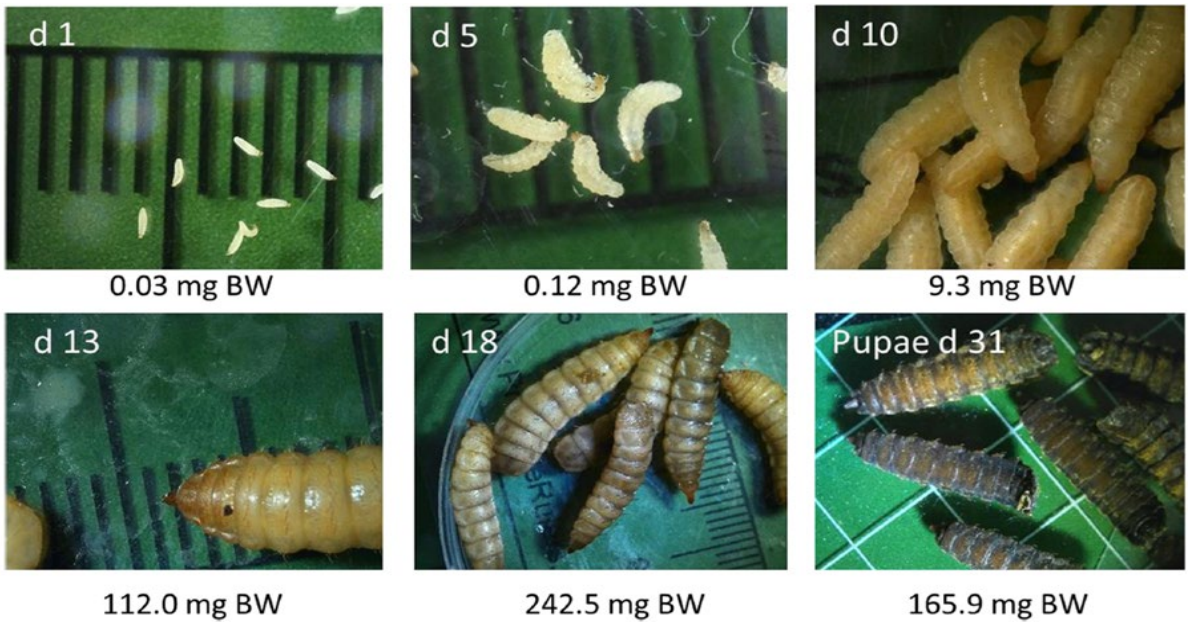

Fig. 2 - Development of BSF larvae from d 1 after hatching up to the pupal stage

(Seyedalmoosavi et al., 2022, under the terms of the Creative Commons Attribution License (CC BY 4.0)

Advantages of BSF over other insects

Other insect species, including *Acheta domestica*, *Alphitobius diaperinus*, *Gryllodes sigillatus*, *Locusta migratoria*, *Musca domestica*, *Schistocerca gregaria*, *Tenebrio molitor*, and *Zophobas morio*, have also been recognized as efficient agents for the bioconversion of organic waste (*Surendra et al., 2020*).

However, *Hermetia illucens* has recently attracted increasing attention as a superior candidate for large-scale bioconversion applications, particularly when compared to species such as *Tenebrio molitor* (mealworms), *Musca domestica* (houseflies), and various beetle larvae (*El Deen et al., 2022*).

One of BSF's major advantages lies in its exceptional substrate flexibility, being capable of converting a wide range of organic waste, such as food scraps, agricultural residues, and animal manure, into valuable larval biomass rich in protein and lipids.

This, along with its rapid biomass accumulation rate, makes BSF particularly suited for scalable waste valorization systems. In addition, BSF larvae demonstrates a high tolerance to environmental fluctuations (e.g., temperature and humidity), offering operational flexibility across different climate conditions. Their short life cycle allows for frequent harvesting and efficient production cycles.

From a sanitary perspective, BSF has clear advantages over insects like the housefly: adult BSFs do not feed and are not vectors of human pathogens, which minimizes biosecurity risks during rearing.

Another key strength is the economic and functional versatility of BSF-derived products. Larval protein can be used in animal feed for poultry, aquaculture, and pets, while the lipid fraction has potential applications in biodiesel and cosmetics. Moreover, BSF frass (a mix of larval excrement and residues) can serve as an organic fertilizer, contributing to nutrient recycling and supporting circular economy strategies.

Finally, BSF receives increasing regulatory acceptance and positive public perception. In several jurisdictions, BSF-based products have already been approved for animal feed, and others are updating legislation accordingly. This growing recognition further strengthens BSF's strategic potential in future waste management and sustainable agriculture systems.

ORGANIC WASTE TYPES USED IN BIOCONVERSION

Food waste, encompassing both edible and inedible fractions discarded at the consumer, retail, and food processing stages, is a highly heterogeneous yet nutrient-rich substrate. Its high moisture content and readily biodegradable organic compounds facilitate rapid larval growth and efficient biomass conversion by BSF larvae (*Ebeneezar et al., 2021*).

The versatility of food waste as a feedstock makes it one of the most utilized substrates in BSF bioconversion research and applications. Nevertheless, challenges arise from the variability in composition and the risk of spoilage and odor generation if not processed promptly and properly managed.

The organic fraction of municipal solid waste typically consists of food scraps, yard trimmings, paper, and other biodegradable materials collected through municipal waste management systems. This mixed organic substrate offers a substantial feedstock for BSF larvae; however, it is often contaminated with plastics, inert materials, or other non-biodegradable components that reduce process efficiency and may require pretreatment steps such as sorting or grinding (*Diener et al., 2011*).

The heterogeneity and seasonal variability of MSW organic fractions also influence larval growth performance and bioconversion yields.

Sewage sludge*,* the semi-solid by-product generated during the treatment of municipal wastewater, contains high levels of organic matter and essential nutrients such as nitrogen and phosphorus, making it a potentially valuable substrate for bioconversion.

Conventional sludge treatment can account for up to 50% of total operating costs in wastewater treatment facilities, posing a significant economic burden. Bioconversion of sewage sludge using BSF larvae emerges as a promising alternative, which not only contributes to sludge volume reduction but also generates value-added larval biomass, potentially offsetting treatment costs (*Bohm et al., 2022*).

The application of BSF larvae has also demonstrated effectiveness in reducing pathogen loads and improving the safety of residual material. However, potential contamination with heavy metals, pharmaceutical residues, or other xenobiotics remains a critical concern due to the risk of bioaccumulation.

Moreover, stringent regulatory frameworks govern the handling and use of sewage sludge and its by-products, requiring thorough risk assessment before implementation.

Agricultural residues, such as crop stalks, husks, and other lignocellulosic by-products, present a more fibrous and recalcitrant substrate for BSF larvae. While BSF can process a wide variety of organic waste, the high cellulose and lignin content of materials like straw and corn stalks limits their digestibility (*Ee et al., 2022*).

Pretreatment strategies, such as mechanical shredding, fermentation, or co-digestion with more easily degradable substrates like fruit or vegetable waste, can significantly improve larval development and bioconversion efficiency. Such interventions are essential to unlock the potential of agricultural residues as a viable feedstock for insect-based recycling systems.

Animal manure, a by-product of livestock production, is rich in nutrients and organic matter but, if mismanaged, serves as a reservoir for pathogens and a source of GHG emissions.

These risks are especially critical in areas with intensive animal husbandry, where manure production exceeds the nutrient uptake capacity of surrounding cropland. Improper handling leads to nutrient runoff, environmental contamination, and public health threats. BSF larvae show great potential in manure treatment, rapidly transforming its physical, chemical, and biological characteristics within one to two weeks (*Bortolini et al., 2020; Sanchez Matos et al., 2020*).

In addition, BSF bioconversion reduces manure odor, pathogen levels, and antibiotic resistance risks (*Beskin et al., 2018*).

BIOCONVERSION PROCESS AND PARAMETERS

The bioconversion of organic waste using BSF larvae is a complex biological process influenced by multiple interrelated parameters. Optimizing these parameters is essential to maximize larval growth, waste reduction efficiency, and the quality of the resultant biomass. BSF larvae exhibit high bioconversion efficiency, with approximately 800 grams of larval biomass produced from 4 kilograms of organic waste, corresponding to a waste reduction rate of around 75% (*Ibadurrohman et al., 2020*).

Sustainable operation of BSF larvae-based biowaste treatment facilities depends on access to diverse and high-quality organic substrates. However, many nutrient-rich waste streams are already allocated to other uses, such as animal feed or energy recovery, while inadequate waste management practices further restrict substrate availability.

Moreover, variability in the composition and supply of feedstock can disrupt daily operations and adversely affect BSF larvae performance, posing challenges to both the sustainability and scalability of this technology (*Mertenat et al., 2019*).

Substrate characteristics

The nutritional composition and physical properties of the substrate are critical determinants of the bioconversion performance of BSF larvae. Essential macronutrients such as organic matter, proteins, lipids,

non-fibrous carbohydrates, and fibers significantly influence larval development and metabolic efficiency (*Lalander et al., 2018*).

Readily digestible components, proteins, non-fibrous carbohydrates, and lipids have been shown to enhance both larval growth and conversion efficiency (*Beniers and Graham, 2019*), whereas fibrous materials like cellulose and lignin are poorly digested and typically inhibit growth (*Liu et al., 2018*). Substrate types vary substantially in nutrient content.

For example, food waste tends to be rich in lipids and easily degradable carbohydrates, making it highly favorable for larval development. In contrast, manures generally exhibit lower levels of organic matter and higher fiber content, while fruit and vegetable residues often lack adequate protein (*Gold et al., 2020*).

BSF larvae adjust their nutrient assimilation and growth dynamics in response to these compositional differences, aiming to accumulate sufficient energy reserves for metamorphosis and adult emergence.

Additionally, substrates that are high in fiber or contain inhibitory compounds can negatively impact BSF larval development and reduce conversion efficiency. This includes materials such as fruit and vegetable pulp, whole grains, grain residues, as well as those with high moisture content like expired milk, beverages, or molasses.

Substrates with unbalanced nutritional profiles may further limit larval growth. To overcome these limitations, pretreatment methods such as grinding, dilution, or homogenization are often employed to enhance substrate uniformity and improve digestibility (*Alyokhin et al., 2019*).

In addition to nutrient content, other substrate parameters such as particle size, moisture content and degradability strongly affect bioconversion outcomes. It is essential to reduce the initial substrate to particles measuring 1–2 cm in diameter, as BSF larvae are unable to break down larger particles with their mouthparts (*Basri et al., 2022*).

Moist, nutrient-rich, and easily degradable substrates, such as bakery or milling residues, are associated with higher larval biomass yields and more efficient waste reduction (*Gold et al., 2020*). However, such substrates are frequently diverted toward other valorization routes, like animal feed or energy production, reducing their availability for BSF-based treatment.

Beyond nutrient and physical characteristics, BSF larvae offer additional benefits through their capacity to mitigate contaminants present in organic waste streams. They have been shown to reduce microbial contaminants and pharmaceutical residues during the bioconversion process, while also demonstrating tolerance to microplastics and elevated levels of heavy metals in the substrate (*Bohm et al., 2022*).

Moreover, BSF larvae can assist in the removal of toxic elements such as zinc from waste streams, although high concentrations of zinc can negatively affect larval development (*Diener et al., 2011*).

Temperature

Temperature is a critical environmental factor influencing the metabolism, growth rate, and overall development of BSF larvae. Due to their high sensitivity to cold, BSF cannot survive in northwestern Europe or in regions where temperatures fall below 5 °C (*Lu et al., 2022*). *Holmes et al. (2016)* further investigated thermal tolerance and reported that BSF eggs can successfully hatch at temperatures between 12 °C and 16 °C, while larvae require a minimum of approximately 19 °C to survive.

These findings are particularly important when designing rearing systems in areas with significant temperature variability. The optimal temperature range for larval growth and development is generally between 25 °C and 30 °C (*Shumo et al., 2019; Ribeiro et al., 2022*).

Temperatures below this range slow down metabolic processes and larval development, leading to extended bioconversion periods and potentially lower biomass yields. Conversely, temperatures exceeding the optimal range may induce heat stress, increasing larval mortality and reducing conversion efficiency.

Maintaining stable temperatures within the optimal range is therefore essential to ensure effective substrate degradation, high larval biomass production, and efficient overall performance.

Additionally, deviations from these thermal limits can adversely affect the microbial communities involved in waste breakdown, thereby compromising bioconversion outcomes.

Moisture content

Maintaining optimal moisture levels within the substrate is essential for effective bioconversion by BSF larvae, as they require a moist environment to sustain feeding and development. The influence of

relative humidity (25%, 40%, 50%, 60%, and 70%) on BSF egg hatching and adult emergence showed that higher humidity levels led to increased hatching and adult emergence rates, while also slowing down the overall development time (*Holmes et al., 2012*).

The ideal moisture content typically ranges between 70% and 85%, although acceptable ranges vary from 50% to 80%, depending on substrate type (*Dortmans et al., 2021; Siddiqui et al., 2022*).

Moisture levels below this range can inhibit larval activity and reduce survival rates, while excessive moisture may create anaerobic conditions, resulting in substrate spoilage, reduced bioconversion efficiency, and odor problems. Additionally, high relative moisture positively influences the hatching success of BSF eggs and the emergence rate of adult flies, while also shortening their developmental period (*Holmes et al., 2012*).

Therefore, maintaining appropriate moisture is critical not only for larval growth but also for optimizing overall bioconversion performance and minimizing operational challenges.

Light

BSF requires adequate light exposure to initiate mating behavior. Since natural light intensity is insufficient during winter, artificial lighting becomes necessary to support reproduction. Various light sources such as fluorescent, halogen, LED, and oxo bulbs have proven effective, whereas rare earth lamps have failed to induce mating. Therefore, the choice of lighting plays a crucial role in successful BSF reproduction under controlled conditions (*Kim et al., 2021*).

Additionally, light wavelength and photoperiod can influence mating efficiency and oviposition rates. Studies suggest that UV-A and blue spectra are more stimulating for adult activity, while prolonged exposure may enhance reproductive outcomes in artificial environments.

Larval density

The initial density of BSF larvae introduced into the substrate significantly affects both waste reduction efficiency and biomass production. While higher larval densities can accelerate the rate of substrate degradation due to increased feeding activity, excessive crowding may intensify competition for nutrients, leading to reduced individual growth rates and higher mortality.

Conversely, lower densities might result in underutilization of the substrate's bioconversion potential. Optimal larval densities depend on substrate type and operational scale but typically range between 5 and 10 larvae per gram of substrate. *Barragán-Fonseca et al. (2018)* found that larval density within breeding containers influences nutrient composition, particularly crude fat content, although it does not significantly affect protein levels.

These findings suggest that managing larval density is crucial not only for maximizing biomass yield but also for modulating the nutritional quality of the larvae. Moreover, larval density can influence the microbial environment within the substrate, potentially affecting both larval health and the hygienic quality of the frass. Therefore, careful regulation of larval numbers is essential to optimize overall bioconversion performance.

Duration of bioconversion

The duration of the bioconversion process significantly influences both the degree of waste reduction and the quality of the larval biomass produced. Typically, larval development cycles range from 10 to 20 days, depending on factors such as substrate composition, moisture content, larval density, and the desired level of larval maturity at harvest.

Shorter cycles may result in incomplete substrate degradation and lower biomass yields, whereas excessively prolonged bioconversion can cause nutrient depletion in the substrate, reducing larval growth rates.

Moreover, extended rearing periods increase the risk of microbial contamination and potential spoilage, which can negatively impact both larval health and product safety.

Optimizing the duration of bioconversion is therefore essential to balance maximal waste reduction with the production of high-quality larval biomass suitable for downstream applications. In addition, the duration of bioconversion can influence the chemical composition of the larvae, including protein and lipid content, which are critical for their intended use as animal feed or bio-based products.

It also affects the characteristics of the residual frass, which may vary in nutrient content and microbial load depending on the rearing time. Therefore, defining an optimal bioconversion period is

essential not only for waste management efficiency but also for the overall quality and safety of the resulting products.

Performance metrics

Key indicators for evaluating the efficiency of BSF bioconversion include larval growth rate, individual larval weight, substrate reduction percentage, and the biochemical composition of the larval biomass, particularly protein and lipid content (*Gold et al., 2020*).

Typically, larval biomass contains 35–45% protein and 15–35% lipids, with variations largely dependent on diet composition and rearing conditions. Substrate reduction rates often exceed 50%, underscoring the substantial capacity of BSF larvae to diminish organic waste volumes effectively.

Monitoring these performance metrics is essential for optimizing process parameters and ensuring consistent production of high-quality biomass for downstream applications such as animal feed or biofuel production.

BSF larvae have been successfully employed for the treatment of various organic waste types, achieving waste reduction rates ranging between 52% and 80%, depending on the substrate, while generating a relatively high biomass yield of approximately 15% of the larval weight relative to the processed waste (*Salam et al., 2022*).

Their voracious feeding behavior allows them to consume up to four times their body weight in organic matter per day, depending on the biowaste composition (*Liu et al., 2018*).

For instance, in the case of food waste, a 14-day bioconversion process resulted in a substrate reduction of 52% and a bioconversion ratio of 28% (dry matter basis) (*Ermolaev et al., 2019*). BSF is considered only moderately effective in biodegrading nutrient-poor substrates such as fruit and vegetable pulp (*Smetana et al., 2019*).

Although fruit and vegetable waste tend to slow larval growth and result in lower waste conversion efficiency compared to mixed food waste (*English et al., 2021*), it may offer the advantage of higher EPA and DHA content relative to other land-based substrates. In poultry farms, BSF larvae have been shown to reduce manure accumulation by up to 60%, with approximately 56% of chicken manure mass being converted into protein- and fat-rich larval biomass suitable for animal feed (*Newton et al., 2005 a*).

Similar outcomes have been documented for dairy and pig manure, with reduction rates of approximately 58% and 56%, respectively (*Newton et al., 2005 b; Myers et al., 2008*). Although animal manure can be effective for waste reduction, its use in large-scale BSF larvae production is limited by the significantly longer development time from hatching to the prepupal stage compared to other feed sources (*English et al., 2021*).

Additionally, BSF larvae have demonstrated the capacity to process lignocellulosic agricultural residues, achieving reduction rates of 32% for rice straw and 49% for corn straw (*Gao et al., 2019*). The effectiveness of waste reduction is strongly dependent on the physico-chemical characteristics of the substrate. Blended waste streams, consisting of multiple organic waste types, tend to yield higher reduction rates than single-stream inputs. This may be attributed to synergistic effects that enhance both larval enzymatic digestion and the microbial activity associated with bioconversion (*Nyakeri et al., 2017*).

COMPARISON WITH CONVENTIONAL TREATMENT METHODS

Bioconversion using BSF larvae offers a biologically driven alternative to traditional organic waste management strategies, including landfilling, composting, and anaerobic digestion.

Compared to landfilling, BSF bioconversion significantly reduces the volume of waste diverted to landfill sites, thereby mitigating long-term environmental risks such as soil and groundwater contamination and GHG emissions, particularly methane, a potent contributor to climate change.

When compared to composting, BSF treatment achieves faster waste reduction rates and produces valuable larval biomass rich in proteins and lipids, which can be utilized as animal feed or for other high-value products. Composting primarily yields stabilized organic matter intended as soil amendment but does not generate such nutrient-dense biomass.

Relative to anaerobic digestion, BSF bioconversion generally requires shorter processing times and results in lower GHG emissions due to the aerobic feeding activity of the larvae, whereas anaerobic digestion produces methane and other gases during organic matter breakdown.

Additionally, the larval biomass produced can offset reliance on conventional protein sources in feed industries, offering economic benefits not attainable through anaerobic digestion alone.

Despite these advantages, integration of BSF bioconversion into existing waste management frameworks necessitates overcoming operational challenges, such as ensuring a consistent substrate supply and meeting regulatory standards. Hybrid approaches combining BSF larvae treatment with composting or anaerobic digestion may optimize resource recovery, reduce environmental footprints, and enhance circular bioeconomy outcomes.

Moreover, BSF bioconversion operates effectively at small to medium scale with minimal land footprint and energy input, making it suitable for decentralized waste management systems, especially in urban or remote settings.

Table 1

Comparative overview of conventional organic waste treatment methods vs. BSF bioconversion

(Authors' own elaboration)

Aspect	Landfilling	Composting	Anaerobic digestion	BSF bioconversion
Duration	Years	Weeks to months	Weeks	10–20 days
Waste volume reduction	Moderate	High	High	High (50–80%)
GHG emissions	Very high (CH_4, CO_2)	Moderate	High (CH_4)	Low (minimal CH_4)
End products	Landfilled waste	Soil amendment	Biogas and digestate	Protein- and lipid-rich larvae biomass, frass fertilizer
Economic value	Negative (management and environmental costs)	Low (low-value amendment)	Moderate (valuable biogas)	High (valuable biomass for feed and other applications)
Health Impact	Risks of contamination and disease vectors	Low	Controlled	Low (non-disease vector species)
Scalability	Large scale	Large scale	Large scale	Growing, dependent on logistics and regulations

ENVIRONMENTAL AND ECONOMIC ASPECTS

Energy efficiency and greenhouse gas emissions

Bioconversion using BSF larvae has demonstrated significant environmental benefits compared to conventional organic waste treatment methods. The process is energy-efficient, requiring relatively low inputs for larval rearing compared to energy-intensive technologies such as incineration or anaerobic digestion.

Moreover, BSF bioconversion substantially reduces GHG emissions by diverting organic waste from landfills, where anaerobic decomposition produces CH_4, a potent GHG. Integrating BSF larvae treatment can lower the overall carbon footprint of organic waste management systems, contributing to climate change mitigation efforts.

Insects represent a rich source of proteins and lipids, positioning them as a promising sustainable protein alternative for both human and animal consumption in the future (*Spranghers et al., 2017*). Their primary advantage compared to traditional livestock production lies in their significantly reduced environmental footprint when scaled to industrial levels (*Bosch et al., 2019*).

Insects exhibit a more efficient feed-to-protein conversion ratio relative to cattle, swine, and in some cases, poultry (*Oonincx and van Loon, 2015*). Industrial-scale insect farming demands considerably less water and land area than conventional animal husbandry, particularly when organic waste streams are utilized as feed (*Allegretti et al., 2018*).

Furthermore, insect rearing results in lower emissions of GHG and ammonia. Life-cycle assessments evaluating the environmental sustainability of insect-derived protein for feed and food applications indicate that insect-based protein powders or meat substitutes may offer an environmental benefit approximately two to five times greater than that of conventional meat products.

Operational and sanitary benefits in waste management

From a waste management perspective, employing BSF for organic waste treatment brings multiple environmental and operational benefits beyond conventional processing methods. These include rapid waste volume reduction, efficient transformation of organic residues into high-value larval biomass and enhanced on-site hygiene.

Unlike other insects, BSF is not associated with disease transmission, making it a biologically safe species for use in controlled waste systems. Moreover, BSF larvae actively suppress pathogenic microorganisms and outcompete other nuisance pests, improving overall sanitary conditions.

A notable advantage is their capacity to reduce malodorous compounds generated by animal manures. *Beskin et al. (2018)* reported odor mitigation rates of up to 87% in poultry, swine, and dairy waste. These attributes make BSF a practical option for improving environmental hygiene in decentralized and small-scale waste facilities.

Economic costs and benefits

From an economic perspective, BSF bioconversion offers promising opportunities. The process converts low-value organic residues into high-value products, such as protein-rich larvae and nutrient-dense frass, which can generate revenue streams in animal feed and fertilizer markets. Initial investments include infrastructure for rearing facilities, substrate preparation, and processing equipment, but operational costs are generally lower compared to chemical or thermal treatments.

Profitability depends on factors like scale, substrate availability, and market demand for insect-derived products. Pilot projects and commercial operations worldwide are increasingly demonstrating the financial viability of BSF bioconversion in circular bioeconomy contexts.

CURRENT CHALLENGES AND RESEARCH GAPS

Despite the growing interest in *Hermetia illucens* as a sustainable solution for organic waste bioconversion, several challenges still hinder its large-scale implementation and full integration into circular bioeconomy models. Scalability remains one of the most pressing obstacles.

While laboratory and pilot-scale studies have demonstrated the efficiency of BSF larvae in converting diverse organic substrates, upscaling the process to industrial levels poses technical and economic difficulties. Factors such as space requirements, automation of larval handling, feedstock logistics, and climate control have become increasingly complex in high-volume facilities.

Moreover, maintaining consistent bioconversion efficiency across variable waste streams remains a technical challenge under commercial conditions.

Emerging risks associated with pathogen transfer, heavy metals, and chemical residues must be closely monitored when rearing BSF larvae on waste substrates. Continuous risk assessment and robust biosecurity protocols are crucial to ensure product safety. Harmonized international regulations are urgently needed to facilitate trade and attract investment in BSF technologies.

However, legislative and regulatory barriers remain a major challenge. In many regions, insects are still ambiguously classified, and the use of substrates like manure or sewage sludge is restricted or lacks clear legal guidance. Within the EU, specific organic waste streams such as food waste and animal manure are subject to regulatory constraints (*Lalander and Vinnerås, 2022*).

Moreover, end-products like insect protein and frass face varying safety and quality standards across markets. Clear, science-based guidelines and legal definitions are needed to support the safe and sustainable scaling of BSF-based systems. Encouraging collaboration between researchers, policymakers, and industry stakeholders is key to overcoming these regulatory hurdles.

Social acceptability and public perception represent additional hurdles, especially in regions where the use of insects in food chains or waste management is culturally unfamiliar or stigmatized. Public awareness campaigns and transparent risk communication strategies are essential to foster acceptance and ensure market uptake of insect-derived products.

Finally, there is a pressing need for process standardization and harmonization of evaluation metrics. Variability in experimental designs, feedstock types, larval densities, and performance indicators across studies makes it difficult to compare results and formulate best practices.

Establishing standardized protocols for BSF larvae rearing, waste treatment efficiency, and product quality assessment is crucial for the scientific advancement and industrial scalability of this technology.

Additionally, long-term environmental impact assessments and techno-economic analyses are lacking, which hinders full understanding of sustainability profiles and investment risks associated with BSF larvae bioconversion. Addressing these research gaps will support evidence-based policy making and business development.

A summary of these key challenges and their potential mitigation strategies is provided in Table 2.

Table 2

Key challenges in BSF larvae-based organic waste bioconversion systems

(Authors' own elaboration)

Challenge	Description	Potential solutions
Scalability	Difficulty in upscaling BSFL systems due to technical constraints (e.g., automation, space, climate control) and cost of operations.	Development of modular, automated systems; optimization of process parameters for industrial scale.
Regulatory barriers	Ambiguous or restrictive legislation regarding insect farming, substrate types (e.g., sludge, manure), and product safety.	Clear legal frameworks; harmonization of regulations across regions; safety protocols for feed/product.
Social acceptance	Cultural resistance or lack of public trust in insect-based waste management and insect-derived products.	Public awareness campaigns; education; transparency in production and safety standards.
Standardization	Inconsistent methodologies, metrics, and performance indicators across studies and facilities.	Establishment of standardized protocols for rearing, efficiency assessment, and product characterization.

Despite these multifaceted challenges, the potential of BSF larvae bioconversion remains substantial. Continued interdisciplinary research, supported by targeted funding and inclusive policy development, will be essential to unlock scalable and safe applications.

Advancements in biotechnology, engineering, and waste management practices are expected to enhance system robustness and efficiency. If these obstacles are systematically addressed, BSF-based systems could become a cornerstone of future circular bioeconomies, contributing simultaneously to waste reduction, resource recovery, and sustainable food and feed production.

CONCLUSIONS AND PERSPECTIVES

The BSF has demonstrated significant potential as a sustainable and efficient bioconversion agent for a wide range of organic waste substrates. Its remarkable capacity to transform diverse residues, including food waste, animal manure, sewage sludge, and agricultural by-products, into valuable biomass, lipids, and frass positions as a promising tool for integrated waste valorization within circular bioeconomy frameworks.

The process is highly influenced by factors such as substrate moisture content, nutrient composition, larval density, and ambient conditions, which must be carefully controlled in scaled-up systems. BSF-based systems offer considerable environmental benefits, such as reduction of greenhouse gas emissions, decreased reliance on conventional protein sources, and nutrient recycling through organic fertilizer production.

However, to fully realize the potential of BSF bioconversion on an industrial scale, further research is required to address existing challenges.

Priority areas include optimizing large-scale rearing protocols, ensuring feedstock safety and consistency, and establishing harmonized regulatory frameworks that facilitate commercialization while safeguarding public health. Moreover, comprehensive life cycle assessments and techno-economic analyses are needed to strengthen the evidence base and promote sustainable implementation globally.

Looking ahead, BSF bioconversion is poised to play a pivotal role in the future of organic waste management, particularly as global waste volumes continue to rise and sustainability targets become more urgent. Integration of BSF technologies into decentralized and urban waste treatment systems can enhance resource efficiency and contribute significantly to achieving SDGs, especially SDG 12.

Continued interdisciplinary collaboration between researchers, policymakers, and industry stakeholders will be essential to accelerate innovation, improve acceptance, and scale up this promising biotechnology for a more sustainable and circular future.

REFERENCES

[1] Adebayo, H. A., Kemabonta, K. A., Ogbogu, S. S., Elechi, M. C., & Obe, M. T. (2021). Comparative assessment of developmental parameters, proximate analysis and mineral compositions of black soldier fly (*Hermetia illucens*) prepupae reared on organic waste substrates. *International Journal of Tropical Insect Science, 41*(3), 1953–1959. https://doi.org/10.1007/s42690-020-00404-4.

[2] Allegretti, G., Talamini, E., Schmidt, V., Bogorni, P. C., & Ortega, E. (2018). Insect as feed: an emergy assessment of insect meal as a sustainable protein source for the Brazilian poultry industry. *Journal of Cleaner Production*, *171*, 403–412. https://doi.org/10.1016/j.jclepro.2017.09.244.

[3] Alyokhin, A., Buzza, A., & Beaulieu, J. (2019). Effects of food substrates and moxidectin on development of black soldier fly, *Hermetia illucens*. *Journal of Applied Entomology, 143*, 137–143. https://doi.org/10.1111/jen.12557.

[4] Basri, N. E. A., Azman, N. A., Ahmad, I. K., Suja, F., Jalil, N. A. A., & Amrul, N. F. (2022). Potential applications of frass derived from black soldier fly larvae treatment of food waste: a review. *Foods*, *11*(17), 2664. https://doi.org/10.3390/foods11172664.

[5] Barragán-Fonseca, K. B., Dicke, M., & van Loon, J. J. A. (2018). Influence of larval density and dietary nutrient concentration on performance, body protein, and fat contents of black soldier fly larvae (*Hermetia illucens*). *Entomologia Experimentalis et Applicata, 166*(9), 761–770. https://doi.org/10.1111/eea.12716.

[6] Beniers, J. J. A., & Graham, R. I. (2019). Effect of protein and carbohydrate feed concentrations on the growth and composition of black soldier fly (*Hermetia illucens*) larvae. *Journal of Insects as Food and Feed.* https://doi.org/10.3920/JIFF2018.0001.

[7] Beskin, K. V., Holcomb, C. D., Cammack, J. A., Crippen, T. L., Knap, A. H., Sweet, S. T., & Tomberlin, J. K. (2018). Larval digestion of different manure types by the black soldier fly (Diptera: Stratiomyidae) impacts associated volatile emissions. *Waste Management, 74*, 213–220. https://doi.org/10.1016/j.wasman.2018.01.019.

[8] Bohm, K., Hatley, G. A., Robinson, B. H., & Gutierrez-Gines, M. J. (2022). Black Soldier Fly-based bioconversion of biosolids creates high-value products with low heavy metal concentrations. *Resources, Conservation & Recycling, 180*, 106149. https://doi.org/10.1016/j.resconrec.2021.106149.

[9] Bortolini, S., Macavei, L. I., Saadoun, J. H., Foca, G., Ulrici, A., Bernini, F., Malferrari, D., Setti, L., Ronga, D., & Maistrello, L. (2020). *Hermetia illucens* (L.) larvae as chicken manure management tool for circular economy. *Journal of Cleaner Production*, *262,* 121289. https://doi.org/10.1016/j.jclepro.2020.121289 121289.

[10] Bosch, G., van Zanten, H. H. E., Zamprogna, A., Veenenbos, M., Meijer, N. P., van der Fels-Klerx, H. J. & van Loon, J. J. A. (2019). Conversion of organic resources by black soldier fly larvae: legislation, efficiency and environmental impact. *Journal of Cleaner Production*, *222*, 355–363. https://doi.org/10.1016/j.jclepro.2019.02.270.

[11] Brisolara, K. F., & Bourgeois, J. (2019). Biosolids and sludge management. *Water Environment Research, 91*(10), 1168–1176. https://doi.org/10.1002/wer.1212.

[12] Chia, S. Y. (2019). *Black soldier fly larvae as a sustainable animal feed ingredient in Kenya* [PhD thesis, Wageningen University, Wageningen, the Netherlands]. DOI: 10.18174/502357. https://research.wur.nl/en/publications/black-soldier-fly-larvae-as-a-sustainable-animal-feed ingredient-.

[13] Chia, S. Y., Tanga, C. M., Osuga, I. M., Alaru, A. O., Mwangi, D. M., Githinji, M., Subramanian, S., Fiaboe, K. K. M., Ekesi, S., van Loon, J. J. A., & Dicke, M. (2019). Effect of dietary replacement of fishmeal by insect meal on growth performance, blood profiles and economics of growing pigs in Kenya. *Animals*, *9*(10), 705. https://doi.org/10.3390/ani9100705.

[14] Demetriou, J., Kalaentzis, K., Kazilas, C., Kunz, G., Muller, B., Mostovski, M. B., & Koutsoukos, E. (2022). An “alien” species on the loose: new records and updated distribution of the black soldier fly *Hermetia illucens* in the Western Palearctic. *Bulletin of Insectology, 75*, 125–130.

[15] Diener, S., Studt Solano, N. M., Roa Gutierrez, F., Zurbrügg, C., & Tockner, K. (2011). Biological treatment of municipal organic waste using black soldier fly larvae. *Waste Biomass Valorization, 2*(4), 357–363. https://doi.org/10.1007/s12649-011-9079-1.

[16] Dortmans, B. M. A., Egger, J., Diener, S., & Zurbrügg, C. (2021). Black Soldier Fly Biowaste Processing - A Step-by-Step Guide (2nd edition). Swiss Federal Institute of Aquatic Science and Technology, Dübendorf, Switzerland, Eawag.

[17] Ebeneezar, S., Linga Prabu, D., Tejpal, C. S., Jeena, N. S., Summaya, R., Chandrasekar, S., Sayooj, P., & Vijayagopal, P. (2021). Nutritional evaluation, bioconversion performance and phylogenetic assessment of black soldier fly (*Hermetia illucens*, Linn. 1758) larvae valorized from food waste. *Environmental Technology & Innovation, 23*, 101783 https://doi. org/10.1016/j.eti.2021.101783.

[18] Ee, K. Y., Lam, M. Q., Mah, J. K., & Merican, A. (2022). Black soldier fly (*Hermetia illucens* L.) larvae in degrading agricultural waste as a sustainable protein production: feedstock modification and challenges. *International Journal of Tropical Insect Science, 42*, 3847–3854. https://doi.org/ 10.1007/s42690-022-00916-1.

[19] El Deen, S. N., Spranghers, T., Baldacchino, F., Deruytter, D. (2022). The effects of the particle size of four different feeds on the larval growth of *Tenebrio molitor* (Coleoptera: Tenebrionidae). *European Journal of Entomology, 119,* 242–249. DOI: 10.14411/eje.2022.026.

[20] English, G., Wanger, G., & Colombo, S. M. (2021). A review of advancements in black soldier fly (*Hermetia illucens*) production for dietary inclusion in salmonid feeds. *Journal of Agriculture and Food Research, 5,* 100164. https://doi.org/10.1016/j.jafr.2021.100164.

[21] Ermolaev, E., Lalander, C., & Vinnerås, B. (2019). Greenhouse gas emissions from small-scale fly larvae composting with *Hermetia illucens*. *Waste Management, 96*, 65–74. https://doi.org/10.1016/j.wasman.2019.07.011.

[22] Gao, Z., Wang, W., Lu, X., Zhu, F., Liu, W., Wang, X., & Lei, C. (2019). Bioconversion performance and life table of black soldier fly (*Hermetia illucens*) on fermented maize straw. *Journal of Cleaner Production*, *230*, 974–980. https://doi.org/10.1016/j.jclepro.2019.05.074.

[23] Gladun, V. V. (2019). The first record of *Hermetia Illucens (Diptera, stratiomyidae*) from Russia. *Nature Conservation Research*, *4*(4), 111–113. https://doi.org/10.24189/ncr.2019.063.

[24] Gold, M., Cassar, C. M., Zurbrugg, C., Kreuzer, M., Boulos, S., Diener, S., & Mathys, A. (2020). Biowaste treatment with black soldier fly larvae: increasing performance through the formulation of biowastes based on protein and carbohydrates. *Waste Management, 102*, 319–329. https://doi.org/10.1016/j.wasman.2019.10.036.

[25] Holmes, L. A., Vanlaerhoven, S. L., & Tomberlin, J. K. (2012). Relative humidity effects on the life history of *Hermetia illucens* (Diptera: Stratiomyidae). *Environmental Entomology, 41*(4), 971–978. https://doi.org/10.1603/EN12054.

[26] Holmes, L. A., Vanlaerhoven, S. L., & Tomberlin, J. K. (2016). Lower temperature threshold of black soldier fly (Diptera: Stratiomyidae). *Journal of Insects as Food and Feed, 2*, 255–262. https://doi.org/10.3920/JIFF2016.0008.

[27] Ibadurrohman, K., Gusniani, I., Hartono, D. M., & Suwartha, N. (2020). The potential analysis of food waste management using bioconversion of the organic waste by the black soldier fly (*Hermetia illucens*) larvae in the cafeteria of the Faculty of Engineering, Universitas Indonesia. *Evergreen, 7*(1), 61–66. DOI: 10.5109/2740946.

[28] Kim, C. H., Ryu, J., Lee, J., Ko, K., Lee, J. Y., Park, K. Y., & Chung, H. (2021). Use of black soldier fly larvae for food waste treatment and energy production in Asian countries: a review. *Processes, 9*, 161. https://doi.org/10.3390/pr9010161.

[29] Lalander, C., Diener, S., Zurbrügg, C., & Vinnerås, B. (2018). Effects of feedstock on larval development and process efficiency in waste treatment with black soldier fly (*Hermetia illucens*). *Journal of Cleaner Production*, *208*, 211–219. https://doi.org/10.1016/j.jclepro.2018.10.017.

[30] Lalander, C., & Vinnerås, B. (2022). Actions needed before insects can contribute to a real closed-loop circular economy in the EU. *Journal of Insects as Food and Feed, 8,* 337–342. https://doi.org/10.3920/JIFF2022.x003.

[31] Liu, Z., Minor, M., Morel, P. C. H., & Najar-Rodriguez, A. J. (2018). Bioconversion of three organic wastes by black soldier fly (Diptera: Stratiomyidae) larvae. *Environmental Entomology, 47*, 1609–1617. DOI: 10.1093/ee/nvy141.

[32] Lu, S., Taethaisong, N., Meethip, W., Surakhunthod, J., Sinpru, B., Sroichak, T., Archa, P., Thongpea, S., Paengkoum, S., Purba, R. A. P., & Paengkoum, P. (2022). Nutritional composition of black soldier fly larvae (*Hermetia illucens* L.) and its potential uses as alternative protein sources in animal diets: a review. *Insects*, *13*(9), 831. https://doi.org/10.3390/insects13090831.

[33] Mahmood, S., Bari Tabinda, A., Ali, A., & Zurbrügg, C. (2021). Reducing the space footprint of black soldier fly larvae waste treatment by increasing waste feeding layer thickness. *Polish Journal of Environmental Studies, 30*(1), 771–779. https://doi.org/10.15244/pjoes/122618.

[34] Mertenat, A., Diener, S., & Zurbrügg, C. (2019). Black soldier fly biowaste treatment – assessment of global warming potential. *Waste Management, 84*, 173–181. https://doi.org/10.1016/j.wasman.2018.11.040.

[35] Myers, H. M., Tomberlin, J. K., Lambert, B. D., & Kattes, D. (2008). Development of black soldier fly (Diptera: Stratiomyidae) larvae fed dairy manure. *Environmenal Entomology, 37*(1), 11–15. https://doi.org/10.1093/ee/37.1.11.

[36] Newton, G. L., Sheppard, D. C., Watson, D. W., Burtle, G. J., Dove, C. R., Tomberlin, J. K., & Thelen, E. E. (2005 a). The black soldier fly, *Hermetia illucens*, as a manure management/resource recovery tool. *Symposium on the State of the Science of Animal Manure and Waste Management, 57*, 275–296.

[37] Newton, L., Sheppard, C., Watson, D. W., & Burtle, G. (2005 b). Using the black soldier fly, *Hermetia illucens*, as a value-added tool for the management of swine manure. Report for North Carolina State University, Raleigh, NC.

[38] Nguyen, T. T. X., Tomberlin, J. K., & Vanlaerhoven, S. (2015). Ability of black soldier fly (*Diptera: Stratiomyidae*) larvae to recycle food waste. *Environmental Entomology*, *44*(2), pp. 406–410. DOI: 10.1093/ee/nvv002.

[39] Nyakeri, E. M., Ogola, H. J. O., Ayieko, M. A., & Amimo, F. A. (2017). Valorisation of organic waste material: growth performance of wild black soldier fly larvae (*Hermetia illucens*) reared on different organic wastes. *Journal of Insects for Food and Feed, 3*(3), 193–202. https://doi.org/10.3920/JIFF2017.0004.

[40] Oonincx, D. G. A. B., van Huis, A., & van Loon, J. J. A. (2015). Nutrient utilisation by black soldier flies fed with chicken, pig, or cow manure. *Journal of Insects as Food and Feed*, *1*(2), 131–139. https://doi.org/10.3920/JIFF2014.0023.

[41] Parodi, A., Gerrits, W. J. J., Van Loon, J. J. A., De Boer, I. J. M., Aarnink, A. J. A., & Van Zanten, H. H. E. (2021). Black soldier fly reared on pig manure: bioconversion efficiencies, nutrients in the residual material, greenhouse gas and ammonia emissions. *Waste Management, 126*, 674–683. https://doi.org/10.1016/j.wasman.2021.04.001.

[42] Raihan, I., Ayuni, J. D., Salmah, Surya, R. M., & Fadhillah, H. (2023). Utilization of black soldier fly's larvae for integrated waste management at farmer household. *Russian Journal of Agricultural and Socio-Economic Sciences, 5*(137), 56–65. DOI: 10.18551/rjoas.2023-05.06.

[43] Ribeiro, N., Costa, R., & Ameixa, O. M. C. C. (2022). The influence of non-optimal rearing conditions and substrates on the performance of the black soldier fly (*Hermetia illucens*). *Insects, 13*, 639. https://doi.org/10.3390/insects13070639.

[44] Salam, M., Shahzadi, A., Zheng, H., Alam, F., Nabi, G., Dezhi, S., Ullah, W., Ammara, S., Ali, N., & Bilal, M. (2022). Effect of different environmental conditions on the growth and development of Black Soldier Fly Larvae and its utilization in solid waste management and pollution mitigation. *Environmental Technology & Innovation, 28*, 102649. https://doi.org/10.1016/j.eti.2022.102649.

[45] Sanchez Matos, J., Barberino, A. T. M. S., de Araujo, L. P., Lôbo, I. P., & de Almeida Neto, J. A. (2020). Potentials and limitations of the bioconversion of animal manure using fly larvae. *Waste Biomass Valorization, 12,* 3497–3520. https://doi.org/10.1007/s12649-020-01141-y.

[46] Seyedalmoosavi, M. M., Mielenz, M., Veldkamp, T., Daș, G., & Metges, C. C. (2022). Growth efficiency, intestinal biology, and nutrient utilization and requirements of black soldier fly (Hermetia illucens) larvae compared to monogastric livestock species: a review. *Journal of Animal Science and Biotechnology, 13*, 31. https://doi.org/10.1186/s40104-022-00682-7.

[47] Shumo, M., Khamis, F. M., Tanga, C. M., Fiaboe, K. K. M., Subramanian, S., Ekesi, S., van Huis, A., & Borgemeister, C. (2019). Influence of temperature on selected life-history traits of black soldier fly (*Hermetia illucens*) reared on two common urban organic waste streams in Kenya. *Animals, 9*, 79. https://doi.org/10.3390/ani9030079.

[48] Siddiqui, S. A., Ristow, B., Rahayu, T., Putra, N. S., & et al. (2022). Black soldier fly larvae (BSFL) and their affinity for organic waste processing. *Waste Management, 140,* 1–13. https://doi.org/10.1016/j.wasman.2021.12.044.

[49] Smetana, S., Schmitt, E., & Mathys, A. (2019). Sustainable use of *Hermetia illucens* insect biomass for feed and food: attributional and consequential life cycle assessment. *Resources, Conservation & Recycling, 144*, 285–296. https://doi.org/10.1016/j. resconrec.2019.01.042.

[50] Spranghers, T., Ottoboni, M., Klootwijk, C., Ovyn, A., Deboosere, S., De Meulenaer, B., Michiels, J., Eeckhout, M., De Clercq, P., & De Smet, S. (2017). Nutritional composition of black soldier fly (*Hermetia illucens*) prepupae reared on different organic waste substrates. *Journal of the Science of Food and Agriculture*, *97*(8), 2594–2600. https://doi.org/10.1002/jsfa.8081.

[51] Statista. (2024). *The Scale of Food Waste in Europe*. https://www.statista.com/chart/31072/food-wasted-per-capita-in-european-countries/.

[52] Surendra, K. C., Tomberlin, J. K., van Huis, A., Cammack, J. A., Heckmann, L. -H., & Khanal, S. K. (2020). Rethinking organic wastes bioconversion: evaluating the potential of the black soldier fly (*Hermetia illucens* (L.) (Diptera: Stratiomyidae) (BSF). *Waste Management, 117*, 58–80. https://doi.org/10.1016/j.wasman.2020.07.050.

[53] United Nations Climate Change. (2024). *Food loss and waste account for 8–10% of annual global greenhouse gas emissions; cost USD 1 trillion annually*. https://unfccc.int/news/food-loss-and-waste-account-for-8-10-of-annual-global-greenhouse-gas-emissions-cost-usd-1-trillion.

[54] United Nations Environment Programme. (2024 a). *UNEP Food Waste Index Report 2024*. https://www.unep.org/resources/publication/food-waste-index-report-2024.

[55] United Nations Environment Programme. (2024 b). *Global Waste Management Outlook 2024*. https://wedocs.unep.org/bitstream/handle/20.500.11822/44939/global_waste_management_outlook_2024.pdf?sequence=3.

[56] van Huis, A., & Tomberlin, J. K. (2017). The potential of insects as food and feed. In: *Insects as Food and Feed: From Production to Consumption*. 1 ed.; van Huis, A., Tomberlin, J. K. (Eds.); Wageningen Academic Publishers, Wageningen, the Netherlands; 25–58.

[57] Wang, Y.-S., & Shelomi, M. (2017). Review of black soldier fly (*Hermetia illucens*) as animal feed and human food. *Foods*, *6*(10), 91. https://doi.org/10.3390/foods6100091.

THE EFFECTS OF PRUNING SHEAR DESIGN ON HAND FORCES DURING HAZELNUT SUCKERS CUTTING

/

FINDIK SÜRGÜNLERININ KESIMI SIRASINDA BUDAMA MAKASI TASARIMININ EL KUVVETLERI ÜZERINDEKI ETKILERI

Kemal Çağatay SELVI*[1)], Mehmet Ali ERDOĞAN[2)], Ehsan Fartash NAEIMI[1)]
[1)] Ondokuz Mayıs University, Department of Agricultural Machinery and Technologies Engineering, Samsun / Turkey;
[2)] Minos Agricultural Machinery, İzmir / Turkey.
**Tel: +90 507 926 28 29; *E-mail: kcselvi@omu.edu.tr*

Keywords: *Pruning shear, shear force, hazelnut sucker, ergonomic design*

ABSTRACT

This study was conducted to comparatively evaluate the cutting force requirements and design characteristics of ten different pruning shears during hazelnut sucker cutting. Hazelnut suckers were used as the plant material, and cutting tests were performed using a Lloyd universal testing machine at a constant speed of 300 mm/min. The tests were repeated ten times for each of five branch diameter groups (5.36, 8.00, 9.21, 10.87, and 12.35 mm). Cutting force data were collected using NEXYGEN software. Covariance analysis was conducted with branch diameter included as a covariate, isolating the effect of pruner design on hand force. Mean comparisons were performed using the LSD test at a 1% significance level. The results showed that the Ergopro pruner required the lowest cutting force in most diameter groups, especially for medium and thick branches, whereas Bossini DS-709 consistently required the highest force across all sizes. The greatest relative increase in hand force was observed in the Bulmaks BMX-286 pruner with a 504% rise from the smallest to the largest branch diameter, while the smallest increase was found in Herly HM204 at 177.5%. These findings highlight the influence of pruner design features—such as blade type, thickness, and weight—on cutting efficiency and ergonomic performance, offering valuable insights for tool selection in orchard management.

ÖZET

Bu çalışma, fındık sürgünlerinin kesilmesi sırasında kullanılan on farklı budama makasının kesme kuvveti gereksinimleri ile tasarım özelliklerini karşılaştırmalı olarak değerlendirmek amacıyla yürütülmüştür. Bitki materyali olarak fındık sürgünleri kullanılmış, kesme testleri 300 mm/dak sabit hızda Lloyd marka evrensel test cihazı ile gerçekleştirilmiştir. Her biri beş farklı dal çapı grubuna (5,36; 8,00; 9,21; 10,87 ve 12,35 mm) ait olmak üzere onar tekrarlı testler yapılmıştır. Kesme kuvveti verileri NEXYGEN yazılımı kullanılarak kaydedilmiştir. Kovaryans analizi, dal çapı kovaryet olarak dahil edilerek, budama makası tasarımının el kuvveti üzerindeki etkisini izole etmek amacıyla uygulanmıştır. Ortalama karşılaştırmaları ise %1 anlamlılık düzeyinde LSD testi ile yapılmıştır. Sonuçlar, özellikle orta ve kalın dallarda, Ergopro model budama makasının çoğu çap grubunda en düşük kesme kuvveti gereksinimine sahip olduğunu; buna karşın Bossini DS-709 modelinin tüm çap gruplarında sürekli olarak en yüksek kuvvet gereksinimine sahip olduğunu göstermiştir. En yüksek oransal artış, Bulmaks BMX-286 modelinde %504'lük bir artışla görülürken, en düşük artış Herly HM204 modelinde %177,5 olarak tespit edilmiştir. Bulgular, bıçak tipi, kalınlığı ve ağırlığı gibi budama makası tasarım özelliklerinin kesme verimliliği ve ergonomik performans üzerindeki etkisini ortaya koymakta olup, bahçe yönetiminde alet seçiminde önemli bilgiler sunmaktadır.

INTRODUCTION

The required shear force to cut vegetative materials is associated with the material's physico-mechanical properties and the blade's structure. It required performing proper cutting operation changes depending on various factors *(Zhang et al., 2023; Wilczyński et al., 2023).*

The most important of these factors are; the material's shear stress, properties of the material, the structure and usage of the blade (*Song et al., 2022; Pekitkan et al., 2020)*. Failure to take into account some basic factors in the design of a pruning shear to perform cutting may result in the worker's musculoskeletal disorders of the upper limbs due to the physical effort required to cut branches and repetitive actions *(Zahid et al., 2022; Minaei et al., 2023).* Lakshmi and Kumari (2016) also highlighted in their research that manual

pruning can place considerable strain on the tendons, bones, and nerves in workers' hands, wrists, and elbows.

For this reason, some limit values for human health have been reported for manual repetitive work, such as pruning used in agricultural production and maintenance.

According to the EN-1005-3 standard, the force to be applied by the hand shouldn't be above 300 N and desirable values should be in the range of 150-200 N, if possible *(Selvi, 2023).*

There are many references to pruning and pruning shears in the literature, but they do not address hand force for repetitive actions or design effect on efficiency. There are many comparative studies in this area. Some of them are; Parish (1998), Romano et al. (2010), Marini et al. (2020), Ramanjineyulu et al. (2024), Sessiz et al. (2015), Selvi and Kabaş (2016).

From a design point of view, it will be seen that a classical pruning shear consists of the following main parts (Figure 1). In addition, some descriptive sizes of the pruning shears are shown in Figure 2.

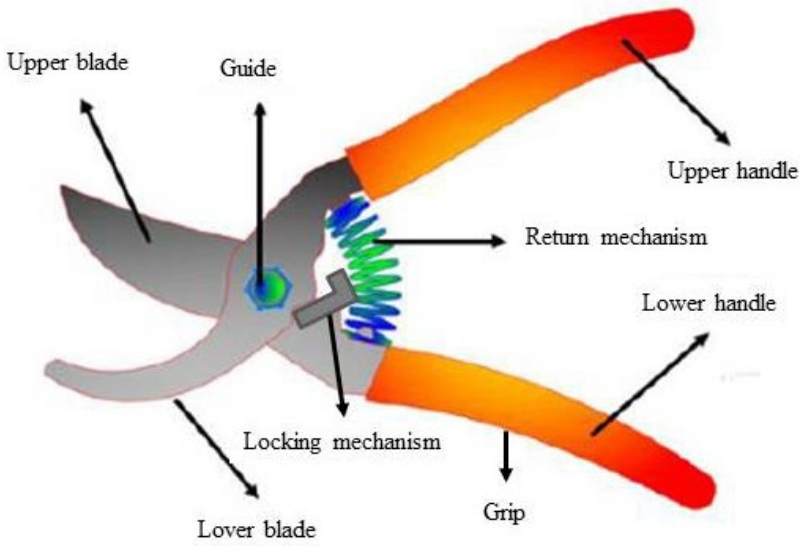

Fig. 1 - Main parts of pruning shear

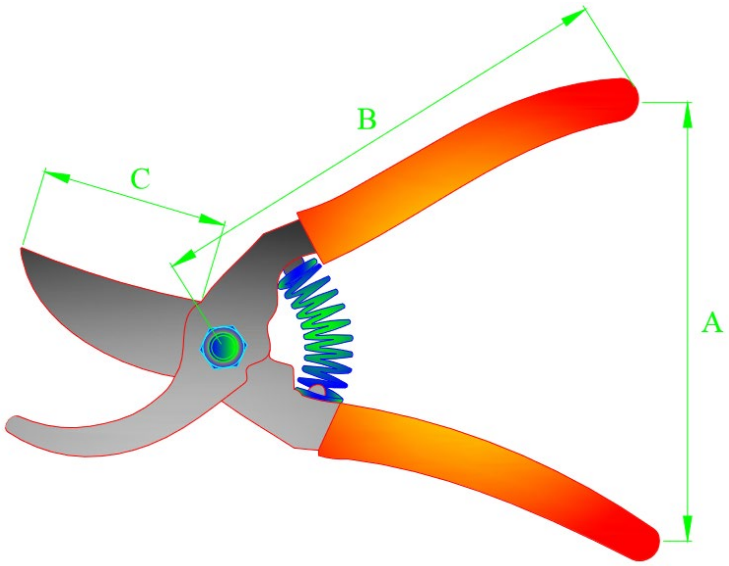

Fig. 2 - Some descriptive sizes of the pruning shears
A- Handle Spacing B- Handle Length C- Blade Length

In addition to this basic representation, it is also seen that pruning shears are examined in two groups: anvil (one blade cuts down against a flat surface) and bypass (two blades pass each other, like scissors). In the design of both types of pruning shears; different return mechanisms such as coil spring, leaf spring and telescopic spring can be used.

In addition, in a comprehensive study carried out by Paivinen (2000), besides the factors such as the locking mechanism, the force transfer mechanism, the guide, weight, stiffness, the returning mechanism is also specified as a design parameter.

The objective of this study was to compare low cost hand pruning shears, both types and returning mechanism, to determine which ones required the low hand force especially in terms of their design and also for hand health according repetitive works such as pruning.

MATERIALS AND METHODS

PLANT MATERIAL

In the shear tests, hazelnut suckers were obtained from a commercial hazelnut garden in Samsun province located in North of the Turkey from the pruning of the autumn period (October-November) between 2018 and 2019 (Figure 3).

The test samples were randomly cut by hand from vineyards. The cut and collected suckers were transported to the laboratory at the Department of Agricultural Machinery and Technologies Engineering, University of Ondokuz Mayıs which were then placed in a refrigerator at 5 °C until the time of the cutting tests.

The test procedure consisted of measuring the force on the handle required to cut hazelnut suckers of several diameters: 5.36, 8.00, 9.21, 10.87 and 12.35 mm.

Fig. 3 - Hazelnuts suckers

Pruning shears

Ten low cost hand pruning shears were selected for evaluation. The models are listed in table 1 and include an anvil and nine bypass pruners.

Table 1

Some information of pruning shears evaluated

Pruners	Figure	Type	Pruners sizes / mm	Blade thickness / mm	Weight / g	Retail Price
Yeniay	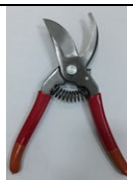	Bypass	A= 150 B= 150 C= 60	4.4	365	24.69
Unknown-1		Bypass	A= 127 B= 133 C= 50	2.1	147	34.67

Akman		Bypass	A= 123 B= 136 C= 52	3.7	187	31.10
Herly HM204	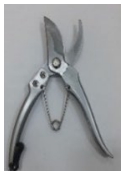	Bypass	A= 132 B= 130 C= 50	2.5	214	49.53
Ergopro		Anvil	A= 102 B= 146 C= 42	2.6	280	59.31
Bulmaks BMX-286		Bypass	A= 150 B= 156 C= 67	2.2	471	33.89
Unknown-2		Bypass	A= 120 B= 136 C= 57	2.95	167	17.90
Akman SNR		Bypass	A= 103 B= 142 C= 50	3.2	168	29.90
Bossini DS-308		Bypass	A=120 B=141 C= 59	5.2	268	20.00
Bossini DS-709		Bypass	A=158 B=146 C= 71	7.4	422	20.00

All of the pruning shears were purchased new for this evaluate. The plant materials were pre-experimented to simulate manual cutting, with a repetition of 300 mm / min at constant speed and 5 different diameter groups (5.36 mm, 8.00 mm, 9.21 mm, 10.87 mm and 12.35 mm) with 10 replications. This cutting velocity value was determined by a preliminary experiment with a pruning shears outside the trial, depending on the way taken during cutting.

Testing device and aparatus

The force required to cut hazelnut suckers with different pruning shears was measured by a Lloyd Instrument Universal Testing Machines (Lloyd Instrument LRX Plus, Lloyd Instruments Ltd, An AMATEK Company). The device has three main parts: moving head, driving unit and data acquisition system (load

cell, note book and connections and NEXYGEN Plus software). The device was equipment with a load cell of 1000 N and measurement accuracy of load cell was 0.5%. Load cell was fixed to moving head (Figure 4).

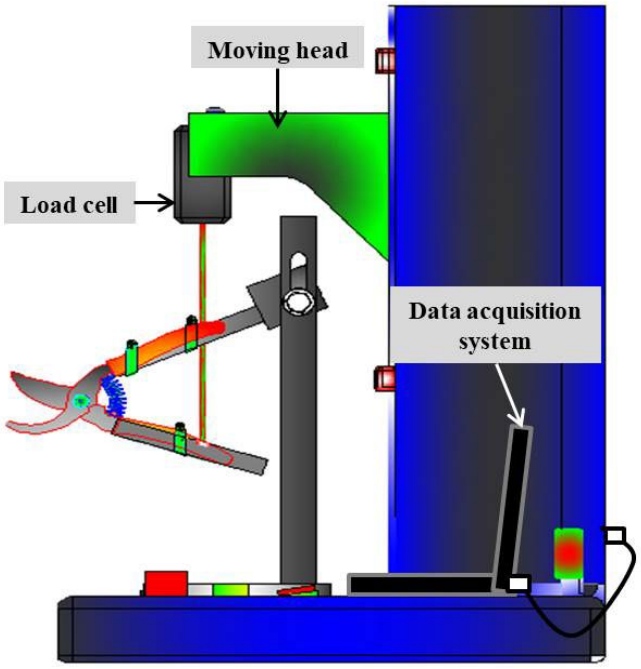

Fig. 4 - View of the universal testing machine used to measure the cutting force required for hazelnut sucker pruning

In the experiments, a clamping apparatus has been manufactured in order to enable the cutting shears to perform the correct cutting operation and to be mounted on the test device. The detail picture and dimensions of the clamping apparatus is shown in Figure 5. Pre-trials were performed to represent the cutting process with pruning shears and the cutting speed was chosen as 300 mm/min. The apparatus was guided vertically to assure that the force would be applied vertically with minimal lateral friction effects.

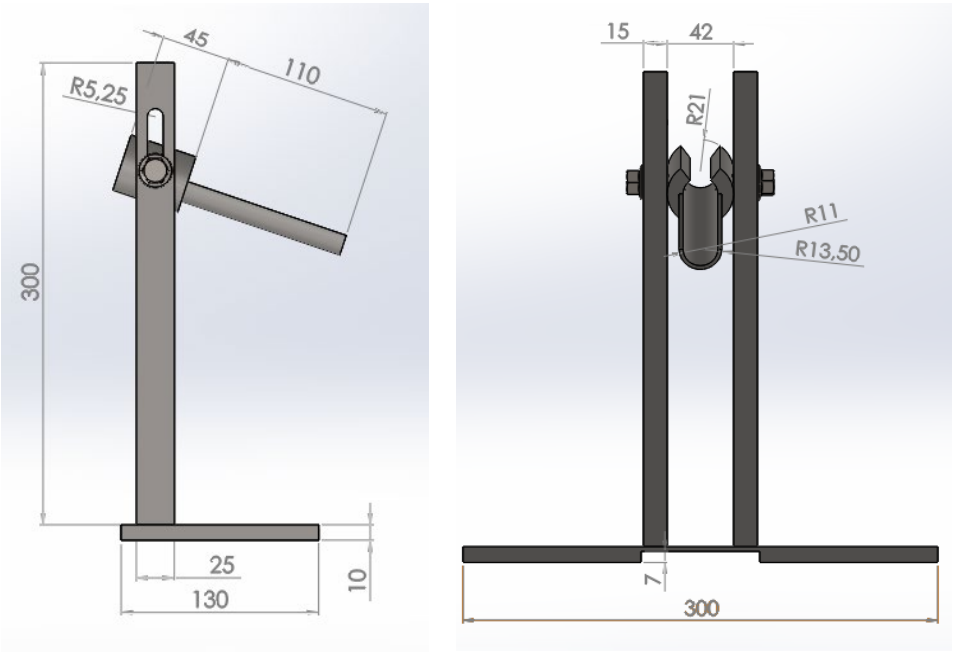

Fig. 5 - Clamping apparatus to the Lloyd LRX Plus tester

In statistical analyzes, moisture and diameter values of hazelnut suckers were included in the model as covariates and their effect was eliminated from the model and only the effect of ergonomic design effect

on force values was investigated. The LSD test was used for comparisons between means, while univariate analysis of variance was used for data analysis.

RESULTS AND DISCUSSION

The pruning shear type and design had a significant effect on the hand force required to cut hazelnut suckers across different branch diameters. Table 2 and Figure 6 presents the mean hand force (N) exerted by users to cut branches of varying diameters using ten different pruning shears.

The results reveal clear trends associated with blade type, handle design, weight, and blade sharpness.

Table 2

Mean hand force for pruning shears to cut hazelnut suckers (figures are the mean of cuts on 10 branches)

Model	Mean Hand Force, N				
	5.36 mm Branch	8.00 mm Branch	9.21 mm Branch	10.87 mm Branch	12.35 mm Branch
Akman	121 ^{bc}	250 ^{b}	333 ^{a}	334 ^{b}	357 ^{c}
Akman-SNR	92 ^{de}	203 ^{c}	222 ^{bc}	284 ^{c}	352 ^{c}
Bossini DS-308	111 ^{cd}	192 ^{cd}	236 ^{b}	363 ^{b}	438 ^{b}
Bossini DS-709	182 ^{a}	321 ^{a}	368 ^{a}	451 ^{a}	561 ^{a}
Bulmax BMX-286	50 ^{f}	144 ^{ef}	184 ^{c}	236 ^{de}	302 ^{d}
Ergopro	51 ^{f}	94 ^{g}	99 ^{d}	153 ^{g}	167 f
Herly	80 ^{e}	149 ^{def}	187 ^{c}	201 ^{ef}	222 ^{e}
Unknown-1	74 ^{e}	177 ^{cde}	209 ^{bc}	269 ^{cd}	323 ^{cd}
Unknown-2	140 ^{b}	216 ^{bc}	247 ^{b}	293 ^{c}	409 ^{b}
Yeni ay	50 ^{f}	124 ^{fg}	188 ^{c}	193 ^{f}	233 ^{e}

*Means in each column followed by the same letter are not significantly different at the 0.05 level

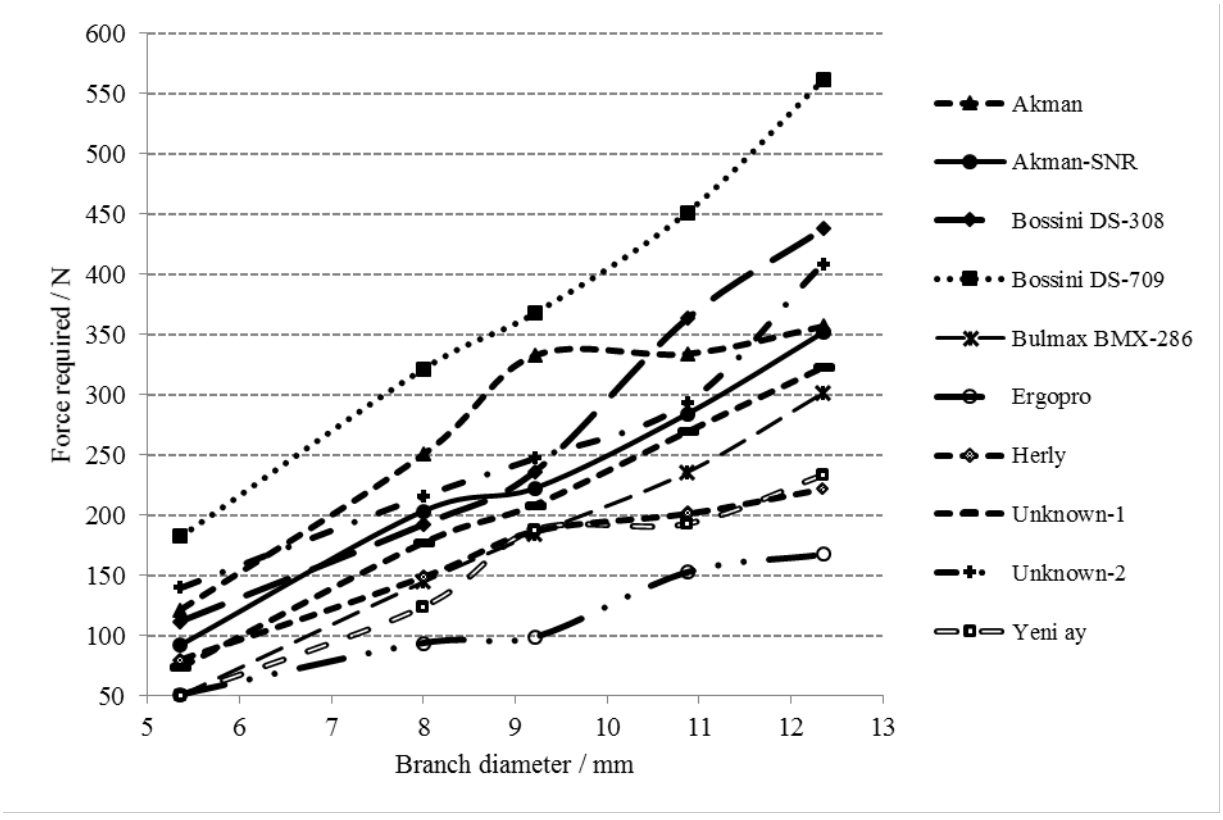

Fig. 6 - Force required to cut hazelnut suckers

For the smallest branch size (5.36 mm), the lowest mean hand force was observed with the Bulmax BMX-286, Ergopro, and Yeniay models (50–51 N), which were statistically similar ($p < 0.05$) and significantly lower than other models. In contrast, Bossini DS-709 required the highest force (182 N), suggesting that despite its larger dimensions and greater blade thickness (7.4 mm), its design does not facilitate ease of cutting in small-diameter branches.

This might be due to its heavier weight (422 g) and relatively wide blade, which could increase friction during initial cutting. As branch diameter increased to 8.00 mm and beyond, the trend in required hand force followed a similar pattern, though differences between models became more pronounced. At 8.00 mm, the Ergopro (94 N) and Yeniay (124 N) remained among the most efficient tools, while Bossini DS-709 and Akman required significantly higher forces (321 N and 250 N, respectively). The anvil-type Ergopro, despite its different cutting mechanism, consistently showed low force requirements, especially in thinner branches, indicating that its blade design and ergonomics were well-suited for ease of use.

For thicker branches (9.21–12.35 mm), the Bossini DS-709 consistently required the highest hand forces (368–561 N), which can be attributed to its high blade thickness (7.4 mm) and possibly suboptimal ergonomic design.

The excessive force requirement for this model may increase the risk of musculoskeletal strain during prolonged use, making it less suitable for large-scale orchard operations. Conversely, Bulmax BMX-286 continued to perform favorably with relatively low force values across all branch sizes (184 N to 302 N), suggesting that its combination of long blade length (C=67 mm) and lightweight design (471 g) contributes to a more efficient force transmission during cutting. However, the Ergopro showed a notable limitation in cutting thicker branches (≥10.87 mm), where the force requirement increased steeply to 153–167 N. While still low compared to some models, this sharp rise suggests that the anvil mechanism may be less effective on thicker woody branches due to the lack of a bypass action that reduces crushing.

A key observation is the consistent performance of Akman-SNR, which offered a good balance between cutting efficiency and ergonomic performance. It required moderate force levels across all diameters (92–352 N), significantly lower than the Akman model, despite their similar design and dimensions. This indicates that even minor design variations (e.g., blade sharpness, joint resistance, handle angle) can result in meaningful differences in user experience and efficiency.

Overall, bypass pruners generally required more force than the anvil-type Ergopro on smaller branches, though they performed better in thicker branch cutting due to their slicing action. Among bypass pruners, Bulmax BMX-286 and Yeniay demonstrated the most ergonomic performance. Weight and blade thickness also showed clear influence: heavier shears with thicker blades (e.g., Bossini DS-709) tended to require more hand force, likely due to increased resistance and less precise blade alignment.

These findings are critical for tool manufacturers and agricultural workers. Selecting pruners with appropriate weight, blade type, and ergonomic handle design can significantly reduce physical effort and fatigue, enhancing productivity and reducing the risk of repetitive strain injuries. For hazelnut sucker cutting, tools like Bulmax BMX-286, Yeniay, and Ergopro are recommended based on their lower required hand forces and ease of use across a range of branch diameters.

CONCLUSIONS

This study demonstrated that the design and structural properties of pruning shears significantly affect the hand force required during hazelnut sucker cutting. Among the evaluated models, the Ergopro pruner required the lowest cutting forces overall, particularly in medium and thick branch diameters, making it the most ergonomically favorable option. In contrast, the Bossini DS-709, characterized by its higher weight and blade thickness, consistently demanded the highest hand forces across all diameter groups, indicating lower efficiency and increased user fatigue risk.

Furthermore, the analysis of force variation across different branch sizes revealed that the Bulmaks BMX-286 had the greatest relative increase (504%), while the Herly HM204 showed the smallest (177.5%), emphasizing the impact of shear design on adaptability to branch thickness. The bypass-type pruners generally performed better than expected in small diameters, but their performance varied significantly based on weight, blade thickness, and handle dimensions.

The findings of this research provide practical insights for tool manufacturers and orchard workers by identifying key design features that influence cutting performance. Selecting ergonomically designed pruners can reduce musculoskeletal strain, improve productivity, and enhance user comfort during repetitive

agricultural tasks. Future studies may expand this work by including muscle activity analysis (EMG), operator fatigue assessment, or long-term field trials to further validate laboratory-based findings

REFERENCES

[1] Lakshmi, P. R., & Kumari, D. R. (2016). Ergonomics of bread making tools–A Review. *IJSR*, 5, 185-191.

[2] Marini, R. P., Sherif, S. M., & Smith, A. H. (2020). Physiology of pruning fruit trees. Virginia Cooperative Extension. http://hdl.handle.net/10919/100448

[3] Minaei, S., Safvati, M., & Mahdavian, A. (2023). Determination of Suitable Shearing Conditions for Effective Pruning of Tree Branches. *International Congress on Agricultural Mechanization and Energy in Agriculture*, 31-38.

[4] Päivinen, M., Haapalainen, M., & Mattila, M. (2000). Ergonomic design criteria for pruning shears. *Occupational Ergonomics*, *2*(3), 163-177. https://doi.org/10.3233/OER-2000-2304

[5] Parish. R. L. (1998). Operating Force Requırements for Manuel Pruning Shears. *Applied Engineering in Agriculture*. *14*(4), 349-352. https://doi.org/10.13031/2013.19393

[6] Pekitkan, F. G., Sessiz, A., & Esgici, R. (2020). Effects of blades types on shear force and energy requirement of paddy stem. *International Journal of Agriculture Environment and Food Sciences*, *4*(3), 376-383. https://doi.org/10.31015/jaefs.2020.3.18

[7] Ramanjineyulu, M., Rao, M. S., Siddiqua, A., & Khayum, A. (2024). Pruning in Horticulture: A Blend of Art and Science. *Journal of Scientific Research and Reports*, *30*(10), 313-329. https://doi.org/10.9734/jsrr/2024/v30i102458

[8] Romano, E., Bonsignore, R., Camillieri, D., Caruso, L., Conti, A., & Schillaci, G. (2010). Evaluation of hand forces during manual vine branches cutting. *International Conference Ragusa SHWA2010,* 465-470.

[9] Selvi, Ç. (2023). The Effects of Blade Coatings on Corce Demand When Pruning Grape. *Black Sea Journal of Engineering and Science*, *6*(2), 111-116. https://doi.org/10.34248/bsengineering.1256088

[10] Selvi, K. Ç., & Kabas, Ö. (2016). Bending and shearing properties of some standard carnation (dianthus caryophyllus l.) varieties stem. *Acta Technica Corviniensis-Bulletin of Engineering*, *9*(4), 133.

[11] Sessiz, A., Esgici, R., Özdemir, G., Eliçin, A. K., & Pekitkan, F. G. (2015). Cutting properties of different grape varieties. *Poljoprivreda i Sumarstvo*, *61*(1), 211. https://doi.org/10.17707/AgricultForest.61.1.27

[12] Song, S., Zhou, H., Jia, Z., Xu, L., Zhang, C., Shi, M., & Hu, G. (2022). Effects of cutting parameters on the ultimate shear stress and specific cutting energy of sisal leaves. *Biosystems Engineering*, *218*, 189-199. https://doi.org/10.1016/j.biosystemseng.2022.03.011

[13] Wilczyński, D., Wałęsa, K., Talaśka, K., & Wojtkowiak, D. (2023). Experimental study on the mechanical behavior of dry corn stalk cutting. *Materials*, *16*(8), 3039. https://doi.org/10.3390/ma16083039

[14] Zahid, A., Mahmud, M. S., He, L., Schupp, J., Choi, D., & Heinemann, P. (2022). An apple tree branch pruning analysis. *HortTechnology*, *32*(2), 90-98. https://doi.org/10.21273/HORTTECH04924-21

[15] Zhang, Q., Liu, F., Wu, D., Qu, S., Liu, W., & Chen, Z. (2023). A comprehensive understanding of knife cutting: effects of hardness, blade angle and the micro-geometry of blade edge on the cutting performance. *Materials*, *16*(15), 5375. https://doi.org/10.3390/ma16155375

APPLICATION OF UAV MULTISPECTRAL IMAGERY FOR VINEYARD MANAGEMENT THROUGH VEGETATION STATUS ASSESSMENT

/

APLICAREA IMAGINILOR UAV MULTISPECTRALE PENTRU MANAGEMENTUL VITICOL PRIN EVALUAREA STĂRII DE VEGETAȚIE

Dan CUJBESCU, Cătălin PERSU*, Mihai MATACHE, Iuliana GĂGEANU, Iulian VOICEA
National Institute of Research - Development for Machines and Installations Designed to Agriculture and Food Industry - INMA Bucharest / Romania.
**Tel: 0784 636 431; *E-mail: persucatalin@yahoo.com*

Keywords: *vineyard, UAV, NDVI, multispectral imagery, precision viticulture*

ABSTRACT

This paper presents a methodology for assessing vineyard vegetative condition using vegetation indices derived from high-resolution unmanned aerial vehicle (UAV) multispectral imagery. Aerial monitoring campaigns were conducted using agricultural UAV equipped with MAPIR Survey 3 multispectral camera. Flight paths and navigation waypoints were planned in Mission Planner software to ensure uniform ground sampling distance and adequate image overlap. Acquired imagery was processed in Agisoft to produce georeferenced orthomosaics, dense point clouds, and digital elevation models (DEMs). The normalized difference vegetation index (NDVI) was subsequently calculated to map intra-plot variability in vine vigor. NDVI maps revealed spatial heterogeneity at the row level, enabling the delineation of management zones and early identification of low-vigor areas. This approach supports the implementation of precision viticulture strategies by providing detailed canopy condition information, reducing field labor and allowing optimized input management.

REZUMAT

Lucrarea prezintă o metodologie pentru evaluarea stării vegetative a viței de vie utilizând indici de vegetație derivați din imagini multispectrale de înaltă rezoluție achiziționate prin intermediul unui vehicul aerien fără pilot (UAV), echipat cu camere multispectrale MAPIR Survey 3. Traseele de zbor și punctele de navigație au fost planificate în software-ul Mission Planner pentru a asigura o distanță uniformă de eșantionare la sol și o suprapunere adecvată a imaginilor. Imaginile achiziționate au fost prelucrate în Agisoft pentru a obține ortofotoplanuri georeferențiate, nori de puncte denși și modele digitale de elevație (DEM). Ulterior, a fost calculat indicele diferențial normalizat de vegetație (NDVI) pentru a cartografia variabilitatea intraparcelară a vigorii butucilor. Hărțile NDVI au evidențiat heterogenitatea spațială la nivel de rând, permițând delimitarea zonelor de management și identificarea timpurie a zonelor cu vigurozitate scăzută. Această abordare sprijină implementarea strategiilor de viticultură de precizie prin furnizarea de informații detaliate despre starea coronamentului, reducerea muncii pe teren și optimizarea aplicării inputurilor.

INTRODUCTION

Precision viticulture (PV) is a site-specific management approach aimed at optimizing grape quality and yield by monitoring spatial and temporal variability in vineyard conditions. Recent advances in remote sensing technologies have significantly improved the ability to characterize canopy vigor and variability at multiple scales (*Matese et al., 2015; Sassu et al., 2021).*

Satellite platforms such as Sentinel-2 have been widely used in viticulture because of their temporal frequency and multispectral capabilities. However, their spatial resolution (10–20 m) is often insufficient for discriminating individual vine rows, especially in narrow-spacing vineyards (*Di Gennaro et al., 2019; Campos et al., 2021*). UAV (Unmanned Aerial Vehicle) platforms equipped with multispectral cameras overcome this limitation by providing centimeter-level resolution, which allows detailed assessment of vine vigor, canopy structure, and missing plants (*Pádua et al., 2018; Vélez et al., 2023; Gavrilović et al., 2024*).

The normalized difference vegetation index (NDVI) is among the most widely used vegetation indices in viticulture for evaluating canopy density, leaf area index (LAI), and chlorophyll content (*Rouse et al., 1974; Campos et al., 2021; Reynolds et al., 2018*). NDVI-derived vigor maps facilitate the delineation of

management zones and the detection of low-vigor or stressed plants, enabling variable-rate application of fertilizers and crop protection products (*Primicerio et al., 2012; Kandylakis et al., 2020; Serrano et al., 2023*).

UAV-based multispectral sensing also supports the estimation of canopy geometric parameters such as canopy height, tree row volume (TRV), and leaf wall area (LWA), which are critical for optimizing pesticide dose and irrigation scheduling (*Poblete-Echeverría et al., 2017; Campos et al., 2021; Mesas-Carrascosa et al., 2019; Gavrilović et al., 2024*). Moreover, UAV-derived data have been successfully employed for water stress estimation (*Kandylakis et al., 2020*), multi-temporal vigor mapping (*Pádua et al., 2019*), and detection of Botrytis cinerea incidence (*Vélez et al., 2023*).

Recent studies underscore the operational benefits of UAV-based NDVI maps in precision viticulture, demonstrating their role in reducing field scouting requirements, improving the accuracy of vineyard management decisions, and enabling cost-effective site-specific strategies (*Comba et al., 2019; Poblete-Echeverría et al., 2017; Sassu et al., 2021; Reynolds et al., 2018*).

The aim of this study is to present a robust UAV-based methodology for determining vineyard vegetative condition by producing NDVI maps at centimeter-level resolution. This approach enables accurate detection of intra-plot canopy variability and supports the implementation of site-specific management strategies without relying on external satellite data sources.

MATERIALS AND METHODS

The initial phase in generating spectral maps of the vineyard crop through the aerial monitoring system based on an agricultural drone involved the precise planning and autonomous execution of the UAV flight over the targeted vineyard area. This step was implemented using the Mission Planner software, a ground control station application that allows for the configuration of flight parameters, georeferenced mission planning, and onboard navigation automation.

Within Mission Planner, the flight route was defined by inputting a set of waypoints that ensured full coverage of the vineyard parcel with adequate image overlap. Specific flight parameters included:

- Altitude: set between 40–60 meters AGL (Above Ground Level);
- Forward and side overlap: maintained above 80% to ensure sufficient stereoscopic coverage for photogrammetric processing;
- Flight speed and camera trigger interval: calibrated to match the resolution of the MAPIR Survey 3 multispectral sensor.

The mission planning accounted for environmental conditions (e.g., solar angle, wind) and GNSS signal quality to ensure accurate geotagging of the captured imagery. Upon take-off, the drone autonomously followed the programmed flight path in “AUTO” mode, navigating to the designated waypoints and triggering the camera at predefined intervals to acquire high-resolution multispectral data of the vine canopy. Once the mission was completed, the UAV automatically returned to the predefined “HOME” location for landing.

Fig. 1 - UAV agricultural monitoring platform

To generate the spectral maps using the aerial spectral monitoring system based on an agricultural drone, the following steps were carried out:

- real-time UAV flight monitoring;

Fig. 2 - Mission Planner "FLIGHT DATA" interface showing real-time UAV flight monitoring.

- flight path planning;

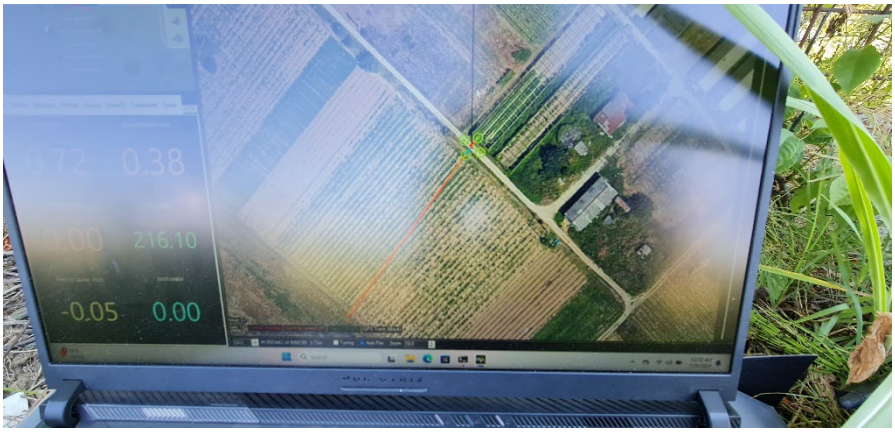

Fig. 3 - Flight path planning

- defining the flight path

Fig. 4 - Flight path planning using polygonal waypoint definition

- start of the agricultural drone flight ("LOITER" mode);

Fig. 5 - UAV take-off phase in "LOITER" mode

- after the drone take-off, the flight switched to "AUTO" mode;

Fig. 6 - UAV take-off

- the drone headed toward the intermediate waypoints, after which it began the actual mission of monitoring the vineyard crop;

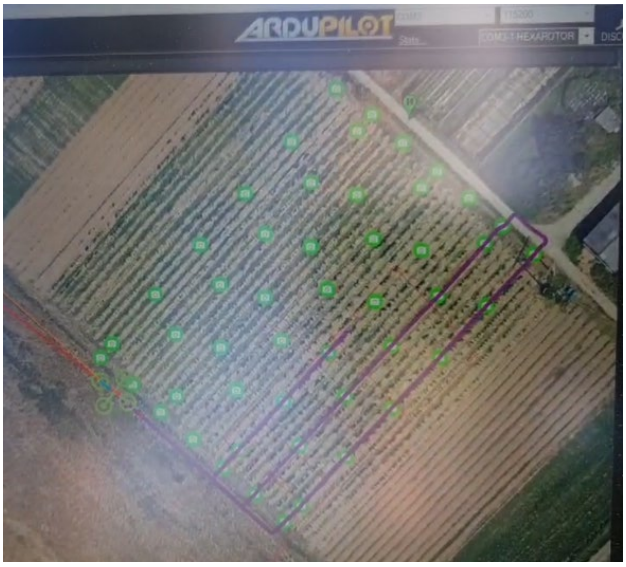

Fig. 7 - Transition to "AUTO" flight mode for mission execution.

- completion of the monitoring mission and return of the drone to the take-off/landing point "HOME".

Following the flight over the monitored vineyard crop, the images obtained using the MAPIR Survey 3 agricultural multispectral camera with integrated GPS were processed using the Agisoft Photoscan photogrammetry software by following these steps:

- the files captured by the MAPIR Survey 3 agricultural multispectral camera with integrated GPS were copied;
- the Agisoft software was launched;
- the photographs captured by the MAPIR Survey 3 multispectral camera were imported into Agisoft;

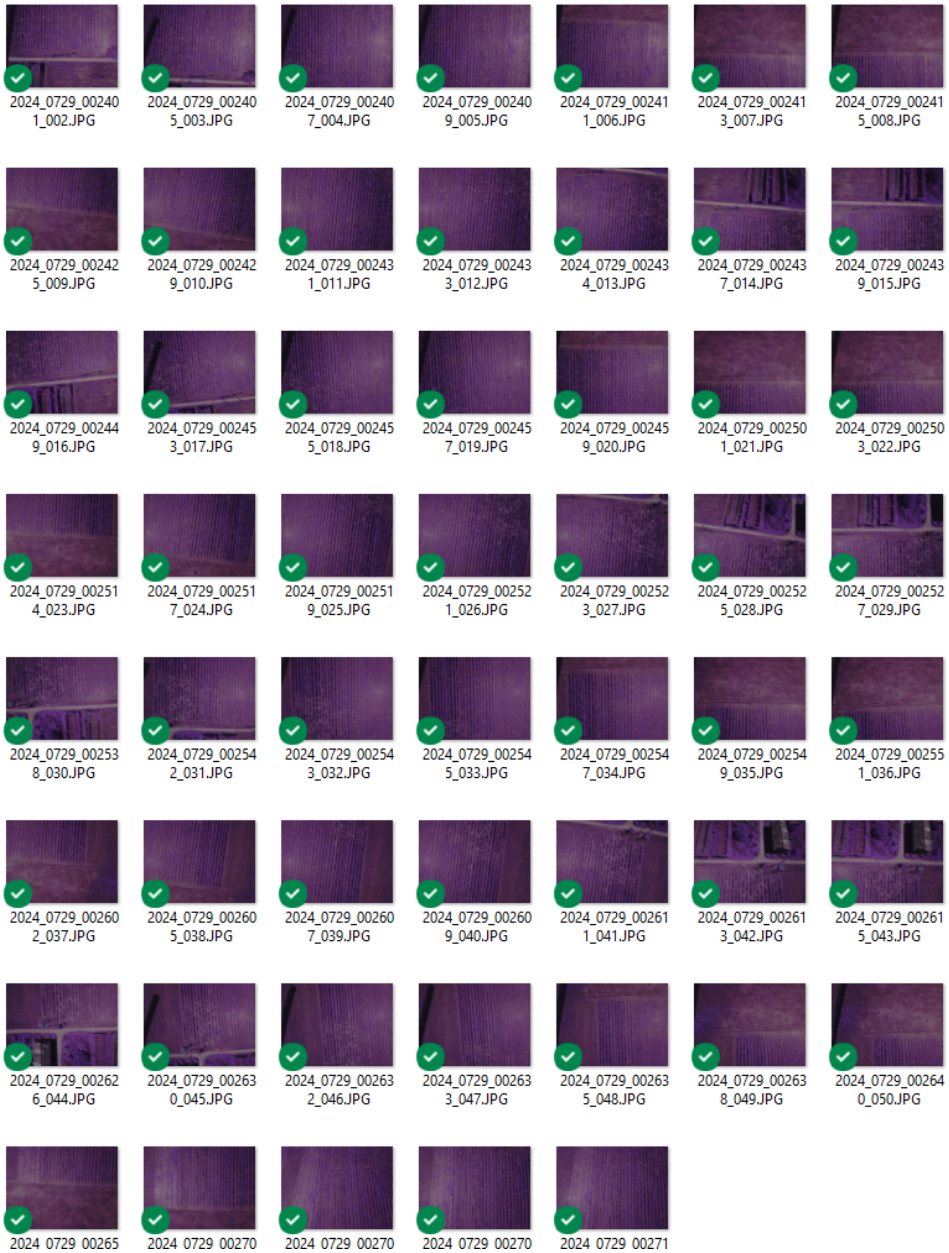

Fig. 8 - Photographs taken with the multispectral camera

- unsuitable images were removed;
- from the “Photos - Change View” menu, the images were displayed in detail;
- the image quality was checked using the “Estimate Image Quality – All Cameras” menu;
- the “Show Cameras” menu was used to display the image acquisition layout and their location;
- proper alignment of the image locations and the horizon was performed via the “Workflow – Align Photos – High” option (“Reference preselection” was enabled as GPS information was available in the photographs);
- the image alignment and the UAV flight path were obtained;
- the three-dimensional dense cloud (Dense Cloud – containing more details) was displayed and transformed into a 3D model;
- the “Workflow – Build Mesh” menu was accessed;

- the “Workflow – DEM” menu was accessed;

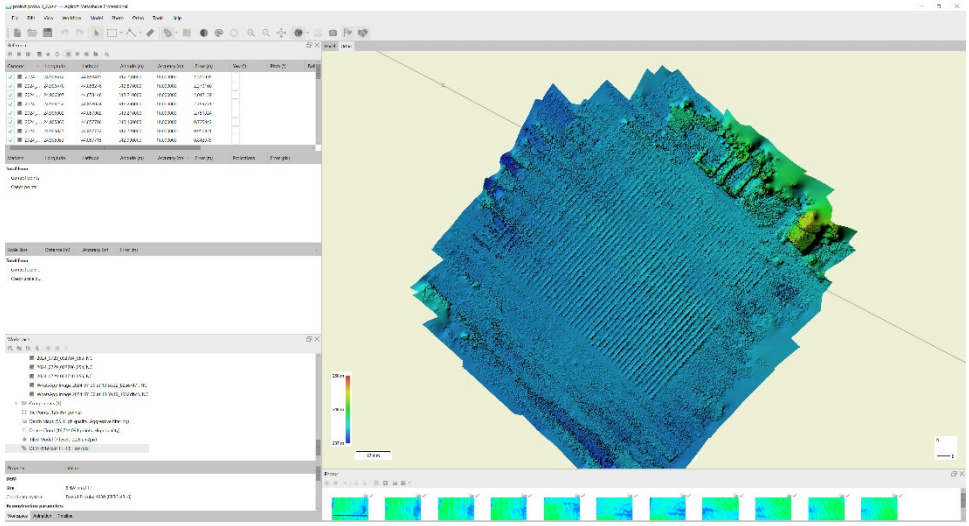

Fig. 9 - Digital Elevation Model (DEM) image

- the “Workflow – Build Orthomosaic” menu was accessed and data were processed;

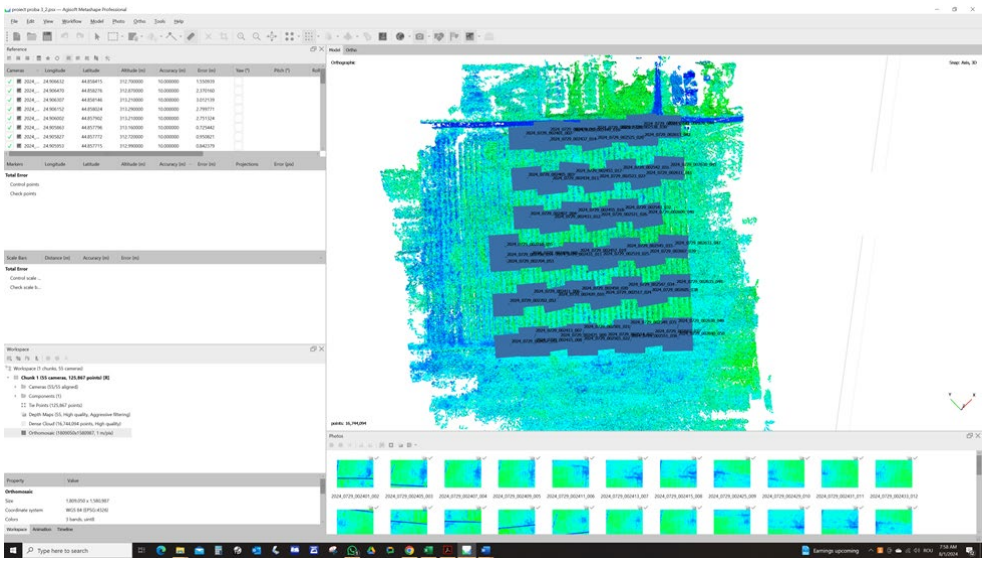

Fig. 10 - Orthomosaic image showing the identified images positioned according to GPS coordinates

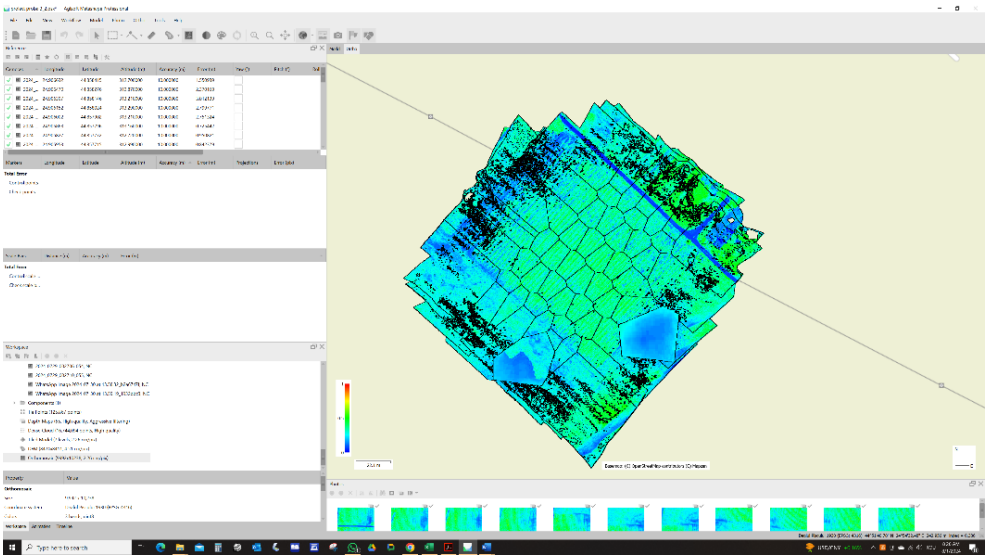

Fig. 11 - Orthomosaic image showing the alignment of processed photographs

- the orthomosaic was exported and saved in tiff format;

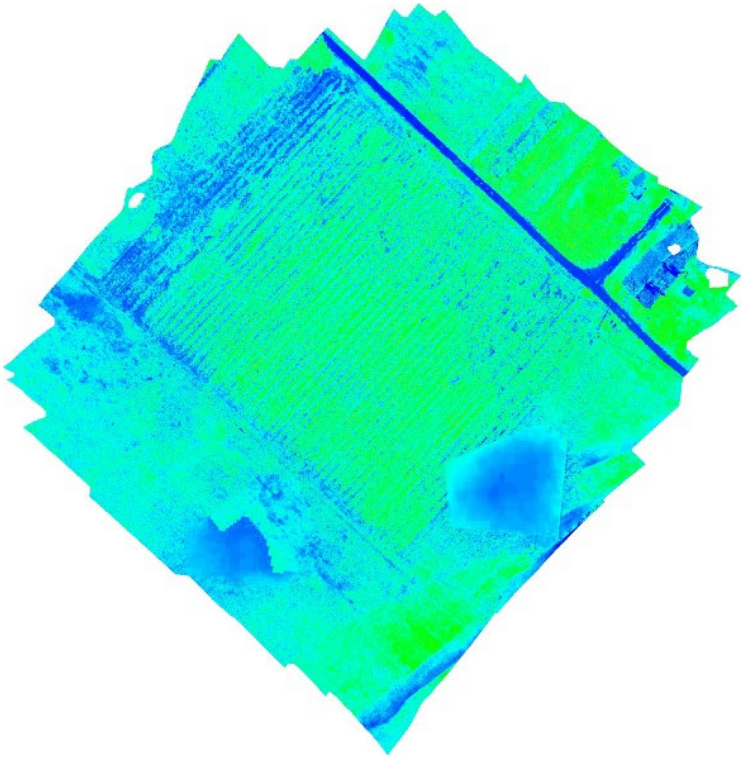

Fig. 12 - Orthomosaic image saved in JPEG format using the software

- the NDVI (Normalized Difference Vegetation Index) map was obtained, which is a non-linear transformation of the visible (RED) and near-infrared (NIR) bands defined as the difference between these two bands divided by their sum – using the "Tools – Set Raster Transform" menu.

The NDVI (Normalized Difference Vegetation Index) is a widely used indicator in remote sensing and environmental monitoring. It measures vegetation amount and health based on data derived from satellite images or ground-based sensors. NDVI is calculated using information from two different spectral bands, typically a red (RED) band and a near-infrared (NIR) band. The NDVI formula is as follows:

$$NDVI = \frac{NIR-RED}{NIR+RED}, \quad [-] \qquad (1)$$

where:

NIR - represent reflectance values in the near-infrared, [-];
RED - represent reflectance values in the red bands, [-].
The resulting value ranges from -1 to +1. Interpretation of NDVI values is as follows:

- Negative values (close to -1): Indicate surfaces covered by water or other non-vegetated areas such as snow, rock, or buildings. Negative NDVI suggests an absence of vegetation or very sparse vegetation;
- Low values (close to 0): Indicate very little vegetation, arid agricultural land, or regions with stressed or diseased vegetation;
- High values (close to +1): Indicate healthy and abundant vegetation. The closer NDVI is to +1 (>0.6), the healthier and denser the vegetation.

RESULTS

The use of NDVI in table grape crops can provide valuable information about vine health and overall condition and can be applied at various stages of crop management, such as:

- monitoring vine growth throughout the growing season;
- detecting vegetative stress: NDVI values lower than expected may indicate stress in the crop caused by water deficits, nutrient deficiencies, diseases, or pests. Early detection allows timely interventions to improve plant health;

- irrigation planning: NDVI can be used to determine irrigation needs based on the current vegetation status. Low NDVI values may indicate the need for additional water to avoid drought stress;
- assessing grape ripeness: prior to harvest, NDVI can be used to evaluate grape ripeness. Specific NDVI values can indicate the optimal harvest time, helping to ensure superior grape quality;
- identifying plant health issues: NDVI values can reveal areas with plant health problems, such as disease infections or pest infestations;
- production monitoring: collecting NDVI data over time can help estimate production potential and assess yields in table grape crops.

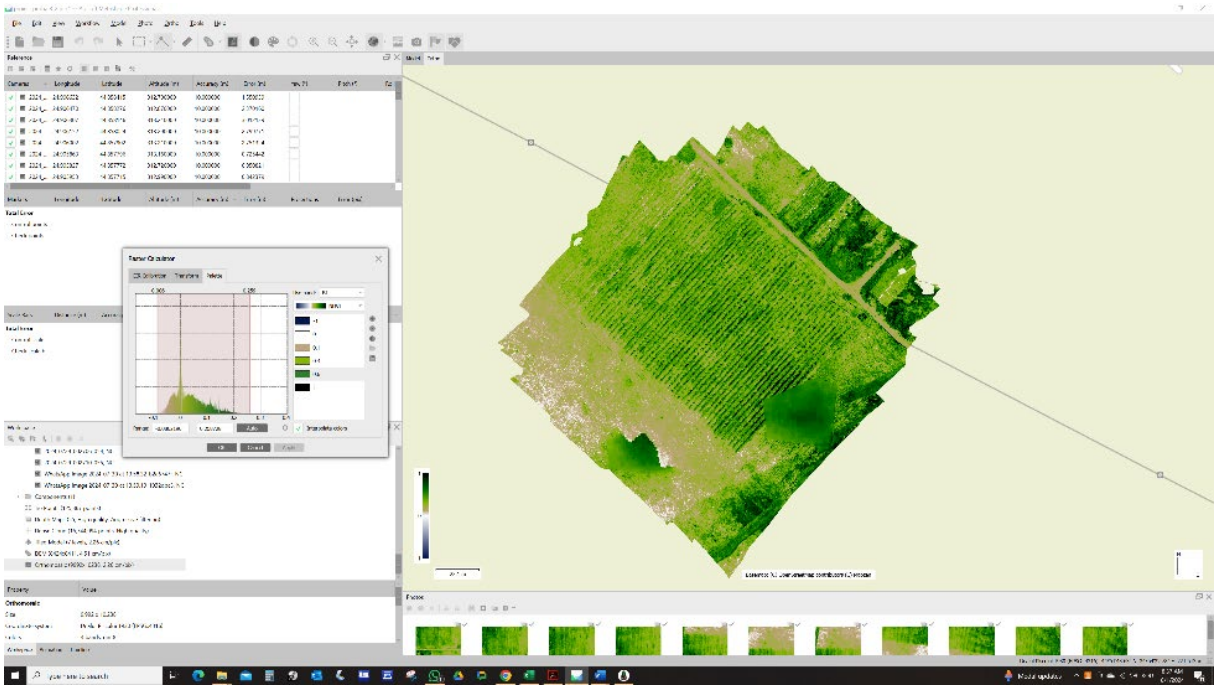

Fig. 13 - NDVI map of the monitored area

Color interpretation:

- Green areas: High NDVI values indicating healthy, dense vegetation. The darker the green, the healthier and denser the vegetation;
- Light green to yellow areas: Moderate NDVI values indicating less dense or stressed vegetation;
- White or very bright areas: Low NDVI values indicating bare soil, built-up areas, or non-vegetated surfaces.

Histogram and statistics:

- The histogram shows the distribution of NDVI values in the mapped area;
- A peak at higher NDVI values (closer to +1) indicates that most of the area is covered with healthy vegetation;
- A significant portion of the histogram at lower values (closer to 0 or negative) indicates non-vegetated areas or stressed vegetation.
- Parcel analysis:
- The studied parcel is predominantly green, suggesting that most of the area is covered with vegetation (healthy vine rows and inter-row vegetation);
- Some lighter green or yellow areas may indicate lower vegetation density or stressed plants, which could be due to factors such as soil quality, water availability, or crop health;
- White patches may correspond to roads, paths, or bare soil within the field.

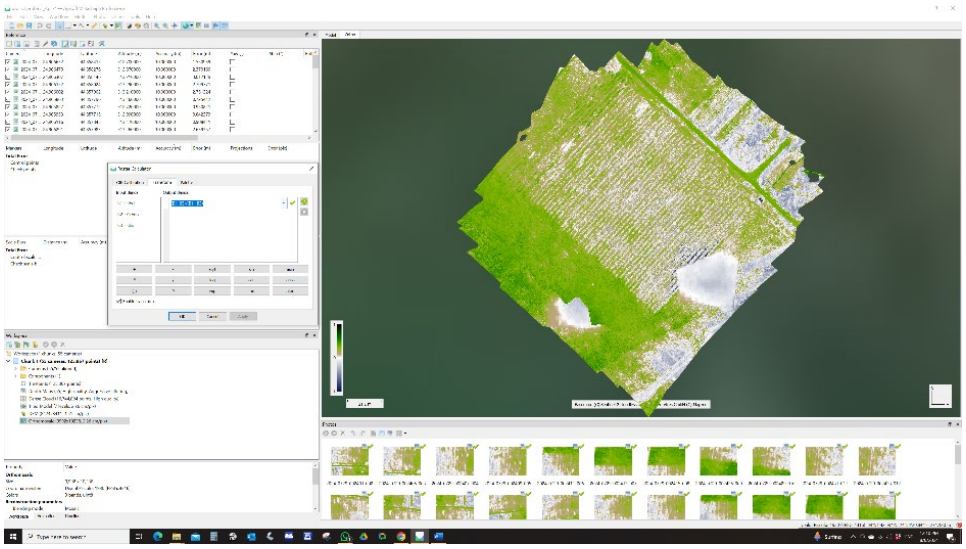

Fig. 14 - Red–Blue / (Red + Blue) map of the monitored area

The formula (Red - Blue) / (Red + Blue) is a type of vegetation index that emphasizes the difference between the red and blue spectral bands normalized by their sum. This specific index can provide information about vegetation characteristics, although it is less commonly used compared to indices such as NDVI.

Index interpretation:

- Numerator (Red - Blue):
  - The red band is typically absorbed by chlorophyll in healthy vegetation, leading to lower reflectance values in this spectral region;
  - The blue band is also absorbed by chlorophyll but generally less than the red band, depending on vegetation health and type;
  - The difference between red and blue can help highlight areas where vegetation absorbs these wavelengths differently.
- Denominator (Red + Blue):
  - Normalizes the difference, accounting for variations in lighting conditions or surface reflectance that could affect overall reflectance intensity.
  - Vegetation characteristics:
  - High index values: Indicate a greater difference between red and blue bands, suggesting strong absorption in the red band (due to high chlorophyll content) and relatively lower absorption in the blue band. These areas likely correspond to healthy vegetation;
  - Low index values: Occur when the difference between red and blue bands is small, suggesting either low absorption in both bands (possibly due to stressed vegetation, bare soil, or non-vegetated surfaces) or similar reflectance in both bands. This could also indicate water bodies, as water typically reflects both red and blue light.

Applications and limitations: This index can help differentiate vegetated from non-vegetated surfaces and may be useful in detecting vegetation stress, soil exposure, or water presence. However, it may not be as sensitive or specific as other vegetation indices, such as NDVI, which specifically use the near-infrared band in combination with the red band to highlight vegetation vigor and biomass.

CONCLUSIONS

Satellite- and UAV-based remote sensing, through the use of multispectral measurements, has significant applications in viticulture as in precision agriculture. These technologies enable detailed assessment of vine health and soil conditions, which are essential for quality wine production. Soil reflectance spectra can provide information about moisture content and organic matter, which are crucial for effective irrigation and fertilization management.

Identifying specific soil constituents, such as clay minerals and iron oxides, helps viticulturists better understand soil fertility and its influence on grape characteristics. Narrow-band or hyperspectral imagery,

together with advanced analytical techniques, can facilitate monitoring vine conditions and early detection of water stress or diseases.

However, current spaceborne instruments have limitations in resolution and spectral bands. This highlights the need to improve remote sensing technologies to support modern viticulture, thereby enhancing wine quality and optimizing cultivation practices

ACKNOWLEDGEMENT

This research was supported by the Ministry of Agriculture and Rural Development – Romania - MADR through the Sectoral Project ADER 25.2.1 "Digital system designed for monitoring orchard crops", Ctr. 20.07.2023.

REFERENCES

[1] Campos, J., García-Ruíz, F., & Gil, E. (2021). Assessment of vineyard canopy characteristics from vigour maps obtained using UAV and satellite imagery. *Sensors*, 21(7), 2363,
[2] https://doi.org/10.3390/s21072363
[3] Comba, L., Biglia, A., Ricauda Aimonino, D., & Gay, P. (2019). Unsupervised detection of missing vines using UAV images in precision viticulture. *Computers and Electronics in Agriculture*, 162, 142–151
[4] Di Gennaro, S. F., Toscano, P., Cinat, P., Berton, A., & Matese, A. (2019). Sentinel-2 validation for detection of within-field variability of vineyards in different phenological stages. *Remote Sensing*, 11(16), 1853
[5] Gavrilović, M., Jovanović, D., Božović, P., Benka, P., & Govedarica, M. (2024). Vineyard Zoning and Vine Detection Using Machine Learning in Unmanned Aerial Vehicle Imagery. *Remote Sensing*, 16(3), 584. https://doi.org/10.3390/rs16030584, https://doi.org/10.3390/rs16030584
[6] Kandylakis, Z., Falagas, A., Karakizi, C., & Karantzalos, K. (2020). Water stress estimation in vineyards from aerial SWIR and multispectral UAV data. *Remote Sensing*, 12(15), 2499,
[7] https://doi.org/10.3390/rs12152499
[8] Matese, A., Di Gennaro, S. F., Fiorillo, E., Vaccari, F. P., Primicerio, J., Belli, C., Zaldei, A., Bianconi, R., & Gioli, B. (2015). Intercomparison of UAV, aircraft and satellite remote sensing platforms for precision viticulture. *Remote Sensing*, 7(3), 2971–2990, https://doi.org/10.3390/rs70302971
[9] Mesas-Carrascosa, F. J., Pérez-Porras, F. J., de la Orden, M. S., Aguilar, F. J., & García-Ferrer, A. (2019). Canopy height models from UAV imagery for site-specific management in vineyards. *Precision Agriculture*, 20(6), 1283–1296. https://doi.org/10.1007/s11119-019-09641-8
[10] Pádua, L., Marques, P., Adão, T., Guimarães, N., Sousa, A., Peres, E., & Sousa, J. J. (2019). Vineyard variability analysis through UAV-based vigour maps to assess climate change impacts. *Agronomy*, 9(10), 581, https://doi.org/10.3390/agronomy9100581
[11] Poblete-Echeverría, C., Olmedo, G. F., Ingram, B., & Bardeen, M. (2017). Classification approaches for vineyard canopy monitoring using UAV-based RGB imagery. *Remote Sensing*, 9(3), 268, https://doi.org/10.3390/rs9030268
[12] Primicerio, J., Di Gennaro, S. F., Fiorillo, E., Genesio, L., Lugato, E., Matese, A., & Vaccari, F. P. (2012). A flexible UAV-based system for vineyards monitoring. *Sensors*, 12(3), 2879–2896
[13] Reynolds, A. G., Lee, H. S., Dorin, B., Brown, R., Jollineau, M., Shemrock, A., Crombleholme, M., Poirier, E. J., Zheng, W., Gasnier, M., Shabanian, M., & Meng, B. (2018). Mapping Cabernet Franc vineyards by UAVs for variability in vegetation indices, water status, and virus titer. *E3S Web of Conferences*, 50, 02010. https://doi.org/10.1051/e3sconf/20185002010
[14] Rouse, J. W., Haas, R. H., Schell, J. A., & Deering, D. W. (1974). Monitoring vegetation systems in the Great Plains with ERTS. *NASA Special Publication*, 351, 309–317
[15] Sassu, A., Gambella, F., Ghiani, L., Mercenaro, L., Caria, M., & Pazzona, A. L. (2021). Advances in unmanned aerial system remote sensing for precision viticulture. *Sensors*, 21(3), 956,
[16] https://doi.org/10.3390/s21030956
[17] Serrano, L., Fernández, P., & Ortega, R. (2023). Monitoring vineyard variability using UAV-derived multispectral imagery. *Environments*, 10(2), 117
[18] Vélez, S., Ariza-Sentís, M., & Valente, J. (2023). Dataset on UAV multispectral images acquired over a vineyard affected by *Botrytis cinerea* in northern Spain. Data in Brief, 46, 108876,
[19] https://doi.org/10.1016/j.dib.2022.108876

ASPECTS REGARDING THE REMEDIATION OF SOILS POLLUTED WITH POLYCYCLIC AROMATIC HYDROCARBONS THROUGH OZONATION
/
ASPECTE PRIVIND REMEDIEREA SOLURILOR POLUATE CU HIDROCARBURI AROMATICE POLICICLICE PRIN OZONARE

Carmen-Otilia RUSĂNESCU[1)], Gigel PARASCHIV[1)], Irina Aura ISTRATE*[1)], Gabriel Alexandru CONSTANTIN[1)], SORIN-Ştefan BIRIŞ[1)], Gheorghe VOICU[1)], Andrei-Marian RUSĂNESCU*[2)], Maria GHEORGHE[3)], Anca Ștefania MAXIM[1)]

[1)] National University of Science and Technology POLITEHNICA Bucharest - Faculty of Biotechnical Systems Engineering / Romania;
[2)] National University of Science and Technology POLITEHNICA Bucharest -Faculty of Computer Science / Romania;
[3)] Department of Training for Teaching Career and Socio-Human Sciences, POLITEHNICA Bucharest / Romania.
E-mail: ia_istrate@yahoo.com; rusanescuandreimarian@gmail.com

Keywords: *polycyclic aromatic hydrocarbons (PAH), ozonation, soil remediation, biodegradation*

ABSTRACT

This study investigates the effectiveness of ozone treatment, with and without toluene, for the remediation of soils contaminated with polycyclic aromatic hydrocarbons (PAHs). The results highlight complex mechanisms of both direct and indirect oxidation, influenced by the contaminant composition and the organic matter content of the soil. Ozonation in the presence of toluene enhanced contaminant mobilization through desorption and the formation of surfactant-like intermediates, facilitating oxidation. After 18 hours of treatment, a significant reduction in hydrocarbon was observed, particularly for highly unsaturated PAHs. Moreover, ozone proved effective not only in degrading easily oxidizable fractions but also resistant hydrocarbon biomarkers, indicating the potential of this technology for treating persistent residual hydrocarbons. The combined ozone–biodegradation treatment demonstrated higher efficiency in removing PAHs, including recalcitrant compounds, compared to individual methods, offering a promising solution for bioremediation of soils contaminated with complex pollutant mixtures. It was also noted that ozonation can generate poorly soluble intermediate products, such as asphaltenes, resulting from partial degradation of other fractions. Therefore, careful process management is essential to maximize treatment efficacy.

REZUMAT

Prezenta lucrare investighează eficiența tratamentului cu ozon, cu și fără adăugarea toluenului, în remedierea solurilor contaminate cu hidrocarburi policiclice aromatice (PAH). Rezultatele au evidențiat mecanisme complexe de oxidare directă și indirectă, influențate de compoziția contaminanților și conținutul de materie organică din sol. Ozonarea, în prezența toluenului, a condus la o mobilizare crescută a contaminanților prin desorbție și formarea unor produse intermediare surfactante, facilitând astfel oxidarea. După 18 ore de tratament, s-a înregistrat o reducere semnificativă a speciilor hidrocarburice, în special a PAH-urilor cu grad ridicat de nesaturare. În plus, ozonul s-a dovedit eficient nu doar în degradarea fracțiilor ușor oxidabile, ci și a unor biomarkeri hidrocaburi rezistenți, ceea ce indică potențialul acestei tehnologii în tratarea hidrocarburilor reziduale persistente. Tratamentul combinat ozonare – biodegradare s-a dovedit a fi mai eficient în eliminarea PAH-urilor, inclusiv a celor greu degradabile, comparativ cu metodele individuale, oferind o soluție promițătoare pentru bioremedierea solurilor contaminate cu amestecuri complexe de poluanți. Totodată, s-a observat că ozonarea poate genera produse intermediare greu solubile, cum ar fi asfaltenele, rezultate din degradarea parțială a altor fracții. Astfel, o gestionare atentă a procesului este esențială pentru maximizarea eficienței tratamentului.

INTRODUCTION

The contamination of sediments with polycyclic aromatic hydrocarbons (PAHs) represents a major environmental issue, given the toxicity, persistence, and bioaccumulation potential of these compounds. In this context, the development of effective remediation methods is essential. In the study conducted by Yu Zeng and P.K. Andrew Hong, the authors investigated the application of slurry-phase ozonation as a treatment technique for a PAH-contaminated sediment originating from a boat launch area polluted with coal tar. The results showed that a 2-hour ozonation led to a significant reduction (50–100%) in PAHs, while also

improving their bioavailability and biodegradability. Furthermore, the authors demonstrated the feasibility of an integrated chemical-biological approach, in which ozonation serves as a pretreatment for subsequent biological processes *(Zeng, Y., and Andrew Hong, P.K. 2011)*.

Another study highlighted that organochlorine pesticides mainly originate from pesticide use in ongoing agricultural activities, while PAH pollution stems from industrial sources (such as fossil fuel combustion, transportation, and technological processes), as well as from food packaging, processing, and transportation. The spatial distribution of these pollutants was significantly influenced by geo-climatic factors, such as precipitation, and by the physicochemical characteristics of the soil (including organic matter content and soil texture). Although the individual and cumulative carcinogenic risks of these compounds were below the critical threshold of 10^{-4}, children were found to be at higher risk compared to adults, indicating increased vulnerability within this population group. (*Liu, Y. et al, 2025)*.

A significant influence of soil properties—such as pH and clay content—on the behavior of PAHs has been observed. With the acceleration of urbanization and industrial development, intense anthropogenic activities over the past decades have led to a substantial increase in environmental contamination with hazardous organic pollutants. Among these, polycyclic aromatic hydrocarbons (PAHs) stand out due to their persistence, toxicity, mutagenic and carcinogenic potential, being considered a major threat to both the environment and human health (*Rusanescu, C.O. et al., 2023*). PAHs are frequently detected in various environmental media—air, water, soil—as well as in food products. In particular, the accumulation of PAHs in soil has a profound impact on terrestrial organisms, negatively affecting the growth, reproduction, and survival of plants, invertebrates, microorganisms, and even vertebrates. These toxic effects occur through two main exposure pathways: direct contact with contaminated soil and trophic transfer through the food chain. Moreover, due to their bioaccumulative capacity, PAHs can cause ecological imbalances and the loss of essential ecosystem functions (*Rusanescu, C.O. et al, 2024*).

Many developed countries have established ecological thresholds for PAHs in soil, taking into account both human health and ecological risks. Existing regulations primarily focus on protecting human health, while international ecological standards—such as Eco-SSL (USA, Ecological Soil Screening Levels), SQGE (Canada, Environmental and Human Health Soil Quality Guidelines), EILs (Australia, Investigation Levels for Soil and Groundwater), Eco-SGVs (New Zealand, Development of Soil Guideline Values for the Protection of Ecological Receptors), and ERL (Netherlands, Environmental Risk Limits)—integrate both direct exposure and trophic transfer through the food chain (*Han, G. et al. 2025).*

Given the toxic potential of these pollutants, this paper presents ozonation techniques as effective methods for treating environmental contaminants. Despite advances in pollution management, heteroatom-substituted polyaromatic compounds (PAXHs, where X = N, S, or O) remain toxic, often overlooked, yet widely distributed contaminants. Due to their stable structures, these compounds strongly adsorb to soil, significantly hindering remediation processes. Biodegradation has been successfully used for remediating soils contaminated with low-molecular-weight PAHs. However, bioremediation strategies have limited applicability in soils and aquifers contaminated with mixtures of high-molecular-weight PAHs. This limitation arises from the strong adsorption of these compounds to soil organic matter, the high structural stability resulting from resonance energy, and their low water solubility.

Ozone is a very powerful oxidizing agent (redox potential E_0 = +2.07 V) and has been successfully used in wastewater treatment for the oxidation of organic contaminants. It can oxidize organic compounds either directly or through the generation of hydroxyl radicals—or through both mechanisms. Following ozonation treatment, organic compounds are transformed into oxygenated intermediates, which are more water-soluble and more readily biodegradable *(Nam, K. and Kukor, J. 2000).*

MATERIALS AND METHODS

This paper synthesizes key aspects related to the remediation of soils contaminated with polycyclic aromatic hydrocarbons (PAHs) through ozonation. For this purpose, various specialized databases from recent years were consulted.

In the study conducted by Satilmis and Schrader (2023), toluene (≥99.8%) and ultrapure water were used for the ozonation process. The contaminated soil sample was collected from an industrial site, air-dried, homogenized, and sieved to 2 mm. In 25 mL vials, 85 mg of soil, 8 mL of toluene, and 10 mL of water were added. Ozone was continuously bubbled at room temperature for either 6 or 18 hours using a BMT 803N generator (1 L/h). Excess ozone was neutralized with manganese dioxide (MnO_2). After ozonation, the soil samples were filtered, dried, and subjected to Soxhlet extraction for 24 hours using 50 mL of

dichloromethane. The solvent was removed under reduced pressure, and the resulting residues were preserved for analysis. The liquid phases (water and toluene) were separated by liquid-liquid extraction. The organic phase was dried over magnesium sulfate, filtered, concentrated, and stored for further characterization *(Satilmis, I. and Schrader, W., 2023).*

RESULTS

It was found that direct ozonation of the contaminated soil, without the use of an organic solvent, did not lead to a significant removal of pollutants—most likely due to the strong binding of PAHs to the soil matrix. To increase contaminant accessibility, toluene was added as a solvent, which significantly improved ozonation efficiency. High-resolution mass spectrometry (APPI-UHRMS) enabled detailed characterization of the initial contaminants and the resulting oxidation products, revealing clear differences between the control sample and the solvent-assisted ozonated samples (with toluene), aimed at facilitating reactions between ozone and soil-adsorbed contaminants (at both 6 h and 18 h exposure times).

Following ozonation in the presence of toluene, new oxygenated species were detected, while signals corresponding to heavy PAHs and nitrogen-containing compounds decreased or were completely eliminated. For instance, the compound $C_{28}H_{17}N$ was almost entirely removed after 18 hours. Oxygenated compounds such as $C_{21}H_{18}O_6$, $C_{25}H_{18}O_3$, and $C_{22}H_{22}O_5$ were identified in increased concentrations.

The results indicated continued degradation of oxidized compounds and the formation of a wide range of oxidation products, highlighting the potential of ozonation as an effective method for remediating soils contaminated with PAXHs (*Satilmis, I. and Schrader, W., 2023*).

The distribution of compounds by heteroatom class showed the presence of various species in all three analyzed phases (organic, aqueous, and soil extract), confirming the transformation of PAHs into more polar oxidation products *(Satilmis, I. and Schrader, W. 2023).*

Analysis of the control sample showed that hydrocarbons (HC class) were the most abundant compounds, followed by nitrogen-containing species (NO, NO_2, N_2). Compared to the control, ozonation—particularly with the addition of toluene for 18 hours—led to a significant decrease in the number of hydrocarbons (from 3,211 to 2,183 species) and nitrogen-containing aromatic compounds (PANHs—from 2,052 to 522 species). However, after 6 hours of ozonation, a temporary increase in hydrocarbons was observed, likely due to more efficient extraction facilitated by toluene.

Ozonation generated a wide range of oxygenated compounds (up to O_{13}), but their number decreased after 18 hours, indicating the gradual degradation of intermediate products. The longer reaction time allowed for the transformation of high-molecular-weight compounds into smaller species *(Satilmis, I. and Schrader, W. 2023).*

After 6 hours of ozonation in the presence of toluene, hydrocarbons with up to 95 carbon atoms were detected in the organic phase (toluene), indicating the extraction of strongly adsorbed PAHs from the soil. In the aqueous phase, only a few hydrocarbon species were detected after both 6 and 18 hours of reaction. After 18 hours of ozonation, highly aromatic PAHs were completely eliminated from the soil. High-molecular-weight (HMW) PAHs appeared to degrade faster than low-molecular-weight (LMW) PAHs, possibly due to their lower concentrations in the soil (*Satilmis, I. and Schrader, W., 2023*).

The efficiency of toluene-assisted ozonation for treating soils contaminated with substituted polycyclic aromatic compounds (PAXHs) was demonstrated. In the absence of an organic solvent, direct ozonation did not result in significant contaminant reduction, suggesting strong adsorption in the soil matrix and limited accessibility for oxidation reactions. The addition of toluene increased contaminant mobilization through desorption and the formation of surfactant-like intermediates, thereby facilitating contact with ozone.

After 18 hours of ozonation, a significant reduction in hydrocarbon species (from 3,211 to 2,183) and nitrogen-containing compounds (from 2,052 to 522) was achieved, particularly for highly unsaturated PAHs.

Another study investigated the efficiency of a combined treatment method for PAH-contaminated soils using ozonation followed by biodegradation to overcome limitations related to bacterial bioavailability of contaminants (*Nam, K. and Kukor, J., 2000*).

The results showed that ozonation is effective in removing low-molecular-weight PAHs such as naphthalene, fluorene, phenanthrene, and anthracene. However, for higher molecular weight PAHs like pyrene, chrysene, and benzo(a)pyrene, the ozonation efficiency was reduced due to their strong binding to soil organic matter and low water solubility (*Nam, K. and Kukor, J., 2000*). Additionally, the presence of organic carbon in the soil (even at low levels, 0.03%) negatively affected the efficiency of the ozone treatment. By applying the combined treatment—ozonation followed by biodegradation—a significant

increase in the degradation of PAHs was observed, including resistant compounds such as chrysene and benzo(a)pyrene, which were not efficiently degraded by the bacterial consortium alone. This increased efficiency was more pronounced in soils contaminated with coal tar, likely due to enhanced bacterial activity (*Nam, K. and Kukor, J., 2000*).

Polycyclic aromatic hydrocarbons (PAHs) are important pollutants, toxic to humans and the environment. Ozone is a strong oxidant capable of transforming PAHs into more soluble and more easily biodegradable compounds. Thus, combining ozonation with biodegradation can increase the removal efficiency of heavy PAHs (*Nam, K. and Kukor, J., 2000*).

The study used sterilized soil and soil contaminated with coal tar, into which seven different PAHs were added. It was demonstrated that the combined ozonation + biodegradation treatment is more effective in eliminating PAHs—including those that are hard to degrade—than biodegradation alone (*Nam, K. and Kukor, J., 2000*). This combined method could be a promising solution for bioremediation of soils contaminated with complex PAH mixtures, such as those from former gasworks.

Combined ozonation and biodegradation treatments for removing PAHs from artificially contaminated soil (*Nam, K. and Kukor, J., 2000*) were tested in two variants: biodegradation followed by ozonation and ozonation followed by biodegradation. Biodegradation lasted 4 weeks, while ozonation was 2 days (Nam, K. and Kukor, J., 2000). In both cases, naphthalene (NAP) and fluorene (FLU) were completely eliminated. For other PAHs (phenanthrene, anthracene, pyrene, chrysene, benzo(a)pyrene), degradation increased by 6–18% compared to ozonation alone. Ozonation followed by biodegradation was more efficient than the reverse order, significantly reducing concentrations of phenanthrene, anthracene, pyrene, and chrysene. Benzo(a)pyrene (BaP) was difficult to degrade, likely due to strong binding to the soil. Ozonation produces oxygenated metabolites that are more water-soluble and biodegradable, thereby facilitating subsequent biological degradation. However, there is a risk that some intermediate metabolites may be more toxic than the original compounds (*Nam, K. and Kukor, J., 2000*). PAH degradation negatively correlates with the number of benzene rings; the larger the ring number, the harder the degradation. Combining treatments offers a better chance for complete contaminant degradation in soil (*Nam, K. and Kukor, J., 2000*).

Ozonation for 2 days effectively reduces light PAHs (NAP, PHE) but not heavy PAHs (PYR, CHR, BaP) (*Nam, K. and Kukor, J., 2000*). Biodegradation alone efficiently degrades light PAHs but struggles with heavy PAHs. Ozonation followed by biodegradation enhances degradation of 4-ring PAHs and partially BaP. BaP degradation remains limited, probably due to low ozone concentration (*Nam, K. and Kukor, J., 2000*). Nutrients are required in soil for effective biodegradation.

Ozone treatment efficiently removed 2-3 ring PAHs but less effectively those with 4-5 rings. By combining ozonation with biodegradation, approximately 95% of NAP, FLU, and PHE and about 65% of PYR and CHR were degraded in contaminated soil. BaP was reduced by ~17%, and combined biodegradation enabled BaP mineralization, which alone was not degradable. This combined method is promising for treating soils contaminated with hard-to-degrade PAHs (*Nam, K. and Kukor, J., 2000*).

The combined ozonation and biodegradation technology represents a promising solution for remediation of soils contaminated with complex PAH mixtures, such as those from former manufactured gas plant sites (*Nam, K. and Kukor, J., 2000*). After prolonged bioremediation, residual petroleum in soil was highly degraded—no alkanes below C14 remained, and concentrations of alkanes and PAHs were much lower than in crude oil. Long-chain alkanes (C34–C40) and 4–6 ring PAHs became predominant, while easily degradable compounds disappeared.

Biomarkers (terpanes, steranes, and triaromatic steranes) were very resistant to bioremediation (losses <35%) (*Wang, J. et al., 2013*). During ozonation (15 hours), total solvent-extractable materials (TSEM) decreased by nearly 69%. Hydrocarbon fractions (saturates, aromatics, and resins) decreased significantly. Ventilation with oxygen without ozone had no effect, indicating ozone's essential role in degradation (Wang, J. et al., 2013). This confirms that ozonation effectively reduces residual hydrocarbons in already bioremediated soils, especially resistant fractions (*Wang, J. et al., 2013*).

Figure 1 shows changes in SARA fractions (Saturates, Aromatics, Resins, Asphaltenes) during ozonation. During the ozonation process of hydrocarbon-contaminated soil, a significant decrease in the total solvent-extractable materials (TSEM) content was observed, reduced by approximately 69% after 15 hours of treatment. This indicates a high efficiency of ozone in oxidizing and decomposing residual hydrocarbons.

Analysis of the SARA fractions (Saturates, Aromatics, Resins, and Asphaltenes) revealed the following changes:

Saturates decreased from 33.6% to 21.6%, indicating degradation of saturated fractions in the soil.

Aromatics decreased from 28.6% to 20.8%, reflecting the oxidation of polycyclic aromatic compounds.

Resins decreased from 36.4% to 28.5%, showing a reduction of intermediate polar fractions.

Asphaltenes increased significantly, from 1.5% to 28.5%, suggesting accumulation of oxygenated and poorly soluble intermediate products formed during ozonation.

These changes indicate that ozonation not only reduces the total amount of hydrocarbons but also transforms chemical structures, leading to the formation of oxygenated compounds with reduced solubility, which may influence subsequent biological degradation (*Wang, J. et al., 2013*).

Figure 2 displays changes in five hydrocarbon groups during ozonation (n-alkanes, terpanes, steranes, PAHs, TAS).

During 15 hours of ozonation, all five groups of hydrocarbons in the soil were degraded to varying degrees:

TAS (Triaromatic Steranes): showed the highest degradation with a 94% removal.

Steranes: decreased by 86.4%.

PAHs (Polycyclic Aromatic Hydrocarbons): reduced by 84.5%.

Terpanes: declined by 80.4%.

Alkanes: experienced the least degradation, with a 59.1% reduction.

The order of reactivity to ozone, from most sensitive to most resistant, was:

TAS > Steranes > PAHs > Terpanes > Alkanes

Although TAS, steranes, and terpanes are typically very stable and resistant to biodegradation, ozonation proved to be an effective treatment for degrading these compounds (*Wang, J. et al., 2013*).

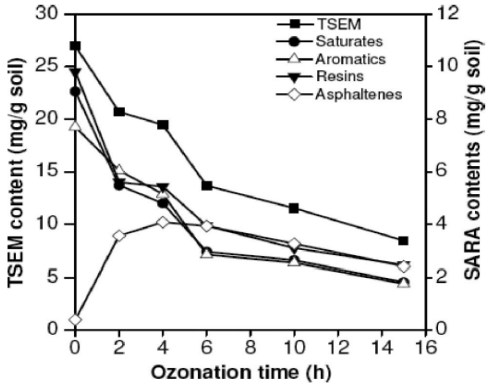

Fig. 1 - Changes in TSEM and SARA Fractions Content During Ozonation

(Wang, J. et al, 2013).

SARA stands for saturated fatty acids, aromatic resins and asphaltenes. TSEM (total solvent extractable matters)

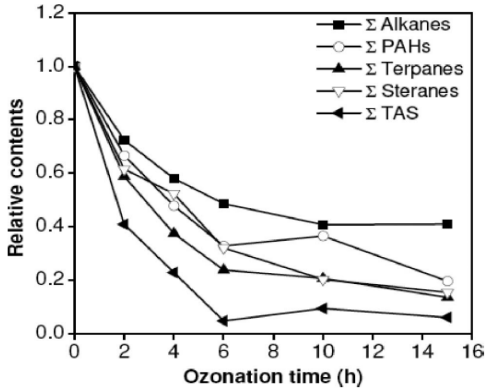

Fig. 2 - Changes in the Content of Five Hydrocarbon Groups (Alkanes, PAHs, Terpanes, Steranes, and TAS) in Soil During Ozonation

(Wang, J. et al, 2013)

TAS - triaromatic steranes

Ozone has been demonstrated to be an effective oxidant for the remediation of soils contaminated with polycyclic aromatic hydrocarbons (PAHs). The reactivity of PAHs with ozone is influenced by the soil

matrix, with higher ozone concentrations enhancing oxidation efficiency, while ozone flow rate appears to have minimal impact. The majority of PAH removal occurs during the initial stages of treatment. Ozone decomposition in soil involves interactions with easily oxidizable organic compounds, stable reaction intermediates, and inorganic soil components, which catalyze ozone breakdown and enhance the overall oxidation process (*Rivas, J. et al., 2009*).

Oxidative treatment is particularly advantageous for PAH-contaminated soils due to the following reasons:

Sole extraction methods are insufficient, as they primarily mobilize but do not degrade PAHs.

Bioremediation is cost-effective and environmentally friendly but limited by the strong sorption of PAHs to soil particles, resulting in slow degradation rates.

Chemical oxidation offers:

Rapid reaction kinetics.

Access to otherwise biologically inaccessible contaminants.

Applicability in situ, on site, or ex situ.

Transformation of hydrophobic PAHs into more soluble and biodegradable oxidation products.

However, chemical oxidation has drawbacks, including higher operational costs relative to bioremediation, potential reagent losses, and the need for careful management of solvents and secondary reaction products.

Common oxidative technologies include ozone treatment, Fenton's reagent, supercritical water oxidation, permanganate, and persulfate oxidation. For enhanced remediation performance, a combined approach integrating chemical oxidation as a pretreatment step followed by bioremediation as a polishing step is recommended. According to Rivas (2006), soil remediation using ozone is a versatile technology deployable in situ, on site, or off site.

Ozone can be introduced as a gas or aqueous phase, with gaseous ozone exhibiting superior diffusivity and higher local concentrations, thus improving contaminant destruction efficacy, especially for PAHs. Ozone treatment efficiency diminishes with increasing soil moisture content, highlighting the necessity of thorough soil characterization to optimize ozone distribution and prevent preferential flow paths that cause uneven treatment. Reaction rates of PAHs with ozone are slower in soil matrices compared to aqueous systems.

Additionally, soil organic matter and metal oxides can modulate ozone consumption; these components may facilitate the generation of highly reactive hydroxyl radicals, further accelerating oxidation processes.

Table 1

Ozone soil remediation technologies

Variables studied	Parameters measured	PAHs oxidised	Notes	References
Combination of chemical oxidation +biodegradation	PAH removal, biodegradability	Fluoranthene, phenanthrene, fluorene, pyrene, triphenylene, benz(*a*)anthracene, chrysene	In the single ozonation process, high molecular weight PAHs exhibit higher removal efficiency compared to low molecular weight PAHs. Conversely, biodegradation experiments show greater degradation rates for low molecular weight PAHs than for their high molecular weight counterparts.	Kulik, N. et al, 2006
Two and three phases ozonation, soil nature, PAH molecular weight	PAH removal, biodegradability	Phenanthrene, anthracene, fluoranthene, pyrene, triphenylene, benz(*a*)anthracene, chrysene, perylene, benzo(*e*)pyrene, benzo(*a*)pyrene, benzo(*g*,*h*,*i*)perylene	Two-phase ozonation demonstrates higher efficiency compared to three-phase ozonation. The combined treatment of ozone followed by biodegradation proves to be effective for remediating contaminated soils. PAHs with a lower number of aromatic rings	Goi,A. and Trapido, M. 2006

			are more readily degraded than their higher molecular weight counterparts.	
Soil nature, radical scavengers, zone dose, humic substances	PAHs removal,ozone uptake	Phenanthrene, benzo(*a*)pyrene	Ozone dosage exhibits a positive effect on the treatment efficiency, while the presence of tert-butanol and humic substances negatively impacts the process. The influence of carbonates is inconclusive, showing no definitive trend.	Choi, H. et al, 2001
Presence of organic matter, soil moisture, soil texture	Ozone demand, PAH removal, toxicity	Pyrene, naphthalene, chrysene, phenenthrene	Soil moisture increases the ozone demand compared to dry soils. The rate of PAH ozonation in soil is lower than expected based on aqueous-phase experiments.	Masten, S.J. and Davies SHR, 1997
Feasibility to treat sediments from a freshwater boat slip subjected to coal tar contamination	PAH removal, biodegradability, chemical oxygen demand, by-products	Naphthalene, phenanthrene, pyrene, benzo[*a*]pyrene	A 2-hour ozonation treatment achieves 50–100% removal of various PAHs present in both the solid and aqueous phases of the sediment. The ozonation process alters the sediment's organic and inorganic composition. Additionally, ozonation enhances the biodegradability of the contaminants, making an integrated chemical-biological remediation approach a viable and effective strategy.	Zeng, Y., and Hong P.K.A. 2002

CONCLUSIONS

This study demonstrates the effectiveness of both direct and indirect oxidation mechanisms during ozonation in treating soils contaminated with complex mixtures of PAHs and organic matter. The presence of organic solvents such as toluene enhances remediation by increasing contaminant bioavailability and facilitating oxidation reactions.

Ozone efficiently degrades not only easily oxidizable fractions but also highly resistant hydrocarbon biomarkers, making it a promising technology for reducing residual hydrocarbons in contaminated soils.

During ozonation, saturated compounds, aromatics, and resins undergo transformation, while the observed increase in asphaltenes indicates the formation of partially oxidized, poorly soluble intermediate products.

The combined ozone-biological treatment represents an optimized approach for remediating soils contaminated with complex PAH mixtures, achieving higher degradation rates compared to individual methods.

In the absence of an organic solvent, the efficiency of direct ozonation is limited due to strong contaminant adsorption onto the soil matrix. The addition of toluene promotes contaminant mobilization through desorption and surfactant-like intermediate formation, enhancing contact with ozone.

After 18 hours of ozonation in the presence of toluene, a significant reduction of hydrocarbon and nitrogen-containing compounds was observed, particularly for highly unsaturated PAHs, confirming the potential of this treatment for persistent soil pollution remediation.

ACKNOWLEDGEMENT

This work was supported by the project, Establishment and operationalization of a Competence Center for Soil Health and Food Safety-CeSoH, Contract no.: 760005/2022, specific project no. 1, with the title, Soil health and food safety by introducing a soil remediation protocol and developing mobile remediation equipment to reduce the concentration of organic/inorganic pollutants, Code 2, financed through PNRR-III-C9-2022–I5 (PNRR-National Recovery and Resilience Plan, C9 Support for the private sector, research, development, and innovation, I5 Establishment and operationalization of Competence Centers).

REFERENCES

[1] Choi, H., Y. Kim, H. Lim, J. Cho, J. Kang, K. Kim, (2001). Oxidation of polycyclic aromatic hydrocarbons by ozone in the presence of sand, *Water Sci. Technol*. 43, 349–356.

[2] Goi, A., Trapido, M., (2004). Degradation of polycyclic aromatic hydrocarbons in soil: the Fenton reagent versus ozonation, *Environ. Technol*. 25, 155–164.

[3] Han, G., Huang, Y., Yang, M., Meng, D, Xia, H., Cui, H., Du, D., (2025). Ecological risk-based soil thresholds for polycyclic aromatic hydrocarbons (PAHs) addressing direct contact and food chain exposure in China, *Science of The Total Environment*, 992, 179978.

[4] Liu, Y., Wang, Z., Liu, M., Zhang, T., Liu, S., Lu, K., (2025). Characterization, sources and risk assessment of organochlorine pesticides (OCPs), organophosphorus pesticides (OPPs) and polycyclic aromatic hydrocarbons (PAHs) in agricultural soils from Jilin Province in Northeast China, *Stochastic Environmental Research and Risk Assessment*, Volume 39, 1741–1755.

[5] Kulik, N., Goi, A., Trapido, M., Tuhkanen, T. (2006). Degradation of polycyclic aromatic hydrocarbons by combined chemical pre-oxidation and bioremediation in creosote contaminated soil, *J. Environ. Manage*. 78. 382–391.

[6] Masten, S.J., Davies, S.H.R. (1997). Efficacy of in-situ ozonation for the remediation of PAH contaminated soils, J. *Contamin. Hydrol.* 28, 327–335.

[7] Nam, K., Kukor, J. (2000). Combined ozonation and biodegradation for remediation of mixtures of polycyclic aromatic hydrocarbons in soil, *Biodegradation* 11: 1–9.

[8] Rivas, J., Gimeno, O., Ruth G. de la Calle, Beltrán, F. (2009). Ozone treatment of PAH contaminated soils: Operating variables effect, *Journal of Hazardous Materials* 169, 509–515

[9] Rivas, J., (2006). Polycyclic aromatic hydrocarbons sorbed on soils: A short review of chemical oxidation based treatments, *Journal of Hazardous Materials* B138, 234–251.

[10] Rusănescu, C.O., Istrate, I.A., Constantin, G.A. Paraschiv, G., Voicu, G., Biriș, S.St., Rusănescu, A.M., Moiceanu, G., Bratu, A.C., Găgeanu, I., (2023) Remedy of soils contaminated with petroleum hydrocarbons using biodegradable absorbent, *ISB-INMATEH*, 180-186, Print: ISSN 2344 - 4118 CD-ROM: ISSN 2344 - 4126 Online: ISSN 2537 – 3773, ISSN-L 2344 – 4118.

[11] Rusănescu, C.O., Istrate, I.A., Constantin, G.A. Paraschiv, G., Voicu, G., Biriș, S.St., Rusănescu, A.M., Marin, E., Bălănescu, S.M., Purdea, L., Sorică, C., (2024). Remedy of polluted soils with polycyclic aromatic hydrocarbons using nanomaterials, *ISB-INMATEH*, Print: ISSN 2344 – 4118, CD-ROM: ISSN 2344 - 4126 Online: ISSN 2537 – 3773 ISSN-L 2344 – 4118, pp.94-102.

[12] Satilmis, I., Schrader, W. (2023). Investigation of the Ozonation of Highly PAXHs Contaminated Soil Using Ultrahigh Resolution Mass Spectrometry, *Environments,* 10, 18.

[13] Wang, J., Zhang, X., Li, G. (2013). Compositional Changes of Hydrocarbons of Residual Oil in Contaminated Soil During Ozonation, *Ozone: Science & Engineering*, 35:5, 366-374.

[14] Zeng, Y., Hong, P.K.A. (2002). Slurry-phase ozonation for remediation of sediments contaminated by polycyclic aromatic hydrocarbons, *J. Air Waste Manage. Assoc*. 52, 58–68.

[15] Zeng, Y., Andrew Hong, P.K. (2011). Slurry-Phase Ozonation for Remediation of Sediments Contaminated by Polycyclic Aromatic Hydrocarbons, *J. Air & Waste Manage. Assoc.* 52:58-68, ISSN 1047-3289.

BIOREMEDIATION OF SOILS CONTAMINATED WITH HYDROCARBONS USING MICROBIAL CONSORTIA

/

BIOREMEDIEREA SOLURILOR CONTAMINATE CU HIDROCARBURI UTILIZÂND CONSORȚII MICROBIENE

Mirela-Nicoleta DINCĂ*, Mariana FERDEȘ, Irina - Aura ISTRATE, Gabriel - Alexandru CONSTANTIN, Gigel PARASCHIV, Mariana IONESCU, Bianca - Ștefania ZĂBAVĂ, Gabriel MUȘUROI, Georgiana MOICEANU, Carmen-Otilia RUSĂNESCU

National University of Science and Technology Politehnica Bucharest / Romania.

**Tel: +40761 938 017; *E-mail: mirela.dinca@upb.ro*

Keywords: *petroleum hydrocarbons, agricultural soil, bioremediation, microbial consortia*

ABSTRACT

The petroleum industry is one of the major industrial sectors, and its activities lead to the pollution of agricultural land. Environmental pollution associated with petroleum hydrocarbons, and their refined products is a serious concern because it harms the ecosystems, human health, groundwater quality and soil fertility. The main soil pollutants include polycyclic aromatic hydrocarbons, petroleum and related products, pesticides, chlorophenols and heavy metals. Polluted soil can be remediated using both biological and physico-chemical methods. Among the treatment methods, bioremediation has gained particular attention because it is an economical, effective and environmentally friendly method of remediation for soils contaminated with petroleum hydrocarbons. This review focuses on the bioremediation of hydrocarbon-contaminated soils using microbial consortia. In addition, the main classes of petroleum hydrocarbons, the types of microorganisms involved, and the bioremediation techniques applied to hydrocarbon-polluted soils are described.

REZUMAT

Industria petrolieră reprezintă unul dintre principalele sectoare industriale, însă activitățile sale conduc la poluarea terenurilor agricole. Poluarea mediului asociată cu hidrocarburile petroliere și produsele lor rafinate reprezintă o preocupare serioasă, deoarece afectează ecosistemele, sănătatea umană, calitatea apelor subterane, precum și fertilitatea solului. Principalii poluanți ai solului includ hidrocarburile aromatice policiclice, petrolul și produsele conexe, pesticidele, clorofenolii și metalele grele. Solul poluat poate fi remediat utilizând atât metode biologice, cât și metode fizico – chimice. Printre metodele de tratament, bioremedierea a câștigat o atenție deosebită datorită faptului că este o metodă de remediere a solurilor contaminate cu hidrocarburi petroliere economică, eficientă și ecologică. Acest review tratează bioremedierea solurilor contaminate cu hidrocarburi utilizând consorții microbiene. În plus, în lucrare sunt descrise principalele clase de hidrocarburi petroliere, tipuri de microorganisme utilizate în procesul de bioremediere, precum și tehnici de bioremediere utilizate pentru solurile poluate cu hidrocarburi petroliere.

INTRODUCTION

Lately, the pollution of agricultural lands has become a major problem worldwide and is associated with industrial development. The oil industry is one of the major industrial sectors and its activities lead to the pollution of agricultural lands. The environmental pollution associated with petroleum hydrocarbons and their refined products is a serious concern as it affects the ecosystem and human health, groundwater quality and soil fertility *(Varjani, S., Upasani, V. N., Pandey, A., 2020).*

Due to the huge demand as an energy source, contamination with petroleum hydrocarbons occurs quite often as a result of exploration, production, maintenance, transportation, storage, and accidental release, leading to significant environmental impacts (*Ahmed F., Fakhruddin A.N.M., 2018*). Petroleum hydrocarbons and heavy metals are classified as major pollutants that represent a serious environmental threat *(Haque, S., Srivastava, N., Pal, D.B. et al, 2022).*

The concentration of total petroleum hydrocarbons in soil was reported to be approximately 44,600 mg/kg dry soil. Total petroleum hydrocarbons are composed of aliphatic hydrocarbons and aromatic compounds, which have harmful effects on humans and other organisms. In addition, oil released on soils

involves serious pollution problems *(Feng, L., Jiang, X., Huang, Y. et al, 2021)*. When entering the soil, hydrocarbons alter soil properties such as electrical conductivity, pH, hydrophobicity, destroy soil texture and structure, or may affect soil biological properties, in particular microbial population and enzyme activity, indirectly affecting the availability of nutrients to plants *(Ambaye, T.G., Chebbi, A., Formicola, F. et al, 2022)*.

Polluted soil can be remediated using both biological and physical-chemical methods. Biological techniques are more energy-efficient than physico – chemical methods, but less effective in treating oil spills. Some forms of micro-organisms can break down oil and use it as a source of carbon and energy. The unique breakdown of hydrocarbons into simpler products is due to the genetic characteristics of microbes (*Ajona, M., Vasanthi, P., 2021*). Among the treatment methods, bioremediation has gained particular attention because it is an economical, efficient and environmentally friendly method to remediate soils contaminated with petroleum hydrocarbons *(Feng, L., Jiang, X., Huang, Y. et al, 2021)*.

Microbial communities, such as heterotrophic bacteria and fungi, can metabolize and convert complex petroleum hydrocarbon-based pollutants into simple, less toxic forms and are widely used as bioremediation agents to remove petroleum hydrocarbons from the environment *(Ambaye, T.G., Chebbi, A., Formicola, F. et al, 2022)*. Microbial consortia have a higher degradation capacity than a single microbial species, the use of a single micro-organism limits the efficiency of the process *(Lázaro-Mass, S., Gómez-Cornelio, S., Castillo-Vidal, M. et al, 2023)*.

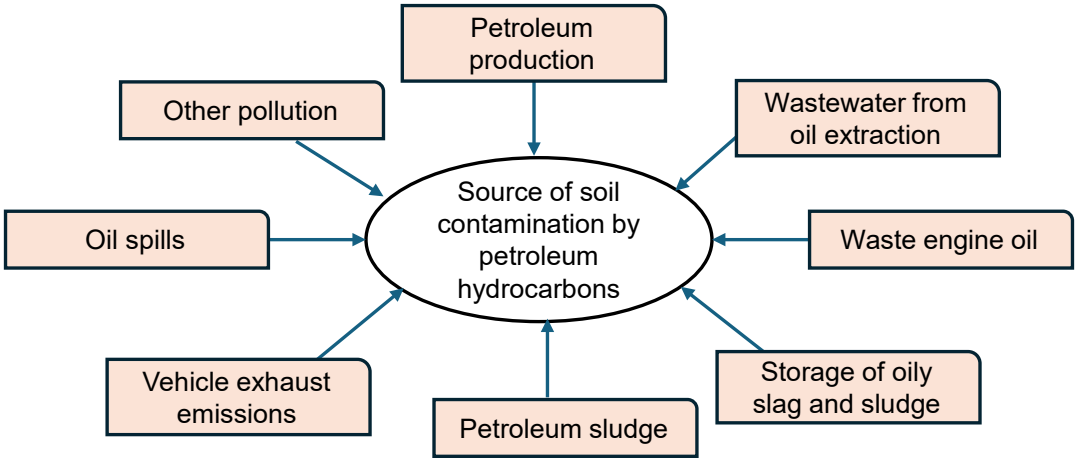

Fig. 1 - The main sources of soil contamination by petroleum hydrocarbons
(adapted from Ambaye, T.G., Chebbi, A., Formicola, F. et al, 2022 and Sui, X., Wang, X., Li, Y. et al, 2021)

The present review focuses on the bioremediation of hydrocarbon contaminated soils using microbial consortia. In addition, the main classes of petroleum hydrocarbons, types of microorganisms used in the bioremediation process, and bioremediation techniques used for hydrocarbon-polluted soils are described.

CLASSIFICATION OF PETROLEUM HYDROCARBONS

Petroleum hydrocarbons as contaminants are a highly toxic mixture of paraffinic, aliphatic and aromatic compounds and have become a serious environmental concern because of their ability to pollute soil and water (*Ambaye, T.G., Chebbi, A., Formicola, F. et al, 2022*).

Total petroleum hydrocarbons (TPH) include *(Mekonnen, B. A., Aragaw, T. A., Genet, M.B., 2024; Ferdeș, M., Dincă, M. N., Istrate, I. A. et al, 2024)*:

1. saturated hydrocarbons (aliphatic)
2. aromatic fraction
3. resins
4. asphaltene.

In general, the structure of petroleum hydrocarbons consists of about 57% aliphatic hydrocarbons, followed by about 29% aromatic hydrocarbons and about 14% as asphaltenes with various polar compounds *(Haque, S., Srivastava, N., Pal, D.B. et al, 2022)*. Based on their chemical structure, saturated hydrocarbons are classified into groups including alkanes (paraffins) and cycloalkanes (naphthenes). Longer chain aliphatic hydrocarbons (C20-C40) are more persistent in soil, do not volatilize easily and are difficult to degrade due to their low water solubility, biological availability and structure *(Koshlaf, E., Ball, A.S., 2017)*.

There are two main categories of compounds: volatile petroleum hydrocarbons and petroleum extractable hydrocarbons. The first group includes short-chain hydrocarbons (C6-C10), which include

benzene, toluene, ethylbenzene and xylene (BTEX). The second group includes long-chain aliphatic hydrocarbons (C10-C40) and polycyclic aromatic hydrocarbons (PAHs) *(Mayans, B., Anton-Herrero, R., García-Delgado, C. et al, 2024)*. These contaminants cause physico-chemical changes in soil properties such as texture, moisture, conductivity, total organic carbon, permeability and compaction and as well as in the biological properties (biomass and enzymes) *(Daâssi, D., Almaghribi, F. Q., 2022)*. In addition, through the soil and, consequently, through plants, these contaminants can be introduced directly into the food chain and are capable of altering physiological or biological processes in many species, including humans, thereby causing serious chronic diseases. In addition, of the various contaminants of petroleum hydrocarbons, BTEX compounds are known to be the most toxic *(Haque, S., Srivastava, N., Pal, D.B. et al, 2022)*. The main soil pollutants include PAHs, petroleum and related products, pesticides, chlorophenols and heavy metals *(Chen, M., Xu, P., Zeng, G. et al, 2015)*.

BIOREMEDIATION TECHNIQUES FOR PETROLEUM HYDROCARBONS POLLUTED SOILS

Soil contamination with petroleum products is a major problem for both the environment and public health, with global implications. Naturally, the process of petroleum degradation in contaminated soil is slow, and complete removal of contaminants is often impossible to achieve. Currently, contaminated soil remediation is achieved through a variety of techniques, including physical methods such as incineration, thermal desorption, landfilling, and electrokinetic treatment, as well as chemical methods such as chemical oxidation and washing extraction *(Yan, Z. F., Fei, Y., Wang, Z. Q. et al, 2024)*. Given the adverse effects associated with other methods, bioremediation has gained considerable attention in recent years, as it is considered a more environmentally friendly alternative.

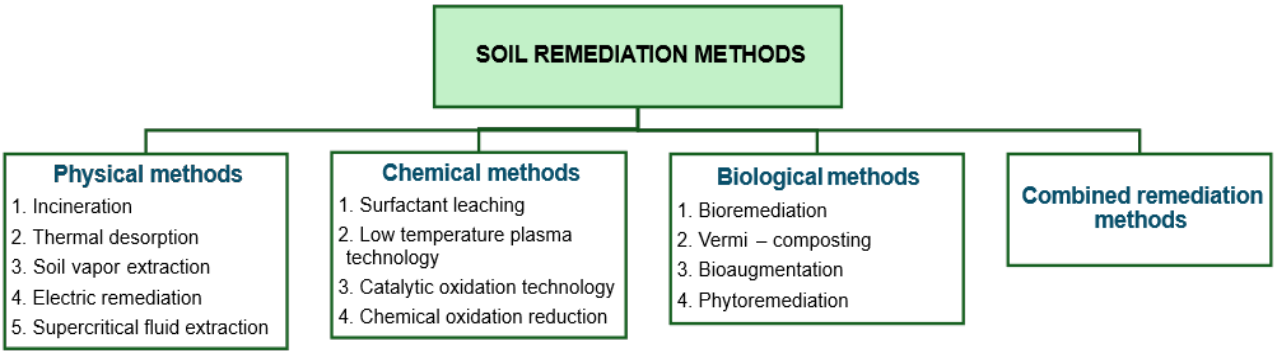

Fig. 2 - Remediation methods for petroleum contaminated soils
(based on Lv, Y., Bao, J., Zhu, L., 2022)

Bioremediation (biological remediation) is an effective, economical and environmentally friendly method that has become widely used for the mineralization of organic contaminants in soil and wastewater. Bioremediation is based on microbial metabolic activities in the presence of optimal ecological factors and the necessary nutrients to transform organic pollutants such as petrogenic hydrocarbons. It has been shown in the literature that bacteria, fungi and some microalgae can completely mineralize petroleum hydrocarbons to carbon dioxide (CO_2), water (H_2O), inorganic compounds, cellular proteins and simple organic compounds found in soil and water *(Mekonnen, B. A., Aragaw, T. A., Genet, M. B., 2024; Koshlaf, E., Ball, A. S., 2017)*

Based on the place of application, bioremediation techniques can be grouped into *ex-situ* and *in-situ* bioremediation. Bioremediation methods are economical and environmentally friendly especially when applied *in-situ* (*Alori E.T., Gabasawa A.I., Elenwo C.E. et al, 2022)*.

For *ex-situ* bioremediation methods, the polluted soil is transported from the site of pollution to another site for treatment, considering the concentration of the pollutant, the level of contamination, the type of pollutant, the cost of treatment, and the geographical location of the polluted site. By *in-situ* bioremediation techniques, the pollutants from the soil are removed right at the pollution site; the soil is treated directly at the pollution site, which makes the method more cost-effective than *ex-situ* bioremediation techniques. Some *in-situ* bioremediation techniques are enhanced by the microbes present in the polluted soil (*Alori E.T., Gabasawa A.I., Elenwo C.E. et al, 2022; Hussain, A., Rehman, F., Rafeeq, H. et al, 2022*).

Different types of biological remediation methods are used to treat hydrocarbon polluted soils. The classification of the bioremediation techniques is presented in Figure 3.

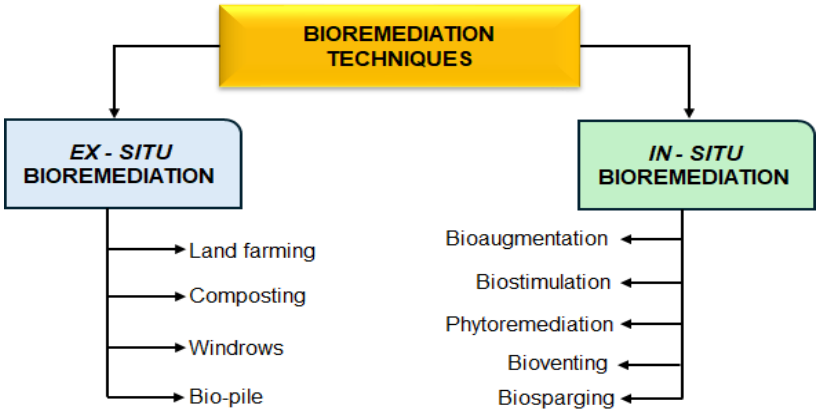

Fig. 3 - Bioremediation techniques for petroleum hydrocarbons polluted soils
(adapted from *Mekonnen, B. A., Aragaw, T. A., Genet, M. B., 2024; Alori E.T., Gabasawa A.I., Elenwo C.E. et al, 2022; Koshlaf, E., Ball, A. S., 2017)*

The choice of bioremediation method depends on different factors including: the affected area, the type, concentration and nature of the pollutant, the cost of remediation method, the depth of contamination, environmental policies, oxygen concentrations, ambient temperature, soil characteristics, amount of nutrients and soil pH and moisture (*Koshlaf, E., Ball, A. S., 2017; Alori E.T., Gabasawa A.I., Elenwo C.E. et al, 2022; Micle, V., Sur, I.M., 2021*).

Bioremediation strategies are based on the introduction of nutrients and oxygen to stimulate the growth and activity of native microflora (biostimulation) or the addition of previously selected indigenous or genetically modified microflora to support native microbial species (bioaugmentation). In biostimulation, nutrients, O_2 or other oxidizing agents are added as biostimulants to stimulate the growth of indigenous microorganisms to remove contaminants. Nutrients such as nitrogen (N), phosphorus (P) and potassium (K) are essential for the successful biodegradation of petroleum hydrocarbons. Studies have shown high removal efficiency of total petroleum hydrocarbons (TPH), n-alkanes or PAHs after spraying nutrient-enriched liquid solution on contaminated soils *(Tsai, W. H., Chen, T. W., Liu, Y. H. et al., 2025).*

For example, Tsai W.H. *et al, (Tsai, W. H., Chen, T. W., Liu, Y. H. et al., 2025)* tested two biostimulants, soil bioremediation nutrients (SBNs) and nutrient solution (NS), in order to assess their effects on the degradation of petroleum hydrocarbons from contaminated soil and changes in bacterial community compositions. Their results indicated that the highest total petroleum hydrocarbons degradation rate (96%) were shown for biopiles with SBNs addition, particularly for 0.5% SBNs – S3), (Figure 4).

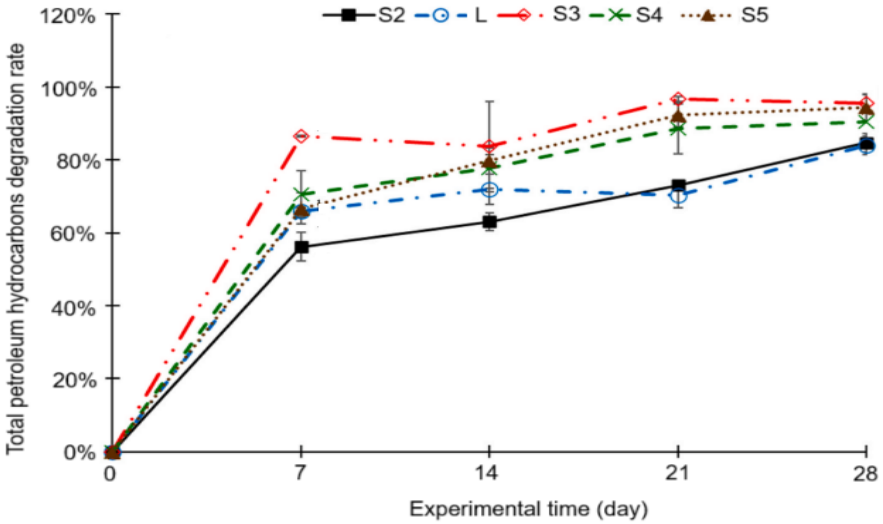

Fig. 4 - Degradation rates of total petroleum hydrocarbons in contaminated soils
(Tsai, W. H., Chen, T. W., Liu, Y. H. et al., 2025)

Michael-Igolima and colab., (Michael-Igolima, U., Abbey, S. J., Ifelebuegu, A. O., 2022) in their study, realised a comparative analysis of remediation methods. As can be seen from figure 5, the combined remediation is the most effective soil remediation method, followed by biological method.

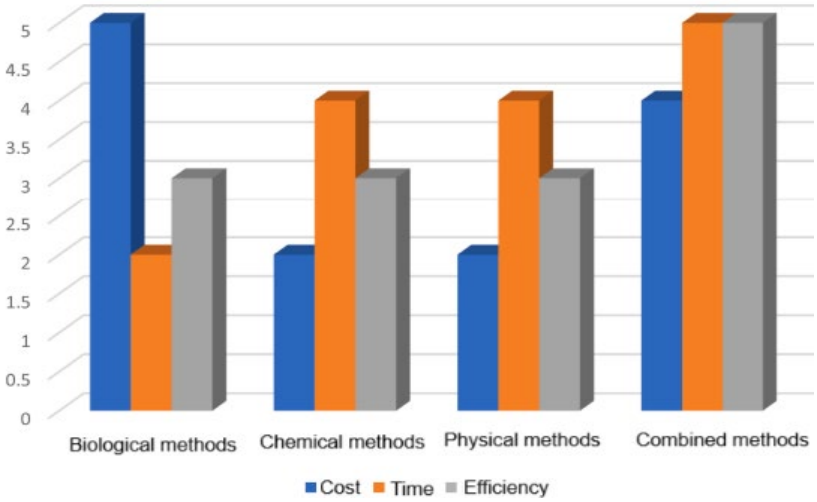

Fig. 5 - Comparative analysis of polluted soil remediation methods
(Michael-Igolima, U., Abbey, S. J., Ifelebuegu, A. O., 2022)

THE USE OF MICROORGANISMS IN THE BIOREMEDIATION PROCESS

The biodegradable degradation of complex hydrocarbons usually involves the collaboration of several bacterial species. This is particularly important in the case of pollutants made up of a variety of compounds (crude oil or petroleum), where the aim is to convert them completely into CO_2 and H_2O *(Ghazali, F. M., Rahman, R. N. Z. A., Salleh, A. B. et al, 2004).*

Microorganisms seem to be the most efficient in the bioremediation process, which can be explained by their structure and size, the diversity of substrates and metabolic pathways involved in the attack on pollutants, and their high resistance to the environmental factors. Depending on the type of pollutants in the bioremediation process, species of bacteria, fungi or microalgae are used single or in combinations (*Ferdeș, M., Dincă, M. N., Istrate, I. A. et al, 2024*).

Among the microorganisms used for the bioremediation process, bacteria occupy the dominant place. In most cases, the native microflora of the polluted area can constitute the source of the microorganisms needed for bioremediation. Among the best-known microorganisms such as bacteria, and fungi that can biodegrade petroleum hydrocarbons are *Aspergillus, Pseudomonas, Trichoderma, Bacillus, Staphylococcus, Penicillium and Rhodotorula (Mekonnen, B. A., Aragaw, T. A., Genet, M.B., 2024).*

Micle and Sur (*Micle, V., Sur, I.M., 2021*), in their research, determined the efficiency of *ex-situ* bioremediation of petroleum hydrocarbon-contaminated soils using a pilot-scale treatment that controls soil aeration time, moisture and microorganism content. During the experiment, they added *Pseudomonas and Bacillus* microorganisms every two weeks. The soil samples were coded according to their location, sampling depth and week in which they were taken (Figure 6).

The authors reported that soils contaminated with petroleum hydrocarbons can be effectively remediated by daily aeration for 8 hours in combination with inoculation of microbial strains of the genera *Pseudomonas* and *Bacillus*. This treatment increases the total number of germs (colony forming units–CFU) from 151 x 10^5 to 213 x 10^7 CFU g^{-1} soil, after 12 weeks of soil treatment, leading to a remediation efficiency of 83%.

In another study, *Varjani et al.* (*Varjani, S., Upasani, V. N., Pandey, A., 2020)* studied bioremediation of soil polluted with petroleum hydrocarbons using a new strain of *Pseudomonas aeruginosa* NCIM 5514. The authors compared five different methods for remediation of polluted soil, namely: bioaugmentation + biostimulation, bioaugmentation, biostimulation, natural attenuation and abiotic factors. In addition, they studied germination of *Vigna radiata* (mung bean) using natural agricultural soil, polluted agricultural soil and bioremediated agricultural soil.

The results showed that the degradation of hydrocarbons was greatest when *Pseudomonas aeruginosa* NCIM 5514 and nutrients were added to the microcosms at the same time, compared with the use of abiotic factors, bioaugmentation, biostimulation, and natural attenuation separately. The results also showed that the bioremediation approach improved seed germination in soil contaminated with oily sludge.

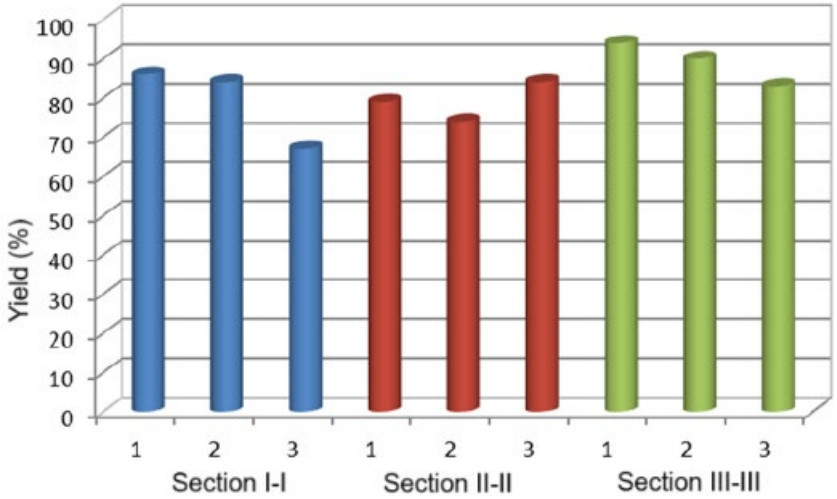

Fig. 6 - Depollution efficiency for petroleum hydrocarbons contaminated soils

(Micle, V., Sur, I.M., 2021)

In the study conducted by *Ma X.k et al. (Ma, X. k., Mao, D., Chen, J. et al, 2024)*, different fungal-bacterial consortia were analyzed, as well as inoculation strategies applied in soils contaminated with petroleum sludge with a total petroleum hydrocarbon concentration of 124,000 mg/kg. Their results demonstrated that strategies using sequential inoculation, with one dose administered at the beginning and another on day 30, of a consortium consisting of either *Bacillus sp.* and *Acremonium sp.* (treatment 1) or *Bacillus sp.* and *Phanerochaete sp.* (treatment 3), had a higher removal efficiency compared to discontinuous inoculation treatments.

Removal of total petroleum hydrocarbons in a pilot system (*on-site*) was investigated by *Martínez-Rabelo F. et. al (Martínez-Rabelo, F., Gómez-Guzmán, L. A., García-Segura, D. R. et al, 2023).* A combination of three simultaneous technologies was applied to oil-contaminated soil, namely: bioaugmentation (bacterial consortium: *Bacillus* sp., *Pseudomonas* sp., and *Shigella* sp.), phytoremediation (*Panicum maximum* grass), and vermiremediation (*Pontoscolex corethrurus* earthworm*)*. Bioremediation treatments were compared with natural attenuation. Authors reported that after 112 days, the bioremediation treatments significantly removed more alkanes (76%), polycyclic aromatic hydrocarbons (68%), and total petroleum hydrocarbons (76%) compared to the natural attenuation treatment (23%, 19%, and 24%, respectively).

Sharma et al. (2016) (Sharma, A., Singh, S. B., Sharma, R. et al, 2016) describe the use of a microbial consortium consisting of *Serratia marcescens* L-11, *Streptomyces rochei* PAH-13, and *Phanerochaete chrysosporium* VV-18 for the *in-situ* bioremediation of polyaromatic hydrocarbons. Within 7 days, the polyaromatic hydrocarbons degradation rate significantly increased to 56–98% under *in-situ.*

CONCLUSIONS

Soil contamination with petroleum products is a major problem for both the environment and public health, with global implications. Naturally, the process of petroleum degradation in contaminated soils is slow, and complete removal of contaminants is often difficult to achieve.

Bioremediation is a non-invasive and cost-effective technology used to remediate sites polluted with petroleum compounds. This method is widely used because it is applicable over large areas and can significantly reduce the concentration of contaminants. The biodegradation process carried out by natural microbial consortia is one of the main mechanisms for removing petroleum and other hydrocarbon-based pollutants from the soil and is cheaper than other remediation technologies.

ACKNOWLEDGEMENT

This research was supported by *the project Establishment and operationalization of a Competence Center for Soil Health and Food Safety – CeSoH, Contract no.: 760005/2022, specific project no.1, with the title: Soil health and food safety by introducing a soil remediation protocol and developing a mobile remediation equipment to reduce the concentration of organic/inorganic pollutants, Code 2, financed through PNRR-III-C9-2022 – I5 (PNRR-National Recovery and Resilience Plan, C9 Support for the private sector,*

research, development and innovation, I5 Establishment and operationalization of Competence Centers) and by *the project CNFIS-FDI-2025-F-0108 "Ensuring the sustainability of an application base for biotechnical systems in orchards, vineyards, gardens and solariums (SISBIOSUS)", from the Ministry of Education and Research through the Executive Agency for Financing Higher Education, Research, Development and Innovation.*

REFERENCES

[1] Ahmed, F., Fakhruddin, A. N. M. (2018). A review on environmental contamination of petroleum hydrocarbons and its biodegradation. International Journal of Environmental Sciences & Natural Resources, 11(3):555811. DOI: 10.19080/IJESNR.2018.11.555811

[2] Ajona, M., Vasanthi, P. (2021). Bioremediation of petroleum contaminated soils – A review. Materials Today: Proceedings, 45(Part 7), 7117–7122. https://doi.org/10.1016/j.matpr.2021.01.949

[3] Alori, E. T., Gabasawa, A. I., Elenwo, C. E., Agbeyegbe, O. O. (2022). Bioremediation techniques as affected by limiting factors in soil environment. Frontiers in Soil Science, 2, 937186. https://doi.org/10.3389/fsoil.2022.937186

[4] Ambaye, T.G., Chebbi, A., Formicola, F., Prasad, S., Gomez, F.H., Franzetti, A., Vaccari, M. (2022). Remediation of soil polluted with petroleum hydrocarbons and its reuse for agriculture: Recent progress, challenges, and perspectives. Chemosphere, 293, 133572, ISSN 0045-6535. https://doi.org/10.1016/j.chemosphere.2022.133572

[5] Ambaye, T.G., Chebbi, A., Formicola, F., Rosatelli, A., Prasad, S., Hernan Gomez, F., Sbaffoni, S., Franzetti, A., Vaccari, M. (2022). Ex-situ bioremediation of petroleum hydrocarbon contaminated soil using mixed stimulants: Response and dynamics of bacterial community and phytotoxicity. Journal of Environmental Chemical Engineering, 10(6), 108814, ISSN 2213-3437. https://doi.org/10.1016/j.jece.2022.108814

[6] Chen, M., Xu, P., Zeng, G., Yang, C., Huang, D., Zhang, J. (2015). Bioremediation of soils contaminated with polycyclic aromatic hydrocarbons, petroleum, pesticides, chlorophenols and heavy metals by composting: Applications, microbes and future research needs. Biotechnology Advances, 33(6), Part 1, 745-755, ISSN 0734-9750, https://doi.org/10.1016/j.biotechadv.2015.05.003

[7] Daâssi, D., Almaghribi, F. Q. (2022). Petroleum-contaminated soil: environmental occurrence and remediation strategies. 3 Biotech, 12, 139. https://doi.org/10.1007/s13205-022-03198-z

[8] Ghazali, F. M., Rahman, R. N. Z. A., Salleh, A. B., Basri, M. (2004). Biodegradation of hydrocarbons in soil by microbial consortium, International Biodeterioration & Biodegradation, 54(1), 61-67, ISSN 0964-8305. https://doi.org/10.1016/j.ibiod.2004.02.002

[9] Feng, L., Jiang, X., Huang, Y., Wen, D., Fu, F., Fu, R. (2021). Petroleum hydrocarbon-contaminated soil bioremediation assisted by isolated bacterial consortium and sophorolipid. Environmental Pollution, 273, 116476, ISSN 0269-7491. https://doi.org/10.1016/j.envpol.2021.116476

[10] Ferdeș, M., Dincă, M. N., Istrate, I. A., Mușuroi, G., Paraschiv, G., Vlăduț, E. V. (2024). Microbial communities involved in the bioremediation of hydrocarbon polluted soil. International Symposium Agricultural and Mechanical Engineering, ISB-INMA TEH 2024, 314-319.

[11] Haque, S., Srivastava, N., Pal, D. B., Alkhanani, M. F., Almalki, A. H., Areeshi, M. Y., Naidu, R., Gupta, V. K. (2022). Functional microbiome strategies for the bioremediation of petroleum-hydrocarbon and heavy metal contaminated soils: A review. Science of The Total Environment, 833, 155222, ISSN 0048-9697. https://doi.org/10.1016/j.scitotenv.2022.155222

[12] Hussain, A., Rehman, F., Rafeeq, H., Waqas, M., Asghar, A., Afsheen, N., Rahdar, A., Bilal, M., Iqbal, H.M.N. (2022). In-situ, Ex-situ, and nano-remediation strategies to treat polluted soil, water, and air – A review. Chemosphere, 289, 133252, ISSN 0045-6535. https://doi.org/10.1016/j.chemosphere.2021.133252

[13] Koshlaf, E., Ball, A.S. (2017). Soil bioremediation approaches for petroleum hydrocarbon polluted environments. AIMS Microbiology, 3(1), 25-49, doi: 10.3934/microbiol.2017.1.25

[14] Lázaro-Mass, S., Gómez-Cornelio, S., Castillo-Vidal, M., Alvarez-Villagomez, C. S., Quintana, P., De la Rosa-García, S. (2023). Biodegradation of hydrocarbons from contaminated soils by microbial consortia: A laboratory microcosm study. Electronic Journal of Biotechnology, 61, 24-32, ISSN 0717-3458. https://doi.org/10.1016/j.ejbt.2022.10.002

[15] Lv, Y., Bao, J., Zhu, L. (2022). A comprehensive review of recent and perspective technologies and challenges for the remediation of oil-contaminated sites. Energy Reports, 8, 7976-7988, ISSN 2352-4847. https://doi.org/10.1016/j.egyr.2022.06.034

[16] Ma, X. k., Mao, D., Chen, J., Wang, Q., Dong, Z., Zhang, H., Liang, J., Peterson, E. C. (2024). Enhancing bioremediation of petroleum sludge-polluted soil: The impact of fungal-bacterial consortium's application strategy, Applied Soil Ecology, 195, 105267, ISSN 0929-1393, https://doi.org/10.1016/j.apsoil.2023.105267

[17] Martínez-Rabelo, F., Gómez-Guzmán, L. A., García-Segura, D. R., Villegas-García, E., Rodriguez-Campos, J., Velázquez-Fernández, J. B., Hernández-Castellanos, B., Barois, I., Contreras-Ramos, S. M. (2023). Hydrocarbon bioremediation in a pilot-scale: A combination of bioaugmentation, phytoremediation, and vermiremediation. Environmental Technology & Innovation, 31, 103210, ISSN 2352-1864. https://doi.org/10.1016/j.eti.2023.103210

[18] Mayans, B., Anton-Herrero, R., García-Delgado, C., Delgado-Moreno, L., Guirado, M., Perez-Esteban, J., Escolastico, C. Eymar E. (2024). Bioremediation of petroleum hydrocarbons polluted soil by spent mushroom substrates: Microbiological structure and functionality. Journal of Hazardous Materials, 473 134650, https://doi.org/10.1016/j.jhazmat.2024.134650

[19] Mekonnen, B. A., Aragaw, T. A., Genet, M.B. (2024). Bioremediation of petroleum hydrocarbon contaminated soil: a review on principles, degradation mechanisms, and advancements. Frontiers in Environmental Science, 12, 1354422. https://doi.org/10.3389/fenvs.2024.1354422

[20] Michael-Igolima, U., Abbey, S. J., Ifelebuegu, A. O. (2022). A systematic review on the effectiveness of remediation methods for oil contaminated soils. Environmental Advances, 9, 100319, ISSN 2666-7657. https://doi.org/10.1016/j.envadv.2022.100319

[21] Micle, V., Sur, I. M. (2021). Experimental Investigation of a Pilot-Scale Concerning Ex-Situ Bioremediation of Petroleum Hydrocarbons Contaminated Soils. Sustainability, 13(15), 8165. https://doi.org/10.3390/su13158165

[22] Sharma, A., Singh, S. B., Sharma, R., Chaudhary, P., Pandey, A.K., Ansari, R., Vasudevan, V., Arora, A., Singh, S., Saha, S., Nain, L. (2016). Enhanced biodegradation of PAHs by microbial consortium with different amendment and their fate in in-situ condition. Journal of Environmental Management, 181, 728-736, ISSN 0301-4797. https://doi.org/10.1016/j.jenvman.2016.08.024

[23] Sui, X., Wang, X., Li, Y., Ji, H. (2021). Remediation of petroleum-contaminated soils with microbial and microbial combined methods: advances, mechanisms, and challenges. Sustainability, 13(16), 9267. https://doi.org/10.3390/su13169267

[24] Tsai, W. H., Chen, T. W., Liu, Y. H., Shen, S. M., Chen, C. S., Tien, C. J. (2025). A field-scale assessment of the efficacy of bioremediation of petroleum hydrocarbon-contaminated soils using two biostimulants. International Biodeterioration & Biodegradation, 196, 105942, ISSN 0964-8305. https://doi.org/10.1016/j.ibiod.2024.105942

[25] Varjani, S., Upasani, V. N., Pandey, A. (2020). Bioremediation of oily sludge polluted soil employing a novel strain of Pseudomonas aeruginosa and phytotoxicity of petroleum hydrocarbons for seed germination. Science of the Total Environment, 737, 139766. DOI: 10.1016/j.scitotenv.2020.139766

[26] Yan, Z. F., Fei, Y., Wang, Z. Q., Yang, J., Zhou, X. Y., Huang, Q. S., Chen, S., Wu, J. (2024). Synergistic bioremediation of petroleum-contaminated soil using immobilized consortium of Rhodococcus rhodochrous and Bacillus subtilis laccase. Journal of Environmental Management, 370, 123049, ISSN 0301-4797. https://doi.org/10.1016/j.jenvman.2024.123049

ENGINEERING MEASURES FOR SOIL EROSION CONTROL: A MECHANISM-BASED SYNTHESIS

/

CONSIDERAȚII PRIVIND PRINCIPALELE METODE UTILIZATE ÎN CONTROLUL EROZIUNII SOLULUI

Roxana Patricia IONAȘCU[1)], Remus Marius OPRESCU*[2)], Dan CUJBESCU[2)], Iulian VOICEA[2)]
[1)] Development Research Station for Combating Soil Erosion "Mircea Moțoc" Perieni, Vaslui County / Romania;
[2)] National Institute of Research - Development for Machines and Installations Designed to Agriculture and Food Industry - INMA Bucharest / Romania.
**Tel: 0766 580 791; *E-mail: oprescu.remusmarius@gmail.com*

Keywords: *vegetative cover, organic and biodegradable mulching, geotextile silt fences, check dams, biopolymer soil stabilization, runoff attenuation; sediment yield*

ABSTRACT

Land degradation is a major driver of the decline in agricultural land, dominated by water and wind erosion and by the reduction of soil organic matter. The spread of these processes—amplified by natural and anthropogenic drivers—lowers fertility, strips the upper soil horizon, and increases sediment loads in receiving waters. The paper presents a coherent set of preventive and control measures, grouped by mechanism of action and context of use. We analyze vegetative solutions (cover crops, green manures) and surface protections—organic or biodegradable mulches, geotextile meshes, and rock-fiber blankets—alongside flow-path barriers (check dams, stone berms, silt fences) and near-surface stabilization using chemical/biopolymeric binders to consolidate the topsoil. These directions reflect current trends in erosion control, with emphasis on integration from plot to watershed scale and on maintenance. Defined as permeable barriers installed along contour, silt fences temporarily retain sediment by decelerating overland flow and promoting deposition; effectiveness depends on siting, toe-trenching/anchorage, and routine inspection. In parallel, polymers and biopolymers increase near-surface cohesion and resistance to raindrop impact, creating a stable bed for vegetation establishment while offering a smaller environmental footprint than conventional cementitious agents. The guiding principle is twofold: reduce runoff volume and/or surface velocity, and combine source, pathway, and receptor measures. A decision matrix and monitoring recommendations support adaptive, long-term implementation.

REZUMAT

Degradarea solului reprezintă o cauză majoră a declinului terenurilor agricole, fiind dominată de eroziunea hidrică și eoliană și de diminuarea conținutului de humus. Extinderea acestor procese, amplificată de factori naturali și antropici, conduce la scăderea fertilității, la pierderi de sol superior și la creșterea încărcăturii de sedimente în corpurile de apă. Lucrarea prezintă un set coerent de măsuri pentru prevenirea și controlul eroziunii, grupate după mecanismul de acțiune și contextul de utilizare. Sunt analizate soluții vegetative (acoperire, culturi verzi) și de suprafață — mulcire cu materiale organice sau biodegradabile, plase geotextile și fibre de rocă — alături de bariere fizice pe traseul scurgerii (baraje de control, diguri de piatră, garduri de nămol) și de stabilizatori chimici/biopolimerici pentru consolidarea stratului superficial. Aceste direcții reflectă tendințele actuale în controlul eroziunii, cu accent pe integrarea măsurilor la scară de parcelă–bazin și pe mentenanță. Definite ca bariere permeabile instalate pe contur, gardurile de nămol rețin provizoriu sedimentele prin încetinirea scurgerii și depunere, eficiența depinzând de amplasare, ancorare și întreținere. În paralel, polimerii/biopolimerii pot crește coeziunea și rezistența la impactul picăturilor de ploaie, oferind un mediu stabil pentru instalarea vegetației, cu o amprentă ecologică mai redusă decât lianții tradiționali. Principiul general urmărit este dublu: reducerea volumului de scurgere și/sau a vitezei sale la suprafață, prin combinarea măsurilor de la sursă, pe cale și la receptor.

INTRODUCTION

Ensuring a sustainable and secure food supply is a defining challenge of the twenty-first century as global population approaches nine billion by mid-century; at the same time, agriculture faces intensifying constraints from climate variability and land-degradation processes, especially soil erosion, with documented

impacts on production stability and food prices (*Kumarasinghe, 2021*). Soil erosion—displacement of the fertile upper horizon by natural agents—may proceed gradually and remain unnoticed, or accelerate abruptly under extreme events, stripping substantial volumes of topsoil and mobilizing fine sediments and nutrients (*Psomiadis et al., 2008*).

Classical classifications distinguish natural erosion, driven by water, snow/ice, wind and biotic activity, from accelerated erosion linked to human actions such as deforestation, improper tillage and overgrazing, which markedly increase soil losses (*Koerner, 2005; Psomiadis et al., 2008*).

The consequences propagate from field to watershed: topsoil removal and organic-matter depletion reduce fertility and water-holding capacity, while sediment-laden runoff elevates turbidity, clogs conveyance systems and degrades channels and reservoirs, particularly where fine, non-cohesive soils coincide with high-intensity rainfall (*Psomiadis et al., 2008*). Climate-change stressors—higher temperatures, altered precipitation regimes and more frequent extremes—further depress yields via increased evapotranspiration and flood damage, and interact with recurrent wildfires that remove protective cover, alter soil properties and challenge post-fire recovery (*Wittenberg et al., 2023*).

In response, erosion control has increasingly adopted integrated portfolios that combine source, pathway and receptor measures. Geotextile-based sediment barriers (silt fences) remain ubiquitous on disturbed slopes; their performance depends on installation details and hydraulic management rather than fabric filtration alone, as shown by large-flume and full-scale studies (*Farias et al., 2006; Bugg et al., 2017; Whitman et al., 2018; Palmeira, 2020; Koerner, 2005*). Complementary practices include vegetative cover and mulching, contour-aligned interventions, check dams and near-surface stabilization to bridge the establishment period of vegetation (*Kumarasinghe, 2021*).

This paper aims to synthesize principal erosion-control mechanisms and practices (vegetative cover, mulching, geotextile sediment barriers, check dams and near-surface stabilization), relate them to site and climate contexts, and provide a decision-oriented framework—consistent with the article's own reference list—for selecting, sizing and maintaining effective, context-appropriate measures.

MATERIALS AND METHODS

One cause of the decline in agricultural land is the degradation of soils. The principal processes that drive soil degradation are erosion by water and wind and the decline of soil humus content; when these natural and anthropogenic stressors spread across the landscape, they precipitate a critical loss of soil fertility *(Kumarasinghe, 2021)*. Washing of the upper fertile horizon and the formation of large rills due to improper tillage accelerate topsoil loss *(Psomiadis et al., 2008)*. To prevent soil erosion, field operations should adopt contour-aligned tillage and seeding (i.e., perpendicular to the slope) to shorten flow paths and reduce overland-flow energy *(Kumarasinghe, 2021)*.

Erosion control denotes a portfolio of measures intended to prevent water- and wind-driven erosion during land development and cropping. In practice, water erosion is mitigated by runoff control (e.g., contour practices, check dams, drainage conveyance), while wind erosion is mitigated by reducing near-surface wind speed and protecting the soil against deflation (e.g., residue cover, vegetative barriers) *(Kumarasinghe, 2021; Koerner, 2005)*.

These measures are central to preventing water pollution, soil loss, habitat degradation, financial damages, and asset risks, and are used on farmland, natural areas, and urban settings. In construction and road works, erosion control measures are integral to stormwater programs and slope stabilization, often combining physical barriers (vegetation strips, rock terraces), field and site drainage systems, and sediment controls such as settling basins and silt-fence barriers *(Koerner, 2005; Adachi et al., 2024; Psomiadis et al., 2008)*.

Problems caused by soil erosion and subsequent sedimentation are responsible for significant environmental impacts on reservoir slopes and silted rivers, particularly in regions with intense rainfall and fine, non-cohesive soils *(Toy, Foster, & Renard, 2002)*. *Witheridge (2012)* highlights several primary impacts of erosion and surface runoff: clogging of stormwater pipes and channels, sedimentation and elevated turbidity in receiving waters, splash (raindrop-impact) erosion, and sheet (laminar) erosion.

Accordingly, preventing and controlling erosion is essential to minimize these consequences. In practical terms, erosion control aims to reduce both the gradual and abrupt wear of soil by integrating source, pathway, and receptor measures suited to site hydrology, soil texture, and rainfall regime *(Toy, Foster, & Renard, 2002)*.

A wide array of soil-erosion countermeasures is therefore deployed against water, wind, and other disturbance agents (including livestock and human activity), with current technical trends consolidating the above practices into site-specific, multi-measure portfolios *(Kumarasinghe, 2021)*.

Fig. 1 - Methods used in soil erosion control
(Wittenberg and Shtober-Zisu, 2023)

Figure 2 presents the principal soil-erosion control methods with reference to runoff drivers. Two fundamental approaches are recognized: (1) reducing runoff volume and (2) reducing flow velocity (*Witheridge, 2012; Koerner, 2005*).

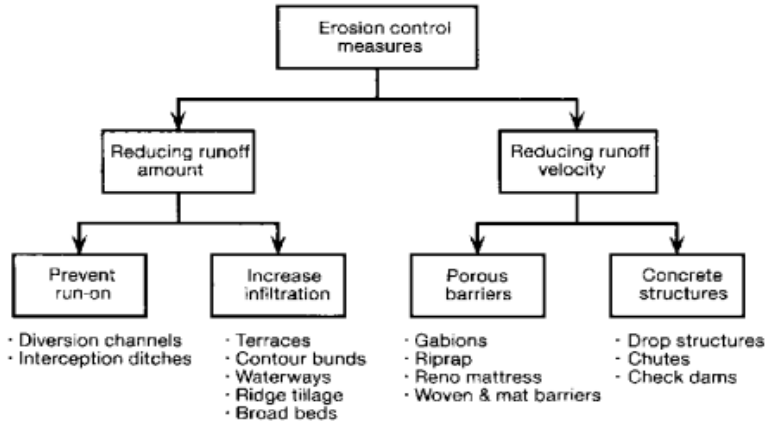

Fig. 2 - Soil erosion control measures
(Witheridge, 2012)

The most effective erosion-control strategy is to minimize the disturbed footprint by preserving as much existing vegetation as possible. This is especially critical on steep slopes or near receiving waters, where no single treatment will adequately control erosion and where receptors are highly sensitive *(Witheridge, 2012)*. Match land development to site sensitivity: avoid wetlands and springs, and exclude areas with steep or fragile soils; delineate and respect all disturbance limits *(Witheridge, 2012)*.

Landslide-hazard management, prevention, and control are essential to reduce risks to life and property; in standard hazard management workflows, mitigation is the final stage that provides the technical means to control natural hazards. Mitigating an existing landslide hazard—or preventing future failures—boils down to reducing driving components and/or increasing resisting forces. The influence of vegetation on slope stability remains an active research challenge, with studies differentiating canopy effects (rain interception, wind shielding) from root-reinforcement mechanisms, while also emphasizing the role of surface runoff over vegetative cover *(Kumarasinghe, 2021)*.

Rainfall-generated overland flow is a practical indicator of slope water loss: it occurs when rainfall intensity exceeds infiltration capacity, producing excess water that cannot infiltrate *(Toy, Foster, & Renard, 2002)*. In this context, implementing sediment-control systems (e.g., sediment barriers) is typically far less costly than repairing downstream damage *(Witheridge, 2012; Adachi et al., 2024)*.

A range of measures is available for erosion control—including mulching, contour seeding, check dams, soil amendments, stone berms, chemical stabilizers, and sediment barriers (silt fences) *(Witheridge, 2012; Koerner, 2005)*. Geosynthetics specifically designed for erosion control have become increasingly

common; their efficiency has been evaluated in both laboratory and field programs *(Farias, Palmeira, & Carvalho, 2006; Adachi et al., 2024)*.

A silt fence is a linear, contour-aligned temporary sediment barrier composed of geotextile supported by wood or metal posts; it slows sheet flow and promotes deposition from disturbed soils on construction sites. The method is cost-effective and readily removable *(Witheridge, 2012; Koerner, 2005; Farias, Palmeira, & Carvalho, 2006)*. Performance depends primarily on siting, toe-trenching/anchorage, and maintenance; large-scale tests show that structural configuration governs sediment capture *(Bugg, Zech, & Perez, 2017; Whitman, Zech, & Donald, 2018; Adachi et al., 2024)*.

Among the constituent materials, geotextiles are central. Over the last five decades, geotextiles have been used as filters because they offer cost and environmental advantages over granular filters *(Koerner, 2005; Palmeira, 2020)*. Filtration is the retention of soil particles subjected to hydrodynamic forces while allowing fluid passage through or around the geosynthetic; filtration behavior depends on hydraulic conditions and soil characteristics (particle-size distribution, density, plasticity), and differs between woven (predominantly two-dimensional pore network) and nonwoven (three-dimensional thickness-scale flow paths) geotextiles *(Palmeira, 2020; Koerner, 2005)*.

Design and construction guidance for silt-fence systems emphasizes configuration, hydraulic capacity, and maintenance; full-scale and flume studies document the benefits of improved anchorage details, post spacing, and controlled dewatering to limit undermining and overtopping *(Whitman, Zech, & Donald, 2018; Bugg, Zech, & Perez, 2017; Farias, Palmeira, & Carvalho, 2006; Adachi et al., 2024)*.

Mulching—the application of materials such as residue, biodegradable films, or mineral cover prior to, during, or immediately after seeding—targets reduced evaporation and water-erosion, improved soil temperature and water-supply capacity, and weed suppression, thereby improving crop production and reducing water use *(Kumarasinghe, 2021)*.

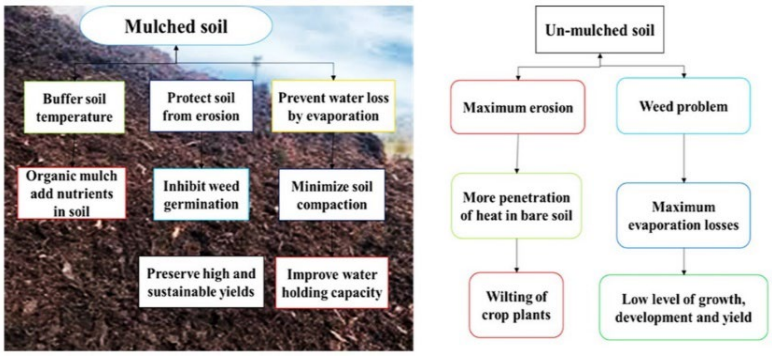

Fig. 3 - Comparative approach with mulched and unmulched soil/crops
(Kumarasinghe, 2021)

Mulch materials are commonly grouped into three classes: organic, inorganic, and specialty. Organic mulches are produced from agricultural residues, wood-processing by-products, processed plant wastes, and animal manures (*El-Beltagi et al., 2022*). Inorganic mulches include polyethylene plastic films and other synthetic polymer sheets, while specialty mulches encompass biodegradable and photodegradable films as well as spray-on/bio-based surface covers that improve ease of application and flexibility and are intended as environmentally friendly options (*Kasirajan & Ngouajio, 2012; El-Beltagi et al., 2022*).

Mulching improves soil properties, increases soil-moisture availability, and enhances soil productivity; key effects are summarized in Figure 4 (*El-Beltagi et al., 2022*). In cropped fields, mulching delivers multiple co-benefits: it reduces soil-water loss, suppresses weed germination, dampens raindrop kinetic energy, and limits water-erosion.

Organic mulches foster soil-structure development and stimulate earthworm activity, with knock-on benefits for porosity and infiltration (*Jiménez et al., 2017*). They may also lower soil pH locally and increase nutrient availability as decomposition proceeds, supplying a slow-release nutrient source over time (*El-Beltagi et al., 2022*).

Plastic and biodegradable mulches can improve soil health and pest management by modifying the microclimate and acting as a barrier to splash, thereby reducing fertilizer leaching and keeping nutrients near the root zone for more efficient uptake (*Kasirajan & Ngouajio, 2012; El-Beltagi et al., 2022*).

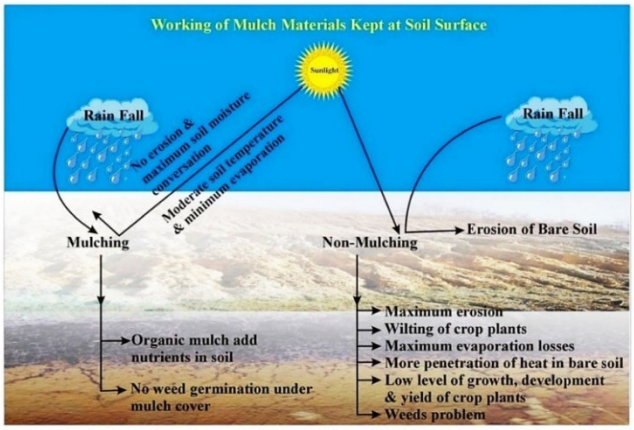

Fig. 4 - Effects between mulching and non-mulching

(El-Beltagi et al., 2022)

In agricultural fields, a wide range of mulching materials is deployed in diverse application modes and layouts, as schematically illustrated in Fig. 5 *(Kasirajan & Ngouajio, 2012; Kader et al., 2017; El-Beltagi et al., 2022)*.

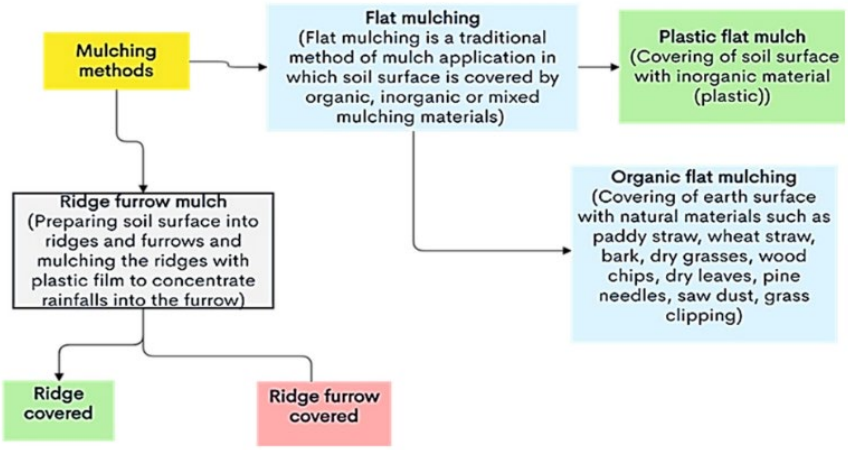

Fig. 5 - An illustration of different mulching techniques

(*El-Beltagi et al., 2022*)

Mulching is widely regarded as beneficial under stressful environments (heat, drought, salinity) because it modifies the evaporation–transpiration balance and the soil–plant microclimate *(Kader et al., 2017)*. Its effectiveness depends on climate and rainfall regime, chiefly by reducing surface evaporation and thus raising near-surface water availability.

In field crops, mulches increase soil-moisture retention, improve soil structure, and suppress weeds, while damping the raindrop kinetic energy that initiates detachment *(El-Beltagi et al., 2022; Jiménez et al., 2017)*. That said, the magnitude of moisture gain varies with mulch material, soil type, and local climate; across studies, mulched treatments generally retain more water than bare soil *(Kader et al., 2017)*.

Over the last decade, substantial research has evaluated traditional soil stabilizers (cement, lime, fly ash, bituminous binders) through direct shear, unconfined compression, and triaxial testing to enhance the strength of natural soils; these approaches can markedly improve mechanical properties but may entail brittle failure modes and environmental trade-offs that limit vegetation establishment *(Chang et al., 2015; Hataf, Ghadir, & Ranjbar, 2018)*.

As an alternative, polymer/biopolymer treatments show attractive mechanical gains with a smaller environmental footprint. Laboratory and field studies report improved resistance to raindrop impact and sheet erosion due to inter-particle bridging and continuous surface coatings; on sandy slopes, water-based polyurethane forms a thin hardened crust that resists rilling under intense rainfall *(Chang et al., 2015; Hataf, Ghadir, & Ranjbar, 2018; Liu, Chen, & Kanungo, 2019)*.

Importantly, eco-engineering trials that pair polymer treatment with vegetation indicate that polymer-treated soils can provide a stable growth medium for seed germination and seedling establishment, supporting integrated stabilization of exposed slopes *(Hataf, Ghadir, & Ranjbar, 2018; Chang et al., 2015)*.

RESULTS

Mulching effectiveness across materials and layouts

Across the reviewed studies, mulching consistently reduced raindrop impact, surface sealing, and net soil loss relative to bare soil. Organic mulches (crop residues, manures, wood by-products) and newer biodegradable films demonstrated higher near-surface water availability by suppressing evaporation; field trials also reported weed suppression and soil structure improvement via increased macroporosity and earthworm activity *(El-Beltagi et al., 2022; Jiménez et al., 2017; Kasirajan & Ngouajio, 2012; Kader et al., 2017)*.

Performance varied with climate and rainfall regime: under hotter/drier conditions the moisture-retention benefit was larger, while under cool/wet regimes thermal moderation and splash reduction dominated. Schematic variants and placement patterns used in agriculture are illustrated in Figs. 4–5 and yielded comparable qualitative outcomes when surface cover exceeded ~60%.

Silt-fence (geotextile) sediment barriers: performance drivers and failure modes

Results from large flume and full-scale testing converge on a central finding: sediment capture is governed mainly by impoundment and controlled dewatering, not by fabric "filtration" alone *(Farias, Palmeira, & Carvalho, 2006; Bugg, Zech, & Perez, 2017; Whitman, Zech, & Donald, 2018; Palmeira, 2020; Koerner, 2005)*. Configurations featuring proper toe-trenching/anchorage, reduced post spacing, and overflow/dewatering elements showed markedly fewer undermining and overtopping events and retained higher fractions of introduced sediment.

Conversely, inadequate trench compaction, long unsupported spans, and uncontrolled bypass led to premature failure. In practice, the placement along contour and the ability to repeatedly store ~0.3 m of ponded water without structural distress were associated with the highest efficiencies.

Geotextile filtration mechanisms relevant to performance.

Nonwoven and woven geotextiles behaved differently under comparable hydraulic and soil conditions: nonwovens provided three-dimensional flow paths through the thickness, whereas wovens relied on two-dimensional pore networks within the plane of the fabric. Effective retention required matching soil gradation and plasticity with apparent opening size and ensuring hydraulic compatibility; where this was satisfied, clogging risk decreased and long-term flow was more stable *(Palmeira, 2020; Koerner, 2005)*. These mechanistic results explain the superior field performance of well-designed systems despite similar nominal fabric parameters.

Vegetation-first and footprint minimization on sensitive sites.

Case syntheses emphasized that minimizing the disturbed area and preserving existing vegetation on steep slopes or near sensitive receptors consistently outperformed any single engineered measure applied post-disturbance. Where disturbance limits were respected and drainage lines/wetlands avoided, the downstream sediment signal and maintenance burden dropped substantially *(Witheridge, 2012)*. These findings support a hierarchy of controls—source measures first (vegetation, mulching), then pathway controls (contour drains, check dams), and finally receptor traps (silt fences, basins).

Polymer/biopolymer and water-based polyurethane (PU) stabilizers.

Laboratory and pilot-scale data showed that low-dosage biopolymers (e.g., xanthan, chitosan) increased near-surface cohesion and delayed rill initiation; treated plots resisted raindrop impact and sheet erosion more effectively than untreated controls *(Chang et al., 2015; Hataf, Ghadir, & Ranjbar, 2018)*. On sandy slopes, water-based PU produced a thin crust that limited rilling during intense storms *(Liu, Chen, & Kanungo, 2019)*. Importantly, pairing polymer treatment with seeding/vegetation provided a stable substrate for germination, indicating that chemical stabilization can bridge the establishment window without the brittleness and ecological trade-offs typical of high-dosage cementitious binders.

Integrated portfolios and cost-avoidance.

Comparative assessments indicated that combined portfolios—mulching + contour interventions + silt-fence trapping—reduced turbidity peaks and sediment delivery more reliably than any single control. Implementing sediment barriers upstream was repeatedly shown to be less costly than post-event remediation of clogged conveyances and silted water bodies *(Witheridge, 2012; Adachi et al., 2024)*. These results reinforce the design principle presented earlier (Fig. 2): pursue runoff-volume reduction and flow-velocity attenuation in tandem for resilient outcomes.

Evidence-based design implications.

(i) Target ≥ 60% post-application surface cover for mulches; anchor on slopes steeper than 1V:3H.

(ii) For silt fences, design for storage and dewatering (height ~0.45–0.60 m; offset trench; robust fastening) rather than relying on fabric filtration alone.
(iii) Select geotextiles by hydraulic/soil compatibility (AOS vs. gradation, plasticity), not just by nominal weight.
(iv) Use biopolymers/PU as temporary surface stabilizers to enable vegetation, with environmental compliance checks. *(Bugg, Zech, & Perez, 2017; Whitman, Zech, & Donald, 2018; Palmeira, 2020; Chang et al., 2015)*.

CONCLUSIONS

Drawing on the experimental evidence and field practice synthesized herein, the following conclusions translate the review into decision-oriented guidance for selecting, sizing, and maintaining soil-erosion controls across source, pathway, and receptor scales.

1. Preserve vegetation and minimize the disturbed footprint first. On steep slopes and near sensitive receptors, preventing disturbance consistently outperforms any single post-disturbance measure. Define and respect disturbance limits; avoid drainage lines and wetlands.
2. Mulching is a high-leverage, low-cost source control—when coverage is sufficient. Target ≥ 60% immediate surface cover; performance scales with climate and rainfall regime. On slopes steeper than 1V:3H, mulch and rolled erosion-control products should be anchored (anchor trench, staples/tackifiers) to prevent wind and runoff displacement.
3. Silt fences work by storage and controlled dewatering, not fabric filtration alone. Efficient systems provide repeatable impoundment (≈ 0.3 m typical), robust toe-trenching/anchorage, reduced post spacing, and overflow/dewatering details to avoid undermining and overtopping. Placement along contour is critical.
4. Select geotextiles by hydraulic compatibility with the soil, not by weight. Woven and nonwoven filters exhibit different pore-network geometries (2-D vs 3-D). Apparent opening size, soil gradation/plasticity, and expected hydraulic gradients govern retention and clogging risk.
5. Polymer/biopolymer and water-based polyurethane (PU) treatments can bridge the vegetation-establishment window. Low-dosage applications increase near-surface cohesion and resistance to raindrop impact/rilling, with fewer brittleness and footprint penalties than high-dosage cementitious binders—provided environmental compliance is verified.
6. Integrated portfolios outperform single measures. Combining source (vegetation, mulch), pathway (contour drains, check dams), and receptor controls (silt fences, basins) reduces peak turbidity and sediment delivery more reliably across site and storm variability.
7. Upstream controls are cheaper than downstream fixes. Proactive sediment barriers and surface protection typically cost less than post-event remediation of clogged conveyances, silted reservoirs, and habitat damage.
8. Design should be decision-oriented and context-specific. Use a matrix keyed to slope, soil texture/plasticity, rainfall intensity, drainage area, and constructability to select feasible measures and their parameter ranges (mulch rate, AOS, post spacing, polymer dosage).
9. Quality assurance and monitoring are non-negotiable. Specify anchor-trench details, fastener density, and installation tolerances; inspect after design storms for ponding depth, dewatering time, fence deflection/undermining, and trapped-sediment height. Maintain photo logs and corrective-action records.
10. Limitations and future work. Field performance remains sensitive to installation quality, maintenance, and extreme-event sequences. Priority research includes (i) long-term field trials for polymer/biopolymer and PU treatments under diverse soils/climates, (ii) standardized dewatering-enabled silt-fence designs for high-intensity rainfall, and (iii) life-cycle and microplastic assessments for mulch materials—particularly biodegradable films.

ACKNOWLEDGEMENT

This research was supported by the Ministry of Agriculture and Rural Development – Romania - MADR through the Sectoral Project ADER 20.1.2. "Enhanced Utilization of Agricultural Land Subject to Erosion through the Conservation of Water and Soil Resources under Climate Change Conditions", Ctr. 27.07.2023.

REFERENCES

[1] Adachi, V. Y. G.; Lukiantchuki, J. A.; Luciano, R. F.; Palmeira, E. M. (2024). Sediment barriers' performance in the laboratory: evaluation of clogging and filtration characteristics in geotextiles subjected to discharge cycles. *Water*, 16(1), 107.

[2] Bugg, R. A.; Donald, W.; Zech, W.; Perez, M. (2017). Performance evaluations of three silt fence practices using a full-scale testing apparatus. *Water*, 9, 502.

[3] Chang, I.; Im, J.; Prasidhi, A. K.; Cho, G.-C. (2015). Effects of xanthan gum biopolymer on soil strengthening. *Construction and Building Materials*, 74, 65–72.

[4] El-Beltagi, H. S.; Basit, A.; Mohamed, H. I.; *et al.* (2022). Mulching as a sustainable water and soil-saving practice in agriculture: a review. *Agronomy*, 12(8), 1881.

[5] Farias, R. J. C.; Palmeira, E. M.; Carvalho, J. C. (2006). Performance of geotextile silt fences in large flume tests. *Geosynthetics International*, 13, 133–144.

[6] Hataf, N.; Ghadir, P.; Ranjbar, N. (2018). Investigation of soil stabilization using chitosan biopolymer. *Journal of Cleaner Production*, 170, 1493–1500.

[7] Jiménez, M. N.; Pinto, J. R.; Ripoll, M. Á.; Sánchez-Miranda, Á.; Navarro, F. B. (2017). Impact of straw and rock-fragment mulches on soil moisture and early growth of holm oaks in a semiarid area. *Catena*, 152, 198–206.

[8] Kader, M. A.; Senge, M.; Mojid, M. A.; Onishi, T.; Ito, K. (2017). Effects of plastic-hole mulching on effective rainfall and readily available soil moisture under soybean (*Glycine max*) cultivation. *Paddy and Water Environment*, 15, 659–668.

[9] Kasirajan, S.; Ngouajio, M. (2012). Polyethylene and biodegradable mulches for agricultural applications: a review. *Agronomy for Sustainable Development*, 32, 501–529.

[10] Koerner, R. M. (2005). *Designing with Geosynthetics* (5th ed.). Upper Saddle River, NJ: Pearson/Prentice Hall.

[11] Kumarasinghe, U. (2021). A review on new technologies in soil erosion management. *Journal of Research in Technology and Engineering*, 2, 120–127.

[12] Liu, J.; Chen, Z.; Kanungo, D. P.; *et al.* (2019). Topsoil reinforcement of sandy slope for preventing erosion using water-based polyurethane soil stabilizer. *Engineering Geology*, 252, 125–135.

[13] Palmeira, E. M. (2020). A review on some factors influencing the behaviour of nonwoven geotextile filters. *Soils and Rocks*, 43(3), 351–368.

[14] Psomiadis, E.; Papazachariou, A.; Soulis, K.X.; Alexiou, D.S.; Charalampopoulos, I. Landslide mapping and susceptibility assessment using geospatial analysis and earth observation data. *Land* 2020, *9*, 133.

[15] Toy, T. J.; Foster, G. R.; Renard, K. G. (2002). *Soil Erosion: Processes, Prediction, Measurement, and Control*. New York: John Wiley & Sons, pp. 10–20.

[16] Whitman, J. B.; Zech, W. C.; Donald, W. N.; LaMondia, J. J. (2018). Full-scale performance evaluations of various wire-backed nonwoven silt fence installation configurations. *Transportation Research Record*, 2672, 68–78.

[17] Whitman, J. B.; Perez, M. A.; Zech, W. C.; Donald, W. N. (2021). Practical silt fence design enhancements for effective dewatering and stability. *Journal of Irrigation and Drainage Engineering*, 147, 04020039.

[18] Whitman, J. B. (2023). Improving the design and performance of double-row sediment barriers used during highway construction. *Transportation Research Record*, 2677, 1241–1252.

[19] Witheridge, G. (2012). *Erosion and Sediment Control—A Field Guide for Construction Site Managers* (Version 4). Brisbane, Australia: Catchments & Creeks Pty Ltd., pp. 7–15.

[20] Wittenberg, L.; Shtober-Zisu, N. (2023). Restoring fire-affected soils: the potential of nature-based solutions. *Current Opinion in Environmental Science & Health*, 100520.

[21] Zech, W. C.; Halverson, J. L.; Clement, T. P. (2008). Intermediate-scale experiments to evaluate silt fence designs to control sediment discharge from highway construction sites. *Journal of Hydrologic Engineering*, 13, 497–504.

THE STAGE OF POSSIBILITY OF SIMPLIFICATION AND MODERNIZATION OF HYDRAULIC SYSTEM CONTROLS FOR COMBINE HARVESTERS

/

STADIUL POSIBILITĂȚII DE SIMPLIFICARE ȘI MODERNIZARE A COMENZILOR SISTEMULUI HIDRAULIC AL COMBINELOR DE RECOLTAT

Stefano-Andrea MANTOVANI*[1)], Vasilica STEFAN[1)], Radu CIUPERCA[1)], Lucretia POPA[1)], Ana ZAICA[1)], Dragos DUMITRU[1)], Alin HARABAGIU[1)], Melania CISMARU[1)], Catalin DUMITRESCU[2)]

[1)] National Institute of Research - Development for Machines and Installations Designed to Agriculture and Food Industry - INMA Bucharest / Romania;

[2)] INOE 2000 - IHP / Romania.

**Tel: (+40) 723 814 202; *E-mail: stefanoandreamantovani@gmail.com*

***Keywords**: combine harvester, hydraulics components, power steering, ECU.*

ABSTRACT

As the need for greater efficiency, reliability, and ease of maintenance grows, traditional hydraulic control methods often encounter limitations in complexity and flexibility. This study reviews modern control approaches, focusing on electronic and digital innovations, and assesses how feasible it is to incorporate these into existing hydraulic systems. It emphasizes identifying key technological advances, evaluating their effects on system performance, and exploring ways to develop more streamlined, automated control solutions. The results indicate that there are considerable opportunities to reduce the complexity of hydraulic controls while improving their capabilities through digital technologies, leading to more efficient, cost-effective, and widely adaptable hydraulic systems.

REZUMAT

Pe măsură ce nevoia de o eficiență, fiabilitate și ușurință în întreținere sporite crește, metodele tradiționale de control hidraulic se confruntă adesea cu limitări în ceea ce privește complexitatea și flexibilitatea. Acest studiu analizează abordările moderne de control, concentrându-se pe inovațiile electronice și digitale și evaluează cât de fezabil este să le încorporăm în sistemele hidraulice existente. Se pune accent pe identificarea progreselor tehnologice cheie, evaluarea efectelor acestora asupra performanței sistemului și explorarea modalităților de dezvoltare a unor soluții de control mai simplificate și automatizate. Rezultatele indică faptul că există oportunități considerabile de a reduce complexitatea controalelor hidraulice, îmbunătățind în același timp capacitățile acestora prin intermediul tehnologiilor digitale, ceea ce duce la sisteme hidraulice mai eficiente, rentabile și adaptabile pe scară largă.

INTRODUCTION

Modern agriculture is undergoing rapid transformation through the integration of advanced technologies aimed at enhancing productivity and operational efficiency. Among these innovations, automation and digitalization have markedly improved the execution of complex agricultural tasks, thus enabling reduced resource consumption and increased processing speed.

Key examples of this technological advancement include high-performance harvesting machinery, which incorporate sophisticated engineering solutions designed to address the evolving demands of contemporary farming systems.

A critical subsystem within such machinery, particularly in combine harvesters, is the hydraulic system. This system is integral to the operation of numerous components, including the positioning and alignment mechanisms, motion and orientation of cutting devices, transportation, and cleaning of harvested material.

The performance and adaptability of hydraulic systems are therefore vital to maintaining efficient harvesting operations across diverse terrains and varying field conditions *(Blagoi and Mitroi, 2003)*.

Hydraulic Drive System Architecture in Combine Harvesters

The hydraulic drive system in combine harvesters is a critical subsystem that converts hydraulic energy into mechanical energy for the operation of key functional components. This system consists

primarily of a power source (internal combustion engine), a hydraulic pump (generator), and associated auxiliary equipment. The hydraulic pump generates flow by pressurizing a working fluid, which transmits energy to actuators and motors that perform mechanical tasks throughout the machine.

The hydraulic system drives multiple essential assemblies of the harvester, including the reaper, cutting platform, variable speed drive, and steering mechanism. The operation and synchronization of these subsystems are fundamental for efficient harvesting, particularly under varying field and crop conditions.

Reaper Unit (header)

The reaper is responsible for uniformly feeding crop material into the threshing system. Its operation is hydraulically driven, allowing adaptive control under variable terrain and harvesting conditions. Through hydraulic actuation, a coupling attached to the reaper can automatically adjust. to difficult working conditions, such as uneven fields or crops. Hydraulic cylinders modulate the position and angle of the reaper in response to crop density, ensuring a consistent flow of material.

Hydraulic motors enable precise control over rotational direction and speed, enhancing adaptability and efficiency. Coordination with the cutting platform is critical, and modern systems utilize sensors to monitor parameters such as height and speed, allowing real-time adjustments to optimize material intake and reduce loss.

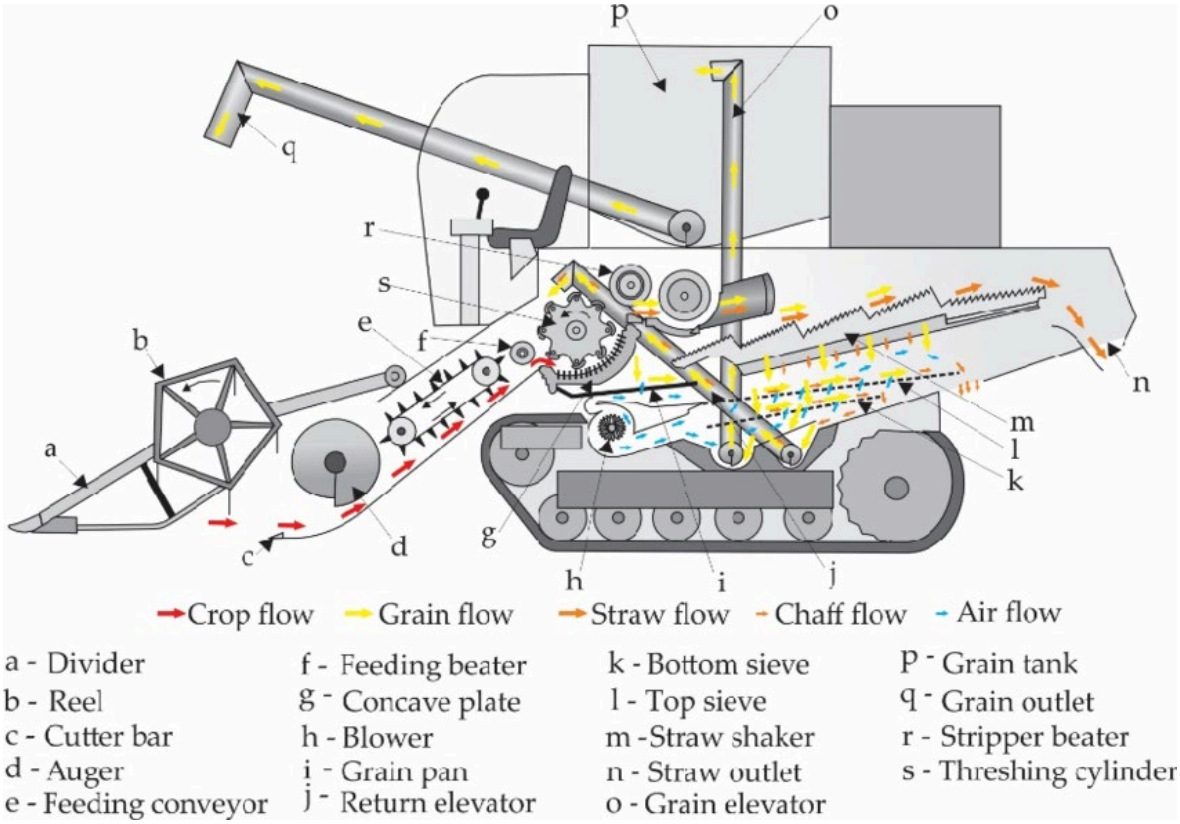

Fig. 1 - Major components and material flow of a combine harvester

(Kahandage et al, 2023)

Cutting Platform

The cutting platform ensures a uniform cut of the crop, which is essential for effective downstream processing. Hydraulic lifting and leveling mechanisms enable dynamic adjustment of the platform height and tilt to maintain optimal cutting conditions across varying terrain.

The cutting blades themselves are often driven by hydraulic motors, which allow fine control over cutting speed based on crop characteristics.

Advanced platforms incorporate parallel guidance systems—mechanical or hydraulic—that enhance stability and tracking performance. Sensor-based feedback systems automatically regulate cutting height and angle in real time, improving efficiency across diverse environmental and operational scenarios.

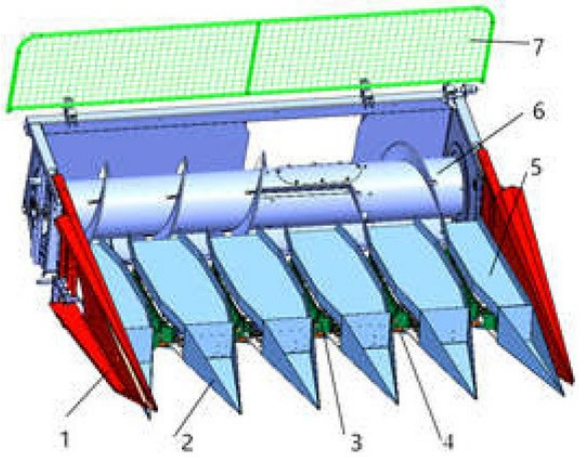

Fig. 2 - Sunflower oil combine harvester header

1-External crop divider. 2-Crop divider header. 3-Clamping and conveying device. 4-Cutting systems. 5-Crop divider. 6-Screw conveyor. 7-Antispatter net.

(Yang et al, 2021)

Variable Speed Drive (Speed Variator)

The variable speed drive system enables adjustment of component functional parameters in response to the specific harvesting conditions and crop types. This functionality is particularly important for optimizing the performance of cutting, threshing, and conveying mechanisms. Speed regulation is achieved by modifying hydraulic pressure through electronically controlled pumps, thereby adjusting the transmission ration in real time.

The system supports dynamic working mode adaptation for components such as the harvester head and cutting blades. For instance, threshing speed can be increased for lighter crop materials or reduced for denser varieties to ensure effective separation without excessive damage.

Power Steering Mechanism

Modern combine harvesters utilize hydraulically actuated steering systems to provide precise rolling, maneuverability and control during operation. A closed-loop hydraulic circuit—comprising pumps, valves, and steering cylinders—facilitates accurate directional changes, even on uneven or sloped terrain.

Steering is typically controlled via a wheel or joystick, which actuates a directional control valve. This input translates into hydraulic pressure that moves the front wheels through connected cylinders. Advanced systems integrate electronic control units (ECUs) and feedback sensors for responsive, real-time steering adjustments, contributing to machine stability and operator ease-of-use *(Catană et al, 1996).*

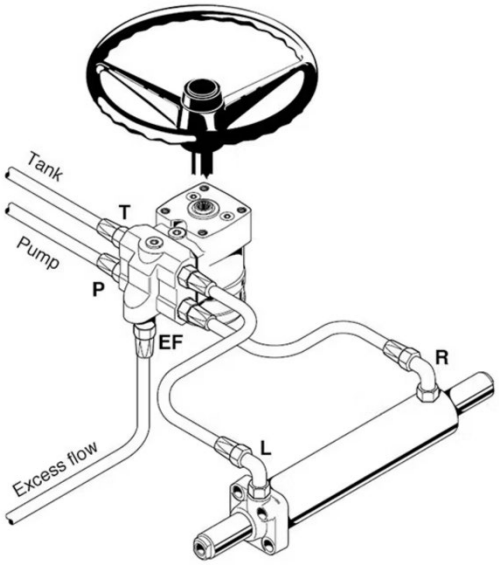

Fig. 3 - Diagram of a hydraulic power steering system

(shijiazhuanghanjiu.en.made-in-china.com)

Integration of Hydraulic Systems Across Functional Subsystems

The hydraulic system functions as the integrative framework that synchronizes the operation of all major components within the combine harvester. Its architecture ensures seamless interaction between the reaper, cutting platform, steering mechanism, and speed variator:

- The reaper and cutting platform operate in tandem to collect and prepare crop material for processing.
- The steering mechanism maintains proper machine alignment in the field, ensuring effective engagement of the harvesting units with the crop rows.
- The variable speed drive ensures optimal synchronization of mechanical components by dynamically adjusting operating speeds based on sensor feedback and crop conditions.

The interdependence of these systems underlines the hydraulic system's role as a central coordinating network, vital for achieving high-performance harvesting with minimal energy consumption and material loss.

MATERIALS AND METHODS

Modeling and simulation are fundamental methodologies widely employed in the analysis, comparison, evaluation, and optimization of both the structural and functional parameters of complex systems. In engineered systems, a defined set of input variables is processed to yield specific outputs that fulfill a predetermined operational objective. When such systems are coupled with control mechanisms, they form control systems designed to achieve desired responses and maintain performance levels in accordance with varying input conditions.

In most practical applications, these systems comprise multiple interacting subsystems, each responsible for executing specialized functions in a coordinated manner, either concurrently or sequentially. When system outputs are time-dependent and exhibit continuous variation relevant to real-time operation, the system is classified as dynamic. Agricultural combine harvesters exemplify such dynamic systems due to their involvement in diverse, time-sensitive, and interrelated processes across multiple functional units. These machines are inherently multifunctional and are designed to handle various crop types and field conditions through integrated and coordinated operations.

The effective automation of such systems relies heavily on robust process modeling and control strategies. Emphasis is placed on the development of mathematical models and simulation tools that support the design and real-time control of subsystem functions. These models form the foundation for designing control architectures and physical components, particularly control units, which are central to system automation and performance optimization.

The objective of this study is to contribute to the advancement of knowledge in functional process analysis, mathematical modeling, computer-aided simulation, and automatic control of self-propelled agricultural machinery, with a particular focus on combine harvesters. The complexity of this subject necessitates an interdisciplinary approach that bridges mechanical, electrical, hydraulic, and control engineering domains.

Although the present work does not offer an exhaustive treatment of all related topics, it aims to provide a framework for understanding key concepts, methods, and techniques. Readers are encouraged to engage critically with the content to build a solid foundation for further study and practical application in automated machine design and system integration.

Modern combine harvesters exhibit high material processing capacity, with travel speeds adjustable according to crop type, variety, and soil conditions. To maintain consistent processing performance, the engine typically operates at a constant speed. Simultaneously, the travel speed must be variable, ranging from slow speeds during harvesting to higher velocities for transport on public roads. These operational requirements are met through the integration of multiple energy and drive systems—mechanical, hydraulic, pneumatic, electrical, and electronic—each serving specific roles in propulsion, functional actuation, and control of the harvesting processes.

A considerable portion of the engine's output is allocated not only to the execution of the core technological operations but also to auxiliary systems that enhance operator comfort, such as climate control within the cabin. This underscores the multifaceted nature of modern combine harvesters, which must balance energy efficiency, control precision, and operator ergonomics within a single, highly integrated system *(Nicolae and Coteanu, 1973*).

The control of agricultural machinery operations can be achieved either manually or through automated systems employing various types of controllers. In contemporary combine harvesters, automatic control is predominantly implemented using electrohydraulic actuators, which offer both precision and responsiveness under variable working conditions.

Key functional components of modern combines are increasingly supported by automated control systems designed for load management and process quality assurance. These systems are frequently integrated with visual and acoustic warning mechanisms, enhancing both operator awareness and system safety. For example, monitoring and signaling subsystems are commonly deployed to supervise the operation of conveyors, crop and grain elevators, straw and chaff handling systems, grain storage and transfer mechanisms, threshing units, and straw walkers.

The integration of such signaling and alert systems enables early detection of malfunctions or suboptimal performance, thereby facilitating timely intervention and preventive maintenance. This not only mitigates the risk of severe mechanical failure and financial loss but also contributes to a significant improvement in operational safety and field efficiency. As such, the investment in advanced diagnostic and warning technologies is fully justified by the measurable gains in productivity and system reliability.

Control, regulation, and automation systems within combine harvesters can be classified into several major categories:

- Hydraulic actuation and control systems, responsible for powering and coordinating the mechanical functions of key components.
- Automatic leveling systems, which maintain the horizontal orientation of the header to ensure optimal cutting performance across uneven terrain.
- Steering control systems, which include electrohydraulic power steering mechanisms.
- Automatic regulation systems, which adjust machine parameters in real time based on load or environmental inputs.
- Electromechanical signaling systems, designed to alert operators to abnormal operating conditions.

A notable advancement in steering automation involves the integration of electrohydraulic steering systems with positioning sensors, forming the basis of GPS-assisted navigation systems. These automated steering systems enable precise guidance of the combine during field operation, real-time positional tracking, and data acquisition related to harvesting performance metrics such as crop yield and area coverage.

Such integration of automation, sensor technology, and real-time monitoring represents a key step toward precision agriculture, enabling machines to operate more efficiently, adapt to variable field conditions, and support data-driven decision-making for farm management.

The operation of combine harvesters on uneven terrain presents significant challenges due to their complex structure, variable center of gravity, and the interaction of multiple moving subsystems. These machines must accurately follow predefined trajectories while performing a series of interconnected tasks on crops and plant materials, all while maintaining high standards of work quality and operational efficiency *(Vasiliu N. and Vasiliu D., 2004)*.

In the context of increasing demands for productivity, consistency, and quality control—alongside efforts to reduce variability in human operator performance—there is a growing need for the implementation of automated control systems during field operations. Concurrently, the development of autonomous agricultural vehicles is rapidly advancing, with increasing emphasis on remote operation capabilities. This emerging field envisions remote human supervision combined with autonomous task execution, enhancing both operational flexibility and labor efficiency.

This section has two primary objectives:

1. To outline the general development concept, functional architecture, and block representation of a simulation framework designed to model both the movement of the combine and its operational behavior during field tasks.
2. To propose a flexible and customizable simulation environment that can be adapted by end users according to the specific requirements of their research or application.

The conceptual model underpinning this simulation package has been developed with core principles of modularity, flexibility, and portability in mind. A hierarchical and reconfigurable modular structure allows for the simulation environment to be tailored to various operational modes, including system behavior

analysis and prediction, subsystem testing and validation, operator training, and hardware-in-the-loop or software-in-the-loop simulations *(Miu P., 2016).*

To facilitate advanced simulation and control—whether the equipment is operated via a human-in-the-loop simulator or an autonomous GPS-guided system—a simulation manager must be established. This system component is responsible for the initialization and provision of all essential input parameters, including vehicle configuration, terrain characteristics, processing subsystems, crop type, and spatial positioning data.

The general simulation framework consists of three main modules:

- Data Input Module: Manages the acquisition and preprocessing of simulation parameters.
- Core Simulation Module: Executes the primary computational tasks, including system dynamics, task coordination, and control algorithms.
- Output Module: Presents the results of the simulation, including performance metrics, trajectory data, and system diagnostics.

The simulation manager plays a distinct role in this architecture, separate from traditional human operators or virtual assistants. Within this framework, the simulation manager is tasked with configuring and managing the full range of available simulation options based on user-defined criteria and available datasets. It also oversees the organization, processing, and transmission of these inputs to the core module for real-time or batch simulation execution.

This framework provides a scalable and adaptable toolset for researchers, developers, and equipment manufacturers to analyze and optimize combine harvester behavior under diverse field conditions, supporting the advancement of autonomous and semi-autonomous agricultural technologies.

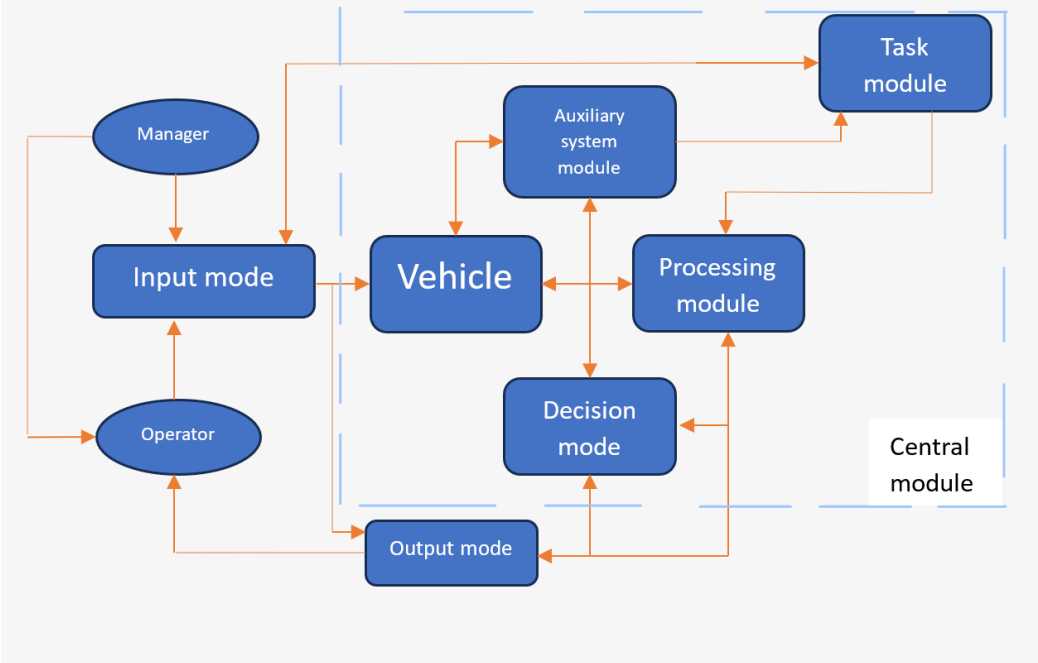

Fig. 4 - Block diagram of a general simulation

For a combine harvester to operate autonomously, it must execute a sequence of complex, interrelated tasks while maintaining a continuous communication interface with a human supervisory system. Upon receiving a pre-programmed task or mission profile from the human operator, the autonomous harvester must be capable of performing the following core functions:

- Automated navigation across mixed environments, including public roadways and agricultural fields, with seamless transitions between the two.
- Autonomous response to dynamic environmental conditions, such as the detection and avoidance of obstacles, adaptation to variable terrain, and interaction with other vehicles or machinery operating within the same environment.
- Self-regulation of harvesting parameters, adjusted in real time based on the specific characteristics of the crop (e.g., density, moisture content, or variety) and local field conditions.

Achieving full autonomy in a combine harvester requires the complete automation of the entire technological workflow—from mobility and perception to processing and decision-making. Such integral automation serves to optimize operational efficiency, ensure consistency in product quality, and support effective harvesting in geographically fragmented or agronomically heterogeneous areas.

The realization of these capabilities relies on the integration of advanced mathematical modeling techniques, real-time control algorithms, and the principles of automatic control theory. Furthermore, the effectiveness of autonomous systems is enhanced by leveraging both internal design expertise and empirical data obtained through extensive field operation.

This convergence of control theory, sensor fusion, artificial intelligence, and mechanized agricultural engineering is pivotal for enabling next-generation autonomous harvesting systems that are not only efficient but also adaptive, robust and scalable to diverse farming scenarios.

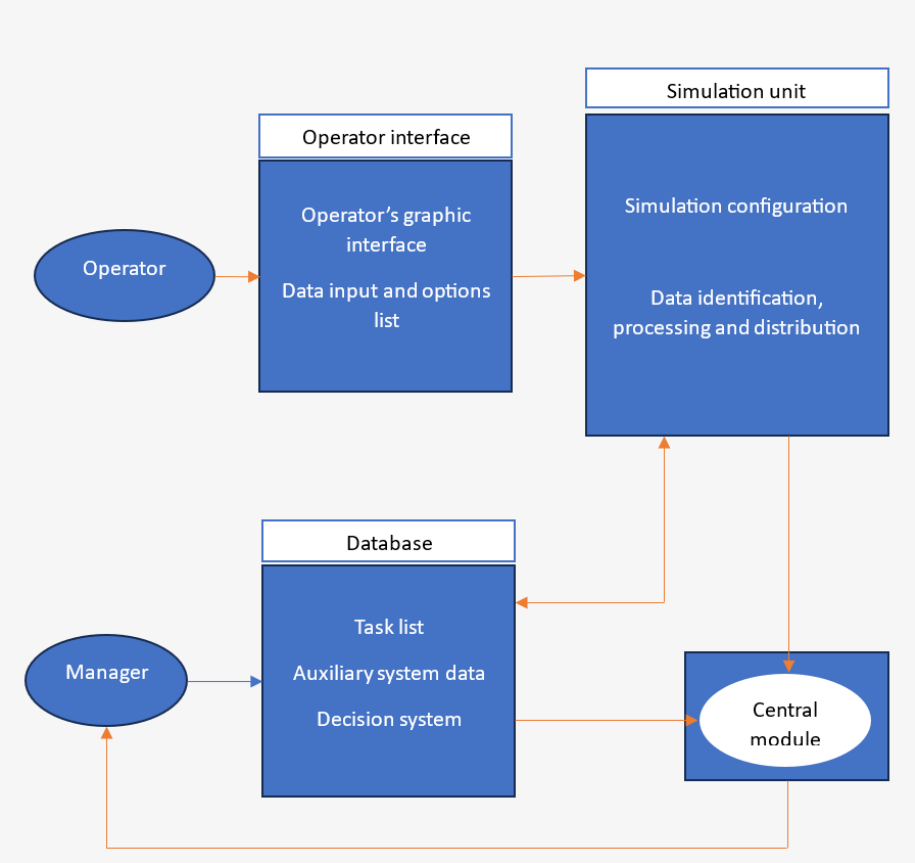

Fig. 5 - Input command diagram

A critical component in the development of autonomous agricultural machinery is the implementation of an automated guidance system capable of accurately controlling the vehicle's direction, speed, and acceleration. To achieve robust and precise navigation under varying environmental conditions, a multi-sensor fusion approach is required—most notably the integration of vision-based systems and satellite-based positioning technologies.

An effective solution involves combining a camera-based visual system with a Global Positioning System (GPS) into a unified control platform. The visual system, utilizing onboard cameras mounted on the agricultural vehicle, enables real-time detection of obstacles and navigational cues without relying on pre-generated digital terrain maps. This system plays a critical role in local navigation and obstacle avoidance, particularly in unstructured or dynamically changing environments.

Complementing this, the GPS module provides accurate geospatial positioning and long-range navigational support. It plays a pivotal role in route planning, path following on public roads, and reducing cumulative positioning errors during extended operation periods.

These two systems operate synergistically to enhance reliability and operational robustness. For example, in scenarios involving low visibility, such as during dusk, fog, or adverse weather, the visual system may degrade in performance—conditions under which GPS-based guidance can maintain navigational

accuracy. Conversely, in environments where satellite signals are obstructed or intermittent (e.g., near tree lines or in remote valleys), the visual system ensures continued trajectory control. Some implementations further integrate geomagnetic positioning sensors to enhance spatial localization, particularly in GPS-denied environments.

The strategic integration of these heterogeneous sensor systems significantly enhances the redundancy, adaptability, and precision of the vehicle's guidance framework. However, the increased complexity of these systems also introduces new challenges related to system maintenance, diagnostics, and lifecycle cost.

As agricultural machinery grows in sophistication, ensuring high reliability of the electronic and hydraulic subsystems becomes imperative. Unplanned equipment downtime due to failures in guidance or control systems can result in substantial financial losses, especially during time-critical harvesting operations. Therefore, improving system reliability—through both design robustness and intelligent maintenance strategies—represents a central focus in the evolution of automated field machinery.

While complexity in maintenance protocols may offer operational benefits by extending equipment lifespan and performance, it must be carefully managed. Excessive maintenance overhead or cost-ineffective solutions may undermine overall system viability. Consequently, a balanced approach that considers both technical performance and economic efficiency is essential for sustainable deployment of autonomous agricultural technologies.

RESULTS

In the development of complex agricultural systems, particularly autonomous or semi-autonomous combine harvesters, system designers must prioritize reliability, maintainability, and operational efficiency from the earliest design stages. A series of well-defined design principles can significantly reduce the probability of failure, simplify maintenance procedures, and enhance the long-term performance of the system. The following measures outline a comprehensive framework for reliability-oriented design:

1. **Minimization of System Complexity**

The initial design phase should aim to produce functional schematics that are as simple as possible, utilizing a minimal number of interdependent components. Unnecessary elements introduce additional failure points, increase the likelihood of malfunction, complicate maintenance, and elevate associated costs. Configurations that result in functional ambiguity or introduce unwarranted automation complexity should be eliminated at the conceptual stage.

2. Selection of High-Reliability Components

The choice of components with proven reliability is fundamental. Prioritizing parts with high mean time between failures (MTBF) contributes to stable system performance and reduces maintenance frequency. This facilitates predictive maintenance scheduling and supports cost-effective, long-duration operational cycles.

3. Strategic Placement of High-Failure-Probability Components

Components with a statistically higher likelihood of failure should be positioned in locations that ensure easy access for inspection and replacement. This approach avoids the need for partial or complete disassembly of complex assemblies, thereby minimizing service time and reducing equipment downtime.

4. Leak Prevention and Fluid Quality Management

Design solutions must address fluid containment, acoustic comfort, and environmental integrity. Key measures include the use of appropriately selected sealing elements (e.g., gaskets and O-rings) that are compatible with the system's working fluids and operational pressures. These solutions help prevent external leakage and maintain fluid quality over time.

5. Reduction of Energy Losses and Thermal Overload

To improve system efficiency and control operating costs, components and conduits should be dimensioned to minimize flow resistance. Increasing the nominal diameters of pipelines and hydraulic elements reduces pressure losses, mitigates overheating, and enhances overall energy efficiency.

6. Modular System Architecture

Adopting a modular design—where the system is composed of semi-independent subassemblies—improves fault tolerance and serviceability. In such architectures, localized failures (e.g., damage to a single seal) are less likely to cause systemic malfunctions, allowing for partial system functionality and isolated repairs.

7. Integration of Compact Functional Blocks

Where feasible, compact functional blocks should replace traditional interconnections made via pipes and mounting plates. This design practice reduces the number of joints and potential leakage points, improves structural compactness, and increases reliability by simplifying component integration and reducing service intervention complexity.

8. Preventive and Predictive Maintenance Planning

A robust preventive maintenance strategy must be embedded into the system from the design phase. This includes scheduling service intervals and specifying inspection procedures. Where applicable, the design should support integration with predictive or proactive maintenance tools, enabling early detection and mitigation of potential failures.

9. Provision of Diagnostic and Monitoring Access Points

Control points for measuring critical system parameters—such as flow rate, pressure, and temperature—should be included in the system layout. These diagnostic interfaces enable real-time monitoring and facilitate the integration of control equipment, ensuring consistent performance and simplifying troubleshooting during operation.

By incorporating these design strategies, engineers can significantly enhance the reliability, serviceability, and overall lifecycle performance of agricultural machinery systems, aligning technological advancement with practical field requirements.

CONCLUSIONS

The evolution of modern agricultural machinery, particularly combine harvesters, is increasingly defined by the integration of advanced automation, control systems, and reliability-centered design strategies. As these machines operate in complex, dynamic, and often unstructured field environments, their performance depends on the seamless coordination of hydraulic, mechanical, electrical, and electronic subsystems. Hydraulic systems, in particular, play a pivotal role in ensuring the synchronized operation of key components such as the reaper, cutting platform, variable speed drive, and steering mechanism.

The transition toward autonomous and semi-autonomous harvesting systems demands robust modeling, simulation, and control frameworks capable of capturing the multifaceted behavior of the machine and its interaction with varying crop and terrain conditions. Through hierarchical, modular simulation environments and real-time sensor integration—particularly GPS and camera-based navigation systems—harvesters are becoming increasingly capable of performing complex tasks with minimal human intervention while maintaining operational precision and safety.

At the core of these advances lies a deliberate focus on system reliability and maintainability. From simplifying functional schematics and selecting high-durability components, to designing modular architectures and embedding predictive maintenance capabilities, each design decision plays a critical role in reducing downtime, optimizing energy use, and minimizing the total cost of ownership. Complementary sensor fusion, preventive diagnostics, and real-time monitoring further contribute to enhancing both the performance and resilience of automated systems in the field.

Ultimately, the convergence of mechanical engineering, control theory, sensor technology, and agricultural science offers a powerful pathway toward the realization of highly efficient, intelligent, and autonomous harvesting platforms. As the agricultural sector continues to demand higher productivity, quality, and sustainability, these integrated engineering approaches provide the foundation for the next generation of self-propelled machines, enabling more informed, adaptable, and efficient field operations.

REFERENCES

[1] Blagoi O., Mitroi A., (2003) General hidraulics. Compendiu
[2] Catană I., Vasiliu, D., Vasiliu, N. (1996) Electrohidraulic servomechanisms. Politechnical University of Bucharest
[3] Kahandage P. D., Piyathissa S. D. S., (2023) Comparative Analysis of Paddy Harvesting Systems Toward Low-carbon Mechanization in the Future: A Case Study in Sri Lanka.
[4] Kassen D. M. (2016) Combine harvester header height control through robust linearization with feedback. Iowa State University
[5] Miu P. (2016) Theory, modeling and design of combine harvesters. CRC Press.

[6] Neculaiasa V., Danila I., Fratila A. I. (1995) Hydraulic systems of tractors and agricultural machinery. Editura A92
[7] Nicolae M. I., Coteanu H. R. (1973) C12 Combine harvester. Notita tehnica editia III
[8] Scripnic V., Babiciu P., Fratila A. I. (1984) Hydraulic systems of tractors and agricultural machinery. CERES
[9] Seyyedhassani H., Jafari A., Rafiee S., Mohtasebi S. S. (2011) Hydraulic System of JD 955 Combine Harvester as Well as Presented Services Based on Statistical Analysis. ResearchGate
[10] Vasiliu N., Vasiliu D., (2004) Hidraulic and pneumatic actuators
[11] Wang H., Cao S., Xu X., Han T., Guo H. (2019) Design and analysis of the leveling hydraulic system of the combine harvester. ResearchGate
[12] Wang H., Wuyun Z., Wei S., Xiaolong L., Ruijie S. (2024) The Design and Experimentation of a Wheeled-Chassis Potato Combine Harvester with Integrated Bagging and Ton Bag-Lifting Systems. MDPI
[13] Woodruff K. A. (1971) Evaluating header height control mechanisms. Iowa State University
[14] Yang L., Chenming L., Wangyuan Z., Xiaomao H., Lina M., Guodang L. (2021) Optimization of Clamping and Conveying Device for Sunflower Oil Combine Harvester Header. MDPI
[15] *** http://www.deere.co.uk/common/docs/products/.
[16] *** https://www.mdpi.com/2077-0472/14/9/1461
[17] *** https://ro.wikipedia.org/wiki/Sistem_de_ac%C8%9Bionare_hidraulic%C4%83
[18] *** shijiazhuanghanjiu.en.made-in-china.com/product/xNhQEZpdAIcw/China-Combine-Harvester-Hydraulic-Steering-Units-101s-1-Steering-Drive.html

ASSESSMENT OF AIRBORNE POLLUTION IN INDUSTRIAL CITIES OF THE DNIPROPETROVSK REGION AND PROSPECTS FOR THE CREATION OF GREEN PROTECTIVE BELTS

/

ОЦІНКА ЗАБРУДНЕННЯ ПОВІТРЯ В ПРОМИСЛОВИХ МІСТАХ ДНІПРОПЕТРОВСЬКОЇ ОБЛАСТІ ТА ПЕРСПЕКТИВИ СТВОРЕННЯ ЗЕЛЕНИХ ЗАХИСНИХ СМУГ

Mykola KHARYTONOV*[1)], Nadia MARTYNOVA[2)], Liubov MATUSHEVYCH[3)], Svitlana SYTNYK[4)]

[1)] Ecology Department, Dnipro State Agrarian and Economic University, Dnipro / Ukraine;

[2)] Botanical Garden, Oles Honchar Dnipro National University, Dnipro / Ukraine;

[3)] Department of Forest Mensuration and Forest Management, National University of Life and Environmental Sciences, Kyiv / Ukraine;

[4)] Laboratory of Forest Management, Dnipro State Agrarian and Economic University, Dnipro / Ukraine.

**Tel: +38-0973 456 227; *E-mail: kharytonov.m.m@dsau.dp.ua*

Keywords: *air borne pollution, nitrogen and sulfur dioxides, urban forest parks, protection strips*

ABSTRACT

The level of air pollution with PM 10 particles in two industrial cities exceeded the recommended annual concentration of PM10 up to 10-15 times. Pollution of the atmosphere of Dnipro city with sulfur dioxide is almost twice as high as the data for Kamyanske. The maximum permissible concentration of nitrogen dioxide in the air of Dnipro and Kam'yanske was exceeded by 1.5-3 times. The gradual replacement of the most vulnerable tree species with other, non-invasive and more resistant ones, for implementation in urban forest parks and shelterbelts is justified. *Phellodendron amurense, Eucommia ulmoides, Koelreuteria paniculata, Sorbus torminalis, Cladrastis kentukea, Gymnocladus dioicus* and some others, which are still rarely used, have great potential for urban park landscaping in steppe zone of Ukraine.

ТЕЗИ

Рівень забруднення повітря частинками PM10 у двох промислових містах перевищив рекомендовану річну концентрацію PM10 до 10-15 разів. Забруднення атмосфери міста Дніпро діоксидом сірки майже вдвічі перевищує дані для Кам'янського. Гранично допустима концентрація діоксиду азоту в повітрі Дніпра та Кам'янського була перевищена в 1,5-3 рази. Обгрунтована поступова заміна найбільш вразливих видів іншими неінвазивними та більш стійкими породами дерев для покращення міських парків та захисних лісосмуг. *Phellodendron amurense, Eucommia ulmoides, Koelreuteria paniculata, Sorbus torminalis, Cladrastis kentukea, Gymnocladus dioicus* і деякі інші, які поки що рідко використовуються, мають великий потенціал для міського озеленення в степовій зоні України.

INTRODUCTION

Constant exceeding of the MPC for the level of technogenic dust, nitrogen dioxide, sulfur and other pollutants in the atmosphere of urban agglomerations leads to the formation of acid rain, photochemical smog and an increase in the number of diseases among the local population *(Karnaukh and Lugovskoy, 2008; Stankevich et al., 2016; Kharytonov et al., 2017).*

It is known that the first metallurgical enterprises of the cities of Dnipro and Kamianske were built at the end of the 19th century on the banks of the Dnipro River in close proximity to the residential areas.

Therefore, at the end of the 20th century, the environmental situation in these cities deteriorated. The metallurgical plants located here have switched to modernization, replacement of equipment and technological processes only in the last two decades *(Babiy et al., 2003).*

The main task of solving the problem of reducing aero-technogenic pollution of industrial cities is to organize a network of posts for regional and local monitoring *(Kharytonov et al., 2015; Batur and Babii, 2022).*

The second task concerns the creation of a network of urban forest parks in residential areas, landscaping of enterprise territories and the creation of green belts from forest plantations around industrial agglomerations *(Khan and Abbasi, 2002).*

Tree plantings 30 m high ensure almost complete dust capture and a significant reduction in the concentration of gaseous pollutants In this regard, many studies are devoted to finding promising species for urban landscaping that are tolerant to the effects of pollutants. For example, experiments by Zhang et al. (2013) with fumigation chambers made it possible to assess the sensitivity of forest trees to air pollutants in subtropical climate. Two of the six species were selected after SO_2 fumigation to create green belts near industrial agglomerations *Ilex rotunda* remained green and absorbed the largest amount of SO_2, while *Cassia surattensis* can be used to improve the oxygen/carbon dioxide ratio in polluted areas.

Another study showed that deciduous trees are relatively sensitive to SO_2 during early growth and become more tolerant with age, while conifers are relatively tolerant during early growth and become very sensitive at peak wood growth, with this sensitivity persisting until early maturity *(Be and Baciak, 2015).*

The accumulation of various air emissions in areas with a high concentration of industrial facilities results in the appearance of more than one harmful substance, and the vegetation is constantly exposed to changing combinations of various toxic substances of varying concentrations *(Mohrena et al., 1992; Paoletti et al., 2010; Geiser et al., 2019).*

In this case the susceptibility of vegetation to damage in areas with exposure to many toxic substances became higher than in the presence of only one harmful substance. A floristic variety of native tree species in a steppe zone of southeast Ukraine is rather poor and totals no more than 40 species. And only some of them are used for urban forest establishment as many of natural species do not endure urbanistic pressure.

Therefore the overwhelming majority of urban forest species are introduced from other geographical areas. It was shown that planting fast growing tree species such as *R. pseudoacacia and A. platanoides* can be an environmentally appropriate and cost-effective measure to mitigate the toxic effects of heavy metals in the park areas *(Lovynska et al, 2024; Lakyda et al., 2025).* Unfortunately, global climate change and increasing anthropogenic pressure lead to destruction of urban ecosystem balance. It makes urban trees vulnerable to damaging by pests and pathogens, leads to life length reduction.

An example is leaf spot caused by the leaf miner Cameraria ohridella (*Lepidoptera, Gracillariidae*), which limits the use of *Aesculus* in urban landscaping *(Sytnyk et al., 2025).* Therefore new resistant trees without invasive risk can be studied and considered as alternative solution to introduction in urban forest assortment.

The main objective of this article was to estimate the man-made atmospheric pollution in industrial cities of the Dnipropetrovsk region and prospects for the creation of green protective belts.

MATERIALS AND METHODS

The tree plantings are natural barrier which protects atmosphere from harmful emissions. However natural woods in a steppe zone of Ukraine take up only 6 % of its territory. That's why artificially created forests carry out important water-retaining, phytomeliorative and recreational functions, increase biodiversity, and serve as reserves for valuable plant and animal species. However, today many of these ecosystems are in a destructive state. It is related both with anthropogenic influence and region environmental conditions. The climate of the southeast of Ukraine becomes more arid. Obvious insufficiency of water supply is observed. Total annual precipitation is small (400-500 mm) and varies significantly over the course of the warm season. Frequent droughts and high average daily temperatures of air during plant vegetation strengthen negative influence on artificial forest ecosystems. The assessment of air pollution was carried out in two urban cities: Dnipro and Kam'yanske, and was based on data from monitoring stations and the Earth Remote Sensing Center.

A review of tree species that are promising for urban park landscaping is based on many years of introduction research conducted in the Oles Honchar Dnipro National University Botanical Garden. It is located in the central part of the Dnipro city, occupies an area of 27 hectares, is one of the structural elements of the city wide greening system and along with other city forests is fully exposed to different stress factors.

RESULTS

The technogenic dust, dioxides of nitrogen and sulphur are main parameters connected with damage to forest trees. An average annual data on respirable particulate matters (PM) PM10, SO_2 and NO_2 observed for Dnipro and Kam'yanske cities are shown in the figure 1-3.

According to the World Health Organization's guidelines on air quality, the recommended annual concentration of PM10 should not exceed 0.02 mg/m^3 (World Health Organization 2005). The level of air pollution with PM 10 particles in two industrial cities was 10-15 times higher. Pollution of the atmosphere of Dnipro city with sulfur dioxide is almost twice as high as the data for Kam'yanske. However, excess of the maximum concentration was not recorded in the atmosphere of both cities. At the same time, the maximum permissible concentration of nitrogen dioxide in the air of Dnipro and Kam'yanske was exceeded by 1.5-3 times.

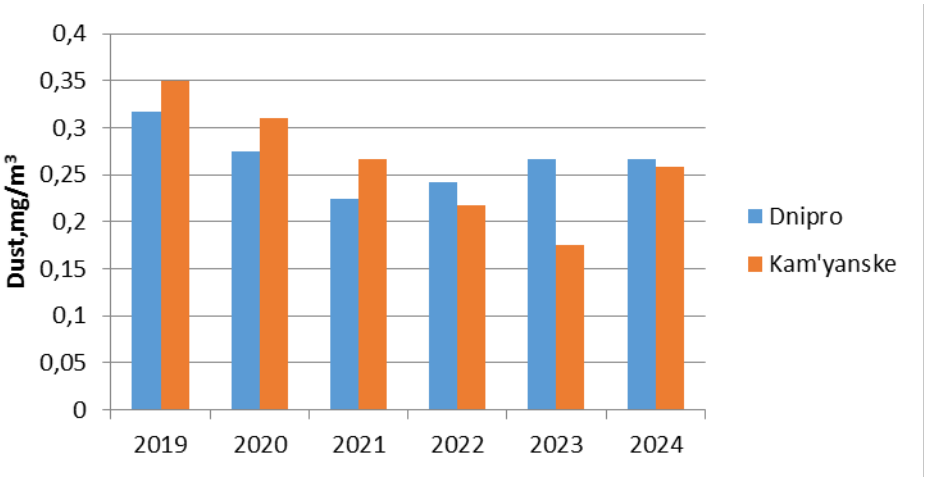

Fig. 1 - An average annual data on PM10 for two cities

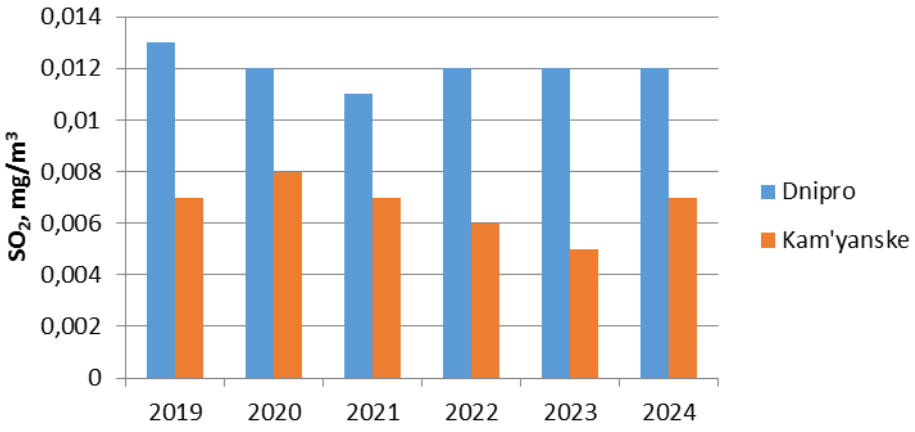

Fig. 2 - An average annual data on SO_2 for two cities

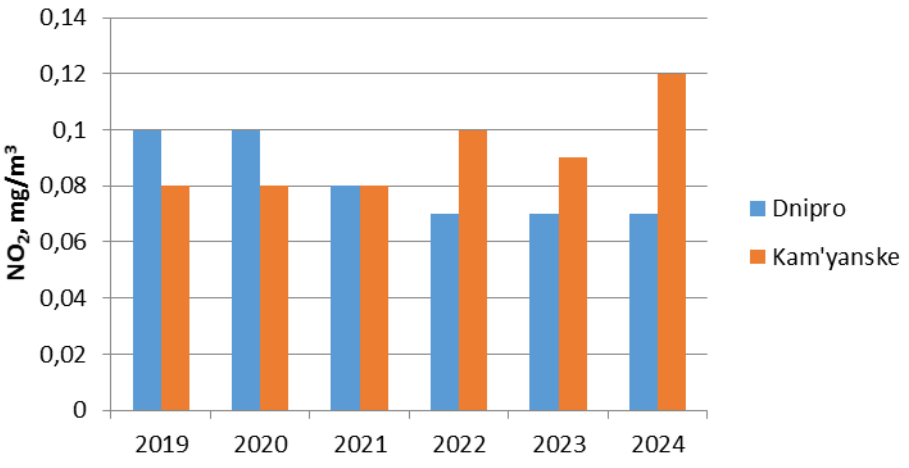

Fig. 3 - An average annual data on NO_2 for two cities

Based on the results of determining the content of nitrogen and sulfur dioxides in the atmosphere of the Dnipro and Kam'yanske cities, the method of overlaying maps was applied. It should be noted that nitrogen dioxide and sulfur dioxide have a summation effect. In the presence of many dispersed sources, individual emissions are superimposed and a total flare is formed, which spreads over industrial agglomerations.

As a result, maps of the risks of total man-made pollution of the atmosphere of two industrial agglomerations NO_2 and SO_2 were made (Fig. 4).

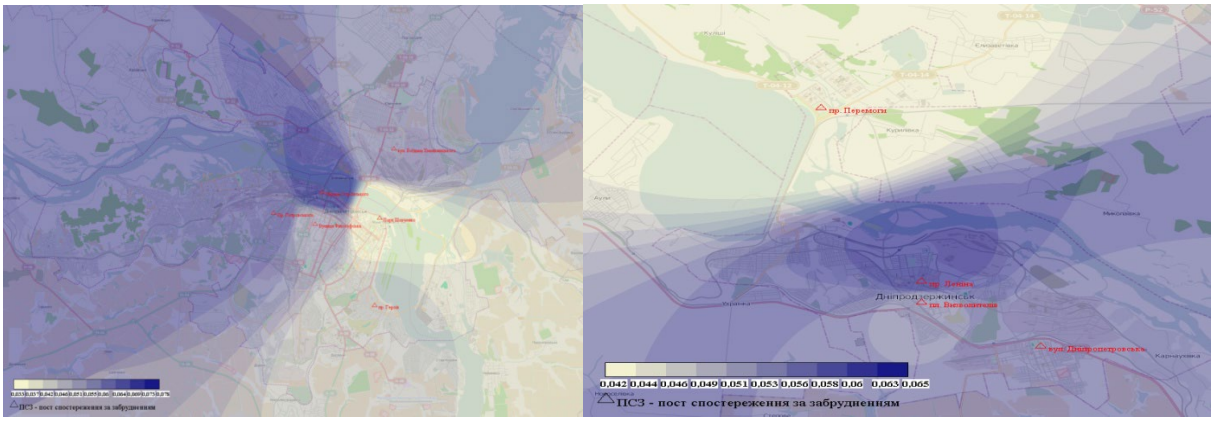

Fig. 4 - Maps of the cumulative assessment of atmospheric pollution risks in Dnipro (left) and Kam'anske (right) with nitrogen and sulfur dioxides

Analysis of maps of the distribution of NO_2 and SO_2 in the atmosphere of two cities in the Dnipropetrovsk province indicates the formation of certain aerosol circulation flows. It is obvious that the greatest attention to greening the territory of these two cities should be directed to the places of formation of smog of nitrogen and sulfur dioxides reflected on the prepared GIS maps.

The degree of damage to plants from the accumulation of toxic substances in them can vary greatly between individual species. Some of them are damaged by low accumulation of pollutants in the air of leaves, while others are damaged by their amount, which is 10-30 times higher *(Nowak et al., 2014; Sonwani et al., 2022)*.

In this regard, it is necessary to create protective green plantings from more resistant species; use gas-resistant plants with high gas-absorbing capacity as a natural filter; take into account the nature of pollution in a particular area when planting urban forest plantations.

Introduction of resistant plants in urban forest structure allows opening in full their ornamental features, to increase longevity and functionality. Today, the main problems of urban plantings are damage by pests and diseases, as well as a reduction of lifespan due to anthropogenic load. Monitoring of Dnipro city urban forests has shown that only 12 from 50 dominant species had no signs of any damages. Trees of *Aesculus hippocastanum* are often damaged by chestnut borer, *Ulmus sp.* by graphiosis, *Acer platanodes, Populus sp*. by tinder fungus.

Another problem of urban forests is the presence of adventitious species with a high potential for expansion and naturalization: *Acer negundo, Ulmus pumila, Robinia pseudoacacia, Celtis occidentalis, Ailanthus altissima* etc. These types of trees often spread from artificial plantings to local ecosystems, where they make serious competition to native species.

One of the methods for improving the state of urban forests may be the introduction and gradual replacement of the most vulnerable species by other more stable in the current conditions, and which do not have an invasive threat. Long-term monitoring of the woody plants collections in the DNU botanical garden allows us to pick out promising species for enriching the biodiversity in urban forests (table 1).

Table 1

Tree species that can be recommended for improving the state of urban forests in the steppe zone of Ukraine

Name	Origin	Height, category
Sorbus torminalis	indigenous	I
Carpinus betulus	indigenous	II
Acer campestre	indigenous	II
Catalpa speciosa	North America	II
Gymnocladus dioicus	North America	II

Cladrastis kentukea	North America	II
Juglans mandshurica	Far East Asian region	I
Phellodendron amurense	Far East Asian region	I, II
Eucommia ulmoides	Far East Asian region	II
Koelreuteria paniculata	Far East Asian region	II

The species presented in the table showed high resistance and viability in arid steppe conditions, as well as tolerance to anthropogenic pressure. Adding some exotic species (*Ginkgo biliba, Liriodendron tulipifera, Pseudotsuga mensiensii*) to the offered range can help enhance the ornamental effect of park plantings.

CONCLUSIONS

The territory of the industrial agglomerations in the Dnipropetrovsk region exposed to severe anthropogenic influence caused by intensive chemical, metallurgical and mining industries concentrated in the region. Constant excess of maximum permissible concentration level of technogenic dust, nitrogen and sulfur dioxides and other pollutants in atmosphere of urban agglomerations leads to formation of acid rains and a photochemical smog.

The total toxicity of these pollutants can be much more in consequence of summation effect. A floristic variety of tree species in a steppe zone of southeast Ukraine is rather poor and totals no more than 40 species. And only some of them are used for urban forest establishment as many of native species do not endure urbanity pressure. Therefore the overwhelming majority of urban forest species are introduced from other geographical areas.

Unfortunately, global climate change and increasing anthropogenic pressure lead to destruction of urban ecosystem balance. It makes urban trees vulnerable to damaging by pests and pathogens, leads to lifespan reduction. As alternative solution we consider introduction in urban forest assortment a few resistant tree species of North American and Asian origin, and three indigenous species as well.

ACKNOWLEDGEMENT

This study was funded by Ministry of Education and Science of Ukraine.

REFERENCES

[1] Babiy, A. P., Kharytonov, M. M., Gritsan, N. P. (2003). Connection between emissions and concentrations of atmospheric pollutants. Melas, D., & Syrakov, D. (eds.). Air Pollution Processes in Regional Scale, NATO Science Series, IV: *Earth and environmental sciences*. Kluwer Academic Publishers. Printed in the Netherlands, p. 11–19.

[2] Batur, M., & Babii, K. (2022). Spatial assessment of air pollution due to mining and industrial activities: a case study of Kryvyi Rih, Ukraine. IOP Conf. Series: *Earth and Environmental Science* 970 012004.doi:10.1088/1755-1315/970/1/012004

[3] Be, A., & Baciak, M. (2015). The effect of sulfur dioxide on selected deciduous forest trees. *Scientific Review Engineering and Environmental Sciences (SREES)* 24(2):155-166

[4] Geiser, L.H., Nelson, P.R., Jovan, S.E., Root, H.T., & Clark, C.M. (2019).Assessing Ecological Risks from Atmospheric Deposition of Nitrogen and Sulfur to US Forests Using Epiphytic Macrolichens. *Diversity*. 11(6):87. https://doi.org/10.3390/d11060087

[5] Karnaukh, M., & Lugovskoy, S. (2008). Social, medical and environmental consequences of mining and metallurgical complex activity in the Krivorozhsky region and decision making. In: Barnes I., Kharytonov M., editors. Simulation and assessment of chemical processes in a multiphase environment NATO science for peace and security series C: *Environmental security*. Dordrecht, Netherlands: Springer, 377–384

[6] Khan, F., & Abbasi, S. A. (2002). Design of Greenbelt for an Industrial Complex Based on Mathematical Modelling. *Environmental Technology* 23(7):799-811.DOI: 10.1080/09593332308618374

[7] Kharytonov, M., Benselhoub, A., Shupranova,L., Kryvakovska, R., & Khlopova, V. (2015).Environmental assessment of atmospheric pollution in Dnipropetrovsk province (Ukraine). *Studia Universitatis Vasile Goldis Seria Stiintele Vietii (Life Sciences Series)* 25(2), 125-130

[8] Kharytonov, M., Benselhoub, A., Kryvakovska, R., Klimkina, I., Bouhedja, A., Bouabdallah, S., Chaabia, R., & Vasylyeva, T. (2017). Risk assessment of aerotechnogenic pollution generated by industrial enterprises in Algeria and Ukraine. *Studia Universitatis Vasile Goldis Arad, Seria Stiintele Vietii* 27(2), 99-104

[9] Lakyda, P., Matushevych, L., Sakharuk, H. Lovynska, V., Holoborodko, K., & Sytnyk, S. (2025). The influence of Robinia pseudoacacia plantations on soil in the park areas of Dnipro contaminated with heavy metals. Ukrainian Journal of Forest and Wood Science 16(2),115–135.

[10] Lovynska, V., Holoborodko, K., Ivanko I.A., Sytnyk, S., Zhukov O.V., Loza I.G., Wiche O., & Heilmeier H. (2023). Heavy metal accumulation by Acer platanoides and Robinia pseudoacacia in an industry city (Northern Steppe of Ukraine). Biosystems Diversity, 31(2), 246–253

[11] Mohrena, G.M.J., Jorritsmaa, I.T.M., Vermetten, & A.W.M. (1992).Quantifying the direct effects of SO_2 and 0_3 on forest growth. Forest Ecology and Management, 51 137-150.

[12] Nowak D.J., Hirabayashi S., Bodine A., & Greenfield E. (2014). Tree and forest effects on air quality and human health in the United States, *Environmental Pollution* 193,119-129, https://doi.org/10.1016/j.envpol.2014.05.028.

[13] Paoletti, E., Schaub, M., Matyssek, R., Wieser, G., Augustaitis, A., Bastrup-Birk, A.M.; Bytnerowicz, A.; Günthardt-Goerg, M.S.; Müller-Starck, G., & Serengil, Y. (2010). Advances of air pollution science: From forest decline to multiple-stress effects on forest ecosystem services. *Environ. Pollut.158*, 1986–1989.

[14] Sonwani, S., Hussain, S., & Saxena, P. (2022). Air pollution and climate change impact on forest ecosystems in Asian region – a review. *Ecosystem Health and Sustainability* 8(1). https://doi.org/10.1080/20964129.2022.2090448.

[15] Stankevich, S.. Titarenko, O., Svideniuk, M., Kharytonov, M., Benselhoub, A., Khlopova V. (2016). Air pollution mapping with nitrogen and sulfur dioxides in the south-eastern part of Ukraine using satellite data. *Mining Science* 23, 21-31

[16] Sytnyk, S., Holoborodko, K., Palchykov, V., Ivanko, I., Dobrovolska, O., Seliutina, O., Bandura, L., & Lovynska, V. (2025). Component composition of organic compounds of the assimilative apparatus of different species of the genus Aesculus affected by Cameraria ohridella (Lepidoptera, Gracillariidae). *Biosystems Diversity* 33(2), e2522.

[17] World Health Organization (2005). Air quality guidelines: global update 2005: particulate matter, ozone, nitrogen dioxide, and sulfur dioxide World Health Organization.

[18] Zhang, X., Zhou, P., Zhou, P., Zhang, W., & Wang, Y., (2013). Selection of Landscape Tree Species of Tolerant to Sulfur Dioxide Pollution in Subtropical China. *Open Journal of Forestry* 03(04),104-108. DOI: 10.4236/ojf.2013.34017.

POTENTIAL AND PERSPECTIVES OF ORCHARD LIGNOCELLULOSIC BIOMASS AS A SOURCE OF RENEWABLE ENERGY IN THE REPUBLIC OF MOLDOVA

/

POTENȚIALUL ȘI PERSPECTIVELE BIOMASEI LIGNOCELULOZICE POMICOLE CA SURSĂ DE ENERGIE REGENERABILĂ ÎN REPUBLICA MOLDOVA

Grigore MARIAN*[1)], Alexandru BANARI[1)], Andrei GUDÎMA[1)], Boris NAZAR[1)], Leonid MALAI[1)], Nicolae DARADUDA[1)], Andrei PAVLENCO[2, 1)], Teodor MARIAN*[2, 1)]

[1)] Scientific Laboratory of Solid Biofuels, Technical University of Moldova, 56 Mircești str., 2049, Chisinau / Republic of Moldova;

[2)] CC „BASADORO AGROTEH" LLC / Republic of Moldova (PhD student TUM).

**Tel: (+37) 379 446 342; *E-mail: grigore.marian@if.utm.md*

Keywords: *fruit tree biomass; pruning residues; solid biofuels; sustainable energy potential; calorific value; ash content; Republic of Moldova*

ABSTRACT

The utilization of residues resulting from orchard pruning represents a promising solution for diversifying renewable energy sources and reducing dependence on fossil fuels in the Republic of Moldova. This study assesses the availability, quality, and sustainable energy potential of lignocellulosic biomass from seed and stone fruit species cultivated in different economic regions, based on samples collected from orchards larger than 10 ha. The analyses included biomass yield, moisture content, net calorific value, and ash content. Results indicate high sustainable energy potential values for peach (33.50 ± 6.54) GJ/ha*, apple (29.67 ± 5.17)* GJ/ha*, and pear (29.45 ± 2.51)* GJ/ha*. The Northern region, dominated by apple orchards, accounts for the largest share of the national potential (467.73 – 665.13)* TJ/yr*, while the Central region stands out for plum and pear, and the Southern region for peach and apricot. Cherry residues show the lowest sustainable energy potential 17.61* GJ/ha *and the highest predictive uncertainty Up = 8.99* GJ/ha*. At the national level, the total sustainable energy potential is estimated between 806.50 and 1161.46* TJ/yr*, and the use of this biomass could substitute significant amounts of coal, natural gas, and fuel oil, reducing greenhouse gas emissions and supporting the transition to a sustainable energy system.*

REZUMAT

Valorificarea reziduurilor provenite din tăierile de întreținere ale plantațiilor pomicole constituie o soluție promițătoare pentru diversificarea surselor de energie regenerabilă și reducerea dependenței de combustibili fosili în Republica Moldova. Studiul evaluează disponibilitatea, calitatea și potențialul energetic sustenabil) al biomasei lignocelulozice de la specii sământoase și sâmburoase cultivate în diferite zone economice, pe baza probelor colectate din livezi de peste 10 ha. Analizele au vizat producția de biomasă, umiditatea, valoarea calorifică netă și conținutul de cenușă. Rezultatele indică valori ridicate ale potențialul energetic sustenabil pentru piersic (33.50 ± 6.54) GJ/ha*, măr (29.67 ± 5.17)* GJ/ha *și păr (29.45 ± 2.51)* GJ/ha*. Nordul țării, dominat de livezi de măr, deține cea mai mare pondere a potențialului național (467.73 – 665.13)* TJ/yr*, Centrul se remarcă prin prun și păr, iar Sudul prin piersic și cais. Cireșul prezintă cel mai redus potențialul energetic sustenabil 17.61* GJ/ha *și cea mai mare incertitudine Up = 8.99* GJ/ha*. La nivel național, potențialul energetic sustenabil total este estimat între 806.50 și 1161.46* TJ/yr*, iar utilizarea biomasei ar putea substitui combustibili fosili, reducând emisiile de gaze cu efect de seră și susținând tranziția spre un sistem energetic durabil.*

1. INTRODUCTION

Renewable energy plays a crucial role in the current context of the Republic of Moldova, a country that imports approximately 70% of its energy resources *(NBSRM., 2024, pp. 338 - 346)*. In this context, the identification and utilization of local renewable energy sources represent a strategic priority for ensuring energy security and sup-porting the transition towards a sustainable energy system. One of the most promising renewable sources in the Republic of Moldova is biomass, which can make a significant contribution to this transition.

To stimulate the use of biomass for energy purposes, the Republic of Moldova has adopted several policies and strategies aimed at promoting renewable energy sources. Among these are the Energy Strategy of the Republic of Moldova until 2030 *(GRM, 2013)* and the Energy Strategy of the Republic of Moldova until

2050 *(GRM, 2024*). These strategies pursue the development of a sustainable and competitive energy sector through market reforms and integration into the European Union's energy market.

The strategies target a series of objectives aimed at strengthening energy security, increasing the efficiency of energy resource use, and diversifying the energy mix, with a particular emphasis on promoting renewable energy and reducing dependence on imports, in the context of the transition towards a sustainable energy system and the commitments undertaken to combat climate change.

In parallel, the National Energy and Climate Plan 2025 – 2030 was developed by the Ministry of Energy, with support from the European Union provided through the program "Addressing the Impact of the Energy Crisis in the Republic of Moldova", implemented by UNDP Moldova *(GRM, 2025)*.

This plan sets out the priorities, objectives, and policies necessary to ensure a sustainable and affordable energy system for all consumers, while also defining the national targets in the fields of renewable energy, energy efficiency, and greenhouse gas emission reduction.

To achieve these objectives, the Government of the Republic of Moldova, in collaboration with international partners, has launched and implemented financial support programs focused on the development of biomass-fueled heating plants and the expansion of capacities for the production of densified solid biofuels, such as pellets and briquettes. Academic and research institutions in the Republic of Moldova are actively involved through research and innovation projects dedicated to the development of advanced technological solutions for the valorization of biomass resources. These efforts represent a key factor in promoting and consolidating the use of renewable energy sources derived from plant biomass, a locally abundant resource with low environmental impact.

Among plant biomass sources, those originating from the agricultural sector play a particularly important role *(Janiszewska & Ossowska, 2024)*. The use of agricultural residues as raw material for solid biofuel production contributes not only to reducing dependence on fossil energy resources and decarbonizing the energy sector, but also to supporting the transition towards sustainable production and consumption models, in line with the principles of the circular economy applied to the agri-food sector *(Ciloci & Țurcan, 2023; Silvestri et al., 2024)*.

Within this category of residues, orchard lignocellulosic biomass shows the greatest potential for use as feedstock in the production of densified solid biofuels *(Aliaño et al., 2022; Cavalaglio et al., 2024; Ciolacu et al., 2022; Marian & Banari, 2025).*

Orchard biomass comprises the totality of organic materials derived from fruit trees and shrubs, generated through orchard maintenance and exploitation activities. This includes residues from formative and maintenance pruning, annual fruiting cuts, tree thinning, the removal of dry or diseased branches, the clearing of trees at the end of their productive cycle, as well as soil cleaning and care operations.

From a compositional perspective, orchard biomass consists of wood, branches and twigs, leaves, bark, as well as other wastes resulting from the industrial processing of fruits *(Cavalaglio et al., 2024; Winzer et al., 2017)*. These residues are characterized by promising energy properties, which make them suitable for direct use in the production of pellets and briquettes, offering advantageous energy characteristics *(Alakangas, 2016; Marian et al., 2022).*

The present study aims to provide a detailed qualitative and quantitative analysis of plant biomass resources derived from fruit-growing in the Republic of Moldova, with a focus on their use for the production of densified solid biofuels. In this context, it is important to note that both the quantity and the quality of orchard biomass vary significantly depending on factors such as climatic conditions, harvesting time and method, geographical characteristics, moisture and mineral content, or conditioning methods *(Ibitoye et al., 2023)*. This variability is frequently highlighted in the specialized literature, underlining the need for detailed local analyses.

For example, researchers from the Czech Republic and Poland established that apple orchards planted at a density of 3.5 × 1.2 m generate approximately 6762 kg/ha of woody biomass (*Burg et al., 2017)*. Although the amount of biomass per tree is relatively low (2.84 kg/tree), the high overall value is explained by the high planting density per unit area. This highlights the essential role played by orchard density in maximizing the total biomass yield at the field level.

Furthermore, Polish researchers, based on an analysis of data reported by five different authors, found that the biomass potential harvested from one hectare of apple orchard varies significantly depending on tree age, year of cultivation, variety, and planting density, with values ranging between 1000 and 9800 kg/ha *(Dyjakon et al., 2016, tab.1)*.

According to the same authors, the theoretical energy potential of biomass derived from apple tree pruning in Poland is estimated at 12.52 PJ/yr, calculated for a total orchard area of 193.44 · 10^3 ha (*Dyjakon et al., 2016, tab.2)*.

A similar trend is observed in other fruit tree species. For instance, based on the analysis of biomass quantities obtained from pear pruning, Živković reported a significant variation among cultivars planted at the same density (500 trees/ha), with values ranging from 9.36 kg/tree (equivalent to 4680 kg/ha) for the 'Red-haven' cultivar to 4.85 kg/tree (2425 kg/ha) for the 'Summerset' cultivar *(Živković et al., 2013)*.

Significant amounts of woody biomass can also be recovered from orchard removal. In this regard, researchers in Germany estimated an annual biomass production potential of 10.6 Mg/ha *(Winzer et al., 2017)*. To determine the total area of cleared orchards, the authors applied a clearance coefficient of 0.05. It is noteworthy that some researchers employ conversion coefficients to estimate the biomass potential obtained from fruit tree maintenance works in relation to the total fruit yield. For example, *(Pence et al., 2024)* proposed such coefficients for several fruit species: apple – 0.19; pear – 0.22; apricot – 0.19; cherry – 0.19; peach – 0.50.

Gudîma also applied a unit conversion factor related to the mass of the main production *(Gudîma, 2017)*, using a coefficient of 0.28 for pome fruit trees and 0.26 for stone fruit trees. These coefficients were adjusted according to the availability of biomass for energy purposes and the inevitable losses occurring during its collection, transport, and processing. The author applied an availability coefficient of 0.8 and a loss coefficient of 0.9. Thus, the effective conversion coefficients, calculated for a biomass moisture content of 10%, were 0.202 and 0.187, respectively.

A similar methodology was adopted by Pavlenco, who provided detailed unit conversion factors for each species. For the pome group, the proposed values are: apple – 0.28 ± 0.02, pear – 0.20 ± 0.03, and quince – 0.14 ± 0.04; for the stone fruit group: sour cherry – 0.16 ± 0.02, sweet cherry – 0.24 ± 0.03, apricot – 0.26 ± 0.05, peach and plum – 0.26 ± 0.04 *(Pavlenco et al., 2018)*. Similarly, the authors applied an availability coefficient of 0.8 and a loss coefficient of 0.9.

The analysis of the data presented by the aforementioned authors highlights that the average production of woody mass resulting from fruit tree maintenance works varies significantly, being influenced by a range of objective and subjective factors. On average, these variations may reach values between 1.5 and 10 Mg/ha. In this context, knowledge of the average amount of biomass available, suitable for use as raw material in different regions of the country, is essential for substantiating decisions regarding the organization of solid biofuel production in specific localities.

At the same time, modern standards for solid biofuel quality (e.g., EN ISO 17225 series) require detailed knowledge of the physico-chemical properties of biomass, in order to ensure compliance with the accepted quality classes on both domestic and international markets. These requirements particularly refer to the calorific value and ash content, parameters strongly influenced by the origin of the biomass used as raw material for producing densified solid biofuels *(Toscano et al., 2023)*.

There are few studies dedicated to an integrated assessment of the sustainable energy potential (SEP), understood as the annual amount of energy obtainable from orchard biomass under real conditions of harvesting, processing, and utilization, in the Republic of Moldova, and the available data remain fragmented and uncorrelated with the geographical distribution of orchards as well as with the specific features of the country's economic development zones.

For instance, data published by Marian and Banari *(Marian & Banari, 2025)* refer to the energy potential of nut crop residues, expressed in GJ/ha, for three species—walnut, hazelnut, and almond—differentiated into two categories of biomass: woody biomass and endocarp. A more detailed evaluation of the energy potential of lignocellulosic biomass is presented for residues from vineyard plantations *(Marian et al., 2024)*.

However, there is a lack of well-substantiated data based on detailed studies concerning the energy potential of biomass derived from fruit tree plantations in the Republic of Moldova, as well as comparative analyses between different fruit species in terms of biomass productivity, calorific value, ash content, and estimation uncertainty.

In this context, the present study addresses an urgent need to substantiate, using experimental data and validated methodologies, the SEP of fruit-tree lignocellulosic biomass, differentiated by species and by regions. The results obtained can provide a scientific basis for the development of regional strategies for the collection, processing, and integration of orchard biomass into the national energy mix, thereby reducing dependence on fossil fuels and supporting decarbonization and circular economy objectives.

2. MATERIALS AND METHODS

2.1. Study area and sampling design

The research was conducted in the main fruit-growing regions of the Republic of Moldova: North, Center (including the municipality of Chișinău), and South (including the Autonomous Territorial Unit of Gagauzia). Orchards belonging to agricultural enterprises and family farms with areas larger than 10 ha were selected, as they are considered representative of the orchard structure in each region. The investigated species included fruit trees from the pome group (apple, pear, quince) and the stone fruit group (plum, cherry, sour cherry, apricot, peach), thus covering the typological diversity of orchards across the country.

The study focused on biomass generated from the annual maintenance and rejuvenation pruning of fruit trees. Samples were collected from representative plots, and the data were extrapolated to larger orchard areas. Tree sampling was carried out using the quarter method.

2.2. Biomass collection and measurement

Annual residues resulting from maintenance pruning were collected during the standard pruning period (February–March). For each orchard, tree density (number of trees/ha) and the average fresh biomass yield per tree were recorded. Moisture content at the time of collection was determined according to ISO 18134-2 by oven-drying the samples at 105 ± 2 °C until constant weight, with weighing differences ≤ 1 mg.

Based on these data, biomass yield per hectare and dry matter yield at the standard 10% moisture content were calculated.

2.3. Biomass characterization

Subsamples of each biomass type were analyzed to determine the net calorific value (NCV) at 10% moisture content, based on the gross calorific value (GCV) measured with an IKA C6000 isoperibolic bomb calorimeter, under constant volume conditions, according to ISO 18125:2017. The ash content (A, % dry basis) was determined according to ISO 18122:2015.

For comparative analysis among species, weighted averages were calculated according to the share of each species in the total orchard area.

2.4. Estimation of the sustainable energy potential

The SEP was calculated by correcting the theoretical energy potential (TEP) with factors reflecting technical losses, logistical constraints, and ecological limitations, according to the following equation:

$$SEP = TEP \cdot A_i \cdot (1-k_{il}) \quad (1)$$

where:

TEP represents the theoretical energy potential, calculated as the product between the biomass yield per hectare (dry basis at 10% moisture content) and the net calorific value of the biomass (determined at 10% moisture and constant pressure); A_i – is the availability coefficient of biomass for energy use; k_{il} - the implementation loss coefficient.

The total SEP values [TJ/yr] at regional and national levels were obtained by multiplying SEP values per hectare by the cultivated areas of each species, according to official data from the National Bureau of Statistics of the Republic of Moldova. Minimum and maximum SEP estimates were derived from the variability of field-measured biomass yields.

3. RESULTS

3.1. Assessment of the availability of orchard biomass for densified solid biofuel production

Table 1 presents the estimated amounts of biomass obtained from pome fruit plantations. The study included apple, pear, and quince varieties, which are widely cultivated in the Republic of Moldova. Samples were collected from traditional, semi-intensive, and intensive orchards, following the methodology described in Section 2.

The data show that the analyzed apple varieties vary considerably in terms of biomass generated per tree, with values ranging from 2.67 kg/tree (Fuji) to 6.23 kg/tree (Florina). A similar pattern was observed for pears, where values range from 1.21 kg/tree (Celina) to 5.27 kg/tree (Conference). These differences can be explained primarily by plantation density as well as orchard management and regeneration practices. Generally, trees from intensive orchards generate smaller amounts of biomass per tree, while more vigorous varieties grown at moderate densities (e.g., Florina, Golden, Reinette Simirenko) appear to be the most energy-efficient.

Table 1

Average biomass yield, calorific value, and ash content from pruning of pome fruit species

Species	Type	n_{th}*	m_t	M_h	m_h	$m_{M=10\%}$	$q_{Pnet\ M=10\%}$	A	$m_{sp\ M-10\%}$	$q_{sp\ Pnet\ M=10\%}$	A_{sp}
Apple	Idared	1250	2.84	43.17	3550.00	2241.63	15.58	3.93	2639 ± 456	15.61 ± 0.33	3.03±0.61
	Idared	833	5.48	42.15	4564.84	2934.18	15.63	3.82			
	Reinette Simirenko	1250	3.06	43.59	3825.00	2397.43	15.76	4.11			
	Reinette Simirenko	833	6.03	42.73	5022.99	3196.30	15.76	4.15			
	Florina	833	6.23	43.97	5189.59	3230.81	15.67	2.21			
	Golden Delicious	833	5.68	42.42	4731.44	3027.07	15.97	2.82			
	Gala	1250	3.12	43.21	3900.00	2460.90	14.93	2.96			
	Fuji	1250	2.67	43.11	3337.50	2109.67	15.58	1.96			
	Jonathan	570	5.97	43.11	3402.90	2151.01	15.63	3.16			
Pear	Conference	833	5.27	45.58	4389.91	2654.43	15.89	3.55	2620 ± 212	15.58 ± 0.41	3.35±0.31
	Noyabrskaya (Xenia)	1428	3.33	47.77	4755.24	2759.62	15.63	3.24			
	Celina	2800	1.24	42.24	3472.00	2228.25	15.57	3.27			
	Doyenné d'Hiver	833	5.21	47.28	4339.93	2542.23	16.00	3.35			
	Passe Crassane	1250	3.75	47.46	4687.50	2736.46	15.57	2.89			
	Clapp's Favourite	1428	3.10	43.12	4426.80	2797.74	14.82	3.81			
Quince	Auriu	800	3.21	43.21	2568.00	1620.41	15.39	3.49	1338±215	15.37±0.37	3.46±0.06
	Yantarnaya Moldavii	834	2.14	42.98	1784.76	1130.74	15.37	3.36			
	Zarea	800	3.04	44.21	2432.00	1507.57	15.74	3.47			
	Cometa	800	2.32	43.11	1856.00	1173.20	15.61	3.53			
	Olga	800	2.45	42.14	1960.00	1260.06	14.76	3.46			

**n_{th} – Number of trees per hectare* [trees/ha]*; m_t – Average biomass yield per tree* [kg/tree]*; M_h – Moisture content of the biomass at harvest, percent wet basis* [$\%_W$]*; m_h – Average biomass yield per hectare at harvest* [kg/ha]*; $m_{M=10\%}$ – Average biomass yield per hectare calculated to 10% moisture* [kg/ha]*; $q_{PnetM=10\%}$ - Net calorific value at constant pressure, calculated for 10% moisture content* [MJ/kg]*; A - Ash content on a dry basis* [%]*;$m_{spM=10\%}$ – Average biomass yield per species calculated to 10% moisture* [kg/ha]*; $q_{spPnetM=10\%}$ - Species average of the net calorific value at constant pressure, calculated for 10% moisture content* [MJ/kg]*;A_{sp} – Average ash content on a dry basis* [%]

At the area level, pear orchards produce on average similar amounts of biomass as apple orchards. Thus, the average usable biomass yield, adjusted to a 10% moisture content, is 2620 ± 212 kg/ha for pear and 2639 ± 456 kg/ha for apple. Quince, by contrast, generates a significantly smaller amount of biomass compared with the other two species. The mean quantity per tree is only 2.63 kg, while at the hectare level the average yield is 1339 ± 215 kg/ha, estimated at 10% moisture content. The moisture content of the biomass, determined immediately after collection, did not vary significantly among the analyzed species, averaging around 44%. This highlights the need for pre-conditioning of the biomass through drying before its energetic utilization.

Among the analyzed species, apple and pear provide the highest potential for the production of densified solid biomass (briquettes, pellets), with comparable average yields of around 2,600–2,700 kg/ha (at 10% moisture content). Therefore, it is recommended to correlate biomass productivity data with economic and ecological factors in order to enable an optimal selection of cultivars for energy purposes, also taking into account the specific calorific value of biomass from different fruit tree species.

It was found that the calorific value of biomass obtained from the 9 samples of different apple cultivars, 6 of pear, and 5 of quince did not differ significantly between the fruit tree species.

Based on the average values determined for each fruit tree cultivar, the mean value for the entire group of pome fruit trees was calculated. The analysis of the results indicates that biomass at 10% moisture content presents an average net calorific value of 15.61 ± 0.33 MJ/kg for apple, 15.58 ± 0.41 MJ/kg for pear, and 15.37 ± 0.37 MJ/kg for quince.

These values highlight only a minor variation between the analyzed species, the difference being about 0.24 MJ/kg, while the overall mean for the pome group is 15.52 MJ/kg.

With reference to the requirements specified in the SM EN ISO 17225 standards, it can be stated that the woody residues from fruit trees of the pome group are suitable for briquette production, fitting into

quality classes A1, A2, and B in terms of calorific value. However, the use of these residues is restricted by the relatively high ash content, which exceeds the 3% threshold. In this context, the analyzed biomass is more suitable for the production of B-class wood briquettes, meeting the criteria related to calorific value and ash content.

The physico-mechanical parameters of the final product are essentially influenced by the technology applied in the biofuel production process. In addition, this raw material has high potential for the manufacture of pellets and briquettes from non-woody biomass, including in mixtures (blends), thus expanding the possibilities of energy valorization.

Table 2 presents the characteristics of biomass from stone fruit trees, collected in March. Peach generated the highest amount of biomass ($m_{spM=10\%}$ = 2909 ± 564 kg/ha), followed by plum ($m_{spM=10\%}$ = 1980 ± 246 kg/ha) and sour cherry ($m_{spM=10\%}$ = 1854 ± 246 kg/ha), while apricot recorded the lowest value ($m_{spM=10\%}$ = 1504 ± 130 kg/ha).

Table 2

Average biomass yield, calorific value, and ash content from pruning of various stone fruit spe-cies

Species	Type	n_{th}*	m_t	M_h	m_h	$m_{M=10\%}$	$q_{Pnet\ M=10\%}$	A	$m_{sp\ M-10\%}$	$q_{sp\ Pnet\ M=10\%}$	A_{sp}
Plum	Stanley	444	7.81	47.01	3467.64	2041.67	16.21	1,7	1981 ± 246	16.21 ± 0.52	2,06 ± 0.20
	Valor	889	4.21	48.12	3742.69	2157.45	15.61	2,19			
	President	800	3.28	47.17	2624.00	1540.29	16.47	2,24			
	Ana Spath	1000	3.77	47.97	3770.00	2179.48	16.95	2,16			
	Piteştean	800	3.82	45.44	3056.00	1852.62	15.63	2,06			
	Renclod Althan	667	5.32	46.38	3548.44	2114.08	16.41	1,99			
Cherry	Kordia	333	5.91	45.58	1968.03	1190.00	15.75	2,64	1566 ± 798	15.78 ± 0.51	2.65 ± 0.31
	Regina	833	3.94	47.77	3282.02	1904.67	15.85	3,04			
	Grace Star	330	6.02	46.21	1986.60	1187.32	15.61	2,29			
	Ferrovia	330	4.02	44.79	1326.60	813.80	15.08	3,02			
	Sweet Heart	830	6.23	47.32	5170.90	3026.70	16.65	2,41			
	Bigarreau Burlat	330	6.23	44.16	2055.90	1275.57	15.77	2,52			
Sour Cherry	Oblačinska	404	7.03	48.01	2840.12	1640.64	15.56	2,61	1854 ± 289	15.58 ± 0.45	2.81 ± 0.20
	Morella	500	6.53	43.91	3265.00	2034.82	16.16	2,58			
	Crișana	833	4.23	46.18	3523.59	2107.11	15.74	2,87			
	Nordh Star	833	4.01	45.23	3340.33	2032.78	15.52	3,03			
	Mărioara	404	6.43	49.62	2597.72	1454.15	14.91	2,96			
Apricot	Kyoto	500	5.12	41.89	2560.00	1652.91	15.9	3,91	1504 ± 130	15.87 ± 0.40	2.70 ± 0.68
	Krasnoshchyokiy	280	7.98	47.77	2234.40	1296.70	15.57	2,45			
	Platimoon	500	5.37	48.28	2685.00	1542.98	16.53	2,28			
	Orange Rubis	330	7.21	42.24	2379.30	1526.98	15.58	2,38			
	Big Red	502	5.13	47.53	2575.26	1501.38	15.79	2,49			
Peach	Cardinal	500	7.74	44.55	3870.00	2384.35	15.97	2,44	2909 ± 564	16.00 ± 0.36	1.90 ± 0.47
	Maycrest	1250	4.94	47.21	6175.00	3621.98	16.6	1,34			
	Moldova	500	7.42	42.24	3710.00	2381.00	15.76	1,57			
	Redhaven	1200	4.04	47.98	4848.00	2802.14	15.97	1,85			
	Stark Sunglo	1250	4.62	47.74	5775.00	3353.35	15.69	2,32			

Moisture content at harvest varied insignificantly among species, while the net calorific values (at 10% moisture) were similar: highest for plum (16.21 ± 0.52 MJ/kg) and lowest for sour cherry (15.58 ± 0.39 MJ/kg), with a difference of 0.63 MJ/kg. Ash content ranged from 1.90 ± 0.41% (peach) to 2.81 ± 0.18% (sour cherry).

The results confirm the literature *(Burg et al., 2017; Matłok et al., 2024)*, according to which stone fruit biomass, although having lower density, exhibits a calorific value comparable to other species, a fact correlated with lignin content: 23.31 ± 2.21% for peach and 24.26 ± 1.25% for plum *(Burg et al., 2017; Matłok et al., 2024)*.

3.2. Energy potential of available orchard biomass for solid biofuel production in different regions of the Republic of Moldova

The Republic of Moldova has 85.6 thousand hectares of orchards (pome and stone fruits), including 38.4 thousand hectares of plantations larger than 10 ha *(NBSRM, 2025)* with specific concentrations across Economic Development Zones:

- Northern Zone – districts such as Edineț, Briceni, Dondușeni, Soroca, Florești (mainly apple, plum, and cherry);
- Central Zone – districts such as Orhei, Hâncești, Strășeni, Călărași, Ialoveni (apple, plum, apricot, cherry);
- Southern Zone – districts such as Cimișlia, Cahul, Taraclia, Ștefan Vodă (peach, apricot, sour cherry).

The species structure directly influences the quantity and quality of biomass obtained from orchard maintenance. Table 3 presents the results of estimating the energy potential of biomass generated from different fruit tree species, distributed by the Economic Development Zones of the Republic of Moldova. The calculations were based on the experimental data presented in subsection 3.1.

Table 3

Energy potential of fruit tree pruning residues

Parameters		Pome fruit			Stone fruit				
		Apple	Pear	Quince	Plum	Sweet cherry	Sour cherry	Apricot	Peach
$m_{b\ M=10\%}$* [kg/ha]	$\bar{m}$	2639	2620	1338	1981	1566	1854	1504	2909
	σ	456	212	215	246	798	289	130	564
$q_{Pnet\ M=10\%}$ [MJ/kg]	$\bar{m}$	15.615	15.579	15.372	16.211	15.784	15.578	15.873	15.995
	σ	0.329	0.414	0.374	0.519	0.506	0.449	0.396	0.360
A_i		0.8	0.8	0.8	0.8	0.8	0.8	0.8	0.8
k_{il}		0.1	0.1	0.1	0.1	0.1	0.1	0.1	0.1
TEP [GJ/ha]		41.21	40.91	20.90	30.93	24.46	28.95	23.49	46.53
Up [GJ/ha]		7.19	3.49	3.40	3.99	12.49	4.59	2.12	9.08
PED [GJ/ha]		32.97	32.73	16.72	24.75	19.57	23.16	18.79	37.22
Up [GJ/ha]		5.75	2.79	2.72	3.19	9.99	3.67	1.69	7.27
SEP [GJ/ha]		29.67	29.45	15.05	22.27	17.61	20.84	16.91	33.50
Up [GJ/ha]		5.17	2.51	2.45	2.87	8.99	3.30	1.52	6.54

**$m_{bM=10\%}$ - average biomass yield converted to a moisture content of 10%; $q_{Pnet\ M-10\%}$ - net calorific value of biomass at 10% moisture content, calculated at constant pressure; TEP - theoretical energy potential; PED - available energy potential; SEP - sustainable energy potential; A_i – availability coefficient, equal to 0.8; k_{il} - implementation loss coefficient, equal to 0.1; Up – predictive uncertainty; m – mean value, σ – standard deviation.*

It was found that residues from peach, apple, and pear pruning exhibit the highest exploitable energy potential and are the most suitable species for energy valorization among the analyzed orchard residues. The exploitable energy — considering the efficiency of technological processes and the sustainability of biomass harvesting — is estimated at 33.50 ± 6.54 GJ/ha for peach, 29.67 ± 5.17 GJ/ha for apple, and 29.45 ± 2.51 GJ/ha for pear.

It is noteworthy that although cherry residues show a lower SESP index, they exhibit the highest predictive uncertainty (Up = 8.99 GJ/ha), which indicates significant variability of the data, most likely due to differences between species, planting schemes, pruning methods, growth conditions, and sampling locations.

The lowest values were recorded for quince (15.05 ± 2.45 GJ/ha), apricot (16.91 ± 1.52 GJ/ha), and cherry (17.71 ± 8.99 GJ/ha), which also had lower uncertainties in estimation.

This suggests a higher probability of obtaining more constant quantities of biomass from these plantations. At the same time, these species show favorable calorific values, indicating that they should not be neglected as raw material for solid biofuel production. The correlation between uncertainty and energy potential shows that species with higher yields also exhibit greater variations in the estimates, which requires more precise assessments at the level of specific orchards and localities before initiating the production of densified solid biofuels from these pruning residues. The analysis of the SEP of biomass derived from fruit trees in the Republic of Moldova (Table 4) highlights significant differences in SEP between economic development zones (Northern Zone, Central Zone including Chișinău municipality, and Southern Zone including ATU Gagauzia), as well as among the fruit species.

Table 4

Sustainable energy potential of fruit tree biomass from orchards belonging to agricultural enterprises and household farms in the Republic of Moldova, by region

Fruit tree species	Northern Zone			Central Zone + Chișinău Municipality			Southern Zone + ATU Gagauzia			National total	
	St* [ha]	SEP [TJ/yr]		St [ha]	SEP [TJ/yr]		St [ha]	SEP [TJ/yr]		SEP [TJ/yr]	
		max	min		max	min		[ha]	max	min	[ha]
Apple	13787	480.34	337.78	3302	115.04	80.90	2002	69.75	49.05	665.13	467.73
Pear	64	2.05	1.72	269	8.60	7.25	35	1.12	0.94	11.76	9.91
Quince	7	0.12	0.09	21	0.37	0.26	28	0.49	0.35	0.98	0.71
Plum	2365	59.46	45.88	5311	133.52	103.03	2634	66.22	51.10	259.19	200.01
Chery	1370	36.44	11.81	1492	39.69	12.86	502	13.35	4.33	89.48	29.00
Sour Cherry	542	13.08	9.51	856	20.66	15.01	593	14.32	10.40	48.06	34.92
Apricot	459	8.46	7.06	966	17.80	14.87	502	9.25	7.73	35.51	29.66
Peach	70	2.80	1.89	352	14.09	9.49	860	34.43	23.19	51.33	34.56
National total										***1161.46***	***806.50***

** St - total orchard area at agricultural enterprises and household farms with agricultural land holdings of 10 hectares and above.*

The total cultivated area with apple orchards is dominant in the Northern Zone (13787 ha), generating an annual SEP estimated between 337.78 and 480.34 TJ, followed by the Central Zone (3302 ha; 80.90 – 115.04 TJ/yr) and the Southern Zone (2002 ha; 49.05 – 69.75 TJ/yr). In total, the SEP of apple orchards available at agricultural enterprises and household farms in the Republic of Moldova ranges between 467.73 and 665.13 TJ/yr at the national level. For other species, such as pear, plum, and cherry, the energy potential varies according to cultivated area and local conditions, but it is noteworthy that orchards in the Central Zone generally generate higher values compared to the other regions.

For example, in the case of plum, the SEP varies between 45.88 – 59.46 TJ/yr in the North, 103.03 – 133.52 TJ/yr in the Center, and 51.10–66.22 TJ/yr in the South, summing up to a national potential between 200.01 and 259.19 TJ/yr. Overall, the orchard biomass from all the studied species provides an energy potential estimated at approximately 806.50 to 1161.46 TJ/yr for the entire country. This renewable resource can substantially contribute to the diversification of the energy mix and to the reduction of dependency on fossil fuels. Harnessing this potential would result in significant savings of fossil resources such as coal, oil, and natural gas, currently used for thermal and electrical energy generation. In addition, the integration of orchard biomass into the national energy mix supports sustainable strategies, contributing to greenhouse gas emission reductions and environmental protection.

To maximize the positive impact, detailed regional planning is required, considering the specific features of each zone, in order to ensure sustainable harvesting and efficient utilization of orchard biomass for the production of densified solid biofuels.

CONCLUSIONS

The results obtained in this study indicate that pruning residues from peach, apple, and pear orchards exhibit the highest SEP among the analyzed species, with values of 33.50 ± 6.54 GJ/ha for peach, 29.67 ± 5.17 GJ/ha for apple, and 29.45 ± 2.51 GJ/ha for pear. These findings are consistent with research carried out in Central and Eastern Europe (*Burg et al., 2017; Dyjakon et al., 2016)*, where pome and stone fruit species have been identified as promising feedstocks for solid biofuel production.

The regional distribution of biomass potential highlights clear differences determined by orchard structure and agroclimatic conditions. The Northern Zone, dominated by apple orchards, accounts for the largest share of the national potential, while the Central Zone stands out with higher values for plum and pear, and the Southern Zone for peach and apricot.

These results emphasize the need for adopting region-specific strategies for biomass collection and utilization, in order to optimize logistics and processing capacities. Although cherry residues show a lower SEP (17.61 GJ/ha), they also recorded the highest predictive uncertainty (Up = 8.99 GJ/ha). This high

variability is influenced by the biological characteristics of the species, planting schemes, and pruning practices, which necessitate additional monitoring and standardization of maintenance operations. From a practical perspective, the sustainable use of this biomass could substitute significant amounts of fossil fuels—particularly coal, natural gas, and fuel oil—currently employed for heat generation.

Depending on calorific values and available quantities, replacing fossil fuels with orchard biomass would directly contribute to reducing national greenhouse gas emissions and to fulfilling the Republic of Moldova's commitments under the European Green Deal. However, certain constraints must be considered.

The relatively high ash content (> 3% for some species) may limit direct use for premium-quality briquette and pellet production, requiring either blending with low-ash feedstocks or adapting combustion systems. Furthermore, the moisture content of biomass at harvest (~44–48%) necessitates a drying stage, which increases processing costs and affects the overall energy efficiency.

Future research directions should include:

- the development of logistic models for biomass collection adapted to the regional distribution of orchards;
- techno-economic analyses of integrated pellet and briquette production chains;
- life cycle assessments to quantify the environmental benefits resulting from large-scale substitution of fossil fuels with pruning residues from fruit orchards.

ACKNOWLEDGEMENT

This research was funded by the Government of the Republic of Moldova through the National Agency for Research and Development, within the framework of the projects addressing issues of critical interest, under the theme "Resilience of the Republic of Moldova to Crisis Situations", project no. 23.70105.7007.08, contract no. 7/08R. Additional support was provided through project no. 20.80009.5107.15 "Development and implementation of good practices for sustainable agriculture and climate resilience / GREEN/020407", which offered technical and logistical assistance. The authors would like to thank the "Management of Scientific Research" Directorate of the Technical University of Moldova for providing logistical support in carrying out this study. Special thanks are extended to SC "BASADORO AGROTEH" SRL and "Agrisolution" SRL for their free assistance with the mechanized collection and transportation of vine residues to the analysis site, as well as to all the agricultural enterprises that permitted the collection of biomass samples used in this study.

REFERENCES

[1] Alakangas, E. (2016). Biomass and agricultural residues for energy generation. In *Fuel Flexible Energy Generation: Solid, Liquid and Gaseous Fuels* (pp. 59–96). 2016 (Woodhead Publishing). https://doi.org/10.1016/B978-1-78242-378-2.00003-1

[2] Aliaño, M., Gabaston, J., Ortiz, V., & Cantos, E. (2022). Wood Waste from Fruit Trees: Biomolecules and Their Applications in Agri-Food Industry. *Biomolecules*, *12*(2), 1–46. https://doi.org/https://doi.org/10.3390/biom12020238

[3] Burg, P., Mašán, V., Dušek, M., Zemánek, P., & Rutkowski, K. (2017). Review of energy potential of the wood biomass of orchards and vineyards in the Czech Republic. *Research in Agricultural Engineering*, *63*(December 2017), S1–S7. https://doi.org/10.17221/30/2017-RAE

[4] Cavalaglio, G., Fabbrizi, G., Cardelli, F., Lorenzi, L., Angrisano, M., & Nicolini, A. (2024). Lignocellulosic Residues from Fruit Trees: Availability, Characterization, and Energetic Potential Valorization. *Energies* , *17*(11), 1–14. https://doi.org/10.3390/en17112611

[5] Ciloci, R., & Țurcan, I. (2023). *The need for the Republic of Moldova to transition to a circular economy*. 78–83. https://doi.org/10.52326/csd2023.12

[6] Ciolacu, F., Ianuș, G., Marian, G., Munteanu, C., Paleu, V., Nazar, B., Istrate, B., Gudîma, A., & Daraduda, N. (2022). A Qualitative Assessment of the Specific Woody Biomass of Fruit Trees. *Forests*, *13*(3), 405. https://doi.org/10.3390/f13030405

[7] Dyjakon, A., Boer, J. Den, Bukowski, P., Adamczyk, F., & Frąckowiak, P. (2016). Wooden biomass potential from apple orchards in Poland. *Drewno*, *59*(198), 73–86. https://doi.org/10.12841/wood.1644-3985.162.09

[8] GRM. (2013). *Decision No. 102 on the Energy Strategy of the Republic of Moldova until 2030*. Official Gazette No. 27-30 Art. 146. https://www.legis.md/cautare/getResults?doc_id=68103&lang=ro

[9] GRM. (2024). Energy Strategy of the Republic of Moldova until 2050 (SEM 2050) - Concept. In *GRM*

(Vol. 20, Issue Sem 2050). https://energie.gov.md/sites/default/files/concept_strategia_enenergetica_act._-clean_1.pdf

[10] GRM. (2025). *The integrated national energy and climate plan for the period 2025-2030*. https://www.legis.md/cautare/getResults?doc_id=147685&lang=ro

[11] Gudîma, A. (2017). Evaluation of the use of agricultural residues for energy purposes. Case study for Soroca district, Republic of Moldova / Evaluarea utilizării reziduurilor agricole pentru scopuri energetice. Studiu de caz pentru raionul Soroca, Republica Moldova. *Meridian Ingineresc*, *1*, 26–29. https://doi.org/http://repository.utm.md/handle/5014/291

[12] Ibitoye, S. E., Mahamood, R. M., Jen, T. C., Loha, C., & Akinlabi, E. T. (2023). An overview of biomass solid fuels: Biomass sources, processing methods, and morphological and microstructural properties. *Journal of Bioresources and Bioproducts*, *8*(4), 333–360. https://doi.org/10.1016/j.jobab.2023.09.005

[13] Janiszewska, D., & Ossowska, L. (2024). The Potential Diversity of Agricultural Biomass in the Context of the Organization of Agricultural Production and Circular Agriculture in Poland. *Energies*, *17*(14). https://doi.org/10.3390/en17143368

[14] Marian, G., & Banari, A. (2025). Comparative evaluation of energy potential and composition of walnut, hazelnut, and almond residues for solid biofuel production. *Journal of Engineering Science*. https://doi.org/https://doi.org/10.52326/jes.utm.2025.32(1).09

[15] Marian, G., Gelu, I., Gudima, A., Nazar, B., Istrate, B., Banari, A., Pavlenco, A., & Daraduda, N. (2022). Calorific Value of Pellets Produced From Raw Material Collected From Both Sides of the River Prut. *Journal of Engineering Science*, *29*(4), 126–137. https://doi.org/10.52326/jes.utm.2022.29(4).10

[16] Marian, G., Ivanova, T. A., Gudîma, A., Nazar, B., Malai, L., Marian, T., & Pavlenco, A. (2024). Biomass Resources from Vineyard Residues for the Production of Densified Solid Biofuels in the Republic of Moldova. *Agronomy*, 1–13. https://doi.org/. https://doi.org/10.3390/agronomy14102183

[17] Matłok, N., Zaguła, G., & Gorzelany, J. (2024). *Analysis of the Energy Potential of Waste Biomass Generated from Fruit Tree Seedling Production*.

[18] NBSRM. (2024). *Statistical yearbook of the Republic of Moldova*. https://statistica.gov.md/files/files/publicatii_electronice/Anuar_Statistic/2024/15_AS.pdf

[19] NBSRM. (2025). *Economic statistics-Agriculture, Perennial plantations by Plants*. https://statbank.statistica.md/PxWeb/pxweb/en/40_Statistica_economica/40_Statistica_economica__16_AGR__AGR020/AGR020070.px/

[20] Pavlenco, A., Marian, G., & Gudîma, A. (2018). Energy potential of agricultural residues: Case study for the northern development region, Republic of Moldova / Potenţialul energetic al reziduurilor agricole: Studiu de caz pentru regiunea de dezvoltare nord, Republica Moldova. *Ştiinţa Agricolă*, *2*(2), 141-148 [in Romanian]. https://doi.org/http://repository.utm.md/handle/5014/23382

[21] Pence, I., Kumas, K., Siseci Cesmeli, M., & Akyüz, A. (2024). Detailed analysis of Türkiye's agricultural biomass-based energy potential with machine learning algorithms based on environmental and climatic conditions. *Clean Technologies and Environmental Policy*, *0123456789*. https://doi.org/10.1007/s10098-024-02822-1

[22] Silvestri, C., Silvestri, L., Piccarozzi, M., & Ruggieri, A. (2024). Toward a framework for selecting indicators of measuring sustainability and circular economy in the agri-food sector: a systematic literature review. In *International Journal of Life Cycle Assessment* (Vol. 29, Issue 8). Springer Berlin Heidelberg. https://doi.org/10.1007/s11367-022-02032-1

[23] Toscano, G., De Francesco, C., Gasperini, T., Fabrizi, S., Duca, D., & Ilari, A. (2023). Quality Assessment and Classification of Feedstock for Bioenergy Applications Considering ISO 17225 Standard on Solid Biofuels. *Resources 2023, 12*. https://doi.org/https://doi.org/10.3390/resources12060069

[24] Winzer, F., Kraska, T., Elsenberger, C., Kötter, T., & Pude, R. (2017). Biomass from fruit trees for combined energy and food production. *Biomass and Bioenergy*, *107*(September), 279–286. https://doi.org/10.1016/j.biombioe.2017.10.027

Živković, M., Urošević, M., Oljača, S., Oljača, M., Gligorević, K., Zlatanović, I., & Koprivica, R. (2013). *Aspects of Using Potential Energy Products of Biomass After Pruning Fruit and Grape Plantations in the Republic of Serbia.* Agriculture & Forestry. https://www.agricultforest.ac.me/paper.php?journal_id=173&id=2160.

METHODS OF OBTAINING BIOCHAR
/
METODE DE OBȚINERE A BIOCHARULUI

Nicoleta-Alexandra VANGHELE*[1, 2)], Nicolae - Valentin VLĂDUȚ[1)], Andreea MATACHE[1)], Augustina PRUTEANU[1)], Florin NENCIU[1)], Laurențiu VLĂDUȚOIU[1)], Ana-Maria TĂBĂRAȘU[1, 2)], Dragoș ANGHELACHE[1, 2)], Alexandru IONESCU[1, 2)], Elena-Melania CISMARU[2)], Cristian RADU[2, 3)]

[1)] National Institute of Research - Development for Machines and Installations Designed for Agriculture and Food Industry - INMA Bucharest, Romania;

[2)] National University of Science and Technology Polytechnic Bucharest Biotechnical Systems Engineering / Romania;

[3)] University of Craiova, Craiova, Dolj County / Romania.

**Tel: (+40) 212 693 457; *E-mail: vanghelelrc@gmail.com*

Keywords: *biomass, transformation, strategy, production processes*

ABSTRACT

In recent decades, biochar has attracted attention in both the political and academic spheres because it is easy to obtain and is beneficial for the environment. It can be used for soil stabilization, wastewater treatment, greenhouse gas management, in climate change mitigation strategies, and power generation. Biochar is the result of the thermochemical transformation of biomass. Its yield and quality are very different depending on the production technology and process parameters. They also have an impact on its performance in agricultural and forestry systems but also in other areas where it is used. This review compared different technologies for biochar production, such as slow pyrolysis, rapid pyrolysis, gasification, and roasting.

REZUMAT

În ultimele decenii biocharul a atras atenția atât în sfera politică, cât și în cea academică pentru că este ușor de obținut și este benefic pentru mediu. Poate fi folosit pentru stabilizarea solului, tratarea apelor uzate, gestionarea gazelor cu efect de seră, în strategiile de atenuare a schimbărilor climatice, și generarea de energie. Biocharul este rezultatul transformării termochimice a biomasei. Randamentul și calitatea sa sunt foarte diferite în funcție de tehnologia de producție și de parametrii de proces; acestea au, de asemenea, un impact asupra performanței sale în sistemele agricole și forestiere dar și în alte domenii în care este utilizat. Această revizuire a comparat diferite tehnologii pentru producția de biochar, cum ar fi piroliza lentă, piroliza rapidă, gazeificarea și torrefacția.

INTRODUCTION

Biochar is produced by the thermal breakdown of plant or animal biomass that is thermally decomposed in the absence of oxygen. It is a porous, aromatic and decay-resistant carbonic solid material. It has gained significant interest in recent years as it is used in a wide range of agricultural and industrial operations *(Rangabhashiyam and Balasubramanian 2019).*

Plant waste, manure, agricultural and forestry by-products, sludge, waste from paper mills, etc., can be used in the production of biochar *(Saletnik et al, 2019; Cobos-Torres et al, 2025; Su et al, 2025*). Biochar, or charcoal, is a sustainable solution for agriculture and the environment, which saw a surge in research in the 1990s.

Researchers investigated how biochar can improve soil quality while reducing greenhouse gas emissions. Since then, interest in biochar has grown, and research into its manufacture is constantly expanding.

Biochar is currently used to improve soil, produce energy, and capture carbon from the atmosphere. It is also a viable alternative to chemical fertilizers. *(Shyam et al, 2025; Kabir et al, 2023; Luo et al, 2023; Amalina et al, 2022; Allohverdi et al, 2021; Weber and Quicker 2018)*.

Biochar is mainly used to improve agricultural soil, improve the environment, and as part of several industrial applications. It improves soil fertility, improves water retention, and may help sequester carbon, which contributes to climate change mitigation *(Ayaz et al, 2025; Xiong et al, 2025).*

Biochar also has the ability to filter liquids and gases, remove pollutants, and be incorporated into textiles and other products *(Yaashikaa et al, 2020; Montanarella et al, 2013; Dong et al, 2025).*

The main areas in which biochar is used are:

1. **Improvement of agricultural soil** by:
   - ***Higher yields***. Biochar increases crop yields by improving soil structure, water-holding capacity, and nutrient availability *(Mak-Mensah, et al, 2021; Feng, et al, 2023; Hussain. et al, 2020)*
   - ***Soil health***. It can improve overall soil health by increasing soil aeration, reducing nutrient leaching, reducing soil acidity, soil decontamination *(Luo et al, 2021; Wei et al, 2019).*
   - ***Carbon sequestration***. The stable carbon content of biochar can remain in the soil for a long time. This makes it a carbon sink and helps reduce the effects of climate change *(Osman et al, 2024; Jafri et al, 2018)*.

2. **Remediating the environment means eliminating pollutants:**
   - ***Removal of pollutants***. Biochar has the ability to extract heavy metals, pesticides, organic and inorganic contaminants from soil and water.
   - ***Wastewater and water management***. It can be used as a filter to remove impurities and pollutants from water sources.
   - ***Odor management***. Biochar is useful in wastewater treatment and waste management because it can absorb odor-causing substances *(Murray 2021; Farah et al, 2022; Amalina et al, 2022)*.

3. **Industrial Applications**:
   - ***Textile:*** Biochar can be used in underwear fabrics that provide thermal insulation and reduce odors *(Schmidt 2012).*
   - ***Materials used in construction***: Potentially, biochar can be added to building materials to improve insulation and reduce the carbon footprint.
   - ***Energy production***: Biochar can be used as a fuel or as a catalyst in a variety of industrial processes *(Yaashikaa et al, 2020; Curcio et al, 2025).*
   - ***Materials required for electrodes***: Biocarbon can be used in supercapacitors and batteries *(Novak 2019).*
   - ***Adsorbent***: Biochar is good for adsorption of pollutants, gases, and other substances due to its large surface area and porosity *(Yaashikaa et al, 2020).*

4. ***In animal management***,
   - ***Animal health.*** Biochar is added to feed to improve animal health and reduce the amount of methane in manure *(Schmidt et al, 2019; O'Toole et al, 2016).*
   - ***Livestock***. Animals are healthier and agriculture more sustainable thanks to the detoxification of the digestive system *(www.causeartist.com)*

Although initially biochar was mainly used in agriculture, currently its use has expanded to a wide range of fields due to its properties, apart from those listed above, biochar is also used in the food industry, as a dye or in the manufacture of packaging, in the pharmaceutical and cosmetic industries in the manufacture of creams, soaps and deodorants *(Lin and Chang 2008).* Figure 1 shows a picture of the main uses of biochar.

Fig. 1 - Main uses of biochar
(www.biochar-industry.com)

The production of biochar is usually achieved through a series of thermochemical conversion processes, which are carried out under different process conditions. The four main processes of obtaining biochar are torification, gasification, slow pyrolysis, and rapid pyrolysis *(Leng et al, 2019; Adeniyi et al, 2024)*.

In addition to slow and fast pyrolysis that are most used, there are several types of pyrolysis, namely: microwave pyrolysis, hydropyrolysis, vacuum pyrolysis, flesh pyrolysis, copirolyrolysis, and intermediate pyrolysis *(Dilipkumar et al, 2021; Kwaku et al, 2023; Ahmed et al, 2025)*.

METHODS OF OBTAINING BIOCHAR

1. Pyrolysis

Pyrolysis is a thermochemical method that creates biochar, biooil, and syngas from biomass *(Bridgwater et al, 2000).* The process involves heating and thermally decomposing biomass under anaerobic conditions or with a limited oxygen supply, known as a low-oxygen stoichiometric atmosphere. Process temperatures range from 400°C to 1200°C (*Amin et al, 2016).*

1.1 Slow pyrolysis: As the name suggests, the slow pyrolysis process requires a long residence time (more than 1 hour), and the end result is biochar (*Liu et al, 2015).* Slow pyrolysis, also known as conventional pyrolysis, involves heating the biomass to 300–600°C and a heating rate of 5–7°C/min *(Li et al, 2020).*

1.2. Rapid pyrolysis: It is a direct thermochemical process that produces high-energy liquid bio-oil from solid biomass. a highly efficient thermochemical method that uses biomass to produce biofuels with reduced amounts of gases and solids produced *(Dai et al, 2017; Chang et al, 2021).* Without oxygen, rapid pyrolysis is carried out at temperatures above 500°C and heating rates of over 300°C/min. A rapid method of obtaining biochar is rapid pyrolysis, which takes only a few seconds. According to other studies, rapid pyrolysis creates 20% biochar, 60% biooil, and 20% syngas *(Dai et al, 2017; Huang et al, 2016).*

1.3 Microwave Pyrolysis: Microwave pyrolysis uses microwave radiation to heat materials, converting electromagnetic energy into heat during this process. The constant heating speed, along with cost efficiency, easy control, and safety features, have made microwave pyrolysis a viable option compared to traditional pyrolysis. A microwave oven is used to carry out this process. Two key factors for this method are power output and frequency. The standard frequency used in this process is 2.45 GHz. The temperature at which the process takes place varies between 400 and 600 °C *(Omoriyekomwan et al, 2017).*

Following the use of microwave pyrolysis to obtain biochar, the carbon content was 77.8% *(Kostas et al, 2020)*. Although the yield increases with temperature, the yield obtained from the use of microwave pyrolysis has been found to be lower than with the use of conventional pyrolysis *(Omoriyekomwan et al, 2017).*

1.4 Vacuum Pyrolysis: This method involves the decomposition of biomass by a thermal process in an oxygen-free environment, either under vacuum or under a fairly low pressure *(Lam.et al.2019).* Usually, the pressure is set between 0.5 and 2 bar, and the temperature is kept between 450 and 600 °C *(Carrier et al, 2011)*. Just like in slow pyrolysis, vacuum pyrolysis has lower heating speeds. However, these two methods generate very different products.

The reason is that the vapors created during vacuum pyrolysis are constantly and efficiently removed through a condensing system. The rapid removal of organic vapors produced in the main pyrolysis phase significantly reduces the time they remain, which helps to decrease side reactions and ensures a good percentage of liquid product during the pyrolysis secondary phase. For this reason, the vacuum or low-pressure extraction technique is exclusively used to remove the vapors released during pyrolysis, which greatly influences the quality and quantity of the product by preventing the release of inorganic substances *(Chen et al, 2017)*.

The carbon content remains low throughout this process, compared to standard pyrolysis, due to the intense reactions that take place in a vacuum. Increasing the temperature reduces the amount obtained, while increasing the size of the biochar with a longer residence time. Due to the presence of vacuum, more volatilization occurs. An extension of the residence time causes further volatilization, but reduces the amount of biochar. A pyrolysis time of 30 minutes generated 67.6% magnetic biochar, which was significantly less compared to 85.9% at 10 minutes *(Thines et al. 2017).*

1.5 Hydropyrolysis: This is a fairly recent method, used to transform biomass into high-quality products by introducing hydrogen or hydrogen-derived substances into the reactor at a high pressure, usually higher than that of the atmosphere, between 50 bar and 200 bar *(Stummann et al, 2021).* The presence of hydrogen allows hydrogenation and polycondensation reactions. This processing is carried out

faster at high temperatures. Pyrolysis takes place at temperatures between 250 and 550 °C. It is essential to maintain a controlled flow of hydrogen gas *(Zheng et al, 2017; Stummann et al, 2020)*. High temperatures reduce both the concentration and volume of biochar obtained. The total amount of ash does not vary according to temperature, but is based on the base materials used *(Rombolà et al, 2016)*. The oxygen content of biochar can be decreased by using a catalyst during hydropyrolysis, which facilitates hydrocracking and thus improves the volume of biochar. A shorter residence time and high hydrogen pressure are recommended to enhance the amount of biochar. A hydrogen pressure of 1 MPa resulted in 26.1% of biochar, compared to higher hydrogen pressures *(Zheng et al, 2017; Chen et al, 2020)*.

1.6 Flash Pyrolysis: Flash pyrolysis is a thermochemical process that converts low-quality materials into high-quality biochar. This method is carried out with very fast heating speeds, thousands of degrees per second. Only certain types of reactors can withstand such high heating speeds, the most used being a special reactor. When raw materials are exposed to these high heating rates and an intense heat source, they move quickly and hit the inner walls of the reactor.

This leads to pyrolysis, a process by which materials are transformed into high-quality biochar. Rapid pyrolysis occurs at temperatures exceeding 400 °C. An increase in temperature can reduce the amount of biochar obtained, but it increases the amount of volatile substances. At 900 °C, biochar production was found to be 14,89 % by weight for palm kernel shell and 18,31 % for chlorella vulgaris microalgae, both of which were less than those obtained at 600 °C.

Since rapid pyrolysis takes place at high temperatures and with high heating rates, the surface of the carbon becomes smoother and the biochar particles become rounder. This process also leads to the formation of large aromatic structures in the resulting biochar *(Eibner et al, 2017; Maliutina et al, 2017)*.

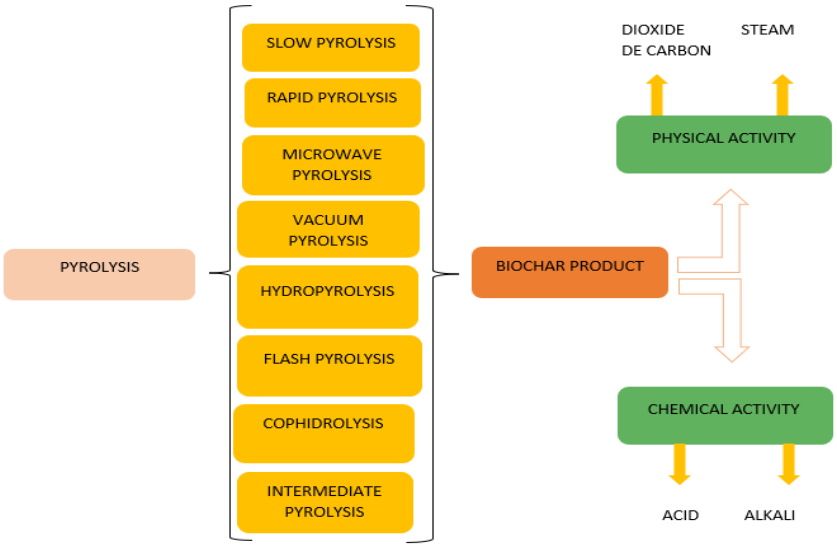

Fig. 2 - Types of pyrolysis to obtain biochar
(adapted from Dilipkumar 2021)

1.7 Co-pyrolysis: Co-pyrolysis is an efficient technique that combines two types of raw materials. This technique helps reduce heavy metal pollution by decreasing the amount of heavy metals in the material used. As a result, biochar obtains a hierarchical porous structure thanks to an environmentally friendly carbon additive. This helps to improve the physical and chemical characteristics of the biochar created. One of the main reasons for this is the efficient balancing of the elements in the raw material used by this method *(Zhao et al, 2017, 2018)*.

To achieve co-pyrolysis, a plug furnace is used. The two raw materials are mixed in appropriate proportions, depending on the type of materials used. During the process, the temperature is increased to a higher level, between 300-700 °C. It has been observed that the maximum yield for biochar from manure is 61%.

High temperatures help increase the strength of biochar *(Meng et al, 2018a)*. It is important that there are limited oxygen conditions during the process. After the material has been heated for a certain time, it cools rapidly to maintain the purity of the biochar. The 0:1 ratio had a yield of 54.87% for biochar, which was found to be maximum compared to other proportions of biomass feedstocks *(Huang et al, 2017; Meng et al, 2018b)*.

The amount of biochar produced depends on three aspects: temperature, ash content and the proportion of raw materials. The temperature and amount of ash are directly related to the yield of biochar. Co-pyrolysis positively influences pH, with biochar having higher pH values than the feedstock *(Meng et al, 2018a).* At high temperatures, the decomposition of raw materials is significant, and the aromatic degree of biochar improves *(Wang et al, 2018; Zhao et al, 2018).*

1.8. Intermediate pyrolysis: Intermediate pyrolysis depends on three process conditions, namely pyrolysis temperature, vapor residence time, and raw material residence time. Generally, intermediate pyrolysis is carried out under moderate temperature conditions, and the temperature between 450 and 550 °C is suitable for the complete conversion of raw materials into biochar. The overall performance for intermediate pyrolysis is higher than other conventional pyrolysis methods. A pyrolysis reactor is used to perform intermediate pyrolysis *(Ahmed et al, 2018; Luz et al, 2018).*

The pore size of the produced biochar is affected by the cell structure of the biomass, the maximum pyrolysis temperature, and the residence time. The BET surface area of biochar has been found to increase with increasing pyrolysis temperatures. The BET surface area (determined using the Brunauer-Emmett-Teller (BET) method indicating its porosity and adsorption capacity) of 128.706 was observed at 550 °C, which was greater than 121.377 at 450 °C *(Luz et al, 2018).* An increase in temperature increases the aromaticity of the biochar produced and the productivity rate of the biochar. Energy efficiency is inversely proportional to temperature *(Ahmed et al, 2018; Luz et al, 2018).*

2. Gasification

It is a chemical thermal process by which carbon-rich materials are broken down into gaseous products, including CO, CO2, CH4, H2 and trace amounts of hydrocarbons; these gases are known as syngas *(Dasappa et al, 2022).*

Gasification takes place at high temperatures, in the range of 700 to 900°C, in an environment with restricted oxidizing agents, such as oxygen, air, nitrogen, steam, carbon dioxide or a combination of these gases. It has been observed that as the temperature rises, the production of carbon monoxide and hydrogen increases, while other substances, such as methane, carbon dioxide and hydrocarbons, decrease. The main result of this process is syngas (mostly hydrogen), while coal is considered a by-product (or waste) with a lower efficiency, along with ash, tar and part of the oil. The partial oxidation of biomass, contrary to the combustion process, captures the energy available in biomass and brings it together in chemical bonds in the form of gaseous products. The inherent chemical energy of carbon in biomass is converted into combustible gases, which are more efficient and easier to use than raw biomass *(Matilo et al, 2022).*

Also, the commercial use of the gasification technique has been recorded. Due to its low emissions and higher volume of syngas, gasification outperforms traditional methods, including pyrolysis, combustion, and fermentation. The O/C ratio is crucial to achieve increased efficiency in gasification. High efficiency is achieved by using biomass with a low O/C ratio in the gasification process. The O/C ratio of biomass can be lowered by the roasting method. Before standard gasification, roasting can be seen as a preparatory step for achieving a higher quality of the product. It is a process carried out at low temperatures, between 200 and 300°C, with a heating rate of about 50°C/min, varying depending on the composition and type of biomass *(Sarker et al, 2021).*

Pyrolysis and gasification are interconnected processes. When these two methods are combined, there is no clear delineation between them.

The low proportion of oxygen used in the gasification process causes a partial oxidation of the biomass, affecting the characteristics of the final product. The type of product is among the most significant differences between pyrolysis and gasification. Gasification generates about 85% gaseous products, 10% solid coal and 5% liquid products. The diagram of the gasification process is illustrated in Figure (*Tripathi et al, 2016; Bisht et al, 2020*).

3. Torrefaction

It is a thermal processing process that improves the characteristics of biomass. The main process of torification from a chemical perspective consists of removing oxygen to create a solid product used as a combustible material or as a soil amendment. Torified biomass exhibits a lower O/C ratio compared to the original biomass *(Barskov et al, 2019).*

As a rule, torification is carried out by directly or indirectly heating the biomass to a temperature between 200 and 300 °C, applying a slow heating rate, up to 50 °C/min, for a duration of 20–120 minutes *(Wang et al, 2017).*

There are several types of torification, depending on the environment, which can be wet or dry, and depending on the method of production, which can be classified into four distinct techniques: oxidative, non-oxidative, acid tartar or steam explosion (fig.3) *(Chen, 2015).*

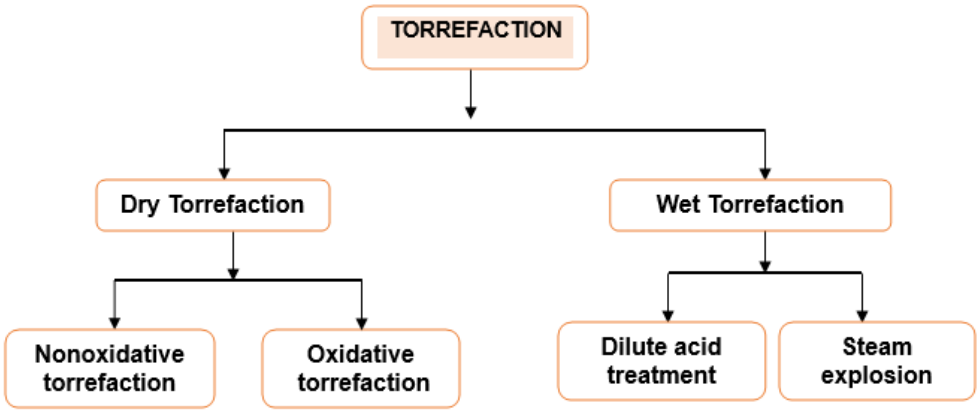

Fig. 3 - Types of torrefaction

The most common methods used for processing solid biomass are non-oxidative or conventional spinning. Realizing that non-oxidative torification is carried out under conditions similar to pyrolysis, except for lower temperatures, thermal processing is often referred to as light pyrolysis as well.

Regardless of the method or raw material used to obtain biochar, the moisture requirements and size are different for each method, but the process of obtaining biochar includes the following steps: First, the biomass raw material must be dried (the humidity should not exceed 15%).

Then, depending on the field of application, the material is shredded to the desired dimensions (the optimum is 8–12 mm). A belt conveyor is used to introduce the resulting biomass into a reactor, where it undergoes the heat treatment process.

This process removes moisture and volatile substances from biomass and produces biochar and other by-products such as syngas, tar, wood vinegar, and biogas. The usual process of obtaining biochar is illustrated in Figure 4.

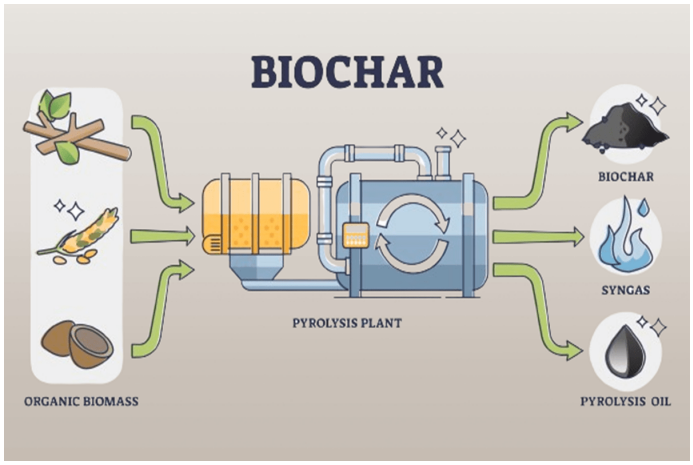

Fig. 4 - The standard process of obtaining biochar
(https://energytheory.com/wp-content/uploads/2023/12/biochar.png)

CONCLUSIONS

Biochar is a crucial component of the coming industrial revolution, helping to create a sustainable future and generating greater economic prosperity, increasing employment opportunities and improving the quality of life for people.

Due to its characteristics, biochar can be applied in multiple sectors, including agriculture, the food industry, construction, as well as in the pharmaceutical and cosmetic fields.

Depending on the type of raw material used for its production and the sector of application, it is necessary to carry out studies to determine the manufacturing method and the selection of the appropriate equipment.

Since the applications of biochar are closely related to its characteristics, future research needs to clarify the impact of the manufacturing process on biochar attributes. Biochar used for water purification will have distinctions from that intended for the energy sector or agriculture. In addition, there are numerous studies in the literature that analyze the influences of biochar on agriculture, especially in terms of agricultural production, influenced by different types of soil. For example, adding biochar can lead to an increase or decrease in crop yields, depending on soil types and fertilization management.

ACKNOWLEDGEMENT

This paper was supported: by one funding source the NUCLEU Programme, carried out with the support of ANCSI, Project 9N/ 01.01.2023 "Technology for the valuation of vegetable residues in the form of biochar for the improvement of soil quality" and NUCLEU Program, through Project 9N/ 23 04 02 01, "Innovative technology for the production of biofertilizers to restore soil biodiversity and reduce the effects of drought on agricultural land".

REFERENCES

[1] Adeniyi, A.G., Iwuozor, K.O., Emenike. E.C., Amoloye M. A., Adeleke J. A., Omonayin, E. O., Bamigbola J. O., Ojo H. T., Ezzat, A. O. (2024). Leaf-based biochar: A review of thermochemical conversion techniques and properties. *Journal of Analytical and Applied Pyrolysis, Volume 177*, 106352, https://doi.org/10.1016/j.jaap.2024.106352;

[2] Ahmed, A., Abu Bakar, M.S., Azad, A.K., et al., (2018). Intermediate pyrol- ysis of Acacia cincinnata and Acacia holosericea species for bio-oil and biochar production. *Energy Convers Manag* 176:393–408. https://doi.org/10.1016/j.enconman.2018.09.041;

[3] Ahmed, S.S., Joshi, S.J. et al. (2025). Biochar as a Soil amendment: implications for soil health, carbon sequestration, and climate resilience. *Discov. Soil 2*, 18. https://doi.org/10.1007/s44378-025-00041-8;

[4] Allohverdi, T., Mohanty, A.K., Roy, P., Misra, M. (2021). A Review on Current Status of Biochar Uses in Agriculture. *Molecules*, *26*, 5584. https://doi.org/10.3390/molecules26185584;

[5] Amalina, F., et al. (2022). A comprehensive assessment of the method for producing biochar, its characterization, stability, and potential applications in regenerative economic sustainability – A review. *Cleaner Materials, Volume 3*, https://doi.org/10.1016/j.clema.2022.100045;

[6] Amin, F.R., Huang, Y., He, Y., Zhang, R., Liu, G., Chen C. (2016). Biochar applications and modern techniques for characterization. *Clean Technologies and Environmental Policy* ;*18(5)* pp.1457-1473;

[7] Ayaz, M., Muntaha, S.T., Baltrėnaitė-Gedienė, E. et al, (2025). Biochar and carbon-negative technologies: exploring opportunities for climate change mitigation. *Biochar* 7, 17. https://doi.org/10.1007/s42773-024-00421-3;

[8] Barskov, S., Zappi, M., Buchireddy, P., Dufreche, S., Guillory, J., Gang, D., Hernandez, R., Bajpai, R. Baudier, J., Cooper, R., Sharp, R.(2019). Torrefaction of biomass: a review of production methods for biocoal from cultured and waste linocellulosic feedstocks. *Renewable Energy*, (), S096014811930552X–. doi:10.1016/j.renene.2019.04.068;

[9] Bisht, A.S., Thakur, N. (2020). Pine needles biomass gasification based electricity generation for Indian Himalayan region: Drivers and barriers. In: *Green Buildings and Sustainable Engineering*. New York, United States of America: Springer, pp. 47-59;

[10] Bridgwater, A., Peacocke, G. (2000). Fast pyrolysis processes for biomass. *Renewable and Sustainable Energy Reviews; 4*(1) pp. 1-73;

[11] Carrier, M, Hugo, T, Gorgens, J, Knoetze, H. (2011). Comparison of slow and vacuum pyrolysis of sugar cane bagasse. *Journal of Analytical and Applied Pyrolysis.; 90*(1) pp. 18-26

[12] Chang, C. et al. (2021). Study on products characteristics from catalytic fast pyrolysis of biomass based on the effects of modified biochars. *Energy. 229*:120818;

[13] Chen, N., Ren, J., Ye, Z., Xu, Q., Liu, J., Sun. S., (2017). Study on vacuum pyrolysis of coffee industrial residue for bio-oil production. In: IOP *Conference Series: Earth and Environmental Science. Vol. 59*, no. 1. United Kingdom: IOP Publishing; p. 012065;

[14] Chen, W., Lu, J., Zhang, C., et al. (2020). Aromatic hydrocarbons produc- tion and synergistic effect of plastics and biomass via one-pot catalytic co-hydropyrolysis on *HZSM-5. J Anal Appl Pyrolysis* 147:104800. https://doi.org/10.1016/j.jaap.2020.104800;

[15] Chen, Wei-Hsin (2015). Pretreatment of Biomass || *Roasting*. , (), 173–192. doi:10.1016/B978-0-12-800080-9.00010-4;

[16] Cobos-Torres, J.-C., Idrovo-Ortiz, L.-H., Cobos-Mora, S. L., & Santillan, V. (2025). Renewable Energies and Biochar: A Green Alternative for Reducing Carbon Footprints Using Tree Species from the Southern Andean Region of Ecuador. *Energies, 18(5*), 1027. https://doi.org/10.3390/en18051027;

[17] Curcio, I., Gigli, R., Mormile, F., Mormile, C. (2025). A comprehensive review on biochar, with a particular focus on nano properties and applications, *Nano Trends, Volume 10*, 100117, ISSN 2666-9781, https://doi.org/10.1016/j.nwnano.2025.100117;

[18] Dai, L. et al. (2017). Production of bio-oil and biochar from soapstock via microwave-assisted co-catalytic fast pyrolysis. *Bioresource Technology*. 225:1-8;

[19] Dasappa, S., Shivapuji, A.M. (2022). Biomass gasification: Thermochemical route to energetic bio-chemicals. *Advanced Biofuel Technologies: Elsevier*. 12; pp. 305-332;

[20] Dilipkumar, A., Divya L., Ashokkumar, K., et al. (2021). Production, characterization, activation and environmental applications of engineered biochar: a review . *Environmental Chemistry Letters*, (), –. doi:10.1007/s10311-020-01167-7;

[21] Dong, M., Jiang, M., He, L., et al. (2025). Challenges in safe environmental applications of biochar: identifying risks and unintended consequence. *Biochar* **7**, 12 . https://doi.org/10.1007/s42773-024-00412-4;

[22] Eibner, S., Margeriat, A., Broust, F. et al. (2017). Catalytic deoxygena- tion of model compounds from flash pyrolysis of lignocellu- losic biomass over activated charcoal-based catalysts. *Appl Catal B about* 219:517–525. https://doi.org/10.1016/j.apcat b.2017.07.071;

[23] Farah, A., Santhana, K., A.W. Zularisam, Mohd, N. (2022). Recent advancement and applications of biochar technology as a multifunctional component towards sustainable environment. *Environmental Development, Volume 46*, 100819, ISSN 2211-4645;

[24] Feng, W., Wang, T., Yang, F., et al. (2023). Effects of biochar on soil evaporation and moisture content and the associated mechanisms. *About Sci eur* 35, 66;

[25] Huang, H., Yang, T., Lai, F., Wu G., (2017). Co-pyrolysis of sewage sludge and sawdust/rice straw for the production of biochar. *J Anal Appl Pyrolysis* 125:61–68. https://doi.org/10.1016/j.jaap.2017.04.018;

[26] Huang, Y.F., Chiueh P.T., Kuan W.H., Lo S.L. (2016). Microwave pyrolysis of lignocellulosic biomass: Heating performance and reaction kinetics. *Energy*. 100:137-144;

[27] Hussain, R.; Ravi, K.; Garg, A. (2020). Influence of biochar on the soil water retention characteristics (SWRC): Potential application in geotechnical engineering structures. *Soil Till. Res., 204*, 104713;

[28] Jafri N., Wong W.Y., Doshi V., Yoon L.W., Cheah K.H. (2018). A Review of Biochar Production and Characterization for Application in Direct Carbon Fuel Cells. *Process Saf Medium Prot* 118:152–166;

[29] Kabir, E., Kim, K.H., Kwon, E.E. (2023). Biochar as a tool for the improvement of soil and environment. *Front about Sci*. https://doi.org/10.3389/fenvs.2023.1324533;

[30] Kostas, E.T., Durán-Jiménez, G., Shepherd, B.J., et al (2020). Micro- wave pyrolysis of olive pomace for bio-oil and bio-char pro- duction. *Chem Eng J 387*:123404. https://doi.org/10.1016/j.CEJ.2019.123404;

[31] Kwaku Armah, E., Chetty, M., Adebisi Adedeji, J., Erwin Estrice, D., Mutsvene, B., Singh, N., & Tshemese, Z. (2023). Biochar: Production, Application and the Future. *IntechOpen.* doi:10.5772/intechopen.105070;

[32] Lam S.S. et al. (2019). Microwave vacuum pyrolysis conversion of waste mushroom substrate into biochar for use as growth medium in mushroom cultivation. *Journal of Chemical Technology & Biotechnology.; 94*(5) pp.1406-1415;

[33] Leng, L., Huang, H. Li, H. Li, J. Zhou, W. (2019). Biochar stability assessment methods: A review, *Science of The Total Environment*, ISSN: 0048-9697, Vol: 647, pp. 210-222;

[34] Li, W. et al. (2020). Mechanistic insight into lignin slow pyrolysis by linking pyrolysis chemistry and carbon material properties. *ACS Sustainable Chemistry & Engineering. 8*(42) pp. 15843-15854;

[35] Lin, C.M., Chang, C.W. (2008). Production of Thermal Insulation Composites Containing Bamboo Charcoal. *Textile Research Journal. 78*(7):555-560. doi:10.1177/0040517507085397;

[36] Liu, W.J., Jiang, H., Yu, H.Q. (2015). Development of biochar-based functional materials: Toward a sustainable platform carbon material. *Chemical Reviews. 115*(22) pp. 12251-12285;

[37] Luo, L., Wang, J., Lv, J., Liu, Z., Sun, T., Yang, Y, et al. (2023). Carbon sequestration strategies in soil using biochar: advances, challenges, and opportunities. *Environ Sci Technol.57*:11357–72. https://doi.org/10.1021/acs.est.3c02620.;

[38] Luo, W., e.al. (2021). A potential Mg-enriched biochar fertilizer: Excellent slow-release performance and release mechanism of nutrients. *Science of The Total Environment*, 768, 144454;

[39] Luz, F.C., Cordiner, S., Manni, A., et al. (2018). Ampelodesmos mauritanicus pyrolysis biochar in anaerobic digestion process: evaluation of the biogas yield. *Energy, 161*, pp. 663–669. https://doi.org/10.1016/j. energy.2018.07.196;

[40] Maitlo, G., Ali, I., Mangi, K. H., Ali, S., Maitlo, H. A., Unar, I. N., & Pirzada, A. M. (2022). Thermochemical Conversion of Biomass for Syngas Production: Current Status and Future Trends. *Sustainability*, *14*(5), 2596. https://doi.org/10.3390/su14052596;

[41] Mak-Mensah, E., Obour, P.B., Essel, E., Wang, Q., Ahiakpa, J.K. (2021). Influence of plastic film mulch with biochar application on crop yield, evapotranspiration, and water use efficiency in northern China: A meta-analysis. *PeerJ 9:e10967*. doi:10.7717/peerj.10967;

[42] Maliutina, K., Tahmasebi, A., Yu, J., Saltykov, S.N. (2017). Comparative study on flash pyrolysis characteristics of microalgal and lig- nocellulosic biomass in entrained-flow reactor. *Energy Con- vers Manag* 151:426–438. https://doi.org/10.1016/j.encon man.2017.09.013;

[43] Martínez-Gómez ,Á. Poveda, J. and Escobar, C. (2022) Overview of the use of biochar from main cereals to stimulate plant growth. *Front. Ski Plant*. 13:912264. doi:10.3389/fpls.2022.912264;

[44] Meng, J., Liang, S., Tao, M., et al. (2018a). Chemical speciation and risk assessment of Cu and Zn in biochars derived from co-pyrolysis of pig manure with rice straw. *Chemosphere, 200*, pp. 344–350. https://doi.org/10.1016/j.chemosphere.2018.02.138;

[45] Meng, J., Tao, M., Wang, L., et al. (2018b). Changes in heavy metal bio- availability and speciation from a Pb–Zn mining soil amended with biochars from co-pyrolysis of rice straw and swine manure. *Sci Total About 633*. pp. 300–307. https://doi.org/10.1016/j.scito tenv.2018.03.199;

[46] Montanarella, L.; Lugato, E. (2013). The Application of Biochar in the EU: Challenges and Opportunities. *Agronomy 3*, pp. 462-473. https://doi.org/10.3390/agronomy3020462;

[47] Murray, M. (2021). What Is Biochar and How Is It Used?, Utah State University logo *Plant Health Extension*, available at https://extension.usu.edu/planthealth/research/biochar;

[48] Novak, J.M. (2019). *Biochar from Biomass and Waste || Future Biochar Research Directions. (), pp. 423–435.* doi:10.1016/B978-0-12-811729-3.00022-4;

[49] O'Toole, A., Andersson, D., Gerlach, A., Glaser, B., Kammann, C.I., Kern, J., Kuoppamäki, K., Mumme, J., Schmidt Hans-Peter Schulze, M., Srocke Franziska Stenrød M. (2016). Current and future applications for biochar. In: Shackley S, Ruysschaert G, Zwart K, Glaser B, eds. *Biochar in European Soils and Agriculture*: Science and Practice. Abington: Taylor & Francis Group. 253-280;

[50] Omoriyekomwan, J.E., Tahmasebi, A., Zhang, J., Yu, J. (2017). Forma- tion of hollow carbon nanofibers on bio-char during micro- wave pyrolysis of palm kernel shell. *Energy Convers Manag 148* pp. 583–592. https://doi.org/10.1016/j.enconman.2017.06.022;

[51] Osman, A.I., Farghali, M., Dong, Y., et al., (2024). Reducing the carbon footprint of buildings using biochar-based bricks and insulating materials: a review. *Environ Chem Lett 22*. pp. 71–104 https://doi.org/10.1007/s10311-023-01662-7;

[52] Rangabhashiyam, S., Balasubramanian, P. (2019). The potential of lignocellulosic biomass precursors for biochar production: Performance, mechanism and wastewater application—A review. *Industrial Crops and Products, 128*. pp. 405–423. doi:10.1016/j.indcrop.2018.11.041;

[53] Rombolà, A.G., Fabbri, D., Meredith, W. et al. (2016). Molecular characteri- zation of the thermally labile fraction of biochar by hydropyroly- sis and pyrolysis–*GC/MS. J Anal Appl Pyrolysis 121.* pp. 230–239. https://doi.org/10.1016/j.jaap.2016.08.003;

[54] Saletnik, B.; Zaguła, G.; Bajcar, M.; Tarapatskyy, M.; Bobula, G.; Puchalski, C. (2019). Biochar as a Multifunctional Component of the Environment—A Review. *Appl. Sci. 9*, 1139. https://doi.org/10.3390/app9061139;

[55] Sarker, T.R., Nanda, S., Dalai, A.K., Meda, V. (2021). A review of torrefaction technology for upgrading lignocellulosic biomass to solid biofuels. *Bioenergy Research. 14(2)*; pp. 645-669;

[56] Schmidt, H, Hagemann, N, Draper, K, Kammann, C. (2019). The use of biochar in animal feeding. *PeerJ* 7:e7373 https://doi.org/10.7717/peerj.7373;
[57] Schmidt, H.P. (2012). 55 Uses of Biochar. *Ithaka-Journal Arbaz, Switzerland*, pp. 450-454, www.ithaka-journal.net/en/ct/143;
[58] Stummann, M.Z., Høj M., Gabrielsen, J., Clausen, L.R., Jensen, P.A., Jensen, A.D. (2021). A perspective on catalytic hydropyrolysis of biomass. *Renewable and Sustainable Energy Reviews; 143:* 110960;
[59] Su, Y., Fu, W., Zhang, X. et al. (2025). Study on the Preparation of Biochar from Xinjiang Biomass Pyrolysis and Its Adsorption Characteristics for Water Pollutants. *Water Air Soil Pollut 236*, 320. https://doi.org/10.1007/s11270-025-07810-9;
[60] Thines, K.R., Abdullah, E.C., Mubarak, N.M. (2017). Effect of process parameters for production of microporous magnetic bio- char derived from agriculture waste biomass. *Microporous Mesoporous Mater 253:29–39*. https://doi.org/10.1016/j.micro meso.2017.06.031;
[61] Tripathi, M, Sahu, J.N., Ganesan, P. (2016) Effect of process parameters on production of biochar from biomass waste through pyrolysis: A review. *Renewable and Sustainable Energy Reviews. 55.* pp. 467-481;
[62] Wang, S., Jiang, D., Cao, B., et al. (2018). Bio-char and bio-oil character- istics produced from the interaction of Enteromorpha clathrate volatiles and rice husk bio-char during co-pyrolysis in a sectional pyrolysis furnace: a complementary study. *J Anal Appl Pyrolysis 135*. pp.219–230. https://doi.org/10.1016/j.jaap.2018.08.030;
[63] Wang, Y, Liu, R. (2017). Comparison of characteristics of twenty-one types of biochar and their ability to remove multi-heavy metals and methylene blue in solution. *Fuel Process Technol 160.* pp. 55–63. https://doi.org/10.1016/j.fuproc.2017.02.019;
[64] Weber, K. & Quicker, P. (2018). Properties of biochar. *Fuel, 217. pp.240–261. doi:10.1016/j.fuel.2017.12.054*;
[65] Wei, Tu J.C., Yuan, G.D., Liu, Y., Bi, D.X., Xiao, L.J., Lu, Theng, B.K.G., Wang, H.L., Zhang, L.J., Zhang, X.Z. (2019). Assessing the effect of pyrolysis temperature on the molecular properties and copper sorption capacity of a halophyte biochar, *Environ. Pollut., 25*. pp. 56-65;
[66] Xiong, X., Liu, J., Xiao, T., et al. (2025). Remediation of uranium-contaminated water and soil by biochar-based materials: a review. *Biochar 7, 41.* https://doi.org/10.1007/s42773-025-00438-2;
[67] Yaashikaa, P.R., Senthil Kumar, P., Varjani S., Saravanan, A. (2020). A critical review on the biochar production techniques, characterization, stability and applications for circular bioeconomy, *Biotechnology Reports Volume 28*. https://doi.org/10.1016/j.btre.2020.e00570;
[68] Zhao, B., Xu, X,. Xu, S. et al. (2017). Surface characteristics and potential- tial ecological risk evaluation of heavy metals in the bio-char produced by co-pyrolysis from municipal sewage sludge and hazelnut shell with zinc chloride. *Bioresour Technol 243*. pp. 375–383. https://doi.org/10.1016/j.biortech.2017.06.032;
[69] Zhao, B., Xu, X., Zeng, F., et al. (2018). The hierarchical porous structure bio-char assessments produced by co-pyrolysis of munici- pal sewage sludge and hazelnut shell and Cu(II) adsorption kinetics. *Environ Sci Pollut Res 25*. pp.19423–19435. https://doi. org/10.1007/s11356-018-2079-y;
[70] Zheng, N., Zhang, J., Wang, J. (2017) Parametric study of two-stage hydropyrolysis of lignocellulosic biomass for production of gaseous and light aromatic hydrocarbons. *Bioresour Technol 244*. pp.142–150. https://doi.org/10.1016/j.biortech.2017.07.103;
[71] *** www.biochar-industry.com/;
[72] *** www.causeartist.com;
[73] *** https://energytheory.com/wp-content/uploads/2023/12/biochar.png

EVALUATION OF NETTLE PARTS FOR FUNCTIONAL FOODS, BASED ON A NOVEL ANTIOXIDANT-DIETARY ELEMENT INDEX (ADEI)

/

EVALUAREA PĂRȚILOR DE URZICĂ PENTRU ALIMENTE FUNCȚIONALE, PE BAZA UNUI INDICE NOU DE ANTIOXIDANȚI ȘI ELEMENTE NUTRITIVE

Patricia-Cristina TARKANYI[1)], Nicolae-Valentin VLADUȚ[*2)], Mihaela LĂCĂTUȘ[1)], Laura RĂDULESCU[1)], Liana Maria ALDA[*1)], Georgeta Sofia POPESCU[1)], Ioan Ladislau CABA[2)], Despina Maria BORDEAN[1)]

[1)] University of Life Sciences "King Mihai I" from Timisoara, Calea Aradului 119, Timisoara, Timis County / Romania;

[2)] National Institute of Research - Development for Machines and Installations Designed to Agriculture and Food Industry - INMA Bucharest / Romania.

**Tel: 0748 283 409; *E-mail: valentin_vladut@yahoo.com*

**Tel: 0726 612 460; *E-mail: lianaalda@usvt.ro*

Keywords: *Urtica dioica, polyphenols, antioxidants, essential minerals, synthetic indicator*

ABSTRACT

Stinging nettle (Urtica dioica L.) is a widespread and sturdy plant with ancient value as a food and medicinal crop. The tight antioxidant and dietary profile of the plant suggests high potential as a food functional ingredient. For all that, limited comparative data are known on the nutritional value of nettle organs. In this contribution, the Antioxidant–Dietary Element Index (ADEI) is introduced as a simple method of ranking plant material by nutritional-related quality. Plant samples were collected from three sources to capture natural variation. Antioxidant activity was measured with the CUPRAC assay, polyphenol content with the Folin–Ciocalteu method, and the minerals iron (Fe) and zinc (Zn) with X-ray fluorescence (XRF).All results were combined in the ADEI index to provide a single comparative score for leaves, stems, and roots. The analysis demonstrated marked variations among plant organs. Leaves consistently exhibited the highest values, indicating superior antioxidant potential and enhanced mineral levels, whereas stems and roots showed comparatively lower functional properties. ADEI presents a simple but integrative way to highlight the nutritional value of plant material. Applied to nettle, it confirms the leaves as the most appropriate organ for functional food production and demonstrates the use of ADEI to valorize other medicinal and edible plants.

REZUMAT

Urzica (Urtica dioica L.) este o plantă răspândită și rezistentă, cu o valoare tradițională importantă atât ca aliment, cât și ca plantă medicinală. Profilul său bogat în antioxidanți și nutrienți sugerează un potențial ridicat ca ingredient funcțional pentru alimente. Cu toate acestea, există puține date comparative referitoare la valoarea nutrițională a diferitelor organe ale plantei. În această lucrare este introdus Indicele elementelor nutriționale-antioxidante (IENA din engl. ADEI) ca metodă simplă de ierarhizare a materialului vegetal în funcție de calitatea nutrițională. Probele de plante au fost colectate din trei surse pentru a surprinde variația naturală. Activitatea antioxidantă a fost măsurată prin metoda CUPRAC, conținutul de polifenoli prin metoda Folin–Ciocalteu, iar mineralele fier (Fe) și zinc (Zn) prin fluorescență de raze X (XRF). Toate rezultatele au fost combinate în indicele ADEI pentru a oferi un scor comparativ unic pentru frunze, tulpini și rădăcini. Analiza a evidențiat variații semnificative între organele plantei. Frunzele au prezentat în mod constant cele mai ridicate valori, indicând un potențial antioxidant superior și niveluri mai mari de minerale, în timp ce tulpinile și rădăcinile au arătat proprietăți funcționale mai reduse. ADEI oferă o metodă simplă, dar integratoare, de evidențiere a valorii nutriționale a materialului vegetal. Aplicat la urzică, acesta confirmă frunzele ca fiind cele mai potrivite pentru producerea de alimente funcționale și demonstrează utilitatea indicelui ADEI pentru valorizarea altor plante medicinale și comestibile.

INTRODUCTION

Stinging nettle (*Urtica dioica* L.) is a widespread wild plant that has long been valued both as food and as a natural remedy. In recent years, it has gained growing attention for its high content of bioactive compounds and essential minerals, which contribute to its many health benefits *(Bhusal, 2022)* Nettle has traditionally been appreciated in both nutrition and phytotherapy for its rich content of polyphenols, vitamins,

and antioxidants, as well as essential minerals including iron, calcium, magnesium, and zinc. Together, these elements account for their well-documented health-promoting effects *(Maietti et al., 2021).*

In recent years, the growing interest in functional foods has emphasized the need for systematic approaches that evaluate plant-based resources not only for their antioxidant capacity but also for their nutritional mineral composition. Although many studies have investigated the phytochemical profile of nettle roots, stems, and leaves, comprehensive comparisons that consider both antioxidant activity and mineral nutritional content remain relatively scarce *(Adhikari et al., 2015).* To advance knowledge in this area, we apply the Antioxidant–Dietary Element Index (ADEI) as a novel integrative approach. This tool unites antioxidant properties and mineral content into a single evaluative criterion, offering a more complete assessment of nettle organs. Such an approach helps highlight the most useful components for functional food design and opens new avenues for food and nutrition research.

Iron stands out as one of the most critical essential minerals. It is fundamental to the formation of hemoglobin and myoglobin, thereby supporting oxygen transport and energy production, while also playing a key role in maintaining immune defense and cognitive performance *(NIH, 2022; Hurrell, 2010).* Iron deficiency continues to be the most widespread nutritional disorder worldwide, leading to anemia, reduced vitality, and hindered development, with the greatest impact seen in vulnerable groups (*WHO, 2001).*

While iron derived from plant foods is absorbed less efficiently than heme iron, nettle still makes a noteworthy dietary contribution and stands out as a potential resource for reducing micronutrient deficiencies *(Adhikari et al., 2015; Bhusal, 2022)*. Iron is an essential trace element for plants, playing key roles in photosynthesis, respiration, and in the synthesis of cofactors required for electron transport and numerous enzymatic processes *(Connorton et al., 2017)*. Since iron is often poorly available in soils and can become harmful when present in excess, plants have evolved sophisticated mechanisms for their uptake, translocation, storage, and regulation in order to maintain internal balance *(Connorton et al., 2017).*

Zinc represents another vital trace element and is the second most prevalent metal in the human body after iron. It acts as a cofactor for over 300 enzymes and is indispensable for immune function, growth and development, neurological activity, and reproductive processes *(Prasad, 2013; NIH, 2021).* Zinc deficiency is considered a major global health problem, linked to reduced immune function, slower growth, and a higher risk of infections (*Wessells & Brown, 2012).* The zinc present in nettle enhances its value as a functional food, complementing antioxidant effects with important nutritional benefits *(Maietti et al., 2021).*

The aim of this study is to present and apply a new Antioxidant–Dietary Element Index (ADEI) as a comprehensive tool for evaluating nettle parts, according to their nutritional and functional significance. By integrating antioxidant capacity with essential mineral content into a single indicator, the ADEI offers a clearer understanding of how various plant parts contribute to human health. This method not only highlights the nettle fractions with the greatest potential for functional food development but also enhances our knowledge of the relationship between dietary minerals and antioxidant activity in shaping the plant's overall health value.

Integrating antioxidant activity with essential dietary minerals in the ADEI highlights the nutritional value and functional potential of nettle.

MATERIALS AND METHODS

Collection and preparation of nettle plants

Soil and nettle samples were collected during the autumn of 2023 and 2024 from three locations in Romania: L1 - Timișoara (Timiș County), L2 - Vadu-Dobrii (Hunedoara County) and L3-Turcinești (Gorj County). At each location, materials were carefully separated into four categories: soil, roots, stems and leaves, and thoroughly rinsed with distilled water. The samples were then air-dried at room temperature to constant weight, ground into a fine homogeneous powder, and subsequently prepared for analysis.

Samples analysis

The moisture content [%] of the soils and nettle samples were determined by thermogravimetric analysis using a Sartorius balance, as described by Bordean et al, 2013. The determination of total polyphenolic content (TPC) was performed using Folin–Ciocalteu colorimetric method, which remains one of the most widely employed assays for polyphenol quantification in plant-derived materials *(Bordean, 2016).* Total antioxidant capacity (TAC) was determinate using CUPRAC method which measures how the antioxidants in the samples reduce copper ions and form a coloured complex. The intensity of this colour reflects the strength of the antioxidant activity, making the method simple, reliable, and suitable for evaluating a wide range of natural compounds *(Apak et al., 2004).* For the XRF (X-ray fluorescence)

analysis, powdered samples were examined using a Hitachi X-MET8000 portable spectrometer *(Tarkanyi et al., 2023*). XRF spectrometry is highly valuable as it allows the rapid and precise determination of both the concentration and presence of chemical elements in a sample *(Yonehara et al., 2010).* All determinations and measurements were performed in triplicate and reported to fresh weight (FW).

Definition and calculation of Antioxidant-Dietary Element Index (ADEI)

ADEI is not a standardized indicator but more a composite indicator concept proposed by the authors for functional food assessment based on the indicators described by Wang et al., 2022 and Vahid et al., 2020.

The ADEI (equation 1) combines bioactive compounds (equation 2) and essential dietary minerals (equation 3) into a single score, enabling direct comparison across samples. This approach makes it possible to rank plant organs or locations by their nutritional and functional potential, to identify the most suitable candidates for functional food development, and to present results in a clear and integrative manner *(Vahid et al, 2020)*.

ADEI was calculated as:

ADEI = Antioxidant score × Micronutrient factor

ADEI > 1 → High functional potential (antioxidants + essential minerals combined)

ADEI ≈ 0 → Very low nutritional/functional relevance (either very low TPC/TAC or Fe/Zn)

Ranking helps sorting ADEI descending, highlighting which samples are most promising for functional food applications.

Where:

$$\mathbf{ADEI} = \frac{TPC_{norm} + TAC_{norm}}{2} \times (1 + \frac{Fe_{norm} + Zn_{norm}}{2}) \quad (1)$$

$$Antioxidant\ Score = \frac{TPC_{norm} + TAC_{norm}}{2} \quad (2)$$

$$Micronutrient\ Factor = 1 + \frac{Fe_{norm} + Zn_{norm}}{2} \quad (3)$$

- TPC_{norm} = Total Polyphenol Content normalized to 0–1 by dividing by the maximum value in the dataset.

- TAC_{norm} = Total Antioxidant Capacity normalized.

- Fe_{norm}, Zn_{norm} = Iron and Zinc concentrations normalized.

Normalization of each variable is described by equation 4.

$$X_{norm} = \frac{X}{X\ max} \quad (4)$$

Where X_{max} *is the highest value in the dataset for that variable.*

RESULTS

The calculated results for ADEI are presented in table 1.

Table 1

Antioxidant, micronutrient and ADEI values of nettle samples

Sample	TAC_{norm}	TPC_{norm}	Fe_{norm}	Zn_{norm}	Antioxidant Score	Micronutrient Factor	ADEI
NL3	1	1	0.052	0.361	1	1.207	1.207
NL2	0.75	0.8	0.039	0.892	0.775	1.465	1.135
							Table 1 continued
NL1	0.697	0.485	0.028	0.227	0.591	1.128	0.666
NS3	0.352	0.337	0.038	0.689	0.345	1.363	0.47
NS2	0.111	0.337	0.067	1	0.224	1.533	0.344
NR2	0.118	0.194	0.075	0.463	0.156	1.269	0.198
NS1	0.148	0.174	0	0.186	0.161	1.093	0.176
NR1	0.135	0.168	0.01	0.06	0.151	1.035	0.157
NR3	0.066	0.194	0.062	0.332	0.13	1.197	0.155
SO1			0.396	0.363		1.379	
SO2			1	0.569		1.785	
SO3			0.266	0.122		1.194	

Legend: NR = nettle roots; NL = nettle leaves, NS= nettle stems; 1,2,3 =collection areas; TPC= total polyphenols contents; TAC = total antioxidant capacity normalization; Fe_{norm}= iron concentrations normalized, Zn_{norm}=zinc concentrations normalized; ADEI= Antioxidant-Dietary Element Index

Based on the calculated ADEI values, the leaf samples (NL3, NL2, NL1) obviously rank highest, confirming that nettle leaves combine both strong antioxidant potential (TPC and TAC) and appropriate levels of Fe and Zn. Among them, NL3 reached the top score, indicating the most promising balance between polyphenol content, antioxidant activity, and micronutrient density. Stem and root samples (NS3, NS2, NR2, NR3) show intermediate ADEI values, suggesting they still contribute functional compounds but at lower effectiveness compared to leaves. For soil TAC and TPC were not analyzed (ND).

Our results demonstrate that integrating polyphenol content (TPC), antioxidant capacity (TAC), and essential minerals (Fe, Zn) into a single composite score (ADEI) provides a powerful way to rank nettle samples by their nutritional and functional potential (Figure 1).

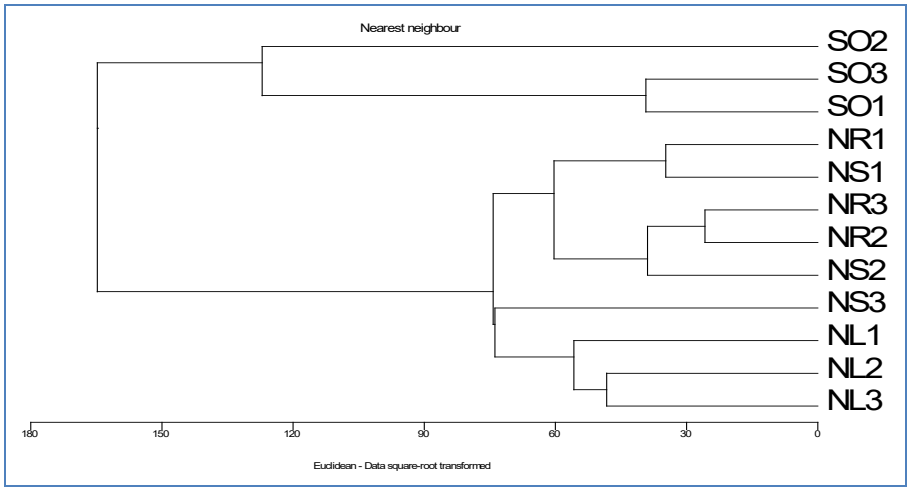

Fig. 1 - Dendrogram as a result of cluster analyses

Legend: NR = nettle roots; NL = nettle leaves, NS= nettle stems; 1,2,3 =collection areas;

This figure presents a graphical representation of clusters obtained by using cluster analyses based on squared root transposed data and Euclidian nearest neighbor equation. The dendrogram groups soil data in cluster 1(SO2, SO3, SO1) and cluster 2 where the plant parts corresponding to roots and stem appear mixt while the vectors corresponding to leaves data NL1, NL2, NL3 are grouped together.

The same cluster analyses offer a second dendrogram figure 2 which groups the antioxidant characteristics together TPC and TAC parameters well connected to Fe and Zn and the indicator ADEI showing a direct link to water content.

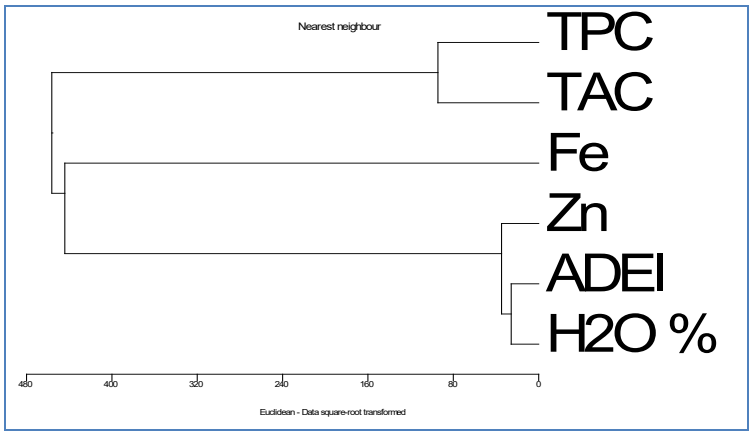

Fig. 2 - Dendrogram of antioxidant and minerals based on cluster analyses

Legend: H2O% = moisture content of samples; TPC= total polyphenols contents;
TAC = total antioxidant capacity normalization; Fe= iron concentrations, Zn=zinc concentrations;
ADEI= Antioxidant-Dietary Element Index

As we can observe from both figures, the leaves exhibited the highest ADEI values, highlighting them as the most promising plant parts for incorporation into functional food formulations. As a comprehensive and user-friendly indicator, ADEI facilitates the evidence-based selection of plant organs and

collection locations, offering meaningful guidance for product formulators and nutrition specialists in determining the most appropriate raw materials.

Iron content generally increases from the root to the leaf, although at location 3 higher amounts were found in both roots and leaves. In the case of zinc, the greatest concentration occurred in the stem at location 2, while at location 3 the stem contained more zinc than the leaf, and the root had the lowest levels.

Arial 10 pt, Paragraph Multiple 1.15 pt

Figure 3 and Table 1 show that iron strongly influences mineral composition and bioactive compounds (TAC and TPC). In Timiș (location 1), lower iron levels correspond to moderate TAC and TPC values. Whereas in Hunedoara (location 2), the highest iron concentrations are associated with increased antioxidant capacity and polyphenol content, suggesting a direct correlation. In location 3 (Gorj), although iron levels are lower than in Hunedoara, TAC and TPC record the highest values, confirming that, in addition to iron, other local factors contribute to the antioxidant potential. These results therefore highlight a complex relationship between iron and bioactive compounds, specific to each collection area.

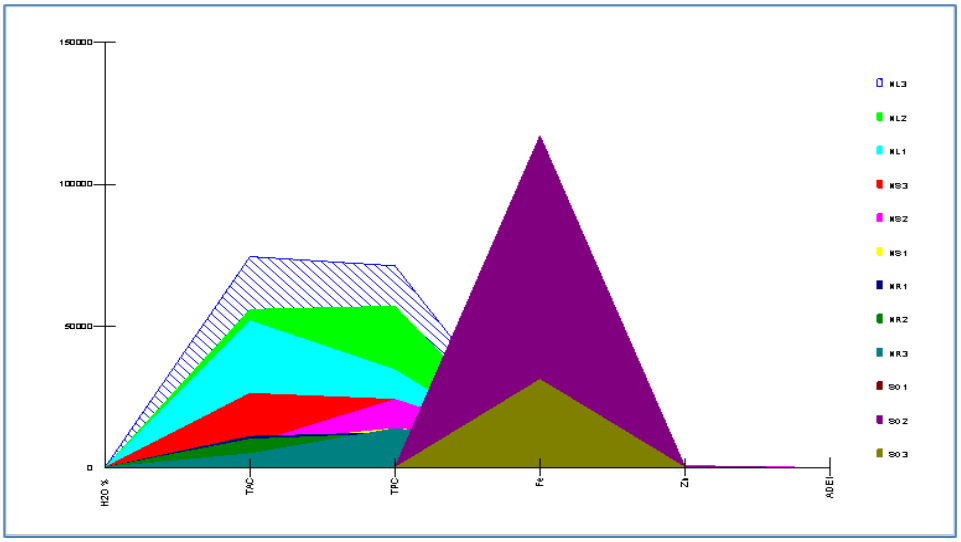

Fig. 3 - Fingerprint-influence of essential minerals and antioxidants on TAC and TPC

Legend: H2O= moisture content of plant samples (%); TPC= total polyphenols contents; TAC = total antioxidant capacity; NR = nettle roots; NL = nettle leaves, NS= nettle stems; 1,2,3 =collection areas;

The fingerprint of nettle illustrated in figure 3 highlights the variations in mineral and bioactive compounds across plant organs and collection areas. The biochemical fingerprint defines the plant's identity, reflecting the diversity of compounds expressed in different organs and growing regions. More than a simple compositional profile, it allows samples to be distinguished, ensures traceability and authentication of raw materials, and highlights their nutritional and therapeutic importance. In this way, biochemical fingerprint functions both as a research tool and as a practical standard for quality assessment and applied purposes.

CONCLUSIONS

Stinging nettle (*Urtica dioica* L.) exhibits notable nutritional and functional potential, and the Antioxidant–Dietary Element Index (ADEI) offered an integrative view of the differences among roots, stems, and leaves. Of these organs, leaves consistently proved to be the most valuable, combining greater antioxidant capacity with higher levels of essential minerals, thus representing the most suitable fraction for functional food applications.

The evaluation across the three collection sites highlighted the influence of soil composition and mineral availability, especially iron, on the levels of bioactive compounds. At the same time, variations observed between locations indicate that additional environmental factors also shape the biochemical profile of nettle, giving each site a distinctive "fingerprint."

By combining different parameters into a single index, ADEI has proven to be an effective and straightforward tool, bringing together antioxidant activity and mineral content in one comprehensive score.

This method makes data easier to interpret while also supporting evidence-based choices in the use and valorization of plant resources.
Nettle shows once again that it is a valuable plant, with its leaves being the main part used for developing functional foods. In addition, the ADEI approach can also be applied to other edible and medicinal plants, giving researchers, nutritionists, and product developers a useful tool to explore and make full use of natural resources.

ACKNOWLEDGEMENT

The research was performed with the support of the Interdisciplinary Research Platform belonging to the University of Life Sciences "King Michael I" from Timisoara and National Institute of Research-Development for Machines and Installations Designed to Agriculture and Food Industry-INMA, 013813 Bucharest, Romania

The results of the scientific study will be included in the PhD Thesis of Patricia Cristina Tarkanyi.

REFERENCES

[1] Adhikari B. M., Bajracharya A., Shrestha A. K. 2015. Comparison of nutritional properties of stinging nettle (Urtica dioica) flour with wheat and barley flours. *Food Science & Nutrition*, 3(1), 126–131.
[2] Apak R., Güçlü K., Özyürek M., Karademir S. E. 2004. Novel total antioxidant capacity index for dietary polyphenols and vitamins C and E, using their cupric ion reducing capability in the presence of neocuproine: CUPRAC method. *Journal of Agricultural and Food Chemistry*, 52(26), 7970–7981. https://doi.org/10.1021/jf048741x
[3] Bhusal K. K. 2022. Nutritional and pharmacological importance of stinging nettle (Urtica dioica). *Journal of Food Biochemistry*, 46(7), e14136.
[4] Bordean D.-M. 2016. *Food Analysis*. ArtPress Publishing House, Timișoara, pp. 52–92.
[5] Bordean D.-M., Borozan A. B., Cojocariu L., Moigrădean D., Cojocariu A., Nica D., Pîrvulescu I., Alda S., Horablaga M. 2013. Seasonal variation in nutrient content of some leafy vegetables from Banat County, Romania. *Review on Agriculture and Rural Development*, 2(1), 170–174.
[6] Connorton J. M., Balk J., Rodríguez-Celma J. 2017. Iron homeostasis in plants – a brief overview. *Metallomics*, 9(7), 813–823. https://doi.org/10.1039/c7mt00136c
[7] Hurrell R. F. 2010. Iron bioavailability and dietary reference values. *The American Journal of Clinical Nutrition*, 91(5), 1461S–1467S.
[8] Maietti A., et al. 2021. Polyphenol content, antioxidant and nutritional properties of stinging nettle (Urtica dioica L.). *Foods*, 10(5), 938.
[9] NIH. 2021. Zinc—Fact Sheet for Health Professionals. Office of Dietary Supplements, U.S. Department of Health & Human Services.
[10] NIH. 2022. Iron—Fact Sheet for Health Professionals. Office of Dietary Supplements, U.S. Department of Health & Human Services.
[11] Prasad A. S. 2013. Discovery of human zinc deficiency: Its impact on human health and disease. *Advances in Nutrition*, 4(2), 176–190.
[12] Tarkanyi P. C., Popescu G. S., Rădulescu L., Dragomirescu M. C., Bordean D. M. 2023. Urtica dioica plants: a possibility to evaluate climate change. *International Multidisciplinary Scientific GeoConference: SGEM*, 23(4.2), 389–396.
[13] Vahid F., Rahmani D., Davoodi S. H. 2020. Validation of Dietary Antioxidant Index (DAI) and investigating the relationship between DAI and the odds of gastric cancer. *Nutrition & Metabolism*, 17(1), 102.
[14] Wang W., Wang X., Cao S., Duan Y., Xu C., Gan D., He W. 2022. Dietary antioxidant indices in relation to all-cause and cause-specific mortality among adults with diabetes: a prospective cohort study. *Frontiers in Nutrition*, 9, 849727.
[15] Wessells K. R., Brown K. H. 2012. Estimating the global prevalence of zinc deficiency: Results based on zinc availability in national food supplies and the prevalence of stunting. *PLoS ONE*, 7(11), e50568.
[16] WHO. 2001. *Iron deficiency anemia: Assessment, prevention and control. A guide for programme managers*. World Health Organization.
[17] Yonehara T., Yamaguchi M., Tsuji K. 2010. X-ray fluorescence imaging with polycapillary X-ray optics. *Spectrochimica Acta Part B: Atomic Spectroscopy*, 65(6), 441–444.

CFD-BASED INVESTIGATION OF A COUNTER-ROTATING VERTICAL AXIS WIND TURBINE FOR LOW-WIND AGRICULTURAL ENVIRONMENTS

/

INVESTIGAȚIE NUMERICĂ BAZATĂ PE CFD A UNEI CONFIGURAȚII CONTRAROTATIVE DE TURBINE EOLIENE CU AX VERTICAL PENTRU MEDII AGRICOLE CU VÂNT REDUS

Adrian PANDELE*[3, 1)], Bogdan Ovidiu DURAN[2, 3)], Dragos Mihail PREDA[2, 3)], Robert BILA[2)], Elena VILCU*[1)], Andrei VULPE*[1)], Gheorghe VOICU[3)]

[1)] ARROW SRL / Romania;

[2)] ROLIX IMPEX SERIES SRL / Romania;

[3)] National University of Science and Technology Politehnica Bucharest / Romania.

**Tel: (+40) 722 655 056; *E-mail: adrian.pandele@arrows.ro*

Keywords: *Lenz, numerical simulation, vorticity magnitude, tip speed ratio*

ABSTRACT

This paper reports a computational fluid dynamics (CFD) analysis of a counter-rotating Lenz-type vertical axis wind turbine (VAWT) that can be used in low-wind agricultural settings. The main aim was to quantitatively assess the aerodynamic performance and flow behaviour of the suggested configuration. An unsteady Reynolds-averaged Navier–Stokes (URANS) model considering shear stress transport (SST) turbulence was used in conjunction with ANSYS Fluent to solve the unsteady rotor–stator interaction. The turbine configuration consisted of two counter-rotating three-bladed rotors with a diameter of 0.3 m, a rotor height of 0.6 m, and a blade chord length of 0.12 m. Simulations were performed for a uniform inlet wind speed of 12 m/s at a tip speed ratio of 0.2 to 1.2. Results indicate the counter-rotating configuration achieved power output readings between 50 W and 120 W with their corresponding variability in torque coefficient, which reflected the best operating conditions for the tested TSR range. Flow field visualisation demonstrated extreme vorticity magnitude in the rotors' region, indicating intense wake interaction that impacted entire turbine performance. The outcome of these tests illuminates the potentiality of counter-rotating Lenz-type VAWTs as a feasible small-scale power alternative for decentralised energy supply in low-wind agricultural settings. Future activities will consider three-dimensional simulations to simulate spanwise flow effects and contrast the two-dimensional results with experimental results from wind tunnel testing. Parametric optimisation of spacing between rotors, blade shape, and rotational speed ratio between the two rotors for maximum efficiency over a range of wind conditions will also be considered.

REZUMAT

Această lucrare prezintă o analiză computațională de dinamica fluidelor (CFD) a unei configuratii contra-rotative de turbine eoliene cu ax vertical (VAWT) de tip Lenz, care poate fi utilizată în medii agricole cu vânt slab. Scopul principal a fost evaluarea cantitativă a performanței aerodinamice și a comportamentului de curgere al configurației sugerate. Un model Navier-Stokes nestaționar, cu mediere Reynolds (URANS) si model de turbulenta SST, a fost utilizat împreună cu ANSYS Fluent pentru a rezolva interacțiunea rotor-stator. Configurația consta insuprapunerea a două rotoare cu trei pale, care se rotesc în sens inverssi care au un diametru de 0,3 m, o înălțime a rotorului de 0,6 m și o lungime a corzii palelor de 0,12 m. Simulările au fost efectuate pentru o viteză uniformă a vântului la intrare de 12 m/s, la un raport al vitezei la vârf de 0,2 până la 1,2. Rezultatele indică faptul că configurația a atins valori de putere de ieșire între 50 W și 120 W, cu variabilitatea corespunzătoare a coeficientului de cuplu, ceea ce a reflectat cele mai bune condiții de funcționare pentru gama TSR testată. Vizualizarea câmpului de curgere a demonstrat o magnitudine extremă a vorticității în regiunea rotoarelor, indicând o interacțiune intensă care a influentat întreaga performanță a turbinei. Rezultatul acestor teste evidențiază potențialul turbinelor de tip VAWT contrarotative de tip Lenz ca o alternativă energetică fezabilă la scară mică pentru alimentarea descentralizată cu energie în medii agricole cu vânt redus. Activitățile viitoare vor lua în considerare simulări tridimensionale pentru a simula efectele de curgere pe lungime și vor compara rezultatele bidimensionale cu rezultatele experimentale din testele în tunelul aerodinamic. De asemenea, se va lua în considerare optimizarea

parametrică a distanței dintre rotoare, a formei palelor și a raportului vitezei de rotație dintre cele două rotoare pentru o eficiență maximă într-o gamă largă de condiții de vânt.

INTRODUCTION

Wind turbines are a key technology for harnessing wind energy, and quantifying their efficiency is crucial to enhance performance and reduce costs. As the demand for renewable energy increases, wind energy is emerging as a dominant force in the world energy mix (*Gielen D.et al., 2019)*.

The classical theory offers a simplification analytical approach to determine the efficiency of wind turbines basically based on Betz's Law and momentum theory (*Sørensen, J. N, 2016)*. It makes simplifying assumptions and fails to accurately depict complex aerodynamic phenomena such as turbulence and eddy interactions.

Figure 1 shows wind speed (in m/s) with wind power density (in W/m²) on a graph with a logarithmic scale. It shows how quickly power density increases with increasing wind speed since power in winds is related cubically to speed. Principal indicators, such as the mean annual value, maximum hourly and ten-minute means, and maximum hundred-year, are depicted to represent the extremely large variations in wind speed and theoretical energy.

The graph illustrates how minimal increases in wind speed significantly raise available wind energy.

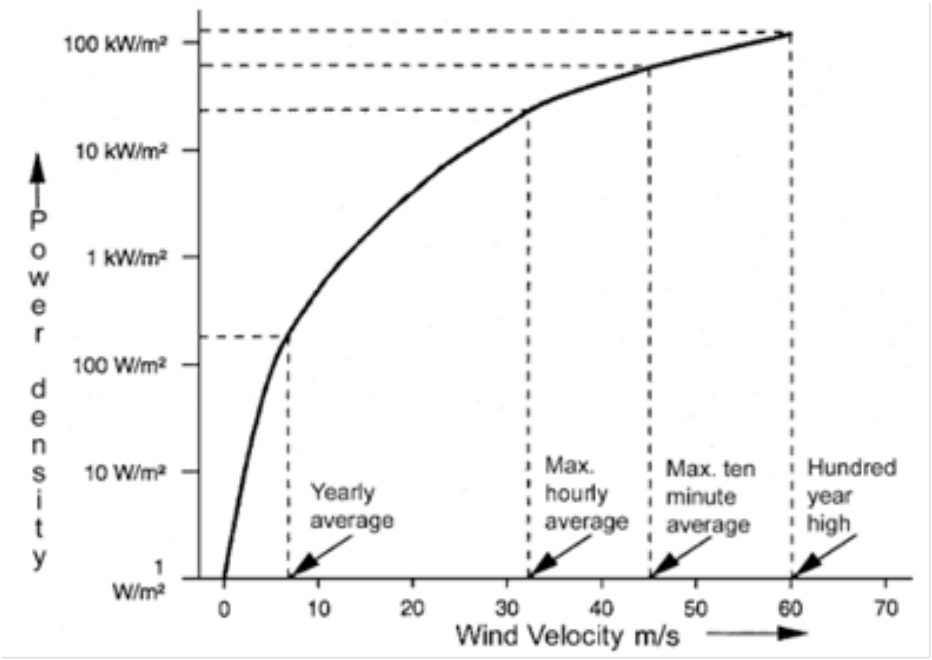

Fig. 1 - Power curve of a wind turbine showing the relationship between wind speed and power output
(Wagner, H. J., 2020)

In Figure 2 are illustrated the lift and drag forces on wind turbine blade and how the airfoil shape and direction of the wind produce torque for power production. The wind strikes the blade at an angle of attack to the chord line (a straight line connecting the leading and trailing edges).

This encounter generates two main aerodynamic forces: lift perpendicular to the wind direction (this is the main force responsible for spinning the blade) and drag in the same direction as the wind and opposing the movement of the blade.

The wind drag force manifests itself as a horizontal force component and one that assists in energy extraction. Even though the point of pressure is the point upon which the resultant aerodynamic force acts, gravity and the plane along which the turbine revolves are incorporated to place the forces the turbine feels when rotating into perspective.

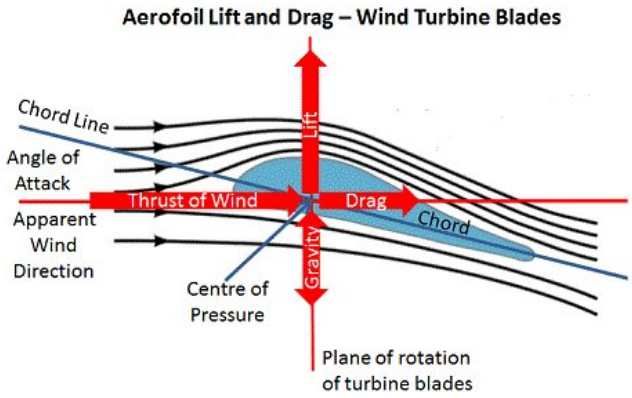

Fig. 2 - Aerodynamic lift and drag force on the blade
(*Chintan Kariya, 2017)*

Computational Fluid Dynamics (CFD) is a numerical method to simulate fluid flow and evaluate in detail the aerodynamic performance of wind turbines. CFD is different from BEM and classical theory because it accounts for intricate effects such as vortex effects, turbulence, and flow separation (*Bianchini, A. et al., 2017)*. The Navier-Stokes equations are the governing equations for the simulation of CFD, which describe the motion of fluids:

$$\rho\left(\frac{\partial v}{\partial t} + v \cdot \nabla v\right) = -\nabla p + \mu \nabla^2 v + f \tag{1}$$

where: v is the fluid velocity field, ρ is the fluid density, p is the pressure, μ is the dynamic viscosity, and f represents body forces, such as gravity.

CFD simulations allow for detailed, high-resolution modelling of the interactions between wind turbine blades and the wind, providing insights into blade shape optimization, turbine spacing, and the effects of vortex interaction (*Calautit, K. et al., 2018)*, (*Chowdhury, A. M. et al., 2016)*, (*Delafin, P. L., 2017)*.

The image below shows a computational fluid dynamics (CFD) simulation showing the magnitude of vorticity around a wind turbine rotor. The colour scale on the left indicates the magnitude of vorticity (in s^{-1}), from blue (low) to red (high). The circular boundary represents the area swept by the rotor, with the turbine hub at the center. Regions of high vorticity (yellow, red) appear near the blade tips and behind them, indicating strong vortex shedding - typical of rotating blades.

The downstream structure behind the rotor exhibits complex flow interactions that are crucial for understanding trailing losses, turbine efficiency, and turbine spacing in wind farms. These flow patterns are important in evaluating aerodynamic performance and in load predictions.

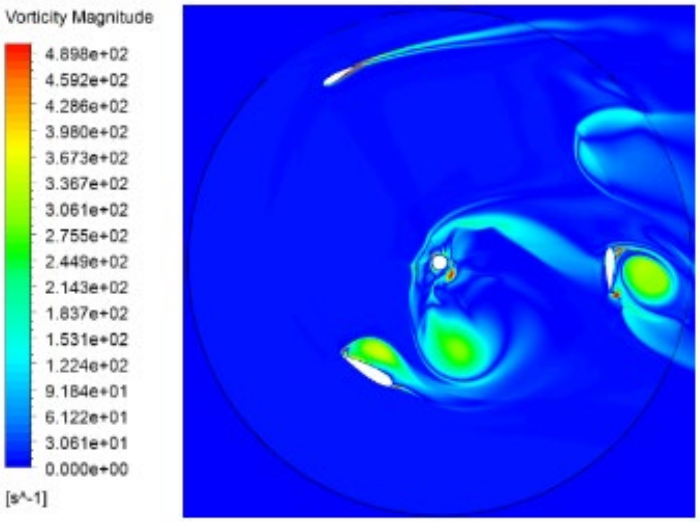

Fig. 3 - CFD simulation showing wind flow over turbine blades
(*Malael, I. et al., 2021)*

Recent advances in wind turbine performance evaluation have led to the development of hybrid models, which combine the advantages of BEM theory and CFD simulations. These hybrid models allow for rapid performance estimates (from BEM) while providing accurate aerodynamic analysis (from CFD). In addition, Artificial Intelligence (AI) (*Al Noman, A. et al., 2022)* and Machine Learning (ML) (*Cheng, B. et al., 2022)* are used to analyze large data sets, predict turbine performance, and optimize operational parameters.

Fig. 4 illustrates the structure and shape evolution of a wind turbine, both in instantaneous and time-averaged perspectives. The top view shows the tip and hub vortices generated by the rotating blades. These vortices create complex and dynamic flow patterns.

This turbulent, unsteady flow has significant implications for the downstream turbines (e.g., fluctuating loads and power). While the bottom view shows the flow divided into three regions: the induction region: just upstream of the rotor, where the wind slows down due to the turbine resistance; the near region: directly behind the rotor, showing a velocity deficit Δu^- and coherent vortex structures; the far region: further downstream, where the wake expands and partially recovers its velocity u^-.

The velocity deficit is most significant near the turbine and gradually decreases downstream.

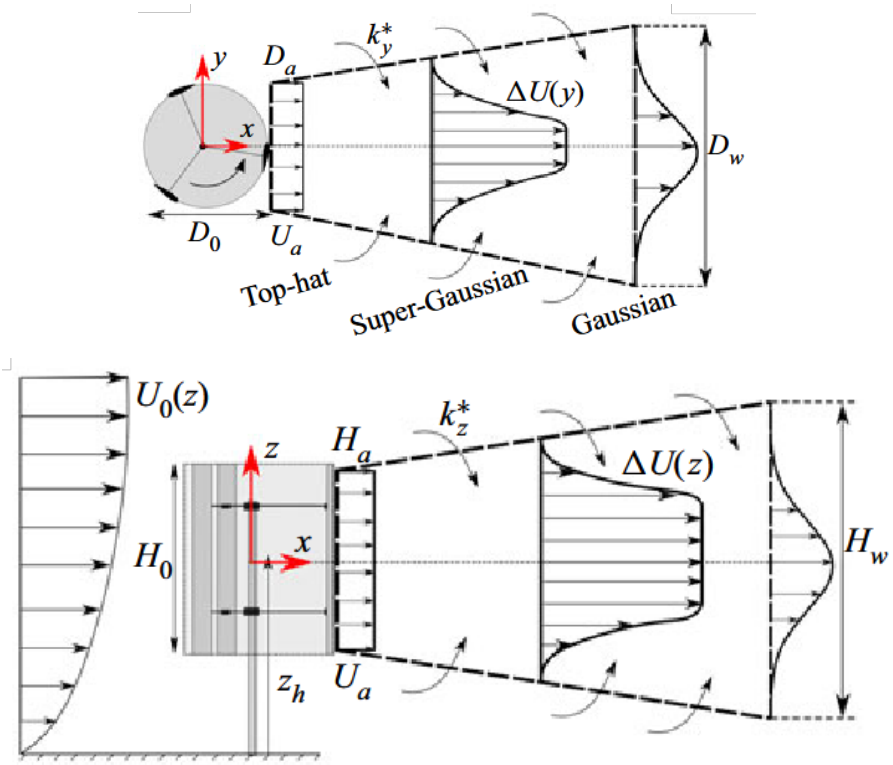

Fig. 4 - Schematic figure showing the flow regions resulting from the interaction of a wind turbine and the turbulent inlet boundary layer

(*Ouro, P.et al., 2021)*

CFD allows the prediction of aerodynamic forces on wind turbine blades, including lift and drag (*Qi, Y, et al., 2025),* (*Huish, C. et al., 2025)*. The main challenge in wind turbine CFD is to capture the effects of turbulence, the transient nature of the wind, and the interaction of the rotating turbine blades with the wind.

Fig. 5 illustrates the computational grid used to simulate the flow over the airfoil of a wind turbine blade, showing several zoom levels from the domain scale to the blade surface. The global grid view (a) shows the overall computational domain, with a fine grid resolution concentrated around the airfoil (center) and coarser cells in the opposite direction.

This is a typical grid structure, designed to save computational resources. The in-focus region (b) is a zoomed-in view of the refined area surrounding the airfoil. A tighter grid grouping can be observed, especially where accurate flow prediction (e.g., vortex generation) is crucial.

The airfoil neighbourhood (c) shows unstructured grid elements around the airfoil, capturing the complex boundary layer behavior and flow separation zones, while the airfoil surface grid (d) is a further zoom in close to the airfoil surface with dense triangular grid elements, essential for resolving the boundary layer flow. Finally, the LE and TE insets show close-ups of the leading edge (LE) and trailing edge (TE),

which feature an extremely fine grid—essential for accurate modelling of pressure gradients and flow separation.

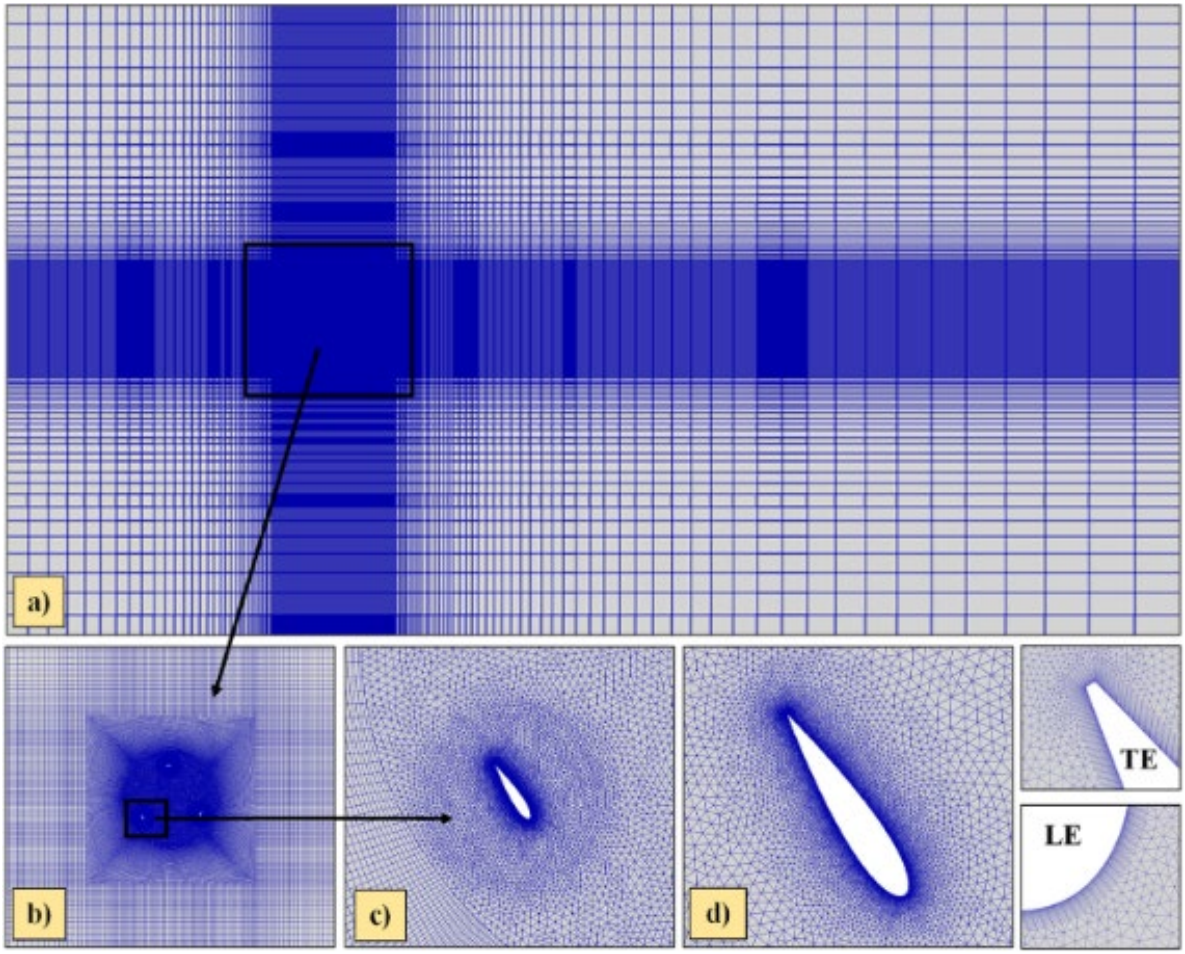

Fig. 5 - Hybrid computational grid for a vertical axis wind turbine of type H: a) structured stationary domain; b) blocks around the rotational domain; c) fine unstructured grids inside the rotational domain; d) grid density on the blade surfaces, leading edge (LE) and trailing edge (TE)
(*Fatahian, E. et al., 2024)*

For wind turbine simulations, accurate turbulence models are essential to predict velocity profiles and power losses (*Cabezon, D. et al., 2011)*. Some commonly used models include:

- model k-ε (Reynolds-Averaged Navier-Stokes (RANS)),
- model k-ω,
- Large Eddy Simulations (LES), which resolves large turbulence scales.

Turbulence models, such as the k-ε, are often used in simulations to approximate the effects of turbulence on flow:

$$\frac{\partial k}{\partial t} + u \cdot \nabla k = \nabla \cdot (v_t \nabla \mathrm{k}) + P_k - \varepsilon \quad (2)$$

where: k is the turbulent kinetic energy (m2/s2), ε – the dissipation rate (m2/s3) and Pk – the turbulent production term.

The predictions of the turbulent wake behind a body (or a section of a wind turbine blade) for different computational models are shown in Fig. 6. This figure highlights the superiority of LES over RANS in capturing the unsteady and turbulent wake dynamics, aligning more closely with experimental data.

This is important for accurate prediction of behavior in wind turbine panels and aerodynamic applications.

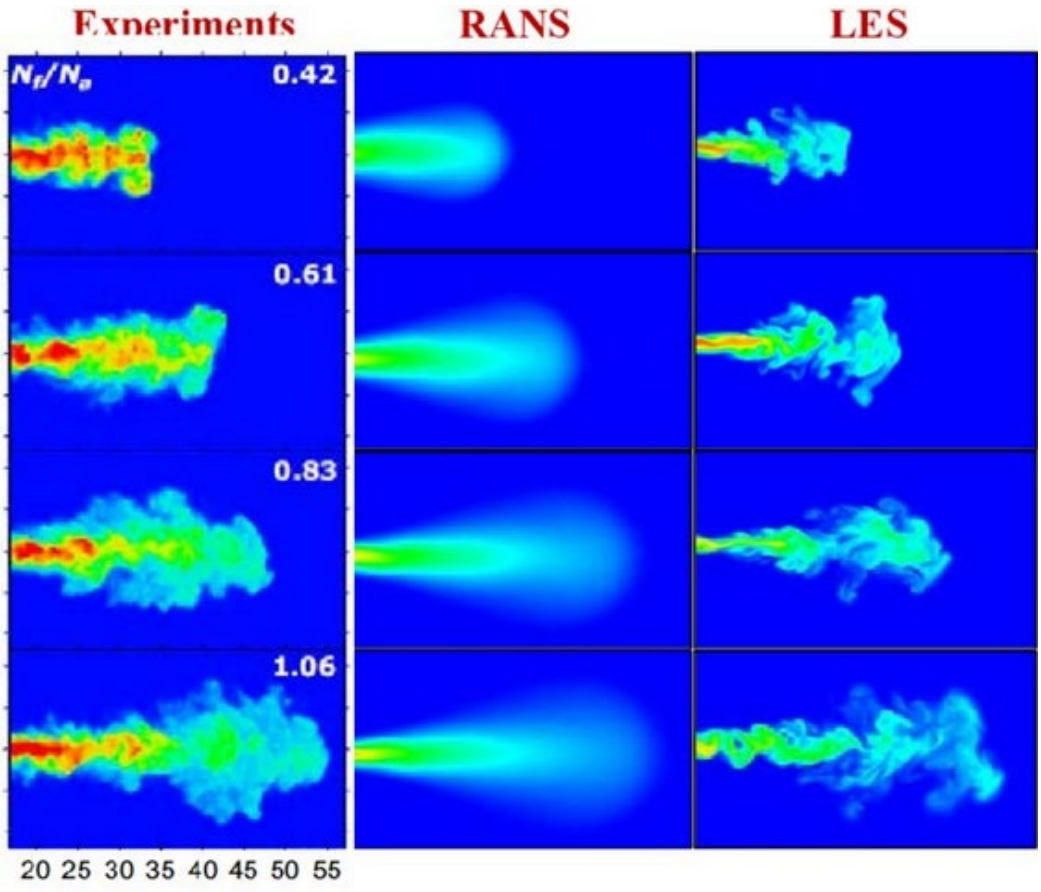

Fig. 6 - Images comparing the equivalence ratio calculated using RANS and LES models
(Som, S. et al., 2012)

In this article, the efficiency of a new vertical axis wind turbine configuration consisting of two counter-rotating Lenz-type wind turbines which will be tested in a wind tunnel was numerically analyzed. The analysis was performed using CFD methods.

MATERIALS AND METHODS

For the development of the counter-rotating vertical axis turbine, its operating parameters were established. This wind turbine is vertical axis and is of the Lenz type (*Gall, M. et al., 2022)*, based on the drag force.

The system of vertical axis wind turbines with dual counter-rotating rotor (Fig. 7), consisting of an upper rotor (1) formed by a set of Lentz-2 type blades (2), which rotates in one direction and a lower rotor (13) with a second set of Lentz-2 type blades (*Bucur, I. O. et al., 2021)* (11), mounted coaxially and rotating in the opposite direction, having coaxial counter-rotating axes (4) which allow the independent rotation of the two sets of blades, characterized in that the coaxial counter-rotating axes (4) are connected to a double-rotation electric generator (6) whose stator and rotor rotate in opposite directions to obtain a double relative speed, thus optimizing the mechanical conversion into electricity and which is provided with a conductive slip ring with inductive coupling (8) which makes possible the contactless transfer of electrical energy from the generator to the electrical box on the support being fixed to the turbine support pole (12) by means of a support flange (7) comprising vibration damping mechanisms (3) and (10) on which UFC type oscillating bearings are mounted, fixed to the turbine support column (12) by means of support flanges (5) and (9), to reduce mechanical stresses.

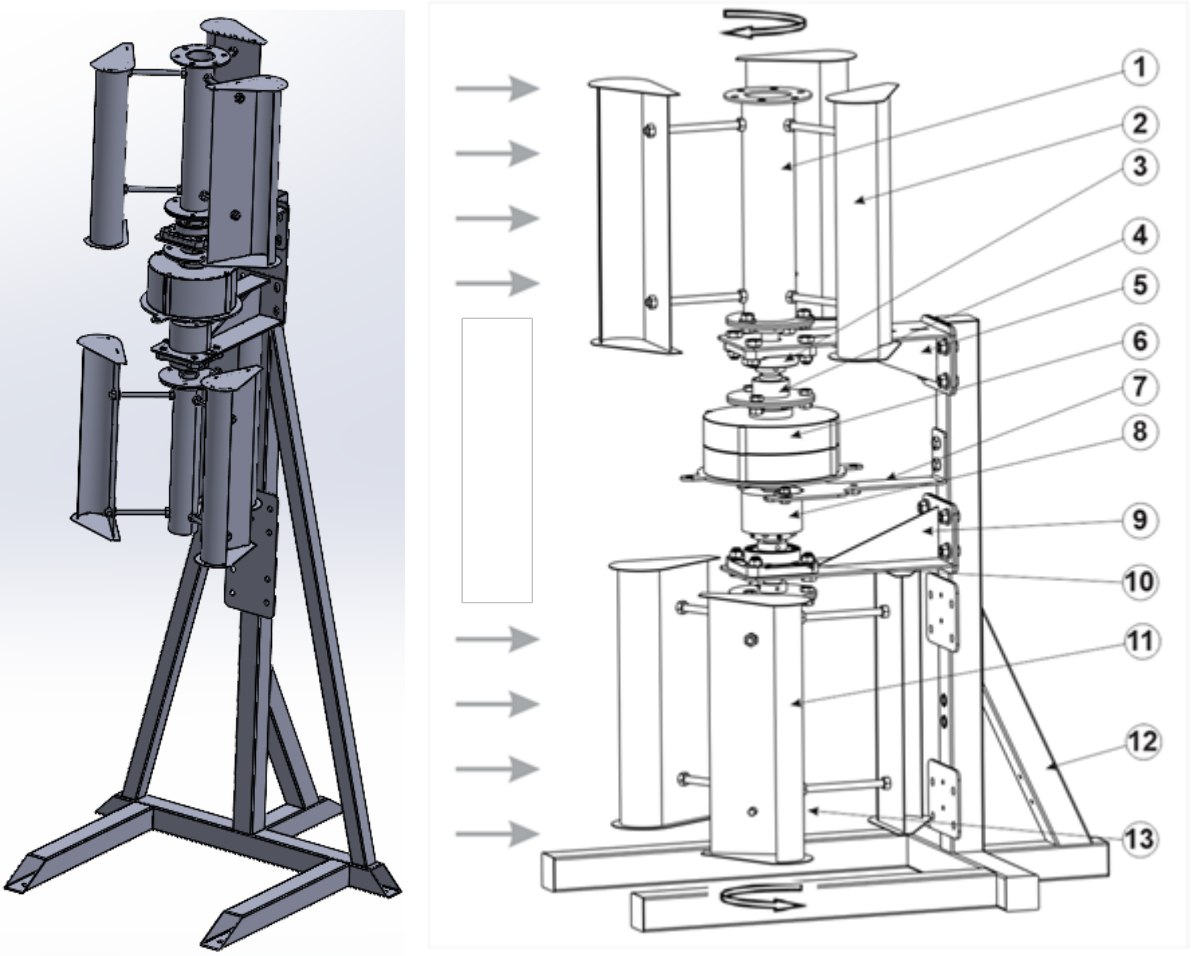

Fig. 7 - CAD model for Lenz type counter-rotating wind turbine

The power coefficient (performance) Cp is determined from the wind power at the turbine shaft. The equations below represent the formula for estimating the power of a wind turbine.

$$P_{wind} = \frac{1}{2}\rho \cdot S \cdot V_{\infty}^{3} \cdot C_p \tag{3}$$

where: P_{wind} is the wind power, ρ 1.225 kg/m3 is the air density, S (m2) is the reference surface, V_{∞} is the wind speed and Cp is the power coefficient.

$$C_{pT} = \frac{P_T}{P_{wind}} = \frac{M \cdot \omega}{\frac{1}{2}\rho S V_{\infty}^{3}} = \frac{\frac{1}{2}\rho S V_{\infty}^{2} L C_m \omega}{\frac{1}{2}\rho S V_{\infty}^{3}} = C_m \frac{L \cdot \omega}{V_{\infty}} = C_m \cdot \lambda < 0.593 \tag{4}$$

To determine the turbine blade chord length, the relative solidity of the turbine rotor radius was expressed, resulting in the parameters in Table 1.

Table 1

Operating parameters for vertical axis wind turbine

V[m/s]	D[m]	c[m]	N	TSR	omega[rad/s]	delta t(2 deg)	it (8 spins)	N [rpm]
12	0.3	0.12	3	0.2	16	0.002182	1440	152.788746
				0.4	32	0.001091		305.577491
				0.6	48	0.000727		458.366237
				0.8	64	0.000545		611.154982
	H[m]			1	80	0.000436		763.943728
	0.6			1.2	96	0.000364		916.732473

The computational domain and grid are created in Ansys Meshing 2024 R1. Using CFD (Computational Fluid Dynamics) simulations, the moment coefficient that will be used to determine the power coefficient can be determined. The equations are solved using the commercial code Fluent. The computational grid for this study is shown in Fig. 8.

The images show the mesh used for the CFD (computational fluid dynamics) simulations of the vertical axis wind turbine (VAWT) model. This mesh was used to discretize the flow domain so that the Navier-Stokes equations governing fluid flow can be solved numerically. The refinement near the turbine ensures an accurate capture of flow separation, vortices, and other aerodynamic effects around the blades.

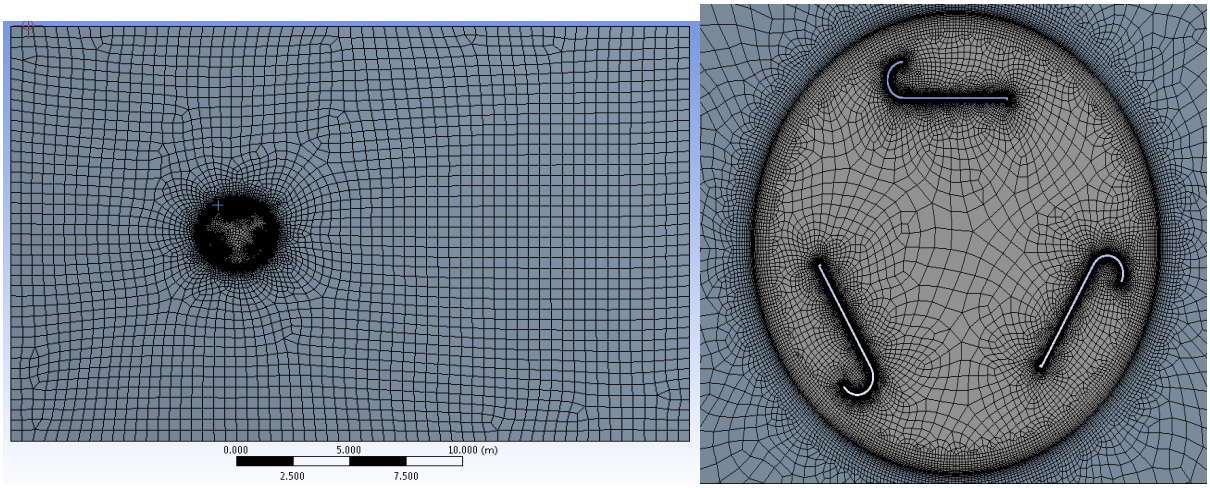

Fig. 8 - The grid made with Ansys Meshing

The first complete turbulence model was introduced by Kolmogorov in 1941 - k-ω, where ω is the specific rate of dissipation of turbulent kinetic energy. The form in which it is defined eliminates the wall functions used to calculate the parameters governing the flow in the vicinity of the walls. This model involves the use of a more efficient calculation grid in the boundary layer area.

The model is extremely sensitive to the variation of the initial conditions, so small variations of ω in the inlet section drastically influence the final results. F.R. Menter built the k-ω SST (Shear Stress Transport) model in 1999.

This is a combination of the standard k-ε model and the k-ω model, using k-ε for the free flow area considered totally turbulent and the k-ω model for the boundary layer.

The transition from one model to the other is ensured by using some fitting functions that activate the k-ε or k-ω formulation depending on the area and by introducing a diffusive term in the transport equation of ω.

For the analysis, the Reynolds number was calculated to be 1e06 and the Menter's Shear Stress Transport (SST) turbulence model was used to perform transient simulations. This model consists of 2 transport equations, which are part of the classical k-omega formulation.

The transport equation for turbulent kinetic energy k:

$$\frac{\partial k}{\partial t}+\bar{u}\frac{\partial k}{\partial x}+\bar{v}\frac{\partial k}{\partial y}+\bar{w}\frac{\partial k}{\partial z}=\frac{1}{\rho}\left[\frac{\partial}{\partial x}\left(\Gamma_k\frac{\partial k}{\partial x}\right)+\frac{\partial}{\partial y}\left(\Gamma_k\frac{\partial k}{\partial y}\right)+\frac{\partial}{\partial z}\left(\Gamma_k\frac{\partial k}{\partial z}\right)\right]+\widetilde{G_k}-Y_k \quad (5)$$

Transport equation for specific dissipation ω:

$$\frac{\partial \omega}{\partial t}+\bar{u}\frac{\partial \omega}{\partial x}+\bar{v}\frac{\partial \omega}{\partial y}+\bar{w}\frac{\partial \omega}{\partial z}=\frac{1}{\rho}\left[\frac{\partial}{\partial x}\left(\Gamma_{\omega}\frac{\partial \omega}{\partial x}\right)+\frac{\partial}{\partial y}\left(\Gamma_{\omega}\frac{\partial \omega}{\partial y}\right)+\frac{\partial}{\partial z}\left(\Gamma_{\omega}\frac{\partial}{\partial z}\right)\right]+G_{\omega}-Y_{\omega}+D_{\omega} \quad (6)$$

where: Γ_k and $\Gamma_\omega$represent the effective diffusivity of k and ω; D_ω^+- the positive portion of the cross-diffusion term; $\widetilde{G_k}$- turbulent kinetic energy production; G_ω – generation of ω.

A first step in setting up the case in the CFD software Ansys Fluent is represented by importing the calculation grid, checking the quality and setting the type of analysis (steady or unsteady). The settings of the case in Ansys Fluent are presented below in Table 2.

Table 2

Case settings in the ANSYS-Fluent 2024 R1 solver

Models	Solver	Pressure Based	Unsteady	3d
	Viscous Model	k-ω SST		
Materials	Air	Density, constat		
Operating conditions	Pressure 101325 [Pa]			
Boundary Condition	Intrare	Velocity inlet: V_x=12m/s		
	Pale	wall		
	Ax	wall		
	Interfata	Interface rotor-stator		
	Rotor	Mesh motion		
	Stator	Stationary		
Solve	Controls	Solution	Courant nr=2	Discretization 2nd order upwind
	Initialize	Intrare		
	Monitors	Residuals	10^{-6}	
		Force	Momentum coeficient	
	Iterate	10^6 Steps	0.001s time step size	
Report	Reference values	Intrare	Length=raza turbinii	

The residuals for all variables decrease rapidly in the first few hundred iterations, indicating that the solution converges well initially (Fig. 9). After about 200 iterations, the residuals level off and oscillate around small values (between 1e-04 and 1e-06 for most variables). The plot indicates that the solution “converges” at iteration 1840, with residuals in the order of 1e-04 to 1e-07, which is generally acceptable for CFD simulations. Oscillations and stagnation at small residual values are common in unsteady simulations or when dealing with complex flow physics such as turbulence.

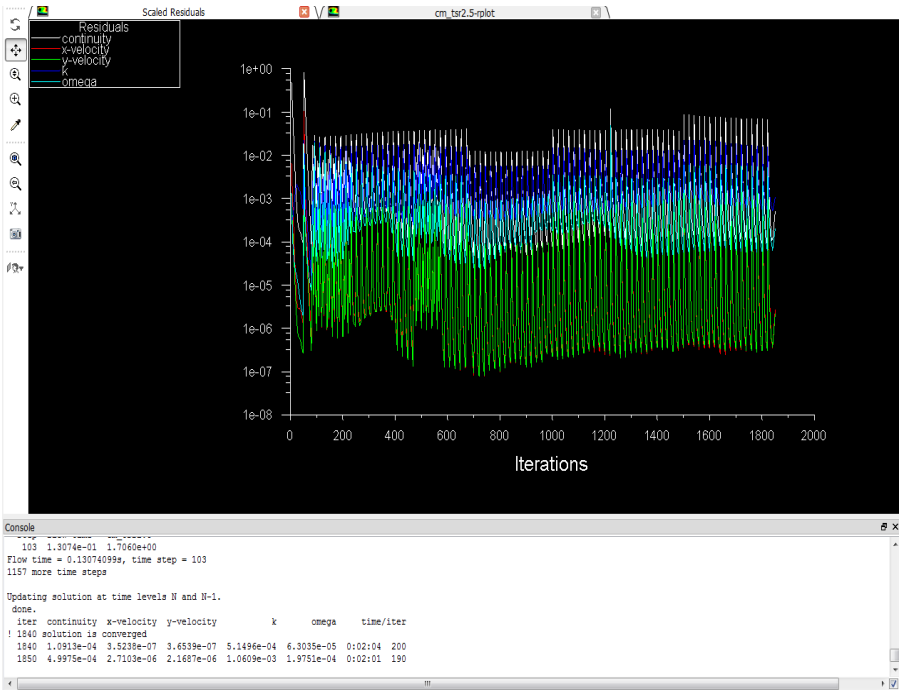

Fig. 9 - Evolution of residues

RESULTS

In the post-processing stage of the numerical data obtained from the unsteady analyses, the recirculation zones and their influence on the wind turbine performance were analyzed. The variation of the moment coefficient for different values of the TSR was also monitored. Following this step, the turbine operating characteristic was obtained, which consists of the graphic representation of the variation of the power coefficient as a function of the TSR (tip speed ratio).

The graph below represents the variation of the torque coefficient Ct as a function of the azimuth angle θ for different tip speed ratios (TSR) of the vertical axis wind turbine. On the X axis is represented the azimuth angle (theta) in degrees, varying from 0° to 360°, representing a complete rotation of the turbine blade, and on the Y axis is represented the torque coefficient (Ct), which measures the momentum generated in relation to the available wind energy. Each curve corresponds to a different TSR value, ranging from 0.2 to 1.2.

At lower TSRs (0.2; 0.4), the power factor exhibits more pronounced peaks and troughs. As the TSR increases, the peaks become less sharp and the curve smooths out. The highest Ct values appear to be close to TSRs of 0.2 and 0.4, indicating a good performance even at these low TSRs.

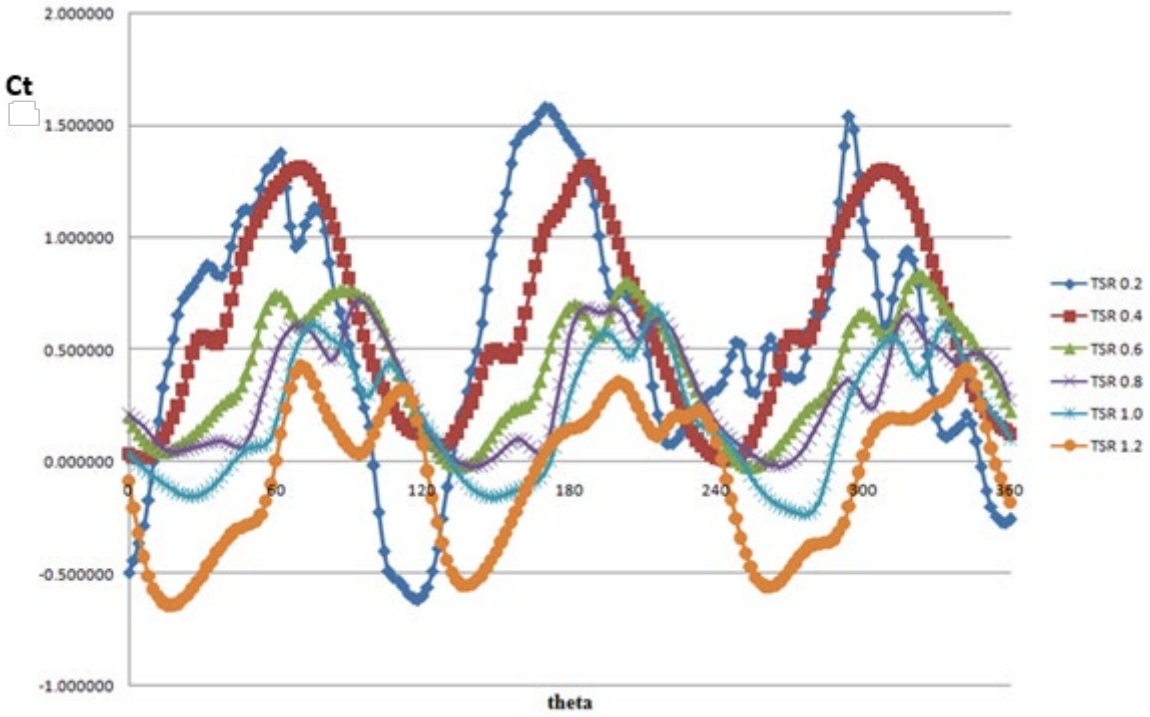

Fig. 10 - Variation of the torque coefficient

Fig. 11 and Fig. 12 show CFD (Computational Fluid Dynamics) visualizations of the vorticity magnitude around the vertical axis wind turbine, captured at different blade positions. The vorticity magnitude is represented by the colour scale at the bottom, ranging from low (blue) to high (red) values. Vortex indicates local rotation of fluid particles, related to turbulence and vortex structures.

Each panel (a, b, c, d) shows the flow field and vortex formation around the turbine blades at different angles. The turbine rotor area is delimited by a circle, showing the blade positions and the flow wake inside.

The regions near the blade tips and leading/trailing edges show high vorticity (yellow to red), indicating strong vortex shedding. Vortices form and break up downstream, creating a complex wake of interacting vortex structures. The differences between the panels show how the vorticity evolves as the blades rotate, highlighting unstable aerodynamic phenomena.

Vortex break-up influences the aerodynamic forces on the blades, affecting power output and structural loads. Understanding the distribution of vorticity helps optimize blade design and spacing to reduce losses and fatigue.

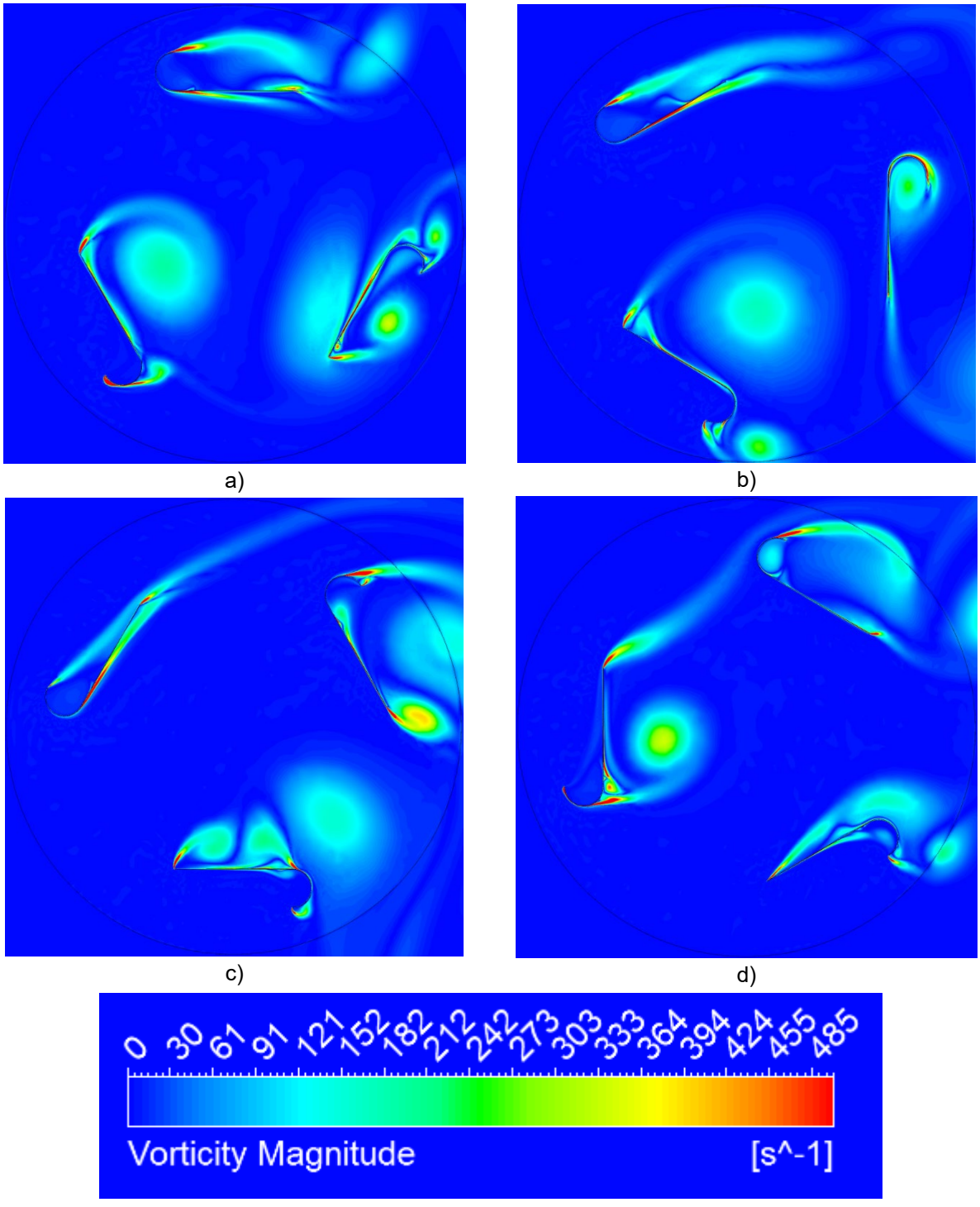

Fig. 11 - Variation of vorticity magnitude for TSR 0.4
a) 0 degree; b) 30 degrees; c) 60 degrees; d) 90 degrees.

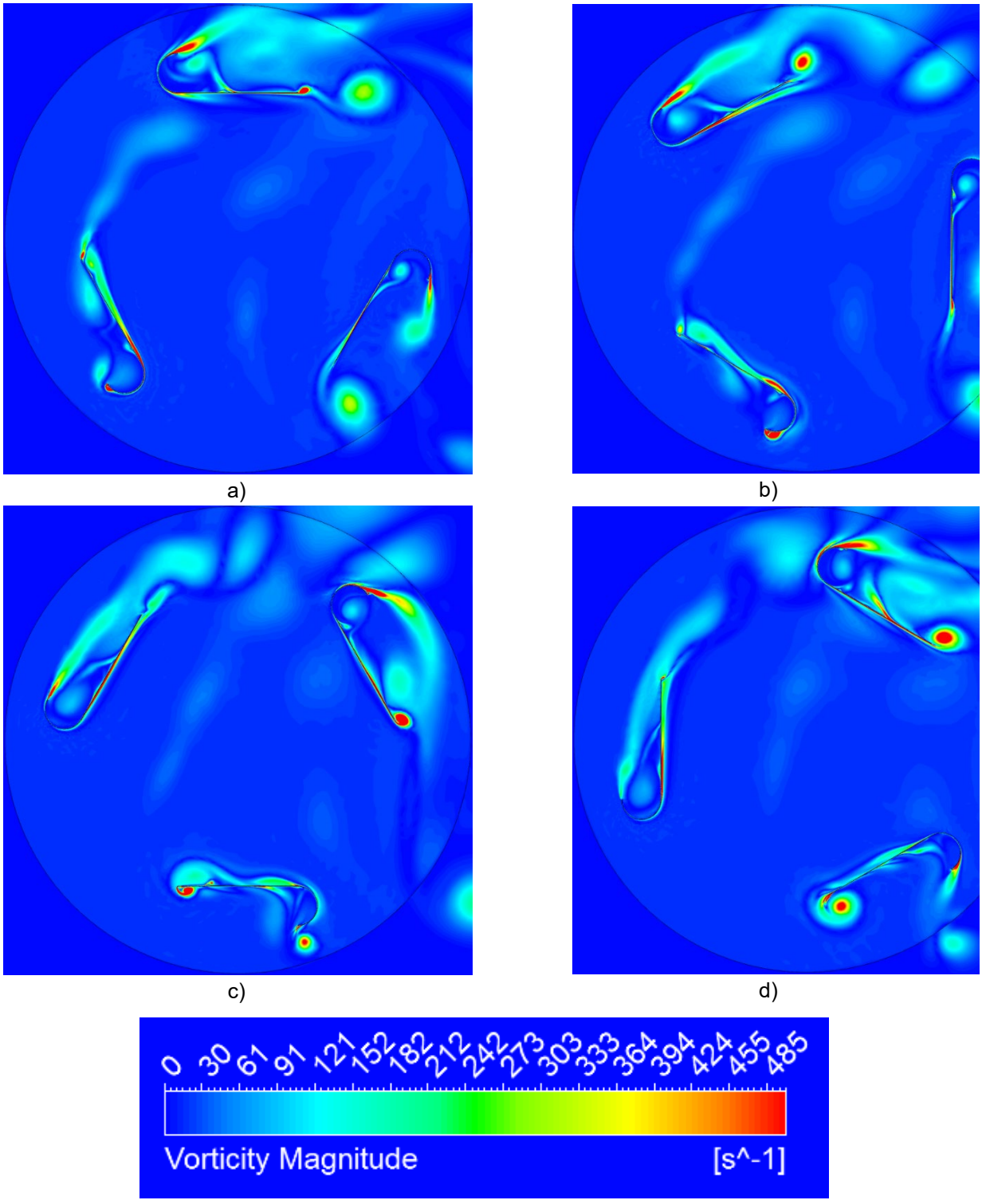

Fig. 12 - Variation of vorticity magnitude for TSR 0.8
a) 0 degree; b) 30 degrees; c) 60 degrees; d) 90 degrees.

CONCLUSIONS

This research presented a numerical investigation of a novel vertical axis wind turbine (VAWT) design featuring two Lenz-type turbines rotating in opposite directions. The study objective was the aerodynamic performance and flow features of this new configuration by means of three-dimensional (3D) Computational Fluid Dynamics (CFD) simulations with ANSYS Fluent 2024 R1.

Simulations were conducted at a steady wind speed of 12 m/s and a range of changing tip speed ratios (TSR) from 0.2 up to 1.2. The SST (Shear Stress Transport) turbulence model was employed in order to capture the unsteady and separated flow around the rotating blades.

Torque fluctuation throughout a full revolution was analyzed for each TSR. The results show that under low TSRs (i.e., 0.2–0.4), the turbine experienced high torque fluctuations due to dominant unsteady flow effects and periodic flow separation. As the TSR increased, the torque behavior became stabilized, with the optimal performance at 0.8, which represented an optimal operating range for the configuration. The counter-rotation arrangement appeared to reduce torque asymmetry and phase lag between the two turbines, resulting in a smoother mechanical output.

The vorticity magnitude contours provided insightful information on the dynamics of the interaction flow between the two counter-rotating rotors. At mid-to-high TSRs, vortex interaction between the rotors created more evenly distributed wake structures and interference zones that were reduced in size. This imply that there are aerodynamic benefits of the opus configuration, particularly in terms of wake loss reduction and improvement in downstream flow quality.

Despite the positive results, there were certain limitations to the study. The simulations were restricted to 10 full revolutions owing to computational cost, and this can limit the long-term evolution of the flow and statistical convergence of unsteady phenomena. In addition, only one wind speed was analyzed, and the rotor geometry was not optimized.

To overcome these restrictions, a physical model of the turbine has been designed and will be wind tunnel tested. Future work will include experimental verification of CFD predictions, as well as further parametric studies including blade profile optimization, rotor spacing, and dynamic stall modeling. More simulations at varied inflow conditions and yaw angles are also on the horizon to check the design's robustness under realistic operating scenarios.

In conclusion, the proposed turbine concept design has positive aerodynamic characteristics, including stable torque generation and constructive vortex interactions under design operating conditions. The findings confirm the feasibility of the configuration as an efficient and compact wind energy product for distributed power systems, particularly for variable direction and moderate wind speed conditions.

REFERENCES

[1] Al Noman, A., Tasneem, Z., Sahed, M. F., Muyeen, S. M., Das, S. K., & Alam, F. (2022). Towards next generation Savonius wind turbine: Artificial intelligence in blade design trends and framework. Renewable and Sustainable Energy Reviews, 168, 112531.

[2] Bianchini, A., Balduzzi, F., Bachant, P., Ferrara, G., & Ferrari, L. (2017). Effectiveness of two-dimensional CFD simulations for Darrieus VAWTs: a combined numerical and experimental assessment. Energy Conversion and Management, 136, 318-328.

[3] Bucur, I. O., Malael, I., & Preda, D. (2021, May). Numerical investigation of a reduced scale Lenz wind turbine model for aerodynamic tunnel applications. In IOP Conference Series: Earth and Environmental Science (Vol. 664, No. 1, p. 012027). IOP Publishing.

[4] Cabezon, D., Migoya, E., & Crespo, A. (2011). Comparison of turbulence models for the computational fluid dynamics simulation of wind turbine wakes in the atmospheric boundary layer. Wind Energy, 14(7), 909-921.

[5] Calautit, K., Aquino, A., Calautit, J. K., Nejat, P., Jomehzadeh, F., & Hughes, B. R. (2018). A review of numerical modelling of multi-scale wind turbines and their environment. Computation, 6(1), 24.

[6] Cheng, B., & Yao, Y. (2022). Design and optimization of a novel U-type vertical axis wind turbine with response surface and machine learning methodology. Energy Conversion and Management, 273, 116409.

[7] Chintan Kariya, Energy Production By Vertical Axis Wind Turbine ,Technical Report April 2017, DOI: 10.13140/RG.2.2.10994.04801

[8] Chowdhury, A. M., Akimoto, H., & Hara, Y. (2016). Comparative CFD analysis of vertical axis wind turbine in upright and tilted configuration. Renewable energy, 85, 327-337.

[9] Delafin, P. L., Nishino, T., Kolios, A., & Wang, L. (2017). Comparison of low-order aerodynamic models and RANS CFD for full scale 3D vertical axis wind turbines. Renewable Energy, 109, 564-575.

[10] Fatahian, E., Mishra, R., Jackson, F. F., & Fatahian, H. (2024). Optimization and analysis of self-starting capabilities of vertical axis wind turbine pairs: A CFD-Taguchi approach. Ocean Engineering, 302, 117614.

[11] Gall, M., Mălăel, I., & Preda, D. (2022, July). Computational analysis of fence-type vertical axis wind turbines array suitable for urban architecture integration. In 2022 26th International Conference on Circuits, Systems, Communications and Computers (CSCC) (pp. 204-210). IEEE.
[12] Gielen D., Boshell F., Saygin D., Bazilian M.D., Wagner N., Gorini R., The role of renewable energy in the global energy transformation, Energy strategy reviews, 2019, 24, 38-50.
[13] Huish, C., Shakya, P., Seibi, A. C., Arias, D., Shekaramiz, M., & Masoum, M. A. (2025). Comparison of applied loads on horizontal axis wind turbine blades using an open-source software Qblade and CFD solver ANSYS-FLUENT. Wind Engineering, 49(4), 910-924.
[14] Malael, I., & Bucur, I. O. (2021). Numerical Evaluation of the Flow around a New Vertical Axis Wind Turbine Concept. Sustainability, 13(16), 9012.
[15] Ouro, P., & Lazennec, M. (2021). Theoretical modelling of the three-dimensional wake of vertical axis turbines. Flow, 1, E3.
[16] Qi, Y., Hong, J., Wang, H., & Qian, W. (2025). Analysis of the Connection between Aerodynamic Force, Deformation, Flow, and Structure of Wind Turbine Blades Using Dynamic Mode Decomposition. Journal of Engineering Mechanics, 151(11), 04025071.
[17] Som, S., Longman, D. E., Luo, Z., Plomer, M., Lu, T., Senecal, P. K., & Pomraning, E. (2012). Simulating flame lift-off characteristics of diesel and biodiesel fuels using detailed chemical-kinetic mechanisms and large eddy simulation turbulence model.
[18] Sørensen, J. N. (2016). General momentum theory for horizontal axis wind turbines (Vol. 4). New York: Springer.
[19] Wagner, H. J. (2020). Introduction to wind energy systems. In EPJ web of conferences (Vol. 246, p. 00004). EDP Sciences.

CHICKPEA PRODUCTIVITY UNDER BIOTIC AND ABIOTIC STRESSES: CURRENT STATUS AND PERSPECTIVES

/

PRODUCTIVITATEA NĂUTULUI ÎN CONDIȚII DE STRES BIOTIC ȘI ABIOTIC: SITUAȚIA ACTUALĂ ȘI PERSPECTIVE

Costin MIRCEA*[1)], Florin NENCIU[1)], Alexandru IONESCU[1)], Iulian DUMITRU[1)], Raluca-Adriana ZOTA[2)]
[1)] National Institute of Research - Development for Machines and Installations Designed to Agriculture and Food Industry – INMA Bucharest / Romania;
[2)] National University of Science and Technology POLITEHNICA Bucharest / Romania.
**Tel: 0766.420.952; *E-mail: costinmircea@yahoo.com*

***Keywords*:** *chickpea, biotic stress, abiotic stress*

ABSTRACT

Chickpea (Cicer arietinum L.) is the second most important legume crop globally, playing a vital role in food security and sustainable agriculture. Its productivity is significantly affected by biotic stresses such as diseases and pests, as well as abiotic stresses including drought, salinity, and extreme temperatures. This article reviews the physiological, biochemical, and molecular mechanisms underlying chickpea responses to these adverse conditions, alongside current breeding strategies and agronomic practices aimed at improving resilience. Integrated understanding of these factors is essential for developing high-performing varieties capable of stable yields under changing climatic conditions.

REZUMAT

Năutul (Cicer arietinum L.) este a doua cea mai importantă leguminoasă cultivată la nivel global, cu un rol esențial în securitatea alimentară și agricultura durabilă. Productivitatea sa este însă afectată semnificativ de stresuri biotice, precum boli și dăunători, și abiotice, cum ar fi seceta, salinitatea și temperaturile extreme. Acest articol sintetizează principalele mecanisme fiziologice, biochimice și moleculare prin care năutul răspunde acestor condiții adverse, precum și strategiile actuale de ameliorare genetică și practici agronomice pentru creșterea rezilienței. Înțelegerea integrată a acestor aspecte este esențială pentru dezvoltarea unor soiuri performante, capabile să asigure o producție stabilă în contextul schimbărilor climatice globale.

INTRODUCTION

Chickpea (*Cicer arietinum* L.) (Figure 1) holds the esteemed position of being the second most cultivated and consumed legume crop globally *(FAOSTAT. FAO)*. It is widely distributed in the tropics, subtropics, and temperate regions *(Anbessa, Y. et al, 2009)*, and is believed to have originated in present-day southeastern Turkey and the surrounding regions of Syria *(Van der Maesen, L.J.G., 1987; Negusse, H. et al, 2025)*. Chickpea is an annual herbaceous crop belonging to the genus *Cicer*, with cultivation extending to more than 50 countries worldwide, covering a total area of 12.14 million hectares and an annual production of 11.30 million tons *(Food and Agriculture Organization of the United Nations, 2012)*. Major producing countries include Canada, India, Myanmar, Pakistan, Turkey, Ethiopia, Iran, Mexico, Australia, and the USA *(Singh, V. et al, 2020)*, with northwestern Mexico representing one of the key regions of production. Ethiopia, for instance, ranks among the six largest chickpea-producing countries globally and is the leading producer, consumer, and exporter of chickpeas in Africa, accounting for more than 14% of its legume production, with 0.46 million tons produced on 0.22 million hectares *(Rawal, V.N.D.K. et al, 2019; Akpo, E. et al, 2021; CSA 2021; Sori, A. et al, 2025)*.

Chickpea plays a crucial role in global food security. Legume seeds are a staple in the diet of many people worldwide, particularly in poorer regions where access to animal protein such as meat, fish, and dairy is limited *(Martín-Cabrejas M. A., 2019; Castañeda, A.L. et al, 2025)*. Chickpeas are highly nutritious, with seeds containing 20–30% protein, 40% carbohydrates, and 3–6% oil *(Gil, J. et al, 1996)*. They also provide a rich source of bioactive compounds, including amino acids, fatty acids, polysaccharides, phenolic compounds, antioxidants, and other phytochemicals *(Johnson, N.A.N. et al, 2024; Kaur, R., Prasad, K., 2021; Khalid, W. et al, 2025)*. In addition to human nutrition, chickpea stover serves as a nutrient-rich

supplement for livestock during lean seasons *(Li, H. et al, 2015)*. Beyond its nutritional value, chickpea is an important crop in sustainable farming systems, being often grown in rotation with cereals as a disease break and contributing to soil fertility through atmospheric nitrogen fixation *(Singh, K. B., 1997).*

Fig. 1 - Chickpea (*Cicer arietinum* L.) *(The Global Bean Project)*

Despite its global importance and adaptability, chickpea productivity is seriously constrained by multiple stresses. Growth, development, and yield are strongly influenced by climatic and environmental conditions *(Saeed, M., 2024)*.

This legume is particularly sensitive to heat stress during the reproductive stage, leading to reduced flowering, flower abortion, and poor pod formation, which collectively represent a major limiting factor for yield *(Naveed, M. et al, 2025)*.

Furthermore, chickpea productivity is hindered by both biotic and abiotic factors, including diseases, insect pests, drought, salinity, and heavy metal toxicity *(Shehzadi, K. et al, 2025)*. These stresses remain the major bottlenecks for achieving yield stability and expanding chickpea production worldwide.

MATERIALS AND METHODS

1. Major Abiotic Stresses in Chickpea Cultivation

Chickpea productivity is strongly influenced by climatic and pedological conditions of the cultivation environment, with abiotic stresses such as drought, salinity, and extreme temperatures representing the main yield-limiting factors. These conditions trigger complex physiological and biochemical responses that negatively affect germination, vegetative growth, pod formation, and seed filling.

1.1. Drought

Drought is the most frequent and severe abiotic stress affecting chickpea cultivation (Table 1), particularly in the semi-arid regions of South Asia, East Africa, and the Middle East. During the reproductive stages—especially flowering and seed-filling—water deficit leads to a reduction in the number of fertile flowers, increased flower abortion, and a drastic decrease in pod formation.

Table 1

Major abiotic stresses affecting chickpea and their effects

Stress Type	Region/Example	Effect on Plant	Tolerant Mechanisms	References
Drought	South Asia, East Africa, Middle East	Reduced flowering, flower abortion, poor pod formation	Deep roots, osmolyte accumulation (proline, soluble sugars), LEA proteins	*Negusse, H. et al, 2025; Kashiwagi, J. et al, 2006.*
Salinity	Global (20% agricultural land)	Reduced photosynthesis, chlorophyll, nutrient imbalance	Ion exclusion (Na^+/Cl^-), K^+/Na^+ homeostasis, antioxidant enzymes (SOD, CAT)	*Eyasu, W. et al, 2025*
Heat	India, Pakistan, Ethiopia	Pollen sterility, ovule inviability, reduced pod set	Heat shock proteins (HSPs), membrane stability, transpiration cooling	*Soren, K. R. et al, 2021*
Heavy Metals / UV	Mining areas, polluted soils	Reduced germination, impaired metabolism	Detoxifying enzymes, restricted uptake	–

According to studies by *Negusse, H. et al, 2025*, severe drought can reduce chickpea yield by up to 70%, depending on the genotype and the timing of stress occurrence. Tolerant genotypes are characterized by deep rooting, rapidly responsive stomata, and increased accumulation of osmolytes such as proline and soluble sugars. In addition, tolerance is often associated with the activation of genes involved in free radical detoxification, osmotic stress regulation, and the synthesis of LEA (Late Embryogenesis Abundant) proteins.

1.2. Salinity

Soil salinization affects over 20% of global agricultural land, and chickpea is moderately sensitive to this stress. The presence of toxic ions such as Na^+ and Cl^- interferes with the uptake of essential nutrients (K^+, Ca^{2+}), reducing the plant's ability to maintain osmotic balance and optimal photosynthetic function.

Several studies have shown that salinity decreases photosynthetic efficiency and chlorophyll content while increasing lipid peroxidation, indicating cellular membrane damage. Tolerant genotypes respond by accumulating proline, regulating ion transport (maintaining a favorable K^+/Na^+ ratio), and activating antioxidant enzymes such as SOD and CAT. A recent study by *Eyasu, W. et al, 2025,* demonstrated that the application of natural biostimulants can mitigate the effects of salinity by enhancing the antioxidant system and improving growth parameters.

1.3. High Temperatures

Heat waves associated with climate change increasingly affect chickpea growing regions, particularly in India, Pakistan, and Ethiopia. Temperatures above 35°C during the flowering period lead to pollen sterility, reduced ovule viability, and impaired synthesis of hormones involved in pod development.

Heat stress triggers the accumulation of reactive oxygen species (ROS) and causes denaturation of structural and enzymatic proteins. Thermotolerant genotypes maintain better cooling capacity through transpiration, exhibit high membrane stability, and have increased levels of heat shock proteins (HSPs). Additionally, QTL loci associated with high-temperature tolerance have been identified and can be utilized in molecular breeding programs.

1.4. Other Relevant Abiotic Stresses

Although less frequent, stresses caused by UV radiation, heavy metal pollution (e.g., Cd and Pb), or unsuitable soil pH can also affect chickpea development and productivity. In particular, in areas affected by mining activities or excessive irrigation, the accumulation of sodium or toxic metals reduces plant viability and interferes with fundamental metabolic processes.

2. Biotic Stresses: Major Diseases and Pests in Chickpea Cultivation

Although chickpea is relatively tolerant to unfavorable environmental conditions, its productivity is severely affected by a range of biotic stresses, particularly diseases caused by fungi, bacteria, and viruses,

as well as attacks by specific insect pests (Figure 2). Under favorable conditions for the pathogens or pests, these factors can lead to yield losses of up to 100% in untreated cases or in the absence of resistant genotypes.

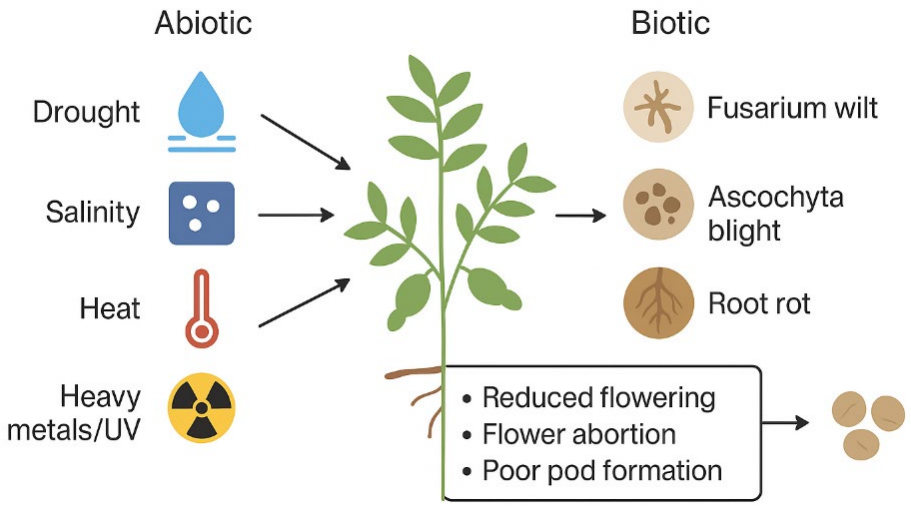

Fig. 2 - Major Abiotic and Biotic Stresses Affecting Chickpea Productivity

2.1. Vascular Wilt – Fusarium oxysporum f. sp. Ciceris

This is one of the most devastating diseases of chickpea, prevalent in hot and dry regions of South Asia, East Africa, and the Middle East. The pathogen invades the root system and colonizes the vascular tissues, leading to gradual wilting of the plant. Symptoms include chlorosis, browning of vascular tissues, and eventual collapse of the entire plant.

Physiological races vary by region, complicating the selection of resistant genotypes. Genetic tolerance is controlled by one or more major loci, and breeding efforts include the introgression of resistance genes from traditional genotypes or wild species *(Jimenez-Gasco, M. M. et al, 2004)*.

2.2. Ascochyta Blight – Ascochyta rabiei

Ascochyta blight is a destructive foliar disease, common in regions with relatively high humidity. The pathogen produces circular lesions on leaves, stems, and pods, accompanied by visible pycnidia. In advanced stages, the infection leads to complete necrosis of the aerial parts.

The plant's response to *Ascochyta rabiei* involves the rapid activation of genes related to phytoalexin synthesis, accumulation of phenolic compounds, and strengthening of cell walls. Disease management relies on a combination of resistant cultivars, crop rotation, and fungicide treatments *(Varshney, R. K. et al, 2019)*. *Fusarium* wilt and *Ascochyta* blight are the most devastating diseases (Table 2).

Table 2

Major biotic stresses affecting chickpea productivity

Stress Type	Causal Agent	Symptoms	Yield Loss	Control Strategies	References
Vascular wilt	Fusarium oxysporum f. sp. ciceris	Chlorosis, browning, wilting	Up to 80%	Resistant genotypes, crop rotation	*Jimenez-Gasco, M. M. et al, 2004*
Ascochyta blight	Ascochyta rabiei	Leaf, stem, pod lesions; necrosis	High	Resistant varieties, fungicides, rotation	*Varshney, R. K. et al, 2019*
Root rot	Rhizoctonia solani, Sclerotium rolfsii	Necrotic roots, stunted seedlings	Moderate to high	Biocontrol (Trichoderma spp.), resistant varieties	-
Insect pests	Helicoverpa armigera	Flower, pod, seed damage	Up to 90%	Selective insecticides, pheromone monitoring, transgenic lines	-
Storage pest	Sitophilus spp., Callosobruchus chinensis	Seed weight loss, reduced germination	Post-harvest losses	Drying <9% moisture, bioinsecticides, hermetic storage	-

2.3. Root Rot – Rhizoctonia solani, Sclerotium rolfsii

This disease affects young plants, especially in warm and moist soils, causing necrosis of roots and basal stems. Early infections result in poor emergence or death of seedlings. Effective control involves the use of biocontrol agents (*Trichoderma* spp.), soil sterilization, and the cultivation of partially resistant varieties.

2.4. Viruses and Phytoplasmas

Although less frequent, viral infections such as Chickpea stunt disease (transmitted by leafhoppers – *Orosius albicinctus*) or Bean yellow mosaic virus can have a major impact on yield. These infections cause stunting, chlorosis, leaf deformation, and reduced pod formation. No effective treatments exist, making preventive measures essential, including off-season planting to avoid vector activity and the use of certified seeds.

2.5. Major Pests

Helicoverpa armigera (pod borer)

This species is considered the most important chickpea pest worldwide. The larvae feed on flowers, pods, and developing seeds. Damage can reach up to 90% in the absence of control measures. Management strategies include the use of selective insecticides, pheromone-based monitoring, and the development of transgenic lines (e.g., Bt-chickpea, still under research).

Sitophilus spp. and Callosobruchus chinensis (storage pests)

They affect seeds during storage. These beetles reduce seed weight, germination viability, and nutritional quality. Control measures include drying seeds to below 9% moisture, applying bioinsecticidal treatments, and using hermetic packaging.

3. Physiological and Biochemical Responses of Chickpea to Stress

Chickpea adaptation to biotic and abiotic stresses involves a range of integrated responses at the morphophysiological, biochemical, and molecular levels. These mechanisms enable the plant to survive and partially maintain productivity under stress conditions by conserving water, reducing oxidative losses, and regulating hormonal balance. This section presents the main adaptations documented in recent scientific literature.

3.1. Responses to Water Stress

Under drought conditions, chickpea activates a series of mechanisms to conserve water and maintain essential physiological functions (Figure 3):

- **Stomatal closure** – reduces transpiration but also limits photosynthesis;
- **Decrease in osmotic potential** – through accumulation of compatible osmolytes (proline, glycine betaine, soluble sugars);
- **Deeper roots** – tolerant genotypes (e.g., ICC 4958) exhibit an extensive root system, efficient in extracting water from deep soil profiles *(Kashiwagi, J. et al, 2006)*;
- **Reduction of leaf area** – minimizes water loss through transpiration.

3.2. Regulation of Oxidative Balance

Most stresses (drought, salinity, heat, pathogens) lead to the accumulation of reactive oxygen species (ROS) – unstable molecules that damage lipids, proteins, and DNA.

To counteract this, plants activate antioxidant systems, such as:

- **Superoxide dismutase (SOD) –** converts superoxide (O_2^-) into hydrogen peroxide (H_2O_2);
- **Catalase (CAT) and peroxidase (POD) –** decompose H_2O_2 into water and oxygen;
- **Ascorbate peroxidase (APX) –** plays a key role in defense against oxidative stress;
- **Non-enzymatic compounds –** glutathione, ascorbic acid, flavonoids, carotenoids *(Ahmad, P. et al, 2022)*.

3.3. Biochemical Changes Specific to Salinity Stress

In saline soils, chickpea responses include:

- **Exclusion of toxic ions (Na^+ and Cl^-)** from aerial tissues;
- **Maintenance of a favorable K^+/Na^+** ratio in meristematic cells;
- **Deposition of lignin and callose** in cell walls to limit the entry of harmful ions;
- **Increase in proline content** and reduction of osmotic stress *(Negusse, H. et al, 2025)*.

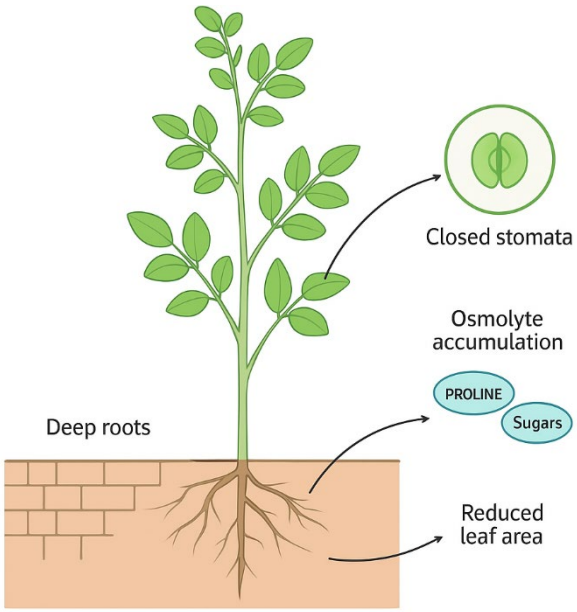

Fig. 3 - Physiological responses of chickpea to drought stress

3.4. Hormonal Responses

Plant hormones regulate numerous adaptive responses:

- **Abscisic acid (ABA) –** increases during drought and salinity; induces stomatal closure and expression of tolerance-related genes;
- **Salicylic acid (SA) and jasmonate (JA) –** involved in defense against pathogens;
- **Ethylene –** regulates senescence and activation of stress responses;
- **Auxins and cytokinins –** influence growth and developmental balance under stress.

3.5. Gene Expression and Stress Proteins

Chickpea copes with stress through regulation of gene expression:

- **LEA proteins (Late Embryogenesis Abundant) –** stabilize membranes and proteins during dehydration;
- **Heat shock proteins (HSPs) –** protect enzymes and cellular structures under high temperatures;
- **Transcription factors (TFs) –** such as DREB, MYB, NAC, WRKY – regulate the stress response cascade *(Soren, K. R. et al, 2021)*.

3.6. Morphological Adaptations

- **Leaf pubescence –** reflects excessive solar radiation;
- **Thick and waxy cuticle –** reduces water evaporation;
- **Reduced leaf angle –** minimizes overheating.

RESULTS

4.1. Impact of Biotic and Abiotic Stresses on Chickpea Productivity

Biotic stresses (diseases, pests) and abiotic stresses (drought, salinity, heat, acidic soils) significantly reduce the production potential of chickpea, affecting all stages of plant development, from germination to seed formation. Vascular wilt caused by *Fusarium oxysporum* f. sp. *ciceris* and Ascochyta blight remain the most frequent and severe diseases, causing yield losses of up to 80% under unfavorable conditions *(Varshney, R. K. et al, 2019)*. Pests such as *Helicoverpa armigera* further reduce yield by damaging pods and developing seeds.

Abiotic stresses, particularly water deficit and salinity, directly influence photosynthetic processes, nutrient uptake, and cellular metabolism. The relative impact of major abiotic and biotic stresses on chickpea yield is illustrated in Figure 4. In semi-arid regions, terminal drought particularly affects the reproductive stages, severely impacting pod number and size *(Kashiwagi, J. et al, 2006)*. Salinity limits plant growth through ion toxicity and osmotic stress, disrupting ionic balance and enzymatic processes *(Negusse, H. et al, 2025)*.

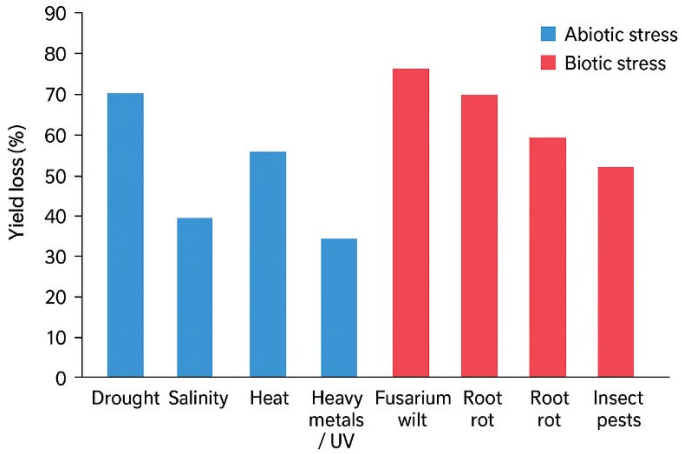

Fig. 4 - Impact of Major Abiotic and Biotic Stresses on Chickpea Yield

4.2. Adaptive Mechanisms of Chickpea to Stress

Chickpea plants have developed a range of physiological and biochemical responses to counteract stress effects:

- **Drought adaptations:** deep roots, osmolyte accumulation, stomatal closure, and morphological modifications (cuticle, leaf pubescence) *(Kashiwagi, J. et al, 2006)*.
- **Oxidative stress management:** activation of antioxidant systems (SOD, CAT, APX), synthesis of phenolic compounds and other antioxidants *(Ahmad, P. et al, 2022)*.
- **Hormonal responses:** increased ABA levels to regulate stomatal closure and stress-related gene expression, involvement of SA and JA in defense against pathogens *(Soren, K. R. et al, 2021)*.
- **Stress protein expression:** LEA proteins and HSPs that stabilize cellular structures under dehydration and high-temperature conditions.

These mechanisms are interconnected, providing multifactorial tolerance that varies among genotypes. The adaptive responses of chickpea under combined biotic and abiotic stresses are summarized in Figure 5.

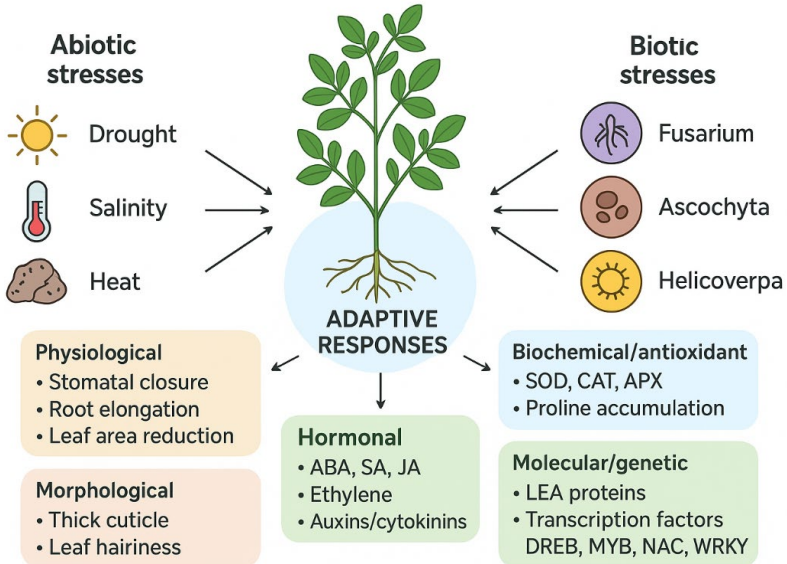

Fig. 5 - Integrated Adaptive Mechanisms of Chickpea under Combined Biotic and Abiotic Stresses

4.3. Modern Breeding and Management Strategies

Technological advances have enabled the integration of effective strategies to enhance chickpea resilience:

- **Marker-assisted breeding:** identification of genes and QTLs associated with tolerance to multiple stresses facilitates rapid and precise selection *(Varshney, R. K. et al, 2019)*.
- **Utilization of local and wild genetic resources:** the genetic diversity of landraces and related species is exploited to introduce stress-tolerance traits *(Negusse, H. et al, 2025)*.
- **Integrated agronomic practices:** crop rotation, targeted fungicide applications, optimized irrigation and fertilization improve plant stress responses.
- **Emerging biotechnologies:** genome editing (e.g., CRISPR-Cas9) and the use of beneficial microorganisms (rhizobacteria, mycorrhizae) are at the experimental stage but offer promising sustainable solutions.

4.4. Challenges and Perspectives

Despite significant progress, major challenges remain:

- **Genetic complexity of multifactorial tolerance:** requires holistic and collaborative approaches among geneticists, physiologists, and agronomists.
- **Impact of climate change:** may exacerbate simultaneous multiple stresses, necessitating the development of cultivars with broad resilience.
- **Adoption of innovative technologies:** remains limited in vulnerable regions due to costs and infrastructure constraints.

CONCLUSIONS

Chickpea (Cicer arietinum L.) is a crucial legume crop for global food security due to its high nutritional value and important role in sustainable agricultural systems. However, its productivity is severely constrained by a wide range of biotic and abiotic stresses, which directly affect plant development and yield.

Biotic stresses, such as fungal diseases and pest attacks, continue to cause significant losses, while **abiotic factors**—drought, salinity, extreme temperatures, and unfavorable soil conditions—impose constant pressure on chickpea's adaptive capacity.

Chickpea's **physiological and biochemical responses** to these stresses are complex and involve stomatal regulation, accumulation of osmoprotective compounds, activation of antioxidant systems, and modulation of gene expression. Understanding these mechanisms is essential for developing effective breeding strategies.

Advances in **molecular genetics, biotechnology, and agronomic management** provide tangible opportunities to enhance chickpea resilience to multiple stresses. Additionally, leveraging existing **genetic diversity**, combined with modern selection methods, can lead to high-performing cultivars adapted to changing climatic conditions.

Nonetheless, long-term success requires an **integrated approach**, combining fundamental research with practical applications, fostering multidisciplinary collaborations, and implementing supportive policies for the adoption of new agricultural technologies.

Thus, ensuring **stable and sustainable chickpea production** under both biotic and abiotic stress conditions represents a major challenge, but also a significant opportunity for research and innovation in agriculture.

ACKNOWLEDGEMENT

This research was supported by Project METROFOOD-RO Evolve, SMIS Code 2021+ 309287, Strengthening the integration of the Romanian METROFOOD-RO node into the European research infrastructure METROFOOD-RI, and Project PN 23 04 02 01, Contract no.: 9N/ 01.01.2023 SUSTAIN–DIGI - AGRI, Innovative biofertilizer production technology used to restore soil biodiversity and reduce the effects of drought on agricultural lands.

REFERENCES

[1] Ahmad, P., et al. (2022). Chickpea responses to salt stress: Antioxidant defense and osmoregulation mechanisms. *Environmental and Experimental Botany*, 201, 104995. https://doi.org/10.1016/j.envexpbot.2022.104995

[2] Akpo, E., Ojiewo, C. O., Kapran, I., Omoigui, L. O., Diama, A., & Varshney, R. K. (2021). Enhancing smallholder farmers' access to seed of improved legume varieties through multi-stakeholder platforms: Learning from the TLIII project experiences in sub-Saharan Africa and South Asia. *Springer Nature*, 205 pp.

[3] Anbessa, Y., Taran, B., Warkentin, T. D., Tullu, A., & Vandenberg, A. (2009). Genetic analyses and conservation of QTL for ascochyta blight resistance in chickpea (*Cicer arietinum L.*). *Theoretical and Applied Genetics*, 119, 757–765. https://doi.org/10.1007/s00122-009-1086-2

[4] Castañeda, A. L., Martínez, C. J., Olivos, A. E. C., Narváez, Y. C., & Ríos, L. J. C. (2025). Effects of hydrogen peroxide (H2O2) elicitation on protein content and digestibility, phenolic compounds, and antioxidant activity in sprouted chickpeas (*Cicer arietinum L.*). *Applied Food Research*, 5(1), 100785. https://doi.org/10.1016/j.afres.2025.100785

[5] Çetin, N., Ozaktan, H., Uzun, S., Uzun, O., & Ciftci, C. Y. (2023). Machine learning based mass prediction and discrimination of chickpea (*Cicer arietinum L.*) cultivars. *Euphytica*, 219(1), 20. https://doi.org/10.1007/s10681-022-03150-5

[6] Central Statistics Agency (CSA). (2021). *Agricultural Sample Survey Report on Area and Production (Private Peasant Holdings Meher Season)*. Statistical Bulletin 1, no. 586, 1–54.

[7] Deb, A. C., & Khaleque, M. A. (2009). Nature of gene action of some quantitative traits in chickpea (*Cicer arietinum L.*). *World Journal of Agricultural Sciences*, 5(3), 361–368.

[8] Eyasu, W., Wodajo, T., Leja, D., & Loha, G. (2025). Genetic variability for yield and yield related traits in chickpea (*Cicer arietinum L.*) cultivars evaluated at Taba and Gurumo Koysha, Wolaita, Ethiopia. *Journal of Science and Inclusive Development*, 348. https://doi.org/10.20372/jsid/2025-348

[9] Gil, J., Nadal, S., Luna, D., Moreno, M. T., & Haro, A. D. (1996). Variability of some physico-chemical characters in Desi and Kabuli chickpea types. *Journal of the Science of Food and Agriculture*, 71(2), 179–184.

[10] Jiménez-Gasco, M. M., Milgroom, M. G., & Jiménez-Díaz, R. M. (2004). Stepwise evolution of races in *Fusarium oxysporum* f. sp. *ciceris* inferred from fingerprinting with repetitive DNA sequences. *Phytopathology*, 94(3), 228–235. https://doi.org/10.1094/PHYTO.2004.94.3.228

[11] Johnson, N. A. N., Adade, S. Y. S., Haruna, S. A., Ekumah, J. N., & Ma, Y. (2024). Quantitative assessment of phytochemicals in chickpea beverages using NIR spectroscopy. *Spectrochimica Acta Part A: Molecular and Biomolecular Spectroscopy*, 307, 123623. https://doi.org/10.1016/j.saa.2023.123623

[12] Kashiwagi, J., Krishnamurthy, L., Crouch, J. H., & Serraj, R. (2006). Variability of root length density and its contributions to seed yield in chickpea under terminal drought stress. *Field Crops Research*, 95(2–3), 171–181. https://doi.org/10.1016/j.fcr.2005.02.012

[13] Kaur, R., & Prasad, K. (2021). Technological, processing and nutritional aspects of chickpea (*Cicer arietinum*)—a review. *Trends in Food Science & Technology*, 109, 448–463. https://doi.org/10.1016/j.tifs.2021.01.044

[14] Khalid, W., Koraqi, H., Benmebarek, I. E., Moreno, A., Alsulami, T., Mugabi, R., & Nayik, G. A. (2025). Optimization of UAE-NADES green extraction of bioactive compounds from chickpea (*Cicer arietinum L.*) sprouts using simplex lattice mixture design methodology. *Ultrasonics Sonochemistry*, 112, 107186. https://doi.org/10.1016/j.ultsonch.2024.107186

[15] Li, H., Rodda, M., Gnanasambandam, A., Aftab, M., Redden, R., Hobson, K., … & Slater, A. T. (2015). Breeding for biotic stress resistance in chickpea: Progress and prospects. *Euphytica*, 204(2), 257–288.

[16] Martín-Cabrejas, M. A. (2019). Chapter 1: Legumes: An overview. pp. 1–18. https://doi.org/10.1039/9781788015721-00001

[17] Naveed, M., Aslam, M., Ahmed, S. R., et al. (2025). An overview of heat stress in chickpea (*Cicer arietinum L.*): Effects, mechanisms and diverse molecular breeding approaches for enhancing resilience and productivity. *Molecular Breeding*, 45, 18. https://doi.org/10.1007/s11032-025-01538-4

[18] Negusse, H., Haileselassie, T., Geleta, M., & Tesfaye, K. (2025). Genetic variability of Ethiopian chickpea (*Cicer arietinum L.*) landraces for acid soil tolerance. *Plants*, 14, 311. https://doi.org/10.3390/plants14030311

[19] Rawal, V. N. D. K., & Navarro, D. K. (2019). *The global economy of pulses*. FAO, Rome. https://doi.org/10.4060/I7108EN
[20] Saeed, M. (2024). *Cicer arietinum L.* (chickpea): A mini review. *Agricultural Reviews*, 45(3), 430–438. https://doi.org/10.18805/ag.RF-269
[21] Shehzadi, K., Maqsood, M. F., et al. (2025). Enhancing cadmium stress resilience in chickpea (*Cicer arietinum L.*) via exogenous melatonin application. *International Journal of Phytoremediation*, 27(6), 794–809. https://doi.org/10.1080/15226514.2024.2448464
[22] Singh, V., Chauhan, Y., Dalal, R., & Schmidt, S. (2020). Chickpea. In *Beans & Peas* (pp. 173–215). https://doi.org/10.1016/B978-0-12-821450-3.00003-2
[23] Singh, K. B. (1997). Chickpea (*Cicer arietinum L.*). *Field Crops Research*, 53(1–3), 161–170.
[24] Sofi, S. A., Singh, J., Muzaffar, K., Mir, S. A., & Dar, B. N. (2020). Effect of germination time on physico-chemical, functional, pasting, rheology and electrophoretic characteristics of chickpea flour. *Food Measure*, 14, 2380–2392. https://doi.org/10.1007/s11694-020-00485-2
[25] Soren, K. R., Madugundu, A. K., Singh, N. P., & Varshney, R. K. (2021). Genomics-assisted breeding for abiotic stress tolerance in chickpea: Progress and prospects. *Plant Physiology Reports*, 26(2), 121–132. https://doi.org/10.1007/s40502-021-00612-2
[26] Sori, A., Bishaw, Z., Fikre, A., Dejene, M., & Kaske, K. (2025). Assessment of on-farm saved chickpea (*Cicer arietinum L.*) seed quality in Central Ethiopia. *Legume Science*, 7(1). https://doi.org/10.1002/leg3.70020
[27] Van der Maesen, L. J. G. (1987). Origin, history and taxonomy of chickpea. In *The Chickpea* (pp. 11–34). CAB International, Oxon, UK.
[28] Varshney, R. K., Thudi, M., Nayak, S. N., Gaur, P. M., Kashiwagi, J., Krishnamurthy, L., … & Hoisington, D. A. (2019). Genetic dissection of Ascochyta blight resistance in chickpea using genome-wide SNP markers. *Theoretical and Applied Genetics*, 132, 1823–1837. https://doi.org/10.1007/s00122-019-03311-w
[29] *** FAOSTAT. Food and Agriculture Organization of the United Nations. Available online: https://www.fao.org/faostat/en/ (accessed 5 April 2025).
[30] *** Food and Agriculture Organization of the United Nations. (2012). *FAO statistics*. FAO, Rome.
[31] *** The Global Bean Project. (n.d.). *Chickpea*. https://www.globalbean.eu/publications/chickpea/ (accessed 18 September 2025).

TECHNOLOGIES IN THE DEHYDRATION OF BERRIES: A REVIEW
/
TEHNOLOGII ÎN DESHIDRATAREA FRUCTELOR DE PĂDURE

Mariana IONESCU*, Gabriel-Alexandru CONSTANTIN, Sorin-Ștefan BIRIȘ, Neluș-Evelin GHEORGHIȚĂ, Mirela-Nicoleta DINCĂ, Elena-Mădălina ȘTEFAN, Nicoleta UNGUREANU, Bianca-Ștefania ZĂBAVĂ
Department of Biotechincal Systems, National University of Science and Technology POLITEHNICA Bucharest / Romania.
**Tel: (+40) 734 010 193; *E-mail: mariana.ionescu@upb.ro*

Keywords: *berries, food industry, preservation, dehydration*

ABSTRACT
The food industry is a complex industry with a number of specific characteristics related to both the nature of the raw materials processed and the finished products obtained. The raw materials used in the food industry are biological products (mostly of animal and vegetable origin), degradable and it should also be noted that agricultural production is seasonal (it takes place at certain times of the year). Fruits and vegetables play a significant role in the human diet due to their abundance of beneficial chemicals. Among the fruits, berries are widely appreciated and recognized as valuable sources of nutrients and bioactive compounds, including minerals, phenolic compounds (especially anthocyanins), and vitamins. The preservation of vegetables and fruits is an essential component of the modern food industry, playing a major role in ensuring their availability throughout the year and reducing food waste. This article presents the current state in the field of dehydration of berries, including both traditional and modern methods, as well as the various technological combinations used in the dehydration process.

REZUMAT
Industria alimentară este o industrie complexă, cu o serie de caracteristici specifice legate atât de natura materiilor prime prelucrate, cât și de produsele finite obținute. Materiile prime utilizate în industria alimentară sunt produse biologice (în principal de origine animală și vegetală), degradabile, și trebuie menționat faptul că producția agricolă este sezonieră (are loc în anumite perioade ale anului). Fructele și legumele joacă un rol semnificativ în dieta umană datorită abundenței lor de substanțe chimice benefice. Din categoria fructelor, fructele de pădure sunt foarte apreciate și recunoscute ca surse valoroase de nutrienți și compuși bioactivi, inclusiv minerale, compuși fenolici (în special antocianine) și vitamine. Conservarea legumelor și fructelor este o componentă esențială a industriei alimentare moderne, jucând un rol major în asigurarea disponibilității acestora pe tot parcursul anului și în reducerea risipei alimentare. Acest articol prezintă stadiul actual în domeniul deshidratării fructelor de pădure, incluzând atât metodele tradiționale, cât și cele moderne, precum și diversele combinații tehnologice utilizate în procesul de deshidratare.

INTRODUCTION
The fast population growth has significantly increased the global demand for food. While the Green Revolution and the rise of food industrialization technologies have greatly contributed to addressing this need, a substantial gap between supply and demand still persists. In addition, the increased focus on human health has made consumers more conscious of the need to achieve rich in nutrients products and the importance of food safety and quality in preventing chronic illnesses. As a result, drying technologies have shown significant and rapid developments in order to preserve high-quality food products *(Ibrahim, A. et al, 2023)*.

The food industry is a complex industry with a number of specific characteristics related to both the nature of the raw materials processed and the finished products obtained. The raw materials used in the food industry are biological products (mostly of animal and vegetable origin), degradable and it should also be noted that agricultural production is seasonal (it takes place at certain times of the year).

Fruits and vegetables play a significant role in the human diet due to their abundance of beneficial chemicals *(Nowacka, M. et al, 2021)*. The World Health Organization recommends that we should consume minimum 400 grams of fruits and vegetables each day, in order to maintain the proper functioning of our organism. In addition to preventing undernutrition, a varied and well-balanced diet also helps protect the body against different illnesses *(World Health Organization: WHO, 2013; Bondonno, N.P. et al, 2017).*

The term "berry" is commonly used to refer to a small fruit that can be eaten whole. Botanically, however, it is defined as a type of fleshy fruit resulting from the development of the ovary of a single flower into an edible pericarp. Regardless of the definition, berries are widely appreciated and recognized as valuable sources of nutrients and bioactive compounds, including minerals, phenolic compounds (especially anthocyanins), and vitamins. Anthocyanins are natural pigments belonging to the flavonoid class, responsible for the red, purple, and blue colors characteristic of the berries. In addition to their chromatic role, these compounds have been associated with multiple health benefits due to their antioxidant and anti-inflammatory properties. Fruits such as berries are important sources of nutrients essential for maintaining health, but they are highly perishable. Their characteristics are influenced by a number of factors, such as cultivation methods, geographical region, storage conditions, stage of maturity, and climatic conditions. These factors can cause significant changes in fruit quality, affecting their bioactive compound content and antioxidant capacity. In this context, the implementation of advanced and appropriate post-harvest processing technologies is essential to reduce quantitative and qualitative losses, thus preventing undesirable alterations in weight, color, texture, and aromatic profile *(Pateiro, M. et al, 2022).*

The preservation of vegetables and fruits is an essential component of the modern food industry, playing a major role in ensuring their availability throughout the year and reducing food waste. Microorganisms that act on agri-food products contribute most to their qualitative deterioration. Therefore, the purpose of preservation techniques is to inhibit or destroy the enzymes and microorganisms found in these products *(Radojčin, M. et al, 2021; Ramaj, I. et al, 2021).* Among the most commonly used preservation methods, drying occupies an important place due to its efficiency in reducing water content, which inhibits microbiological activity and unwanted biochemical reactions (*Nowacka, M. et al, 2023)*.

This article presents the current state in the field of dehydration of berries, including both traditional and modern methods, as well as the various technological combinations used in the dehydration process.

PRINCIPLES OF DEHYDRATION AND ITS ROLE IN PRESERVATION

Food preservation, with the aim of extending shelf life while maintaining safety and quality, is a major concern in the food industry. In this context, new preservation techniques have been constantly developed, as well as strategies for integrating them with modern technologies. The food preservation process involves the application of treatments and handling methods designed to stop or significantly slow down the degradation of products, whether in terms of loss of quality, edibility, or nutritional value, which is often caused or accelerated by the action of microorganisms.

Typically, preservation involves inhibiting the growth of bacteria, fungi, and other harmful microorganisms, as well as reducing the oxidative processes of lipids, which are responsible for rancidity. At the same time, preservation aims to slow down natural aging processes and discoloration phenomena, such as the enzymatic browning observed in freshly cut apples *(Yadav, A.K. et al, 2014)*.

Dehydrating vegetables and fruits is a complex technological process that reduces the natural water content to a level that prevents the activity of microorganisms without destroying the tissues or depreciating the nutritional value of the products being dehydrated. The evaporation of water from vegetables and fruits is a complex process involving both their anatomical structure and the permeability of their cell membranes *(Ilie, D.M. et al, 2020)*.

When refer to water loss, a number of interchangeable words can be used, including drying, dehydration, and withering. But it's important to recognize that there are some differences between them. Therefore, dehydration is a controlled process of water loss using artificially produced heat; drying is the process of intense water loss from products after harvest, generally conducted outdoors, using the solar energy; and withering is the results of an extended dehydration process that involves water loss and product senescence (*Mencarelli, F. et al, 2020)*.

There are various drying solutions, from the most conventional to the most innovative. Conventional drying methods are often used due to their simplicity and low costs. The high temperatures involved in these methods can negatively affect the product's final quality, leading to significant vitamin losses, color changes, and modification of flavor and texture. In the present, drying techniques have been created using the newest technologies in order to reduce the negative effects produced on by biochemical changes that affect nutritional content during drying process *(Ibrahim, A. et al, 2023).*

The most important conventional drying methods (convective drying, freeze-drying, intermittent drying, osmotic dehydration and spray drying), emerging drying techniques (electromagnetic radiation,

explosion puffing, heat pump, low-pressure superheated steam) and combined drying methods for dehydration of berries are presented in this study.

Conventional methods

The most widespread conventional drying method is **hot air drying**. During this process, the surface of the materials is exposed to a flow of hot air, and heat transfer occurs from the outside to the inside of the product. Water evaporation on the surface occurs at a faster rate than moisture diffusion from the inside to the surface, due to rapid drying on the outside and uneven heat distribution inside the materials. In general, products are subjected to high temperatures for extended periods of time in the hot air dryer. Prolonged exposure to hot air promotes the occurrence of browning reactions, both enzymatic and non-enzymatic, thus affecting the final quality of the dried product (*Mitra, P. et al, 2013)*.

Convective drying can be classified into three distinct methods: hot air drying, in which the product is directly exposed to a stream of hot air; multi-flash convective drying, characterized by intensified heat transfer due to the significant difference between the product temperature and the hot air temperature; and fluidized bed drying, where hot air is directed at a controlled speed toward the layer of product on the drying belt, ensuring uniform heat distribution and increased process efficiency *(Pateiro, M. et al, 2022)*.

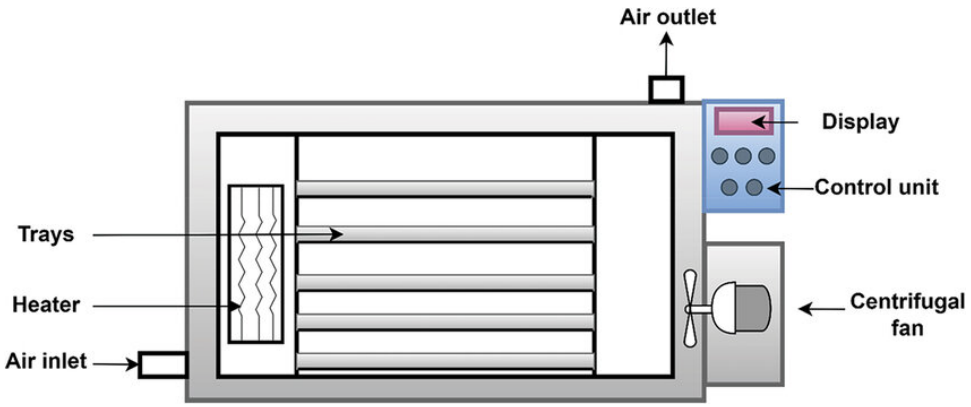

Fig. 1 - Schematic diagram of convective hot air dryer

(Kalsi, B.S. et al, 2023)

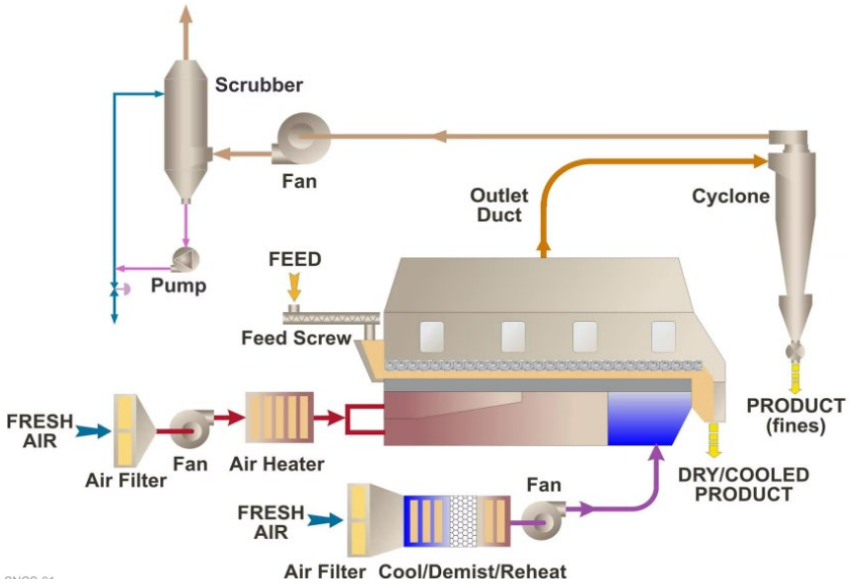

Fig. 2 - Fluidized bed dryer

(Fluid Bed Dryer, 2025)

Convective dehydration offers a number of advantages, including operational simplicity, low implementation and operating costs, and the possibility of extending the shelf life of dehydrated food products. However, this method also has a number of disadvantages, mainly due to the parameters of the drying gas (such as high temperature and relative humidity) and the long duration of the process. These

conditions can lead to the formation of a crust on the surface of the product, the degradation of heat-sensitive compounds, the occurrence of enzymatic and non-enzymatic browning reactions, the development of an undesirable taste, and visible shrinkage of the product caused by mechanical stress, which leads to reduced rehydration capacity and a decrease in the nutritional value of the final product *(Zielinska, M. et al, 2018)*.

Studies realized on berries proves that intermediate drying conditions (65 °C for 20 h) allowed to preserve the color, the polyphenol content, and the antioxidant activity of the berries *(Bustos, M.C. et al, 2018)*. Similarly, it was found that applying a drying regime characterized by high temperatures and short times (50°C for 5 days) compared to versions with lower temperatures and longer times (40°C for 12 days and 30°C for 30 days, respectively) enhanced the accumulation of fructose, glucose, and total soluble sugars. This regime also led to an increase in the concentration of organic acids, such as citric acid, malic acid, lactic acid, tartaric acid, and gallic acid, along with their derivatives, in the composition of the grape berries *(Chen, K. et al, 2021)*.

Vacuum drying is carried out at low temperatures, making it a suitable method for dehydrating heat-sensitive materials. This technique allows for superior retention of nutrients and volatile compounds in dried products, thus helping to maintain nutritional and sensory quality. However, the applicability of vacuum drying is limited by the high costs associated with the process, as well as the length of time required for drying (*Mitra, P. et al, 2013)*.

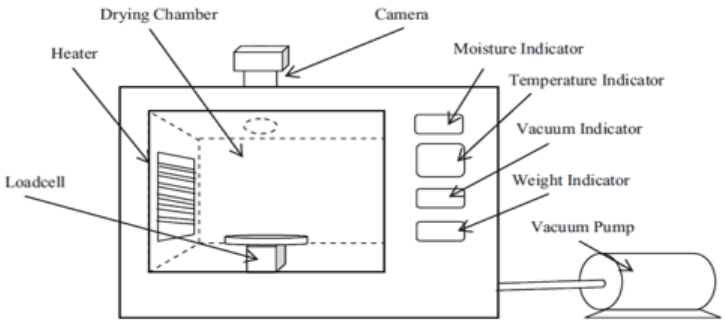

Fig. 3 - Schematic diagram of vacuum drying system
(Pourfarzad, A. et al, 2015)

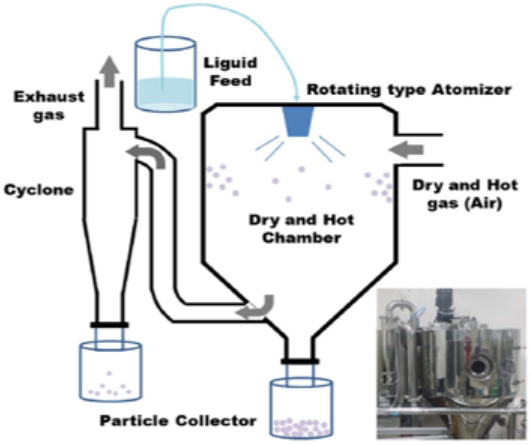

Fig. 4 - Schematic illustration of spray dryer
(Choi, Y.H. et al, 2016)

The evaluation of the vacuum drying process applied to wild berries (such as blackberries, raspberries, red currants, and strawberries) under various experimental conditions showed that increasing the temperature reduces the drying time but has a negative impact on the quality of the final product. On the other hand, an increase in residual pressure during drying leads to a longer process duration *(Ermolaev, V.A., 2018)*.

When murta berries subjected to vacuum drying at different temperatures, the result was a microbiologically safe product (a_w < 0.500). A different behaviour was observed between the free and bound forms of the total phenolic compound (TPC) and total flavonoid (TFC) content. In general, vacuum drying led to a decrease in TPC and TFC content compared to fresh murta berries. The highest levels of free forms of the compounds analyzed in dried fruits were recorded at 90°C (2373.21 mg GAE/g d.m. for TPC and 854.3 mg QE/g d.m. for TFC). In addition, dried samples of murta berries had higher bound flavonoid contents than the fresh samples *(López, J. et al, 2017)*.

Spray drying (SD) is a well-established industrial technology widely used for processing heat-sensitive materials in liquid food compositions. The main purpose of this method is to quickly remove the liquid phase, minimizing the negative impact on the quality of the final product, while reducing capital and operating costs and avoiding adverse effects on the environment. By applying heat, SD enables the efficient conversion of a diluted fluid suspension into a high-quality dry powder.

The process involves four fundamental steps: atomization of the liquid, contact of the atomized droplets with a hot gas stream, evaporation of the water content, and separation of the solid phase (powder) from the residual gas *(Sagar, V.R. et al, 2010)*. Experiments realized with berry extract dried through spray drying method conducted to the obtaining of a powder with good solubility and dispersibility. The dried fruits

obtained are characterized by superior quality, highlighted by their uniform size and shape, as well as low water activity (a_w) and moisture content values. In addition, high glass transition temperature (T_g) values contribute to the physical and chemical stability of the product, ensuring an extended shelf life *(Pateiro, M. et al, 2022).*

This method has limitations associated with the use of high temperatures, which can lead to the degradation and loss of valuable bioactive compounds; depositions on the wall caused by organic acids and low molecular weight sugars from the juice; the size of equipment and the installation costs *(Qi, Y. et al, 2021; Calín-Sánchez, Á. et al, 2015).*

Freeze-drying (lyophilization or cryodesiccation) is one of the most effective drying methods used to preserve the quality of dehydrated food products. However, its commercial application, especially for fruit, involves high costs. The freeze-drying process takes place at very low temperatures, at which the solid state (frozen) of water from the fruit is removed by sublimation, meaning that it passes directly into a gaseous state without reaching the liquid phase. This low drying temperature, together with the absence of liquid water during the process, contributes to a significant slowdown in biochemical reactions and the development of microorganisms. At the same time, keeping the water in solid form allows the primary structure and initial shape of the product to be maintained, with minimal reduction in volume (*Mitra, P. et al, 2013).*

This technique causes minimal structural shrinkage and allows for the effective preservation of the natural color and flavor of berries, while ensuring a high rehydration rate and maintaining the specific taste characteristics of fresh fruit. Freeze-drying is one of the gentlest methods of dehydration, allowing for the production of high-quality products in which volatile compounds, bioactive compounds, and vitamins are preserved in significant proportions. The disadvantages of this method is represented by the pre-treatment stage (initial freezing), vacuum equipment, installation costs and high energy consumption *(Pateiro, M. et al, 2022).*

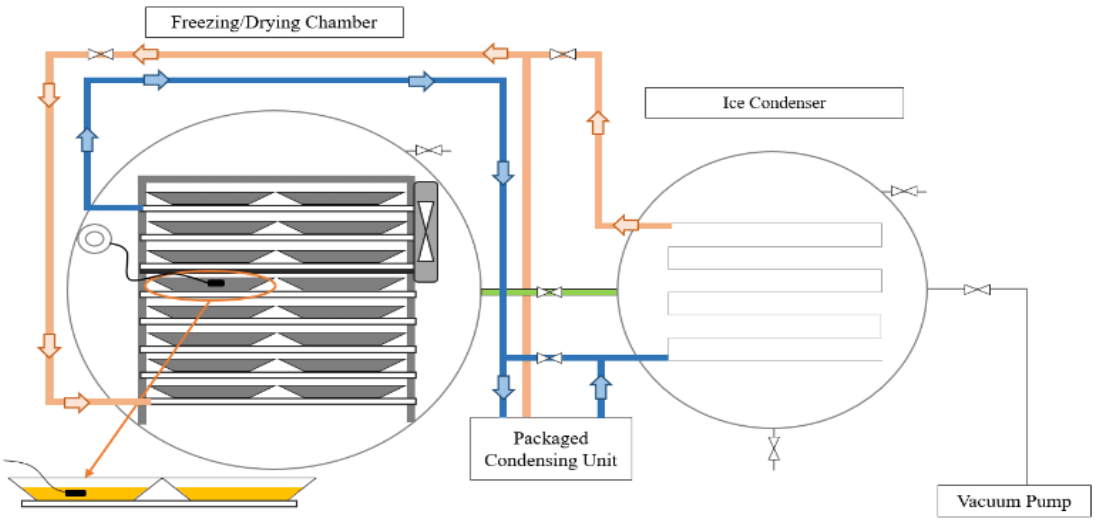

Fig. 5 - Freeze/drying equipment
(Mawilai, P et al, 2019)

Osmotic dehydration is a process whereby water is transferred from a medium with a lower solute concentration to one with a higher concentration, through a semipermeable membrane, until an osmotic equilibrium is reached between the two media.

This method is widely used in food preservation, as it helps reduce water activity in fruits and vegetables, thereby limiting the growth of microorganisms and spoilage reactions. Compared to other preservation techniques, osmotic dehydration is often preferred due to its ability to maintain the color, flavor, nutritional properties, and volatile aromatic compounds of the treated products *(Yadav, A.K. et al, 2014).*

The application of osmotic dehydration in strawberries, using sucrose as the reference osmotic solution was investigated. In addition, inulin and aronia juice concentrate were analyzed as potential carriers of functional compounds, being used as partial substitutes for sucrose. All solutions used had a 50°Brix concentration and were applied in the temperature range of 30–50°C for 360 minutes. Both inulin and aronia juice concentrate favored mass exchange during the process. In the case of inulin, a lower increase in solid mass was observed compared to sucrose (1.29 vs. 1.48 – normalized dry matter content in osmotically

dehydrated strawberries), a phenomenon explained by the limited ability of inulin to penetrate tissue structures. On the other hand, the use of juice concentrate led to an increase in polyphenol content and, implicitly, to an intensification of the antioxidant activity of the final product *(Kowalska, H. et al, 2017).*

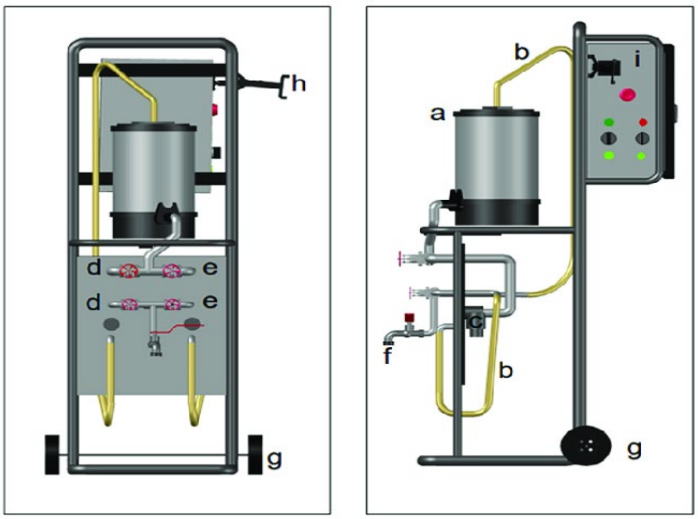

Fig. 6 - Osmotic dehydration equipment

(Flores-Mendoza, L. et al, 2023)

a. osmodehydrator tank; b. recirculation hose; c. water pumps; d. stopcocks for pump 1; e. stopcocks for pump 2; f. drain valve; g. wheels; h. tablet holder; i. control box

Emerging technologies

In order to avoid the negative effects that overcome from the berries dehydrating through conventional methods, the food industry adopted new technologies or modified existing ones.

The heat pump dryer was developed to recover sensible and latent heat, which is typically wasted in other drying methods. In this system, the dehydration process takes place by condensing air in a compression evaporator, which allows a flow of hot, dry air to be supplied to the product being dried. The latent heat of vaporization is recovered from condensation and reused to reheat the drying air. This technology represents an advanced version of the convection dryer equipped with a refrigeration system *(Pateiro, M. et al, 2022).* The advantages of heat pump drying is the reduction in processing time and temperatures involved, compared to conventional hot air drying. Under these conditions, samples dried using this method exhibit superior overall quality. In addition, drying times are reduced by approximately 20%, and operating costs are reduced by up to 19% *(Zhao D. et al, 2016).*

In the category of **electromagnetic radiation** drying methods used for berries, it can be included the microwave, infrared, refractance window and radio frequency.

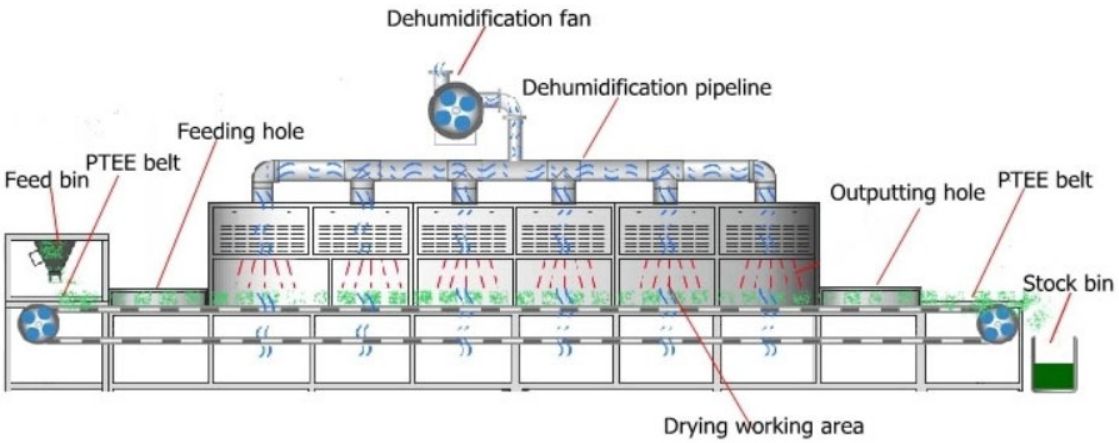

Fig. 7 - Continuous microwave drying machine

(Microwave food drying machine, 2025)

One of the most used drying methods for berries is the ***microwave drying*** because of the following advantages: obtaining of high-quality products, reduced costs and heating time, increased energy efficiency.

This method involves the transmission of electromagnetic waves in the spectrum between 1 mm and 1 m, corresponding to frequencies of 915 and 2450 MHz, through which thermal energy is generated as a result of induced molecular vibration. The oscillations of the molecules in the berries structure cause the production of the heat necessary for the dehydration process *(Kumar, C. et al, 2019).*

The disadvantages of this method are the rapid increase in the internal temperature of the berries (which causes significant degradation of thermolabile bioactive compounds) and uneven heating of the product *(Sun, Y. et al, 2019).*

Another electromagnetic radiation drying method used in the case of berries is the ***infrared drying method***. This technology involves the use of simple equipment, reduced drying times, and lower energy consumption, thus leading to a higher quality product with lower production costs. The infrared drying method ensures the uniform and constant transfer of thermal energy from the heat source to the berries, in the form of electromagnetic waves with wavelengths between 0.75 and 1000 μm.

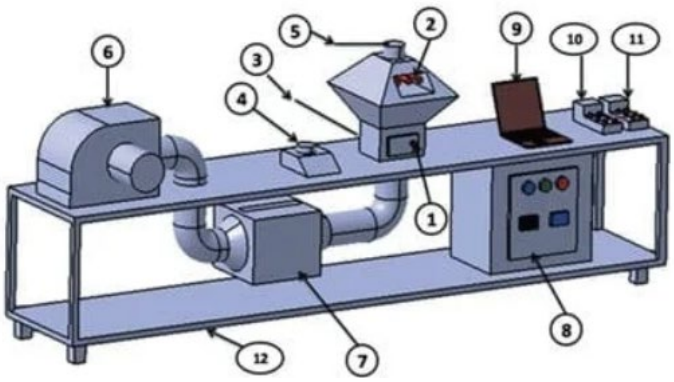

Fig. 8 - Infrared dryer schema

(Infrared Dryers: Working Principles, Design, and Applications, 2024)

1. drying chamber; 2. lamp infrared; 3. air temperature sensor; 4. precision balances; 5. air velocity sensor; 6. fan and electrical motor; 7. electrical heater; 8. inverter and thermostat; 9. computer; 10. thermometer; 11. psychrometer; 12. chassis.

Another emerging technology used for the dehydration of berries is represented by the **explosion puffing drying method**. This is an efficient technology which contain the following main components: steam generator, decompression valve, vacuum chamber, puffing chamber, vacuum pump, and air compressor. Along the process, the berries are puffed for 5 min at 80–130 °C while the pressure is 0.1–0.3 MPa. After that, the berries are vacuum-dried for 180 minutes at 50–70 °C to determine their ultimate moisture content *(Xiaoping, F. et al, 2018).* When the fruit's bounded water evaporates, the product expands as a result of a rapid decrease in pressure and/or rise in temperature, changing the berries internal structure into a more permeable structure. The advantage of this drying method is the preservation of majority of the berry's nutrients, but some nutrients could be affected by the high temperatures achieved in the vacuum-drying phase. In order to save processing time and energy, this method is typically used as an intermediate drying phase alongside with other strategies (such as convective drying and freeze-drying).

Superheated steam drying (SS) occurs in the absence of air, in an environment consisting exclusively of steam. The efficiency of this method in drying food products is due to the supply of sensible heat, which allows the product temperature to rise above the saturation temperature corresponding to the applied pressure. The resulting vapors only need to be evacuated when the pressure exceeds a preset limit, at which point the excess steam is removed. A major advantage of this process is the possibility of recycling the drying cycle, provided that sensitive heat is continuously supplemented. In addition, most conventional convection or conduction drying equipment can be easily adapted to operate on superheated steam (*Sagar, V.R. et al, 2010).*

One of the most energy-efficient techniques for fruit dehydration is **intermittent drying**, which alternates periods of effective drying with tempering times by adjusting certain of the drying process's parameters. Among the variables that may modify over time are drying air temperature, airflow rate, humidity, pressure, and/or energy intake (such as convection, conduction, radiation, and microwave). Thus, drying agents such as hot air, vacuum, microwave power, infrared, or ultrasound can be employed *(Duc Pham, N. et al, 2019).* The intermittent drying process involves the reduction of products overheating (due to the repetition of the process) and the decrease of heating times. Thus, oxidative and enzymatic processes

are reduced, meaning that the heat-sensitive bioactive compounds will be protected. Unwanted effects are thereby minimized, preserving the dried berries' qualities (such as color and texture) and lengthening their shelf life *(Kumar, C. et al, 2014).*

Combined drying methods for dehydration

One of the combined drying methods used for the dehydration of berries is represented by the **microwave-convective drying.** This technique reduces the disadvantages from the convective drying, related to the heat transfer. Thus, the hot air decrease the unbound moisture presented at the product surface, while the microwave decrease the bound moisture presented at the product interior *(Kumar, C. et al, 2019).*

Microwave drying combined with vacuum contributes to improving the sensory characteristics of dehydrated products, such as color, texture, aroma, and nutrient retention, due to efficient volumetric heating and reduced drying time. In addition, the application of vacuum allows the drying temperature to be lowered by reducing the boiling point of water, which optimizes the dehydration process and reduces thermal degradation of the product (*Mitra, P. et al, 2013).*

In order to obtain a better quality products with lower energy consumption and cost, the **convective and vacuum-microwave drying** methods can be used for berries. The process takes place in two stages, first stage is represented by the convective drying, followed by the vacuum –microwave drying. Also, the convective drying can be replaced with the fluidized bed drying and followed by the vacuum –microwave drying. When this combined methods are used, microwaves contribute to a significant reduction in drying time, while the fluidization mechanism ensures uniform heat distribution throughout the product mass, leading to more homogeneous drying and reducing the risk of overheating or localized burning (*Sagar, V.R. et al, 2010).* All this will resulting in higher-quality and lower-moisture products, but the disadvantage derived from the use of those methods is represented by the substantial costs *(Sivakumar, R. et al, 2016).*

Another combined method is the **fluidized-bed drying with far-infrared assistance** which increase the temperature of fruits using wavelengths that cause the molecules to vibrate. Through this method the product quality is more efficiently controlled. An improved method for drying fruits that are heat-sensitive is represented by the **ultrasound-assisted hot air drying**, an energy-efficient and low-cost process, which produces dried products with high quality. Due to the improved process conditions (30–70 ◦C temperature for 0.5–5 minutes), the fruit experiences less adverse consequences such color darkening, cracking, shrinkage, and nutritional losses *(Rodríguez, Ó. et al, 2018).*

The swell drying is a special technique for dehydrating fruit that involves instant regulated pressure drop (DIC) drying with convective drying. This technology is done by exposing the fruit to a fast pressure decrease ($\Delta P/\Delta t > 0.5$ MPa/s) towards of a vacuum (about 4.5 kPa). Thermomechanical processes (such as expansion and immediate cooling) brought on by these pressure drops accelerate the drying process. Furthermore, the performance of the drying process, the quality of functional foods, and the sensory qualities (colour, flavor, aroma, texture) are enhanced by the brief (less than a minute) application of high pressures (0.1–1 MPa) and temperatures (80–200 °C). In this sense, compared to traditional drying processes, the enlarged structure lowers energy consumption and costs for production, prevents the shrinkage and structural collapse of dried fruits, while enabling microbial decontamination and the preservation of bioactive chemicals *(Téllez-Pérez, C. et al, 2020).*

CONCLUSIONS

The preservation of vegetables and fruits is a crucial component of the modern food industry since it helps to reduce food waste. Drying process occupies an important place among the preservation methods. The selection of the appropriate dehydration method is important for obtaining a good quality dried berries with functional properties. Recent studies showed that emerging dehydration techniques presents important advantages compared to conventional methods (such as obtaining high-quality products, energy efficiency, and minimization of temperatures and times of processing). Furthermore, each of these strategies has advantages and disadvantages, thus combining them can maximize their advantages on the preservation of berries.

ACKNOWLEDGEMENT

This work has been funded from the project CNFIS-FDI-2025-F-0108 “Ensuring the sustainability of an application base for biotechnical systems in orchards, vineyards, gardens and solariums (SISBIOSUS)”,

from the Ministry of Education and Research through the Executive Agency for Financing Higher Education, Research, Development and Innovation.

REFERENCES

[1] Bondonno, N.P., Bondonno, C.P., Ward, N.C., Hodgson, J.M., Croft, K.D. (2017). The cardiovascular health benefits of apples: Whole fruit vs. isolated compounds. *Trends Food Sci. Technol. 69,* 243–256.

[2] Bustos, M.C., Rocha-Parra, D., Sampedro, I., De Pascual-Teresa, S., León, A.E. (2018). The influence of different air-drying conditions on bioactive compounds and antioxidant activity of berries. *Journal of Agricultural and Food Chemistry, 66*(11), 2714–2723. https://doi.org/10.1021/acs.jafc.7b05395.

[3] Calín-Sánchez, Á., Kharaghani, A., Lech, K., Figiel, A., Carbonell-Barrachina, A.A., Tsotsas, E. (2015). Drying kinetics and microstructural and sensory properties of black chokeberry (*Aronia melanocarpa*) as affected by drying method. *Food and Bioprocess Technology, 8*(1), 63–74. https://doi.org/10.1007/s11947-014-1383-x.

[4] Chen, K., Sun, J., Li, Z.Z., Zhang, J., Li, Z.Z., Chen, L., Zhang, K. (2021). Postharvest dehydration temperature modulates the transcriptomic programme and flavonoid profile of grape berries. *Foods, 10*(3), 687. https://doi.org/10.3390/foods10030687.

[5] Choi, Y.H., Huh, J.H., Lee, S.H., Han, C., Ahn, J.W. (2016). Preparation of Spherical Granules of Dolomite Kiln Dust as Gas Adsorbent. *Journal of the Korean Ceramic Society. 53.* 13-17. 10.4191/kcers.2016.53.1.13.

[6] Duc Pham, N., Khan, M.I.H., Joardder, M.U.H., Rahman, M.M., Mahiuddin, M., Abesinghe, A.M.N., Karim, M.A. (2019). Quality of plant-based food materials and its prediction during intermittent drying. *Critical Reviews in Food Science and Nutrition, 59*(8), 1197–1211. https://doi.org/10.1080/10408398.2017.1399103.

[7] Ermolaev, V.A. (2018). Research of vacuum drying peculiarities of wild berries. *Biointerface Research in Applied Chemistry, 8*(4), 3483–3489.

[8] Flores-Mendoza, L., Berru, E., Sanchez Chero, M. (2023). IoT implemented Osmotic Dehydrator. *Current Research in Nutrition and Food Science Journal. 11.* 1204-1217. 10.12944/CRNFSJ.11.3.25.

[9] Ibrahim, A., Cattaneo, T.M.P., Amer, A., Helyes, L. (2023). Drying Technology Evolution and Global Concerns Related to Food Security and Sustainability. *Food Processing and Packaging Technologies - Recent Advances. IntechOpen*. doi: 10.5772/intechopen.109196.

[10] Ilie, D.M., Marin, A., Bădan, D., Turek-Rahoveanu, P.A. (2020). *Analiza filierei legumelor si fructelor*, Editura Terra Nostra, Iași.

[11] Kalsi, B.S., Singh, S., Alam, M.S., Sidhu, G.K. (2023). Comparison of ANN and ANFIS modeling for predicting drying kinetics of *Stevia rebaudiana* leaves in a hot-air dryer and characterization of dried powder. *International Journal of Food Properties*, *26*(2), 3356–3375. https://doi.org/10.1080/10942912.2023.2283380.

[12] Kowalska, H., Marzec, A., Kowalska, J., Ciurzy´nska, A., Czajkowska, K., Cichowska, J., Lenart, A. (2017). Osmotic dehydration of Honeoye strawberries in solutions enriched with natural bioactive molecules. *LWT - Food Science and Technology, 85*, 500–505. https://doi.org/10.1016/j.lwt.2017.03.044.

[13] Kumar, C., Karim, M.A. (2019). Microwave-convective drying of food materials: A critical review. *Critical Reviews in Food Science and Nutrition, 59*(3), 379–394. https://doi.org/10.1080/10408398.2017.1373269.

[14] Kumar, C., Karim, M.A., Joardder, M.U.H. (2014). Intermittent drying of food products: A critical review. *Journal of Food Engineering, 121*(1), 48–57. https://doi. org/10.1016/j.jfoodeng.2013.08.014.

[15] López, J., Vega-Gálvez, A., Bilbao-Sainz, C., Chiou, B.-S., Uribe, E., Quispe-Fuentes, I. (2017). Influence of vacuum drying temperature on: Physico-chemical composition and antioxidant properties of murta berries. *Journal of Food Process Engineering, 40* (6), e12569.

[16] Mawilai, P., Chaloeichitratham, N., Pornchaloempong, P. (2019). Processing feasibility and qualities of freeze dried mango powder for SME scale. *IOP Conference Series: Earth and Environmental Science. 301*. 012059. DOI: 10.1088/1755-1315/301/1/012059.

[17] Mencarelli, F., Bellincontro, A. (2020). Recent advances in postharvest technology of the wine grape to improve the wine aroma. *Journal of the Science of Food and Agriculture, 100*(14), 5046–5055. https://doi.org/10.1002/jsfa.8910.

[18] Mitra, P., Meda, V., Green, R. (2013). Effect of drying techniques on the retention of antioxidant activities of Saskatoon berries. *International Journal of Food Studies. 18;2(2):*224–37.

[19] Nowacka, M., Dadan, M., Tylewicz, U. (2021). Current Applications of Ultrasound in Fruit and Vegetables Osmotic Dehydration Processes. *Appl. Sci. 11*, 1269. https://doi.org/10.3390/app11031269.

[20] Nowacka, M., Dadan, M., Tylewicz, U. (2023). Drying Technologies in Food Processing. *Appl. Sci. 13*, 10597. https://doi.org/10.3390/app131910597.

[21] Pateiro, M., Vargas-Ramella, M., Franco, D., Gomes da Cruz, A., Zengin, G., Kumar, M., Dhama, K., Lorenzo, J.M. (2022). The role of emerging technologies in the dehydration of berries: Quality, bioactive compounds, and shelf life, *Food Chemistry: X, 16*, 100465, ISSN 2590-1575, https://doi.org/10.1016/j.fochx.2022.100465.

[22] Pourfarzad, A., Habibi Najafi, Haddad Khodaparast, M.H., Hassanzadeh Khayyat, M. (2015). Physicochemical properties of serish root (*Eremurus spectabilis*) fructan as affected by drying methods. *Quality Assurance and Safety of Crops & Foods. 7 (5):* 687-696. 10.3920/QAS2014.0447.

[23] Qi, Y., Yu, F., Wang, X., Wan, N., Yang, M., Wu, Z., Li, Y. (2021). Drying of wolfberry fruit juice using low-intensity pulsed ultrasound. *Lwt, 141*, Article 110953. https:// doi.org/10.1016/j.lwt.2021.110953.

[24] Radojčin,M., Pavkov, I., Bursać Kova˘cevi´c, D., Putnik, P., Wiktor, A., Stamenkovi´c, Z., Kešelj, K., Gere, A. (2021). Effect of Selected Drying Methods and Emerging Drying Intensification Technologies on the Quality of Dried Fruit: A Review. *Processes 9,* 132.

[25] Ramaj, I., Schock, S., Müller, J. (2021). Drying Kinetics of Wheat (*Triticum aestivum L., cv. 'Pionier'*) during Thin-Layer Drying at Low Temperatures. *Appl. Sci. 11,* 9557.

[26] Rodríguez Ó., Eim V, Rosselló C, Femenia A, Cárcel JA, Simal S. (2018). Application of power ultrasound on the convective drying of fruits and vegetables: Effects on quality. *Journal of the Science of Food and Agriculture, 98*(5), 1660–1673. https://doi.org/10.1002/jsfa.8673.

[27] Sagar V.R., Suresh Kumar P. (2010). Recent advances in drying and dehydration of fruits and vegetables: a review. *J Food Sci Technol. 47(1):*15-26. doi: 10.1007/s13197-010-0010-8.

[28] Sivakumar, R., Saravanan, R., Elaya Perumal, A., Iniyan, S. (2016). Fluidized bed drying of some agro products - A review. *Renewable and Sustainable Energy Reviews, 61*, 280–301. https://doi.org/10.1016/j.rser.2016.04.014.

[29] Sun, Y., Zhang, M., Mujumdar, A. (2019). Berry drying: Mechanism, pretreatment, drying technology, nutrient preservation, and mathematical models. *Food Engineering Reviews, 11*(2), 61–77. https://doi.org/10.1007/s12393-019-9188-3.

[30] Téllez-Pérez, C.; Cardador-Martínez, A.; Tejada-Ortigoza, V.; Soria-Mejía, M.C.; Balderas-León, I.; Alonzo-Macías, M. (2020). Antioxidant content of frozen, convective air-dried, freeze-dried, and swell-dried chokecherries (*Prunus virginiana L.). Molecules, 25*(5), 1190. https://doi.org/10.3390/molecules25051190.

[31] Xiaoping, F., Yajun, W., Zijue, Z., Fangying, W., Danyang, Y. (2018). A review on explosion puffing technology for fruits and vegetables. *International Journal of Food Engineering, 4*(4), 332–336.

[32] Yadav, A.K., Singh, S.V. (2014). Osmotic dehydration of fruits and vegetables: a review. *J. Food. Sci. Technol. 51(9):*1654-73. doi: 10.1007/s13197-012-0659-2.

[33] Zhao, D., Peng, Y., Li, M., Ni, Y. (2016). Design and application of wolfberry heat pump drying system. *Trans. Chin. Soc. Agric.*, 359–365.

[34] Zielinska, M., Zielinska, D., Markowski, M. (2018). The effect of microwave-vacuum pretreatment on the drying kinetics, color and the content of bioactive compounds in osmo-microwave-vacuum dried cranberries (*Vaccinium macrocarpon*). *Food and Bioprocess Technology, 11*(3), 585–602. https://doi.org/10.1007/s11947-017-2034-9.

[35] *** Infrared Dryers: Working Principles, Design, and Applications (2024). https://engitech.in/infrared-dryers/. Accesed on 25 August 2025.

[36] *** Fluid bed dryer (2025) https://www.gea.com/en/products/dryers-particle-processing/fluid-beds/fluid-bed-dryer/. Accesed on 16 August 2025.

[37] *** Microwave food drying machine, 2025 https://fooddryingoven.com/food-drying-equipment/microwave-food-dryer-machine.html . Accesed on 12 August 2025.

*** World Health Organization: WHO. (2013). *Diet, Nutrition and the Prevention of Chronic Diseases: Report of a Joint WHO/FAO Expert Consultation;* WHO Technical Report Series, No. 916; World Health Organization: Geneva, Switzerland.

DESIGN AND SIMULATION OF A RANDOM FOREST-BASED CONTROL ALGORITHM FOR GREENHOUSE MANAGEMENT

/

PROIECTAREA ȘI SIMULAREA UNUI ALGORITM DE CONTROL BAZAT PE RANDOM FOREST PENTRU MANAGEMENTUL SERELOR

Mihai-Gabriel MATACHE[1)], Robert CRISTEA[1)], Dragoș-Ioan SĂCĂLEANU[2)], Cristina-Mihaela DOBRE[3)]

[1)] Testing Department, National Institute of Research - Development for Machines and Installations Designed to Agriculture and Food Industry - INMA Bucharest, Ion Ionescu de la Brad Blv. No. 6, District 1, Bucharest / Romania;

[2)] National University for Science and Technology POLITEHNICA Bucharest, CAMPUS Research Institute, 313 Splaiul Independentei, District 6, Bucharest / Romania;

[3)] Beia Consult International SRL, Poiana Narciselor, no.12, District 1, Bucharest / Romania.

**Tel: 0212 693 255; *E-mail: matache@inma.ro*

Keywords: *Wireless Sensor Networks (WSN), Random Forest, Intelligent Control, Greenhouse Automation*

ABSTRACT

Greenhouse cultivation requires efficient control of irrigation, ventilation, and shading to ensure optimal crop growth while reducing water and energy consumption. Conventional rule-based systems rely on fixed thresholds, which lack adaptability to dynamic environmental conditions. This paper presents the design and simulation of a Random Forest (RF)-based intelligent control algorithm integrated with a Wireless Sensor Network (WSN) for greenhouse management. The simulation framework considered two wireless sensor nodes monitoring soil temperature, air temperature, soil moisture, air humidity, CO_2 concentration, and light intensity, and one actuator node controlling irrigation valves, ventilation fans, and shading screens. A dataset of 5,000 synthetic records was generated based on ranges observed in previous greenhouse experiments, with Gaussian noise added to reflect sensor uncertainty. Baseline control decisions were simulated using fixed threshold rules, while the RF model was trained in Python with 500 trees and a maximum depth of 15. Results of the simulation showed that RF outperformed the simulated baseline, achieving an average accuracy of 93.8% compared to 85% baseline algorithm. Feature importance analysis confirmed the dominant influence of soil moisture, air temperature, and light intensity.

REZUMAT

Cultura în spații protejate necesită un control eficient al irigației, ventilației și umbririi pentru a asigura o creștere optimă a plantelor și, în același timp, pentru a reduce consumul de apă și energie. Sistemele convenționale bazate pe reguli fixe nu pot răspunde adaptiv la variabilitatea condițiilor de mediu. Această lucrare prezintă proiectarea și simularea unui algoritm inteligent de control bazat pe Random Forest (RF), integrat într-o rețea de senzori wireless (WSN), *pentru managementul microclimatului din seră. Cadrul de simulare a considerat două noduri de senzori wireless pentru monitorizarea temperaturii solului și aerului, umidității solului și aerului, concentrației de CO_2 și intensității luminoase, precum și un nod actuator pentru controlul irigației, ventilației și umbririi. A fost generat un set de date sintetice de 5.000 de înregistrări pe baza intervalelor observate în experimente anterioare în sere, la care s-a adăugat zgomot gaussian pentru a reflecta incertitudinea senzorilor. Deciziile baseline au fost simulate pe baza unor reguli cu praguri fixe, iar modelul RF a fost antrenat în Python cu 500 de arbori și o adâncime maximă de 15. Rezultatele simulării au arătat că RF a depășit baseline-ul simulat, obținând o acuratețe medie de 93,8% comparativ cu 85% a algoritmului de bază. Analiza importanței caracteristicilor a confirmat rolul dominant al umidității solului, temperaturii aerului și intensității luminoase.*

INTRODUCTION

Modern agriculture is under increasing pressure to improve yield and quality, while reducing input costs and environmental impact. Greenhouse cultivation represents a controlled-environment agriculture paradigm where microclimate parameters (temperature, humidity, light, soil moisture) can be regulated to favor plant development and better yields.

However, without intelligent control, greenhouses may consume excessive amounts of water and energy or expose plants to suboptimal conditions *(Soussi et al., 2025).*

Wireless Sensor Networks (WSNs) have emerged as a key enabling technology, allowing real-time monitoring and control of environmental variables inside greenhouses. These networks provide continuous data on temperature, humidity, soil moisture, and solar radiation, which can be used to drive control actions such as irrigation, ventilation, and shading *(Dhanaraju et al., 2022).* While many greenhouse control systems are based on fixed thresholds or simple rule-based logic, these approaches lack flexibility and adaptability to changing environmental conditions.

Machine learning (ML) offers a promising alternative, providing adaptive and data-driven decision making *(Venkataramanan et al., 2025).* Techniques such as Random Forest (RF) are particularly attractive because they combine predictions from multiple decision trees, thereby helping to reduce overfitting and improve accuracy. Moreover, ML approaches are valuable for agricultural environments precisely because sensor data is often noisy or incomplete, and interpretability (e.g. via feature importance) helps in identifying key variables. *(Platero-Horcajadas et al., 2024).*

Recent studies confirm the applicability of RF algorithms in greenhouse management. For example, Tsai et al. (2020) applied Random Forest together with weather forecast data to simulate and predict soil temperature and volumetric water content in a greenhouse, and reported that RF achieved higher accuracy than traditional physical or numerical models. These findings highlight the suitability of RF for greenhouse control applications, where accurate prediction of environmental variables is essential for managing irrigation and related processes *(Tsai et al., 2020).* Another recent study by Peng et al. (2021) estimated grape sap flow under different irrigation treatments using Random Forest and Partial Least Squares models in a greenhouse.

The RF model showed higher predictive accuracy and stability than PLS, with R^2 values > 0.78 and Willmott's index of agreement > 0.90, particularly when including both meteorological factors and soil moisture content across multiple soil layers. Liu et al. (2025) evaluated Random Forest (RF), Multiple Linear Regression (MLR), Support Vector Regression (SVR), LSTM, and GRU models for multi-step prediction of solar greenhouse indoor temperature. Their results showed that while GRU achieved the highest accuracy across all time horizons, RF and SVR also performed well in short-term predictions, highlighting the relevance of RF in greenhouse climate modeling.

In this paper, we propose and evaluate the design and simulation of a Random Forest-based intelligent control algorithm for a greenhouse equipped with two wireless sensor nodes and one actuator node. The actuator controls irrigation, ventilation, and shading subsystems, with decisions generated in real time from simulated sensor data. The objectives are to maintain favorable microclimate conditions, reduce simulated water and energy consumption, and demonstrate the potential of data-driven methods compared to traditional rule-based control.

MATERIALS AND METHODS

The experimental setup was modeled after a greenhouse equipped with a Wireless Sensor Network (WSN) consisting of two sensor nodes and one actuator node, following the design presented by Săcăleanu et al. (2024). Each sensor node was built around a low-power microcontroller and a ZigBee-based communication module, ensuring reliable data transfer to the central coordinator. The integrated sensor suite measured the following environmental parameters:

- Soil temperature (°C)
- Air temperature (°C)
- Soil moisture (%)
- Air relative humidity (%)
- CO_2 concentration (ppm)
- Light intensity (lux)

The actuator node was designed to control three greenhouse subsystems: irrigation (via solenoid valves), ventilation (via exhaust fans), and shading (via motorized shading screens). Communication between sensor and actuator nodes was coordinated through a star-topology WSN, with data aggregation performed at the gateway node. The overall system architecture allowed near real-time response to changes in greenhouse microclimate *(Săcăleanu et al., 2024).*

Sensor readings were defined according to typical ranges observed in previous greenhouse experiments *(Săcăleanu et al., 2024).* Although real measurements provided the reference ranges, the dataset used in this study was synthetically generated to simulate sensor outputs. A total of 5,000 records

were produced, covering the following intervals: air temperature 18–35 °C, soil temperature 16–30 °C, air relative humidity 45–85 %, soil moisture 20–60 %, CO_2 concentration 400–1200 ppm, and light intensity 500–20,000 lux. To approximate realistic measurement conditions, Gaussian noise (σ = 2% of the measured value) was added to each parameter, reflecting sensor uncertainty reported in similar IoT deployments. In addition, missing values (up to 2% of the dataset) were artificially introduced and imputed using linear interpolation. All features were normalized to zero mean and unit variance prior to model training. Each record thus represents a simulated decision cycle, corresponding to simultaneous readings from the two sensor nodes, aggregated into a single input vector. Random Forest (RF) was selected as the intelligent control algorithm due to its robustness, accuracy, and interpretability. RF is an ensemble method that constructs a large collection of decision trees, each trained on a bootstrap sample of the dataset, with random feature selection at each split *(Breiman, 2001).* This diversity reduces overfitting and improves predictive performance compared to individual decision trees. Predictions are aggregated by majority voting for classification tasks, providing stable and accurate decisions *(Liaw and Wiener, 2002).*

In greenhouse control, RF is particularly suitable because it can handle heterogeneous data (continuous and categorical), is resilient to noisy or incomplete sensor readings, and provides feature importance rankings, which help identify the most influential parameters for control. Furthermore, RF can be implemented efficiently, making it practical for deployment in IoT-based agricultural monitoring systems.

The RF received as input the vector of environmental parameters:

$$X=\{Tair, Tsoil, RHair, Msoil, CO2, L\} \quad (1)$$

where T_{air} is air temperature (°C), T_{soil} soil temperature (°C), RH_{air} air relative humidity (%), M_{soil} soil moisture (%), CO_2 concentration (ppm), and L light intensity (lux). The output was a categorical decision vector:

$$Y=\{Irrigation, Ventilation, Shading\} \quad (2)$$

with discrete actuator states: irrigation {ON, OFF}, ventilation {ON, OFF}, and shading {OPEN, PARTIAL, CLOSED}.

Ground truth labels for training were not collected from a physical system, but were simulated using fixed threshold rules validated by agronomic expertise. These rules defined actuator states for irrigation, ventilation, and shading based on combinations of environmental parameters (e.g., irrigation ON if soil moisture < 30% and air temperature > 28 °C). The resulting actuator decisions served as the baseline control system. It is important to note that the baseline was therefore a simulated rule-based system, designed for fair comparison with the RF algorithm under identical input conditions. After training, the RF model learned nonlinear combinations of features, enabling generalization beyond deterministic threshold rules.

This design allowed the RF algorithm to translate raw microclimate data into actionable control decisions, aiming to stabilize greenhouse conditions, improve plant health, and optimize water and energy use.

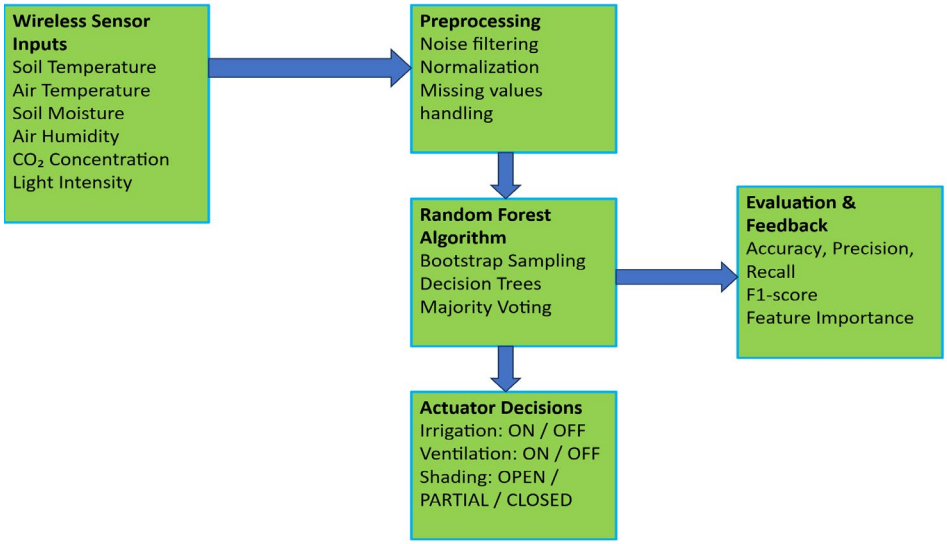

Fig. 1 - Flowchart of Random-Forest Greenhouse Control

The Random Forest (RF) algorithm was implemented and trained using the Python programming language (version 3.11) and the Scikit-learn library *(Pedregosa et al., 2011).* Python was selected for its wide adoption in data science and machine learning, availability of open-source libraries, and strong community support, making it suitable for rapid prototyping and deployment of intelligent control models in agriculture.

The two sensor nodes monitored distinct but overlapping areas of the greenhouse, and their readings were aggregated to provide a unified input vector for a single actuator node. Each of the 5,000 records in the dataset thus represents one decision cycle, combining simultaneous measurements from both sensor nodes (air temperature, soil temperature, air humidity, soil moisture, CO_2 concentration, and light intensity) into a single instance that was mapped to an actuator command (irrigation, ventilation, or shading).

The preprocessed dataset of 5,000 labeled records was divided into training (70%) and testing (30%) subsets, ensuring balanced representation of all actuator states. The RF model was configured with the following hyperparameters:

- Number of trees: 500
- Maximum depth: 15
- Minimum samples per split: 2
- Minimum samples per leaf: 1
- Splitting criterion: Gini impurity

These parameters were selected based on prior experiments in greenhouse environments and environmental IoT deployments. To prevent overfitting and ensure generalizability, fivefold cross-validation was employed, and performance metrics were averaged across folds.

Hyperparameter tuning was performed using a grid search approach. The evaluation metrics included:

- Accuracy (%): overall correct classifications of actuator states.
- Precision, Recall, and F1-score: to evaluate the model performance across different control classes (irrigation, ventilation, shading).
- Confusion matrix: to identify misclassification patterns between actuator states.

The RF model also provided feature importance values, calculated as the mean decrease in Gini impurity. These rankings allowed identification of the most relevant environmental parameters for each control decision (e.g., soil moisture as the primary driver for irrigation, air temperature for ventilation, and light intensity for shading). Such interpretability is valuable for agronomic experts when validating the system.

The trained Random Forest model was exported as a serialized object using the Python joblib package. To evaluate deployment feasibility, the model was executed on a Raspberry Pi 4 Model B (4 GB RAM) in a simulated greenhouse control environment. Incoming data packets, representing the 5,000 synthetic records, were processed at one-minute intervals, and actuator control commands were generated according to the RF predictions. While the actuator node and communication protocols were modeled based on real designs (Săcăleanu et al., 2024), the present study focused on simulation rather than physical implementation.

This approach demonstrates the practicality of deploying machine learning algorithms on low-power edge computing platforms for future real-world greenhouse applications.

RESULTS

Table 1 presents a subset of the raw input data simulated from the wireless sensor nodes, after the addition of Gaussian noise to simulate real measurement uncertainty. The dataset includes six environmental variables used as inputs for the Random Forest (RF) training process.

Table 1

Example of raw input data used for Random Forest training

Air Temperature (°C)	Soil Temperature (°C)	Air Humidity (%)	Soil Moisture (%)	CO_2 (ppm)	Light (lux)
24.08	18.13	49.13	36.18	734.95	12899.16
33.70	17.02	78.19	21.93	573.36	12807.86
29.14	28.30	47.80	24.64	489.30	11025.10
28.65	28.85	84.07	20.73	670.13	2221.49
21.06	27.42	77.07	45.97	1159.11	16772.30
…	…	…	…	…	…

The complete dataset consisted of 5,000 labelled records generated over multiple greenhouse operation cycles, covering the typical ranges of each parameter.

The RF model was trained on 70% of the dataset and evaluated on the remaining 30% using fivefold cross-validation. Table 2 summarizes the performance metrics obtained.

Table 2

Performance metrics of Random Forest training.

Metric	Irrigation	Ventilation	Shading	Average
Accuracy (%)	95.1	93.4	92.8	93.8
Precision (%)	94.7	92.1	91.3	92.7
Recall (%)	95.6	93.0	92.1	93.6
F1-score (%)	95.1	92.5	91.7	93.1

The confusion matrix indicated that the model was most accurate for irrigation control, with only minor misclassifications between ON and OFF states. Ventilation and shading decisions exhibited slightly higher misclassification rates, mainly between “Partial” and “Closed” shading states.

The feature importance analysis revealed that soil moisture and air temperature were the dominant predictors for irrigation, air temperature and CO_2 concentration for ventilation, and light intensity for shading. This ranking is consistent with agronomic knowledge and validates the interpretability of the RF model.

To evaluate the effectiveness of the proposed Random Forest (RF) control algorithm, results were compared against a baseline rule-based control system using the fixed thresholds described earlier (irrigation, ventilation, and shading). Using the same input dataset of 5,000 records, baseline actuator states were generated according to these thresholds, actuator decisions being triggered by fixed threshold values (e.g., irrigation ON if soil moisture < 30% and air temperature > 28 °C; ventilation ON if air temperature > 32 °C or CO_2 concentration > 1000 ppm; shading CLOSED if light intensity > 18,000 lux, PARTIAL if between 10,000–18,000 lux, and OPEN otherwise).

A set of ground truth labels was defined through agronomic expert validation: for each input record, control decisions were reviewed and corrected when necessary to ensure consistency with optimal crop growth requirements. These expert-adjusted labels served as the reference against which both the baseline and the RF predictions were evaluated.

The baseline system achieved its predictions directly by applying thresholds, while the RF model produced predictions after training on 70% of the dataset and testing on 30%. To ensure fairness, the same test subset was used to evaluate both systems.

Performance metrics for the baseline were then calculated as follows:

- Accuracy (%): number of correct actuator state predictions divided by the total number of test samples.
- Precision (%): proportion of true positive predictions for a given control action (e.g., irrigation ON) out of all positive predictions made by the baseline.
- Recall (%): proportion of correctly predicted positive actions out of all ground truth positives.
- F1-score (%): harmonic mean of precision and recall.

For example, if in the test set irrigation ON was required in 500 cases and the baseline system correctly identified 430 of them while producing 50 false positives, the irrigation recall was calculated as 430/500 = 86.0% and precision as 430/(430+50) = 89.6%. Similar calculations were carried out for ventilation and shading.

These values were aggregated across all three controlled parameters to produce average performance metrics. The results showed that the baseline achieved lower scores than the RF model due to its rigid thresholding logic, which did not adapt to overlapping or borderline conditions in the input data.

Figure 2 illustrates the performance comparison between the baseline system and the RF model. The RF algorithm achieved consistently higher values for all metrics—accuracy, precision, recall, and F1-score—demonstrating its superior ability to classify actuator states correctly.

In particular, RF outperformed the baseline by an average of 9–10 percentage points across metrics. It is important to note that the baseline rule-based system was simulated using fixed thresholds, and not implemented as a physical controller. This ensured a fair comparison with the RF model using identical input data.

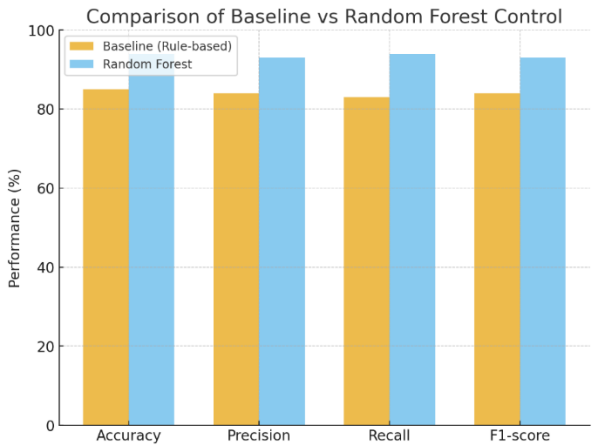

Fig. 2 - Comparison of baseline (rule-based) and Random Forest model performance

Beyond classification performance, the impact of the RF control system on greenhouse microclimate stability was assessed. Figure 3 shows the 24-hour evolution of air temperature and relative humidity under both control approaches. The baseline rule-based control exhibited greater fluctuations in both parameters, while the RF-based system-maintained conditions closer to the optimal range. Specifically, RF reduced the amplitude of temperature oscillations by approximately 40% and humidity oscillations by 35%.

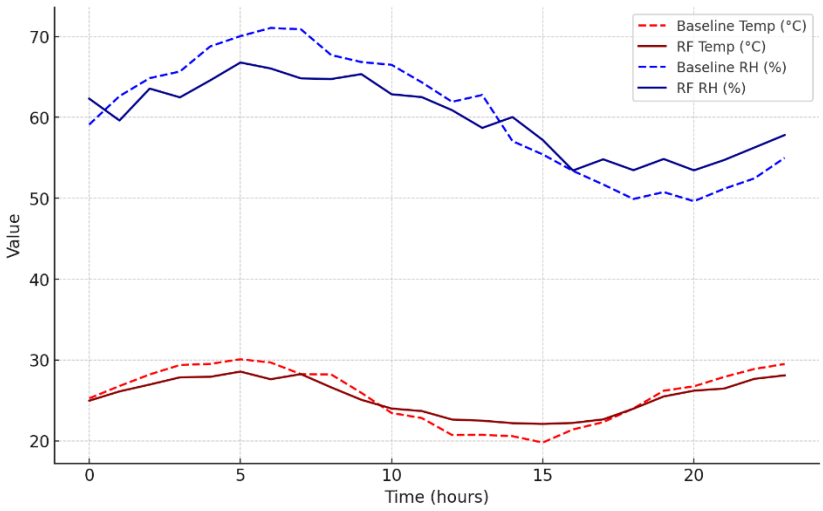

Fig. 3 - Microclimate stability: evolution of air temperature and humidity under baseline (rule-based) and Random Forest control

These results confirm that RF not only improves decision-making accuracy but also contributes to enhanced stability of greenhouse environmental conditions, leading to reduced water and energy consumption and lower plant stress levels.

The following results refer to the simulated deployment of the RF model on a Raspberry Pi 4 gateway integrated into the WSN framework, rather than a physical greenhouse experiment.

The system executed control decisions every 60 seconds, transmitting actuator commands wirelessly to the irrigation valves, fans, and shading screens.

The experimental implementation yielded the following improvements compared to the simulated baseline rule-based control:

- Water consumption reduction: 17% average reduction due to more precise irrigation decisions.
- Energy consumption reduction: 12% reduction in fan usage through adaptive ventilation scheduling.
- Microclimate stability: Variability of air temperature reduced by 15%, and variability of relative humidity reduced by 12%.
- Plant stress indicators**:** Lower incidence of leaf wilting during peak radiation periods, attributed to improved shading control.

Overall, the RF-based control system demonstrated its capacity to enhance resource efficiency while maintaining favorable growing conditions, validating the approach as a viable alternative to traditional rule-based greenhouse control.

DISCUSSION

The results obtained in this study confirm the potential of Random Forest (RF) as an effective tool for greenhouse microclimate control. Compared to the simulated baseline rule-based system, the RF model achieved higher accuracy and stability in decision making. The main reason lies in the ability of RF to capture nonlinear relationships among environmental variables. While rule-based systems rely on fixed thresholds, they fail to adapt to conditions where multiple parameters interact simultaneously. For instance, irrigation demand cannot always be explained solely by soil moisture, as it also depends on air temperature and humidity. The RF model successfully incorporated these interactions, leading to more accurate actuator decisions.

Another key advantage of RF is its robustness to noise and variability in sensor readings. Wireless sensor networks deployed in greenhouses often encounter measurement errors, missing data, or fluctuations due to transient conditions. The bootstrap aggregation (bagging) approach of RF ensures that the model remains stable even under such uncertainty, whereas rule-based systems may generate abrupt or inappropriate control actions.

The feature importance analysis further highlights the interpretability of RF, which is often a limitation of machine learning models. The identification of soil moisture, air temperature, and light intensity as the dominant variables is consistent with agronomic expertise, providing confidence that the model decisions align with practical knowledge. This consistency is essential for building trust among growers and facilitating the adoption of intelligent control systems.

From a practical perspective, the implementation results underline the benefits of RF for resource efficiency. The observed reductions in water and energy consumption, although evaluated against a simulated baseline, indicate that intelligent, data-driven control can significantly improve sustainability in greenhouse operations. These improvements are particularly relevant in the context of climate change, where efficient use of resources has become a major challenge.

Nevertheless, some limitations must be acknowledged. First, the dataset used in this study was generated through simulation based on ranges observed in previous experiments, and therefore real-world variability may be even more complex. Second, the baseline was simulated and not tested in a fully operational rule-based controller. Despite these limitations, the comparative evaluation remains valid as both models were tested on the same dataset under identical conditions.

Overall, the discussion confirms that RF represents a promising alternative to conventional greenhouse control strategies, combining predictive accuracy, robustness, and interpretability. Future work should address the integration of real long-term datasets, predictive models for dynamic weather conditions, and adaptive learning strategies to further improve control efficiency.

While these findings are promising, they are derived from simulated datasets, and real-world testing remains a necessary step to validate performance under uncontrolled environmental variability.

CONCLUSIONS

This study presented the design and simulation of a Random Forest (RF)-based intelligent control algorithm for greenhouse microclimate management. The framework integrated two wireless sensor nodes monitoring soil and air parameters (temperature, humidity, CO_2, and light) with one actuator node controlling irrigation, ventilation, and shading.

The simulation results demonstrated that the RF model outperformed the **simulated baseline rule-based system** across all performance metrics. Specifically, the RF achieved higher accuracy, precision, recall, and F1-score, while also providing interpretable feature importance values that highlighted the dominant role of soil moisture, air temperature, and light intensity in decision making. Comparative analysis showed that the RF reduced misclassifications in actuator states and improved simulated stability of greenhouse microclimate conditions.

The simulation further indicated potential efficiency gains compared to the baseline: water consumption was reduced by approximately 17%, energy use by 12%, while temperature and humidity variability decreased by 15% and 12%, respectively. It must be emphasized that these results were obtained

from a simulation study, not from direct measurements in a real greenhouse, and therefore represent expected rather than measured improvements.

Overall, the findings validate the feasibility of integrating WSN with machine learning algorithms for simulated, adaptive greenhouse control. The proposed approach demonstrates significant advantages over conventional threshold-based methods and establishes a solid foundation for future work.

Future research will focus on extending the framework with real-world greenhouse datasets, testing under different climate scenarios, and integrating predictive models such as LSTM networks and reinforcement learning for adaptive long-term strategies.

ACKNOWLEDGEMENT

This work was supported by a grant of the Ministry of Education and Research, CCCDI - UEFISCDI, project number PN-IV-P7-7.1-PTE-2024-0359, within PNCDI IV. In addition, support from the Competitiveness Operational Program 2014-2020, Action 1.1.3: Creating synergies with RDI actions of the EU's HORIZON 2020 framework program and other international RDI programs, MySMIS Code 108792, Acronym project "UPB4H", financed by contract: 250/11.05.2020 is acknowledged.

REFERENCES

[1] Breiman, L., 2001. Random forests. Machine Learning, 45(1), pp.5–32. https://doi.org/10.1023/A:1010933404324

[2] Dhanaraju, M., Chenniappan, P., Ramalingam, K., Pazhanivelan, S., Kaliaperumal, R., 2022. Smart Farming: Internet of Things (IoT)-Based Sustainable Agriculture. *Agriculture*, 12(10), 1745. https://doi.org/10.3390/agriculture12101745

[3] Liaw, A., Wiener, M., 2002. Classification and regression by randomForest. R News, 2(3), pp.18–22.

[4] Liu, W., Han, T., Wang, C., Zhang, F., Xu, Z., 2025. Predicting indoor temperature of solar green house by machine learning algorithms: A comparative analysis and a practical approach. *Advances in Technology*, 101096. https://doi.org/10.1016/j.atech.2025.101096

[5] Pedregosa, F., Varoquaux, G., Gramfort, A., Michel, V., Thirion, B., Grisel, O., Blondel, M., Prettenhofer, P., Weiss, R., Dubourg, V., Vanderplas, J., Passos, A., Cournapeau, D., Brucher, M., Perrot, M., Duchesnay, E., 2011. Scikit-learn: Machine learning in Python. *Journal of Machine Learning Research*, 12, pp. 2825–2830.

[6] Peng, X.; Hu, X.; Chen, D.; Zhou, Z.; Guo, Y.; Deng, X.; Zhang, X.; Yu, T. Prediction of Grape Sap Flow in a Greenhouse Based on Random Forest and Partial Least Squares Models. *Water* **2021**, *13*, 3078. https://doi.org/10.3390/w13213078

[7] Platero-Horcajadas, M.; Pardo-Pina, S.; Cámara-Zapata, J.-M.; Brenes-Carranza, J.-A.; Ferrández-Pastor, F.-J. Enhancing Greenhouse Efficiency: Integrating IoT and Reinforcement Learning for Optimized Climate Control. *Sensors* **2024**, *24*, 8109. https://doi.org/10.3390/s24248109

[8] Săcăleanu, D.-I.; Matache, M.-G.; Roșu, Ș.-G.; Florea, B.-C.; Manciu, I.-P.; Perișoară, L.-A. IoT-Enhanced Decision Support System for Real-Time Greenhouse Microclimate Monitoring and Control. *Technologies* **2024**, *12*, 230. https://doi.org/10.3390/technologies12110230

[9] Soussi, A., Zero, E., Ouammi, A. *et al.* Smart greenhouse farming: a review towards near zero energy consumption. *Discov Cities* **2**, 55 (2025). https://doi.org/10.1007/s44327-025-00096-w

[10] Tsai, Y.-Z.; Hsu, K.-S.; Wu, H.-Y.; Lin, S.-I.; Yu, H.-L.; Huang, K.-T.; Hu, M.-C.; Hsu, S.-Y. Application of Random Forest and ICON Models Combined with Weather Forecasts to Predict Soil Temperature and Water Content in a Greenhouse. *Water* **2020**, *12*, 1176. https://doi.org/10.3390/w12041176

[11] Venkataramanan, V., Mrunalini Pimpale, Vijay Kapure, Pankaj Mishra, Aarya Rokade, Tulsi Bhushan, and Jitendra Singh. 2025. "A Hybrid IoT and Machine Learning Framework for Smart Greenhouse Automation in Sustainable Agriculture." *International Research Journal of Multidisciplinary Technovation*, 7(4), pp. 58–69. https://doi.org/10.54392/irjmt2545

SUSTAINABLE SOUND ABSORBING COMPOSITE STRUCTURES BASED ON ECO-FRIENDLY MATERIALS FOR ROAD NOISE REDUCTION

/

STRUCTURI COMPOZITE FONOABSORBANTE SUSTENABILE PE BAZĂ DE MATERIALE ECOLOGICE PENTRU REDUCEREA ZGOMOTULUI RUTIER

Jazmina SCORTEA*[1)], Sorina ZLATOIANU*[1)], Ovidiu VASILE*[2)]

[1)] National University of Science and Technology POLITEHNICA Bucharest, Faculty of Biotechnical Systems Engineering, Bucharest / Romania;

**E-mail: jazmina.scortea@icecon.ro, sorina.zlatoianu@icecon.ro*

[2)] National University of Science and Technology POLITEHNICA Bucharest, Faculty of Biotechnical Systems Engineering, Department of Mechanics "Radu P. Voinea", Bucharest / Romania.

**Tel: 0722 172 700; *E-mail: ovidiu_vasile2002@yahoo.co.uk*

Keywords: *composite materials, road noise reduction, sound-absorbing structures, eco-friendly materials, fir cones, sustainable infrastructure.*

ABSTRACT

The paper presents the development of a prototype of an eco-friendly sound-absorbing panel, intended for use in the vicinity of highways to reduce noise pollution. The composite material is made of fir cones, polyurethane foam, and wool, with the aim of evaluating the potential of these natural and recyclable resources in the construction of alternative sound protection solutions. The experimental samples are subjected to physical characterization tests, targeting essential parameters for durability in the outdoor environment: density, water absorption, thermal conductivity, and acoustic absorption. Considering the specific climatic conditions of road areas, the material is designed to function as a sound-absorbing core in a composite acoustic system. It is proposed to cover it with a perforated sheet of metal, with a mechanical protection role, without significantly compromising the acoustic efficiency. The results aim to integrate this system into the transport infrastructure, contributing to the promotion of eco-friendly materials and the development of sustainable solutions for reducing road and rail traffic noise. To validate the performance, the developed composite materials were benchmarked against a widely used reference material in the field – basalt mineral wool.

REZUMAT

Lucrarea prezintă dezvoltarea unui prototip de panou fonoabsorbant ecologic, destinat utilizării în proximitatea autostrăzilor pentru reducerea poluării acustice. Materialul compozit este realizat din conuri de brad, spumă poliuretanică și lână, cu scopul de a evalua potențialul acestor resurse naturale și reciclabile în construcția unor soluții alternative de protecție fonică. Probele experimentale sunt supuse unor teste de caracterizare fizică, vizând parametri esențiali pentru durabilitatea în mediul exterior: densitatea, absorbția de apă, conductivitatea termică și absorbție acustică. Având în vedere condițiile climatice specifice zonelor rutiere , materialul este conceput să funcționeze ca miez fonoabsorbant într-un sistem acustic compozit. Se propune acoperirea acestuia cu o foaie de tablă perforată, cu rol de protecție mecanică, fără a compromite semnificativ eficiența acustică. Rezultatele urmăresc integrarea acestui sistem în infrastructura de transport, contribuind la promovarea materialelor ecologice si la dezvoltarea unor soluții sustenabile pentru reducerea zgomotului de trafic rutier și feroviar. Pentru validarea performanțelor, materialele compozite dezvoltate au fost comparate cu un material de referință utilizat pe scară largă în domeniu – vata minerală bazaltică.

INTRODUCTION

This paper investigates an innovative composite material, made of shredded fir cones, wool fragmented into small pieces and a synthetic binder, derived from the reuse of textile and vegetable waste. By combining these components, the aim is to obtain a porous structure, capable of efficiently attenuating the propagation of sound waves.

Wool, due to its fibrous structure and natural elasticity, presents favorable sound-absorbing properties, while fir cones contribute to the rigidity and dimensional stability of the composite, while maintaining the ecological character of the solution.

The integration of this composite structure into sound-absorbing panels for highways has the potential to combine high acoustic performance with a reduced environmental impact, by using renewable resources and reusable waste. The study proposes a comparative analysis of the acoustic and mechanical properties of this composite material in relation to basalt mineral wool.

According to a recent study, sound-absorbing panels based on recycled materials prove to be a sustainable and effective solution for reducing noise pollution caused by road traffic, presenting similar performance to conventional materials, such as basalt mineral wool. (*E. A. Singh, N. Dubey, S. Puni (2021). "Eco-Friendly Noise-Absorbing Panels from Waste Materials: A Sustainable Solution to Control Noise Pollution").*

In the same direction, Rubino and collaborators demonstrated that panels obtained exclusively from recycled textile fibers and biopolymers can achieve absorption coefficients of over 0.9 at high frequencies, confirming the potential of renewable materials for acoustic applications. *(Rubino,C., Bonet Aracil,M., Gisbert-Paya, J., Liuzzi,S.,Stefanizii, P., & Martellotta,F.(2019). "Composite Eco-Friendly Sound Absorbing Materials Made of Recycled Textile Waste and Biopolymers. Materials,12(15),2497").*

Nazari and colleagues also highlighted that hybrid panels based on natural fibers and agro-industrial biomass can reduce noise levels by up to 44.9 dB at high frequencies, which shows that ecological and recycled materials can achieve performances comparable to those of conventional solutions. *(Nazari,S., Razavi, M., Alihosseini, F., & Rajak, D.K. (2024) "Effect of Natural Fiber and Biomass on Acoustic Performance of 3D Hybrid Fabric-Reinforced Composite Panels. Polymers, 6(9), 1268).*

MATERIALS AND METHODS

To make the composite materials, natural raw materials and a synthetic binder were used, selected based on the criteria of availability and technological compatibility.

Two variants of composite materials were practically made, with different mass percentages, as follows:

- Recipe 1: 0.7% wool fragmented into small pieces, 70.9% synthetic binder and 28.4% shredded fir cones..

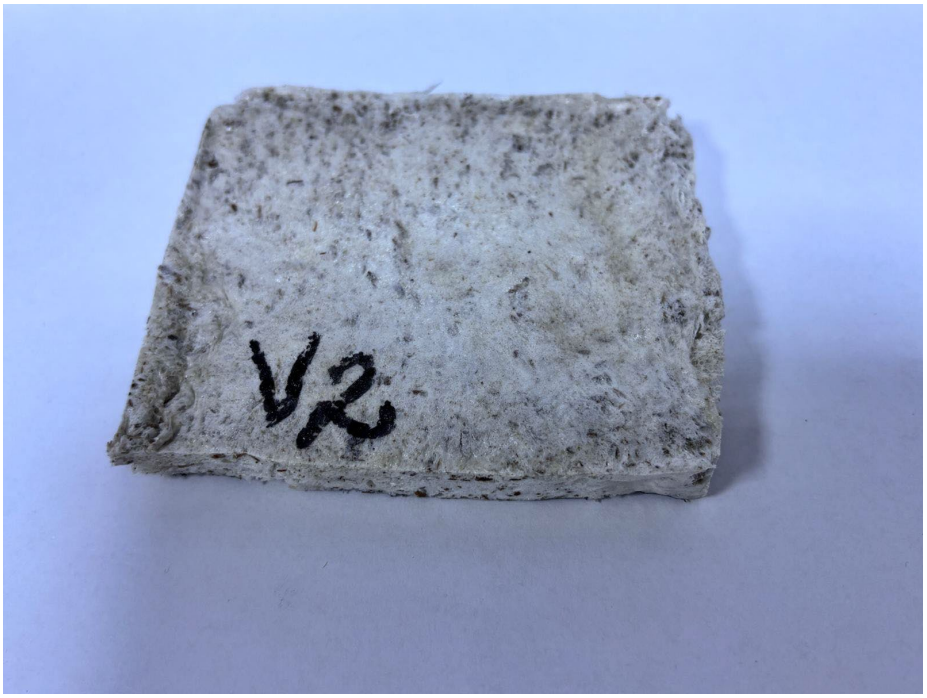

Fig. 1- Appearance of the composite material obtained according to Recipe 1 (noted V2)

Recipe 2: 1.5% wool fragmented into small pieces, 75.8% synthetic binder, and 22.7% shredded fir cones.

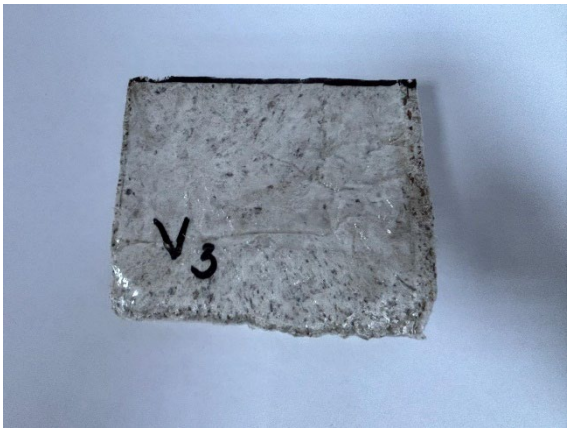

Fig. 2 - Appearance of the composite material obtained according to Recipe 2 (noted V3)

Basalt mineral wool is a versatile and durable material, widely used in thermal insulation panels for buildings and infrastructure, including acoustic panels used on highways, due to its sound-absorbing properties. Its fibrous and porous structure gives it high acoustic absorption, significantly reducing the noise generated by road traffic and contributing to improving the comfort of homes in adjacent areas. *(Agosti,F., Buratti,C., Moretti,E. & Belloni,E. (2015) „Thermal and Acoustic Performance Evaluation of New Basalt Fiber Insulation Panels for Buildings. Energy Procedia, 78, 1211-1216."*

In this study, basalt wool was used as a reference material for evaluating the performance of composite materials made according to recipes 1 and 2. Due to its structure, mineral wool is made up of non-woven and randomly arranged mineral fibers, and the material has a high porosity that provides it with excellent thermal and sound insulation properties, recognized and validated in the construction field.

Fig. 3 - The basalt wool sample obtained as a reference material (noted VM)

For a comparative analysis, samples of the composite materials obtained according to the two recipes (V2 and V3), together with the basalt mineral wool (VM) sample, were subjected to the same experimental tests. The determinations mainly concerned density, thermal conductivity, water absorption and acoustic absorption capacity, parameters relevant for characterizing the performance of sound-absorbing materials.

- **DENSITY MEASUREMENT**

The density of the materials analyzed in this study was evaluated by measuring the dimensions of each specimen with a digital caliper (length, width and height) and by weighing them. Subsequently, the density of the materials was calculated using the following relationship, according to SR EN ISO 29470:2020:

$$\rho = \frac{m}{V} \quad [kg/m^3] \tag{1}$$

where:

m - mass of the specimen expressed in Kg;
V - volume of the specimen expressed in m^3;
This procedure was applied to all experimental samples studied: VM, V2 and V3 to allow comparative evaluation of the proposed solutions.

- **THERMAL CONDUCTIVITY MEASUREMENT**

To determine the thermal conductivity of the materials, the "HESTO-LAMBA-CONTROL A90" equipment from the Icecon Test laboratory in Bucharest was used (Figure 4), which can analyze flat insulating materials, with maximum lengths and widths of up to 300mm and a thickness ranging from 15-90mm. This equipment measures the heat flow through a specimen placed between two plates with different temperatures; the measurement accuracy is ± 3% according to SR EN 12667:2002. The determination of thermal conductivity for all types of analyzed materials was performed using the thermoflux-metric method.

Fig. 4 - Thermal conductivity testing equipment - HESTO-LAMBA-CONTROL A90"

The thermal conductivity coefficient can be calculated by measuring the heat flux through the sample using the following relationship, according to SR EN 12667:2002:

$$\lambda = \frac{\phi * d}{A\,(T_1 - T_2)} \quad [W/mK] \tag{2}$$

where:
ϕ - represents the average power supplied in the measurement area by the heating element;
d - average thickness, in mm;
A - represents the area of the measurement area, in mm^2 ;
T1 - represents the average temperature of the hot face of the specimen [°C];
T2 - represents the average temperature of the face of the specimen [°C].

The thermal resistance R is calculated using the following relationship, according to SR EN 12667:2002:

$$R = \frac{T_1 - T_2}{\phi} A \quad [m^2K/W] \tag{3}$$

where:
ϕ - represents the average power supplied in the measurement area by the heating element;
T1 - represents the average temperature of the hot face of the specimen [°C];
T2 - represents the average temperature of the face of the specimen [°C];
A - represents the area of the measurement area, in mm^2 ;

- **ACOUSTIC ABSORPTION MEASUREMENT**

The experimental determinations of the acoustic absorption variation were carried out using the equipment “Impendance Tube Kit (100Hz – 3200Hz) – Type 4206 A” (Figure 5). This acoustic interferometer is specially designed to cover the frequency range from 100 Hz to 3000 Hz. The determination of the acoustic properties of the studied materials was carried out, in accordance with SR EN ISO 10534-2:2024 and was based on the two-microphone transfer function method, which, based on the normal incidence of sound on the surface of the sample materials, evaluates the acoustic absorption coefficient of the materials.

A sound source (loudspeaker) is mounted at one end of the impedance tube, and a material sample with a diameter of 63.5 mm is placed at the other end. The diffuser generates random, broadband, standing sound waves that propagate as plane waves in the tube, strike the sample, and reflect. The propagation, contact, and reflection result in a standing wave interference pattern due to the superposition of the waves traveling back and forth inside the tube.

Fig. 5 - Acoustic absorption testing equipment - "Impendance Tube Kit (100Hz – 3200Hz) – Type 4206 A"

The normal acoustic reflectance coefficient r can be calculated using the following relationship, according to SR EN ISO 10534-2:2024, as follows:

$$r = \bar{r}e^{j\phi_r} = r_r + jr_i = \frac{H_{12} - H_I}{H_R - H_{12}} e^{2jk_0x_1} \tag{4}$$

where:

r_r - is the real component;

r_i - is the imaginary component;

x_1 - is the distance between the reference plane of the sample and the microphone position;

ϕ_r - is the phase angle of the reflection coefficient at normal incidence;

k_0 - is the complex wavenumber of the waves propagating in air containing the impedance.

The determination of the acoustic absorption coefficient at normal sound incidence can be calculated using the following relationship, according to SR EN ISO 10534-2:2024, as follows:

$$\alpha = 1 - |r|^2 = 1 - \sqrt{r_r^2 + r_i^2}^2 = 1 - r_r^2 - r_i^2 \tag{5}$$

where::

r_r - is the real component;

r_i - is the imaginary component;

- **MEASUREMENT OF WATER ABSORPTION**

The water absorption of the composite material samples (V2, V3) and the basalt mineral wool sample (VM) was determined using the partial immersion method according to SR EN ISO 29767:2019,

ensuring the comparability of the results between materials with different structure and porosity. The samples were conditioned for 6 hours at a temperature of 23°C ±2°C and a controlled relative humidity of 50% RH. Each sample was placed in a container with water so that it was partially immersed for 24 hours. The water level was maintained constant throughout the test.

The water absorption W_p was calculated according to the relationship:

$$Wp = \frac{m_{24} - m_0}{A_p} \quad (6)$$

where:
m_0 - initial mass of the sample, in Kg;
m_{24} - mass of the sample after 24h immersion, in Kg;
A_p - area of the immersed surface, in m^3.

The results were expressed in Kg/m^2 .

EXPERIMENTAL RESULTS

The density of the samples was determined by weighing them and measuring the volume, applying the formula [1]. An electronic scale with an accuracy of 0.01g was used to determine the mass, and the volume was calculated based on dimensional measurements with a digital caliper.

The tests were performed in the laboratory at a temperature of 23±2°C and a relative humidity of 50±5% (Figure 6).

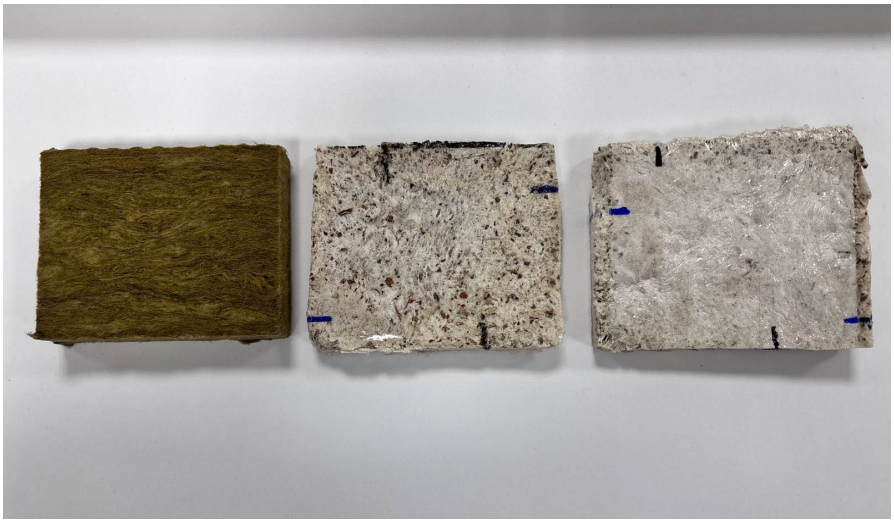

Fig. 6 - Samples prepared for density determination

Following dimensional determinations and weighing of the samples, the density of sample V2 was obtained to be 138.0 kg/m3, the density of sample V3 to be 122.2 kg/m3, and the density of mineral wool to be 100.5 kg/m3, as can be seen in the graph in figure 7.

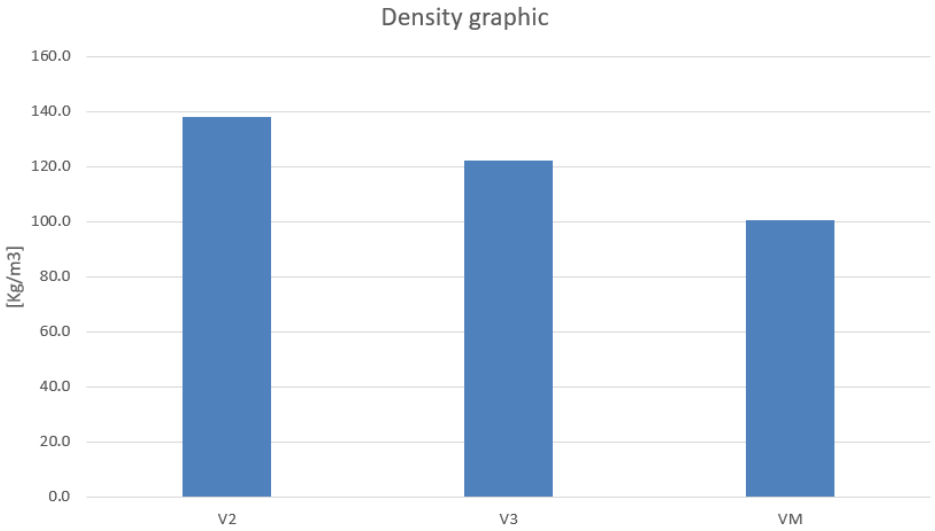

Fig. 7 - Density evaluation of the three materials

In order to evaluate the potential use of the composite material obtained from shredded fir cones, wool fragmented into small pieces and a synthetic binder (V2 and V3), a comparative analysis of **thermal conductivity** with a widely used insulating material – basalt mineral wool (VM) was carried out.

This comparative analysis provides an overview of the thermal performance of the two new recipes and allows highlighting both the advantages and possible limitations.

The following are the **thermal conductivity** values determined for the analyzed materials, obtained from the tests carried out according to the method described above.

Tabel 1

The thermal conductivity values determined for the studied materials are presented in Table 1.

Number of samples	Thermal conductivity coefficient, [W/mK]	Thermal conductivity coefficient, 10°C
V2	0.0450	0.0419
V3	0.0441	0.0410
VM	0.0357	0.0336

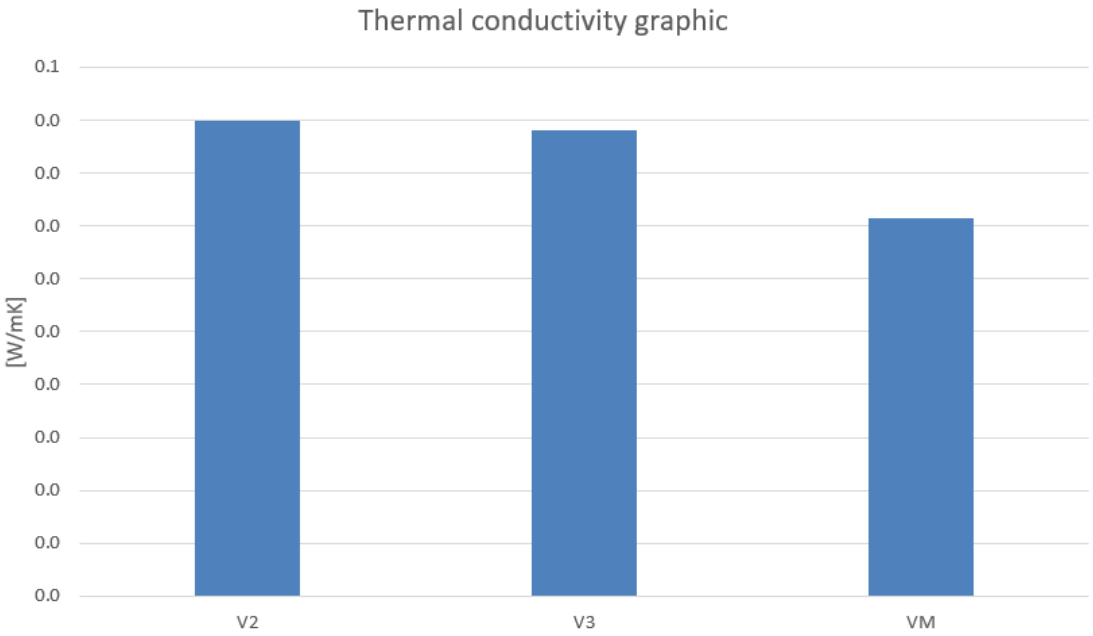

Fig. 8 - Thermal conductivity evaluation of the three types of material

The graph in figure 8 clearly shows the difference between the two composite material recipes (V2 and V3) and the reference material (VM). The values of the thermal conductivity coefficient for V2 and V3 are higher than those of basalt mineral wool, which indicates a lower thermal insulation.

However, it is noted that sample V3 has lower values than V2, confirming a slightly improved thermal performance due to the high proportion of wool. Overall, the graph highlights the positioning of the tested ecological materials between the optimal values offered by basalt mineral wool and the acceptable thresholds for insulating materials usable in construction.

Acoustic absorption coefficient

To determine the acoustic absorption coefficient, the samples were cut into circular shapes with a diameter of 63.5 mm specific to the medium acoustic interferometer, Type 4200 A (Fig.8). The average thickness of the samples is: VM - 20.30 mm, V3 – 14.72 mm and V2 – 13.80 mm

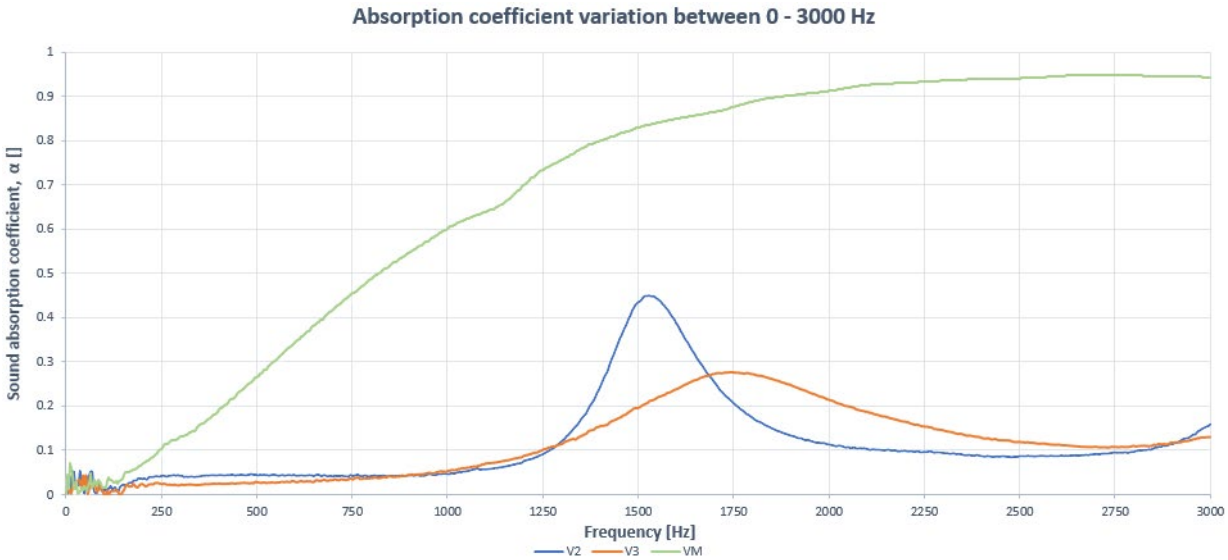

Fig. 9 - Variation of acoustic absorption coefficient, α []

The graph in figure 9 illustrates the variation of the acoustic absorption coefficient for the tested materials (V2, V3 and VM) in the range of 100-3000 Hz. It is observed that basalt mineral wool (VM) shows the best performance over the entire frequency range, reaching values close to 0.9-1.0.

The experimental composite materials (V2 and V3) show lower acoustic absorption, but highlight a differentiated behavior: sample V2 shows a significant peak around the frequency of 1500 Hz (~0.45), while sample V3 has a more uniform, but lower acoustic absorption (~0.25-0.3).

These results suggest that ecological materials can be effective in narrow frequency bands and that optimizing their structure could lead to improved acoustic performances.

Short-term water absorption by partial immersion

The three samples (V2, V3 and VM) were placed together in a clean and airtight container (figure 10). Water was poured into the container to a level of 1 cm, so that the lower part of the samples was in contact with the water.

The samples were left in this position for 24 h to achieve absorption, and were then weighed at predetermined time intervals to determine the increase in mass due to the absorbed water.

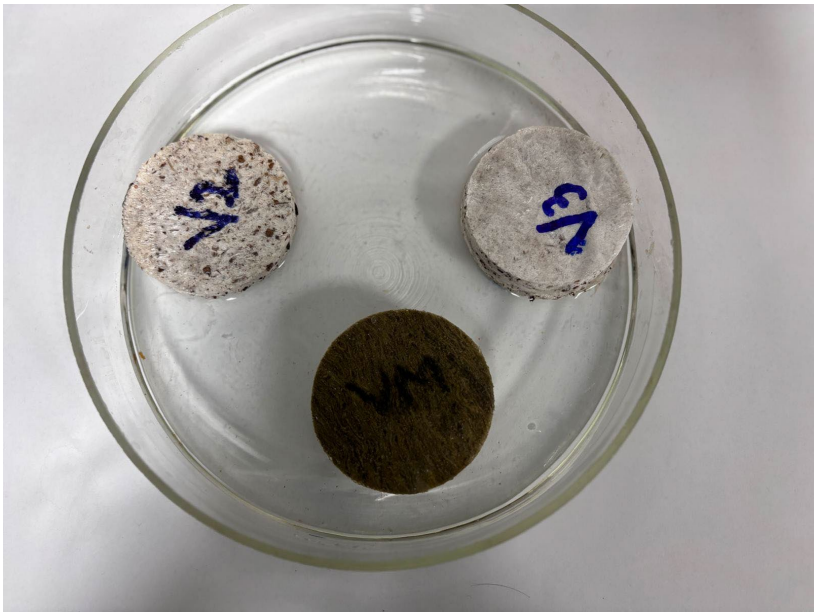

Fig. 10 - Samples V2, V3 and VM on water absorption

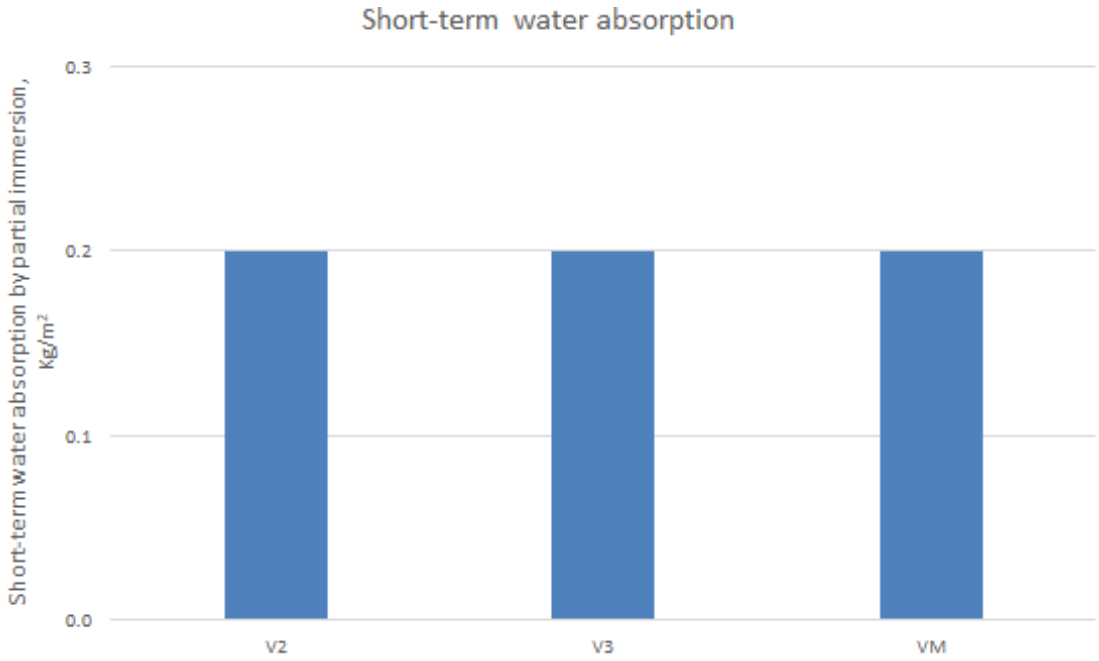

Fig. 11- Water absorption assessment

In the graph in figure 11 it is observed that the three samples presented the same degree of absorption (0.2). This indicates a uniformity of the tested material, which suggests a homogeneous structure and similar physical properties regarding permeability and porosity.

CONCLUSIONS

Based on the tests carried out in this study, the following conclusions are highlighted:

- Basalt mineral wool (VM) presents the best acoustic properties across the entire frequency range, reaching absorption coefficients of 0.9 – 1.0.
- Materials made from crushed fir cones, wool fragmented into small pieces and synthetic binder (V2 and V3) presented higher densities than basalt mineral wool (122-138 Kg/m^3 compared to 100,5 Kg/m^3), but their acoustic efficiency is limited to a narrow frequency band (approximately 1500-1700 Hz).
- The values obtained for thermal conductivity for V2 and V3 (0,041-0,045 W/mK) are comparable, but higher than for basalt mineral wool (0,033 - 0,036 W/mK), which indicates a lower thermal insulation capacity.

- The water absorption of the three analyzed samples (V2, V3 and VM) had the same value, which indicates a uniformity of the materials.
- Even if the acoustic and thermal performances of the experimental materials are inferior to basalt mineral wool, the use of renewable resources and waste highlights a significant potential in the development of ecological solutions, with an impact on the environment.
- The integration of the composite material (V2 or V3) in a panel covered with perforated sheet metal or the combination with other materials could increase both the acoustic performance and the mechanical resistance.

REFERENCES

[1] SR EN ISO 10534-2:2024 Acoustics - Determination of acoustic properties in impedance tubes - Part 2: Two-microphone method for sound absorption coefficient at normal incidence and acoustic impedance of the normal surface; https://magazin.asro.ro/

[2] Agosti,F., Buratti,C., Moretti,E. & Belloni,E. (2015) „ *Thermal and Acoustic Performance Evaluation of New Basalt Fiber Insulation Panels for Buildings. Energy Procedia, 78, 1211-1216";*

[3] Nazari,S., Razavi, M., Alihosseini, F., & Rajak, D.K. (2024) "*Effect of Natural Fiber and Biomass on Acoustic Performance of 3D Hybrid Fabric-Reinforced Composite Panels. Polymers,16(9), 1268*. doi: 10.3390/ma17235695; https://pmc.ncbi.nlm.nih.gov/articles/PMC11642230/;

[4] SR EN 12667:2002 Thermal performance of building materials and products. Determination of thermal resistance by the guarded hot plate method and by the thermofluxmeter method. Products with high and medium thermal resistance; https://magazin.asro.ro/ ;

[5] Thermal insulation products for use in buildings - Determination of bulk density, SR EN ISO 29470:2020 https://magazin.asro.ro/

[6] Rubino,C., Bonet Aracil,M., Gisbert-Paya, J., Liuzzi,S.,Stefanizii,P.,&Martellotta,F.(2019). *"Composite Eco-Friendly Sound Absorbing Materials Made of Recycled Textile Waste and Biopolymers. Materials,12(15),2497* doi: 10.3390/ma12234020; https://pmc.ncbi.nlm.nih.gov/articles/PMC6926769/;

[7] Singh, E. A., Dubey N., Puni S. (2021). *" Eco-Friendly Noise-Absorbing Panels from Waste Materials: A Sustainable Solution to Control Noise Pollution;*

[8] Strazdas , E., Janusevicius T.,(2023) " *A review ot the acoustic properties of noise barriers made from waste and plant-based materials"* . http://dx.doi.org/10.3846/enviro.2023.869

[9] Tao, Y., Ren, M., Zhang, H., & Peijs, T. (2021). "Recent progress in acoustic materials ans noise control strategies – A review. doi.org/10.1016/j.apmt.2021.101141

[10] SR EN ISO 29470:2020 Thermal insulation products for use in buildings - Determination of bulk density.

[11] *** https://icecon.ro/

VALORIZATION OF RENEWABLE RESOURCES FOR THE PRODUCTION OF BIOPLASTICS IN A CIRCULAR ECONOMY

/

VALORIFICAREA SURSELOR REGENERABILE PENTRU PRODUCEREA BIOPLASTICELOR ÎNTR-O ECONOMIE CIRCULARĂ

Ana-Maria TĂBĂRAȘU*[1)], Iuliana GĂGEANU[1)], Dragoș-Nicolae ANGHELACHE[1)], Alin-Teofil ONCESCU[1)], Doru-Relu ANTON[3)], Nicoleta-Alexandra VANGHELE[1)], Melania-Elena CISMARU[2)], Alexandru CIOACLĂ[1)], Alexandru IONESCU[1)], Cristian RADU[2)]

[1)] National Institute of Research - Development for Machines and Installations Designed for Agriculture and Food Industry - INMA Bucharest / Romania;

[2)] National University of Science and Technology POLITEHNICA Bucharest / Romania;

[3)] Ion Ionescu de la Brad Iasi University of Life Sciences / Romania

**Tel: 0730 417 449; *E-mail: anamariatabarasu22@yahoo.com.*

Keywords: *bioplastics, renewable resources, biodegrability, circular economy*

ABSTRACT

The alarming growth in the production and consumption of conventional plastics, coupled with low recycling rates and their severe environmental impact, has driven increasing interest in sustainable alternatives. Bioplastics, derived either from renewable resources or designed with biodegradability, represent a promising solution to reduce dependence on fossil fuels and to support circular economy strategies. Their classification is based on the origin of raw materials and biodegradation capacity, including polymers such as PLA, PHA, TPS, bio-PE, and PBAT. Recent literature highlights the relevance of mechanical strength, barrier performance, biodegradability, and compostability, which are essential factors for expanding their applications in packaging, agriculture, medicine, textiles, and electronics. Numerous studies also demonstrate the valorization of agro-industrial residues (starch, cellulose, proteins, lignocellulosic materials) for the development of functional bioplastics, confirming both the advantages and the current limitations of these materials. This paper aims to synthesize recent findings on renewable feedstocks used for bioplastic production, the main processing steps, key properties, and application domains, with a particular emphasis on their contribution to the circular economy.

REZUMAT

Creșterea alarmantă a producției și consumului de plastice convenționale, asociată cu rata scăzută de reciclare și impactul negativ asupra mediului, a stimulat interesul pentru dezvoltarea unor alternative sustenabile. Bioplasticele, obținute fie din resurse regenerabile, fie prin procese care le conferă biodegradabilitate, reprezintă o soluție promițătoare pentru reducerea dependenței de combustibili fosili și integrarea în economia circulară. Clasificarea lor se bazează pe originea materiilor prime și pe capacitatea de degradare biologică, fiind incluse materiale precum PLA, PHA, TPS, bio-PE sau PBAT. Literatura recentă evidențiază importanța proprietăților mecanice, de barieră, biodegradabilitate și compostabilitate, factori esențiali pentru extinderea aplicațiilor în ambalaje, agricultură, medicină, textile și electronică. De asemenea, numeroase studii au demonstrat posibilitatea valorificării deșeurilor agroindustriale (amidon, celuloză, proteine, lignocelulozice) pentru obținerea de bioplastice funcționale, confirmând atât avantajele, cât și limitele acestor materiale. Lucrarea urmărește să sintetizeze informațiile recente privind sursele regenerabile utilizate în producerea bioplasticelor, etapele de procesare, proprietățile esențiale și domeniile de aplicare, cu accent pe contribuția lor la o economie circulară.

INTRODUCTION

Conventional plastics, primarily derived from petroleum, have become ubiquitous due to their durability, low cost, and versatility. However, these very properties make them highly problematic for the environment. Their degradation can take hundreds or even thousands of years, during which the resulting fragments, including microplastics and nanoplastics, contaminate water, soil, and food chains, with adverse effects on ecosystems and human health. Moreover, their entire life cycle accounts for approximately 15% of the global carbon budget, contributing significantly to climate change (*Venkatachalam H. and Palaniswamy*

R., 2020; Atiwesh G. et al., 2021; Chilote M.O. and Dhakal H.N.; Mishra S. et al., 2024). Global plastic production exceeds 300 million tons per year, while the recycling rate is only 7%. The remaining share is either incinerated or disposed of in dedicated landfill sites (*Atiwesh G. et al., 2021*). In 2015, approximately 407 million tons were produced, and projections indicate that by 2050 this amount could exceed 1,600 million tons annually if no decisive measures are implemented (*Mishra S. et al., 2024*).

In this context, bioplastics have emerged as a promising alternative. They are polymeric materials that are either biodegradable or produced from renewable biological resources such as corn or potato starch, cellulose, chitosan, or polyhydroxyalkanoates (*Chauhan K. et al., 2024; Pooja N. et al., 2023; Narmatha J. and Amritkumar P., 2021*).

The major difference from conventional plastics lies in the origin of the raw materials and, in many cases, in their ability to decompose more rapidly, thereby reducing the carbon footprint and the dependence on fossil fuels *(Venkatachalam H. and Palaniswamy R., 2020.; Pooja N. et al., 2023*). However, it is important to emphasize that bioplastics are not universally biodegradable. For instance, bio-PE and bio-PP demonstrate degradation resistance comparable to that of their petrochemical analogues, despite being derived from renewable raw materials (*Pooja N. et al., 2023*).

Although research on bioplastics began many years ago, their production has not yet reached a significant industrial scale. In 2019, approximately 1.95 million tons were produced, representing only 0.6% of the global plastic output. According to the data in Figure 1, the evolution of these volumes in recent years can be observed, as well as the anticipated growth trends for the coming period (*Costa A. et al., 2023*).

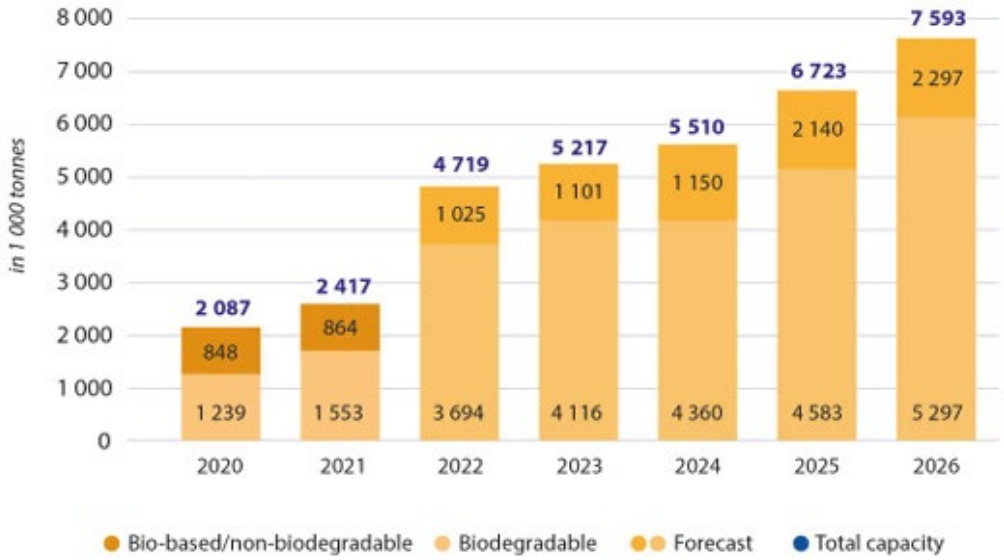

Fig. 1 - Estimates of global bioplastics production for the period 2021–2026
(*Costa A. et al., 2023*)

Figure 1 illustrates the projected evolution of global bioplastics production capacities between 2020 and 2026, including both biodegradable types and those derived from biological resources that do not naturally decompose. In 2020, total production was approximately 2.1 million tons, and by 2026 it is expected to reach around 7.6 million tons. Both categories will expand, although biodegradable bioplastics are projected to grow at a faster rate. Nevertheless, bio-based but non-biodegradable plastics will remain dominant. The most significant increase is anticipated during the period 2024–2026.

MATERIALS AND METHODS

The diversity of existing bioplastics arises both from the variety of raw materials used and from the processes by which they are transformed. To better understand their characteristics and potential applications, bioplastics can be classified according to several criteria, the most common being the origin of the resources and their biodegradability, as well as the chemical composition of the base material.

Bioplastics can first be classified according to the source of the raw material and their biodegradability:

- Bio-based and biodegradable: obtained from renewable resources and capable of decomposing under specific conditions. Examples include polylactic acid (PLA),

polyhydroxyalkanoates (PHA), and thermoplastic starch (TPS) *(Costa A. et al., 2023; Ahsan W.A. et al., 2023).*

- Bio-based and non-biodegradable: produced from renewable raw materials but exhibiting resistance to degradation similar to that of conventional plastics. Examples include bio-based polyethylene (bio-PE), bio-based polyethylene terephthalate (bio-PET), and bio-based polyamides (bio-PA) *(Costa A. et al., 2023; Ahsan W.A. et al., 2023).*
- Fossil-based and biodegradable: derived from fossil resources but with properties that allow biological decomposition. Examples include polybutylene adipate-co-terephthalate (PBAT), polycaprolactone (PCL), and polybutylene succinate (PBS) *(Ahsan W.A. et al., 2023).*

From the perspective of composition, bioplastics can be derived from a wide range of natural raw materials:

- Starch-based: produced from cereals or tubers (corn, potatoes, wheat), usually combined with other biodegradable polymers such as PLA, PBS, PBAT, PCL, or PHA.
- Cellulose-based: derived from wood, plant fibers, or bamboo, in the form of esters such as acetate, nitrate, butyrate, or propionate.
- Protein-based: produced from gluten, casein, albumin, whey, or soy protein *(Dalmia J. and Wadiye G., 2020)*.
- Aliphatic polyesters: obtained through bacterial fermentation of low-cost carbon sources, including PHA, PHB, PLA, PGA, and PCL.
- Bio-based polyamides: formed through the reaction between diamines and dicarboxylic acids, for example from ricinoleic acid or sebacic acid.
- Bio-based polyethylene: derived from ethylene obtained through the fermentation of ethanol sourced from sugarcane or corn.
- Lipid-based polymers: obtained from vegetable or animal triglycerides, such as sunflower oil, soybean oil, or castor oil *(Dalmia J. and Wadiye G., 2020).*

At the global level, agricultural activities and related industries (such as food processing, alcohol production, forestry, and sugar manufacturing) generate very large amounts of plant residues, estimated at nearly 933 million tons annually. Although these wastes can be used as fertilizers, in paper production, or as sources of biofuels, most are incinerated or landfilled, with negative environmental impacts.

Their integration into the circular economy through conversion into bioplastics offers valuable opportunities, particularly due to their high content of polysaccharides such as starch, cellulose, chitin, and pectin. Figure 2 briefly illustrates the transformation stages of these resources, from extraction and processing to applications and end-of-life management, a process influenced by the type of biomass and its chemical composition (*Negrete-Bolagay D. and Guerrero V.H., 2024*).

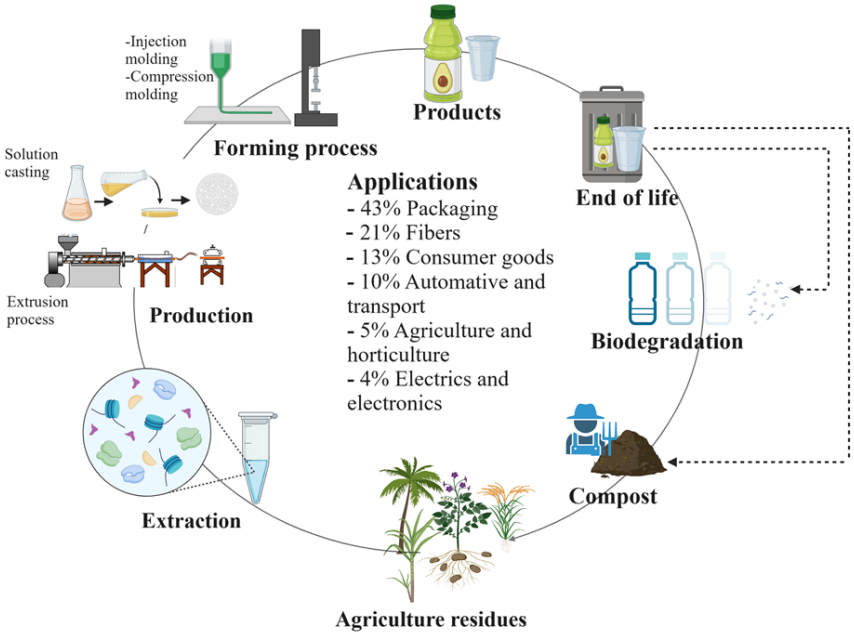

Fig. 2 - Bioplastic production and applications derived from agricultural residues
(*Negrete-Bolagay D. and Guerrero V.H., 2024*)

The performance of bioplastics is closely linked to their physical properties and behavior in the environment. Among the most important are mechanical properties, which determine strength and durability, barrier properties, which are essential for applications such as food packaging, as well as biodegradability and compostability, which define how they are integrated at the end of their life cycle within the circular economy.

Table 1 summarizes these characteristics based on recent studies.

Table 1

Properties of bioplastics

Mechanical properties	Barrier properties	Biodegrability	Compostability	References
Tensile strength, Young's modulus, elongation at break	Oxygen, CO_2, water vapor permeability; UV protection	Discussed for PLA, PHA, TPS	Addressed in relation to food packaging standards	(*Somoghi R. et al., 2025*)
Effect of plasticizers on strength and flexibility	Barrier to oxygen and moisture	Tested under different environmental conditions	Mentioned for PLA, PHA and blends	(*Shi X. et al., 2025*)
Tensile strength, elongation, structural changes during composting	-	Monitored via mass loss and property degradation	Long-term composting studies (90–365 days)	(*Myalenko D. and Fedotova O., 2023*)
Comparative analysis of mechanical reinforcement strategies	Permeability and stability considerations	Degradation in soil and water	Theoretical discussion of compostability	(*Attallah O.A. et al., 2021*)
-	-	Tested in soil, freshwater, marine, and industrial environments	Compared between industrial composting and natural settings	(*Gadaleta G. et al., 2025*)

Due to their structural and functional diversity, bioplastics can be applied across a wide range of fields, from packaging and agriculture to medicine and emerging industries such as textiles and electronics. Each sector leverages specific properties of these materials, such as mechanical strength, barrier performance, or biodegradability.

Table 2 summarizes the main application areas and representative examples reported in the scientific literature.

Table 2

Examples of bioplastic applications in packaging, agriculture, medicine, and electronics

Packaging	Agriculture	Medicine and Biotechnology	Textiles and Electronics
PLA and PHA films, active/smart packaging, food trays, disposable films, bioplastic food packaging materials (*Shi X. et al., 2025 ; Ibrahim N.I. et al., 2021; Elkaliny N.E. et al., 2024*)	PLA and PHA films, active/smart packaging, food trays, disposable films, bioplastic food packaging materials (*Ibrahim N.I. et al., 2021*; *Negrete-Bolagay D. and Guerrero V.H., 2024)*	Drug delivery coatings, wound dressings, sutures, scaffolds for tissue engineering, biomedical implants and prosthetics (*Ibrahim N.I. et al., 2021*; *Negrete-Bolagay D. and Guerrero V.H., 2024.*; *Elkaliny N.E. et al., 2024.*)	Biopolymer fibres for clothing, electronics casings, biodegradable electronic components, textile additives, biopolymer composites (*Ibrahim N.I. et al., 2021*; *Negrete-Bolagay D. and Guerrero V.H., 2024.*; *Elkaliny N.E. et al., 2024.*)

In addition to classifications and functional properties, bioplastics exhibit both significant advantages and limitations that influence their large-scale adoption. The main benefits include the use of renewable resources, integration into the circular economy, and the potential to reduce plastic pollution. At the same time, high production costs, sometimes lower performance compared to conventional materials, and the requirement for specific conditions for biodegradation remain major challenges.

Figure 3 illustrates these aspects in a comparative manner (*Gadaleta G. et al., 2025; Pires J.R.A. et al., 2022; Di Bartolo A. et al., 2021 ; Nicolau A.-M. and Petcu P., 2025; Jha S. ET AL., 2024 ; Abe M.M. et al., 2021; Stasiškiene Ž.; B. et al., 2022 ; Bartolucci L. et al., 2023*).

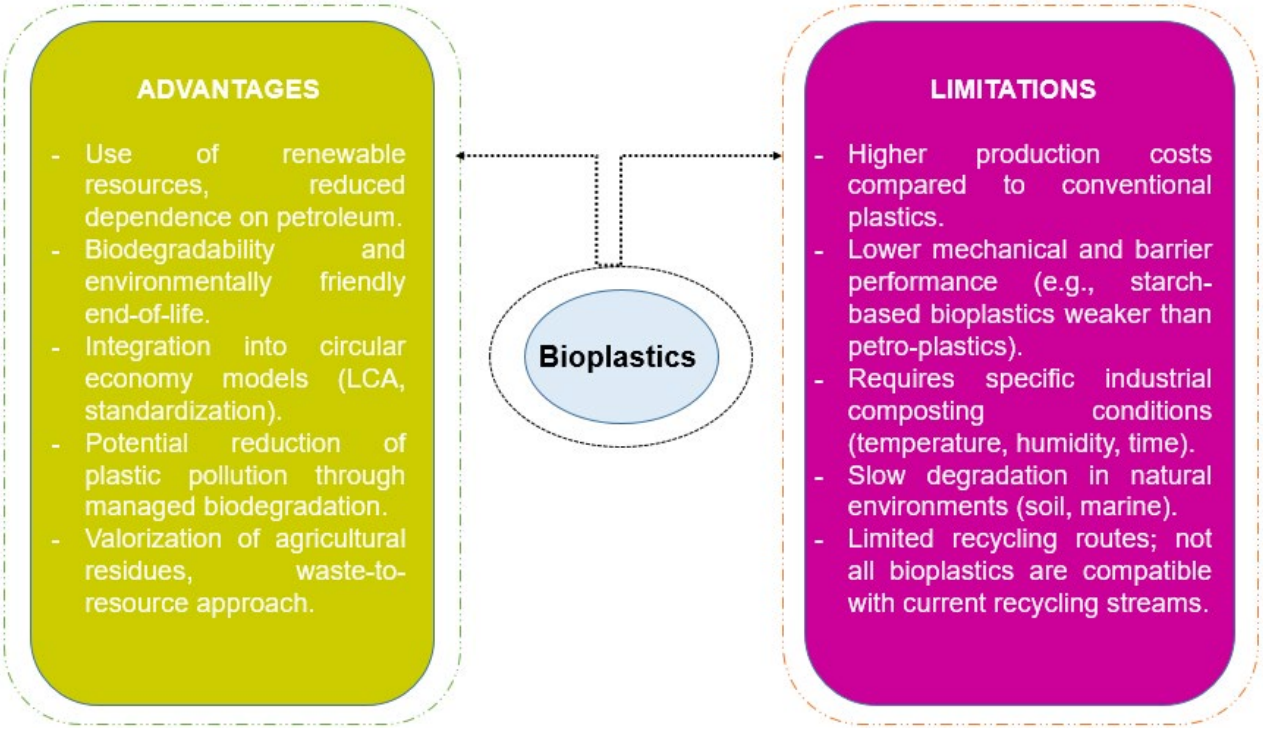

Fig. 3 - Comparative summary of the advantages and limitations of bioplastics

RESULTS

The scientific literature provides multiple examples demonstrating that plant residues and by-products can be converted into bioplastics with functional and environmentally friendly properties. The following section presents several recent studies that are relevant to the application of circular economy principles.

The study (*Torche A. et al., 2025*) utilized cassava starch in combination with onion peel powder, an agro-industrial by-product often discarded as waste, to develop bioplastics intended for food packaging. By

optimizing the composition through statistical methods, films were obtained with tensile strength values of up to 3.87 MPa and a biodegradability rate of approximately 30% after 30 days.

Recent research (*Alves L.T.d.O et al., 2024*) focused on producing biofilms based on proteins extracted from sunflower seeds, a renewable and abundant resource often obtained as a by-product of the vegetable oil industry. To enhance the material's properties, these proteins were combined with locust bean gum, a natural polysaccharide used as a thickening and stabilizing agent.

Analyses showed that higher proportions of gum led to more uniform film structures, increased mechanical strength, and improved barrier performance against water vapor and oxygen, which are essential features for food packaging. At the same time, solubility and biodegradability tests confirmed that these films maintained their eco-friendly profile, degrading rapidly under natural conditions.

Another recent study (*Santos J.F. et al., 2025*) investigated the improvement of cassava starch-based bioplastics by incorporating an alcoholic extract from the Amazonian plant *Vismia guianensis*, which is rich in polyphenolic compounds with antioxidant and antimicrobial effects. Films obtained by the casting method, with extract concentrations ranging from 0.2% to 1.0%, were characterized using physicochemical and mechanical techniques.

The results showed that the extract interacts with starch chains through hydrogen bonding, leading to improved flexibility, thermal stability, and mechanical strength, particularly at the 0.2% concentration. In addition, the films acquired extra functional properties, such as antioxidant and antimicrobial activity, making them promising not only for sustainable packaging but also for biomedical applications.

Waisarikit, A. et al. (*Waisarikit A. et al., 2025*) explored the use of spent coffee grounds from the coffee industry as a natural additive to enhance polylactic acid (PLA), a biopolymer employed in the production of biodegradable horticultural bags. By extracting residual oils from the coffee grounds, stable particles (exSCG) were obtained and incorporated at concentrations of 5–15% into the PLA matrix, followed by processing through extrusion and film blowing. The results showed that the addition of exSCG increased material flexibility, reduced UV light transmission, and accelerated soil biodegradability, while maintaining mechanical properties suitable for practical use. The optimal composition was identified at 10% exSCG, providing a balance between processability, mechanical performance, and controlled degradation.

Another material that can be valorized is corn husk (*Motshabi N. et al.,2025*), which represents an important source of cellulose nanofibrils. These can enhance the mechanical strength, thermal stability, and barrier properties of bioplastics while preserving their biodegradability. Similarly, sugarcane bagasse (*Hassan S. et al., 2024*), an abundant lignocellulosic residue, can be converted through microbial processes into polyhydroxyalkanoates (PHA). These bioplastics are fully biodegradable and provide a sustainable alternative to conventional plastics.

The study (*Ugozor A.O. et al., 2025*) demonstrated the potential for producing biodegradable bioplastics from agricultural residues such as bean husks, plantain peels, and cork stoppers from wood. Cellulose was extracted from these materials through acid-alkaline treatments and subsequently converted into cellulose acetate via acetylation reactions. Yields varied depending on the source used, with the highest recorded for bean husks (45.5% cellulose and 80% cellulose acetate).

Tests confirmed significant biodegradability within approximately four weeks, highlighting the potential of these waste streams to serve as raw materials for sustainable bioplastics.

CONCLUSIONS

Bioplastics are emerging as a sustainable alternative to conventional plastics, playing a key role in reducing dependence on fossil resources and limiting pollution caused by traditional plastic.

The use of renewable resources and agro-industrial residues, such as starch, cellulose, proteins, and lignocellulosic materials, demonstrates the potential of these streams to be transformed into value-added raw materials, directly contributing to the development of the circular economy.

Mechanical and barrier properties, together with biodegradability and compostability, are decisive factors for the large-scale adoption of bioplastics, particularly in sectors such as packaging, agriculture, medicine, textiles, and electronics. However, current limitations, including high production costs, sometimes lower performance compared to conventional materials, and the need for specific conditions for biodegradation, require intensified research and process optimization.

The integration of bioplastics into global economic chains can be accelerated through innovation, standardization, and supportive public policies, paving the way for a genuine transition to a circular economy.

REFERENCES

[1] Abe, M.M., Martins, J.R., Sanvezzo, P.B., Macedo, J.V., Branciforti, M.C., Halley, P., Botaro, V.R., Brienzo, M. (2021). Advantages and Disadvantages of Bioplastics Production from Starch and Lignocellulosic Components. *Polymers*, 13, 2484. https:// doi.org/10.3390/polym13152484.

[2] Ahsan, W.A., Hussain, A., Lin, C., Nguyen, M.K. (2023). Biodegradation of Different Types of Bioplastics through Composting—A Recent Trend in Green Recycling. *Catalysts*, 13, 294. https:// doi.org/10.3390/catal13020294.

[3] Alves, L.T.d.O., Fronza, P., Gonçalves, I., da Silva, W.A., Oliveira, L.S., Franca, A.S. (2024). Development of Polymeric Films Based on Sunflower Seed Proteins and Locust Bean Gum. *Polymers*, 16, 1905. https://doi.org/10.3390/polym16131905.

[4] Attallah, O.A., Mojicevic, M., Garcia, E.L., Azeem, M., Chen, Y., Asmawi, S., Brenan Fournet, M. (2021). Macro and Micro Routes to High Performance Bioplastics: Bioplastic Biodegradability and Mechanical and Barrier Properties. *Polymers*, 13, 2155. https://doi.org/10.3390/ polym13132155.

[5] Atiwesh, G., Mikhael, A., Parrish, C.C., Banoub, J. (2021). Environmental impact of bioplastic use: A review. *Heliyon,* 7.

[6] Bartolucci, L., Cordiner, S., DeMaina, E., Kumar, G., Mele, P., Mulone, V., Igliński, B., Piechota, G. (2023). Sustainable Valorization of Bioplastic Waste: A Review on Effective Recycling Routes for the Most Widely Used Biopolymers. *Int. J. Mol. Sci*., 24, 7696. https://doi.org/ 10.3390/ijms24097696.

[7] Chauhan, K., Kaur, R., Chauhan, I. (2024). Sustainable bioplastic: a comprehensive review on sources, methods, advantages, and applications of bioplastics. *Polymer-plastics technology and materials*, https://doi.org/10.1080/25740881.

[8] Chilote, M.O., Dhakal, H.N. (2025). Plastic Pollution and Framework Towards Sustainable Plastic Waste Management in Nigeria: Case Study. *Environments*, 12, 209. https://doi.org/10.3390/environments12060209.

[9] Costa, A., Encarnação, T., Tavares, R., Todo Bom, T., Mateus, A. (2023). Bioplastics: Innovation for Green Transition. *Polymers*, 15, 517. https://doi.org/10.3390/polym 15030517.

[10] Dalmia, J., Wadiye, G. (2020). Review of types and applications of bioplastics. *IARJSET*, Vol. 7, Issue 6.

[11] Di Bartolo, A., Infurna, G., Dintcheva, N.T. (2021). A Review of Bioplastics and Their Adoption in the Circular Economy. *Polymers*, 13, 1229. https://doi.org/10.3390/ polym13081229.

[12] Elkaliny, N.E., Alzamel, N.M., Moussa, S.H., Elodamy, N.I., Madkor, E.A., Ibrahim, E.M., Elshobary, M.E., Ismail, G.A. (2024). Macroalgae Bioplastics: A Sustainable Shift to Mitigate the Ecological Impact of Petroleum-Based Plastics. *Polymers*, 16, 1246. https://doi.org/ 10.3390/polym16091246.

[13] Gadaleta, G., Andrade Chapal, J.C., López-Ibáñez, S., Mozo Toledo, M., Navarro-Calderón, Á. (2025). Biodegradability of Bioplastics in Managed and Unmanaged Environments: A Comprehensive Review. *Materials*, 18, 2382. https://doi.org/10.3390/ ma18102382.

[14] Hassan, S., Ngo, T., Ball, A.S. (2024). Valorisation of Sugarcane Bagasse for the Sustainable Production of Polyhydroxyalkanoates. *Sustainability*, 16, 2200. https:// doi.org/10.3390/su16052200.

[15] Ibrahim, N.I., Shahar, F.S., Sultan, M.T.H., Shah, A.U.M., Safri, S.N.A., Mat Yazik, M.H. (2021). Overview of Bioplastic Introduction and Its Applications in Product Packaging. *Coatings*, 11, 1423. https:// doi.org/10.3390/coatings11111423.

[16] Jha, S., Akula, B., Enyioma, H., Novak, M., Amin, V., Liang, H. (2024). Biodegradable Biobased Polymers: A Review of the State of the Art, Challenges, and Future Directions. *Polymers*, 16, 2262. https: //doi.org/10.3390/polym16162262.

[17] Mishra, S., Bauri, K.P., Panigrahi, S. (2024). Addressing plastic pollution: Sustainable alternatives and advanced waste management. *World Journal of Advanced Research and Reviews*, 23(02), 1948-1957.

[18] Motshabi, N., Lenetha, G.G., Malimabe, M.A., Gumede, T.P. (2025). Cellulose Nanofibril-Based Biodegradable Polymers from Maize Husk: A Review of Extraction, Properties, and Applications. *Polymers*, 17, 1947. https://doi.org/ 10.3390/polym17141947.

[19] Myalenko, D., Fedotova, O. (2023). Physical, Mechanical, and Structural Properties of the Polylactide and Polybutylene Adipate Terephthalate (PBAT)-Based Biodegradable Polymer during Compost Storage. *Polymers*, 15, 1619. https:// doi.org/10.3390/polym15071619.

[20] Narmatha, J., Amritkumar, P. (2021). Classification of Bioplastics Based on Sources. *Indian Journal of Natural Sciences*, Vol.12, Issue 69.

[21] Negrete-Bolagay, D., Guerrero, V.H. (2024). Opportunities and Challenges in the Application of Bioplastics: Perspectives from Formulation, Processing, and Performance. *Polymers*, 16, 2561. https://doi.org/10.3390/ polym16182561.

[22] Nicolau,A.-M., Petcu, P. (2025). A Systemic View of Biodegradable Materials: Analyzing the Environmental Performance of Compostable Coffee Capsules in Real Infrastructural Contexts. *Sustainability*, 17, 7736. https://doi.org/ 10.3390/su17177736.

[23] Pires, J.R.A., Souza, V.G.L., Fuciños, P., Pastrana, L., Fernando, A.L. (2022). Methodologies to Assess the Biodegradability of Bio-Based Polymers—Current Knowledge and Existing Gaps. *Polymers*, 14, 1359. https://doi.org/10.3390/ polym14071359.

[24] Pooja, N., Chakraborty, I., Rahman, M.H., Mazmuder, N. (2023). An insight on sources and biodegradation of bioplastics: A review. Biotech, 13:220, https://doi.org/10.1007/s13205-023-03638-4.

[25] Santos, J.F., Silva, C.W.C., Silva, B.P.G., Britto-Costa, P.H., Costa, C.S., Otubo, L., Carbonari, A.W., Cabrera-Pasca, G.A. (2025). Enhancing Cassava Starch Bioplastics with Vismia guianensis Alcoholic Extract: Characterization with Potential Applications. Polymers, 17, 419. https://doi.org/10.3390/ polym17030419.

[26] Shi, X., Cui, L., Xu, C., Wu,S. (2025). Next-Generation Bioplastics for Food Packaging: Sustainable Materials and Applications. Materials, 18, 2919. https://doi.org/10.3390/ ma18122919.

[27] Somoghi, R., Mihai, S., Oancea, F. (2025). An Overview of Bio-Based Polymers with Potential for Food Packaging Applications. Polymers, 17, 2335. https://doi.org/ 10.3390/polym17172335.

[28] Stasiškienė, Ž., Barbir, J., Draudvilienė, L., Chong, Z.K., Kuchta, K., Voronova, V., Leal Filho, W. (2022). Challenges and Strategies for Bio-Based and Biodegradable Plastic Waste Management in Europe. Sustainability, 14, 16476. https:// doi.org/10.3390/su142416476.

[29] Torche, A., Toufik,C., Djeghim,F., Sanah, I., Arhab, R., D'Elia, M., Rastrelli, L. (2025). Optimization of Cassava Starch/Onion Peel Powder Based Bioplastics: Influence of Composition on Mechanical Properties and Biodegradability Using Central Composite Design. Foods, 14, 2414. https://doi.org/10.3390/foods14142414.

[30] Ugozor, A. O., Udebuani, A. C., & Nnorom, O. O. (2025). Production of bioplastic from waste agricultural biomass. European Journal of Sustainable Development Research, 9(2), em028. https://doi.org/10.29333/ejosdr/16248.

[31] Venkatachalam, H., Palaniswamy, R. (2020). Bioplastic world: A review. Journal of Advanced Scientific Research, 11 (3), 2020.

[32] Waisarikit, A., Suadaung, N., Khantho,B., Hadad,B., Ross,G.M., Topham,P.D., Ross,S., Mahasaranon, S. (2025). Extracted Spent Coffee Groundsasa Performance-EnhancingAdditivefor Poly(Lactic Acid) Biodegradable NurseryBagsinAgriculture. Polymers, 17, 561. https://doi.org/ 10.3390/polym17050561.

CURRENT STATE OF RESEARCH ON THE INFLUENCE OF VIBRATIONS ON THE HUMAN BODY OF VEHICLE OPERATORS

/

STADIUL ACTUAL AL CERCETĂRILOR PRIVIND INFLUENȚA VIBRAȚIILOR ASUPRA ORGANISMULUI UMAN AL CONDUCĂTORULUI AUTO

Teofil-Alin ONCESCU*[1)], Nicolae-Valentin VLADUT[1)], Iuliana GAGEANU[1)], Ioan Catalin PERSU[1)], Gabriel-Mihai MATACHE[1)], Oana Elena MILEA[1)], Ana-Maria TABARASU[1)], Lavinia Madalina MICU[2)]

[1)] National Institute of Research - Development for Machines and Installations Designed for Agriculture and Food Industry - INMA Bucharest, 013811 Bucharest / Romania;

[2)] University of Life Sciences "King Mihai I" from Timisoara, Timis County / Romania.

**Tel: (+40) 786 848 903; *E-mail: alin.oncescu93@gmail.com*

Keywords: *Whole Body Vibration (WBV), ISO2631-1, Root Mean Square acceleration, agricultural vehicles, vibration analysis*

ABSTRACT

Exposure to mechanical vibrations represents a major occupational health and safety risk, particularly in sectors that involve prolonged operation of road vehicles or heavy machinery. This review article provides a comprehensive and critical analysis of the current scientific literature concerning the influence of vibrations on the human body, with a specific focus on Whole-Body Vibration (WBV) exposure. It defines the fundamental concepts related to vibration, including physical characteristics (frequency, amplitude, and direction), predominant sources of vibration within the vehicle–driver system, and the pathways through which these vibrations are transmitted to the human body. This paper explores biomechanical and physiological correlations between vibration parameters and human anatomical structures, highlighting both acute and chronic health effects such as musculoskeletal disorders, intervertebral disc degeneration, accelerated fatigue, and decreased cognitive performance. It also reviews international exposure assessment criteria in accordance with ISO 2631-1 standards and current occupational health regulations. Ultimately the current state of research in the field of whole-body vibration (WBV) is synthesized, highlighting emerging investigative directions, existing knowledge gaps, and the pressing need to develop advanced methods for monitoring and mitigating vibrations transmitted to the human body in the context of increasingly technologized mobility. In this regard, modern systems for the acquisition and processing of experimental vibration data affecting the human body—specifically the vehicle operator—are presented and analysed, aiming to substantiate practical solutions for reducing the risks associated with occupational exposure.

REZUMAT

Expunerea conducătorilor auto la vibrații mecanice reprezintă un factor de risc major pentru sănătatea și siguranța ocupațională, în special în sectoarele care implică operarea prelungită a vehiculelor rutiere sau utilajelor grele. Acest articol de tip review oferă o analiză comprehensivă și critică a literaturii de specialitate privind influența vibrațiilor asupra organismului uman, cu accent pe expunerea de tip Whole-Body Vibration (WBV). Sunt definite conceptele fundamentale legate de vibrații, incluzând caracteristicile fizice (frecvență, amplitudine, direcție), sursele predominante ale vibrațiilor în sistemul vehicul–șofer și modalitățile de transmitere a acestora către corpul uman. Lucrarea abordează corelațiile biomecanice și fiziologice dintre parametrii vibrațional și structura anatomică a organismului uman, evidențiind efectele acute și cronice ale expunerii, precum: tulburări musculo-scheletale, afectarea discurilor intervertebrale, oboseală accelerată și diminuarea performanței cognitive. De asemenea, sunt analizate criteriile internaționale de evaluare a expunerii la WBV, în conformitate cu standardele ISO 2631-1 și reglementările în vigoare privind sănătatea ocupațională. În final, este realizată o sinteză a stadiului actual al cercetărilor în domeniul WBV, punând în evidență direcțiile emergente de investigare, lacunele de cunoaștere existente și necesitatea dezvoltării unor metode avansate de monitorizare și atenuare a vibrațiilor transmise întregului corp în contextul unei mobilități din ce în ce mai tehnologizate. În acest sens, sunt prezentate și analizate sisteme moderne de achiziție și prelucrare a datelor experimentale privind vibrațiile la care este supus organismul uman – conducătorul auto, în scopul fundamentării unor soluții practice de reducere a riscurilor asociate expunerii ocupaționale.

INTRODUCTION

The present review article aims to provide a comprehensive and well-documented analysis of the scientific literature concerning the influence of vehicle-induced vibrations on the human body of the driver, with the purpose of positioning this research topic within the current context of the field. In order to achieve the proposed objectives, several essential directions of investigation are addressed, structured as follows: the definition of vibrations and identification of their generation sources within driver–vehicle systems; the analysis of physiological and biomechanical effects of vibrations on the human body; the assessment of exposure levels to Whole-Body Vibrations (WBV) according to current international standards; the examination of relevant anatomical characteristics influencing vibration transmission; and the synthesis of the current state of research regarding WBV and its implications on occupational health.

This approach aims to establish a scientific foundation for understanding the relationship between vibration parameters and the human biological structure in the context of vehicle operation under mechanically demanding environments.

Vibrations experienced by drivers represent a ubiquitous phenomenon resulting from the complex interaction between vehicle systems and road surface irregularities. These vibrations affect a wide range of operators — from commercial vehicle drivers and agricultural machinery operators to heavy equipment operators — exposing them to mechanical stressors that may, over time, lead to musculoskeletal disorders and neurological impairments. Vibrations are defined as mechanical oscillations of a body around its equilibrium position, characterized by specific parameters such as frequency, amplitude, and direction, which are influenced by both internal and external dynamic factors *(Blanks, A. M., et al. 2022; Shen, C.-L., et al. 2022; Zhou, Y., et al. 2022; Mester, J., et al. 2021; Ramoneda-Rabat, M., et al. 2024)*.

In the context of motor vehicles, the main sources of vibration include the engine, transmission, suspension system, road surface irregularities, and the interaction between the tires and the contact surface. The transmission of vibrations to the human body occurs through contact points such as the seat, steering wheel, and floor, while the biomechanical response depends on both the vibration parameters and the posture adopted during driving. Under Whole-Body Vibration (WBV) conditions, the body movements occur in a synchronous manner, manifesting as a global dynamic response of the human mass relative to the excitation source *(Mirakhorlo, M. et al. 2022; Desai, R. et al. 2024; Desai, R. et al. 2023; Cvetković, M. et al. 2023; Happee, R. et al. 2023)*.

The analysis of whole-body transmitted vibrations focuses on the critical frequency range of [0–80] Hz, as specified by ISO 2631, considering their significant impact on the physiological functions of exposed operators (ISO 2631-1, 1997). In the case of Whole-Body Vibrations (WBV), various anatomical regions of the human body come into direct contact with the vibration source — a representative example being the operating environment of agricultural vehicles such as tractors — where the transfer of mechanical energy disturbs physiological homeostasis, induces discomfort, and affects long-term health. Prolonged exposure may lead to musculoskeletal disorders, particularly affecting the spinal column and joint structures.

The assessment of vibration severity is based on three fundamental criteria: reduction of comfort, interference with task performance, and deterioration of health status. The health effects are influenced by three primary factors: the threshold value of exposure without adverse effects, the dose–response relationship between vibration magnitude and the severity of outcomes, and the latency period between the initial exposure and the onset of symptoms. High-risk exposure environments include off-road vehicles (tractors, agricultural machinery) and heavy road vehicles (trucks, buses), in which vibrations are recognized sources of discomfort and potential occupational injuries *(Singh, R. et al. 2022; Barač, G. et al. 2025; Melo, R. 2019)*. The vibrational behavior of the vehicle, perceived as driving dynamics, manifests predominantly within the frequency range below 20 Hz, with acceleration amplitudes sufficiently high to be transmitted and perceived by the driver. Vibrations generated by the vehicle structure — particularly those associated with pitch, roll, and yaw motions — are directly correlated with the dynamic characteristics of the suspension system, chassis, and body, representing key components of the vehicle–terrain interaction. These vibrations are transmitted through the wheels as a result of contact with surface irregularities and subsequently propagate through the vehicle structure toward the driver's contact points *(Vlădut, N., V., et al. 2024; Burdzik, R. 2023; Dumitriu, M. et al. 2023; Zhang, Y. et al. 2021; Zhou, Y. 2023)*.

For the purpose of contextualizing the analyzed experimental data, it is necessary to provide a technical characterization of the vehicle employed in the studies concerning the influence of vibrations on the human body.

The vehicle of interest is the agricultural tractor — a self-propelled machine, equipped with either wheels or tracks, designed to provide traction and power for mounted, semi-mounted, or towed implements. The construction characteristics, total mass, axle load distribution, suspension stiffness, seat geometry, and cabin configuration are determining factors of the overall vibrational behavior of the system, directly influencing both the level and nature of the operator's exposure to Whole-Body Vibrations (WBV) *(Guruguntla, V. et al.2023; Mei, Y. et al. 2023; Barrie, A. et al 2024)*.

Self-propelled agricultural vehicles of the tractor type can be classified according to the type of engine with which they are equipped, as follows: thermal engine tractors and electric engine tractors, as illustrated in Figure 1.

a) **b)**

Fig. 1 - Self-propelled agricultural vehicle of the tractor type: (a) equipped with a thermal engine; (b) equipped with an electric engine

Studies conducted by various authors (*Mitroi, M. F., 2020; Deulgaonkar, V. R., 2012; Harikrishnan, P., 2017; Hiemstravan, M., 2014*) highlight that vibrations and shocks transmitted through the vehicle structure — particularly via the floor, seat, and other cabin components — are directly perceived by the driver, influencing both biomechanical comfort and physiological exposure. The specialized literature examines the behavior of the tire–wheel system, schematically illustrated in Figure 2, emphasizing the transmission path of random vibrations from the tire–ground contact to the suspension system (*Mitroi, M., 2016*).

Vibrations are partially attenuated by the elastic elements of the tire and suspension before being retransmitted through the vehicle's supporting structure and, ultimately, to the seat. Irregularities in the driving surface induce initial shocks at the wheels, which are subsequently transformed into lower-frequency oscillations that have a direct impact on the perception of comfort and driving safety.

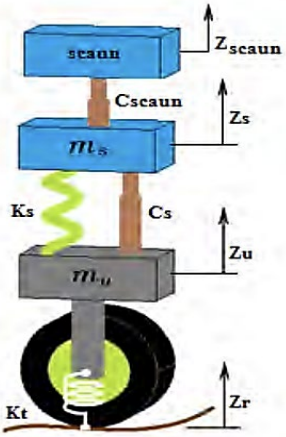

Fig. 2 - Transmission of random vibrations through the tire–wheel system

MATERIALS AND METHODS

This chapter provides a systematic overview of the essential aspects related to the assessment of vibration impact on driver health, with a focus on describing the human body's resonance frequencies in functional positions (standing and seated), determining the exposure levels to Whole-Body Vibrations (WBV), and presenting the methods and equipment employed for experimental data acquisition and processing.

Current methodologies for quantifying accelerations transmitted to the human body are described, along with the measurement systems used to capture vibrational signals at critical contact points (seat, floor,

backrest), in accordance with the applicable international standard (ISO 2631-1). This integrated approach enables an accurate characterization of biomechanical exposure and facilitates the evaluation of health risks to drivers as a function of the measured dynamic parameters.

From a physical and anatomical perspective, the human body represents a highly complex system subjected to shocks and vibrations, which, under certain conditions, may adversely affect health status. When seated, the human body is exposed to vibrations generated by the type of vehicle used during operation on different terrain surfaces and at varying driving speeds. The factors influencing the impact of vibrations on the human body include vibration amplitude, the distance between the subject and the vibration source, body posture, mode and duration of exposure, frequency range, and the direction of vibration propagation. Mechanical influences become significant when vibration amplitudes exceed specific critical thresholds, leading to potential damage to internal organs. In cases where excitation of the nervous system induces a biological response, the consequences may include reduced concentration capacity during driving, the onset of fatigue, and diminished attention levels. Table 1 presents the main resonance frequencies of the human body in standing and seated positions *(Griffin, M., J.2006)*.

Table 1

Resonance frequencies of the human body in standing and seated positions

Position	Frequency [Hz]	Results
Standing	1 Hz	The displacement amplitudes of the pelvis, shoulders, and head range between 20% and 30% of the amplitude of the vibrating surface movements and progressively decrease with increasing vibration frequency
	2-3 Hz	It can be observed that relative maxima occur in the oscillation amplitudes at the shoulder and head levels, indicating localized resonance effects
	Peste 5 Hz	The head movement occurs predominantly along the vertical axis, with an amplitude corresponding to approximately 10–30% of the horizontal movement amplitude of the vibrating surface
Seated	1,5 Hz	The results indicate a significant amplification of oscillations in the hip and pelvic regions, suggesting localized resonance effects
	3 Hz	The results reveal a considerable increase in oscillation amplification at the head level, indicating a higher susceptibility to vertical resonance effects
	1-3 Hz	At specific critical resonance frequencies, the system exhibits a significant amplification of its dynamic response to vibrations
	Peste 5 Hz	Head motion is predominantly manifested along the vertical axis, with an amplitude accounting for approximately 10–30% of the horizontal vibration amplitude of the surface

The specialized literature summarizes the health effects caused by whole-body vibration exposure, particularly at resonance frequencies. These effects are presented in Table 2, highlighting the direct relationship between resonance frequencies and the various associated physiological disorders *(Rasmussen, G., 1996)*.

Table 2

Health effects associated with whole-body vibration exposure

Frequency [Hz]	Adverse health effects
4-9	General discomfort sensation
13-20	Head-related symptoms
6-8	Mandibular symptoms
13-20	Impact on speech
12-16	Sensation of a lump in the throat
5-7	Chest pain
4-10	Abdominal pain
10-18	Urge to urinate
13-20	Increased muscle tone
4-8	Impact on respiratory movements
4-9	Muscle contractions

The phenomenon of resonance occurs when the frequency of vibrations generated by the tractor coincides with the natural frequency of certain tissues or organs of the operator. In such situations, even vibrations with relatively small amplitudes can cause significant displacements of internal organs, which may

lead to pronounced discomfort and the development of serious health disorders *(Gao, R. et al. 2021; Peretti, A. et al. 2023)*.

To comprehensively evaluate the effects of vibrations on the human body, it is essential to measure acceleration along well-defined axes and to correlate these measurements with the analysis of vibration frequencies, amplitudes, and exposure duration.

Acceleration is assessed along three principal axes corresponding to the directions of motion and the orientation of the human body: longitudinal axis (Z): extending from the feet or pelvis to the head, responsible for evaluating vertically transmitted vibrations, which have the greatest impact on the spinal column and torso; transverse left–right axis (X): measures lateral accelerations that affect the operator's balance and lateral stability; transverse front–back axis (Y): measures vibrations in the antero–posterior direction, influencing stability and forward–backward body movements. These directions are perpendicular to the three principal planes of the human body, as illustrated in Figure 3, providing a comprehensive view of how vibrations propagate through the body.

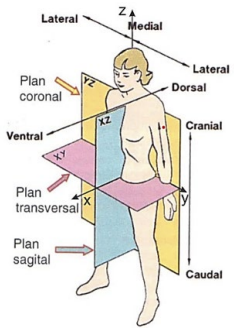

Fig. 3 - Principal planes of the human body and measurement axes according to ISO 2631-1

An essential method for measuring whole-body transmitted vibrations is based on compliance with the guidelines provided by the most widely used standards in this field. These standards offer precise instructions for the accurate assessment of vibration exposure and are summarized in Table 3.

Table 3

Main international standards for the assessment of whole-body vibration exposure

Applicable international standards	Description
ISO 2631-1(2001)	Mechanical vibration and shock — Evaluation of human exposure to whole-body vibration. Part 1: General requirements
ISO 2631-2(1989)	Part 2: Continuous and shock-induced vibrations in buildings (1 to 80 Hz)
ISO 2631-4(2001)	Part 4: Guidelines for the evaluation of the effects of vibration and rotational motion on passenger and crew comfort in fixed-guideway transport systems
ISO 2631-5(2004)	Part 5: Method for evaluation of vibration containing multiple shocks

ISO 2631-1 defines the exposure limits for vibrations transmitted to the human body within the following frequency ranges:

a) 0.5 Hz to 80 Hz for health, comfort, and perception of vibration;
b) 0.1 Hz to 0.5 Hz for the prevention of motion sickness.

The main variables describing the measurement of whole-body vibration exposure are:

a) The vibration measurement directions (or measurement axes) are presented in Figure 4;
b) Measurement location;
c) Measurement duration.

Fig. 4 - Illustration of vibration measurement directions on the tractor and the operator

The vibrations transmitted to the human body must be monitored at the contact points between the body and the vibrating surface. These main contact areas may vary and are not always immediately apparent. According to ISO 2631-1, for seated persons, three main measurement zones are used:

- The vehicle floor (seat support surface and the contact surface of the operator's feet);
- The horizontal surface of the vehicle seat;
- The seat backrest.

The measurement duration must be sufficiently long to ensure adequate statistical accuracy and to accurately reflect the characteristics of the vibrations to which the operator is exposed. The vibration level, expressed as the root mean square (r.m.s.) value, represents the mean acceleration measured at the seat level during the operator's driving activity in the seated position. The analysis of mechanical vibrations involves measuring the weighted average acceleration, represented by the root mean square (r.m.s.), along the X, Y, and Z measurement axes. The formula used to calculate this value is expressed in Equation (1).

$$a_{w\,\text{r.m.s}} = \left[\frac{1}{T}\int_0^T a_w^2(t)dt\right]^{1/2} \quad (1)$$

where: $a_w^2(t)$ - is the frequency-weighted acceleration at time t;

T — is the measurement duration.

The overall magnitude of the oscillatory motion is determined using the formula expressed in Equation (2):

$$a_{W_v} = \sqrt{k_x\,a_{W_x}^2 + k_y\,a_{W_y}^2 + k_z\,a_{W_z}^2} \quad (2)$$

where: k_x, k_y și k_z represent multiplication factors applied to the measurement axes X, Y și Z.

To assess the impact of vibration exposure on human health, it is necessary to determine the frequency-weighted root mean square (r.m.s.) acceleration within the range of [0–80] Hz. This parameter must be measured for periodic, random, or transient vibrations transmitted to the human body in the seated position through the seat surface. According to ISO 2631-1, the Health Guidance Caution Zone (HGCZ) is defined based on this frequency-weighted acceleration, measured along the dominant Z-axis, and is illustrated in the red-highlighted area in Figure 5 *(de la Hoz-Torres, M. L. et al. 2022; Plewa, K. M. et al. 2012)*.

The Health Guidance Caution Zone (HGCZ) is based on the principle of energy conservation. Assuming that the human body's response is directly proportional to the total energy of the vibrations to which it is exposed, two different daily vibration exposures can be considered equivalent when the condition expressed by the formula in Equation (3) is satisfied.

$$a_{w1}T_1^{1/2} = a_{w2}T_2^{1/2} \quad (3)$$

where: a_{w1} şi a_{w2} – represent the frequency-weighted root mean square (r.m.s.) acceleration values corresponding to the first and second whole-body vibration exposures, respectively;

T_1 şi T_2 – represent the exposure durations corresponding to the first and second vibration events, respectively.

As reported in the specialized literature, the equation defined in Relation (4) reveals a time-dependent behavior:

$$a_{w1}T_1^{1/4} = a_{w2}T_2^{1/4} \quad (4)$$

Figure 5 illustrates the Health Guidance Caution Zone (HGCZ), as defined by the health-related indications derived from the application of Equations (3) and (4). This zone emphasizes the frequency range in which additional protective measures are required to prevent potential health risks.

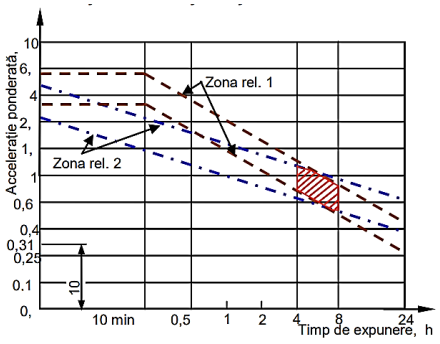

Fig. 5 - Health Caution Zone

At the end of this chapter, the process of experimental data acquisition concerning the vibrations transmitted to the driver is described, using accelerometer-type sensors from the Biometrics Ltd range [BIOM]. The measurement systems were configured to record the three-dimensional components of acceleration (X, Y, Z axes) at critical contact points (seat, backrest, and floor), in accordance with current international standards. The raw data obtained were processed using the specialized software VATS – Vibration Analysis ToolSet (NexGen Ergonomics), which provides advanced functionalities for spectral analysis, frequency weighting calculations according to ISO 2631-1, identification of dominant frequency components, and determination of root mean square (RMS) acceleration values.

The data acquisition system developed by Biometrics Ltd enables the collection of both analog and digital data from a wide range of sensors. The DataLog MWX8 equipment used in the study is illustrated in Figure 6 and represents a modern device capable of collecting experimental data at sampling frequencies of up to 20,000 Hz..

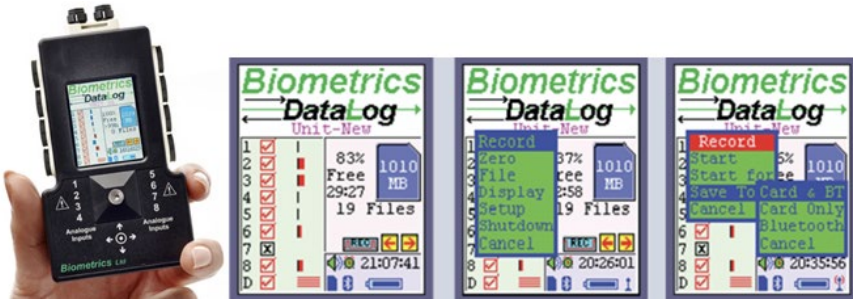

Fig. 6 - DataLog MWX8 data acquisition equipment (Biometrics Ltd)

The triaxial accelerometer sensors (illustrated in Figure 7) are high-precision 3-axis sensors rated at 10 G, featuring factory-set offset and sensitivity, thermal signal isolation, and adjustable filters for each channel. They connect directly to the DataLog data acquisition device, with each channel linked to the host instrument via a separate connector.

Fig. 7 - Triaxial accelerometer sensors from the Biometrics Ltd range used for vibration data acquisition

A vibration analysis toolkit used for data processing is VATS™ (Vibration Analysis Tool Set), developed by NexGen Ergonomics, which is designed for whole-body vibration analysis. The system integrates the MWX8 DataLog data acquisition unit, which collects data from accelerometer-type sensors. The interface of this software is presented in Figure 8.

The DataLog equipment includes a real-time clock, allowing each recording to be time-stamped with an exact start date and time, as well as its total duration. VATS performs whole-body vibration analysis for the health, comfort, and perception domains, in accordance with the ISO 2631-1 standard.

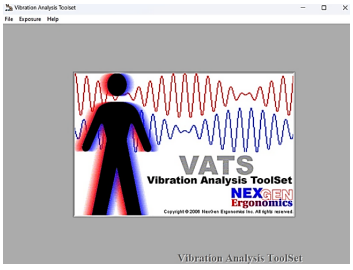

Fig. 8 - Software interface of NexGen Ergonomics VATS™ used for whole-body vibration analysis

RESULTS

This chapter presents the current research directions in the field of whole-body vibrations (WBV), with a focus on their influence on the human body, particularly in the context of operating agricultural

vehicles. The present study integrates relevant findings from the specialized literature published over the last decade, highlighting the progress made in biomechanical modeling of the human body, identification of critical resonance frequencies, analysis of physiological responses to vibrational exposure, and the development of professional risk assessment methodologies.

Recent research reflects a clear trend toward deepening experimental studies through the use of advanced measurement and simulation systems, as well as the application of international standards (ISO 2631-1, ISO 2631-5) as benchmarks for exposure quantification. In particular, the literature emphasizes the significant impact of vibrations generated by self-propelled agricultural vehicles, such as tractors, on the lumbar and spinal segments and the vestibular system, underlining the need for corrective measures regarding workstation ergonomics, seat suspension design, and exposure time management.

During the operation of various types of vehicles, vibrations are primarily generated by the interactions between the tires and the road surface. Several studies have been conducted to analyze the impact of vibrations on the driver, caused by different terrain types ranging from plowed fields to flat surfaces *(Singh, A. et al. 2019; Park, D.J. et al. 2019; Oncescu, T.A. et al. 2022; Oncescu, T.A. et al. 2024)*. Whole-body vibrations (WBV) transmitted to the driver represent one of the most influential factors affecting health and comfort, and the specialized literature documents numerous studies in which tractor operators are exposed to high levels of WBV and mechanical shocks *(Kabir, M. S. N. et al. 2015; Sun, L. et al. 2024; Cvetanovic, B. et al. 2017; Fethke, N. B. et al. 2022)*.

Exposure to high levels of vibration is associated with multiple health disorders, including musculoskeletal conditions such as lower back pain, as discussed in the studies by *(Bovenzi, M. et al. 2021; Jithendar, K. et al. 2023; Benos, L. et al. 2020)*, general muscle fatigue (Huang, Q.et al. 2023). Recent studies have also emphasized the psychological effects of vibration exposure, such as increased stress and anxiety levels, which can impair driver attention and operational performance *(Bhuiyan, M.H.U.et al. 2022; Vosoughi, S. 2019; Sorosh, A. 2019; Jalilian, H. et al. 2019; Johnson, P. W. et al. 2017)*.

Several specialized studies have addressed these safety concerns, with a primary focus on the technical design and performance characteristics of agricultural tractors *(Biris, S.S. et al. 2020; Ayers, P. et al. 2018)*, vibrations *(Vallone, M. et al. 2016)* and vehicle ergonomics *(Jamshidi, N. et al. 2016)*. Among these elements are the tractor cabin, tires and tire pressure, chassis, axles, and seat suspension systems, *(Choi, H.-J. et al. 2018; Deboli, R. et al. 2017; Poczwardowski, A. et al. 2022; Brusl, H. et al. 2021)*.

The specialized literature investigates how various types of running surfaces affect tractor operation *(Singh, A. et al. 2022; Cuong, D. M. et al. 2015; Zhang, J. et al 2022)*. The specialized literature has examined the behavior and posture of tractor operators through studies assessing whole-body vibration exposure, following the methodologies defined by specific international standards *(Caffaro, F. et al 2018; Irwin, J. D. et al. 2019; Fargnoli, M.et al. 2019)*.

Figure 9 illustrates the diagram of the geographical distribution of organizations and institutions involved in this field, contributing to the improvement of vehicle ergonomics, particularly for self-propelled agricultural vehicles such as tractors.

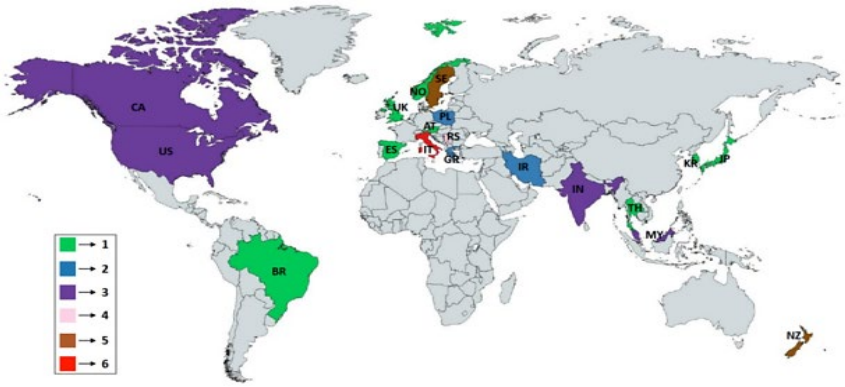

Fig. 9 - Geographical distribution of research organizations contributing to vehicle ergonomics improvement

CONCLUSIONS

This review article has provided a comprehensive and structured analysis of the specialized literature concerning the influence of vibrations on the human body, with particular emphasis on drivers of self-propelled agricultural vehicles such as tractors. Through a rigorous documentation of vibration sources

and their transmission phenomenology to the human body, the study highlighted the critical resonance frequencies and their implications for operator health. A systematic presentation of the main methodological approaches for evaluating whole-body vibration exposure levels was achieved, complemented by a detailed description of the equipment and procedures used for the acquisition and processing of relevant experimental data.

The current state of research in the field of Whole-Body Vibrations (WBV) has been outlined, emphasizing development trends, persistent scientific gaps, and the need for interdisciplinary approaches. This review contributes to strengthening the theoretical and practical framework required for the development of effective strategies for monitoring, prevention, and ergonomic optimization in the field of occupational vibration exposure.

REFERENCES

[1] Ayers, P., Khorsandi, F., Wang, X., Araujo, G. (2018).ROPS designs to protect operators during agricultural tractor rollovers. *J. Terramech.*, vol. 75, pp. 49–55, DOI: 10.1016/j.jterra.2017.05.003

[2] Barač, G., Milinković, D., & Mandić, L. (2025). Machine Learning Based Prediction of Whole-Body Vibration Exposure Levels in Agricultural Vehicles. *Agriculture*, 7(3), 72. https://doi.org/ 10.3390/ agriculture 7030072

[3] Barrie, A., Govers, M., Habegger, J., Hassan, M., & Oliver, M. (2024). Smart whole-body vibration attenuation, cushion for heavy equipment seating: Model and simulation. *Journal of Low Frequency Noise, Vibration and Active Control*, 43(1), 1–15. https://doi.org/10.1177/14613484241279542

[4] Benos, L., Tsaopoulos, D., Bochtis, D., (2020). A Review on Ergonomics in Agriculture, Part I: Manual Operations. *Appl. Sci.*, vol.10, pp. 1905, https://doi.org/10.3390/app10061905

[5] Bhuiyan, M.H.U., Fard, M., Robinson, S.R., (2022). Effects of whole-body vibration on driver drowsiness: A review, *Journal of Safety Research*, vol. 81 (1), pp. 175-189, DOI: 10.1016/j.jsr.2022.02.009

[6] Biris, S.S., Cristea, M., Matache, M.G., Sorica, C., Ungureanu, N., (2020). Study on the behavior of a battery mounted on an electric tractor prototype, *INMATEH Agricultural Engineering*, vol. 62 (3), pp. 19-28, DOI:10.35633/inmateh-62-02

[7] Blanks, A. M., et al. (2022). The Clinical Utility of Whole-Body Vibration: A Review of the Different Types and Dosing for Application in Metabolic Diseases. *Journal of Clinical Medicine*, 11(18), 5361. https://doi.org/10.3390/jcm11185361

[8] Bovenzi, M., & Schust, M. (2021). A prospective cohort study of low-back outcomes and alternative measures of cumulative external and internal vibration load on the lumbar spine of professional drivers. *Scandinavian Journal of Work, Environment & Health*, 47(4), 277–286. https://doi.org/10.5271/sjweh.3947

[9] Brusl, H., Donati, P., & Christ, E. (2021). Whole Body Vibration Analysis for Drivers of Suspended Cabin Tractor Semitrailer. *Experimental Techniques*, 38(1), 47–53. https://doi.org/10.1111/j.1747-1567.2011.00786

[10] Burdzik, R. (2023). Impact and Assessment of Suspension Stiffness on Vibration Propagation into Vehicle.

[11] Caffaro, F., Micheletti Cremasco, M., & Cavallo, E. (2018). Whole-body vibration exposure in agricultural tractor drivers: A systematic review. *International Journal of Environmental Research and Public Health*, 15(4), 627. https://doi.org/10.3390/ijerph15040627

[12] Choi, H.-J., & Lee, S.-H. (2018). Experimental Study of the Dynamic Characteristics of Rubber Mounts for Agricultural Tractor Cabin. *Journal of Biosystems Engineering*, 43(4), 256–263. https://koreascience.or.kr/article/JAKO201809454741550

[13] Cuong, D. M., Zhu, S. H., & Zhu, Y. (2013). Effects of tyre inflation pressure and forward speed on vibration of an unsuspended tractor. *Journal of Terramechanics*, 50(3), 185–198. https://doi.org/10.1016/j.jterra.2013.03.003

[14] Cvetanovic, B., Cvetković, D., Praščević, M., Cvetković, M., & Pavlović, M. (2017). An analysis of the impact of agricultural tractor seat cushion materials to the level of exposure to vibration. Proceedings of the Institution of Mechanical Engineers, Part D: *Journal of Automobile Engineering*, 231(9), 1234–1245. https://journals.sagepub.com/doi/full/10.1177/0263092317711983

[15] Cvetković, M., Desai, R., Papaioannou, G., & Happee, R. (2023). Kinematic body responses and perceived discomfort in a bumpy ride: Effects of sitting posture. *arXiv preprint*, arXiv:2310.05923. https://arxiv.org/abs/2310.05923

[16] de la Hoz-Torres, M. L., Aguilar, A. J., Ruiz, D. P., & Martínez-Aires, M. D. (2022). Whole Body Vibration Exposure Transmitted to Drivers of Heavy Equipment Vehicles: A Comparative Case According to the Short- and Long-Term Exposure Assessment Methodologies Defined in ISO 2631-1 and ISO 2631-5. *International Journal of Environmental Research and Public Health*, 19(9), 5206. https://doi.org/10.3390/ijerph19095206

[17] Deboli, R., Calvo, A., Preti, C., & Preti, G. (2017). Whole Body Vibration Exposure Transmitted to Drivers of Heavy Equipment Vehicles: A Comparative Case According to the Short- and Long-Term Exposure Assessment Methodologies Defined in ISO 2631-1 and ISO 2631-5. *International Journal of Environmental Research and Public Health*, 14(11), 1424. https://doi.org/10.3390/ijerph14111424

[18] Desai, R., Cvetković, M., Papaioannou, G., & Happee, R. (2023). Modelling human seat contact interaction for vibration comfort. *arXiv preprint*, arXiv:2307.05496. https://arxiv.org/abs/2307.05496

[19] Desai, R., Papaioannou, G., & Happee, R. (2024). Vibration transmission through the seated human body captured with a computationally efficient multibody model. *Multibody System Dynamics*, 56, 345–352. https://doi.org/10.1007/s11044-024-10025-1

[20] Deulgaonkar, V.,R., Kallurkar, S.,P., Mattani, A.,G., (2012). Review and Diagnostics of noise and vibrations in automobiles, *International Journal of Modern Engineering Research*, vol.1(2), pp. 242-246.

[21] Dumitriu, M., Apostol, I. I., & Stănică, D. I. (2023). Influence of the Suspension Model in the Simulation of the Vertical Vibration Behavior of the Railway Vehicle Car Body. *Vibration*, 6(3), 512–535. https://doi.org/10.3390/vibration6030032

[22] Fargnoli, M., Lombardi, M., Puri, D., (2019). Applying Hierarchical Task Analysis to Depict Human Safety Errors during Pesticide Use in Vineyard Cultivation. *Agriculture*, vol. 9, pp. 158, https://doi.org/10.3390/agriculture9070158

[23] Fethke, N. B., & Prater, L. F. (2022). Back Pain Can Be Attributed to Whole-body Vibration. *Successful Farming*, August 6, 2022. https://www.agriculture.com/family/health-safety/back-pain-can-be-attributed-to-whole-body-vibration

[24] Gao, R., Yan, H., & Yang, Z. (2021). Evaluation of tractor driving vibration fatigue based on multiple physiological parameters. *PLoS ONE*, 16(7). DOI: 10.1371/journal.pone.0254636

[25] Griffin, M., J., Huang, Y., (2006). Effect of voluntary periodic muscular activity on nonlinearity inthe aarent mass of the seated human body during vertical random whole-body vibration, *Journal of Sound and Vibration*, vol. 298 (23), pp. 824-840, DOI: 10.1016/j.jsv.2006.06.028

[26] Guruguntla, V., & Lal, M. (2023). Multi-body modelling and ride comfort analysis of a seated occupant under whole-body vibration. *Journal of Vibration and Control*, 29(3), 1–15. https://doi.org/10.1177/10775463221091089

[27] Happee, R., Desai, R., & Papaioannou, G. (2023). Simulating vibration transmission and comfort in automated driving integrating models of seat, body, postural stabilization and motion perception. *arXiv preprint*, arXiv:2306.16344. https://arxiv.org/abs/2306.16344

[28] Harikrishnan, P., M., Gopi, V., P., 2017. Vehicle Vibration Signal Processing for Road Surface Monitoring", *IEEE Sens. J.*, vol. 17 (16), pp. 5192–5197, DOI: 10.1109/JSEN.2017.2719865

[29] Hiemstravan, M., S., Groenesteijn, L., Vink, P., et al., (2014). Predicting passenger seat comfort and discomfort on the basis of human, context and seat characteristics: a literature review, *Ergonomics*, vol. 60, pp. 889–911, DOI: 10.1080/00140139.2016.1233356

[30] Huang, Q., Gao, M., Guo, M., Wei, Y., Zhang, J., Jin, X, (2023). Vibration comfort assessment of tractor drivers based on sEMG and vibration signals, *Computer Methods in Biomechanics and Biomedical Engineering*, vol. 13, pp. 1875-1892, DOI: 10.1080/10255842.2023.2263126

[31] International Organisation for Standardisation (2001) ISO 2631-1. Mechanical vibration and shock – Evaluation of human exposure to whole-body vibration Part 1: General requirements. https://www.iso.org/standard/7612.html

[32] Irwin, J. D., & Graf, E. (2019). Human response to whole-body vibration: A review of current standards and research. *Applied Ergonomics*, 80, 103–113. https://doi.org/10.1016/j.apergo.2019.05.001

[33] Jalilian, H., Zamanian, Z., Gorjizadeh, O., Riaei, S., Monazzam, M. R., & Abdoli-Eramaki, M. (2019). Autonomic nervous system responses to whole-body vibration and mental workload: A pilot study.

International Journal of Occupational and Environmental Medicine, 10(4), 174–184. https://pmc.ncbi.nlm.nih.gov/articles/PMC7975586/

[34] Jamshidi, N., Abdollahi, S.M., Maleki, A.,(2016). A survey on the actuating force on brake and clutch pedal controls in agricultural tractor in use in Iran. Pol. Ann. Med., vol. 23, pp. 113–117, DOI: 10.1016/j.poamed.2016.01.007

[35] Jithendar, K., Singh, S., Kumar, P., Karmakar, N.C., (2023). Role of contributing factors on health risks of whole-body vibration exposure of heavy equipment and vehicle operators: A critical review, *Sage Journals*, vol. 30, pp. 11-12, DOI: 10.1177/10775463231185627

[36] Johnson, P. W., Zigman, M., Ibbotson, J., Dennerlein, J. T., & Kim, J. H. (2017). The impact of different seats and whole-body vibration exposures on truck driver vigilance and discomfort. *Annals of Work Exposures and Health*, 62(8), 990–999. https://pubmed.ncbi.nlm.nih.gov/28845747

[37] Kabir, M. S. N., Chung, S.-O., Kim, Y.-J., Sung, N.-S., & Hong, S.-J. (2014). Measurement and evaluation of whole body vibration of agricultural tractor operator. International *Journal of Agricultural and Biological Engineering*, 7(2), 13–20. https://www.ijabe.org/index.php/ijabe/article/view/2113

[38] Mei, Y., Liu, H., Renqiang, J., Ding, Y., & Nguyen, V. (2023). Development of vibration isolation models in vibratory roller's seat and cabin: A survey. Journal of Low Frequency Noise, *Vibration and Active Control*, 42(2), 1–15. https://doi.org/10.1177/14613484241279542

[39] Melo, R. B., Miguel, A. S., & Perestrelo, G. (2019). A Comparison of ISO 2631-5:2004 and ISO 2631-5:2018 Standards for Whole-Body Vibrations Exposure: A Case Study. În P. Arezes et al. (Eds.), *Occupational and Environmental Safety and Health* (pp. 711–719). Springer, Cham. DOI: 10.1007/978-3-030-14730-3_74

[40] Mester, J., et al. (2021). Lower Body Acceleration and Muscular Responses to Rotational and Vertical Whole-Body Vibration at Different Frequencies and Amplitudes. *Journal of Musculoskeletal & Neuronal Interactions*, 21(1), 32–45. https://www.ncbi.nlm.nih.gov/pmc/articles/PMC6327349/

[41] Mirakhorlo, M., Kluft, N., Shyrokau, B., & Happee, R. (2022). Effects of seat back height and posture on 3D vibration transmission to pelvis, trunk and head. *International Journal of Industrial Ergonomics*, 91, 103327. https://doi.org/10.1016/j.ergon.2022.103327

[42] Mitroi, M. F., (2020). Considerații privind influența vibrațiilor aleatoare induse de vehicule și calea de rulare organismului uman – *Știință și Inginerie*, pp. 29-91.

[43] Mitroi, M., (2016). Referat, "Echipamente și proceduri destinate evaluării confortului autovehiculelor, Universitatea Transilvania Brașov.

[44] Oncescu, T.A., Persu, C., Tarnita, D., Vilceleanu, M.V., Biris, S.S.,(2024). Study of the effects of vibration transmission In operators of electric tractors driven at constant speed on different types of roads, Acta Technica Corviniensis – *Bulletin of Engineering*, vol. 1, pp. 119-122, e–ISSN: 2067 – 3809

[45] Oncescu, T.A., Persu, C., Tarnita, D., Biris, S., Tunsoiu, N., Fudulache, O.,(2024). The measurement and evaluation of the large agricultural tractor operator's whole-body vibration for four types of land and two running speeds, ANNALS of Faculty Engineering Hunedoara – *International Journal of Engineering*, vol. 1, pp. 130-136, ISSN 2601 – 2332

[46] Oncescu, T.A., Persu, C., Dumitru, I., Prunoiu, D., Grigore, L., Tarnita, D., (2022). Influence of the road type on the whole body vibrations transmitted to the driver of an electric tractor, ACTA Special Issue II , vol. 65 (2S), pp. 387-392, DOI: 10.2991/978-94-6463-152-4_31

[47] Park, D.J., Choi, M.G., Song, J.T., Ahn, S.J. Jeong, W.B, (2019). Analysis of driving seat vibrations in high forward speed tractors. *Ind. Ergon.*, vol. 72, pp. 363-371, DOI: 10.1016/j.biosystemseng.2007.03.004

[48] Peretti, A., Carletti, E., & Pedrielli, F. (2023). Whole-Body Vibration in Farming: Background Document for Creating a Simplified Procedure to Determine Agricultural Tractor Vibration Comfort. *Agriculture*, 7(10), 84. https://doi.org/10.3390/agriculture7100084

[49] Plewa, K. M., Eger, T. R., Oliver, M. L., & Dickey, J. P. (2012). Comparison between ISO 2631–1 Comfort Prediction Equations and Self-Reported Comfort Values during Occupational Exposure to Whole-Body Vehicular Vibration. *Vehicle System Dynamics*, 31(1), 43–56. https://doi.org/10.1260/0263-0923.31.1.43

[50] Poczwardowski, A., & Knapczyk, J. (2022). Multi-Body Model of Agricultural Tractor for Vibration Transmission Investigation. *Applied Sciences*, 12(18), 8451. https://www.mdpi.com/2076-3417/12/18/8451

[51] Ramoneda-Rabat, M., et al. (2024). Effects of Different Vibration Frequencies on Muscle Strength, Bone Turnover and Walking Endurance in Chronic Stroke. *Journal of Rehabilitation Medicine*, 56(6), 345–352. https://doi.org/10.2340/jrm.v56.345

[52] Rasmussen, G., (1996). Human Body Vibration Exposure and its Measurement, in: *Journal of the Acoustical Society of America*, DOI:10.1121/1.389513

[53] *Sensors*, 23(4), 1930. https://doi.org/10.3390/s23041930

[54] Shen, C.-L., et al. (2022). On the Optimal Whole-Body Vibration Protocol for Muscle Strength. *Journal of Functional Morphology and Kinesiology*, 7(4), 43. https://doi.org/10.3390/jfmk7040043

[55] Singh, A., Samuel, S., Singh, I., & Singh, J. (2022). Measurement and Analysis of Vibration Transmissibility through Tractor Seat. În Proceedings of the 13th International Conference on Applied Human Factors and Ergonomics (AHFE 2022). https://www.researchgate.net/publication/361246365

[56] Singh, A., Singh, L.P., Singh, S., Singh, H., Chhuneja, N.K., Singh, M., (2019). Evaluation and analysis of occupational ride comfort in rotary soil tillage operation, *Measurement*, vol. 131, pp. 19-27, DOI: 10.1016/j.measurement.2018.08.046

[57] Singh, R., Verma, N., & Shukla, A. (2022). Assessment of Whole-Body Vibration Exposure on Agricultural Tractor Operators Using ISO 2631-5: A Field Study. *Applied Sciences*, 12(4), 1745. https://doi.org/10.3390/app12041745

[58] Sorosh, A., Naserkhaki, S., Parnianpour, M., (2019). Effect of whole-body vibration and sitting configurations on lumbar spinal loads of vehicle occupants, *Computers in Biology and Medicine*, vol. 107, pp. 292-301, https://doi.org/10.1016/j.compbiomed.2019.02.019

[59] Sun, L., Shang, T., Chen, H., Wang, Z., Wang, C., & Luo, F. (2024). Development of a model for the optimization of the main factors influencing a 162kW wheeled tractor driver's whole body vibration. Proceedings of the Institution of Mechanical Engineers, Part D: *Journal of Automobile Engineering*, 238(1), 123–135. https://journals.sagepub.com/doi/full/10.1177/14613484231190286

[60] Vallone, M., Bono, F.; Quendler, E., Febo, P., Catania, P. (2016). Risk exposure to vibration and noise in the use of agricultural track-laying tractors. Ann. Agric. Environ. Med., vol. 23, pp. 591–597, DOI: 10.5604/12321966.1226852

[61] Vlădut, N., V., et al. (2024). Beyond Agriculture 4.0: Design and Development of Modern Agricultural Machines and Production Systems. Agriculture, Vol 14, Issue 7, p991. 10.3390/agriculture14070991

[62] Vosoughi, S., Rostamzadeh, S., Asghar Farshad, A., Taheri, F., Vahabzadeh-Monshi, H., (2019). Whole-body vibration exposure study in intercity mini-bus drivers-the risk of musculoskeletal disorders, Irania Journal of Health, *Safety and Environment*, vol 6 (1), pp. 1198-1205.

[63] Zhang, J., Yao, H., Chen, L., Zheng, E., Zhu, Y., & Xue, J. (2022). Vibration characteristics analysis and suspension parameter optimization of tractor/implement system with front axle suspension under ploughing operation condition. *Journal of Terramechanics*, 102, 49–64. https://doi.org/10.1016/j.jterra.2022.05.001

[64] Zhang, Y., Li, Y., & Wang, H. (2021). Unified Chassis Control of Electric Vehicles Considering Wheel Vertical Vibrations. *Sensors*, 21(11), 3931. https://doi.org/10.3390/s21113931

[65] Zhou, Y., & Wang, H. (2023). Dynamic Analysis of a Vehicle–Bridge System Under Excitation of Random Road Irregularities. *Buildings*, 14(11), 3413. https://doi.org/10.3390/buildings14113413

[66] Zhou, Y., et al. (2022). Effects of Whole-Body Vibration Training with Different Body Positions and Amplitudes on Lower Limb Muscle Activity in Middle-Aged and Older Women. International Journal of *Environmental Research and Public Health*, 19(15), 9289. https://doi.org/10.3390/ijerph19159289

THE INFLUENCE OF STORAGE CONDITIONS ON THE QUALITY OF CANNED MEAT
/
INFLUENȚA CONDIȚIILOR DE DEPOZITARE ASUPRA CALITĂȚII CONSERVELOR DE CARNE

Andreea Ioana BADIU, Sorin-Ștefan BIRIȘ, Florentina BRATOSIN, Alexandru Ionuț CÎRÎC, Mihaela BEGEA*
National University of Science and Technology POLITEHNICA Bucharest / Romania
**E-mail: mihaela.begea@gmail.com*

Keywords: *canned meat products, storage, unregulated conditions, protein degradation.*

ABSTRACT
The objective of this study was to evaluate the quality of the canned beef, which was stored under four temperature conditions for a period of 14 days. The samples were analyzed at three distinct time points (Day 1, 7, and 14), namely at temperatures of 4-25°C (manufacturer's recommendation), 0-8°C, -16°C, and 44±1°C respectivelly, to simulate improper transport and storage conditions. For all these temperature regimes, physico-chemical analyses were performed, including the determination of pH, easily hydrolyzable nitrogen (EHN), water activity (a_w), total nitrogen, nitrite and nitrate content, fat oxidation by the Kreiss reaction, the presence of ammonia with Nessler's reagent, along with organoleptic analysis. The results showed a significant increase in easily hydrolyzable nitrogen content, especially at extreme temperatures (-16°C and 44°C), suggesting a degradation of the protein fractions. The study demonstrated that storage temperature have a direct impact on the quality of canned meat products, leading to accelerated degradation of the nitrogen compounds when stored outside of recommended conditions.

REZUMAT
Obiectivul prezentului studiu a constat în evaluarea calității conservelor de carne de vită care au fost depozitate în condiții diferite de temperatură, pe o perioadă de 14 zile. Probele au fost analizate la trei momente distincte (ziua 1, 7 și 14), în condiții de depozitare la 4-25°C (recomandarea producătorului), precum și la 0-8°C, -16°C și 44±1°C, pentru a simula un transport și o depozitare necorespunzătoare. Pentru aceste regimuri de temperatură au fost efectuat analize fizico-chimice, incluzând determinarea pH-ului, azotului ușor hidrolizabil (AUH), activității apei (a_w), azotului total, conținutului de nitriți și nitrați, a oxidării grăsimilor, a amoniacului cu reactiv Nessler, alături de analiza organoleptică. Rezultatele au evidențiat o creștere semnificativă a conținutului de AUH, în special la temperaturile extreme (-16°C și 44°C), sugerând o degradare a fracțiunilor proteice. Studiul a demonstrat că temperatura de depozitare are un impact direct asupra calității conservelor, ducând la o degradare accelerată a compușilor cu azot, în condiții de depozitare diferite de cele recomandate.

INTRODUCTION
Preservation of meat is a fundamental process in the food industry, with a long history, which has evolved from traditional methods to complex technologies, essential for ensuring global food security and market diversification *(Sholpan et al., 2022).* Canned meat is a stable product on the shelf, the quality and safety of which critically depends on the maintenance of integrity throughout the entire life cycle, from production to the consumer *(Haouet et al., 2018).*

The shelf life of a food product defines the period during which it retains its sensory, chemical, physical and microbiological characteristics to an acceptable level while remaining safe for consumption *(Torrieri et al., 2016).* This term is influenced by a multitude of intrinsic (product composition, pH, water activity) and extrinsic (temperature, humidity, light) factors *(Simpson et al., 2012).* Among extrinsic factors, temperature is considered the most important parameter, since it governs the speed of most chemical and biochemical degradation reactions *(Mizrahi et al. 2004).* Despite manufacturers' recommendations for specific storage conditions, typically a dry and cool environment (4-25°C), products are often subjected to unsuitable conditions during transit and subsequent storage, including at the final consumer stage.

The quality and freshness of meat products are closely related to the proportion of nitrogen fractions. Total nitrogen (N_T) is an indicator of the general protein content, while EHN, which includes low molecular weight compounds such as ammonia, amines and free amino acids, represents a sensitive indicator of the

proteolysis processes *(Simpson et al., 2012, Khalid et al., 2022).* An increase in the content of EHN indicates a degradation of the protein structure and, implicitly, a loss of the nutritional and sensory quality of the product *(Motoc et al., 1966).*

The mechanisms by which proteinaceous compounds degrade at extreme temperatures are well-documented in the scientific literature. High temperatures accelerate thermal protein denaturation and residual enzymatic reactions *(Khalid et al., 2022).*

In contrast, frost, although it slows most chemical reactions, induces severe mechanical stress on the structure of the meat product. The formation of ice crystals in the product matrix leads to the physical destruction of muscle fibers, the release of previously bound water in protein structures, and the exposure of proteins to the action of endogenous enzymes, which can lead to accelerated post-defreezing degradation *(Kuznetsova et al., 2022).* However, the impact of such short term stress conditions on the chemical stability of canned meat is a less explored area.

The objective of this study was the quantitative assessment of the evolution of nitrogen fractions and several other associated parameters in canned beef, subjected for 14 days to storage conditions that simulate non-compliant scenarios (refrigeration, freezing, and exposure to high temperatures), compared to standard ones.

MATERIALS AND METHODS

Samples of canned beef in its own juice were utilised in this study. To ensure the homogeneity of the experimental material and the comparability of findings, all samples were sourced from a single production batch, with all units sharing identical identification data, such as the batch number, manufacturing date, and best-before date.

The study was designed to evaluate the impact of four different storage conditions over a period of 14 days on some relevant physical-chemical parameters, including the nitrogen-related characteristics of canned meat. The samples were stored under the following conditions: in a dry and cool place at a temperature between 4 and 25°C, as recommended by the manufacturer; under refrigeration at 0–8°C; under freezing conditions at a temperature of -16°C; and at a controlled high temperature of 44±1°C.

Analyses were carried out at three different time points to observe the evolution of the quality parameters: T1 (day 1), T2 (day 7), and T3 (day 14). Standard analytical methods were applied to evaluate the changes, as detailed in the specialized literature. pH determination was carried out directly on the homogenized sample, utilizing a digital pH-meter equipped with a penetration probe suitable for semi-solid products. Water activity (a_W) determination involved the measuring of the a_w value with a water activity analyzer, by placing the homogenized sample into the equipment's measuring crucible.

For the easily hydrolyzable nitrogen determination, the method was based on the release of volatile nitrogenous compounds through steam distillation in the presence of magnesium oxide.

The liberated ammonia was captured in a boric acid solution and subsequently titrated with a 0.1 N hydrochloric acid solution. Total nitrogen (N_T) determination employed the standard Kjeldahl method, which encompasses three stages: sample mineralization with concentrated sulfuric acid in the presence of a catalyst, ammonia distillation after alkalization, and titration of the distillate. The total protein content was calculated using the standard conversion factor of 6.25. Nitrite and nitrate determination involved the Griess spectrophotometric method.

This method relies on the diazotization reaction in an acidic medium and the formation of a coloured compound, whose absorbance was measured at 520 nm. To complete the quantitative evaluation, qualitative analyses were also performed: organoleptic analysis consisted of an assessment of the samples' sensory characteristics, including the can appearance, as well as the appearance, taste, and smell of the meat, according to a standard evaluation grid. Fat oxidation determination is based on the qualitative Kreis reaction to detect the presence of aldehydes, which are secondary products of oxidative rancidity.

Finally, the ammonia identification, as an indicator of advanced degradation of proteins, was verified through the qualitative Nessler reaction.

All quantitative determinations were performed in duplicate. The results were presented as mean, and for the EHN and the protein content, as mean ± the calculated uncertainty value.

RESULTS

General product stability: qualitative and organoleptic analysis

The qualitative evaluation of the samples of canned beef during the 14 days of study revealed a noteworthy stability from a sensory point of view. Regardless of the storage conditions, all samples showed normal organoleptic characteristics and complied with the product specifications and legal requirements: intact, non-swollen can, as well as specific appearance, colour, taste and smell. In addition, the qualitative tests to detect degradation were negative in all cases.

No evidence of fat oxidation was detected by the Kreiss reaction, and the absence of free ammonia - a marker of advanced spoilage - was confirmed using Nessler's reagent.

These results suggest that, at the macroscopic and sensory level, the product maintained its quality during the experiment, even under severe thermal stress. However, this apparent stability contrasts with the measurable chemical changes discussed in the following sections. It is important to outline that the protein and other chemical compounds degradation may reach chemically significant levels before the product becomes organoleptically unacceptable to the consumer.

This discrepancy highlights the limitations of sensory analysis as the only quality control tool and validates the need for the use of chemical markers, which are much more sensitive and are recommended as early indicators of quality loss for the meat products. In terms of the food industry, this implies that the assessment of the impact of an incident in the cold chain (for example, a failure of the cooling system) or the establishing of a realistic shelf life should not be based solely on sensory tests, but requires a complementary quantitative physico-chemical approach.

Changes in the physical-chemical matrix: pH and water activity (a_w)

Changes within the internal environment of the studied canned beef, reflected by the pH and water activity, provide valuable information about the degradation processes. The data obtained are summarised in Table 1.

Table 1

Change in pH and water activity (aw) depending on storage conditions and time

Storage conditions	Time point	pH	Water activity (a_w)
Control (4-25 °C)	T1	6.15	0.928
	T2	6.16	0.925
	T3	6.11	0.927
Refrigeration (0–8°C)	T2	6.15	0.942
	T3	6.24	0.954
Freezing (-16°C)	T2	6.18	0.956
	T3	6.15	0.962
High Temperature (44±1°C)	T2	6.15	0.957
	T3	6.13	0.961

A general trend of slight acidification (decrease in pH) is observed in most samples of canned beef, a phenomenon that can be associated with the slow continuation of Maillard-type reactions or the partial hydrolysis of the meat components, with acid formation. A notable exception is the samples stored at 0-8°C, in which the pH rises to T3 up to the value of 6.24. This increase in pH is probably the result of the activity of psychrotrophs, which, although slowed down by the cold, can continue to break down proteins, releasing amines and ammonia *(Triki et al., 2018).*

The most significant change is noticed for the water activity. The canned beef samples subjected to extreme conditions, both freezing (-16°C) and high temperature (44°C), show a sharp increase in the value a_w, reaching 0.962 and 0.961 at the end of the study, respectively. This increase should not be seen as a simple effect, but an active factor in the process of degradation.

Thermal stress, either by heat or by the mechanical action of ice, induces proteins denaturation in the meat matrix and leads to the relaxation of their tertiary and quaternary structure and the release of water that was previously "bound" inside these structures *(Kerth et al., 2013).*

The released water increases the "free" fraction of the system, which is measured by a higher a_w value. The increased water activity signifies a greater molecular mobility and increased availability of water as solvent and reactant, creating a more favourable environment for further acceleration of hydrolytic

reactions such as proteolysis. This establishes a causal relationship, namely the thermal stress causes protein distortion, which leads to increased a_w, which in turn accelerates other degradation reactions.

Nitrogen faction degradation: easily hydrolyzable nitrogen (EHN) and total nitrogen (N_T)

The analysis of nitrogen fractions provides a direct picture of protein integrity. The results are presented in Table 2.

Table 2

Evolution of protein and easily hydrolyzable nitrogen

Storage conditions	Time point	Protein	Easily hydrolyzable nitrogen
		[g/100g]	[mg/100g]
Control (4-25 °C)	T1	11.93±0.33	29.63±1.66
	T2	12.08±0.34	29.67±1.66
	T3	12.22±0.34	31.61±1.77
Refrigeration (0–8°C)	T2	11.99±0.34	30.56±1.71
	T3	12.32±0.35	35.08±1.96
Freezing (-16°C)	T2	11.82±0.33	42.00±2.35
	T3	11.79±0.33	45.57±2.55
High Temperature (44±1°C)	T2	12.08±0.34	33.31±1.87
	T3	12.21±0.34	36.69±2.05

The protein content, determined from total nitrogen, was relatively constant, indicating that the total nitrogen, in all its forms present in the product, constituted a closed system. In contrast, the evolution of easily hydrolyzable nitrogen is dependent on storage conditions. At 44°C, the EHN content increases by about 24% from the initial value, an explainable result due to the thermal acceleration of the hydrolysis reactions *(Krylova et al., 2017)*.

The most significant finding was the over 50% increase in EHN content in the samples stored at -16°C. This apparently counterintuitive phenomenon does not reflect the intense chemical activity at freezing temperature but rather highlights a distinct degradation mechanism initiated by a physical factor. The formed ice crystals cause irreversible mechanical damage to muscle fibres *(Kuznetsova et al., 2022)*.

This structural damage exposes numerous normally protected cleavage sites. When the sample is analyzed at room temperature, these vulnerable proteins hydrolyze much more easily. Therefore, the high EHN value at -16°C quantifies the increased vulnerability to degradation induced by the physical stress of freezing.

The evolution and stability of nitrites and nitrates

Nitrites and nitrates are essential additives in meat products, with a role in stabilising colour, flavour and inhibiting the growth of the pathogenic bacteria *Clostridium botulinum (Banu, 2022, Chira et al, 2005)*, therefore their stability is crucial to the safety of the product (Table 3).

Table 3

Monitoring the content of nitrites and nitrates during storage

Storage conditions	Time point	Nitrites	Nitrates
		[mg/kg]	**[g/100g]**
Control (4-25 °C)	T1	10.90	2.89
	T2	10.91	3.21
	T3	10.97	3.29
Refrigeration (0–8°C)	T2	10.90	1.10
	T3	10.97	1.94
Freezing (-16°C)	T2	10.88	2.38

Storage conditions	Time point	Nitrites	Nitrates
		[mg/kg]	[g/100g]
	T3	12.63	3.58
High Temperature (44±1°C)	T2	10.74	1.49
	T3	12.51	1.76

It can be noticed that an increase in nitrite concentration to T3 is observed in samples subjected to heat stress (-16°C and 44°C), while nitrates exhibit wide fluctuations. These variations suggest that thermal stress disrupts the chemical balance of the conservation system. The increase in nitrites concentration could be the result of the decreasing of residual nitrates by thermostable microbial enzymes or by non-enzymatic chemical reactions.

Regardless of the overall mechanism affecting the quality of canned meat products during storage, the instability of this system has implications for long-term food safety of canned meat. Uncompliant storage could compromise secondary chemical barriers that inhibit the development of heat-resistant spores *(Wang et al., 2020).*

CONCLUSIONS

According to the analysis carried out over a period of 14 days in non-compliant scenarios, the evolution of nitrogen fractions and other relevant quality indicators in meat cans reveals relevant aspects that could be exploited to be further recommmended for industrial practices. As regards the total nitrogen, there was an insignificant variation in its content regardless of storage conditions. This result indicates the noteworthy protein stability during the 14 days of the study, suggesting that the nutritional integrity of the product is well maintained under the simulated conditions.

The analysis of water activity revealed a direct correlation with storage temperature. It has been observed that water activity increases at higher temperatures and decreases at lower temperatures, which is a crucial aspect for food stability and safety, as high levels of water can favour microbial growth and degradation reactions. Regarding the nitrite and nitrate content, the study showed significant variations depending on storage conditions.

Fluctuations in their concentration can be associated with different rates of chemical conversion and degradation, influenced by the temperature and humidity of the environment. A positive finding was obtained from tests to identify ammonia with the Nessler reagent and fat oxidation by the Kreis reaction, both of which yield negative results.

This finding is very relevant in terms of food quality and safety, as the absence of ammonia and signs of oxidation confirms that the stability of the product is maintained during the experiment. EHN levels showed significant variations depending on storage conditions.

Although there were notable differences between samples, the highest value of 45.57 mg/100 g was obtained at time point T3 in the case of beef can stored at -16 °C. This value is below the maximum permissible limit of 55 mg/100 g, as specified in Romanian Order No. 560/2006 from the Ministry of Agriculture, Forests and Rural Development.

While higher levels of EHN suggest possible product degradation or changes, careful monitoring of this parameter is recommended to ensure the quality and safety of canned foods, in particular the canned meat products.

ACKNOWLEDGEMENT

This work was supported by ICA Research & Development S.R.L., where part of the laboratory analyses were conducted. The authors are grateful for the access to the necessary equipment and expertise that made this research possible.

REFERENCES

[1] Haouet MN, Tommasino M, Mercuri ML, Benedetti F, Di Bella S, Framboas M, et al. Experimental accelerated shelf life determination of a ready-to-eat processed food. Ital J Food Saf. 2018;7(2):6919. doi: 10.4081/ijfs.2018.6919.

[2] Khalid W, Maggiolino A. Dynamic alterations in protein, sensory, chemical, and oxidative properties occurring in meat during thermal and non-thermal processing techniques: A comprehensive review. Front Nutr. 2022;9:1057457. doi: 10.3389/fnut.2022.1057457.
[3] Kerth CR, editor. The Science of Meat Quality. Wiley-Blackwell; 2013.
[4] Krylova VB, Gustova TV. Comparative dynamics of protein destruction in canned foods in sauce at different thermal treatment regimes and subsequent storage. Theory and practice of meat processing. 2017;2(1):37-46. doi: 10.21323/2414-438X-2017-2-1-37-46.
[5] Kuznetsova T, Krylova V, Gustova T. The effect of storage conditions on the microstructure of sterilized canned meat. Potravinarstvo Slovak J Food Sci. 2022;16:1714. doi: 10.5219/1714.
[6] Mizrahi S. Accelerated shelf-life tests. În: Kilcast D, Subramaniam P, editori. Understanding and Measuring the Shelf-Life of Food. Woodhead Publishing; 2004. p. 317-39. doi: 10.1533/9781855739024.2.317.
[7] Sholpan A, Gulshat Z, Talgat K, Lyazzat B, Zhanar N. Application of functional ingredients in canned meat production. *Food Sci Technol*. 2022;42:e61122. doi: 10.1590/fst.61122.
[8] Simpson BK, Nollet LML, Toldrà F, Benjakul S, Paliyath G, Hui YH, editori. Food Biochemistry and Food Processing. 2nd ed. John Wiley & Sons; 2012.
[9] Torrieri E. Storage Stability: Shelf Life Testing. *Food Eng Rev*. 2016;8(1):85-98.
[10] Triki M, Herrero AM, Jiménez-Colmenero F, Ruiz-Capillas C. Quality Assessment of Fresh Meat from Several Species Based on Free Amino Acid and Biogenic Amine Contents during Chilled Storage. *Foods*. 2018;7(9):132. doi: 10.3390/foods7090132.
[11] Wang J, Qu Y, Liu Z, Zhou H. Formation, Analytical Methods, Change Tendency, and Control Strategies of Biogenic Amines in Canned Aquatic Products: A Systematic Review. *J Food Prot*. 2021;84(11):2020-36. doi: 10.4315/JFP-21-120.
[12] Banu C, Alexe P, Vizireanu C. Procesarea industrială a cărnii / Industrial meat processing. București: Editura Tehnică; 1997.
[13] Banu C, editor. Aditivi și ingrediente pentru industria alimentară / Additives and ingredients for the food industry. București: Editura Tehnică; 2000.
[14] Chira A, Niculescu N. Ghid pentru managementul siguranței alimentului conform principiilor sistemului HACCP cu exemplificare pentru industria cărnii / Guide for food safety management according to HACCP principles with examples for the meat industry. București: Editura YES srl; 2005.
[15] Moțoc BC. Biochimia Cărnii și a Subproduselor / Biochemistry of Meat and By-products. București: Editura Tehnică; 1966.
[16] Romanian Order 560/2006 for the approval of the Norms on the marketing of meat products.

STUDY ON OPTIMIZING THE PERFORMANCE OF ROW CROP SEEDERS
/
STUDIU PRIVIND OPTIMIZAREA PERFORMANȚELOR SEMĂNĂTORILOR DE PLANTE PRĂȘITOARE

Eugen MARIN*, **Nicolae-Valentin VLĂDUȚ, Mihai-Gabriel MATACHE, Dan-Iulian CUJBESCU, Mario CRISTEA, Alexandru IONESCU**

National Institute of Research - Development for Machines and Installations Designed for Agriculture and Food Industry - INMA Bucharest / Romania.

**Tel. 0758 437 214; *Email: marineu61@yahoo.com*

Keywords: *automated system, seeding depth control, row crops*

ABSTRACT

This paper presents a study aimed at designing an automated seeding depth control system for row crop seeders, ensuring the optimal and uniform placement of seeds in the soil, with real-time adjustments directly from the tractor cabin. The intelligent system will be adapted to variable soil conditions, maintaining consistent optimal germination conditions across the entire working width. The row crop seeder equipped with this automated system will provide precise seed placement at recommended agrotechnical depths, promoting uniform emergence and maximizing crop yields. Such a system is essential for modern farms utilizing precision agriculture to optimize agricultural processes.

REZUMAT

Lucrarea cuprinde un studiu realizat în scopul proiectării unui sistem automat de control al adâncimii de semănat la mașinile de semănat plante prășitoare, pentru a asigura plasarea semințelor la o adâncime optimă și uniformă în sol, în timp real direct din cabina tractorului. Sistemul inteligent va fi adaptat la condițiile variabile ale solului, asigurând aceleași condiții optime de germinare pe întreaga lățime de lucru. Semănătoarea de plante prășitoare echipată cu acest sistem automat va asigura o plasare precisă a semințelor la adâncimi agrotehnice recomandate, favorizând o răsărire uniformă și maximizând randamentului culturilor. Un astfel de sistem este esențial pentru fermele moderne care folosesc agricultura de precizie pentru optimizarea proceselor agricole.

INTRODUCTION

Global food production is facing profound challenges due to complex factors such as population growth, climate change, a condensed period of multiple crises (e.g. wars, geopolitical conflicts and pandemic effects) and changing consumer preferences *(Galanakis, C.M. 2020; Galanakis, C.M. et al., 2021; Galanakis, C.M., 2023).*

For example, the world population is projected to reach approximately 9.7 billion by *2050 (Bahar, N.H. et al, 2020)*, requiring resource management and creating an increasingly urgent need for the production of safe, nutritious and sustainable food.

The rapid growth in global food demand is accompanied by urbanisation, a corresponding increase in environmental impacts and the expansion of agriculture, all of which require the sustainability and resilience of our food systems *(Boyaci-Gunduz, C.P. et al., 2021; Tilman, D.; Balzer et al., 2011).*

Agriculture, as the main source of sustainable food, is significantly affected by climate change and extreme weather events, such as temperature variations, erratic rainfall and the availability of surface and groundwater resources *(Markou, M. et al., 2020).*

As the population grows, it is essential to improve food production. Technological advancement is crucial for the agricultural sector to minimise the conventional seeding process and produce high quality food products to better meet the basic food needs of humanity *(Bhujangarao, A. et al., 2023).* Seed drills are specialized agricultural equipment designed for precision seeding of various row crops such as corn, sunflower, soybean, sugar beet, etc.

These machines are at the heart of the seeding process in agriculture and play a critical role in crop yield and efficiency *(Yadav, N.K. and Meena, S.S., 2024).* The most commonly used seed drills today are pneumatic seed drills, which use an air pressure system to distribute the seed. The distributors are driven by

the drive wheel through various transmission components such as chains, gears, shafts and belts *(Soyoye, B. O., 2020)*.

Figure 1 shows the functional diagram of a row crop planter (precision sowing of crops such as maize, sunflower, etc.). The planter is of the pneumatic type *(Cujbescu, D. et al., 2022; Marin, E. et al., 2010)*.

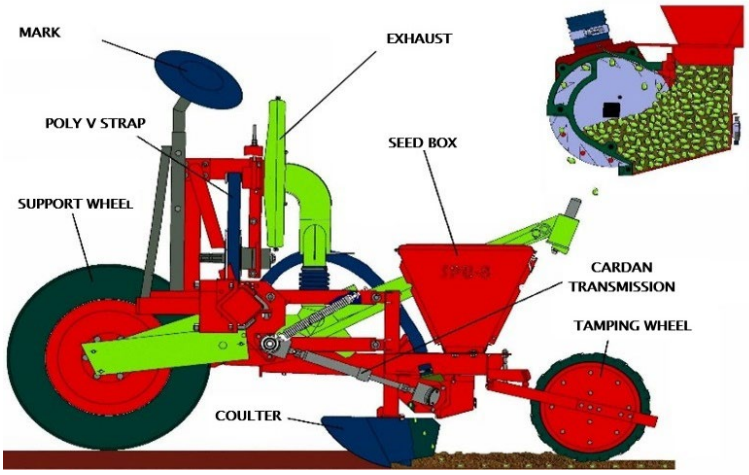

Fig. 1 - Functional diagram of a row crop seeder

During operation, the exhaust fan creates a vacuum which is transferred to the seed distribution units via suction tubes. The vacuum holds the seed in the supply chambers against the openings of the distributor discs. As the row planter moves, the support wheels transmit motion through a gearbox with sprockets and cardan shafts to the distributor shafts which rotate the discs, sending the seeds into the furrows and from there into the open grooves created by them. Only one seed is fixed to each disc hole due to the limited space around the hole. The packer wheels close the furrows and compact the soil to the sides of the planted row. The planter is guided across the field by the tracks left on the ground by the marker *(Bahar, N.H. et al.; 2020)*.

Ensuring uniform distribution along the row within the specified interval, minimizing seed damage, accurate dosing regardless of travel speed, and proper seed placement at the correct depth of the furrow are current requirements aimed at improving the quality indicators of crop sowing *(Zahariev, I. and Kehayov, D., 2022)*.

The utilization of row crop planters (corn, sunflower) in contemporary agriculture is imperative, as they facilitate precise seed distribution, optimize row spacing, and promote the cultivation of uniform crops, thereby fostering high and efficient yields *(Nielsen, S. K., et al., 2018)*.

Precision pneumatic seeders, which are instrumental in ensuring optimal crop germination, must place seeds with exactitude at the depth where soil moisture is present to facilitate seed germination *(Thalmann, G., 1983)*.

The current stage in monitoring and controlling sowing depth involves research aimed at using sensors to control sowing depth in real time, allowing for automatic adjustments directly from the tractor cabin. This system integrates with moisture sensors, such as the Correvit-H400/250, manufactured by Pessl Instruments, to ensure that seeds are placed at optimal depths with adequate moisture. The overarching objective of these systems is to minimize variability between rows and ensure uniform sowing depth across the entire field *(Iqbal, T. et al, 2022; Li, Y. et al., 2015)*.

International companies with a reputation for innovation, such as Ag Leader, have developed advanced technology to optimize the down Force of seeders during operation using the ISOBUS Hydraulic Down Force Row Module Detection. Utilizing the SureForce sensor, this technology instantly provides the necessary downforce to maintain depth in no-till conditions and across different soil types, through heavy residues and compacted areas. This technology is part of a broader trend in agriculture of automation and digitalization, which is having a significant impact on efficiency and productivity *(Zhou, L. et. Al., 2023)*.

Ag Leader Technology, Inc. is a recognized leader in the field of precision farming hardware and software. Headquartered in Ames, Iowa, USA, the company specializes in the design, manufacture and marketing of precision technology, with the objective of assisting farmers in making informed decisions that

lead to profitable outcomes. Since its establishment in 1992, the company has experienced consistent growth and expansion by offering products that provide added value to farmers, thereby contributing to their sustained profitability. Further information can be found at www.agleader.com.

In a move that exemplifies its commitment to innovation, John Deere has developed FurrowVision™, a state-of-the-art technology integrated into its planter seeders. This technology is designed to enhance the precision and efficiency of the seeding process by verifying seed depth and providing a visualization of the seeding channel directly from the tractor cab. This is achieved by incorporating a video camera within the actual plant furrow. This technology focuses on monitoring and controlling planting depth and seed positioning in seed rows, ensuring uniform and optimal germination *(https://www.futurefarming.com/crop-solutions/john-deere-announces-furrow-vision/).*

The implementation of precision sowing technology, which involves the meticulous adjustment of sowing depth, necessitates the integration of sensors of various types, along with PID (Proportional Integral Derivative) controllers. These controllers are instrumental in ensuring the seamless operation of automation and control systems, where they function as critical components in maintaining process values within the desired range.

The sensors, which can be classified as laser, ultrasonic, or angle types, can be mounted in different positions on the sowing section (Fig. 2, a, b, and c) *(Wang, S. et al., 2024).*

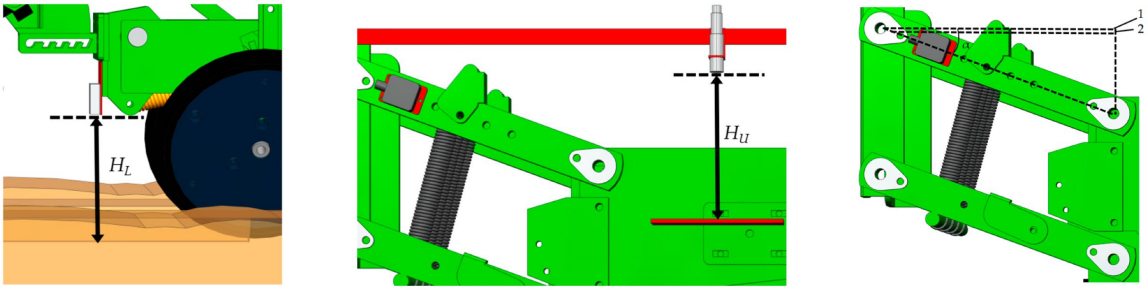

a. b. c.

Fig. 2 - Diagrams of the sensor detection principle in the seeding depth control system
a. Principle of monitoring with a laser sensor; b. Principle of monitoring with an ultrasonic sensor; c. Principle of monitoring with an angle sensor, 1. Horizontal plane. 2. Initial height
(Wang, S. et al., 2024)

The following table presents the main characteristics of the sensor types.

Table 1

Main parameters of the sensors used

Sensor type	Parameter	Value
Laser sensor	Measurement accuracy/mm	0.5
	Measurement range/m	0.05~80
	Spot size/mm	6
Ultrasonic sensor	Beam angle/(°)	10
	Detection range/cm	7~100
	Blind measurement zone/cm	0~7
Angle sensor	Measurement resolution/(°)	0.01
	Measurement accuracy/(°)	0.05
	Measurement range/(°)	±90

Recent research endeavours have culminated in the formulation of intelligent seeding systems that leverage artificial intelligence and optimisation algorithms to dynamically adjust seeding depth in real time. Precision Planting is recognised for its innovations in agricultural technologies, which assist farmers in improving the accuracy and efficiency of seeding, fertilisation and crop monitoring.

Utilising advanced sensors, electronic control systems and data analytics, the company provides solutions that optimise resource utilisation and enhance crop yield. One such example is the SmartDepth™ *(https://www.precisionplanting.com/products/planters/smartdepth)* system, which integrates advanced sensors and an automated control system to optimise seed placement based on soil conditions. A second example is DeltaForce® coulter pressure control, which optimises the force applied to the seeding unit to maintain a constant seed depth in any soil type *(Cloete, S., 2019).*

The sections of precision pneumatic seed drills are mounted to the frame bar by means of a deformable parallelogram mechanism, and to control the sowing depth they are provided with different mechanisms for adjusting the pressing force of the depth wheel drive system (see Figures 3a, b and c) *(Li, H. et al., 2023)*.

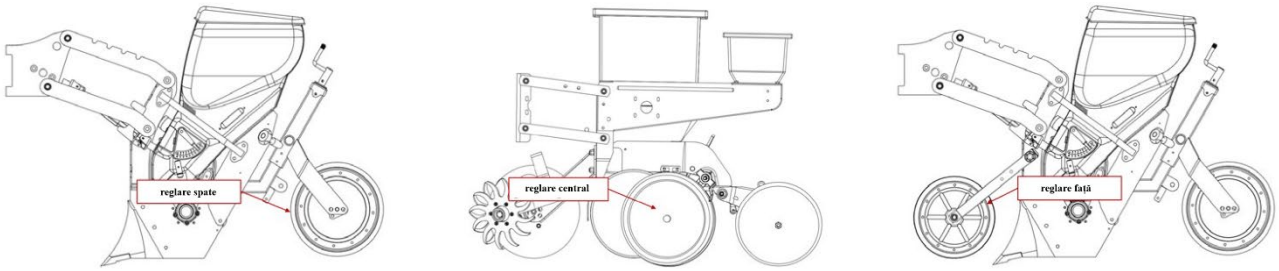

Fig. 3 - Downforce adjustment mechanisms for the depth wheel drive system
a. Rear adjustment mechanism; b. Central roller adjustment mechanism; c. Front adjustment
(Tilman, D. et al., 2011)

The pressing force adjustment mechanism of the passive type depth wheel drive system primarily employs a mechanical spring, while the pressing force adjustment mechanism of the active type depth wheel drive system predominantly utilises a hydraulic drive or a pneumatic drive, as illustrated in Table 2 *(Li, H. et al., 2023)*.

Table 2

Common methods of the downforce adjustment mechanism for the depth wheel system

Type	Partial view	Description
Mechanical adjustment		- Simple structure, high reliability, wide range of applications; - Easy to install and adjust; - Preload must be empirically adjusted based on soil conditions before operation; unstable aerodynamic force on the soil.
Hydraulic adjustment		- Requires sensor-assisted adjustment; - Complex structure; - Fast response time, suitable for high-speed operation; - Provides greater force and torque, adjustable range, and high stability.
Pneumatic adjustment	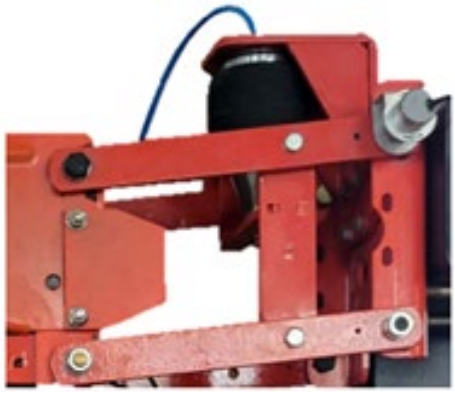	- Requires sensor-assisted adjustment; requires an external air supply unit; - Can withstand very high pressure and vibration impact; - Good vibration damping effect; high stability for seed drop.

MATERIALS AND METHODS

The research undertaken for the design of an intelligent control and monitoring system for the sowing depth was conducted on a seeder equipped with sowing sections procured from S.C. Mecanică Ceahlău S.A. Piatra Neamţ. The sowing sections are mounted to the frame bar by means of a system of articulated bars and a plate that is fixed to the square bar with two clamps. The sowing sections are equipped with a seed hopper, a pneumatic distribution device, a skid coulter, a zero-pressure tire compaction wheel and a chain transmission mechanism.

The compaction wheel shaft is capable of mounting four sprockets (z=9, z=10, z=11, z=16), while the distributor shaft can accommodate two sprockets (z=22, z=30). The configuration of the seeder ensures the accurate and consistent sowing of grains at regular intervals. This is facilitated by the pneumatic-mechanical distributor, which enables precise distribution, and the uniformity of the sowing depth is ensured by the left and right support wheels, which are supported on the frame bar by means of arms. The seed distributor transmission and the tamping wheel, equipped with a 0-pressure tire and a V-profile, ensure the conditions for optimal sowing. Figure 4 shows the main components of the equipment for sowing weed plants.

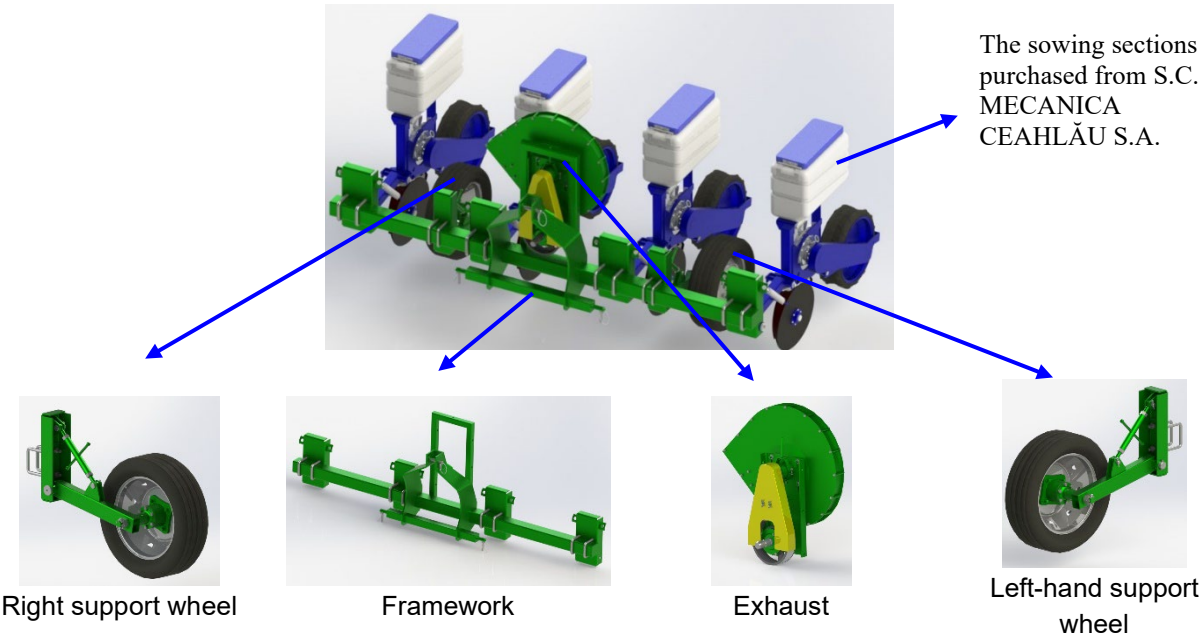

Fig. 4 - Main components of the row crop seeding machine

The working depth adjustment of the seed drill is accomplished through the utilisation of a double-threaded tie rod (equipped with two opposite threads, one on the right and one on the left), which facilitates the elevation or depression of the support wheel on the right or left side relative to the ground level. Consequently, the position of the coulter undergoes a proportional alteration, and the effective working depth is derived from the adjustment made. The soil settlement, estimated at 2-3 cm (due to the wheel sinking into the ground), is then subtracted from this.

The initial phase of this study involved the identification of contemporary solutions for replacing the double-threaded tie rod, thereby enabling automation of the working depth adjustment process through the integration of an intelligent control and monitoring system.

The following solutions are proposed:

- The electro-hydraulic system with depth sensors will consist of the following main components:
  - The double-threaded tie rod is replaced by an electronically controlled hydraulic cylinder.
  - Depth sensors (e.g. ultrasonic or LIDAR sensors) measure the position of the coulters relative to the ground in real time.
  - The hydraulic cylinder's optimal operating depth is automatically regulated by the control unit.
  - It is possible to integrate this with tractor ISOBUS systems for the purpose of in-cab control.
- The electric motor system with linear actuator will comprise the following main components:

- The installation of an electric actuator in lieu of the tie rod facilitates precise adjustment of the working depth.
- The implementation of intelligent software control facilitates the adjustment of the coulter position, a function that is informed by the readings received from the sensors.

In the final stage of this study, three-dimensional geometric models of the primary subassemblies, i.e. the constituent elements of the seeder for grass seeds, were developed. The Workstation 22H2, equipped with an Intel(R) Xeon(R) W-2123 CPU @ 3.60GHz, was utilized for this purpose. The parametric design program SOLIDWORKS® Premium 2018 S.P. 0.1 was used for 3D modelling.

Initially, each component was modelled in three dimensions individually, and subsequently assembled using the Assemblies module.

RESULTS

As illustrated in Figure 6, both support wheels are equipped with a hydraulic cylinder of the CS00503220 type, manufactured by Hidraulica Industrial *(https://hidraulica-center.ro/toate-produsele/cilindri-hidraulici/dubla-actiune/cilindri-cs/).*

Fig. 5 - Left support wheel

Fig. 6 - Right support whee

Figure 7 presents the functional diagram, and Table 3 details the primary parameters of a hydraulic cylinder of type CS00503220.

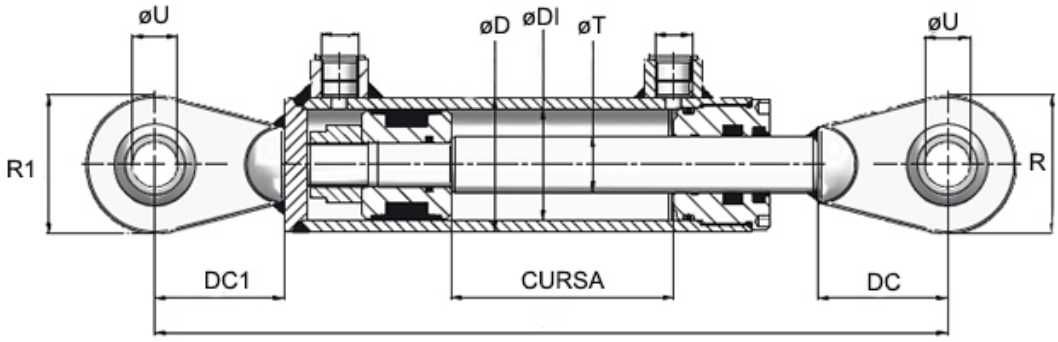

Fig. 7 - Functional diagram of a hydraulic cylinder type CS00503220

Table 3

Main parameters of the hydraulic cylinder type CS00503220

Cod	D	DI	T	Cursa	LT	U	R	DC	R1	DC1	F
CS00503220	42	32	20	50	275	16	46	60	46	60	¼”

As illustrated in Figure 8, the equipment for sowing weedy plants comprises two support wheels, each equipped with a hydraulic cylinder type CS00503220.

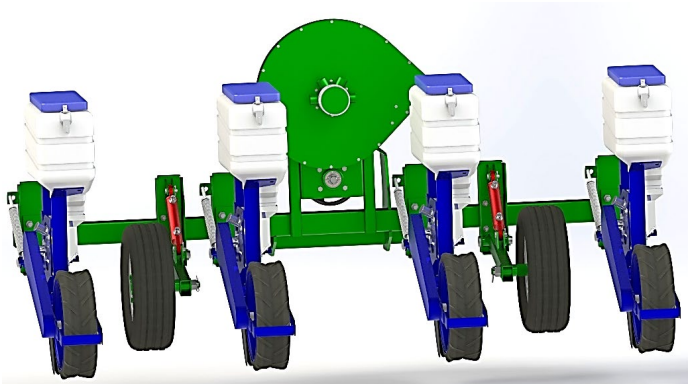

Fig. 8 - Row crop seeding machine equipped with a left support wheel and a right support wheel, each fitted with a hydraulic cylinder type CS00503220

As illustrated in Figures 9 and 10, each support wheel is fitted with a CONCENTRIC LACT4P-12V-20 linear electric actuator manufactured by Pololu Robotics and Electronics *(https://www.pololu.com/).*

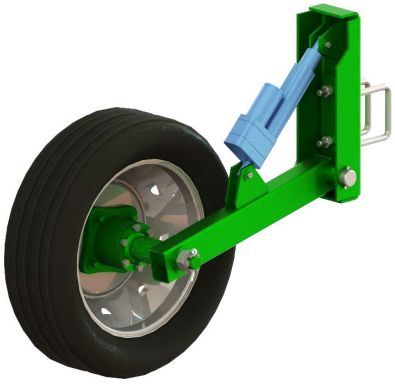

Fig. 9 - Left support wheel

Fig. 10 - Right support wheel

Figure 11 shows the diagram with the main dimensions, and table 4 shows the main parameters of a linear electric actuator type LACT4P-12V-20.

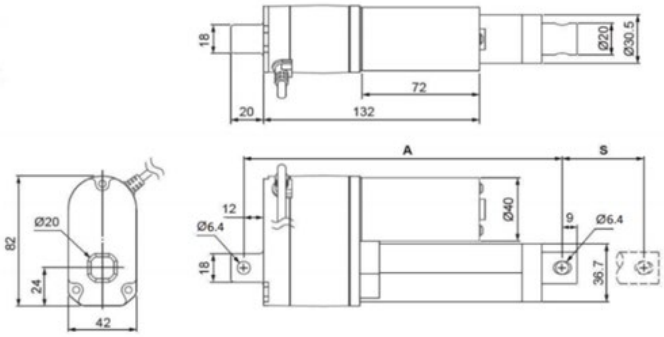

Fig. 11 - Diagram with the main dimensions of a linear electric actuator type LACT4P-12V-20

Table 4

Main parameters of the linear electric actuator type LACT4P-12V-20

Cod	Cursa S, mm	Lungimea retasă A, mm	Viteza de lucru, mm/s	Viteza de lucru în sarcina, mm/s
LACT4P-12V-20	100	246	14,6	12,3

Figure 12 presents a schematic illustration of the apparatus employed for the cultivation of weedy vegetation, consisting of the left and right support wheels, with each being equipped with a linear electric actuator designated LACT4P-12V-20.

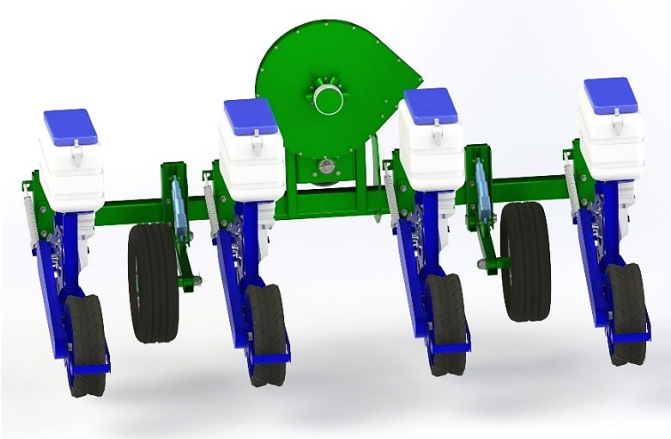

Fig. 12 - Row crop seeding machine equipped with a left support wheel and a right support wheel, each fitted with a linear electric actuator type LACT4P-12V-20

The automation of the CS00503220 hydraulic cylinder for seeding depth control encompasses the following components:

1. The Danfoss PVG 32 proportional hydraulic distributor (cf. fig. 13) is a device that regulates the oil flow to the cylinder depending on the signal received from the control unit.

Fig. 13 - Danfoss PVG 32 proportional hydraulic valve distributor
(https://lyra.ro/produs/distribuitor-danfoss-pvg-32-o-sectiune-proportionala-flotanta/)

2. The Temposonics MH magnetostrictive cylinder position sensor (see Figure 14) is a device that measures the position of the cylinder piston and transmits a signal to the control unit.

Fig. 14 - Temposonics MH magnetostrictive position sensor for cylinders
(https://www.infinitrade-romania.ro/produs/marcicomercializate/mts-sensors/senzori-de-pozitie-hidraulica-mobila-mts/senzor-de-pozitie-aplicatii-hidraulice-mh-mts/)

3. The distance sensor (ultrasonic/laser) quantifies the actual distance between the sowing unit and the ground, compensating for unevenness. The SICK UM30-213113 sensor (fig. 15) is a viable option, manufactured by SICK AG, a German company specialising in industrial sensors, automation and measurement systems.

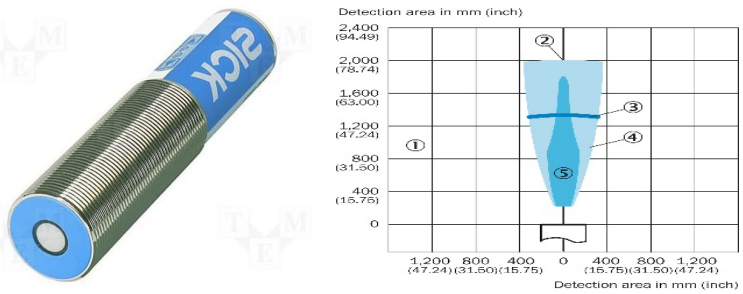

① Detection range dependent on reflection properties, size, and alignment of the object
② Limiting range
③ operating range
④ example object: aligned plate 500 mm x 500b mm
⑤ example object: pipe with 27 mm diameter

Fig. 15 - SICK UM30-213113 distance sensor

(https://www.sick.com/cl/en/catalog/products/distance-sensors/ultrasonic-distance-sensors/um30/um30-213113/p/p222357)

4. The Siemens LOGO! PLC electronic control unit (ECU) (fig. 16), which receives the signal from the position sensor and controls the proportional valve to adjust the cylinder position.

Fig. 16 - Electronic Control Unit (ECU) PLC Siemens LOGO!

(https://www.siemens.com/global/en/products/automation/systems/industrial/plc/logo/logo-basic-modules.html)

5. Additional sensors (optional):

5.1. The WIKA A-10 pressure sensor (fig. 17) is employed to monitor the pressure in the system for the purposes of protection and diagnostics.

Fig. 17 - WIKA A-10 pressure sensor

(https://www.infinitrade-romania.ro/produs/marcicomercializate/wika-instrumente-de-masura/masurarea-presiunii-wika/wika-senzori-de-presiune/senzor-de-presiune-wika-model-a-10/)

5.2. The Danfoss DST P92 flow sensor (see Figure 18) is utilised for the purpose of measuring oil flow, thus facilitating fine adjustments.

Fig. 18 - Danfoss DST P92 flow sensor

(https://www.danfoss.com/en/products/sen/sensors-and-transmitters/industrial-pressure-transmitters/dst-p92s/)

6. Cable and electrical connectors required to connect the sensors and distributor to the control unit.

Operating principle:

- The operator sets the desired depth on the Siemens LOGO! PLC interface.
- The Temposonics MH magnetostrictive cylinder position sensor measures the cylinder position in real time and sends data to the Siemens LOGO! PLC.
- The Siemens LOGO! PLC compares the value measured by the distance sensor with the desired setting and sends a signal to the Danfoss PVG 32 proportional valve.
- The Danfoss PVG 32 proportional hydraulic valve adjusts the oil flow to position the cylinder as commanded.

The automation of the linear electric actuator (Concentric LACT4P-12V-20) for seeding depth control comprises the following components:

1. The Pololu Jrk G2 18v19 Pololu Jrk G2 18v19 actuator controller (fig. 19), which controls the direction and speed of movement. This actuator has an internal potentiometer, which measures the exact position of its stroke and transmits the signal to the controller.

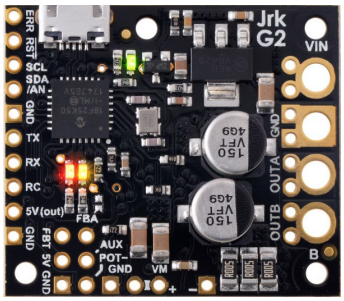

Fig. 19 - Pololu Jrk G2 18v19 actuator controller

(https://www.pololu.com/product-info-merged/3146)

2. Siemens LOGO! PLC control unit (fig.15), which processes the sensor data and controls the actuator.

3. Power supply with motorcycle battery The Exide 12V 12Ah, EB12AL-A2 (fig. 20) Exide 12V 12Ah motorcycle battery (fig. 20), which provides the power for the actuator and controller.

Fig. 20 - Exide 12V 12Ah motorcycle battery, EB12AL-A2

(https://www.baterii-acumulatoare.ro/baterie-exide-moto-12ah-eb12al-a2)

Operating principle:

- Setting the desired depth – The operator enters the value on a control panel or it is predefined in the Siemens LOGO! PLC.
- Actuator position measurement – The internal potentiometer transmits the current position to the ECU.
- Comparing values – The Siemens LOGO! PLC checks whether the current position corresponds to the desired setting.
- Actuator control – If there is a difference, the Siemens LOGO! PLC sends a signal to the actuator controller to extend/retract it.
- Automatic corrections – The system continuously monitors the seeding depth and makes adjustments in real time.

CONCLUSIONS

1. Ensuring a constant planting depth in crops of grass crops such as maize and sunflowers is essential for uniform emergence, whereas an incorrect depth can lead to uneven crop growth. If seeds are placed too close to the surface (below 3 cm), they risk drying out quickly in arid soil. When seeds are placed at the optimum depth (4-6 cm), they benefit from optimal contact with the soil, which ensures rapid and uniform germination. If the seeds are placed too deep (over 7 cm), sprouting is delayed and uneven, as the seeds use more energy to reach the surface.
2. The left-right screw-pull coulter depth adjustment is notable for its simplicity of construction and low cost. However, it is also characterized by a protracted adjustment time and a tendency to err on the side of under-correction with regard to ensuring the correct sowing depth.
3. The hydraulic cylinder seeding depth adjustment offers the advantage of being able to make quick and accurate adjustments directly from the tractor cab; however, there is a risk of oil leakage from the hydraulic circuit.
4. The seed depth adjustment with an electric linear actuator provides precise adjustment with full automation possible, has low power consumption and minimum maintenance, but there is a possible delay in response compared to a hydraulic system.
5. The validation of the design of an automatic seed depth control system (hydraulic cylinder or electric linear actuator) shall be carried out by conducting performance tests to confirm that the seed depth control is effective under varying field conditions. The following tests shall be conducted:
   - checking uniformity of sowing;
   - testing sowing depth on different sowing depths on different fields;
   - measuring impact on sowing quality (uniform plant germination).
6. The utilization of a hydraulic cylinder or electric linear actuator seed depth adjustment system has been demonstrated to be advantageous for a number of individuals and entities within the agricultural sector. These include farmers seeking to enhance the accuracy of their seeding operations, equipment manufacturers developing advanced technologies, machine operators seeking greater control, and agricultural researchers studying seeding efficiency. The integration of this technology has been demonstrated to enhance productivity, reduce financial expenditure and safeguard the environment.

ACKNOWLEDGEMENT

The results presented in this article were obtained with the support of MADR through the "Sectoral Plan - ADER 2026", financing contract no. 25.1.2 / 14.07.2023, ADER project 25.1.2. Tehnologie inovativă de prelucrare minimă a terenului agricol adaptată la schimbările climatice actuale – TEHCONS.

REFERENCES

[1] Cloete, S. (2019). Precision planting technology: Designed to maximise farm ouput. Farmer's Weekly, 2019(19031), 50-51.

[2] Cujbescu, D., Găgeanu, I., Persu, C. & Gheorghe, G. (2022). Numerical simulation of seed distribution of a pneumatic seed meter. INMATEH-Agricultural Engineering, 66(1).

[3] Bahar, N.H., Lo, M., Sanjaya, M., Van Vianen, J., Alexander, P., Ickowitz, A. and Sunderland, T., 2020. Meeting the food security challenge for nine billion people in 2050: What impact on forests?. *Global Environmental Change*, *62*, p.102056.

[4] Bhujangarao, A., Vidyasagar, K., Surya Prasad Rao, B. and Suryaprakash, G., 2023. Design of a Corn Seed Sowing Machine for Uniform Distribution of Corn Seeds Using Optimum Seed Distribution Algorithm. In Modern Approaches in IoT and Machine Learning for Cyber Security: Latest Trends in AI (pp. 293-309). Cham: Springer International Publishing.

[5] Boyaci-Gunduz, C.P.; Ibrahim, S.A.; Wei, O.C.; Galanakis, C.M. Transformation of the food sector: Security and resilience after the COVID-19 pandemic. *Foods 2021, 10*, 497.

[6] Galanakis, C.M. The Food Systems in the Era of the Coronavirus (COVID-19) Pandemic Crisis. *Foods 2020,* 9, 523.

[7] Galanakis, C.M.; Rizou, M.; Aldawoud, T.M.S.; Ucak, I.; Rowan, N.J. Innovations and technology disruptions in the food sector within the COVID-19 pandemic and post-lockdown era. *Trends Food Sci. Technol. 2021, 110*, 193–200.

[8] Galanakis, C.M. The “Vertigo” of the food sector within the triangle of climate change, the post-pandemic world, and the Russian-Ukrainian war. *Foods 2023, 12*, 721.
[9] Iqbal, T., Ghaffar, A. M., ur Rehman, U., Saeed, Y., Aqib, M., Iqbal, F., & Saleem, S. R. (2022). Development of Real Time Seed Depth Control System for Seeders. Environmental Sciences Proceedings, 23(1), 7.
[10] Li, Y., Xiantao, H., Tao, C., Dongxing, Z., Song, S., Zhang, R., & Mantao, W. (2015). Development of mechatronic driving system for seed meters equipped on conventional precision corn planter. International Journal of [11]. Li, H., He, J., Wang, C., Yang, W., Lin, H., Wang, Q., ... & Tan, L. (2023). Research progress on the development of the planter unit for furrowing control and the depth measurement technology. Applied Sciences, 13(21), 11884.
[11] Markou, M.; Moraiti, C.A.; Stylianou, A.; Papadavid, G. Addressing Climate Change Impacts on Agriculture: Adaptation Measures for Six Crops in Cyprus. Atmosphere 2020, 11, 483.
[12] Marin, E., Sorică, C., Manea, D., & Vezirov, Z. (2010). Echipament tehnic destinat tehnologiei inovative de lucrare a solului si înfiinţare a culturilor de prăsitoare, bază a promovării agriculturii durabile. *INMATEH–Agricultural Engineering, 31(2)*.
[13] Nielsen, S. K., Munkholm, L. J., Lamandé, M., Nørremark, M., Edwards, G. T., & Green, O. (2018). Seed drill depth control system for precision seeding. Computers and electronics in Agriculture, 144, 174-180
[14] Soyoye, B. O. (2020). Development of the instrumentation unit of a motorized precision planter. European Journal of Engineering and Technology Research, 5(4), 403-407.
[15] Thalmann, G. (1983). Systematik und Gestaltung der Arbeitsphasen einer Einzelkornsämaschine. agrartechnik, 33(1).Agricultural and Biological Engineering, 8(4), 1-9.
[16] Tilman, D.; Balzer, C.; Hill, J.; Befort, B.L. Global food demand and the sustainable intensification of agriculture. *Proc. Natl. Acad. Sci. USA 2011*, 108, 20260–20264.]
[17] Wang, S., Yi, S., Zhao, B., Li, Y., Li, S., Tao, G., ... & Sun, W. (2024). Sowing depth monitoring system for high-speed precision planters based on multi-sensor data fusion. Sensors, 24(19), 6331.
[18] Yadav, N.K. and Meena, S.S., 2024. Advancements in Mechanized Techniques for Sweet Corn Cultivation: A Review. Asian Research Journal of Agriculture, 17(4), pp.47-63.
[19] Zahariev, I. and Kehayov, D., 2022. Determining of the parameters for movement on a vacuum sowing apparatus of seeder section for pneumatic precision seed drill. Scientific Papers. Series A. Agronomy, 65(2).
[20] Zhou, L., Ma, Y., Zhou, H., Niu, K., Zhao, B., Wei, L., ... & Zhang, W. (2023). Design and test of sowing depth measurement and control system for no-till corn seeder based on integrated electro-hydraulic drive. Applied Sciences, 13(10), 5823.
[21] *** https://www.baterii-acumulatoare.ro/baterie-exide-moto-12ah-eb12al-a2
[22] *** https://www.danfoss.com/en/products/sen/sensors-and-transmitters/industrial-pressure-transmitters/dst-p92s/
[23] *** https://hidraulica-center.ro/toate-produsele/cilindri-hidraulici/dubla-actiune/cilindri-cs/
[24] *** https://www.infinitrade-romania.ro/produs/marcicomercializate/mts-sensors/senzori-de-pozitie-hidraulica-mobila-mts/senzor-de-pozitie-aplicatii-hidraulice-mh-mts/
[25] *** https://www.infinitrade-romania.ro/produs/marcicomercializate/wika-instrumente-de-masura/masurarea-presiunii-wika/wika-senzori-de-presiune/senzor-de-presiune-wika-model-a-10/
[26] *** https://lyra.ro/produs/distribuitor-danfoss-pvg-32-o-sectiune-proportionala-flotanta/
[27] *** https://www.pololu.com/
[28] *** https://www.pololu.com/product-info-merged/3146
[29] *** https://www.precisionplanting.com/products/planters/deltaforce
[30] *** https://www.precisionplanting.com/products/planters/smartdepth
[31] *** https://www.siemens.com/global/en/products/automation/systems/industrial/plc/logo/logo-basic-modules.html
[32] *** https://www.sick.com/cl/en/catalog/products/distance-sensors/ultrasonic-distance-sensors/um30/um30-213113/p/p222357

VIBRATORY CULTIVATORS FOR SUSTAINABLE AGRICULTURE: A REVIEW OF DESIGN, PERFORMANCE, AND SMART TECHNOLOGIES

/

CULTIVATOARELE VIBRATOARE ÎN AGRICULTURA SUSTENABILĂ: ANALIZĂ A PROIECTĂRII, PERFORMANȚEI ȘI TEHNOLOGIILOR INTELIGENTE

Neluș-Evelin GHEORGHIȚĂ*[1)], Sorin-Ștefan BIRIȘ[1)], Raluca-Adriana ZOTA[1)], Mariana IONESCU[1)], Daria-Ioana SICARU[1)], Dragoș ANGHELACHE[2)]

[1)] Faculty of Biotechnical Systems Engineering, National University of Science and Technology POLITEHNICA Bucharest / Romania;
[2)] National Institute of Research - Development for Machines and Installations Designed to Agriculture and Food Industry - INMA Bucharest / Romania.
*Tel: 0726 453 269; *E-mail: evelin_gheorghita@yahoo.com*

Keywords: *Vibratory cultivators, Soil compaction, Energy efficiency, Sustainable agriculture, Precision agriculture*

ABSTRACT

In terms of energy consumption and its effect on the long-term health of the soil, tillage is one of the most demanding farming practices. The usage of vibratory cultivators, which lessen the draft power needed, improve soil breakdown, and can consume less energy overall, has shown promise. When vibration frequencies are appropriately set, field testing have demonstrated certain advantages, including lower clod sizes and less need for traction. Similar research on tractor-rotary tiller systems shows improvements in soil performance as well as the significance of vibration control for the operator's and the machine's safety.Simple vibration has not been the focus of study in recent years. In order to increase efficiency and lessen adhesion issues in wet soils, new systems now employ cameras to assess soil roughness and only activate vibration when necessary. Using nature as inspiration, other research has demonstrated that biomimetic tool designs may reduce resistance by almost 10%. On the digital side, real-time soil compaction estimation has been successfully achieved through the use of machine learning and vibration data.When combined, these developments suggest that vibratory tillage, bio-inspired designs, and smart sensors will be used in the future to improve the sustainability and efficiency of soil management.

REZUMAT

În ceea ce privește consumul de energie și efectele asupra sănătății solului pe termen lung, prelucrarea solului este una dintre cele mai solicitante practici agricole. Utilizarea cultivatoarelor vibratoare, care reduc puterea de tracțiune necesară și îmbunătățesc fragmentarea solului, scăzând consumul total de energie, s-a dovedit promițătoare. Testele din câmp au arătat anumite avantaje atunci când frecvențele vibrațiilor sunt setate corect, inclusiv brazde de pământ mai mici și o nevoie redusă de tracțiune. Cercetări similare privind sistemele tractor–freză rotativă arată atât îmbunătățiri ale performanței solului, cât și importanța controlului vibrațiilor pentru siguranța operatorului și a utilajului.În ultimii ani, vibrațiile simple nu au mai fost în centrul studiilor. Pentru a crește eficiența și a reduce problemele de aderență în solurile umede, sisteme noi folosesc camere pentru a evalua rugozitatea solului și activează vibrația doar atunci când este necesar. Inspirându-se din natură, alte cercetări au demonstrat că uneltele cu design biomimetic pot reduce rezistența la înaintare cu aproape 10%. Pe partea digitală, estimarea în timp real a compactării solului a fost realizată cu succes prin utilizarea datelor vibraționale și a algoritmilor de învățare automată.Luate împreună, aceste progrese sugerează că în viitor lucrările solului cu organe de lucru vibratoare, designurile bio-inspirate și senzorii inteligenți vor fi integrate pentru a crește sustenabilitatea și eficiența gestionării solului.

INTRODUCTION

One of the most important aspects of agricultural productivity is land preparation. The soil in the field can be improved for crop development by land preparation techniques. Tractor traction is necessary for traditional farming equipment like share plows and disc harrows. On the other hand, because of their many useful functions and reduced power load needs, tractor rotational tillage devices have taken over as the primary technique for land preparation. Thus, the study of a rotary tiller's operating performance will contribute to raising crop output and final operation quality *(Gao Y.. et al, 2024)*. Because of the complex

field working environment, agricultural machinery frequently experiences intense vibrations from multisource excitations while in use, which lowers the machinery's dependability and lowers the quality of the job produced.(*Chen, S.R. et al, 2020*)

A revolutionary approach to contemporary farming, precision agriculture (PA) uses sophisticated sensing, data analytics, and decision-support technology to handle the temporal and geographical variability seen in agricultural areas (*Alfred. et al., 2021*). In contrast to contemporary planters, sprayers, and harvesters, tillage equipment has remained less sophisticated in agricultural operations. However, tillage is becoming more widely acknowledged as a crucial area for innovation to include into precision agricultural systems due to the rise of herbicide-resistant weeds, the requirement for residue management, field smoothing, and data-centric farming (*Janbazi Alamdari et al, 2025*).

Soil compaction is becoming a major issue on a global scale. Compaction now affects over 68 million hectares of land globally (*Oldeman, 1992*), and in the ensuing decades, this amount is predicted to rise. Land use and heavy machinery have been highlighted as key causes to compaction, which the European Union has acknowledged as a serious type of soil deterioration (*Jones, 2004*). Compaction is the most common kind of deterioration in Central and Eastern Europe, where high soil loading is the main cause of the widespread degradation *(Van den Akker, 2004).* These issues highlight how critical it is to precisely determine the degree of compaction on commercial agricultural areas and implement mitigation strategies.

By physically loosening the soil, adding organic matter, creating a uniform planting surface, controlling residue, adding herbicide, and fostering root growth, effective tillage enhances soil conditions for seedbed preparation. Additionally, it's essential for controlling soil compaction, which can hinder downward root development, water penetration, crop production, and nutrient uptake (*Nawaz et. al, 2013*). Tillage and herbicide inputs frequently work in opposition to one another in integrated weed management systems because decreasing herbicide use usually necessitates more mechanical intervention, whereas decreasing tillage intensity tends to increase reliance on herbicides to maintain efficient weed control and minimize yield loss (*Mason et. al, 2020*).

In agriculture, interactions between soil and tools often take place at several stages of crop growth, such as tillage, sowing, crop management, and harvesting. In order to accomplish the shearing, upheaval, failure, movement, loosening, overturning, and fracturing of the soil, agricultural soil-engaging tools (ASETs) and soil engage mechanically, usually with a tractor (*Gursoy et. al, 2017*). The energy required for the overall cropping system is mostly derived from the energy utilized in the soil's operational activities.

Biomimetic, experimental, oscillatory, high-pressure-gas splitting (HGS), line element design (LED), and other techniques are among the tillage resistance reduction techniques used by ASETs. Depending on the power supply, the oscillation technique may be divided into two categories: forced and self-oscillation (*Shagoli et. al, 2010*). By adding a vertical movement to the ASET, this technique can lower the horizontal resulting draught force in line with the mechanical qualities of the soil.

The broad definition of biomimetics is bio-inspired design that is adapted or derived from nature (*Pu et.al, 2016*). Designing and producing a variety of tools by imitating diverse animals has advanced quickly in recent years. The use of biomimetic ASETs to reduce tillage resistance is an excellent example of biomimetic approaches in action. This may be achieved through a variety of processes, such as lowering adhesion and friction on the soil (*Ren et. al, 2008*). The moving mechanisms of bionic prototypes, the integration of biomimetic design, the agronomic requirements, and other methods are just a few of the difficulties that still exist in relation to the selection of effective bionic factors, as biomimetic methods are typically restricted to a specific soil status or tool parameter.

MATERIALS AND METHODS

This review was conducted in order to identify, compare, and synthesize recent research on vibratory cultivators, biomimetic design strategies, and smart sensing technologies for sustainable soil management. The methodology followed a structured approach to literature selection and analysis.

The experiment of Esehaghneygi et. al aimed to investigate how a twin bent-share cultivator's field performance was affected by introducing vibrations at various frequencies. Additionally, the effects on the tool draught force and soil parameters of an additional vibratory motion at two frequencies and constant amplitudes are examined. The impact of lowering the draught force required in the event of longitudinal oscillations has been somewhat demonstrated in a prior research; however, the outcome of lowering the traction force in the case of transverse oscillations of a twin bentshare cultivator has not yet been documented. Based on the sideway failure zone reported by, the trials were carried out on a practical scale

using a vibrating dual bent-share cultivator with a 120 mm overlap of soil disturbance reported by *Salar et al. 2013*.(Figure 1).

The two bent-share combinations had identical descriptions. The experimental tools had a shared length of 350 mm (perpendicular to the moving direction), a share width of 110 mm, an attack angle of 15° (the angle of the leading edge), and a bent angle of 10° (the angle of the trailing edge). Because of the tool-tip's location in relation to the pivot point, the oscillation angle for this forward blade twin bent-share cultivator would be quite small. A Ck45 steel plate that was 10 mm thick was used to make the tools' shank and share. The tool oscillated thanks to a crank follower mechanism.

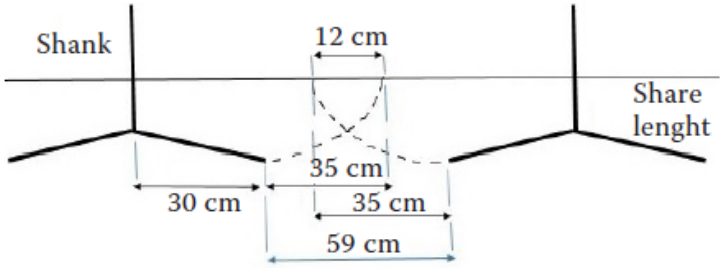

Fig. 1 - The soil failure zone overlap for the vibrating twin bent-share cultivator's tool spacing

Since the motion of the reciprocating tools was therefore perpendicular to that of the tractor, the tools were supported by two slider bearings on an upper pivot (Figure 2).

The field trials were carried out at the Research Farm of Isfahan University of Technology (Iran) using a split-plot factorial design with three replicates. Barley stubble from the previous season was present, and plots (3 m × 50 m) were arranged within randomized blocks. The dual bent-share cultivator was tested in vibrating (0.88 and 2 Hz) and non-vibrating modes, at two depths (100 and 200 mm) and two soil moisture levels (0.7 and 0.9 of PL). Tractor speed was kept constant (0.28 m·s–1) and a control with non-vibration tools was also included. Measurements included draught force, specific draught, disturbed soil cross-sectional area, mean weight diameter (MWD), soil bulk density, cohesion, adhesion, and friction angles. Soil properties such as water content, plastic limit, and texture were determined using standard methods.

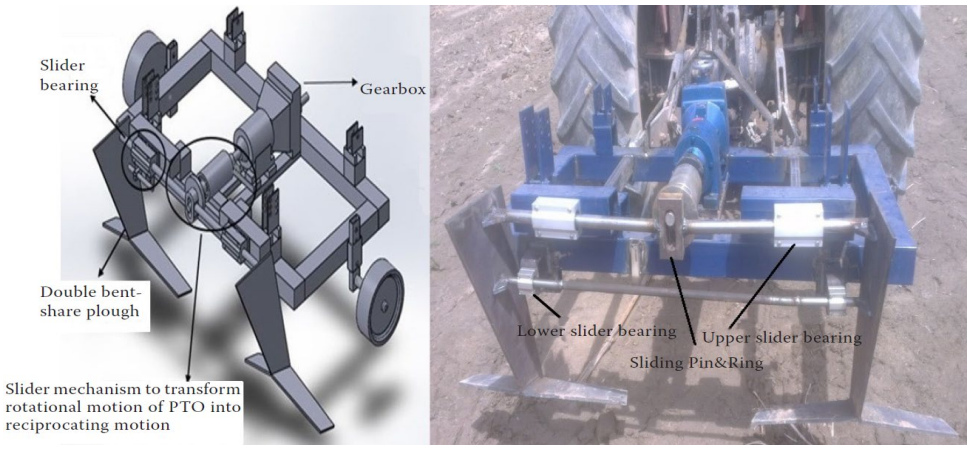

Fig. 2 - Overview of the vibrating dual bent-share cultivator

The study by Gao et al. (2024) proposed a novel methodological framework for analyzing vibrations during tractor–rotary tiller operations. Instead of treating the tractor and tiller separately, the authors investigated the combined interaction of the tractor, the three-point suspension mechanism, and the rotary tiller as a single system (Figure 3). To capture vibration transfer comprehensively, multiple tri-axial acceleration sensors were mounted at key locations, and tests were conducted under real field conditions at forward speeds of 2.1, 3.6, and 4.5 km/h.

The vibration signals were processed in both the time and frequency domains, enabling assessment of acceleration amplitudes, resonance frequencies, and vibration transmission pathways. This approach not only provided insights into how speed influences system dynamics but also revealed structural assembly

issues such as asymmetry in tractor cab vibrations, demonstrating the potential of vibration monitoring as both an operational analysis and diagnostic tool.

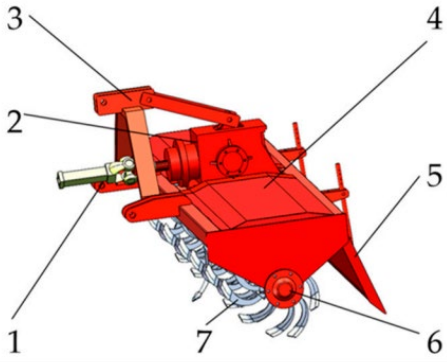

Fig. 3 - Main structure of rotary tiller:
1-Transmission system, 2- Gear box, 3- Linkage frame, 4- Cover,
5- Soil leveling board, 6- Rotary tiller shaft, 7- Rotary tiller blade

Overall, the methodology highlights how integrating multi-point sensor data with dual-domain analysis can uncover both performance-related and structural issues in tractor–tiller systems. This provides a valuable reference for optimizing implement design, reducing vibration-induced resistance, and improving operator comfort. Such an approach expands the role of vibration testing from simple measurement to a comprehensive diagnostic and design-support tool.

The article by Wang et al. (2024) provides a comprehensive methodological synthesis of biomimetic approaches for reducing tillage resistance in agricultural soil-engaging tools (ASETs). Unlike earlier studies that often tested isolated prototypes, this work systematically compared results from 148 paired experiments across 38 studies, quantifying tillage resistance reduction rates (TFRRs) for different tool categories under varying soil conditions.

A key methodological contribution was the identification of three core biomimetic strategies—reducing soil disturbance area, optimizing soil particle movement direction, and improving soil–tool contact conditions—as a framework for evaluating design effectiveness.The review also highlighted the importance of selecting appropriate biological prototypes (e.g., claws, heads, skin textures) based on local soil environments, as well as integrating biomimetic methods with other resistance-reduction techniques such as oscillation

By combining statistical comparisons with design insights, the study advanced a methodology that not only benchmarks past achievements but also guides future tool development toward energy efficiency and sustainability.

For cultivators, biomimetic designs have primarily focused on claw/leg and skin structures inspired by organisms such as mole crickets, dung beetles, and shark skin, with emphasis on reducing soil disturbance and improving contact conditions. Subsoilers, by contrast, have been designed using shanks and cutting shares inspired by bear claws, mole forepaws, and anteater claws, with influencing factors including soil properties, working depth, and soil–tool contact conditions.

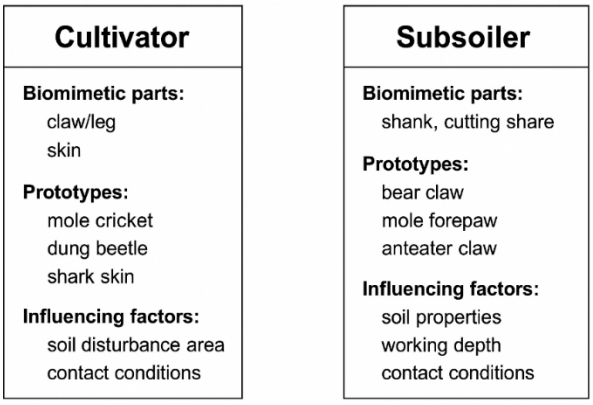

Fig. 4 - Comparative schematic highlighting the biomimetic approaches applied to cultivators and subsoilers

RESULTS

In Esehaghneygi et. al, 2020 study, the draught force was significantly impacted by the working depth. Increasing the working depth from 100 to 200 mm resulted in a 54% increase in the draught force. When the working depth was raised from 300 to 400 mm, the draught force showed the same trend (Guillen-Sanchez et al. 2017). Higher soil surcharge pressure and increased soil-metal friction are the causes of the increase in draught force. Based on the coefficient of determination and the F-values, it seems that the vibration frequency had a greater impact on the draught force than the working depth. The only factor that significantly affected the draught force was the combination of vibration frequency and working depth.

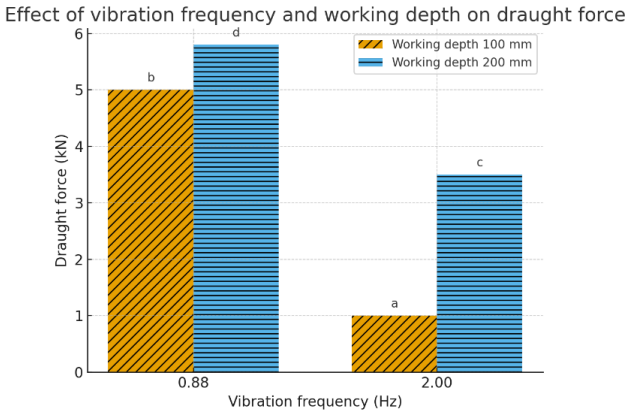

Fig. 5 - Effect of vibration frequency and working depth on the draught force of the vibrating dual bent-share cultivator

(Esehaghneygi et. al, 2020)

According to the study's findings, a twin bentshare cultivator's specific draught and clod MWD are considerably reduced when a vibration at a frequency of 2 Hz is applied. A 1.9 reduction in the draught force and a 13% rise in the soil-disturbed area were the causes of the drop in the specific draught. Because the vibrating cultivator transferred energy to the soil more efficiently, the clod size was less during the soil disturbance process.

The results of Gao et al. 20 study showed that vibration accelerations of the rotary tiller, three-point suspension, and tractor components generally increased with higher forward speeds (2.1, 3.6, and 4.5 km/h), although not uniformly across all frequency bands. The three-point suspension mechanism exhibited the highest vertical acceleration changes (standard deviation 5.914 m/s²), indicating its role as a key transmission path of vibration between the tiller and tractor. Asymmetry in left–right vibration responses suggested possible structural or assembly issues in the tractor. Frequency domain analysis revealed that the rotary tiller resonated around 350 Hz, which could be exploited to reduce soil resistance, whereas the tractor cab resonance at ~280 Hz should be avoided to protect operator comfort and machine durability. At low frequencies (0–80 Hz), cab vibrations remained relatively small, which may be beneficial for driver health. Overall, the study highlighted the dual effect of vibration: moderate excitation can aid tillage efficiency, but excessive transfer to the tractor impairs stability, comfort, and long-term reliability.

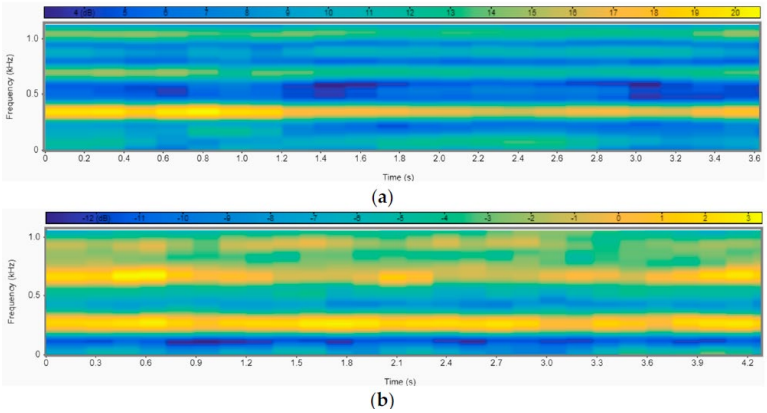

Fig. 6 - Local time−frequency analysis of working condition 1: (a) Gearbox and (b) Cab

In their study, Wang et al. (2024) presented as a result the successful application of shark skin riblet structures to the cutting share of a subsoiler shank, as shown in Figure 7. By mimicking the micro-riblet geometry of the shortfin mako shark (*Isurus oxyrinchus*), characterized by its spacing, height, and angle, the authors demonstrated an effective reduction in soil adhesion and draught force. This biomimetic modification improved soil–tool contact conditions and contributed to enhanced penetration efficiency and lower energy consumption during deep tillage operations.

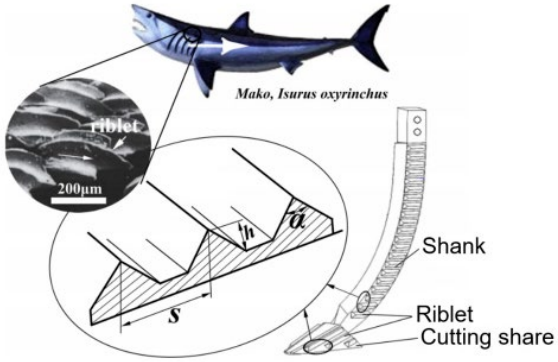

Fig. 7 - Example of a biomimetic design inspired by the skin surface of the shortfin mako shark
(Wang et al., 2024)

The authors also illustrated in Figure 8 how natural structures such as the anteater's claw (8a), the mole's forepaw (8b), the mole cricket's leg (8c) , and the pangolin's claw (8d) can be used as design inspirations for improving soil penetration efficiency.

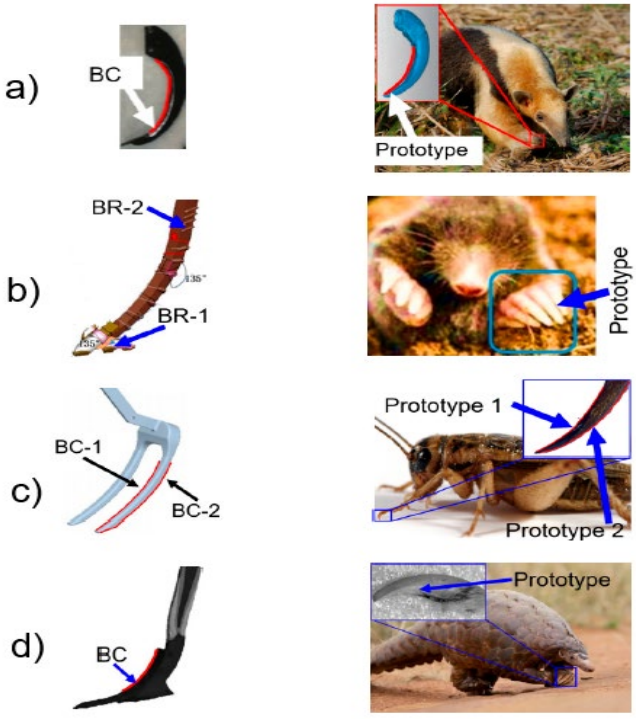

Fig. 8 - Biomimetic parts (BMPs) and their bionic prototypes for subsoiling tools (SSTs)
(Wang et al. 2024)

By translating these biological features into engineered components—such as modified bending radii, claw-like cutting edges, and optimized curvature of the share—subsoiler tools were able to better disrupt compacted soil layers while reducing draught force. These results confirmed that selecting appropriate prototypes from digging and burrowing animals provides a practical pathway for enhancing the performance of deep tillage equipment.

The authors analyzed the factors limiting tool improvement, explained the internal mechanisms by which biomimetic strategies reduce resistance, and summarized performance evaluations across existing

studies. Their conclusions confirmed that biomimetic design provides a promising approach for enhancing the efficiency of ASETs and offers a useful reference for future tool optimization and development.

In their experimental work, Sun et al. (2018**)** applied biomimetic tooth profile (BTP) and biomimetic polygonal convex curve (BPCC) elements to the design of subsoilers.

The authors developed six different configuration modes: a shank with BTP in the normal direction of the shank curve (S-T-N), a shank with BPCC in the normal direction of the shank curve (S-C-N), a shank with BTP in the horizontal direction of motion (S-T-H), a shank with BPCC in the horizontal direction of motion (S-C-H), a tine with BTP parallel to its centerline (T-T), and a tine with BPCC parallel to its centerline (T-C).

These variants provided a comparative basis for assessing how biomimetic modifications influence soil disturbance, draught force, and overall tool performance under subsoiling conditions.

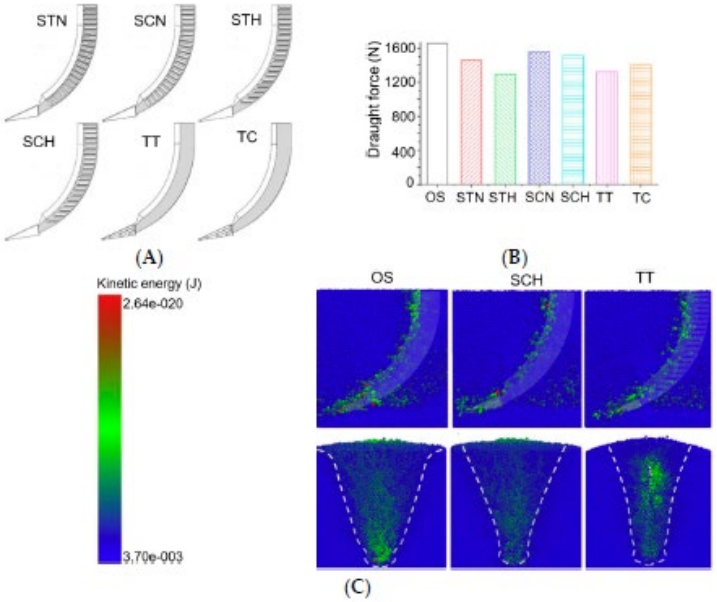

Fig. 9 - Biomimetic subsoiling tool optimization using experimental method: (A) six biomimetic subsoiling tools with various biomimetic riblets, (B) draught forces from various subsoiling tools, and (C) soil disturbance profiles from various subsoiling tools (STN, SCN, STH, SCH, TT, and TC represent six different biomimetic subsoiling tools; OS represents ordinary subsoiling tool)

CONCLUSIONS

Experimental results have shown that applying vibration to cultivators can effectively reduce draught force, decrease clod size, and enlarge the disturbed soil area, demonstrating the advantages of oscillatory tillage. Research on tractor–rotary tiller systems highlights the strong vibration interactions between components, where controlled excitation improves efficiency, while excessive resonance threatens operator comfort and machine durability.

Biomimetic approaches, including riblet-inspired surfaces and claw-like geometries, have proven effective in lowering soil resistance and enhancing penetration efficiency. Further experimental work with biomimetic tooth profiles and convex curves confirmed improvements in subsoiler performance by reducing draught and increasing soil disruption.

Overall, these findings indicate that vibratory mechanisms, bio-inspired designs, and smart technologies represent complementary strategies for reducing energy consumption and supporting sustainable soil management.

ACKNOWLEDGEMENT

This work has been funded from the project CNFIS-FDI-2025-F-0108 “Ensuring the sustainability of an application base for biotechnical systems in orchards, vineyards, gardens and solariums (SISBIOSUS)”, from the Ministry of Education and Research through the Executive Agency for Financing Higher Education, Research, Development and Innovation.

REFERENCES

[1] Alfred, R., Obit, J.H., Chin, C.P.Y., Haviluddin, H., Lim, Y. (2021). *Towards Paddy Rice*

[2] Chen, S.R.; Zhou, Y.P.; Tang, Z.; Lu, S.N., (2020) Modal vibration response of rice combine harvester frame under multi-source excitation.*Biosystems Engineering*, 194, 177–195.

[3] Esehaghbeygi, A., Abedi, M., Razavi, J., Hemmat, A., (2020), Field evaluation of a vibrating dual bent-share cultivator, *Research in Agricultural Engineering*, 66(4), 123–130

[4] Gao Y. , Yang Y., Fu S., Feng K. , Han X. , Hu Y., Zhu Q. and Wei X., (2024). Analysis of Vibration Characteristics of Tractor–Rotary Cultivator Combination Based on Time Domain and Frequency Domain). *Agriculture*, 14, 1139.

[5] Guillen-Sanchez J., Campos-Magana S.G., Sanchez-Lopez C., Gonzalez-Brambila O.M., Ramirez-Fuentes G. (2017), Experimental apparatus to determine the power applied in vibrating vertical tillage. *Agricultural Engineering International:CIGR Journal*, 19: 680–675.

[6] Gursoy, S.; Chen, Y.; Li, B. Measurement and modelling of soil displacement from sweeps with different cutting widths. *Biosyst.Eng*. 2017, 161, 1–13.

[7] JanbaziAlamdari, S., Brokesh, E., Ridder, E., Flippo, D., (2025), Soil compaction prediction in precision agriculture using cultivator shank vibration and soil moisture data, *Preprints.org*

[8] Jones, R. A. L. (2004). Soft machines: nanotechnology and life. *Oxford University Press.*

[9] Mason-Jones, K., Vrehen, P., Koper, K., Wang, J., van Der Putten, W. H., & Veen, G. C. (2020). Short-term temperature history affects mineralization of fresh litter and extant soil organic matter, irrespective of agricultural management. *Soil Biology and Biochemistry*, 150, 107985.

[10] Nawaz, M. F., Bourrie, G., & Trolard, F. (2013). Soil compaction impact and modelling. A review.

[11] *Agronomy for sustainable development*, 33, 291-309.

[12] Oldeman, R. A. (1992). Architectural models, fractals and agroforestry design. *Agriculture, ecosystems & environment*, 41(2), 179-188.

[13] Pu, X.; Li, G.J.; Huang, H.L. Preparation, anti-biofouling and drag-reduction properties of a biomimetic shark skin surface. *Biol.Open* 2016, 5, 389–396.

[14] Ren, L.Q. Progress in bionic research on drag reduction of ground mechanical desorption. *Chin. Sci. Tech. Sci*. 2008, 38, 1353–1364.

[15] Shahgoli, G.; Fielke, J.; Desbiolles, J.; Saunders, C. Optimising oscillation frequency in oscillatory tillage. *Soil Till. Res*. 2010, 106, 202–210.

[16] Sun, J., Wang, Y., Ma, Y., Tong, J., Zhang, Z., (2018), DEM simulation of bionic subsoilers (tillage depth >40 cm) with drag reduction and lower soil disturbance characteristics, *Advances in Engineering Software*,119, 30-37

[17] Van den Akker, J. J. (2004). SOCOMO: a soil compaction model to calculate soil stresses and the subsoil carrying capacity. *Soil and Tillage Research*, 79(1), 113-127.

REMEDIATION METHODS OF CONTAMINATED SOILS - REVIEW
/
METODE DE REMEDIERE A SOLURILOR CONTAMINATE - REVIEW

Mariana Gabriela MUNTEANU*[1)], Irina Aura ISTRATE[1)], Gheorghe VOICU[1)], Georgiana MOICEANU[2)], Elena Mădălina ȘTEFAN[1)], Mihai Sabin MAGUREAN[3)], Gabriel GHEORGHE[4)]

[1)] National University of Science and Technology Politehnica Bucharest, Faculty of Biotechnical Systems Engineering, Bucharest / Romania;

[2)] National University of Science and Technology Politehnica Bucharest, Faculty of Entrepreneurship, Engineering and Business Management, Bucharest / Romania;

[3)] Colentina Clinical Hospital, Bucharest / Romania;

[4)] National Institute of Research – Development for Machines and Installations Designed for Agriculture and Food Industry - INMA Bucharest / Romania.

*Tel: (+40) 767 236 522; *E-mail: mariana.munteanu@upb.ro*

Keywords: *pollution, heavy metals, remediation, soil*

ABSTRACT

Soil contamination is one of the major global environmental problems, with direct effects on ecosystem quality, agricultural productivity, and human health. The main sources of pollution includes industrial activities, intensive agricultural practices, inadequate waste management and urbanization processes. Pollutants associated with these activities, such as heavy metals, persistent organic compounds, or pesticide residues, can lead to the degradation of the physical, chemical and biological properties of the soil, reducing its functionality. In recent decades, numerous studies have been dedicated to the development and optimization of methods for remediating contaminated soils. They are broadly divided into physical, chemical, and biological methods, each category having specific applicability depending on the type and level of contamination. Conventional ex-situ technologies offer high efficiency but involve considerable costs and energy impact. In contrast, approaches based on biological processes, such as bioremediation and phytoremediation, are increasingly being studied due to their sustainability and compatibility with the principles of the circular economy. This paper aims to highlight the main methods for remediating contaminated soils, the mechanisms by which they work and their effectiveness in different types of contamination. A better understanding of these technologies is essential for promoting sustainable solutions capable of restoring the ecological and economic functions of soils.

REZUMAT

Contaminarea solurilor reprezintă una dintre problemele majore de mediu la nivel global, având efecte directe asupra calității ecosistemelor, productivității agricole și sănătății umane. Sursele principale de poluare includ activități industriale, practici agricole intensive, gestionarea inadecvată a deșeurilor și procesele de urbanizare. Poluanții asociați acestor activități, precum metalele grele, compușii organici persistenți sau reziduurile de pesticide, pot conduce la degradarea proprietăților fizice, chimice și biologice ale solului, reducându-i funcționalitatea. În ultimele decenii, numeroase cercetări au fost dedicate dezvoltării și optimizării metodelor de remediere a solurilor contaminate. Acestea se împart, în linii mari, în metode fizice, chimice și biologice, fiecare categorie având aplicabilitate specifică în funcție de tipul și nivelul contaminării. Tehnologiile convenționale, de tip ex-situ, oferă o eficiență ridicată, însă presupun costuri și impact energetic considerabile. În contrast, abordările bazate pe procese biologice, cum sunt bioremedierea și fitoremedierea, sunt tot mai studiate datorită caracterului sustenabil și a compatibilității cu principiile economiei circulare. Această lucrare își propune să evidențieze principalele metode de remediere a solurilor contaminate, mecanismele prin care acestea acționează și eficiența lor în diferite tipuri de contaminare. O mai bună înțelegere a acestor tehnologii este esențială pentru promovarea unor soluții sustenabile, capabile să redea solurilor funcțiile lor ecologice și economice.

INTRODUCTION

Environmental pollution is one of the most pressing and intensely debated issues globally today. Industrial and urban expansion has led to a significant increase in the degradation of environmental components, manifested in particular by the accumulation of potentially toxic pollutants. Heavy metal

contamination is recognized as a major challenge, with serious implication s for human health and ecosystem balance. In the context of growing demand for a higher standard of living, there is increasing exposure of the population to the harmful effects of environmental pollutants (*Vasilachi, I.C. et al., 2021*). Soil contamination is one of the most persistent and difficult forms of pollution to remedy, caused by the accumulation of hazardous chemicals and imbalances in the natural structure of the soil.

The main sources of pollution include industrial emissions, intensive use of agrochemicals, but also leaching of pollutants from landfills or infiltration of contaminated water (*Santos, M. et al., 2025; Meena, P. M. et al., 2024*). At European level, heavy metals and petroleum hydrocarbons are the most common contaminants, together accounting for almost 60% of all reported cases of soil pollution (*Santos, M. et al., 2025*).

These contaminants include in particular heavy metals such as lead, chromium, arsenic, zinc, cadmium, copper, mercury and nickel, known for their high persistence in soil and low capacity for natural degradation. Their long-term presence has serious implications, affecting human health, ecosystem balance, and food safety. Exposure can occur directly, through contact with contaminated soil, indirectly through the consumption of contaminated food, or through the infiltration of pollutants into groundwater used for consumption or irrigation (*Meena, P. M. et al., 2024*). Industrial activities, such as mining and processing, have consistently been major sources of soil pollution (*Moghimi Dehkordi, M. et al., 2024; Food and Agriculture Organization of the United Nations*).

Fig. 1- Different types of soil pollution

Industrial regions generally have significantly higher concentrations of trace elements and organic pollutants as a result of direct or accidental emissions generated during technological processes. These emissions frequently end up in the soil, nearby surface waters, or the atmosphere, contributing to long-term environmental contamination. Soil also continues to be affected by abandoned industrial sites, persistent historical pollution, and environmentally unmanaged waste disposal sites.

These residual sources remain active factors in contamination (*Food and Agriculture Organization of the United Nations*). The authors of the paper (*Crăciun, A.I. et al., 2024*) highlighted that industrial activities carried out in the past at the former chemical plant in Turda caused soil and water contamination with pesticides and heavy metals, generating persistent risks to the environment and human health. The situation requires continuous monitoring and the implementation of effective remediation strategies to limit the impact

on ecosystems and protect the exposed population. Copșa Mică is another example of extreme industrial pollution, where uncontrolled activities in the metallurgical industry have led to severe contamination of the air, water, and soil with heavy metals and toxic gases, profoundly affecting the health of ecosystems and the local population (*Rotaru A., 2010*). On an urban scale, heavy metal contamination is not limited to industrial areas, but also affects green spaces such as public parks.

The study (*Ene, A. et al., 2024*) shows that factors such as intense traffic, the age of parks, the long-term use of pesticides, as well as urbanization and rehabilitation processes contribute to the progressive accumulation of pollutants in the soil. Thus, soil contamination becomes a systemic problem with a cumulative impact on public health and the quality of the urban environment. The paper (*Onakpa, M. M. et al., 2018*) highlights that high levels of lead concentration in soil can reduce its fertility, while very low levels can negatively affect essential plant processes such as photosynthesis, cell division (mitosis), and water absorption. These imbalances can cause toxicity symptoms, such as darkening of leaves, wilting of mature leaves, reduced foliage development, and the appearance of short, brown roots.

Human activities can cause soil pollution both directly and indirectly. For example, inefficient drainage and increased runoff can contaminate nearby land and waterways. Uncontrolled waste disposal leads to its decomposition in the soil, releasing various chemicals and pollutants. These pollutants can seep into groundwater or be carried into the local water supply. Excessive waste storage also promotes the growth of bacteria in the soil, which, through decomposition processes, generate methane gas, a major contributor to global warming and air quality degradation. In addition, this process produces unpleasant odors and negatively affects quality of life (*Verma A., 2021*).

The use of pesticides, herbicides, and fertilizers in agricultural practices can contribute to the accumulation of toxic chemical compounds in the soil. These compounds often persist in the soil environment, affecting soil quality and reducing its ability to support optimal plant growth (*Crăciun, A.I. et al., 2024*; *Tăbăraşu, A. et al., 2021*).

In addition, the accumulation of toxic substances in plants can have adverse effects on human and animal health. Excessive application of chemical fertilizers contributes to soil acidification and the formation of soil crust, which leads to a decrease in organic matter content and beneficial microorganism activity. These changes in soil pH favor the proliferation of pests and can amplify greenhouse gas emissions (*Das, H. et al., 2023*).

The main sources of hydrocarbon contamination, which include production processes, transport pipeline and refinery failures, as well as tank leaks or accidents, can seriously affect soil quality, disrupting the ecological balance. This contamination negatively affects the structure and functioning of soil ecosystems by destroying beneficial microorganisms and altering the physical and chemical properties of the soil, generating long-lasting effects on the environment (*Crăciun, A.I. et al., 2024*). In fine soils, hydrocarbon contamination can cause significant changes in textural and structural properties, affecting particle size distribution, particle shape, and porosity. These changes lead to a substantial reduction in the number of micropores and specific surface area, while the characteristics of macropores remain relatively constant. In coarse-grained soils, hydrocarbons can adhere to the surface of particles, forming hydrophobic films and clogging both macropores and micropores. Due to the predominance of physical interactions between particles in this type of soil, properties such as texture, porosity, capillary retention capacity (cerosity), and cohesion are significantly affected (*Gonçalves Sales da Silva, I. et al. 2020*). Globally, approximately 8.8 million metric tons of oil are spilled into the aquatic environment each year, with most (approximately 90%) coming from human activities, making petroleum hydrocarbons persistent and dangerous pollutants for the ecosystem (*Ambaye, T. G.et al., 2022*). Soil pollution with oil promotes the transfer of certain oil pollutants to food, causing the biological accumulation and amplification of these toxic substances. This affects not only the nutritional and organoleptic quality of vegetables, but also the integrity of the food chain, generating significant risks to human health and perpetuating a vicious cycle of environmental degradation (*Hu, M., 2020*; *Bouruc, D. et al., 2020*).

Given the major impact of pollution on soil quality, food safety, and public health, there is a growing need to implement effective remediation measures capable of reducing contaminant levels and restoring soil ecosystem functions. Soil remediation is the practice of cleaning contaminated land to reduce the concentration of pollutants to a safe level, prevent their spread, and make the land suitable for agriculture (*https://www.pollutionsolutions-online.com/news/bioremediation/197/breaking-news/what-methods-are-used-for-soil-remediation/58120*). Therefore, in order to reduce exposure risk, restore soil functionality, and ensure ecosystem services, it is essential to implement risk-based remediation strategies aimed at restoring and

recovering contaminated soils for various uses, including agriculture (*Ambaye, T. G. et al., 2022*). The choice of remediation method for a contaminated environment is tailored to each individual site. It takes into account variables such as the nature and composition of the pollutants, the physical, chemical, and biological characteristics of the affected environment, as well as the existing microbial community or the need to supplement it. The selection of the appropriate remediation technique also involves consideration of the mechanisms involved, regulatory requirements, and cost and time constraints (*Ossai, I.C. et al. 2020*).

MATERIALS AND METHODS

The materials for this paper are represented by the review articles, research manuscripts of scientific journals, conference proceedings, scientific books and other online publications and sources of information. All these collected articles were explored, consulted, studied, analyzed and the most important and relevant information was summarized about the impact of soil organic pollutants on the environment. All materials used are cited in the text and presented in the list of references.

RESULTS

Remediation of contaminated areas involves the application of specialized techniques designed to remove or isolate hazardous substances so that the land can be safely reused, in accordance with accepted risk limits for human health and environmental protection. An optimal remediation process should either completely remove contaminants from the soil or reduce their levels below thresholds considered safe, while preventing the spread of pollutants to other adjacent areas (*Bastão de Souza, R. et al., 2013*). In this context, the chapter aims to analyze the techniques used to eliminate or degrade pollutants.

Physical-chemical methods - Physical-chemical treatments play a crucial role in remediating contaminated soils, especially in the case of persistent pollutants such as heavy metals, petroleum hydrocarbons, and pesticides. These methods include a variety of physical, chemical, electrochemical, thermal, and acoustic processes designed to remove, immobilize, or degrade contaminants. The choice of the appropriate method depends on factors such as the nature and concentration of the pollutants, soil properties, site conditions, and specific remediation objectives. In many cases, combining several types of treatments can significantly increase the effectiveness of the intervention (*Coreia, A. A. S. et al., 2025*). Thermal treatment is an effective and frequently used method for remediating oil-contaminated soil, as, depending on operating conditions, a temperature of approximately 600 °C can reduce a concentration of 5,000 ppm below regulatory limits, while for more severe contamination, up to 10,000 ppm, temperatures of up to 900 °C are required to meet the required standards. (*Weng, M.C. et al., 2020*). The use of thermally treated soils in the manufacture of building materials, such as bricks, is an effective solution for both reducing soil contamination and promoting sustainability and efficient use of resources. Although scaling up this method to an industrial level poses challenges related to energy consumption and emissions control, the economic benefits and high potential for soil reuse make it a viable alternative for environmental remediation (*Heidari, S. A., et al., 2025*).

Chemical methods aim to modify the behavior of pollutants by adding substances (amendments or inhibitors) that reduce their solubility in water, limit their diffusion, and decrease their bioavailability in the environment *(Liu, X. et al., 2023).* Soil washing is a remediation method that involves injecting aqueous solutions into contaminated soil in order to dissolve and mobilize pollutants, which are then extracted by pumping. The solutions used are enriched with special additives, such as acids, bases, chelating agents, surfactants, or organic solvents, which facilitate the desorption and transport of contaminants from the soil (*Coreia, A. A. S. et al., 2025*). Based on the data obtained in the study (*Effendi, A.J. et al. 2020*), potassium iodide (KI) proved to be an effective solution for washing mercury-contaminated soil, achieving a removal efficiency of over 88% under optimal conditions (pH = 2, KI concentration = 0.25 M, solid/liquid ratio = 1:15). Following a comparative study on the efficiency of different chelating agents in removing heavy metals from contaminated soil (Table 1), it was found that EDTA (ethylenediaminetetraacetic acid) is the most effective agent, demonstrating a superior solubilization capacity for removing heavy metals, especially lead (*Karthika, N. et al., 2016*).

Another study (*Moutsatsou, A. et al. 2006*) shows that the effectiveness of methods for washing heavy metal-contaminated soils depends significantly on the nature of the metals and the type of extraction agent used, and among the reagents tested, 1 M HCl proved to be the most effective for removing Pb, Zn, Cu, and Mn, but the additional costs generated by the treatment of the resulting acid solutions are a major limitation of this method.

The processes of washing soils contaminated with heavy metals have been extensively studied by the authors of the paper (*Choi, J. et al. 2021*), including through the combined application of conventional mechanical mixing and ultrasound under various operating conditions. The parameters investigated included: HCl solution concentration (0.1; 0.5 and 1.0 M), EDTA concentration (0.01; 0.05, and 0.10 M), liquid:soil ratio (3:1, 5:1, and 10:1), and soil particle size (~4.75 mm; 2.00–4.75 mm; 0.30–2.00 mm, and <0.30 mm).

The results in Figures 2 indicated that the integration of ultrasound with mechanical mixing causes a significant increase in the efficiency of the metal removal process. Furthermore, the use of ultrasound proved to be particularly advantageous under less aggressive washing conditions, characterized by lower concentrations of HCl or EDTA, lower liquid:soil ratios, and smaller soil particles.

Table 1

Comparative Evaluation of Different Agents for Heavy Metal Removal from Contaminated Soils

(Karthika, N. et al., 2016)

Types of metal	Chelating agents	Contamination type	Removal efficiency (%)
Cd Pb Ni Zn Cu	EDTA	Both Artificial and Natural	97-100% 45-100% 24% 54-100% 47-98%
Cd Pb N	HCL	Both Artificial and Natural	98% 94% 55%
Cd Pb Ni	Acetic acid	Artificial	5.2-31.1% 42.2-100% Not exceeds 1%
Cu Ni Zn	Texapon N-40		83.2% 82.8% 86.6%
Cd Zn Cu	Tween 80		85.9% 85.4 % 81.5%
Ni Zn As	Polafix CAPB		79% 83.2% 49.7%
Pb	Citric acid	Artificial	50%

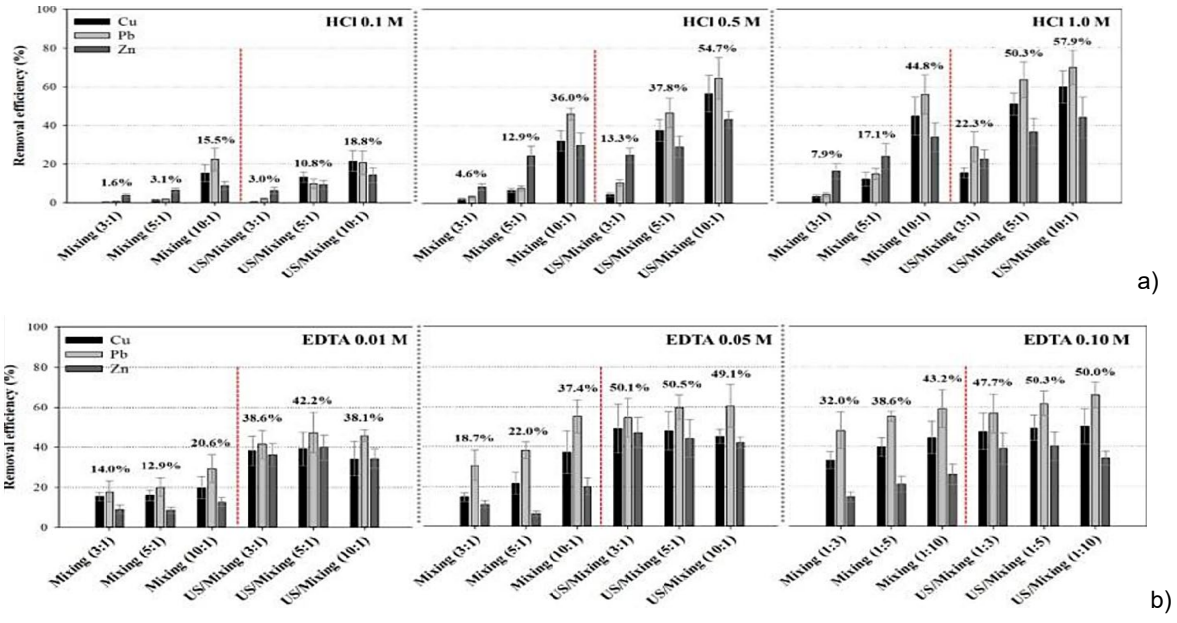

Fig. 2 - Removal efficiency of Cu, Pb, and Zn by mechanical and hybrid (US/Mixing) washing with a) HCl and b) EDTA

(Choi, J. et al. 2021)

Biological methods (Bioremediation) - Bioremediation techniques rely on natural biological processes, such as plants, algae, and microorganisms, capable of effectively degrading a wide range of pollutant compounds, including persistent organic contaminants. By stimulating the growth of microorganisms that use pollutants such as oil, solvents, or pesticides as a source of food and energy, these methods offer a sustainable and effective alternative for remediating contaminated soils. The optimal selection of bioremediation technology, whether in-situ or ex-situ, requires a complex preliminary characterization of the site, including analysis of the type and concentration of contaminants, the physical and chemical properties of the soil, hydrogeological conditions, as well as economic and time-related factors relevant to the implementation of the treatment. (*Gonçalves Sales da Silva, I. et al. 2020*).

Ex-situ bioremediation involves removing contaminated soil for treatment at another location, but it is a complex, risky, and less commonly used method due to logistical difficulties and the risk of spreading contaminants during transport (*Verma A., 2021*).

In situ bioremediation is a biological process carried out directly at the site of contamination and is the preferred method due to the reduction in mechanical operations and the risk of spreading pollutants. The process involves the degradation of organic pollutants by microorganisms, transforming them into inorganic end products such as CO_2, CH_4, H_2O and inorganic salts, under natural or controlled conditions. (*Verma A., 2021*).

In recent years, the use of bacteria capable of degrading hydrocarbons has become a frequently used, effective, and cost-effective method for remediating soil contaminated with petroleum products. Research has shown that various microbial species, such as *Pseudomonas spp.*, *Bacillus spp.*, *Micrococcus spp.*, *Rhodococcus spp.*, *Enterobacter spp.*, *Mycobacterium spp.*, *Modococci spp.* și *Acinetobacter spp.*, have the ability to degrade petroleum compounds. (*Ghoreishi, G. et al., 2017*). Conform (*Qattan S. Y. A., 2025*) *Cupriavidus metallidurans* stands out for its resistance to cadmium and mercury, being able to efficiently break down benzene, which makes it a promising microorganism for the bioremediation of oil sites contaminated with heavy metals. Similarly *Bacillus* strains that produce exopolysaccharides have been shown to be highly effective in adsorbing cadmium and lead from contaminated soils, contributing both to reducing the bioavailability of heavy metals and stimulating plant growth.

The authors of the research (*Nwaehiri, U.L. et al., 2020*) sed two types of treatment containing groups of bacteria to remediate the soil and effluent water from a paper mill. The first type of treatment consisted of *Serratia marcescens, Pseudomonas pyogenes, Erwnia amylovora, Enterobacter cloacae* for the remediation of polluted soi land *Escherichia coli, Acinetobacter baumannii, Erwnia amylovora, Citrobacter freundii for effluent samples, while the second treatment consisted of Bacillus subtilis and Staphylococcus aureus for the contaminated soil samples and Streptococcus pneumoniae for effluent samples.*

The study demonstrated that certain bacteria have the ability to survive in contaminated environments and transform heavy metals into less toxic forms. Although the soil and effluent were not pretreated, the bacteria isolated from the paper mill environment showed a remarkable ability to adsorb toxic heavy metals in a time-dependent manner. Metals such as lead, arsenic, chromium, zinc, and nickel were successfully remediated from the analyzed samples, with treatment 1 showing superior efficiency compared to treatment 2.

Plants used in phytoremediation have the ability to accumulate significant amounts of heavy metals in their root systems, exhibiting tolerance to a wide range of metals and possessing physiological adaptations that allow them to thrive in diverse environmental conditions. Phytoremediation involves several essential mechanisms, including phytoextraction, phytostabilization, phytodegradation, phytovolatilization, and rhizofiltration. These processes are based on the natural metabolic functions of plants, including root absorption, microbial interactions in the rhizosphere, and enzymatic degradation of contaminants (*Ahmad H., 2024*).

The study (*Antoniadis, V. et al. 2021*) concluded that, of the eight plants used in soil remediation research, *Artemisia vulgaris* stood out as the species with the highest heavy metal absorption capacity among the 12 elements analyzed. It was particularly effective in accumulating zinc and cadmium and, to a lesser extent, copper and nickel (Figure 3).

Another study showed that Betula papyrifera can accumulate approximately twice as much copper as most of the other trees analyzed, but only translocates 20% of this element to the foliage, compared to 60% in the case of the other species studied (*https://www.botanyeveryday.com/online-classes/2012-plant-talk-15-plants-for-phytoremediation*).

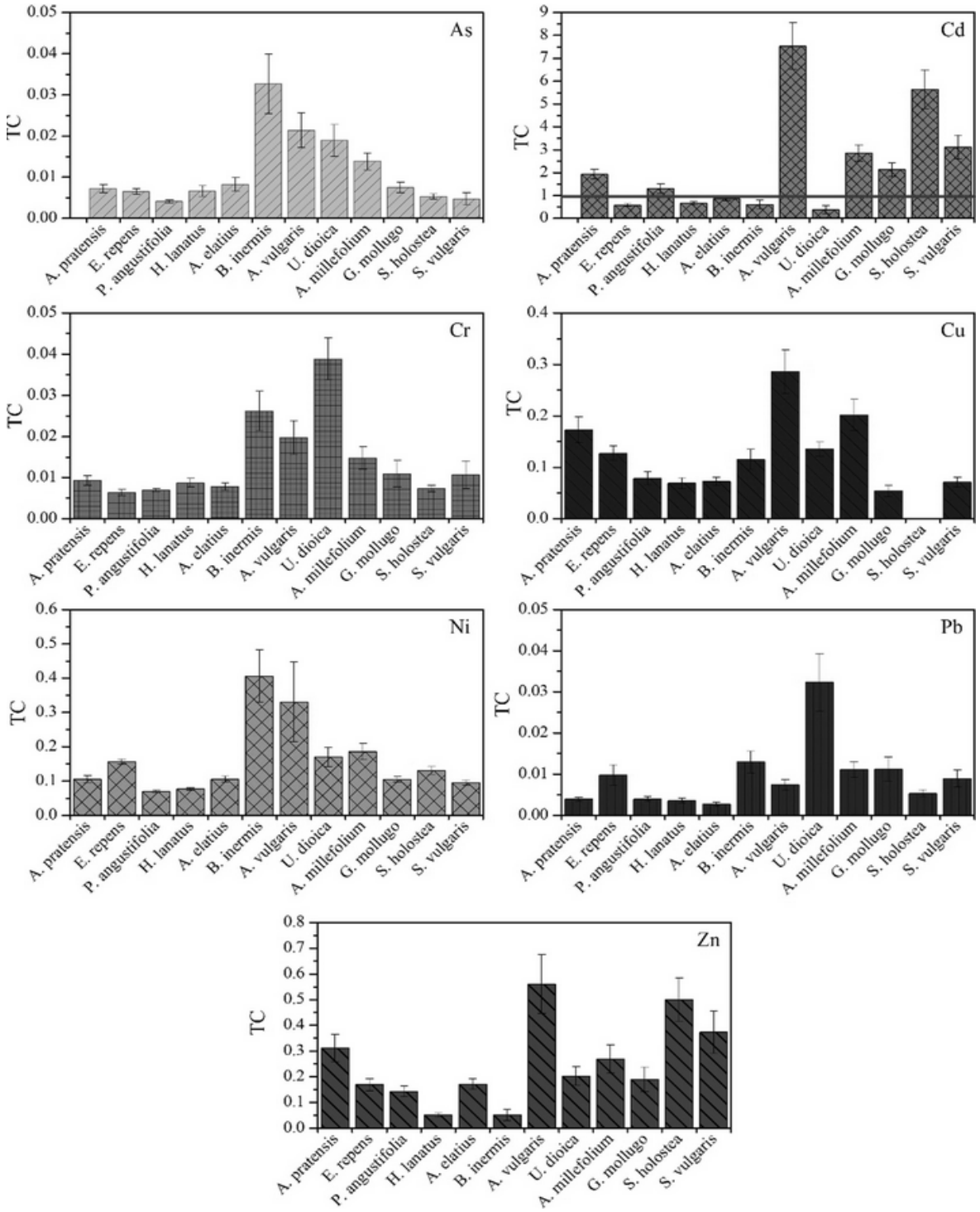

Fig. 3 - The transfer coefficient of potentially toxic elements (As, Cd, Cr, Cu, Ni, Pb and Zn) to the 12 plants
(Antoniadis, V. et al. 2021)

The authors of the study (*Lu., N. et al., 2021*) evaluated the effectiveness of four medicinal plant species, such as *Artemisia capillaris, Taraxacum mongolicum*. *Medicago sativa*, *Plantago asiatica L.* in remediating lead-contaminated soils. The results showed that all four plants contributed to reducing the concentration of lead in the soil, and their effectiveness varied depending on the level of contamination.

Thus, under conditions of slight pollution, the order of effectiveness in removing lead was *Artemisia capillaris*, *Plantago asiatica*, *Medicago sativa* and *Taraxacum mongolicum*. At a level of mild to moderate pollution, the order changed to *Taraxacum mongolicum*, *Medicago sativa*, *Plantago asiatica* and *Artemisia capillaris*. The specific rates of lead removal from the soil were 26.25% for *Artemisia capillaris*, 19.72% for *Plantago asiatica*, 17.71% for *Medicago sativa*, and 13.01% for *Taraxacum mongolicum*.

CONCLUSIONS

Soil pollution remains one of the most complex and persistent environmental problems, with direct implications for ecosystems and human health. A comparative analysis of remediation methods highlights that there is no single, universally applicable solution, but rather a set of technologies that can be adapted to the nature and level of contamination.

Physical-chemical methods, although effective in rapidly reducing pollutants, are often limited by high costs and secondary environmental impacts. In contrast, biological techniques, such as bioremediation and phytoremediation, offer sustainable alternatives with long-term benefits, but require longer application periods and careful monitoring.

The results analysed highlight the importance of combining traditional methods with modern approaches to maximise efficiency and minimise adverse effects. The choice of remediation strategy should be based on a comprehensive site assessment, including soil characteristics, pollutant speciation, economic factors and regulatory requirements.

The development of integrated, low-cost technologies with minimal environmental impact is the main direction for restoring the functionality of contaminated soils and ensuring food security and public health.

ACKNOWLEDGEMENT

This research was supported by the project, Establishment and operationalization of a Competence Center for Soil Health and Food Safety-CeSoH, Contract no.: 760005/2022, specific project no. 1, with the title, Soil health and food safety by introducing a soil remediation protocol and developing mobile remediation equipment to reduce the concentration of organic/inorganic pollutants, Code 2, financed through PNRR-III-C9- 2022–I5 (PNRR-National Recovery and Resilience Plan, C9 Support for the private sector, research, development, and innovation, I5 Establishment and operationalization of Competence Centers).

REFERENCES

[1] Ahmad H. (2024). Phytoremediation: The Green Solution. Bioremediation for Environmental Sustainability, ISBN978-1-83634-289-2, DOI: 10.5772/intechopen.1007671

[2] Ambaye, T. G., Chebbi, A., Formicola, F., Prasad, S., Gomez, F. H., Franzetti, A., Vaccari, M. (2022). Remediation of soil polluted with petroleum hydrocarbons and its reuse for agriculture: Recent progress, challenges, and perspectives. Chemosphere, 293, 133572, https://doi.org/10.1016/j.chemosphere.2022.133572

[3] Antoniadis, V., Shaheen, S. M., Stärk, H.-J., Wennrich, R., Levizou, E., Merbach, I., Rinklebe, J. (2021). Phytoremediation potential of twelve wild plant species for toxic elements in a contaminated soil. Environment International, 146, https://doi.org/10.1016/j.envint.2020.106233

[4] Bastão de Souza, R., Maziviero T. G., Christofoletti, C. A., Pinheiro, T.G., Fontanetti C.S.(2013). Soil Contamination with Heavy Metals and Petroleum Derivates: Impact on Edaphic Fauna and Remediation Strategies. Soil Processes and Current Trends in Quality Assessment. ISBN978-953-51-1029-3, DOI: 10.5772/52868

[5] Choi, J., Lee, D. Son,. Y. (2021). Ultrasound-assisted soil washing processes for the remediation of heavy metals contaminated soils: The mechanism of the ultrasonic desorption. Ultrason Sonochem, 74, 105574, doi: 10.1016/j.ultsonch.2021.105574

[6] Coreia, A. A. S., Rasteiro M. G. (2025). A Review of Persistent Soil Contaminants: Assessment and Remediation Strategies. Environments, 12(7), 229, https://doi.org/10.3390/environments12070229

[7] Crăciun, A. I., Ozunu, A. (2024).Comprehensive analysis and review of soil contamination and the associated risks at the Poșta-Rât Industrial Site in Turda, Cluj, Romania. Journal of Engineering Sciences and Innovation, 9(4),p.383 - 392

[8] Das, H., Devi, N.S., Venu, N., Borah, A. (2021). Research and ReviewinAgriculture Sciences. Bright Sky Publications, Vol. 7, Chpater 3 - Chemical Fertilizer and its Effects on the Soil Environment, New Delhi

[9] Effendi, A.J., Lestari V., Irsyad, M. (2020). Optimizing soil washing remediation of mercury contaminated soil using various washing solutions and solid/liquid ratios. E3S Web of Conferences, 148, https://doi.org/10.1051/e3sconf/202014 04 2019 8050

[10] Ene, A., Sion, A, Stihi, C., Gheboianu, A. I., Basliu V., Ceoromila, A. M., Gosav, S. (2024). Metal Contamination and Human Health Risk Assessment of Soils from Parks of Industrialized Town (Galati, Romania). Appl. Sci. 2024, 14(22), 10379; https://doi.org/10.3390/app142210379

[11] Gabriel-Alin Iosob, Alexandru Bute, Mariana Calara, Andreea Antal Tremurici, Carmina Mihaela Benchea, Bouruc, D., Avasiloaiei, D.-I., Muscalu, S.-P. (2020). Heavy metals contamination of soil and vegetables in three regions from Romania: a review. Studii şi Cercetări, 29/1, 79-87, Universitatea"Vasile Alecsandri" din Bacău

[12] Ghoreishi, G., Alemzadeh, A., Mojarrad, M., Djavaheri M. (2017). Bioremediation capability and characterization of bacteria isolated from petroleum contaminated soils in Iran. Sustainable Environment Research, 27(4), pp.195-202, https://doi.org/10.1016/j.serj.2017.05.002

[13] Gonçalves Sales da Silva, I., Gomes de Almeida, F. C., Padilha da Rocha e Silva, N. M., Casazza, A. A., Converti, A., Sarubbo, L. A. (2020). Soil Bioremediation: Overview of Technologies and Trends. Energies, 13(18):4664, doi:10.3390/en13184664

[14] Heidari, S. A., Amiri, M., Harifi, A., Wu, W. (2025). Effect of thermal treatment on stabilization and solidification of heavy metal contaminated clayey soil. Scientific Reports, 15, 17197, https://doi.org/10.1038/s41598-025-01155-3

[15] Hu, M. (2020). Environmental Behavior of Petroleum in Soil and its Harmfulness Analysis. IOP Conf. Series: Earth and Environmental Science, 450, 012100, doi:10.1088/1755-1315/450/1/012100

[16] Karthika, N., Jananee K., Murugaiyan V. (2016). Remediation of contaminated soil using soil washing-a review. Int. Journal of Engineering Research and Applications, 6 (1), pp. 13-18

[17] Liu, X., Qi, W., Cui, S., Lv, L., Jiang, J., Jiang, J., Zhu, Z. (2023). A Comparison of Different Remediation Technologies of Contaminated Agricultural Soils. 9th International Conference on Energy Materials and Environment Engineering (ICEMEE 2023), 406, https://doi.org/10.1051/e3sconf/202340603018

[18] Lu., N., Li, G., Sun, Y., Wei, Y., He, L., Li, Y. (2021). Phytoremediation Potential of Four Native Plants in Soils Contaminated with Lead in a Mining Area. Land, 10(11), 1129, https://doi.org/10.3390/land10111129

[19] Meena, P. M., Aggarwal, R.K., Meena, R., Rathore, M. S. (2024). Soil Contamination, Risk Assessment, and Remediation. The Future of Risk Management, DOI: 10.5772/intechopen.1005045

[20] Moghimi Dehkordi, M., Pournuroz Nodeh, Z., Soleimani Dehkordi, K., Salmanvandi, H., Rasouli Khorjestan, R., Ghaffarzadeh, M. (2024). Soil, air, and water pollution from mining and industrial activities: Sources of pollution, environmental impacts, and prevention and control methods. Results in Engineering, 23, https://doi.org/10.1016/j.rineng.2024.102729

[21] Moutsatsou, A., Gregou M., Matsas, D., Protonotarios, V. (2006). Washing as a remediation technology applicable in soils heavily polluted by mining–metallurgical activities. Chemosphere, 63(10), pp. 1632-1640, https://doi.org/10.1016/j.chemosphere.2005.10.015

[22] Nwaehiri, U.L., Akwukwaegbu, P. I., Nwoke, B. E. B. (2020). Bacterial remediation of heavy metal polluted soil and effluent from paper mill industry. Environ Anal Health Toxicol, 35(2), doi: 10.5620/eaht.e2020009

[23] Onakpa, M. M., Anoka, A. N., Ogbureke C. K. (2018). A Review of Heavy Metal Contamination of Food Crops in Nigeria. Ann Glob Health, 84(3), pp. 488-494, doi: 10.29024/aogh.2314

[24] Ossai, I.C., Ahmed, A., Hassan, A., Hamid, F. S. (2020). Remediation of soil and water contaminated with petroleum hydrocarbon: A review. Environmental Technology & Innovation. 17, 100526, https://doi.org/10.1016/j.eti.2019.100526

[25] Qattan S. Y. A. (2025). Harnessing bacterial consortia for effective bioremediation: targeted removal of heavy metals, hydrocarbons, and persistent pollutants. Environmental Sciences Europe, 37, https://doi.org/10.1186/s12302-025-01103-y

[26] Rotaru, A. (2010). Most contaminated soils in Romania's urban areas. 2nd International Conference on Geotechnical Engineering, Innovative Geotechnical Engineering ICGE'10, Hammamet, Tunisia

[27] Santos, M., Rebola, S., Evtuguin, D. V. (2025). Soil Remediation: Current Approaches and Emerging Bio-Based Trends. Soil Systems, 9(2), Article 35. https://doi.org/10.3390/soilsystems9020035

[28] Tăbăraşu, A., Matsche, M., Grigore, I., Vlăduţoiu, L.C., Ungureanu, N., Biriş, S. S. (2021). Environmental pollution caused by agricultural activities. ACTA TECHNICA CORVINIENSIS – Bulletin of Engineering, Tome XIV, Fascicule 2

[29] Vasilachi, I. C., Gavrilescu, M. (2021). Methods for the remediation of soils polluted with heavy metals. Buletinul Institutului Politehnic din Iaşi, Seria Chimie şi Inginerie Chimică, 67(4), Universitatea Tehnică „Gheorghe Asachi" din Iași
[30] Verma A. (2021). Bioremediation Techniques for Soil Pollution: An Introduction. Biodegradation Technology of Organic and Inorganic Pollutants, DOI: 10.5772/intechopen.99028
[31] Weng, M.C., Lin, C.L., Lee, C.H. (2020). Effect of Heat-Treatment Remediation on the Mechanical Behavior of Oil-Contaminated Soil. Appl. Sci.,10(9), 3174, https://doi.org/10.3390/app10093174
[32] ***Food and Agriculture Organization of the United Nations, Chapter 3 - Sources of soil pollution https://openknowledge.fao.org/server/api/core/bitstreams/fe5df8d6-6b19-4def-bdc6-62886d824574/content/src/html/chapter-03-5.html accesed in july 2025
[33] What Methods Are Used for Soil Remediation? https://www.pollutionsolutions-online.com/news/bioremediation/197/breaking-news/what-methods-are-used-for-soil-remediation/58120
[34] *** https://www.botanyeveryday.com/online-classes/2012-plant-talk-15-plants-for-phytoremediation

STUDY OF JERK FOR A ROBOTIC ARM
/
STUDIUL DERIVATEI ACCELERAŢIEI PENTRU UN BRAȚ ROBOTIC

Florinel LUPU*[1], Andrei CRAIFALEANU*[2], Sorin NEGROIU*[3]
[1] National University of Science and Technology POLITEHNICA Bucharest, Faculty of Biotechnical Systems Engineering / Romania;
[2] National University of Science and Technology POLITEHNICA Bucharest, Faculty of Biotechnical Systems Engineering / Romania;
[3] National University of Science and Technology POLITEHNICA Bucharest, Faculty of Biotechnical Systems Engineering / Romania.
*[1] *Tel: 0758.727.272; E-mail: autokingdomlupu@gmail.com;*
*[2] *Tel: 021.402.92.50; E-mail: ycraif@yahoo.com;*
*[3] *Tel: 0729.076.640; E-mail: negroiu_sorin@gmail.com*

Keywords: *kinematic, 6-axis industrial robot, relative motion*

ABSTRACT
This paper studies the jerk (the derivative of angular acceleration), which is present in the motion of a 6-axis industrial robot used for the manipulation of heavy and elongated shafts. This parameter describes the smoothness of the robot's motion. Higher values of jerk are associated with increased wear of the joints, as well as with vibrations, which lead to reduced motion precision.

REZUMAT
Prezenta lucrare analizează jerk-ul (derivata acceleraţiei unghiulare) ce apare în mişcarea unui robot industrial cu 6 axe destinat manipulării arborilor grei şi alungiţi. Acest parametru caracterizează continuitatea mişcării robotului. Valori ridicate ale jerk-ului sunt corelate cu o uzură accelerată a articulaţiilor, precum şi cu apariţia vibraţiilor, care conduc la diminuarea preciziei de mişcare.

INTRODUCTION

The paper continues the studies presented by the authors in reference *(Lupu and Craifaleanu, 2024)* and focuses on the analysis of the jerk, defined as the time derivative of angular acceleration, in the context of a 6-axis industrial robot designed for the manipulation of heavy and elongated shafts. Jerk is a higher-order kinematic parameter that plays a critical role in describing the smoothness of motion executed by robotic manipulators *(Gasparetto and Zanotto, 2010).* While position, velocity, and acceleration are traditionally considered sufficient to characterize a robot's motion, jerk provides an additional and more refined measure of motion quality. Specifically, it captures the rate of change in acceleration, which directly influences the dynamic stresses experienced by the robot's mechanical structure and drive systems *(Angeles, 2007; Asada and Slotine, 1986; Doroftei and Grosu, 2003; Mihăilă, 2015).*

The importance of jerk minimization becomes evident when considering the practical implications of excessive values of this parameter. High jerk measures abrupt changes in acceleration that generate undesirable mechanical effects, including vibrations in the robot's joints and supporting structures. These vibrations not only compromise the precision of motion and positioning accuracy but also contribute to accelerated wear of components, such as bearings, gears, and actuators. Over time, this leads to reduced operational reliability and increased maintenance requirements. Moreover, in applications involving the manipulation of heavy and elongated shafts, the effects of jerk are amplified, since the payload introduces significant inertial forces. Sudden variations in acceleration can induce oscillations in the load, causing instability and further decreasing the accuracy of the task being performed *(Hogan, 1985).*

Therefore, controlling jerk is a practical necessity in industrial contexts where both productivity and equipment longevity are critical. By minimizing jerk, smoother robot motion, reduced mechanical stress, and higher levels of safety during operation are ensured.

MODEL OF ROBOTIC ARM

Figure 1 illustrates the 3D CAD model of a 6-axis industrial robot, equipped with a custom-designed gripper for handling long and heavy cylindrical shafts. The robot geometry was created using Dassault Systèmes CATIA software and includes six rotational joints. The links and joints are colored distinctly to

improve visualization of the kinematic structure. The end-effector, shown gripping a shaft, consists of two symmetrical jaws, designed to provide secure and balanced clamping along the length of the object.

The model is used for kinematic and dynamic simulations, as well as for trajectory optimization under payload constraints.

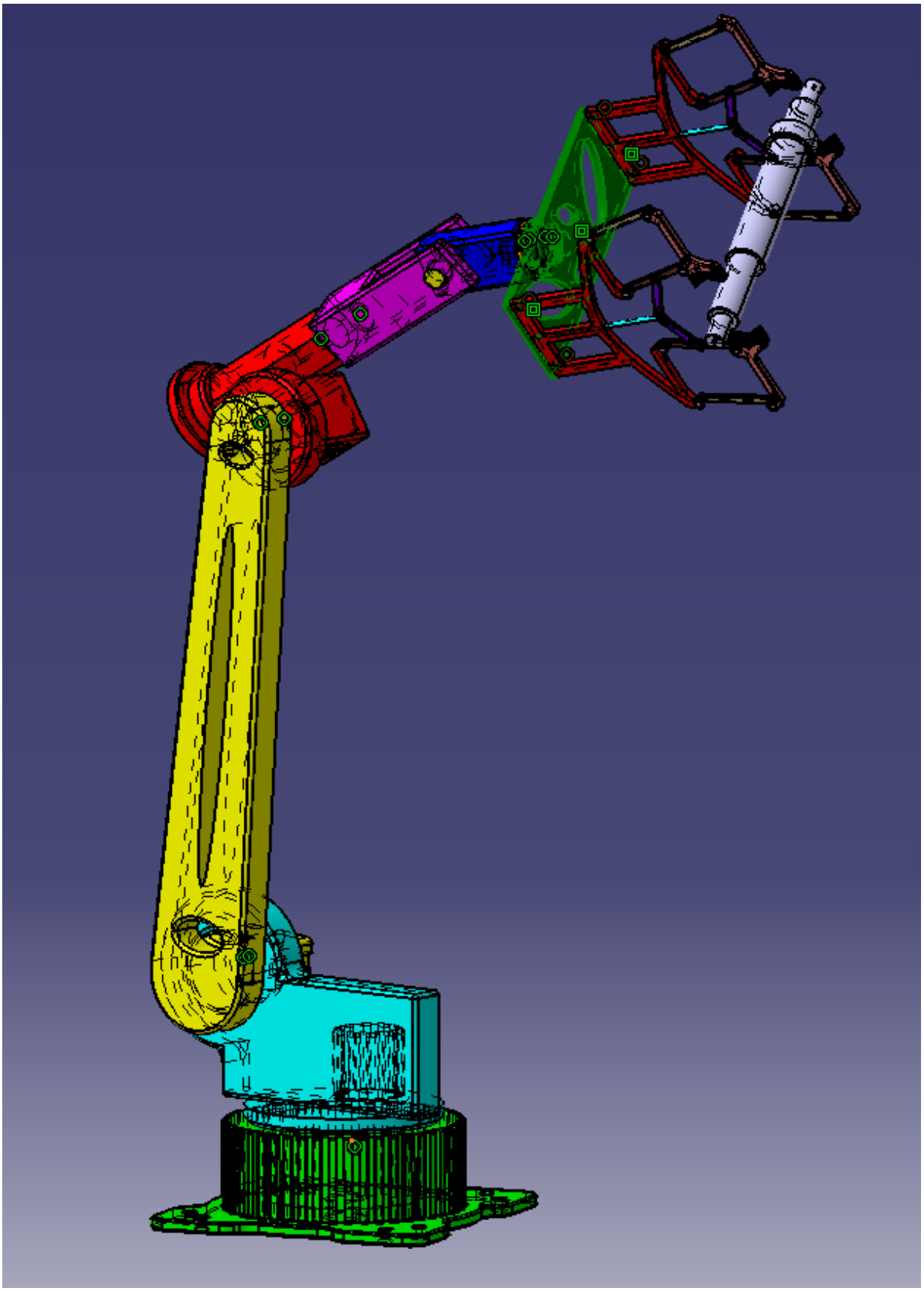

Fig. 1 - 3D model of a 6-axis industrial robot with gripper for long shafts (CAD assembly in CATIA)

Figure 2 presents the kinematic model of the industrial robot manipulator. Each joint and link is represented schematically, with rotational joints denoted by the connecting axes between origin points O_0 to O_7. The rotated coordinate systems $O_ix_iy_iz_i$ (i=1,2,…,7) are displayed in black, while the translated ones, $O_ix'_iy'_iz'_i$, are displayed in red.

The end-effector is not represented, in order to focus on the manipulator structure.

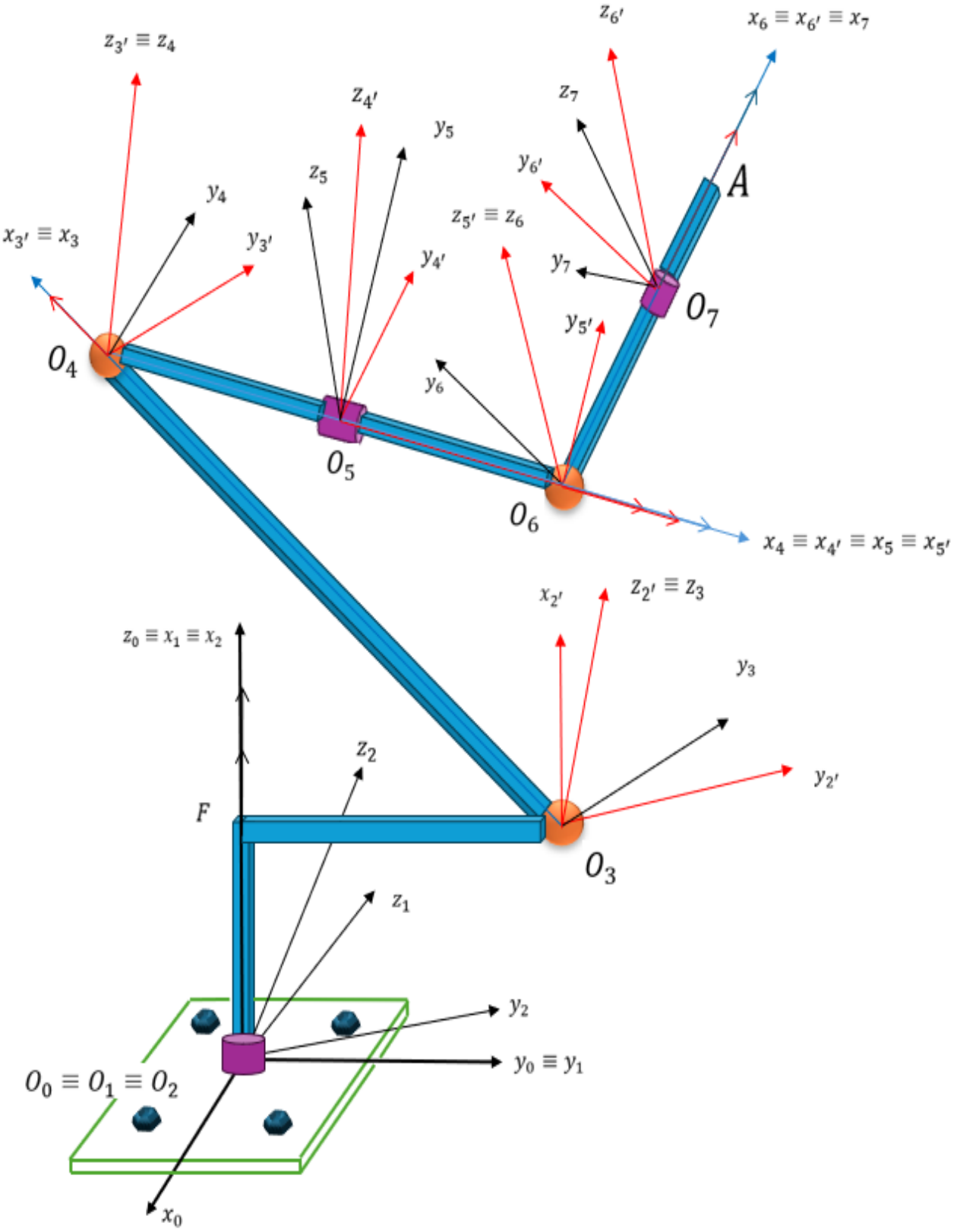

Fig. 2 - Kinematic diagram of a 6-axis industrial robot with reference frames

EQUATIONS OF MOTION

The motion of a robotic arm element is defined by the following law (Fig. 3),

$$q(t)=q_0+\frac{q_1-q_0}{2}\left(1-\cos\pi\frac{t-t_0}{t_1-t_0}\right), \tag{1}$$

where parameter *q* represents the rotation angle of the joint connecting the element to the preceding one.

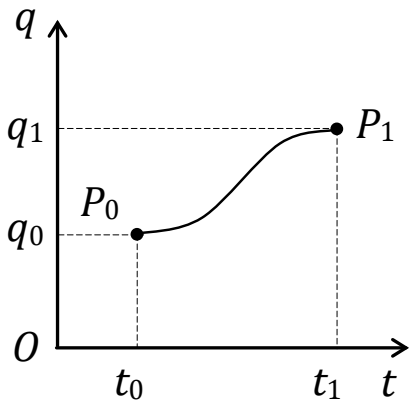

Fig. 3 - Motion law representation of the joint rotation angle

The angular velocity is

$$\dot{q}(t)=\frac{\pi}{2}\frac{q_1-q_0}{t_1-t_0}\sin\pi\frac{t-t_0}{t_1-t_0}, \tag{2}$$

The angular acceleration is

$$\ddot{q}(t)=\frac{\pi^2}{2}\frac{q_1-q_0}{(t_1-t_0)^2}\cos\pi\frac{t-t_0}{t_1-t_0}, \tag{3}$$

The jerk (the derivative of angular acceleration) is

$$\dddot{q}(t)=-\frac{\pi^3}{2}\frac{q_1-q_0}{(t_1-t_0)^3}\sin\pi\frac{t-t_0}{t_1-t_0}, \tag{4}$$

The global effect of the derivative of acceleration, over a time interval [t_0, t_1] is measured by the parameter *(Gasparetto and Zanotto, 2010)*.

$$J=\int_{t_0}^{t_1}\dddot{q}^2(t)\mathrm{d}t. \tag{5}$$

For the law of motion chosen in the present paper, this parameter takes the expression

$$J=\int_{t_0}^{t_1}\frac{\pi^6}{4}\frac{(q_1-q_0)^2}{(t_1-t_0)^6}\sin^2\pi\frac{t-t_0}{t_1-t_0}\mathrm{d}t=\frac{\pi^6}{8}\frac{(q_1-q_0)^2}{(t_1-t_0)^6}\int_0^{t_1}\left(1-\cos2\pi\frac{t-t_0}{t_1-t_0}\right)\mathrm{d}t= \tag{6}$$

$$=\frac{\pi^6}{8}\frac{(q_1-q_0)^2}{(t_1-t_0)^6}\left[t-\frac{t_1-t_0}{2\pi}\sin2\pi\frac{t-t_0}{t_1-t_0}\right]\Bigg|_{t_0}^{t_1}=\frac{\pi^6}{8}\frac{(q_1-q_0)^2}{(t_1-t_0)^5}=120.17\frac{(q_1-q_0)^2}{(t_1-t_0)^5}.$$

NUMERICAL STUDY

A numerical study was performed, considering the values

$$t_0 = 0,$$

$$t_1 = 2\text{s},$$

$$q_0 = 0.2\text{rad},$$

$$q_1 = 0.8\text{rad}.$$

The time variations of parameters (1)-(4) are ploted in Figure 4.

Parameter (6) takes the value

$$J = 1.352\text{rad}^2/\text{s}^3. \tag{7}$$

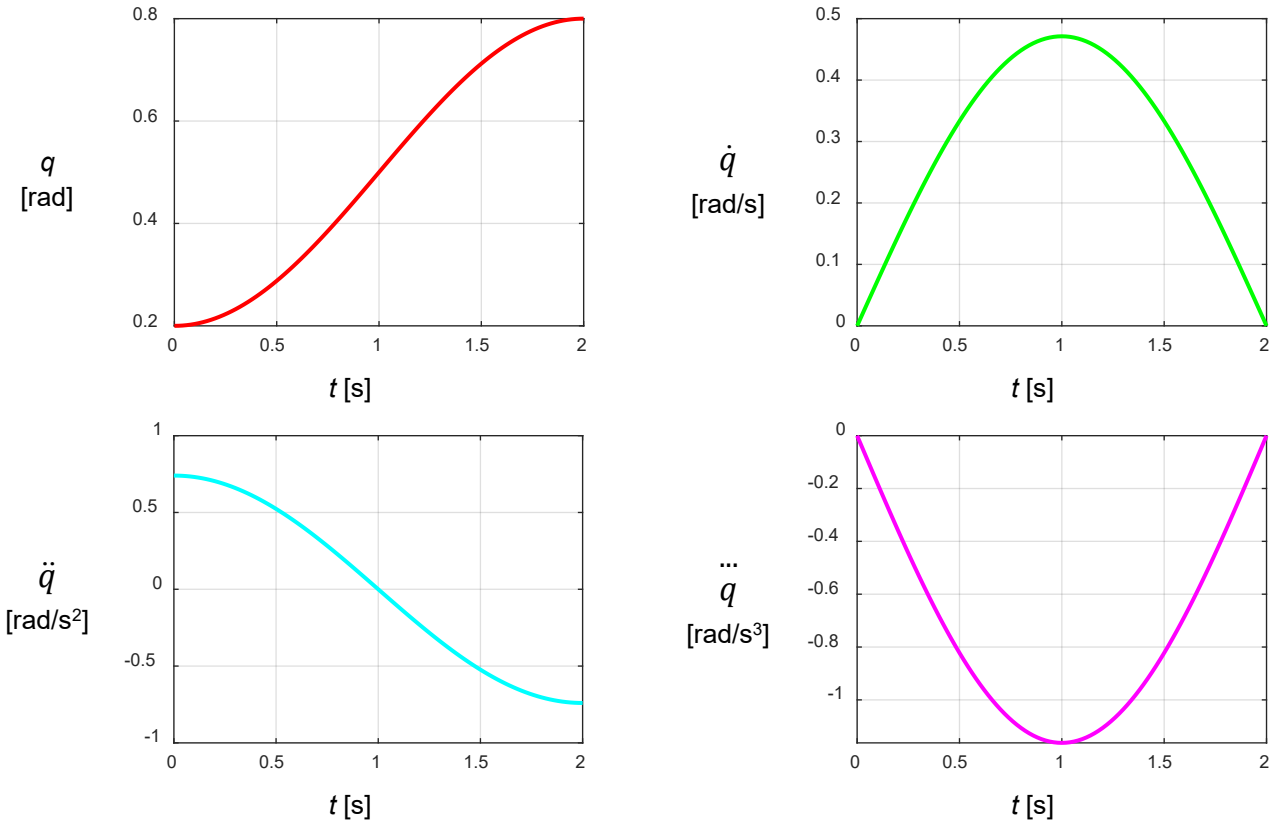

Fig. 4 - Time variation of the rotation angle and of its first three derivatives

CONCLUSIONS

In this paper the jerk (time derivative of angular acceleration) developed in a joint of a 6-axis industrial robot was determined.

A simple sinusoidal law of motion was considered for the rotation angle.

The angular velocity, angular acceleration and jerk were determined analytically.

A parameter J defined as the integral of the jerk squared, calculated on the time interval of the motion, was introduced as a measure of the global jerk effect.

The time variations of the kinematic parameters were plotted as a numerical application.

Future work should be done in order to determine other laws of motion, between the start value q_0 and the final value q_1 which lead to lower values of parameter J.

REFERENCES

[1] Angeles J., *Fundamentals of Robotic Mechanical Systems: Theory, Methods, and Algorithms*, Springer, New York, 2007.

[2] Asada H., Slotine J.J. E., *Robot Analysis and Control*, John Wiley & Sons, New York, 1986.

[3] Doroftei I.,Grosu C., *Modelling and Control of Industrial Robots*, Editura Politehnium, Iași, 2003.

[4] Gasparetto A., Zanotto V., *A technique for time-jerk optimal planning of robot trajectories*, Robotics and Computer-Integrated Manufacturing, 26(3), 2010, pp. 361–371.
[5] Hogan N., *Impedance control: An approach to manipulation,* ASME Journal of Dynamic Systems, Measurement, and Control, 107(1), 1985, pp. 1–24.
[6] Lupu F., Craifaleanu A., *Kinematic Study of a robotic component with relative motion*, ISB-INMA TEH' 2024, ISSN 2537 – 3773, Bucharest.
[7] Mihăilă S. N., *Trajectory Planning for 6-DOF Serial Robots*, Journal of Automation and Computer Science, 42(4), 2015, pp. 215–220.

THE IMPORTANCE OF PNEUMATIC DEDUSTING SYSTEMS IN CEREAL MILLS
/
IMPORTANȚA SISTEMELOR PNEUMATICE DE DESPRĂFUIRE ÎN MORILE DE CEREALE

Liliana-Caliopi ISCRU*[1)], Daniel-Mirel DUMITRESCU[2)], Gheorghe VOICU[1)]
[1)] National University of Science and Technology POLITEHNICA Bucharest / Romania;
[2)] Pietrosani Middle School, Teleorman County / Romania.
**Tel: (+40) 765 914 811; *E-mail: dumitresculilianacaliopi@gmail.com*

Keywords: *milling industry, grain dust, pneumatic dedusting systems, occupational health, explosion prevention, dust control, industrial safety, sustainable milling, dust emission reduction, process optimization.*

ABSTRACT

In milling units, technological processes such as transport, cleaning, grinding, and sifting of cereals generate significant amounts of organic dust, characterized by heterogeneous composition and variable granulometry. The accumulation of these dust particles poses a critical risk factor, impacting both facility safety and worker health, as well as the quality of the final product. In this context, the implementation of pneumatic dedusting systems represents a fundamental technological requirement, essential for the safe operation of milling facilities. From a theoretical perspective, the analysis of dust formation and dispersion phenomena serves as the foundation for designing and optimizing capture systems. A comprehensive examination of the implications of grain dust highlights the strategic importance of these installations, which are not merely auxiliary technical solutions but integral components with direct effects on occupational health, facility safety, economic efficiency, and environmental protection. By reducing respirable particle concentrations below the thresholds permitted by European and national legislation, pneumatic systems help mitigate medical risks associated with occupational exposure. Furthermore, by eliminating hazardous dust accumulations, these systems minimize the likelihood of deflagrations and explosions, which can have devastating effects on technological installations. From an economic standpoint, the recovery of raw material losses and the reduction of premature equipment wear enhance the overall efficiency of the milling process. The ecological role is equally significant, as these systems limit atmospheric emissions and contribute to sustainable development. Thus, theoretical and experimental research dedicated to improving pneumatic dedusting systems confirms efficiencies exceeding 95% and falls within a multidisciplinary framework, offering substantial applied value for the modernization and sustainability of the milling industry.

REZUMAT

În unitățile de morărit, procesele tehnologice de transport, curățire, măcinare și cernere a cerealelor generează cantități semnificative de praf organic, caracterizat printr-o compoziție eterogenă și o granulometrie variabilă. Acumularea acestor pulberi constituie un factor critic atât din punct de vedere al securității instalațiilor, cât și al sănătății lucrătorilor și al calității produsului finit. În acest context, implementarea unor sisteme pneumatice de desprăfuire reprezintă o cerință tehnologică fundamentală, indispensabilă funcționării în condiții sigure a unităților de morărit. Din perspectivă teoretică, analiza fenomenelor de formare și dispersie a prafului constituie fundamentul pentru dimensionarea și optimizarea sistemelor de captare. Analiza complexă a implicațiilor generate de praful de cereale subliniază caracterul strategic al acestor instalații, care nu reprezintă doar soluții tehnice auxiliare, ci elemente integrative, cu un impact direct asupra sănătății ocupaționale, securității instalațiilor, eficienței economice și protecției mediului. Prin reducerea concentrațiilor de particule respirabile sub pragurile admise de legislația europeană și națională, sistemele pneumatice contribuie la diminuarea riscurilor medicale asociate expunerii profesionale. De asemenea, prin eliminarea acumulărilor periculoase de praf, se minimizează probabilitatea producerii deflagrațiilor și exploziilor, cu efecte devastatoare asupra instalațiilor tehnologice. Din perspectivă economică, recuperarea pierderilor de materie primă și reducerea uzurii premature a utilajelor conduc la creșterea randamentului global al procesului de măcinare. Funcția ecologică este la fel de importantă, întrucât aceste sisteme limitează emisiile atmosferice și contribuie la dezvoltarea durabilă. Astfel, cercetările teoretice și experimentale dedicate perfecționării sistemelor pneumatice de desprăfuire confirmă eficiențe de peste 95% și se înscriu într-un cadru multidisciplinar, cu valoare aplicativă majoră pentru modernizarea și sustenabilitatea industriei de morărit.Praful rezultat în timpul procesării cerealelor este o problemă centrală pentru sănătatea ocupațională, siguranța instalațiilor și sustenabilitatea proceselor industriale. Format din

particule fine, combustibile, praful de cereale poate provoca atât afecțiuni respiratorii, cât și explozii devastatoare dacă nu este controlat eficient.

INTRODUCTION

From a worker health perspective, numerous studies have shown worrying effects. For example, in Nigeria, PM10 levels exceeded 1,000 µg/m³ and PM2.5 above 600 µg/m³, well above WHO limits. Respiratory function tests confirmed a significant decrease in lung capacity in millers (FEV1 = 1.61 L compared to 2.1 L in the control group), concluding that chronic exposure leads to serious respiratory diseases (*Iyogun et al., 2019*).

Fig. 1 - Fire and combustible dust hazard inside a flour processing plant
(https://www.freepik.es/fotos/planta-molino-polvo)

Another study, conducted in Turkey, identified 68 occupational hazards in flour mills, of which 38% were classified as “unacceptable”, the greatest hazards being dust exposure and explosion risk (*Özbakır, O., 2024*). Occupational health and safety in flour mills: A research and risk assessment. International Journal of Agriculture, Environment and Food Sciences). The risk of explosion is equally important. In the United States, around 10 grain dust explosions are recorded annually *(Schoeff, 2006).* The international standard NFPA 61 provides measures for preventing fires and explosions in agricultural and grain processing facilities, including the assessment of potentially explosive areas and the implementation of dust removal and suction systems.In addition, dust has a significant economic and ecological impact.

Raw material losses, accelerated wear of machinery and polluting emissions lead to increased production costs and the carbon footprint of the units. Studies based on Life Cycle Assessment have shown that optimizing technological parameters and reducing emissions through modern technologies can considerably reduce the environmental impact (*Tang et al., 2024; Zhao et al., 2023*).

Recent research in the field of multi-objective optimization suggests that advanced algorithms can simultaneously contribute to reducing carbon emissions, costs and processing times in the industry.In this context, pneumatic dust removal systems are no longer just a technological accessory, but a strategic investment. They help protect workers' health, reduce the likelihood of explosions, improve economic efficiency and support sustainability goals. Through cyclones, bag filters or HEPA systems, dust removal efficiency exceeds 95%, which turns them into the "technological lungs" of milling units, capable of ensuring a safe and clean working environment.Modern pneumatic dust removal technologies include cyclones, bag filters, and HEPA filters, each with specific roles. Cyclones are most commonly used in milling for coarse particle separation, having the advantage of low cost and mechanical strength, but their efficiency decreases for particles smaller than 10 µm. In addition, bag filters achieve efficiencies of over 95% in capturing fine respirable particles, making them essential for maintaining concentrations below explosive and occupational exposure limits (*NFPA, 2017*).For advanced control, especially in critical spaces, HEPA filters are used, capable of retaining over 99.97% of particles with a size of 0.3 µm. By combining these technologies, modern mills can ensure a safe environment for workers and operational continuity.

MATERIALS AND METHODS

Technological innovations

In recent years, research has introduced innovative solutions to complement traditional methods. CFD (Computational Fluid Dynamics) simulations allow modeling of dust flows and pressure distribution in equipment, providing a precise picture of vulnerable points and optimizing the design of installations *(Kurukulasuriya et al., 2020).* In parallel, smart sensors integrated into equipment can monitor dust concentration in real time, triggering alarms or automatic shutdowns when safe values are exceeded. In the field of process optimization, recent research has demonstrated the effectiveness of evolutionary algorithms. One example is the INSDBO (Improved Non-dominated Sorting Dung Beetle Optimization) algorithm, applied

to rectification processes. It reduced carbon emissions by 11.7%, costs by 7.7% and processing time by 6.7%, compared to traditional optimization methods *(Zhang et al., 2023).* Although the study focused on rectification, the methodology has potential for application in optimizing the parameters of dedusting plants, to increase energy efficiency and reduce operating costs.

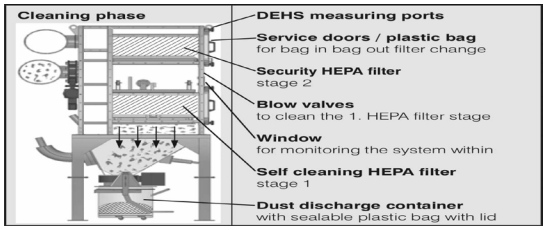

Fig. 2 - Schematic section of a two-stage HEPA filtration system, equipped with cleaning valves, exhaust container and monitoring window

Sustainability and circular economy: Dust recovered from pneumatic systems should not be seen as just a waste, but as a resource. Integrating dust removal into circular economy concepts allows the collected particles to be reused in other production streams, reducing losses and emissions. In addition, reducing energy consumption and carbon footprint is a global priority.

Studies based on Life Cycle Assessment have shown that optimizing process parameters in milling can significantly reduce environmental impact (*Kurukulasuriya et al., 2020*). Therefore, pneumatic dust removal is no longer just a safety measure, but also a tool for sustainable resource management. The work by Solari et al. (2017) constitutes a significant contribution by providing a solid validation of a CFD model applied to air filtration processes in the milling industry. The authors provide detailed experimental data on pressures and velocity distributions inside the pilot plant, which can be subsequently used as benchmarks for similar studies. In addition, the proposed validation methodology – which combines measurements obtained with specialized sensors and numerical simulations performed in ANSYS Fluent – represents a robust framework that can be adapted to other industrial applications where flow phenomena occur through porous media.The 2017 work aimed to develop and validate a CFD numerical model for analyzing the behavior of an air filtration system used in grain mills.

The study was carried out on a pilot plant built within the Industrial Engineering Laboratory of the University of Parma, which reproduces the real conditions in a wheat mill. The analyzed system consisted of a cyclone separator inside which 31 textile filter bags were mounted, a configuration often found in industrial milling units. The methodology involved experimental velocity and pressure measurements using a hot-wire anemometer, a Pilot tube and a differential pressure sensor. These data were compared with the results obtained through CFD simulations in ANSYS Fluent, for different operating conditions. The results showed a very good agreement between the measured and simulated values, both in terms of velocity field distributions and pressure losses.

The validation of the model confirms its applicability as a predictive tool in the design and optimization of dust filtration systems generated by milling processes.Thus, the study demonstrates the potential of using numerical simulation methods in support of the cereal industry, contributing to improving technological performance and reducing dust emissions into the environment. *(Solari, F., Tagliavini, G., Montanari, R., Bottani, E., Malagoli, N., & Armenzoni, M. (2017).*

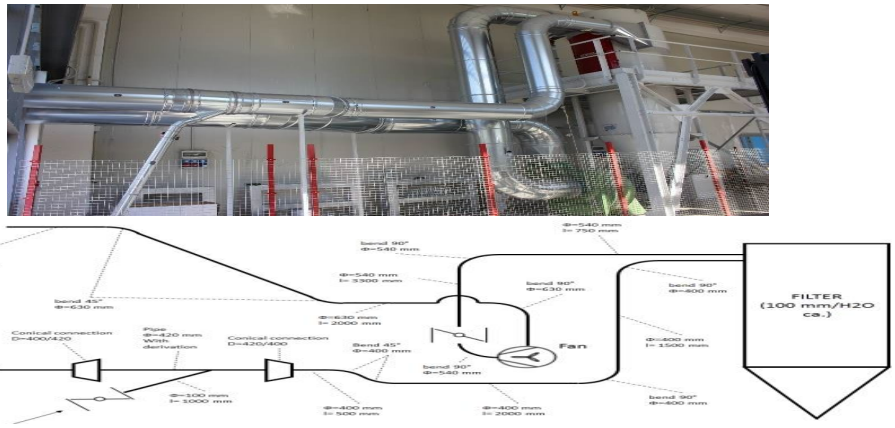

Fig. 3 - Pilot plant used for CFD model validation: (a) photo of the system mounted in the Industrial Engineering laboratory of the University of Parma; (b) technical diagram of the ductwork and bag filter, including the suction fan and the main geometric connections

(after Solari et al., 2017)

The aim of the work was to examine the operation of an air purification system consisting of a cyclone separator and a textile filter equipped with 31 bags. The system was tested in various operating modes to obtain a predictive model useful in the design of industrial facilities. This objective was achieved through CFD simulations, validated through an experimental program carried out on the pilot plant *(Solari, F., Tagliavini, G., Montanari, R., Bottani, E., Malagoli, N. & Armenzoni, M. (2017).*

A first step consisted in the placement and preparation of sensor locations, so that the velocities and pressure differences could be measured both in the filter area and at the inlet and outlet pipes (Figure 2). A hot wire anemometer and a Pitot tube were used to determine the velocities, and the pressure losses were monitored using a differential sensor. In parallel, comparisons were made between the measured air flows and the characteristic curves of the fan, obtained at different inverter frequencies, to confirm the correct operation of the pilot plant *(Solari, F., Tagliavini, G., Montanari, R., Bottani, E., Malagoli, N., & Armenzoni, M. (2017)*. Based on these data, the three-dimensional model of the bag filter was developed, discretized in Ansys MESHING. The computational mesh was designed finely in the narrow areas between the bags, in order to faithfully capture the velocity distribution. CFD simulations were performed in steady-state mode for four inlet velocities: 15 m/s, 19 m/s, 22.5 m/s and 25 m/s *(Solari, F., Tagliavini, G., Montanari, R., Bottani, E., Malagoli, N., & Armenzoni, M. (2017).* The numerical validation consisted of comparing the results obtained by simulation with the experimental measurements. For the velocities in the cyclone volute and in the lower conical part, minimum and maximum values were recorded, subsequently verified by correlation with the numerical curves (*Solari, F., Tagliavini, G., Montanari, R., Bottani, E., Malagoli, N., & Armenzoni, M., 2017*).

RESULTS

The results showed that the CFD predictions fall within the experimental ranges, confirming the correctness of the model from the point of view of the velocity field. Regarding the pressure loss, the values measured with the differential sensor were reported to the inlet velocities determined with the Pitot tube and compared with the simulation results, finding a good agreement from this perspective as well *(Solari, F., Tagliavini, G., Montanari, R., Bottani, E., Malagoli, N., & Armenzoni, M. (2017).*

In conclusion, the study led to the development of a predictive CFD model suitable for the design of air filtration plants in milling. Future research directions include the analysis of the pipe network in terms of velocity distribution and pressure losses, as well as the extension of the model to industrial scale, in order to reproduce real operating conditions *(Solari, F., Tagliavini, G., Montanari, R., Bottani, E., Malagoli, N., & Armenzoni, M. (2017).* The paper by Solari, Lysova and Montanari (2023) describes the development of a digital twin model for the monitoring and predictive maintenance of a cyclone bag filter used in milling plants. The objective of the research was both to detect failures and to estimate the remaining service life of the filter elements. CFD simulations were used to analyze the air flow regimes in various bag clogging states. The results served to identify the optimal position for an additional velocity sensor, intended to complement the differential pressure monitoring, and to define adaptive cleaning procedures with compressed air jets. The integration of experimental and historical data with numerical modeling allowed the construction of the digital twin, connected to the pilot plant through an acquisition system. Validation over a period of one year confirmed its ability to recognize defects such as bag breakage and to provide reliable estimates of the remaining service life.Overall, the study demonstrates that combining CFD simulations with an operational digital twin improves filter efficiency, allows early identification of anomalies, and supports predictive maintenance in wheat mills *(Solari F., Lysova N., Montanari R. (2023).*

The paper highlights several essential contributions:• the possibility of rapid identification of malfunctions, by comparing in real time the measured values with those estimated by the model;• determining the remaining life of the filter elements, an essential aspect in planning maintenance interventions;• optimizing bag cleaning cycles, so as to reduce energy consumption and component wear;• achieving a decrease in operating costs, by avoiding unexpected shutdowns and by using materials efficiently;• ensuring compliance with environmental regulations, by constantly maintaining the emission level below the permitted limits. Through this approach, the filtration system becomes part of an intelligent infrastructure, capable of monitoring its performance, predicting degradation over time, and supporting operational and maintenance decision-making. While the 2017 study focused on the experimental validation of a pilot-scale CFD model, the 2023 research represents a decisive step towards the practical application of digital technologies for predictive management and operational optimization in industrial filtration plants. (*Solari F., Lysova N., Montanari R. 2023*).

Fig. 4 - Integration between the "Physical Twin" (pilot installation equipped with sensors) and the "Digital Twin" (numerical model based on CFD simulations and historical data)

(after Solari, Lysova & Montanari, 2023).

At the bottom, we have the “Physical Twin” – the real pilot plant (cyclone + bag filter) equipped with sensors for real-time data collection. At the top-left, the “Digital Twin” – the numerical model (CFD + historical data + operational data). The information flow is bidirectional: historical and operational data feed the digital model, and the data collected in real time from the physical plant is processed (data logging & data processing). *(Solari F., Lysova N., Montanari R. (2023*).

The processing results allow a series of advanced functionalities:

- evaluation of the degree of clogging of the filter bags.
- detection of anomalies in real time, by comparing the measured values with those estimated by the model.
- analysis of trends to monitor the evolution of the condition of the installation.

Adjustment of the sequence of compressed air jets for cleaning the bags, optimizing energy consumption and reducing wear.Estimation of the remaining life (RUL) of the filter elements, an essential aspect for predictive maintenance. The results obtained show a satisfactory agreement between the CFD simulations and the experimental measurements. The evolutions of the pressure drops, both calculated and experimentally determined, present parallel slopes as the air velocity at the filter inlet changes. The small deviations observed can be associated with the measurement uncertainty generated by the KIMO sensor, positioned near a pipe bend, which influenced the accuracy of the recordings. In case 8, the deviations were more evident, probably due to the fact that the method of simulating clogging by covering with foil does not fully reflect the real situation of a uniformly blocked sleeve. It is worth noting that the differences increase with the intensification of the clogging degree, which explains the more pronounced variation in case 8 compared to case 6. *(Solari F., Lysova N., Montanari R. (2023).* The variation trends of the air velocity at the monitored point inside the filter also confirm the validity of the model, although the deviations are more pronounced.

These differences can be explained by three aspects: (i) the simulations provide only the tangential component of the velocity, while the anemometer captures other components as well, due to constructive limitations; (ii) fixing the sleeves only at the upper part, corroborated with their length of 3 m, allows oscillations that can modify the flow distribution; (iii) the alternation of completely clogged areas with areas unaffected by the foil creates different flow conditions compared to a uniform clogging. (*Solari F., Lysova N., Montanari R. 2023*). Thus, the experimental data confirm the relationships between air flow, pressure drops and velocity at the measuring point, demonstrating that pressure losses increase with the degree of clogging, and the local air velocity intensifies under standardized clogging conditions. However, the model could not be validated regarding the real-time adjustment of the sequence and frequency of compressed air jets (Table 9), since the artificial clogging method used would have compromised the efficiency of the cleaning process. In this regard, future research should aim at testing and validating the model under real industrial conditions, in order to optimally calibrate the cleaning sequence and frequency. (*Solari F., Lysova N., Montanari R., 2023*). The developed digital twin demonstrated the ability to estimate the remaining useful life of the bags (RUL) and identify faults in operation. The model has so far been trained on data corresponding to normal clogging, but its extension to a wider spectrum of operating conditions is necessary to increase its robustness and industrial applicability. In addition, the data generated by the simulations can extend the usefulness of the digital twin by providing information that is difficult to obtain experimentally, such as the distribution of upward velocities inside the bags, the impact velocities on the filter material or the individual flow rate filtered by each element. *(Solari F., Lysova N., Montanari R., 2023*).In 2025, in the paper published in Foods, the characteristics of the materials retained by the bag filtration systems of a wheat mill in southeastern Romania (SC Agro Chirnogi) were analyzed. The study targeted the filters from two technological stages – the cleaning section and the grinding section – by taking samples at the inlet and outlet. The determinations included particle size and distribution (modeled according to the Rosin–Rammler law), apparent and true density, porosity, specific surface area and angle of repose *(Iscru, Voicu G.D., Banu, I. Ungureanu, C., & al. (2025).* The results showed that the particles collected in the grinding section are significantly finer than those in the cleaning section. Although the filters effectively retain the medium and large particle fractions, a considerable part of the very fine particles (PM10 and PM2.5) passes through the filter material. The authors concluded that it is necessary to adjust the technological parameters and implement additional systems for capturing ultrafine particles, in order to reduce emissions and protect the health of operators. (*Iscru, Voicu G. D., Banu, I., Ungureanu, C., & al., 2025*).

CONCLUSIONS

1. Grain dust remains one of the biggest risks in the milling industry. Empirical evidence confirms the effects on workers' health, the vulnerability of plants to explosions and the hidden costs generated by raw material losses and emissions. Modern pneumatic systems – cyclones, bag filters and HEPA – represent the fundamental solution for controlling these risks. Their combination with technological innovations – CFD simulations, smart sensors, evolutionary algorithms – paves the way for a safer, more efficient and environmentally responsible industry. In an integrated vision, dedusting becomes not just a technical requirement, but a strategic investment, indispensable for the sustainable future of the milling sector.
2. Grain dust remains a major risk in milling, but modern dedusting technologies offer efficient and sustainable solutions. - The integration of these systems, in accordance with international standards and supported by applied research, is the key to a safe, efficient and environmentally responsible industry.
3. Textile filters in wheat mills effectively retain medium and large particles, but allow the passage of ultrafine fractions (PM10, PM2.5).
4. CFD validation on pilot plants (2017) demonstrated the accuracy of simulations for flows and pressure losses.
5. The 2023 study introduced the concept of digital twin, useful for fault detection and predictive maintenance.
6. Investigations carried out in Romania (2025) confirm these results and show the need for additional systems for ultrafine particles.
7. The integration of advanced materials, CFD modeling and digital monitoring can increase the efficiency of the filtration process.
8. The implementation of these solutions ensures emission reduction, cost optimization and improved working conditions in the mill.

ACKNOWLEDGEMENT

This paper is written during the doctoral internship of the first author in the Doctoral School of Biotechnical Systems Engineering, from the National University of Science and Technology Politehnica Bucharest.

REFERENCES

[1] Iscru, D., Banu, I., Ungureanu, C., et al. (2025). Aspects of the material characteristics of the filtration system in a wheat mill. Foods.

[2] Iyogun, K. C., Ana, G. R. E. E., Fakunle, G., et al. (2019). Lung Function of Grain Millers Exposed to Grain Dust and Diesel Exhaust in Two Food Markets in Ibadan Metropolis, Nigeria. Annals of Global Health.

[3] Liu, B.D.,Jia, P.Y., et al. (2017).Stability model and simulation of bag dust removal system. Mathematical Modeling and its Applications, 6(1), 39–52.

[4] National Fire Protection Association. (2017). NFPA 61: Standard for the prevention of fires and dust explosions in agricultural and food processing facilities. Quincy, MA: NFPA.

[5] Özbakır, O. (2024). Occupational health and safety in flour mills: A research and risk assessment. International Journal of Agriculture, Environment and Food Sciences.

[6] Schoeff, R. W. (2006). Dust explosions in the grain industry: 2005 annual report. Manhattan, KS: Kansas State University, Department of Grain Science and Industry.

[7] Solari, F., Lysova, N., & Montanari, R. (2023). Digital Twin Based on Historical Data and Simulation Results: Fault Detection and Estimation of the Remaining Useful Life of a Cyclone Bag Filter. Applied Sciences, 13(14), 8297. https://doi.org/10.3390/app13148297.

[8] Solari, F., Tagliavini, G., Montanari, R., Bottani, E., Malagoli, L., & Armenzoni, F. (2017). CFD model validation of a bag filter for air filtration in a milling plant. In Proceedings of the International Food Operations and Processing Simulation Workshop (Barcelona).

[9] Tang, R., Zhu, Y., & Zhang, H. (2024). Multi-objective optimization model for machining process considering carbon emissions and cost. Sustainable Energy Research.

[10] Zhao, Y., Li, J., & Wang, K. (2023). Carbon emission prediction and optimization models in industrial processes. Sustainability.

TESTING METHODOLOGY FOR A MIXED INTELLIGENT CROP BIRD SCARING SYSTEM

/

METODOLOGIE DE TESTARE PENTRU UN SISTEM INTELIGENT MIXT DE SPERIAT PĂSĂRILE DIN CULTURI

Augustina PRUTEANU*[1)], Mihai MATACHE[1)], Alexandru IONESCU[1)], Dorin Andrei CÎRSTEA[1)], Dorin Robert CRISTEA[1)], Simona-Florina ISTICIOAIA[2)]

[1)] National Institute of Research - Development for Machines and Installations Designed to Agriculture and Food Industry - INMA Bucharest / Romania;

[2)] Agricultural Research and Development Station Secuieni, Neamt County / Romania.

**Tel: 0740 690 268; *E-mail: pruteanu_augustina@yahoo.com*

Keywords: *crows, starlings, pigeons, scaring system, acoustic system and light system*

ABSTRACT

This study presents the test methodology for an intelligent mixed system to scare away birds from crops, using modern technologies in the field of precision agriculture. The system consists of distributed components, which can be controlled both locally and centrally, to detect pests early and apply rapid prevention measures. The intelligent mixed protection system uses both acoustic methods (ultrasonic generators and sound emitters at various frequencies and acoustic powers) and light radiation (laser in two colors – red and green – with thousands of patterns and projection intensities). The testing methodology was carried out in the laboratory and in different crops, such as raspberry plantations and apple orchards. The role of the intelligent mixed system developed is to improve crop safety, reduce losses and ensure an effective intervention, with minimal impact on the environment.

REZUMAT

Acest studiu prezinta metodologia de testare pentru un sistem inteligent mixt de speriat pasarile din culturi, folosind tehnologii moderne din domeniul agriculturii de precizie. Sistemul este format din componente distribuite, care pot fi controlate atât local, cât și centralizat, pentru a detecta din timp dăunătorii și a aplica măsuri rapide de prevenire. Sistemul inteligent mixt de protecție utilizeaza atat metode acustice (generatoare de ultrasunete și emițătoare de sunete la frecvențe și puteri acustice variate), cat si radiație luminoasă (laser în două culori – roșu și verde – cu mii de modele și intensități de proiecție). Metodologia de testare s-a realizat in laborator si în culturi diferite, precum plantații de zmeură și livezi de meri. Rolul sistemului intelligent mixt dezvoltat este de a îmbunătăți siguranța culturilor, de a reduce pierderile și de a asigura o intervenție eficientă, cu un impact minim asupra mediului.

INTRODUCTION

Identifying and classifying bird species is a challenge even for ornithologists, due to the high variability in behaviour, morphology, habitat, geographical distribution and adaptability to environmental change (*Gavali et al., 2020; Raj et al., 2020*). The study of bird behavior – such as feeding, reproduction and migration – correlated with habitat changes and specific diseases, is essential for understanding avian ecology. The posture of birds provides valuable information about their behavior (*Lin C.-W., 2022*), But collecting this data involves significant financial resources and efforts.

In this context, modern computer vision technologies based on **deep learning**, especially **convolutional neural networks (CNNs),** have become an important tool in automatic bird recognition, providing outstanding results in numerous studies (*Gavali et al., 2020; Lin et al., 2022*). Unlike sound or video, images are preferred for classification because audio signals can be affected by background noise *(Briggs et al., 2013*).

Frequently used CNN models include:

- **Part-based R-CNN** (*Zhang et al., 2014*) and **Pose Normalized CNN** (*Branson et al., 2014*), which integrate information about bird body parts;
- **D-CNN** (GoogLeNet), used for general classification (*Gavali et al., 2020*);
- **Faster R-CNN,** applied in the automatic detection of bird pests in orchards (*Lee et al., 2018*);

- **YOLO**, specialized in real-time image processing *(Redmon et al., 2016*);
- **HRNet**, which allows the recognition of bird posture by detecting key points (*Lin et al., 2022*);
- Other networks: **CUB-200-2011**, **ImageNet**, **NABirds**, **OverFeat**, as well as specialized sound identification systems such as **BirdNET**.

At the same time, modern machine learning algorithms such as **OpenPose**, **UniPose**, **CPM** and **PifPaf** are used for 2D posture estimation, but their applications to birds are still in the exploratory stage, in the absence of well-defined public datasets (*Lin et al., 2022*).

Therefore, the integration of artificial intelligence in ornithology opens up new perspectives for the efficient and accurate monitoring of avifauna, being of major interest to researchers, farmers and environmental protection institutions.

According to the classification proposed by ***(Micaelo et al., 2023).*** The classic methods of driving away harmful birds from horticultural crops are divided into six main categories:

Visual devices – used to scare birds through visual stimuli, include: scarecrows, reflective strips, kites "hawk's eye" balloons, models of birds, aircraft, drones and flashing lights;

Hearing devices – emit unpleasant or alarming sounds, and include: hunting rifles, pyrotechnic means (pistols and missiles), gas cannons, audio-visual (AV) alarms, predatory bird sounds, high intensity sounds, ultrasound and infrasound;

Chemical deterrents – which affect the behavior of birds or cause them discomfort, such as: tactile repellents, behavioral repellents and the substance methyl anthranilates;

Methods of physical exclusion – which prevent birds from having access to culture, such as: aerial net and foam;

Habitat modification – to make the area less attractive to birds, using: tall grass and application of fungicides;

Active removal methods – which involve capturing or disposing of birds, including: booby traps, live ammunition shooting, falconry (using birds of prey) and surfactants;

Other deterrence techniques – innovative or less used methods, such as: the area of deception, magnets, microwaves and lasers.

Habituation is the most important limiting factor in the effectiveness of classic bird scaring techniques. As they point out (*Pruteanu et al., 2023*), birds can quickly learn that the stimuli used do not pose a real threat. In some cases, these stimuli can even become **conditional clues of the presence of food,** thus attracting birds to the culture and having an effect contrary to the desired one.

To prevent habituation and increase the effectiveness of deterrence methods, it is essential to:

- **the use of a variety of visual** and auditory devices and techniques;
- **activating them as soon as the birds show interest** in the crop, before they form a feeding habit in the area;
- **frequently changing the position and type of devices**, in order to preserve the unpredictability of stimuli.

In addition, **combining different types of control methods** (visual, auditory, chemical, exclusion, habitat modification) have proven to be the most effective strategy in protecting orchards and horticultural crops against harmful birds (*Pruteanu et al., 2023*).

In this context, this paper presents a methodology that has been applied for testing a Mixed Intelligent System for the Protection of Agricultural Crops against pests using acoustic and light rejection elements in order to drive away harmful birds from different crops.

MATERIALS AND METHODS

The Intelligent Mixed Crop Protection System has two different control architectures (acoustic version and acoustic and light version) [11,12] and uses renewable energy sources, digital technologies for pest detection and information processing, acoustic and light repellents for scaring birds.

The system consists of three component modules: power mode, detection mode and rejection mode:

- The power module consists of: solar panels, solar panel system controller, battery and inverter;
- The detection module consists of bird motion detection sensors, smart camera and/or central computer;
- The rejection module consists of various rejection devices, acoustic and light, which work on different principles: sound generator, ultrasonic generator, laser, kites, balloons, reflective tape.

Overview images of the mixed intelligent system for scaring birds from crops in the laboratory (figure 1) and in various crops (figure 2) can be seen below.

Fig. 1 - Experimenting with the system in the laboratory

The intelligent acoustic system in the apple orchard

The intelligent acoustic and light system in raspberry cultivation

Fig. 2 - Experimenting with the system in cultures

1. DESCRIPTION OF THE MIXED INTELLIGENT SYSTEM

1.1. *Hardware components*

*The mixed intelligent system for the protection of agricultural crops (**acoustic version**) is composed of the following physical components:*

◆ **The detection mode** comprises motion sensors (figure 3)

- Sensor Type: PIR
- Operating voltage: 5V – 20V
- Current: 65mA
- TTL digital output: 3.3V/0V
- Adjustable delay: 0.3 sec – 5 min
- Detection range: up to 12 m
- Detection angle: 110°
- Operating temperature: -15°C – +70°C

Fig. 3 - PIR (Passive Infrared) motion sensors

◆ **The rejection mode** comprises sonic generator (figure 4)

- Operating mode: random or sensor-triggered
- Frequency: 3–5 kHz
- Sound power: 105–110 dB at 1 m
- Covered area: approx. 5,000 m²
- Number of speakers: 1
- Power supply: 220V-230V/12V DC
- Dimensions: 15 cm x 22 cm x 10 cm; Weight: 1.4 kg

Fig. 4 - Sound generator for chasing away birds

◆ **Power module** includes: solar panels, solar panel controller, battery, inverter

◆ **Other auxiliary equipment:**

- Holographic tape – for bird-scaring visual reflections
- Kite – imitates the flight of birds of prey for visual discouragement

*The intelligent mixed crop protection system (**acoustic and light version**) is composed of the following physical components:*

◆ **The detection mode comprises the** smart camera (figure 5)

- Type: color, 360° rotation
- Resolution: 1920x1080 pixels (2MP)
- Image sensor: 1/3.7"
- Operating System: Ubuntu Linux
- AI Mode: NVIDIA® Jetson™ Xavier NX
- Digital I/O: 4
- bird detection with YOLOv8 algorithm

Fig. 5 - Smart camera

◆ **The rejection mode** comprises laser system (figure 6) and sound and ultrasonic generator (figure 7):

- Colors: red (650 nm, 100 mW) and green (532 nm, 50 mW)
- Radius Divergence: 60°
- Range: up to 75 m
- Coverage: 10,000 m²
- Classification: Class 3R
- Dimensions: 18.5 x 14.8 x 7.0 cm; Weight: 1.5 kg
- Operating temperatures: -20°C to -40°C

Fig. 6 - Laser system

- Coverage area:
  - Sonic: up to 2–3 ha (30,000 m²)
  - Ultrasonic: up to 400 m²
- Sound pressure: Sonic: 105–110 dB and Ultrasonic: 95–102 dB
- Frequencies: Sonic: 3–5 kHz and Ultrasonic: 15–25 kHz
- Number of speakers: 4 (size 10 x 10 x 15 cm)
- Unit dimensions: 23 x 23 x 13 cm; Weight: 5 kg
- Power supply: 220–240V AC / 12V DC

Fig. 7 - Sound and Ultrasonic Generator

◆ **Power module** includes: solar panels, solar panel controller, battery, inverter

◆ **Other auxiliary equipment:**

- Balloon scarecrows in various colors and drawn with "hawk eyes".

1.2. Detection and reaction algorithms

The acoustic system [11] works in two main operating modes, each governed by a dedicated algorithm:

- **The random mode *(automated via PLC)*** has the following features:
  - controlled by a PLC (programmable logic controller);
  - Activate the sonic generator randomly to prevent birds from getting used to sounds.
  - Interval between activations: 5–30 minutes, with an operating time of 40 seconds.
  - PLC algorithm: uses a pseudo-random number generator to decide the time of the next activation, within the pre-established limits;
  - The advantage of this module is that unpredictably distributed noises increase the efficiency of the system.
- **The Sensor Mode (PIR)** has the following features:
  - PIR sensors detect the movement of birds.
  - Upon detection, the acoustic system is activated instantly, for 40 seconds.
  - It works whenever a movement occurs, as long as there is a natural pause between activations.
  - The sensors are strategically mounted to eliminate blind spots and ensure full coverage.

The change of operating mode is done manually, through a physical selector mounted on the control panel.

The acoustic and lighting system [12] integrates an intelligent algorithm, which combines computer vision with an automatic reaction model based on random logic and adaptivity.

- **Stages of operation:**
  - bird detection through the SMART camera using the YOLOv8 artificial intelligence model, trained for crow recognition;
  - when identifying a bird, the algorithm activates one or both rejection modules (acoustic and light), then a continuous check of the presence of birds is made;
  - if the presence is persistent, the system increases the intensity of the reaction by activating sound/ultrasound and laser, randomly to prevent birds from adapting;
  - the transition between actions (sounds, ultrasounds, laser) is done through a finite state automaton (FSM), which adjusts the response according to the detected behavior.

The YOLOv8 algorithm has algorithmic performance (Precision; Recall; mAP; F1 score: Confidence curve; Confusion Matrix: True Positive; False Negatives).

1.3. Smart functionalities and real-time adaptability

The intelligent acoustic system [11] integrates several functions and adaptation mechanisms to react effectively to dynamic conditions, such as:

- **real-time response** to the presence of birds (through PIR sensors);
- **acoustic adaptability**: the generator can emit various sounds (owl, eagle, heron, etc.) at different frequencies and acoustic pressures;
- **multiple modes of operation** (random or sensor-based) to **prevent birds from adapting;**
- **energy autonomy** thanks to solar panels;
- **modular system**, easy to configure and scalable for larger areas;
- **contribution to Agriculture 4.0**: integrating smart technologies for real-time crop protection, reducing losses and increasing production.

The intelligent acoustic and light system [12] is an advanced implementation of the *Agriculture 4.0 concept*, with intelligent functions that allow automatic adaptation to environmental conditions and adaptable behavior in real time of birds, such as:

- AI Recognition Computer Vision (YOLOv8) for automatic bird detection;
- automatic reaction based on a finite state automaton, which: activates the acoustic, light or combined mode; alternates actions randomly, preventing birds from getting used to it; Variable sounds including distress cries, predatory bird sounds, harassing sounds, configured via toggles (from 1 to 8) for variations;
- continuous monitoring of bird behavior in the protected area;
- automatic adjustment of the intensity and type of reaction;
- continuous evaluation of algorithm performance based on ml metrics (Precision, Recall, mAP, F1);
- immediate response to environmental or behavioral variations;
- solar power, autonomy in areas without electrical infrastructure.

2. METHODOLOGY FOR TESTING INTELLIGENT SYSTEMS FOR DRIVING BIRDS AWAY FROM AGRICULTURAL CROPS

The testing of intelligent acoustic and acoustic and lighting systems had the following objectives:

- evaluation of the functional efficiency of the systems in driving away harmful birds from agricultural crops;
- determination of performance parameters in different environmental conditions (meteorological, soil types, day/night variations);
- checking the adaptability of systems to different types of birds and flight behaviors;
- measuring energy consumption and sustainability of operation based on renewable sources (solar panels and battery);
- identification of technological or site limitations in laboratory and field conditions.

The systems were tested under the following atmospheric conditions, to evaluate the strength and performance of the equipment:

- light / medium / strong wind (0.5 – 15 m/s);
- temperatures ranging from -5°C to +35°C;
- relative humidity: 30 % – 95 %;

- atmospheric pressure: 720 – 780 mmHg;
- Lighting level: sunny / cloudy / dusk day.

The most frequently encountered birds pests in the tested agricultural crops (raspberry crop and apple orchard were monitored), they are shown in the table 1:

Table 1

Bird species monitored

Bird type	Typical behavior	Follow-up reaction
Crow (*Corvus sp.)*	Stationary, repetitive flight	Complete banishment
Common Grass (*Sturnus vulgaris*)	Flock flight, fast movement	Disorientation, dispersion
Pigeon (*Columba livia*)	Stationary, solitary or in pairs	Perimeter avoidance

The measured parameters were: bird scaring efficiency, reaction times and energy consumption.

• **Bird scaring efficiency,** defined as the percentage of birds leaving the protected area at the first activation of the system. Method of visual observation and video recording and calculation, according to the relation (1):

$$Efficiency\ (\%) = \left(\frac{number\ of\ scared\ birds}{total\ number\ of\ birds\ observed}\right) \cdot 100 \quad (1)$$

• **Reaction times,** defined as the time between motion detection and actual system activation. The measuring instruments used were: stopwatch, video camera.

Typical values for the acoustic system of 1.2 – 2.4 seconds and for the acoustic and lighting system of 0.8 – 1.5 seconds.

• **Energy consumption** was estimated by measuring the following parameters: solar energy produced (Wh); energy consumed daily (Wh/day); specific consumption (Wh/m²/day). The measuring instruments used were: network analyzer, digital multimeter, solar controller.

✓ To calculate the solar output of the panel, the relation (2) is used:

E [Wh/day/panel] = P x t .. (2)

where: E is the solar production; - P is the power of the solar panel; - t refers to the hours of sunshine/day.

✓ The relation (3) is for the calculation of energy consumption:

Power [in watts] = Voltage (in volts) x Current (in amps) … (3)

✓ The calculation of the daily electricity consumption for the mixed intelligent system was calculated with the relation (4):

Daily electricity consumption = rated power x average daily usage time …….(4)

✓ the calculation of the kWh consumption, for the mixed intelligent system, was made with the relation (5):

kWh = (rated power in watts x hours of use) / 1000 …….(5)

✓ the specific consumption refers to the energy required to protect a given area, expressed in Wh/m²/day, the calculation relationship (6) is as follows:

$$Specific\ energy\ consumption\ [Wh/m^2/day] = \frac{Daily\ electrical\ energy\ required\ [Wh]}{Protected\ area\ [m^2]} \quad . (6)$$

▪ **Laboratory testing** to verify components under controlled conditions. The aspects analyzed were: functional tests in vacuum (sound, light, power); standardized acoustic measurements (according to SR EN ISO 3744:2011); sensor accuracy and AI validation (YOLOv8) on simulated images.

▪ **Field testing,** in real conditions of use, respectively raspberry crop and apple orchard. The aspects analyzed were: the actual sound/light coverage; birds' response to stimuli; the durability of the system in various weather conditions; energy reliability depending on solar radiation.

The limitations observed during testing are shown in table 2:

Table 2

Limitations observed for the Acoustic System and the Acoustic and Lighting System

Limitation observed	Affected system	Proposed measures
Low noise in strong winds	Acoustic system	Additional sound insulation
Interfering solar reflections with PIR sensors	Acoustic system	Sensor repositioning
Partially shaded solar panel	Acoustic system Acoustic and light system	Position/Tilt Adjustment
Adaptive behavior of birds	Acoustic system Acoustic and light system	Alternating modes

RESULTS

Table 3 shows a structuring of the comparative results between the acoustic system and the acoustic and lighting system, obtained from testing in laboratory and field conditions, with a focus on efficiency, reaction times, coverage, energy consumption and limitations.

Table 3

Results of the tested systems

Parameter	Acoustic system	Acoustic and light system	Observations
Scare efficiency (average)	78–85%	**88–94%**	More effective by combining multiple stimuli
Average reaction time	1.5 – 2.4 seconds	**0.8 – 1.5 seconds**	Light has faster triggering
Efficient covered surface	6000 m²	**6500–7000 m²**	Acoustic-luminous has higher dispersion
Daily energy consumption (average)	120 – 150 Wh/day	**180 – 220 Wh/day**	Grows with LED lighting
Specific energy consumption	0.020 – 0.025 Wh/m²/day	**0.027 – 0.032 Wh/m²/day**	Both in the sustainable area
Bird behavior after 7 days	Observed adaptation trend	**Visible fit reduction**	Light alternation reduces habituation
Reliability in strong wind conditions	Stable, but sound can be attenuated	**More stable, light penetrates visually**	Acoustic and light advantage
Night detection	Limited (PIR sensor and sound)	**Efficient (PIR & Radar & Light)**	Radar and LED increase accuracy
Impact on non-target fauna	Low, but sometimes disturbing to animals	**Minimum (Precisely Directed Light)**	Fine-tuning possible
Estimated cost of implementation	Lower cost	**Higher cost**	Justified cost of superior performance

The comparative testing of the acoustic system and the acoustic and lighting system for the protection of agricultural crops highlighted the fact that:

- The acoustic and lighting system offers superior efficiency in repelling harmful birds, especially due to the combination of visual and sound stimuli, which significantly reduces the birds' adaptation to the system.
- The shorter reaction time and the ability for automatic operation based on detection (PIR, radar and AI analysis with smart camera) allow for rapid and adaptive intervention, improving crop protection.
- The simple acoustic system remains a viable option for small or medium-sized farms, having a lower cost and lower energy consumption, but with limited efficiency in the face of birds that develop tolerance over time.
- Both systems can be integrated into Agriculture 4.0 strategies, with the advantage of renewable power (solar panels), automatic adaptation to field conditions and constant monitoring of wildlife.

The results obtained provide valuable information about how harmful birds react to stimuli and about the efficiency of the system in repelling them, under various agricultural conditions.

CONCLUSIONS

The implementation of mixed intelligent systems, both in acoustic and acoustic and light versions, contributes significantly to the modernization and efficiency of precision agriculture practices, in accordance with the principles of Agriculture 4.0. These systems offer efficient, sustainable and adaptable solutions to combat the presence of bird pests in fruit and shrub crops, reducing production losses and minimizing the use of invasive or polluting methods.

The acoustic model is based on PIR sensors and simple random or reactive triggering algorithms, being effective in areas where rapid detection and audible response are sufficient. It is ideal for orchard applications, offering a good cost-efficiency ratio. On the other hand, the acoustic and light model integrates advanced computer vision technologies (YOLOv8) and real-time analysis, along with multisensory reactions (laser and sound/ultrasound). This approach provides increased automation, adaptability and precision, making it suitable for more sensitive crops (such as raspberries) or areas with high bird pressure.

Both models demonstrate the usefulness of combining smart hardware, adaptive algorithms and renewable energy sources, outlining a clear direction towards sustainable, digitized and ecological

agriculture. The acoustic and humid system is superior in terms of efficiency, reaction speed and territorial coverage, with a moderately increased energy consumption. The simple acoustic system is effective in basic conditions, with low consumption, but risks becoming less efficient over time, due to the adaptation of the birds.

The alternative or combined use of the two models can provide an optimal strategy in large farms or with significant seasonal variations in birds. The work thus supports the smart use of resources and the promotion of sustainable and competitive agriculture.

ACKNOWLEDGEMENT:

The paper has been funded by the Program NUCLEU 2023-2026, PN 23 04 01 06 "Intelligent mixed system for protection of agricultural crops against pests according to the Agriculture Concept 4.0", Contract no. 9N/01.01.2023.

REFERENCES

[1] Branson, S., Van Horn, G., Belongie, S., Perona, P., (2014). Bird species categorization using pose normalized deep convolutional nets. In: BMVC - *Proceedings of the British Machine Vision Conference,* preprint arXiv: 1406.2952.

[2] Briggs, F., Huang, Y., Raich, R., Eftaxias, K., Lei, Z., Cukierski, W., Milakov, M. (2013). New methods for acoustic classification of multiple simultaneous bird species in a noisy environment. In the 9th annual MLSP competition: *IEEE International Workshop on Machine Learning for Signal Processing* (MLSP). doi:10.1109/mlsp.2013.6661934.

[3] Gavali, P., Banu, J.S., (2020). Bird species identification using deep learning on GPU platform. In: 2020 *International Conference on Emerging Trends in Information Technology and Engineering* (ic-ETITE). IEEE, pp. 1–6, doi:10.1109/ic-ETITE47903.2020.85.

[4] Micaelo, E.B.; Lourenço, L.G.P.S.; Gaspar, P.D.; Caldeira, J.M.L.P.; Soares, V.N.G.J., (2023), Bird deterrent solutions for crop protection: approaches, challenges, and opportunities. *Agriculture*, 13, 774. https://doi.org/10.3390/agriculture13040774.

[5] Pruteanu A., Vanghele N., Cujbescu D., Nitu M., Gageanu I., (2023). Review of effectiveness of visual and auditory bird scaring techniques in agriculture, 22nd International Scientific *Conference Engineering for Rural Development* 24-26.05.2023 Jelgava, LATVIA, pp.275 – 281, DOI: 10.22616/ERDev.2023.22.TF056.

[6] Raj S., Garyali S., Kumar S., Shidnal S., (2020). Image based bird species identification using convolutional neural network, *International Journal Of Engineering Research & Technology* (IJERT), Volume 09, Issue 06, DOI:10.17577/IJERTV9IS060279.

[7] Redmon J., Divvala S., Girshick R., Farhadi A., (2016). You only look once: unified, real-time object detection, IEEE *Conference on Computer Vision and Pattern Recognition* (CVPR), Las Vegas, NV, USA, 2016, pp. 779-788, doi: 10.1109/CVPR.2016.91.

[8] Lee C.W., Muminov A., Ko M.C., Oh H.J., Lee J.D., Kwon Y.A., Na D., Heo S.P., Jeon H.S., (2021). Anti-adaptive harmful birds repelling method based on reinforcement learning approach," in *IEEE Access*, vol. 9, pp. 60553-60563, doi:10.1109/ACCESS.2021.3073205.

[9] Lin C.-W., Hong S., Lin M., Huang X., Liu J., (2022). Bird posture recognition based on target keypoints estimation in dual-task convolutional neural networks, *Ecological Indicators* 135, 108506, https://doi.org/10.1016/j.ecolind.2021.108506.

[10] Zhang, N., Donahue, J., Girshick, R., Darrell, T. (2014). Part-based R-CNNs for fine-grained category detection. In: Fleet, D., Pajdla, T., Schiele, B., Tuytelaars, T. (eds) *Computer Vision* – ECCV 2014. ECCV 2014. Lecture Notes in Computer Science, vol 8689. Springer, Cham. https://doi.org/10.1007/978-3-319-10590-1_54.

[11] *** Methodology for testing the intelligent mixed crop protection system (acoustic), INMA Bucharest, Nucleu Program 2023-2026, PN 23 04 01 06, 2025.

[12] *** Methodology for testing the intelligent mixed crop protection system (acoustic and light), INMA Bucharest, Nucleu Program 2023-2026, PN 23 04 01 06, 2025.

EVALUATION OF THE NUTRITIONAL COMPOSITION OF HEMP-BASED DIETARY SUPPLEMENTS AND FUTURE TRENDS

/

EVALUAREA COMPOZIȚIEI NUTRIȚIONALE A SUPLIMENTELOR ALIMENTARE PE BAZĂ DE CÂNEPĂ ȘI TENDINȚELE VIITOARE

Andreea MATACHE*[1)], Nicoleta Alexandra VANGHELE[1)], Florin NENCIU[1)], Augustina Mirabela PRUTEANU[1)], Tatiana ONISEI[2)], Alexandra LEONTE[3)], Lorena-Diana POPA[3)]

[1)] National Institute of Research - Development for Machines and Installations Designed for Agriculture and Food Industry - INMA Bucharest / Romania;

[2)] National Institute for Research and Development of Food Bioresources – IBA Bucharest / Romania;

[3)] Secuieni Agricultural Development Research Station - SCDA Secuieni, Neamt County / Romania.

**Tel: 0212 693 259; *E-mail: andmatache@yahoo.com*

Keywords: *improvet nutrition, alternative medicines, fatty acids, plant extracts*

ABSTRACT

Current trends in promoting a healthier lifestyle have led to an increase in the consumption of clean, (organic) foods and nutrient-rich food supplements. Medicinal plants are the oldest and most widespread form of medicine in the world and are still used today. In recent years, traditional medicine has received increased attention, demonstrating the potential to obtain products with real benefits for human health, in the context of a more sustainable future. Hemp (Cannabis sativa L.) is among the oldest medicinal plants in human history, recognized for its ability to treat various conditions (cardiovascular, neurodegenerative). Hemp extracts, such as cannabidiol (CBD), are currently used as food supplements due to its properties in relieving pain, anxiety, insomnia. This paper describes an overview of the nutritional content of food supplements containing hemp extracts and future trends in optimizing the utilization of the plant.

REZUMAT

Tendintele actuale de promovare a unui stil de viata cat mai sanatos au determinat o crestere a consumului de alimente curate, (bio) precum si a suplimentelor alimentare bogate in nutrienti. Plantele medicinale constituie cea mai veche și mai răspândită formă de medicină din lume fiind utilizata si in prezent. In ultimii ani, medicina traditională s-a bucurat de o atentie crescuta, demonstrand potentialul in obtinerea unor produse cu reale beneficii pentru sanatatea umana, in contextul unui viitor mai sustenabil. Canepa (Cannabis sativa L.) se numara printre cele mai vechi plante medicinale din istoria omenirii, recunoscuta pentru capacitatea sa de a trata diverse afectiuni (cardiovasculare, neurodegenerative). Extractele de cânepă, cum ar fi canabidiolul (CBD), sunt utilizate în prezent ca suplimente alimentare datorita proprietatilor sale in ameloirarea durerii, anxietatii, insomniei. Prezenta lucrare descrie o imagine de ansamblu a continutul nutritional al suplimentelor alimentare ce contin extracte de canepă si tendintele viitoare in optimizarea valorificarii plantei.

INTRODUCTION

It is estimated that 80% of the world's population regularly uses traditional medicine to treat and/or prevent a variety of diseases *(Oyebode, O. et al., 2016).* Cannabis sativa is among the oldest medicinal plants in human history. In the past, even doctors used hemp to relieve various conditions, including pain. The understanding of the complex chemistry of cannabis has had a favorable evolution along with its multiple therapeutic properties *(Liktor-Busa, E. et al., 2025).*

For example, in traditional Chinese medicine, inflorescences have been used for various health problems such as severe pain, insomnia, cough or shortness of breath, and wounds. The leaves have been recommended for treatments in cases of malaria, respiratory distress, roundworm infections, scorpion stings, hair loss and hair whitening. The bark of the strain has been used for therapeutic purposes for body injuries, and the roots against problems related to spots, difficult births, placenta retention, and bodily injury *(Jin, D. et al., 2020)*.

Even though in previous centuries, hemp was mainly used for textiles, and seeds were considered waste, today, due to their exceptional nutritional qualities and versatility, hemp seeds are used in the food

industry, to obtain oils rich in essential fatty acids, proteins with a high biological value and derivatives for fortification, supplementation and nutraceutical purposes *(Miller, A. et al., 2025).*

To establish a connection between traditional and modern evidence-based medicine, it is essential to identify active biochemical compounds, and their molecular mechanisms must be determined through preclinical and clinical studies. Cannabis is presented with a content of several classes of secondary metabolites, including 14 cannabinoids, 47 terpenoids, 3 sterols, and 7 flavonoids, which are found in the flowers, leaves, bark of the stem, and the roots of the plant.

The identification of bioactive substances, followed by well-structured clinical trials, could turn every part of the cannabis plant into a treatment based on scientific evidence *(Jin, D. et al., 2020).* Currently, the marketing of CBD-based dietary supplements, which is the subject of intense debate in the scientific community, is regulated differently in the United States, Europe and the rest of the world *(Cerino, P. et al., 2020).*

Hemp seeds contain THC (tetrahydrocannabinol) or CBD (cannabidiol), molecules responsible for the psychoactive and therapeutic properties of cannabis. These low levels of terpenophenols make it more suitable for use in food. Certain biological activities of phytochemical compounds (mainly polyphenols and terpenoids) present in hemp seeds confer antioxidant, antimicrobial, and anti-inflammatory properties *(Montero, L. et al., 2023)*.

The health benefits of hemp seed oil are mainly attributed to its desirable ratio of n-3 and n-6, 3:1 fatty acids, which is suggested to be optimal for human nutrition. Unbalanced intake of n-3 and n-6 fatty acids has been shown to be associated with many diseases, e.g., diabetes, cardiovascular disease, and cancer *(Mikulcová, V. et al., 2017).*

MATERIALS AND METHODS

Throughout history, cannabis has been indicated for a wide range of conditions related to pain, inflammation, and mental illness *(Jin, D. et al., 2020).*

The growing demand for high-quality healthy foods and dietary supplements with potential in treating various conditions has led to the development of the hemp products market, figure 1 *(Aloo, S.O. et al., 2022).*

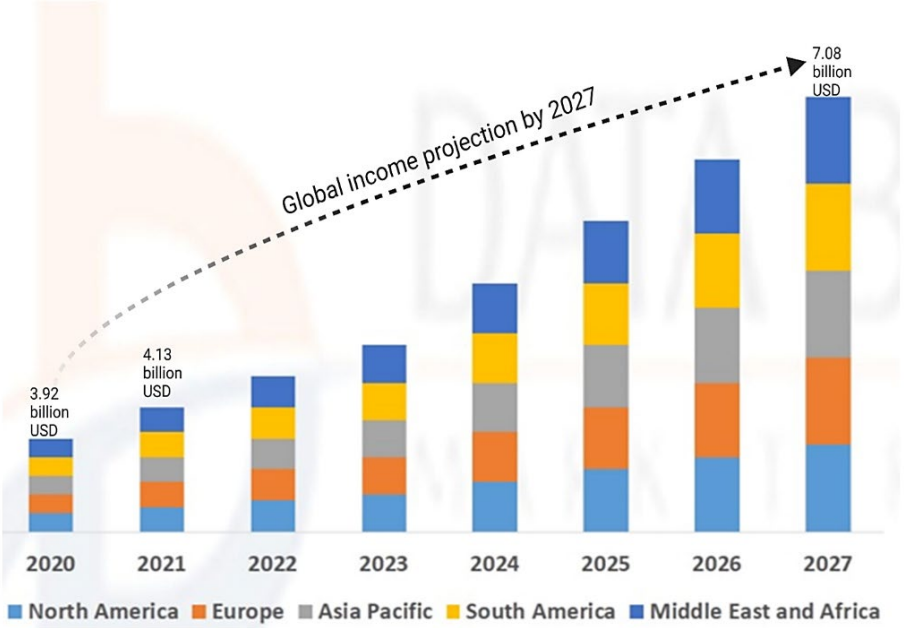

Fig. 1 - Global Hemp Food Market Share, by Regions, Trend, and Revenue Forecast to 2027
(Aloo, S.O. et al., 2022)

The characteristics that make hemp or hemp-derived products suitable for food applications are: solubility (one of the essential properties in determining the potential for incorporation of ingredients into food is their solubility), film formation, emulsification, surface hydrophobicity, nutritional value and bioactive components of hemp seeds (being the only constituent of hemp that can be used as food, hemp seeds have been shown to have great nutritional value). They contain proteins, essential amino acids, carbohydrates *(Aloo, S.O. et al., 2022)*.

Recently published studies, using an optimized method for the chemical characterization of hemp,

identified 189 lipids, including 52 phospholipids and 80 sulfolipids, and 147 compounds belonging to the classes of flavonoids, proanthocyanidins and phenolic acids *(Cerino, P. et al., 2020).* According to the results presented in the literature, hemp terpenes have antidepressant, anti-inflammatory and anxiolytic effects. They participate in photosynthesis and have a protective role in plants *(Salami, S.A. et al., 2020).*

Obtaining phytocannabinoids, which are linked to a variety of medicinal and therapeutic properties with no mentioned adverse effects, is a topic of great interest. The proportion of phytotrope Δ9-tetrahydrocannabinol (THC) remains below 0.2% in industrial hemp varieties, which allows them to be grown legally in many European Union member states.

Harvesting and processing hemp for fiber or seed produces a lot of waste that contains a significant amount of bioactive compounds, such as cannabidiol (CBD), which are the main cannabinoids, along with cannabidiolic acid (CBDA), cannabinol (CBN), cannabigerol (CBG), and cannabichromene (CBC). That is why it is essential to optimize the process of extracting cannabinoids from the residues resulting from the processing of industrial hemp.

Numerous studies demonstrate the beneficial medicinal and therapeutic properties of these non-psychotropic compounds. CBD and CBDA have demonstrated modulating effects on the human endocannabinoid system, possessing analgesic, antibacterial, antidiabetic, antiemetic, antiepileptic, anti-inflammatory, antiproliferative, and antipsychotic properties *(Vági, E. et al., 2019)*.

RESULTS

It is worth noting that numerous cannabinoids, including Δ9 - THC, show their physiological and pharmacological effects via the natural cannabinoid system (endocannabinoid), figure 2 *(Binding, C.A. et al., 2022).*

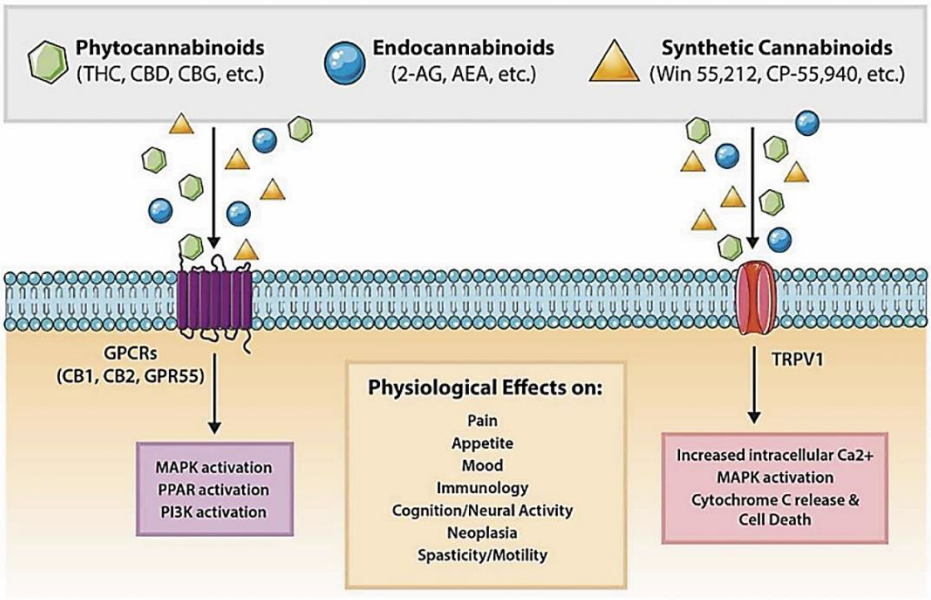

Fig. 2 - Signaling pathways and effects of cannabinoids. Regardless of the type of cannabinoid ligand (phytocannabinoid, endocannabinoid, or synthetic), these compounds mainly interact with GPCR proteins, such as CB1 and CB2 receptors, and GPR55, or with TRP, such as TRPV1, to induce a cellular response. Activated pathways vary depending on receptor activation and have physiological effects on pain, appetite, mood, and many other effects in the body

(Ligare, C.A. et al., 2022)

In addition to endocannabinoids, there are two other sources of cannabinoids, namely phytocannabinoids (produced by plants in the genus Cannabis) and synthetic cannabinoids (lab-generated compounds that can interact with cannabinoid receptors). In the literature there are a number of observations that assess the endocannabinoid system (ligands and receptors), as well as the phytocannabinoids in Cannabis sp. Thus, attention has been directed to medical conditions, disorders and diseases for which cannabis has potential for therapeutic use. In addition, enzymes responsible for breaking down endocannabinoids, such as fatty acid amide hydrolase (FAAH) and monoacylglycerol lipase (MAGL), are also key targets in creating new treatments *(Ligare, C.A. et al., 2022).*

A disproportionate consumption of n-3 and n-6 fatty acids has been shown to be associated with various health problems, including diabetes, cardiovascular disease, and cancer. As a result, aware of the antioxidant and anti-inflammatory effects of hemp seeds and hemp-derived products, the researchers studied whether dietary supplementation with these preparations could have the ability to fight chronic-degenerative diseases, characterized by persistent inflammation and oxidative stress, including cardiovascular and neurodegenerative diseases.

Studies suggest that adding 10% hemp seeds to a high-fat diet led to a significant improvement in serum parameters (i.e., a reduction in total cholesterol, LDL, and triglycerides). Daily consumption of 30 ml of hemp oil for four weeks was able to lower total plasma triglyceride (TG) levels and generate significant changes in the structure of serum cholesterol-esters (ECs) and triglycerides in healthy subjects *(Farinon, B. et al., 2020; Mikulcová, V. et al., 2017).*

Due to the alarming increase in the incidence of cancer globally, *cannabis sativa L* was among the first plants investigated for potential anticancer therapies, knowing the remarkable antioxidant properties of its more than 100 bioactive compounds. Hemp-derived extracts, especially those high in cannabidiol (CBD), exhibit important synergistic biological effects, including blocking cancer cell development, angiogenesis, and metastasis, along with promoting apoptosis. Due to these pharmacological attributes, hemp oils can be considered promising or adjuvant alternatives to conventional chemotherapy.

Figure 3 further illustrates the complexity of the tumor microenvironment (TME) and highlights the inhibitory effects exerted by CBD and THC *(Christodoulou, M.C. et al., 2025).*

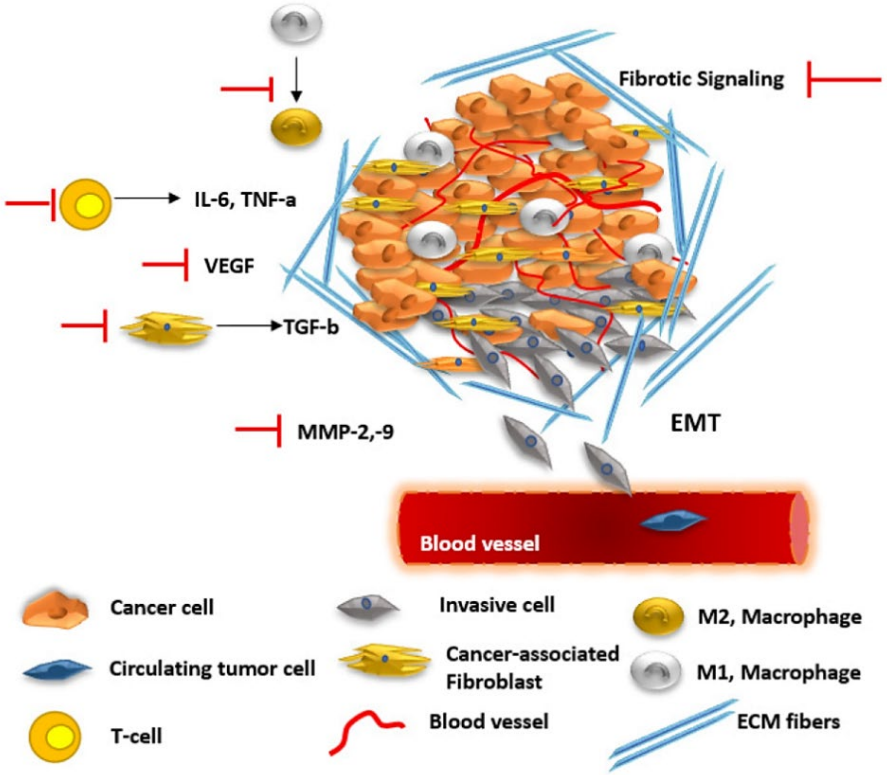

Fig. 3 - Effects of CBD and THC on the tumor microenvironment (TME). CBD suppresses pro-inflammatory cytokines (e.g., IL-6, TNF-α), helping to reduce chronic inflammation associated with tumor progression. CBD also influences macrophage polarization by shifting to the M1, antitumor phenotype (M2→M1 phenotype shift). THC can also be an immunosuppressant at high doses, reducing T cell activation and cytokine production. Both CBD and THC reduce angiogenesis by downregulating VEGF and MMPs. CBD affects EMT and negatively regulates MMP-2/9, limiting the migration and invasion of cancer cells. Limited research suggests that cannabinoids may reduce fibrotic signaling and modulate stromal support for tumors, potentially altering tumor stiffness and invasiveness. Cancer-associated fibroblasts, CAF; Cannabidiol, CBD; interleukin-6, IL-6; epithelial-mesenchymal transition, EMT; matrix metalloproteinases, MMP; tumor necrosis factor alpha, TNF-α; Δ9 - tetrahydrocannabinol, THC; vascular endothelial growth factor, VEGF

(https://www.mdpi.com/cancers/cancers).

The antiviral applications of cannabis and its bioactive compounds have been studied, especially in the context of SARS-CoV-2, while also examining their therapeutic potential. Cannabinoids can prevent virus

penetration, influence immune system responses (e.g., by reducing pro-inflammatory cytokines by activating CB2/PPARγ), and decrease mental stress associated with COVID-19. The finding suggests that CBD could alter the body's immune response by stimulating the CB2 receptor, specifically by reducing inflammation and adjusting immune responses to viral infection, figure 4 *(Qin, X. et al., 2025).*

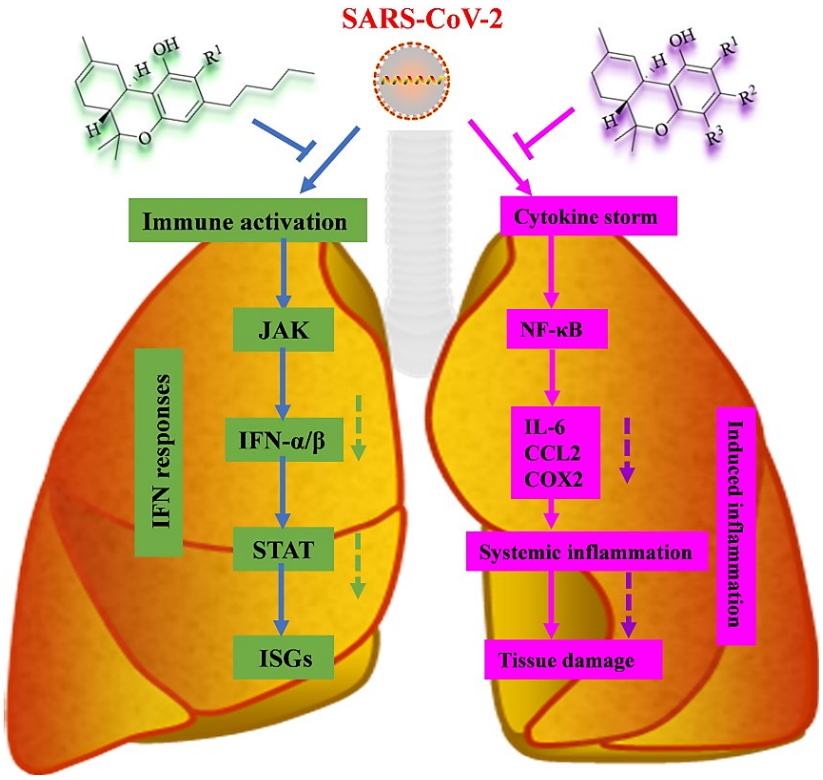

Fig. 4 - An outline of immune signaling (left) and major inflammatory signaling (right) is shown, annotated with the known mechanisms by which SARS-CoV-2 activates and suppresses signals (dotted line)
(Qin, X. et al., 2025)

Another analysis showed that consumption of hemp seed oil for 8 weeks did not decrease plasma concentrations of IL-6 and TNF-α in the group of patients with many patients undergoing maintenance hemodialysis (MHD), instead some clinical studies have shown that Omega-3 polyunsaturated fatty acids have anti-inflammatory effects in HD patients *(Khosravi, M. et al., 2021).*

The benefit of hemp as a nutritional supplement is that it can enrich the consumer's diet. Hemp extracts, such as CBD, are currently used as dietary supplements. There is an interesting pharmaceutical and dietary supplement and can be added to foods to complement the nutritional value *(Lin, Y., et al., 2021).* CBDIt has also been shown that daily oral administration of hemp seed oil on a mouse model with MS can have positive effects on the treatment of this chronic-inflammatory and neurodegenerative disease characterized by extensive demyelination, as it can exert immunomodulatory action, especially anti-inflammatory, and improve the remyelination of the neuronal myelin sheath in the brain, with a protective effect on the central nervous system (CNS) *(Rezapour-Firouzi, S. et al., 2018).*

It is now known that the endocannabinoid system (ECS) plays an essential role in maintaining balance in the body, creating connections between all organs and systems of the body. ECS has been associated with various conditions and essential regulatory functions, including chronic inflammatory conditions and adjustment of immune homeostasis in the gut, as well as anxiety and migraines.

Although the body produces its own endogenous cannabinoids, such as anandamide and 2-arachidonylglycerol, plant-derived cannabinoids (phytocannabinoids) have been studied as promising therapeutic options in numerous fields, due to their ability to influence ECS *(Harrison, J. et al., 2019).* Figure 5 summarizes the basic molecular biology of the ECS, as well as some of the molecular effects of phytocannabinoids *(https://ars.els-cdn.com/content/image)*.

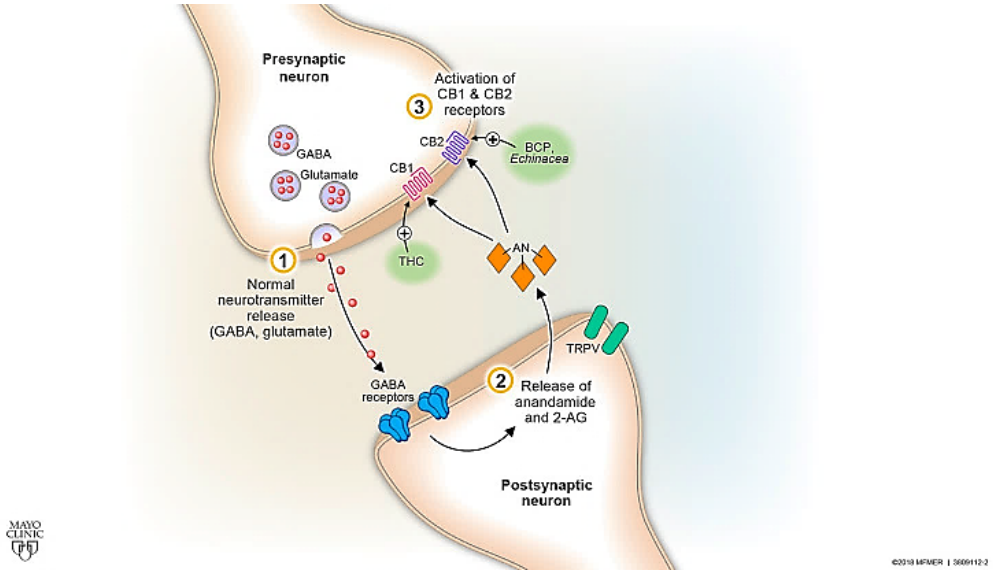

Fig. 5 - Modulation of the endocannabinoid system by phytocannabinoids. The figure illustrates how the endogenous cannabinoids anandamide (AN) and 2-arachidonylglycerol (2-AG) interact with cannabinoid receptors 1 and 2 (CB1 and CB2) that are associated with the G protein in presynaptic neurons in both the central and peripheral nervous systems. The compounds marked in green represent common plant cannabinoids and other plant components in hemp oils, which have been shown to influence natural endocannabinoids in one way or another, either by altering the activity of CB receptors (e.g., the agonist effect of tetrahydrocannabinol [THC] on CB1 receptors) or through as yet unexplained mechanisms, such as inhibition of enzymatic degradation of endocannabinoids or other forms of receptor modification. BCP stands for β-caryophyllene; GABA stands for γ-aminobutyric acid; and TRPV represents the potential transient vanilloid receptor

(https://ars.els-cdn.com/content/image)

Cannabis sativa *seeds* are low in phytocannabinoids, but are instead rich in omega-6 and omega-3 essential fatty acids, substantial amounts of γ-linolenic acid, and other nutritious antioxidants. In addition, there are also products based on "cannabis oil", which are oils derived from the marijuana plant that have high levels of THC. Table 1 summarizes these differences *(Harrison, J. et al., 2019).*

Table 1

Hemp Seed, CBD, and Cannabis Oils

(Harrison, J. et al., 2019)

Variable name:	Hemp seed oils	Hemp/CBD oils	Cannabis oils
Part of plant extracted	Seeds	Flowers and leaves of hemp plant	Flowers and leaves of marijuana plant
Main components	Omega-6 and omega-3 fatty acids, γ-linolenic acid, nutritious antioxidants	Mostly CBD and BCP with other smaller-quantity phytocannabinoids and terpenoids	Mostly THC with some CBD and other phytocannabinoids and terpenoids
THC levels	None	<0.3% Dry weight	>0.3% Dry weight (often very high amounts such as 80%)
CBD levels	Little to none	More than average cannabis plants (12%-18% CBD, often higher due to postextraction enrichment)	Lower levels (10%-15%)
Uses	Nutritional supplement, other uses of hemp such as clothing and fibers	Medicinal uses of CBD and full-spectrum hemp oils	Medicinal uses of THC

BCP = β-caryophyllene; CBD = cannabidiol; THC = tetrahydrocannabinol.

The products can be marketed as "full-spectrum" formulas, dietary supplements, hemp oils or CBD-enriched products, in the form of oils, capsules, soft gelatin capsules, conditioners, sprays, even chew toys

for pets. These products are marketed for a variety of uses, such as sleeping pills, pain relief, or stress reduction *(Harrison, J. et al., 2019).*

As an active, plant-based, easily extractable biological compound with a high therapeutic index and a good safety profile, CBD is currently marketed both as a dietary supplement derived mainly from hemp, subject to ever-evolving legislation and regulatory actions, and as a medicine, such as Epidiolex (CBD only) and Sativex (THC and CBD in a 1:1 ratio), with specific indications of worldwide approval. Epidiolex is currently approved by both the European Medical Agency and the Food and Drug Administration (FDA) against seizures associated with Lennox-Gastaut syndrome or Dravet in patients 2 years of age and older, based on high-quality scientific evidence from randomized controlled clinical trials *(Cerino, P. et al., 2021; EMCDDA, 2018*).

CONCLUSIONS

The growing demand for dietary supplements with increased efficiency in managing various health problems and the complexity of the structure of hemp (Cannabis sativa L.) have contributed to the increase in its use in the nutraceutical field. The plant has also received increased attention from scientists who have been looking at potential alternatives to conventional medicines.

Numerous studies confirm the antioxidant and anti-inflammatory effects of hemp seeds and hemp products. Hemp seeds stand out for their remarkable content of quality proteins, including albumin and edestine which contribute to an exceptional nutritional value. They are also rich in healthy lipids with a high content of polyunsaturated fatty acids, such as linoleic acid (omega-6), alpha-linolenic acid (omega-3) and some vitamins (vitamins E, D and A).

Extracts made from hemp, especially those containing a high amount of cannabidiol (CBD), have important complex biological effects, including blocking the growth of cancer cells.

The antiviral applications of cannabis and its bioactive compounds have been studied especially in the context of SARS-CoV-2, as cannabinoids can prevent the penetration of the virus and influence immune system responses. Hemp seed oil may have positive effects on the treatment of chronic-inflammatory and neurodegenerative diseases.

The results of research suggest that traditional medicine is used as an adjunct therapy to modern medicine. The bioactive compounds in each part of the hemp plant lead to a future trend to capitalize on the entire plant, in the context of changing the diet globally and managing waste as efficiently as possible.

ACKNOWLEDGEMENT:

This research was supported by Project ADER 16.1.1 /29.01.2024 Research on the potential for superior exploitation of the Cannabis sativa species for food purposes, funded by Ministry of Agriculture and Rural Development. The research was also financed by Project PN 23 04 02 01, Contract no.: 9N/ 01.01.2023 SUSTAIN–DIGI -AGRI, Innovative biofertilizer production technology used to restore soil biodiversity and reduce the effects of drought on agricultural lands.

REFERENCES

[1] Aloo, S.O., Mwiti, G., Ngugi, L. W., & Oh, D. H. (2022). Uncovering the secrets of industrial hemp in food and nutrition: The trends, challenges, and new-age perspectives. Critical Reviews in Food Science and Nutrition, 64(15), 5093–5112. https://doi.org/10.1080/10408398.2022.2149468

[2] Cerino, P., Buonerba, C., Cannazza, G., D'Auria, J., Ottoni, E., Fulgione, A., Di Stasio, A., Pierri, B. and Gallo, A. (2020). A Review of Hemp As Food and Nutritional Supplement, Cannabis and Cannabinoid Research, vol. X, Number X, *Mary Ann Liebert*, Inc., DOI: 10.1089/can.2020.0001

[3] Christodoulou, M.C., Rodosthenous, P., Neophytou, C.M. (2025). Unveiling the Antioxidant Role of Hemp Oils in Cancer Prevention and Treatment. Cancers, 17, 2128. https://doi.org/10.3390/cancers17132128

[4] European Monitoring Centre for Drugs and Drug Addiction (EMCDDA), (2018). Cannabis Legislation in Europe; EMCDDA: Lisbon, PortugalISBN 978-92-9497-328-3

[5] Farinon, B., Molinari, R., Costantini, L., Merendino, N. (2020). The Seed of Industrial Hemp (Cannabis sativa L.): Nutritional Quality and Potential Functionality for Human Health and Nutrition. Nutrients, 12, 1935. https://doi.org/10.3390/nu12071935

[6] Harrison, J., VanDolah, B.A., Brent, A., Bauer, M.D., Karen, F., Mauck, M.D. (2019). Clinicians' Guide to Cannabidiol and Hemp Oils, Mayo Clinic Proceedings, vol. 94, Issue 9, pp. 1840-1851

[7] Jin, D., Dai, K., Xie, Z. et al. (2020). Secondary Metabolites Profiled in Cannabis Inflorescences, Leaves, Stem Barks, and Roots for Medicinal Purposes. Ski Rep 10, 3309 https://doi.org/10.1038/s41598-020-60172-6

[8] Khosravi, M., Asadikaram, G., Mehdiabadi, F.M., Nikvarz, N. (2021). The Effect of Hempseed Oil on Markers of Systemic Inflammation in Hemodialysis Patients: a single-blind randomized trial, Journal of Kerman University of Medical Sciences, 28(3): 236-242, 10.22062/JKMU.2021.91663

[9] Legare, C.A., Raup-Konsavage, W.M., Vrana, K.E. (2022). Therapeutic Potential of Cannabis, Cannabidiol, and Cannabinoid-Based Pharmaceuticals, Pharmacology, 107(3–4): 131–149, https://doi.org/10.1159/000521683

[10] Liktor-Busa, E., Largent-Milnes, T.M. (2025). Natural Products Derived from Cannabis sativa for Pain Management. In: Wainwright, C.L., Schini-Kerth, V.B. (eds) Natural Products as Sources of Novel Drugs. Handbook of Experimental Pharmacology, vol 287. Springer, Cham. https://doi.org/10.1007/164_2024_710

[11] Lin, Y., P. Pangloli, and V. P. Dia. (2021). Physicochemical, functional and bioactive properties of hempseed (Cannabis sativa L.) meal, a co-product of hempseed oil and protein production, as affected by drying process. Food Chemistry 350:129188. doi:10.1016/j.foodchem.2021.129188

[12] Mikulcová, V., Kašpárková, V., Humpolíček, P., Buňková, L. (2017). Formulation, Characterization and Properties of Hemp Seed Oil and Its Emulsions. *Molecules*, 22, 700. https://doi.org/10.3390/molecules22050700

[13] Miller, A., Kwiecień, I., Bednarski, M., Zygmunt, M., Sapa, J., Sablik, M., Lombardo, G.P., Condurso, C., Merlino, M., Kotańska, M. (2025). Promising Dietary Supplements with Potential Senotherapeutic Effects: Aqueous Extracts from Enzymatically Hydrolysed Hemp Seed Cake Flour and Hemp Seed Protein Concentrate. *Antioxidants*, 14, 734. https://doi.org/10.3390/antiox14060734

[14] Montero, L., Ballesteros-Vivas, D, Gonzalez-Barrios A.F. and Sánchez-Camargo Ad.P. (2023). Hemp seeds: Nutritional value, associated bioactivities and the potential food applications in the Colombian context. Front. Nutr. 9:1039180. doi:10.3389/fnut.2022.1039180

[15] Oyebode, O., Kandala, N.B., Chilton, P.J., Lilford, R.J. (2016). Use of traditional medicine in middle-income countries: a WHO-SAGE study, Health Policy and Planning, vol.31, Issue 8, pp. 984–991, https://doi.org/10.1093/heapol/czw022

[16] Qin, X., Yang X., Deng Y., Guo L., Li, Z. (2025). Cannabis Derivatives as Ingredients of Functional Foods to Combat the COVID-19 Pandemic, Foods, 14(16), 2830; https://doi.org/10.3390/foods14162830

[17] Rezapour-Firouzi, S., Shahabi, S., Mohammadzadeh, A., Tehrani, A., Kheradmand, F., Mazloomi, E. (2018). The potential effects of hemp seed/evening primrose oils on the mammalian target of rapamycin complex 1 and interferon-gamma genes expression in experimental autoimmune encephalomyelitis. Res. Pharm. Sci., 13, 523

[18] Salami, S.A., Martinelli, F., Glovino, A., Bachari, A., Arad, N., Mantri, N. (2020). It is our turn to get Cannabis high: Put cannabinoids in food and health baskets. Molecules, 25, 4036.

[19] Vági, E., Balázs, M., Komóczi, A., Kiss, I., Mihalovits, M., Székely, E. (2019). "Cannabinoids Enriched Extracts from Industrial Hemp Residues," Journal of Polytechnic Chemical Engineering, 63(2), pp. 357–363, https://doi.org/10.3311/PPch.12896

[20] *** https://www.mdpi.com/cancers/cancers-17-02128/article_deploy/html/images/cancers-17-02128-g003.png

[21] *** https://ars.els-cdn.com/content/image/1-s2.0-S0025619619300072-gr1.jpg

STUDIES AND RESEARCH ON THE TECHNOLOGICAL PROCESS OF REMOVING SOLID PARTICLES FROM WASTEWATER OF A RECIRCULATING AQUACULTURE FISH FARMING SYSTEM, BY USING TECHNICAL MECHANICAL FILTRATION EQUIPMENT

/

STUDII ȘI CERCETĂRI ASUPRA PROCESULUI TEHNOLOGIC DE ÎNDEPĂRTARE AL PARTICULELOR SOLIDE DIN APĂ REZIDUALĂ A UNUI SISTEM ACVACOL RECIRCULANT DE CREȘTERE A PEȘTILOR, PRIN UTILIZAREA UNUI ECHIPAMENT TEHNIC DE FILTRARE MECANICĂ

Evelin-Anda LAZA*[1)], Dragoș Vasile NICA[1)], Ioan Ladislau CABA[1)], Ana-Cristina VASILE[2)], Aurelian GRUIN[2)]

[1)] National Institute of Research - Development for Machines and Installations Designed for Agriculture and Food Industry - INMA Bucharest / Romania;

[2)] NIRD URBAN-INCERC Timisoara Branch, 2 Traiana Lalescu Street, Timisoara, Timis County / Romania.

**Tel: 0741 122 570; *E-mail: eveline-anda@yahoo.com*

Keywords: *aquaculture, mechanical filtration, water filtration*

ABSTRACT

For recirculating aquaculture system (RAS) maintaining physico-chemical characteristics of the water at an optimum level for breeding species, is one of the main goals to be achieved in order to talk about what a successful aquaculture means. Technological developments in the field of mechanical filtration in recent decades have contributed in a decisive way in terms of waste water filtration process within a recirculating system, with the aim to improve its quality, but not least significant reduction of waste that are released into the environment. This paper aims to develop a description of the situation that exists both global and national levels on the range of mechanical water filtration equipment that are used in a RAS.

REZUMAT

Pentru sistemul de acvacultură cu recirculare (SAR), menținerea caracteristicilor fizico-chimice ale apei la un nivel optim pentru speciile de reproducere este unul dintre principalele obiective care trebuie atinse pentru a vorbi despre ce înseamnă o acvacultură de succes. Dezvoltările tehnologice în domeniul filtrării mecanice din ultimele decenii au contribuit într-un mod decisiv în ceea ce privește procesul de filtrare a apelor uzate în cadrul unui sistem de recirculare, cu scopul de a îmbunătăți calitatea acestora, dar nu în ultimul rând de a reduce semnificativ deșeurile care sunt eliberate în mediu. Această lucrare își propune să dezvolte o descriere a situației existente atât la nivel global, cât și național, privind gama de echipamente mecanice de filtrare a apei utilizate într-un SAR.

INTRODUCTION

In order that a recirculating acvacol system to be economic, it must have reliable and efficient technology that are able to maximize the production *(Steven T. Summerfelt, 1998)*. The technological installations that are found in a recirculating system must ensure the optimal conditions for the growth and development of crop species, by reconditioning the water which is recycled within the system (*Interdonato Filippo, 2012; Victor Cristea, Iulia Grecu, Cornel Ceapa, 2002)*.

One of the main problems of recirculating systems is the problem of removing of solid particles. It was estimated that around 60% of the food introcuced into the system remains unconsumed and is transformed in residual solids *(Michael P. Masser, James Rakocy and Thomas M. Losordo, 1999).*

According to him *(Ariel. E and Jutta. P, 2014),* the quantity of waste from a recirculating system is directly proportional to the fish production within the system *(Interdonato Filippo, 2012).*

Still from the design stage of a recirculating system, focus must fall on controlling and removing the solid particles coming from the unconsummated feed, faecal matter and bacterial biomass, to prevent in this way the supplementary consumption of oxygen, the uncontrolled increase of the amount of carbon dioxide

and of the ammoniacal nitrogen, compounds particularly toxic for fish *(Joanna G. Twarowska, 1997; Keith Jeffery, 2011; Steven T. Summerfelt, 1998)*.

To reduce the amount of solids in the tanks for growth, solids that can negatively affect the physical and chemical factors of the water, is needed the use of mechanical filtration equipment, dimensioned so as to be capable of removing the organic matter accumulated in the system *(Thomas M. Losordo, Michael P. Masser and James Rakocy, 1998)*.

Mechanical filtration is one of the major processes of controlling the solid particles from the recirculating system *(Shulin Chen și Ronald F. Malone 1991)*. The role of mechanical filtration as the first water filtration process of RAS is all the more important because of it depends the success of all other stages which will follow in the filtering process *(James M. Ebeling).*

The principle underlying the mechanical filtration refers to the fact that the wastewater coming from the growing tanks passes through a filtering material which is intended to retain the solid particles from water *(Samir Ahmad Ali, 2012).* The filtering material present in filters consists of: sand, gravel or various types of sieves made textile materials or non-corrosive metals *(Michel Couturier et. all 2009).*

To remove suspended solids in recirculating systems *(Losordo et al., 1998)* affirm that are specifically used two types of mechanical filters: drum filter and sand filter *(Pop Augustin, colab.2009; Alessandro Moretti, 2005)*.

MATERIALS AND METHODS

In the field of mechanical filtration at present there are a number of devices that can cover a wide range of applications in the acvacol field, the way in which are classified the filtering processes which are used particularly in aquaculture is made according on the nature of the filtering medium: filtration with sieves and filtration with granular agents *(Brinker, A., Bergheim, A.., 2005).*

As regards the equipments for mechanical filtering with sieves, the largest shares are occupied by the following types of filters: axial filters with rotating sieves, radial filters with rotating sieves and chain filters with sieve. Among the consecrated companies manufacturing mechanical filters for recirculating acvacole systems we mention: Hydrotech - Sweden, FIAP – Germany, Faivre – France, Akva- Denmark.

Nationally one of the companies producing installations designed to the acvacol sector is the company EuroCar - Oradea, and one of the products made by them, which was successfully implemented in several fish farms in Romania is the drum filter.

Mechanical filtration with sieves is the most common method in the filtering process widely in commercial Aquaculture and research.

The mode of action of these type of filters is that the water loaded with solid particles passes through a system of sieves, the sieves retaining only the particles of equal size or larger than the sieve meshes *(Fred Wheaton, 2002)* Sieves dimensioning is based on the charging degree of the water with solid particles (TSS) and of the granulometric composition of them *(Bura Marian, 2008).*

Currently at a worldwide there are no farms with the recirculation of the water evacuated from the tanks which does not use the filters with microsieves, this and because they occupy a relatively small space, not require the same physical effort as in the case of the sumps when carrying out the maintenance and cleaning works *(Fred Wheaton, 2002).* In the case of filtering with sieves the filtering capacity is given by the mesh size of the sieve ranging between 40 – 100 μm, and according to Jelenna Stokic, 2012 between 60 - 200 μm *(Jelena Stokic, 2012).* Cripps and Bergheim, 2000 quoted by *(Couturier et al., 2009),* concluded that the use of filtration equipment with microsieves with a mesh size less than 60 mm, are not recommended due to the risk of the clogging phenomenon *(Keith Jeffery, Nicholas Stinton & Tim Ellis, 2011).*

The filters with rotary sieves, according to (Tchobanoglous and Burton, 1991), represent the most efficient solution to the conventional alternative by sedimentation of solid particles and for this reason these have been successfully implemented on the acvacole farms *(Samir Ahmad Ali, 2012).*

The functioning of the filters with rotary sieves, no matter if we speak of the axial or radial ones in both cases these will work only if they are partially immersed in the water to be filtered *(James H. Tidwell, 2012).* To clean strainers, both the radial filters with rotary sieve and the axial filters with rotary sieve are equipped with a system of spraying nozzles disposed above the drum or in the case of axial filter the nozzles are fixed on the downstream side of the sieve, in this way it is done the washing of the retained solid particles *(Odd- Ivar Lekang, 2007).*

Drum filtering is the predominant technology for the removal of solids with the widest spread worldwide and as the degree of use in recirculating *systems (James M. Ebeling, Carla F. Welsh, Kata L.*

Rishel, 2006). This is due primarily to the filtering capacity that can be adjusted according to the charging with solid suspensions of the recirculating system. Normally, the mechanical filters are able to remove the solid particles larger than 40 - 100 μm, whilst states that the mechanical filters are designed to remove only can particles larger than 80 μm *(Odd- Ivar Lekang, 2007)*. It is specified in the literature that a drum filter can remove about 40% of the total of solids in suspension *(Henrik Mortensen, 2014*).

The working principle of the drum filter is relatively simple, water loaded with solid particles in suspension (TSS) is entering the drum filter in an axial direction and is coming out filtered in a radial direction. During the filtering process as the network mesh of sieve from the drum filter is loaded with solids the water level rises, switching on the spray equipment. Then washed solid material is collected in a trough and discharged outside the system *(Bura Marian, 2008).*

Usually, to wash the sieves of a drum filter is used an amount of 0.2 to 2% of the volume of water through the use of the high-pressure water jet [3]. The main disadvantage of this type of filter is the costs of maintenance and operation of it *(James H. Tidwell, 2012).*

Fig. 1 - Radial filter with rotating

RESULTS

The experiments on the mechanical water filtration installation were carried out under laboratory conditions by integrating this technical equipment into the circuit of an aquaculture system. The utilities necessary for the experiments, namely the electricity supply, fresh water supply and waste water evacuation, were provided.

The mechanical water filtration system has the role of ensuring the proper quality of the water supplied to the growth tanks. This is achieved using a rotating drum type filter.

The rotating screen is a high-capacity filter with much smaller dimensions than other screens used in solid-liquid separation. The filtration rate is five times higher in the case of this type, compared to static screens, and the possibility of it being blocked by residues is practically nil because they have a self-cleaning system.

The water flow with suspended solid particles enters the drum axially and exits filtered in a radial direction, through the mesh network of the screen.

The maximum filtration capacity of this screen is 50 m^3/hour.

The physical and chemical characteristics of the water at the exit of the mechanical filter are presented in table 1.

Table 1

The physical and chemical characteristics of the water at the exit of the mechanical filter

Waste	40 μm	60 μm	90 μm
Total phosphorus	65 – 84 %	50 – 80 %	45 – 75 %
Total nitrogen	25 – 32 %	20 – 27 %	15 – 22 %
Solids in suspensions	60 – 91 %	55 – 85 %	50 – 80 %

CONCLUSIONS

To have a successful aquaculture first of all of performant equipments, competitive, that to maximize the fish production.

To increase the fish production and minimize any loss, we need that the water recycled through system to be correctly filtered.

For this reason it is essential to know which are the most efficient equipment for the removal of the solid particles within a recirculating system and for this we must to know what exist today on the market.

One of the most appreciated filtration equipment within a RAS, due to its effectiveness is the drum filter.

REFERENCES

[1] Alessandro Moretti, (2005), *Manual on Hatchery Production of Seabass and Gilthead Seabream* http://www.fao.org/docrep/008/y6018e/y6018e04.htm.

[2] Ariel E Turcios, Jutta Papenbrock, (2014), *Sustainable Treatment of Aquaculture Effluents—What Can We Learn from the Past for the Future?* , Sustainability, Volume 6, Issue 2, pp 836.

[3] Brinker, A., Bergheim, A., (2005), *Waste treatment in fish farms. In: Water encyclopedia 1: Domestic, municipaland industrial water supply and waste disposal* (eds Lehr, J.H., Keeley, J.). pp. 681–684. Wiley- Interscience.

[4] Bura Marian., (2008). *Manual for the presentation and use of sturgeon farming technology in a super-intensive system with recirculated water*, Edt. EUROBIT.

[5] Fred Wheaton, (2002) *Recirculating Aquaculture Systems: An Overview ofWaste Management*, University of Maryland, http://www.aces.edu.

[6] Henrik Mortensen, (2014), *Microscreens, Efficiencies in Aquaculture Systems*, http://www.atlantech.ca

[7] Interdonato Filippo, (2012), *Recirculating aquaculture system (RAS) biofilter: focusing on bacterial communities complexity and activity*, Universita DegliStudi Di Messina, http://archimer.ifremer.fr.

[8] James M.Ebeling, Brian Vinci – *Solid Capture*, https://ag.arizona.edu

[9] James M. Ebeling, Carla F. Welsh, Kata L. Rishel ,(2006), *Performance Evaluation of the Hydrotech Belt Filter in Intensive Recirculating Filter in Intensive Recirculating Aquaculture SystemsAquaculture Systems*, http://ag.arizona.edu.

[10] James H. Tidwell, (2012), *Aquaculture Production Systems*, ISBN 978-0-8138-0126-1, Wiley-Blackwell.

[11] Jelena Stokic (2012), *Particle size distribution in the Tilapia Recirculating Aquaculture System*, Norway.

[12] Joanna G. Twarowska, Philip W. Westrrman, Thomas M.Losordo,(1997), *Water Treatment and Waste Characterization Evaluation of an Intensive Recirculating Fish*, Aquacultural Engineering, Volume 16, Issue 3, pp 133- 147.

[13] Keith Jeffery, Nicholas Stinton & Tim Ellis, (2011), *A review of the land- based, warm-water recirculation fish farm sector in England and Wales*, http://www.fishfrom.com

[14] Michael P. Masser, James Rakocy and Thomas M. Losordo, (1999), *Recirculating Aquaculture Tank Production Systems Management of Recirculating Systems* - SRAC Publication No. 452.

[15] Michel Couturier, Therese Trofimencoff, Jose´ Utge Buil, Jessica Conroy, (2009), *Solids removal at a recirculating salmon-smolt farm*, Aquacultural Engineering, Volumes 41, www.elsevier.com.

[16] Odd- Ivar Lekang (2007), *Aquacultural Engineering*, ISBN: 978-1-4051-2610-6, Blackwell Publishing Ltd,pp 47.

[17] Pop Augustin, colab. (2009), *Considerations upon energetic efficiency of a recirculating aquatic system (RAS) for super intensive fish culture*, edt. Bioflux pag 155, Vol 2(2).

[18] Ronald Malone, (2013), *Recirculating Aquaculture Tank Production Systems A Review of Current Design Practice*, SRAC Publication No.453.

[19] Samir Ahmad Ali, (2012), *Design and evaluate a drum screen filter driven by undershot waterwheel for aquaculture recirculating systems*, Aquacultural Engineering, AQUE – 1658, pp 38-44, ELSEVIER .

[20] Steven T. Summerfelt, (1998), *An Integrated Approach to Aquaculture Waste Management in Flowing Water Systems, Recirculating Aquaculture*, pp 98, SYMPOSIUM 4 - Waste Management.

[21] Steven T.Summerfelt,(1998), *Engineering Design of Modular and Scalable Recirculating Systems ContainingCircular Tanks, Microscreen Filters, Fluidized-Sand Biofilters, Cascade Aerators, and Low-Head or U-Tube Oxygenators*, pp 421.

[22] Shulin Chen și Ronald F. Malone (1991), *Suspended Solid Control In Recirculating Aquacultural Systems, Engineering Aspects of Intensive Aquaculture,* p 170 – 186.

[23] Thomas M. Losordo, Michael P. Masser and James Rakocy (1998), *Recirculating Aquaculture Tank Production Systems An Overview of Critical Considerations*, SRAC Publication No.451.

[24] Victor Cristea, Iulia Grecu, Cornel Ceapa (2002), *Recirculating Aquaculture Systems Engineering,* Edt. Didactică și pedagogică, R.A.

INTEGRATED MECHANICAL AND METABOLIC ENGINEERING STRATEGIES FOR HIGH-CELL-DENSITY CULTIVATION OF *SACCHAROMYCES CEREVISIAE* IN STIRRED-TANK BIOREACTORS: A CRITICAL REVIEW

/

STRATEGII INGINEREȘTI MECANICE ȘI METABOLICE INTEGRATE PENTRU CULTIVAREA LA DENSITATE RIDICATĂ A SACCHAROMYCES CEREVISIAE ÎN BIOREACTOARE CU AGITARE MECANICĂ: O ANALIZĂ CRITICĂ

Elena-Valeria VLĂDUȚ*, Sorin-Ștefan BIRIȘ, Mariana FERDEȘ, Adrian IOSIF, Alina-Daiana IONESCU, Raluca Adriana ZOTA

National University of Science and Technology Politehnica Bucharest / Romania.

**Tel: (+40) 739 960 285; *E-mail: elena.vladut@upb.ro*

Keywords: *saccharomyces cerevisiae, bioreactor, agitation speed, optical density, oxygen transfer, process analytical technology*

ABSTRACT

Saccharomyces cerevisiae remains the dominant eukaryotic model in industrial biotechnology, with extensive applications in food, beverage, pharmaceuticals, and biofuels. Achieving high-cell-density cultivation (HCHC) in stirred-tank bioreactors requires a delicate integration of mechanical engineering strategies (impeller design, hydrodynamics, gas-liquid mass transfer) with metabolic regulation (substrate feeding, nutrient balance, mitigation of the Crabtree effect). This review provides a comprehensive and critical synthesis of recent advances in STR design and operation for yeast cultivation, highlighting the interplay between oxygen transfer dynamics, shear forces, and metabolic adaptations. Recent advances highlight the role of process analytical technology (PAT) and computational fluid dynamics (CFD) in enhancing real-time monitoring, improving predictive modelling, and facilitating more reliable scale-up of yeast cultivation processes.

REZUMAT

Saccharomyces cerevisiae rămâne modelul eucariotic dominant în biotehnologia industrială, având aplicații extinse în domeniul alimentar, farmaceutic și energetic. Obținerea unor culturi la densitate celulară ridicată (HCDC) în bioreactoare cu agitare mecanică presupune integrarea atentă a strategiilor inginerești mecanice (designul agitatoarelor, hidrodinamica, transferul de masă gaz-lichid) cu reglarea metabolică (hrănirea cu substrat, echilibrul nutrițional, reducerea efectului Crabtree). Această analiză oferă o sinteză cuprinzătoare și critică a progreselor recente în proiectarea și operarea bioreactoarelor cu agitare mecanică pentru cultivarea drojdiilor,subliniind interacțiunea dintre dinamica transferului de oxigen, forțele de forfecare și adaptările metabolice. Se evidențiază rolul tehnologiilor PAT și al dinamicii fluidelor computaționale (CFD) în monitorizarea avansată, modelarea predictivă și susținerea scalării fiabile a proceselor de cultivare a drojdiilor.

INTRODUCTION

The yeast *Saccharomyces cerevisiae* has been the heart of human civilization for millennia. Its use in bread, beer, and wine production dates back to ancient Egypt and Mesopotamia *(Parapouli et al., 2020*). Today, it remains indispensable not only for traditional food and beverage fermentation but also for modern biotechnology sectors, including bioethanol, biopharmaceuticals, fine chemicals, and heterologous protein-production *(Nandy & Srivastava, 2018; Stanbury et al., 2016)*. The global industrial yeast market has grown steadily, with bioethanol alone accounting for more than 100 bilion liters annually, much of it produced by *S. cerevisiae (Mussatto, 2010)*.

Saccharomyces cerevisiae was the first eukaryotic organism to have its entire genome sequenced *(Goffeau et al., 1996)*, reinforcing its status as both a model organism and an industrial workhorse. Its Generally Recognized As Safe (GRAS) designation makes it particularly attractive for pharmaceutical and food applications *(Parapouli et al., 2020)*. However, high-cell-density cultivation (HCDC), often targeting biomass concentrations >50 g/L dry cell weight (DCW), remains technically demanding. The major

engineering bottleneck in STR-based cultivation is oxygen transfer. Oxygen solubility in aqueous broths is extremely low (~7–8 mg/L at 30 °C), while yeast demands high oxygen uptake rates for biomass and metabolite production *(Garcia-Ochoa et al., 2010)*. Scale-up from 5 L laboratory STRs to >5000 L industrial bioreactors typically reduces kLa by more than 50%, while increasing mixing times tenfold *(van't Riet & Tramper, 1991; Shuler & Kargi, 2017)*. These gradients create metabolic heterogeneity, limiting process robustness *(Arulrajah et al., 2025)*.

On the metabolic side, yeast exhibits the Crabtree effect: when glucose concentrations exceed ~40 g/L, fermentative metabolism dominates even the presence of oxygen, resulting in ethanol accumulation and reduced biomass yields *(Malairuang et al., 2020)*. Overcoming this requires controlled feeding strategies, nutrient supplementation, and, in some cases, immobilization approaches *(Călinescu et al., 2012)*.

And of course, recent advances in digitalization are reshaping the engineering of yeast bioprocesses. Computational fluid dynamics (CFD) has emerged as a powerful tool to resolve spatial heterogeneities by simulating oxygen distribution, mixing patterns, and localized shear environments within large-scale bioreactors *(Susukida et al., 2025)*. In parallel, process analytical technology (PAT) provides real-time, data-rich monitoring of key variables such as dissolved oxygen, pH, and biomass, enabling dynamic adjustments of cultivation conditions *(Brudes et al., 2016; Yousefi- Darani et al., 2021*).

The convergence of CFD-based modelling with PAT-driven monitoring establishes the foundation for predictive and adaptive control strategies, thereby bridging classical fermentation engineering with modern data-driven approaches for robust STR-based yeast cultivation.

BIOREACTOR HYDRODYNAMICS AND OXYGEN TRANSFER

Stirred-tank bioreactors (STRs) continue to represent the benchmark configuration for aerobic yeast processes owing to their scalability and operational flexibility. Within these systems, hydrodynamic performance is largely dictated by impeller geometry, baffle arrangement, and power input, all of which govern oxygen transfer and mixing efficiency. Radial-flow impellers such as Rushton turbines are capable of delivering high gas dispersion, achieving kLa values in the range of 200-400 h^{-1} at 600 rpm in laboratory-scale reactors; however, this performance is often accompanied by elevated shear stresses than can compromise cell viability *(van't Riet & Tramper, 1991; Garcia-Ochoa et al., 2010)*. In contrast, axial-flow shear loads, though at the expense of lower oxygen transfer rates, typically around 150 h^{-1}. Pitched-blade turbines provide an intermediate solution, balancing mixing efficiency with shear tolerance, while multi-impeller arrangements are frequently employed in tall industrial vessels to ensure homogeneity across large working volume *(Stanbury et al., 2016)*.

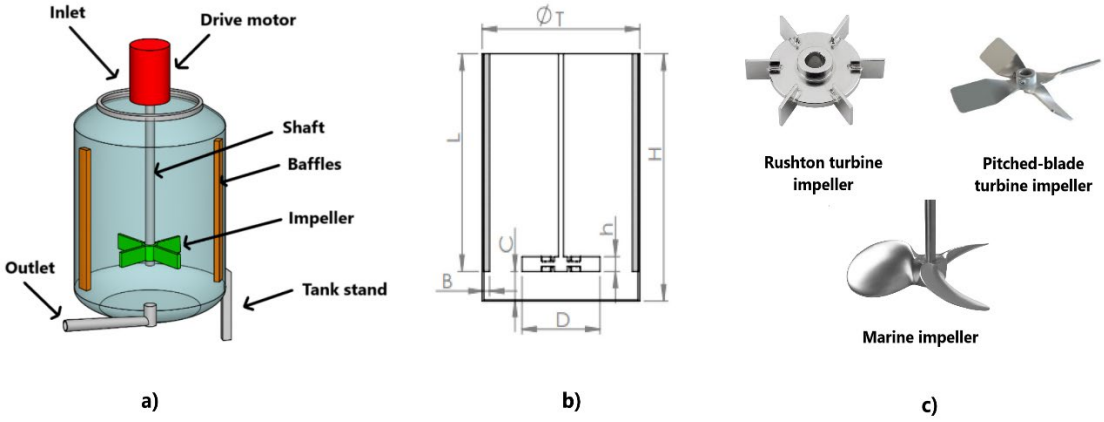

Fig. 1 - Schematic representation and dimensional drawing of the stirred-tank bioreactor (a–b), and examples of impeller geometries: (a) Rushton turbine impeller (radial-flow), (b) pitched-blade turbine impeller (mixed-flow), and (c) marine impeller (axial-flow)
(adapted from Torotwa, I. et al. 2018)

As illustrated in Figure 1, the stirred-tank bioreactor is typically equipped with baffles and a centrally mounted impeller, whose geometry plays a decisive role in shaping the hydrodynamic environment. Among the most widely adopted designs, the Rushton turbine (radial-flow) is recognized for its ability to promote intense gas dispersion and high oxygen transfer rates, though often at the cost of increased shear stress. In contrast, pitched-blade turbines generate a mixed-flow pattern that provides a more balanced compromise between oxygen availability and mechanical stress, making them suitable for processes involving moderately

shear-sensitive microorganisms. Marine impellers, characterized by their axial-flow configuration, are frequently applied when reduced shear conditions are prioritized, albeit with comparatively lower kLa values.

The selection of impeller design thus directly influences mixing efficiency, oxygen transfer capacity, and ultimately the physiological response of *Saccharomyces cerevisiae*. In this context, Tabel 1 summarizes reported kLa values for *Saccharomyces cerevisiae* in stirred-tank bioreactors of different scales, explicitly highlighting the influence of impeller design in conjunction with agitation and aeration conditions.

Tabel 1

Reported kLa values in stirred-tank bioreactors for Saccharomyces cerevisiae and related systems (with impeller types)

Scale / Bioreactor	Agitation (rpm)	Aeration (vvm)	kLa (h^{-1})	Impeller type / configuration	Notes / Organism & medium	Reference
5 L laboratory STR	300	1.0	~120	Rushton turbine (radial-flow)	Standard yeast cultivation / aqueous medium	Zhuang et al., 2021
5 L laboratory STR	600	1.5	300–350	Rushton turbine (radial-flow)	High agitation, enhanced oxygen transfer	Garcia-Ochoa et al., 2010
20 L pilot STR	450	1.0	~200	Pitched-blade turbine (mixed-flow)	Pilot-scale yeast cultivation	Suresh et al., 2009
5000 L industrial STR	150	0.5	< 50	Marine impeller (axial-flow)	Industrial scale, low shear operation	van't Riet & Tramper, 1991
5 L laboratory STR	250	~5 L/min airflow	~20	Rushton / propeller impeller	Bench-top STR, reported kLa in s^{-1} converted to h^{-1}	Ramírez et al., 2020
Laboratory fermenter	Variable	-	-	Rushton vs pitched-blade	Comparative analysis of kLa under different setups	Paciello & Parascandola, 2020
STR (general review)	-	-	-	Hollow-blade impeller	Improved gas handling reported	Schaepe et al., 2013
STR with multiple impellers	400-800	-	+23–77% (gain)	Dual Rushton turbines	Performance increase compared to single impeller	Karimi et al., 2013

As shown in Tabel 1, reported kLa values for *Saccharomyces cerevisiae* in stirred-tank bioreactors vary substantially across scales and impeller designs. Laboratory-scale systems equipped with Rushton turbines often achieve high oxygen transfer rates. They can exceed 300 h^{-1} under high agitation *(Garcia-Ochoa et al., 2010)*, while moderate conditions yield ~120 h^{-1} *(Zhuang et al., 2021)*. Pitched-blade turbines in pilot reactors typically reach ~200 h^{-1} *(Suresh et al., 2009)*, whereas industrial STRs with marine impellers operate below 50 h^{-1} due to lower agitation and aeration *(van't Riet & Tramper, 1991)*. Comparative studies confirm the influence of geometry, with pitched-blades providing lower shear than Rushtons *(Paciello & Parascandola, 2020)*, dual Rushtons improving transfer efficiency *(Karimi et al., 2013)*, and hollow-blade designs enhancing gas handling *(Schaepe et al., 2013)*. Overall, impeller selection remains a key determinant of oxygen transfer and shear environment in yeast bioprocesses.

MECHANICAL STRESS AND YEAST PHYSIOLOGY

In stirred-tank systems, the physiological impact of hydrodynamics on *Saccharomyces Cerevisiae* depends strongly on energy dissipation and the flow field set by impeller design. Continuous-culture

experiments spanning mean specific energy dissipation rates from ~0.045 to 6 W kg^{-1} reported only transient, sublethal perturbations at the upper end, indicating high shear tolerance of brewing yeast under STR conditions *(Boswell et al., 2003)*. High-cell-density runs with dual Rushton turbines at 2–4 W kg^{-1} likewise maintained robust growth and productivity, consistent with yeast's resilience to the shear levels typical of laboratory STRs *(Malairuang et al., 2020)*.

Conversely, low-shear scale-up strategies that fix $\bar{\varepsilon}$ at ~0.10 W kg^{-1} across 5–3000 L have achieved comparable ethanol productivities, illustrating that oxygen supply can be decoupled from aggressive mixing when mass-transfer is engineered appropriately (*Beigbeder et al., 2021)*. Local stress still matters: controlled devices show viability drops beyond ~1.3–2.8 kPa shear stress, and regions behind radial turbines can exhibit very high local dissipation compared with the vessel average *(Daub et al., 2014)*. Together these data indicate that impeller choice governs the shear/oxygen trade-off, but yeast remains comparatively tolerant over the $\bar{\varepsilon} \approx$ 0.1–4 W kg^{-1} window commonly used in aerobic processes.

Tabel 2

Shear tolerance of *Saccharomyces cerevisiae*

Energy dissipation / Shear	Impeller / System	Observed effect on viability / growth	Notes	Reference
0.045–6 W kg^{-1}	Aerated STR (continuous)	No lasting viability loss; only transient sublethal signals at >~4.5 W kg^{-1}	Brewing yeast; multiparameter flow cytometry	Boswell et al., 2003
2–4 W kg^{-1}	Dual Rushton turbines (5 L)	High-cell-density growth sustained	Robust performance	Malairuang et al., 2020
~0.10 W kg^{-1} (fixed across scales)	STRs 5–3000 L	Comparable ethanol productivities across scales; no evidence of shear-related loss	Low-shear scale-up criterion	Beigbeder et al., 2021
1.3–2.8 kPa (local shear stress)	Controlled shear device	Onset of viability decrease above threshold	Shear reported as stress (Pa), not W kg^{-1}	Lange et al., 2001
-	STR/shake systems	Highlights heterogeneity of local dissipation; relevance for hot-spots	Method to estimate e_{max} in small vessels	Daub et al., 2014
local dissipation behind blades	Rushton region	Very high local dissipation possible near blades vs vessel average	-	Hewitt et al., 2010

Overall, hydrodynamic control, rather than agitation intensity alone, governs *Saccharomyces cerevisiae* performance, with impeller geometry setting the operative trade-off between oxygen delivery and mechanical load. Practical scale-up should target the required oxygen transfer at the lowest feasible mean dissipation while limiting local hot-spots via impeller selection, multi-impeller configurations, and baffling.

METABOLIC AND NUTRITIONAL STRATEGIES

Metabolic control must be co-engineered with hydrodynamics. In batch cultivation on high initial glucose (≈50 g L^{-1}), *S. cerevisiae* rapidly enters the Crabtree regime, diverting carbon to ethanol at the expense of biomass, a pattern well documented in standard practice *(Stanbury et al., 2016)*. Glucose-limited fed-batch strategies that maintain the residual substrate below the Crabtree threshold (<0.5g L^{-1}) suppress overflow metabolism and substantially increase cell density, an outcome mirrored by maltodextrin/dextrin feeding that delivers glucose gradually and supports high-cell-density cultivation *(Malairuang et al., 2020)*.

Beyond suspended cultures, immobilization (e.g., calcium-alginate or polyacrylamide matrices) stabilizes the biocatalyst and can improve ethanol productivity under industrial conditions *(Călinescu et al., 2012)*, consistent with classic reports of higher production rates and multi-cycle reusability for alginate-entrapped yeast.

Meanwhile, cell-retention membrane bioreactors (MBRs) provide an alternative route to HCDC and product accumulation; although widely deployed for oleaginous yeasts, they illustrate how decoupling growth from washout can outperform conventional STRs for certain products *(Koruyucu et al., 2023)*.

Tabel 3

Feeding and immobilization strategies

Strategy	Substrate/ Control Target	Max DCW (g L^{-1})	Ethanol accumulation	Reference
Batch	Glucose 50 g L^{-1}	25-30	High	Stanbury et al., 2016
Fed-batch	Glucose maintained <0.5 g L^{-1}	45-50	Low	Malairuang et al., 2020
Fed-batch	Maltodextrins / dextrin feeding	55-60	Minimal	Malairuang et al., 2020
Immobilized	Glucose 80 g L^{-1}	>40	Moderate	Călinescu et al., 2012

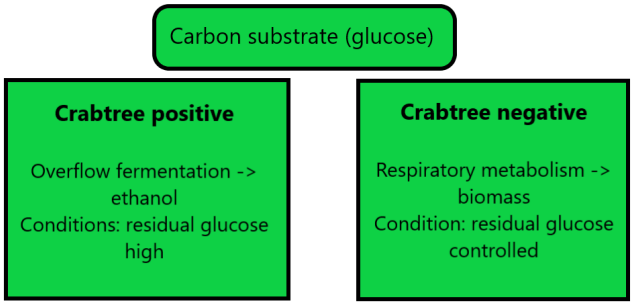

Fig. 2 - Metabolic routing under high vs controlled residual glucose: overflow fermentation versus oxidative growth in S. cerevisiae

(adapted from Dashko, S.et al.2014)

SCALE-UP AND INTEGRATIVE SOLUTIONS

Scaling to m^3 vessels amplifies transport non-linearities: mixing slows and DO/pH/substrate gradients appear, driving metabolic heterogeneity as cells cycle through aerobic-anaerobic microenvironments *(Arulrajah et al., 2025)*. CFD helps localize the origin of these hot and cold spots and predicts shear/mixing distributions around impellers and gas cavities *(Zhang et al., 2019; Susukida et al., 2025)*. Practically, two levers dominate: (i) oxygen transfer, improved by oxygen enrichment of moderate overpressure, and (ii) bulk mixing, improved by axial or multi-impeller shafts and CFD guided sparger/impeller placement *(Garcia-Ochoa et al., 2010; Zhuang et al., 2021)*.

In parallel, PAT (Raman/fluorescence probes with soft sensor models) enables real-time state estimation and faster corrective action; coupled with data-driven control, “smart” bioreactors move from reactive to predictive operation *(Bruder et al., 2016; Yousefi-Darani et al., 2021; Zhuang et al., 2021)*. Finally, hybrid configurations mitigate scale constraints: immobilized yeast stabilizes performance under stresses, while cell-retention membrane systems sustain high cell density and product accumulation (Călinescu et al., 2012; Koruyucu et al., 2023).

To illustrate how the engineering maneuvers proposed here (CFD-guided impeller/sparger design and PAT-assisted control) address scale-dependent heterogeneity, we include two CFD examples. Figure 3 visualizes where dissipation and shear concentrate in a double-impeller STR, explaining hot spots, recirculation boundaries, and low-shear cores. Blade-wake/tip-vortex hot spots and the impeller-impeller interaction zone delineate recirculation boundaries and a low-shear core, providing a mechanistic basis for axial or multi-impeller layouts, spacing/clearance optimization, and targeted sparger placement *(Ebrahimi et al., 2019)*.

Meanwhile, figure 4 shows logarithmic shear-rate fields with streamlines across geometries and speeds, highlighting boundary layers at baffles, recirculation cells, and stagnation pockets. High shears localizes near impeller blades and within the baffle boundary layer, while recirculation cells and stagnation pockets appear in the bulk and depend on impeller geometry/clearance; these patterns motivate CFD-guides choices of impeller type/spacing and sparger layout, completemented by PAT for real time supervision *(Šafarič et al., 2019)*.

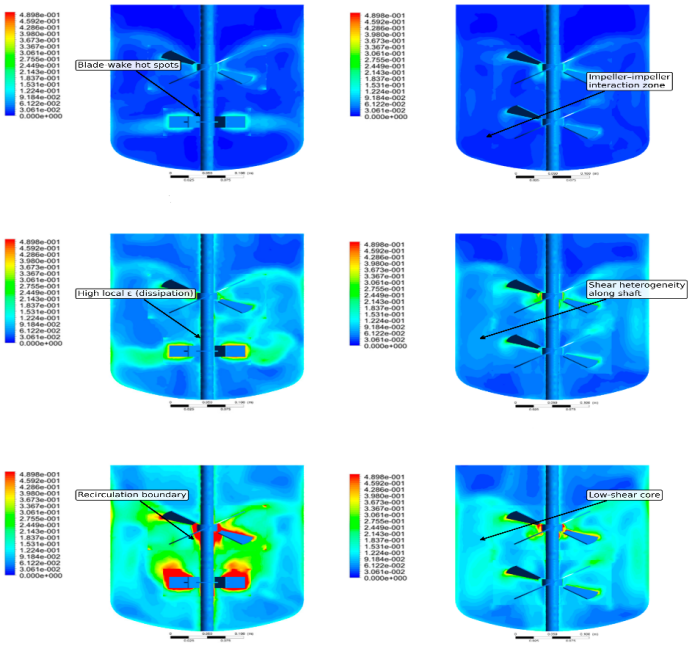

Fig. 3 - CFD-derived turbulence/energy-dissipation fields in a double-impeller STR
(adapted from Ebrahimi,M. et al. 2019)

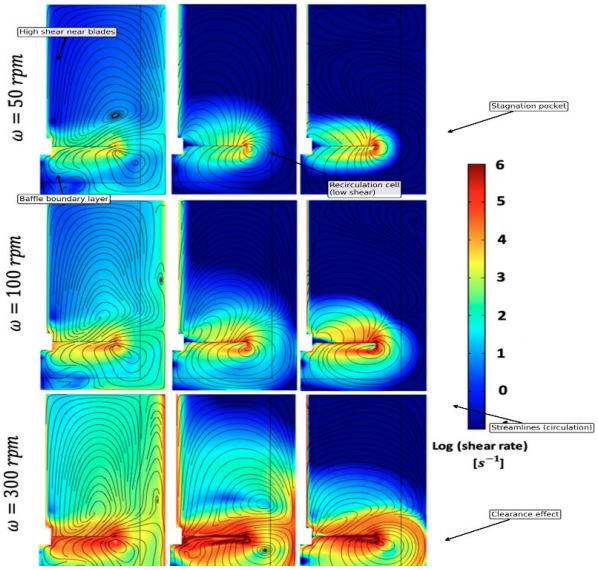

Fig. 4 - Log shear-rate contours with in-plane streamlines in a stirred vessel
(adapted from Šafarič et al., 2019)

CONCLUSIONS

High-cell-density cultivation of Saccharomyces cerevisiae in stirred-tank bioreactors represents a complex interplay between hydrodynamic performance and metabolic regulation. The synthesis of available data indicates that impeller geometry is a primary determinant of the balance between oxygen transfer efficiency and mechanical stress. Rushton turbines (radial-flow) consistently deliver the highest volumetric oxygen transfer coefficients (kLa values often exceeding 300 h^{-1} under laboratory conditions), yet they impose elevated local shear stresses than can compromise cell viability at scale, while marine impellers ensure gentle mixing at the expense of oxygen transfer. Evidence indicates that pitched-blade turbines, or hybrid multi-impeller systems, represent the most effective compromise, sustaining robust growth and minimizing ethanol overflow. From a metabolic standpoint, the most effective strategy remains glucose-limited fed-batch cultivation, witch consistently suppresses the Crabtree effect and allows biomass concentrations above 50 g/L dry cell weight. Also, immobilization and retention systems further stabilize culture performance under stress conditions, enabling multi-cycle operation and supporting product accumulation in case of high-density regimes. Supported by advanced CFD modelling and PAT- driven

monitoring, these configurations provide a scientifically robust basis for a reliable scale-up and a sustainable operation of industrial yeast bioprocesses.

ACKNOWLEDGEMENT

This paper is written during the doctoral internship of the first author in the Doctoral School of Biotechnical Systems Engineering, from the National University of Science and Technology POLITEHNICA Bucharest.

REFERENCES

[1] Arulrajah, P., Wu, D., Moresi, M., Zhang, H., & Wang, Z. (2025). Scale-down bioreactors: gradients and process heterogeneity. Bioprocess and Biosystems Engineering, 47, 103–118. https://doi.org/10.1007/s00449-025-03182-w.

[2] Beigbeder, J.-B., de Medeiros Dantas, J. M., & Lavoie, J.-M. (2021). Optimization of yeast, sugar and nutrient concentrations for high ethanol production rate using industrial sugar beet molasses. Fermentation, 7(2), 86. https://doi.org/10.3390/fermentation7020086.

[3] Boswell, C. D., Nienow, A. W., Gill, N. K., Kocharunchitt, S., & Hewitt, C. J. (2003). The impact of fluid mechanical stress on Saccharomyces cerevisiae. Food and Bioproducts Processing, 81(1), 23–32. https://doi.org/10.1205/096030803765208665.

[4] Bruder, S., Reifenrath, M., & Takors, R. (2016). Process analytical technologies for high cell density cultivations with yeast. Applied Microbiology and Biotechnology, 100(19), 8229–8240. https://doi.org/10.1007/s00253-016-7644-5.

[5] Călinescu, I., Chipurici, P., Trifan, A., & Bădoiu, C. (2012). Immobilisation of Saccharomyces cerevisiae for the production of bioethanol. U.P.B. Scientific Bulletin, Series B: Chemistry and Materials Science, 74(1), 33–40.

[6] Chen, X., Li, Y., Wang, T., Zhao, H., Liu, J., & Sun, W. (2025). Evaluation of stress tolerance in high-cell-density yeast fermentation. Frontiers in Microbiology, 16, 11720210. https://doi.org/10.3389/fmicb.2025.11720210.

[7] Dashko, S., Zhou, N., Compagno, C., & Piškur, J. (2014). Why, when and how did yeast evolve alcoholic fermentation? FEMS Yeast Research, 14(6), 826–832. https://doi.org/10.1111/1567-1364.12161.

[8] Daub, A., Böhm, M., Delueg, S., Mühlmann, M., Schneider, G., & Büchs, J. (2014). Characterization of hydromechanical stress in aerated stirred tanks. Journal of Biological Engineering, 8, 17. https://doi.org/10.1186/1754-1611-8-17.

[9] Ebrahimi, M., Jahanmiri, A., & Haghighi, M. (2019). CFD analysis of mixing and energy dissipation in stirred bioreactors. Chemical Engineering Research and Design, 148, 262–275. https://doi.org/10.1016/j.cherd.2019.06.019.

[10] Garcia-Ochoa, F., Gomez, E., Santos, V. E., & Merchuk, J. C. (2010). Oxygen uptake rate in microbial processes: An overview. Biochemical Engineering Journal, 49(3), 289–307. https://doi.org/10.1016/j.bej.2010.01.011.

[11] Goffeau, A., Barrell, B. G., Bussey, H., Davis, R. W., Dujon, B., Feldmann, H., Galibert, F., Hoheisel, J. D., Jacq, C., Johnston, M., Louis, E. J., Mewes, H. W., Murakami, Y., Philippsen, P., Tettelin, H., & Oliver, S. G. (1996). Life with 6000 genes. Science, 274(5287), 546–567. https://doi.org/10.1126/science.274.5287.546.

[12] Karimi, A., Moghaddas, J. S., & Raisi, A. (2013). Effect of multiple impellers on oxygen transfer in stirred tanks. Chemical Engineering and Processing: Process Intensification, 67, 75–83. https://doi.org/10.1016/j.cep.2013.02.005.

[13] Koruyucu, M., Alkan, M., Ozturk, S., & Demirci, A. (2023). High-cell-density yeast oil production with diluted substrates imitating microalgae hydrolysate. Energies, 16(4), 1757. https://doi.org/10.3390/en16041757.

[14] Lange, H. C., Heijnen, J. J., & van Gulik, W. M. (2001). Shear sensitivity of Saccharomyces cerevisiae in controlled devices. Biotechnology and Bioengineering, 73(4), 326–335. https://doi.org/10.1002/bit.1066.

[15] Levin, D. E. (2011). Regulation of cell wall biogenesis in Saccharomyces cerevisiae: the cell wall integrity signaling pathway. Genetics, 189(4), 1145–1175. https://doi.org/10.1534/genetics.111.128264.

[16] Malairuang, K., Intawong, B., Sangwattana, S., & Laopaiboon, P. (2020). High cell density cultivation of Saccharomyces cerevisiae with novel fed-batch strategies. Processes, 8(10), 1321. https://doi.org/10.3390/pr8101321.

[17] Mishra, R., van Drogen, F., Dechant, R., Oh, S., Jeon, N. L., Lee, S. S., & Peter, M. (2017). Protein kinase C and calcineurin mediate survival under compressive stress in yeast. Proceedings of the National Academy of Sciences, 114(51), 13471–13476. https://doi.org/10.1073/pnas.1717406114.

[18] Mishra, R., Minc, N., & Peter, M. (2022). Cells under pressure: how yeast responds to mechanical forces. Trends in Microbiology, 30(5), 495–510. https://doi.org/10.1016/j.tim.2021.09.009.

[19] Mussatto, S. I. (2010). Biomass and bioenergy production from yeast processes. Renewable and Sustainable Energy Reviews, 14(9), 2777–2785. https://doi.org/10.1016/j.rser.2010.07.056.

[20] Nandy, S. K., & Srivastava, R. K. (2018). Sustainable yeast bioprocessing: A review. Renewable and Sustainable Energy Reviews, 81, 436–444. https://doi.org/10.1016/j.rser.2017.08.026.

[21] Neeli-Venkata, R., Municio-Diaz, C., Celador, R., Sanchez, Y., & Minc, N. (2021). Detection of surface forces by the Wsc1 mechanosensor in Saccharomyces cerevisiae. Developmental Cell, 56(20), 2856–2870. https://doi.org/10.1016/j.devcel.2021.09.023.

[22] Nielsen, J. (2019). Yeast systems biology: Model organism and cell factory. Biotechnology Journal, 14(9), e1800421. https://doi.org/10.1002/biot.201800421.

[23] Nienow, A. W. (1998). Hydrodynamics of stirred bioreactors. Applied Mechanics Reviews, 51(1), 3–32. https://doi.org/10.1115/1.3098989.

[24] Paciello, L., & Parascandola, P. (2020). Comparative analysis of impellers for yeast fermentation. Journal of Chemical Technology and Biotechnology, 95(5), 1241–1249. https://doi.org/10.1002/jctb.6315.

[25] Parapouli, M., Vasileiadis, A., Afendra, A. S., & Hatziloukas, E. (2020). Saccharomyces cerevisiae and its industrial applications. AIMS Microbiology, 6(1), 1–31. https://doi.org/10.3934/microbiol.2020.1.1.

[26] Salari, R., & Salari, R. (2017). Investigation of the best Saccharomyces cerevisiae growth conditions. Electronic Physician, 9(1), 3592–3597. https://doi.org/10.19082/3592.

[27] Schaepe, S., Kuprijanov, A., Blümich, B., & Büchs, J. (2013). Hollow-blade impellers improve gas handling in stirred tanks. Chemical Engineering Journal, 215–216, 224–231. https://doi.org/10.1016/j.cej.2012.11.077.

[28] Shuler, M. L., & Kargi, F. (2017). Bioprocess Engineering: Basic Concepts (3rd ed.). Prentice Hall, New Jersey.

[29] Stanbury, P. F., Whitaker, A., & Hall, S. J. (2016). Principles of Fermentation Technology (3rd ed.). Elsevier, Oxford.

[30] Su, Y., Xu, C., Shea, J., DeStephanis, D., Li, J., Yan, M., Wu, X., & Su, Z. (2023). Transcriptomic changes in yeast under mechanical stress. BMC Genomics, 24, 88. https://doi.org/10.1186/s12864-023-09310-3.

[31] Susukida, R., Tanaka, Y., Kondo, A., & Matsuda, F. (2025). Improved mixing properties of stirred fermentation analyzed by CFD and omics. Frontiers in Bioengineering and Biotechnology, 13, 12322652. https://doi.org/10.3389/fbioe.2025.12322652.

[32] Suresh, S., Srivastava, V. C., & Mishra, I. M. (2009). Techniques for oxygen transfer measurement in bioreactors. Journal of Chemical Technology & Biotechnology, 84(8), 1091–1103. https://doi.org/10.1002/jctb.2104.

[33] Torotwa, I., & Ji, C. (2018). A study of the mixing performance of different impeller designs in stirred vessels using computational fluid dynamics. Designs, 2(1), 10. https://doi.org/10.3390/designs2010010.

[34] van't Riet, K., & Tramper, J. (1991). Basic Bioreactor Design. CRC Press, New York.

[35] Yousefi-Darani, A., Karimzadeh, I., Behroozi, J., & Farid, S. S. (2021). Online biomass monitoring using unscented Kalman filter. Biochemical Engineering Journal, 174, 108118. https://doi.org/10.1016/j.bej.2021.108118.

[36] Zhang, Y., Wu, J., & Wang, Z. (2019). Magnetic induction spectroscopy for biomass monitoring in yeast cultivation. Sensors and Actuators B: Chemical, 285, 649–656. https://doi.org/10.1016/j.snb.2019.01.116.

[37] Zhuang, S., Renault, N., & Archer, I. (2021). Multidisciplinary engineering in yeast fermentation. Journal of Biotechnology, 339, 32–41. https://doi.org/10.1016/j.jbiotec.2021.08.002

GIS TECHNOLOGY AND ITS APPLICATIONS IN ENVIRONMENTAL ENGINEERING
/
TEHNOLOGIA GIS ȘI APLICAȚIILE ACESTEIA ÎN INGINERIA MEDIULUI

Bianca-Ștefania ZĂBAVĂ*[1)], Gheorghe VOICU[1)], Mirela - Nicoleta DINCĂ[1)], Gigel PARASCHIV[1)], Mariana IONESCU[1)], Georgiana MOICEANU[2)], Mariana FERDEȘ[1)]

[1)] Department of Biotechnical Systems, National University of Science and Technology Politehnica of Bucharest / Romania;

[2)] Department of Management and Entrepreneurship, National University of Science and Technology Politehnica of Bucharest / Romania.

**Tel: (+40) 731 538 941; *E-mail: bianca.dragoiu@upb.ro*

Keywords: Geographic Information Systems, environmental, technology, monitoring system

ABSTRACT

Geographic Information Systems (GIS) technology plays an increasingly important role in environmental engineering, providing an efficient framework for collecting, managing, analyzing, and visualizing spatial data. This technology enables environmental professionals to better understand the relationships between natural phenomena and human activities, thus contributing to informed and sustainable decision-making. The present article analyzes the fundamental concepts of GIS technology and highlights its main applications in the field of environmental engineering. Concrete examples are presented to demonstrate how GIS can support predictive modeling, real-time monitoring of resources, and the assessment of the environmental impact of human activities. The conclusion emphasizes that GIS technology is essential not only as a technical tool but also as a strategic support mechanism for the development of environmental policies and for adaptation to climate change.

REZUMAT

Tehnologia Sistemelor Informaționale Geografice (GIS) joacă un rol tot mai important în ingineria mediului, oferind un cadru eficient pentru colectarea, gestionarea, analiza și vizualizarea datelor spațiale. Această tehnologie permite profesioniștilor din domeniul mediului să înțeleagă mai bine relațiile dintre fenomenele naturale și activitățile umane, contribuind astfel la luarea unor decizii informate și sustenabile. Articolul de față analizează conceptele fundamentale ale tehnologiei GIS și evidențiază principalele sale aplicații în ingineria mediului. Sunt prezentate exemple concrete recente care demonstrează modul în care GIS poate sprijini modelarea predictivă, supravegherea în timp real a resurselor și evaluarea impactului activităților antropice asupra mediului. Concluzia subliniază că tehnologia GIS este esențială nu doar ca instrument tehnic, ci și ca suport strategic în elaborarea politicilor de mediu și în adaptarea la schimbările climatice.

INTRODUCTION

With the development of human society, it has become evident that human activity influences the environment and is, in turn, influenced by it. Through various stages of organization, environmental quality protection, and more recently, integrated environmental management, has become a vital necessity to ensure societal prosperity and sustainable development.

Environmental management has become an essential aspect of any type of development, regardless of the scale at which environmental impacts may occur.

To ensure effective governance of all social activities, even when environmental aspects sometimes seem secondary, the need for a system of continuous monitoring and assessment of environmental quality has emerged in the form of an environmental monitoring system *(Mihăiescu, R., 2014).*

As pressures on the environment increase, it becomes increasingly clear that effective decision-making cannot be achieved without accurate and integrated information.

Within the course of human evolution, the major challenges we face today are the protection of the natural environment and the preservation of a high quality of life. In the pursuit of development activities, the assimilative capacity of environmental components (air, water, and soil) toward various forms of pollution is seldom considered.

The chaotic and unregulated nature of these activities leads to resource overexploitation, congestion, inappropriate land use, and, consequently, the deterioration of living conditions. As a result, environmental pollution has become a central issue, closely associated with high-risk areas and contexts.

Environmental Engineering constitutes a critical discipline focused on assessing, mitigating, and managing the impacts of environmental contaminants, encompassing the integrated management of water, air, and waste systems. Given the inherently spatial nature of environmental phenomena, which manifest across specific geographic locations and landscapes, it is imperative to capture and analyze their spatial dimensions.

It plays a key role today because it addresses major challenges caused by human activities on the environment and the need to move towards a sustainable development model. Through this field, innovative technological solutions and strategies are developed to prevent and reduce pollution, manage natural resources responsibly, and protect biodiversity.

The importance of this engineering discipline comes from its ability to balance economic progress with environmental conservation, thus contributing to public health and the resilience of ecosystems. In this context, using modern tools for analyzing and managing information has become essential.

Geographic Information Systems (GIS) stand out for their ability to collect, organize, analyze, and visualize complex spatial data, offering an integrated view of natural and human processes.

By combining various sources of information, such as climate, hydrological, geological, or biological data GIS helps understand ecosystem dynamics and supports decision-making based on scientific evidence *(Gajos, M., & Sierka, E., 2012*).

The integration of GIS into environmental management is increasingly necessary for a rigorous, data-driven approach. These technologies enable detailed monitoring of natural resources, precise assessment of the impacts of human activities, and identification of vulnerable areas.

Furthermore, GIS facilitates the analysis of complex interactions among demographic, socioeconomic, and environmental factors, providing support for the development of mitigation strategies and sustainable management plans *(Calka, B., & Szostak, M., 2025).* Thus, the use of GIS significantly contributes to environmental protection and the promotion of sustainable societal development. In this regard, GIS have emerged as a robust and accessible technology, capable of efficiently acquiring, integrating, and analyzing complex spatial datasets.

The convergence of GIS and environmental engineering thus facilitates the development of sophisticated environmental models and engineering solutions, underpinning the construction of adaptive decision support systems for sustainable environmental management and conservation *(Joao, E., & Fonseca, A., 1996)*.

Accordingly, GIS provides an indispensable framework for researchers, environmental managers, and engineers to investigate dynamic environmental processes, systematically monitor ecological phenomena, and simulate the responses of natural systems to both anthropogenic and natural perturbations *(GIS for civil engineering, 2010)*.

The Environmental Systems Research Institute defines Geographical Information Systems (GIS) as “a structured collection of computer hardware, software, geographic data, and personnel designed to efficiently capture, store, update, manipulate, analyze, and display all types of geographically referenced information”.

Building on this, Goodchild (1995) outlined additional defining characteristics of GIS, including: **(i)** the capacity to store and analyze spatial relationships among objects—such as intersection, adjacency, connectivity, or overlap—and to compute these relationships when required; **(ii)** the ability to manage and analyze an unlimited range of attributes associated with each object; **(iii)** a primary focus on analysis rather than on simple data storage and retrieval; and **(iv)** the integration of data from multiple sources, potentially at different scales and using diverse modes of representation *(Hamal, S., 2020).*

GIS supports environmental monitoring, assessment, and mitigation, and can also facilitate the development of environmental models. It is especially effective for organizing and analyzing environmental data. GIS serves as a core tool in environmental data systems for data transfer, retrieval, validation, and analysis. Its main components—software, hardware, data, procedures, and methods—enable people to make location-based decisions and analyses.

Fig. 1 - The components of GIS
(Perumal, M., Velumani, B., Sahasivam, A., & Kamaswany, K., 2015)

Geographic Information Systems (GIS) represent a fundamental technology in environmental engineering, due to their capacity to manage, correlate, and analyze complex spatial data. By integrating heterogeneous sources of information – from satellite imagery and digital terrain models to climatic and hydrological data – GIS facilitates the assessment of anthropogenic impacts on ecosystems and supports the development of evidence-based environmental policies.

In fields such as water resource management, pollution control, biodiversity protection, and sustainable land-use planning, GIS enables the modeling of natural processes, the identification of risk areas, and the optimization of engineering interventions. Therefore, the use of GIS in environmental engineering goes beyond mere cartography, making a significant contribution to the development of sustainable strategies for environmental protection and management.

The usefulness of GIS, particularly for decision-making and addressing environmental issues, increases with the complexity and scale of these problems. In high-risk environments, GIS can facilitate the rapid and efficient development and analysis of mitigation plans. New spatial interrelationships allow for overlays that integrate diverse demographic, socioeconomic, and environmental data, as well as information on environmental outcomes *(Shaw, N. T., & Mcguire S. K., 2017).*

The present article provides a comprehensive analysis of the fundamental concepts underlying Geographic Information Systems (GIS) technology, examining its theoretical foundations, key components, and operational principles.

MATERIALS AND METHODS

The range of GIS applications is extensive, encompassing any context in which spatial features must be represented and analyzed. GIS provides the capability to acquire, store, manage, manipulate, and interpret spatially referenced data, as well as to communicate the outcomes of such analyses through thematic cartographic representations.

The adoption of a GIS is typically informed by jurisdictional considerations (e.g., at the level of a municipality), specific objectives, or the requirements of a given application. In practice, GIS implementations are frequently customized to address the particular needs and operational contexts of individual organizations *(Khandve, P., & Mokadam. A.M., 2011).*

GIS can play a crucial role in the analysis and rapid development of intervention strategies for high-risk areas. GIS constitutes a central tool in environmental data management, facilitating data validation, adherence to digital data transfer standards, as well as the collection, dissemination, and analysis of information.

Moreover, GIS serves as a platform for communicating environmental information to both the public and decision-makers, providing the technical foundation for integrating multimedia approaches within the environmental decision-making process.

From the analysis of Figure 2, the main fields of application of GIS technologies in environmental engineering can be highlighted.

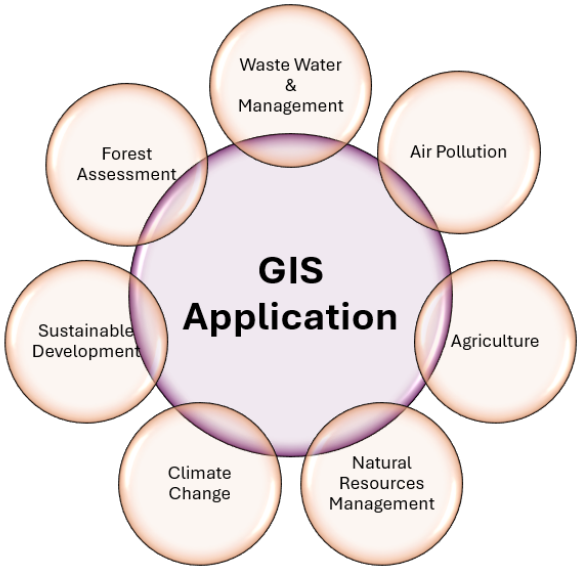

Fig. 2 - Application of GIS for various environmental solutions

RESULTS

GIS has many uses, especially where spatial features need to be created and studied. It helps in collecting, storing, changing, analyzing, and showing information that is connected to a location, and also in sharing the results through special maps. The way a GIS is set up usually depends on the area it covers, like a city, or the goal it serves. Often, a GIS system is made to fit the specific needs of an organization.

Ramroop grouped GIS uses in water resources into these categories: water resources management, watershed management, flood management, groundwater management, water quality, biodiversity and habitat, pollution prevention and control, following rules and regulations, sustainable development, and working with agencies and organizations *(Ramroop, S., 2010).*

Regarding agriculture, GIS and RS (remote sensing) technologies can improve agricultural decisions and policies. They allow for a more efficient analysis of spatial factors that influence productivity, contributing to sustainable agricultural policies and evidence-based interventions. However, in many low- and middle-income countries, the use of GIS is limited due to a lack of reliable spatial data and limited analytical skills *(Tu, L. H.; & Ha, N. T., 2023)*.

This is problematic given the urgent need to modernize agriculture and food production. For optimal use, governments, farmers, and other stakeholders (researchers, consultants, decision-makers, distributors, etc.) must collaborate and have access to up-to-date spatial data.

This information is essential for planning and implementing agricultural policies, as well as for supporting small farmers in their decision-making. GIS and RS have important applications in precision agriculture, crop monitoring, soil fertility management, drought prevention, and disease detection, all of which contribute to food security. To realize this potential, it is necessary to develop comprehensive and up-to-date spatial databases, along with advanced analytical methods capable of providing useful insights for agricultural policies and practices *(Asif, R., 2024).*

Environmental engineering focuses on reducing pollution and finding solutions for managing water, air, and waste. Since environmental issues have a spatial dimension, GIS is essential for collecting and analyzing geographic data. Integrating GIS into environmental engineering allows for modeling phenomena, supports decision-making, and provides tools for protecting the environment.

Through digital maps with layers of information (such as environmental trends, soil stability, pesticide use, pollution sources, etc.), GIS helps researchers and engineers understand and manage the environment more efficiently.

GIS plays a key role in analyzing high-risk environments and in quickly developing mitigation plans. It is a crucial tool for validating, transferring, recovering, and analyzing environmental data. Additionally, GIS helps communicate information to the public and decision-makers, becoming a technical basis for environmental decisions. With the development of spatial standards, the internet, and modern technologies,

environmental information becomes accessible to all users in a relevant spatial context *(Sharma, V.N., Mohammmed, J., & Uppuluri, S., 2009).*

Regarding climate changes, GIS plays a key role in field. It gives scientists, leaders, and local groups the tools and knowledge they need to learn about how the environment is changing. With spatial data, GIS helps people look at and analyze a lot of information, making it easier to spot patterns, trends, and possible impacts.

By placing data like temperature readings, rainfall levels, and plant coverage on maps, GIS helps researchers better understand how climate change is affecting different regions and natural systems (GIS in Climate Change Analysis) *(Le Hoangtu, P. T., 2023).*

Motor vehicles are closely linked to rising air pollution in cities around the world. In addition to releasing large amounts of CO2, these vehicles also emit significant levels of CO, HC, NOx, SPM, and other harmful air pollutants into the atmosphere, which have serious effects on both the environment and human health.

Air quality is crucial for our health and the environment, but it can be hard to track down the exact sources of pollution. GIS technology helps by collecting and organizing data in a way that shows how poor air quality is connected to problems in human and environmental health. This makes it easier to monitor pollutant emissions. With GIS, we can find out where pollutants come from and keep track of those areas to help protect the air we breathe *(Khandve, P., & Mokadam, A.M., 2011).*

CONCLUSIONS

GIS technology is a critical tool in environmental engineering. It integrates and analyzes complex spatial data, helping us better understand natural events and the effects of human activities. GIS aids sustainable decision-making through predictive modeling, real-time monitoring, and identifying vulnerable areas. Its applications include water resource management, pollution control, biodiversity protection, sustainable agriculture, and analyzing climate change.

However, using GIS comes with challenges, especially in places that lack up-to-date databases and analytical skills. Still, its potential to help create effective environmental policies and support societal adaptation to climate change means GIS is more than just a technical tool. It also serves as a key support for environmental protection and sustainable development.

REFERENCES

[1] Asif, R. (2024). A Systematic Review of Geographic Information Systems (GIS) in Agriculturefor Evidence-Based Decision Making and Sustainability. Global Sustainability Research 3(1). DOI 10.56556/gssr.v3i1.636

[2] Calka, B., & Szostak, M. (2025). GIS-Based Environmental Monitoring and Analysis. Appl. Sci., 15, 3155. https://doi.org/10.3390/app15063155

[3] Gajos, M., & Sierka, E. (2012). GIS Technology in Environmental Protection: Research Directions Based on Literature Review. Polish Journal of Environmental Studies, 21(2), 241–248.

[4] Hamal, S. (2020). GIS Technology and its Applications in Water Resources and Environmental Engineering. J Hydrogeol Hydrol Eng 9:3

[5] Joao, E., & Fonseca, A. (1996). The role of GIS in improving environmental assessment effectiveness: Theory vs. Practice. Impact Assessment. 14: 371–387.

[6] Khandve, P., & Mokadam, A.M. (2011). Application of GIS in environmental engineering. Proceedings of National Conference on Environment Pollution and Management Aurangabad pp: 244–250

[7] Le Hoangtu, P. T. (2023). GIS Application in Environmental Managment: A Review. VNU Journal of Science: Earth and Environmental Sciences, 39(2), 1-15. doi:https://doi.org/10.25073/2588-1094/vnuees.4957

[8] Mihăiescu, R. (2014) Integrated Environmental Monitoring/ Monitoringul Integrat Al Mediului, Cluj-Napoca

[9] Perumal, M., Velumani, B., Sahasivam, A., & Kamaswany, K. (2015). Spatial data mining approaches for GIS – A brief review," Springer International Publishing Switzerland. 338(2), pp. 579 – 580. doi:10.1007/978-3-319-13731-5_63

[10] Ramroop, S. (2010). GIS Applications in Water Resources and Environmental Engineering

[11] Shaw, N. T., & Mcguire S. K. (2017). Understanding the use of geographical information systems (GISs) in health informatics research: A review. Journal of Innovation Health Informatics. 24, (2), pp. 228 – 233, doi:10.14236/jhi. v24i2.940
[12] Sharma, V.N., Mohammmed, J., & Uppuluri, S. (2009). GIS in environmental studies- an overview. Geospatial World.
[13] Tu, L. H.; & Ha, N. T. (2023). GIS Application in Environmental Management: A Review. J. Environ. Sci. Eng. 67, 112–130.
[14] *** GIS for civil engineering (2010) Environmental Systems Research Institute (ESRI).

STONE PAPER AS A SUSTAINABLE ALTERNATIVE: APPLICATIONS, CHALLENGES AND OPPORTUNITIES

/

STONE PAPER CA ALTERNATIVĂ SUSTENABILĂ: APLICAȚII, PROVOCĂRI ȘI OPORTUNITĂȚI

Andreea-Nicoleta BURCEA[1)], Daniel ȘIPU[2)], Cristina-Ileana COVALIU-MIERLĂ*[3)]

[1)] Biotechnical System Engineering Doctoral School, National University of Science and Technology Politehnica Bucharest / Romania;

[2)] Adam Stone SA / Romania;

[3)] Faculty of Biotechnical Systems Engineering, National University of Science and Technology Politehnica Bucharest / Romania.

**Tel: 40 722 791 791; *E-mail: cristina_covaliu@yahoo.com*

Keywords: *Stone Paper, calcium carbonate, sustainable production*

ABSTRACT

Stone Paper, produced mainly from micronised calcium carbonate derived from recycled marble residuals, offers a sustainable alternative to traditional cellulose-based paper and plastic-based packaging solutions. By utilizing industrial by-products, it reduces deforestation, water consumption, and the environmental impacts of waste disposal. This review explores innovative strategies for integrating recycled marble residuals into Stone Paper production, highlighting its role in promoting resource efficiency and circular economy principles. A comprehensive literature review was conducted to examine manufacturing techniques, environmental benefits, and market adoption. Case studies and life cycle assessments were analyzed to compare Stone Paper with conventional paper. Stone Paper production demonstrates significant potential to valorize residual materials, lower carbon emissions, and conserve water resources. The public–private partenership illustrate the feasibility of large-scale adoption while addressing challenges such as recycling pathways and production scalability. Stone Paper represents a high-performance, eco-friendly material that transforms recycled marble residuals into a valuable resource. Its adoption can mitigate environmental challenges, enhance material efficiency, and support sustainable industrial practices.

REZUMAT

Hârtia din piatră, produsă în principal din carbonat de calciu micronizat, derivat din praf de marmură rezidual, oferă o alternativă sustenabilă la hârtia tradițională pe bază de celuloză, precum și la soluțiile de ambalare pe bază de plastic. Prin utilizarea produselor secundare industriale se reduc defrișările, consumul de apă și impactul asupra mediului cauzat de eliminarea necorespunzătoare a deșeurilor. Această lucrare trece în revistă strategii inovatoare pentru integrarea prafului de marmură rezidual în producția de stone paper, subliniind rolul său în promovarea eficienței utilizării resurselor și a principiilor economiei circulare. A fost realizată o analiză a literaturii de specialitate pentru a examina tehnicile de fabricație, beneficiile de mediu și adoptarea pe piață. Au fost analizate studii de caz și evaluări ale ciclului de viață pentru a compara hârtia din piatră cu produsele convenționale. Producția de hârtie din piatră demonstrează un potențial semnificativ de valorificare a reziduurilor industriale, reducere a emisiilor de carbon și conservare a resurselor de apă. Parteneriatul public–privat ilustrează fezabilitatea adoptării la scară largă, abordând în același timp provocări precum opțiunile de reciclare și scalabilitatea producției. Hârtia din piatră reprezintă un material performant și ecologic care transformă praful de marmură rezidual într-o resursă valoroasă. Adoptarea sa poate atenua provocările de mediu, poate îmbunătăți eficiența materialelor și poate sprijini practicile industriale sustenabile.

INTRODUCTION

Global demand for paper and packaging continues to rise, creating environmental pressures such as deforestation, water scarcity, and plastic pollution (*Kaushani, K. G., Rathnasinghe, N. L., Katuwawila et al, 2022*). Conventional pulp and paper production consumes substantial water and energy and generates chemical effluents (*Hawanis, H. S. N., Ilyas, R. A., Jalil et al, 2024*).

Stone Paper, also known as mineral paper or rock paper, replaces cellulose fibers with finely ground calcium carbonate ($CaCO_3$) and incorporates a polymer binder, typically high-density polyethylene (HDPE)

(*Indriati, L., Nugraha, M. A., & Perng, Y. S.,2020; Swain, N., Saini, P., Bhati et al, 2023*). Commercial formulations are generally ~80% $CaCO_3$ and ~20% HDPE.

This composition imparts water and tear resistance, dimensional stability, and a smooth surface suitable for printing, while altering environmental impacts compared to conventional papers (*Indriati, L., Nugraha, M. A., & Perng, Y. S.,2020; Swain, N., Saini, P., Bhati et al, 2023; Akpolat, C., & Akgül, A., 2024*).

Research methodology surrounding Stone Paper examines its durability, water resistance, and recyclability, showcasing advantages over traditional paper in various applications (*Indriati, L., Nugraha, M. A., & Perng, Y. S.,2020; Swain, N., Saini, P., Bhati et al, 2023*). For instance, studies have demonstrated that Stone Paper can outperform standard paper in durability, positioning it as a viable option for sectors ranging from packaging to education.

This fundamental transition toward using alternative fibers encapsulates a shift toward sustainability that is crucial for the future of material production (*Li, J., Sun, J., Zhang, L et al, 2025, Fathi, Y., Abdulkhani, A., Hamzeh, Y et al 2024*).

This review synthesizes recent literature (technical studies, LCAs, and case reports) on Stone Paper manufacturing, environmental performance, applications, limitations, and policy/market opportunities with a focus on materials derived from recycled marble residuals (an important waste stream in regions with active stone industries).

MATERIALS AND METHODS

A structured literature search was performed in Scopus, Web of Science, Google Scholar and publisher sites (Elsevier, Springer, MDPI, AIP Proceedings). Search terms included: “Stone Paper”, “mineral paper”, “Terraskin”, “calcium carbonate paper”, “life cycle assessment Stone Paper”, “Stone Paper recycling”, and combinations with “marble residuals” and “industrial by-products”. Inclusion criteria prioritized peer-reviewed articles, conference proceedings, and technical LCA reports; manufacturer LCAs and recognized technical reports were used when peer-reviewed LCA studies were sparse.

Where possible, case studies and LCAs comparing Stone Paper to cellulose paper and plastic films were extracted and summarized. Because Stone Paper literature is a mixture of peer-reviewed studies and industry reports, each source type is noted in the reference list and when used in the text.

Stone paper: materials and manufacturing

The exploration of innovative materials has led to the emergence of Stone Paper, a unique product synthesized primarily from calcium carbonate, bounded by a non-toxic polymer (*Indriati, L., Nugraha, M. A., & Perng, Y. S.,2020; Swain, N., Saini, P., Bhati et al, 2023*).

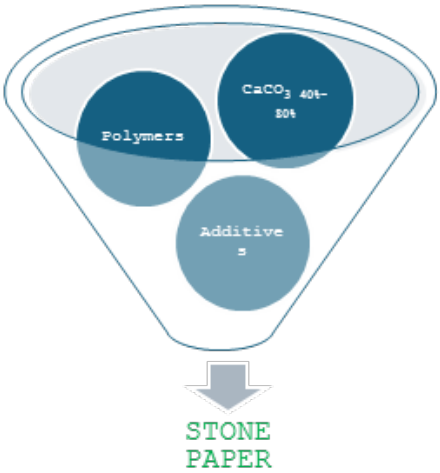

Fig. 1 - The components of Stone Paper

This material is notable for its environmentally friendly production process; the manufacturing of Stone Paper employs no water, no trees, and significantly reduces carbon emissions compared to traditional paper methods.

Multiple studies highlight its superior characteristics, including water resistance, tear durability, and the ability to withstand challenging environmental conditions, which make it a viable alternative for various

applications, from packaging to stationery (*Indriati, L., Nugraha, M. A., & Perng, Y. S.,2020; Swain, N., Saini, P., Bhati et al, 2023*).

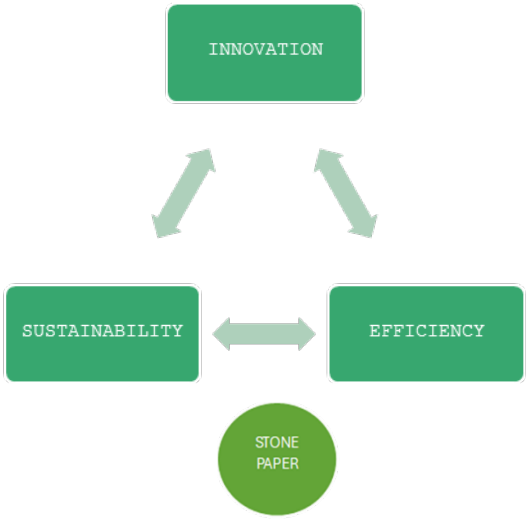

Fig. 2 - The values of Stone Paper

Furthermore, researchers have employed methodologies that assess the life cycle of Stone Paper, revealing a less detrimental impact on ecosystems compared to conventional papers (citing its ability to reduce deforestation and energy consumption) *(Affeldt, C., Leung, A., & Yang, K., 2016).* The versatility and sustainability of Stone Paper underline its potential as a transformative material in the context of increasing environmental awareness and the necessity for sustainable solutions *(Swain, N., Saini, P., Bhati et al, 2023).*

A typical industrial process includes: collection and preparation of stone residuals → micronization (ultrafine grinding to produce $CaCO_3$ powder) → mixing with binder and additives → extrusion and calendaring to form sheets → surface finishing for printability and coating as required (Figure 3).

The production avoids conventional digestion, pulping and bleaching steps used in cellulose paper mills, significantly reducing process water demand *(Hawanis, H. S. N., Ilyas, R. A., Jalil, R et al, 2024).*

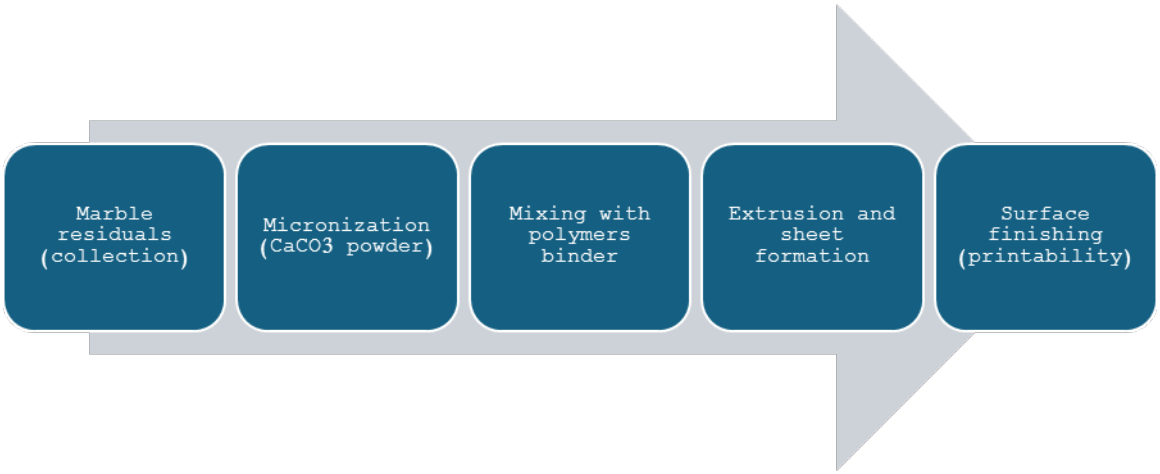

Fig. 3 - Industrial production process for Stone Paper

Environmental performance (lca insights)

As the pursuit of sustainable alternatives intensifies, innovative materials like Stone Paper present significant potential to lessen ecological footprints associated with traditional paper production. Traditional paper relies heavily on wood pulp, consuming vast quantities of water, energy, and chemicals, leading to deforestation and habitat destruction (*Swain, N., Saini, P., Bhati et al, 2023, Affeldt, C., Leung, A., & Yang, K., 2016*). In contrast, Stone Paper is composed primarily of calcium carbonate, using far less water and no trees, which minimizes biodiversity loss and reduces greenhouse gas emissions (*Fathi, Y., Abdulkhani, A., Hamzeh, Y et al, 2024*).

One of the most consistent advantages reported for Stone Paper is drastically lower process water use relative to conventional wood-pulp paper production — the stone-based process typically requires

negligible process water, since pulping/bleaching stages (which consume the bulk of water in conventional paper) are absent. This outcome is emphasized in technical and industry LCA summaries *(Swain, N., Saini, P., Bhati et al, 2023, Affeldt, C., Leung, A., & Yang, K., 2016).*

Results for greenhouse gas (GHG) emissions and primary energy vary by study and depend on the polymer source, electricity grid, and whether $CaCO_3$ feedstock is from quarrying or recycled marble residuals (*Ippolito, F., Hübner, G., Claypole, T et al, 2021, Bilir, T., Karadağ, Ö., & Aygün, B. F., 2022*).

Some LCAs indicate Stone Paper can reduce certain impact categories compared to coated papers and some plastic films, while others point out that the polymer binder (HDPE) and crushing/grinding energy can increase fossil-based impacts if not managed. Thus, LCA outcomes are context-dependent: processing technology, binder selection, electricity mix and end-of-life scenarios strongly influence results (*Swain, N., Saini, P., Bhati et al, 2023, Affeldt, C., Leung, A., & Yang, K., 2016*).

Traditional pulp bleaching can generate chlorinated phenolics and other toxic effluents (e.g., studies on chlorophenolic compounds from wheat straw pulp bleaching) (*Indriati, L., Nugraha, M. A., & Perng, Y. S., 2020*).

Stone Paper avoids those bleaching effluents but introduces considerations related to microplastic shedding, additive residues, and potential release of particles if sheets degrade. Comparative risk profiles therefore differ rather than uniformly “improve” across all endpoints (*Indriati, L., Nugraha, M. A., & Perng, Y. S., 2020*).

Stone Paper is recyclable in principle: it can be treated as a plastic-rich stream and processed using appropriate polymer-recycling pathways (separation, re-extrusion), or in some cases collected for recovery into composite products (*Swain, N., Saini, P., Bhati et al, 2023*).

However, in practice, Stone Paper is often misidentified as cellulose paper in mixed paper collection streams, leading to contamination issues and limited recycling. Where dedicated collection streams exist, producers and recyclers report good recovery rates, but infrastructure is the bottleneck.

Applications

The exploration of innovative materials has yielded significant insights into the practical applications of Stone Paper, particularly in various industries seeking sustainable alternatives. Research methodology often involves comparative analyses with traditional papers, highlighting characteristics such as superior water resistance, durability, and the absence of wood pulp (*Indriati, L., Nugraha, M. A., & Perng, Y. S.,2020; Swain, N., Saini, P., Bhati et al, 2023*).

By employing experimental frameworks similar to those detailed in which examines structural resilience of materials under stress, scholars can assess Stone Papers capacity to withstand harsh environmental conditions. For instance, studies have demonstrated its potential in packaging, where its moisture-resistant properties enhance product longevity and reduce waste (*Liendo, F., Arduino, M., Deorsola, F. A et al, 2022; Li, J., Sun, J., Zhang, L., Gao, C et al, 2025*).

Furthermore, the application of stone paper in educational contexts, such as notebooks and writing materials, showcases its feasible transition from concept to market. This suite of applications elucidates not only the versatility of Stone Paper but also its alignment with contemporary sustainability goals, affirming its role as a pivotal material in the ongoing quest for eco-friendly solutions (*Indriati, L., Nugraha, M. A., & Perng, Y. S.,2020; Swain, N., Saini, P., Bhati et al, 2023*).

The exploration of packaging methodologies reveals significant potential for integrating Stone Paper into various consumer products. Stone Paper, characterized by its durability, water resistance, and decreased reliance on trees, presents an alternative to traditional packaging materials.

Research indicates that effective packaging strategies can enhance sustainability by addressing the complexities of material choice and resource interdependencies within supply chains *(Kaushani, K. G., Rathnasinghe, N. L., Katuwawila, N et al, 2022*).

For example, studies on wine labels have highlighted the competitive appeal of alternative substrates, yet they also underscore challenges in fully integrating stone paper into existing frameworks where it may not outperform conventional materials in specific physical properties (*Affeldt, C., Leung, A., & Yang, K., 2016*).

This duality of opportunity and limitation emphasizes the necessity for further research in developing tailored specifications that can elevate stone papers viability in packaging applications, ultimately contributing to more sustainable consumer practices while navigating the embedded resource complexities inherent in e-commerce.

In assessing the impact of Stone Paper on educational materials and stationery, it is crucial to consider its unique characteristics that promote sustainability. Unlike traditional paper made from trees, stone paper is derived from calcium carbonate, offering a water permeable quality that enhances durability and resistance to tearing and wet conditions. This resilience makes it an ideal medium for educational tools such as notepads, textbooks and art supplies (*Indriati, L., Nugraha, M. A., & Perng, Y. S., 2020; Swain, N., Saini, P., Bhati et al, 2023*).

Challenges and limitations

The dominant practical obstacle is end-of-life management: Stone Paper often requires either recognition and routing into plastic recycling streams, or dedicated mono-streams. Because municipal collection systems are typically optimized for paper vs. plastic separation, widespread adoption requires adjustments to collection, labeling and public guidance. Where dedicated recycling streams exist, stone paper recycling can be efficient; where not, contamination and landfill remain likely. Even though $CaCO_3$ replaces cellulose, the binder is often fossil-based HDPE. This creates tradeoffs in GHG and fossil resource impacts unless the polymer is bio-sourced or recycled.

Research into bio-polymers and lower binder fractions is ongoing. The complexity of contemporary research is underscored by the necessity for interdisciplinary collaboration, particularly in fields such as sustainability, which includes innovative materials like Stone Paper.

Researchers often grapple with navigating differing institutional logics, which encompass varied goals such as societal impact, commercial viability, and the generation of academic knowledge. This divergence can inhibit effective collaboration, thereby slowing progress in addressing critical issues (*Indriati, L., Nugraha, M. A., & Perng, Y. S., 2020; Swain, N., Saini, P., Bhati et al, 2023*).

Stone Paper may face higher production costs (micronization energy, specialized extrusion) depending on scale and local supply. Market acceptance and willingness-to-pay for sustainable alternatives are also a factor; policy incentives and procurement standards may accelerate adoption. Hibiki & Managi's work on information provision and market incentives (PRTR systems) suggests that better environmental disclosure and market signals can influence firm choices and could be leveraged to support materials like Stone Paper (*Hibiki, A., & Managi, S., 2010*).

Opportunities and future research

One of the most promising avenues to improve Stone Paper sustainability is the development of bio-based or degradable binders to replace conventional fossil-based polymers. By substituting with bio-binders derived from renewable sources, the environmental footprint of Stone Paper can be significantly reduced, particularly regarding fossil fuel consumption and end-of-life disposal challenges. Such bio-binders could also enhance biodegradability, enabling Stone Paper to be incorporated into composting or organic waste streams where feasible, thus advancing circular economy objectives (*Swain, N., Saini, P., Bhati et al, 2023*).

Industrial symbiosis represents another opportunity to increase the sustainability of Stone Paper production. Regions with active stone, marble, or mining industries can valorize mineral residuals locally, using them as a source of calcium carbonate for paper production. This approach reduces the need for long-distance transport of raw materials, lowers associated greenhouse gas emissions, and creates closed-loop material supply chains that integrate existing industrial waste streams into the Stone Paper value chain.

As the urgency for sustainable materials intensifies, the research trajectory for Stone Paper must adapt to emerging ecological challenges and technological advancements. Future investigations could delve into material properties such as biodegradability and the recycling potential of Stone Paper, particularly in comparison to traditional alternatives. This could involve experimental studies that evaluate the environmental impact of stone paper throughout its lifecycle.

CONCLUSIONS

Stone Paper — produced mainly from micronized $CaCO_3$ and a polymer binder — is an emerging, high-performance, and potentially more resource-efficient alternative to conventional cellulose paper for many applications. Its main environmental strengths are near-zero process water use and the potential to valorize marble residuals, while its principal limitations are related to polymer dependence and end-of-life infrastructure. To realize the full environmental benefits, efforts must focus on binder innovation, transparent LCA reporting, and the development of dedicated recycling streams (public-private partnerships

and procurement incentives will speed adoption). With coordinated technical and policy actions, Stone Paper can take an important role in sustainable material portfolios.

REFERENCES:

[1] Affeldt, C., Leung, A., & Yang, K. (2016). *Life cycle assessment of stone paper, polypropylene film, and coated paper for use as product labels*. http://deepblue.lib.umich.edu/handle/2027.42/117675

[2] Akpolat, C., & Akgül, A. (2024). Print quality analysis of stone paper and coated sticker paper used in screen printing. *Applied Sciences*, *14*(15), 6668. https://doi.org/10.3390/app14156668

[3] Baraketi, S., & Khwaldia, K. (2024). Nanoparticles from agri-food by-products: Green technology synthesis and application in food packaging. *Current Opinion in Green and Sustainable Chemistry*, *49*, 100953. https://doi.org/10.1016/j.cogsc.2024.100953

[4] Bilir, T., Karadağ, Ö., & Aygün, B. F. (2022). Waste marble powder. În Sustainable Concrete Made with Ashes and Dust from Different Sources (pp. 479–506). Elsevier. https://doi.org/10.1016/B978-0-12-824050-2.00015-2

[5] Fathi, Y., Abdulkhani, A., Hamzeh, Y., Ashori, A., Mortha, G., & Chiani, E. (2024). Physico-chemical characterization and degradation analysis of mineral paper: Impact of accelerated weathering and aerobic biodegradation. *Polymer Composites*, *45*(1), 111–121. https://doi.org/10.1002/pc.27698

[6] Hawanis, H. S. N., Ilyas, R. A., Jalil, R., Ibrahim, R., Majid, R. A., & Ab Hamid, N. H. (2024). Insights into lignocellulosic fiber feedstock and its impact on pulp and paper manufacturing: A comprehensive review. *Sustainable Materials and Technologies*, *40*, e00922. https://doi.org/10.1016/j.susmat.2024.e00922

[7] Hibiki, A., & Managi, S. (2010). Environmental information provision, market valuation, and firm incentives: An empirical study of the japanese prtr system. *Land Economics*, *86*(2), 382–393. https://ideas.repec.org//a/uwp/landec/v86y2010i2p382-393.html

[8] Indriati, L., Nugraha, M. A., & Perng, Y. S. (2020). Stone paper, an eco-friendly and free-tree papers. 030010. https://doi.org/10.1063/5.0001753

[9] Ippolito, F., Hübner, G., Claypole, T., & Gane, P. (2021). Calcium carbonate as functional filler in polyamide 12-manipulation of the thermal and mechanical properties. *Processes*, *9*(6), 937. https://doi.org/10.3390/pr9060937

[10] Kaushani, K. G., Rathnasinghe, N. L., Katuwawila, N., Jayasinghe, R. A., Nilmini, A. H. L. R., & Priyadarshana, G. (2022). Trends in smart packaging technologies for sustainable monitoring of food quality and safety. *International Journal of Research and Innovation in Applied Science*, *07*(07), 07–30. https://doi.org/10.51584/IJRIAS.2022.7702

[11] Li, J., Sun, J., Zhang, L., Gao, C., Luo, S., Chen, X., Wu, X., & Nie, W. (2025). Research on the impact of active calcium carbonate on the performance of degradable composite films. *Journal of Polymer Engineering*, *45*(1), 50–57. https://doi.org/10.1515/polyeng-2024-0169

[12] Liendo, F., Arduino, M., Deorsola, F. A., & Bensaid, S. (2022). Factors controlling and influencing polymorphism, morphology and size of calcium carbonate synthesized through the carbonation route: A review. *Powder Technology*, *398*, 117050. https://doi.org/10.1016/j.powtec.2021.117050

[13] Malinowski, R., Fiedurek, K., Rytlewski, P., Puszczykowska, N., Kaczor, D., & Stasiek, A. (2023). The structure and selected properties of poly (E-caprolactone)-based biodegradable composites with high calcium carbonate concentration. *Science of The Total Environment*, *867*, 161528. https://doi.org/10.1016/j.scitotenv.2023.161528

[14] Swain, N., Saini, P., Bhati, S. S., & Rastogi, V. K. (2023). Biodegradable stone paper as a sustainable alternative to traditional paper: A review. *Journal of Inorganic and Organometallic Polymers and Materials*, *33*(8), 2240–2251. https://doi.org/10.1007/s10904-023-02644-6

ADSORPTION EFFICIENCY OF COOPER FROM WASTEWATER BY USE SOME ALTERNATIVE ADSORBENT MATERIALS

/

EFICIENȚA DE ADSORBȚIE A CUPRULUI DIN APE UZATE PRIN UTILIZAREA UNOR MATERIALE ADSORBANTE ALTERNATIVE

Cristina-Ileana COVALIU-MIERLĂ*, Maria RÂPĂ, Sorin IONESCU
National University of Science and Technology Politehnica Bucharest, 313 Splaiul Independentei, 060042, Bucharest / Romania
**E-mail: cristina_covaliu@yahoo.com*

Keywords: *adsorption, adsorbent materials, copper ions, wastewater*

ABSTRACT

The removal of heavy metals is an important aspect in wastewater treatment. This is achieved, in particular, through the adsorption process, using activated carbon as an adsorbent material. Since activated carbon is a rather expensive material, some research has been focused on finding and developing adsorbent materials from industrial and agricultural waste, which are cheap, available and in large quantities. In this work, four such adsorbent materials were used, namely blast furnace slag, walnut shells, hazelnut shells, sawdust, to monitor the efficiency of removing copper ions from wastewater. It was observed, following laboratory experiments, a high efficiency of removing copper ions in the case of the adsorbent materials studied, from 21.66%, in the case of sawdust, to 99.96%, in the case of blast furnace slag. The aim of this work is to deepen the discovery of alternative adsorbent materials, derived from industrial and agricultural waste, to remove heavy metals, in this case copper ions, from wastewater.

REZUMAT

Eliminarea metalelor grele este un aspect important în epurarea apelor uzate. Acest lucru se realizează, în special, prin procesul de adsorbție, utilizând ca material adsorbant cărbunele activ. Întrucât cărbunele activ este un material destul de scump, unele cercetări s-au orientat spre găsirea și dezvoltarea unor materiale adsorbante provenite din deșeurile industriale și agricole, care sunt ieftine, disponibile și în cantitate mare. În această lucrare s-au utilizat patru astfel de materiale adsorbante, și anume zgură de furnal, coji de nucă, coji alune de pădure, rumeguș, pentru a urmări eficiența de îndepărtare a ionilor de cupru din apele uzate. S-a observat, în urma experimentelor de laborator, o eficiență de îndepărtare a ionilor de cupru ridicată în cazul materialelor adsorbante studiate, de la 21,66%, în cazul rumegușului, până la 99,96%, în cazul zgurii de furnal. Scopul acestei lucrări este de a aprofunda descoperirea unor materiale adsorbante alternative, provenite din deșeurile industriale și agricole, pentru a îndepărta metalele grele, în acest caz ionii de cupru, din apele uzate.

INTRODUCTION

Water is a vital resource for sustaining life and for this reason water quality must be protected and maintained in parameters as close as possible to natural ones. The existence of wastewater, resulting from the use of water in various anthropogenic processes, has led to the development of processes for eliminating pollutants from this wastewater. Heavy metals are some of the strongest water pollutants because they are chemical elements with a high toxicity in small quantities. In this work, the efficiency of copper removal from wastewater by adsorption was investigated, using various materials derived from industrial and agricultural waste.

Adsorption is one of the most widely used methods for wastewater treatment, as it presents multiple advantages, such as simplicity of use, simple implementation, use of a variety of substances as adsorbents, which leads to a high efficiency of the purification process (*Senthil Rathia, B. et al., 2024*).

. Activated carbon is the most well-known and used adsorbent material in the adsorption process, but, since it is a rather expensive material (*Mishra, P.C. et al., 2009*), the use of alternative materials derived from various types of waste (*Wang, Z. et al., 2016*) has been pursued, such as blast furnace slag (*Dong, Q.G. et al., 2024*), hazelnut shells, walnut shells (*Rawlins, C.H. et al., 2017*), sawdust (*Majid, H. et al., 2022*). Considering the major concern related to the toxicity of heavy metals, as well as the existence of strict

requirements regarding the removal of heavy metals from wastewater, it is necessary to develop adsorption materials that are efficient and economical (*Covaliu, C. et al., 2014*).

To observe the efficiency of removing heavy metals from wastewater using alternative adsorbent materials, a laboratory experiment was conducted to investigate the possibility of the four materials listed above to be used in the adsorption of copper ions. Copper is a heavy metal with a density of 8.96 g/cm^3, a good conductor of heat and electricity, originating from various sources such as metal manufacturing, chemical manufacturing, steel industry, fertilizers and pesticides. It is necessary to remove copper ions from wastewater, as too high a copper content can have undesirable effects on human health, such as anemia, hair loss, kidney problems, headaches (*Senthil Rathia, B. et al., 2024*).

MATERIALS AND METHODS

The adsorbent materials, derived from industrial and agricultural waste, used to test the removal of copper ions from wastewater were blast furnace slag, walnut shells, hazelnut shells, and sawdust. The samples from the four materials used were dried, crushed, ground and sieved through a set of filters to obtain a sample size of 45 µm.

This is because adsorption is the purification process based on the phenomenon of retention on the surface of a body of molecules of a substance dissolved in water, and it is desirable that the granulation of the adsorbent materials be as small as possible in order to have a larger contact surface.

Adsorption experiments were performed using a multi-element solution of heavy metals to obtain wastewater samples. Samples of slag, walnut shells, hazelnut shells, sawdust, with a particle size of 45 µm, in quantities of 10 mg, 25 mg and 50 mg were immersed in 30 mL of heavy metal solution with a concentration of 5 mg/L. Magnetic stir plates were used for homogenization, at 60 rpm, for 60 minutes. All experiments were performed at room temperature.

To determine the concentration of copper ions, a contrAA 800 atomic absorption spectrophotometer was used, where the sample solution to be analyzed is sprayed into the flame, taking place a series of processes through which free atoms are obtained. The analytical characteristics by which the analysis of copper ions was performed, using an atomic absorption spectrophotometer, are specified in the table below (Table 1).

Table 1

Analytical characteristics of the determination of copper ions

Analytical characteristics / Heavy metals	Wavelength (nm)	Linear regression	Detection limit (mg/L)	Limit of quantification (mg/L)	Flame type
Cu^{2+}	324.754	y=0.0187+0.0954x R^2=0.9941	0.0093	0.0280	acetilenă - aer

The Cu^{2+} removal efficiency from wastewater of the four materials studied was calculated as follows:

$$\textit{Removal efficiency, (\%)} = \frac{C_i - C_t}{C_i} \cdot 100 \quad (1)$$

where:

Ci (mg/L) is the initial concentration, and

Ct is the total concentration at a given time, of the Cu^{2+}

RESULTS

All experiments were performed three times, and the average data were used in data analysis. Following examination of 10 mg, 25 mg and 50 mg samples with the contrAA 800 atomic absorption spectrophotometer, the following amounts of Cu^{2+} were found (Table 2):

Table 2

Amounts of Cu^{2+} found in the analyzed samples

Adsorbent material	Heavy metal	Contact time (minutes)	Concentration (mg/L)		
			10 mg	25 mg	50 mg
Blast furnace slag	Cu^{2+}	60	0,0048	0,0023	0,0002
Walnut shells			0,2110	0,2127	0,2425
Hazelnut shells			0,1812	0,1988	0,3021

Sawdust	0,2221	0,3870	0,3917

The efficiency of removing copper ions from wastewater, using the adsorbent materials taken into work, was evaluated as follows (Table 3):

Table 3

The efficiency of removing copper ions from wastewater

Adsorbent material	Heavy metal	Contact time (minutes)	Removal efficiency (%)		
			10 mg	25 mg	50 mg
Blast furnace slag	Cu^{2+}	60	99,04	99,54	99,96
Walnut shells			57,80	57,46	51,50
Hazelnut shells			63,76	60,24	39,58
Sawdust			55,58	22,60	21,66

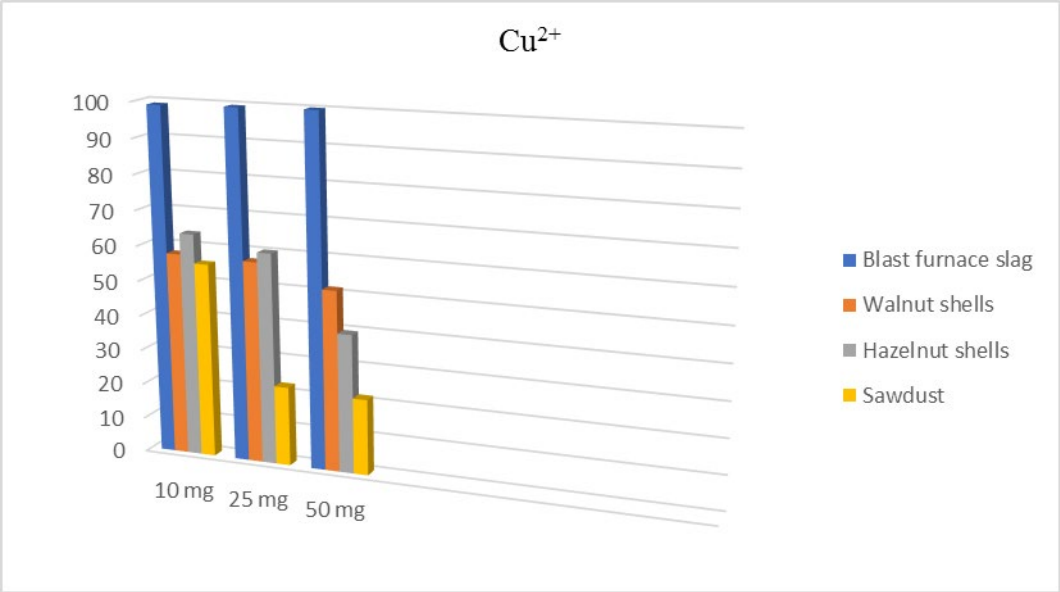

Fig. 1 - Copper ion adsorption efficiency by adsorbent materials

As can be seen from Figure 1, the highest value of the copper ion removal efficiency from the wastewater sample was obtained in the case of blast furnace slag, and the lowest removal efficiency value was obtained in the case of sawdust. Thus, in the case of a quantity of 50 mg of blast furnace slag, the copper ion removal efficiency was 99.96%, for 25 mg of blast furnace slag, the efficiency was 99.54%, and for the quantity of 10 mg there was a removal efficiency of 99.04%.

For hazelnut shells, a removal efficiency of 63.76%, 60.24% and 39.58% was obtained for the quantities of 10 mg, 25 mg and 50 mg of hazelnut shells. In the case of walnut shells, there was an efficiency of 57.80%, 57.46%, 51.50% for the amounts of 10 mg, 25 mg and 50 mg of walnut shells, and by using sawdust as an adsorbent material, a removal efficiency of 55.58%, 22.60%, 21.66% was obtained for the same amounts of 10 mg, 25 mg and 50 mg.

The contact time between adsorbent and adsorbate was 60 minutes for each adsorbent material used.

The amount of adsorbent material used influenced the efficiency of removing copper ions from the wastewater sample. Thus, the best efficiency was for a quantity of 50 mg, in the case of blast furnace slag 99.96%, respectively a quantity of 10 mg, in the case of walnut shells 57.80%, hazelnut shells 63.76 and sawdust 55.58%.

The lowest removal efficiency, for each adsorbent material used, was for the amount of 50 mg, in the case of sawdust 21.66%, hazelnut shells 39.58% and walnut shells 51.50%, and for the amount of 10 mg, in the case of blast furnace slag 99.04%. As can be seen, blast furnace slag, in the case of each amount of adsorbent material, i.e. 10 mg, 25 mg and 50 mg, had a high copper ion removal efficiency, i.e. 99.04%, 99.54% and 99.96%.

The high efficiency of copper removal, using blast furnace slag as an adsorbent material, can be explained by the possibility of copper to form alloys with silicon, calcium, zinc, sulfur, etc. elements that are found in the composition of blast furnace slag.

CONCLUSIONS

Adsorbent materials derived from industrial and agricultural waste offer a reliable and efficient alternative in wastewater treatment. Following laboratory testing, a high efficiency of the adsorbent materials used, namely blast furnace slag, walnut shells, hazelnut shells and sawdust, was observed in the removal of copper ions from wastewater.

These adsorbent materials were used at a fine granulation of 45 μm, because in order to have a large contact surface between the adsorbent and the adsorbate, the granulation of the adsorbent materials must be as small as possible.

The most efficient adsorbent material for copper ions was blast furnace slag, and the adsorbent material with the lowest removal efficiency was sawdust. Thus, in the case of blast furnace slag, in an amount of 50 mg, the removal efficiency was 99.96%, and sawdust, in an amount of 50 mg, presented a removal efficiency of 21.66%.

A promising result, in terms of the removal of copper ions from wastewater, was also obtained in the case of walnut shell, in an amount of 10 mg, an efficiency of 57.80%, respectively, in the case of hazelnut shell, in an amount of 10 mg, an efficiency of 63.76%.

This aspect indicates the possibility and necessity of using such adsorbent materials, derived from industrial and agricultural waste, in wastewater treatment, as they are accessible, cheap and efficient and, at the same time, reduce the amount of waste that may occur.

REFERENCES

[1] Covaliu C., Bunghez I.R., Biriş S.Şt., Paraschiv G. - *Research on copper ions removal from industrial wastewater using environmental friendly nanomaterials*, International Symposium ISB-INMA TEH 2014 "Agricultural and Mechanical Engineering"

[2] Qing-Guo Dong, Jing Li, Zhi-Qing Kang, Muhammad Imran Anwar, Muhammad Asad, Baoji Miao, Shuanghu Wang, Ayesha Younas - *Unlocking the potential: A comprehensive review on blast furnace slag and silica analog adsorbents for sustainable industrial and pharmaceutical pollution control and resource utilization*, Emerging Contaminants 10 (2024) 100387

[3] Haneen Majid, Ghayda Yaseen Al Kindi, Jwad K. Al Refaaec - *A sawdust Filter is Used to Remove Oil From The Kitchen Wastewater*, IOP Conf. Series: Earth and Environmental Science 1120 (2022) 012028.

[4] Mishra P.C., Patel R.K. - *Removal of lead and zinc ions from water by low cost adsorbents*, Journal of Hazardous Materials 168 (2009) 319-325.

[5] Rawlins C.H., Sadeghi F. - *Experimental Study on Oil Removal in Nutshell Filters for Produced-Water Treatment*, 2017 SPE Production & Operations.

[6] Senthil Rathia B., Senthil Kumar P., Natanya Ida Susana J., Francia Virgin J., Dharani R., Sanjay S., Gayathri Rangasamy - *Recent research progress on the removal of heavy metals from wastewater using modified zeolites: A critical review*, Desalination and Water Treatment 319 (2024) 100573.

[7] Wang Z., Huang G., An C., Chen L., Liu J. - *Removal of copper, zinc and cadmium ions through adsorption on water-quenched blast furnace slag*, Desalination and Water Treatment 57 (2016) 22493–22506.

EXPERIMENTAL STUDY ON THE DYNAMIC BEHAVIOR OF THE 3SLP SPRINGBOARD IN RUNNING TESTS

/

STUDIU EXPERIMENTAL PRIVIND COMPORTAMENTUL DINAMIC AL TRAMBULINEI 3SLP ÎN TESTELE DE ALERGARE

Daniel-Mirel DUMITRESCU*[1)], Gheorghe VOICU[2)], Nicolaie ORĂȘANU[2)], Liliana-Caliopi ISCRU[2)], Gabriel-Alexandru CONSTANTIN[2)], Adrian IOSIF[2)]

[1)] Pietrosani Middle School, Teleorman County / Romania;

[2)] National University of Science and Technology POLITEHNICA Bucharest / Romania.

**Tel: 004-0764 050 608; *E-mail: dumitrescudanielmirel@gmail.com*

***Keywords**: springboard, dynamic behavior, gymnastics equipment, impact testing, elasticity*

ABSTRACT

Gymnastics, as a complex and highly educational sport, plays a central role in both physical development and elite athlete training. The quality and safety of gymnastics equipment are critical factors in achieving optimal performance and preventing injuries in schools and sports clubs. Among various apparatuses, the springboard (or vaulting board) serves as a key technical component, converting the athlete's kinetic energy into vertical and horizontal momentum essential for proper acrobatic execution. Its performance depends directly on elastic properties and component reliability, influencing both movement execution and user safety.Specialized studies indicate that optimal springboard elasticity is not an absolute parameter but rather a balance between frame stiffness, elastic element characteristics (coil springs, leaf springs), and assembly. Reliability—defined as durability and consistent performance—depends on the elastic system's behavior under repeated and varied loads.This study experimentally evaluates the dynamic behavior of a 3SLP springboard through controlled tests involving three participants with different body masses (40 kg, 58.5 kg, and 68 kg). Tests included controlled drops from heights of 30 cm and 60 cm at specified impact points, as well as running approaches from a 5 m distance. The results highlight the relationship between impact conditions, elastic response, and performance consistency, providing insights for equipment optimization and safety standards in gymnastics training.

REZUMAT

Gimnastica, ca sport complex și extrem de educativ, joacă un rol central atât în dezvoltarea fizică, cât și în antrenamentul sportivilor de elită.Calitatea și siguranța echipamentului de gimnastică sunt factori critici în obținerea performanței optime și prevenirea accidentărilor în școli și cluburi sportive. Printre diversele aparate, trambulina(sau placa de sărituri) servește drept componentă tehnică cheie, transformând energia cinetică a sportivului în impuls vertical și orizontal, esențial pentru o execuție acrobatică corectă.Performanța sa depinde direct de proprietățile elastice și de fiabilitatea componentelor, influențând atât execuția mișcării, cât și siguranța utilizatorului. Studiile specializate indică faptul că elasticitatea optimă a unei trambuline nu este un parametru absolut, ci mai degrabă un echilibru între rigiditatea cadrului, caracteristicile elementelor elastice (arcuri elicoidale, arcuri lamelare)și asamblare.Fiabilitatea definită ca durabilitate și performanță constantă - depinde de comportamentul sistemului elastic sub sarcini repetate și variate.Acest studiu evaluează experimental comportamentul dinamic al unei trambuline 3SLP prin teste controlate care au implicat trei participanți cu mase corporale diferite (40 kg, 58,5 kg și 68 kg). Testele au inclus căderi controlate de la înălțimi0 de 30 cm și 60 cm în puncte de impact specificate, precum și abordări de alergare de la o distanță de 5 m.Rezultatele evidențiază relația dintre condițiile de impact, răspunsul elastic și consecvența performanței, oferind informații pentru optimizarea echipamentului și standardele de siguranță în antrenamentul de gimnastică.

INTRODUCTION

Dimensions and characteristics of the trampoline used in the determinations

The trampoline analyzed in the experiments was made of curved laminated plywood, a material chosen for its robustness and optimal elasticity, capable of ensuring both mechanical resistance and the flexibility necessary for dynamic behavior. The contact surface is upholstered with a layer of polyethylene

and covered with carpet, which improves comfort and increases grip during jumps, reducing the risk of slipping and contributing to the safety of the user. The elastic system is made up of spiral springs made of nickel-plated steel, arranged in such a way as to ensure controlled deformability of the assembly. These include two types of coils:

- a conical spring, consisting of 6 turns, with a total length of 137 mm, an upper diameter of 52.5 mm, a lower diameter of 85 mm and a material thickness of 5.9 mm;
- a cylindrical spring, with 4 turns, with a thickness of 6 mm, a diameter of 65 mm and a total length of 78 mm.

The upper plate of the assembly has a thickness of 16.5 mm, while the lower plate has a thickness of 26.5 mm, both having a width of 142.8 mm. Additional elasticity is provided by a metal slat with a thickness of 5 mm, a width of 50 mm and a length of 595 mm, which reinforces the structure

The overall dimensions of the trampoline are 1200 × 600 × 200 mm (length × width × height), with a front threshold of 20 mm and an extension of 600 mm.

The constructive curves of the plates were defined as follows: the lower lamella has a curvature of 50 mm, and the upper threshold also has a curvature of 50 mm. Through these characteristics, the trampoline offers an optimal combination of rigidity and flexibility, ensuring an elastic behavior suitable for experimental tests on the absorption and redistribution of kinetic energy.

MATERIALS AND METHODS

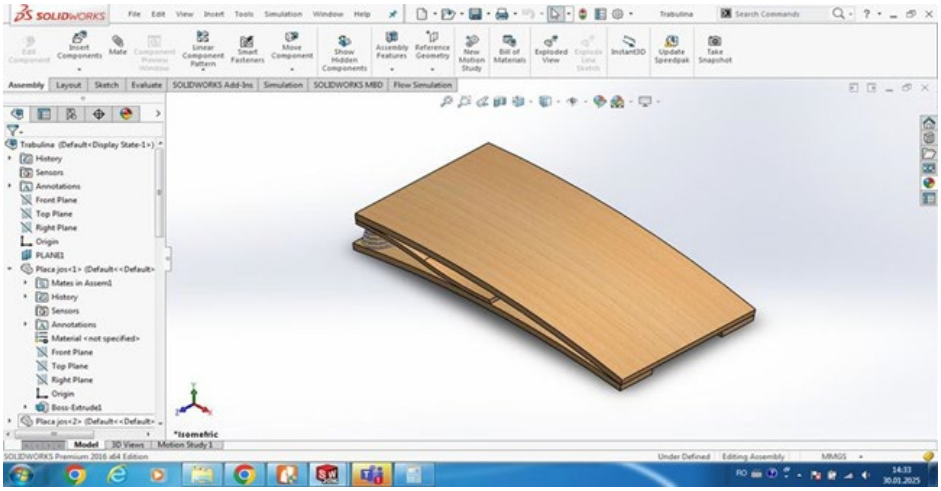

Fig. 1 - Three-dimensional model of the 3SLP trampoline-type elastic structure made in SolidWorks

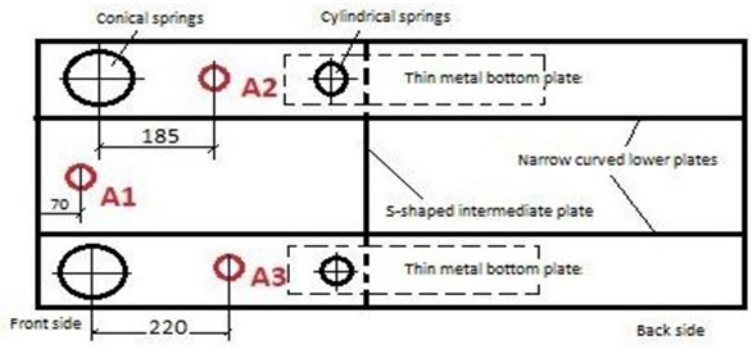

Fig. 2 - Mounting of accelerometers and configuration of the acquisition system

To perform dynamic measurements, three metal plates were fixed on the lower part of the 3SLP elastic structure, acting as supports for the piezoelectric accelerometers. The recordings were made with CCLD sensors, model 4507-B-001 with integrated TEDS, characterized by a sensitivity of 10 mV/g (equivalent to 1 mV/(m s²), a frequency range of 0.1–6000 Hz and a working temperature range between −54 °C and +121 °C, parameters that make them suitable for precision vibration measurements.

The arrangement of the sensors was chosen to capture the differentiated behavior of the structure depending on the monitored area:A1 – located under the front of the upper plate curved in "S", corresponding to position P1, responsible for the direct interaction with the conical springs (*Di Rocco, F., Papale, O., Festino, E., De Maio, M., Cortis, C., & Fusco, A. (2023).*

A2 – positioned in the middle area, on the lower part of the curved plates, at the transition between the truncated conical and cylindrical springs;A3 – installed in the rear part (P3), where the structural response is dominated by the cylindrical springs.

The accelerometers were connected to an NI USB-9233 acquisition system, designed for vibration and noise analysis, and the data were processed using dBFA Suite 4.8.1 software (01dB-METRAVIB, Areva Group), which allowed the recording, integration and visualization of dynamic signals.

RESULTS

To obtain the kinematic parameters, the raw data were subjected to a first-order numerical integration, to determine the instantaneous velocities, and a second- order integration, to calculate the displacements of the measured points *(Eager, D., Zhou, S., Ishac, K., Hossain, I., Richards, A., & Sharwood, L. N. (2022*).

The acquisition system was activated a few seconds before contact, so that the resulting graphs include both the natural oscillations of the structure before impact (of higher frequency) and their modification at the moment of contact, when the amplitudes increase considerably.

The present study analyzes the recordings provided by accelerometers mounted on a 3SLP trampoline, used by a subject with a mass of 40 kg. The main objective is to characterize the elastic behavior of the structure under variable dynamic conditions, which correspond to jumps performed after a 3 m and 5 m run, respectively, within three successive tests (Tests 1, 2 and 3).The data collected by accelerometers A1 and A2 allow the investigation of both the impact zone itself and the way in which the oscillations propagate in the trampoline structure.

Accelerometer A1, located in the frontal area (P1), provides direct information on the local response of the truncated conical springs, while accelerometer A2, positioned in the medial area (P2), captures the combined effects of the two types of springs and the elastic transition phenomenon.

The comparison of the signals recorded in the two positions highlights significant differences in the amplitude and phase of the oscillations suggesting a progressive attenuation of the energy as it propagates from the impact point to the rest of the structure. These results contribute to a more detailed understanding of the distribution of stresses and the role of each elastic zone in the process of absorption and restitution of kinetic energy.

Description of the experimental procedure

To evaluate the dynamic behavior of the structure, tests were carried out with the participation of three volunteer students, with different body masses (40 kg, 58.5 kg and 68 kg). They were subjected to tests consisting of:

- controlled falls from heights of 30 cm and 60 cm, at predetermined impact points (previous figure);
- lunge jumps, after 5 m runs.

The recorded data allowed the analysis of the acceleration evolution in the three measurement positions (A1, A2, A3). For the present study, the results obtained for the 40 kg subject, who performed jumps after 3 m and 5 m runs, within three successive repetitions (Trials 1–3), are presented in particular. The A1 accelerometer, located frontally (P1), provided relevant information regarding the local response of the conical springs, while the A2 accelerometer, positioned medially (P2), recorded the combined effects of the conical and cylindrical springs, highlighting the elastic transition zone *(Križaj, D., & Čuk, I. (2015).*

The comparison of the signals measured in the two positions revealed significant differences in amplitude and phase, which confirms a progressive attenuation of the energy as it propagates from the point of impact to the rest of the structure. These results contribute to a deeper understanding of how the dynamic load is distributed and of the specific role of each elastic zone in the absorption and return of kinetic energy *(Kobayashi, S., & Hasegawa, T. (2021).*

To ensure the full capture of the dynamic phenomenon, the acquisition system was activated a few seconds before the moment of the ball's release.

Thus, in the resulting graphs, relatively high-frequency initial oscillations are observed, associated with the structure's own vibrations before impact.At the moment of contact, these oscillations significantly change their character, becoming more frequent and with a higher amplitude. The first pronounced oscillation in this new regime corresponds to the actual moment of impact between the ball and the trampoline surface.

In this study, the recordings obtained from accelerometers mounted on a 3SLP trampoline, used by a subject with a mass of 40 kg, are analyzed. The main objective is to characterize the elastic behavior of the structure under various dynamic conditions, corresponding to jumps performed after a 3 m and, respectively, 5 m run, within three successive tests (Tests 1, 2 and 3).

The data provided by accelerometers A1 and A2 allow the investigation of both the actual impact zone and the way in which the oscillations propagate in the trampoline structure. Accelerometer A1, located in the frontal area (P1), provides direct information on the local response of the truncated conical springs, while accelerometer A2, positioned in the medial area (P2), captures the combined effects of the two types of springs and the elastic transition phenomenon.

Comparison of the signals recorded at the two positions highlights significant differences in the amplitude and phase of the oscillations, suggesting a progressive attenuation of the energy as it propagates from the point of impact to the rest of the structure. These results contribute to a better understanding of the stress distribution and the role of each elastic zone in the absorption and return of kinetic energy.

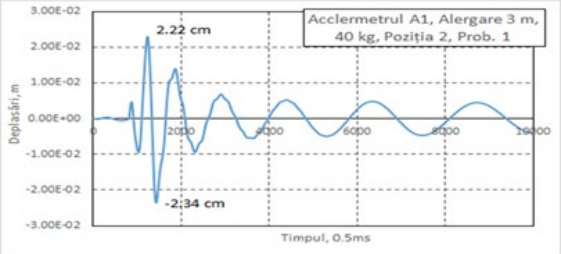

Fig. 3 - Accelerometer A1

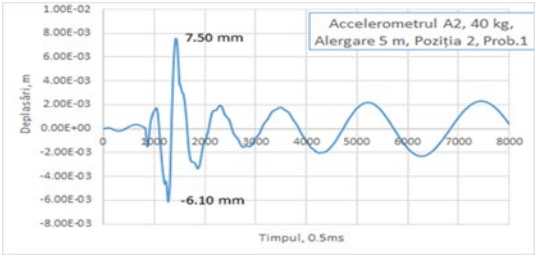

Fig. 4 - Accelerometer A2

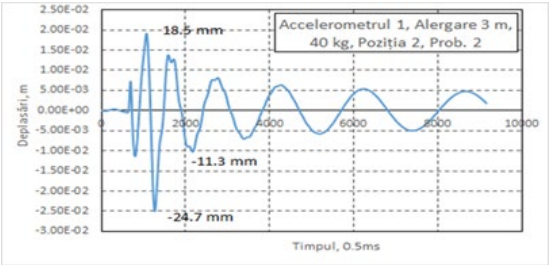

Fig. 5 - Accelerometer A1

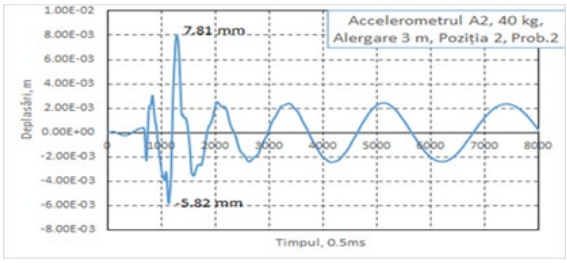

Fig. 6 - Accelerometer A2

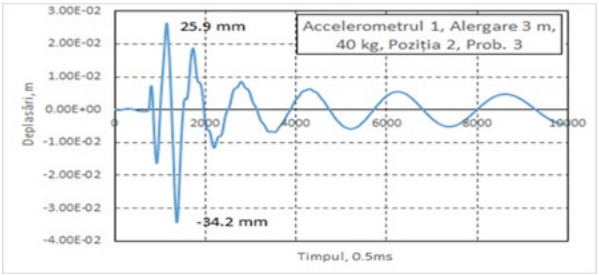

Fig. 7 - Accelerometer A1

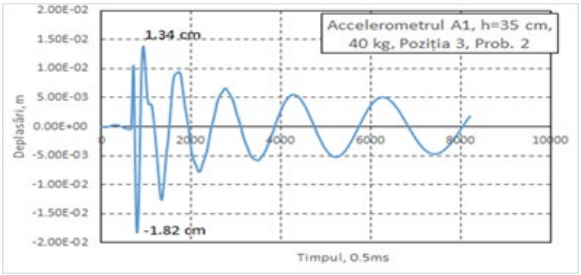

Fig. 8 - Accelerometer A2

Experimental results and interpretationAccelerometer A1 response – 3 m run, subject 40 kg, position P2, sample 1The graph in figure 3 illustrates the response of accelerometer A1 recorded after a jump performed after a 3 m run, by a subject with a mass of 40 kg. The maximum displacements obtained, of +2.22 cm and −2.34 cm, highlight a pronounced and almost symmetrical dynamic behavior with respect to the equilibrium position.

The temporal evolution of the signal shows a progressive decrease in amplitude, which confirms the existence of an efficient damping mechanism in the frontal area. The regular shape of the waves suggests a

rapid and controlled elastic return, and the proximity of the positive and negative extreme values indicates a uniform application of force in the impact area. These characteristics confirm the ability of the frontal plate to take over and redistribute kinetic energy in a balanced way.

Accelerometer A2 response – 5 m run, subject 40 kg, position P2, sample 1.

The graph in figure 4 shows the displacements recorded by the accelerometer A2, located in the median zone, for a jump performed after a 5 m run. The maximum measured values, of +7.50 mm and −6.10 mm, reflect a relatively moderate response of the structure in this zone, despite the higher kinetic energy associated with running over a longer distance. This finding suggests that the P2 position benefits from a higher stiffness or a more efficient constructive support, which limits the amplitude of the deformations. The oscillations are clear, regular and present a visible damping, indicating a predictable and stable elastic behavior. The persistence of the waveform throughout the measurement interval confirms the role of the median zone in dissipating energy without generating local resonance phenomena.

Accelerometer A1 response – 3 m run, subject 40 kg, position P2, sample 2In this experimental repetition, the maximum amplitudes reached +18.5 mm and −24.7 mm, significantly higher than in the previous sample. The difference between the positive and negative displacements suggests an asymmetric impact, most likely determined by a lateral landing of the subject. The initial oscillations are characterized by high amplitudes, and their decrease is relatively slow, which indicates a weaker energy dissipation. This finding confirms the increased sensitivity of the frontal area to the variations in the subject's positioning on the surface. Compared to the tests performed under symmetric impact conditions, sample 2 highlights the importance of load distribution in the overall behavior of the structure *(Lehmann, T., Schleichardt, A., Naundorf, F., & Knoll, K. (2017).*

Accelerometer A2 response – 3 m run, subject 40 kg, position P2, test 2In this test, accelerometer A2 recorded maximum values of +7.81 mm and −5.82 mm, considerably lower than those obtained by A1 under similar conditions. The relatively small difference between the extremes suggests a more uniform impact and a more balanced distribution of the dynamic load in the median area.The oscillations, although with low amplitude, are well-defined and with constant periodicity, which denotes a robust elastic behavior and a good capacity of the structure to respond in a controlled manner. The positioning of sensor A2, less exposed to direct contact, explains both the reduced amplitudes and the stability of the response. This result emphasizes the importance of choosing the measurement points for the correct characterization of the dynamic response.

Accelerometer A1 response – 3 m run, subject 40 kg, position P2, test 3In the third test, accelerometer A1 recorded the largest displacements of all the tests performed: +25.9 mmnand −34.2 mm. These very high values indicate either a particularly violent impact or the occurrence of a local resonance phenomenon.

The shape of the graph suggests unstable initial oscillations, with large amplitudes and relatively slow attenuation, which confirms the intense stress on the frontal area. This behavior can be correlated with a particular positioning of the subject or with an uneven application of force.

The results could also indicate the beginning of a material fatigue process or a reduction in the elastic performance of the elements in the monitored area.

Comparative analysis between dynamic responses. Maximum displacement amplitude: In all cases, A1 recorded larger displacements than A2. For example, in Sample 1, A1 reached ±22.2– 23.4 mm, while A2 only ±6–7.5 mm.

This contrast highlights the fact that the frontal area takes the direct load, while the median area is less affected. Evolution of amplitudes on samples: In A1, a constant increase in maximum displacements between samples is noted (2.22 cm → 2.47 cm, 3.42 cm), which can be explained by a more energetic application of force or by the accumulation of structural fatigue effects. In A2, the values remain stable, with minor variations, confirming the stability of the median area.Influence of running distance:

For A2, the difference between the 3 m and 5 m runs was insignificant (7.50 mm vs. 7.81 mm), indicating that the additional energy is not efficiently transmitted to the edge of the structure.Symmetry of response: In Trial 2, A1 recorded asymmetric values (+18.5 mm vs. −24.7 mm), confirming the sensitivity of the frontal zone to lateral landings. In contrast, A2 maintained a more balanced response, indicating a reduced influence of the impact position.Oscillation damping: In A1, the damping became progressively slower between trials, suggesting a decrease in the damping efficiency in the frontal zone.

In A2, oscillations were consistently well controlled, confirming its stabilizing role *(Middelkoop, C. (2019)*. The results show that the elastic structure exhibits different behavior depending on the impact

position. The frontal zone (A1) is more sensitive, registers large amplitudes and is strongly influenced by the exact position of the contact. The middle zone (A2) exhibits a stable behavior, with low amplitudes and constant damping, demonstrating its role as a buffer and dissipative zone.These findings highlight the importance of a differentiated design of stiffness and damping, so that the structure can respond uniformly and safely to varying dynamic loads

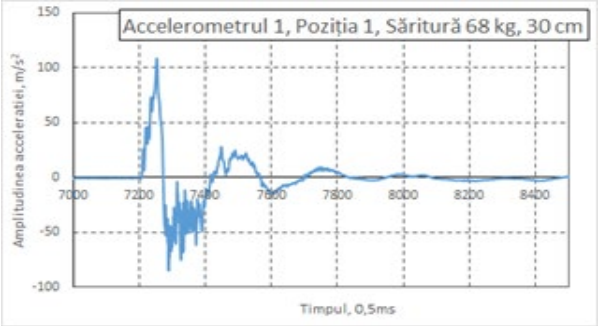

Fig. 9 - Accelerometer A1

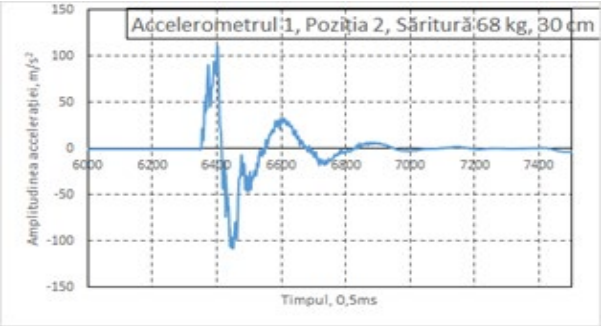

Fig. 10 - Accelerometer A1

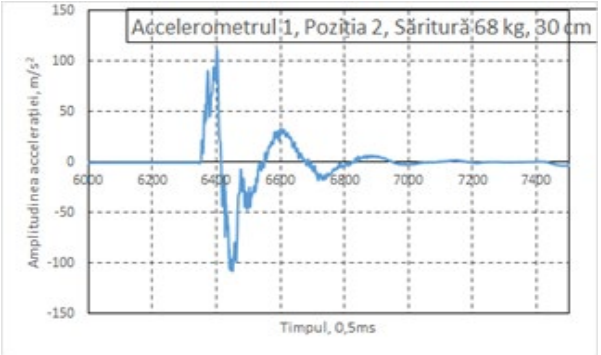

Fig. 11 - Accelerometer A1

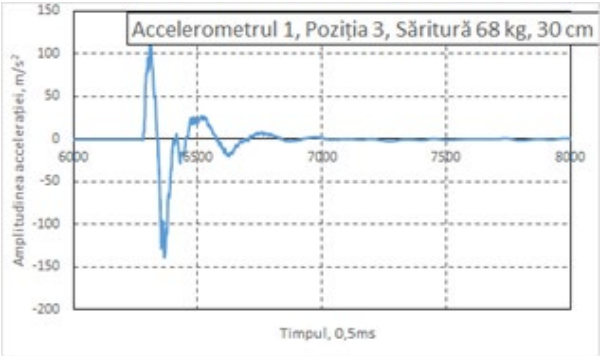

Fig. 12 - Accelerometer A1

Interpretation of experimental resultsAnalysis of the signals obtained for the subject with a mass of 68 kg, in the case of a controlled fall from 30 cm.From the evaluation of the signals recorded by the accelerometer A1, centrally located 70 mm from the front edge of the elastic structure, for a jump from a height of 30 cm (lateral position at 35 cm), it is found that acceleration values of over 100 m/s² are reached in all three positions investigated (140 mm, 330 mm and 530 mm from the front end).

However, the amplitudes and the vibration regime differ, indicating a progressive damping from position 1 to position 3.Position 1 (above accelerometer A1): the maximum acceleration reached values of +108.6 m/s² and −84.2 m/s².² *(Lehmann, T., Lorz, A., Schleichardt, A., Naundorf, F., Knoll, K., Eckardt, F., & Witte, K. (2020).*

The initial oscillation is pronounced, especially under the upper plate, and the duration of the damping was about 1200 ms.Position 2 (≈260 mm from A1): the amplitudes increase to +110.8 m/s² and −105.2 m/s², but the number of undulations is reduced, and the damping occurs more quickly, in about 1000 ms.Position 3 (≈460 mm from A1, close to the free end): the accelerometer recorded maximum values of +115.9 m/s² and −139.2 m/s².

However, the damping is accelerated (≈800 ms), and the positive/negative alternations are less, which suggests more efficient energy dissipation in the free area of the structure. In conclusion, the amplitudes increase from position 1 to position 3, but the damping duration decreases significantly, confirming the existence of zonal differences in stiffness and energy dissipation.

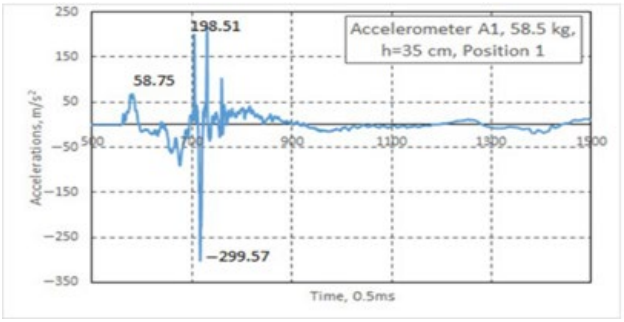

Fig. 13 - Accelerometer A1

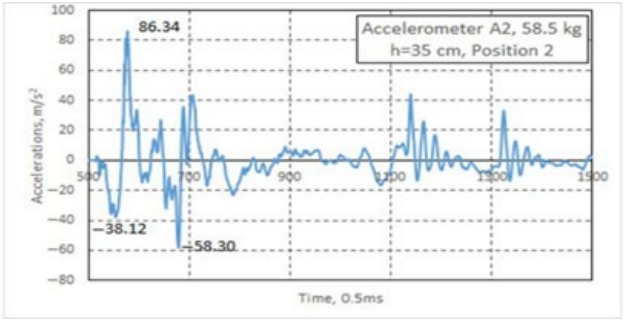

Fig. 14 - Accelerometer A2

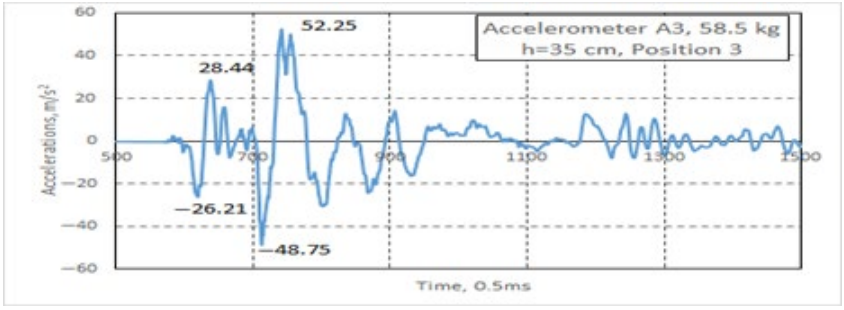

Fig. 15 - Accelerometer A2

Experimental resultsFor Position 1 (A1, frontal area) maximum amplitudes of +198.51 m/s² and −299.57 m/s² were recorded, preceded by an initial oscillation of +58.75 m/s². The signal shows sudden variations immediately after impact, followed by a progressive damping, which confirms the intense stress on the conical springs responsible for absorbing the shock.In Position 2 (A2, medial area) the maximum values were +86.34 m/s², −38.12 m/s² and −58.30 m/s².

The oscillations had a lower amplitude than in A1, but with a more complex structure, marked by multiple alternations. This behavior reflects the role of the medial area as a transitional element, where the conical and cylindrical springs interact.For Position 3 (A3, posterior area) the amplitudes reached +52.25 m/s² and −48.75 m/s², with moderate initial values (+28.44 m/s² and −26.21 m/s²).The signal attenuated more quickly, presenting low intensity and relatively regular oscillations, characteristic of energy dissipation through the cylindrical springs.

Comparative analysisThe results show a progressive decrease in amplitudes from the front to the rear of the structure. Position A1 highlights the maximum amplitudes, corresponding to direct shock absorption; A2 reflects the transfer and redistribution of energy; and A3 confirms the dissipation and subsequent stabilization. This distribution demonstrates the existence of distinct local stiffnesses and the differentiated role of conical and cylindrical springs in the dynamic behavior of the assembly.

CONCLUSIONS

1. The 3SLP elastic structure exhibits its dynamic behavior through the balance between the stiffness of the plates, the characteristics of the conical and cylindrical springs and the assembly method, elements that determine the overall performance.
2. The athlete's mass directly influences the amplitude and duration of the oscillations; the values increase proportionally with the weight, which confirms the sensitivity of the assembly to variable dynamic loads.
3. The fall height has a major effect on the maximum amplitudes: the tests at 60 cm produced larger and more difficult to dampen oscillations compared to those at 30 cm.
4. The frontal zone (A1) absorbs the initial shock and presents the largest displacements, confirming the dominant role of the conical springs in absorbing the impact energy.
5. The median zone (A2) reflects a stable elastic transition, with moderate amplitudes and constant damping, due to the interaction between the conical and cylindrical springs.
6. The posterior area (A3) has a predominantly dissipative role, the amplitudes being reduced and the oscillations quickly die out, which contributes to the stabilization of the entire assembly.
7. The experimental results provide a basis for optimizing the design and standardizing gymnastics equipment, ensuring both increased performance and increased user safety.

ACKNOWLEDGEMENT

This paper is written during the doctoral internship of the first author in the Doctoral School of Biotechnical Systems Engineering, from the National University of Science and Technology Politehnica Bucharest.

REFERENCES

[1] Bradshaw, E. (2004). Target-directed running in gymnastics: A preliminary exploration of vaulting.Sports Biomechanics, 3*(1), 125–144. https://doi.org/10.1080/14763140408522834.

[2] Di Rocco, F., Papale, O., Festino, E., De Maio, M., Cortis, C., & Fusco, A. (2023). Acute effects of mini trampoline training session on leg stiffness and reactive power. *Applied Sciences, 13*(17), 9865. https://doi.org/10.3390/app13179865.

[3] Eager, D., Zhou, S., Ishac, K., Hossain, I., Richards, A., & Sharwood, L. N. (2022). Investigation into the trampoline dynamic characteristics and analysis of double bounce vibrations.Sensors, 22*(8),2916. https://doi.org/10.3390/s22082916.

[4] Kobayashi, S., & Hasegawa, T. (2021). Detection of motion on a trampoline with a smartwatch. *Sensors, 21*(24), 8413. https://doi.org/10.3390/s21248413.

[5] Križaj, D., & Čuk, I. (2015). Can miniature accelerometers attached to the gymnastics springboard be used for take-off analysis? *Science of Gymnastics Journal, 7*(3), 69–79.

[6] Lehmann, T., Schleichardt, A., Naundorf, F., & Knoll, K. (2017). Modeling a springboard in gymnastics. In *Proceedings of the 35th Conference of the International Society of Biomechanics in Sports* (pp. 284–287). Cologne, Germany.

[7] Lehmann, T., Lorz, A., Schleichardt, A., Naundorf, F., Knoll, K., Eckardt, F., & Witte, K. (2020). A multi-body model of a springboard in gymnastics. *Science of Gymnastics Journal, 12*(3), 265–275.

[8] Middelkoop, C. (2019). *Evaluation of artistic gymnastics vault board design* (Master's thesis). Iowa State University, Ames, IA, USA.

[9] Park, S.-K., Park, J.-K., Won, H.-I., Choi, S.-H., Kim, C.-H., Lee, S., & Kim, M. Y. (2022). Three-dimensional foot position estimation based on footprint shadow image processing and deep learning for smart trampoline fitness system. *Sensors, 22*(17), 6922. https://doi.org/10.3390/s22176922

[10] Radeș, M. (2008). Mechanical vibrations. Bucharest: Printech Publishing House.

KINEMATIC ANALYSIS OF A DISINFECTION SPIDER ROBOT
/
ANALIZA CINEMATICĂ A UNUI ROBOT PĂIANJEN DE DEZINFECȚIE

Sorin NEGROIU*[1)], Andrei CRAIFALEANU[1)], Florinel LUPU[2)]
*[1)] Student, Department of Mechanics, National University of Science and Technology POLITEHNICA Bucharest / Romania;
[1)] Associate Professor, Department of Mechanics, National University of Science and Technology POLITEHNICA Bucharest / Romania;
[2)] Student, Department of Mechanics, National University of Science and Technology POLITEHNICA Bucharest / Romania.
*[1)] *Tel: 0729 076 640; E-mail: sorin.negroiu@stud.mec.upb.ro*
[1)] *Tel: 0724 896 306; E-mail: andrei.craifaleanu@upb.ro*
*[2)] *Tel: 0758 727 272; E-mail: florinel.lupu@stud.isb.upb.ro*

Keywords: *arachnids, structure, kinematics, rotation angle.*

ABSTRACT
In the medical domain, surface disinfection has been a critical factor in the performance of all procedures. In this regard, it has been found that the use of robots specifically designed for this purpose is the best option. This paper examines the kinematics of a spider robot used in the disinfection process of a room. It has a robotic arm attached, which could be used to disinfect surfaces less accessible to conventional robots. The kinematic analysis was performed both on the body of the robot and on the robotic arm, at the end of which an ultraviolet light lamp was attached.

REZUMAT
În domeniul medical, dezinfectarea suprafețelor a reprezentat un factor foarte important în desfășurarea tuturor procedurilor. În acest sens, s-a constatat că utilizarea roboților special proiectați pentru acest scop este cea mai bună opțiune. În cadrul acestui articol, s-a studiat cinematica unui robot păianjen, utilizat în procesul de dezinfecție a unei camere. Acesta are atașat un braț robotic, cu care poate dezinfecta suprafețe mai puțin accesibile roboților convenționali. Analiza cinematică a fost realizată atât asupra corpului robotului, cât și asupra brațului ce are atașat la capăt o lampă cu lumină ultravioletă.

INTRODUCTION

A robot is a system capable of performing autonomous tasks, which can be operated by an operator or by a computer program *(Karakurt et al., 2015; Kyrarini and Lygerakis, 2021)*. Disinfection robots have been an essential aid for medical staff, both during and after the COVID-19 pandemic, as sanitization of medical wards is necessary for proper patient care.

One effective method is the use of robots which utilize ultraviolet (UV) light for disinfection *(Gasparetto and Vidoni, 2008).* The most widely used type of robot on the market is the wheeled robot model, as shown in *(Gasparetto and Vidoni, 2008).* However, it has been found that for some more difficult to reach places, it would be ideal to use another type of robot, as shown in various articles.

The spider robot, an alternative to the conventional type of robots with wheels, comes with a number of additional advantages over other models on the market.

The spider robot can replicate the motion of the arachnids *(Ikhar and Lanjewar, 2023),* having better flexibility and a wide variety of movements. Over the years, many such robotic systems have been created and studied.

In *(Karakurt et al., 2015),* a simplified mechanical model was developed for a spider robot with a specific structure: six limbs and three segments. This model was created since it is very difficult to synthesize an exact model for a robot which has limbs based on a multi-link structure, such as one with a total of twenty-four mobilities *(Karakurt et al., 2015; Craifaleanu and Negroiu, 2024).*

In *(Chen et al., 2023; Craifaleanu and Negroiu, 2024; Karakurt et al., 2015; Kravchenko, 2023; Manikandan and Sandeep, 2023),* more models of quadrupedal spider robots have been designed, in order to mimick the spider walk. These models have similar mechanical structures, but different electronic control systems *(Craifaleanu and Negroiu, 2024).*

MATERIALS AND METHODS

The paper presents a spider robot, which uses UV light devices to disinfect various surfaces. The spider robot kit BITMI 10158 (Fig. 1) was used as a model, to which a stand with four UV lamps and a robotic arm were attached (Fig. 2, 3).

The improvement is represented by the addition of the robotic arm, which has a lamp and a sensor attached at the end. This device is more convenient for disinfection in places that are difficult to reach for other types of robots, such as the underside of a chair or a toilet seat.

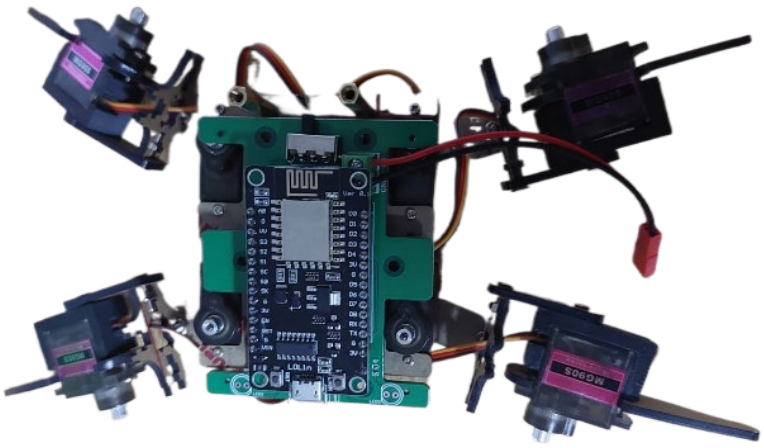

Fig. 1 - BITMI 10158 robot kit

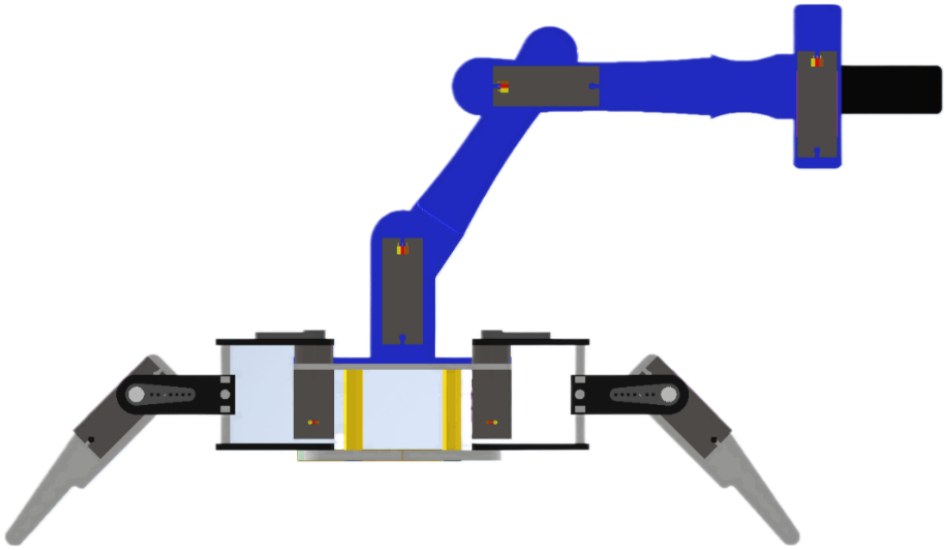

Fig. 2 - 3D model of presented robot

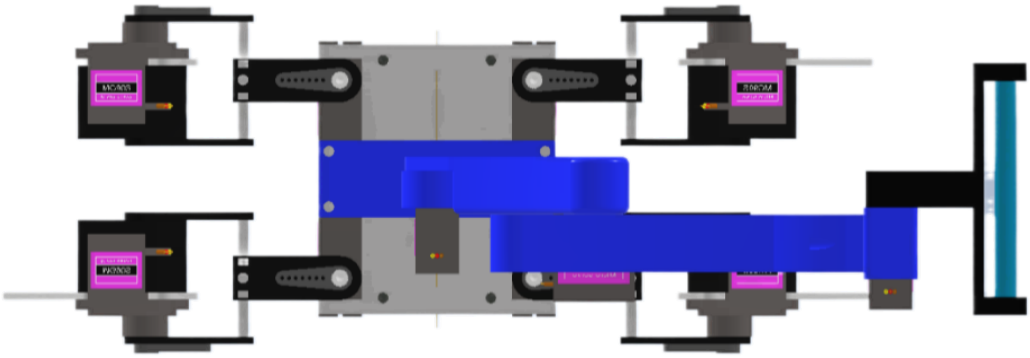

Fig. 3 - A top view of the 3D model of the robot

A kinematic analysis for the entire system is presented, in which the velocities and accelerations of the robot legs and the arm attached to the robot are determined.

In the following pages, some of the study methods used for kinematic calculations were presented *(Radoi and Deciu).*

The first method involves the kinematics of the relative motion of a rigid body. For this method, three coordinate systems were defined: T_0, fixed, T_1, in motion with respect to T_0 and T_2, which is connected to the rigid body. System T_2 is in motion with respect to both T_0 and T_1. A point M of the rigid body is considered (Fig. 4).

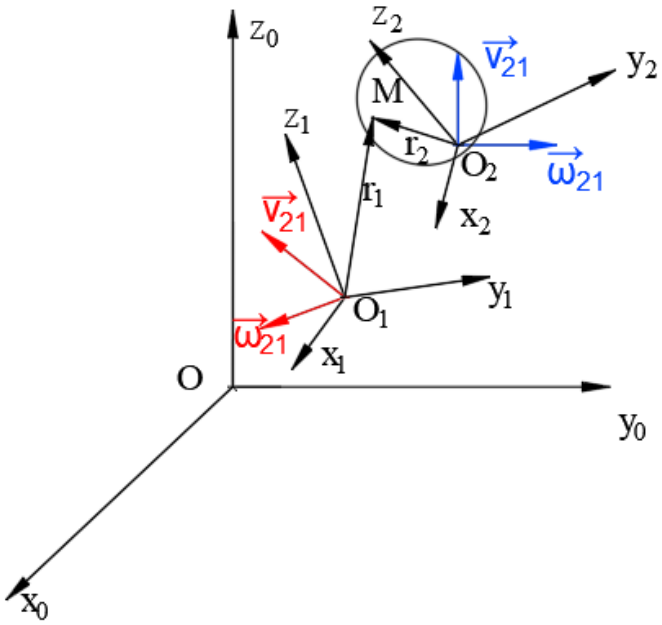

Fig. 4 - The three systems and their respective elements *(Radoi and Deciu)*

The motion of an arbitrary system T_j with respect to another system, T_i is defined by the velocity $\vec{v}_{ji}$ and by the acceleration $\vec{a}_{ji}$ of the origin O_j with respect to T_i, as well as by the angular velocity vector $\vec{\omega}_{ji}$ and by the angular acceleration vector $\vec{\varepsilon}_{ji}$ [9, p.274-275].

The composition formula of the velocities in the relative motion of a material point *(Radoi and Deciu)*,

$$\vec{v}_a = \vec{v}_r + \vec{v}_t, \tag{1}$$

Leads to the following relation:

$$\vec{v}_{20}^{M} = \vec{v}_{10} + \vec{v}_{21} + \vec{\omega}_{10} \times \vec{r}_1 + \vec{\omega}_{21} \times \vec{r}_2. \tag{2}$$

In this relation, $\vec{r}_i$ represents the position vector of point *M*, with respect to origin O_i.

For an arbitrary number *n* of reference systems, formula (2) can be generalized as

$$\vec{v}_{n0}^{M} = \sum_{i=1}^{n} \vec{v}_{i,i-1} + \sum_{i=1}^{n} \vec{\omega}_{i,i-1} \times \vec{r}_i. \tag{3}$$

Similarly, the absolute acceleration of point *M* is

$$\vec{a}_a = \vec{a}_r + \vec{a}_t + \vec{a}_c, \tag{4}$$

which leads to

$$\begin{aligned} \vec{a}_{20}^{M} = {} & \vec{a}_{10} + \vec{a}_{21} + \vec{\varepsilon}_{10} \times \vec{r}_1 + \vec{\varepsilon}_{21} \times \vec{r}_2 + \\ & + \vec{\omega}_{10} \times (\vec{\omega}_{10} \times \vec{r}_1) + \vec{\omega}_{21} \times (\vec{\omega}_{21} \times \vec{r}_2) + 2\vec{\omega}_{10} \times (\vec{v}_{21} + \vec{\omega}_{21} \times \vec{r}_2). \end{aligned} \tag{5}$$

Similarly to formula (2), formula (5) can be generalized for an arbitrary number *n* of reference systems *(Radoi and Deciu)*:

$$\vec{a}_{n0}^{M} = \sum_{i=1}^{n} \vec{a}_{i,i-1} + \sum_{i=1}^{n} \vec{\varepsilon}_{i,i-1} \times \vec{r}_i + \sum_{i=1}^{n} \vec{\omega}_{i,i-1} \times \left(\vec{\omega}_{i,i-1} \times \vec{r}_i\right) + \\ + 2\sum_{i=1}^{n}\sum_{j=1}^{i-1} \vec{\omega}_{j,j-1} \times \left(\vec{v}_{i,i-1} + \vec{\omega}_{i,i-1} \times \vec{r}_i\right). \tag{6}$$

The second method involves numerical derivation. The relationships for *x* components of velocity and acceleration of a point are *(Radoi and Deciu)*:

$$v_{x_i} \cong \frac{x_{i+1} - x_{i-1}}{t_{i+1} - t_{i-1}} \quad (i = 1,...,n), \tag{7}$$

$$a_{x_i} \cong \frac{x_{i+1} - 2x_i + x_{i-1}}{(t_{i+1} - t_i)^2} \quad (i = 1,...,n). \tag{8}$$

For *y* and *z* components, similar relations are valid:

$$v_{y_i} \cong \frac{y_{i+1} - y_{i-1}}{t_{i+1} - t_{i-1}} \quad (i = 1,...,n), \tag{9}$$

$$a_{y_i} \cong \frac{y_{i+1} - 2y_i + y_{i-1}}{(t_{i+1} - t_i)^2} \quad (i = 1,...,n), \tag{10}$$

$$v_{z_i} \cong \frac{z_{i+1} - z_{i-1}}{t_{i+1} - t_{i-1}} \quad (i = 1,...,n), \tag{11}$$

$$a_{z_i} \cong \frac{z_{i+1} - 2z_i + z_{i-1}}{(t_{i+1} - t_i)^2} \quad (i = 1,...,n). \tag{12}$$

The kinematic analysis is performed for the robotic arm and for one leg of the spider robot. First, the motions of the servomotors that drive the robot will be defined.

The robot (Fig. 5) has eleven servomotors built into its structure. The servomotors in points O_2, O_3, O_4, O_5, are designed to drive the legs of the robot (as shown in Fig. 6). Those in O_2 and O_4 rotate about O_iZ_i axis with angles ψ_i (*i* = 2, 4), respectively, while servomotors in O_3 and O_5 rotate about the O_iY_i axis, with angles θ_i (*i* = 3, 5), respectively (Fig. 7).

The servomotors in points O_6, O_7, O_8 are used to operate the robot arm. These servomotors rotate about O_iY_i axis with angles θ_i (*i* = 6, 7, 8).

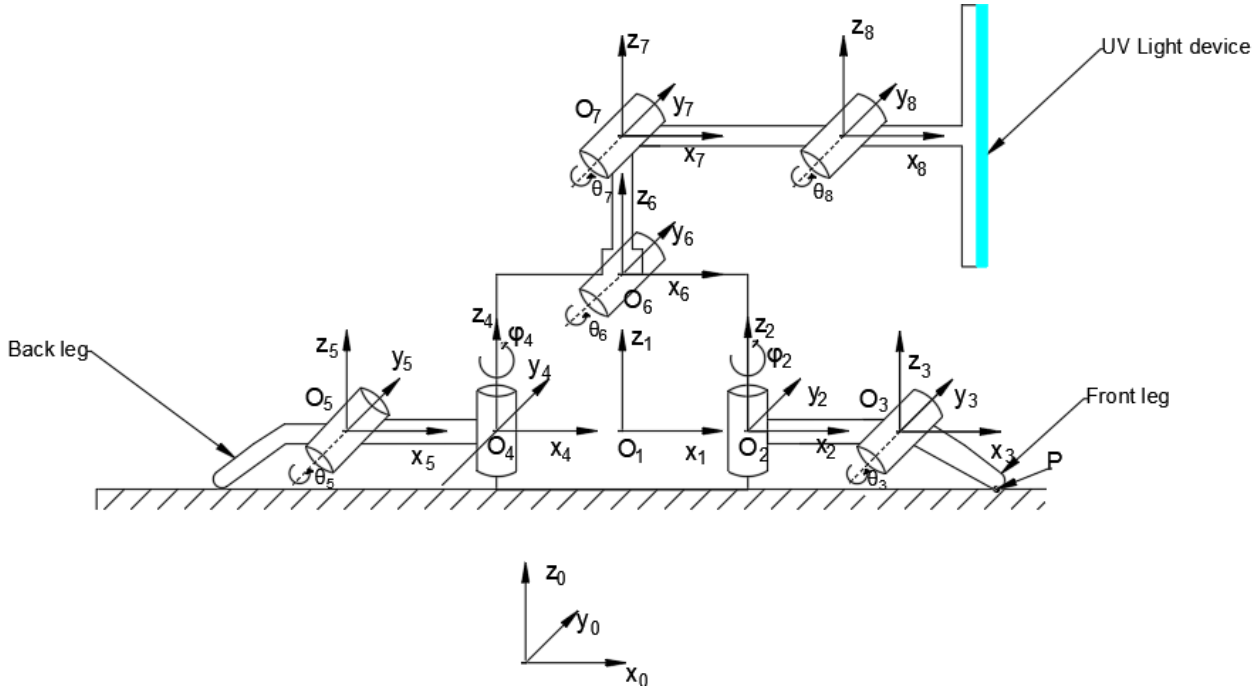

Fig. 5 - Kinematic structure of the robot

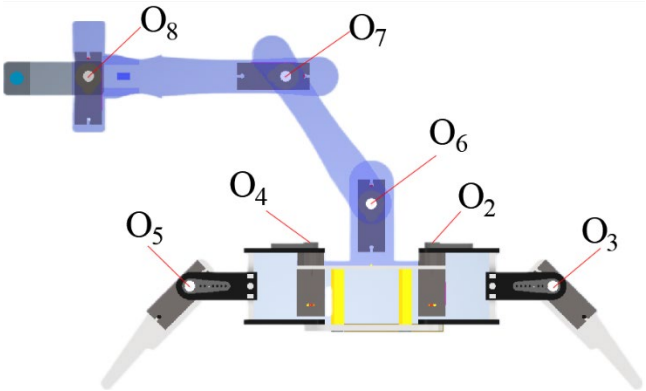

Fig. 6 - The location of the servomotors

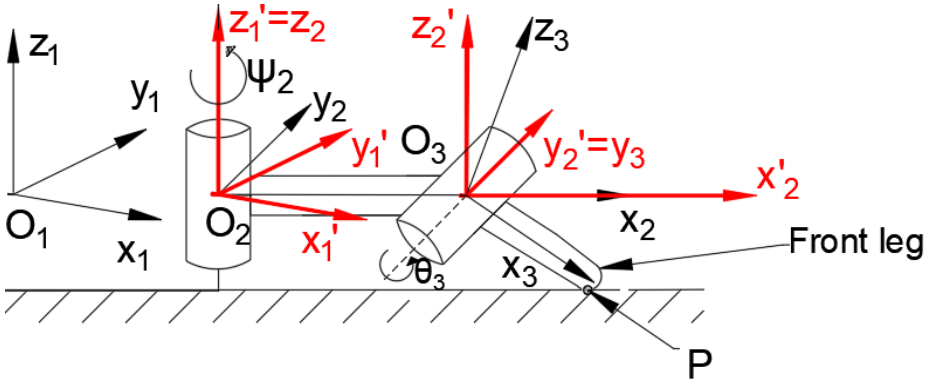

Fig. 7 - Kinematic model of the robot leg

The velocity of point P (Fig. 7) (which is the tip of the foot, i.e. the point of the robot leg which touches the fixed surface), with respect to reference system $O_1x_1y_1z_1$ (connected to the chassis) is:

$$\vec{v}_{31}^{P} = \sum_{i=2}^{3} \vec{v}_{i,i-1} + \sum_{i=2}^{3} \vec{\omega}_{i,i-1} \times \vec{r}_i \qquad (13)$$

The acceleration of point *P* is

$$\vec{a}_{31}^{P}=\sum_{i=2}^{3}\vec{a}_{i,i-1}+\sum_{i=2}^{3}\vec{\varepsilon}_{i,i-1}\times\vec{r}_i+\sum_{i=2}^{3}\vec{\omega}_{i,i-1}\times\left(\vec{\omega}_{i,i-1}\times\vec{r}_i\right)+$$
$$+2\sum_{i=1}^{3}\sum_{j=1}^{i-1}\vec{\omega}_{j,j-1}\times\left(\vec{v}_{i,i-1}+\vec{\omega}_{i,i-1}\times\vec{r}_i\right), \quad (14)$$

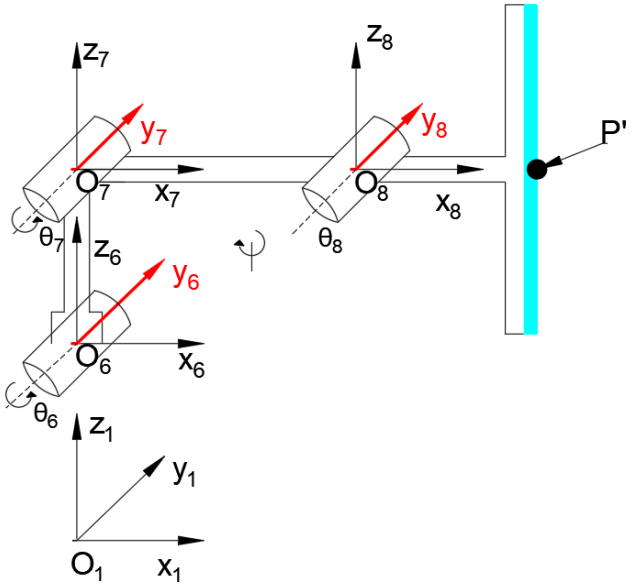

Fig. 8 - Kinematic schematics for the robot arm

The velocity and acceleration of point P' (Fig. 8) (which is the tip of the end effector), with respect to reference system $O_1x_1y_1z_1$ are, according to formulae (3) and (6), respectively:

$$\vec{v}_{81}^{P'}=\vec{v}_{61}+\sum_{i=7}^{8}\vec{v}_{i,i-1}+\vec{\omega}_{61}\times\vec{r}_1+\sum_{i=7}^{8}\vec{\omega}_{i,i-1}\times\vec{r}_i \quad (15)$$

$$\vec{a}_{81}^{P'}=\vec{a}_{61}+\vec{\varepsilon}_{61}\times\vec{r}_6+\vec{\omega}_{61}\times\left(\vec{\omega}_{61}\times\vec{r}_6\right)+2\sum_{i=7}^{8}\vec{\omega}_{61}\times\left(\vec{v}_{i,i-1}+\vec{\omega}_{i,i-1}\times\vec{r}_i\right)+$$
$$+\sum_{i=7}^{8}\vec{a}_{i,i-1}+\sum_{i=7}^{8}\vec{\varepsilon}_{i,i-1}\times\vec{r}_i+\sum_{i=7}^{8}\vec{\omega}_{i,i-1}\times\left(\vec{\omega}_{i,i-1}\times\vec{r}_i\right)+ \quad (16)$$
$$+2\sum_{i=7}^{8}\sum_{j=7}^{i-1}\vec{\omega}_{j,j-1}\times\left(\vec{v}_{i,i-1}+\vec{\omega}_{i,i-1}\times\vec{r}_i\right).$$

Table 1

Rotation angles for the active joints of the robot leg

Rotation angles	ψ_2	θ_3
Values	$0.....\frac{\pi}{2}$	$0.....\frac{\pi}{2}$

Table 2

Rotation angles for the active joints of the robot arm

Rotation angles	θ_6	θ_7	θ_8
Values	$0.....\frac{\pi}{4}$	$0.....\frac{\pi}{4}$	$0.....\frac{\pi}{2}$

Each angle varies in the time interval t_1=0.... t_n=10s, according to a special law of motion. For example, the law of motion for angle θ_3 is:

$$\theta_3 = a_3 + 0.5 \cdot (b_3 - a_3) \cdot [1 - \cos(\omega_3 t)], a_3 = 0; b_3 = \frac{\pi}{2} \quad (17)$$

In the following paragraphs, the results of the kinematic analysis for the front leg of the robot are shown. Figure 9 displays the variations of the rotation angles of joints O_2 and O_3 of the leg, with respect to time.

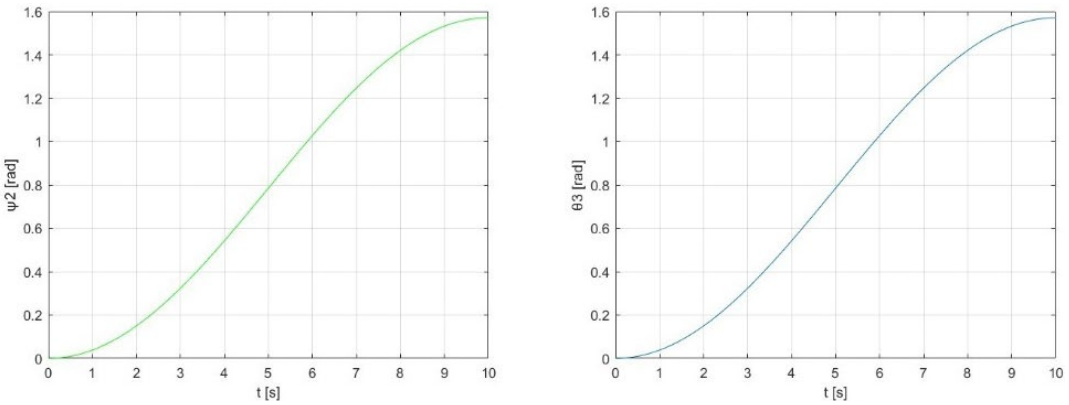

Fig. 9 - Time variations of rotation angles for O_2 and O_3, respectively

The variations of the angular velocities and accelerations of joints O_2 and O_3 of the leg can be displayed in a similar manner.

Next, the variations of the coordinates of point P, with respect to time are displayed in Figure 10. Also, the variations of the velocity and acceleration components of the same point are displayed in Figure 11 and 12, respectively.

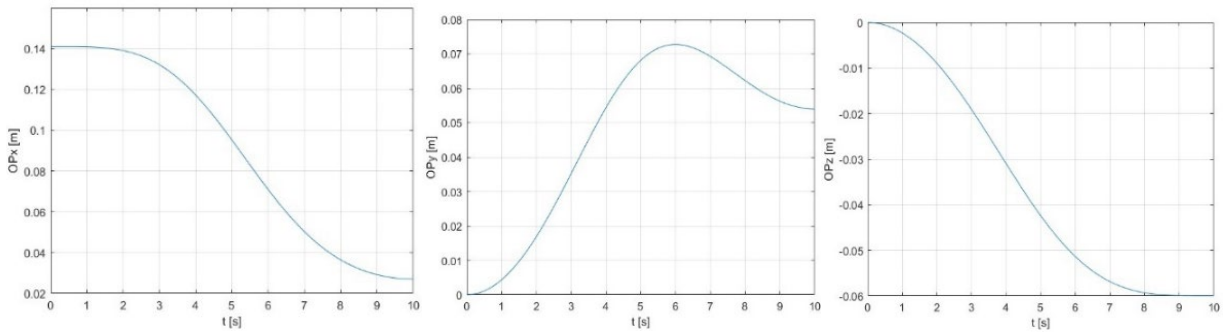

Fig. 10 - Time variations of coordinates of point *P*

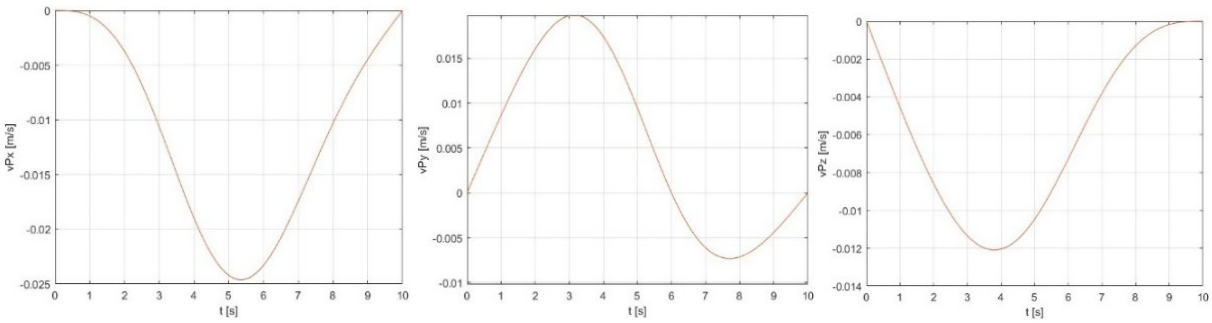

Fig. 11 - Time variations of velocity components of point *P*

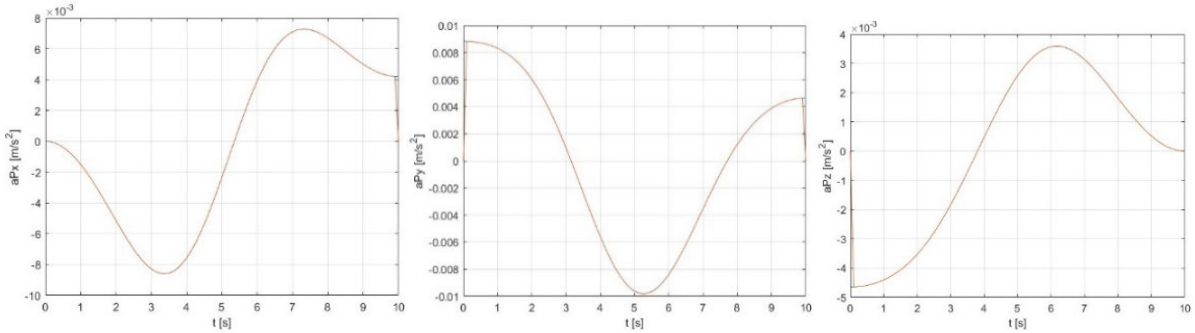

Fig. 12 - Time variations of acceleration components of point *P*

For the arm attached to the robot, Figure 13 displays the variations of the rotation angles of the joints. The velocity and acceleration components of joints O_6, O_7 and O_8 can be displayed in a similar manner.

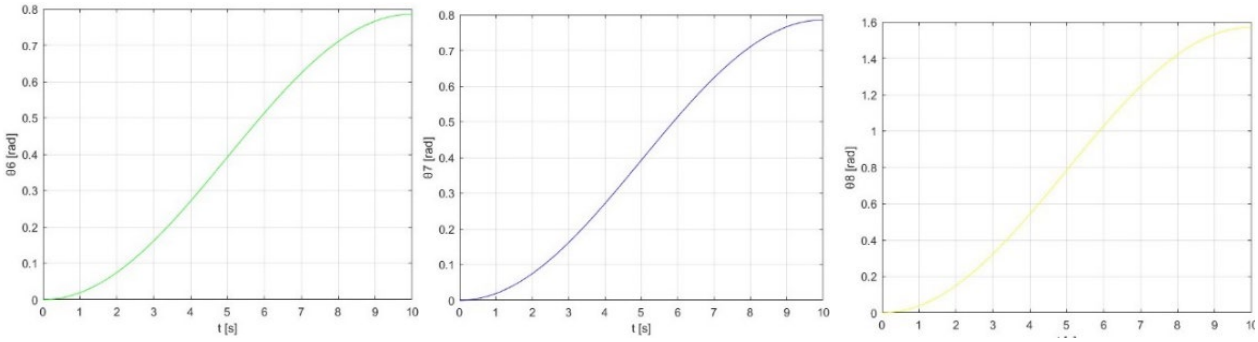

Fig. 13 - Time variations of rotation angles for O_6, O_7 and O_8, respectively

Figure 14 displays the variation of the coordinates of point P', with respect to time. The variations the of velocity and acceleration components of the same point are displayed in Figures 15 and 16.

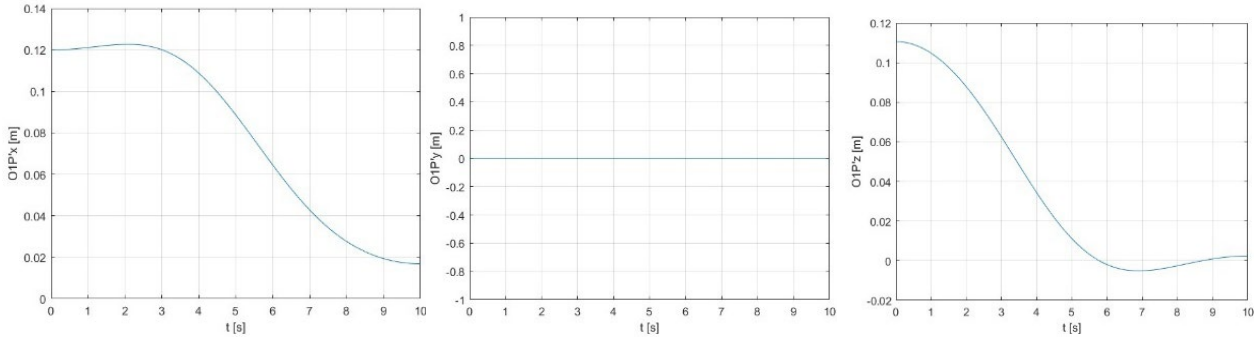

Fig. 14 - Time variations of coordinates of point *P'*

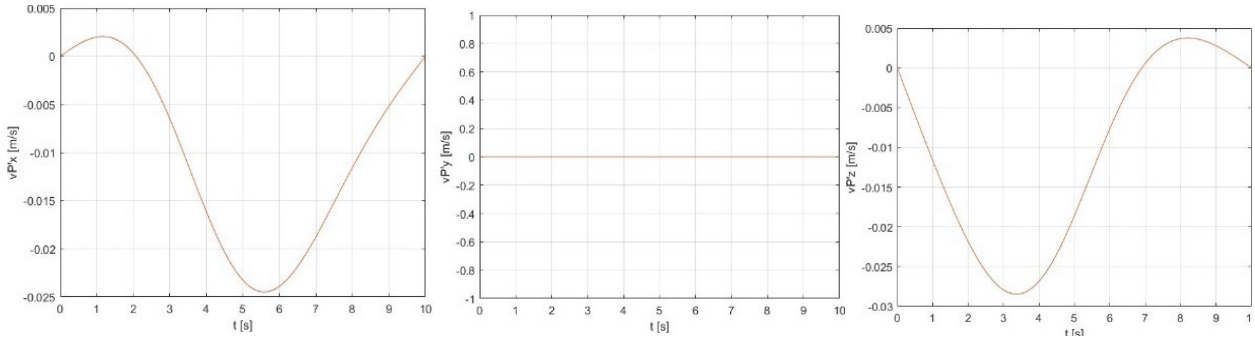

Fig. 15 - Time variations of velocity components of point *P'*

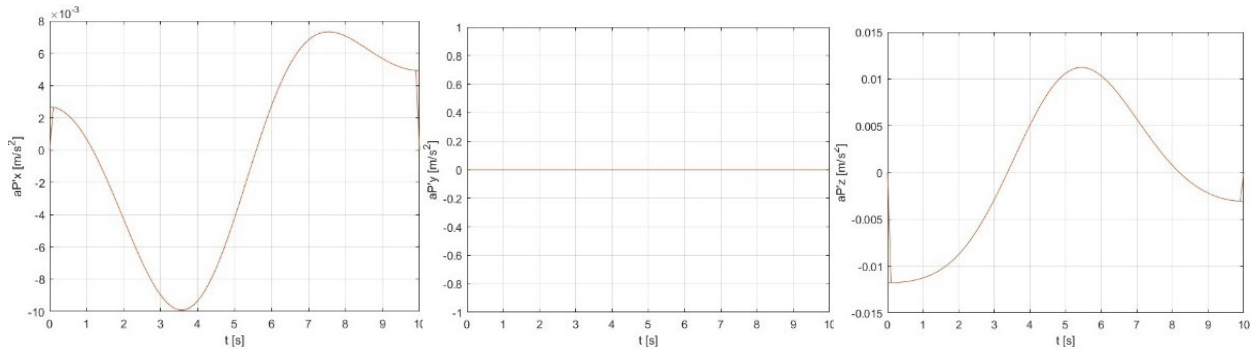

Fig. 16 - Time variations of acceleration components of point *P'*

The variations of the velocity and acceleration components with respect to time have been calculated using two derivation methods: analytical (with blue) and numerical (with orange). It can be seen in each figure, that, at the chosen representation scales, the two variation curves are superimposed, which verifies the accuracy of the calculations. Figure 17 shows a zoomed view of the curves in the first part of Figure 16.

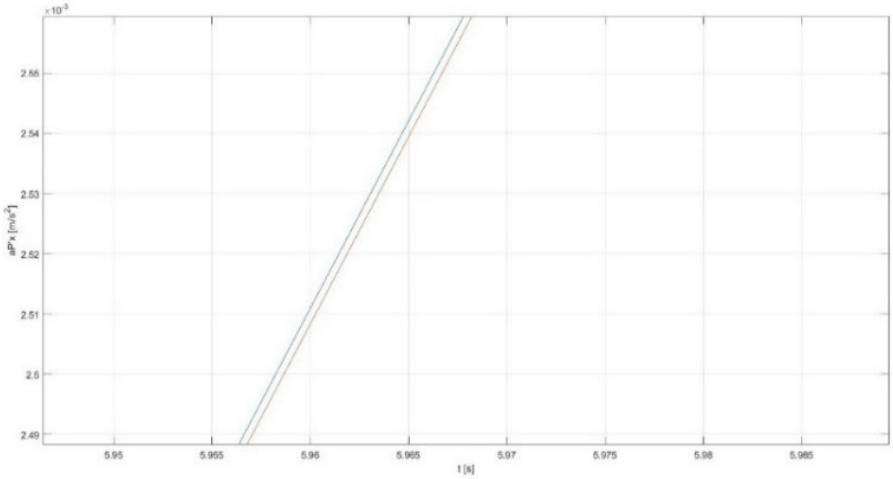

Fig. 17 - A close-up view of the first graph

CONCLUSIONS

The presented robot is designed for disinfection of hard-to-reach areas.

This disinfection process can be performed using the RRR robotic arm attached to a four-legged spider robot, which represents the improved version of a commercial model.

The chassis has been designed to be simple to assemble and repair, and the robot arm attached to it is made of 3D printed parts. In terms of construction and maintenance, the robot is affordable and can be easily upgraded.

A kinematic analysis of a leg and of the robotic arm has been performed and the results obtained by two different methods are in very good agreement.

REFERENCES

[1] Chen, Q., Li, C. & Hao, X., 2023. *A micro quadruped crawling robot manufactured from.* Udaipur, India, s.n., p. 6. https://doi.org/10.21595/vp.2023.23694

[2] Craifaleanu, A. & Negroiu, S., 2024. KINEMATIC ANALYSIS OF THE LEG OF A SPIDER ROBOT, *ANALIZA CINEMATICĂ A PICIORULUI UNUI ROBOT PĂIANJEN*. Bucuresti, s.n.

[3] Gasparetto, A. & Vidoni, R., 2008. Kinematic study of the spider system in a biomimetic perspective. Nice, France, s.n., p. 6. HYPERLINK "https://doi.org/10.1109/IROS.2008.4650677" \t "_blank" 10.1109/IROS.2008.4650677

[4] Ikhar, S. & Lanjewar, H., 2023. Design and Synthesis of Eight-Legged Spider Robot. *International Journal for Research in Applied Science & Engineering Technology (IJRASET)*, 11(3), p. 9. https://www.ijraset.com/best-journal/design-and-synthesis-of-eight-legged-spider-robot

[5] Karakurt, T., Durdu, A. & Yilmaz, N., 2015. Design of Six Legged Spider Robot and Evolving Walking Algorithms. *International Journal of Machine Learning and Computing*, 5(2), p. 5. HYPERLINK "http://dx.doi.org/10.7763/IJMLC.2015.V5.490" \t "_blank" 10.7763/IJMLC.2015.V5.490

[6] Kravchenko, V. V., 2023. Comparison of Spider-Robot Information Models. Journal of Robotics and Control (JRC), 4(5), p. 7., 10.18196/jrc.v4i5.19533.

[7] Kyrarini, M. & Lygerakis, F., 2021. A Survey of Robots in Healthcare. Technologies, 9(8), p. 26. HYPERLINK "https://doi.org/10.3390/technologies9010008" https://doi.org/10.3390/technologies9010008

[8] Manikandan, V. & Sandeep, B., 2023. Design and Fabrication of 8 Legged Spider Robot. International Journal for Research in Applied Science & Engineering Technology (IJRASET), May.11(5). https://doi.org/10.22214/ijraset.2023.51372

[9] Radoi & Deciu, Mechanics, Kinematics, Dynamics; Mecanica, Cinematica, Dinamica. s.l., s.n.

DEEP LEARNING - POWERED APP FOR EARLY DETECTION OF TOMATO AND PEPPER LEAF DISEASES

/

APLICAȚIE BAZATĂ PE DEEP LEARNING PENTRU DETECTAREA TIMPURIE A BOLILOR FRUNZELOR DE ROȘII ȘI ARDEI

Robert-Dorin CRISTEA[1)], Ionel Lucian DUMITRESCU[*2)], Alexandru-Cristian CIOACLA[1)], Dorin-Andrei CÎRSTEA[1)]

[1)] National Institute of Research - Development for Machines and Installations Designed for Agriculture and Food Industry - INMA Bucharest / Romania;

[2)] Research and Development Institute for Processing and Marketing of Horticultural Products - HORTING / Romania.

**E-mail: lucian.dumitrescu@horting.ro*

Keywords: *image analysis, plant* phenotyping*, computer vision, leaf classification*

ABSTRACT

This paper presents the development of an innovative deep learning-based application for automatic and real-time detection of tomato and pepper leaf diseases in protected environments. The application uses the YOLO9 (You Only Look Once version 9) algorithm trained on diversified datasets from Roboflow and Kaggle platforms, totaling over 10,000 labeled images. The integrated system includes an HD webcam for image capture, preprocessing modules for visual data optimization, and an alert system for user notifications. The application performs real-time detection with optimized processing rates, implementing advanced functions for automatic incident recording in CSV format for subsequent analysis. Results demonstrate system efficiency in early identification of diseases such as Early Blight, Late Blight, Septoria Leaf Spot, and Leaf Miner, contributing to improved disease management in protected crops.

REZUMAT

Această lucrare prezintă dezvoltarea unei aplicații inovatoare bazate pe deep learning pentru detectarea automată și în timp real a bolilor frunzelor de tomate și ardei în spații protejate. Aplicația utilizează algoritmul YOLO9 (You Only Look Once versiunea 9) antrenat pe seturi de date diversificate provenite din platformele Roboflow și Kaggle, totalizând peste 10.000 de imagini etichetate. Sistemul integrat include o cameră web HD pentru capturarea imaginilor, module de preprocesare pentru optimizarea datelor vizuale, și un sistem de alertă pentru notificarea utilizatorilor. Aplicația realizează detectarea în timp real cu o rată de procesare optimizată, implementând funcții avansate de salvare automată a incidentelor într-un format CSV pentru analiză ulterioară. Rezultatele demonstrează eficiența sistemului în identificarea precoce a bolilor precum Early Blight, Late Blight, Septoria Leaf Spot și Leaf Miner, contribuind la îmbunătățirea managementului bolilor în culturile protejate.

INTRODUCTION

Leaf diseases are one of the main threats to the productivity of tomato and pepper crops, causing significant yield losses globally (*Jelali, 2024*). Early and accurate detection of these diseases is essential to implement appropriate control measures and minimize the economic impact on agricultural producers (*Jafar et al., 2024*). Traditional methods of disease identification, based on visual observation and the experience of specialists, are often limited by subjective factors, high costs, and time required for diagnosis (*Wang & Liu, 2024*).

Recent advances in artificial intelligence, especially in deep learning and computer vision technologies, offer promising solutions for automating the process of plant disease detection (*Pacal et al., 2024; Abdullah et al., 2024*).

Algorithms based on convolutional neural networks (CNNs) have demonstrated remarkable capabilities in recognizing and classifying medical and agricultural images, achieving comparable or superior human performance in many specific cases. Due to limited dataset availability in machine learning-based research, studies on plant recognition and disease detection are significantly affected, however, recent efforts have made notable progress in bridging this gap (*Jelali, 2024*).

The YOLO (You Only Look Once) algorithm, in its evolutionary versions, has revolutionized the field of real-time object detection, offering an optimal balance between accuracy and processing speed (*Guo,*

2024; Zayani et al., 2024). Unlike traditional detection methods that process the image in multiple stages, YOLO analyzes the entire image in a single pass, making simultaneous predictions for the location and classification of detected objects. This approach makes it ideal for applications that require real-time response, such as continuous monitoring of plant health in protected spaces.

Tomato and pepper crops are vulnerable to a wide range of fungal, bacterial and viral pathogens that primarily affect the leaves (*Mathew & Mahesh, 2022; Suryaprabha, 2024*). Common diseases include Early Blight, Late Blight, Septoria Leaf Spot and Leaf Miner, each with distinctive visual characteristics that can be exploited by computer vision algorithms for automatic identification.

Implementing automated detection systems in protected spaces offers significant advantages over conventional methods. Continuous 24/7 monitoring, reduced need for frequent manual inspections, early detection before significant visible symptoms appear, and automated incident documentation for epidemiological analysis are just some of the benefits of this advanced technological approach (*Sun et al., 2025*).

This paper describes the development and implementation of an innovative application based on the YOLO9 algorithm for the automatic detection of tomato and pepper leaf diseases in greenhouse conditions.

The integrated system combines high-resolution video capture technologies with advanced image preprocessing and real-time detection algorithms, providing a complete solution for plant health monitoring in precision agriculture.

MATERIALS AND METHODS

System configuration and application architecture

The application developed for the detection of tomato and pepper leaf diseases is based on a modular architecture that integrates several advanced technological components. The system operates on a laptop platform equipped with an Intel Core i5-13600h processor, 16 GB RAM, and a dedicated Nvidia RTX 4060 graphics card for accelerating deep learning calculations.

The image acquisition component consists of an HD webcam with a minimum resolution of 1920x1080 pixels, capable of video capture at 30 fps. The camera is strategically positioned within the protected space to ensure optimal coverage of the monitoring areas, with automatic adjustments for the variable lighting conditions specific to greenhouses.

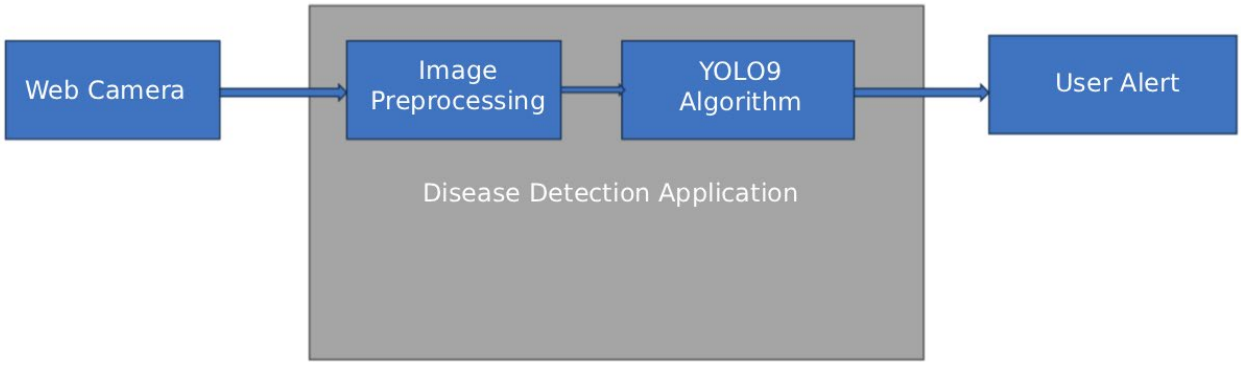

Fig. 1 - Block diagram of the application for detecting leaf diseases

Dataset preparation and processing

Two main datasets, specifically optimized for leaf disease detection, were used to train the YOLO9 model. For tomato crops, the "Tomato Leaf Disease" dataset available on the Roboflow platform was used, which contains 10,269 images distributed as follows: 9,236 images for training (90%), 867 images for validation (8%), and 166 images for testing (2%).

For pepper disease detection, a "superset" was created by concatenating multiple data sources from the Roboflow and Kaggle platforms. The resulting set contains 1,256 images, divided into: 1,130 images for training (90%), 100 images for validation (8%), and 26 images for testing (2%). This approach ensured the diversity necessary for robust training of the algorithm under varied conditions of capture and symptom manifestation.

Fig. 2 - Examples of images of tomato leaves affected by various diseases

All images were subjected to a standardized preprocessing process that includes auto-orientation to automatically correct image position, resizing to the standard 640x640 pixel size compatible with the YOLO9 architecture, and applying augmentations to improve the generalization ability of the model. The augmentations applied include 90° rotations in both directions and exposure adjustments within the range of ±8% to simulate the variable lighting conditions in the greenhouse.

Fig. 3 - Example image of an affected pepper leaf

Implementing and configuring the YOLO9 algorithm

The YOLO9 algorithm used represents the latest evolution of the YOLO family, optimized for real-time object detection with superior performance in terms of accuracy and speed *(Dai et al., 2024)*. The neural network architecture is based on an advanced convolutional backbone that extracts hierarchical features from images, followed by a feature aggregation neck and a detection head that generates final predictions.

The hyperparameter configuration for training included: batch size of 16 images to optimize GPU memory, initial learning rate of 0.001 with adaptive programming, 300 epochs for full training with early

stopping in case of overfitting, and loss functions optimized for multi-class detection. Training was performed on an NVIDIA RTX 4090 GPU configuration, with a total time of approximately 15 hours for each model (tomatoes and peppers).

Image preprocessing and optimization system

The preprocessing module implements several techniques to optimize image quality before analysis by YOLO9. Auto-orientation uses edge detection algorithms to identify the correct leaf orientation and automatically correct unwanted rotations. Resizing is performed using bicubic interpolation to maintain the quality of fine details, essential for identifying early symptoms.

The system also includes advanced brightness and contrast normalization functions to compensate for variable lighting conditions in the greenhouse, which are often encountered due to changes in time or day *(Kaur et al., 2024).* Noise filtering and sharpness enhancement are achieved by applying adaptive filters that preserve information relevant for disease detection.

Alert system architecture and data storage

The notification system implements a multi-level strategy to inform users about disease detection. Visual alerts appear as pop-ups on the graphical interface, containing information about the type of disease detected, the time of detection, and the coordinates of the affected area on the image. Optional sound alerts can be activated for situations that require immediate attention.

An innovative aspect of the application is the automatic incident recording system. Each confirmed detection is saved in a local CSV file, recording the following information: the exact timestamp of the detection, the type of disease identified, and the configuration parameters active at the time of detection. This data allows for subsequent statistical analysis to identify trends and optimize disease management strategies.

User interface and interactive features

The application's graphical interface is developed in an intuitive design that allows easy access to all system functionalities. Users can select their preferred capture device from the list of available cameras and configure the interface language (Romanian or English).

A key functionality consists of selecting the type of plant being monitored (tomatoes or peppers), which activates the corresponding YOLO model.

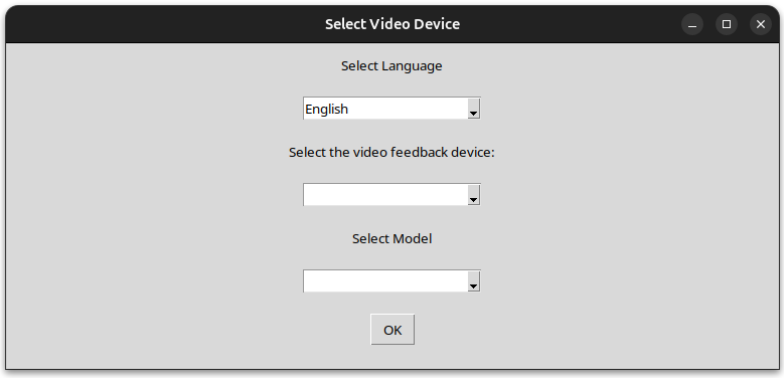

Fig. 4 - The initial application configuration interface

The control panel offers real-time adjustments for the detection confidence threshold (sensitivity), frame rate (FPS), and the threshold time for confirming persistent detections. Users can enable or disable audible alerts and configure pop-up notification suppression based on their work preferences and specific monitoring environment requirements.

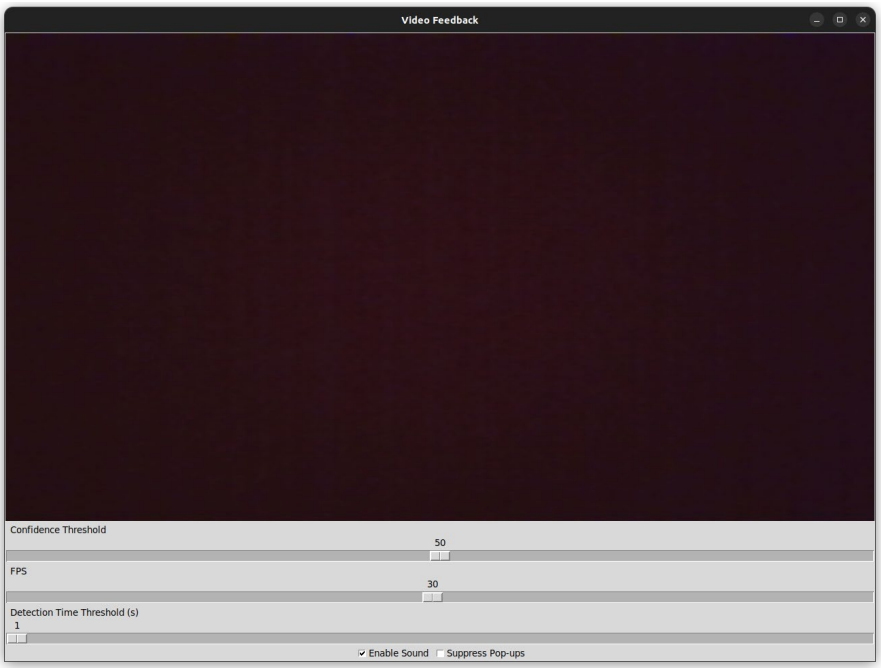

Fig. 5 - Main screen of the application during monitoring

The user also has the option to enable or disable sound alerts via a checkbox and can choose to suppress pop-up messages that appear when diseases are detected. The application is also equipped with a notification system that, once a disease is detected, sends a warning message in the form of a pop-up on the screen once the threshold time has been exceeded.

This message includes details about the type of disease detected and the time during which it has been continuously observed. The user can choose to suppress these notifications if they wish.

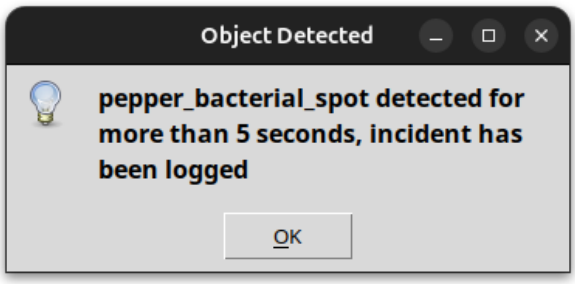

Fig. 6 - Notification pop-up with details about the detected disease and observation time

RESULTS

The results obtained from training and testing the YOLO9 models for leaf disease detection demonstrate the high efficiency of the developed system. For the model for tomato disease detection, trained on the Roboflow dataset with 10,269 images, remarkable performances were obtained in identifying the main pathologies: Early Blight, Late Blight, Septoria Leaf Spot, Leaf Miner, Leaf Mold, Mosaic Virus, Spider Mites and Yellow Leaf Curl Virus.

The evaluation on the test set showed an average accuracy (mAP@0.5) of 97% for the detection of all disease classes, with a mAP@0.5:0.95 value of 93%, indicating excellent robustness at various IoU (Intersection over Union) thresholds. The final training losses were: box loss = 0.36, class loss = 0.27, and DFL (Distribution Focal Loss) = 0.15, while the validation losses were: box loss = 0.36, class loss = 0.33, and DFL = 0.93.

The analysis of the normalized confusion matrix (Fig. 9) reveals exceptional performances per class: Leaf Miner achieved a perfect accuracy of 100%, Late Blight and Spider Mites recorded 96% and 98%, respectively, Early Blight demonstrated 96% accuracy, Mosaic Virus 95%, Leaf Mold 94%, Septoria 92%, and Yellow Leaf Curl Virus 90%. The model also showed a good ability to identify healthy leaves with 91% accuracy, essential for reducing false positives.

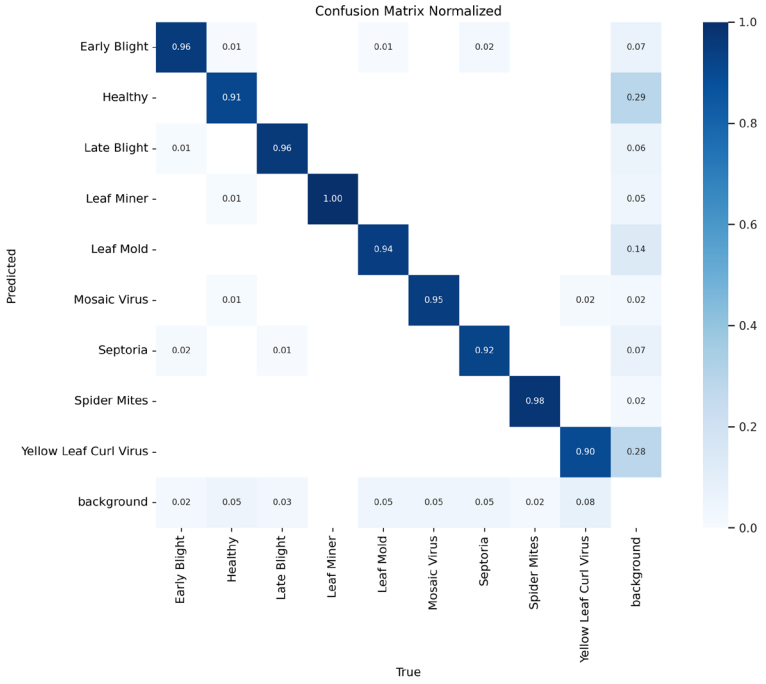

Fig. 7 - Normalized confusion matrix for tomato disease detection model

For pepper crops, the model trained on the concatenated superset of 1,256 images showed satisfactory results, with an average accuracy (mAP@0.5) of 66% and mAP@0.5:0.95 of 51%. Although these values are more moderate compared to the tomato model, they reflect the inherent challenges due to the smaller dataset and lower diversity of the training images. The final training losses were: box loss = 0.46, class loss = 0.34, and DFL = 0.23, with validation losses of: box loss = 0.46, class loss = 0.47, and DFL = 0.83.

The confusion matrix for pepper (Fig. 10) reveals differential performance between classes: Pepper Blossom End Rot was detected with the highest accuracy (99%), followed by Pepper Bacterial Spot (80%), Pepper Powdery Mildew (53%), and Pepper Frogeye Leaf Spot (49%). The main challenges were in differentiating between Pepper Frogeye Leaf Spot and Pepper Bacterial Spot, with cross-confusions of 49% for both classes, indicating significant visual similarities between these two diseases.

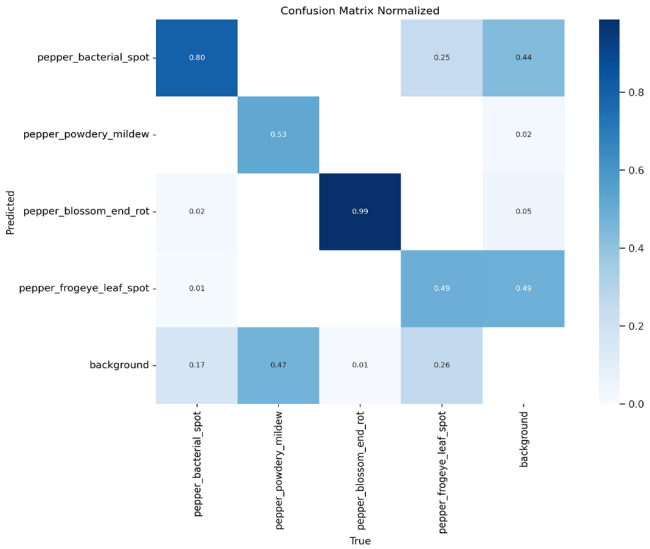

Fig. 8 - Normalized confusion matrix for tomato disease detection model

The pepper model presented greater challenges in differentiating between certain disease classes, particularly between Pepper Frogeye Leaf Spot and Pepper Bacterial Spot, where the mutual confusion was 49%, according to the confusion matrix.

This highlights the need to enrich the database for these specific classes and possibly implement additional augmentation techniques to improve discrimination between similar symptoms. However, detections for Pepper Blossom End Rot were exceptionally accurate (99%), providing a reliable tool for identifying this common disease.

The automatic incident saving functionality has been proven functional under laboratory testing conditions. The system generates detailed CSV records for each confirmed detection, including precise information on the time of the incident, the type of disease, the spatial coordinates of the affected area, and the level of confidence of the prediction.

07:20:36	pepper_bacterial_spot	pepper_bacterial_spot detected for more than 1 seconds
07:20:51	pepper_bacterial_spot	pepper_bacterial_spot detected for more than 5 seconds
07:41:23	Leaf Miner	Leaf Miner detected for more than 1 seconds
07:41:25	Leaf Miner	Leaf Miner detected for more than 1 seconds
07:44:58	pepper_bacterial_spot	pepper_bacterial_spot detected for more than 5 seconds
07:45:07	pepper_bacterial_spot	pepper_bacterial_spot detected for more than 5 seconds
07:47:57	pepper_frogeye_leaf_spot	pepper_frogeye_leaf_spot detected for more than 5 seconds, incident has been logged
07:47:58	pepper_blossom_end_rot	pepper_blossom_end_rot detected for more than 5 seconds, incident has been logged

Fig. 9 - Automatic recording of detected incidents with timestamp and technical details

Performance tests under laboratory conditions demonstrated the system's ability to process images at a constant rate of 25 fps on the specified standard hardware configuration. The average processing time for a 640x640 pixel image, including preprocessing, YOLO9 inference, and post-processing of the results, was 40-48 ms, with most of the time spent waiting for a new image to be acquired, allowing for real-time monitoring without noticeable delays.

CONCLUSIONS

This article demonstrates that the YOLO9 algorithm, integrated into a tomato and pepper leaf disease recognition application, provides fast and accurate automatic detection. The tomato model achieved high performance (up to 97% mAP), confirming the usefulness of deep learning in phytosanitary monitoring. The pepper model had more modest results (66% mAP), highlighting the need for larger and more varied datasets.

The system reduces manual inspections, detects diseases before visible symptoms appear, and allows for continuous 24/7 monitoring. Major limitations relate to data quality and hardware requirements, but the solution has high potential for practical application in greenhouses and commercial farms, contributing to the digitalization and efficiency of precision agriculture.

ACKNOWLEDGEMENT

This work was supported by Ministry of Agriculture and Rural Development (MARD) - under the name: Project: ADER 6.3.19 – Research on Improving Management and Implementing Digitalization in Vegetable Production Farms through the Use of "HIGH TECH" and "SMART" Technologies; coordinator: Research and Development Institute for Processing and Marketing of Horticultural Products - HORTING București.

REFERENCES

[1] Abdullah, A., Amran, G. A., Tahmid, S. M. A., Alabrah, A., AL-Bakhrani, A. A., & Ali, A. (2024). A Deep-Learning-Based Model for the Detection of Diseased Tomato Leaves. *Agronomy*, 14(7), 1593. https://doi.org/10.3390/agronomy14071593.

[2] Dai, M., Sun, W., Wang, L., Dorjoy, M. M. H., Zhang, S., Miao, H., Han, L., Zhang, X., & Wang, M. (2023). Pepper leaf disease recognition based on enhanced lightweight convolutional neural networks. *Frontiers in Plant Science*, 14. https://doi.org/10.3389/fpls.2023.1230886.

[3] Guo, X. (2024). Automatic detection of tomato leaf disease using an adopted deep learning algorithm. *Journal of Intelligent & Fuzzy Systems*, *46*(4), 236905. https://doi.org/10.3233/JIFS-236905}.

[4] Jafar, A., Bibi, N., Naqvi, R. A., Sadeghi-Niaraki, A., & Jeong, D. (2024). Revolutionizing agriculture with artificial intelligence: plant disease detection methods, applications, and their limitations. *Frontiers in Plant Science*, 15. https://doi.org/10.3389/fpls.2024.1356260.

[5] Jelali, M. (2024). Deep learning networks-based tomato disease and pest detection: a first review of research studies using real field datasets. *Frontiers in Plant Science*, 15. https://doi.org/10.3389/fpls.2024.1493322.

[6] Kaur, R., Mittal, U., Wadhawan, A., Almogren, A., Singla, J., Bharany, S., Hussen, S., Rehman, A. U., & Al-Huqail, A. A. (2025). YOLO-LeafNet: a robust deep learning framework for multispecies plant disease detection with data augmentation. *Scientific Reports*, 15(1). https://doi.org/10.1038/s41598-025-14021-z.

[7] Mathew, M. P., & Mahesh, T. Y. (2021). Leaf-based disease detection in bell pepper plant using YOLO v5. *Signal, Image and Video Processing*, *16*, 841–847. https://doi.org/10.1007/s11760-021-02024-y.

[8] Pacal, I., Kunduracioglu, I., Alma, M.H. et al. A systematic review of deep learning techniques for plant diseases. *Artif Intell Rev* 57, 304 (2024). https://doi.org/10.1007/s10462-024-10944-7.

[9] Sun, H., Fu, R., Wang, X. et al. Efficient deep learning-based tomato leaf disease detection through global and local feature fusion. *BMC Plant Biol* 25, 311 (2025). https://doi.org/10.1186/s12870-025-06247-w

[10] Suryaprabha, D., Kumar, A., & Ravi, V. (2024). Bell pepper leaf disease classification using support vector machine. *International Journal of Computer Engineering and Technology*, *15*(2), 379616178.

[11] Wang, X., Liu, J. An efficient deep learning model for tomato disease detection. *Plant Methods 20*, 61 (2024). https://doi.org/10.1186/s13007-024-01188-1.

[12] Zayani, H. M., Ammar, I., Ghodhbani, R., Maqbool, A., Saidani, T., Slimane, J. B., Kachoukh, A., Kouki, M., Kallel, M., Alsuwaylimi, A. A., & Alenezi, S. M. (2024). Deep learning for tomato disease detection with YOLOv8. *Engineering, Technology & Applied Science Research*, 14(2), 13584–13591. https://doi.org/10.48084/etasr.7064.

MODERN METHODS FOR PROCESSING FERMENTED DAIRY PRODUCTS
/
METODE MODERNE DE PROCESARE A PRODUSELOR LACTATE FERMENTATE

Florentina BRATOSIN, Sorin-Ștefan BIRIȘ, Andreea-Ioana BADIU, Alexandru Ionuț CÎRÎC, Mihaela BEGEA*
National University of Science and Technology POLITEHNICA Bucharest / Romania.
**E-mail: mihaela.begea@gmail.com*

Keywords: *fermented dairy products, yogurt, kefir, non-thermal technologies.*

ABSTRACT

Fermented milk products represent one of the most appreciated food categories, valued for their distinct sensory and physicochemical characteristics, as well as their health-promoting properties. The production of fermented dairy products, which began with the ancient practice of acidifying milk, has significantly increased milk's shelf life. This study provides a concise review of modern technologies used in the production of fermented milk products, with a focus on yogurt and kefir. The article presents innovative fermentation methods that improve safety, sensory quality, and shelf life, such as the Maroyaka Tannen technique and non-thermal technologies including CO_2 addition, high-pressure processing (HPP), and ultrasound technology. Additionally, equipment like the APV Cavitator and CaviMaster are explored for their efficiency in homogenization, thermal control, and the optimization of functional properties.

REZUMAT

Produsele lactate fermentate reprezintă una dintre cele mai apreciate categorii de alimente, apreciate pentru caracteristicile lor senzoriale și fizico-chimice distincte, precum și pentru proprietățile lor benefice pentru sănătate. Producția de produse lactate fermentate, care a început cu practica antică de acidificare a laptelui, a crescut semnificativ durata de valabilitate a laptelui. Acest studiu oferă o trecere în revistă concisă a tehnologiilor moderne utilizate în producția de produse lactate fermentate, cu accent pe iaurt și chefir. Articolul prezintă metode inovatoare de fermentare care îmbunătățesc siguranța, calitatea senzorială și durata de valabilitate, cum ar fi tehnica Maroyaka Tannen și tehnologiile non-termice, inclusiv adaosul de CO_2, procesarea la presiune înaltă (HPP) și tehnologia cu ultrasunete. În plus, echipamente precum APV Cavitator și CaviMaster sunt explorate pentru eficiența lor în omogenizare, control termic și optimizarea proprietăților funcționale.

INTRODUCTION

Recent advances in food science have led to the emergence of innovative methods for processing fermented dairy products, aiming to preserve their nutritional value while enhancing their sensory and functional characteristics. While traditionally, fermented milk was obtained using starter cultures at controlled temperatures modern consumer demand for milder products with a smooth texture and enhanced bioactive properties has driven the development of non-thermal technologies and adapted fermentation approaches.

According to reports, the global yogurt market has followed steady growth in recent years, with notable differences between regions and countries. In 2020, the global value was slightly over USD 90 billion, supported by large markets such as China and the United States, where consumption of functional dairy products increased in the context of the pandemic. In 2021, the market surpassed USD 95 billion, with significant contributions from Germany and France, where the tradition of yogurt consumption is strongly established. In 2022, the market reached around USD 100 billion, driven by convenient formats and drinking yogurts, with rapid expansion in India and Brazil, emerging markets with high potential (*Mordor Intelligence, 2025).* In 2023, the value approached USD 103 billion, supported by the popularity of high-protein diets, especially in the United States and the United Kingdom, where “high-protein” and “low-sugar” yogurts have become highly sought after. For 2024, the report estimated a value of USD 105.61 billion, reinforced by rising demand in China—the largest market in the Asia-Pacific region—and stable demand in Western Europe. In the medium term, by 2029, the global market is projected to reach USD 135.84 billion, with a compound annual growth rate (CAGR) of 5.16%. The Asia-Pacific region will remain the main driver of expansion, through countries such as China, India, and Japan, while mature markets in Europe (Germany, France, the

United Kingdom) and North America (the United States, Canada) will continue to dominate through innovation and a focus on probiotic and functional products (*Mordor Intelligence, 2025).*

Fig. 1 - Estimated global yogurt consumption per capita, 2017–2030
(source: Mordor Intelligence, 2025)

According to the latest report entitled *"Yogurt Market: Size, Share, Trends and Forecast by Product Type, Flavor, Distribution Channel, and Region, 2025–2033"*, the global yogurt market was valued at approximately USD 127.4 billion in 2024. Estimates indicate that it will reach USD 203.8 billion by 2033, registering a compound annual growth rate (CAGR) of around 5.4% during the period 2025–2033 (*Mordor Intelligence, 2025).*

Regarding the production technologies Maroyaka Tannen technique was developed by Hiroshi Horiuchi at Meiji and is based on reducing the dissolved oxygen content in milk and carrying out fermentation at lower temperatures than conventional ones. This favors optimal metabolic activity of lactic acid bacteria and leads to a fine texture and moderate acidity. The method gives yogurt a smooth texture and mild flavor, closely replicating the traditional Bulgarian style. Using this fermentation approach, it becomes possible to reproduce on an industrial scale the specific flavor of Bulgarian yogurt. This production method is currently applied in yogurts such as LB81 Zero-Fat Plain, Meiji Probio Yogurt R-1 Low-Fat, and others. The research was initially inspired by the technology behind Meiji Oishii Gyunyu milk, which achieved a unique taste by removing oxygen from the milk before pasteurization. The process also proceeded at a much faster pace considering the fermentation time *(Horiuchi, H., 2014).*

REVIEW OF MODERN PROCESSING TECHNOLOGIES

The Maroyaka Tannen Technique

The Maroyaka Tannen technique, developed by Hiroshi Horiuchi at Meiji, is based on reducing the dissolved oxygen content in milk and fermenting at lower than conventional temperatures. This method favors the optimal metabolic activity of lactic acid bacteria, resulting in a fine texture and moderate acidity. The technique allows for the reproduction on an industrial scale of the smooth texture and mild flavor characteristic of traditional Bulgarian yogurt *(Horiuchi, H., 2014).*

It is currently used in products such as LB81 Zero-Fat Plain and Meiji Probio Yogurt R-1 Low- Fat. The research was inspired by the unique taste achieved by removing oxygen from milk before pasteurization. This process significantly reduces fermentation time. Traditionally, yogurt is fermented at temperatures above 40°C. While traditional Bulgarian yogurt ferments at a much lower temperature, past attempts to scale this method failed due to slow fermentation and a soft curd. In the Maroyaka Tannen technique, deoxygenated milk is inoculated with Lactobacillus delbrueckii subsp. bulgaricus and Streptococcus thermophilus. Deoxygenating the milk before adding the cultures stimulates bacterial activity under low-temperature conditions, thereby reducing fermentation time and improving the yogurt's texture *(Horiuchi, H., 2014).*

Technologies Developed by SPX

Technologies from SPX, such as the APV Cavitator and CaviMaster, offer significant innovations in dairy processing. The APV Cavitator is a modular unit that uses controlled cavitation for highly efficient mixing and flameless heating, ensuring a smooth texture, uniform heating, and effective aeration. This method improves the hydration of powder ingredients and the functionalization of milk proteins and whey protein concentrate (WPC), which increases product viscosity and stability. The technology also reduces fouling, lowers costs, and increases productivity, enabling a creamy texture even in low-fat products. The new CaviMaster combines the benefits of the Cavitator and LeanCreme to facilitate the development of

innovative, low-fat yogurts with high nutritional value using whey proteins. This recombination concept supports sustainable production that is less dependent on the quality of raw milk *(SPX FLOW, 2013).*

Non-Thermal Technologies - addition of carbon dioxide

Adding CO_2 to milk lowers the pH by forming carbonic acid. While *Lactobacillus bulgaricus* is relatively tolerant to CO_2, the CO_2 produced by *Streptococcus thermophilus* stimulates the growth of *Lactobacillus bulgaricus*, as the latter requires CO_2 for cell growth. Supercritical carbon dioxide (sCO_2) is a liquid state of CO_2 achieved above a critical temperature of 31.1°C and a critical pressure of 7.4 MPa. The benefits of using sCO_2 include its low viscosity and high solubility in both the aqueous and fat phases of food materials. Its use for inactivating alkaline phosphatase and *Escherichia coli* in milk has been investigated, with one study finding that a ratio of 0.05 sCO_2:milk, at 70°C, 80 bar, and a holding time of 30 minutes, inactivated *E. coli* and 94.5% of the enzyme *(Marella, C., et al., 2015).*

High-Pressure Processing (HPP)

High-Pressure Processing (HPP) can be implemented as either a batch or a semi-continuous process. In the batch process, food is placed in a vessel filled with a pressure-transmitting liquid. The target pressure, which can range from 50 to 1000 MPa, is applied by a pump or piston and maintained for a set period before depressurization. A current application of HPP in the yogurt industry is post-packaging treatment, which inactivates yeasts and molds for up to three months and reduces *Lactobacillus bulgaricus* counts, preventing post-acidification. Research on set yogurt from HPP-processed milk showed that milk treated at 193 MPa had no disruptive effect on casein micelles or whey protein denaturation. In contrast, milk treated at 676 MPa exhibited smaller casein micelles than thermally treated milk *(Krystian M., Paul D., Szymon S. et al, 2019).*

Low-Frequency Ultrasound Technology

Ultrasound refers to sound waves with a frequency above 16 kHz. Low-frequency ultrasound (20–100 kHz) is used to modify the physical properties of products and inactivate microorganisms, while high-frequency ultrasound (20 kHz to 2 MHz) is primarily a non-destructive analytical method. Cavitation, the formation and implosion of microbubbles in liquid media, is a key mechanism of action. Low-frequency ultrasound produces high acoustic pressure, resulting in a high cavitation rate. One study found that ultrasound treatment had a homogenizing effect on milk fat globules, reducing their size *(Prosekov, A., et al., 2025).* Treatment at 90 W (20 kHz) for 10 minutes achieved a homogenization effect similar to conventional methods. Higher power levels resulted in a more uniform dispersion of smaller fat globules. This reduction in fat globule size also enhanced the milk's water-holding capacity *(Prosekov, A., et al., 2025).*

Table 1

Comparative table about the advantages and disadvantages for Maroyaka Tannen, CO_2, HPP and ultrasound

Technology	Advantages	Disadvantages	Mechanism of action
The Maroyaka Tannen	– Reduces astringent taste – Improves clarity and stability of beverages – Gentle, natural method	– Limited effect only on phenolic compounds – Extra cost for tannin extracts – May subtly alter flavor	Treatment with natural tannins (usually plant extracts) that bind proteins and polyphenols, reducing astringency and improving stability.
CO_2 (carbonation / supercritical)	– Recognized, safe method – Improves microbiological stability – Can preserve aroma and color – Supercritical CO_2 also acts as a selective solvent	– High cost (high- pressure equipment) – May slightly alter taste via acidification – Requires strict pressure control	Dissolved or supercritical CO_2 inhibits enzymes and microorganisms, lowers pH, and improves stability.
HPP (High Pressure Processing)	– Preserves color, flavor, and nutrients – Effective microbial inactivation – No additives needed	– Very high cost (complex equipment) – Does not inactivate all enzymes – Unsuitable for products with gas/air (packaging may burst)	Hydrostatic pressure (300–600 MPa) inactivates microorganisms and some enzymes without thermal treatment.
Ultrasound	– Can reduce microbial load – Enhances extraction of bioactive compounds – Versatile technology, combinable with others	– Limited effectiveness as a stand-alone method – May generate oxidation compounds – Can affect texture or flavor if not controlled	Acoustic cavitation: bubble formation and collapse generate localized temperature and pressure, disrupting microbial cells and modifying proteins/polyphenols.

DISCUSSION FINDINGS

The **Maroyaka Tannen technique** demonstrates that fermentation time can be significantly shortened by controlling dissolved oxygen levels, even at lower temperatures. The symbiotic relationship between *Lactobacillus bulgaricus* and *Streptococcus thermophilus* is essential for this process, as the deoxygenation stimulates their activity.

In the case of **HPP**, the results indicate that the treatment parameters are crucial. While high pressure at 676 MPa for 30 minutes produced a yogurt with firmness similar to that of a thermally treated one, a lower pressure (193 MPa) or a shorter duration (5 minutes) resulted in a weaker gel. Both HPP at high pressure and thermal treatment were found to alter whey proteins, which then bound to κ-casein. Furthermore, HPP-treated yogurt gels lost minimal water-holding capacity after 20 days of storage, on par with thermally treated gels.

For the **addition of CO_2,** the data shows that this method leads to a significantly higher lactic acid content after seven days of storage compared to a control sample. This supports the conclusion that pre-acidification with CO_2 can accelerate the fermentation process.

Finally, the **Low-Frequency Ultrasound** technology has proven effective in improving milk's physical properties. It has a homogenizing effect on fat globules and enhances water-holding capacity by increasing the surface area for interactions with casein. A key finding is that the beneficial effects on the gel's texture and water-holding capacity are caused by physical changes (homogenization) or heat generated during the treatment, not by the ultrasound or pressure itself. This highlights the importance of controlling the temperature during ultrasound treatment to achieve desired results.

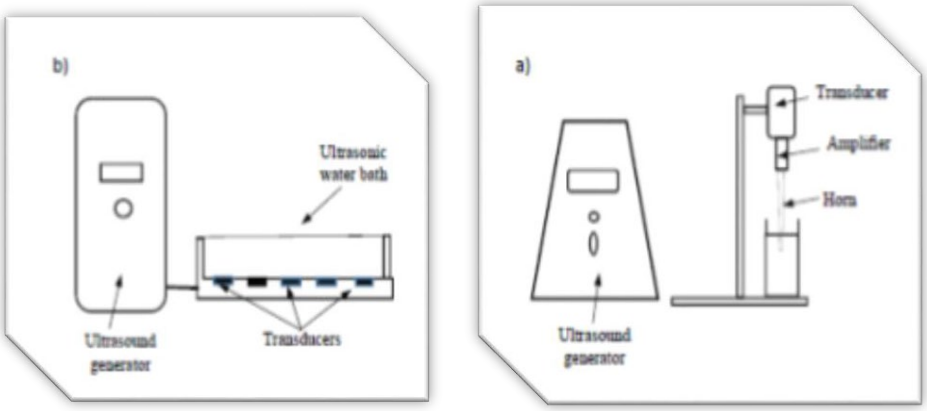

Fig. 2 - Ultrasound setup: (a) ultrasound probe; (b) ultrasonic bath
(adapted from Horiuchi, H. 2023)

During the study, the temperature was maintained at 20 or 40°C (below the denaturation temperature of whey proteins), and no whey protein denaturation was observed, indicating that any whey protein denaturation was attributed to heat generation rather than an effect of ultrasound. The resulting acid gels exhibited low firmness at these temperatures (20 and 40°C). When the temperature was maintained at 60°C, the acid gels reached a final firmness of up to 260 Pa *(Schorsch, B. C., & Haug, W., 2001).*

The costs and scalability of each technology

Regarding CO_2, the costs are relatively low because the equipment required for injection and pressure control is simple and does not involve major energy or maintenance expenses. This technology is highly scalable and can be easily integrated into existing dairy production lines. Additionally, CO_2 allows precise control of acidification and colloidal calcium phosphate solubilization, which influences gel firmness, texture, and syneresis *(Anne K. L., Tijs A.M. R., et al., 2022).*

High Pressure Processing (HPP) is a significantly more expensive technology. The equipment requires investments ranging from hundreds of thousands to millions of dollars, with considerable energy consumption and maintenance. Scalability is possible, but the high cost limits commercial adoption for small-scale production. At the molecular level, HPP partially denatures proteins and solubilizes colloidal calcium phosphate, modifying the gel network and affecting firmness and water-holding capacity *(Chawla, R., et al., 2010).*

Ultrasound has moderate costs, with equipment requirements depending on frequency, power, and batch size. Scalability is good for medium and large facilities, though process efficiency depends on the uniform distribution of ultrasound waves. Molecularly, cavitation generated by ultrasound fragments micelles,

exposes colloidal calcium phosphate, and accelerates ion transfer, resulting in more uniform and elastic gels *(Sutariya, S., Sunkesula, V., Kumar, R., & Shah, K. 2018).*

For **tannins (Maroyaka Tannen**), costs range from low to moderate, depending on the type and purity of polyphenols used, and the technology is highly scalable. Tannins can be easily incorporated into existing processes and influence gel structure through protein–polyphenol complex formation and calcium ion chelation, modulating firmness, texture, and syneresis *(Sutariya, S., Sunkesula, V., Kumar, R., & Shah, K. 2018).*

Health-promoting properties

Regarding the **health-promoting properties** discussed in the introduction, each technology influences the viability of probiotics or the formation of bioactive peptides to varying degrees. The technologies used in dairy processing not only affect texture and gelation but also have a direct impact on health benefits by influencing the viability of probiotic microorganisms and the generation of bioactive peptides *(Singh, P., et al., 2012).*

In the case of CO_2, acidification resulting from carbonic acid formation can lower the medium's pH and influence the enzymatic activity of lactic bacteria. However, CO_2 allows very fine control of pH and the acidification rate, which can protect probiotic viability if the process is properly adjusted. Additionally, moderate acidity promotes the activation of endogenous proteases from both milk and bacteria, potentially leading to the formation of bioactive peptides, such as antihypertensive or immunomodulatory peptides *(Singh, P., et al., 2012).*

High Pressure Processing (HPP) has a more complex effect on probiotics and bioactive peptides. High pressure can partially inactivate sensitive microorganisms, reducing the viability of some probiotic cultures, but certain resistant species may survive and even benefit from a more favorable environment due to Ca^{2+} release and protein structure modifications. Moreover, HPP can induce partial protein denaturation, exposing protein fragments to proteases and stimulating bioactive peptide formation, without affecting thermolabile compounds such as vitamins or unsaturated fatty acids *(Siddiqui, S. A., et al., 2024).*

Regarding **ultrasound**, cavitation and mechanical forces can affect both microflora and milk proteins. Ultrasound applied at moderate intensity can stimulate probiotic activity by increasing nutrient availability and enhancing the transfer of oxygen or ions, thereby improving viability. At the same time, micelle fragmentation and exposure of colloidal calcium phosphate can facilitate protease action, promoting the generation of bioactive peptides, while excessive exposure or high intensity may reduce the viability of sensitive bacteria *(Silva, M., et al., 2022).*

In the case of tannins **(Maroyaka Tannen**), the effects are indirect and dose-dependent. Tannins can form complexes with proteins and cations, modifying gel structure and nutrient accessibility. At moderate levels, tannins can create a protective environment for probiotics by reducing oxidative stress and safeguarding bacterial cells. Simultaneously, protein complexation can influence how proteases act on the protein matrix, potentially stimulating or modulating the formation of bioactive peptides, such as those with antioxidant or antimicrobial effects *(Ojo, M. A., et al., 2022).*

CONCLUSIONS

The Maroyaka Tannen Technique

In this technique, tannins (polyphenols) interact strongly with proteins through multiple bonds (hydrophobic interactions) and can chelate metal ions (Ca^{2+}), resulting in the formation of complexes, precipitation, or reorganization of protein networks. In parallel, they can chelate calcium ions, reducing the Ca^{2+}–phosphate bridges responsible for micellar aggregation.

The result is a different gel network: sometimes more stable and less prone to syneresis (due to additional cross-linking), and other times softer if calcium binding weakens micellar junctions. Thus, tannins can act as "modulators" of the gel's texture and firmness, depending on their dose and type. This concept for yogurt and fresh cheese categories is based on recombined powder formulations that can be integrated with liquid milk, milk concentrate, or whey components.

The use of this technology enables sustainable production, which is less dependent on the quality or availability of raw milk. The resulting products exhibit creaminess and a smooth mouthfeel, providing a solution that can be tailored to precisely meet consumer taste preferences *(Giordano, I., et al., 2022).*

Addition of carbon dioxide

Pre-acidification of milk before fermentation (at 40 °C until reaching pH 4.6) showed a linear increase in the solubilization of colloidal calcium phosphate with decreasing pre-acidification pH. The solubilized

colloidal calcium phosphate reduced the number of cross-links between it and casein within the casein micelle, thereby decreasing the number of reticulated colloidal calcium phosphates during gelation, which results in a weaker gel. Regarding the effect on the gel at the molecular level following the addition of carbon dioxide, the pH decrease caused by carbonic acid protonates the phosphate groups in colloidal calcium phosphate and the acidic residues of caseins, reducing the net charge of the micelles *(Marella, C., et al., 2015).*

In acid coagulation (yogurt), the pH decrease reduces electrostatic repulsion between micelles and promotes aggregation through hydrophobic interactions, while the amount of ionic calcium (resulting from the dissolution of colloidal calcium phosphate) can accelerate the formation of junction points between caseins, thereby producing a faster or firmer gel, but also a more contractile one (increased syneresis). In rennet coagulation, ionic calcium is essential for the formation of Ca^{2+} bridges between caseinates; the dissolution of colloidal calcium phosphate before cleavage reduces the initial structural integrity of the micelles and can alter the texture of the resulting network *(Marella, C., et al., 2015).*

High-Pressure Processing (HPP)

High-pressure treatment of milk, particularly at 676 MPa for 30 minutes, can produce yogurt structures and properties similar to those obtained through conventional thermal treatment, affecting casein micelle size and whey protein denaturation. The final effect depends on the process parameters and the initial pH of the milk. High pressure partially denatures proteins, disrupts the internal cavities of micelles, and can solubilize colloidal calcium phosphate.

High Pressure Processing can solubilize colloidal calcium phosphate, similar to acidification, releasing ionic calcium and altering micelle size and stability. As a result, aggregations may occur between whey proteins and pressure- modified caseins *(Siddiqui, S. A., et al., 2024).*

Low-Frequency Ultrasound Technology

High-pressure or ultrasound treatment of milk can improve yogurt texture and stability by reducing fat globule size and accelerating fermentation. Most of the beneficial effects on the gel are caused either by physical changes (homogenization and protein interactions) or by heat generated during the treatment, rather than by the ultrasound or pressure itself. Thus, these technologies can be used to produce firmer yogurts with improved water-holding capacity while maintaining product safety.

Cavitation generated by ultrasound produces mechanical forces and microturbulence, such as micelle fragmentation that exposes more colloidal calcium phosphate to the solution and accelerates the transfer of CO_2 into the micelle. The impact on the gel is that CO_2 can dissolve colloidal calcium phosphate more efficiently due to enhanced transport, resulting in a more uniform and elastic gel network, with faster micelle aggregation *(Prosekov, A., et al., 2025).*

Table 2

Interaction with CCP, effect on the gel, and control parameters

Technology	Interaction with CCP / Proteins	Effect on Gel	Control Parameters
The Maroyaka Tannen	Forms carbonic acid → protonates and partially dissolves CCP → releases Ca^{2+} → micelles become more prone to aggregation	Accelerates micellar aggregation; gel can be firmer or contractile; syneresis increases if dissolution is too fast	CO_2 pressure (pCO_2), temperature, injection rate, contact time
CO_2 (carbonation / supercritical)	Partial protein denaturation, CCP solubilization, redistribution of Ca^{2+} bridges, oligomer dissociation	Gel networks vary: finer, more fragile, or denser; firmness and water-holding capacity are modified	Pressure (MPa), holding time, temperature; combining with CO_2 or mild heat can modify effects
HPP (High Pressure Processing)	Cavitation → micelle fragmentation, CCP exposure; enhances ion and CO_2 transfer	Produces more uniform, elastic gels; affects porosity and aggregation kinetics	Frequency (kHz), amplitude, duration, temperature, presence of gases/particles
Ultrasound	Forms protein–polyphenol complexes; chelates Ca^{2+}, reducing micellar bridges	Modulates gel network: can increase stability or produce softer gel; affects firmness, texture, and syneresis	Type of tannin (condensed vs. hydrolyzable), dosage, timing of addition in the process

REFERENCES

[1] Akdeniz, V., et al. (2024). High-Energy Ultrasound Improves Culture Activity and Protein Digestibility in Probiotic Yogurts. Food Research International, 164, 112349, https://doi.org/10.1016/j.ifset.2024.103573.

[2] Ali, M. A., et al. (2021). Functional Dairy Products as a Source of Bioactive Peptides and Probiotics: Current Trends and Future Prospectives. Foods, 10(11), doi: 10.1007/s13197-021-05091- 8.

[3] Anne K. L., Tijs A.M. R., et al. (2022). Texture and microstructure of heat and acid induced gels from buffalo and cow milk: Effect of thermal treatment and fat content of milk. International Dairy Journal, 129, 105299, https://doi.org/10.1016/j.idairyj.2021.105299.

[4] Cauduro, V. H., et al. (2023). Ultrasound-Assisted Encapsulation of Phytochemicals for Functional Dairy Products. Foods, 12(20), 3859, https://doi.org/10.3390/foods12203859.

[5] Chawla, R., Patil, G. R., & Singh, A. K. (2011). High hydrostatic pressure technology in dairy processing: A review. Journal of Food Science and Technology, 48, 260–268, https://doi.org/10.1007/s13197-010-0180-4.

[6] Cheng, Y., et al. (2024). Effect of multi-mode divergent ultrasound pretreatment on the properties of whey protein gels. Preprints, 202405.1609, doi: 10.20944/preprints202405.1609.v1.

[7] Cheftel, J. C. (1996). Effects of high pressure on dairy proteins: a review. Trends in Food Science & Technology, 8(4), 124-131, doi: 10.1016/j.idairyj.2005.11.007.

[8] Cognitive Market Research. (2025). Yogurt Market Report 2025 (Global Edition).

[9] Deeth, H. C., & Tamime, A. Y. (2020). Yoghurt: Science and Technology (3rd ed.). CRC Press.

[10] Dimitreli, G., & Antoniou, K. (2018). Texture and microstructure of strained yogurt: a review. Journal of Texture Studies, 49(2), 187–199, doi: 10.33263/BRIAC103.56568.

[11] Data Bridge Market Research. (2025). Global Yogurt Market Size, Share, and Trends Analysis.

[12] Fox, P. F., McSweeney, P. L. H., Cogan, T. M., & Guinee, T. P. (2017). Fundamentals of Cheese Science (2nd ed.). Springer.

[13] Frontiers in Food Science and Technology. (2025). Enhancing Functional Dairy Foods: Bioactive Compounds in Dairy Products, https://doi.org/10.3389/frfst.2025.168515.

[14] Gevaudan, S., & Rémond, D. (1996). Effect of Treatment by Gaseous Carbon Dioxide on the Solubilization of Calcium Phosphate in *Milk*. Journal of Dairy Science, 79(4), 653–659, https://doi.org/10.3168/jds.S0022-0302(96)76537-2.

[15] Giordano, I., et al. (2022). *Application of Ultrasound and Microencapsulation on Probiotic Delivery Systems in Dairy Products*. Heliyon, 8(5), e09757, doi: 10.1016/j.heliyon.2022.e10969.

[16] Giordano, I., et al. (2023). *Microencapsulation and Sonication: A Multiple Physical Approach for Probiotic Delivery*. Food Research International, https://doi.org/10.1016/j.foodres.2023.112634.

[17] Grandison, A. S., & Lewis, M. J. (2012). *Separation Processes in the Food and Biotechnology Industries: Principles and Applications*. CRC Press.

[18] Gutiérrez-Álzate, K., et al. (2024). *Micro- and Nanoencapsulation of Probiotics: Exploring Their Potential in Dairy Products*. ACS Food Science & Technology, 4(5), 1234–1245, https://doi.org/10.1021/acsfoodscitech.4c00776.

[19] Habiba, M. U., et al. (2025). *Probiotic Dairy Innovations: Exploring Buffalo Milk Potential for Functional Foods*. Comprehensive Reviews in Food Science and Food Safety, https://doi.org/10.1111/1541-4337.70236.

[20] Horiuchi, H. (2023). *Reviving Traditional Yogurt with Modern Fermentation Technology*, https://www.meiji.com/global/wellness-stories/revising_traditional_yogurt.html.

[21] Joao L.A.D., et al. (2013). *Influence of Acidification Method on Composition, Texture, Psychrotrophs, and Lactic Acid Bacteria in Minas Frescal Cheese*. Food and Bioprocess Technology, doi: 10.1007/s11947-012-1029-9.

[22] Kaur, H., et al. (2022). *Dairy-Based Probiotic-Fermented Functional Foods*. Foods, 8(9), 425, https://doi.org/10.3390/foods8090425.

[23] Kazemi, S., et al. (2025). *Selection of Appropriate Probiotic Yeasts for Use in Dairy Products*. Food Production, Processing and Nutrition, 7(1), 1–10, https://doi.org/10.1186/s43014-024-00293-x.

[24] Krystian M., Paul D., Szymon S., et al. (2019). *Comparative effect of supercritical carbon dioxide and high pressure processing on structural changes and activity loss of oxidoreductive enzymes*. Journal of CO2 Utilization, 29, 46–56, https://doi.org/10.1016/j.jcou.2018.11.007.

[25] Lee, W. J., & Lucey, J. A. (2010). *Formation and physical properties of yogurt*. Journal of Dairy Science, 93(10), 3861–3873, doi: 10.5713/ajas.2010.r.05.

[26] Li, Y., et al. (2025). *Research progress on flavor of fermented dairy products*. Food Science and Applied

Processing, https://doi.org/10.26599/FSAP.2025.9240129.
[27] Marella, C., et al. (2015*). Manufacture of modified milk protein concentrate utilizing injection of carbon dioxide. Journal of Dairy Science, 98(6), 3677–3686, https://doi.org/10.3168/jds.2014-8946*.
[28] Mari Varhaug. (n.d.). "Smart Yoghurt" – *Combining innovative technologies towards more efficient yoghurt manufacturing.*
[29] McSweeney, P. L. H., & Fox, P. F. (2013). *Advanced Dairy Chemistry (Vols. 1–4). Springer*
[30] Mizuta, A. G., et al. (2025). *Improving Probiotic Strawberry Dairy Beverages with High-Intensity Ultrasound. Foods, 14(4), 616, doi: 10.3390/foods14040616.*
[31] Mordor Intelligence. (2025). *Yogurt Market Size & Share Analysis.*
[32] Nath, K. G., et al. (2023). *High-Pressure Processing: Effect on Textural Properties of Dairy Products*. Trends in Food Science &Technology, 124, 1–10, https://doi.org/10.1016/j.tifs.2022.12.001.
[33] Ogrodowczyk, A. M., et al. (2023). *Recent Advances in Fermented Milk and Meat Products: Non- thermal methods including high-pressure processing*, https://doi.org/10.3390/ani13132048.
[34] Ozaybi, N., et al. (2024). *High-Pressure Processing of Milk and Dairy Products: Review of advancements*. Processes, 12(10), https://doi.org/10.3390/pr12102073.
[35] Ojo, M. A., et al. (2022). *Tannins in Foods: Nutritional Implications and Processing Technologies*. Foods, 11(2), doi: 10.3746/pnf.2022.27.1.14.
[36] Park, Y. W. (2015). *Bioactive Peptides in Milk and Dairy Products: A Review*. Food Research International, 74, 1–10, https://doi.org/10.1016/j.foodres.2015.05.029.
[37] Prosekov, A., et al. (2025). *The Effect of Ultrasound on the Functionality and Health-Improving Properties of Dairy Products*. Food Production, Processing and Nutrition, 7(1), 36, doi:10.1186/s43014-025-00311-6.
[38] Rao, J., & Chen, B. (2015). *Novel applications of ultrasonics in dairy processing*. Journal of Dairy Research, 82(3), 399–406, https://doi.org/10.1051/dst/2009044.
[39] Ravash, N., Peighambardoust, S. H., Soltanzadeh, M., Pateiro, M., & Lorenzo, J. M. (2022). *Impact of high-pressure treatment on casein micelles, whey proteins, fat globules and enzyme activity in dairy products: a review*. Critical Reviews in Food Science and Nutrition, 62(11), 2888–2908, https://doi.org/10.1080/10408398.2020.1860899.
[40] Saputra, A., et al. (2025). *High-Pressure Processing as an Emerging Technology for Dairy Products*. Critical Reviews in Food Science and Nutrition, https://doi.org/10.1080/10408398.2025.2499623.
[41] Schorsch, B. C., & Haug, W. (2001). *Effects of heating whey proteins alone or in the presence of casein micelles on acid-induced gelation*. Journal of Dairy Science, 84(11), 2411–2417, doi: 10.1017/s0022029901004915.
[42] Siddiqui, S. A., et al. (2024). *Impact of High-Pressure Processing on the Bioactive Components of Dairy Products*. Journal of Dairy Science, 107(4), 1–12, doi: 10.1007/s13197-024-05938-w.
[43] Silva, M., et al. (2022). *Encapsulation of Nutraceuticals in Yoghurt and Beverage Systems: A Review*. Foods, 11(19), 2999, doi: 10.3390/foods11192999.
[44] Silva, R., Xavier, L. S., et al. (2024). *Strategies to Improve the Quality of Goat Yogurt: Whey Protein Isolate, Ultrasound, High Shear Dispersion*. Foods, 13(10), https://doi.org/10.3390/foods13101558.
[45] Singh, P., et al. (2012). *The use of carbon dioxide in the processing and packaging of milk and dairy products: A review*. International Journal of Dairy Technology, 65(1), 1–8, doi: 10.1111/j.1541-4337.2006.00008.x.
[46] SPX FLOW. (2013). *APV Cavitator Technology in Functionalization of WPC and other Food Ingredients.*
[47] Sutariya, S., Sunkesula, V., Kumar, R., & Shah, K. (2018). *Emerging applications of ultrasonication and cavitation in dairy industry: a review*. Cogent Food & Agriculture, 4(1), 1549187, https://doi.org/10.1080/23311932.2018.1549187.
[48] Ume R., Afeera A., et al. (2021). *Impact of high-pressure treatments on enzyme activity of fruit- based beverages: an overview*. International Journal of Food Science and Technology, 57(2), 801– 815, https://doi.org/10.1111/ijfs.15492.
[49] Vinderola, G., et al. (2000). *Characteristics of carbonated fermented milk and survival of probiotic bacteria*. International Dairy Journal, 10(7), 457–463, https://doi.org/10.1016/S0958-6946(00)00031-5.
[50] Wróblewska, B., et al. (2023). *Bioactive Dairy-Fermented Products and Phenolic Compounds: Health Benefits and Applications*. Foods, 12(5), 1120, doi: 10.3390/molecules28248081.
[51] Zhao, Y., et al. (2024). *Ultrasound-induced structural changes of different milk fat globules*. Food Research International, 162, 112634, doi: 10.1016/j.ultsonch.2024.106799.

EXTRUSION FABRICATION OF SHEEP-WOOL REINFORCED PLA/PBAT/PA BIOCOMPOSITES FOR AGRICULTURE 4.0/5.0 APPLICATIONS

/

FABRICAREA PRIN EXTRUDARE A BIOCOMPOZITELOR DIN PLA/PBAT/PA RANFORSATE CU LÂNĂ DE OAIE PENTRU APLICAȚII ÎN AGRICULTURA 4.0/5.0

Teodor Gabriel FODOREAN[1)], Elena Mihaela NAGY[1)], Dragos-Vasile NICA[1)], Eveline Anda LAZA[1)], Ioan KABA[1)], Valentin VLADUT[1)], Teodor VINTILA[2)]

[1)] National Institute of Research – Development for Machines and Installations Designed for Agriculture and Food Industry - INMA Bucharest, 6 Ion Ionescu de la Brad Blvd, District 1, 013813.Bucharest / Romania;

[2)] University of Life Sciences "King Mihai I" from Timişoara, 119 Aradului Path, 300645, Timişoara, Timis County / Romania.

*Tel: (+40)741 212 696; *E-mail: gabriel.fodorean@gmail.com

Keywords: *sheep wool, PLA, PBAT, PA, extrusion, bio-composite, Agriculture 4.0/5.0*

ABSTRACT

Sheep wool is an abundant keratinous waste with agronomic and material potential (Alexander P., Earland C., 1952, Process for the Treatment of Keratin and Related Materials, US Patent, No. 2622036). This work presents a reproducible processing and characterization workflow to obtain extruded bio-composites using PLA/PBAT/PA ternary matrices reinforced with sheep-wool fibres (5–25 wt%) (Fodorean G., Cota C., Cioica N., Influence of rotation speed during extrusion to the properties and morphology of biopolymers blend, Acta Technica Napocensis, Series: Applied Mathematics and Mechanics nr.56/2013, vol. III, pag. 493-496, ISSN 1221-5872; Fodorean T.G., Nagy E.M., Boeru A.I., Luca L., Marica M. (2024). Biocompozit pe bază de aminoacizi proveniți din materiale proteice keratinoase și procedeu de realizare, patent request OSIM A/00754 from 28 November 2024). Processing windows, reactive extrusion dosing of wool hydrolysates, and characterization methods (FT-IR, NMR relaxometry, SEM, DSC/TGA, mechanical testing and soil-burial assays) are integrated into a complete protocol. Target applications include biodegradable mulch films, seedbed modules and sensor housings for Agriculture 4.0/5.0 (Hunter and all 2017, Agriculture în 2050: Recalibrating targets for sustainable intensification, Bioscience, 67, 386–391). Expected outcomes are improved water buffering, adjustable mechanical properties and controlled biodegradability.

REZUMAT

Lâna de ovină reprezintă un deșeu keratinos abundent cu potențial agronomic și material (Alexander P., Earland C., 1952, Process for the Treatment of Keratin and Related Materials, US Patent, No. 2622036). Lucrarea prezintă un protocol reproductibil de procesare și caracterizare pentru obținerea bio-compozitelor extrudate pe bază de matrice ternară PLA/PBAT/PA armate cu fibre din lână de ovină (5–25% din greutate) (Fodorean G., Cota C., Cioica N., Influence of rotation speed during extrusion to the properties and morphology of biopolymers blend, Acta Technica Napocensis, Series: Applied Mathematics and Mechanics nr.56/2013, ISSN 1221-5872; Fodorean T.G., Nagy E.M., Boeru A.I., Luca L., Marica M. (2024). Biocompozit pe bază de aminoacizi proveniți din materiale proteice keratinoase și procedeu de realizare, patent request OSIM A/00754 from 28 November 2024). Sunt integrate ferestrele de procesare, dozarea hidrolizatului de lână în extrudare reactivă și metodele de caracterizare (FT-IR, relaxometrie NMR, SEM, DSC/TGA, teste mecanice și studii de degradare în sol). Aplicațiile vizate includ folii biodegradabile, module de support pentru semințe și carcase pentru senzori pentru Agricultura 4.0/5.0 (Hunter and all, 2017, Agriculture în 2050: Recalibrating targets for sustainable intensification, Bioscience, 67, 386–391).

INTRODUCTION

Global wool production and textile processing generate significant wool waste *(IWTO, 2021, Wool Production, International Wool Textile Organization),* often landfilled despite valuable material and agronomic properties. Keratinous wool offers water retention, slow nutrient release and biodegradability *(Alexander P., Earland C., 1952, Process for the Treatment of Keratin and Related Materials, US Patent, No. 2622036; Bhavsar, P. S. (2020).*

Green hydrolysis of waste wool), making it a candidate reinforcement and functional additive for biodegradable polymer matrices. Combining wool with PLA/PBAT/PA blends processed by extrusion can

produce materials suitable for precision agriculture applications *(Fodorean G., Cota C., Cioica N., Influence of rotation speed during extrusion to the properties and morphology of biopolymers blend, Acta Technica Napocensis, Series: Applied Mathematics and Mechanics nr.56/2013, ISSN 1221-5872; Fodorean T.G., Nagy E.M., Boeru A.I., Luca L., Marica M. (2024).* Biocompozit pe bază de aminoacizi proveniți din materiale proteice keratinoase și procedeu de realizare, patent request OSIM A/00754 from 28 November 2024).

The paper aims to: (1) develop extrusion protocols for PLA/PBAT/PA matrices reinforced with sheep-wool fibres (5–25 water percentage); (2) define characterization methods to assess mechanical, hydric and biodegradation behaviour; (3) propose application pathways in Agriculture 4.0/5.0 for mulches, seedbed modules and transient sensor housings *(Hunter and all, 2017, Agriculture în 2050: Recalibrating targets for sustainable intensification, Bioscience, 67, 386–391; Nagy E.M., Fodorean G.,Cota C., Cioica N., Gyorgy Z., 2017, Influence of natural fibers on the mechanical properties of starch-based bioplastics PROCEEDINGS OF THE 45th INTERNATIONAL SYMPOSIUM ON AGRICULTURAL ENGINEERING "Actual Tasks on Agricultural Engineering", ISSN 1848-4425, Opatija – Croaţia; Fodorean T.G., Nagy E.M., Cioica N., Deac T., 2024, Study regarding the influence of the mechanical properties by the processing parameters in the case of ternary biopolymer blends, ISB-INMA TEH' 2024 Agricultural and Mechanical Engineering).*

MATERIALS AND METHODS

Materials: industrial-grade PLA, PBAT and a compatibilizing PA were selected as the ternary matrix (baseline 60/20/20 %). Sheep-wool feedstock was used as milled short cut fibres and alkaline hydrolysates for liquid dosing. Processing: twin-screw extrusion mixers were used with typical temperatures between 160–205 °C and rotor/screw speeds 50–100 rpm. Hydrolysates were dosed via peristaltic pump in reactive extrusion *(Nagy E.M., Fodorean T. G, Deac T., Fechete-Tutunaru L.V., 2024 - Research on wool waste processing technologies for use in agricultural crops, ISB-INMA TEH' - Agricultural and Mechanical Engineering).* Samples were granules or specimen-cast for tests *(Nagy E.M., Fodorean T.G., Nica D.V., Laza E.A., Vintila T., 2024, Researches for the physico-chemical characterization of some granular fertilizers obtained from native wool waste, in order to use them in agriculture, Scientific Papers. Series E. Land Reclamation, Earth Observation & Surveying, Environmental Engineering, Vol. XIII, 320-325; Onifade, A., Al-Sane, N., Al-Musallam, A. and Al-Zarban, S. (1998). A review: potentials for biotechnological applications of keratin-degrading microorganisms and their enzymes for nutritional improvement of feathers and other keratins as livestock feed resources. Bioresource Technology; Schwan, A., J. Herrling, and H. Zahn (1986). Characterization of internal lipids from wool. Colloid and Polymer Science).*

In order avoid excessive wool fibres degradation and to maximize interfacial bonding, was use low shear feeding and consider a mild compatibilizer (maleic anhydride grafted PLA/PBAT or a coupling agent). Pre-treatments (alkaline wash or mild hydrolysis) can increase surface polarity and potential bonding with the matrix, and allow wool to function as a nutrient carrier if loaded with hydrolysate during extrusion. The agronomic work shows protein hydrolysates obtained from wool are feasible reagents.

Formulations (recipes): B1 (60/20/20 + 5 % wool), B2 (60/20/20 + 10 % wool milled), B3 (60/20/20 + 15 % wool), B4 (60/20/20 + 10% wool + 4 % wool hydrolysate). Drying to <3% moisture before extrusion and use of mild compatibilizers (e.g., MA-grafted agents) are recommended to improve interface adhesion and dispersion.

Table 1

Formulations (recipes)

Formulation (recipe)	Biopolymers matrix (%)	Wool (%)
B1	PLA 60 / PBAT 20 / PA 20	5 (milled)
B2	PLA 60 / PBAT 20 / PA 20	10 (milled)
B3	PLA 60 / PBAT 20 / PA 20	15 (milled)
B4	PLA 60 / PBAT 20 / PA 20	10 (milled) + 4 wool hydrolysate

The processing was made by extrusion using a Collin ZK25 extruder (Fig. 1). The mixture was dosed through the extruder feed point is taken up by the two corotating screws which homogenize it and process it by shearing and heating while it is moved towards the die provided with a 7 mm diameter. The extruder has two co-rotating modular screws, with a productivity of approx. 15 kg/h, screw diameter D=25 mm, screw length: L=30xD, screw speed: max. 400 rpm.

The extruder barrel is also modular and has 6 removable and interchangeable zones, each zone having independent heating and cooling systems. The dosage of the mixture of solid components in the extruder hopper was done using a two-screw dispenser.

Fig. 1 - Collin ZK25 extrusion machine used for processing

Relating properties methods of characterization (Fig.2), a multi-technique suite is planed: FT-IR for chemical bonding; SEM/EDX for morphology and dispersion; DSC/TGA for thermal behaviour; tensile, flexural and impact tests for mechanical performance; gravimetric water uptake and dynamic nutrient-release assays for hydric function; and soil-burial compost tests for biodegradation.

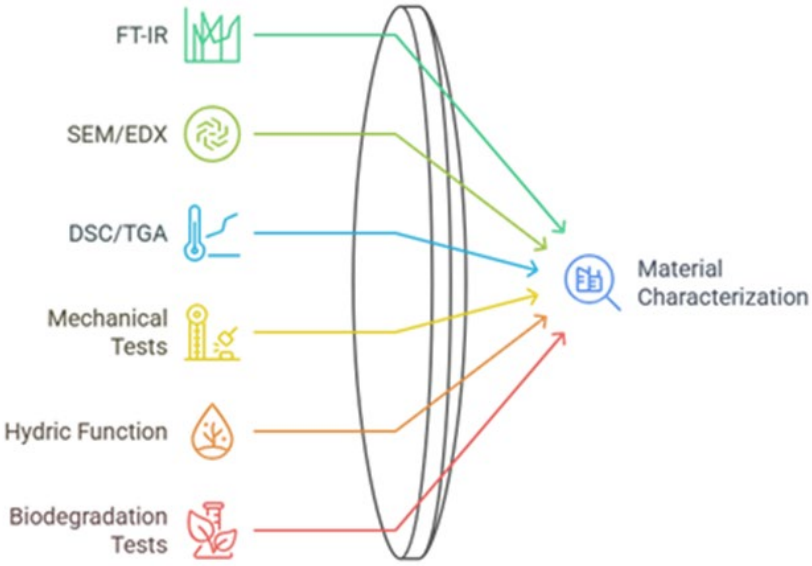

Fig. 2 - Designed protocol for establishing the properties and behaviour of the new obtained bio-composite material

On the Fig. 3 we have an example of the obtained extruded bio-composite material having wool fibers.

RESULTS

Based on literature and preliminary laboratory experiments the ternary PLA/PBAT/PA matrix is extrudable with up to around 15 % wool content without severe processing issues when rotor speeds and temperature profiles are optimized.

Wool increases water-retention and introduces porosity beneficial for mulch films and seedbed modules but may reduce tensile strength unless compatibilized. Reactive extrusion with hydrolysate

dosing enables nutrient-carrier functionality and supports agronomic compatibility with beneficial microbes.

Fig. 3 - Obtained extruded bio-composite material

Potential/planed applications case studies:

1. Smart biodegradable mulch film (25–100-500 μm): retains soil moisture via wool-induced porosity; degrades after one crop cycle; can be co-extruded with a protective top layer and inner wool-rich layer for moisture buffering. Integration of passive humidity tags enables remote monitoring of field moisture (Agriculture 4.0).
2. Seedbed modular blocks: 3D-printed or extruded thicker elements (bio-composite blocks) containing wool as nutrient and moisture reservoirs; loaded with beneficial microbial lyophilizates during extrusion for targeted early root microbiome enrichment. Compatibility of wool hydrolysate with beneficial microbes supports this route.
3. Biodegradable sensor housings: for in-soil sensor nodes that must disappear post-season, fabricated from the PLA/PBAT/PA matrix tuned for necessary strength and controlled biodegradability.

Limitations and challenges – while PLA-PBAT-PA ternary blends reinforced with sheep wool fibres offer improved biodegradability, enhanced toughness, and better thermal insulation, their integration also presents significant issues such as fibre-matrix interfacial adhesion, moisture uptake from wool, and the trade-off between stiffness and ductility. The presence of natural fibres like wool often reduces thermal stability and increases heterogeneity in mechanical behaviour across samples. Also, the complexity of blending three polymer phases (PLA, PBAT, PA) complicates achieving uniform phase dispersion, and the wool content tends to accelerate hydrolysis under humid or composting conditions.

Manufacturing new products from this bio-composite introduces further challenges: extrusion processes must be carefully optimized to prevent thermal degradation of both polymer phases and wool fibres, and high shear or temperature can damage wool keratin or cause depolymerization of the matrices. Moreover, ensuring repeatability in product quality is difficult, given variability in wool fibre properties (length, diameter, cleanness) polymer batch differences, and processing parameters; scale-up will likely require fibre pre-treatment or compatibilizers, and stringent control over blending, drying, and extrusion schedules.

CONCLUSIONS

Sheep-wool reinforced PLA/PBAT/PA bio-composites produced by extrusion present a feasible route toward biodegradable, water-buffering agricultural materials for Agriculture 4.0/5.0 applications.

The proposed processing windows, reactive extrusion dosing strategies, and characterization matrix provide a roadmap for experimental validation and scale-up. Next steps are full lab validation following the experimental plan above; results will quantify trade-offs between mechanical performance, water buffering, nutrient release kinetics, and biodegradation.

ACKNOWLEDGEMENT

The authors would like to express their gratitude to the Laboratory of Bio-polymers and Bio-composites Materials, National Institute of Research – Development for Machines and Installations Designed for Agriculture and Food Industry – INMA Cluj-Napoca and Timisoara branches, to University of Life Sciences Timisoara for their valuable support, resources, and collaborative environment that contributed to the development of this research.

REFERENCES

[1] Alexander P., Earland C., (1952), Process for the Treatment of Keratin and Related Materials, US Patent, No. 2622036.

[2] Bhavsar, P. S. (2020) Green hydrolysis of waste wool.

[3] Crainic R., Nagy E.M., Fodorean G., et al (2024). Advanced NMR, FT-IR, VIS-NIR and XRD methods used for characterization of organo-mineral fertilizers based on biosolids. *Agriculture, 14(10), 1826*; https://doi.org/10.3390/agriculture14101826

[4] Das, O., N. K. Kim, A. K. Sarmah, and D. Bhattacharyya. (2017). Development of waste-based biochar/wool hybrid biocomposites: Flammability characteristics and mechanical properties. Journal of Cleaner Production 144:79–89.

[5] Fodorean G. - Influenţa regimului termic asupra procesării materialelor bioplastice. Dezvoltarea materialelor bioplastice, Editura GlobeEdit, Berlin, 2016, ISBN: 978-3-330-71379-6

[6] Fodorean G., Cota C., Cioica N., Influence of rotation speed during extrusion to the properties and morphology of biopolymers blend, Acta Technica Napocensis, Series: Applied Mathematics and Mechanics nr.56/2013, vol. III, pag. 493-496, ISSN 1221-5872, [Indexed by: IndexCopernicus™ International].

[7] Fodorean G., Fu Y., Peuvrel-Disdier E. - Research regarding optimal resistance at impact of a binary biopolymer blend and optimal PLA/PBAT blends percentage, Acta Techvnica Napocensis-series: applied mathematics, mechanics, and engineering, vol. 56, 2013.

[8] Fodorean T.G., Nagy E.M., Boeru A.I., Luca L., Marica M. (2024). Biocompozit pe bază de aminoacizi proveniți din materiale proteice keratinoase și procedeu de realizare, patent request OSIM A/00754 from 28 November 2024.

[9] Fodorean T.G., Nagy E.M., Cioica N., Deac T. (2024). Study regarding the influence of the mechanical properties by the processing parameters in the case of ternary biopolymer blends, ISB-INMA TEH' 2024 Agricultural and Mechanical Engineering.

[10] Fodorean T.G., Nica D.-V., Nagy E.M., Laza E.A., Vintila T. (2023). Cercetări privind utilizarea deșeurilor de lână la obținerea unor fertilizanți organici pentru agricultură în vederea îmbunătățirii proprietăților solului şi reducerii poluării mediului – research project: PN 23 04 02 02, Romania.

[11] Fu Y., Fodorean G., Navard P., Peuvel-Disdier E. - Study of the partial wetting morphology in polylactide/poly[(butylene adipate)-co-terephthalate]/polyamide ternary blends: case of composite droplets, Polymer International (impact score 3.44), pp. 1378-1385, 2018, ISSN 10970126, 09598103, Marea Britanie; https://mc.manuscriptcentral.com/pi-wiley

[12] Hunter and all (2017) Agriculture în 2050: Recalibrating targets for sustainable intensification, Bioscience, 67, 386–391.

[13] Maria, A., and Păcurar I. (2015). Study on the use sheep wool, in soil and fertilization as the mixture into cubes nutrients. Proenvironment 8:290-292.

[14] Nagy E.M., Fodorean G.,Cota C., Cioica N., Gyorgy Z. Influence of natural fibers on the mechanical properties of starch-based bioplastics PROCEEDINGS OF THE 45th INTERNATIONAL SYMPOSIUM ON AGRICULTURAL ENGINEERING "Actual Tasks on Agricultural Engineering", pp. 573-579, 2017, ISSN 1848-4425, Opatija - Croaţia; http://atae.agr.hr

[15] Nagy E.M., Fodorean T. G, Deac T.,Fechete-Tutunaru L.V.(2024) - Research on wool waste processing technologies for use in agricultural crops, ISB-INMA TEH' 2024 Agricultural and Mechanical Engineering

[16] Nagy E.M., Fodorean T.G., Nica D.V., Laza E.A., Vintila T., (2024) Researches for the physico-chemical characterization of some granular fertilizers obtained from native wool waste, in order to use them in agriculture, Scientific Papers. Series E. Land Reclamation, Earth Observation & Surveying, Environmental Engineering, Vol. XIII, 320-325.
[17] Onifade, A., Al-Sane, N., Al-Musallam, A. and Al-Zarban, S. (1998). A review: potentials for biotechnological applications of keratin-degrading microorganisms and their enzymes for nutritional improvement of feathers and other keratins as livestock feed resources. Bioresource Technology 66: 1-11.
[18] Schwan, A., J. Herrling, and H. Zahn (1986). Characterization of internal lipids from wool. Colloid and Polymer Science 264 (2):171–75.
[19] *** IWTO (2021) Wool Production, International Wool Textile Organization. https://www.iwto.org/wool-production
[20] *** www.statista.com/statistics/263154/worldwide-production-volume-of-textile-fibers-since-1975

EFFECT OF FRUITS POWDERS ADDITION ON WHEAT FLOUR DOUGH RHEOLOGICAL PROPERTIES - REVIEW

/

INFLUENȚA ADAOSULUI PUDREI DE FRUCTE ASUPRA PROPRIETĂȚILOR REOLOGICE ALE ALUATULUI DIN FĂINĂ DE GRÂU - REVIEW

Elena-Mădălina ȘTEFAN[1)], Aura-Irina ISTRATE*[1)], Gabriel-Alexandru CONSTANTIN[1)], Mariana-Gabriela MUNTEANU[1)], Gheorghe VOICU[1)], Gabriel MUȘUROI[1)], Alina-Daiana IONESCU[1)], Elena-Melania CISMARU[2)]

[1)] National University of Science and Technology POLITEHNICA Bucharest / Romania;
[2)] National Institute of Research - Development for Machines and Installations Designed for Agriculture and Food Industry - INMA Bucharest / Romania.
**Tel: (004) 0723 542 609; *E-mail: irina_aura.istrate@upb.ro*

Keywords: *fruit powders, wheat flour, dough, rheological properties, functional ingredients, bakery products*

ABSTRACT

In today's food industry, there is increasing interest in improving the quality of bakery products through the use of functional raw materials. The quality and safety of these products are influenced both by environmental factors and by technological innovations in the food sector. Fruit powders or flours obtained from pulp or from processing by-products such as peels and seeds are valuable sources of fiber, antioxidants, and bioactive compounds. Their incorporation enables the development of innovative products with superior nutritional profiles, enhanced functional properties, and extended shelf life. In contrast, soil contamination with heavy metals affects cereal crops through physiological and biochemical changes, reducing flour quality and threatening food safety. The addition of fruit powders such as chokeberry, sea buckthorn, currants, cranberries, rosehip, raspberry, apple, or grape can help counterbalance these adverse effects by providing antioxidants, fibers, and protective compounds. Moreover, these ingredients improve the rheological properties of dough, including hydration capacity, development time, elasticity, extensibility, and gas retention, which positively influence texture, flavour, and nutritional value. This research highlights the potential of fruit powders as a sustainable solution for obtaining functional bakery products with high added value, despite the negative effects of environmental stressors.

REZUMAT

În industria alimentară actuală există un interes tot mai mare pentru îmbunătățirea calității produselor de panificație prin utilizarea materiilor prime funcționale. Calitatea și siguranța acestor produse sunt influențate atât de factorii de mediu, cât și de inovațiile tehnologice din sectorul alimentar. Pudrele sau făinurile obținute din pulpă de fructe sau din subproduse rezultate în urma procesării, precum coji și semințe, reprezintă surse valoroase de fibre, antioxidanți și compuși bioactivi. Integrarea lor permite dezvoltarea unor produse inovatoare, cu profil nutrițional superior, proprietăți funcționale îmbunătățite și termen de valabilitate extins. În schimb, contaminarea solului cu metale grele afectează culturile de cereale prin modificări fiziologice și biochimice, reducând calitatea făinurilor și punând în pericol siguranța alimentară. Adăugarea pulberilor de fructe precum aronia, cătină, coacăze, merișoare, măcește, zmeură, mere sau struguri poate contrabalansa aceste efecte negative prin aportul de antioxidanți, fibre și compuși cu rol protector. De asemenea, aceste ingrediente îmbunătățesc proprietățile reologice ale aluatului, inclusiv capacitatea de hidratare, timpul de dezvoltare, elasticitatea, extensibilitatea și retenția de gaze, influențând pozitiv textura, aroma și valoarea nutrițională. Această direcție de cercetare evidențiază potențialul pulberilor de fructe ca soluție sustenabilă pentru obținerea unor produse de panificație funcționale și cu valoare adăugată ridicată, în ciuda efectelor negative generate de factorii de mediu.

INTRODUCTION

The bakery industry is one of the most important food production sectors, providing staple products that supply carbohydrates, proteins, dietary fiber, and bioactive compounds essential for human nutrition. In recent years, its role has expanded due to consumer demand for functional foods, health-promoting ingredients, and sustainable production systems *(Galanakis, 2021; Zarzycki et al., 2024)*.

In this context, fruit powders obtained from whole fruits or processing by-products (peels, seeds) have gained particular interest for their fiber, vitamins, polyphenols, and other bioactive compounds *(Salehi, 2020; Krakowska-Sieprawska et al., 2024)*. Unlike extracts or juices, fruit powders offer higher stability, preservation of bioactives, and easier handling, while also supporting circular economy principles by valorizing by-products *(Krakowska-Sieprawska et al., 2024)*. Meanwhile, wheat flour quality is increasingly affected by climate change, intensive agricultural practices, and environmental pollution, which alter protein, gluten, and starch content, with direct impact on dough stability and rheological behavior. The addition of fruit powders represents a promising strategy to counterbalance these effects, as their antioxidants, fibers, and bioactive compounds contribute to maintaining quality, nutritional value, and shelf life *(Han et al., 2025; Murariu et al., 2025)*.

Fruit powders also provide functional health benefits, including antioxidant and anti-inflammatory activity, cardiovascular protection, glycemic regulation, and support for gut microbiota. Fruits such as chokeberry, cranberry, blueberry, pomegranate, and sea buckthorn have been widely studied, showing improvements in nutritional and sensory profiles through natural color, flavor, and preservation properties *(Meng et al., 2019; Kasprzak-Drozd et al., 2021)*. However, their incorporation modifies dough rheology, development time, elasticity, extensibility, and gas retention, which in turn determines loaf volume, crumb structure, and texture. These changes require technological adjustments to preserve desirable quality *(Fadiji and Pathare, 2023; Cacak-Pietrzak et al., 2023; Kolesárová et al., 2025)*.

Examples such as the addition of chokeberry, sea buckthorn, or rosehip demonstrate both nutritional and functional benefits, as well as technological challenges. In the case of chokeberry, although its high anthocyanin and fiber content enhances nutritional value and extends shelf life, it significantly affects dough rheological properties *(Fadiji and Pathare, 2023; Cacak-Pietrzak et al., 2023)*. Sea buckthorn, rich in vitamins and antioxidants, provides important functional benefits but requires optimization of addition levels to avoid compromising bread texture and flavor *(Bal et al., 2011; Wang et al., 2016; Stanciu et al., 2023)*. Similarly, rosehip seed flour (Rosa canina L.) can enrich bakery products with fibers, proteins, and minerals, but it also modifies dough rheology, necessitating adjustments in formulation and processing *(Gül and Şen, 2017; Cingöz and Şahin, 2023; Sanfilippo et al., 2025)*. Moreover, currants, due to their high vitamin C and anthocyanin content, have been linked to enhanced antioxidant capacity and color stability in baked goods.

Raspberries and blackberries, rich in bioactive compounds such as fibers and polyphenols, contribute to higher nutritional value while improving natural aroma and color, whereas grapes and their by-products (pomace) are valuable sources of resveratrol and fibers, successfully applied to increase product stability, functional properties, and shelf life *(Kierońska et al., 2024; Mandache et al., 2025; Salehi, 2020)*. From a technological perspective, these challenges have prompted strategies to balance enrichment with processing performance, including optimization of addition levels, the use of functional improvers (vital gluten, enzymes), and adjustments of fermentation conditions *(Lauková et al., 2016; Murariu et al., 2025)*.

Considering the increasing demand for functional bakery products and the complexity of dough systems, understanding the mechanisms behind fruit powder-induced rheological modifications remains a research priority. In addition, fruit powders may play a dual role: enhancing nutrition while helping mitigate the negative impact of environmental contaminants on wheat-based products by improving antioxidant content, dough stability, and product safety.

MATERIALS AND METHODS

This paper is a review based on the analysis of scientific articles, conference papers, books, and relevant online publications. Sources were retrieved from international databases (Scopus, Web of Science, Google Scholar) for the period 1999-2025, with emphasis on the most recent contributions (2020-2025). Keywords used were “fruit powders,” “wheat flour,” “dough rheology,” “functional bakery products,” “antioxidants,” and “bioactive compounds.” Publications focusing on the effect of fruit powders on the rheological, nutritional, and technological properties of wheat flour dough were selected. The information was synthesized and grouped into key categories: gluten hydration, dough development time, elasticity and extensibility, gas retention, viscoelastic properties, and functional benefits.

RESULTS

The literature consistently reports that the addition of fruit powders influences both the rheological behavior of dough and the nutritional and sensory quality of bakery products. The effects depend on fruit type, chemical composition, and incorporation level, being largely driven by the interactions of fibers,

polyphenols, anthocyanins, vitamins, and the gluten network in wheat flour. In general, moderate additions (3-8%) improve the functional and nutritional profile of bread, whereas higher concentrations (>10%) often cause undesirable changes in dough volume, texture, and rheological performance *(Djeghim et al., 2021)*.

Impact of fruit powder addition on dough rheological behaviour

Existing studies show that fruit powders induce significant changes in wheat dough properties, primarily through their content of soluble and insoluble fibers, polyphenols, organic acids, and sugars *(Della Valle et al., 2022)*. Key rheological parameters affected include water absorption, dough development time, elasticity, extensibility, gas retention capacity, and viscoelastic properties, all of which directly influence bread quality.

Water absorption capacity and gluten hydration

Dough quality refers to the set of properties that determine its technological performance in the breadmaking and baking process, including softness, extensibility, stretchability, elasticity, stability, and the balance between moisture, stickiness, and dryness *(AbuDujayn et al., 2022)*. These characteristics largely depend on flour composition, especially gluten proteins (glutenin and gliadins), fiber content, hydration, and water absorption capacity, as well as on mixing, fermentation, and baking conditions.

High-quality dough must be extensible enough to expand during fermentation/proofing, but also elastic enough to retain the produced gases without tearing or becoming too rigid. Farinographic parameters, such as water absorption, dough development time, dough stability, mixing tolerance index, and degree of softening, are key indicators commonly used for evaluating dough quality. These were determined using a Farinograph Brabender (Duisburg, Germany), according to ISO 5530-1:2013 *(Lauková et al., 2016)*.

The chemical composition of commercial apple powder and fine wheat flour was reported in a previous study by *Lauková et al., (2016)*. The apple powder contained 46.1% total dietary fiber, of which 20.4% was pectin. Gluten hydration and water absorption capacity are decisive for dough functionality and loaf volume. Gluten, formed from gliadin and glutenin, provides the viscoelastic network that stabilizes gas cells. Any ingredient competing for water or altering protein interactions will therefore influence dough development and stability (*Schopf and Scherf, 2021; Almutawah et al., 2007)*.

Fruit powders enrich bakery products nutritionally, but their bioactive compounds and fibers inevitably compete with gluten for water, altering hydration dynamics *(Isaak et al., 2019).* Additions rich in insoluble fibers, such as rosehip powder or grape pomace, tend to reduce water absorption and gluten hydration capacity, leading to a less developed protein network (*Sanfilippo et al., 2025; Šporin et al., 2017)*. By contrast, powders high in soluble fibers (e.g., blackcurrant, raspberry) exert more moderate effects, retaining water in a gel-like form and contributing to a more uniform dough texture *(Alba et al., 2020; Cacak-Pietrzak et al., 2023)*.

Moreover, the high pectin content of certain fruits (citrus, apples) may increase water-holding capacity, though often accompanied by reduced gluten elasticity due to interference with protein bonding *(Sharoba et al., 2013; Mudgil, 2017)*. Other polysaccharides, such as β-glucans and arabinoxylans, redistribute water and destabilize protein structures, resulting in doughs with reduced elasticity and extensibility *(Welc-Stanowska et al., 2023)*. In the study of *Schopf and Scherf (2021)*, ten commercial vital gluten samples were analyzed to determine the factors underlying their variable baking performance.

Protein composition (gliadins and glutenins), free thiols, and disulfide bonds were quantified, and micro-baking trials were performed using both a complex bread mix and a weak wheat flour. The authors demonstrated that bread quality was not determined by protein composition, but rather by water absorption capacity, with each sample showing a distinct optimal hydration level for maximum loaf volume.

As illustrated in Figure 1, samples hydrated at or near their optimal level produced larger, well-aerated breads, while those under- or over-hydrated yielded smaller, denser loaves. This highlights that industrial baking performance can only be ensured by adjusting water addition to the hydration properties of each gluten batch, even though this practice is rarely applied.

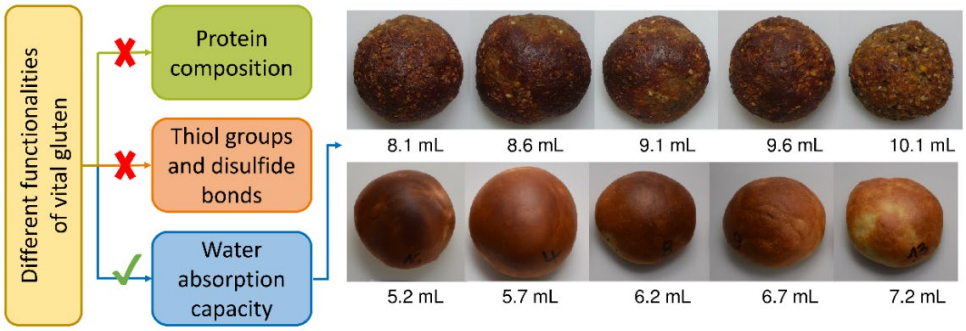

Fig. 1 - Functional performance of different vital gluten samples in breadmaking. Bread volumes varied as a consequence of differences in water absorption capacity, while protein composition and disulfide bonding were not decisive factors

(Schopf and Scherf, 2021)

Therefore, assessing the impact of fruit powders on water absorption and gluten hydration is critical for understanding dough rheology and for adjusting processing conditions to maintain both nutritional and sensory quality. A synthesis of literature findings is presented in Table 1, which summarizes the effects of different fruit powders on water absorption, gluten hydration, and baking outcomes.

Table 1

Effect of fruit powders on water absorption and gluten hydration

Fruit powder / additive	Effect on water absorption	Effect on gluten hydration	Consequences for dough / bread quality	References
Rosehip, chokeberry	Decrease (due to high insoluble fiber content)	Limit gluten hydration	Increased dough stability but reduced extensibility; lower loaf volume	*Matas et al., 2022; Cacak-Pietrzak et al., 2023*
Berries (e.g., blackcurrant, raspberry)	Moderate effect on water absorption	Partial preservation of gluten hydration	Stiffer dough with slower fermentation and reduced loaf volume; pre-hydration mitigates negative effects	*Stanciu et al., 2023; Reißner et al., 2020*
Apple powder (hydrated)	Significant increase (e.g., from ~58% to ~75%)	Extended dough development time, reduced mixing tolerance	More stable dough, but less resistant to mechanical stress	*Lauková et al., 2016*
Apple pomace (dried)	Increased water absorption	Weakened gluten network at high inclusion levels	Firmer texture of final products, lower loaf volume, impaired crumb quality	*Usman et al., 2020; Jannati et al., 2018*
Pomegranate powder	Moderate increase in water absorption	Improved cohesiveness and elasticity	Enhanced dough viscoelasticity and texture at 4-12% addition; high levels may deteriorate structure	*Zhang et al., 2023*
Sprouted wheat	Decrease (due to higher enzymatic activity, e.g., amylases and proteases)	Lower gluten index, weaker aggregation	Softer, less viscoelastic dough	*Annor et al., 2015*
β-glucans (barley, yeast)	Redistribution of water (effective decrease for gluten)	Formation of a weaker, less elastic protein network	Decreased elasticity, cohesion, and dough stability	*Welc-Stanowska et al., 2023*
Fruit/vegetable by-products (fiber-rich)	Moderate increase at low levels; decrease at high levels	Interaction with gluten proteins, limiting hydration	Good dough performance at moderate levels; impaired gluten network at higher doses	*Djeghim et al., 2021*
Technological	Decrease (salt	Salt strengthens the	May mask or amplify the	*Isaak et al., 2019*

Fruit powder / additive	Effect on water absorption	Effect on gluten hydration	Consequences for dough / bread quality	References
factors (salt, water level)	reduces water absorption)	gluten network but modifies perceived gluten strength	effects of fruit powder additions	
Spectroscopic studies on gluten hydration	Changes depending on water content	Hydration alters protein conformation	Direct impact on rheological behavior and bread volume	*Almutawah et al., 2007; Schopf and Scherf, 2021*

Table 1. Synthesis of literature findings on the effects of fruit powders and related factors on dough rheology. The table summarizes how different fruit-derived ingredients influence water absorption and gluten hydration, highlighting their technological consequences for dough handling, bread volume, and crumb quality.

Dough development time

The dough development time is defined as the interval required, during kneading, for the dough to reach the maximum consistency corresponding to the optimal development of gluten. It is one of the central parameters analyzed with the farinograph, usually reported together with stability and degree of softening *(Fig. 2)*. This parameter reflects the process of hydration and alignment of gluten proteins into a viscoelastic network capable of retaining fermentation gases *(Suprabha Raj et al., 2023)*, being recognized as a reliable indicator of flour performance *(*Oyeyinka *et al., 2023)*. From a mechanical perspective, dough development progresses through the increase in apparent viscosity under shear and extensio0n, until over-kneading leads to network degradation.

Development time thus marks the transition from the progressive accumulation of rheological properties to an apparent equilibrium state of a fully developed dough *(Zheng et al., 2000)*.

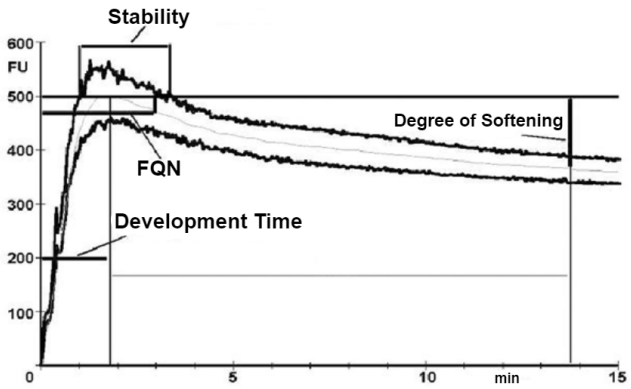

Fig. 2 - Schematic presentation of Farinograph parameters, Brabender Measurement
(Mekuria and Emire, 2015)

The presence of fibers and polyphenolic compounds retards the interactions between glutenins and gliadins, resulting in a less cohesive protein network. Consequently, the development time is often reduced as the level of functional additives increases, with the gluten network reaching maximum stability more quickly but with lower qualitative properties.

Recent studies on bread enriched with chokeberry powder and rosehip powder have reported significant decreases in development time, especially with additions above 8-10% *(Cacak-Pietrzak et al., 2023; Chochkov, 2023)*. Similar findings were reported by Murariu et al. (2025), who investigated the effect of integrating wheat flour with blueberry fruits on French-type bread.

The study showed that blueberry addition modified gluten development parameters and dough structure, reducing dough stability and mixing tolerance, while also influencing bread volume and texture. At moderate substitution levels, however, the breads were enriched with bioactive compounds, exhibited enhanced antioxidant activity, and achieved favorable sensory scores, demonstrating the potential of antioxidant-rich fruits to improve functional bakery products.

As shown in Figure 3, clear differences in appearance and structure were observed between control samples and those supplemented with 5% and 10% fruit powder, according to standardized technological protocols for French-type bread *(ISO 6820-1985; Foods, 2024)*.

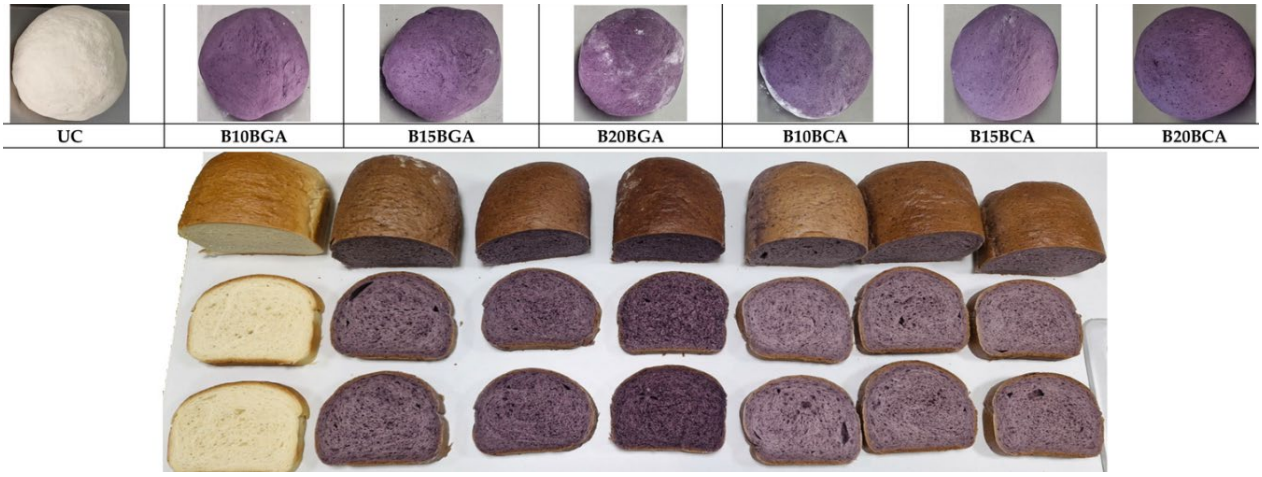

Fig. 3 - The aspect of the dough and developed bread samples obtained with different fruit powder additions (control, 5%, and 10%)
(Murariu et al., 2025)

When comparing instruments, the development time determined with the farinograph strongly correlates with Mixolab parameters, particularly with C1 development and protein weakening at C2. Thus, the profiles obtained for medium- and low-strength flours highlight clear differences in mixing kinetics and protein resistance under the combined action of kneading and controlled temperature *(Koksel et al., 2009) (Fig. 4)*.

Consistent correlations between development time, dough stability, and bread volume have been reported by *Singh et al. (2019)*, while previous studies *(Dabčević et al., 2009; Zhang and Shen, 2021)* confirmed the robustness of the parameter across various types of flours and blends.

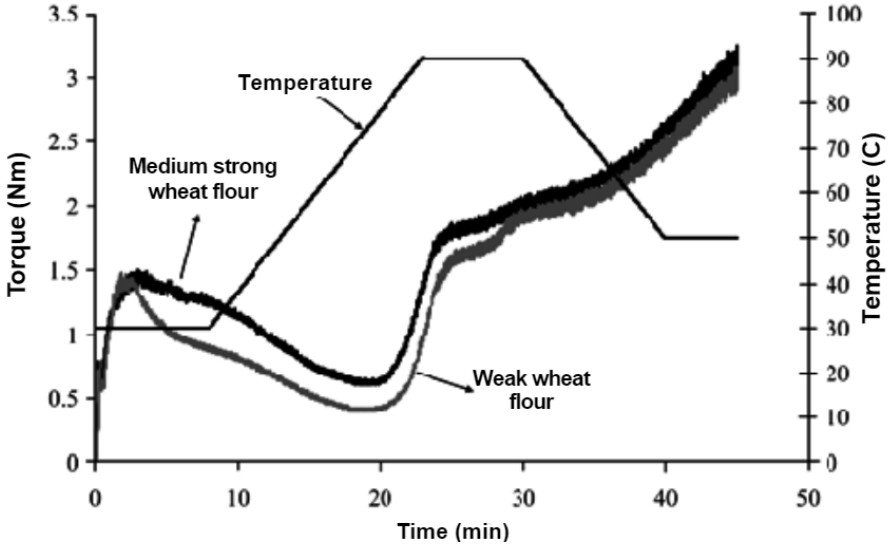

Fig. 4 - Representative Mixolab curves showing torque development for medium-strong and weak wheat flours under simultaneous mixing and controlled temperature conditions
(Koksel et al., 2009)

Agronomic factors such as heat and water stress during wheat grain filling also influence hydration kinetics and, implicitly, development time *(Lama et al., 2022)*. This sensitivity explains the widespread use of the parameter both in wheat breeding and in flour quality control and technological process adjustments (water level, kneading time, and energy).

In addition, numerous studies have highlighted the influence of composition on development time: fiber additions interfere with gluten network formation and significantly modify kneading kinetics *(Rosell et al., 2010)*, while changes in salt concentration have shown direct effects on gluten hydration and strength *(Kim et al., 2023)*. More recently, *Mahmoud et al. (2025)* showed that fiber-rich by-products, such as flour obtained from oat drink residue, significantly extend development time, with correlations confirmed through multivariate analyses.

Elasticity and extensibility

Dough elasticity and extensibility are strongly modulated by the interactions between dietary fibers and gluten proteins. In general, additions of aronia and rosehip powders increase resistance to extension and stability, but reduce extensibility, leading to stiffer doughs that are more difficult to process. This effect stems largely from polyphenol, protein interactions, which restrict the formation of flexible disulfide bonds. In contrast, softer-fleshed fruits such as raspberries and blackberries, though also polyphenol-rich, exert a less pronounced impact on extensibility due to their relatively lower insoluble fiber content *(Schefer et al., 2021)*.

Elasticity and extensibility together determine a dough's capacity to deform during processing while recovering sufficiently to maintain structural integrity, with direct consequences for sheetability, gas-cell stabilization, and final product quality. As highlighted by *Patel and Chakrabarti-Bell (2013)*, sheetability can be viewed as a practical expression of elasticity: excessive elastic recoil impedes smooth passage through rollers, whereas adequate extensibility permits thinning without rupture. Consequently, flour quality assessments often prioritize extensibility metrics over elasticity itself. Classic cereal chemistry studies have similarly shown that high resistance to extension coupled with insufficient extensibility penalizes loaf volume and processing performance *(Anderssen et al., 2004)*.

Formulation factors further modulate the elastic–viscous balance. *Catherine et al. (2012)* demonstrated that emulsifiers, hydrocolloids, and enzymes can be used to fine-tune extensibility, thereby improving both handling and volume outcomes. Chemometric analyses also support that the relative amounts and quality of gluten fractions, particularly the gliadin-to-glutenin ratio, are strong predictors of extensibility and resistance, linking molecular composition with macroscopic deformation behavior.

Empirical indices derived from instruments such as the alveograph reinforce these findings: the P/L ratio and deformation energy consistently correlate with breadmaking performance. When elasticity dominates at the expense of extensibility, doughs become harder to sheet and more prone to rupture. Conversely, balanced elasticity combined with sufficient extensibility yields smoother dough flow during processing and improved loaf quality *(Gómez et al., 2003)*.

In addition to these aspects, the incorporation of fruit and vegetable powders can significantly affect elasticity and extensibility. In the article Recent applications of powdered fruits and vegetables as novel ingredients in biscuits: a review, *Salehi (2020)* analyzed the use of dried fruit and vegetable powders such as mango, apple, carrot, pumpkin, guava, pomegranate, blueberry, or grape as innovative ingredients in biscuit production. The author showed that such additions can markedly improve the nutritional value of products through fiber, vitamins, minerals, and antioxidant compounds, while at the same time influencing rheological, physicochemical, and sensory properties.

The most notable changes occur in dough color, texture, and stability, effects primarily attributed to the fiber and polyphenol content of the powders. The conclusions emphasize that moderate incorporation of these ingredients can provide a balance between nutritional enrichment and the maintenance of acceptable sensory characteristics for consumers.

Gas retention and bread volume

Gas retention capacity represents one of the most critical determinants of bread quality, being directly associated with loaf volume, crumb porosity, and overall texture. This parameter reflects the ability of the gluten, starch viscoelastic matrix to capture and stabilize carbon dioxide generated during yeast fermentation and retained throughout proofing and baking *(Dobraszczyk and Morgenstern, 2003)*. A weakened network results in the collapse of gas bubbles, ultimately reducing bread volume.

Fruit powder incorporation into wheat-based formulations markedly influences this parameter. At high substitution levels (>5-10%), almost all fruit powders lead to reduced bread volume *(Bravo, 1999; Tong et al., 2010).* This decline arises primarily from the dilution of gluten proteins and the competition for water by insoluble dietary fibers, which hinder gluten hydration and continuity. As highlighted by *Vitrac et al., (2007)*, such fibers produce thinner gas-cell walls, thereby lowering the gas-holding capacity. Similar effects have been observed with berry pomace, where impaired fermentation and reduced loaf volume were reported unless the pomace was pre-hydrated to release water back into the system *(Reißner et al., 2020).*

Beyond the mechanical effects of gluten dilution and water competition, polyphenols and organic acids present in fruits interact with gluten proteins and starch granules, destabilizing the thin films surrounding CO_2 bubbles and weakening interfacial properties *(Lauková, 2016).* Non-starch polysaccharides, such as arabinoxylans, also interfere with gluten crosslinking, yielding fragile bubble walls *(Goesaert et al., 2005).* Likewise, β-glucans can increase dough viscosity but compromise bubble stabilization, leading to reduced volume *(Mastromatteo et al., 2011).*

Nevertheless, moderate additions (3-5%) of fruit powders can preserve loaf volume while enriching the product with bioactive compounds and dietary fibers *(Djeghim et al., 2021).* At these levels, sensory attributes such as color, aroma, and antioxidant capacity are enhanced without dramatic technological drawbacks. Examples include apple or berry pomace, which provide functional enrichment while maintaining acceptable structural quality.

Importantly, the adverse effects of fruit powders on gas retention can be mitigated through technological adjustments. Pre-hydration of pomace reduces direct competition for water, while the use of vital gluten, oxidizing agents (e.g., ascorbic acid, glucose oxidase), or polysaccharide-degrading enzymes (xylanases, cellulases) strengthens the gluten matrix and limits fiber, induced disruption. Process modifications, such as adjusting fermentation time, hydration levels, or mixing energy-can also help restore the rheological properties necessary for efficient gas entrapment *(Al-Marazeeq et al., 2024)*.

General viscoelastic properties

The incorporation of fruit powders consistently modifies the viscoelastic profile of wheat doughs, with a common observation being dough stiffening, reflected by increased values of the storage modulus (G′) and loss modulus (G″), which describe the elastic and viscous components of the system, respectively. A higher G′ indicates a more rigid, solid-like behavior, while an increase in G″ reflects stronger energy dissipation during deformation. These shifts are primarily attributed to dietary fibers and non-starch polysaccharides, which absorb water, compete with gluten proteins for hydration, and disrupt the continuity of the protein–starch network *(Meng et al., 2020; Reißner et al., 2020)*.

As a result, dough extensibility and elasticity are generally reduced, limiting the gluten network's capacity to expand and retain gas during fermentation. Studies on berry pomace and apple powders confirm that G′ and G″ values increase in small-amplitude oscillatory tests, indicating more rigid and less deformable doughs *(Lauková et al., 2016; Usman et al., 2020)*. Similar effects have been reported for arabinoxylan- and β-glucan-rich powders, where polysaccharide, protein interactions generate fragile, discontinuous networks with diminished viscoelastic recovery *(Liburdi et al., 2023; Welc-Stanowska et al., 2023)*.

At the macroscopic scale, these rheological changes translate into smaller bread volumes, denser crumb structures, and altered texture. Nevertheless, moderate additions can improve technological and nutritional attributes such as water retention, fiber enrichment, and antioxidant capacity without severely impairing dough functionality *(Zhang et al., 2023; Djeghim et al., 2021)*.

From a technological standpoint, bakers often need to compensate for the stiffening effect by adjusting hydration levels, adding functional improvers such as xylanases, cellulases, proteases, or vital gluten, or by optimizing fermentation time, mixing energy, and formulation blends. Thus, fruit powders act as a double-edged ingredient: while enriching breads with fibers, polyphenols, and bioactive compounds, they simultaneously shift dough rheology toward a stiffer, more solid-like state.

Monitoring viscoelastic parameters such as G′, G″, and tan δ (G″/G′) provides valuable insight into the balance between elasticity and viscosity, supporting formulation strategies that reconcile nutritional enhancement with desirable technological and sensory qualities *(Dobraszczyk* and *Morgenstern, 2003; Goesaert et al., 2005; Mastromatteo et al., 2011; Zykwinska et al., 2005)*.

These rheological modifications are closely related to the nutritional and technological impacts described in recent research on fruit and vegetable powders. *Salehi (2019)* reviewed the incorporation of mango, apple, carrot, pumpkin, guava, pomegranate, blueberry, and grape powders in biscuits, highlighting their ability to enrich products with fibers, vitamins, minerals, and antioxidants, while simultaneously modifying dough stability, texture, and color due to the presence of fibers and polyphenols. Similarly, *Zahid et al. (2022)* demonstrated that mango peel powder (MPP) and banana peel powder (BPP) significantly increased total phenolic content and probiotic viability in fortified yogurts but altered sensory parameters such as color, decreasing lightness (L*) from 88.42 in control samples to 59.07 with BPP.

The study of *Moraes Crizel et al., (2016)* further supports the technological relevance of fruit byproduct powders, reporting that olive powder exhibited the highest fiber content (≈53.68%), papaya powder had favorable water-holding capacity (≈8.93 g/g) and solubility (≈59.91%), while blueberry powder contained exceptionally high anthocyanin levels (≈2063.4 mg/100 g). These findings underline both the functional potential and the strong influence of bioactive compounds and fibers on dough viscoelasticity. *Ramírez-Pulido et al., (2021)* emphasized the use of fruit processing residues (peels, seeds, pulp) converted into powders rich in dietary fibers, polyphenols, and carotenoids, noting their capacity to improve antioxidant activity but also to alter sensory and functional attributes such as texture, color, and water retention capacity.

More recent contributions reaffirm these trends. *Kurćubić et al. (2025)* highlighted that fruit and vegetable powders act as functional food supplements, improving antioxidant content and nutritional value, but affecting sensory acceptance depending on concentration and formulation. *Jiang (2013)* also observed that fruit and vegetable powders can extend shelf life and retain nutritional quality, aroma, and color, but processing and storage conditions are critical for maintaining bioactive integrity.

Together, these findings corroborate that the viscoelastic modifications observed at the rheological level, dough stiffening, increased G′ and G″, reduced extensibility, are manifestations of the high dietary fiber and polyphenol contents in fruit powders. They act both as enhancers of nutritional and antioxidant properties and as disruptors of gluten hydration and network formation, confirming their role as multifunctional yet technologically challenging ingredients.

Nutritional and functional benefits of fruit powders

Fruit powders are increasingly recognized as multifunctional ingredients that combine nutritional enrichment with technological functionality in food systems. As highlighted by *Kaur and Kapoor (2001)*, fruits are valuable sources of bioactive compounds, particularly phenolics, vitamins, and minerals, that underpin their antioxidant capacity and health-promoting effects.

Converting fruits into powders preserves these compounds while extending shelf life, improving handling, and facilitating incorporation into cereal-based products. In addition, fruit and vegetable powders valorize by-products, reduce food waste, and supply fibers, phytochemicals, and natural pigments, thereby contributing to sustainable food chains *(Galanakis et al., 2020)*.

A major nutritional advantage of fruit powders lies in their high content of polyphenols and flavonoids, compounds widely documented for their antioxidant, anti-inflammatory, and antidiabetic activities. For instance, *Kunyanga et al. (2012)* reported that indigenous fruit powders markedly increase radical-scavenging activity, while *Zhangping Liao et al., (2017)* emphasized their role in glycemic regulation and oxidative stress reduction. Powders derived from tropical fruits such as durian also provide bioactive compounds associated with immune support, cardiovascular health, and improved digestion *(ChenLang Bio, 2023)*.

Beyond their nutritional profile, fruit powders deliver functional attributes relevant to food formulation. Drying methods, including spray-drying and freeze-drying, influence the retention of antioxidants and fibers, as well as solubility and powder stability *(Carrasco-Castilla et al., 2012)*. According to *Sagar and Kumar (2010)*, fruit powders act as natural stabilizers, color enhancers, and flavoring agents, thereby improving both technological and sensory performance. Their prebiotic potential has also been highlighted, with studies showing that fermentable fibers and oligosaccharides present in fruit powders stimulate beneficial gut microbiota *(Fan and Roos, 2019)*.

From a functional food perspective, incorporating fruit powders into breads, snacks, and beverages enhances nutritional density by increasing levels of dietary fiber, vitamins C and E, carotenoids, and phenolic acids. At the same time, they raise consumer appeal through attractive color, flavor, and aroma *(Giri and Mangaraj, 2012; Rivero-Pino et al., 2023)*. Furthermore, *Savaş and Demir, (2025)* demonstrated that fruit powders can act as natural alternatives to synthetic additives by contributing to oxidative stability, microbial safety, and textural improvements.

Overall, the scientific literature consistently demonstrates that fruit powders represent an efficient tool for the development of functional products. They meet consumer demand for healthy, sustainable, and sensorially attractive foods. Successful application, however, depends on the careful choice of fruit source, processing technology, and incorporation level, in order to preserve bioactive compounds while maintaining desirable rheological and technological properties.

Beyond nutritional enrichment, fruit powders may also play a compensatory role in dough systems affected by environmental stressors. Studies have shown that heavy metal contamination and environmental pollutants can impair protein functionality and gluten quality, reducing dough stability. The addition of fruit powders, through their antioxidants and fibers, may help counteract these negative effects, supporting gluten hydration, improving rheological behavior, and maintaining product safety.

Table 2 provides a comparative summary of the main studies on fruit powder supplementation in breadmaking, highlighting the typical levels of addition, their impact on bread volume, and the main rheological effects observed. This synthesis complements the narrative review by allowing a quick comparison across fruit types.

Table 2

Comparative effects of fruit powders on bread dough and bread quality

Fruit / By-product	Percentage used (%)	Effect on bread volume	Main rheological effects
Apple (powder / pomace)	5-15	Moderate decrease (>10%) at higher levels	Increases water absorption, decreases gluten elasticity
Sea buckthorn	2-10	Slight decrease, but improves nutritional value	Reduces dough development time, increases dough firmness
Aronia (black chokeberry)	2-8	Significant decrease (>15%)	Decreases extensibility, increases dough tenacity
Rosehip	3-10	Moderate decrease, but acceptable sensorially	Reduces dough stability, increases viscosity
Blackcurrant	2-6	Small decrease, tolerable	Improves gas retention, slightly decreases elasticity
Mixed berry fruits (lyophilized)	2-5	Slight decrease, compensated by enzyme addition	Reduces farinograph stability, increases dough hydration
Prune powder	5-10	Moderate decrease, still accepted by consumers	Reduces dough elasticity, increases viscosity

The role of environmental factors and contaminants on the quality of flour and dough

Flour and dough quality are shaped not only by intrinsic compositional and genetic factors, but also by environmental influences and potential contaminants encountered during cultivation, processing, and storage.

From an environmental perspective, the study by *Mikhaylenko et al. (2000)* demonstrated that wheat growing conditions have a decisive effect on flour composition, dough rheology, and baking quality. In Washington State, wheat cultivated in Lind (semi-arid) exhibited higher protein content, superior micro-SDS sedimentation values, and higher water absorption compared with Fairfield (high-rainfall). These differences translated into greater bread volumes for hard wheat grown in Lind, but larger biscuit diameters for soft wheat from Fairfield. Similarly, *Peña (2002)* highlighted the interaction between genetic background and environment, showing that breeding programs may enhance gluten quality and protein composition, but climatic and soil factors can significantly offset or modify these gains, underscoring the need for testing under diverse conditions.

Expanding this view, *Filip et al. (2023)* provided a comprehensive overview of the factors that determine the functional quality of common wheat (*Triticum aestivum L.*). Their review emphasizes that the interplay between genetic factors (protein fractions, gluten composition, enzymatic activity), environmental stresses (temperature, water availability, soil quality), and processing conditions collectively shape dough rheology and baking performance. The authors underline that even small variations in asparagine content, starch properties, or gluten protein distribution can significantly influence technological outcomes such as loaf volume, dough stability, and extensibility, reinforcing the importance of integrated genetic–environmental assessments.

Beyond agronomic conditions, environmental and technological factors can also introduce contaminants. *Maher et al. (2022)* investigated chemical contaminants in bread, identifying acrylamide, furans, polycyclic aromatic amines, 3-monochloropropanediol esters (3-MCPDE), glycidyl esters, as well as natural contaminants such as mycotoxins, heavy metals, and pesticide residues. Acrylamide levels were reported to range from tens to hundreds of µg/kg, with crust containing up to ~80 µg/kg when baked at 270 °C for 15 minutes. Similarly, 3-MCPDE concentrations of ~120 µg/kg and mycotoxin levels exceeding permissible limits were observed, stressing the importance of rigorous monitoring of raw materials and processing conditions.

Complementing this, *Varzakas (2016)* emphasized that acrylamide formation, mycotoxin contamination, and other safety risks in wheat products require the integration of advanced analytical methods (e.g., near-infrared spectroscopy) alongside strict quality controls across the processing chain. In line with this, the study *"The role of flours and leavening systems on the formation of acrylamide in the technological process of baked products: Case studies of bread and biscuits"* by *Marianelli et al. (2025)* investigated how flour type and leavening systems influence acrylamide formation in bread and biscuits. Their aim was to identify natural mitigation strategies without compromising product quality.

They examined different wheat flours and leavening systems (e.g., yeast vs. alternative agents) in combination with technological parameters such as baking temperature and time, as well as the levels of

reducing sugars and asparagine, the main Maillard reaction precursors leading to acrylamide. The study showed that flour selection, combined with leavening system choice and adjustments in baking conditions, can significantly reduce acrylamide formation in bakery products. Their findings suggest that low-asparagine flours and leavening systems that limit the accumulation of reducing sugars before baking are promising strategies for controlling acrylamide levels.

Microbiological and fungal contamination further complicates flour and dough safety. *Sami et al. (2020)* reported microbial loads from 240 samples (flour, dough, bread) collected in Isfahan, Iran. Total bacterial counts ranged from 2.83 ± 0.99 to 6.43 ± 1.12 log cfu/g, while molds varied between 0.00 ± 0.00 and 1.63 ± 0.63 log cfu/g. Bulk breads exhibited higher bacterial counts, whereas flat breads were more susceptible to molds, with species including *Penicillium* (24.4%), *Cladosporium* (20.1%), *Mucor* (20.1%), *Aspergillus* (19.0%), and *Alternaria* (3.8%).

Although levels remained below Iranian legal limits, the high consumption of bread highlights the need for continuous microbial surveillance.

In addition to chemical and microbial hazards, bakery products are vulnerable to physical contaminants. *Mutlu (2025)* reviewed the occurrence of foreign objects such as glass, metal, and plastic fragments, as well as insect and pest residues, arising during packaging, storage, and handling. The study underlined the necessity of preventive measures including visual inspections, storage monitoring, supply chain verification, and good manufacturing practices to safeguard consumer health.

Altogether, these studies converge on the notion that wheat flour and dough quality cannot be evaluated solely through compositional and rheological parameters. Environmental factors shape protein content, gluten functionality, and end-product performance *(Mikhaylenko et al., 2000; Peña, 2002; Filip et al., 2023)*, while chemical, microbial, and physical contaminants *(Maher et al., 2022; Sami et al., 2020; Mutlu, 2025; Varzakas, 2016; Marianelli et al., 2025)* pose safety and technological challenges.

Effective management therefore requires an integrated approach, breeding for resilience, cultivating under optimal agro-ecological conditions, applying strict processing controls, and implementing advanced monitoring technologies. Such strategies enable the simultaneous pursuit of high-quality and safe wheat-based products.

CONCLUSIONS

The integration of fruit powders into wheat flour dough represents a promising strategy for the development of functional bakery products with enhanced nutritional and technological properties. Scientific evidence shows that moderate additions (3-8%) of fruit powders improve fiber, antioxidant, and bioactive content, while maintaining acceptable dough rheology and bread quality. However, higher levels (>10%) often compromise gluten hydration, extensibility, and gas retention, leading to reduced loaf volume and altered texture.

The variability of effects depends strongly on fruit type, composition, and processing conditions, which highlights the need for optimized formulations and the use of technological improvers (enzymes, vital gluten, pre-hydration techniques). From a sustainability perspective, fruit powders valorise processing by-products, reduce waste, and provide natural alternatives to synthetic additives, while also contributing to food security in the context of environmental stressors and soil contamination.

Future research should focus on refining processing strategies, identifying optimal incorporation levels, and exploring consumer acceptance, to fully exploit the potential of fruit powders in next-generation bakery products.

ACKNOWLEDGEMENT

This research was supported by project Establishment and operationalization of a Competence Center for Soil Health and Food Safety – CeSoH, Contract no.: 760005/2022, specific project no.1, with the title: Soil health and food safety by introducing a soil remediation protocol and developing a mobile remediation equipment to reduce the concentration of organic/inorganic pollutants, Code 2, financed through PNRR-III-C9-2022 – I5 (PNRR-National Recovery and Resilience Plan, C9 Support for the private sector, research, development and innovation, I5 Establishment and operationalization of Competence Centers), and by the project CNFIS-FDI-2025-F-0108 “Ensuring the sustainability of an application base for biotechnical systems in orchards, vineyards, gardens and solariums (SISBIOSUS)”, from the Ministry of Education and Research through the Executive Agency for Financing Higher Education, Research, Development and Innovation.

REFERENCES

[1] AbuDujayn, A. A., Mohamed, A. A., Alamri, M. S., Hussain, S., Ibraheem, M. A., Qasem, A. A. A., Shamlan, G., and Alqahtani, N. K. (2022). Relationship between Dough Properties and Baking Performance of Panned Bread: The Function of Maltodextrins and Natural Gums. Molecules, 28(1), 1. https://doi.org/10.3390/molecules28010001.

[2] Alba, K., Rizou, T., Paraskevopoulou, A., et al. (2020). Effects of Blackcurrant Fibre on Dough Physical Properties and Bread Quality Characteristics. Food Biophysics, 15, 313-322. https://doi.org/10.1007/s11483-020-09627-x.

[3] Al-Marazeeq, K., Saleh, M., Angor, M., and Lee, Y. (2024). Cookie dough functional properties of partially replaced all-purpose wheat flour with powdered fruit skins and the hedonic perception of the resulting cookies. Frontiers in Sustainable Food Systems, 8, Article 1445206. https://doi.org/10.3389/fsufs.2024.1445206.

[4] Almutawah, A., Barker, S. A., and Belton, P. S. (2007). Hydration of gluten: A dielectric, calorimetric, and Fourier transform infrared study. Biomacromolecules, 8(5), 1601-1606. https://doi.org/10.1021/bm061206g.

[5] Anderssen, R., Bekes, F., Gras, P. W., Nikolov, A., and Wood, J. (2004). Wheat-flour dough extensibility as a discriminator for wheat varieties. Journal of Cereal Science, 39, 195-203. https://doi.org/10.1016/j.jcs.2003.10.002.

[6] Annor, G. A., Marcone, M., Corredig, M., Bertoft, E., and Seetharaman, K. (2015). Effects of the amount and type of fatty acids present in millets on their in vitro starch digestibility and expected glycemic index (eGI). Journal of Cereal Science, 64, 76-81. https://doi.org/10.1016/j.jcs.2015.05.004.

[7] Bal, L. M., Meda, V., Naik, S. N., and Satya, S. (2011). Sea buckthorn berries: A potential source of valuable nutrients for nutraceuticals and cosmoceuticals. Food Research International, 44(7), 1718-1727. https://doi.org/10.1016/j.foodres.2011.03.002.

[8] Bravo, L. (1999). Effect of processing on the non-starch polysaccharides and in vitro starch digestibility of legumes / Efecto del procesado en el contenido de polisacáridos no amiláceos y la digestibilidad in vitro del almidón de legumbres. Food Science and Technology International, 5(5), 415-423. https://doi.org/10.1177/108201329900500507.

[9] Cacak-Pietrzak, G., Dziki, D., Gawlik-Dziki, U., Parol-Nadłonek, N., Kalisz, S., Krajewska, A., and Stępniewska, S. (2023). Wheat Bread Enriched with Black Chokeberry (Aronia melanocarpa L.) Pomace: Physicochemical Properties and Sensory Evaluation. Applied Sciences, 13(12), 6936. https://doi.org/10.3390/app13126936.

[10] Carrasco-Castilla, J., Hernández-Álvarez, A. J., Jiménez-Martínez, C., et al. (2012). Use of Proteomics and Peptidomics Methods in Food Bioactive Peptide Science and Engineering. Food Engineering Reviews, 4, 224-243. https://doi.org/10.1007/s12393-012-9058-8.

[11] ChenLang Bio. (n.d.). Health benefits of durian fruit powder. ChenLang Bio Knowledge Center. Retrieved September 30, 2025, from https://www.chenlangbio.com/knowledge/health-benefits-of-durian-fruit-powder.

[12] Chochkov, R., Zlateva, D., Ivanova, P., and Stefanova, D. (2023). Effect of rosehip flour on the properties of wheat dough and bread. Ukrainian Food Journal, 11, Article 6. https://doi.org/10.24263/2304-974X-2022-11-4-6.

[13] Cingöz, A., and Şahin, N. (2023). Determination of Rheological and Chemical Properties of Hemp, Rosehip Seed and Safflower Flours. Journal of Agricultural Sciences, 29(4), 914-923. https://doi.org/10.15832/ankutbd.1178258.

[14] Dabčević, T., Hadnađev, M., and Pojić, M. (2009). Evaluation of the Possibility to Replace Conventional Rheological Wheat Flour Quality Control Instruments with the New Measurement Tool - Mixolab. Agriculturae Conspectus Scientificus (ACS), 74, 133-138.

[15] de Moraes Crizel, T., Hermes, V. S., de Oliveira Rios, A., et al. (2016). Evaluation of bioactive compounds, chemical and technological properties of fruits byproducts powder. Journal of Food Science and Technology, 53, 4067-4075. https://doi.org/10.1007/s13197-016-2413-7.

[16] Della Valle, G., Dufour, M., Hugon, F., Chiron, H., Saulnier, L., and Kansou, K. (2022). Rheology of wheat flour dough at mixing. Current Opinion in Food Science, 47, 100873. https://doi.org/10.1016/j.cofs.2022.100873.

[17] Djeghim, F., Bourekoua, H., Różyło, R., Bieńczak, A., Tanaś, W., and Zidoune, M. N. (2021). Effect of By-Products from Selected Fruits and Vegetables on Gluten-Free Dough Rheology and Bread Properties. Applied Sciences, 11(10), 4605. https://doi.org/10.3390/app11104605.

[18] Dobraszczyk, B. J., and Morgenstern, M. P. (2003). Rheology and the breadmaking process. Journal of Cereal Science, 38(3), 229-245. https://doi.org/10.1016/S0733-5210(03)00090-0.

[19] Fadiji, T., and Pathare, P. B. (2023). Technological Advancements in Food Processing and Packaging. Processes, 11(9), 2571. https://doi.org/10.3390/pr11092571.

[20] Fan, F., and Roos, Y. H. (2019). Physicochemical properties, structural transformation, and relaxation time in strength analysis for honey powder models. Food Research International, 122, 137–148. https://doi.org/10.1016/j.foodres.2019.04.003.

[21] Filip, E., Woronko, K., Stępień, E., and Czarniecka, N. (2023). An Overview of Factors Affecting the Functional Quality of Common Wheat (Triticum aestivum L.). International Journal of Molecular Sciences, 24(8), 7524. https://doi.org/10.3390/ijms24087524.

[22] Galanakis, C. M. (2021). Functionality of Food Components and Emerging Technologies. Foods, 10(1), 128. https://doi.org/10.3390/foods10010128.

[23] Giri, S. K., and Mangaraj, S. (2012). Processing Influences on Composition and Quality Attributes of Soymilk and its Powder. Food Engineering Reviews, 4, 149–164. https://doi.org/10.1007/s12393-012-9053-0.

[24] Gkekas, I., Gioran, A., Boziki, M. K., Grigoriadis, N., Chondrogianni, N., and Petrakis, S. (2021). Oxidative Stress and Neurodegeneration: Interconnected Processes in PolyQ Diseases. Antioxidants, 10(9), 1450. https://doi.org/10.3390/antiox10091450.

[25] Goesaert, H., Brijs, K., Veraverbeke, W. S., Courtin, C. M., Gebruers, K., and Delcour, J. A. (2005). Wheat flour constituents: how they impact bread quality, and how to impact their functionality. Trends in Food Science and Technology, 16(1-3), 12-30. https://doi.org/10.1016/j.tifs.2004.02.002.

[26] Gómez, M., Ronda, F., Blanco, C. A., et al. (2003). Effect of dietary fibre on dough rheology and bread quality. European Food Research and Technology, 216, 51-56. https://doi.org/10.1007/s00217-002-0632-9.

[27] Gül, H., and Şen, H. (2017). Effects of rosehip seed flour on the rheological properties of bread dough. Scientific Bulletin. Series F. Biotechnologies, XXI, 330-335. ISSN 2285-1364.

[28] Han, P., Wang, Y., and Sun, H. (2025). Impact of Temperature Stresses on Wheat Quality: A Focus on Starch and Protein Composition. Foods, 14(13), 2178. https://doi.org/10.3390/foods14132178.

[29] Isaak, C., Sapirstein, H., Wu, Y., and Graf, R. (2019). Effects of water absorption and salt on discrimination of wheat gluten strength assessed by dough mixing and protein composition. Journal of Cereal Science, 89, 102794. https://doi.org/10.1016/j.jcs.2019.04.007.

[30] Jannati, N., Hojjatoleslamy, M., Hosseini, E., Mozafari, H., and Siavoshi, M. (2018). Effect of apple pomace powder on rheological properties of dough and Sangak bread texture. Carpathian Journal of Food Science and Technology, 10, 77-84.

[31] Kaur, C., and Kapoor, H. C. (2001). Antioxidants in fruits and vegetables – the millennium's health. International Journal of Food Science and Technology, 36(7), 703-725. *https://doi.org/10.1111/j.1365-2621.2001.00513.x*.

[32] Kierońska, E., Skoczylas, J., Dziadek, K., Pomietło, U., Piątkowska, E., and Kopeć, A. (2024). Basic Chemical Composition, Selected Polyphenolic Profile and Antioxidant Activity in Various Types of Currant (Ribes spp.) Fruits. Applied Sciences, 14(19), 8882. https://doi.org/10.3390/app14198882.

[33] Kim, H. R., Kim, M. R., Ryu, A. R., et al. (2023). Comparison of rheological properties between Mixolab-driven dough and bread-making dough under various salt levels. Food Science and Biotechnology, 32, 193-202. https://doi.org/10.1007/s10068-022-01186-w.

[34] Koksel, H., Kahraman, K., Şanal, T., Ozay, D., and Dubat, A. (2009). Potential Utilization of Mixolab for Quality Evaluation of Bread Wheat Genotypes. Cereal Chemistry, 86, 522-526. https://doi.org/10.1094/CCHEM-86-5-0522.

[35] Kolesárová, A., Bojnanska, T., Solgajová, M., Mendelová, A., Kopcekova, J., and Kolesarova, A. (2024). The effects of the addition of lyophilized berry fruits on the leavening properties of dough and volume properties of bread. Food and Feed Research, 52, 45. https://doi.org/10.5937/ffr0-52510.

[36] Krakowska-Sieprawska, A., Walczak-Skierska, J., Pomastowski, P., Sobolewska, R., Głogowski, J., Bernat, C., and Rafińska, K. (2024). Advanced Extraction Techniques for Bioactive Compounds from

Berry Fruits: Enhancing Functional Food Applications. Foods, 13(24), 4115. https://doi.org/10.3390/foods13244115.

[37] Kurćubić, V., Miletić, N., Petkovic, M., and Stajić, S. (2025). Fruit and Vegetable Powder as a Functional Food Supplement. https://doi.org/10.1007/978-3-031-96610-1_7.

[38] Kunyanga, C. N., Imungi, J. K., Okoth, M. W., Biesalski, H. K., and Vadivel, V. (2012). Total phenolic content, antioxidant and antidiabetic properties of methanolic extract of raw and traditionally processed Kenyan indigenous food ingredients. LWT - Food Science and Technology, 45(2), 269-276. https://doi.org/10.1016/j.lwt.2011.08.006.

[39] Lama, S., Kuzmenkova, M., Vallenback, P., and Kuktaite, R. (2022). Striving for Stability in the Dough Mixing Quality of Spring Wheat under the Influence of Prolonged Heat and Drought. Plants, 11(19), 2662. https://doi.org/10.3390/plants11192662.

[40] Lauková, M., Kohajdová, Z., and Karovičová, J. (2016). Effect of hydrated apple powder on dough rheology and cookies quality. Potravinarstvo, 10. https://doi.org/10.5219/597.

[41] Liburdi, K., Fabrizi, C., and Esti, M. (2023). Catalytic properties of lipoxygenase extracted from nine different Italian olive varieties (Olea europaea L.). International Journal of Food Science and Technology, 58(8), 4464-4472. https://doi.org/10.1111/ijfs.16563.

[42] Liao, Z., He, H., Zeng, G., Liu, D., Tang, L., Yin, D., Chen, D., and He, M. (2017). Delayed protection of Ferulic acid in isolated hearts and cardiomyocytes: Upregulation of heat-shock protein 70 via NO-ERK1/2 pathway. Journal of Functional Foods, 34, 18-27. https://doi.org/10.1016/j.jff.2017.04.012.

[43] Marianelli, A., Pieracci, Y., Scappaticci, G., Macaluso, M., Guazzotti, M., Gualco, S., and Zinnai, A. (2025). The role of flours and leavening systems on the formation of acrylamide in the technological process of baked products: Case studies of bread and biscuits. LWT, 217, 117387. https://doi.org/10.1016/j.lwt.2025.117387.

[44] Mastromatteo, M., Chillo, S., Civica, V., and Del Nobile, M. A. (2011). Formulation optimisation of gluten-free functional spaghetti based on maize flour and oat bran enriched in β-glucans. Food and Bioprocess Technology, 4, 1147-1156. https://doi.org/10.1007/s11947-011-0519-5.

[45] Matas, A., Igual, M., García-Segovia, P., and Martínez-Monzó, J. (2022). Application of 3D Printing in the Design of Functional Gluten-Free Dough. Foods, 11(11), 1555. https://doi.org/10.3390/foods11111555.

[46] Mekuria, B., and Emire, S. (2015). Effects of Vital Gluten Enrichment on Qualities of Value Added Products. Journal of Food Science and Technology, 6, 1-10. https://doi.org/10.4172/2157-7110.1000508.

[47] Meng, L., Zhu, J., Ma, Y., Sun, X., Li, D., Li, L., Bai, H., Xin, G., and Meng, X. (2019). Composition and antioxidant activity of anthocyanins from Aronia melanocarpa cultivated in Haicheng, Liaoning, China. Food Bioscience, 30, 100413. https://doi.org/10.1016/j.fbio.2019.100413.

[48] Mikhaylenko, G., Czuchajowska, Z., Baik, B.-K., and Kidwell, K. (2000). Environmental Influences on Flour Composition, Dough Rheology, and Baking Quality of Spring Wheat. Cereal Chemistry, 77, 507-511. https://doi.org/10.1094/CCHEM.2000.77.4.507.

[49] Mudgil, D. (2017). The Interaction Between Insoluble and Soluble Fiber. In Dietary Fiber: Properties, Recovery, and Applications (pp. 23-38). https://doi.org/10.1016/B978-0-12-805130-6.00003-3.

[50] Murariu, O. C., Caruso, G., Frunză, G., Lipșa, F. D., Ulea, E., Tallarita, A. V., Calistru, A., and Jităreanu, G. (2025). Effect of Wheat Flour Integration with Blueberry Fruits on Rheological, Quality, Antioxidant, and Sensory Attributes of 'French' Bread. Foods, 14(7), 1189. https://doi.org/10.3390/foods14071189.

[51] Mutlu, C., Candal-Uslu, C., Arslan-Tontul, S., and Erbas, M. (2025). Chemical and physical food safety contaminants and preventive control on sourdough and bakery products. In F. Ozogul, J. M. Rocha, and E. Bartkiene (Eds.), Handbook of Sourdough Microbiota and Fermentation (pp. 3-18). Academic Press. https://doi.org/10.1016/B978-0-443-18622-6.00001-3.

[52] Mandache, M. B., Vijan, L. E., and Cosmulescu, S. (2025). Insight into Bioactive Compounds and Antioxidant Activity of Bakery Products Fortified with Fruit Pomace. Foods, 14(5), 806. https://doi.org/10.3390/foods14050806.

[53] Maher, A., and Nowak, A. (2022). Chemical Contamination in Bread from Food Processing and Its Environmental Origin. Molecules, 27(17), 5406. https://doi.org/10.3390/molecules27175406.

[54] Oyeyinka, S. A., and Bassey, I. A. V. (2023). Composition, Functionality, and Baking Quality of Flour from Four Brands of Wheat Flour. Journal of Culinary Science and Technology, 23(1), 87-107. https://doi.org/10.1080/15428052.2023.2191874.

[55] Patel, M., and Chakrabati-Bell, S. (2013). Flour quality and dough elasticity: Dough sheetability. Journal of Food Engineering, 115, 371-383. https://doi.org/10.1016/j.jfoodeng.2012.10.038.

[56] Peña, R. J., Trethowan, R., Pfeiffer, W. H., and van Ginkel, M. (2002). Quality (End-Use) Improvement in Wheat: Compositional, Genetic, and Environmental Factors. Journal of Crop Production, 5(1-2), 1-37. https://doi.org/10.1300/J144v05n01_02.

[57] Rashed, M. S., Gallagher, E., Frias, J. M., Pojić, M., and Pathania, S. (2025). Dough rheology properties as affected by the inclusion of oat drink residue flour: a multivariate analysis approach. International Journal of Food Science and Technology, 60(1), vvae101. https://doi.org/10.1093/ijfood/vvae101.

[58] Reißner, A. M., Beer, A., Struck, S., and Rohm, H. (2020). Pre-Hydrated Berry Pomace in Wheat Bread: An Approach Considering Requisite Water in Fiber Enrichment. Foods, 9(11), 1600. https://doi.org/10.3390/foods9111600.

[59] Rivero-Pino, F., Leon, M. J., Millan-Linares, M. C., and Montserrat-de la Paz, S. (2023). Antimicrobial plant-derived peptides obtained by enzymatic hydrolysis and fermentation as components to improve current food systems. Trends in Food Science and Technology, 135, 32-42. https://doi.org/10.1016/j.tifs.2023.03.005.

[60] Rosell, C. M., Santos, E., and Collar, C. (2010). Physical characterization of fiber-enriched bread doughs by dual mixing and temperature constraint using the Mixolab®. European Food Research and Technology, 231, 535-544. https://doi.org/10.1007/s00217-010-1310-y.

[61] Sharoba, A., Farrag, M., and El-Salam, A. (2013). Utilization of some fruits and vegetables waste as a source of dietary fiber and its effect on the cake making and its quality attributes. Journal of Agroalimentary Processes and Technologies, 19, 429-444.

[62] Schefer, S., Oest, M., and Rohn, S. (2021). Interactions between Phenolic Acids, Proteins, and Carbohydrates-Influence on Dough and Bread Properties. Foods, 10, 2798. https://doi.org/10.3390/foods10112798.

[63] Schopf, M., and Scherf, K. A. (2021). Water Absorption Capacity Determines the Functionality of Vital Gluten Related to Specific Bread Volume. Foods, 10(2), 228. https://doi.org/10.3390/foods10020228.

[64] Sanfilippo, R., Canale, M., Fascella, G., et al. (2025). Nutritional and technological characterization of rosehip seed flours as a functional ingredient in common wheat bread. European Food Research and Technology, 251, 1033–1045. https://doi.org/10.1007/s00217-025-04686-1.

[65] Savaş, E., and Demir, V. (2025). Glutathione-enriched fruit based candies: ingredient optimization impact on storage stability and product quality. Journal of Food Science and Technology. https://doi.org/10.1007/s13197-025-06444-3.

[66] Singh, N., Gujral, H. S., Katyal, M., and Sharma, B. (2019). Relationship of Mixolab characteristics with protein, pasting, dynamic and empirical rheological characteristics of flours from Indian wheat varieties with diverse grain hardness. Journal of Food Science and Technology, 56(5), 2679-2686. https://doi.org/10.1007/s13197-019-03756-z.

[67] Stanciu, I., Ungureanu, E. L., Popa, E. E., Geicu-Cristea, M., Draghici, M., Mitelut, A. C., Mustatea, G., and Popa, M. E. (2023). The Experimental Development of Bread with Enriched Nutritional Properties Using Organic Sea Buckthorn Pomace. Applied Sciences, 13(11), 6513. https://doi.org/10.3390/app13116513.

[68] Suprabha Raj, A., Boyacioglu, M. H., Dogan, H., and Siliveru, K. (2023). Investigating the Contribution of Blending on the Dough Rheology of Roller-Milled Hard Red Wheat. Foods, 12(10), 2078. https://doi.org/10.3390/foods12102078.

[69] Salehi, F. (2020). Recent applications of powdered fruits and vegetables as novel ingredients in biscuits: a review. Nutrire, 45, 1. https://doi.org/10.1186/s41110-019-0103-8.

[70] Sami, M., Abedi, R., Mohammadi, R., and Mirlohi, M. (2020). Microbial and Fungal Contamination of Wheat Flour, Dough, and Bread Samples Collected from Isfahan, Iran. Egyptian Journal of Veterinary Sciences, 51(2), 163-170. https://doi.org/10.21608/ejvs.2020.19056.1118.

[71] Sagar, V. R., and Suresh Kumar, P. (2010). Recent advances in drying and dehydration of fruits and vegetables: a review. Journal of Food Science and Technology, 47, 15-26. https://doi.org/10.1007/s13197-010-0010-8.

[72] Tong, Q., Zhang, X., Wu, F., Tong, J., Zhang, P., and Zhang, J. (2010). Effect of honey powder on dough rheology and bread quality. Food Research International, 43, 2284–2288. https://doi.org/10.1016/j.foodres.2010.08.002.

[73] Usman, M., Ahmed, S., Mehmood, A., Bilal, M., Patil, P. J., Akram, K., and Farooq, U. (2020). Effect of apple pomace on nutrition, rheology of dough and cookies quality. Journal of Food Science and Technology, 57(9), 3244-3251. https://doi.org/10.1007/s13197-020-04355-z.

[74] Varzakas, T. (2016). Quality and Safety Aspects of Cereals (Wheat) and Their Products. Critical Reviews in Food Science and Nutrition, 56(15), 2495–2510. https://doi.org/10.1080/10408398.2013.866070.

[75] Vitrac, O., Mougharbel, A., and Feigenbaum, A. (2007). Interfacial mass transport properties which control the migration of packaging constituents into foodstuffs. Journal of Food Engineering, 79(3), 1048-1064. https://doi.org/10.1016/j.jfoodeng.2006.03.030.

[76] Welc-Stanowska, R., Karp-Paździerska, S., Kurek, M., Miś, A., and Nawrocka, A. (2023). Effect of β-glucans on water redistribution and gluten structure in a model dough during the mixing process. International Agrophysics, 37, 151–158. https://doi.org/10.31545/intagr/159209.

[77] Wang, D., Zhang, L., Wen, M., Du, L., Gao, X., Xue, C., Xu, J., and Wang, Y. (2016). Enhanced neuroprotective effect of DHA and EPA-enriched phospholipids against 1-methyl-4-phenyl-1,2,3,6-tetrahydropyridine (MPTP) induced oxidative stress in mice brain. Journal of Functional Foods, 25, 385-396. https://doi.org/10.1016/j.jff.2016.06.014.

[78] Zheng, H., Morgenstern, M., Campanella, O., and Larsen, N. (2000). Rheological Properties of Dough During Mechanical Dough Development. Journal of Cereal Science, 32, 293-306. https://doi.org/10.1006/jcrs.2000.0339.

[79] Zhang, M., Peng, H., Li, B., and Tian, J. (2023). Impact of pomegranate fruit powder on dough, textural and functional properties of fresh noodle. Journal of the Science of Food and Agriculture, 103(14), 6895-6904. https://doi.org/10.1002/jsfa.12772.

[80] Zhang, F., and Shen, Q. (2021). The impact of endogenous proteins on hydration, pasting, thermal and rheology attributes of foxtail millet. Journal of Cereal Science, 100, 103255. https://doi.org/10.1016/j.jcs.2021.103255.

[81] Zarzycki, P., Wirkijowska, A., and Pankiewicz, U. (2024). Functional Bakery Products: Technological, Chemical and Nutritional Modification. Applied Sciences, 14(24), 12023. https://doi.org/10.3390/app142412023.

[82] Zahid, H. F., Ranadheera, C. S., Fang, Z., and Ajlouni, S. (2022). Functional and Healthy Yogurts Fortified with Probiotics and Fruit Peel Powders. Fermentation, 8(9), 469. https://doi.org/10.3390/fermentation8090469.

[83] Zykwinska, A., Rondeau-Mouro, C., Garnier, C., Thibault, J. F., and Ralet, M. C. (2005). Alkaline extractable pectins from sugar beet cell walls. Carbohydrate Polymers, 60(3), 527-538. https://doi.org/10.1016/j.carbpol.2005.02.019.

[84] Šporin, M., Avbelj, M., Kovač, B., and Možina, S. S. (2017). Quality characteristics of wheat flour dough and bread containing grape pomace flour. Food Science and Technology International, 24(3), 251-263. https://doi.org/10.1177/1082013217745398.

[85] Ramírez-Pulido, B., Bas-Bellver, C., Betoret, N., Barrera, C., and Seguí, L. (2021). Valorization of vegetable fresh-processing residues as functional powdered ingredients: A review on the potential impact of pretreatments and drying methods on bioactive compounds and their bioaccessibility. Frontiers in Sustainable Food Systems, 5, 654313. https://doi.org/10.3389/fsufs.2021.654313.

OBTAINING FORTIFIED WINES WITH GRAPE POMACE BIOCOMPOUNDS OBTAINED BY MAE EXTRACTION METHOD

/

OBȚINEREA VINURILOR FORTIFIATE CU BIOCOMPUȘI DIN TESCOVINĂ OBȚINUȚI PRIN METODA DE EXTRACȚIE MAE

Petronela Anca ONACHE[1)], Irina Elisabeta GEANĂ[*2)], Corina Teodora CIUCURE[2)], Iulia Cristina CIOBANU[3)], Victoria ARTEM[3)], Georgiana CÎRSTEA[4)], Alina FLOREA[1)], Dorin Ioan SUMEDREA[1)], Mircea NEGRUTA[5)]

[1)] National Research & Development Institute for Biotechnology in Horticulture
Bucharest-Pitesti Street, no.37, Stefanesti, Arges County / Romania;
[2)] National Research and Development Institute for Cryogenic and Isotopic Technologies,
Uzinei no 4, Ramnicu Valcea, Valcea County / Romania;
[3)] Research and Development Resort for Viticulture and Winemaking Murfatlar,
Calea Bucuresti, no 2, Murfatlar, Constanta County / Romania;
[4)] National University of Science and Technology Polytechnic Bucharest University- Pitesti University Center,
Targul din Vale No 1, Pitesti, Arges County / Romania;
[5)] SC Mancora Ocean S.R.L/ Romania.
**E-mail:* irina.geana@icsi.ro

Keywords: *Grape pomace/marc, wine, MAE extraction, polyphenolic compounds, antioxidant activity*

ABSTRACT

In order to encourage the development of the sustainable food system in the wine industry, it is necessary to recover and reuse winemaking by-products such as pomace. The research carried out in this article provides compelling evidence on the prospects of using marc as an abundant source of bioactive chemicals for the creation of new functional ingredients, such as fortified wine with bioactive compounds from marc. The pomace being one of the most important waste results of winemaking, it has been subject to research with very good results in ingredients with high potential of functional bioingredients. The pomace was subjected to drying by the microwave method and followed by shredding. In order to extract the active biocompounds, the flour from the pomace from red grapes was subjected to MAE microwave extraction, and the extracts (1:10) were used to fortify the wine, with 50 ml of extract per litter of wine. Our research has been carried out on seven varieties of wine and the pomace from Stefanesti and Murfatlar wine centres in the 2023 production year. The active biocompounds in the red wine were assessed in parallel with the fortified 5% wine. The active component analysis (PCA) of the pomace has been evaluated using XLSTAST. Correlation values were evaluated using Pearson correlation. Differences in $p < 0.05$ were considered significant.

REZUMAT

Pentru a încuraja dezvoltarea sistemului alimentar durabil în industria vinicolă este necesar de a recupera și reutiliza subprodusele de vinificație, cum ar fi tescovina. Cercetările realizate în cadrul acestui articol oferă dovezi convingătoare asupra perspective utilizării tescovinei ca sursă abundentă de substanțe chimice bioactive pentru crearea de noi ingrediente funcționale, cum ar fi vinul fortifiat cu compuși bioactivi din tescovină. Tescovina fiind unul din cele mai importante deșeuri rezultate vinificării, ea a fost supusă cercetărilor având rezultate foarte bune în ingredientele cu potential ridicat de bioingrediente funcționale. Tescovina a fost supusă uscării prin metoda microundelor și urmată de mărunțirea. Pentru a extrage biocompușii active, făina din tescovina din struguri roșii a fost supusă extracției cu microunde MAE, iar extractele (1:10) s-au folosit la fortifierea vinului, cu 50 ml de extract la un litru de vin. Cercetările noastre s-au realizat pe șapte soiuri de vin și tescovină din centrele viticole Ștefănești și Murfatlar anul de producție 2023. S-au evaluat biocompușii activi din vinul martor în paralel cu vinul fortifiat 5%. Analiza activă a componentelor (APC) a tescovinei a fost evaluată utilizând XLSTAST. Valorile de corelație au fost evaluate utilizând corelația Pearson. Diferenţele la $p < 0,05$ au fost considerate semnificative.

INTRODUCTION

Currently, humanity faces one of the great challenges of the century, namely achieving a balance between economic development and environmental protection *(Diaconu, 2022).* This challenge is known as sustainability or achieving sustainable agriculture *(Diaconu, 2022).* The achievement of sustainable

viticulture and wine-making, as well as the methods to be applied to achieve sustainability, are confusing to both winegrower and winemakers companies and consumers *(Baiano, 2021; Szolnoki, 2011).* In order to define the sustainability concept applied to viticulture and wine production, both the International Organisation of Vine and Wine (OIV) have developed methodologies for sustainable wine growing (OIV 2008) and the Global Principles of Sustainability of the Wine Sector *(Diaconu, 2022; OIV, 2021; FIVS, 2016).*

According to the OIV (2021), sustainable viticulture is a "global strategy on the scale of grape production and processing systems, which at the same time incorporates the economic sustainability of structures and territories, producing quality products, taking into account the precision requirements in sustainable viticulture, environmental risks, product safety and consumer health *(Diaconu, 2022; OIV, 2021).*

The main environmental issues are: land use, water management, energy management, the use of chemicals in vine and wine treatments, waste generation, leading to greenhouse gas emissions *(Montalvo-Falcón, 2023; Diaconu, 2022; OIV, 2021)*. Viticulture, as with other types of agriculture, makes extensive use of pesticides having an important effect on the environment *(Montalvo-Falcón, 2023; Springmann, 2018).* In most vineyards around the world, technologies conventional viticulture use synthetic herbicides on soil for weeds and pesticides to control diseases and insects harmful to vines *(Montalvo-Falcón, 2023; Dumitriu, 2021).* According to Gilinsky *(Dumitriu, 2021; Gilinsky, 2016)*, by achieving sustainable agriculture in the wine sector, future generations will benefit from it *(Baiano, 2021; Dumitriu, 2021; Gilinsky, 2016).*

In the wine industry, most of the waste generated by the winemaking process is organic in nature, which means that it can be reintroduced into the natural circuit *(Diaconu, 2022).* In recent decades, economic and environmental problems have increased concerns about the high volume of waste generated in the food industries. In this respect, one of the current challenges is framing such waste as „by-products" that can be reprocessed, aiming to reduce their negative impact, as well as obtaining high benefit materials *(Caldas, 2018).*

The wine industry generates a large amount of residues, which are generally used as organic fertilizer for land or for animal feed *(Rivera, 2021).* In the wine industry, most of the waste generated by the winemaking process is organic in nature, which means that it can be reintroduced into the natural circuit *(Diaconu, 2022).*

Due to its antioxidant rich composition, the use of grape marc has numerous benefits for human health, reducing the risk of developing chronic diseases such as cancer, diabetes, inflammatory and cardiovascular diseases *(Yu, 2013)*. In Europe, many countries have begun to capitalize on winemaking waste by obtaining various valuable products for the pharmaceutical, cosmetic, food and not only industries *(Diaconu, 2022; Yu, 2013)*.

Consequently, grape pomace is considered a valuable source of phytochemicals that can be recovered in the form of functional compounds or extracts for the pharmaceutical, cosmetic and food industries. In this way, the recovery of phenolic substances from grape by-products in the wine industry has attracted increasing attention in recent years. According to the current assessments 1 kg of grape marc is generated for obtaining each 6 L of wine *(Spinei, 2021, Dávila, 2017; Mendes, 2013).*

One tonne of grape marc contains 425 kg of grape skins, 225 kg of grape seeds, 249 kg of bunch and other minor constituents *(Spinei, 2021).* Grape seed accounts for about 15% of the solid waste produced in wine *(Luque-Rodríguez, 2005),* and depending on the grape variety, the seeds are between 2% and 6% by weight of the grapes and 1% to 4% by weight of the grapes. Dried pomace seeds contain 40-65% and have an oil content of 12-22% *(Passos, 2009).* Modern techniques have demonstrated their suitability for extracting bioactive compounds by obtaining the recovery of bioactive compounds similar to or better than conventional methods *(Onache 2023; Yammine, 2020; Ahmad, 2011)*.

Therefore, it is necessary to have effective and durable extraction technologies in order to achieve a good recovery of compounds. There are many factors that influence the extraction efficiency, such as: extraction method, solvent type and concentration, temperature and extraction time *(Ahmad, 2011).* Unlike traditional extraction methods such as maceration or percolation, which require long periods of time and large amounts of solvent *(Tellez-Robles, 2024),* MAE allows for rapid and efficient extraction due to the ability of microwaves to directly heat polar molecules from the extraction material and solvent *(da Rocha, 2021; Bagade, 2019)*. This direct and uniform heating significantly reduces the processing time and at the same time improves the yield and quality of the extract obtained.

Microwave assisted extraction (MAE) is an advanced technique that uses electromagnetic radiation to facilitate and optimize the extraction process of active compounds from various materials, such as plants, food, or even industrial waste *(Bagade, 2019)*. MAE represents a significant improvement in the field of

extraction techniques, providing an optimal balance between efficiency, durability and quality of the final product *(da Rocha, 2021).*

In this article, the microwave-assisted extraction method (MAE) was used on 7 varieties of marc obtained in the 2023 production year from two wine-growing areas. With these extracts, wines obtained in the same year of production, 2023, were fortified. The wines were fortified with 50 ml of extract per 1 litter of wine.

MATERIALS AND METHODS

Chemicals and Reagents

Ethanol (pharmaceutical), Folin–Ciocalteu phenol reagent, radical scavenging assay reagents DPPH, -6-hydroxy-2,5,7,8- tetramethyl-2- carboxylic acid (Trolox) were purchased from obtained from Alfa Aesar (ThermoFisher GmbH Kandel, 76870 Kandel, Germany). All solvents were of HPLC quality, and all chemicals were of analytical grade (>99%). Analytical standards (gallic acid, abscisic acid, p-coumaric acid, caffeic acid, 3,4-dihidroxibenzoic acid, 4-hidroxibenzoic acid, shkimic acid, chlorogenic acid, siringic acid, azelaic acid, elagic acid, 2,5-dihydroxybenzoic acid, t-resveratrol, (+)-catechin, (-)–epicatechin, oenina, polidatin, t-polidatin, quercetin) from Sigmainheim.

Raw material

Grape pomace (*Vitis vinifera* varieties 'Cabernet Sauvignon', 'Burgund', 'Pinot Noir' and 'Merlot') was collected from the winery in INCDBH Stefanesti and from the SCDVV Murfatlar winery ('Mamaia', 'Pinot Noir' and 'Băbească Neagra'), the harvest 2023. The grape pomace samples were frozen and stored before the analysis. The grape pomace was dried at 45 ◦C for 5 minutes at tunnel microwave drying tape JW-MW-6 KW *(Onache, 2022)*. The grape pomace samples before drying had humidity between 85-75%, and after drying they reached between 5-8%, after which the samples were shredded using the mill with Fritsch Pulverisetti 16 hammers.

Extraction Procedures

Microwave-assisted extraction (MAE) was performed using the NEOS GR system with the following parameters: 10 g pomace/100 ml solvent (alchool), 10 minutes extraction time, power delivered in the environment 330 W. To obtain the targeted extractive fraction (polyphenols), a solvent based on distilled water and pharmaceutical ethyl alcohol (10:100 v/v) was used. With these extracts were fortified wines obtained in the same year of production 2023. The wines were fortified with 50 ml of extract per 1 litter of wine.

Analytical Investigations

Quantitative UV-Vis Spectrophotometric Determinations. In order to investigate the bioactive characteristics from wine and fortified wines were determined: total polyphenols compounds - TPC (mgGAE/L), catechins – TC (mg/L), tannins - TT (mg/L), polymerized tannins – TPT (mg/L) Total anthocianins - TA (mg/L); antioxidant activity (AA) expressed as mmol TE/L. The total polyphenolic compound content (TPC) were determined by Folin-Ciocaltu method, the absorbance was measured with Analytik Jena Specord 205 UV/VIS spectrophotometer at 765 nm and data were expressed as gallic acid equivalent (GAE)·per mg/l for sample *(Onache, 2022; Vignoli, 1960).*

Total anthocyanins were evaluated as reported by Ribereau-Gayon in 1965, the absorbance at 520 nm was read with Analytik Jena Specord 205 UV/VIS spectrophotometer, and results were expressed as mg/l *(Onache, 2023).* Catechins, monomer flavanolic units, were determined with the method by which the reaction of catechins with vanillin assay *(Onache, 2022)* (1% alchohol solution).

The absorbance was measured with Analytik Jena Specord 205 UV/VIS spectrophometer at 500 nm. Tannins have been determined by the leukocytanidins (LA) method, based on the property of tannins to transform on hot (100°C) and strongly acidic (concentrated HCl) environment into cyanidin, which is red in color *(Onache, 2023; Onache, 2022).* The optical density at a wavelength of 550 nm is directly proportional to the concentration of tannins. The evaluation of the antioxidant activity was carried out by testing free radical scavenger property. The antioxidant activity of the extracts was measured in terms of hydrogen-donating or radical-scavenging ability by means of the radical 2,2-diphenyl-1-picrylhydrazyl (DPPH•), according to a the method described by Sanchez-Moreno et al. (1999). The reaction mixtures were shaken and incubated for 45 min in the dark at room temperature *(Onache, 2022; Sanchez-Moreno et al., 1999).* The absorbance was read at 517 nm using the AnalytikJena Specord 205 UV/VIS spectrophotometer. *Polyphenolic Profile by UHPLC-HRMS.* The quantitative analysis of individual polyphenols (phenolic acids, flavonoids, and stilbens) was performed by UHPLC–ESI/HRMS (ultra-high-performance liquid chroma-

tography electrospray ionization tandem mass spectrometry) using a high-resolution Q Exactive mass spectrometer™ Focus Hybrid Quadrupole—OrbiTrap equipped with HESI, coupled to a high-performance liquid chromatograph UltiMate 3000 UHPLC (Thermo Fisher Scientific, City, State, Country).

Wine Samples

The wine was obtained from the winemaking of the 7 varieties from which the grape pomace resulted, in the same year of production, 2023. The wine was enriched with 5% extract from the grape pomace of each variety. (Stefanesti wine-centre: Burgund, Cabernet Sauvignon, Pinot Noir, Merlot and Murfatlar wine-centre: Babeasca Neagra, Mamaia, Pinot Noir).

RESULTS

Phytochemicals content of MAE extract, wine and fortified wine

Table 1 shows the results of polyphenolic compounds in the pomace extracts of the 7 grape varieties obtained by the MAE method. Total polyphenols and anthocyanins in the extracts are highlighted according to the antioxidant activity of the pomace. It is noted that the extracts have a very low content of anthocyanins, by fermenting the wine on the breastbone and by the treatments suffered by the grape pomace, most anthocyanins are destroyed. The concentration of biocompounds in the pomace was expressed in g per 100mg pomace (dry matter - DM). As observed quantities of anthocyanins after microwave extraction is reduced. The lowest amount of anthocyanins is observed in Babeasca Neagra from Murfatlar (36.108 mg/100g DM), and the highest at Pinot Noir from Stefanesti (266.175 mg/100g DM). Different from anthocyanins are found total polyphenols in very high concentrations. The highest value of PFT is found in the Burgund variety from Stefanesti (2198.7 mg GAE/100g DM), and the lowest in all the Badeasca Neagra from Murfatlar variety (1523.7mg GAE/100g DM). The concentration of total polyenols is in the same range as at (Yammine, 2020), where the total content of polyphenolic compounds varies from 0.59 ± 0.05 to 3.66 ± 0.19 g gallic acid GA/100 g dry matter for Cabernet Franc, Merlot, Pinot Noir (6.070 g/100 g DM).

Table 1

Total polyphenolic biocompound content of tescovina extract obtained by MAE method

Varieties	TPF mg GAE/100mg	TA mg/100 g	TC mg/100 g	TT mg/100g	TPT, mg/100 g	AA, mmol TE/g
M_St MAE	1926.2	57.458	3.93	73.37	0.0536	206.20
CS_St MAE	1779.9	121.217	4.11	61.33	0.0669	244.62
B_St MAE	2198.7	110.658	6.10	100.58	0.0607	120.85
PN_St MAE	1588.4	266.175	5.33	224.09	0.0238	353.17
M_Mf MAE	1651.6	105.525	3.62	69.81	0.0518	104.91
BN_Mf MAE	1523.7	36.108	2.42	38.94	0.0623	90.04
CS_Mf MAE	1530.7	57.283	3.99	71.02	0.0562	74.81
PN_Mf MAE	1543.8	76.242	4.32	105.61	0.0409	164.76

The polyphenolic profile of extracts (Table 2) made by UHPLC-HRMS is shown below.

Table 2 presents the results obtained from grape pomace extracts using MAE method, for all the compounds found. Flavonols are found in fresh grape pomace, but degrade as they undergo treatments, drying and extraction with organic solvents. The catechins are between 9.63 mg/L (MM-Mf_MAE) and 181.03 mg/L (PN_M_MAE).

Table 2

Individual phenolic compounds of pomace extracts obtained by MAE method

Extracts, mg/L	B_St_MAE	CS_St_MAE	M_St_MAE	PN_St_MAE	BN-Mf_MAE	CS-Mf_MAE	MM-Mf_MAE	PN-Mf_MAE
SHK	33.84	15.97	24.77	69.65	54.67	24.94	91.57	26.35
GAL	65.08	28.30	31.85	64.04	124.06	77.86	107.91	23.42
3,4-DHBA	11.04	2.74	3.11	17.03	24.90	17.99	44.53	2.7
2,5-DHB	0.32	0.09	0.23	1.19	1.65	0.00	2.76	0.1
4-HDB	2.11	0.95	0.77	2.75	3.47	0.00	3.79	0.71
CAT	107.31	39.72	125.93	95.82	46.70	25.62	9.63	181.03
CFA	1.08	0.99	0.31	0.47	0.24	1.23	1.15	0.39
ECAT	21.96	8.07	24.23	33.83	15.55	6.68	3.50	56.14
SYR	84.21	119.63	57.58	265.32	373.62	597.08	217.89	64.84
p-CUM	1.26	0.82	1.03	0.88	2.05	1.13	4.58	0.53

polidatin	0.85	0.83	0.66	1.12	0.83	0.61	0.59	0.59
t-RES	14.12	1.19	2.95	1.24	0.00	0.00	7.63	2.51
taxifolin	1.40	1.55	0.54	0.66	0.19	0.94	0.44	1
ferulic_acid	0.28	2.56	1.63	2.05	2.17	0.00	2.13	1.24
rutin	0.82	0.48	0.97	0.47	1.31	0.49	1.09	0.51
PLO	1.07	1.10	0.00	1.76	0.00	1.55	0.49	1.56
ELG	5.32	5.06	2.41	0.64	0.75	2.15	0.94	2.32
AE	10.25	9.25	11.15	9.45	8.15	8.40	3.20	18.31
QUE	5.34	5.08	2.44	0.41	0.27	6.42	0.33	2.35
ABS	1.25	1.18	1.22	1.99	1.80	2.16	2.22	1.38

Epicatechin had values between (3.5 mg/L) in the MM-Mf_MAE variety and 56.14 mg/L in the PN_St_MAE variety. Shikimic acid is an important polyphenolic acid in plant synthesis and was highlighted by large quantities in the grape pomace extract. The highest values were recorded in the extracts obtained from the 'Mamaia' variety (91.57 mg/L) cultivated in the Murfatlar region, (65.08 mg/L) as was recorded in the extracts obtained from the 'Burgund' variety, cultivated in the Stefanesti wine region. Phenolic acids are found in high quantities, for example gallic acid, which is found in the grape pomace extract between 0.05mg/L (BM-St_MAE) and 124.06 mg/L (MM_Mf_MAE). It has a high content for CS_St_MAE (28.30 mg/L) compared to the reference 5,49 mg/100g DW *(Rockenbach, 2011)* for the same variety, but it is low with 'Mamaia' variety, compared to the 'Bordeux' variety in reference *(Rockenbach, 2011).*

Another high phenolic acid is caffeic acid, ranging from 0.03 mg/L (CS_St_MAE) to 38.87 mg/L (MM_Mf_MAE). The syringic acid in pomace is one of the highest value polyphenolic acids. The syringic acid has values between 57.58 mg/L (M_St_MAE) and 597.08 mg/L (CS_Mf_MAE). Resveratrol is the most important polyphenol in the polyphenolic profile of pomace. It is found in the extract of pomace like t-resveratrol (t-RES) and it has values between 0.0 mg/L (BN_Mf_MAE and CS_Mf_MAE) and 7.63 mg/L (MM_Mf_MAE). After the extraction, the wines were fortified with 50 ml/L of MAE extract. Figure 1 and 2 shows the parallel determinations of total polyphenolic compounds with the antioxidant activity of wine varieties before and after fortification with MAE extract. It is observed after fortification the very large increase in the amount of total polyphenol compounds, implicitly of antioxidant activity. The most obvious change (figure 1) is to PNw_St = 1653 mg GAE/L, versus PN_Stw+MAE = 13415 mgGAE/L, it is also seen in the rose wine of PN_St_MAE = 12515 mg GAE/L, but also to wine CS_St w = 5432 mgGAE/L, versus CS_Stw+MAE = 8256 mgGAE/L. In the case of anthocyanins, it is best to observe the fortification of the wine of the variety CS_St = 124.51 mg/L versus CS_Stw+MAE = 378.61 mg/L, t is also seen in the rose wine of PN_St = 48.39 mg/L versus PNr_St _MAE =76.13mg/L. A small growth of anthocyanins is observed in the 'Mamaia' variety, MM_Mf=108.24 mg/L versus MM_Mf_MAE = 151.99 mg/L.

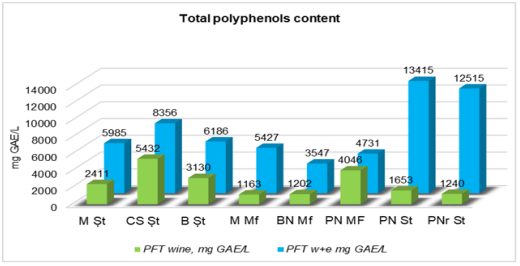

Fig. 1 - Total polyphenol content of wines before and after fortification with extracts obtained by MAE

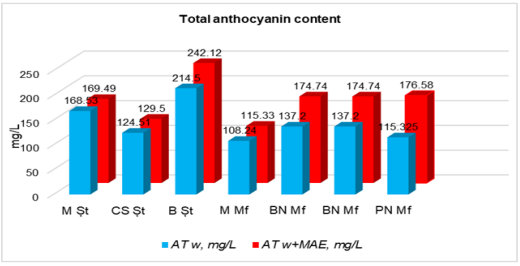

Fig. 2 - Total anthocyanin content of wines before and after fortification with extracts obtained by MAE

The pomace has a high content of catechins, which is observed and figure 3 in which you can see an increase in the concentration of catechins in all wines fortified with MAE extract. The highest content of catechins is observed in wine CS_St_MAE (53.7549 mg/L). In the case of tannin content, it is noted that the highest is the wine MM_Mf_MAE (549.7198 mg/L)

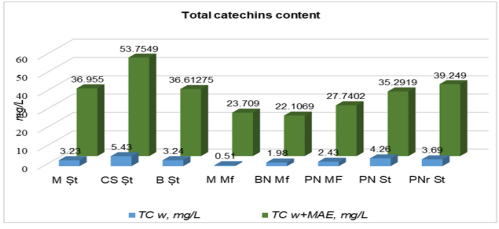

Fig. 3 - Total catechins content of wines before and after fortification with extracts obtained by MAE

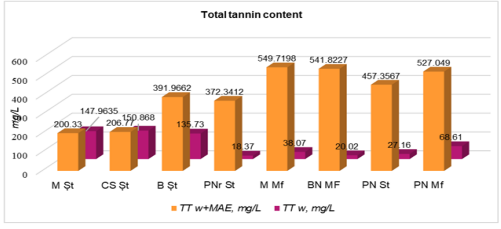

Fig. 4 - Total tannins content of wines before and after fortification with extracts obtained by MAE

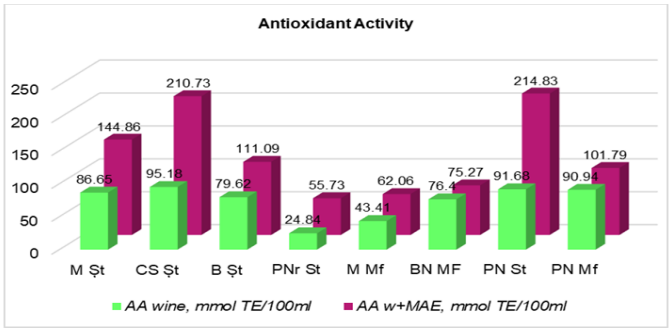

Fig. 5 - The antioxidant activity of wines before and after fortification with extracts obtained by MAE method

As for the antioxidant activity of wines, it grows and takes as much for fortified wines (figure 5). The antioxidant activity at PN_St_MAE is the highest (214.83mmol TE/L), compared to the initial wine PN_Stw= 91.68 mmol TE/L. As a high content of total polyphenols was observed at CS_St, the antioxidant activity being directly proportional to this parameter, CS _ St_MAE (210.73 mmol TE/L) wine has a high antioxidant activity.

The samples were also analysed with HPLC-HRMS to identify individual polyphenolic compounds in wine and fortified wine. Table 3 shows individual polyphenols that were determined from wine before and after fortification with MAE extract.

Table 3

Individual phenolic compounds of of wines before and after fortification with extracts obtained by MAE method

Wine / Individual Polyphenols	B-St	B-St-MAE	CS-St	CS-St-MAE	M-St	M-St-MAE	PN-St	PN-St-MAE	PNr-St	PNr-St-MAE	MM-Mf	MM-Mf-MAE	PN-Mf	PN-Mf-MAE	BN_Mf	BN-Mf-MAE
SHK	31.69	28.05	38.54	39.69	30.41	28.7	20.27	21.31	18.29	21.45	17.67	17.29	27.91	26.63	21.46	23.64
GAL	76.55	69.57	110.7	112.7	67.87	66.84	63.17	62.8	1.93	2.49	14.81	16.57	14.63	16.55	5.78	7.68
3,4-DHBA	6.02	5.01	4.53	4.48	5.85	6.13	4.46	4.61	1.88	1.88	4.31	4.87	5.02	5.2	7.32	7.05
2,5-DHB	1.36	1.16	1.02	1.33	1.01	0.83	0.88	0.89	0.97	0.91	0.72	0.65	1.42	1.58	0.58	0.56
4-HDB	0.89	0.77	0.79	0.8	0.44	0.47	0.68	0.74	0.39	0.38	0.42	0.54	0.92	0.88	0.86	0.91
CFA	8.91	7.97	4.06	3.98	3.7	3.46	1.89	1.67	2.62	2.6	6.39	6.36	13.63	11.7	4.33	4.25
CAT	50.76	49.45	76.05	64.91	30.45	35.64	89.19	78.34	7.24	20.83	15.68	20.58	27.93	37.6	10.10	15.32
ECAT	19.18	17.76	25.56	21.33	12.98	11.59	24.05	24.59	1.21	4.44	3.11	3.85	7.27	10.95	1.24	2.53
SYR	250.1	231.2	406.8	415.5	315.8	283.0	259.3	260.2	10.46	14.07	78.85	81.32	86.61	77.32	33.03	37.78
oenina	8.01	6.22	9.12	6.13	4.64	2.72	4.07	1.95	7.67	4.12	18.64	11.85	38.21	27.01	24.85	17.16
p-CUM	2.29	2.17	1.18	1.37	1.11	1.24	0.99	1.01	0.7	0.74	3.02	3.33	3.75	3.78	4.74	4.87
polidatin	2.06	1.79	0.98	0.85	0.75	0.7	0.96	0.87	0.48	0.41	1.6	1.42	1.23	1.55	0.44	0.56
t-RES	3.03	1.92	1.22	1.05	0.92	1.36	1.63	1.13	0.71	0.39	3.1	3.28	1.95	2.89	1.08	1.15
t-polidatin	442.6	535.7	494.5	474.2	264.8	220.6	710.6	570.5	497.6	391.3	219.7	186.6	625.7	486.1	266.4	209.6
ELG	0.87	0.97	0.92	0.92	0.37	0.59	1.44	1.39	0.09	0.09	0.19	0.55	0.15	0.44	0.23	0.28
AZE	4.54	5.21	4.33	5.08	13.44	4.48	3.88	4.26	7.57	5.33	5.88	4.74	5.21	5.44	6.15	4.76
QEA	0.87	0.97	0.92	0.92	0.37	0.59	1.44	1.39	0.09	0.09	0.19	0.55	0.15	0.44	0.23	0.28

Statistical Data Analysis of *MAE extract, wine and fortified wine*

A distinct interest that conduct to the need to identify and quantify the potential interactions between phytochemical compounds was the large number of results and independent interest variables (figure 6 and 7).

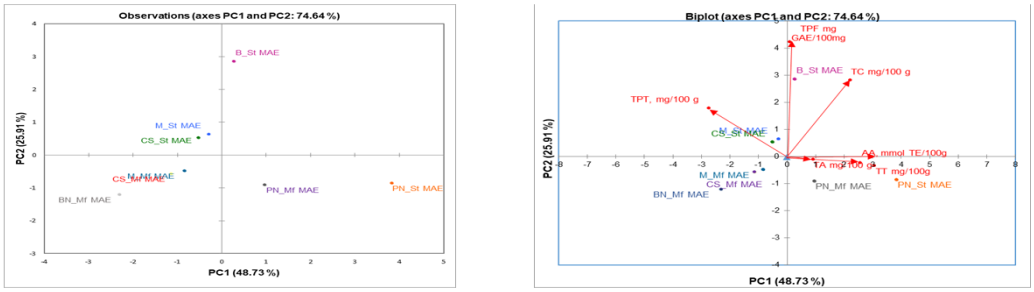

Fig. 6 - Distribution and principal component analyzed (PCA), according to the composition of polyphenolic compounds in the pomace extracts

The influence between the phytochemical elements of grape pomace extracts is shown in Figure 6. The PCA score of 74,64% is a very good score.

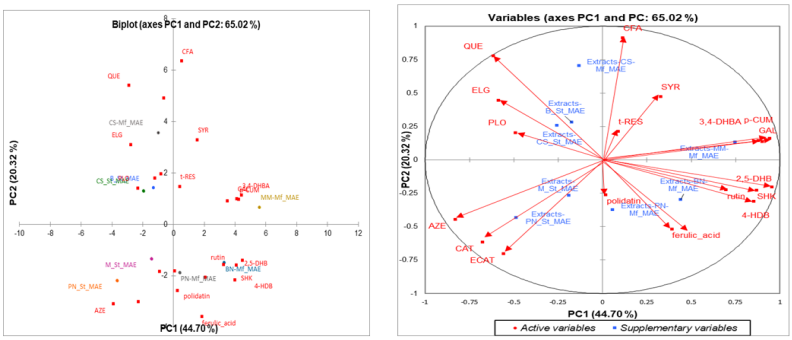

(A) (B)

Fig. 7 - Biplot (A) and distribution (B) of principal component analyzed (PCA), according to the individual polyphenols in pomace extracts

The influence between the individual polyphenols of grape pomace extracts is shown in Figure 7. The PCA score of 65,02% is a very good score.

A distinct interest that conducts to the need to identify and quantify the potential interactions between phytochemical compounds was the large number of results and independent interest variables.

The matrix of the variables of interest in the extract obtained by the microwave assisted extraction method MAE (figure 8,(A)), of the wines before (figure 8(B)) and after fortification with MAE extracts (figure 8(C)) are presented as studied phyto-compound markers (PFT, TA, TC, TT, TTP, AA), respectively, the 8 variants (wine varieties/grape pomace extract).

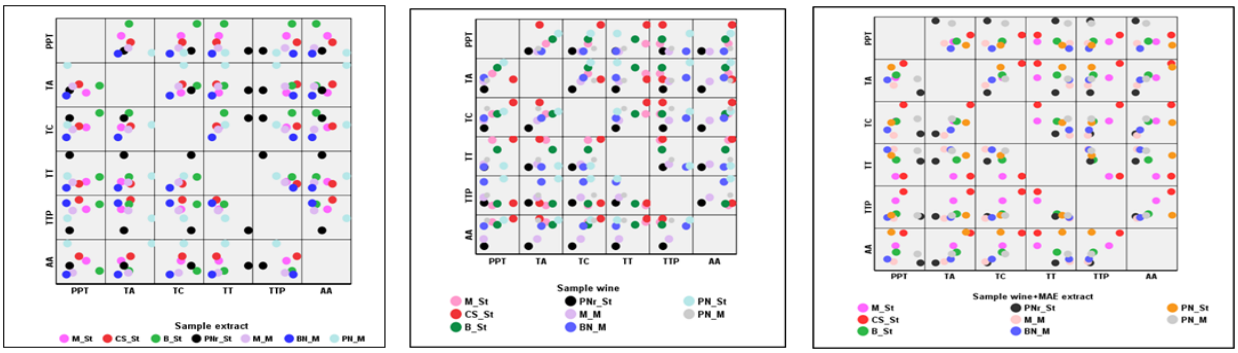

(A) (B) (C)

Fig. 8 - Correlations between the phytochemical compounds of the pomace extract (A), wine before (B) and after (C) fortification (TPF, TA, TC, TT, TPT and AA), depending on the varieties from which they were produced

Within these statistical analyses correlations are made for each matrix: MAE extracts (Table 4), wine (table 5) and fortified wine (Table 6). In the extracts of grape pomace (Table 4) anthocyanins are distinctly positively correlated with the antioxidant activity (0.804*).

Tannins are very significantly negative correlates with polymerized tannins (-0.889**). Total polyphenols in extracts have a significantly positive correlation with catechins (0.605) and polymerized

tannins (0.418), and with antioxidant activity is negatively correlated (-0.184), with tannins (-0.113), as well as anthocyanins (-0.164).

Table 4

Correlations between the polyphenolic compounds of grape pomace extracts

	Phytochemicals	PPT	TA	TC	TT	TTP	AA
PPT	Pearson Correlation	1	-.164	.605	-.113	.418	-.184
TA	Pearson Correlation	-.164	1	.239	.084	-.216	.804(*)
TC	Pearson Correlation	.605	.239	1	.646	-.342	.119
	Sig. (2-tailed)	.150	.605		.117	.452	.799
TT	Pearson Correlation	-.113	.084	.646	1	-.889(**)	.109
	Sig. (2-tailed)	.809	.857	.117		.007	.816
TTP	Pearson Correlation	.418	-.216	-.342	-.889(**)	1	-.229
	Sig. (2-tailed)	.351	.641	.452	.007		.622
AA	Pearson Correlation	-.184	.804(*)	.119	.109	-.229	1
	Sig. (2-tailed)	.692	.029	.799	.816	.622	

** Correlation is significant at the 0.05 level (2-tailed)*
*** Correlation is significant at the 0.01 level (2-tailed)*

The correlations between polyphenolic compounds in wine depend strongly on the wine variety (Figure 8(B). Figure 6 graphically represents the correlation matrix of the phytochemical compounds of wine. Total polyphenols in wine (Table 5) are distinctly positively correlated with catechins (0.763*), significantly positively correlated with anthocyanins (0.502), tannins (0.606), antioxidant activity (0.631) and significantly negatively correlated with polymerized tannins (-0.059). The antioxidant activity in wine (Table 5) is highly significantly correlated with catechins (0.904**).

Table 5

Correlations between polyphenolic compounds of wine

	Phytochemicals	PPT	TA	TC	TT	TTP	AA
PPT	Pearson Correlation	1	.502	.763(*)	.606	-.059	.631
TA	Pearson Correlation		.205	.028	.111	.889	.093
TC	Pearson Correlation	.502	1	.432	.180	.397	.649
	Sig. (2-tailed)	.205		.286	.670	.330	.081
TT	Pearson Correlation	.763(*)	.432	1	.623	.019	.904(**)
	Sig. (2-tailed)	.028	.286		.099	.965	.002
TTP	Pearson Correlation	.606	.180	.623	1	-.648	.528
	Sig. (2-tailed)	.111	.670	.099		.082	.179
AA	Pearson Correlation	-.059	.397	.019	-.648	1	.226
	Sig. (2-tailed)	.889	.330	.965	.082		.591

** Correlation is significant at the 0.05 level (2-tailed)*
*** Correlation is significant at the 0.01 level (2-tailed)*

Correlations in fortified wines (table 6) are not at all similar to correlations in initial wines (table 5) or correlations in extracts (table 4). Significant positive correlations between PPT and TC (0.112) and TTP (0.111) are observed. Significant negative correlations between PPT and TA (-0.375), TT (-0.332) and AA (-0.229). Also in Table 6 there are observed significant strong positive correlations between TA with TC (0.811) and TTP (0.813).

Table 6

Correlations between polyphenolic compounds of fortified wine

Sample wine+MAE extract		PPT	TA	TC	TT	TTP	AA
PPT	Correlation	1.000	-.375	.112	-.332	.111	-.229
	Significance (2-tailed)	.	.407	.811	.467	.813	.621
TA	Correlation	-.375	1.000	.847	-.577	.750	.923
	Significance (2-tailed)	.407	.	.016	.175	.052	.003
TC	Correlation	.112	.847	1.000	-.753	.898	.776
	Significance (2-tailed)	.811	.016	.	.051	.006	.040
TT	Correlation	-.332	-.577	-.753	1.000	-.837	-.760
	Significance (2-tailed)	.467	.175	.051	.	.019	.047

TTP	Correlation	.111	.750	.898	-.837	1.000	.761
	Significance (2-tailed)	.813	.052	.006	.019	.	.047
AA	Correlation	-.229	.923	.776	-.760	.761	1.000
	Significance (2-tailed)	.621	.003	.040	.047	.047	.

** Correlation is significant at the 0.05 level (2-tailed)*
*** Correlation is significant at the 0.01 level (2-tailed)*

Between the antioxidant activity in fortified wines with the other bio compounds is in a significantly strong positive correlation with TA (0.750), with TC (0.898) and the strong negative correlation with TT (-0.837).

Classification and differentiation between samples of wine (Figure 9 (A)) and fortified wine (figure 9 (B)) based on total phenolic compounds was carried out by multivariate data analysis using Principal Component Analysis (PCA). Figure 9 shows a two-dimensional graph of the eight samples of red wine analysed, defined by the first two main components, PC1 and PC2.

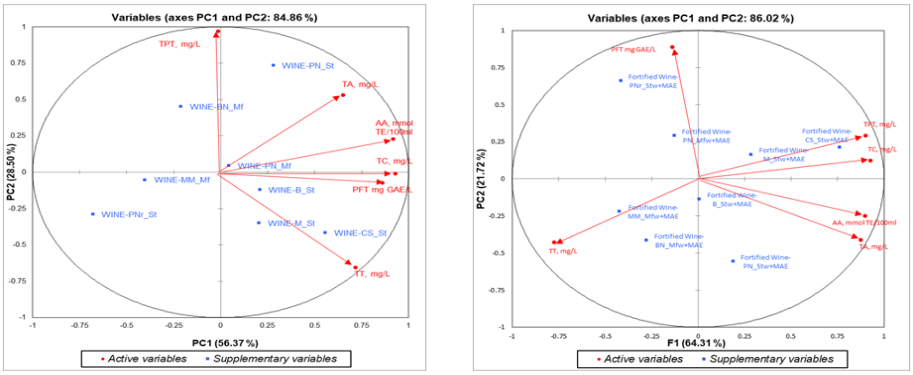

(A) (B)

Fig. 9 - Distribution and principal component analyzed (PCA), according to the composition of total polyphenolic compounds in the wine before (A) and after (B) fortification

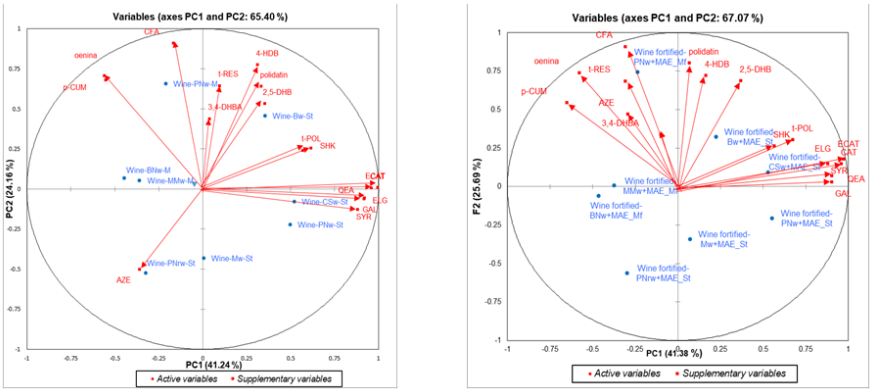

(A) (B)

Fig. 10 - Distribution and principal component analyzed (PCA), according to the composition of individual polyphenols in the wine before (A) and after (B) fortification

The multivariate statistical analysis was carried out by separating wines before fortification (Figure 9 (A)) after fortification (Figure 9 (B)), due to the major difference between the phytocomponents introduced from the extract of pomace from fortified wines. PCA has been applied separately to the two wine collections. The first two axes (shown in the diagram) explain 84.86% of the total variation of the phytochemical composition. The maps defined by PC1 and PC2 for PCA on the polyphenolic data on the original wines analysed and are presented in Figure 9 (A) and, in Figure 9 (B), are the polyphenolic data for fortified wines. The PCA score of 84.86% is a very good score. Figure 9 (A) PC1 main component explained by 56.37% of the total variation is opposed to PFT, TT and TC compounds and the remaining measured polyphenols, explained PC2 by 28.5%. The PCA score of 86.02% is a very good score for polyphenolic compounds

determined from fortified wine (figure (B)). Figure 9 (B) PC1 main component explained by 64.31% of the total variation is opposed to AA, TT and TA and the remaining measured polyphenols, explained PC2 by 21.72%.

The PCA score of 65,40% is a very good score. Figure 10 (A) main component PC1 explained by 41.24% of the total variation is opposed to AZE, GAL, SYR, ELG and content phenols at the remaining measured parameters, PC2 explained by 24,16%. The influence of grape pomace extract on the content of individual polyphenols in fortified wines is underlined in Figure 10 (B). The PCA score of 67,07% is a very good score. Figure 10 (B) main component PC1 explained by 41.38% of the total variation and content in the measured parameters remaining in the main component PC2, explained by 25.69%. Table 7 shows Pearson correlations between individual polyphenols of pomace extracts. As observed in table 7, there are some distinctly significant positive correlations between individual polyphenols, such as: between shkimic acid and 3,4- dihidroxibenzoic acid (r^2=0.876**), 2,5- dihidroxibenzoic (r^2=0.949**), 4- hidroxibenzoic (r^2=0.879**). It is also distinctly positively correlated with p- coumaric (r^2=0.786*) and distinctly negative with quercetin (r^2=-0.754*). The gallic acid in the extract of the pomace is distinctly significantly correlated with 3,4-dihidroxibenzoic acid (r^2=0.869**), significantly correlated with 2,5- dihidroxibenzoic (r^2=0.765*), 4-hidroxibenzoic (r^2=0.737*), p-coumarir acid (r^2=0.709*) and azelaic acid (r^2=0.717*), and significantly negatively correlated with ellagic acid (r^2=-0.712*).

Table 8 correlates individual polyphenols in wine. As expected in red wine, gallic acid is highly correlated with epicatechin (r^2=0.931**) and syringic acid(r^2=0.981**), and with shkimic (r^2=0.803*), catechin (r^2=0.814**), ellagic acid (r^2=0.739**) and quercetin (r^2=0.739**), is significantly positively correlated. The individual compound polydatin (r^2= 0.939**) in wine, being a precursor to resveratrol, is distinctly significantly correlated with t-resveratrol in wine. The individual compound polydatin in wine, being a precursor to resveratrol, is distinctly significantly correlated with t-resveratrol in wine (r^2=0.939**). For fortified wines, the correlation of individual polyphenolic compounds is shown in Table 9. In fortified wines, very significant correlations between individual polyphenolic compounds are preserved. A clear example is epicatechin which correlates very distinctly significantly with catechin (r2=0.834**), gallic acid (r2=0.831**), ellagic acid (r2=0.912**) and quercetin (r2=0.912**). T-polydatin stilbene forms t-resveratrol. The individual compound t-polydatin in fortified wine correlates significantly with catechin and epicatechin. Due to the fortification with polyphenolic compounds from the extracts of pomace, fortified wine has different correlations between the individual polyphenolic components. There may be negative correlations between the stilbene that are normally distinctly positively correlated, as t-polydatin (r^2=-0.202) is related t-resveratrol, although it is its precursor.

Table 7

Correlations between the individual polyphenols of grape pomace extracts

Individual polyphenols		SHK	GAL	3,4-DHBA	2,5-DHB	4-HDB	CAT	CFA	ECAT	SYR	p-CUM	Polydatin	t-RES	taxifolin	ferulic_acid	rutin	PLO	ELG	AE	QUE	ABS
SHK	Pearson Correlation	1	.694	.876(**)	.949(**)	.879(**)	-.375	.023	-.190	.160	.786(*)	.198	.171	-.627	.372	.440	-.158	-.672	-.614	-.754(*)	.706
	Sig. (2-tailed)		.056	.004	.000	.004	.360	.956	.652	.705	.021	.638	.686	.096	.364	.275	.708	.068	.105	.031	.050
GAL	Pearson Correlation	.694	1	.869(**)	.765(*)	.737(*)	-.653	.132	-.522	.600	.709(*)	.050	.057	-.626	.059	.668	-.374	-.536	-.712(*)	-.401	.717(*)
	Sig. (2-tailed)	.056		.005	.027	.037	.079	.756	.184	.116	.049	.907	.893	.097	.890	.070	.361	.171	.048	.325	.045
3,4-DHBA	Pearson Correlation	.876(**)	.869(**)	1	.910(**)	.752(*)	-.671	.313	-.518	.439	.919(**)	-.107	.156	-.583	.164	.531	-.256	-.582	-.788(*)	-.482	.820(*)
	Sig. (2-tailed)	.004	.005		.002	.031	.069	.450	.189	.276	.001	.801	.711	.129	.699	.175	.540	.130	.020	.226	.013
2,5-DHB	Pearson Correlation	.949(**)	.765(*)	.910(**)	1	.910(**)	-.487	.010	-.332	.138	.891(**)	.054	.136	-.671	.487	.631	-.395	-.626	-.683	-.760(*)	.629
	Sig. (2-tailed)	.000	.027	.002		.002	.221	.980	.421	.744	.003	.898	.748	.069	.221	.093	.333	.097	.062	.029	.095
4-HDB	Pearson Correlation	.879(**)	.737(*)	.752(*)	.910(**)	1	-.341	-.107	-.211	-.002	.709(*)	.355	.279	-.542	.484	.645	-.373	-.450	-.573	-.741(*)	.413
	Sig. (2-tailed)	.004	.037	.031	.002		.408	.802	.615	.996	.049	.388	.504	.165	.224	.084	.362	.263	.138	.035	.309
CAT	Pearson Correlation	-.375	-.653	-.671	-.487	-.341	1	-.581	.933(**)	-.618	-.603	.018	.120	.158	-.190	-.253	.207	.145	.900(**)	-.060	-.590
	Sig. (2-tailed)	.360	.079	.069	.221	.408		.131	.001	.102	.113	.966	.776	.708	.652	.545	.623	.732	.002	.888	.124
CFA	Pearson Correlation	.023	.132	.313	.010	-.107	-.581	1	-.621	.270	.332	-.232	.420	.508	-.395	-.256	.310	.422	-.492	.609	.266
	Sig. (2-tailed)	.956	.756	.450	.980	.802	.131		.100	.518	.422	.580	.300	.199	.333	.540	.455	.297	.216	.109	.524
ECAT	Pearson Correlation	-.190	-.522	-.518	-.332	-.211	.933(**)	-.621	1	-.456	-.544	.100	-.049	.049	-.086	-.326	.370	-.085	.883(**)	-.230	-.352
	Sig. (2-tailed)	.652	.184	.189	.421	.615	.001	.100		.256	.163	.814	.908	.908	.840	.430	.367	.842	.004	.584	.392
SYR	Pearson Correlation	.160	.600	.439	.138	-.002	-.618	.270	-.456	1	.138	-.024	-.460	-.311	-.294	-.015	.159	-.447	-.422	.131	.764(*)
	Sig. (2-tailed)	.705	.116	.276	.744	.996	.102	.518	.256		.744	.955	.252	.453	.479	.971	.707	.267	.297	.758	.027
p-CUM	Pearson Correlation	.786(*)	.709(*)	.919(**)	.891(**)	.709(*)	-.603	.332	-.544	.138	1	-.302	.307	-.497	.267	.636	-.457	-.397	-.758(*)	-.457	.574
	Sig. (2-tailed)	.021	.049	.001	.003	.049	.113	.422	.163	.744		.467	.460	.211	.522	.090	.254	.331	.029	.254	.137
Polydatin	Pearson Correlation	.198	.050	-.107	.054	.355	.018	-.232	.100	-.024	-.302	1	-.035	.075	.298	-.175	.250	-.001	-.090	-.206	-.036
	Sig. (2-tailed)	.638	.907	.801	.898	.388	.966	.580	.814	.955	.467		.935	.860	.474	.679	.551	.999	.831	.625	.933
t-RES	Pearson Correlation	.171	.057	.156	.136	.279	.120	.420	-.049	-.460	.307	-.035	1	.311	-.345	.218	-.069	.471	-.132	.162	-.225
	Sig. (2-tailed)	.686	.893	.711	.748	.504	.776	.300	.908	.252	.460	.935		.454	.402	.604	.871	.239	.755	.702	.592
taxifolin	Pearson Correlation	-.627	-.626	-.583	-.671	-.542	.158	.508	.049	-.311	-.497	.075	.311	1	-.308	-.675	.549	.900(**)	.322	.792(*)	-.554
	Sig. (2-tailed)	.096	.097	.129	.069	.165	.708	.199	.908	.453	.211	.860	.454		.459	.066	.158	.002	.437	.019	.154
ferulic_acid	Pearson Correlation	.372	.059	.164	.487	.484	-.190	-.395	-.086	-.294	.267	.298	-.345	-.308	1	.253	-.360	-.279	-.238	-.653	-.040
	Sig. (2-tailed)	.364	.890	.699	.221	.224	.652	.333	.840	.479	.522	.474	.402	.459		.545	.381	.504	.570	.079	.926

rutin	Pearson Correlation	.440	.668	.531	.631	.645	-.253	-.256	-.326	-.015	.636	-.175	.218	-.675	.253	1	-.903(**)	-.322	-.442	-.514	.117
	Sig. (2-tailed)	.275	.070	.175	.093	.084	.545	.540	.430	.971	.090	.679	.604	.066	.545		.002	.436	.273	.193	.782
PLO	Pearson Correlation	-.158	-.374	-.256	-.395	-.373	.207	.310	.370	.159	-.457	.250	-.069	.549	-.360	-.903(**)	1	.151	.357	.368	.140
	Sig. (2-tailed)	.708	.361	.540	.333	.362	.623	.455	.367	.707	.254	.551	.871	.158	.381	.002		.722	.385	.370	.742
ELG	Pearson Correlation	-.672	-.536	-.582	-.626	-.450	.145	.422	-.085	-.447	-.397	-.001	.471	.900(**)	-.279	-.322	.151	1	.232	.769(*)	-.742(*)
	Sig. (2-tailed)	.068	.171	.130	.097	.263	.732	.297	.842	.267	.331	.999	.239	.002	.504	.436	.722		.580	.026	.035
AE	Pearson Correlation	-.614	-.712(*)	-.788(*)	-.683	-.573	.900(**)	-.492	.883(**)	-.422	-.758(*)	-.090	-.132	.322	-.238	-.442	.357	.232	1	.162	-.590
	Sig. (2-tailed)	.105	.048	.020	.062	.138	.002	.216	.004	.297	.029	.831	.755	.437	.570	.273	.385	.580		.702	.123
QUE	Pearson Correlation	-.754(*)	-.401	-.482	-.760(*)	-.741(*)	-.060	.609	-.230	.131	-.457	-.206	.162	.792(*)	-.653	-.514	.368	.769(*)	.162	1	-.334
	Sig. (2-tailed)	.031	.325	.226	.029	.035	.888	.109	.584	.758	.254	.625	.702	.019	.079	.193	.370	.026	.702		.419
ABS	Pearson Correlation	.706	.717(*)	.820(*)	.629	.413	-.590	.266	-.352	.764(*)	.574	-.036	-.225	-.554	-.040	.117	.140	-.742(*)	-.590	-.334	1
	Sig. (2-tailed)	.050	.045	.013	.095	.309	.124	.524	.392	.027	.137	.933	.592	.154	.926	.782	.742	.035	.123	.419	

** *Correlation is significant at the 0.01 level (2-tailed).*

* *Correlation is significant at the 0.05 level (2-tailed).*

Table 8

Correlations between the individual polyphenols of wine

Individual polyphenols		SHK	GAL	3,4-DHBA	2,5-DHB	4-HDB	CFA	CAT	ECAT	SYR	oenina	p-CUM	polydatin	t-RES	t-polydatin	ELG	AZE	QEA
SHK	Pearson Correlation	1	.803(*)	.309	.550	.469	.244	.467	.646	.782(*)	-.114	-.179	.240	-.046	.153	.303	.019	.303
	Sig. (2-tailed)		.016	.456	.158	.242	.560	.243	.084	.022	.789	.672	.566	.915	.718	.465	.965	.465
GAL	Pearson Correlation	.803(*)	1	.165	.298	.225	-.179	.814(*)	.931(**)	.981(**)	-.569	-.519	.289	.032	.251	.739(*)	-.078	.739(*)
	Sig. (2-tailed)	.016		.697	.473	.592	.672	.014	.001	.000	.141	.188	.488	.940	.548	.036	.854	.036
3,4-DHBA	Pearson Correlation	.309	.165	1	-.078	.581	.242	.023	.088	.179	.269	.623	.137	.160	-.316	.081	.073	.081
	Sig. (2-tailed)	.456	.697		.854	.131	.564	.958	.836	.671	.520	.099	.745	.706	.445	.849	.864	.849
2,5-DHB	Pearson Correlation	.550	.298	-.078	1	.402	.686	.224	.333	.263	.139	-.152	.507	.254	.582	.096	-.101	.096
	Sig. (2-tailed)	.158	.473	.854		.324	.061	.594	.420	.529	.742	.720	.199	.543	.130	.821	.813	.821
4-HDB	Pearson Correlation	.469	.225	.581	.402	1	.544	.330	.322	.146	.468	.521	.266	.196	.428	.291	-.584	.291
	Sig. (2-tailed)	.242	.592	.131	.324		.163	.425	.437	.731	.242	.186	.524	.643	.291	.485	.129	.485
CFA	Pearson Correlation	.244	-.179	.242	.686	.544	1	-.195	-.155	-.202	.748(*)	.561	.575	.544	.185	-.314	-.239	-.314
	Sig. (2-tailed)	.560	.672	.564	.061	.163		.643	.714	.631	.033	.148	.136	.163	.660	.449	.569	.449
CAT	Pearson Correlation	.467	.814(*)	.023	.224	.330	-.195	1	.964(**)	.795(*)	-.448	-.469	.237	.075	.628	.956(**)	-.436	.956(**)
	Sig. (2-tailed)	.243	.014	.958	.594	.425	.643		.000	.018	.266	.241	.572	.859	.096	.000	.280	.000
ECAT	Pearson Correlation	.646	.931(**)	.088	.333	.322	-.155	.964(**)	1	.908(**)	-.520	-.519	.304	.079	.533	.908(**)	-.296	.908(**)
	Sig. (2-tailed)	.084	.001	.836	.420	.437	.714	.000		.002	.187	.188	.465	.853	.174	.002	.477	.002
SYR	Pearson Correlation	.782(*)	.981(**)	.179	.263	.146	-.202	.795(*)	.908(**)	1	-.555	-.535	.212	-.035	.201	.702	.050	.702
	Sig. (2-tailed)	.022	.000	.671	.529	.731	.631	.018	.002		.154	.172	.614	.935	.634	.052	.906	.052
oenina	Pearson Correlation	-.114	-.569	.269	.139	.468	.748(*)	-.448	-.520	-.555	1	.840(**)	.040	.186	-.046	-.554	-.234	-.554
	Sig. (2-tailed)	.789	.141	.520	.742	.242	.033	.266	.187	.154		.009	.926	.660	.914	.154	.576	.154
p-CUM	Pearson Correlation	-.179	-.519	.623	-.152	.521	.561	-.469	-.519	-.535	.840(**)	1	.109	.310	-.320	-.446	-.228	-.446
	Sig. (2-tailed)	.672	.188	.099	.720	.186	.148	.241	.188	.172	.009		.797	.455	.440	.268	.587	.268
polydatin	Pearson Correlation	.240	.289	.137	.507	.266	.575	.237	.304	.212	.040	.109	1	.939(**)	.149	.243	-.386	.243
	Sig. (2-tailed)	.566	.488	.745	.199	.524	.136	.572	.465	.614	.926	.797		.001	.725	.562	.345	.562
t-RES	Pearson Correlation	-.046	.032	.160	.254	.196	.544	.075	.079	-.035	.186	.310	.939(**)	1	.006	.119	-.441	.119
	Sig. (2-tailed)	.915	.940	.706	.543	.643	.163	.859	.853	.935	.660	.455	.001		.989	.779	.274	.779
t-polydatin	Pearson Correlation	.153	.251	-.316	.582	.428	.185	.628	.533	.201	-.046	-.320	.149	.006	1	.578	-.560	.578
	Sig. (2-tailed)	.718	.548	.445	.130	.291	.660	.096	.174	.634	.914	.440	.725	.989		.133	.149	.133
ELG	Pearson Correlation	.303	.739(*)	.081	.096	.291	-.314	.956(**)	.908(**)	.702	-.554	-.446	.243	.119	.578	1	-.443	1.000(**)
	Sig. (2-tailed)	.465	.036	.849	.821	.485	.449	.000	.002	.052	.154	.268	.562	.779	.133		.272	.000
AZE	Pearson Correlation	.019	-.078	.073	-.101	-.584	-.239	-.436	-.296	.050	-.234	-.228	-.386	-.441	-.560	-.443	1	-.443
	Sig. (2-tailed)	.965	.854	.864	.813	.129	.569	.280	.477	.906	.576	.587	.345	.274	.149	.272		.272
QEA	Pearson Correlation	.303	.739(*)	.081	.096	.291	-.314	.956(**)	.908(**)	.702	-.554	-.446	.243	.119	.578	1.000(**)	-.443	1
	Sig. (2-tailed)	.465	.036	.849	.821	.485	.449	.000	.002	.052	.154	.268	.562	.779	.133	.000	.272	

** *Correlation is significant at the 0.01 level (2-tailed).*

* *Correlation is significant at the 0.05 level (2-tailed).*

Table 9

Correlations between the individual polyphenols of fortified wine

Individual polyphenols		SHK	GAL	3,4-DHBA	2,5-DHB	4-HDB	CFA	CAT	ECAT	SYR	genina	p-CUM	polydatin	t-RES	t-polydatin	ELG	AZE	QEA
SHK	Pearson Correlation	1	.783(*)	.117	.593	.336	.057	.450	.518	.752(*)	-.094	-.234	-.008	-.267	.312	.245	.255	.245
	Sig. (2-tailed)		.021	.784	.121	.416	.893	.263	.189	.031	.825	.577	.984	.523	.452	.559	.543	.559
GAL	Pearson Correlation	.783(*)	1	.089	.361	.172	-.207	.785(*)	.834(**)	.991(**)	-.509	-.514	.104	-.217	.399	.732(*)	-.213	.732(*)
	Sig. (2-tailed)	.021		.835	.380	.684	.623	.021	.010	.000	.197	.193	.806	.605	.328	.039	.613	.039
3,4-DHBA	Pearson Correlation	.117	.089	1	-.218	.557	.216	-.090	-.057	.119	.362	.639	.153	.303	-.420	.107	-.411	.107
	Sig. (2-tailed)	.784	.835		.604	.152	.608	.832	.892	.779	.378	.088	.717	.465	.300	.801	.312	.801
2,5-DHB	Pearson Correlation	.593	.361	-.218	1	.366	.596	.445	.482	.323	.325	-.136	.463	.182	.701	.193	.634	.193
	Sig. (2-tailed)	.121	.380	.604		.373	.119	.269	.226	.435	.432	.748	.248	.667	.053	.647	.091	.647
4-HDB	Pearson Correlation	.336	.172	.557	.366	1	.430	.300	.301	.135	.570	.591	.337	.194	.334	.299	.117	.299
	Sig. (2-tailed)	.416	.684	.152	.373		.288	.470	.468	.750	.140	.123	.414	.645	.419	.472	.783	.472
CFA	Pearson Correlation	.057	-.207	.216	.596	.430	1	-.187	-.139	-.249	.785(*)	.563	.807(*)	.770(*)	.078	-.168	.616	-.168
	Sig. (2-tailed)	.893	.623	.608	.119	.288		.658	.743	.551	.021	.146	.015	.025	.855	.691	.104	.691
CAT	Pearson Correlation	.450	.785(*)	-.090	.445	.300	-.187	1	.989(**)	.791(*)	-.402	-.530	.160	-.187	.794(*)	.917(**)	-.276	.917(**)
	Sig. (2-tailed)	.263	.021	.832	.269	.470	.658		.000	.019	.324	.176	.705	.657	.019	.001	.508	.001
ECAT	Pearson Correlation	.518	.834(**)	-.057	.482	.301	-.139	.989(**)	1	.831(*)	-.417	-.538	.211	-.186	.775(*)	.912(**)	-.228	.912(**)
	Sig. (2-tailed)	.189	.010	.892	.226	.468	.743	.000		.011	.304	.169	.615	.659	.024	.002	.587	.002
SYR	Pearson Correlation	.752(*)	.991(**)	.119	.323	.135	-.249	.791(*)	.831(*)	1	-.518	-.528	.054	-.210	.370	.740(*)	-.302	.740(*)
	Sig. (2-tailed)	.031	.000	.779	.435	.750	.551	.019	.011		.189	.178	.899	.618	.367	.036	.467	.036
genina	Pearson Correlation	-.094	-.509	.362	.325	.570	.785(*)	-.402	-.417	-.518	1	.840(**)	.372	.594	-.093	-.428	.461	-.428
	Sig. (2-tailed)	.825	.197	.378	.432	.140	.021	.324	.304	.189		.009	.365	.121	.826	.290	.250	.290
p-CUM	Pearson Correlation	-.234	-.514	.639	-.136	.591	.563	-.530	-.538	-.528	.840(**)	1	.293	.546	-.430	-.378	.150	-.378
	Sig. (2-tailed)	.577	.193	.088	.748	.123	.146	.176	.169	.178	.009		.482	.161	.288	.356	.723	.356
polydatin	Pearson Correlation	-.008	.104	.153	.463	.337	.807(*)	.160	.211	.054	.372	.293	1	.802(*)	.202	.318	.313	.318
	Sig. (2-tailed)	.984	.806	.717	.248	.414	.015	.705	.615	.899	.365	.482		.017	.631	.443	.450	.443
t-RES	Pearson Correlation	-.267	-.217	.303	.182	.194	.770(*)	-.187	-.186	-.210	.594	.546	.802(*)	1	-.202	.008	.127	.008
	Sig. (2-tailed)	.523	.605	.465	.667	.645	.025	.657	.659	.618	.121	.161	.017		.632	.984	.765	.984
t-polydatin	Pearson Correlation	.312	.399	-.420	.701	.334	.078	.794(*)	.775(*)	.370	-.093	-.430	.202	-.202	1	.578	.229	.578
	Sig. (2-tailed)	.452	.328	.300	.053	.419	.855	.019	.024	.367	.826	.288	.631	.632		.133	.586	.133
ELG	Pearson Correlation	.245	.732(*)	.107	.193	.299	-.168	.917(**)	.912(**)	.740(*)	-.428	-.378	.318	.008	.578	1	-.476	1.000(**)
	Sig. (2-tailed)	.559	.039	.801	.647	.472	.691	.001	.002	.036	.290	.356	.443	.984	.133		.233	.000
AZE	Pearson Correlation	.255	-.213	-.411	.634	.117	.616	-.276	-.228	-.302	.461	.150	.313	.127	.229	-.476	1	-.476
	Sig. (2-tailed)	.543	.613	.312	.091	.783	.104	.508	.587	.467	.250	.723	.450	.765	.586	.233		.233
QEA	Pearson Correlation	.245	.732(*)	.107	.193	.299	-.168	.917(**)	.912(**)	.740(*)	-.428	-.378	.318	.008	.578	1.000(**)	-.476	1
	Sig. (2-tailed)	.559	.039	.801	.647	.472	.691	.001	.002	.036	.290	.356	.443	.984	.133	.000	.233	

*** Correlation is significant at the 0.01 level (2-tailed).*

** Correlation is significant at the 0.05 level (2-tailed).*

CONCLUSIONS

In order to realize the negative impact of waste from the wine industry on the environment, in order to have a sustainable agriculture, this industry must move from a linear economy to a circular one. For this purpose, it is assumed to valorised the wine by-products from the wine industry.

The wine by-products are considered natural waste, with great potential for processing and its use in fortifying food. Food obtained by fortification with the by-products of winemaking is a predominant source of bioactive compounds such as: flavonoids, anthocyanins, procyanidins, tannins, catechins, resveratrol, etc.

The pomace extracts resulting from advanced MAE techniques give positive results on optimal extraction conditions, including extraction cost, recovery rate and percentage of purity, stability and toxicity to the environment.

As regards the MAE method, the prediction interval at a 95% confidence level for antioxidant activity ranged from 90.04 mMol TE/100 mg (BN_Mf) to 244.62 mMol TE/100 g pomace (CS_St), and for the total polyphenol content, it ranged from 1523.7 mg GAE/100g (also at BN_Mf) to 2198.7 mg GAE/100 g (B_St) pomace the obtained values were higher than those obtained in bibliography by other advanced extraction methods [25].

The TPC of the extracts showed that the Burgund pomace from Stefanesti and AT from the Pinot Noir pomace variety from Murfatlar, have great potential as a source of antioxidant compounds for food applications. In addition, the content of bioactive compounds increased using the MAE extraction method and proved to be effective for the extraction of phenolic compounds from winemaking waste. However, by fortifying wines with extracts obtained by MAE method, very high values were obtained both TPC (CS_Stw+MAE = 8356 mgGAE/L and PN_St_w+MAE = 13415 mg GAE/L), TA (CS_Stw+MAE = 378.61 mg/L and PN_Stw+MAE = 218.05mg/L) and their antioxidant activity were high (PN_Stw+MAE =214.83 mMol TE/L). Although there are high values of biocompounds in fortified wines, the correlations between these bioactive compounds in fortified wine are only positively or negatively correlated at a significant level.

Due to the fortification with polyphenolic compounds from the extracts of pomace, fortified wine has different correlations between the individual polyphenolic components. There may be negative correlations

between the stilbene that are normally distinctly positively correlated, as t-polydatin (r2=-0.202) is related t-resveratrol, although it is its precursor.

Future research may evaluate the use of other methods of clean extractives, organic solvents and dispersion materials to obtain bioactive compounds (tannins, anthocyanins, etc.) for food fortification.

ACKNOWLEDGEMENTS

This research was funded by the ADER 6.5.2.project financed by the Ministry of Agriculture and Rural Development, Romania.

REFERENCES

[1] S. M. Ahmad, B.A. Siahsar. (2011). Analogy of physicochemical attributes of two grape seeds cultivars, *Cie. e Inv.Agraria*, 38(2), 291-301.

[2] S.B Bagade, M. Patil. (2019). Recent advances in microwave assisted extraction of bioactive compounds from complex herbal samples: A review. *Crit. Rev. Anal. Chem.,*51(2), 138–149.

[3] A. Baiano. (2021). An Overview on Sustainability in the Wine Production Chain, *Beverage*, 7 (1),15

[4] Bru R. and Pedreño M. (2003). Method for the production of resveratrol in cell cultures. PCT patent WO 03/062406.

[5] W. Caldas, V. Tonon et al., (2018). Phenolic compounds recovery from grape skin using conventional and non-conventional extraction methods. *Industrial Crops & Products*, 111, 86-91.

[6] I. Dávila, E. Robles, I. Egüés, J. Labidi, P. Gullón. The Biorefinery Concept for the Industrial Valorization of Grape Processing By-Products. In Handbook of Grape Processing By-Products; Galanakis, C.M., Ed.; Academic Press: Cambridge, MA, USA, 2017; pp. 29–53.

[7] C. Diaconu, (2022). Modele de bune practice circulare în industria vitivinicolă mondială, Technical Scientific Conference of Undergraduate, Master, PhD students, Technical University of Moldova, Chisinau, Republic of Moldova, vol. 2, 285-289.

[8] G.D. Dumitriu, C. Teodosiu, V.V. Cotea, Grape and Wine, Chapt: Management of Pesticides from Vineyard to Wines: Focus on Wine Safety and Pesticides Removal by Emerging Technologies, *Intech Open,* London, UK, 2021.

[9] FIVS. (2016). Global Principles of Sustainability of the Wine Sector

[10] A. Gilinsky Jr., S.K. Newton, R.F. Vega, (2016). Sustainability in the Global Wine Industry: Concepts and Cases*. Agric. Agric. Sci. Procedia,* 8, 37–49.

[11] F. De Lillo, F. Cecconi, G. Lacorata, A. Vulpiani, (2008). Sedimentation speed of inertial particles in laminar and turbulent flows, *EPL*, vol. 84 (4).

[12] J.M. Luque-Rodríguez, M.D. Luque de Castro, P. Pérez-Juan. (2005). Extraction of fatty acids from grape seed by superheated hexane *Talanta,* 68 (1), 126.

[13] J.A.S. Mendes, S.O Prozil, D.V. Evtuguin, L.P.C. Lopes. (2013). Integrated utilization of grape skins from white grape pomaces *Industrial Crops Products*, 49, 286-291.

[14] V. Montalvo-Falcón, E. Sánchez-García, artolomé Marco-Lajara andJavier Martínez-Falcó. (2023). Green human resource management and economic, social and environmental performance: Evidence from the Spanish wine industry, Heliyon, 9(10):e20826.

[15] Morales M. (1998). All about *Catharanthus roseus*. Journal of Plant Biotechnology. 53: 179-187.

[16] OIV. State of the World Vine and Wine Sector 2021; OIV: Paris, France, 2022; pp. 3–19.

[17] P.A. Onache, E.I. Geana, C.T. Ciucure, A. Florea, D.I., Sumedrea, R.E. Ionete, O. Tița. (2022). Bioactive Phytochemical Composition of Grape Pomace Resulted from Different White and Red Grape Cultivars *Separations*, 9, 395,

[18] P.A. Onache, E.I. Geana, C.T. Ciucure, A. Florea, D.I., Sumedrea, R.E. Ionete, O. Tița. (2023). Assessment of bioactive compounds in must and wine from different grape cultivars, *Applied Sciences* 13(9):5722.

[19] C. Passos, R.M. Silva, F.A. Da Silva, M.A. Coimbra, C.M. Silva, J. of Sup. Fluids, 48 (2009)

[20] M. Pedreño, R. Bru, M. Morales, (2008). Synergistic and cytotoxic action of indole alkaloids produced from elicited cell cultures of *Catharanthus roseus*. *Pharmaceutical Biology***}**. 51(3):304-310.

[21] P Ribéreau-Gayon, E Stonestreet. (1965). Determination of anthocyanins in red wine, *Bull Soc Chim Fr*. 9:2649-52.

[22] O.M.P. Rivera, M.D.S. Leos, V.E. Solis, J. M. Domínguez, (2021). Recent trends on the valorization of winemaking industry wastes. *Curr.Opin. Green Sustain. Chem*, 27:100415

[23] C. da Rocha, C. Noreña, (2020) Microencapsulation and controlled release of bioactive compounds from grape pomace, Drying Technology, *Int. J. of Food Eng*., 16, ISSN: 0737-3937 (Print) 1532-2300 (Online)

[24] M. Spinei, M. Oroian, (2021). The Potential of Grape Pomace Varieties as a Dietary Source of Pectic Substances, *Foods,* 10(4), 867.

[25] JM. Springmann, K.M. Carlson, D.M.-D'Croz, K. Wiebe, B. L. Bodirsky, L. Lassaletta, W. de Vries, Sonja J Vermeulen, M. Herrero, Kimberly M Carlson, M. Jonell, M. Troell, F.DeClerck, J. Gordon, R. Zurayk, P. Scarborough, M. Rayner, B. Loken, J. Fanzo, H Charles, J. Godfray, D. Tilman, J. Rockström, W. Willett. (2018) Options for keeping the food system within environmental limits, *Nature*, 562.

[26] G. Szolnoki, J. Bosman, O. Samara, M. Iselborn, A. Ferrigato, K. Tari, N. Gálvez Egea, 6th AWBR Int. Conf. Bourdeaux, France (2011)

[27] D. Tellez-Robles, M.S. López-Cortez, F. Santoyo-Tepole, R. Rosales-Martínez, F. García-Ochoa, M.T. Hernández-Botello, M.P. Salgdo-Cruz, (2024). Optimization of the Extraction of Bioactive Compounds from Cabernet Sauvignon Grape Pomace from Querétaro, Mexico, Using MSPD, *Separations*, 11(1), 13.

[28] L. Vignoli, B. Cristau, J.P. Defretin, R. Vignoli. (1960). [Photocolorimetric microdetermination of carbon monoxide in the blood by palladium chloride and the Folin-Ciocalteu phosphomolybdotungsten reagent, *Arch Mal Prof*. 21:432-8

[29] S. Yammine, C. Delsart, X. Vitrac, Martine M. Peuchot, R. Ghidossi, (2020). Characterisation of polyphenols and antioxidant potential of red and white pomace by-product extracts using subcritical water extraction. *OENO One*, 54(2).

[30] J. Yu, M. Ahmedna, (2013). Functional components of grape pomace: their composition, biological properties and potential applications. *J. of F. Sci. and Tech*., 48, 221-237

IMPLEMENTATION OF A MICROHYDROPOWER SYSTEM FOR SUSTAINABLE AERATION OF FISH PONDS

/

REALIZAREA UNUI SISTEM MICROHIDROENERGETIC PENTRU AERAREA SUSTENABILĂ A BAZINELOR PISCICOLE

Marinela MATEESCU*[1)], Dragoș MANEA[1)], Eugen MARIN[1)], Dragoș- Nicolae DUMITRU[1)], Elena-Melania CISMARU[1)], Ioan PAVEL[2)]

[1)] National Institute of Research - Development for Machines and Installations Designed to Agriculture and Food Industry - INMA Bucharest / Romania;

[2)] INOE IHP / Romania.

**Tel: 0756 880 044; *E-mail: marinelamateescu@yahoo.com*

Keywords: micro-hydro energy, fishpond aeration, renewable energy, aquatic ecosystems, sustainability

ABSTRACT

The paper presents the manufacturing technology developed at INMA Bucharest for the experimental model Micro-Hydro Energy System SME 1,5-0, designed for converting hydraulic energy into electrical power used to drive aeration systems in aquaculture basins. By integrating renewable energy sources with aeration technologies, the proposed solution contributes to enhancing water quality, reducing phosphorus loads and algal blooms, eliminating pathogenic bacteria, and mitigating discomfort caused by mosquitoes and odors. Controlled aeration optimizes the aquatic habitat, supporting increased fish productivity and ecosystem stability. The sheet-metal components were manufactured using CNC technologies (cutting, punching, bending, and laser cutting), ensuring high precision and improved reliability of the assembly. The results demonstrate that the system can serve as a viable and sustainable alternative for the efficient utilization of zootechnical and aquaculture resources, with a positive impact on the environment and the circular economy.

REZUMAT

Lucrarea prezintă tehnologia de realizare în cadrul INMA București a modelului experimental Sistem Microhidroenergetic SME 1,5-0, destinat conversiei energiei hidraulice în energie electrică utilizată pentru acționarea sistemelor de aerare în bazinele piscicole. Prin integrarea energiei regenerabile cu tehnologiile de aerare, soluția propusă contribuie la îmbunătățirea calității apei, la reducerea încărcărilor de fosfor și a înfloririlor algale, la eliminarea bacteriilor patogene și la diminuarea disconfortului generat de țânțari și mirosuri. Aerarea controlată optimizează habitatul acvatic, susținând creșterea productivității piscicole și stabilitatea ecosistemului. Execuția componentelor din tablă a fost realizată prin tehnologii CNC (debitare, stanțare, îndoire și tăiere cu laser), ceea ce a permis obținerea unei precizii ridicate și a unei fiabilități sporite a ansamblului. Rezultatele obținute demonstrează că sistemul poate constitui o alternativă viabilă și sustenabilă pentru valorificarea eficientă a resurselor zootehnice și piscicole, cu impact pozitiv asupra mediului și economiei circulare.

INTRODUCTION

The growing global demand for sustainable and decentralized energy solutions has intensified interest in micro-hydropower systems (MHES), which are considered viable options for rural and semi-urban applications. These systems harness the kinetic and potential energy of water currents to generate electricity with minimal environmental impact, representing a valuable component of the local renewable energy mix. (*Boroomandnia et al., 2022; Pokharel et al., 2008*).

In recent years, the increasing impact of climate change on water resources and their quality has become increasingly evident. Among the main indicators of the ecological status of aquatic ecosystems, dissolved oxygen represents a key parameter for maintaining biological balance and water quality. (*Boyd, 1998*). Ensuring optimal oxygen concentrations is achieved mainly through natural or artificial aeration processes, which represent the fundamental method for improving water quality and supporting aquatic life. (*Kahil & Seif, 2014; Roy et al., 2021*).

Recent studies highlight the potential of micro-hydropower installations not only for electricity generation, but also for their integration with other energy-dependent systems, such as aeration technologies used in aquaculture and wastewater treatment. (*Emamipour et al., 2025; Munaaim et al., 2021*).

Micro-hydropower systems represent an efficient and sustainable solution for aquaculture, harnessing the kinetic energy of water to generate on-site electricity. Supplying aeration systems with renewable energy reduces dependence on the electrical grid and optimizes the energy consumption of fish farms. At the same time, these systems help maintain optimal dissolved oxygen levels, supporting fish health and the productivity of fish ponds, while promoting efficient energy and environmental management of aquatic ecosystems. *(Nugraha et al., 2025).*

Technological advances in computer numerical control (CNC) machining and numerical simulations (CFD – Computational Fluid Dynamics) have enabled the design and optimization of high-efficiency micro-hydropower components, including penstocks, turbines and control assemblies. (*Putra et al., 2022*). Sustainability assessments also show that community-scale micro-hydropower systems can contribute to strengthening local economies and promoting the circular use of resources. (*Chhetri et al., 2009*).

In this context, the present paper introduces the fabrication of the experimental model Micro-Hydropower System SME 1.5-0, designed and developed at INMA Bucharest. The system is intended for converting hydraulic energy into electrical energy used to power aeration systems in fish ponds, representing an innovative integration of renewable energy and environmental management technologies.

MATERIALS AND METHODS

Precision in sheet metal component manufacturing is an essential factor that influences the reliability and performance of the experimental system Micro-Hydro Energy System SME 1.5-0. To ensure high dimensional accuracy, increased repeatability, and superior structural integrity, advanced CNC (Computer Numerical Control) technologies were employed.

Two types of sheet metal, S235JR and S275JR, were used for the fabrication of experimental system components, selected according to the mechanical demands of the parts.

- The S235JR sheet metal components were processed according to the following workflow:
  - cutting on the HST-C 6/2500 CNC center (fig. 1);
  - punching on the ALPHA-CADMAN 1012T CNC center (fig. 2);
  - bending on the PPEB-4 C CNC center (fig. 3).
- The S275JR sheet metal components were processed by:
  - CNC laser cutting on the Laser FC 1530-S system (fig. 4);
  - bending on the PPEB-4 C CNC center (fig. 3).

All parts were subsequently subjected to CNC inspection for dimensional and tolerance control.

The validated parts were directed to the assembly stage for integration into the experimental system assembly.

This differentiated approach allowed for the optimization of the manufacturing process, adaptation to the mechanical properties of the materials, and ensured the precision, repeatability, and structural integrity of all components.

Sheet metal cutting was carried out using the HST-C 6/2500 CNC cutting center (fig. 1), which allows processing sheets up to [6 mm] thick with a positioning accuracy of ±0.1 mm. The equipment ensures precise contouring of the parts and minimizes thermal deformation.

Fig. 1 - HST-C 6/2500 cutting center, highlighting the cutting head and the working area

The components were punched on the ALPHA-CADMAN 1012T punching center (fig. 2), which provides high repeatability and enables the creation of complex patterns using various dies. The main parameters include a maximum punching force of [300 kN], a table size of [2000 × 1000 mm], and an operating speed of [15 strokes/min].

Fig. 2 - CNC punching center with key components highlighted

Component bending was performed using the PPEB-4 C bending center (fig. 3), which allows bending sheets up to [4 mm] thick and angles up to [90°]. The system minimizes unwanted deformations and ensures uniformity of the components.

Fig. 3 - CNC bending center in operation, showing the active die and the workpiece

Final cutting and the creation of complex profiles were performed using the Laser FC 1530-S CNC system (Fig. 4), capable of processing sheets up to [12 mm] thick with tolerances of ±0.05 mm. This process ensures clean edges and precise contours of the components.

Fig. 4 - Laser cutting system in operation, highlighting the laser beam and the workpiece

The application of CNC technologies and the use of S235JR and S275JR materials enabled the production of components with precise shapes, high repeatability, and appropriate structural integrity.

After completing the machining processes, the components were dimensionally inspected on a control bench equipped with certified metrological instruments, calibrated in specialized laboratories.

The inspection aimed to confirm compliance with the tolerances and dimensions specified in the design.

Parts that met the compliance criteria were forwarded to the assembly stage of the experimental system.

RESULTS AND DISCUSSION

A sheet metal part with a thickness of 4 mm was produced, featuring a 90° bend and a circular hole on one face. The complete CAD model was created in SolidWorks, shown in Figure 5, and the generated DXF file is presented in figure 6.

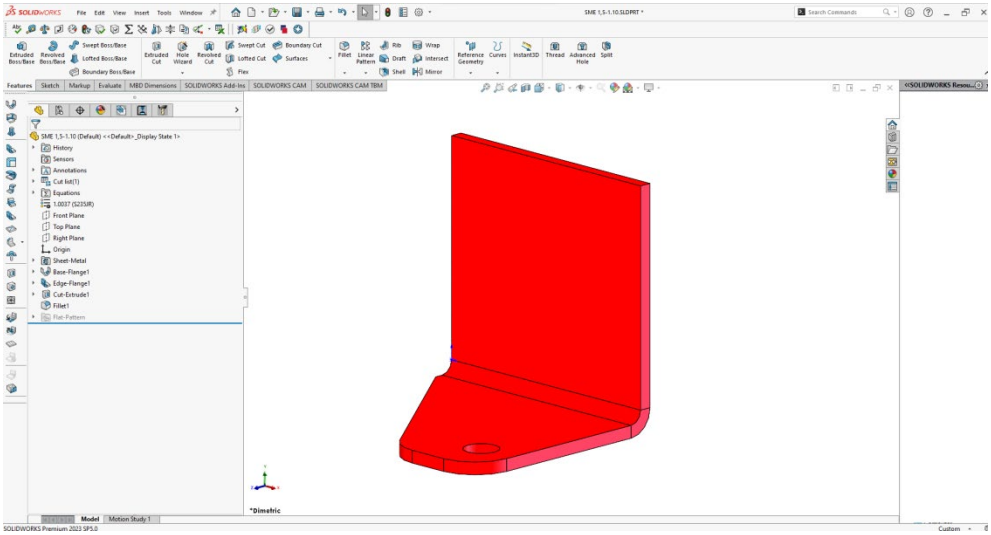

Fig. 5 - CAD model of the machined part, showing the outer contour and the hole position

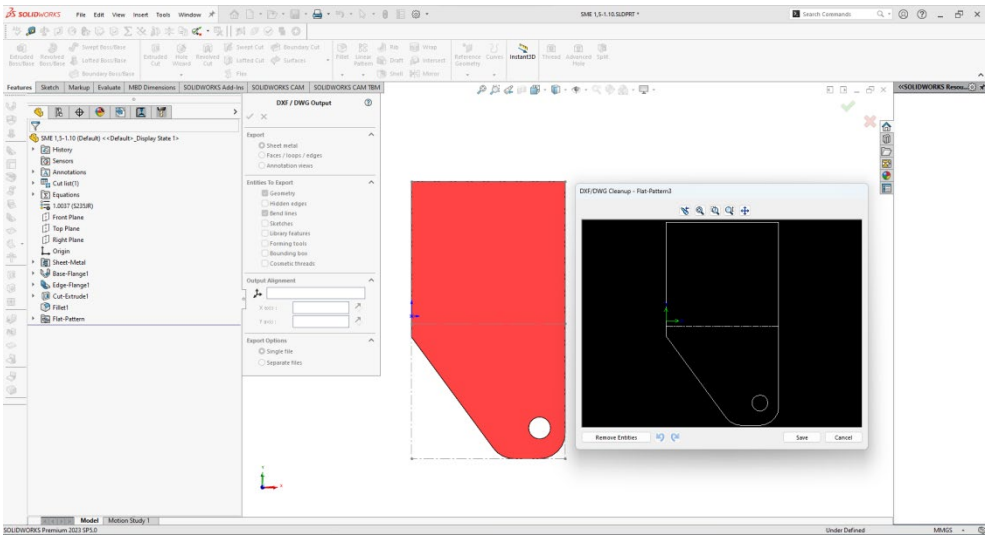

Fig. 6 - DXF file generated for CNC programming of the punching operation

Punching was performed on the ALPHA-CADMAN 1012T machine, first creating the inner hole and then the outer contour, according to the CAM simulation to avoid errors and collisions. CNC bending was carried out on the PPEB-4 C with a 90° angle and optimal processing parameters, verifying the accuracy of the angle and the alignment of the hole.

Following the correct sequence of operations – punching followed by bending – was essential to maintain geometric accuracy and prevent sheet metal deformations.

For the fabrication of the 10 mm thick sheet metal part with holes arranged on two concentric circles, the cutting and drilling operations were carried out using the Laser FC 1530-S CNC. The CAD model of the part is shown in Figure 7, and the 2D DXF file used for CNC programming is presented in Figure 8.

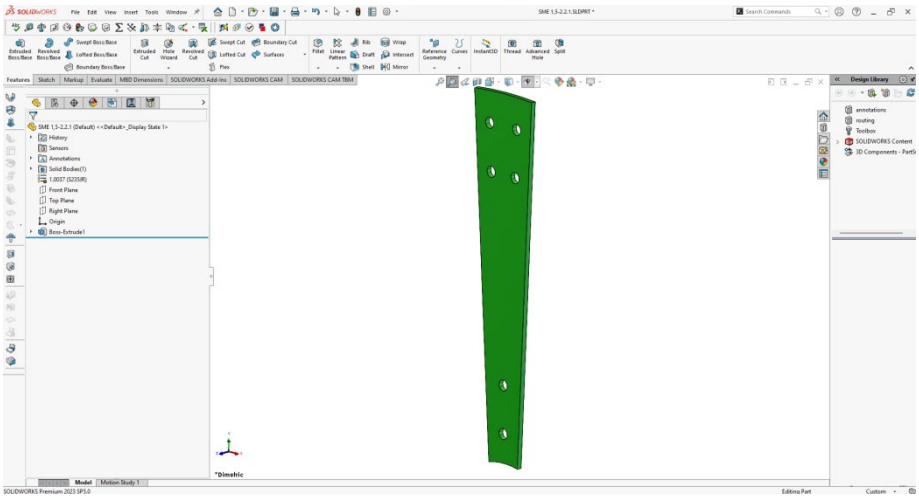

Fig. 7- CAD model of the 10 mm thick sheet metal part, with holes arranged on two concentric circles

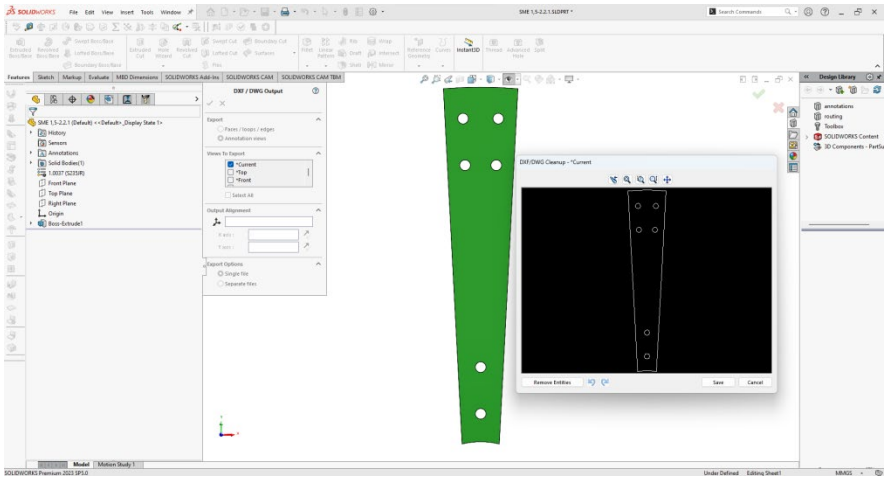

Fig. 8 - DXF file generated for CNC programming of the cutting and drilling operations with the Laser FC 1530-S

The model was checked for geometric correctness and exported in DXF format for import into the laser's CAM software. In CAM, the cutting and drilling parameters were defined, and the operation sequence was set so that the inner holes were made before the outer contour, preventing material deformations. The process was virtually simulated, and subsequently the part was machined on the laser worktable. Aspects of the machine interface and the execution stages of the part are shown in Figure 9.

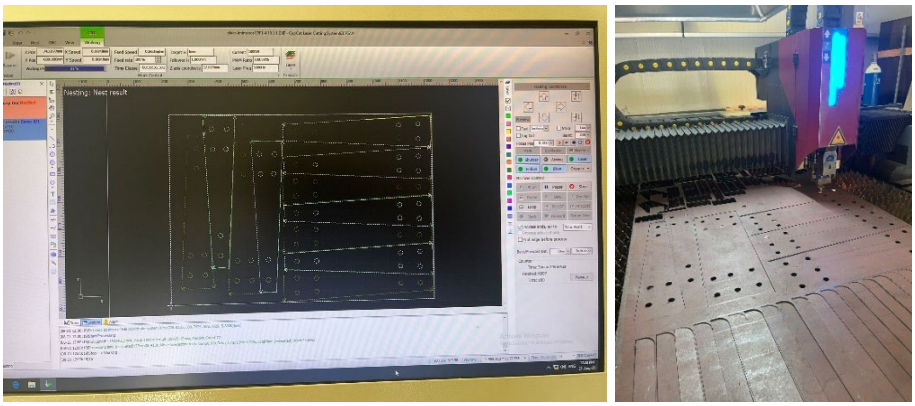

Fig. 9 - Aspects of the CAM software interface and the part execution on the Laser FC 1530-S CNC worktable

All parts were subjected to dimensional inspection on certified metrological equipment, confirming compliance with the project specifications. The accuracy of the holes, contour dimensions, and edge quality were evaluated, ensuring structural integrity and preparing the components for final assembly. Adherence to the operation sequence and CAM simulations prevented sheet metal deformations and guaranteed the precision of the parts, demonstrating the efficiency of the integrated CNC and laser methods for manufacturing components with complex geometry.

It is important to note that this work focuses on presenting the methodology for the design and fabrication of the SME 1.5-0 micro-hydro energy system. At this stage, no experimental tests regarding operational performance were conducted; the primary objective is to demonstrate constructural and technological feasibility, providing a methodological framework for future implementations in fish farms.

CONCLUSIONS

- The components of the *SME 1.5-0 Micro-Hydro Energy* experimental system were successfully manufactured using advanced CNC and CNC laser technologies, ensuring high precision.
- Following the operation sequence – cutting, punching/cutting → drilling → bending – was essential to prevent sheet metal deformations and maintain geometric tolerances.
- Dimensional inspection on certified metrological equipment confirmed that the parts complied with the project specifications, preparing them for the final assembly of the experimental system.
- The integration of CNC and laser technologies demonstrated the efficiency of producing complex components with precision, repeatability, and sustainability, highlighting the potential for applying these methods in micro-hydro energy systems and other industrial applications.

ACKNOWLEDGEMENT

The results presented in this article were obtained with the support of MADR through the "Sectoral Plan - ADER 2026", financing contract no. 13.1.1 / 17.07.2023, ADER project 13.1.1. Research on increasing profitability in aquaculture farms by introducing valuable species with the implementation of specific aquaculture, animal husbandry and agricultural technologies - the realization of the integrated aquaculture farm, managed by the The Research and Development Institute for Aquatic Ecology, Fishing and Aquaculture – Galati.

REFERENCES

[1] Aytac, A., Kelestemur, G. T., & Tuna, M. C. (2024). An effective aeration system for high performance pond aeration at low energy cost. Aquaculture International, 32(5), 6869-6886.

[2] Boyd, C. E. (1998). Pond water aeration systems. Aquacultural engineering, 18(1), 9-40.

[3] Boroomandnia, A., Rismanchi, B., & Wu, W. (2022). A review of micro hydro systems in urban areas: Opportunities and challenges. Renewable and Sustainable Energy Reviews, 169, 112866.

[4] Chhetri, A. B., Pokharel, G. R., & Islam, M. R. (2009). Sustainability of Micro-Hydro Systems — A Case Study. Energy and Environment, 20, 567–580.

[5] Emamipour, H., Eshghi, M. J., & Khan, A. A. (2025). Design of a Hybrid Wind and Micro-Hydro System for Sustainable Water Treatment. Energies, 18(18), 4870.

[6] Kahil, M., & Seif, H. (2014). Mathematical modeling of wastewater aeration efficiency using natural stepped cascades. Civil and Environmental Research, 6(5), 41-47.

[7] Munaaim, M. A. C., et al. (2021). Review on the Potential of Micro Hydro Electric Generator Embedded at Effluent Discharge of Sewerage Treatment Plant. Jurnal Teknologi (Sciences & Engineering).

[8] Nugraha, I. M. A., & Desnanjaya, I. G. M. N. (2025). Energy efficiency in aeration systems for aquaculture ponds: a comprehensive review. Jurnal Riset Akuakultur, 20(1), 1-25.

[9] Pokharel, G. R., Chhetri, A. B., Khan, M. I., & Islam, M. R. (2008). Decentralized Micro-Hydro Energy Systems in Nepal: En Route to Sustainable Energy Development. Energy Sources, Part B: Economics, Planning, and Policy, 3(2), 144–152.

[10] Putra, Y. S., Noviani, E., & Muhardi, M. (2022). Numerical Study of the Effect of Penstock Dimensions on a Micro-Hydro System using a Computational Fluid Dynamics Approach. International Journal of Renewable Energy Development, 11(2), 491–499.

[11] Roy, S. M., P, J., Machavaram, R., Pareek, C. Á., & Mal, B. C. (2021). Diversified aeration facilities for effective aquaculture systems—a comprehensive review. Aquaculture International, 29(3), 1181-1217.

PERFORMANCE EVALUATION OF THE EXPERIMENTAL PLANER-GRADER MODEL FOR PERMANENT GRASSLAND MAINTENANCE

/

EVALUAREA PERFORMANȚELOR MODELULUI EXPERIMENTAL DE RINDEA-GREDER PENTRU ÎNTREȚINEREA PAJIȘTILOR PERMANENTE

Eugen MARIN*[1)], Vasile MOCANU[2)], Tudor-Adrian ENE[2)], Dragoș MANEA[1)], Mihai-Gabriel MATACHE[1)], Laurențiu-Constantin VLĂDUȚOIU[1)], Alexandru IONESCU[1)]

[1)] National Institute of Research - Development for Machines and Installations Designed to Agriculture and Food Industry - INMA Bucharest / Romania;

[2)] Institute of Research-Development for Grasslands-ICDP Brasov, Brasov County / Romania.

**Tel: 0758 437 214; *E-mail: marineu61@yahoo.com*

Keywords: *planer-grader, permanent grasslands, maintenance, environmental protection, biodiversity*

ABSTRACT

The paper presents the results of field testing under real operating conditions of an experimental planer-grader model designed for permanent grassland maintenance, developed within the ADER 15.3.2 project. The study focused on the machine's performance in destroying molehills on an experimental plot located in the Drăguș area (Brașov County, Romania). The research included the determination of pedoclimatic characteristics, soil resistance and moisture analysis, as well as the evaluation of energetic and operational indicators such as working speed, traction force and power, effective working capacity, and specific fuel consumption. The obtained results demonstrated the technical and functional efficiency of the equipment, confirmed by the final expert assessment that highlighted its reliability. The study concludes that the experimental planer-grader model represents a viable solution for permanent grassland maintenance works, contributing to environmental protection and biodiversity conservation.

REZUMAT

Lucrarea prezintă rezultatele testării, în condiții reale de exploatare, a modelului experimental de rindea-greder pentru întreținerea pajiștilor permanente, dezvoltat în cadrul proiectului ADER 15.3.2. Studiul a urmărit comportarea utilajului la lucrările de distrugere a mușuroaielor pe un lot experimental situat în zona Drăguș (județul Brașov). Cercetările au inclus determinarea caracteristicilor pedoclimatice, analiza rezistenței și umidității solului, precum și evaluarea indicatorilor energetici și de exploatare, cum ar fi viteza de lucru, forța și puterea de tracțiune, capacitatea efectivă de lucru și consumul specific de combustibil. Rezultatele obținute au demonstrat eficiența tehnică și funcțională a echipamentului, confirmată și prin expertiza finală, care a evidențiat fiabilitatea acestuia. Concluziile studiului arată că modelul experimental de rindea-greder reprezintă o soluție viabilă pentru lucrările de mentenanță a pajiștilor permanente, contribuind la protecția mediului și menținerea biodiversității.

INTRODUCTION

Grasslands are essential ecosystems representing up to 40% of its land area (*Petermann, J.S. & Buzhdygan, O.Y.,2021*), with a role in conserving biodiversity, maintaining soil fertility, protecting against erosion and capturing atmospheric carbon.

Grasslands, through the integration of grasses and legumes (*Li, Z. et al., 2024*), provide animal feed, raw material for agriculture and contribute to the ecological balance of rural areas.

By maintaining dense and diversified vegetation, grasslands support hydrological functions, reduce the risk of floods and contribute to the conservation of specific flora and fauna (*Jia, H. et al., 2025*).

Sustainable grassland management, where it is currently homogeneous, is an important first step towards improving multifunctionality at the landscape scale (*Richter, F. J. et al., 2024*) and can be achieved by monitoring the state of vegetation and soil, carrying out periodic maintenance work (destruction of weeds, mowing, scarification, fertilization), avoiding overgrazing and maintaining the balance between agronomic use and environmental protection (*Liu, K., & Shao, X., 2024*). These interventions prevent land degradation, loss of soil fertility and the emergence of invasive species, thus the grassland vegetation ecosystem can be protected, preserving its richness and diversity (*Zhang, L., & Li, J., 2024*).

The grassland planer-grader is used for cleaning annual and multi-annual weeds, removing solid manure and micro-leveling the land on degraded permanent grasslands (*Zimmer, A. et al., 2024*). The machine can be towed during work and semi-mounted during transport, providing flexibility and adaptability to different terrain conditions.

The main components of the planer-grader include: assembled frame, left leveling blade, right leveling blade, rear leveling blade, front disc battery, left and right side disc batteries, rear leveling blade lifting-lowering mechanism, hydraulic system, running gear and tow bar. The machine operates in aggregate with wheeled tractors with powers between 59 and 81 kW (80–100 HP), offering high performance and energy efficiency (*Mocanu, V. et al., 2019*).

The experimental model of the 2.0 m planer-grader, used with the New Holland TL100A tractor, was developed by ICDP Brașov (*Mocanu, V. et al., 2024*), and the field experiments for the performance analysis were carried out by the ICDP Brașov team, in collaboration with the INMA Bucharest team.

In the international context, there are several models of planers-graders specialized for the destruction of dunghills and the maintenance of grasslands (*Mocanu, V. et al., 2021*). For example, the Robert DBS Dung Spreader Harrow is equipped with 40 cm leveling blades, effective in destroying dunghills and evenly distributing organic residues on the surface of grasslands. It also includes 10 cm solid manure spreading blades for evening out the residues and flexible tines for aerating and regenerating the soil, allowing for efficient management of stubble and organic residues and helping to improve soil structure (Pasture harrow, dung spreader DBS (atelier-robert.be)).

Another example is the Mole Hill Destroyer, a machine dedicated to destroying molehills, which levels the ground and prevents damage to equipment. It has working widths of 3.05 m and 3.66 m, can be mounted on various types of harrows and is easy to use and maintain. Its efficiency in molehill management helps prevent damage to equipment and improve the quality of grasslands (molehilldestroyer.com). At the same time, the HE-VA Grass Rejuvenator is a multifunctional machine that includes cutting plates and ploughing blades for leveling molehills and rehabilitating grasslands. It has heavy-duty working rods for soil aeration and offers the possibility of adding a seeder for vegetation regeneration. Thus, the machine allows for efficient leveling of molehills and rehabilitating grasslands, contributing to increasing forage production (Grass Rejuvenator, level, scarify, reseed - HE-VA UK). The present study aims to analyze the performance of the 2.0 m experimental planer-grader model, used with the New Holland TL100A tractor, under real operating conditions, focusing on pedoclimatic characteristics, energy indices, working times and fuel consumption, providing useful information for sustainable grassland management.

MATERIALS AND METHODS

Within the Brașov ICDP, a technology was created to improve degraded grasslands by cleaning annual and multi-annual weeds, solid manure and micro-leveling the land with an experimental model of a 2.0 m grassland grader (fig. 1).

Fig. 1 - Experimental model of 2.0 m grassland grader planer

The operating principle is based on the combined action of the leveling blades and the rotating discs. During work, the tractor pulls the machine, and the left, right and rear leveling blades penetrate the surface layer of the soil to destroy annual and perennial weeds and level the land.

The adjustment of the depth and angle of the rear blade, carried out by the hydraulic lifting-lowering mechanism, allows the machine to adapt to different ground conditions and the degree of degradation of the meadow. The disc batteries, located at the front and sides, ensure the uniform breaking and distribution of organic residues and solid manure, contributing to the natural fertilization of the soil and stimulating the regeneration of vegetation. The undercarriage and the drawbar provide stability and maneuverability during work, and the assembled frame ensures the integration and rigidity of all components. Thus, the machine simultaneously combines land leveling, soil aeration, uniform spreading of manure and rehabilitation of degraded grasslands, reducing manual effort and preventing damage to both the land and the equipment.

This integrated operation makes the grader an essential tool for sustainable grassland management and increasing forage productivity.

Table 1 presents the main technical characteristics of the experimental model of the 2.0 m grassland grader planer.

Table 1

The main technical characteristics of the equipment used in the experiment

Characteristic	Value
Working width, [m]	2
Front disc battery	
- number of discs, [pcs.]	12
- disc diameter, [cm]	46
- disc type	dentate
Side disc battery	
- number of discs [pcs.]	4
- disc diameter [cm]	4
- disc type	sleek
Weight, [kg]	1613

The determination of the indices under operating conditions was carried out through experimental field research, on an experimental lot belonging to SC GUSUTRI COM SRL, a collaborating company of ICDP Brașov, located in Drăguș, Brașov County.

In April 2025, in Drăguș, Brașov County, average daytime temperatures were approximately 15°C, and nighttime temperatures around 3°C. Total precipitation was approximately 65 mm, distributed over 15 days, with an average humidity of 79% and wind with an average speed of 11 km/h.

Additional equipment used:

- to determine the degree of soil compaction, a Wile penetrometer was used, an instrument designed to measure soil resistance to penetration (*Ulanov, A. S.,et alea, 2024*). Measurements were made starting from 5 m from the end of the experimental plot and at different points separated in a diagonal direction towards the end;
- for direct measurement of water content, expressed as a percentage of the soil volume, the portable soil moisture meter Extech MO750 (*Hilal et al., 2022*). Soil moisture was determined at the same points where soil resistance to penetration was measured.

Table 2 presents the characteristics of the experimental field on which the experiments were carried out, with the experimental model of machine for overseeding degraded grasslands in aggregate with the TL 100A New Holland tractor.

Table 2

Characteristics of the experimental field

No.	Characteristic	Value
1	Soil type	brown
2	Degree of soil coverage with plants, [%]	70-80
3	Average plant height, [cm]	12
4	Plant mass, [g/m2]	100
5	Average soil moisture in the 0…10 cm layer, [%]	7,02
6	Penetration resistance in 10 cm layer, [MPa]	1,655

Calculation of the slippage δ of the drive wheels of the tractor from the TL 100A New Holland aggregate, slippage that occurs in the process of transmitting the tractor's traction power to carry out the working process of the experimental model, was calculated as follows:

- the slippage of the drive wheels was evaluated by comparing the number of rotations under load (Ns) with the number of rotations under load (Ng), according to the ISO/OECD standard 789-10:2006. The number of rotations under load was recorded separately for the left and right wheels, and the value used in the calculation was the arithmetic mean:

$$N_s = \frac{N_{sst} + N_{sdr}}{2} \quad (1)$$

- the number of idle revolutions was calculated based on the length of the test route (L=50 m) and the developed length of the tractor wheel (Lr):

$$N_g = \frac{L}{L_r} \quad (2)$$

- the slippage of the driving wheels was calculated according to the relationship:

$$\delta = \left(\frac{N_S - N_g}{N_S}\right) \times 100, [\%] \quad (3)$$

This method allowed the assessment of traction losses and the degree of slippage of the drive wheels.

The traction force was determined by the tensometric method using strain gauges, an acquisition system and a computer equipped with a specialized software package. The data that were stored were retrieved and processed by specialized software, after which the average values of the traction force were determined by eliminating the transition regimes during experimental research (*Matache et al., 2020; Persu et al., 2020*).

The traction power Ptr was calculated based on the travel speed vl and the traction force Ftr (*Marin et al., 2012*).

The determination of the exploitation indices (effective working time, time losses, effective working capacity and fuel consumption per hectare) of the experimental model of the overseeding machine in aggregate with the New Holland TL 100A tractor allowed the evaluation of the performance, which would ensure maximum economic effects in the concrete conditions of each farm (*Hunt, 2008*).

The determination of the fuel consumption per hectare was based on the direct measurement of the volume of fuel consumed, which consisted of completely filling the tank before the overseeding operation, carrying out the work on a determined area and finally filling the tank again and measuring the volume of fuel added (*Voicu et al., 2020*).

To ensure the reproducibility of the results, each experiment was carried out in 3 independent repetitions. The data obtained were statistically processed by calculating the mean, standard deviation and coefficient of variation, providing a measure of the variability and consistency of the results.

RESULTS AND DISCUSSION

The soil penetration resistance in the experimental plot was determined according to the procedure using a portable Wile penetrometer. The values obtained were 200 psi for the 0–10 cm layer, 220 psi for 10–20 cm and 240 psi for 20–30 cm. The superficial layer falls within the zone of good growing conditions, while the deeper layers show moderate compaction, which can limit root development and reduce water infiltration and gas exchange.

The average soil moisture, determined simultaneously with the penetration measurements, was 7.03%. Table 3 presents the average values of soil penetration resistance and soil moisture obtained from the measurements.

Table 3

Average values of soil characteristics of the experimental field

No.	Characteristic	Value
1	Average soil penetration resistance, [Kpa]	1517
2	Average soil moisture, [%]	7,03

The high resistance to penetration can be partly attributed to this low humidity. From a grassland management perspective, the results highlight the need for regular monitoring of soil compaction, especially after dry periods, and the application of light aeration or scarification work.

Table 4 presents the average values of the energy indices (average working speed and slippage of the tractor drive wheels of the aggregate) achieved for two speeds of the tractor in the aggregate.

Table 4

Average working speed and slippage of the tractor drive wheels in the aggregate

Speed level	Average speed of travel, [km/h]	Average slippage, [%]
V_1	5,25	11,13
V_2	5,91	10,88

The analysis of the results shows that, with the increase in travel speed, the slip of the drive wheels is slightly reduced, from 11.13% in gear V_1 to 10.88% in gear V_2.

This is explained by the increase in the dynamic stability of the aggregate and by a more uniform distribution of the load on the contact surface with the ground. The recorded values are below the threshold of 15%, considered optimal for surface agricultural work, which confirms good wheel adhesion and satisfactory efficiency of power transmission to the ground.

The determinations regarding the average working speed and the slip of the drive wheels of the tractor in the aggregate were carried out under real operating conditions, and Figure 2 shows an aspect of these measurements.

Fig. 2 - Appearance during measurements to determine the working speed and slippage of the tractor's drive wheels

The tensile force of the 2.0 m experimental planer-grader model was determined by the tensometric method, using 120 Ω strain gauges (type KFG-6-120-C1-11 N15C2) mounted on the tractor's drawbars and a QuantumX 1615 data acquisition system.

Figure 3 shows the materials and equipment used to determine the tensile strength.

Fig. 3 - Aspects during preparation for determining tensile strength

Table 5 presents the average values of working speed, tractive force (F_{tr}) and the calculated values of the required tractive power (P_{tr}) for the experimental model of a 2.0 m grassland planer-grader made for two speeds of the tractor in the aggregate.

Table 5

Average values of working speed, tractive effort and tractive power

Speed level	Working speed average		Average tractive force	Average tractive effort	
	[m/s]	[km/h]	[daN]	[CP]	[kW]
V_1	1,46	5,25	18450	35,88	26,39
V_2	1,64	5,91	18580	40,68	29,91

Table 6 presents the average values of the theoretical working capacity determined in two speed ranges for the experimental model of a 2.0 m planer-grader in aggregate with the New Holland TL 100A tractor on the experimental lot of SC GUSUTRI COM SRL located in Drăguș, Brașov County.

Table 6

Average values of theoretical work capacity

Speed level	Average working speed V_l	Average working width, B_l	Average theoretical working capacity, W_t
	[km/h]	[m]	[ha/h]
V_1	5,25	1,9	0,998
V_2	5,91	1,9	1,23

In the experiments under operating conditions carried out on an area of 0.3762 ha, the experimental model of a 2.0 m grassland planer-grader performed well throughout the period, under these conditions it achieved an operating safety coefficient of 0.96, an hourly performance capacity of 0.548 ha/h and a fuel consumption of 15.02 l/ha.

Figure 4 graphically presents the operating indices achieved during the tests.

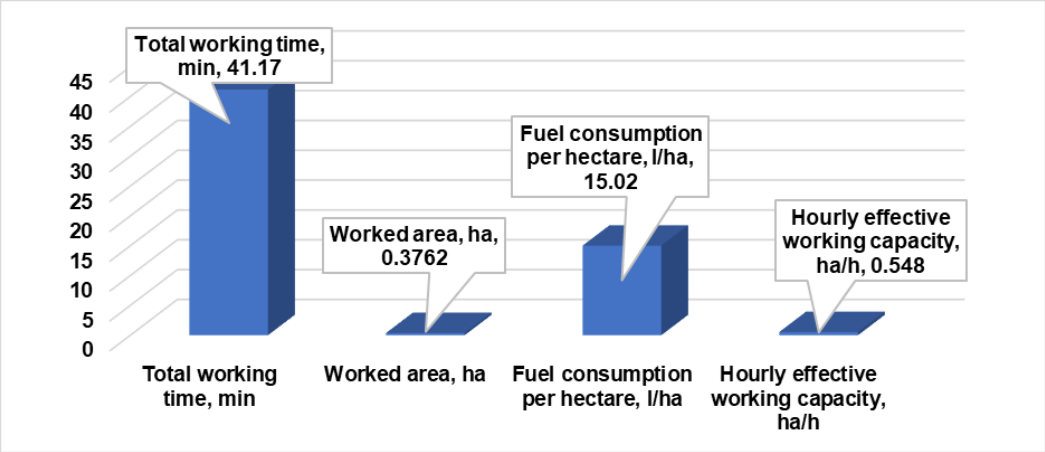

Fig. 4 - Operating indices achieved by the 2.0 m grassland planer-grader

Operating indices obtained:

- Total working time was 41.17 minutes (0.686 h).
- The achieved working capacity was 0.548 ha/h, which represents 50% of the theoretical capacity (1.10 ha/h).

Causes: Long times for turning, short length of the plot and the need for technical interventions.

- Consumption per hectare: 15.02 l/ha – is within normal limits for light work, without high resistance to advancement.

The energy efficiency and organization of the work were good, and time losses were moderate. The indicators obtained confirm that the assembly used is appropriate for this type of work, and productivity can be improved by reducing auxiliary times and combining work on larger areas.

Figure 5 presents some aspects before testing the experimental model of the 2.0 m meadow planer-grader (spring season).

Fig. 5 - Aspects before testing the experimental model of the 2.0 m meadow planer-grader (spring season)

Figure 6 presents some aspects after testing the experimental model of the 2.0 m meadow planer-grader (spring season).

Fig. 6 - Aspects after testing the experimental model of a 2.0 m meadow planer-grader (spring season)

CONCLUSIONS

- The experimental model of a grassland planer-grader for the maintenance of permanent grasslands, tested under real operating conditions on a 0.3762 ha plot in the Drăguș area (Brașov county), demonstrated very good operational performance and reliability.
- The effective working capacity obtained was 0.548 ha/h, representing approximately 50% of the theoretical capacity (1.10 ha/h), the difference being mainly determined by the turning times, the small plot size and the auxiliary adjustments made during operation.
- The specific fuel consumption was 15.02 l/ha, which is within normal limits for light plowing and maintenance of the grassland surface, confirming the energy efficiency of the machine.
- The equipment maintained good traction performance, with wheel slip values below 12%, ensuring efficient power transmission and minimal soil disturbance.
- The overall operational safety coefficient was 0.96, indicating a high level of functional reliability of the prototype grader-planer.
- Compared to other mechanized maintenance works (such as scarification or fertilization), the operation of the grassland planer-grader equipment offers a balanced ratio between fuel consumption and labor efficiency, ensuring both technical efficiency and environmental protection.
- The results obtained confirm that the experimental model of the 2.0 m grassland planer-grader represents a viable technological solution for the sustainable management and rehabilitation of permanent grasslands, contributing to increased productivity, soil protection and biodiversity conservation.

ACKNOWLEDGEMENT

The results presented in this article were obtained with the support of MADR through the "Sectoral Plan - ADER 2026", financing contract no. 15.3.2 / 17.07.2023, ADER project 15.3.2. Research on the

development and promotion of mechanization technologies for the reconstruction, maintenance of permanent meadows, environmental protection and biodiversity maintenance using new specific equipment, managed by the Research -Development Institute for Grasslands Brasov- Mechanization Laboratory.

REFERENCES

[1] Jia, H., Tian, B., Song, X., Sun, W., & Mu, X. (2025). Hydrological shifts from vegetation restoration in semi-arid regions: insights from the typical watersheds of the Yellow River. *Ecological Indicators*, *178*, 113924.

[2] Hilal, Y. Y., Khessro, M. K., van Dam, J., & Mahdi, K. (2022). Automatic water control system and environment sensors in a greenhouse. *Water, 14(7*), 1166

[3] Hunt, D. (2008). *Farm power and machinery management*. Waveland Press.

[4] Li, Z., Li, Y., Yao, B., & Carmona, C. (2024). Optimising management practices to secure grassland agroecosystems' sustainability. *Frontiers in Sustainable Food Systems*, *8*, 1507692.

[5] Liu, K., & Shao, X. (2024). Grassland ecological management and utilization for sustainability. *Agronomy*, *14*(1), 149.

[6] Marin E., Sorica C., Manea D., (2012), The establishing of corn with the equipment for soil tillage and sowing in narrow strips, *40. Symposium "Actual Tasks on Agricultural Engineering", Opatija, Croatia*, 231-241 ref. 9

[7] Matache, M. G., Cristea, M., Găgeanu, I., Zapciu, A., Tudor, E., Carpus, E., & Popa, L. D. (2020). Small power electric tractor performance during ploughing works. *Inmateh-agricultural engineering*, *60*(1).

[8] Mocanu, V., Ene, T. A., Marin, E., & Gheorghita, N. E. (2024). Mechanization of Grassland Farming by Technological Variants with Minimal Inputs: A Review. *INMATEH Agricultural Engineering*, *74*(3), 954-70.

[9] Mocanu, V., Dragomir, N., Tod, M. A., Mocanu, V., Ene, T. A., & Blaj, V. A. (2021). *Pajistile Romaniei-resurse, strategii de imbunatatire si valorificare*. Editura Universitatii Transilvania din Brasov.

[10] Mocanu, V., Ene, T. A., & Blaj, V. A. (2019). Levelling-greder equipment for grassland, RGP-2,0 type. In *Proceedings of the International Symposium ISB-INMA-TEH: Agricultural and Mechanical Engineering* (pp. 305–310). Bucharest, Romania: ISB-INMA-TEH.

[11] Petermann, J. S., & Buzhdygan, O. Y. (2021). Grassland biodiversity. *Current Biology*, *31*(19), R1195-R1201.

[12] Persu, C., Gheorghe, G., Găgeanu, I., Cujbescu, D., Fogoraş, A., & Lateş, D. (2020). Influence on quality and energy indices for a reversible plow equipped with electric vibrators. *" Annals of the University of Craiova-Agriculture Montanology Cadastre Series"*, *50*(2), 453-457.

[13] Richter, F. J., Suter, M., Lüscher, A., Buchmann, N., El Benni, N., Feola Conz, R., ... & Klaus, V. H. (2024). Effects of management practices on the ecosystem-service multifunctionality of temperate grasslands. *Nature communications*, *15*(1), 3829.

[14] Ulanov, A. S., Kupryashkin, V. F., Naumkin, N. I., & Naumkin, D. A. (2024). Investigating the Soil Hardness on Personal Subsidiary and Individual Peasant Farms. *Engineering technologies and systems*, *34*(4), 530-548

[15] Voicu, G., Constantin, G. A., Matache, M. G., Tudor, P., & Poenaru, I. C. (2020). Research on tensile strength and specific fuel consumption for a Miscanthus rhizome planter in different equipping conditions at the four row. *Scientific Papers. Series A. Agronomy*, *63*(1).

[16] Zimmer, A. H., Macedo, M. C. M., Kichel, A. N., & Euclides, V. P. B. (2004). Integrated agropastoral production systems. *Agropastoral systems for the tropical savannas of Latin America. Cali: CIAT*, 253-290.

[17] Zhang, L., & Li, J. (2024). Sustainable land management and degraded grassland restoration: Key measures for vegetation and soil health. *Resources Data Journal*, *3*, 175-178.

SIMPLIFIED MODELING OF ACOUSTIC ATTENUATION FOR SOUND BARRIERS
/
MODELAREA SIMPLIFICATĂ A ATENUĂRII ACUSTICE PENTRU BARIERE SONICE

Ana-Maria GROSU*[1)], Ovidiu VASILE*[2)]
[1)] National University of Science and Technology POLITEHNICA Bucharest, Faculty of Biotechnical Systems Engineering, Bucharest / / Romania;
[2)] National University of Science and Technology POLITEHNICA Bucharest, Faculty of Biotechnical Systems Engineering, Department of Mechanics "Radu P. Voinea", Bucharest / Romania.
*Tel: 0722 172 700; *E-mail: ovidiu_vasile2002@yahoo.co.uk, ana_maria.grosu@stud.isb.upb.ro*

Keywords: *sound barriers, acoustic attenuation, frequency variation.*

ABSTRACT
The paper presents a simplified calculation model for evaluating the acoustic attenuation of two constructive typologies of sound barriers, which highlights the differences in dB of the acoustic level at the receiver depending on the frequency variations. A comparative analysis is carried out for frequencies of 600 Hz, 1200 Hz, 2400 Hz, and 3600 Hz, depending on the distance between the sound barriers and the position of the receiver.

REZUMAT
Lucrarea prezintă un model de calcul simplificat pentru evaluarea atenuării acustice a două tipologii constructive de bariere fonice prin care se evidențiază diferențele în dB a nivelului acustic de la receptor în funcție de variațiile de frecvență. Se realizează o analiză comparativă pentru frecvențe de 600 Hz, 1200 Hz, 2400 Hz și 3600 Hz în funcție de distanța dintre barierele fonice și poziția receptorului.

INTRODUCTION

Noise pollution constitutes a significant environmental concern in urban areas, with road traffic identified as the predominant source. Approximately 70% of urban noise is attributable to transportation activities *(Medina, M. G. O. et al., 2010; Siano D., 2012),* underscoring its substantial contribution to ambient sound levels.

The public health implications of noise exposure are considerable. A report by the World Health Organization (WHO) indicates that Europeans collectively lose at least one million healthy life years annually due to diseases and disabilities induced by environmental noise, with road traffic noise being a primary contributor *(Fritschi, L.; Brown, L. et al., 2011; Gil-Lopez T. et al., 2017).* Beyond direct health impacts, noise pollution detrimentally affects various occupational and institutional settings, including schools, universities, offices, and hospitals, thereby compromising general well-being. For instance, in educational environments, elevated noise levels can disrupt teaching and learning processes by necessitating increased auditory effort in study spaces, potentially impairing concentration and academic performance.

Noise pollution pervades various occupational and institutional settings, including schools, universities, offices, and hospitals, thereby impacting working environments and overall well-being. In educational contexts, for instance, ambient noise can significantly disrupt pedagogical and learning processes, demanding increased auditory effort within study spaces *(Sala E, Rantala L., 2016; Silva LT, Oliveira IS, Silva JF., X)*.

Construction-generated noise represents another critical area of concern, primarily due to the elevated noise exposure levels experienced by workers *(Lee, S.C., et al., 2019; Li, X., et al.,).* This issue has gained amplified significance in recent years, driven by heightened environmental awareness within both the public and corporate sectors. Construction noise is known to induce *discomfort (Lee, S.C., et al.,; Liu, Y.; Xia, B. et al., 2017; Kwon, N. et al., 2018)* and can elicit adverse behavioral effects on surrounding communities. Furthermore, the effective control of on-site construction noise is inherently complex, compounded by several interacting factors: the ubiquitous presence and variability of noise sources, continuous logistical flows of materials, personnel, and vehicles, the inherent scale of construction sites, the limited efficacy of many attenuation solutions at lower frequencies, and the intrinsic difficulty in precisely evaluating the effects of implemented mitigation measures *(Sohrabi, S., Pàmies Gómez, T., & Romeu Garbí, J., 2020).* The modernization of road transport infrastructure has led to the construction of high-capacity

highways primarily designed to bypass residential areas. However, achieving this objective is not always feasible, particularly in regions experiencing intensive urban development where highways are often situated in close proximity to cities to facilitate convenient connectivity between urban and interurban traffic. Furthermore, the development of urban agglomerations along highway corridors can necessitate acoustic monitoring of these newly formed populated areas *(Enescu N., Vasile O.).*

Within the European Union, efforts to mitigate noise levels have been formalized through legislative frameworks. Notably, the EEC Machine Safety Directive of 1989, subsequently augmented by amendments in 1991 and 1993, established regulations pertaining to noise reduction *(Brooks B. M. et al., 1996).*

MATERIALS AND METHODS

In Figure 1, a thin, semi-infinite barrier is illustrated, characterized by a height *H*, with an acoustic source *S* located on the left side at a distance d_s from the barrier and 0,5 m above the ground. On the right side, the receiver *R* is positioned at height y_R and distance x_R. The source generates exclusively pure tones.

This study aims to evaluate the levels of acoustic attenuation achieved through the application of the Moreland–Musa method. The assessment will specifically focus on the spatial distribution of sound level reduction within the immediate proximity of a sound-absorbing panel.

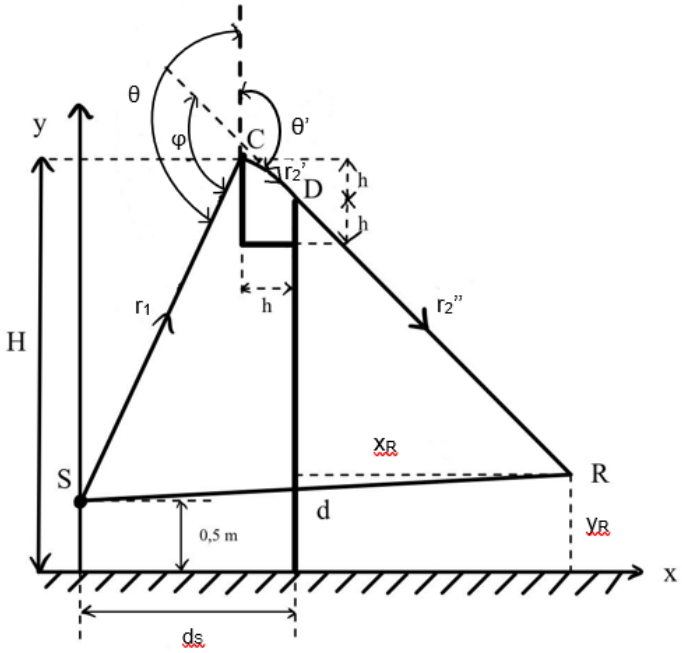

Fig. 1 - Barrier - variant 1

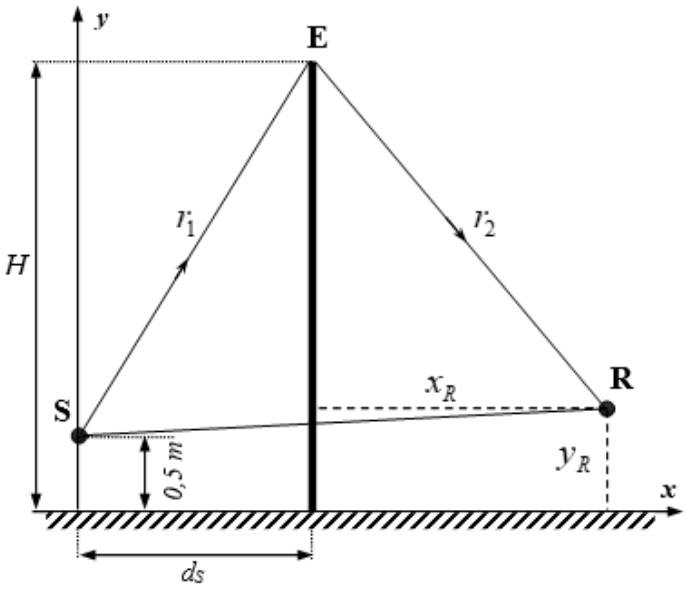

Fig. 2 - Barrier – variant 2

The fixed data are: H=4,6 m, h=0,3 m, d_s=3,2 m, which allows the determination of the coordinates of the points: S(0;0,5), D(3,2;4,3), C(2,9;4,6), and E(3,2;4,6).

In the first variant, based on the coordinates of points ***S***, ***D,*** and ***C*** relative to the axes of the considered system, the following distances are obtained:

$$r_1 = SC = \sqrt{(x_C - x_S)^2 + ({y_C}^2 - {y_S}^2)} = \sqrt{2{,}9^2 + (4{,}6 - 0{,}5)^2} = 5{,}02\,m \quad (1)$$

$${r_2}' = CD = \sqrt{(3{,}2 - 2{,}9)^2 + (4{,}3 - 4{,}6)^2} = 0{,}42\,m \quad (2)$$

In the second approach, given the coordinates of points ***S*** and ***E*** with respect to the chosen reference system, the distance can be calculated as follows:

$$r_1 = SE = \sqrt{3{,}2^2 + (4{,}6 - 0{,}5)^2} = 5{,}2\,m \quad (3)$$

The receiver ***R*** coordinates are comprised in the intervals: $x_R = [3{,}5 \ldots 32]$, $y_R = [1 \ldots 4]$, distances are in meters.

The attenuation was determined using a computational program, with discretization intervals of ***Δx*** = 0,5 m along the *Ox* direction and ***Δy*** = 1 m along the *Oy* direction.

Since the magnitude of the attenuation depends on the sound frequency, calculations were carried out for four distinct frequencies: f = *(600, 1200, 2400,* and *3600) Hz*, as the noise exhibits a continuous distribution over the entire frequency range.

The Moreland–Musa formula, applied for the calculation of the attenuation in the first approach, is given below:

$$A = 10\log\left\{3 + \frac{10}{\pi}k[(r_1 + {r_2}' + {r_2}'') - d]\right\} \text{ [dB]} \quad (4)$$

$${r_2}'' = DR = \sqrt{(x_R - d_S)^2 + (y_R - H + h)^2} \text{ [m]} \quad 5)$$

and in the case of the second variant is:

$$A = 10\log\left\{3 + \frac{10}{\pi}k[(r_1 + r_2) - d]\right\} \text{ [dB]} \quad (6)$$

$$r_2 = ER = \sqrt{(x_R - 3{,}2)^2 + (y_R - 4{,}6)^2} \text{ [m]} \quad (7)$$

For these cases, we compute the distance $d$using the next equation:

$$d = \sqrt{{x_R}^2 + (y_R - 0{,}5)^2} \text{ [m]} \quad (8)$$

k - wave number, *k=f/c*, where *f* is the sound frequency, and $c = 344$ m/s, represents the standard speed of sound.

RESULTS

In variant 1, due to the shape of the upper barrier, an additional reduction occurs caused by the diffraction phenomenon, which adds to the decrease calculated using equation (4). This additional reduction is determined through the supplementary damping factor *E*, whose value depends on the width *h* of the barrier and the angles *θ* and *θ'*.

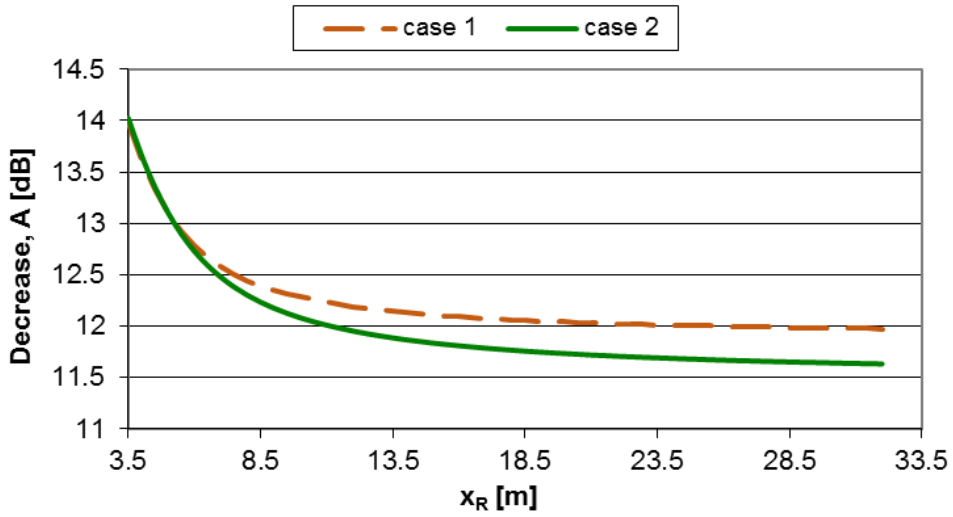

Fig. 3 - Representation of the decrease at 600 Hz for y_R=2m

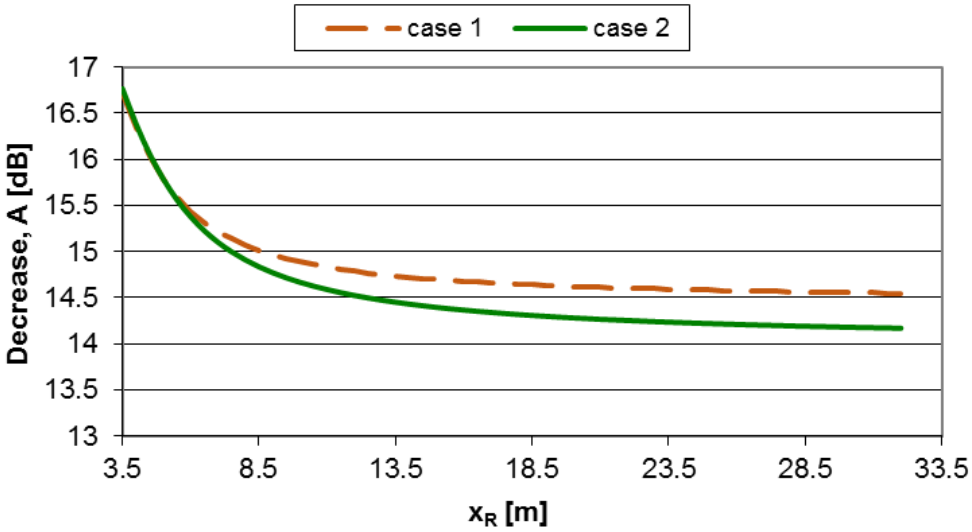

Fig. 4 - Representation of decrease at 1200 Hz for y_R=2m

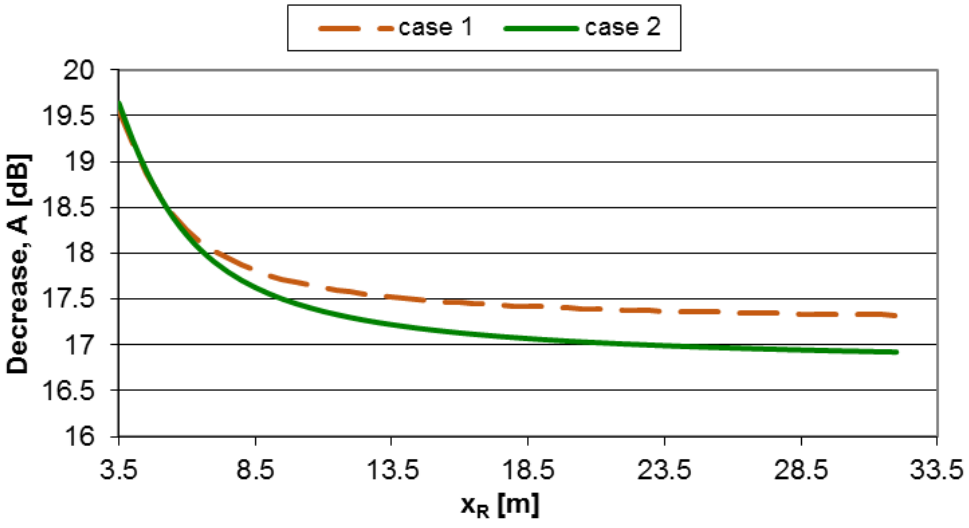

Fig. 5 - Representation of decrease at 2400 Hz for y_R=2m

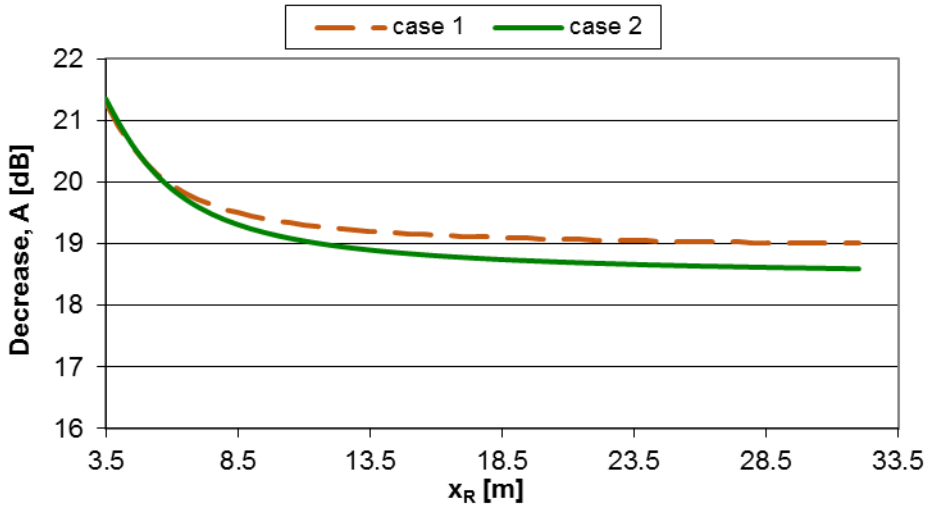

Fig. 6 - Representation of decrease at 3600 Hz for y_R=2m

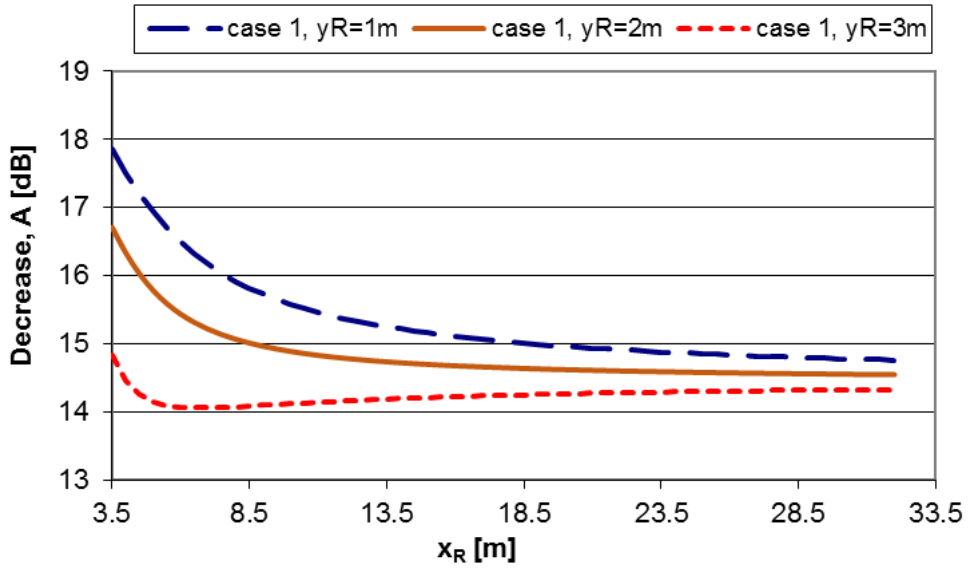

Fig. 7 - Representation of attenuation in case 1 for f=1200 Hz, y_R=1 m, y_R=2 m, y_R=3 m.

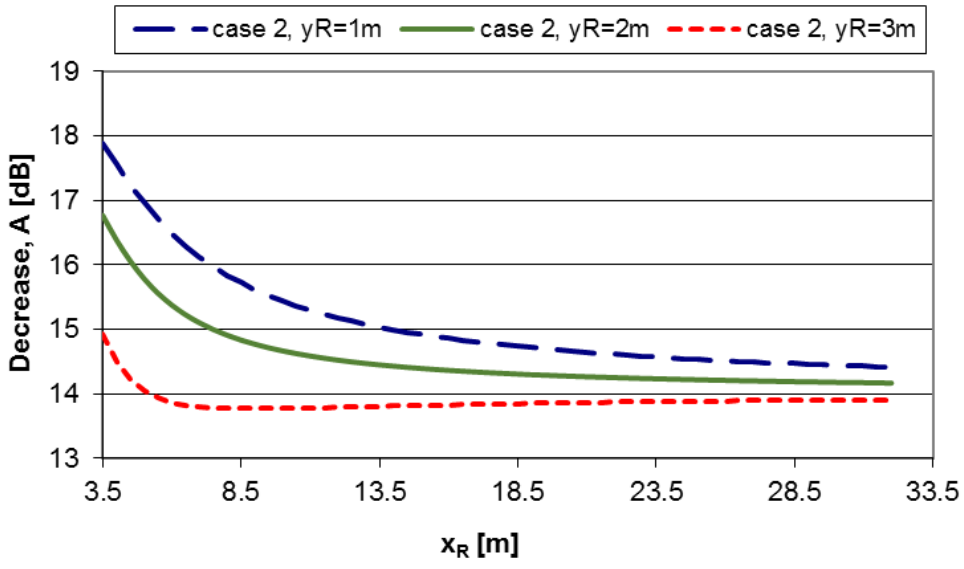

Fig. 8 - Representation of attenuation in case 2 for f=1200 Hz, y_R=1 m, y_R=2 m, y_R=3 m.

CONCLUSIONS

Analyzing the results presented in Figures 3–5, it can be observed that the attenuation produced by the barrier increases with frequency, confirming that acoustic barriers are more effective for higher noise frequencies. In variant 1, due to the shape of the upper part of the barrier, an additional reduction in sound level occurs, caused by the diffraction phenomenon, which adds to the attenuation calculated using the theoretical relation. This difference is quantified by the supplementary damping factor $\boldsymbol{E}$, which depends on the width h of the barrier and the angles of incidence $\boldsymbol{\theta}$ and $\boldsymbol{\theta'}$.

The graphs show that at short distances from the barrier, the variation in attenuation is more pronounced, while at larger distances the values tend toward a constant limit. Furthermore, the position of the receiver $\boldsymbol{y_R}$ slightly influences the attenuation level, with higher values observed at lower heights. Comparing the two analyzed cases, it is evident that variant 1 generally provides higher attenuation, highlighting the importance of the barrier's geometric shape in controlling sound propagation.

The results confirm the significant role of diffraction in noise reduction and indicate that optimizing the upper profile of the barrier can lead to notable acoustic improvements without major structural modifications.

REFERENCES

[1] Brooks, B. M., DuBois, T. J., Hoover, R. M., Maling, G. C., & Sutherland, L. C. (1996). *A global vision for the noise control marketplace*.

[2] Enescu, N., & Vasile, O. (2007). *The decrease of noise with acoustics barriers*. Romanian Journal of Acoustics and Vibration, issue IV, no. 2, pp. 71-74, https://sra.ro/Arhiva/2007/nr2/3.Enescu_Vasile.pdf.

[3] Fritschi, L., Brown, L., Kim, R., Schwela, D., & Kephalopoulos, S. (2011). *Burden of disease from environmental noise – Quantification of healthy life years lost in Europe*. WHO European Centre for Environment and Health, Bonn Office.

[4] Gil-López, T., Molina, M. M., Vázquez, A. V., & Rodríguez, B. M. (2017). Acoustic and economic analysis of the use of palm tree pruning waste in noise barriers to mitigate the environmental impact of motorways. *Science of the Total Environment, 584–585*, 1066–1076, https://doi.org/10.1016/j.scitotenv.2017.01.177

[5] Kwon, N., Song, K., Lee, H.-S., Kim, J., & Park, M. (2018). Construction noise risk assessment model focusing on construction equipment. *Journal of Construction Engineering and Management, 144*(1), 1–12, https://doi.org/10.1061/(ASCE)CO.1943-7862.0001410

[6] Lee, S. C., Kim, J. H., & Hong, J. Y. (2019). Characterizing perceived aspects of adverse impact of noise on construction managers on construction sites. *Building and Environment, 152*, 17–27, https://doi.org/10.1016/j.buildenv.2019.01.010

[7] Lee, S. C., Hong, J. Y., & Jeon, J. Y. (2015). Effects of acoustic characteristics of combined construction noise on annoyance. *Building and Environment, 92*, 657–667, https://doi.org/10.1016/j.buildenv.2015.05.027

[8] Li, X., Song, Z., Wang, T., Zheng, Y., & Ning, X. (n.d.). Health impacts of construction noise on workers: A quantitative assessment model based on exposure measurement. *Journal of Cleaner Production*.

[9] Liu, Y., Xia, B., Cui, C., & Skitmore, M. (2017). Community response to construction noise in three central cities of Zhejiang province, China. *Environmental Pollution, 230*, 1009–1017, https://doi.org/10.1016/j.envpol.2017.07.049

[10] Medina, M. G. O., & Montaño, A. F. (2010, November). Urban noise and transport as a strategy of environmental quality. In *2nd Pan-American and Iberian Meeting on Acoustics, 160th ASA Meeting, 7Congress FIA, 17Congress IMA*. Cancún, México.

[11] Sala, E., & Rantala, L. (2016). Acoustics and activity noise in school classrooms in Finland. *Applied Acoustics, 114*, 252–259. https://doi.org/10.1016/j.apacoust.2016.07.007

[12] Siano, D. (2012). *Noise control, reduction and cancellation solutions in engineering*. InTech.

[13] Silva, L. T., Oliveira, I. S., & Silva, J. F. (n.d.). The impact of urban noise on primary schools: Perceptive evaluation and objective assessment. *(detalii lipsă pentru citare completă – revistă, an, volum etc.)*

[14] Sohrabi, S., Pàmies Gómez, T., & Romeu Garbí, J. (2020). Suitability of active noise barriers for construction sites. *Applied Sciences, 10*(18), 6160. https://doi.org/10.3390/app10186160

ULTRASONIC ASSESSMENT OF MECHANICAL PROPERTIES IN ISOTROPIC AND ORTHOTROPIC MATERIALS

/

EVALUAREA ULTRASONICĂ A PROPRIETĂȚILOR MECANICE ALE MATERIALELOR IZOTROPE ȘI ORTOTROPE

Andreea-Denisa GRIGUȚA*[1)], Mihai Valentin PREDOI[1)], Cristian-Cătălin PETRE[2)], Laura-Mariana BARBU[1)], Gheorghe FLOROIU[1)]

[1)] Department of Mechanics, National University of Science and Technology POLITEHNICA Bucharest - Faculty of Biotechnical Systems Engineering, Bucharest / Romania;

[2)] Department of Strength of Materials, National University of Science and Technology POLITEHNICA Bucharest - Faculty of Biotechnical Systems Engineering, Bucharest / Romania.

**Tel: 0743 861 528; *E-mail: andreea.griguta@upb.ro*

Keywords: *non destructive characterization, mechanical propesties, isotropic and orthotropic material, pulse echo method, Lamb waves, dispersion curves*

ABSTRACT

Material characterization is a fundamental requirement across engineering and applied sciences, as the reliable knowledge of mechanical properties determines both design strategies and performance assessment. While classical methods have long been employed during early development phases, there is an increasing need for non-destructive techniques that can provide accurate and non-invasive evaluation suitable for real applications. This paper presents both theoretical considerations and experimental findings related to non-destructive testing methods applied to isotropic materials as well as to orthotrop materials. The experimental investigations are based on the analysis and overlapping of dispersion curves for isotropic media, which allow the extraction of relevant mechanical characteristics. In addition, a dispersion curve is also obtained for a carbon-epoxy plate, serving as a first experimental step for composites, although in this case no overlap with theoretical predictions is performed. Beyond the experimental results, the study emphasizes the importance of microstructural aspects in composites, such as the alignment of fibers, which strongly affect the observed mechanical response. The paper therefore presents relevant information on the mechanical properties of both isotropic materials and composites, contributing to the refinement of non-destructive testing methodologies adapted to different classes of materials.

REZUMAT

Caracterizarea materialelor reprezintă o cerință fundamentală în inginerie și științele aplicate, deoarece cunoașterea precisă a proprietăților mecanice influențează atât strategiile de proiectare, cât și evaluarea performanțelor. Dacă metodele clasice sunt utilizate frecvent în etapele inițiale, devine din ce în ce mai importantă aplicarea unor tehnici nedistructive, capabile să ofere rezultate precise și neinvazive, adecvate aplicațiilor reale. Lucrarea de față prezintă atât considerații teoretice, cât și rezultate experimentale privind metode de testare nedistructivă, aplicate materialelor izotrope și ortotrope. Investigațiile experimentale se bazează pe analiza și suprapunerea curbelor de dispersie pentru medii izotrope, metodă ce permite obținerea caracteristicilor mecanice relevante. În plus, este prezentată și o curbă de dispersie obținută experimental pentru o placă de carbon-epoxy, constituind un prim pas în direcția caracterizării compozitelor, însă fără realizarea unei suprapuneri cu rezultatele teoretice. Dincolo de aceste rezultate, studiul subliniază importanța aspectelor structurale ale compozitelor, precum alinierea fibrelor, care influențează direct comportamentul mecanic observat. Lucrarea furnizează astfel informații relevante privind proprietățile mecanice ale materialelor izotrope și ale compozitelor, contribuind la dezvoltarea unor metodologii nedistructive adaptate diferitelor categorii de materiale.

INTRODUCTION

The mechanical characteristics of materials represent a fundamental aspect in numerous engineering domains, as they directly influence both the design process and the long-term reliability of structures and devices. In the medical field, for instance, advanced knowledge of material properties is crucial for the development of prosthetics, implants, and biomedical devices, where compatibility with the human body and durability under cyclic loads are essential. In the aerospace and automotive industries, the characterization of materials determines the performance of fuselages, joints, and structural components, where lightweight yet resistant materials are required to ensure both safety and fuel efficiency. Similarly, in the agricultural sector, machinery components such as frames, cutting tools, or transmission elements rely heavily on materials with well-defined mechanical responses to withstand harsh environmental conditions and repeated mechanical stress. Beyond these domains, civil engineering, energy systems, and even consumer electronics increasingly depend on accurate material characterization to optimize functionality, reduce failures, and extend service life. Consequently, the development of reliable techniques for evaluating the mechanical characteristics of materials has become a priority in both research and industry, particularly when moving toward advanced materials such as composites, which introduce new challenges for testing and characterization *(Chulkov, Terekhin, & Dumansky, 2020).*

Real-time characterization of materials has gained increasing importance, as the mechanical characteristics of engineering materials are not static but evolve over time due to processes such as aging, fatigue, environmental exposure, and operational stresses. These changes can significantly alter the structural integrity and functional performance of components, particularly in safety-critical applications such as aerospace, medical implants, or energy systems. Traditional destructive testing methods, while effective for initial evaluations, cannot capture these time-dependent variations during service life, nor can they be applied to components already integrated into complex systems. For this reason, non-destructive characterization methods are essential, as they allow continuous or periodic monitoring of materials without compromising their integrity. Such approaches provide valuable information on the degradation of mechanical properties, enabling predictive maintenance strategies, life-cycle assessment, and early detection of potential failures *(Qiu & Ge, 2025).* In addition, the integration of real-time non-destructive monitoring with advanced data processing and modeling techniques opens the possibility of adaptive control systems, where material behavior is continuously evaluated and compensated for during operation. This paradigm not only enhances safety and reliability but also contributes to cost reduction by minimizing downtime and extending the effective service life of components and structures *(Alqurashi, Alver, Bagci, & Catbas, 2025)*.

The pulse-echo method is one of the most widely used techniques for material characterization, particularly in the case of isotropic materials. It is based on the principle of transmitting an ultrasonic pulse into the material and recording the reflected signal (echo) generated at interfaces or discontinuities. By measuring parameters such as the time-of-flight, amplitude, and frequency content of the reflected waves, it is possible to determine key mechanical characteristics, including elastic moduli, wave velocities, thickness, and the presence of defects such as cracks, voids, or inclusions *(Filho, Moreno, & Luso, 2022).*

The method is highly valued for its simplicity, relatively low cost, and ability to provide fast results with minimal preparation. Its applicability extends across a broad range of engineering fields, from aerospace to civil engineering, where it is routinely used for quality control, defect detection, and verification of uniformity in isotropic media. However, the reliability of the pulse-echo method decreases when applied to more complex materials, such as composites, where directional dependence and heterogeneous structures affect wave propagation and make the interpretation of echoes more challenging *(Shibata & Ishihara, 2001).* Despite these limitations, the pulse-echo technique remains a cornerstone of ultrasonic non-destructive testing and serves as a benchmark for the development of more advanced characterization *methods (Maiyena, Daud, & Ayop, 2025)*.

Another method addressed in this paper is based on ultrasonic guided waves and the interpretation of dispersion curves. In this approach, experimental dispersion data are compared with theoretical predictions, and the degree of overlap provides valuable insight into the mechanical characteristics of the material. In contrast to the pulse-echo technique, which is most effective for isotropic media, the dispersion curve method can be applied to a broader range of materials, including composites, where structural features significantly influence wave propagation. Previous research has demonstrated the reliability of this method for evaluating elastic properties and detecting defects, and likewise, the matching of experimental and

theoretical dispersion curves has been reported as a robust strategy for advanced material characterization *(Griguța & Predoi, 2021), (Mihai Valentin Predoi, 2022), (Griguța A. D., Predoi, Petre, & Rugină, 2025).*

In addition, guided-wave techniques present practical advantages, such as the ability to cover large areas with limited sensing equipment, making them particularly well suited for applications in structural health monitoring and long-term assessment of engineering components *(Griguța, Predoi, & Petre, 2023), (Jiang, et al., 2023).*

THEORETICAL ASPECTS

Fundamental theoretical aspects of wave propagation in isotropic materials are first outlined, followed by key considerations regarding Lamb wave propagation and the formulation of dispersion curves. Subsequently, Hooke's law is introduced for the case of orthotropic materials, from which the authors derive the rotation matrix applicable to laminated composites.

1. Isotropic materials

The constitutive relation may be written as:

$$\begin{bmatrix}\sigma_{xx}\\ \sigma_{yy}\\ \sigma_{zz}\\ \sigma_{yz}\\ \sigma_{xz}\\ \sigma_{xy}\end{bmatrix}=\begin{bmatrix}C_{11} & C_{12} & C_{12} & 0 & 0 & 0\\ C_{21} & C_{11} & C_{12} & 0 & 0 & 0\\ C_{21} & C_{21} & C_{11} & 0 & 0 & 0\\ 0 & 0 & 0 & C_{66} & 0 & 0\\ 0 & 0 & 0 & 0 & C_{66} & 0\\ 0 & 0 & 0 & 0 & 0 & C_{66}\end{bmatrix}\begin{bmatrix}\varepsilon_{xx}\\ \varepsilon_{yy}\\ \varepsilon_{zz}\\ \varepsilon_{yz}\\ \varepsilon_{xz}\\ \varepsilon_{xy}\end{bmatrix} \quad (1)$$

with,

$$C_{66}=\frac{C_{11}-C_{12}}{2} \quad (2)$$

where,

σ_{ii} - Normal stresses component of the stress tensor;

σ_{ij} - Shear stresses component of the stress tensor;

C_{11}, C_{12}, C_{21}, C_{66} - Elastic coefficients;

ε_{ii} - Normal strains of the elastic tensor;

ε_{ij} - Shear terms of the elastic tensor.

The relationships between the Lamé coefficients, Young's modulus, Poisson's ratio, and the elasticity coefficients can be expressed as follows:

$$C_{11}=\lambda+2\mu=\frac{E(1-\nu)}{(1+\nu)(1-2\nu)}$$
$$C_{66}=\mu=\frac{E}{(1+\nu)} \quad (3)$$
$$C_{12}=C_{21}=C_{11}-2C_{66}=\lambda=\frac{\nu E}{(1+\nu)(1-2\nu)}$$

where,

λ, μ - Lame coefficients;

E -Young modulus;

v - Poisson ratio.

The two bulk velocities of longitudinal and transversal wave are expressed with respect to the engineering constants as follows:

$$c_T=\sqrt{\frac{\mu}{\rho}}=\sqrt{\frac{C_{66}}{\rho}}=\sqrt{\frac{E}{2\rho(1+\nu)}}$$
$$c_L=\sqrt{\frac{\lambda+2\mu}{\rho}}=\sqrt{\frac{C_{11}}{\rho}}=\sqrt{\frac{E(1-\nu)}{\rho(1+\nu)(1-2\nu)}} \quad (4)$$

where,

ρ - density of the material.

Therefore, the engineering constants, Young Modulus and Poisson ratio may be expressed as:

$$E=\rho c_T{}^2\frac{3c_L{}^2-4c_T{}^2}{c_L{}^2-c_T{}^2},\nu=\frac{c_L{}^2-2c_T{}^2}{2(c_L{}^2-c_T{}^2)} \quad (5)$$

Furthermore, by particularizing the general wave equation for a thin plate, and by introducing the scalar and vector potential formulation together with the appropriate boundary conditions, the dispersion relations governing Lamb wave propagation can be derived as follows (Griguța & Predoi, 2021), for symmetric modes of propagation:

$$C_s(k_x,\omega) = 4k_x^2 k_{Tz} k_{Lz} \tan(k_{Lz} z) + (k_T^2 - 2k_x^2)^2 \tan(k_{Tz} z) = 0 \quad (6)$$

And for asymmetric modes of propagation:

$$C_a(k_x,\omega) = 4k_x^2 k_{Tz} k_{Lz} \tan(k_{Tz} z) + (k_T^2 - 2k_x^2)^2 \tan(k_{Lz} z) = 0 \quad (7)$$

where,

k_x - Wavenumber component in the propagation direction (x-direction);

ω - Angular frequency of the wave;

k_T - Transverse (shear) bulk wave number;

k_L - Longitudinal bulk wave number;

k_{Tz} - Vertical component of the shear wave vector;

k_{Lz} - Vertical component of the longitudinal wave vector;

z – Half thickness of the plate.

with,

$$k_x^2 + k_{Lz}^2 = k_L^2;\ k_x^2 + k_{Tz}^2 = k_T^2 \quad (8)$$

For the purpose of illustrating the dispersion characteristics of Lamb waves, an aluminum plate with a thickness of 3 mm was considered as the reference structure. The dispersion relations were evaluated and subsequently presented in separate plots corresponding to the symmetric and antisymmetric modes of wave propagation.

In the graphical results, it can be observed that new higher-order modes emerge progressively with increasing frequency. Each of these modes appears only above its respective cut-off frequency, below which propagation is not supported.

The fundamental modes (S0 and A0) are present from the lowest frequency range and display strong dispersive behavior, particularly the antisymmetric A0 mode at low frequencies. In contrast, higher-order modes (S1, A1, etc.) gradually become accessible as the excitation frequency increases, and they exhibit more complex propagation characteristics.

The dispersion curves were obtained through numerical computations carried out in MATLAB, which allowed for an efficient solution of the transcendental equations defining the Lamb wave modes.

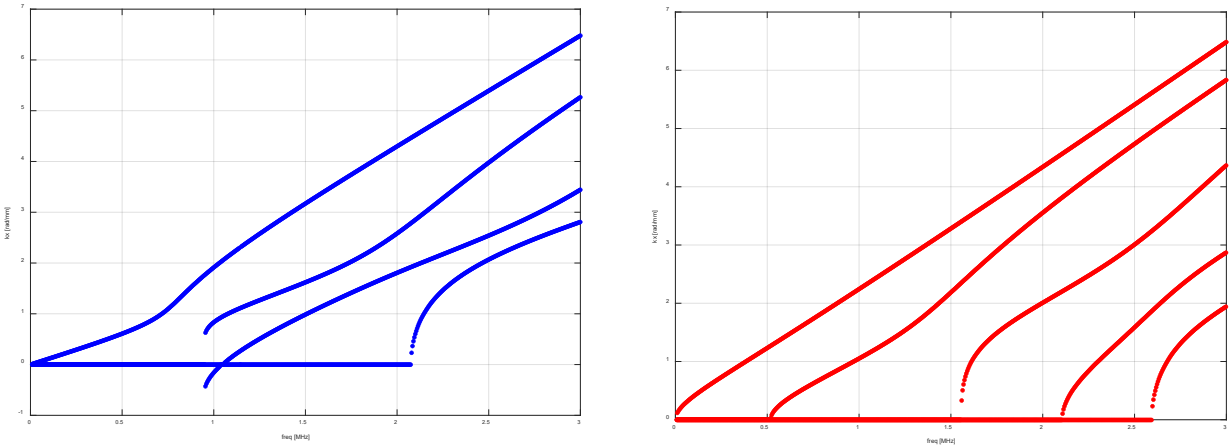

Fig. 1 - Dispersion curves for symmetric (blue) and antisymmetric (red) modes of propagation

2. Orthotropic materials

The constitutive relation for orthotopic materials with respect to elastic coefficients:

$$\begin{bmatrix}\sigma_{xx}\\ \sigma_{yy}\\ \sigma_{zz}\\ \sigma_{yz}\\ \sigma_{xz}\\ \sigma_{xy}\end{bmatrix}=\begin{bmatrix}C_{11} & C_{12} & C_{13} & 0 & 0 & 0\\ C_{21} & C_{22} & C_{23} & 0 & 0 & 0\\ C_{31} & C_{32} & C_{33} & 0 & 0 & 0\\ 0 & 0 & 0 & C_{44} & 0 & 0\\ 0 & 0 & 0 & 0 & C_{55} & 0\\ 0 & 0 & 0 & 0 & 0 & C_{66}\end{bmatrix}\begin{bmatrix}\varepsilon_{xx}\\ \varepsilon_{yy}\\ \varepsilon_{zz}\\ \varepsilon_{yz}\\ \varepsilon_{xz}\\ \varepsilon_{xy}\end{bmatrix} \quad (9)$$

For orthotropic materials, Hooke's law is formulated by explicitly accounting for the directional dependence of the material's elastic response. In this case, the engineering constants—namely the Young's moduli, shear moduli, and Poisson's ratios—are not isotropic but instead vary with respect to the three principal material axes. As a result, the constitutive relations involve different stiffness or compliance coefficients along each axis, leading to a more general representation of stress–strain behavior compared to the isotropic case.

Correlation between elastic constants and engineering constant is presented as:

$$C_{11}=\frac{(1-\nu_{yz}\nu_{zy})E_x}{\Delta};\ C_{22}=\frac{(1-\nu_{xz}\nu_{zx})E_y}{\Delta};\ C_{33}=\frac{(1-\nu_{xy}\nu_{yx})E_z}{\Delta}$$
$$C_{12}=\frac{(\nu_{xy}+\nu_{xz}\nu_{zy})E_x}{\Delta}=C_{21};\ C_{13}=\frac{(\nu_{xz}+\nu_{xy}\nu_{yz})E_x}{\Delta}=C_{31};$$
$$C_{12}=\frac{(\nu_{xy}+\nu_{xz}\nu_{zy})E_x}{\Delta}=C_{21};\ C_{13}=\frac{(\nu_{xz}+\nu_{xy}\nu_{yz})E_x}{\Delta}=C_{31}; \quad (9)$$
$$C_{23}=\frac{(\nu_{yz}+\nu_{yx}\nu_{xz})E_y}{\Delta}=C_{32};\ C_{44}=\mu_{yz};\ C_{55}=\mu_{xz};\ C_{66}=\mu_{xy}$$
$$\Delta=1-\nu_{xy}\nu_{yx}-\nu_{xz}\nu_{zx}-\nu_{yz}\nu_{zy}-2\nu_{xy}\nu_{yz}\nu_{zx}$$

Therefore, the general form of Hooke's Law with respect to engenerring constants looks like:

$$\begin{bmatrix}\sigma_{xx}\\ \sigma_{yy}\\ \sigma_{zz}\\ \sigma_{yz}\\ \sigma_{xz}\\ \sigma_{xy}\end{bmatrix}=\begin{bmatrix}\frac{1}{E_x} & -\frac{\nu_{yx}}{E_y} & -\frac{\nu_{zx}}{E_z} & 0 & 0 & 0\\ -\frac{\nu_{xy}}{E_x} & \frac{1}{E_y} & -\frac{\nu_{zy}}{E_z} & 0 & 0 & 0\\ -\frac{\nu_{xz}}{E_x} & -\frac{\nu_{yz}}{E_y} & \frac{1}{E_z} & 0 & 0 & 0\\ 0 & 0 & 0 & \frac{1}{\mu_{yz}} & 0 & 0\\ 0 & 0 & 0 & 0 & \frac{1}{\mu_{xz}} & 0\\ 0 & 0 & 0 & 0 & 0 & \frac{1}{\mu_{xy}}\end{bmatrix}\begin{bmatrix}\varepsilon_{xx}\\ \varepsilon_{yy}\\ \varepsilon_{zz}\\ \varepsilon_{yz}\\ \varepsilon_{xz}\\ \varepsilon_{xy}\end{bmatrix} \quad (10)$$

A compact form of the previous expression is:

$$\boldsymbol{\sigma}=\boldsymbol{C}\,\boldsymbol{\varepsilon};\ \boldsymbol{\varepsilon}=\boldsymbol{S}\,\boldsymbol{\sigma} \quad (11)$$

where,

σ, ε – Stress and strain tensor;

C, S – Stiffness matric and compliance matrix.

In the case of composite laminated materials, the orientation of each lamina plays a crucial role in determining the overall mechanical response of the laminate. A rotation of the individual layer with respect to the reference coordinate system significantly influences the stiffness properties and, consequently, alters the solution of the governing equations used in the computational analysis.

To correctly account for this effect, a transformation of the material property matrices is required. This is achieved by introducing a rotation matrix, which establishes the relationship between the local material axes of the lamina and the global coordinate system of the laminate The material principal axes of the lamina are assumed to be rotated by an angle θin the counterclockwise direction with respect to the global reference axes. This transformation enables the mapping of stresses and strains from the local

material coordinate system—where the material properties are defined—into the global coordinate system used for structural analysis.

The rotated stiffness matrix is computed by considering a transformation matrix for the strain and stress as follows:

$$[C'] = [T_\sigma]^{-1} \cdot [C] \cdot [T_\varepsilon] \tag{12}$$

with the corresponding transformation matrxis stress:

$$T_\sigma = \begin{bmatrix} cos^2\theta & sin^2\theta & 2sin\,\theta\,cos\,\theta \\ sin^2\theta & cos^2\theta & -2sin\,\theta\,cos\,\theta \\ -sin\,\theta\,cos\,\theta & sin\,\theta\,cos\,\theta & cos^2\,\theta - sin^2\,\theta \end{bmatrix} \tag{13}$$

and for strain:

$$[T_\varepsilon] = \begin{bmatrix} cos^2\theta & sin^2\theta & sin\,2\theta \\ sin^2\theta & cos^2\theta & -sin\,2\theta \\ -\frac{1}{2}sin\,2\theta & \frac{1}{2}sin\,2\theta & cos\,2\theta \end{bmatrix} \tag{15}$$

The authors have indicated that future research will extend the computational framework developed for orthotropic materials in order to present the theoretical dispersion curves corresponding to such media and to investigate, in greater detail, the influence of ply rotation on composite laminated structures. The incorporation of rotation effects is of particular significance, as it directly governs the directional stiffness and wave propagation characteristics of laminates.

MATERIALS AND METHODS

The determination of the mechanical properties of the examined material was carried out by employing two principal experimental approaches: the pulse–echo technique and the correlation of dispersion curves, established through the superposition of theoretical predictions with experimentally acquired data. The experimental configuration and the methodological procedures adopted in this investigation are succinctly outlined.

In the pulse–echo technique, the experimental configuration consists of a pulser–receiver, an oscilloscope, and an ultrasonic transducer. This method requires two distinct measurements in order to determine the full set of elastic engineering constants of the material, including Young's modulus (E), Poisson's ratio (ν), the shear modulus (G), the Lamé parameters (λ and μ, with μ = G), and the bulk modulus (K). Specifically, one measurement is performed with a longitudinal-wave transducer, while a second is carried out with a shear-wave transducer.

During the measurement, the transducer is excited by the pulser–receiver, generating an ultrasonic pulse that propagates into the specimen. The same transducer then acts as a receiver, detecting both the incident (direct) wave and its subsequent reflection after traversing the material. These signals are displayed on the oscilloscope as two distinct peaks corresponding to the forward and reflected waves, see Fig. 2. The time interval between the peaks represents the travel time of the ultrasonic pulse within the specimen. By repeating the procedure with both longitudinal and shear transducers, the respective wave velocities can be determined. These velocities are subsequently employed to calculate the complete set of elastic constants.

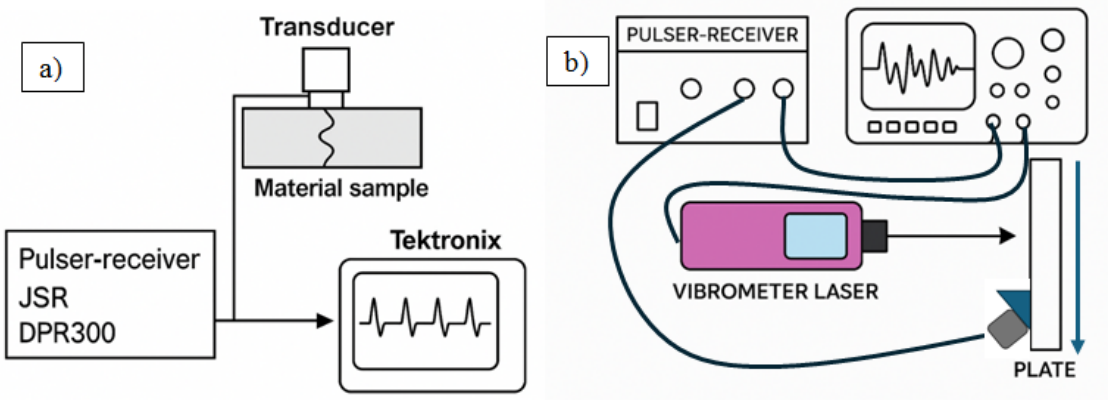

Fig. 2 - Experimental set up for a) pulse echo method b) overlapping of dispersion curves method

The previously described pulse–echo technique provides a relatively straightforward means of deducing the elastic characteristics of a material. Nevertheless, as emphasized earlier, its applicability is limited in the case of more complex materials. To address this limitation, a more sophisticated yet broadly applicable approach is employed, namely the comparison between theoretical and experimental dispersion curves. In this method, the dispersion relations predicted by theory are superimposed onto those extracted from experimental measurements, enabling a comprehensive characterization of the material.

As illustrated in Figure 2 b), the experimental arrangement comprises a pulser–receiver that excites an ultrasonic transducer, which in turn introduces a guided wave into a plate specimen. The out-of-plane surface displacements generated by the propagating wave are measured using a scanning laser vibrometer that records a spatial sequence of points along the plate surface. The positioning of the plate relative to the vibrometer is controlled with a precision displacement system. At each measurement point, the vibrometer output is directed to the oscilloscope, and the corresponding data are subsequently stored for post-processing. In order to efficiently couple the ultrasonic energy into the plate, the transducer is mounted on a polymethyl methacrylate (PMMA) wedge with an incidence angle of 30°, ensuring the correct excitation of guided modes

RESULTS

The experimental results are reported for two distinct specimens: an aluminum plate of 3 mm thickness, representing an isotropic benchmark material with well-established elastic constants, and a thin carbon/epoxy composite plate, selected as a representative complex material. The aluminum plate serves as a validation case, providing a straightforward comparison between experimental measurements and theoretical predictions.

By employing the pulse–echo technique, the authors applied the analytical formulations previously derived in this work in order to extract the elastic constants of the tested specimens. For the isotropic aluminum plate, the procedure yielded quantitative values for the principal engineering parameters, namely Young's modulus (E) and Poisson's ratio (v). The obtained results, 69.7 GPa for Young Modulus and 0.34 for Poisson ratio, serve both to validate the experimental methodology and to provide a direct comparison with reference values reported in the literature for aluminum alloys of similar grade and thickness.

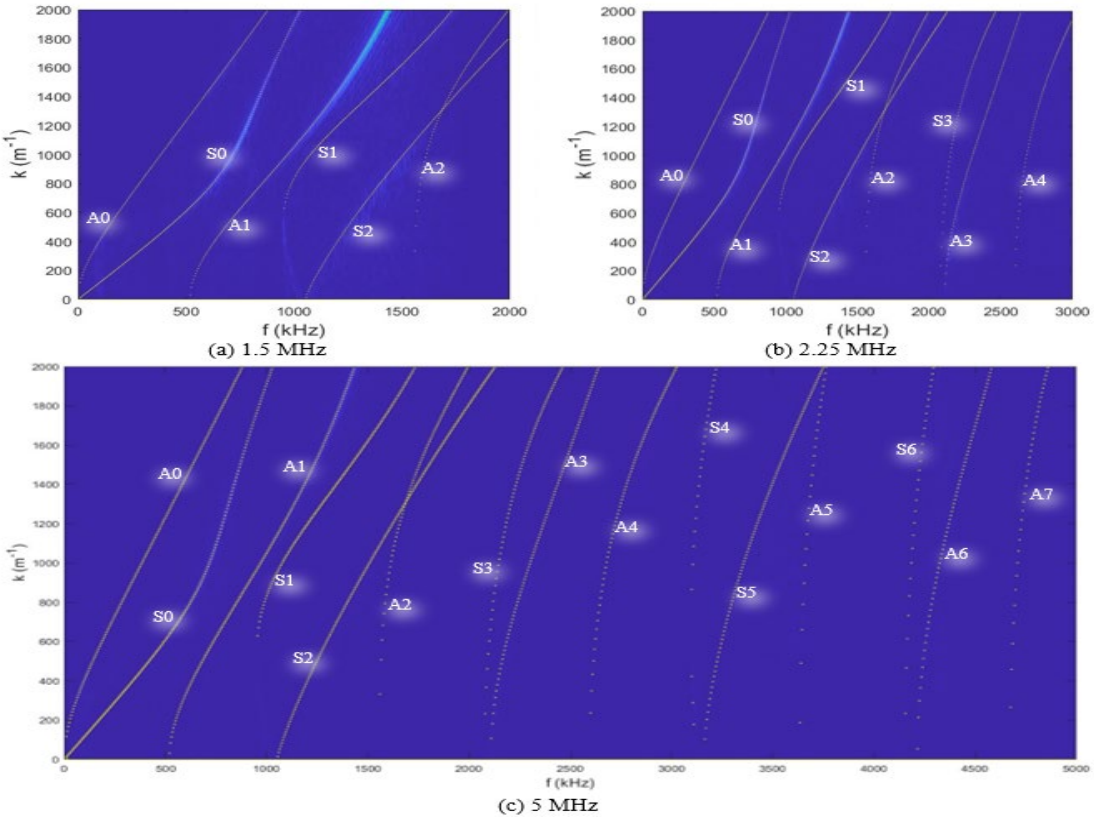

Fig. 3 - Overlapping of theoretical dispersion curves with experimental dispersion curves

(Griguta, et al., 2025)

The results obtained through the dispersion-curve overlapping method for the aluminum plate demonstrate an excellent agreement between the experimentally measured and theoretically predicted

curves see Fig. 3. The experimental campaign was carried out by the authors at the LOMC Laboratory, Le Havre, within the framework of an Erasmus+ collaboration. This high level of correspondence provides strong evidence that the material parameters employed in the theoretical modeling accurately represent those of the tested specimen. Consequently, the procedure confirms that the intrinsic elastic characteristics of the sample can be reliably inferred from the matching of theoretical and experimental dispersion curves.

For the composite specimen, only experimental results are reported, as the complex orthotropic behavior of the material renders the direct analytical derivation of dispersion relations non-trivial.

In this investigation, two excitation frequencies, namely 1 MHz and 1.5 MHz, were employed in order to capture the wave propagation response under different conditions and to enhance the robustness of the experimental observations. In the corresponding graphical representations, a dotted white line has been superimposed solely to facilitate the visualization of the experimental peaks and to guide the interpretation of the measured data, without implying any additional theoretical fitting, see Fig. 4.

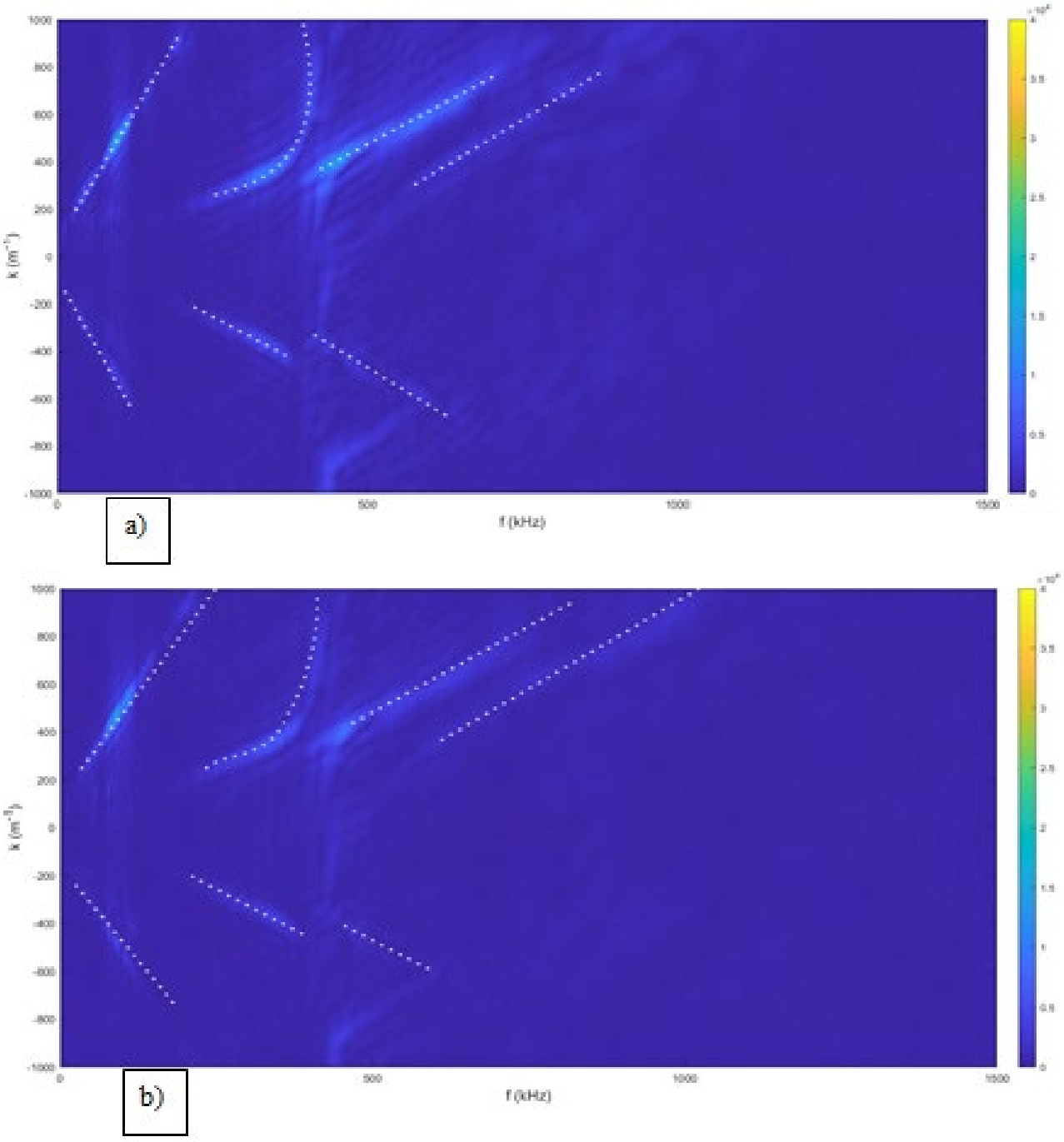

Fig. 4 - Experimental dispersion curves for carbon plate at a) 1MHz b) 2MHz

CONCLUSIONS

This study has presented the theoretical and computational understanding of guided wave propagation in both isotropic and orthotropic materials. By revisiting the governing equations for Lamb waves, the analysis has highlighted the fundamental differences between symmetric and antisymmetric modes of propagation, as well as their dependence on cut-off frequencies. The work has further addressed two nondestructive methods for determining the mechanical properties of materials: the pulse–echo technique, applied to an aluminum plate, and the dispersion curve matching approach, demonstrated through the superposition of theoretical dispersion curves for aluminum with experimentally obtained results for a carbon-fiber-reinforced composite plate. These complementary approaches have shown that guided waves represent a reliable and versatile means of characterizing both metals and composites.

At the same time, the results point toward several avenues for future research. In particular, while the overlapping of theoretical and experimental dispersion curves has been validated for aluminum, extending this procedure to orthotropic carbon-fiber laminates remains a necessary step to fully capture the effect of anisotropy and fiber orientation on wave propagation. Moreover, the computational framework for orthotropic materials requires completion through the incorporation of the rotation matrix formalism, which will allow the accurate treatment of arbitrarily oriented plies within laminated composites. Such an enhancement is essential for ensuring that the anisotropic stiffness contributions of individual layers are correctly represented in the global coordinate system and for improving the predictive capacity of the models.

Overall, the findings emphasize the importance of guided wave methods as nondestructive evaluation tools capable of bridging theory and experiment across a wide range of material classes. By extending the present framework to include complete orthotropic formulations and systematic experimental validation, future studies will strengthen the applicability of these methods in engineering practice, particularly in fields where the structural integrity of advanced composites is critical, such as aerospace, automotive, and civil infrastructure.

ACKNOWLEDGEMENT

The authors gratefully acknowledge *Le Laboratoire Ondes et Milieux Complexes* (LOMC), a joint research unit of the CNRS (UMR 6294), for providing access to the experimental facilities that were essential to the successful realization of this study. Sincere thanks are extended to the scientific and technical staff of LOMC for their invaluable assistance, expert guidance, and continuous support throughout the experimental campaign. The authors also wish to express their special gratitude to the Erasmus+ Program, which enabled the first author, Andreea, to undertake a research placement at LOMC—a formative experience that was instrumental in fostering the international collaboration and experimental work presented herein. Finally, the authors acknowledge the Faculty of Biotechnical Systems Engineering at the National University of Science and Technology POLITEHNICA Bucharest for the financial support provided through the doctoral grant, which facilitated participation in the conference.

REFERENCES

[1] Alqurashi, I., Alver, N., Bagci, U., & Catbas, F. N. (2025). A Review of Ultrasonic Testing and Evaluation Methods with Applications in Civil NDT/E. *Journal of Nondestructive Evaluation, 44*.

[2] Chulkov, D. I., Terekhin, A. B., & Dumansky, A. M. (2020). A study of physical and mechanical characteristics of polymer composite materials by ultrasonic technique. *IOP Conf. Series: Materials Science and Engineering.* Moscow: IOP Publishing.

[3] Filho, M. A., Moreno, C., & Luso, E. (2022). The Use of Ultrasonic Echo Pulse Velocity as an NDT Method to Predict the Concrete Strength and Uniformity. *Russian Journal of Nondestructive Testing*, 277-288.

[4] Graff, K. (1975). *Wave Motion in Elastic Solids.* New York: Dover Publications.

[5] Griguța, A. D., Predoi, M. V., & Petre, C. C. (2023). Detectability of notches in plates using multi-modal lamb waves. *The 10th International Conference on Structural Analysis of Advanced Materials*, (pp. 11-17). Zakynthos.

[6] Griguța, A. D., Predoi, M. V., Petre, C. C., & Rugină, C. (2025). Methodologies for Dataset Analysis in Regard to Obtaining Material Characteristics Using Lamb Waves. *Special Issue MACROMOLECULAR SYMPOSIA - ICSAAM 2025.* Brașov: Wiley.

[7] Griguța, A., & Predoi, M. (2021). Generation of multi-modal Lamb waves for the inspection of thin aeronautical structures. *U.P.B. Scientific Bulletin, Series A, 83*(4).

[8] Jiang, Y., Liu, Y., Zeng, J., Wang, Y., Xie, Q., & Hu, N. (2023). Equivalent elastic modulus measurement of cross-ply composite plates using Lamb waves. *Composite Structures, 321*.

[9] Maiyena, S., Daud, A. N., & Ayop, S. K. (2025). Elastic PropertiesMeasurement ofthe Multi-layeredMaterialsusing the Pulse-Echo Immersion Technique. *Journal of Science and Mathematics Letters, 13*(1), 23-29.

[10] Mihai Valentin Predoi, A.-D. G. (2022). Similarities between guided and longitudinal ultrasonic waves. *U.P.B. Scientific Bulletin, Series A, 84*(4).

[11] Qiu, M., & Ge, X. (2025). Nondestructive Evaluation of Aging Failure in Insulation Coatings by Ultrasonic Guided Wave Based on Signal Processing and Machine Learning. *Coatings, 15*.

[12] Shibata, T., & Ishihara, M. (2001). Ultrasonic signal characteristics by pulse-echo technique and mechanical strength of graphite materials with porous structure. *Nuclear Engineering and Design*, 133-141.

PM_{10} AND $PM_{2.5}$ PARTICLE POLLUTION IN TARGOVISTE CITY, DAMBOVITA COUNTY

/

POLUAREA CU PARTICULE PM_{10} ŞI $PM_{2,5}$ ÎN ORAŞUL TÂRGOVIŞTE, JUDEŢUL DÂMBOVIŢA

Florina Roxana DUMITRU*[1)], Lucica BARBEŞ*[1)], Daniel Emil Constantin DUNEA*[2)]

[1)] Doctoral School Biotechnical Systems Engineering, National University of Science and Technology POLITEHNICA Bucharest, 313 Splaiul Independentei, 060042, Bucharest / Romania;

[2)] VALAHIA University of Targoviste, Aleea Sinaia 13, 130004, Targoviste, Dambovita County / Romania.

**E-mail: dflorina11@protonmail.com (F.R.D.), lucille.barbes2020@gmail.com (L.B.), ddunea@yahoo.com (D.D.)*

Keywords: *PM_{10}; $PM_{2.5}$; air pollution; portable device.*

ABSTRACT

Concentrations of suspended particles (PM_{10} and $PM_{2.5}$) were investigated in various urban and peri-urban areas, using localized measurements performed with the Lighthouse "Handy Man" portable device (Lighthouse Technologies, 2018) *(July-August 2024), supported by comparative data (Casella Microdust Pro)* (Casella, 2020)*. The aim was to identify primary pollution sources and assess the influence of meteorological conditions. The data reveal a persistent air quality problem* (Law no. 104/2011; Directive 2008/50/EC)*, with extremely high pollution peaks, far exceeding legislative limits and WHO recommendations* (Strop de aer, 2024; Vitalia Mediu, 2025) (Romanian language)*. The PM_{10} peak reached 904.35 µg/m³ (OMV Sârbi), and the $PM_{2.5}$ peak reached 80.82 µg/m³ (Zona Piața "1 Mai"). Critical episodes are correlated with heavy road traffic at peak hours, construction activities and dust resuspension. Dry weather and wind massively amplify concentrations, while rain provides only a temporary cleaning effect. The significant discrepancy between low averages and alarming highs underlines the episodic and localized nature of severe pollution. The results require the development of urgent strategies to monitor and manage local sources of dust and combustion.*

REZUMAT

Concentrațiile de particule în suspensie (PM_{10} și $PM_{2,5}$) au fost investigate în diverse zone urbane și periurbane, folosind măsurători localizate efectuate cu dispozitivul portabil Lighthouse "Handy Man" (Lighthouse Technologies, 2018) (iulie-august 2024), susținute de date comparative (Casella Microdust Pro) (Casella, 2020). Scopul a fost identificarea surselor primare de poluare și evaluarea influenței condițiilor meteorologice. Datele relevă o problemă persistentă a calității aerului (Legea nr. 104/2011; Directiva 2008/50/EC), cu vârfuri de poluare extrem de ridicate, depășind mult limitele legislative și recomandările OMS (Strop de aer, 2024; Vitalia Mediu, 2025) (Romanian language). Vârful PM_{10} a atins 904.35 µg/m³ (OMV Sârbi), iar vârful $PM_{2,5}$ a ajuns la 80.82 µg/m³ (Zona Piața "1 Mai"). Episoadele critice se corelează cu traficul rutier intens la ore de vârf, activitățile de construcție și fenomenul de resuspensie a prafului. Vremea uscată și vântul amplifică masiv concentrațiile, în timp ce ploaia oferă doar un efect temporar de curățare. Discrepanța semnificativă dintre mediile scăzute și maximele alarmante subliniază caracterul episodic și localizat al poluării severe. Rezultatele impun dezvoltarea unor strategii urgente de monitorizare și gestionare a surselor locale de praf și ardere.

INTRODUCTION

Air pollution with suspended particles (PM) represents a major risk for public health. *PM_{10}* particles (aerodynamic diameter ≤10 µm) and especially *$PM_{2.5}$* (≤2.5 µm) can penetrate deep into the respiratory system and are associated with cardiovascular and respiratory diseases.

The objective of this study is to characterize the levels of PM_{10} and *$PM_{2.5}$* in an urban area (Targoviște), using rapid and localized sampling techniques with a portable device Lighthouse "Handy Man" *(Lighthouse Technologies, 2018)* and Casella Microdust Pro *(Casella, 2020)*.

By analyzing peak data and correlating them with meteorological conditions and the type of area, the aim is to identify critical sources of pollution and the environmental factors that amplify them.

MATERIALS AND METHODS

The measurements were mainly performed with the Lighthouse "Handy Man" particle counter *(Lighthouse Technologies, 2018),* a laser scattering-based instrument designed for rapid monitoring of PM_{10} and $PM_{2.5}$ concentrations. Comparative data (July 25 and August 2, 2024 and March−June 2025) were also taken from a Casella Microdust Pro device *(Casella, 2020),* which, although operating in a different period, confirms the nature and magnitude of the peak episodes.

The measurements were carried out between July 25 and August 2, 2024 and March-June 2025.

The meteorological conditions included:

- high temperatures (maximum 25.5 ^{0}C−35 ^{0}C).
- extreme weather events on July 25 (strong wind of 50−70 km/h, torrential rains, hail), followed by predominantly sunny and dry weather.
- in the following days, the lack of precipitation favored the resuspension and accumulation of pollutants *(InfoClima, 2025; Climate-ADAPT, 2025).*

RESULTS

1. Exceptional PM_{10} Peaks (Lighthouse "Handy Man")

Data analysis revealed PM_{10} concentrations that massively exceed the daily legal threshold of 50 µg/m^3 (Directive 2008/50/EC; Law no. 104/2011).

Table 1

Measured PM_{10} concentrations and identified possible emission sources

Location	Date	PM_{10} Value (µg/m^3)	Observations/Possible Causes
OMV Sârbi	01.08.2024	904.35	Exceptionally high value, indicating an intense local source (heavy traffic at the intersection, gas station, dust).
Vis-à-vis Crom Steel/NIMET SRL	01.08.2024	358.07	Influence of industrial/truck traffic and industrial area.
County Court Area	27.07.2024	253.71	Heavy traffic in a central area.
Under the pavcom bridge	28.07.2024	167.45	Heavy traffic junction.

The peak of 904.35 µg/m^3 at OMV Sârbi is almost 18 times higher than the daily legal limit (50 µg/m^3), highlighting the existence of local, short-term, highly polluting events.

2. Notable PM2.5 Peaks (Lighthouse "Handy Man")

Although most $PM_{2.5}$ values were below 15 µg/m^3, alarming peaks were also recorded (Table 2).

Table 2

Measured $PM_{2.5}$ concentrations and identified possible emission sources

Location	Date and Period	$PM_{2.5}$ Value (µg/m^3)	Observations/Possible Causes
1 Mai" Square	29.07.2024 (morning)	80.82	Extremely high value, suggesting combustion sources (rush hour traffic, possible uncontrolled burning) and/or morning thermal inversion.
Teiș Area	30.07.2024 (seara)	43.49	Associated with nocturnal atmospheric stability and evening traffic.

The peak of 80.82 µg/m^3 exceeds the WHO recommended daily limit (15 µg/m^3*) (Strop de aer, 2024; Vitalia Mediu, 2025)* (Romanian language) by more than five times, confirming a serious health risk from point exposures.

3. Correlation of weather-pollution and predominant sources

The correlation of data confirms a dual role of meteorological factors:

- Cleaning effect of rain: decrease in PM concentrations observed after precipitation (e.g.: June 9, 2025, afternoon).
- Amplification of pollution: lack of rain and strong wind lead to massive resuspension of dust from roads and construction sites (e.g.: Peak of 1715 µg/m^3 PM_{10} on Cernăuți Street, March 28, 2025*) (InfoClima, 2025)* (Romanian language).

Predominant sources of pollution:

- Road Traffic: constant source of pollution, with clear peaks during peak hours (Calea Domnească, roundabouts).
- Construction/Construction Sites: confirmed by massive peaks of PM10 in Micro 2/Str. Cernăuți and Vulcana Pandele (heavy equipment traffic).
- Combustion: suggested by very high peaks of PM2.5 (Piața "1 Mai", “Groapa de Gunoi”), indicating combustion processes (traffic, uncontrolled fires).

4. Interpretation of the discrepancy between average vs. maximum values

The collected data (including the comparative ones collected with the Casella device) (Casella, 2020) show a major discrepancy between the average values (sometimes very low) and the instantaneous maximum values (extremely high).

For example, on Cernăuți Street (March-June 2025), maximums of 1099 µg/m^3 PM_{10} were recorded, although the corrected averages were only 1 µg/m^3. This indicates that severe pollution problems are predominantly episodic and localized, being triggered by the interaction between a strong local source (construction site, machinery traffic) and a favorable meteorological factor (wind that resuspends dust, lack of rain).

CONCLUSIONS

The study confirms a critical and persistent air quality problem in Targoviște, with numerous episodes of PM_{10} and $PM_{2.5}$ pollution that far exceed national legal limits (Law no. 104/2011; Directive 2008/50/EC) and, especially, WHO guidelines (Strop de aer, 2024; Vitalia Mediu, 2025).

REFERENCES

[1] Casella. (2020). Microdust Pro User Manual. Casella.
[2] Climate-ADAPT.(2025). European platform for climate change adaptation. Available at: https://climate-adapt.eea.europa.eu/
[3] Directive 2008/50/EC of the European Parliament and of the Council of 21 May 2008 on ambient air quality and cleaner air for Europe. (2008). Official Journal of the European Union. Available at: https://eur-lex.europa.eu/eli/dir/2008/50/oj
[4] Government of Romania. (2021). Emergency Ordinance no. 598/2021 on air quality. Official Monitor / Lege5 / Indaco. Available at: https://legislatie.just.ro/public/DetaliiDocument/243063
[5] InfoClima. (2025). Climate information. Available at: https://www.infoclima.ro/
[6] Law no. 104/2011 on ambient air quality. (2011). calitateaer.ro. Available at: https://www.calitateaer.ro/public/legislation-page/national-legislation-page/?__locale=ro
[7] Law no. 104/2011 on ambient air quality. (2011). lege5.ro. Available at: https://lege5.ro/

[8] Lighthouse Technologies. (2018). Handy Man Operating Guide. Lighthouse Technologies.
[9] Ministry of Environment and Forests. (2012). Order no. 195/2012 approving the Methodology for assessing air quality in urban areas and agglomerations. Official Monitor of Romania, Part I, no. 201 of 27 March 2012. Available at: https://lege5.ro/Gratuit/geztsmbqgq/ordinul-nr-195-2012-privind-aprobarea-metodologiei-de-evaluare-a-calitatii-aerului-in-zonele-si-aglomerarile-urbane
[10] PMC. (n.d.). Public Library of Medicine – Articles on air quality. Available at: https://pubmed.ncbi.nlm.nih.gov/
[11] Strop de aer. (Romanian language) (2024). About air quality. Available at: https://stropdeaer.ro/
[12] Vitalia Mediu.(Romanian language) (2025). What are PM2.5 and PM10 particles? Available at: https://www.vitalia-mediu.ro/informatii/pm-2-5/

OPTIMIZING PROCESSES IN AGRICULTURE AND THE FOOD INDUSTRY
/
OPTIMIZAREA PROCESELOR ÎN AGRICULTURĂ ȘI INDUSTRIA ALIMENTARĂ

Gabriel NAE*[1)], Florin NENCIU[1)], Andreea MATACHE[1)], Nicoleta VANGHELE[1)], Diana-Lorena POPA[2)], Floarea SERBANCEA[3)], Cristian SERBANCEA[3)]

[1)] National Institute of Research - Development for Machines and Installations Designed for Agriculture and Food Industry - INMA Bucharest / Romania;

[2)] Secuieni Agricultural Development Research Station - SCDA Secuieni, Neamt County / Romania;

[3)] National Institute for Research and Development of Food Bioresource - IBA, Bucharest / Romania.

**Tel: 0735 906 254; *E-mail: gabi.nae83@yahoo.com*

Keywords: *artificial intelligence, models, sensors, information, optimization*

ABSTRACT

Against the backdrop of global food security issues, influenced by phenomena such as population expansion, climate change, limited resources and geopolitical instability, factors that will generate a significant increase in the need for food, it is necessary to widely adopt digital innovation in agriculture, often referred to as "smart agriculture". By introducing artificial intelligence into agricultural systems, processes in agriculture and the food industry can be optimized, which implies improving efficiency and productivity through the use of advanced technologies and sustainable practices. In this paper, forecasting models and sensors used in agriculture were briefly presented, with an in-depth study of the most common devices, where the focus was on the benefits and limitations of these equipment in order to form a concise representation for stakeholders. Optimizing processes in agriculture and the food industry can lead to increased competitiveness, reduced costs and improved product quality, thus contributing to food security and sustainability.

REZUMAT

Pe fondul problemelor legate de securitatea alimentară la nivel global, influențată de fenomene cum sunt expansiunea populației, schimbările climatice, resursele limitate și instabilitatea geopolitică, factori ce vor genera o creștere semnificativă a nevoii de alimente, este necesară adoptarea pe scară largă a inovației digitale în agricultură, deseori denumită „agricultură inteligentă". Prin introducerea inteligenței artificiale în cadrul sistemelor agricole se pot optimiza procesele în agricultură și industria alimentară, ceea ce implică îmbunătățirea eficienței și productivității prin utilizarea tehnologiilor avansate și a practicilor durabile. În această lucrare au fost prezentate succint modele de prognoză și senzori utilizați în agricultură fiind aprofundat studiul asupra celor mai uzuale dispozitive unde s-a pus accentul pe beneficiile și limitările acestor echipamente pentru a forma o reprezentare cât mai concisă pentru părțile interesate. Optimizarea proceselor în agricultură și industria alimentară poate duce la creșterea competitivității, reducerea costurilor și îmbunătățirea calității produselor, contribuind astfel la securitatea alimentară și sustenabilitate.

INTRODUCTION

The concern about global food security is an extremely sensitive issue, influenced by several factors, including population expansion, climate change, limited resources and geopolitical instability *(Dahlberg, K., 2012)*. With the world population estimated at 9.7 billion by 2050, there will be a significant increase in the need for food, which will put enormous pressure on agricultural systems. In addition, climate change poses a threat to agricultural production, giving rise to severe weather events, changing the timing of growing seasons and damaging natural resources such as soil and water *(Alexandratos, N. and Bruinsma, J., 2012)*.

Digital innovation in agriculture, often referred to as "smart agriculture" or "agriculture 4.0," integrates advanced digital tools and technologies into traditional agricultural practices. The exact origin of the term "smart agriculture" is difficult to trace, given that it emerged from the collective input of researchers and industry experts (Weraikat, D. et al, 2024). However, in the specialized literature, it is considered that precision agricultural technologies began to be used in the late 1980s in the United States and Australia *(Stafford, J., 2000)*.

Artificial Intelligence (AI), automation, and the Internet of Things (IoT) are useful for optimizing agricultural production and increasing sustainability. AI algorithms process data from various sources to help

farmers make informed decisions, while automated devices simplify planting, irrigation, and harvesting. IoT devices collect real-time data from sensors, drones, and other connected equipment, increasing operational efficiency *(Saiz-Rubio, V. and Rovira-Más, F., 2020; Friha, O. et al, 2021; Subeesh, A. and Mehta, C., 2021; Lakshmi, G. et al, 2023).*

One solution for transforming the agricultural sector is IoT-based automation for crop monitoring that includes a wireless sensor network (WSN) for real-time monitoring of crop health and a remote sensing platform for obtaining multispectral images for classifying healthy and unhealthy crops, which has led to increased production with reduced human effort *(Shafi et al, 2019).* Unmanned aerial vehicles (UAVs), used as remote sensing tools, provide aerial imagery that can detect problems early and apply precise interventions, optimizing resources and improving crop management *(Radoglou-Grammatikis, P. et al, 2020).*

An extremely important aspect is the monitoring and optimization of essential environmental and soil parameters (nitrogen (N), phosphorus (P), potassium (K), moisture and temperature), *(Macholdt, J. et al, 2019)* as well as a precise plant management strategy, focused on variable application of nitrogen fertilizers *(Weddell, B.J., 2023).* Regarding irrigation and efficient water management, an automatic irrigation system has been proposed, incorporating sensors for measuring pH, soil moisture and humidity. This system allows farmers to remotely access information from the field, reducing manual work and time, while improving productivity and resource use. The farmer is informed through a GSM (Global System for Mobile Communications) module, which allows real-time updates on field conditions via short message service (SMS), *(Pawar, R.Y. et al, 2021).*

An IoT-based soil nutrient system has also been integrated to help farmers make informed decisions throughout the agricultural process. The model incorporates sensors, cloud computing, and machine learning (ML) tools to collect real-time data on soil conditions and analyze nutrient levels *(Murali, K.S. et al, 2023).*

Another transformative potential of these technologies is how forecasting models can be used to improve both conventional and alternative agricultural systems. Exploring forecasting models can optimize food processing and supply chain management, thereby contributing to the resilience and sustainability of global food systems. Innovations in Food Security and Supply Chain Optimization take a comprehensive analytical approach to explore the integration of AI-based forecasting models in addressing key challenges related to global food security (fig. 1) *(Dhal, S.B. and Kar, D., 2024).*

Fig. 1 - Schematic diagram providing a comprehensive analysis of the challenges and constraints of global food security

(Dhal, S.B. and Kar, D., 2024)

By using artificial intelligence (AI), it is possible to optimize resource use, reduce waste, and minimize environmental impact *(Kennedy, N., 2024).* Data-driven insights help farmers understand the relationship between natural systems, which is essential for achieving both sustainability and food security goals *(Rozenstein, O., 2024).*

Optimization efforts in food processes have relied on simplistic, single-variable experimental approaches. These methods focused on evaluating the effect of a parameter at a given time on a given response, while holding all other factors constant. Although effective for certain scenarios, this approach introduced substantial limitations.

It neglected potential interactions between variables, which are often essential in understanding the complexity of food production systems *(Yolmeh, M. and Jafari, S.M., 2017).* Multi-objective optimization addresses problems that involve multiple responses or variables simultaneously, providing solutions that optimize multiple objectives simultaneously.

This approach is particularly relevant to food science, where competing objectives often require trade-offs *(Carrizosa, E.and Morales, D.R., 2013).*

MATERIALS AND METHODS

The focus of this paper is to assess the literature on advanced AI-based sensor technology that enables monitoring of critical environmental and soil parameters that affect crop yields, as well as forecasting models that can bring benefits to agricultural systems. In addition, through this paper, we aim to increase awareness of smart farming practices among farmers.

The literature suggests that collaboration between various stakeholders in the agricultural supply chain can lead to optimization of processes in agriculture, which produces numerous benefits, including increased efficiency and productivity, cost reduction, and improved product quality.

Artificial Intelligence-Based Forecasting Models

- **Crop Yield Predictions:** Models can predict crop yields with greater accuracy, enabling better planning and risk management *(Benami, E. et al, 2021; Kim, N. et al, 2019).*
- **Climate Monitoring and Real-Time Data:** Models help monitor and respond to changing weather patterns, providing farmers with real-time information to adjust their practices *(Singh, B. and Kaunert, C., 2024).*
- **Supply Chain Optimization:** Models provide optimization solutions for food supply chains by reducing inefficiencies, minimizing costs, and improving food accessibility *(El Jaouhari, A. and Hamidi, L.S.).*

Harnessing forecasting models

- **Climate forecasting models:** The effects of climate change, such as changes in growing seasons and severe weather conditions, pose significant risks to agricultural production. Climate forecasting models predict these changes in weather patterns and environmental changes, helping farmers adapt their practices to prevent crop failures and use resources more efficiently *(Kang, Y. et al, 2009).*
- **Crop yield forecasting models:** The increasing demand for food driven by population growth is putting immense pressure on agricultural systems. Crop yield forecasting models use data on soil quality, precipitation and temperature to predict yields, allowing for better planning and timely interventions to prevent shortages, ensuring food security *(Basso, B. and Liu, L., 2019).*
- **Supply chain forecasting models:** Inefficient distribution contributes to significant problems in food supply chains. Artificial intelligence-based supply chain forecasting models are essential in predicting customer demand, identifying logistical bottlenecks, and optimizing the transportation of food from producers to consumers, improving the operational efficiency of food distribution systems *(Abaku, E.A. et al, 2024).*

The Evolution of Alternative Agriculture and Food Processing in Agricultural Systems

- ***Hydroponics and Aquaponics:*** These soilless farming systems rely on precise control of environmental factors such as water, nutrients, and light. Forecasting models help predict ideal nutrient levels, water conditions, and energy use to optimize plant and fish growth, ensuring efficiency and consistency of yield *(Saikanth, K. et al, 2023; Sharma, N. et al, 2018).*
- ***Vertical Farming:*** Vertical farming offers a sustainable solution for food production in highly urbanized areas, but it is energy-intensive. Forecasting models help balance energy

consumption, optimize harvest cycles, and predict plant growth rates to enhance sustainability *(Beacham, A.M. et al, 2019; Kalantari, F. et al, 2018).*

- **Advanced Food Processing Techniques**:
  In food processing, predictive models, based on real-time data from Internet of Things (IoT) devices and automation, help improve product quality and safety. These models predict spoilage rates, optimize consumption, and ensure efficient processing workflow, leading to improved food quality and reduced waste *(Misra, N.N. et al, 2020; Gao, T. et al, 2020).* Modele esențiale de prognoză pentru optimizarea climei, randamentului și lanțului de aprovizionare
- ***Time Series Models***
  ARIMA and SARIMA are commonly used for yield and price forecasting in agriculture. These models analyze historical data to predict trends and cycles, helping farmers and policymakers make informed decisions about resource allocation *(Suresh, K.K. et al, 2011; Mila, F.A. and Parvin, M.T., 2019; Divisekara, R.W. et al, 2020).* These models also extend to processing programs to ensure that food products are optimally distributed to minimize waste (*Falatouri, T. et al, 2022).*
- ***Machine Learning (ML) Models***
  ML models, including RF and SVM, excel at handling complex, nonlinear relationships between climate, soil quality, and market conditions. These models are widely used for yield forecasting and market prediction, providing robust insights into market dynamics and resource optimization *(Kok, Z.H. et al, 2021; Suresh, N. et al, 2021).*
- ***DL Models***
  - LSTMs, a type of recurrent neural network (RNN), analyze sequential data, such as long-term weather patterns, enabling accurate predictions of environmental and agricultural system impacts *(Jaiswal, R. et al, 2022).*
  - CNNs process spatial data, such as satellite imagery, to monitor crop health and predict supply chain disruptions, providing real-time insights into potential bottlenecks *(Prashanthi, V. and Srinivas, K., 2020).*
  - Integrating LSTMs and CNNs into hybrid models improves prediction accuracy by combining spatial and temporal data, especially in advanced yield prediction and supply chain management *(Gafurov, A. et al, 2023; Suebsombut, P. et al, 2021; Iitsuka, S. et al, 2019).*
- ***The evolution of hybrid models in food security.***
  Hybrid models combine various forecasting methods, such as ML, DL, and time series models, to improve the accuracy of predictions in food systems. These models are especially valuable for addressing complex agricultural challenges.
  - Time series + ML: Combining time series with ML provides a comprehensive understanding of agricultural crop trends, increasing the accuracy of forecasts in terms of yield and prices *(Guo, Y., 2024; Özden, C., 2023).*
  - ML+DL: Hybrid models that combine ML for feature selection with DL for long-term predictions are particularly effective in forecasting complex risks such as pest outbreaks, extreme weather events, and supply chain failures *(Paul, R.K. et al, 2022; Khatraty, Y. et al, 2022).*
  - Clustering + ML: Recent research highlights the application of clustering algorithms with traditional ML models for improved sales prediction in retail environments. The same approach can be adapted to agriculture to group farms with similar environmental and economic characteristics *(Udokwu, C. et al, 2022).*

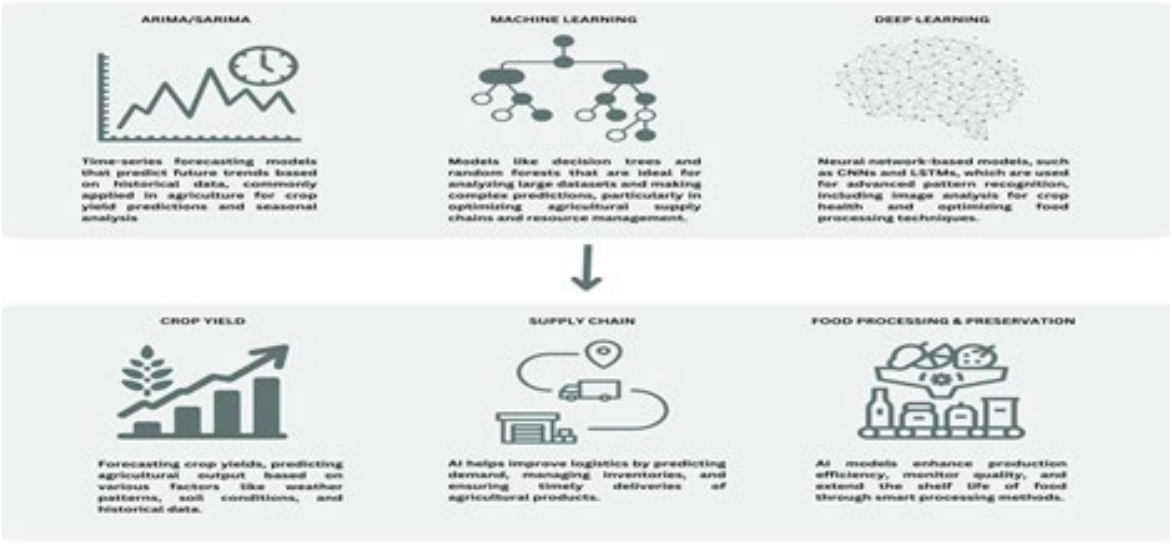

Fig. 2 - Applications of forecasting models based on artificial intelligence in agriculture
(Dhal, S.B. and Kar, D., 2024)

Sensors used in agriculture

In this paper, we present a single device that integrates multiple sensors to facilitate farmer interaction with technology. This approach eliminates the need for the farmer to implement four distinct sensors.

- **IP68 ABS Soil NPK Sensor Taidacent, B08MXXSP59, Guangzhou, China** (fig. 3), high-precision NPK sensor for soil nutrients, intelligent fertilizer detector, tester. Technical specifications: Measurement range: 0-1999 mg/kg; Working humidity: 5-95% (relative humidity), non-condensing; Measurement accuracy: ±2%F.s; Resolution: 1 mg/kg (mg/L); Working temperature: 5-45°C; Power supply: 12 V-24 V DC *(Amazon, 2024)*.
- **The ESP32 microcontroller (SIMAC Electronics HANDEL GmbH, Neukirchen-Vluyn, Germany)** (fig. 4) was used to develop the sensor system, which serves as the central processing unit for controlling the entire system. It incorporates the 5-pin NPK sensor to measure soil parameters such as potassium, phosphorus, moisture, temperature and pH levels. The system is equipped with Wi-Fi connectivity for real-time data transmission and includes local data logging on an SD card to ensure data backup in case of Wi-Fi instability *(McCormick, A., 2017)*.

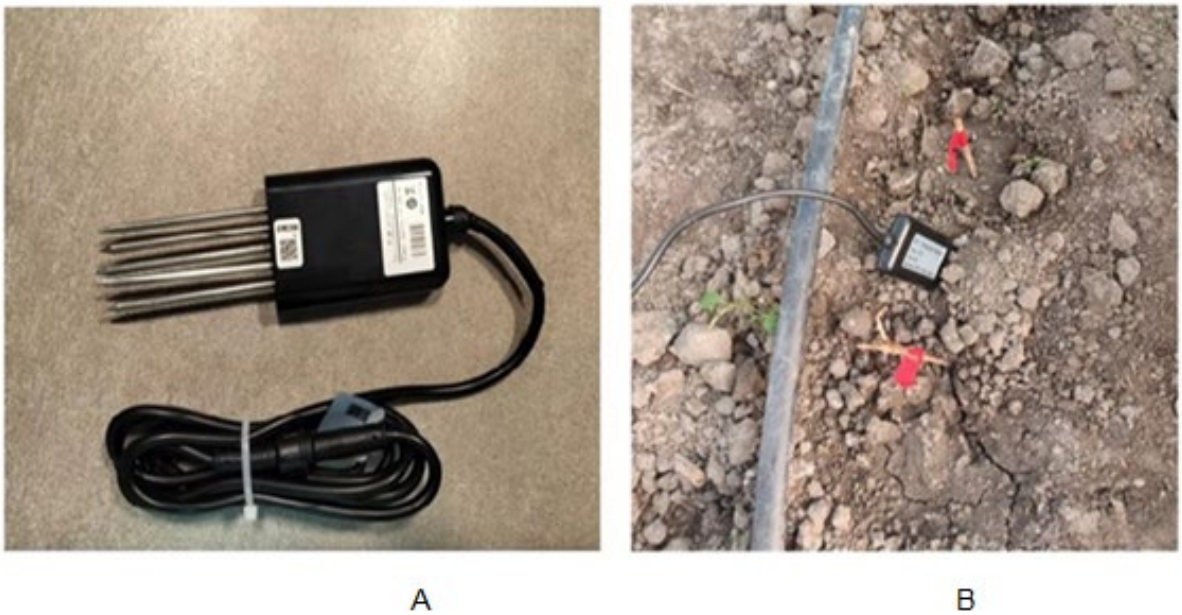

Fig. 3 - (A). A close-up view of the sensor. (B). The NPK sensor installed.
(Amazon, 2024)

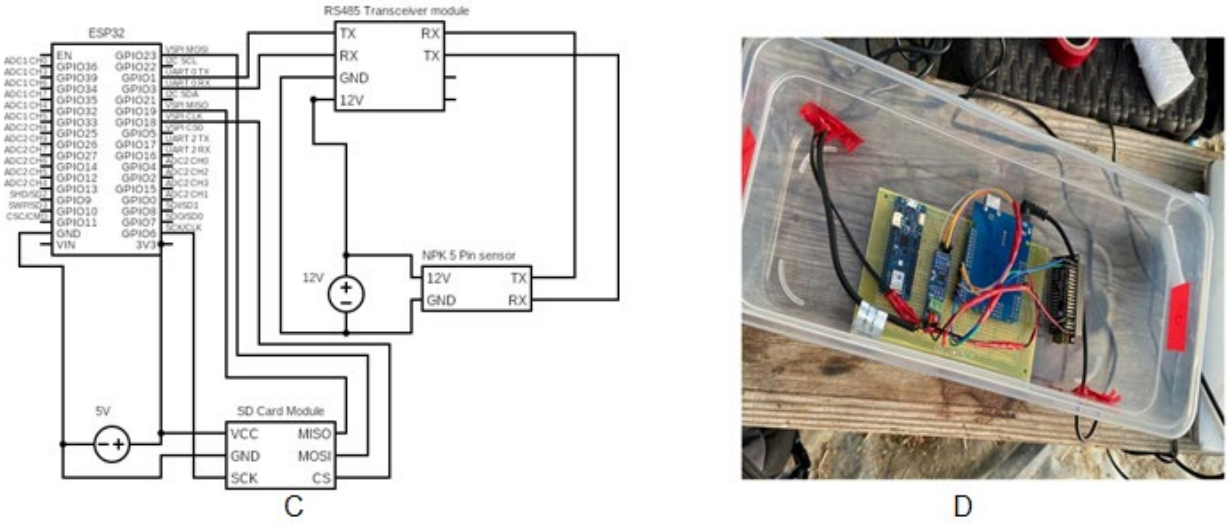

Fig. 4 - Schematic diagram of the system circuit (C) and the actual installed system (D).
(McCormick, A., 2017)

The data collection process was designed to capture comprehensive data on environmental and soil parameters across the entire site. Fig. 5 illustrates the flow chart of the steps involved in this process. The sensors continuously recorded data at set intervals (every 2 minutes) to capture sufficient variations and overall trends. The data was transmitted via Wi-Fi to a central database using IoT communication protocols. A data logger was also used as a backup plan to prevent data loss. The collected data was recorded in a cloud-based storage system, allowing remote access cloud, permițând accesul de la distanță *(Weraikat, D. et al, 2024).*

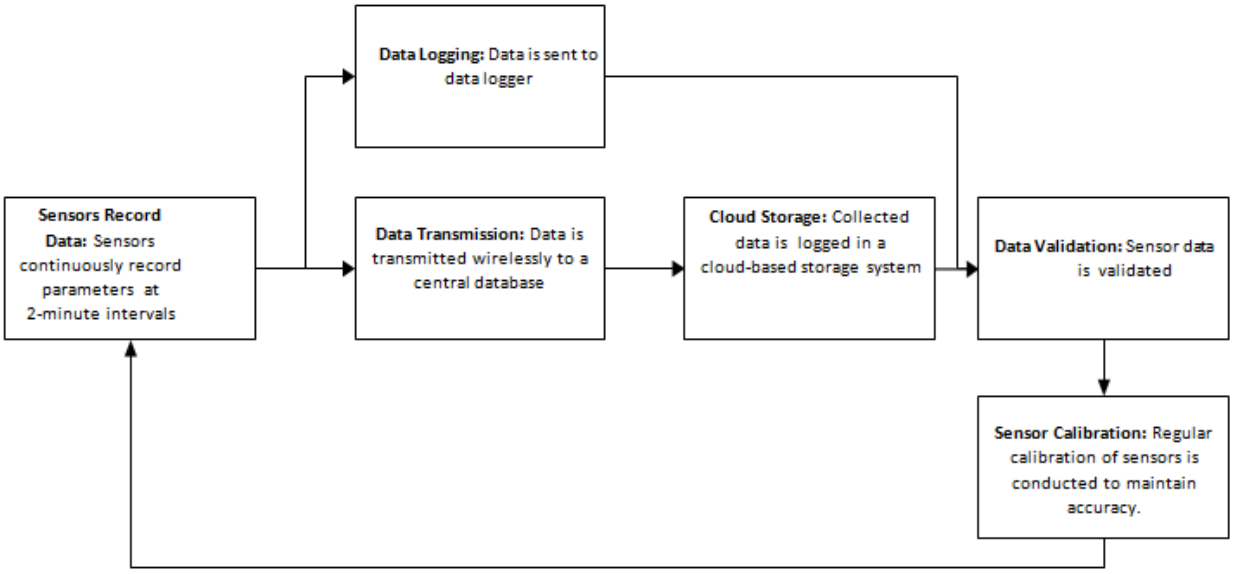

Fig. 5 - Data collection process for environmental and soil parameters.
(Weraikat, D. et al, 2024)

Multi-objective optimization (MOO)

Multi-objective optimization (MOO) is an important strategy to address the multiple challenges of the food industry. This sector operates at the confluence of numerous, often conflicting, objectives, such as economic profitability, nutritional quality, environmental sustainability, and alignment with global frameworks such as the United Nations 2030 Agenda for Sustainable Development. Multi-objective optimization (MOO) provides a structured methodology for balancing diverse objectives, providing a path to innovation, resilience, and sustainability in food production and distribution systems. Ecological sustainability and alignment with global frameworks such as the United Nations 2030 Agenda for Sustainable Development. MOO provides a structured methodology for balancing these diverse objectives, providing a path to

innovation, resilience, and sustainability in food production and distribution systems (*Biegler, L.T. et al, 1995)*.

In fig. 6 presents various applications and objectives of MOO in the food industry, focusing on essential objectives such as reducing operational costs, environmental sustainability, food quality and food safety *(Arteaga-Cabrera, E. et al, 2025).*

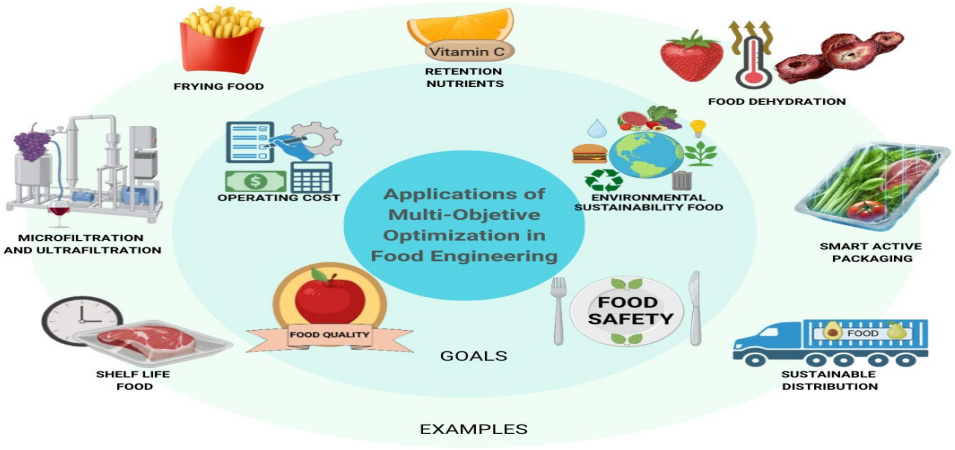

Fig. 6 - Applications of multi-objective optimization in food engineering.
(Arteaga-Cabrera, E. et al, 2025)

RESULTS

By using the information obtained from studying the specialized literature on multi-objective optimization, forecasting models and sensors used in agriculture, the focus was on the benefits and possible limitations of forecasting models and sensors. In Table 1, we have presented the smart devices on which the study of this paper was in-depth, where we presented the applications of each model and also their benefits and limitations in order to form a concise representation for the stakeholders.

Table 1

Benefits and limitations of forecasting models and sensors used in agriculture

Nr. crt.	Smart Agriculture		Instruments	Benefits	Limitation	Reference
1			Time series models (ARIMA and SARIMA)	informed decisions on resource allocation	sensitivity to non-stationary data	*Suresh,K.K.et al, 2011;*
				extension to processing programs	gestmanaging external variables	*Falatouri,T.et al, 2022*
2			Machine Learning (ML) Models (ML Models including RF and SVM)	solid information about market dynamics and resource optimization	Interpretability	*Kok,Z.H.et al, 2021;*
					risk of overadaptation	*Suresh,N.et al, 2021*
					computational requirements	
3		Forecasting models	Models DL (LSTM; CNN)	accurate predictions of impacts on the environment and agricultural systems	high computational cost	*Jaiswal,R.et al, 2022;*
				monitors crop health and predicts supply disruptions	data requirements and difficulty in understanding outputs	*Prashanthi,V. and Srinivas,K., 2020*
4			Time series + ML	accuracy of forecasts regarding yield and prices	for hybrid models there is no concrete data regarding their limitations	*Guo, Y., 2024; Özden,C., 2023*
5			ML+DL	effective in forecasting complex risks (pest outbreaks, extreme weather events)		*Paul,R.K. et al, 2022; Khatraty,Y. et al, 2022*
6			Clustering + ML	improved sales prediction in retail environments		*Udokwu,C.et al, 2022*
7	Sensors used in agriculture	Integrated equipment	Taidacent IP68 ABS Soil NPK Sensor, B08MXXSP59, Guangzhou, China	captures complete data on environmental and soil parameters (potassium, phosphorus, moisture, temperature and pH levels)	high costs: expensive for small or medium-sized farms	*Amazon, 2024; McCormick,A.,2017; Weraikat,D.et al, 2024*
					maintenance and calibration: sensors require periodic maintenance and calibration	
			Microcontrolerul ESP32 (SIMAC Electronics HANDEL GmbH, Neukirchen-Vluyn, Germania)		data security: data collection and transmission may raise security concerns	
					electromagnetic interference: from other devices	
					data interpretation: farmers must have the necessary knowledge and skills	

CONCLUSIONS

The benefits of forecasting models demonstrate their potential to play an instrumental role in addressing global food security challenges by increasing productivity, optimizing resource use, and reducing losses along the food supply chain. While there are limitations to forecasting models, particularly those related to data quality, model scalability, interpretability, and the infrastructure required for real-time forecasting, investing in technological innovation, fostering collaborations, and developing accessible and explainable tools that can be used successfully is essential. Forecasting models can become a vital component in building a sustainable, resilient, and productive global food system.

The benefits of sensors used in agriculture support the collection of accurate and real-time data, which helps farmers make data-driven decisions that optimize resource use, increase crop yields, and promote environmental sustainability. In the case of limitations, to minimize them, it is important to choose

reliable sensors and implement an appropriate maintenance and calibration strategy. It is also essential to ensure data security and provide farmers with training and support to use the technology effectively.

ACKNOWLEDGEMENT

This research was supported by Project METROFOOD-RO Evolve, SMIS Code 2021+ 309287, Strengthening the integration of the Romanian METROFOOD-RO node into the European research infrastructure METROFOOD-RI, and Project PN 23 04 02 01, Contract no.: 9N/ 01.01.2023 SUSTAIN–DIGI -AGRI, Innovative biofertilizer production technology used to restore soil biodiversity and reduce the effects of drought on agricultural lands.

REFERENCES

[1] Abaku, E.A., Edunjobi, T.E., Odimarha, A.C. (2024). Theoretical approaches to AI in supply chain optimization: Pathways to efficiency and resilience. Int. J. Sci. Technol. Res. Arch., 6, 92–107. https://doi.org/10.53771/ijstra.2024.6.1.0033

[2] Alexandratos, N., Bruinsma, J. (2012). World Agriculture Towards 2030/2050: The 2012 Revision. Food and Agriculture Organization: Rome, Italy

[3] Amazon. Xinwoer. (2024). Available online: https://www.amazon.com/Xinwoer-Precision-Nutrient-Intelligent-Fertilizer/dp/B07ZKTK8QR (accessed on 6 June 2024)

[4] Arteaga-Cabrera, E., Ramírez-Márquez, C., Sánchez-Ramírez, E., Segovia-Hernández, J.G., Osorio-Mora, O., Gómez-Salazar, J.A. (2025). Advancing Optimization Strategies in the Food Industry: From Traditional Approaches to Multi-Objective and Technology-Integrated Solutions. Appl. Sci., 15, 3846. https://doi.org/10.3390/app15073846

[5] Basso, B., Liu, L. (2019). Seasonal Crop Yield Forecast: Methods, Applications, and Accuracies. Adv. Agron., 154, 201–255

[6] Beacham, A.M., Vickers, L.H., Monaghan, J.M. (2019). Vertical Farming: A Summary of Approaches to Growing Skywards. J. Hortic. Sci. Biotechnol., 94, 277–283. https://doi.org/10.1080/14620316.2019.1574214

[7] Benami, E., Jin, Z., Carter, M.R., Ghosh, A., Hijmans, R.J., Hobbs, A., Kenduiywo, B., Lobell, D.B. (2021). Uniting remote sensing, crop modelling and economics for agricultural risk management. Nat. Rev. Earth Environ., 2, 140–159. https://doi.org/10.1038/s43017-020-00122-y

[8] Biegler, L.T., Nocedal, J., Schmid, C. (1995). A reduced Hessian method for large-scale constrained optimization. SIAM J. Optim., 5,314–347.

[9] Dahlberg, K. (2012). (Ed.) Beyond the Green Revolution: The Ecology and Politics of Global Agricultural Development; Springer Science & Business Media: New York, NY, USA

[10] Dhal, S.B., Kar, D. (2024). Transforming Agricultural Productivity with AI-Driven Forecasting: Innovations in Food Security and Supply Chain Optimization. Forecasting, 6, 925–951. https://doi.org/10.3390/ forecast6040046

[11] Divisekara, R.W., Jayasinghe, G.J.M.S.R., Kumari, K.W.S.N. (2020). Forecasting the Red Lentils Commodity Market Price Using SARIMA Models. SN Bus. Econ., 1, 20. https://doi.org/10.1007/s43546-020-00020-x

[12] Carrizosa, E., Morales, D.R. (2013). Supervised classification and mathematical optimization. Comput. Oper. Res., 40,150–165. https://doi.org/10.1016/j.cor.2012.05.015

[13] El Jaouhari, A., Hamidi, L.S. (2024). Assessing the influence of artificial intelligence on agri-food supply chain performance: The mediating effect of distribution network efficiency. Technol. Forecast. Soc. Chang., 200, 123149

[14] Falatouri, T., Darbanian, F., Brandtner, P., Udokwu, C. (2022). Predictive Analytics for Demand Forecasting—A Comparison of SARIMA and LSTM in Retail SCM. Procedia Comput. Sci., 200, 993–1003. https://doi.org/10.1016/j.procs.2022.01.298

[15] Friha, O., Ferrag, M., Shu, L., Maglaras, L., Wang, X. (2021). Internet of Things for the Future of Smart Agriculture: A Comprehensive Survey of Emerging Technologies. IEEE/CAA J. Autom. Sin., 8, 718–752. https://doi.org/10.1109/JAS.2021.1003925

[16] Gafurov, A., Mukharamova, S., Saveliev, A., Yermolaev, O. (2023). Advancing Agricultural Crop Recognition: The Application of LSTM Networks and Spatial Generalization in Satellite Data Analysis. Agriculture, 13, 1672. https://doi.org/10.3390/agriculture13091672

[17] Gao, T., Tian, Y., Zhu, Z., Sun, D.-W. (2020). Modelling, responses and applications of time-temperature indicators (TTIs) in monitoring fresh food quality. Trends Food Sci. Technol., 99, 311–322. https://doi.org/10.1016/j.tifs.2020.02.019

[18] Guo, Y. (2024). Integrating Genetic Algorithm with ARIMA and Reinforced Random Forest Models to Improve Agriculture Economy and Yield Forecasting. Soft Comput., 28, 1685–1706. https://doi.org/10.1007/s00500-023-09516-8

[19] Iitsuka, S., Fujii, N., Kokuryo, D., Kaihara, T., Nakano, S. (2019). CNN-Based Growth Prediction of Field Crops for Optimizing Food Supply Chain. In Proceedings of the IFIP WG 5.7 International Conference, APMS 2019, Austin, TX, USA, 1–5 September 2019, Part I. Springer International Publishing: Cham, Switzerland, pp. 148–154.

[20] Jaiswal, R., Jha, G.K., Kumar, R.R., Choudhary, K. (2022). Deep Long Short-Term Memory Based Model for Agricultural Price Forecasting. Neural Comput. Appl., 34, 4661–4676. https://doi.org/10.1007/s00521-021-06621-3

[21] Kalantari, F., Tahir, O.M., Joni, R.A., Fatemi, E. (2018). Opportunities and Challenges in Sustainability of Vertical Farming: A Review. J. Landsc. Ecol., 11, 35–60. https://doi.org/10.1515/jlecol-2017-0016

[22] Kang, Y., Khan, S., Ma, X. (2009). Climate Change Impacts on Crop Yield, Crop Water Productivity and Food Security—A Review. Prog. Nat. Sci., 19, 1665–1674. https://doi.org/10.1016/j.pnsc.2009.08.001

[23] Kennedy, N. (2024). Data-Driven Farming: Key to Agri Success. Agribusiness Strategies. The Farming Insider. 2 March 2024. Available online: https://thefarminginsider.com/data-driven-agri-farming/ (accessed on 6 June 2024).

[24] Khatraty, Y., Mellouli, N., Diallo, M., Nanne, M. (2022). Deep Predictive Models Based on IoT and Remote Sensing Big Time Series for Precision Agriculture. Int. J. Emerg. Technol. Adv. Eng., 12, 79–88. https://doi.org/1010.46338/ijetae1122_09

[25] Kim, N., Ha, K.-J., Park, N.-W., Cho, J., Hong, S., Lee, Y.-W. (2019). A comparison between major artificial intelligence models for crop yield prediction: Case study of the midwestern United States, 2006–2015. ISPRS Int. J. Geo-Inf., 8, 240. https://doi.org/10.3390/ijgi8050240

[26] Kok, Z.H., Shariff, A.R.M., Alfatni, M.S.M., Khairunniza-Bejo, S. (2021). Support Vector Machine in Precision Agriculture: A Review. Comput. Electron. Agric., 191, 106546. https://doi.org/10.1016/j.compag.2021.106546

[27] Lakshmi, G., Asha, P., Sandhya, G., Sharma, S., Shilpashree, S., Subramanya, S. (2023). An intelligent IOT sensor coupled precision irrigation model for agriculture. Meas. Sens., 25, 100608. https://doi.org/10.1016/j.measen.2022.100608

[28] Macholdt, J., Piepho, H.-P., Honermeier, B. (2019). Mineral NPK and manure fertilisation affecting the yield stability of winter wheat: Results from a long-term field experiment. Eur. J. Agron., 102, 14–22. https://doi.org/10.1016/j.eja.2018.10.007

[29] McCormick, A. (2017). Spring Onions—Harvst, 31 May 2017. Available online: www.harvst.co.uk/how-to-grow-spring-onions (accessed on 24 October 2023).

[30] Mila, F.A., Parvin, M.T. (2019). Forecasting Area, Production and Yield of Onion in Bangladesh by Using ARIMA Model. Asian J. Agric. Ext. Econ. Sociol., 37, 1–12. https://doi.org/10.9734/ajaees/2019/v37i430274

[31] Misra, N.N., Dixit, Y., Al-Mallahi, A., Bhullar, M.S., Upadhyay, R., Martynenko, A. (2020). IoT, big data, and artificial intelligence in agriculture and food industry. IEEE Internet Things J., 9, 6305–6324. https://doi.org/10.1109/JIOT.2020.2998584

[32] Murali, K.S., Abhishek, R., Neelamadhab, P. (2023). IoT-Enabled Soil Nutrient Analysis and Crop Recommendation Model for Precision Agriculture. Computers, 12, 61. https://doi.org/10.3390/computers12030061

[33] Özden, C. (2023). Comparative Analysis of CNN, LSTM and Random Forest for Multivariate Agricultural Price Forecasting. Black Sea J. Agric., 6, 422–426. https://doi.org/10.47115/bsagriculture.1304625

[34] Paul, R.K., Yeasin, M., Kumar, P., Kumar, P., Balasubramanian, M., Roy, H.S., Paul, A.K., Gupta, A. (2022). Machine Learning Techniques for Forecasting Agricultural Prices: A Case of Brinjal in Odisha, India. PLoS ONE, 17, e0270553. https://doi.org/10.1371/journal.pone.0270553

[35] Pawar, R.Y., Deshmukh, P.B., Metre, V.A., Ghogardare, S.V. (2021). Improving Plant Yield by Smart Irrigation System Using pH and NPK Sensors. Sensors, 2, 293–303

[36] Prashanthi, V., Srinivas, K. (2020). Plant Disease Detection Using Convolutional Neural Networks. Int. J. Adv. Trends Comput. Sci. Eng., 9, 3633–3637. https://doi.org/10.30534/ijatcse/2020/21932020

[37] Radoglou-Grammatikis, P., Sarigiannidis, P., Lagkas, T., Moscholios, I. (2020). A compilation of UAV applications for precision agriculture. Comput. Netw., 172, 107148. https://doi.org/10.1016/j.comnet.2020.107148

[38] Rozenstein, O., Cohen, Y., Alchanatis, V., Behrendt, K., Bonfil, D., Eshel, G., Harari, A., Harris, W., Klapp, I., Laor, Y., et al. (2024). Data-driven agriculture and sustainable farming: Friends or foes? Precis. Agric., 25, 520–525. https://doi.org/10.1007/s11119-023-10061-5

[39] Saikanth, K., Latha, A.M., Priyadarshini, K., Satya Prasad, M., Suneetha, A., Lakshmi, K.P. (2023). Advancing Sustainable Agriculture: A Comprehensive Review for Optimizing Food Production and Environmental Conservation. Int. J. Plant Soil. Sci., 35, 417–425. https://doi.org/10.9734/ijpss/2023/v35i163169

[40] Saiz-Rubio, V., Rovira-Más, F. (2020). From smart farming towards agriculture 5.0: A review on crop data management. Agronomy,10, 207. https://doi.org/10.3390/agronomy10020207

[41] Shafi, U., Mumtaz, R., García-Nieto, J., Hassan, S., Zaidi, S., Iqbal, N. (2019). Precision agriculture techniques and practices: From considerations to applications. Sensors, 19, 3796. https://doi.org/10.3390/s19173796

[42] Sharma, N., Acharya, S., Kumar, K., Singh, N., Chaurasia, O.P. (2018). Hydroponics as an Advanced Technique for Vegetable Production: An Overview. J. Soil. Water Conserv., 17, 364–371. https://doi.org/10.5958/2455-7145.2018.00056.5

[43] Singh, B., Kaunert, C. (2024). Harnessing Sustainable Agriculture Through Climate-Smart Technologies: Artificial Intelligence for Climate Preservation and Futuristic Trends. In Exploring Ethical Dimensions of Environmental Sustainability and Use of AI, IGI Global: Hershey, PA, USA, pp. 214–239. Available online: https://www.igi-global.com/chapter/harnessing-sustainableagriculture-through-climate-smart-technologies/334962 (accessed on 30 August 2024).

[44] Stafford, J. (2000). Implementing precision agriculture in the 21st century. J. Agric. Eng. Res., 76, 267–275. https://doi.org/10.1006/jaer.2000.0577

[45] Subeesh, A., Mehta, C. (2021). Automation and digitization of agriculture using artificial intelligence and internet of things. Artif. Intell. Agric., 5, 278–291. https://doi.org/10.1016/j.aiia.2021.11.004

[46] Suebsombut, P., Sekhari, A., Sureephong, P., Belhi, A., Bouras, A. (2021). Field Data Forecasting Using LSTM and Bi-LSTM Approaches. Appl. Sci., 11, 11820. https://doi.org/10.3390/app112411820

[47] Suresh, K.K., Priya, S.R.K. (2011). Forecasting Sugarcane Yield of Tamilnadu Using ARIMA Models. Sugar Tech, 13, 23–26. https://doi.org/10.1007/s12355-011-0071-7

[48] Suresh, N., Ramesh, N.V.K., Inthiyaz, S., Priya, P.P., Nagasowmika, K., Kumar, K.V.N.H., Shaik, M., Reddy, B.N.K. (2021). Crop Yield Prediction Using Random Forest Algorithm. In Proceedings of the 2021 7th International Conference on Advanced Computing and Communication Systems (ICACCS), Coimbatore, India, 19–20 March 2021; Volume 1, pp. 279–282.

[49] Udokwu, C., Brandtner, P., Darbanian, F., Falatouri, T. (2022). Improving sales prediction for point-of-sale retail using machine learning and clustering. In Machine Learning and Data Analytics for Solving Business Problems: Methods, Applications, and Case Studies; Springer International Publishing: Cham, Switzerland, pp. 55–73.

[50] Yolmeh, M., Jafari, S.M. (2017). Applications of response surface methodology in the food industry processes. Food Bioprocess Technol., 10, 413–433. https://doi.org/10.1007/s11947-016-1855-2

[51] Weddell, B.J. (2023). Precision Agriculture. Int. J. Comput. Algorithm, 12.

[52] Weraikat, D., Šoriˇc, K., Žagar, M., Sokaˇc, M. (2024). Data Analytics in Agriculture: Enhancing DecisionMaking for Crop Yield Optimization and Sustainable Practices. Sustainability, 16, https://doi.org/10.3390/su16177331

EXTENSIVE GREEN ROOFS FOR SMART BUILDINGS
/
ACOPERIȘURI VERZI EXTENSIVE PENTRU CLADIRI SMART

Dragos Mihail PREDA*[1)], Adrian PANDELE[1)], Bogdan Ovidiu DURAN[1)], Elena VILCU*[2)], Andrei VULPE*[2)], Gheorghe VOICU[3)]
[1)] ROLIX IMPEX SERIES SRL / Romania;
[2)] ARROW SRL / Romania;
[3)] UNST POLITEHNICA Bucharest / Romania.
*Tel: (+40)749 998 642; *Email: dragospreda@yahoo.com*

Keywords: green roof, Subsurface Textile Irrigation (SSTI), water reuse, water efficiency, agrivoltaics.

ABSTRACT
This paper presents a comparative evaluation of innovative irrigation technologies for extensive green roofs integrated into smart buildings. The study analyzes the Pirouz self-irrigated system and the Subsurface Textile Irrigation (SSTI) solution, focusing on water efficiency, moisture distribution, and structural performance. Simulation results show irrigation water savings of up to 70% and improved substrate uniformity compared to conventional systems. Both technologies allow the reuse of filtered greywater, supporting circular resource management. The findings confirm their potential to enhance building sustainability, reduce urban heat, and improve environmental resilience.

REZUMAT
Lucrarea prezintă o evaluare comparativă a tehnologiilor inovatoare de irigare pentru acoperișuri verzi extensive integrate în clădiri inteligente. Studiul analizează sistemul autoirigat Pirouz și soluția de irigare cu textile subterane (SSTI), având ca obiectiv eficiența apei, uniformitatea umidității și performanța structurală. Rezultatele simulărilor arată economii de apă de până la 70% și o distribuție mai uniformă a umidității comparativ cu sistemele convenționale. Ambele tehnologii permit reutilizarea apei gri filtrate, susținând economia circulară. Concluziile confirmă potențialul acestora de a îmbunătăți sustenabilitatea clădirilor și reziliența urbană.

INTRODUCTION
In recent decades, the rapid pace of urbanization and the growing demand for energy-efficient buildings have intensified interest in sustainable architectural solutions. Among these, *green roofs*—vegetated layers installed on the rooftops of buildings—represent one of the most effective nature-based strategies for mitigating urban environmental challenges. *Extensive green roofs*, in particular, are characterized by lightweight substrates (typically 5–15 cm thick), low-maintenance vegetation such as sedums and grasses, and adaptability to a wide range of structural systems. Unlike intensive systems, which function as accessible gardens, extensive green roofs prioritize environmental performance and scalability across large urban surfaces (*Antrop M., 2004; Beradi and Ghaffarian, 2019*).

Integrating extensive green roofs into *smart building* design aligns with contemporary concepts of digitalized and climate-adaptive architecture. These systems contribute to thermal insulation, reduction of the urban heat island effect, stormwater management, and enhancement of air quality, while simultaneously improving building energy performance. When equipped with sensor networks and IoT monitoring tools, green roofs become intelligent components capable of regulating irrigation, detecting substrate moisture, and transmitting real-time environmental data (*Lee et al., 2015; Shafique et al., 2018; Fioretti et al., 2010)*.

The implementation of such hybrid *eco-digital infrastructures* supports the transition toward sustainable cities and aligns with the European Green Deal objectives for climate-neutral buildings by 2050. This paper explores the functional characteristics, environmental benefits, and technological integration of extensive green roofs in the context of smart buildings, focusing on their potential to improve urban resilience, resource efficiency, and long-term sustainability (*European Union, 2015; Getter and Rowe, 2006*).

Systems for extensive green roofs that combine:

- a network of pipes for water storage,
- a innovative multi-chamber filters,

- a optimized drainage layer,
- a and the use of stored water for both irrigation and other domestic and civil uses.

Fig. 1 - Green systems for buildings
(https://www.permagard.co.uk/advice/green-roof-construction)

It also provides a comprehensive analysis of the system's performance compared to conventional green roofs – including water retention, runoff filtration, irrigation needs, etc (*Xu et al., 2012*).

Other relevant complementary technologies

• **Subsurface Textile Irrigation (SSTI)** – an underground system that distributes water and nutrients directly to the roots, reducing evaporation losses and allowing the use of recycled water: o it makes water consumption more efficient with savings between 50–75%; it has an exceptional lifespan; o it can cover large volumes of soil; it ensures uniform distribution through capillary geotextiles; o it is also adapted for commercial areas or urban green projects (*https://en.wikipedia.org/wiki/Subsurface_textile_irrigation*).

• **"Green roof + agrivoltaic" approaches** – plants grown under solar panels on the roof: o the shade created reduces evaporation by up to 50–66% and, by cooling the air, improves the efficiency of photovoltaic panels; o bi-functional system: food production + solar energy + reduction of the urban heat island effect (*https://www.wired.com/story/the-ultra-efficient-farm-of-the-future-is-in-the-sky*).

• **Rainwater and greywater reuse** – controlled use of collected water for rooftop irrigation: o approach through advanced models (MPC) that anticipate weather conditions and optimize pump control; o reduce drinking water consumption and dependence on the municipal network *(https://arxiv.org/abs/2110.13669).*

In Romania, green-roof adoption is still at an early stage; the European Federation of Green Roof Associations reports roughly **~400,000 m²** of green roofs nationwide, with no comprehensive national inventory yet in place, despite strong potential to mitigate urban heat and manage stormwater (*EFB, 2023; Berardi & Ghaffarian Hoseini, 2019*).

This paper presents an approach to green roof, taking into account the pressure on urban green spaces and the need for rooftop use, the challenges regarding water consumption, runoff management and plant efficiency, theoretical foundations, types of green roofs and principles of phytoremediation, retention, and thermoregulation.

MATERIALS AND METHOD

The systems studied in this paper integrate two innovative technologies for extensive green roofs: (i) the Pirouz self-irrigated system with multilayer filters and PVC reservoirs, and (ii) Subsurface Textile Irrigation (SSTI) for optimized water delivery at the root zone.

The modular platform consists of a waterproof membrane, root barrier, and lightweight vegetative substrate (5–15 cm depth). Below the substrate, PVC pipes (Ø 75–110 mm) form a storage and drainage network, allowing rainwater and greywater retention. Above these pipes, multi-chamber ceramic and polypropylene filters ensure sequential sediment capture and purification, enabling the reuse of treated water for irrigation. The SSTI layer—comprising subsurface drip lines covered by a capillary geotextile—distributes moisture laterally by capillarity, maintaining uniform soil humidity while minimizing evaporation losses (*Pirouz et al., 2023)*.

System performance was assessed through simulation and literature-validated parameters (*Pirouz et al., 2023; Sunnylands Foundation, 2017*). Comparative evaluation with conventional green roofs included parameters such as water consumption, moisture uniformity, structural weight, and suitability for integration with photovoltaic (agrivoltaic) modules.

Subsurface Textile Irrigation (SSTI)

Structure: at the base it has an impermeable layer, over which drip tubes and a capillary geotextile are placed, covered by a superficial impermeable layer to avoid water "tunneling" to the surface.

Distribution method: the geotextile captures and spreads water in a capillary manner over distances of up to 2m from the dripper, transforming an emission point into a dispersed source of water under the substrate.

Typical installation: 15–20cm under the substrate in urban applications; 30–50cm in agriculture.

Significant benefits:

- 50–75% reduction in water consumption compared to surface irrigation;
- Allows the use of recycled or treated water – it does not reach the surface;
- Uniform distribution, avoiding evaporation and weed infestation.

Basic components of SSTI systems:

1. Drip tubes – placed under the substrate, transport water.
2. Capillary geotextile – placed above the tubes, takes water and distributes it evenly laterally.
3. Upper waterproof layer – prevents water from evaporating upwards.
4. Lower waterproof layer – isolates the system from the soil or the underlying structure (e.g. roof).

Water drains from the tube into the geotextile → is distributed horizontally by capillarity and moistens the surrounding root zone, without reaching the surface.

Table 1

Advantages of the SSTI System [13, 14, 17]

Advantage	Details
Significant reduction of water losses	Evaporation is minimal (water does not reach the surface).
Uniform distribution	The capillary geotextile ensures constant moisture throughout the entire root zone.
Allows the use of greywater or recycled water	Water does not reach the soil surface, so it does not come into contact with people or animals.
Prevents weed growth	The soil surface remains dry — fewer seeds can germinate.
Long service life	Over 20 years under normal conditions (according to manufacturers such as Irrigation & Water Technologies Australia).
Ideal for green roofs and urban spaces	Easy to install and maintain.

SSTI can be used for:

- Green roofs;
- Living walls;
- Urban green spaces (permeable pavements, public gardens);
- Urban and precision agriculture;
- Sports fields and luxury lawns.

Table 2

Comparison between SSTI and classic irrigation [13, 14, 17, 19]

Characteristic	Conventional Irrigation	SSTI
Evaporation	High	Very low
Runoff losses	Frequent	Minimal
Surface moisture	Yes	No
Risk of fungal diseases	High (due to surface humidity)	Very low
Maintenance requirements	Moderate	Low
Water distribution	Variable	Uniform

The Pirouz self-irrigated system represents an innovative water-management solution designed specifically for extensive green roofs and arid or semi-arid environments. Its core principle is based on multi-layered water retention and capillary redistribution, allowing the roof substrate to remain moist without the need for frequent surface irrigation (*Pirouz et al., 2023*).

The system integrates PVC or polypropylene drainage pipes with perforations that act simultaneously as *water reservoirs and distribution channels*. Above these, a sequence of filtering layers—including coarse gravel, sand, and synthetic textiles—facilitates gradual capillary movement of water toward the root zone. This configuration ensures efficient moisture balance, while preventing waterlogging or nutrient leaching.

A major innovation lies in the self-regulating drainage mechanism, which allows excess rainfall to be stored temporarily and reused during dry periods. The filtration unit removes sediment and organic debris, maintaining water quality suitable for plant uptake and permitting the safe use of recycled or greywater sources. The modular construction makes it adaptable to a variety of roof geometries and structural load limits.

Overall, the Pirouz system enhances hydrological efficiency, reducing irrigation needs by up to 60–70%, improving substrate moisture uniformity, and contributing to the long-term sustainability of vegetated roofs. When combined with digital monitoring tools, it forms an intelligent irrigation platform that supports energy-efficient, climate-resilient urban design.

Table 3

Advantages of the Pirouz Self-Irrigated System (*Pirouz et al., 2023, 20, 15*)

Advantage	Details
Water-saving performance	The multilayer reservoir and capillary redistribution reduce irrigation demand by up to 60–70% compared with conventional green roof systems.
Self-regulating drainage	Automatically retains excess rainwater in PVC reservoirs and gradually redistributes it to the substrate during dry periods.
Improved moisture uniformity	Maintains consistent humidity throughout the root zone, preventing localized drought or oversaturation.
Compatibility with recycled water	Integrated filtering layers allow the safe use of greywater and rainwater, reducing potable water consumption.
Lightweight modular design	Suitable for extensive green roofs due to low structural load and easy installation on flat or slightly sloped roofs.
Reduced maintenance requirements	Filters and reservoirs function autonomously for long periods, requiring minimal servicing.
Extended plant vitality	Stable water availability supports healthy root development and increased vegetation coverage.
Environmental sustainability	Enhances stormwater management, mitigates the urban heat island effect, and supports circular resource use.

The data presented in Table 3 highlight the multifunctional nature of the Pirouz self-irrigated system, which integrates water retention, filtration, and capillary redistribution into a compact modular design. By maintaining optimal substrate humidity and recycling stored rainwater, the system reduces irrigation demand and supports sustainable vegetation growth even under limited water availability. Its lightweight and low-maintenance structure make it particularly suitable for extensive green roofs, while the capacity to utilize greywater enhances environmental performance and aligns with circular resource management principles.

RESULTS AND DISCUSSIONS

Simulation data and previous studies confirm that the proposed system significantly improves hydrological efficiency. Annual irrigation demand decreased by up to **66%** compared with conventional drip systems, while moisture distribution remained uniform throughout the substrate profile. The integrated PVC reservoirs retained 30–70 L/m²/year, depending on pipe diameter, ensuring self-sufficiency during moderate drought periods.

The SSTI layer contributed to 50–75% reductions in evaporation losses, and by isolating water flow from the surface, allowed safe reuse of greywater. When coupled with photovoltaic modules, the system

demonstrated an additional 30–60% decrease in evaporation due to shading and a 4% increase in PV efficiency, confirming the advantages of agrivoltaic integration.

Overall, the combined system maintaines a lightweight structural profile, facilitated installation even on sloped roofs, and provided water treatment through replaceable multi-layer filters. Estimated savings for a 500 m² roof in a temperate-continental climate reached up to 50 m³ of potable water per year.

Table 4

Comparative Table of System Performance [16, 19]

Characteristic	Conventional Green Roof	Pirouz System (Self-Irrigated)	SSTI System
Water retention/storage (volume)	Limited (gravel + substrate)	High (in PVC tubes)	Geotextile + drip system
Irrigation need during dry periods	High	Low (subsurface automatic irrigation)	Very low
Evaporation losses	High	Minimal	Very minimal
Possibility of using recycled water	No	Yes (filtered and treated water)	Yes (does not reach surface)
Moisture uniformity	Variable	Controlled	Excellent
Structural weight	High (gravel + substrate)	Lower (tubes vs. gravel)	Depends on SSTI structure
Integration with PV systems	Without significant benefits	Yes (reduced evaporation and energy synergy)	Depends on integration level

The comparative analysis presented in Table 4 illustrates the operational and functional differences among conventional green roofs, the Pirouz self-irrigated system, and the SSTI subsurface irrigation technology. The Pirouz system demonstrates superior water-retention capacity through the use of PVC reservoirs, ensuring gradual moisture release and significantly lower irrigation requirements. Similarly, the SSTI configuration provides exceptional uniformity of moisture distribution and minimizes evaporation losses due to its capillary geotextile layer. Both advanced systems enable the safe reuse of recycled or treated greywater, contributing to resource efficiency and sustainability. In contrast, traditional green roofs rely on surface irrigation, which increases water consumption and structural weight while offering limited control over moisture dynamics. Overall, the integration of self-irrigated and subsurface systems represents a major step toward high-efficiency, low-maintenance solutions for urban green infrastructure and smart building applications.

Table 5

Simulation Examples with Comparative Real Water Consumption Values (liters/m²/year)

Characteristic	Conventional Green Roof	Pirouz System (Self-Irrigated)	SSTI System
Water retention/storage (volume)	Limited (gravel + substrate)	High (in PVC tubes)	Geotextile + drip system
Irrigation need during dry periods	High	Low (automatic subsurface irrigation)	Very low
Evaporation losses	High	Minimal	Very minimal
Possibility of using recycled water	No	Yes (treated through filters)	Yes (does not reach surface)
Moisture uniformity	Variable	Controlled	Excellent
Structural weight	High (gravel + substrate)	Lower (tubes vs. gravel)	Depends on SSTI structure
Integration with PV systems	Without multiple benefits	Yes (reduces evaporation + increases energy efficiency)	Depends on integration level

The comparative simulation results summarized in Table X clearly demonstrate the superior hydrological performance of the Pirouz and SSTI systems compared to conventional green roof configurations. Both innovative solutions substantially reduce water losses through evaporation and runoff, while maintaining consistent substrate moisture even under dry climatic conditions. The Pirouz self-irrigated system achieves this by storing water within PVC reservoirs and delivering it gradually through a capillary process, whereas the SSTI design ensures uniform distribution via geotextile layers and subsurface drip

lines. Additionally, both systems enable the reuse of treated greywater, lowering the demand for potable water. These findings underline the potential of smart irrigation technologies to enhance the efficiency, sustainability, and adaptability of urban green infrastructure.

CONCLUSIONS

The combined Pirouz + SSTI system represents a scalable, efficient solution for sustainable green roof irrigation. Its modular architecture supports rainwater retention, filtration, and reuse within a self-regulated cycle that drastically lowers potable water demand. Results highlight the potential of integrating smart control and renewable energy components to further enhance system autonomy.

By combining physical water management with digital monitoring, extensive green roofs can evolve into *eco-intelligent* infrastructure units that contribute to climate-resilient cities. Future research should focus on long-term pilot studies, AI-driven irrigation control, and standardization of lightweight materials for large-scale deployment.

REFERENCES

[1] Antrop, M. Landscape change and the urbanization process in Europe. Landsc. Urban Plan 2004, 67, 9–26.
[2] Berardi, U., & GhaffarianHoseini, A. (2019). State-of-the-art analysis of the environmental benefits of green roofs. Applied Energy, 241, 108–129.
[3] European Commission Nature-Based Solutions & Re-Naturing Cities; EU Publications: Brussels, Belgium, 2015; Volume 35, ISBN 9789279460517.
[4] European Federation of Green Roof Associations (EFB). (2023). *Romania country profile & association updates* (Converde).
[5] Fioretti, R., et al. (2010). Green roof energy and water-related performance in Mediterranean climate. Building and Environment, 45(8), 1890–1904.
[6] Getter, K. L., & Rowe, D. B. (2006). The role of extensive green roofs in sustainable development. HortScience, 41(5), 1276–1285.
[7] Lee, J.Y.; Lee, M.J.; Han, M. A pilot study to evaluate runoff quantity from green roofs. J. Environ. Manag. 2015, 152, 171–176.
[8] Pirouz, B.; Palermo, S.A.; Becciu, G.; Sanfilippo, U.; Nejad, H.J.; Piro, P.; Turco, M. A Novel Multipurpose Self-Irrigated Green Roof with Innovative Drainage Layer. Hydrology 2023, 10, 57. https://doi.org/10.3390/hydrology10030057.
[9] Shafique, M.; Kim, R.; Rafiq, M. Green roof benefits, opportunities and challenges—A review. Renew. Sustain. Energy Rev 2018, 90, 757–773.
[10] Xu, T.; Sathaye, J.; Akbari, H.; Garg, V.; Tetali, S. Quantifying the direct benefits of cool roofs in an urban setting: Reduced cooling energy use and lowered greenhouse gas emissions. Build. Environ. 2012, 48, 1–6.
[11] *** https://en.wikipedia.org/wiki/Subsurface_textile_irrigation
[12] *** https://www.wired.com/story/the-ultra-efficient-farm-of-the-future-is-in-the-sky
[13] *** https://arxiv.org/abs/2110.13669
[14] *** https://www.epa.gov/heatislands/using-green-roofs-reduce-heat-islands
[15] *** https://sunnylands.org/wp-content/uploads/2017/08/Irrigation-Fact-Sheet.pdf
[16] *** https://consensus.app/papers/a-novel-multipurpose-selfirrigated-green-roof-with-nejad-pirouz/b0198c873b0d5808b6607026835b2c83/
[17] *** https://consensus.app/papers/a-novel-multipurpose-selfirrigated-green-roof-with-nejad-pirouz/b0198c873b0d5808b6607026835b2c83/
[18] *** https://www.wired.com/story/your-rooftop-garden-could-be-a-solar-powered-working-farm
[19] *** https://www.sciencedirect.com/science/article/abs/pii/S2210670715300081
[20] *** https://www.dripworks.com/blog/subsurface-drip-irrigation-for-lawns?srsltid=AfmBOoo82Adr5G2juwgDjjxz02hqxzyfl-l2_QwVSL8ws07VwUfe65pt&-
[21] *** https://extension.colostate.edu/topic-areas/agriculture/subsurface-drip-irrigation-sdi-4-716/
[22] *** https://www.researchgate.net/figure/More-details-of-the-novel-multipurpose-self-irrigated-GRs-1-Polystyrene-foam-or-other_fig12_368869606
[23] *** https://www.permagard.co.uk/advice/green-roof-construction

COMPARATIVE STUDY ON SOIL TYPES AND AGRICULTURAL POTENTIAL IN THE MAIN REGIONS OF ROMANIA

/

STUDIU COMPARATIV ASUPRA TIPURILOR DE SOL ȘI POTENȚIALULUI AGRICOL ÎN PRINCIPALELE REGIUNI ALE ROMÂNIEI

Iuliana GĂGEANU*[1)], Ana-Maria TĂBĂRAȘU[1)], Teofil-Alin ONCESCU[1)], Lorena-Diana POPA[2)]

[1)] National Institute of Research - Development for Machines and Installations Designed to Agriculture and Food Industry - INMA Bucharest / Romania;

[2)] ARDS Secuieni, Neamt County / Romania.

**E-mail: iulia.gageanu@gmail.com*

Keywords: *soil type; soil parameters; agricultural potential, fertility indicators, pedological diversity, sustainable land management.*

ABSTRACT

This paper presents a comparative assessment of the main soil types characteristic of three major agricultural regions of Romania: South-West Oltenia, South Muntenia, and North-East Moldova. The study integrates data from regional soil reports and typological classifications to evaluate pedological traits, fertility indicators, and agricultural suitability. The analysis reveals a clear spatial differentiation of soil quality and productive potential. Chernozems and Phaeozems exhibit high natural fertility and structural stability, supporting intensive cereal and industrial crop systems. Luvisols and Cambisols show moderate productivity constrained by acidity, compaction, and erosion, while Fluvisols provide favorable conditions for irrigated vegetable and forage crops. In contrast, Arenosols and Regosols are limited by coarse texture and low humus content, suitable mainly for drought-tolerant or perennial crops. The results emphasize the importance of region-specific soil management practices, including liming, organic amendments, and irrigation, to maintain fertility and ensure sustainable agricultural performance in line with European soil health and climate adaptation strategies.

REZUMAT

Lucrarea prezintă o evaluare comparativă a principalelor tipuri de sol specifice celor trei mari regiuni agricole ale României: Sud-Vest Oltenia, Sud Muntenia și Nord-Est Moldova. Studiul integrează date din rapoarte regionale de sol și clasificări pedologice pentru a analiza caracteristicile tipologice, indicatorii de fertilitate și gradul de favorabilitate agricolă. Analiza evidențiază o diferențiere spațială clară a calității solului și a potențialului productiv. Cernoziomurile și faeoziomurile prezintă o fertilitate naturală ridicată și o structură stabilă, susținând sisteme agricole intensive pentru cereale și culturi industriale. Luvisolurile și cambisolurile înregistrează o productivitate moderată, limitată de aciditate, compactare și procese de eroziune, în timp ce fluvisolurile oferă condiții favorabile pentru legume și culturi furajere în sistem irigat. În contrast, arenosolurile și regosolurile, caracterizate prin textură grosieră și conținut redus de humus, sunt potrivite doar pentru culturi perene sau tolerante la secetă. Rezultatele subliniază necesitatea aplicării unor practici de gestionare adaptate condițiilor regionale – amendamente calcaroase, fertilizare organică și irigații – pentru menținerea fertilității și asigurarea unei agriculturi durabile, în concordanță cu obiectivele europene privind sănătatea solului și adaptarea la schimbările climatice

INTRODUCTION

Soil resources represent one of the most important components of Romania's natural capital, underpinning agricultural production, ecosystem services, and rural development. The country's pedological diversity reflects the combined influence of climatic gradients, relief variability, and lithological heterogeneity, leading to the formation of highly productive Chernozems, moderately fertile Cambisols, and more constrained Luvisols and Podzols. Understanding this spatial variability is crucial for optimizing land use and ensuring sustainable crop production (*ICPA, 2012; MADR, 2024*).

Romania's agricultural regions—South-West Oltenia, South-Muntenia, and North-East Moldova—offer representative examples of soil heterogeneity, ranging from drought-prone sandy soils in Oltenia to erosion-sensitive Luvisols in Moldova. Such diversity affects both yield potential and the types of crops best

suited for cultivation. The adaptation of soil management practices to local characteristics, including fertilization, irrigation, and conservation measures, is therefore a key factor in achieving productivity and environmental sustainability (*Bucur et al., 2007*; *European Commission, 2022*).

To illustrate the complex interdependence between soil characteristics and agricultural performance, an integrative conceptual model was developed (Figure 1). This infographic summarizes the main physical, chemical, and biological properties that determine soil quality and how these influence key agricultural outcomes. By linking fundamental soil parameters—such as texture, organic matter, and nutrient balance—to yield potential and resource efficiency, the model emphasizes the functional role of soil as a living system underpinning sustainable crop production.

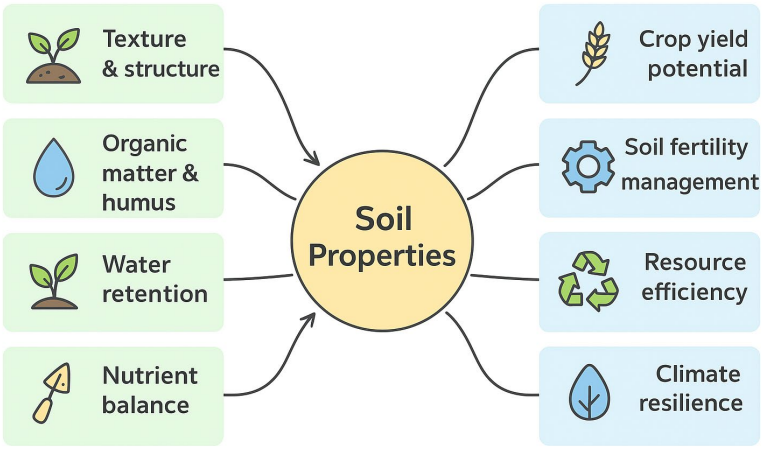

Fig. 1 - Main properties of soils in relation with agricultural potential

As shown in Figure 1, soil properties act as the foundation of agricultural potential. Well-structured soils with adequate organic matter and balanced nutrient content promote effective water retention, root development, and microbial activity, which in turn enhance crop productivity and long-term fertility. Conversely, degradation of any of these properties—through erosion, compaction, or nutrient imbalance—reduces efficiency and resilience. The diagram therefore highlights how maintaining soil health directly supports climate adaptation, resource sustainability, and overall farm performance in agricultural systems.

This study aims to compare the main soil types and their agricultural potential across these regions, identify limiting factors, and propose regionalized management strategies to support sustainable intensification and compliance with CAP 2023–2027 priorities related to soil health and climate adaptation.

MATERIALS AND METHODS

The analysis was conducted using data extracted from regional soil studies for Oltenia, Muntenia, and Moldova (2023–2024), as well as national pedological classifications (*ICPA database*). Parameters considered included soil type distribution, humus content, texture class, reaction (pH), base saturation, available water capacity (AWC), and known limiting factors (erosion, salinity, compactness). The evaluation focused on correlating these characteristics with the main agricultural crops cultivated in each region and their productivity potential.

The South-West Oltenia region is characterized by a predominance of Chernozems, Cambisols, and Arenosols, reflecting a gradual transition from fertile plains to more eroded upland terrains. The Calcaric and Cernic Chernozems found on the terraces of the Danube and Jiu Rivers represent some of Romania's most productive soils, with high humus content (3–5%), balanced structure, and excellent nutrient availability. These soils sustain intensive cultivation of maize, wheat, sunflower, and sorghum, although their fertility is threatened by drought and low water-holding capacity. In contrast, the sandy formations around Dăbuleni and Bechet are dominated by Arenosols and Regosols, where coarse texture, weak aggregation, and rapid drainage create severe moisture deficits during summer. Here, sustainable use depends on irrigation, mulching, and the introduction of drought-tolerant crops. On the piedmont slopes, Eutric Cambisols and Luvisols with medium fertility are present, supporting orchards, vineyards, and pastures when erosion control measures are applied (*Dumitru et al., 2011*).

The soils of the South-Muntenia region display significant variability influenced by relief, parent material, and climatic gradients. The most widespread are Luvisols, Cambisols, and Phaeozems, associated

with the vast plains of Teleorman, Argeș, and Ialomița counties. Luvic soils, often slightly acidic (pH 5.5–6.2), exhibit clay illuviation in the Bt horizon and moderate fertility, suitable for cereals, oilseed rape, and vineyards when properly limed and fertilized. Cambisols predominate in hilly areas and terraces, offering balanced physical properties but showing moderate erosion susceptibility. Phaeozems occur locally in depressions and areas with higher organic matter accumulation, supporting maize, sunflower, and forage crops. Despite favorable climatic conditions, the main limiting factors are periodic droughts, structural compaction, and erosion on slopes, which require conservation tillage, contour farming, and organic amendment practices to preserve productivity and soil structure (*Vintila et al., 2004; Vlad et al., 2010*).

The North-East region of Moldova presents one of Romania's most diverse and complex pedological landscapes, dominated by Luvisols, Chernozems, and Regosols formed under the influence of hilly relief, loessic deposits, and continental climate. Luvisols are the most extensive, especially on the Central Moldavian Plateau, where strong textural differentiation, moderate acidity, and erosion susceptibility limit intensive agriculture. However, with proper fertilization and liming, they can sustain profitable wheat, barley, and sunflower crops. Chernozems occur in the Botoșani–Iași area and remain highly fertile, with humus content above 4% and excellent structure, ideal for cereals and sugar beet cultivation. On steep slopes and recently eroded surfaces, Regosols and Erodosols are common, showing poor horizon development and requiring reforestation or perennial grass establishment to reduce land degradation. Overall, the agricultural potential of Moldova remains significant, provided that erosion control, organic matter restoration, and adaptive crop rotations are implemented (*Patriche et al., 2024; Matei et al., 2020; Niacsu et al., 2015*).

A comparative matrix was developed to highlight similarities and differences between regions. Oltenia's soils were characterized by the prevalence of Chernozems and Arenosols with good fertility but moderate water retention; Muntenia displayed a predominance of Luvisols and Cambisols with variable pH and structural instability; Moldova showed a complex pattern dominated by Luvisols and Chernozems, strongly affected by erosion and slope gradients.

The comparative analysis used qualitative and semi-quantitative indicators to assess soil fertility and potential agricultural use, supported by literature and field data from the Ministry of Agriculture and the National Research-Development Institute for Soil Science (ICPA, 2022).

RESULTS

Soil distribution and regional characteristics

- **South-West (S-W) Oltenia:** Soils are dominated by Chernozems and Cambisols, with moderate to high fertility and good nutrient balance. Arenosols appear in the southern sandy areas (Dăbuleni), where low water-holding capacity and drought risk limit crop productivity. Suitable crops include maize, sunflower, and sorghum, with irrigation required for stability.
- **South (S) Muntenia:** Luvisols and Phaeozems predominate, moderately acidic and rich in clay, favoring cereals, rapeseed, and vineyards. Soil compaction and reduced aeration are local constraints. Cambisols on slopes support orchards and pastures but require erosion control.
- **North-East (N-E) Moldova:** The region has a mosaic of Luvisols, Chernozems, and Regosols. Erosion is the main degradation factor due to the hilly relief. Despite good natural fertility, yield variability is high. Cereals (wheat, barley) and industrial crops (sugar beet, sunflower) are dominant.

The comparative synthesis presented in Table 1 highlights the pedological and agronomic diversity of the analyzed regions.

Table 1

Technological traits of the main soil types in the regions studied

Region	Dominant soil types	Fertility level	Main limiting factors	Recommended crops
South-West Oltenia	Chernozems, Cambisols, Arenosols	Medium–high	Drought, low water capacity	Maize, sunflower, sorghum
South Muntenia	Luvisols, Cambisols, Phaeozems	Medium	Acidity, compaction, erosion	Wheat, barley, rapeseed, vineyards
East Moldova	Luvisols, Chernozems, Regosols	Medium–high	Erosion, acidity, slope	Wheat, barley, sugar beet, sunflower

South-West Oltenia is characterized mainly by highly fertile Chernozems and Cambisols, whose productivity is occasionally limited by drought and low water-holding capacity. In South Muntenia, Luvisols and Cambisols dominate, displaying moderate fertility but structural and acidity constraints that necessitate corrective practices such as liming and organic fertilization. East Moldova mainly exhibits a mixture of Luvisols, Chernozems, and Regosols, where erosion and slope conditions reduce yield stability despite relatively high inherent fertility. The recommended crop systems reflect these constraints, emphasizing cereals and industrial crops in fertile plains, and forage or vineyard crops on more fragile terrains.

To provide a comprehensive understanding of the pedological diversity that shapes Romania's agricultural productivity, Table 2 summarizes the main physical, chemical, and biological parameters of the dominant soil types identified in the analyzed regions (Oltenia, Muntenia, and Moldova). The comparative data highlights the contrasting fertility levels, structural properties, and water retention capacities that determine the suitability of each soil for specific crops and management practices. These indicators represent averaged values derived from regional soil surveys and typological classifications established according to the Romanian Soil Taxonomy System (*Tarau et al., 2012*).

Table 2

Parameters and characteristics of soil types in S-W Oltenia, S – Muntenia and N-E – Moldova Regions

Parameter	Soil type						
	Chernozems	**Luvisols**	**Cambisols**	**Phaeozems**	**Fluvisols**	**Arenosols**	**Regosols**
Texture	Loam–loam-clay; stable granular structure	Loam–clay loam (Ap/E); clayey Bt (argic)	Clay loam to clay; weathering horizon	Loam; intermediate between Chernozems & Luvisols	Sandy loam to loam; stratified alluvium	Fine sand to fine sandy loam; >70% sand	Sandy loam/loamy sand; weak profile
pH	6.8–7.8 (neutral–slightly alkaline)	5.2–6.8 (slightly acidic–neutral)	5.8–6.8 (slightly acidic–neutral)	6.3–7.2 (near neutral)	6.5–7.8 (neutral–slightly alkaline)	5.0–6.2 (acidic to slightly acidic)	5.5–6.8 (slightly acidic–neutral)
Humus content (%)	3.5–5.5	1.8–3.0	2.0–3.2	3.0–4.0	1.8–3.5	0.6–1.5 (very low)	1.0–2.5 (low)
Base saturation (V%)	85–100 (high)	50–75 (moderate)	65–85 (well base-saturated)	70–90 (high)	>75 (often >85)	35–55 (low–moderate)	40–60 (low–moderate)
Water-holding capacity (AWC, %)	12–14	10–12	12–15	11–14	12–17	5–9	8–14
Bulk density (g/cm³)	1.20–1.35	1.35–1.50 (higher in Bt)	1.30–1.45	1.25–1.40	1.30–1.45	1.40–1.65	1.40–1.60
Total porosity (%)	48–55	38–45 (lower in Bt)	48–53	~50	45–52	35–42	—
Biological activity	High (active microbiota, mull humus)	Medium (limited in Bt)	Medium–high	High (humus-rich)	Medium–high	Low	Low–medium
Color & morphology	Dark; deeper; stable structure	Yellowish-brown; reddish with clay coatings	Dark brown; light to reddish	Dark surface horizon; leached subsurface	Stratified alluvial layers; weak profile	Light-colored sands; weak structure	Light brown to grayish; Thin; weakly developed

As shown in Table 2, Chernozems exhibit the highest fertility, reflected by their balanced structure, neutral to slightly alkaline pH, and high humus content, making them ideal for cereal and industrial crops. Luvisols and Cambisols show moderate productivity, constrained by acidity and higher bulk density in the Bt horizon, while Phaeozems represent a transitional type with favourable humus levels and improved structure. Fluvisols display good agricultural potential under irrigation, whereas Arenosols and Regosols are limited by coarse texture, low nutrient reserves, and reduced water-holding capacity. The overall comparison underscores the need for region-specific soil management, including liming, organic amendments, and irrigation, to sustain productivity and prevent degradation.

Figure 2 summarizes the relative compatibility of dominant soil groups with representative crop categories, based on regional soil characteristics described in the S-W Oltenia, S - Muntenia, and N-E - Moldova profiles. Suitability levels (High, Moderate, Low) were established considering each soil's texture, nutrient status, water-holding capacity, and limiting factors (acidity, erosion, salinity, drought susceptibility).

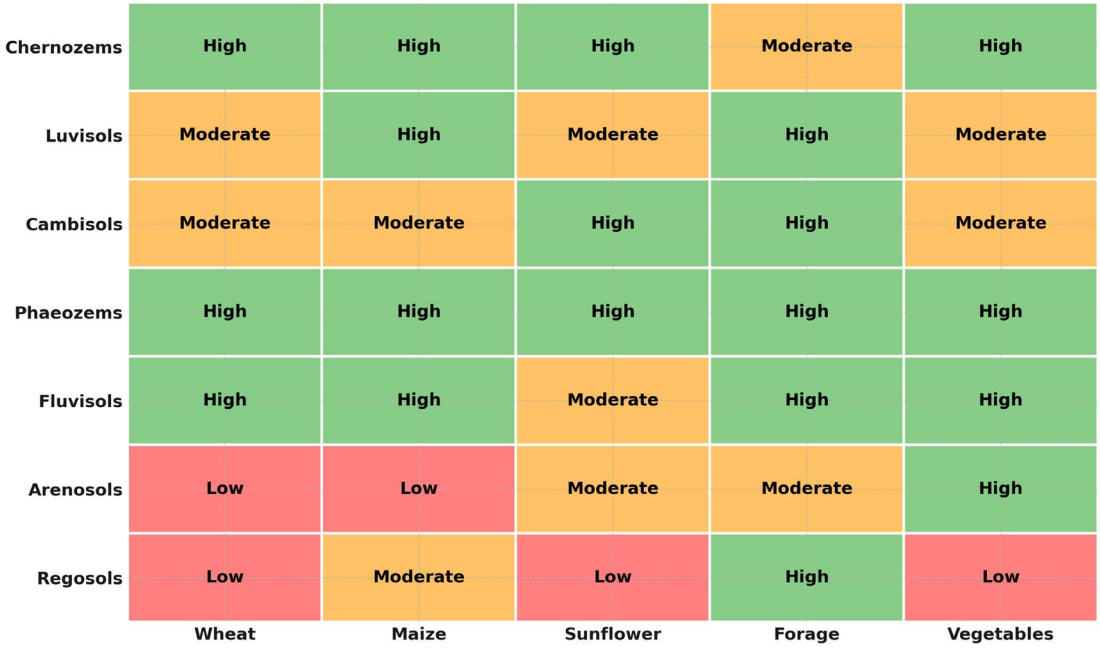

Fig. 2 - Agricultural suitability matrix of main soil types in Romania

Figure 3 presents the relative importance of major soil types in the regions studied, emphasizing their agricultural potential and limitations.

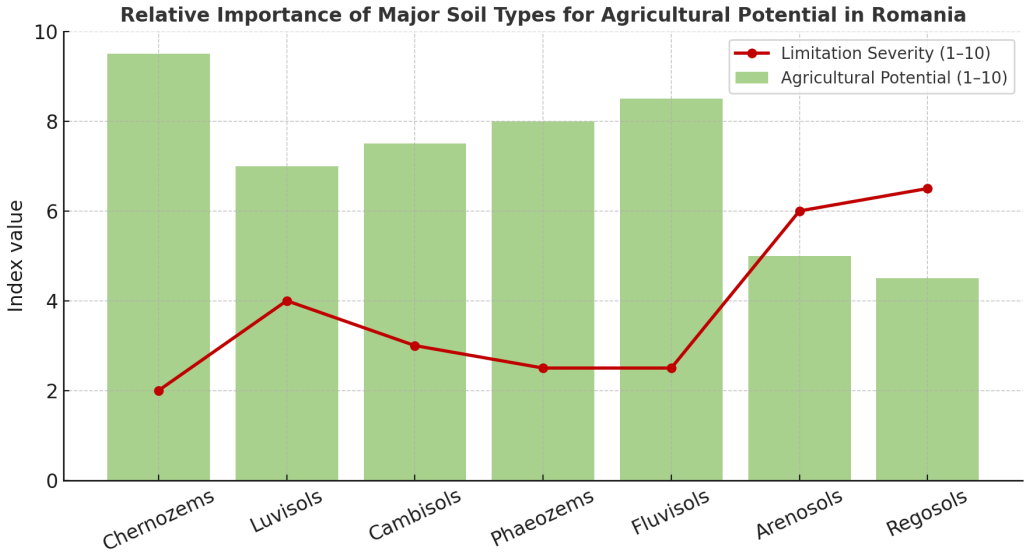

Fig. 3 - Relative importance of major soil types for Agricultural potential in Romania

As it can be observed from Figure 3, Chernozems stand out as the most fertile soils, with the highest potential index and minimal limitations, supporting intensive cereal and industrial crop systems. Luvisols and Cambisols show moderate potential, constrained by acidity and structural issues, while Phaeozems and Fluvisols maintain relatively high productivity under appropriate management. In contrast, Arenosols and Regosols display reduced agricultural value due to poor texture, low water-holding capacity, and erosion susceptibility. Overall, the figure highlights the clear gradient between fertile, structurally balanced soils and those requiring careful conservation and amelioration to sustain productivity.

CONCLUSIONS

The comparative evaluation of soil types in South-West Oltenia, South Muntenia, and East Moldova highlights the strong pedological variability that underpins Romania's agricultural potential. Chernozems and Phaeozems exhibit the highest fertility, with balanced structure, neutral pH, and high humus content, supporting intensive cereal and industrial crop systems. In contrast, Luvisols and Cambisols show moderate productivity, constrained by acidity, compaction, and erosion risks, yet remain valuable under integrated management practices involving liming, organic amendments, and conservation tillage. Arenosols and Regosols represent fragile soil resources, characterized by coarse texture, weak aggregation, and low water retention, limiting their suitability mainly to drought-tolerant or forage crops under irrigation.

Regional patterns confirm that soil fertility and management constraints are closely linked to climatic and geomorphological conditions. Oltenia's productivity is mainly affected by drought, Muntenia by acidity and compaction, and Moldova by erosion and slope gradients. These findings emphasize the necessity of tailored soil conservation and fertility improvement strategies that align with local characteristics and European soil health objectives under the CAP 2023–2027 framework.

Overall, the study demonstrates that sustainable agricultural performance in Romania depends on maintaining soil structure, enhancing organic matter content, and implementing adaptive land management practices. Strengthening monitoring programs and integrating digital mapping tools (e.g., SIGSTAR, BDUST) will be essential for optimizing land use and safeguarding soil resources as part of the national and European agenda for climate-resilient agriculture.

ACKNOWLEDGEMENT

This research was supported by EIT FOOD Program, through project CROSAR 250725 "Crop Rotation Optimisation for Sustainable Agriculture in Romania".

REFERENCES

[1] Bucur, D., Jitareanu, G., Ailincai, C., Tsadilas, C., Ailincai, D., Mercus, A. (2007). Influence of soil erosion on water, soil, humus and nutrient losses in different crop systems in the Moldavian Plateau, Romania. Journal of Food, Agriculture & Environment Vol.5 (2) : 261-264.

[2] Dumitru, M., Manea, A., Ciobanu, C., Dumitru, S., Vrinceanu N., Calciu, I., Tanase V., Preda M., Tanase V., Preda, M., Risnoveanu, I., Mocanu, V., Eftene, M. (2011). Monitoring the quality of soils in Romania. Sitech Publishing House, Craiova.

[3] European Commission (2022). Key Policy Objectives of the CAP 2023–2027. Directorate-General for Agriculture and Rural Development, Brussels. https://agriculture.ec.europa.eu/common-agricultural-policy/cap-overview/cap-glance/key-policy-objectives-cap-2023-27_en

[4] ICPA (2022). National Soil Database and Agrochemical Maps of Romania. Bucharest.

[5] Patriche, C.V.; Roșca, B.; Pîrnău, R.G.; Vasiliniuc, I.; Irimia, L.M. (2024). Digital Mapping of Land Suitability for Main Agricultural Crops in Romania. *Agronomy*, *14*, 2828. https://doi.org/10.3390/agronomy14122828.

[6] MADR – Ministry of Agriculture and Rural Development (2024). Agricultural Production and Soil Monitoring Data 2023–2024. Bucharest.

[7] Matei, I.; Pacurar, I.; Rosca, S.; Bilasco, S.; Sestras, P.; Rusu, T.; Jude, E.T.; Tăut, F.D. (2020). Land Use Favourability Assessment Based on Soil Characteristics and Anthropic Pollution. Case Study Somesul Mic Valley Corridor, Romania. Agronom, 10, 1245.

[8] Niacsu, L.; Ionita, I.; Curea, D. (2015). Optimum agricultural land use in the hilly area of eastern Romania, case study: Pereschiv catchment. Carpath. J. Earth Env. Sci., 10, 183–192

[9] Research Institute for Pedology and Agrochemistry (ICPA) Bucharest. Soil Map of Romania at scale 1:200,000 / 1:500,000.

[10] Tarau, D., Rogobete, G., Dicu, D., Nita, L. (2012). Romanian soil taxonomy systems SRTS-2012. Research Journal of Agricultural Science, 44 (3).

[11] Vintila, R.; Munteanu, I.; Cojocaru, G.; Radnea, C.; Turnea, D.; Curelariu, G.; Nilca, I.; Jalbă, M.; Piciu, I.; Râşnoveanu, I.; et al. (2004). The Geographic Information System of the Soil Resources of Romania SIGSTAR-200: Development and main types of applications. Proc. XVII-th Rom. Natl. Conf. Soil Sci., 34A, 439–449. (In Romanian)

[12] Vlad, V.; Stan, M.G.; Nilca, I. BDUST (2010). The database of the agricultural soil-land units at large scale of Romania: Basic concepts. Lucr. Stiintifice Ser. Agron. 53, 317–323.

[13] https://static.anaf.ro/static/10/Anaf/AsistentaContribuabili_r/preturi_medii/arhiva_preturi_agricole.htm (accessed on August 12, 2025).

MINERAL COMPOSITION AND AROMA QUALITY IN BAY LAUREL *(LAURUS NOBILIS)* LEAVES / *COMPOZIȚIA MINERALĂ ȘI CALITATEA AROMEI FRUNZELOR DE DAFIN (LAURUS NOBILIS)*

Petruta ANDREI[1)], Corina Dana MISCA[1)], Aurica BREICA BOROZAN[1)], Ioan Ladislau CABA[*2)], Diana MOIGRADEAN[1)], Despina - Maria BORDEAN[*1)]

[1)] University of Life Sciences "King Mihai I" from Timisoara, Calea Aradului 119, Timis County / Romania;

[2)] National Institute of Research - Development for Machines and Installations Designed to Agriculture and Food Industry - INMA Bucharest / Romania.

[*1)] *Tel: 00400 724 217 134; E-mail: despinabordean@usvt.ro*

[*2)] *Tel: 0040 744 515 964; E-mail: cabaioan@yahoo.com*

Keywords: *nutritional profile, XRF analysis, sensory observations, plant adaptability*.

ABSTRACT

Bay laurel (Laurus nobilis) is a Mediterranean evergreen plant generally valued for its culinary and medicinal uses. The aim of this study was to evaluate the mineral composition of bay leaves cultivated in Dumbravita, Timis County, Romania, using portable X-ray fluorescence (XRF). Two sets of samples (fresh and dry leaves) were analyzed and compared. Understanding the mineral profile is essential for assessing quality, safety, and plant adaptation to diverse environments. The results established the adaptability of Laurus nobilis to Romanian climatic conditions. In addition to mineral characterization, sensory observations showed that local bay leaves display a spicy and intense aroma, noticeably stronger than that of commercial products. These conclusions suggest that environmental conditions and mineral uptake may influence both the nutritional profile and sensory quality of bay laurel, supporting its potential as a functional and gastronomic resource.

REZUMAT

Dafinul (Laurus nobilis) este o plantă mediteraneană veșnic verde, apreciată în general pentru utilizările sale culinare și medicinale. Scopul acestui studiu a fost de a evalua compoziția minerală a frunzelor de dafin cultivate în Dumbrăvița, județul Timiș, România, cu ajutorul spectrometrului cu fluorescență de raze X (XRF). Au fost analizate și comparate două seturi de probe (frunze proaspete și uscate). Înțelegerea profilului mineral este esențială pentru evaluarea calității, siguranței și adaptării plantelor la diverse medii. Rezultatele au stabilit adaptabilitatea speciei Laurus nobilis la condițiile climatice românești. Pe lângă caracterizarea mineralelor, observațiile senzoriale au arătat că frunzele de dafin locale prezintă o aromă picantă și intensă, vizibil mai puternică decât cea a produselor comerciale. Aceste concluzii sugerează că condițiile de mediu și absorbția mineralelor pot influența atât profilul nutrițional, cât și calitatea senzorială a dafinului, susținând potențialul său ca resursă funcțională și gastronomică.

INTRODUCTION

Laurus nobilis L. (Lauraceae), generally known as bay are shrubs or small trees (*https://greenwoodplants.co.uk/blog/plant-focus-laurus-nobilis-bay-laurel/*), is native to the southern Mediterranean region, commonly cultivated in Europe and the USA as an ornamental plant and as aromatic leaves in countries like Turkey, Algeria, Morocco, Portugal etc. (*Awada, F. at al, 2023, Guenane, H. at al, 2016)*. The bay laurel is unisexual, with male and female flowers on separate plants (https://www.treeguideuk.co.uk/bay-tree-identification/).

All over the world, there is increasing awareness in the importance of dietary minerals in nutrition and for the prevention of several diseases [6]. Although minerals justify for only a small percentage of plant biomass, they are vital for the sensory and nutritional properties of e bay laurel (Laurus nobilis) leaves. The minerals in bay leaves are macro elements like calcium, potassium, magnesium, phosphorus (*Al-Hashimi, A. G. at al, 2016*) and trace elements (iron, zinc, copper, iodine, chromium, manganese, etc.), each serving various scientific and biological objectives.

In Laurus nobilis, potassium and calcium lead the mineral spectrum, regulating osmotic balance in the plant, stabilizing cell walls, and shaping the resilience of leaves under Mediterranean and continental climates

(*Ishimwe, C at al, 2024*). These same minerals, when consumed, contribute to electrolyte balance, skeletal health, and cardiovascular protection in humans. Leading the mineral spectrum in bay plant, potassium and calcium control osmotic balance in the plant, stabilize cell walls, and shape the resilience of leaves under Mediterranean and continental temperatures. Consumed, these same minerals assist people in preserving their cardiovascular health, skeletal structure, and electrolyte balance (*Hasanuzzaman, M. at al, 2018*).

The trace minerals (iron, zinc, copper, and manganese), present in smaller amounts, act as cofactors for enzymatic systems responsible for photosynthesis, respiration, and phenolic biosynthesis, which in turn influence antioxidant potential and aroma compounds (*Trairatapiwan, T. at a, 2025*).

While trace metals like zinc and iron interact with secondary metabolites, influencing the spicy, resinous, and persistent taste, potassium and magnesium manage volatile oil metabolism, a scent that elevates their culinary worth.

The minerals present in bay plant leaves reveal the soil and ecological environment where the tree is grown as well as explains the leaves odor, a stronger smell when set against those commercially brought in. Therefore, bay laurel shows how minerals, however numerically small, are qualitatively critical. Supporting the plant structurally and physically, they improve the nutritional profile of human diets and interact with phytochemicals to provide both health advantages. gastronomic perfection as well as (anti-inflammatory action, digestive stimulation, antioxidant protection).

MATERIALS AND METHODS

Plant material

Bay laurel (Laurus nobilis) leaves were collected from cultivated plants in Dumbravita, Timis County, Romania. We worked with two types of material: dried leaves (1F), obtained by oven-drying at 60 °C until constant weight, and fresh leaves (2F), analyzed immediately after harvesting (*Nica, D. at al, 2012*). To make the results analogous, concentrations from both sets of samples were expressed on a dry weight basis (*Şuian, B. at al,2025*). Before analysis, leaves were carefully rinsed with distilled water. Dried leaves were finely ground and pressed into stable pellets, while fresh leaves were compacted into discs of the similar size to confirm comparable conditions during measurement.

XRF analysis

Elemental composition was determined using a portable X-ray fluorescence spectrometer (Hitachi X-MET8000). Each sample type (1F and 2F) was analyzed in triplicate (*Tarkanyi, P. at al, 2024*).

The pellets and discs were prepared with a manual press to offer a uniform surface, improving precision. The instrument was operated in its soil/plant mode, which is optimized for detecting both major nutrients and trace metals. To bring the results closer to reference laboratory methods such as ICP-AES, we applied element-specific correction factors based on previous work with plant matrices (e.g. K and Ca: 0.8, Fe/Zn/Cu: 0.6, Ni: 0.5, Ti/Mo: 0.2, Ba/Sr: 0.3). All results are presented in ppm (mgkg-1 DW).

Detection limits

The sensitivity of the XRF allowed us to detect trace metals down to ~1–5 ppm (e.g. Cd, Pb, Hg, As), 5–10 ppm for transition metals such as Fe, Cu, and Zn, and around 50–100 ppm for abundant elements like K and Ca. Measurements below the detection limit were reported as “not detected” (ND). Elements close to the quantification limit (roughly three times the LOD) were double-checked through repeated analysis.

Literature data

For comparison, we used published values from ICP-AES and WD-XRF (Sultana S. at al, *2023*) studies of Moroccan bay leaves (*Mrabet et al., 2024*), AAS analyses of Algerian samples (*Guenane et al., 2016*), and compositional values reported in the Foodstruct nutritional database (*https://foodstruct.com/food/bay-leaf*).

Data handling

We compiled our results and literature values into a single comparative dataset. The interpretation of data was made using PAST version 2.17c (*Hammer, O. at al, 2001*) and Microsoft Excel. These tools helped us highlight where local Romanian samples stood out against previously published data.

RESULTS

Our XRF measurements showed that bay laurel leaves grown in Dumbravita, Timis County accumulate a rich and diverse set of minerals, but with some clear differences compared to values reported in the literature. Because we analyzed both dried leaves (1F) and fresh leaves (2F), all results are expressed on a dry weight basis so they can be compared directly (Table 1).

Table 1

Mineral composition of dry and fresh bay leaves (mgkg^{-1})

Element	LAB1F	LAB2F	LIT-ICP-AES [6]	LIT-WD-XRF	LIT-Foodstruct [8]
K	19152	18046.4	4646	6340	5290
Ca	26325.6	18249.6	10013	9730	8340
Fe	258	277.8	124	427	430
Cu	21.96	18.36	3.48	24	4.2
Mn	320	250	72	170	82
Mo	0.28	0.32		-	-
Zn	57.24	45.36		56	37
Ni	ND	5		240	
Ti	1.64	7.88		-	
Ba	12.15	13.5		-	
Zr	0.12	ND		-	
Sr	2.7	1.53		510	
Rb	1.76	1.6			
Cr	7	ND			
Ta	19	26			
Sb	13	21			
Hg	0.13	0.12			
Cd	ND	ND			
Tl	ND	ND			

Legend: LAB1F= dried bay leaves analyzed in our laboratory using XRF; LAB2F= fresh bay leaves analyzed in our laboratory using XRF; LIT-ICP-AES = literature data – minerals detected by ICP-AES, LIT-WD-XRF= literature data – minerals detected by WD-XRF; LIT-Foodstruct = minerals data of bay leaves from Foodstruct.com

As we can observe in Table 1 and Figure 1, potassium (K) and calcium (Ca) were the most abundant elements in our samples, much higher than those typically reported from Morocco or Algeria. This suggests that bay laurel grown under Romanian conditions has a superior capacity to take up and store these elements, possibly because of the soil composition, or climate. Higher K and Ca levels may also contribute to the strong, spicy aroma that local users notice related to imported bay leaves.

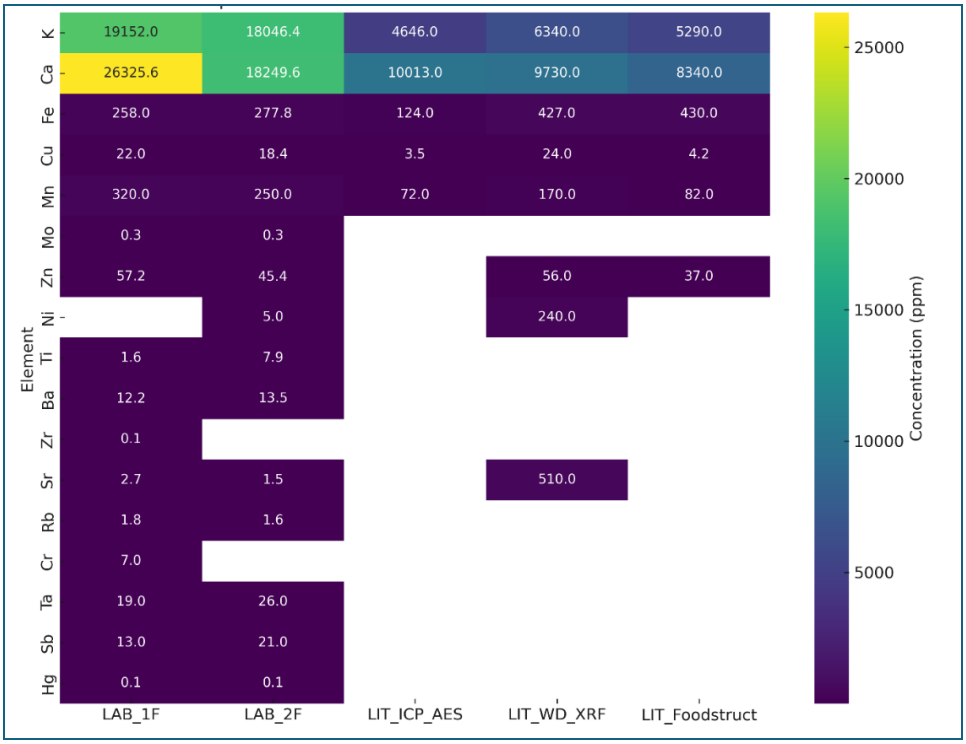

Fig. 1 - Heatmap of LAB versus Literature data for Laurus nobilis leaves

Legend: LAB1F= dried bay leaves analyzed in our laboratory using XRF; LAB2F= fresh bay leaves analyzed in our laboratory using XRF; LIT-ICP-AES = literature data – minerals detected by ICP-AES, LIT-WD-XRF= literature data – minerals detected by WD-XRF; LIT-Foodstruct = minerals data of bay leaves from Foodstruct.com

The laboratory results for the transition elements Fe and Zn were in line with food database data (~430 ppm) and WD-XRF measurements, but higher than some ICP-AES values (124 ppm). Manganese (Mn), however, stood out: our samples contained 250–320 ppm, while literature values rarely exceeded 170 ppm. This suggests a strong local enrichment of Mn, possibly linked to the soil parent material or higher bioavailability.

Regarding trace and minor elements, we also found elements such as nickel (Ni, ~5 ppm), chromium (Cr, ~7 ppm), strontium (Sr, 1–3 ppm), barium (Ba, 12–14 ppm), rubidium (Rb, 1–2 ppm), and titanium (Ti, 1–8 ppm). These were either absent or rarely reported in the literature. In addition, we detected small amounts of antimony (Sb, 13–21 ppm) and mercury (Hg, 0.12–0.13 ppm). While very low, these findings are important because such elements are seldom measured in bay leaves. Their presence likely reflects natural soil background rather than contamination, but they highlight the usefulness of XRF for broad-spectrum screening.

From the toxicological point of view, elements of major concern such as cadmium, lead, thallium, and arsenic were not detected in our samples. Mercury was present, but at levels far below any toxic threshold. This supports the safety of consuming Romanian bay leaves from a mineral contamination perspective.

The comparison of Romanian to Mediterranean bay leaves samples are presented in Figure 2.

When we compared our LAB data with Moroccan (*Mrabet et al., 2024*) and Algerian (*Guenane et al., 2016*) studies, the Romanian bay leaves are consistently richer in macro- and microelements. This observation might be explained by the soils of western Romania, which are relatively fertile and rich in base cations, and by local climate factors that favor mineral uptake. These differences could also contribute to the sensory profile, as many users note that local bay leaves have a stronger, more pungent aroma than imported ones, and mineral nutrition may play a role in essential oil biosynthesis.

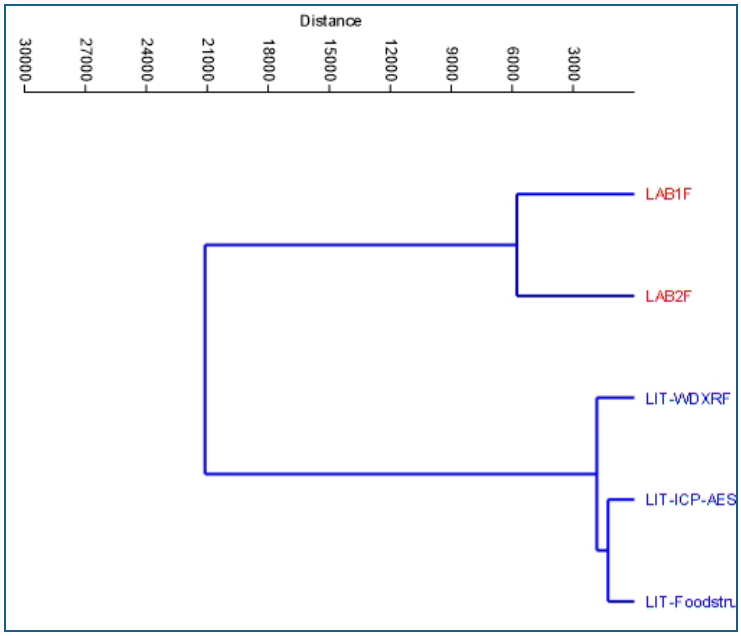

Fig. 2 - Cluster Analysis of Data using Ward's Method based on Euclidian Distances

Legend: LAB1F= dried bay leaves analyzed in our laboratory using XRF; LAB2F= fresh bay leaves analyzed in our laboratory using XRF; LIT-ICP-AES = literature data – minerals detected by ICP-AES, LIT-WD-XRF= literature data – minerals detected by WD-XRF; LIT-Foodstruct = minerals data of bay leaves from Foodstruct.com

Ward's method is a hierarchical clustering technique that groups samples step by step, minimizing the variance within clusters (https://online.stat.psu.edu/stat505/lesson/14/14.7). The Euclidean distance is used as a measure of similarity: samples with smaller "distances" in their mineral composition are considered more identical (*Levy, A. at al, 2025*).

The clustering confirms the distinctive mineral "fingerprint" of Romanian bay leaves, separating them from Mediterranean references (*Guenane, H. at al,2016, Mrabet, A. at al, 2024, https://foodstruct.com/food/bay-leaf)* and also helps which minerals behave in similar ways (e.g., K and Ca

as dominant macronutrients; Zn and Cu as closely related trace metals). Practically it proves that environmental conditions in Dumbrăvița, Timiș county led to a unique mineral and aromatic profile.

Influence of minerals and climatic conditions on adaptation

A unique aspect of our study is that the analyzed bay tree has been growing outdoors in Dumbrăvița (Timiș County) for several winters, surviving cold spells down to –12 °C without damage. This is unusual for a Mediterranean evergreen but can be explained by a combination of mineral nutrition and microclimatic protection. The plant is located just 4–5 m from the house wall, benefiting from residual heat and reduced wind exposure. It is also sheltered by a tulip tree (Liriodendron tulipifera) (*https://www.plante.md/ro/catalog/listvennyie-rasteniya/liriodendron-tulipifera-tulip-tree*), a silver fir (Abies concolor), and a fig tree (Ficus carica), which together act as a living windbreak and buffer against frost. This neighborhood of plants forms a micro-ecosystem that softens temperature extremes, stabilizes humidity, and prevents radiative cooling on cold nights.

Mineral composition may further reinforce this adaptation. High Ca and K improve cell membrane stability and osmotic regulation under cold stress, while Mn and Zn strengthen antioxidant defenses against oxidative bursts triggered by frost (*Zhou L. at al 2025*). In effect, the plant's nutritional richness and its protected microclimate act synergistically to extend its ecological range into temperate Central Europe.

CONCLUSIONS

The present study shows that bay laurel leaves grown in Dumbrăvița, Timiș County are richer in key minerals (potassium, calcium, manganese, and copper), than values commonly reported in Mediterranean studies. This mineral enrichment not only enhances the nutritional value of the leaves but also supports the biosynthesis of volatile compounds, offering a clear explanation for the spicier aroma and stronger flavor noted by consumers.

Ecological observations confirm that the tree has successfully adapted to local winters, surviving temperatures of −12 °C, thanks to both its protective microclimate (neighboring trees and proximity to the house wall) and its robust mineral profile that strengthens stress tolerance. Together, these findings highlight the potential of Romanian bay leaves as a distinctive, safe, and high-quality product with both culinary and functional benefits.

ACKNOWLEDGEMENT

This study was funded by the University of Life Sciences "King Mihai I" from Timisoara". The research was performed with the support of the Interdisciplinary Research Platform belonging to the University of Life Sciences "King Mihai I" from Timisoara. The acquisition of XRF Analyzer was financed by Interreg–IPA Cross–border Cooperation Romania–Serbia Program, through the project "Modern technologies for monitoring land covered with waste in order to restore their initial use", 2019–2021, code e-MS: RORS 365.

REFERENCES

[1] Al-Hashimi, A. G., & Mahmood, S. A. (2016). The nutritional value and antioxidant activity of bay leaves (Laurus nobilis L.)., Basrah Journal of Veterinary Research, 2016, Vol. 15, No. 4, 10-23 ref. 51 https://www.cabidigitallibrary.org/doi/full/10.5555/20173048455;

[2] Awada, F., Hamade, K., Kassir, M., Hammoud, Z., Mesnard, F., Rammal, H., & Fliniaux, O. (2023). Laurus nobilis Leaves and Fruits: A Review of Metabolite Composition and Interest in Human Health. Applied Sciences, 13(7), 4606. https://doi.org/10.3390/app13074606;

[3] Guenane, H., Gherib, A., Carbonell-Barrachina, Á., Cano-Lamadrid, M., Krika, F., Berrabah, M., Maatallah M. & Bakchiche, B. (2016). Minerals analysis, antioxidant and chemical composition of extracts of Laurus nobilis from southern Algeria. J. Mater. Environ. Sci, 7(11), 4253-4261, https://www.jmaterenvironsci.com/Document/vol7/vol7_N11/454-JMES-2349-Guenane.pdf#:~:text=Mineral%20and%20heavy%20metal%20concentration%20of%20Laurus,especially%20Ca%2C%20K%2C%20Fe%20and%20Mg%20.;

[4] Hammer, O., Harper, D. A. T. & Ryan, P. D. – 2001 – Past: Paleontological statistics software package for education and data analysis, Palaeontologia Electronica, 4: 1-9;

[5] Hasanuzzaman, M., Bhuyan, M. H. M. B., Nahar, K., Hossain, M. S., Mahmud, J. A., Hossen, M. S., Masud, A. A. C., Moumita, & Fujita, M. (2018). Potassium: A Vital Regulator of Plant Responses and Tolerance to Abiotic Stresses. Agronomy, 8(3), 31. https://doi.org/10.3390/agronomy8030031;

[6] Imelouane, B., Tahri, M., Elbastrioui, M., Aouinti, F., & Elbachiri, A. (2011). Mineral contents of some medicinal and aromatic plants growing in eastern Morocco. J. Mater. Environ. Sci, 2(2), 104-111. http://www.jmaterenvironsci.com/Document/vol2/13-JMES-52-2010-Emelouane.pdf;

[7] Ishimwe, C., & Deligöz, A. (2024). Drought effects on growth, biochemical changes and leaf gas exchange in laurel (Laurus nobilis L.). Central European Forestry Journal, 70(2), 122-132. https://www.proquest.com/docview/3159469849?pq-origsite=gscholar&fromopenview=true&sourcetype=Scholarly%20Journals;

[8] Levy, A., Shalom, B. R., & Chalamish, M. (2025). A guide to similarity measures and their data science applications. Journal of Big Data, 12(1), 188. https://journalofbigdata.springeropen.com/articles/10.1186/s40537-025-01227-1;

[9] Mrabet, A., Abdelfattah, B., El Mansouri, F., Simou, A., & Khaddor, M. (2024). Bay Laurel of Northern Morocco: A Comprehensive Analysis of Its Phytochemical Profile, Mineralogical Composition, and https://www.mdpi.com/2673-4125/4/2/17 Antioxidant Potential. Biophysica, 4(2), 238-255. https://doi.org/10.3390/biophysica4020017,

[10] Nica, D., Bordean, D.M., Gergen, I., Bura, M., & Vintila, T. (2012). Comparative assessment of trace metal accumulation in celery and nettle leaves. JOURNAL of Horticulture, Forestry and Biotechnology, 16(2), 217-220;

[11] Șuian, B., Amariei, S., & Petraru, A. (2025). Comprehensive Characterization of Armoracia rusticana Roots and Leaves: Physicochemical Properties, Functional Potential, and Nutritional Composition. International Journal of Molecular Sciences, 26(19), 9462. https://doi.org/10.3390/ijms26199462;

[12] Sultana S, Khatun HA, Faruquee M, Islam MMU, Tonny HJ, Islam MR. Comparison between Acid Digestion (ICP-OES) and X-ray Fluorescence (XRF) Spectrometry for Zinc Concentration Determination in Rice (Oryza sativa L.). Foods. 2023 Mar 1;12(5):1044. doi: 10.3390/foods12051044. PMID: 36900565; PMCID: PMC10001123;

[13] Tarkanyi, P., Popescu, G. S., Rădulescu, L., Alda, L. M., Dragomirescu, M. C., Alda, S., Baghina, N., Gh., & Bordean, D. M. (2024). Nettle Plants Fingerprint Based on XRF Analysis. Scientific Papers. Series B. Horticulture, 68(1), https://horticulturejournal.usamv.ro/pdf/2024/issue_1/Art111.pdf;

[14] Trairatapiwan, T., Lertpatarakomol, R., Chotikatum, S., Lukkananukool, A., & Mitchaothai, J. (2025). Influence of Trace Mineral Sources and Levels on Growth Performance, Carcass Traits, Bone Characteristics, Oxidative Stress, and Immunity of Broiler. Animals, 15(15), 2287. https://doi.org/10.3390/ani15152287, https://www.mdpi.com/3435792;

[15] Ward's Method, Applied Multivariate Statistical Analysis, https://online.stat.psu.edu/stat505/lesson/14/14.7;

[16] Zhou L, Ullah F, Zou J, Zeng X. Molecular and Physiological Responses of Plants that Enhance Cold Tolerance. Int J Mol Sci. 2025 Jan 29;26(3):1157. doi: 10.3390/ijms26031157. PMID: 39940925; PMCID: PMC11818088, https://pmc.ncbi.nlm.nih.gov/articles/PMC11818088/

[17] *** https://foodstruct.com/food/bay-leaf;

[18] *** https://greenwoodplants.co.uk/blog/plant-focus-laurus-nobilis-bay-laurel/;

[19] *** https://www.treeguideuk.co.uk/bay-tree-identification/;

[20] *** https://www.plante.md/ro/catalog/listvennyie-rasteniya/liriodendron-tulipifera-tulip-tree;

[21] *** https://www.vdberk.ro/trees/laurus-nobilis/.

CAPITALIZING ON CLIMATE-IMPACTED AGRICULTURAL AREAS WITH *CHAENOMELES* FRUIT SHRUBS
/
VALORIFICAREA SUPRAFEȚELOR AGRICOLE AFECTATE DE SCHIMBĂRILE CLIMATICE CU ARBUȘTI FRUCTIFERI *CHAENOMELES*

Tamara Elena MIHOCIU[1)], Denisa Eglantina DUȚĂ*[1)], Luminița CATANĂ[1)], Gabriela Daniela CRIVEANU-STAMATIE[1)], Monica CATANĂ[1)], Iulia GRIGORE[2)]

[1)] National Research and Development Institute for Food Bioresources, IBA Bucharest, 6 Dinu Vintilă Street, District 2, 021102, Bucharest / Romania;

[2)] National Institute of Research - Development for Machines and Installations Designed to Agriculture and Food Industry - INMA Bucharest / Romania.

**E-mail: denisa.duta@bioresurse.ro*

Keywords: *Chaenomeles japonica, marmalade, sensory analysis*

ABSTRACT

The interest in dietary intake of polyphenolic compounds has motivated the food industry to include new sources in the human diet. Chaenomeles shrubs (Japanese quince), are widespread throughout the world, originating from Southeast Asia, mainly from China and Japan, the fruits of the shrub are valued in traditional Chinese medicine for their medicinal properties, including antioxidant, anti-inflammatory, immunomodulatory, antiviral, antibacterial, antihyperglycemic and antihyperlipidemic effects (Zhang et al., 2014). Since the fruits are unsuitable for fresh consumption (characterized by hardness, high acidity and astringency), their exploitation for food purposes has been achieved by producing processed forms, such as juices, candied fruits, jams, jellies and chips (Rumpunen et al., 2003). It is common practice for developers of new food products in a target market to evaluate their impact on consumers. The simplest possible compositional structures were used, processing the Japanese quince fruits in the form of jam and marmalade. The new product, Japanese quince marmalade, has a positive overall image, with 88.4% of the subjects surveyed appreciating the main sensory characteristics. The overall acceptability score for the reformulated Japanese quince marmalade samples was for the cinnamon sample.The new products have a positive overall image that justifies the establishment of Chaenomeles shrub crops in Romania.

REZUMAT

Interesul pentru aportul alimentar de compuși polifenolici a motivat industria alimentară să includă noi surse în dieta umană. Arbuștii de Chaenomeles (gutui japonez), sunt răspândiți în întreaga lume, originari din Asia de Sud-Est, în principal din China și Japonia, fructele arbustului sunt apreciate în medicina tradițională chineză pentru proprietățile lor medicinale, inclusiv efecte antioxidante, antiinflamatorii, imunomodulatoare, antivirale, antibacteriene, antihiperglicemice și antihiperlipidemice (Zhang et al., 2014). Deoarece fructele sunt improprii consumului în stare proaspătă (caracterizate prin duritate, aciditate ridicată și astringență), valorificarea lor în scopuri alimentare s-a realizat prin producerea de forme procesate, cum ar fi sucuri, fructe confiate, gemuri, jeleuri și chipsuri (Rumpunen et al., 2003). Este o practică obișnuită ca dezvoltatorii de noi produse alimentare pe o piață țintă să evalueze impactul acestora asupra consumatorilor. Au fost utilizate cele mai simple structuri compoziționale posibile, procesând fructele de gutui japonez sub formă de dulceață și marmeladă. Noul produs, marmeladă japoneză de gutui, are o imagine generală pozitivă, 88,4% dintre subiecții chestionați apreciind principalele caracteristici senzoriale. Scorul global de acceptabilitate pentru probele reformulate de marmeladă japoneză de gutui a fost la proba cu scorțișoară. Noile produse realizate au o imagine generală pozitivă ce justifică înființarea culturilor de arbust Chaenomeles în România.

INTRODUCTION

The interest in the dietary intake of polyphenolic compounds has motivated the food industry to include new sources of polyphenolic compounds in the human diet. The shrubs of Chaenomeles (Japanese quince), family Rosaceae, with their four species (Chaenomeles cathayensis, Chaenomeles speciosa, Chaenomeles thibetica, and Chaenomeles japonica) are widespread throughout the world, originating from Southeast Asia, primarily in China and Japan. The fruits of the shrub are valued in traditional Chinese

medicine for their medicinal properties, including antioxidant, anti-inflammatory, immunomodulatory, antiviral, antibacterial, antihyperglycemic, and antihyperlipidemic effects *(Zhang et al., 2014).* Originally cultivated in Europe as an ornamental shrub, the chemical composition of Chaenomeles fruits has been studied. The abundance of phytochemical compounds in the Chaenomeles plant *(Ruoling et al., 2023)* suggests that the plant is suitable for use in the production of dietary supplements for the prevention or early treatment of metabolic syndrome disorders.

As a result, Chaenomeles are used in several industries to drive product innovation and support consumer health *(Hongyue et al., 2024).* A high content of organic acids was found in the extracts, being a rich source of phenolic compounds, the dominant group being polymeric proanthocyanidins in a percentage of up to 79% of total polyphenols *(Turkiewicz et al., 2021),* total phenolic acids 175 mg/g of which chlorogenic acid 4.4%, procyanidins 57.8%, (-)-epicatechin 33% *(Strugała et al., 2016). Baranowska-Bosiacka et al. (2017)* found high levels of microelements in fresh fruit: 0.516 Fe, 0.146 Cu, 0.546 Zn, 0.25 Mn, 16.73 Mg, 22.92 Ca, 64.09 P, 249.74 K, expressed in mg/100g dry matter, ascorbic acid 62.7 – 68.8 g/100g, vitamins and carotenoids *(Haizhao et al, 2024),* tannins, oligosaccharides, fiber 1.35-3.88 g/100g. And in the study conducted by (*Turkiewicz (et al., 2021),* it was confirmed that Chaenomeles fruits can be part of a balanced diet, providing vitamins A and E, as well as essential amino acids necessary for the proper functioning of the human body.

According to another study, Chaenomeles seeds are also rich in potassium and microelements (Fe, Cu, Zn, Mn), with nutritional potential *(Turkiewicz et al., 2021).* The review by Marat et al. (2022) highlights the content of phenolic compounds in 5 Chaenomeles varieties: C. speciosa, C. thibetica, C. cathayensis, C. japonica, and C. sinensis. The nutritional value of Chaenomeles fruits has led to the establishment of crops primarily in Lithuania, Estonia, Latvia, Sweden, Finland, and Poland. Since the fruits are unsuitable for fresh consumption (characterized by hardness, high acidity, and astringency), their exploitation for food purposes was achieved through the production of processed forms, such as juices, candied fruits, jams, jellies, and chips *(Rumpunen et al., 2003; Radenkovs et al., 2024).*

The characteristic aroma of Japanese quinces (a combination of citrus, pineapple, and nut aromas) increases their potential for exploitation in the food industry. In Romania, Japanese quince shrubs are cultivated exclusively for ornamental purposes in landscaping. The low agroclimatic requirements, resistance to pests, and minimal fertilization requirements make the Japanese quince a suitable choice for cultivation, particularly in organic farming *(Marat et al., 2022).* The shrubs can grow on nutrient-poor soils, are resistant to both water excess and deficiency in the soil, as well as to frost and high temperatures, for short periods.

The potential for the development of Chaenomeles crops is high in areas strongly affected by climate change (approximately 30% of the country's agricultural area). These hilly areas are located in Transylvania, Maramureș, and the Subcarpathian hills (approximately 5 million hectares) *(Badiu et al., 2020*). These lands are characterized by natural vegetation (meadows and natural pastures), forested with shrubs and traditional orchard plantations, and intensive cereal crops. In the Eastern Subcarpathians, the climate is sharply continental, with moderately warm summers (averaging 19°C, with an extreme of 40°C) and winters characterized by average temperatures ranging from -5.5°C to -6°C (with an extreme of -25°C) *(Chiţu et al., 2010; Chiţu et al., 2023)*.

The intensification of meteorological phenomena due to climate change has resulted, in recent years, in decreases in fruit production from traditional orchards and in the productivity of cereal crops. *(Coman et al., 2023).* The requirements of the Japanese quince shrub are conducive to establishing crops in the hilly areas of Romania affected by climate change, to valorize agricultural areas economically.

The Japanese quince fruit is not known in Romania as a food, either in fresh or processed form. It is common practice for developers of new food products in a target market to evaluate their impact on consumers. It is necessary to consider the attitudes and expectations of potential consumers, as they influence the sensory quality of products by evaluating the perceived intrinsic and extrinsic characteristics.

This study was conducted to evaluate the potential for valorizing Japanese quince fruits, considering their nutritional value. The simplest possible compositional structures were used, processing Japanese quince fruits in the form of jam and marmalade. The test samples were produced using traditional technology and then reformulated to reduce the sugar content and eliminate the intense sour taste.

MATERIALS AND METHODS

1. Materials

1.1 Raw materials and ingredients for test product execution

Japanese quince fruits were harvested from the landscaping of INCDBA IBA Bucharest in October 2024. The fruits were harvested ripe, with a light-yellow color and a characteristic, persistent aroma. They were processed by removing the seminal cavity and seeds, slicing, vacuum packaging, and freezing at -20°C until use in the test products. The compositional dilution of fruits was made with apples from the local varieties Iohnatan and Golden Delicious, fresh and purchased from the local market. Pectin and stevia extract were purchased from the Food Ingredients Romania branch, and sugar, fructose, lemons, and cinnamon were purchased through the commercial network.

1.2 Reagents

The reagents used, of analytical purity, for the physico-chemical determinations were purchased from the company laboratory Bucharest.

2. Methods

2.1 Processing Japanese quince into food products

a) Three types of jams were obtained according to traditional processes from thawed Japanese quince fruits and: a mixture of fresh apples with sugar (product code 587) / or fructose (product code 340)/ or stevia extract (product code 289), pectin, and lemon juice. The fruit mixture was brought to a boil with sweetener, left to rest for 3 hours to facilitate the osmosis process, finely chopped, and pectin was added and concentrated to a total soluble substance value < 35°Brix. The samples were differentiated by the sweetener used: sugar, fructose and sugar dilution with stevia extract (Table 1).

b) Japanese quince marmalade (product code 578), a traditional product, was produced over an open fire, by immersing thawed Japanese quince fruits and fresh Jonathan apples in sugar syrup, with a fruit:sugar ratio of 1:1 (kg/kg). The mixture was brought to a boil, finely chopped and concentrated to a total soluble substance value of approximately 65°Brix.

Table 1

Compositional structures of test products from Japanese quince

Sample code / Composition, %	587	340	289	578	251	612
Japanese quince fruit	31.50	32.40	33.95	22.12	35.93	35.78
Apples	26.80	27.60	33.95	22.12	29.94	24.66
Sugar	20.40	-	6.35	44.25	14.97	18.13
Fructose	-	15.00	-	-	-	-
Stevia extract	-	-	1.50	-	0.84	1.61
Pectin	1.17	1.50	1.70	-	1.50	1.21

where: 587 = jam with sugar; 340 = jam with fructose; 289 = jam with stevia; 578 = traditional *Japanese quince marmalade*; 251 = stevia *Japanese quince marmalade* with lemon; 612 = stevia Japa*nese quince marmalade* with cinnamon.

c) For the reformulated Japanese quince marmalade samples (product code 251 and product code 612), the compositional dilution was made with Golden Delicious apple, the sugar dilution with stevia extract, pectin, and flavorings: lemon peel and cinnamon. (Table 1) The manufacturing process was the one used for Japanese quince marmalade, a traditional method, up to a total soluble substance value of < 50°Brix.

2.2 Analytical determinations

a) Determination of total soluble substances (%Brix) was carried out with a classic ABBE AR4 Refractometer, manufactured by KRUSS Germany, with a measurement range of 0-95% Brix, accuracy of 0.25% Brix, temperature measurement accuracy ±0.5°C, and temperature measurement resolution 0.1°C. The mass of the sample taken for analysis was 5g, which was diluted with distilled water in a ratio of 1:1 and 1:2, depending on the viscosity of the sample.

The calculation:

$$\%Brix = \%Brix\ read\ X\ dilution \quad (1)$$

The readings were performed in duplicate.

b) pH determination, was performed with a digital laboratory pH meter 827 manufactured by Metrohm Switzerland, series 2013. The readings were performed in duplicate, the average of the readings representing the measurement result.
c) Acidity determination was performed according to SR EN 750/2008.
d) Sensory evaluation
The sensory analysis for assessing the acceptability of the new products was conducted through hedonic tests using scoring scales. The groups of evaluators consisted of untrained individuals, aged between 20 and 65, of both genders.

RESULTS

The test products were subjected to physicochemical and sensory analysis using hedonic acceptability tests and descriptive analysis tests between assortments of the same product (Japanese quince jam) as well as by comparison with a control product (Cydonia oblonga quince jam, sample code 341). Cydonia oblonga quince jam is a traditional product manufactured and marketed by S.C. Annabella Fabrica de Conserve Râureni S.A., Romania.

3.1 Analytical determinations

The chemical characteristics of the test samples (jam and Japanese quince marmalade) are given in Table 2.

Table 2

Chemical characteristics of test products Japanese quince jam and marmalade

Sample code / Chemical characteristics	587 (Z)	340 (F)	289 (S)	341	578	251	612
SST (°Brix)	34.58	33.09	15.81	60.50	67.85	25.80	46.08
pH	2.87	2.94	2.95	3.00	3.02	3.12	3.11
Free acidity (% acid citric)	1.45	1.72	2.0	0.58	1.04	1.68	1.37

where: 340 = fructose jam; 587 = jam sugar; 289 = stevia jam; 341 = control; 578 = traditional *Japanese quince marmalade*; 251 = stevia Japanese quince with lemon; 612 = stevia *Japanese quince marmalade* with cinnamon.

The chemical composition analysis (Table 2) is correlated with the compositional structure (Table 1).

For the test products Japanese quince jam, it is found that by increasing the percentage of Japanese quince fruits in the composition, the pH of the samples has values within very narrow limits: ± 0.04 pH. The free acidity increases proportionally with the increase in the content of Japanese quince fruits, the increase being by a percentage of approximately 27% for each 1% addition of Japanese quince fruits. The difference between the samples was given by the content in SST, where sample 289 (with the addition of stevia extract) was 45.7°Brix compared to sample 587 (with the addition of sugar) and 47.78°Brix compared to sample 340 (with the addition of fructose).

For the reformulated Japanese quince marmalade test samples, the optimization of the compositional structure was considered by increasing the content of Japanese quince fruits and decreasing the level of SST in the product. An increase in the total fruit content by 12.63% (251) and 16.2% (612) and in the content of Japanese quince fruits by 13.8% (251) and 13.66% (612) was obtained compared to sample 578. (Table 1).

The samples were chemically characterized simultaneously with a sample of Cydonia quince marmalade, purchased from the commercial network (sample code 341). Reducing the amount of added sugar by 29.28% (251) and 26.12% (612) reduced the SST content by 42°Brix (251) and 21.77°Brix (612) compared to that of sample 578 (67.85°Brix). (Table 2)

3.2 Sensory analysis

The sensory analysis of Japanese quince products was carried out in three steps according to the scheme in Figure 1.

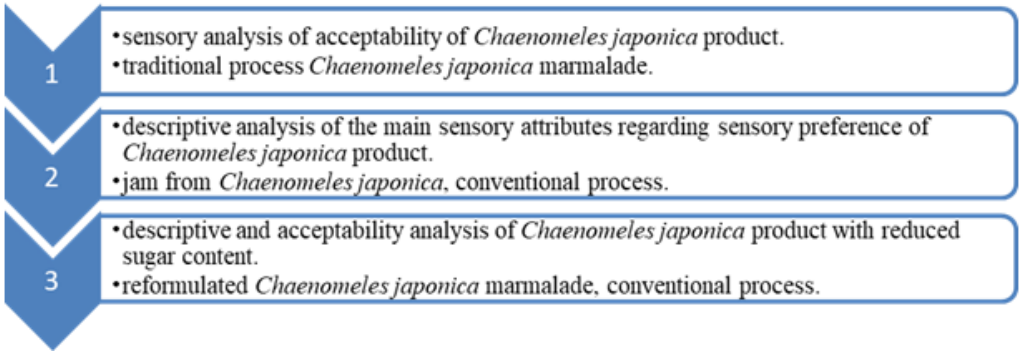

Fig. 1 - Sensory analysis scheme for products made from Japanese quince (*Chaenomeles japonica*)

1) The sensory quality analysis of the Japanese quince marmalade product (code 578), a traditional process, was carried out through a hedonic acceptability test for a unidimensional result. A 5-point Likert scale was used: 1-total disagreement; 2-disagreement; 3-indifferent; 4-agreement and 5-total agreement, through questions of appreciation of the perceptible sensory characteristics of the product: appearance, color, taste, flavor. The test was carried out on a number of 22 untrained subjects, grouped by age (under 30 years (8 subjects) _ 30 - 40 years (8 subjects) _ over 40 years (6 subjects)).
The score of the 4 sensory attributes resulted from calculating the algebraic sum of the opinions of the surveyed subjects. The result classified (Figure 2), in descending order, the sensory quality assessment of the Japanese quince marmalade sample, traditional process, as follows:
Color = 4.64 > Appearance = 4.59 > Flavor = 4.36 > Taste = 4.09;

The Global Score was calculated as the simple arithmetic mean of the partial scores, with a value of 4.42. The product has a positive overall image, with 88.4% of the surveyed subjects appreciating the main sensory characteristics of the new product. The global score, by age group indicates the highest degree of acceptability belonging to the age group under 30 years.

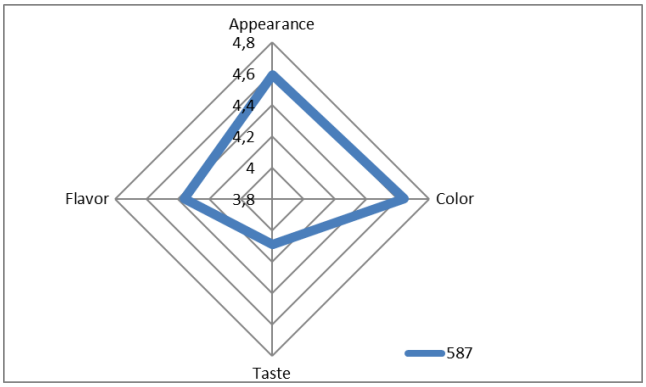

Fig. 2 - Sensory assessment of the Japanese quince marmalade sample

2) In order to establish a relationship between the main sensory attributes of the product (appearance, consistency, color, taste, aroma) and the sensory preference expressed by consumers, a product diversification from Japanese quince fruit was used by making three jam samples: code 587 - with added sugar, code 340 - with added fructose and code 289 - with added sugar and stevia extract. The objective of the test was to identify the perceptions underlying consumer preferences through descriptive assessment. A number of 13 subjects of both genders, aged between 25 and 65 years, participated in the test. The questionnaire used was developed in five stages of appreciation, well defined for each sensory characteristic, in order to identify the perception of each general sensory attribute underlying consumer preference. The information obtained by calculating the average score regarding the assessment of multiple general properties of Japanese quince jam samples is presented in Figure 3.

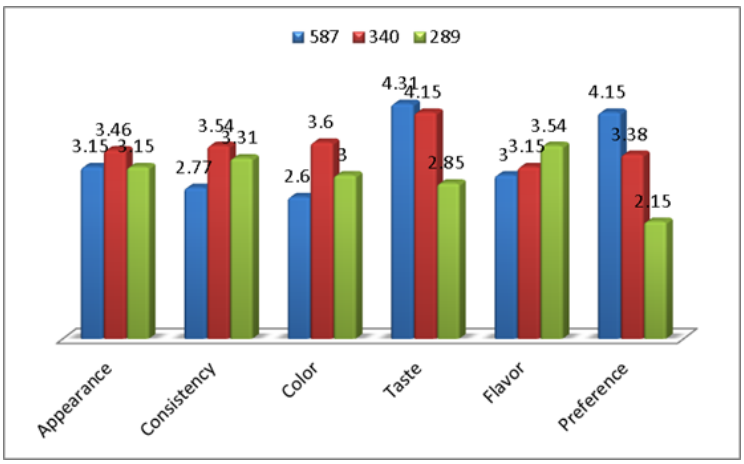

Fig. 3 - Score on the appreciation of multiple general properties of Japanese quince jam samples, where: 587 = Japanese quince jam with added sugar; 340 = Japanese quince jam with added fructose; 289 = Japanese quince jam with added sugar and stevia extract.

It is observed from Figure 4 that in the top of preference for the taste attribute the highest score was assigned to the sample with added sugar (587). The sensory attributes with visual evaluation (appearance, consistency and color) had the best score for the sample with added fructose (340), and the aroma attribute classified, with the best score, the sample with added stevia (251). It was found that the sample with added sugar (587) accumulated the best score regarding preference.

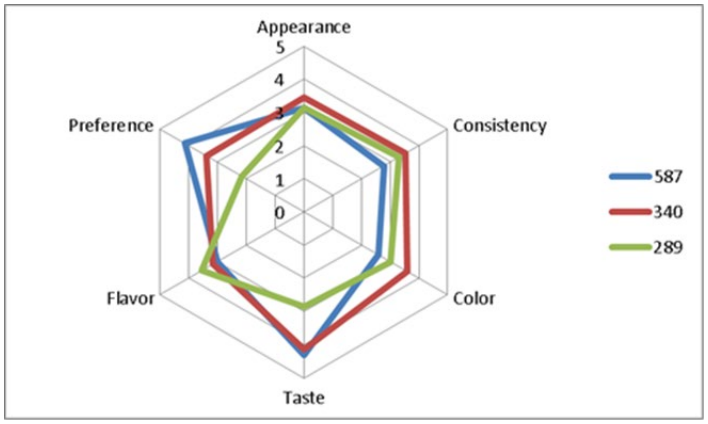

Fig. 4 - Sensory profile descriptive analysis of Japanese quince jam samples, where: 587 = Japanese quince jam with added sugar; 340 = Japanese quince jam with added fructose; 289 = Japanese quince jam with added sugar and stevia extract.

When assessing the sweet and sour taste (Figure 5) the subjects appreciated the perception of sour taste as superior to sweet taste for all samples. The jam sample evaluated with the most balanced ratio of sour taste / sweet taste was the sample with added fructose 340 = 1.11 < 587 = 1.14 < 289 = 1.31.

The Global Product Appetite Score (GPS) was calculated as the simple arithmetic mean of the partial scores. The global score thus calculated ranks the Japanese quince jam samples in the following order: 3.58 (340) > 3.17 (289) > 3.16 (587). Jam sample 340 has a higher score than jam sample 587 for the attribute's appearance (0.31 Pm), consistency (0.77 Pm) and aroma (0.15 Pm) (Figure 5) by 1.07 Pm. for the taste attribute, outperforming sample 587. It is found that the SG of the samples regarding acceptability differs from the expressed option regarding Preference (4.15 (587) > 3.38 (340) > 2.15 (289)).

Overall, the products have a high degree of acceptability, with the surveyed subjects positively appreciating, in percentages of 71.6% (340), 63.4% (289) and 63.2% (587) the main sensory characteristics of the new products, in the three compositional variants.

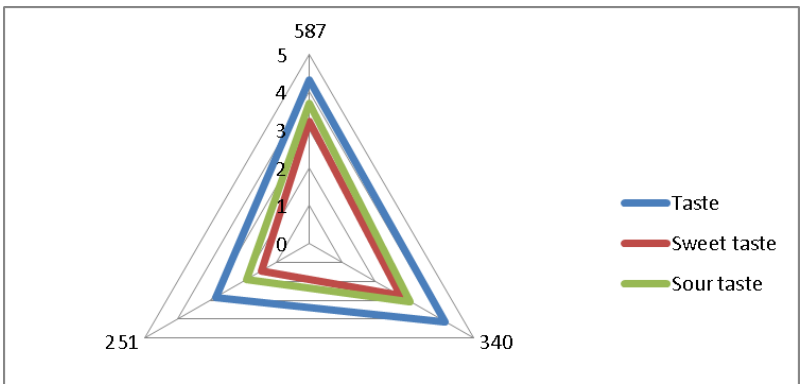

Fig. 5 - Average score of sour taste and sweet taste, where: 587 = Japanese quince jam with added sugar; 340 = Japanese quince jam with added fructose; 289 = Japanese quince jam with added sugar and stevia extract.

3) Sensory analysis of reformulated Japanese quince marmalade samples.

A five-point assessment questionnaire was used to analyze the sensory profile and consumer preference, well-defined for each sensory characteristic. The test was attended by 30 consumers, trained on (the evaluation procedure and questionnaire completion) for the perception of each general sensory attribute), aged < 30 years (18 consumers), 30 – 40 years (6 consumers) and > 40 years (6 consumers), of both genders.

By calculating Pm, the appreciation of the main sensory characteristics (Figure 6) of the reformulated Japanese quince marmalade samples (251 and 612) was evaluated compared to a Cydonia quince marmalade sample (341), purchased from the local market.

The sensory profile obtained is presented in Figure 6.

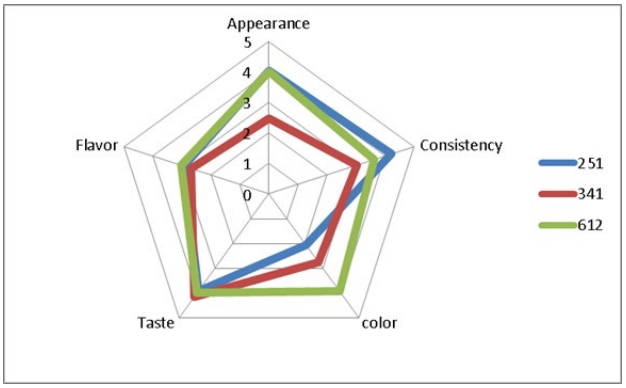

Fig. 6 - Sensory profile descriptive analysis of main sensory attributes of Japanese quince marmalade, where: 251 = Japanese quince marmalade formulation variant 1 (lemon peel), 612 = Japanese quince marmalade formulation variant 2 (cinnamon); 341 = Cydonia quince marmalade (control).

The result of the descriptive sensory analysis classifies the main sensory attributes (Figure 6) of the reformulated Japanese quince marmalade samples as follows:

Appearance: sample 251 was preferred with a slight difference in score (+0.6 Pm) compared to sample 612: described as fine, homogeneous paste, clear visual appearance.

Consistency: sample 251 was the most preferred being the firmest, with a total fruit content of 65.87%, the highest percentage of pectin and the lowest SST content = 25.8°Brix.

Color: sample 612 was the most preferred, the addition of cinnamon imitates the color of Cydonia quince marmalade from the commercial network (341), a traditional product.

Taste: sample 341 was the most preferred, possibly due to its more intense sweet taste with the highest SST content = 60.50°Brix compared to 251 = 25.8°Brix and 612 = 46.08°Brix. The differences in average score obtained by the three samples are not significant (± 0.12):

4.17 (341) > 4 (612) > 3.93 (251)

Aroma: sample 612 obtains the best average score = 3.03, but at a value very close to the two samples 2.93 (251) and 2.67 (341). In traditional cuisine, the aroma of cinnamon is associated with quince and apple fruits, the addition of spice having an important weight in the level of appreciation of the aroma.

The descriptive analysis for the taste attribute, resulting from the average score calculation, has the sensory profile in Figure 7.

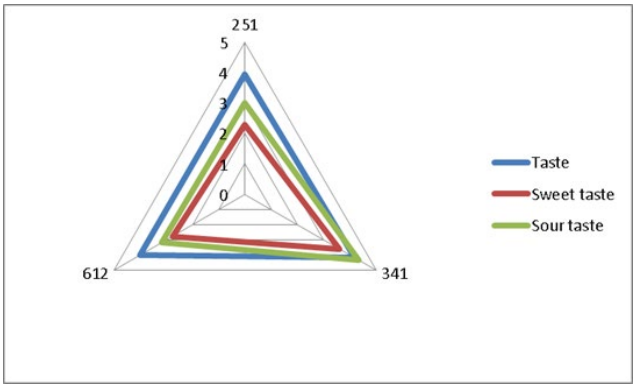

Fig. 7 - Sensory profile of the taste attribute of reformulated Japanese quince marmalade. Where: 251 = reformulated Japanese quince marmalade variant 1 (lemon peel), 612 = reformulated Japanese quince marmalade variant 2 (cinnamon); 341 = Cydonia quince marmalade (control).

It is observed from Figure 7 that the Japanese quince marmalade samples with the most balanced average score of the sour taste / sweet taste ratio were, in ascending order, 1.14 (341) < 1.2 (612) < 1.32 (251), a sensory evaluation that was perceived faithfully to the free acidity value of the samples: 1.04 (341) < 1.37 (612) < 1.68 (251). (Table 2)

The significant differences in sensory quality between the three samples were recorded in the sensory attributes consistency and color as a result of the difference in SST content (Table 2) and the color of the spices.

The global acceptability score was calculated similarly to the jam samples, as a simple arithmetic mean of the partial scores. The overall sensory quality assessment score classifies the reformulated Japanese quince marmalade sample with cinnamon (612) with the best average score (3.72), according to Figure 6.

It can be concluded that consumer preference recommends for reformulating Japanese quince marmalade (by increasing the content of Japanese quince fruits and decreasing the level of SST) a Japanese quince fruit / apple ratio of 1.45 and a reduction in sugar content by approximately 26% compared to the composition of Japanese quince marmalade with the traditional process (578). (Table 1) Consumers participating in the study appreciated the sensory quality of the marmalade samples, in both variants, by a percentage of 74.4% (612) > 68.8% (251) > 60.4% (341), outperforming the Cydonia quince marmalade currently available in the commercial network.

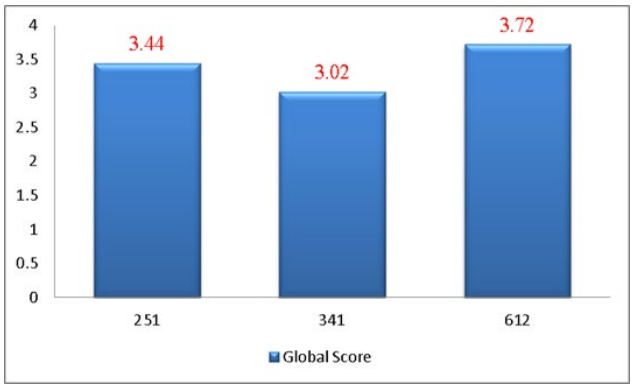

Fig. 8 - Classification, according to the global score, of the sensory quality of the reformulated *Japanese quince marmalade* samples, where: 251 = *Japanese quince marmalade* formulation variant 1 (lemon peel), 612 = *Japanese quince marmalade* formulation variant 2 (cinnamon); 341 = Cydonia quince marmalade (control)

CONCLUSIONS

The fruits of Chaenomeles shrubs (Japanese quince) are a significant source of compounds with high biological value that can contribute to the nutritional increase of the diet, due to the abundance of phytochemical compounds and the high content of microelements. The study evaluated the potential for the exploitation of Japanese quince fruits in Romania, in order to establish Chaenomeles shrub crops. The study

was based on making compositional structures as simple as possible by processing the fruits in the form of jam and marmalade. The sensory analysis of the new products was carried out using the 5-point Likert scale as a sensory study instrument for calculating the Global Score and STAS 12656-88: Sensory Analysis, Scoring Scale Methods, for calculating the average score for classifying the quality of sensory attributes. The study was carried out in three stages on a number of 65 untrained subjects, aged between 20 and 65 years of both genders.

The Japanese quince fruit jam made in three variants (with fructose, sugar and stevia extract) obtained a positive overall score, with the surveyed subjects appreciating the main sensory characteristics of the jam in percentages of 71.6%; 63.2% and 63.4%.

The marmalade product was made in three variants of sugar content: 44.25%; 18.13% and 14.97%. The calculation of the global score on acceptability resulted in a percentage of 88.4%; 74.4% and 68.8% of subjects who positively appreciated the sensory quality of the Japanese quince marmalade product. For the production of Japanese quince marmalade, consumer appreciation recommends a Japanese quince fruit / apple ratio of 1.45 and the possibility of reducing the addition of sugar by approximately 26% - 30% compared to the traditional manufacturing process.

The new products produced have a positive overall image that justifies the establishment of Chaenomeles shrub cultures in Romania.

ACKNOWLEDGEMENT

This work was supported by a grant of the Ministry of Research, Innovation and Digitization, CNCS/CCCDI - UEFISCDI, project number PN-IV-P8-8.1-PRE-HE-ORG-2025-0270, within PNCDI IV (contract 112PHE)".

REFERENCES

[1] Badiu A.F. (2020). Informare privind evoluția condițiilor climatice, a rezervei de umiditate din sol și stării de vegetație la culturile de toamnă în intervalul 01.Sept. 2020 – 15 oct. 2020, în zonele de influențăale unităților de cercetare-dezvoltare din domeniul agricol, ASAS "Gheorghe Ionescu-Șișești"

[2] Baranowska-Bosiacka I., Bosiacka B., Rast J., Gutowska I., Wolska J., Rębacz-Maron E., Dębia K., Janda K., Korbecki J., Chlubek D. (2017). Macro- and Microelement Content and Other Properties of Chaenomeles japonica L. Fruit and Protective Effects of Its Aqueous Extract on Hepatocyte Metabolism, Biol Trace Elem Res 178:327–337.

[3] Chiţu E., Mateescu E., Petcu A., Surdu I., Sumedrea D., Tănăsescu Nicolae, Păltineanu C., Chiţu V., Mladin P., Coman M., Butac, M., Gubandru, V. (2010). Modele de estimare a favorabilităţii climatice pentru cultura pomilor în România, Editura INVEL Multimedia Bucureşti.

[4] Chiţu E., Ivona M., Mirela C., Mihail C., Plăiașu F., Chivu M., Sturzeanu M., Petrescu A., Hera O., (2023). Modelarea favorabilității climatice a Romaniei în vedere extinderii în cultură a unor specii pomicole de climat temperat și subtropical. Institutul de Cercetare-Dezvoltare pentru Pomicultură Pitești – Mărăcineni, Academia de Științe Agricole și Silvice "GHEORGHE IONESCU ȘIȘEȘTI".

[5] Coman V., Rotaru A., Juravlea A., Popa M., Nistorescu M., Doba A. (2023). Raport de mediu „Strategia naţională privind prevenirea şi combaterea deşertificării şi degradării terenurilor 2019-2030".

[6] Haizhao S., Hong L., Jing L., Minfang C., Yubo C., Qiang C. (2024). Chaenomeles sinensis (Thouin) Koehne fruit polyphenols alleviate high-fat diet–induced obesity and liver steatosis by improving lipid metabolism in mice. Nutrition Research, Volume 123, Pages 111-119.

[7] Hongyue T, Xia Li, Lingzhuo An, Shirui W., Zhouyi X., Zhilai Z., Xuemin Z., Guanglu C., Wenyuan G., Lanping G., (2024). Genetic variation, functional composition, biological activity, and diverse applications of Chaenomeles: A review of current knowledge. Food Chemistry, Volume 485, 144404.

[8] Watychowicz K, Janda K, Jakubczyk K, Wolska J, (2017). CHAENOMELES – HEALTH PROMOTING BENEFITS. Rocz Panstw Zakl Hig 2017; 68(3):217-227.

[9] Marat, N., Danowska-Oziewicz, M., Narwojsz, A. (2022). Chaenomeles Species—Characteristics of Plant, Fruit and Processed Products: A Review. Plants 11, 3036.

[10] Rumpunen K., Göransson E. (2003). Consumer Preferences for Japanese Quince (Chaenomeles japonica) Products, Swedish University of Agricutural Sciences p. 177–180

[11] Ruoling X., Mengting K., Ning L. (2023). Phytochemistry and pharmacology of plants in the genus Chaenomeles. Archives of Pharmacal Research, 46, 825 -854.

[12] SR EN 750/2008. Produse din fructe şi legume. Determinarea acidităţii titrabile.

[13] Strugała P., Cyboran-Mikołajczyk S., Dudra A., Mizgier P., Kucharska A.Z., Olejniczak T., Gabrielska J. (2016). Biological Activity of Japanese Quince Extract and Its Interactions with Lipids, Erythrocyte Membrane, and Human Albumin, J Membrane Biol 249:393–410.

[14] Turkiewicz I.P., Tkacz K., Nowicka P., Michalska-Ciechanowska A., Lech K., Wojdyło A., (2021). Physicochemical characterization and biological potential of Japanese quince polyphenol extract treated by different drying techniques, LWT,Vol 152, 112247.

[15] Radenkovs V., Krasnova I., Cinkmanis I, Juhnevica-Radenkova K., Rubauskis E. and Seglina D., (2024). Comparative Analysis of Japanese Quince Juice Concentrate as a Substitute for Lemon Juice Concentrate: Functional Application as a Sweetener, Acidifier, Stabilizer, and Flavoring Agent,, Horticulturae, 10(12), 1362;

[16] Zhang S.Y., Han L.Y., Zhang H., Xin H.L. (2014). Chaenomeles speciosa: A review of chemistry and pharmacology. Biomed Rep. 2(1):12-18.

DESIGN OPTIMIZATION OF CUTTING BLADES FOR MOWING EQUIPMENT THROUGH COMPARATIVE STUDY USING SOLIDWORKS SIMULATION

/

OPTIMIZAREA CONSTRUCTIVĂ A CUȚITELOR PENTRU ECHIPAMENTE DE COSIT PRIN STUDIU COMPARATIV UTILIZÂND SOLIDWORKS SIMULATION

Alin-Nicolae HARABAGIU*[1)], Vasilica ȘTEFAN[1)], Lucreția POPA[1)], Dragoș-Nicolae DUMITRU[1)], Elena-Melania CISMARU[1)], Dragoș MANEA[1)], Polifron CHIRITA[2)]

[1)] The National Institute of Research - Development for Machines and Installations Designed for Agriculture and Food Industry - INMA Bucharest / Romania;

[2)] INOE IHP / Romania.

**Tel: 0040 773 867 656; *E-mail: alinhara04@gmail.com*

Keywords: *design study, blade rotor, mowing equipment, design optimization*

ABSTRACT

This study aims to optimize the design of tractor-mounted rotary mower blades for inter-row mowing by building on insights from prior SolidWorks simulation studies. Previous structural and modal analyses of blade rotors provide critical information on stress distribution, deformation, and material behavior under dynamic operating conditions. Using these findings, the research evaluates how blade geometry—including length, angle of attack, number of blades per drum, and thickness—and material selection influence cutting efficiency, torque, vibration, and overall durability. By applying this knowledge, the study identifies design improvements that enhance performance, reduce mechanical stress, and ensure reliable operation, providing a foundation for developing more efficient and durable rotary mowing equipment suited to modern agricultural demands.

REZUMAT

Acest studiu își propune optimizarea designului lamelor pentru cositori rotative tractate, utilizate la cosirea între rânduri, prin valorificarea rezultatelor studiilor anterioare realizate în SolidWorks. Analizele structurale și modale preexistente ale rotoarelor lamelor furnizează informații esențiale privind distribuția tensiunilor, deformațiile și comportamentul materialelor în condiții de operare dinamice. Pe baza acestor date, cercetarea evaluează modul în care geometria lamelor — inclusiv lungimea, unghiul de atac, numărul de lame pe rotor și grosimea — și selecția materialelor influențează eficiența tăierii, cuplul, vibrațiile și durabilitatea generală. Aplicând aceste cunoștințe, studiul identifică îmbunătățiri de design care cresc performanța, reduc solicitările mecanice și asigură funcționarea fiabilă, oferind un fundament pentru dezvoltarea unor echipamente de cosire rotative mai eficiente și mai durabile, adaptate cerințelor moderne ale agriculturii.

INTRODUCTION

In modern agricultural mechanization, tractor-mounted rotary drum mowers play a vital role in forage harvesting systems. These machines use fast-rotating blades to cut grass and other vegetation efficiently. Compared with traditional sickle-bar mowers, rotary drum mowers offer higher cutting capacity, reduced vibration, and improved stubble uniformity *(Celik et al., 2023; Wu et al., 2023).* The performance of such mowers depends largely on the geometric and structural characteristics of the blades, including length, angle of attack, number of blades per drum, and rotational speed *(Celik et al., 2023).* Figure 1 shows a representative rotary mower blade model illustrating the primary geometric parameters that influence cutting performance.

Fig. 1 - Tractor mounted rotary drum mower model
(Celik et al., 2023)

The geometry and material of mower blades are crucial to both efficiency and durability. Studies have shown that twisted or inclined blades can lift crops before shearing, resulting in cleaner cuts and lower energy demand *(Wu et al., 2023; Uzoma & Briggs, 2019).*

Conversely, worn or sub optimally shaped blades significantly increase drag and fuel consumption; Refai et al., (2023) reported that worn drum mower blades increased fuel use by 67% and carbon dioxide emissions during alfalfa mowing. The mechanical performance of blades, therefore, strongly depends on their material properties—hardened steels and advanced alloys are often selected to improve wear resistance and service life *(El-Baily, 2022; Alkaddour 2025).*

From a mechanical standpoint, mower blades are subjected to intense dynamic loads during operation. Bartoň (2019) demonstrated that the oscillatory motion of drum mower blades is closely linked to vegetation properties and blade stiffness, emphasizing the need for structural and modal analysis in design.

Similarly, in a previous research study performed modal and structural analysis on a mower blade rotor using SolidWorks Simulation, identifying critical stress zones and natural frequencies under working conditions. These findings underscore the value of computer-aided engineering (CAE) in optimizing agricultural cutting equipment, it is also a good starting point for design optimization *(Harabagiu et al., 2024*).

Advancements in simulation technology have facilitated the optimization of mower blades using SolidWorks Simulation and Design Study modules. These tools allow for the variation of geometric and material parameters to evaluate stress distribution, deformation, and natural frequency. For instance, Revi et al., (2016) used computational fluid dynamics (CFD) and finite element analysis (FEA) to refine the aerodynamic profile of a rotary mower blade. Similarly, Pandey et al., (2021) modeled a rotary tiller blade in SolidWorks and performed fatigue analysis in ANSYS to determine optimal dimensions for reducing power consumption.

Figure 2 illustrates key blade geometry parameters—the cutting angle and thickness—both of which strongly influence torque, stress, and energy efficiency *(Uzoma & Briggs, 2019).* Considering the reviewed studies, the present work focuses on the design optimization of cutting blades for a tractor mounted rotary mower through a comparative study using SolidWorks Simulation.

The research aims to identify the optimal combination of blade geometry and material to minimize stress and vibration while maximizing cutting efficiency and structural reliability, building directly on the methodology and findings of our previous study, we now investigate possible design optimization.

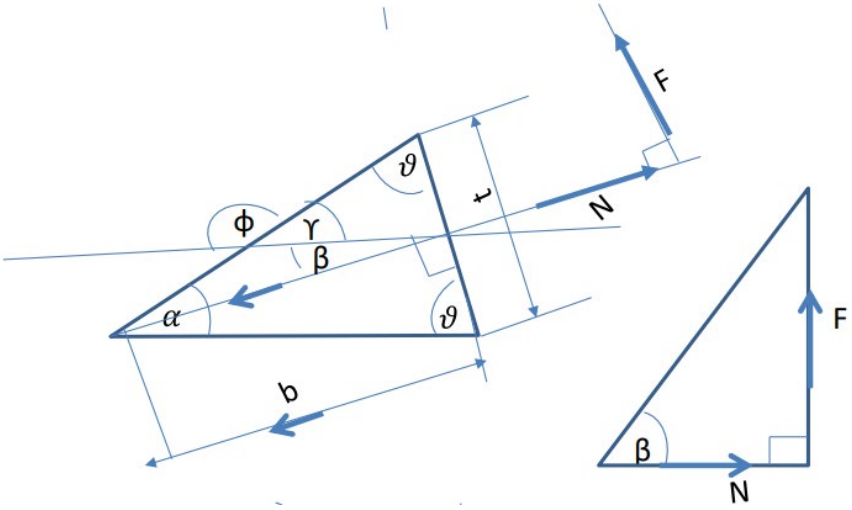

Fig. 2 - Geometric representation of blade cutting angle and thickness
(Uzoma & Briggs, 2019)

MATERIALS AND METHODS

The materials and research methodology for this study involve the analysis of scientific literature, including summaries from specialized sources such as Thomson ISI, ScienceDirect, ResearchGate, and Google Scholar. The research uses an already existing 3D CAD model of the cutting blade designed in SolidWorks and previous simulation results. The optimization process relies heavily on insights obtained from previous studies *(Nandish et al., 2019; Wang et al., 2024)* and prior simulation results of our blade and blade rotor.

These earlier investigations provided detailed information on stress distribution, deformation patterns, vibration behavior, and critical failure zones under operating conditions (Figure 3).

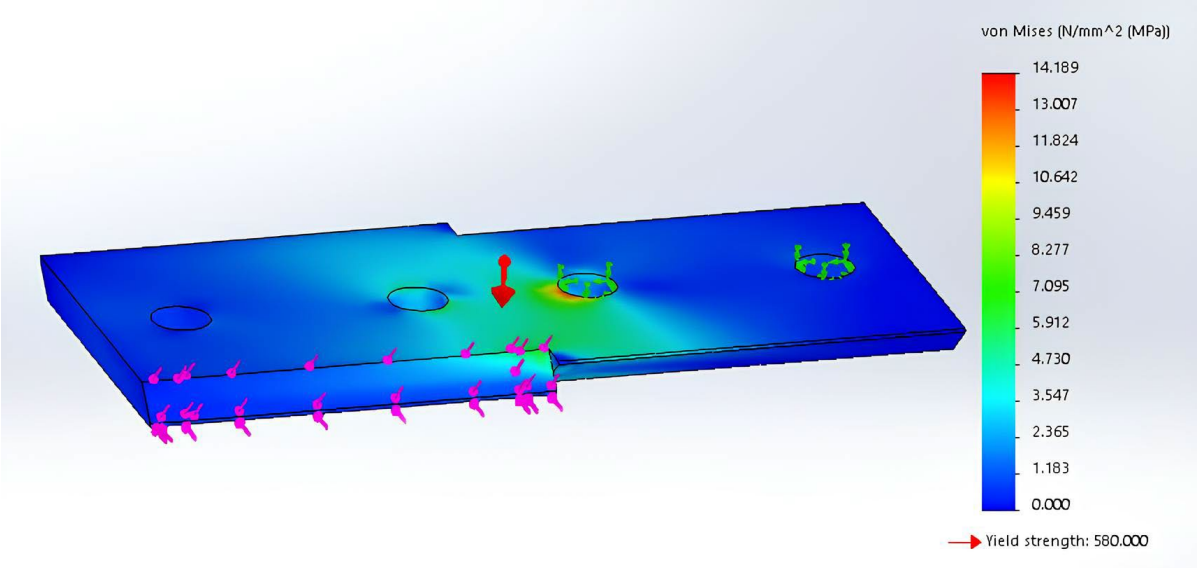

Fig. 3 - Stress results on the cutting blade

All design studies and optimizations reported in this work were created and executed using the Design Study functionality built into SOLIDWORKS. The Design Study environment provides two distinct but related computational paradigms for exploring parametric design spaces: an evaluation paradigm in which discrete sets of parameter values are enumerated to form multiple scenarios that are individually evaluated, and an optimization paradigm in which variables are specified as continuous ranges or discrete choices and the software iteratively searches the design space for combinations that satisfy user-defined constraints while optimizing one or more objectives.

Evaluation is appropriate to exhaustively or selectively test a manageable number of discrete combinations, whereas optimization is more appropriate when continuous exploration and automated search are required to locate optimal subject to constraints (2023 Web Help, Dassault Systèmes).

Prior to the construction of any study, model preparation and prerequisite elements were established within the SOLIDWORKS.

Figure 4 shows the parameters used as variables, they were defined as dimension-driven model parameters and persistent sensors were created to report quantities of interest such as mass properties, key dimensions, or, when required, simulation outputs. Simulation-derived sensors were required, our previous study was used as an initial simulation study, this provides the optimization module with a baseline simulation that it can re-solve for each scenario or iteration. Study metadata (including the results folder and study quality settings) were set at study creation so that output files, intermediate results, and logging followed a reproducible file structure.

The SOLIDWORKS documentation describes the recommended practice of defining parameters and sensors before creating the study, and explains how study properties influence result storage and fidelity.

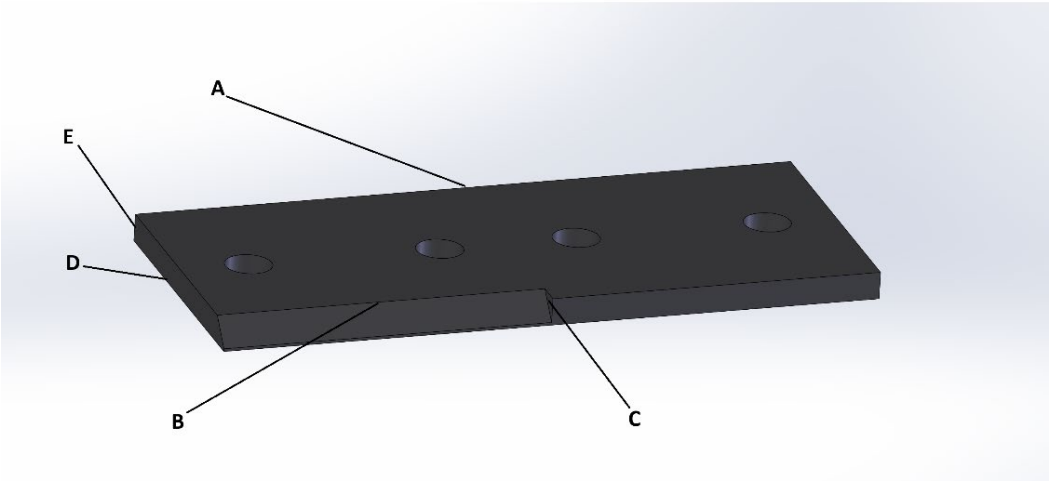

Fig. 4 - Most influential design parameters of the blade

The workflow employed to build each study followed the canonical sequence implemented in the SOLIDWORKS Design Study property managers and user interface. A new Design Study tab was created within the model, after which variables were linked to model parameters and sensors were associated with the physical quantities and simulation outputs of interest; variables were specified as discrete value lists, but also as continuous ranges with different step sizes, and sensors were marked as objectives.

For optimization studies variables were supplied as continuous ranges and as mixed discrete sets, and the Optimization checkbox engaged the solver that iteratively sampled the design space with the aim of satisfying constraints while minimizing the chosen goal sensors, in our case the factor of safety.

Operational parameters and solver limit important to reproducibility and to the interpretation of results were recorded and controlled. The evaluation/design-scenario module imposes a practical upper bound on the number of enumerated scenarios; the documentation specifies that up to 4,096 scenarios can be generated and evaluated in a single evaluation study, for our study 247 scenarios were made. For optimization studies the software imposes limits on the number of design variables and the combined count of goals plus constraints; the official guidance states a maximum of 20 design variables and a total of 20 constraints and goals combined, our study used a total of 5 variables and only 3 constraints and goals combined.

Study quality was set to high, these were chosen to balance computational cost and numerical fidelity; the documentation notes that quality settings affect available post-processing features (for example, certain local-trend graphs are not available under specific combinations of high quality and discrete-only variables) and thereby influence the types of sensitivity analyses that can be performed directly in the Design Study interface.

In the present study, the optimization of the blade design was carried out with five key design variables, as previously mentioned, each selected to capture critical aspects of the geometry and functional performance. The first variable, blade width, was defined over a discrete range from 50 to 150 mm with increments of 50 mm, representing variations in lateral size that influence cutting efficiency and structural rigidity.

The second variable, cutting angle, was considered as three discrete values: 30°, 45°, and 60°, reflecting the angular orientation of the blade edge relative to the material and its effect on cutting performance and load distribution. Blade thickness, the third variable, was varied across 4, 8, and 10 mm, capturing the influence of cross-sectional robustness on mechanical strength and resistance to deformation. Blade length was treated as a continuous variable within the range 240 to 480 mm, incremented in steps of 120 mm, accounting for the longitudinal reach and leverage of the blade during operation.

Finally, the ratio of cutting surface, expressed as the proportion of the blade length that constitutes the effective cutting edge, was varied from 0.25 to 0.75 in steps of 0.25, representing different distributions of cutting versus non-cutting regions along the blade. Together, these variables were systematically incorporated into the SOLIDWORKS Optimization Module, enabling the iterative solver to explore the multidimensional design space and identify configurations that optimize performance objectives while satisfying defined constraints.

Finally, for scientific validity, computational results obtained from Design Study optimization were subjected to independent verification and engineering judgment before being reported. Optimized designs were examined for manufacturability, checked against unmodeled constraints, and re-evaluated with refined mesh or higher study quality in the linked simulation study.

RESULTS

For this study it was used the Design Study Add-in built within SolidWorks. In order to improve the blade design, previous structural simulations using different loads in order to simulate the use of the machine in different environments. We used the original model of the blade with the length of the cutting edge of 120 mm, a width of 100 mm, a thickness of 10 mm and a 45-degree cutting angle.

The first design study takes into account previous results of the stress and deformation on the blade during alfalfa harvesting, our previous study was used in order to determine the value of this stress and deformation, the cutting edge length, the blade width, the cutting angle and blade thickness were modified in order to achieve a much better factor of safety, and less deformation on the blade, the mass of the blade was also monitored during our study in order to find a lighter design possibility to reduce the manufacturing costs.

First step was to define the variables and their specific values within SolidWorks Design Study (Figure 5).

Name	Type	Value	Units
A	Range with Step	Min:50 Max:150 Step:50	mm
B	Discrete Values	30°, 45°, 60°	deg
C	Discrete Values	4, 8, 10	mm
D	Range with Step	Min:240 Max:480 Step:120	mm
E	Range with Step	Min:0.25 Max:0.75 Step:0.25	N/A

Fig. 5 - Setting up the Design Study

The goal of the Design Study was to achieve a much lower Factor of Safety (FOS), while maintaining the structural properties of the blade. At the end of the study process, we achieved a blade design that has a blade thickness of 4, a total length of 360 mm with a cutting edge of 75% of total length, the cutting angle of 45° and a width of 100 (Figure 6).

Component name	Units	Current	Initial	Optimal	Scenario1	Scenario2
A	mm	50	50	100	50	100
B	deg	30°	30°	45°	30°	30°
C	mm	4	4	4	4	4
D	mm	240	240	360	240	240
E	N/A	0.25	0.25	0.75	0.25	0.25
Minimum Factor of Safety1		3.894586	3.894586	3.966846	3.740210	4.978802
Mass1	kg	0.34169	0.34169	1.0664	0.34242	0.71682
Minimum Factor of Safety2		3.894586	3.894586	3.966846	3.740210	4.978802

Fig. 6 - Design study results for the blade model during alfalfa cutting

The results shown above represent significant improvements, lowering the factor of safety by 89,47%, from 38 to a 3.967 value, the weight of our blade was lowered by 39% down to 1.07 Kg allowing us to cut down the costs of manufacturing the blade by 39.2%. To assess the structural performance of the updated design, the earlier simulations were repeated, focusing on the resulting deformation (Figure 7a) and stress distribution on the blade (Figure 7b).

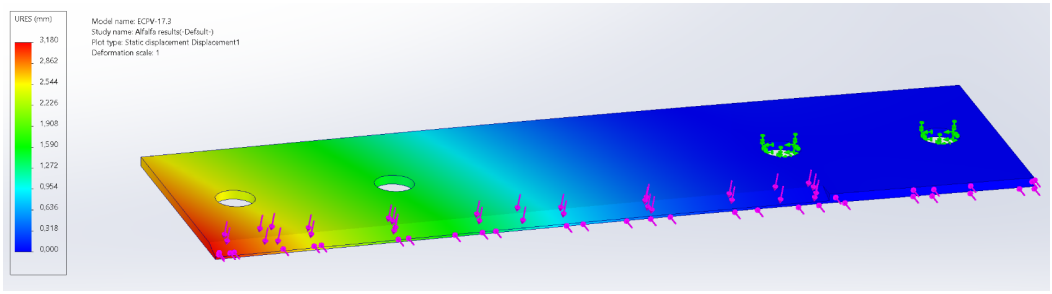

a)

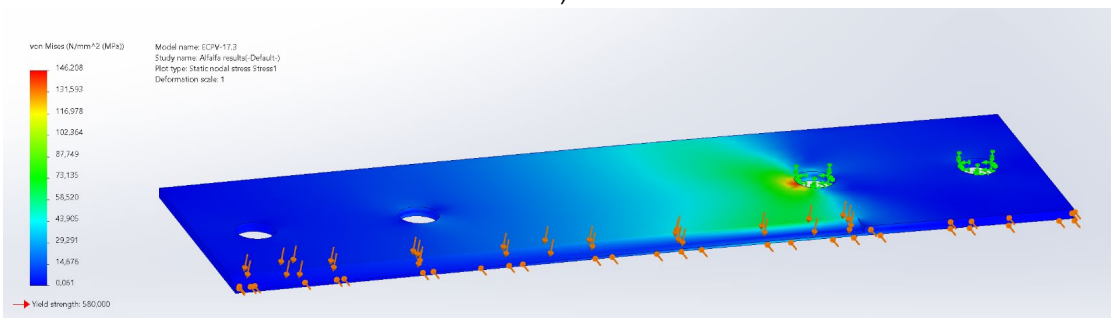

b)

Fig. 7 - Simulation results on the newly updated design

To further evaluate the structural performance of the optimized blade design, previous simulation setup was used to represent the cutting of thicker grass, which introduces greater resistance and load on the cutting edge. This analysis aimed to verify whether the updated design could maintain structural integrity under more demanding operating conditions.

However, the results revealed a significant issue: the Factor of Safety (FOS) decreased to 0.5, a value considerably below the acceptable threshold for safe operation. With such a low FOS indicating a high risk of structural failure under realistic field conditions, it was decided to perform the Design Study once more, this time based on the simulation results of the thicker grass scenario, in order to obtain a safer and more reliable configuration.

As a result of this new optimization process, we achieved a blade design characterized by the following parameters: a blade thickness of 8 mm, a total length of 240 mm with a cutting edge of 75 % of the total length, a cutting angle of 45°, and a width of 100 mm (Figure 8).

Component name	Units	Current	Initial	Optimal	Scenario1	Scenario2
A	mm	100	100	100	50	100
B	deg	45°	45°	45°	30°	30°
C	mm	4	4	8	4	4
D	mm	360	360	240	240	240
E	N/A	0.75	0.75	0.75	0.25	0.25
Minimum Factor of Safety1		4.966	3.966846	3.922	3.740210	4.978802
Mass1	kg	1.06 kg	1.0664	1.4	0.34242	0.71682
Minimum Factor of Safety2		4.966	3.966846	3.922	3.740210	4.978802

Fig. 8 - Design study results for the blade model during millet stems cutting

The results obtained show a clear improvement, increasing the Factor of Safety from 0.5 to 3.9. To assess the structural performance of this updated design, the simulations were repeated, focusing on the resulting deformation (Figure 9a) and stress distribution on the blade (Figure 9b).

These results clearly demonstrate the effectiveness of the Design Study in optimizing the blade's geometry, improving its structural reliability, and achieving a more efficient and cost-effective configuration suitable for varying cutting conditions.

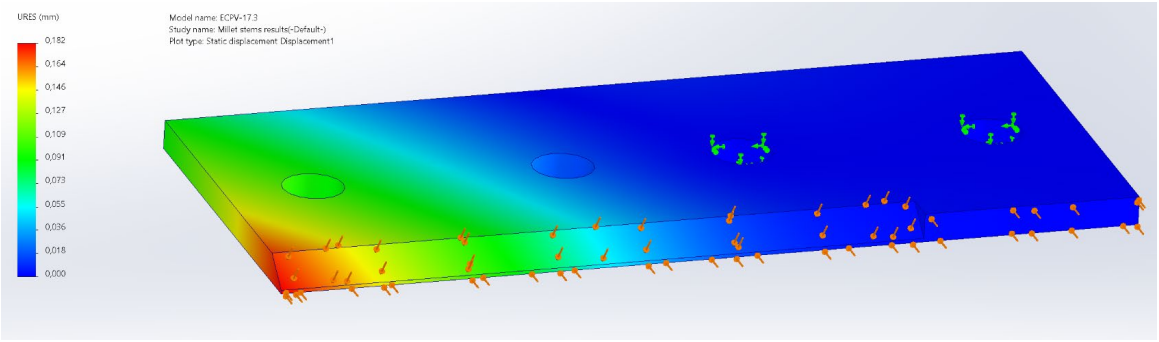

a)

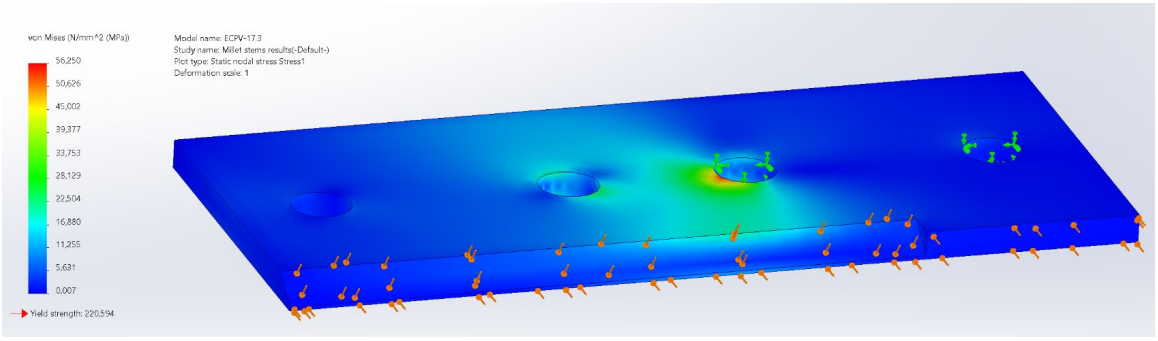

b)

Fig. 9 - Simulation results on the final designed blade

CONCLUSIONS

The study demonstrated that systematic use of SolidWorks Simulation and the Design Study module can significantly enhance the structural performance of the cutting blades for a mowing equipment. By iteratively refining geometric parameters such as thickness, length, cutting angle, and width, the optimized blade achieved a substantial improvement by lowering the Factor of Safety, from 38 to 3.9, while also reducing mass and manufacturing costs. These results confirm the value of simulation-based design as an efficient and reliable method for optimizing agricultural machinery components. Furthermore, integrating real operating conditions into the simulation process ensures that the resulting design maintains durability, efficiency, and cost-effectiveness when exposed to varying vegetation densities and cutting environments.

ACKNOWLEDGEMENT

The results presented in this article were obtained with the support of the MCID through the NUCLEU program, project PN 23 04 02 03, INNOVATIVE TECHNOLOGY FOR GREEDING THE INTERVAL BETWEEN VINEYARD ROWS AND FRUIT TREES TO AVOID SOIL STRUCTURE DEGRADATION, funding contract no. 9N / 01.01.2023 .

REFERENCES

[1] Alkaddour, S. M. (2025). *Simulate four main models of holes to make in the lawn mower cutting blade and find out the least noisy*. *SSRN Electronic Journal*. https://dx.doi.org/10.2139/ssrn.5101574

[2] Bartoň, S. (2019). *The dynamics of the drum mower blade*. In *Proceedings of PANM 2019* (pp.35–44). Institute of Mathematics of the Czech Academy of Sciences. DOI: 10.21136/panm.2018.01

[3] Celik, H. K., Akinci, I., Çaglayan, N., & Rennie, A. E. W. (2023). *Structural strength analysis of a rotary drum mower in transportation position*. *Applied Sciences, 13*(20), 11338. https://doi.org/10.3390/app132011338

[4] El-Baily, M. M. (2022). A study of rotary drum mower blade wear and its effects on forage productivity. *Poljoprivredna Tehnika*, 47, 87-100. https://doi.org/10.5937/PoljTeh2203087E

[5] Harabagiu, A.-N., Prisacariu, E., Mantovani, S.-A., Ștefan, V., Popa, L., Cismaru, E.-M., Dumitru, D.-N., & Zota, A.-R. (2024). *Modal and structural analysis of the blade rotor of a mowing equipment for inter-row spaces using SolidWorks Simulation*. *Agri-INMA, 5*(2), 45–56.

[6] Nandish, B., Muthanna, K. P., Kaveriappa, M. B., & Biddappa, P. S. (2019). Design and analysis of grass mower. *International Journal of Science, Engineering and Management (IJSEM), 6*(4).

[7] Pandey, D., Rangera, D., Bhatia, D., Singh, G., & Chaudhary, R. (2021). *Design optimization and static force analysis of L-type rotary tiller blade*. In *Lecture Notes in Mechanical Engineering* (Vol. 147, pp.147–162). Springer.

[8] Refai, M., Abdelkader, T. K., Sayed, H. A. A., Wan, Q., & Abdelhamid, M. A. (2023). *Wear behavior and CO_2 emissions analysis of drum mower blades during alfalfa harvest*. *SN Applied Sciences, 5*(3), 316. https://doi.org/10.1007/s42452-023-05545-y

[9] Revi, V. P., Akhil, K. A., Vishnu, N. V., Rozario, K., & Rohith, P. (2016). Design and analysis of rotary lawn mower. *International Journal of Engineering Research & Technology (IJERT), 5*(4). DOI: 10.17577/IJERTV5IS040152

[10] Uzoma, S. M., & Briggs, T. A. (2019). *Optimization model of lawn mower blade geometry to attain improved cutting efficiency*. *European Journal of Mechanical Engineering Research, 6*(1), 25–31.

[11] Wang, W., Wang, Z., Pan, B., Cui, Q., Zhang, L., Qiu, S., & Zhang, Y. (2024). Study on the shear and bending mechanical properties of millet stem. *Agriculture, 14*(6), 923. https://doi.org/10.3390/agriculture14060923

[12] Wu, B., Zuo, T., Li, Z., Qian, H., Huang, T., & Xiang, Y. (2023). Numerical simulation and optimization of the airflow field of a forage drum mower. *Applied Sciences*, 13, 5910. https://doi.org/10.3390/app13105910

BIOCHAR IN SUSTAINABLE AGRICULTURE: EFFECTIVE APPLICATION STRATEGIES FOR SOIL IMPROVEMENT AND PRODUCTIVITY INCREASE- REVIEW

/

BIOCHARUL ÎN AGRICULTURA DURABILĂ: STRATEGII EFICIENTE DE APLICARE PENTRU ÎMBUNĂTĂȚIREA SOLULUI ȘI CREȘTEREA PRODUCTIVITĂȚII - REVIEW

Iulian DUMITRU*[1)], Laurențiu VLĂDUȚOIU[1)], Florin NENCIU[1)], Valentin VLADUȚ[1)], Alexandru IONESCU[1)], Oana-Elena MILEA[1)], Gabriel NAE[1)], Costin MIRCEA[1)], Iulian VOICEA[1)], Andreea-Iulia GRIGORE[1)], Adriana BORȘ[2)]

[1)] National Institute of Research – Development for Machines and Installations Designed to Agriculture and Food Industry – INMA Bucharest / Romania;

[2)] INOE 2000 - IHP / Romania

**Tel: 0773 720 468; *E-mail: dumitru.iulian2016@gmail.com*

Keywords: *biochar, soil amendment, soil fertility, soil structure, sustainable development, climate change*

ABSTRACT

The following material analyzes the potential of biochar as a sustainable agricultural amendment, with a focus on how its application influences soil fertility, crop productivity, and agroecological processes. The study explores key aspects such as timing of application, incorporation depth, dosage, type of biochar, as well as the technologies used for its integration into the soil. The paper synthesizes recent experimental results that highlight the effectiveness of composted biochar compared to other forms of application, demonstrating its positive impact on soil pH, microbial activity, and plant yield. It emphasizes the need for adopting biochar as an integral part of a sustainable agricultural system adapted to local conditions, underlining the importance of applied research and institutional support for large-scale implementation.

REZUMAT

In materialul de mai jos este analizat potențialul biocharului ca amendament agricol sustenabil, cu accent pe modul în care aplicarea sa influențează fertilitatea solului, productivitatea culturilor și procesele agroecologice. Sunt dezvoltate aspecte legate de momentul aplicării, adâncimea, cantitatea, tipul de biochar, precum și tehnologiile utilizate pentru încorporare. Lucrarea sintetizează rezultate experimentale recente care indică eficiența biocharului compostat comparativ cu alte forme de aplicare, demonstrând impactul pozitiv asupra pH-ului solului, activității microbiene și randamentului plantelor. Se subliniază nevoia adoptării biocharului ca parte integrantă a unui sistem agricol durabil și adaptat condițiilor locale, subliniind importanța cercetării aplicate și a sprijinului instituțional pentru implementare la scară largă.

INTRODUCTION

In the context of the climate crisis and the depletion of natural resources, modern agriculture is facing increasing pressure to become more sustainable, productive, and resilient. Soil degradation, biodiversity loss, and crop yield volatility (*Chen et al., 2024*) demand the development of innovative solutions. Biochar – a stable, carbon-rich material obtained through the pyrolysis of biomass (*Bruun et al., 2012*) under limited oxygen conditions – is being promoted as a viable option for soil regeneration and reducing agriculture's carbon footprint.

Its physico-chemical properties, such as porosity, water retention capacity, alkaline pH, and recalcitrant carbon content, make it a valuable ally in strategies aimed at improving soil quality. However, the effectiveness of biochar depends on numerous factors: soil type, crop species, climate conditions, feedstock used, and especially the technology and timing of application. This paper explores all these dimensions, offering an up-to-date synthesis of scientific literature and recent experimental data.

Biochar, produced through biomass pyrolysis under reduced oxygen conditions, offers multiple benefits for agriculture and the environment. Due to its porous structure, it retains water and nutrients, enhances soil fertility and structure *(Singh et al., 2023)*, increases pH, reduces greenhouse gas emissions (*Li et al., 2024*), and mitigates heavy metal pollution. It is particularly effective in restoring degraded soils, especially in arid regions or areas with poor-quality soils.

Applying biochar increases crop yields *(Huang et al., 2023*), improves nutrient retention, supports microbial activity, and reduces the need for chemical fertilizers (Wang et al., 2024). It is successfully used in

greenhouses, gardens, agriculture, forestry, construction, and even in water filtration or as a feed additive. An additional advantage is the production of clean energy during the pyrolysis process.

Although the use of biochar may seem like a recent innovation, the technique has been used for thousands of years. Today, biochar is recognized as a key tool for regenerative agriculture and climate change mitigation *(Kumar et al., 2025)*, through carbon sequestration and the reduction of CO_2, CH_4, and N_2O emissions.

The success of thermochemical conversion technologies and biochar adoption depends on local conditions, biomass availability, and market demand. In this context, biochar becomes a key element in the circular economy, transforming organic waste (*Zhao et al., 2025*) into a valuable resource with positive economic and ecological impacts.(*https://www.businessagricol.ro/biocharul-parte-a-economiei-circulare-solutie-ideala-de-transformare-a-deseurilor-organice/*)

To fully harness the potential of biochar, it must be integrated into a set of sustainable agricultural practices. In a circular farming system, biochar can be effectively combined with compost or organic fertilizers (*Schmidt et al., 2021*), contributing to improved soil structure and increased water-holding capacity. In Romania, some farmers have already begun applying these integrated solutions, using biochar alongside crop rotation and cover crops, which helps prevent erosion, soil-borne diseases, and supports long-term soil fertility.

Collaboration between researchers, farmers, and authorities is essential for the effective adaptation of biochar use (*Sohi et al., 2010*) under various agricultural conditions. At the European level, biochar has been successfully integrated into organic farms, contributing to increased yields (*Biederman & Harpole, 2013*) and reduced greenhouse gas emissions. Institutional support, in the form of financial incentives, can accelerate the adoption of this innovative technology, strengthening the transition toward sustainable practices.

Thus, biochar represents a promising solution for enhancing food security, protecting natural resources, and combating the effects of climate change. Its widespread adoption could drive the development of regenerative, sustainable agriculture that is adapted to current challenges. For effective implementation, it is recommended to consult environmental specialists who can assist with obtaining the necessary permits and ensuring compliance with environmental regulations.(*https://stratos.ro/blog-biochar-sau-carbunele-vegetal-un-produs-ideal-pentru-practicile-agricole-sustenabile/*)

Fig.1 - Characteristics of biochar
https://www.bestongroup.com/ro/biochar-production-equipment/amp/

The most important characteristics of biochar are (Fig 1):

a) Porous structure:

Biochar has a dense network of micropores both on the surface and within its internal matrix. This porous structure provides a high specific surface area, typically ranging between 200 and 500 m²/g. Thanks to this feature, biochar exhibits excellent adsorption capacity and effectively contributes to water and nutrient retention in the soil.

b) Rich content of functional groups:

The surface of biochar is covered with various functional groups, such as hydroxyl and carboxyl. These offer multiple active sites for chemical interactions with minerals, microorganisms, or organic matter, thereby enhancing biochar's ability to adsorb beneficial substances.

c) Remarkable stability and durability:

The carbon in biochar is primarily present in stable aromatic forms, giving it high chemical and thermal resistance. Due to this stability, biochar degrades very slowly in the environment and can remain active in the soil for hundreds of years.

Biochar is a carbon-rich material obtained through the pyrolysis of biomass, such as wood, agricultural waste, or other plant residues. Biochar production equipment ensures that the pyrolysis process takes place at high temperatures and in the absence of oxygen. This production method gives biochar a series of distinct properties:

MATERIALS AND METHODS

In general, biochar can be applied to soil through several methods, each with specific characteristics and benefits. One of the simplest approaches is direct application, where biochar is spread on the soil and mechanically incorporated. However, the effectiveness of this method can vary depending on soil type and the crop to be planted. A frequently used alternative is mixing biochar with mature compost (*Agegnehu et al., 2016*), which allows for better homogenization and distribution of nutrients. However, the most effective method, according to recent studies, is composting biochar—a complex biological process in which biochar is integrated into a mix of organic materials (plant residues, manure, green waste, etc.) and subjected to controlled fermentation. In this context, biochar not only acts as a physical support for microbial colonies (*Liu et al., 2024*), but also actively participates in the transformation of organic matter. This interaction enhances humification and mineralization processes, helps stabilize pH, reduces phytotoxic compounds, and increases the accumulation of available nutrients (nitrogen, phosphorus, potassium). Composting also improves the water and nutrient retention capacity of biochar, increasing its efficiency in the soil and ensuring a slow, sustained release of nutrients needed by plants. Thus, composted biochar becomes a complex soil amendment (*Zhang et al., 2025*) with higher agronomic value than other application forms.

The application of biochar to soil is closely linked to the stages of agricultural land preparation, since the efficiency of this amendment largely depends on proper integration into the active soil profile. The most suitable periods for application are autumn, immediately after harvest, and spring, before sowing, as these are the typical times for basic mechanical works such as plowing, disking, or rotary tilling, which allow for deep and uniform incorporation of the material.

Autumn application offers several advantages. After harvest, the soil remains bare until the next crop cycle, providing a time window in which biochar can be applied without interfering with plants. Moreover, biochar has time to interact with the soil and undergo an “activation” process—that is, the absorption of nutrients and colonization by beneficial microorganisms—before the next growing season begins. This “maturation” period in the soil enhances the efficiency of biochar in improving soil structure, water retention, and nutrient availability.

Spring application, before sowing, is also a viable option, especially when a rapid response is desired during the growing season. In this case, it is important for the biochar to be well incorporated before the crop is established to avoid losses through wind or overexposure to sunlight, as well as to prevent possible temporary nutrient lock-up (the so-called “initial adsorption effect”). Therefore, combining biochar with compost or natural fertilizers is often recommended, particularly in spring.

In both cases, synchronizing biochar application with already planned mechanical operations reduces additional costs and minimizes soil disturbance. Thus, biochar becomes an integral part of the agricultural system, contributing sustainably to the long-term improvement of soil fertility.

The amount of biochar applied depends on several factors, including soil type, crop needs, current soil condition, and agronomic goals. Typically, the quantity is expressed in tons of biochar per hectare (t/ha), and recommendations vary between 5 and 20 t/ha depending on each specific situation.

Optimal quantity for carbon-poor soils

In soils with low organic matter or degraded conditions, an application of 10–20 t/ha of biochar is recommended. This helps improve soil structure, increase water retention and aeration, and support the development of beneficial microorganisms. Carbon-poor soils benefit the most from biochar, as it provides stable carbon that remains available long-term.

If the soil is already fertile and well-balanced in terms of organic matter, the amount of biochar can be reduced to 5–10 t/ha. Application at this rate will contribute more to nutrient stabilization and soil structure improvement without risking carbon oversaturation. In such cases, biochar can be used primarily as an amendment to enhance water retention and optimize nutrient availability during drought periods.

In some situations, biochar can be applied in combination with other soil amendments such as compost or organic fertilizers. These combinations enhance the benefits of biochar by increasing nutrient availability and supporting soil microbiology. For example, a combined application of 5–10 t/ha of biochar and 20–30 t/ha of compost can be effective in boosting microbial activity and improving soil structure.

It is important to monitor the impact of biochar application on soil and crops to adjust the amount based on the results. For instance, if biochar effects are visible within one year but not sufficiently strong, the amount can be increased in subsequent years. On the other hand, if the soil becomes too rich in carbon or if nutrient imbalances occur, future applications can be reduced.

The depth at which biochar is applied is a key factor that directly influences its efficiency in the soil. To obtain maximum benefits, biochar must be incorporated into the active soil layer, where biological activity is highest and plant roots develop most effectively. Generally, this zone corresponds to the top 10–30 cm of soil, depending on the crop type and farming system used.

For annual crops (wheat, corn, (*Wijitkosum et al., 2025*), soybeans, etc.), the optimal incorporation depth is 15–25 cm, as the roots of these plants mainly develop in the upper layer. Incorporation at this depth allows biochar to improve soil structure, increase water retention, and regulate nutrient availability precisely where plants need it.

For perennial crops or fruit trees, a deeper or localized application around the root zone is recommended—down to 30–40 cm—to directly influence the mature root absorption area. In such cases, biochar can be introduced either through pits or fertilization bands.

Too shallow an application (0–5 cm) may lead to wind erosion losses, especially in light soils or arid zones, and reduces contact with soil microorganisms. Conversely, incorporation that is too deep (>40 cm) may reduce effectiveness, as the biochar no longer interacts efficiently with plant roots and the biologically active layer.

Modern application techniques, such as plowing, rotary tilling, or strip tillage, enable precise and uniform incorporation of biochar at the desired depth. This ensures optimal distribution and effective interaction between biochar, soil, and plants.

Particle size and feedstock type are essential factors influencing the interaction of biochar with soil and plants, determining its efficiency and long-term benefits. In terms of particle size, this affects the dynamics of biochemical and physical reactions in the soil. Fine biochar (under 2 mm) has a large specific surface area, meaning higher chemical reactivity. It promotes fast biochemical reactions, improves microbial activity in the soil, and has a significant impact on nutrient availability and water retention. Due to its smaller particles, fine biochar may be more effective in stimulating biological activity and enhancing the soil's capacity to support microbial life.

In contrast, coarse biochar (2–10 mm) offers greater porosity, contributing to the improvement of physical soil structure (Glaser et al., 2002). It is not as chemically reactive but helps improve soil aeration and prevent compaction. Thanks to its larger particle size, coarse biochar provides longer durability in soil, being more stable over time, and can be useful in areas where maintaining a stable soil structure long-term is desired.

The type of feedstock used to produce biochar also influences its physico-chemical properties, stability, and biodegradability. Biochar made from hardwood (such as beech or oak) is chemically more stable and has higher durability in the soil, as it decomposes much more slowly than other types of biochar. This makes it ideal for long-term soil structure improvement and carbon stabilization in the soil, providing lasting impact. Hardwood biochar is low in nutrients at production but contributes to improved physical structure and soil stability, often used in organic farming where long-term stability is essential.

On the other hand, biochar made from plant residues (such as straw or corn stover) is richer in nutrients and more biodegradable. It decomposes faster in the soil, meaning it supplies nutrients more quickly and supports rapid plant growth. Plant-residue biochar significantly contributes to microbial activity

and improves nutrient availability for plants, although it has lower durability than hardwood biochar. This type is useful in soils requiring a quick nutrient supply and where an immediate impact on soil fertility is desired.

Choosing between fine or coarse biochar, and between hardwood or plant-residue biochar, depends on agronomic goals, soil type, and crop needs. Combining these characteristics can optimize the benefits of biochar according to the specific conditions of each farm.

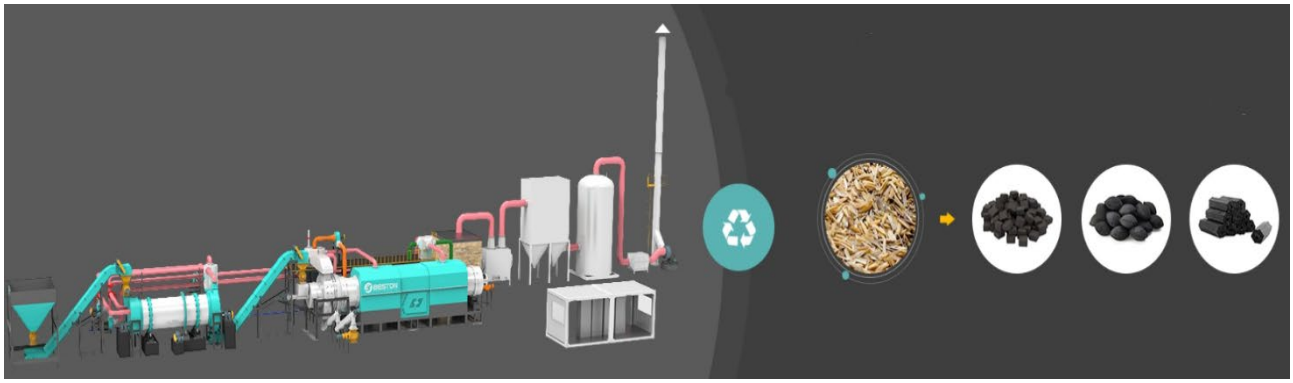

Fig. 2 - Rice husk biochar production machine

(https://www.bestongroup.com/ro/charcoal-making-machine/rice-husk/)

The rice husk carbonization machine (Fig. 2) provides an efficient and sustainable solution for the valorization of agricultural biomass waste. Over time, the rice industry has faced challenges regarding the optimal use of rice husks. Today, thanks to carbonization technology, these plant residues can be transformed into biochar, a valuable product with multiple uses. Thus, the process not only increases the economic value of this agricultural by-product but also opens up new income opportunities for the rice industry while supporting sustainable farming practices.

Sawdust biochar production machine

The sawdust biochar production machine converts sawdust into high-quality charcoal through pyrolysis technology. It offers an efficient solution for waste disposal in the wood processing industry. This sawdust charcoal has wide applications in industry, agriculture, and other sectors, presenting profitable prospects for investors.

Wood biochar production machine

The wood biochar production machine provides an effective solution for the disposal of wood waste generated by the forestry and wood processing industries. Using high-temperature pyrolysis technology under low-oxygen conditions, it transforms wood residues into high-value charcoal. The entire process is environmentally friendly, ensuring minimal environmental impact. There is also the coconut shell charcoal machine, an efficient solution for recycling coconut shell waste.

Fig. 3 - Palm kernel shell biochar production machine

(https://www.bestongroup.com/ro/charcoal-making-machine/palm-kernel-shell/)

The palm kernel shell biochar production machine is gaining increasing popularity in the market (Fig.3). Using pyrolysis technology, this equipment efficiently transforms palm kernel shells into high-value

charcoal. Due to the high demand and multiple uses of this type of charcoal, investing in such equipment can bring considerable profits.

Fig. 4 - Bamboo biochar production machine
(https://www.bestongroup.com/ro/charcoal-making-machine/bamboo/)

The Beston bamboo charcoal production machine efficiently transforms bamboo into valuable charcoal (Fig. 4). Similar to that obtained from wood or coconut shells, bamboo charcoal has multiple uses and a considerable market value.

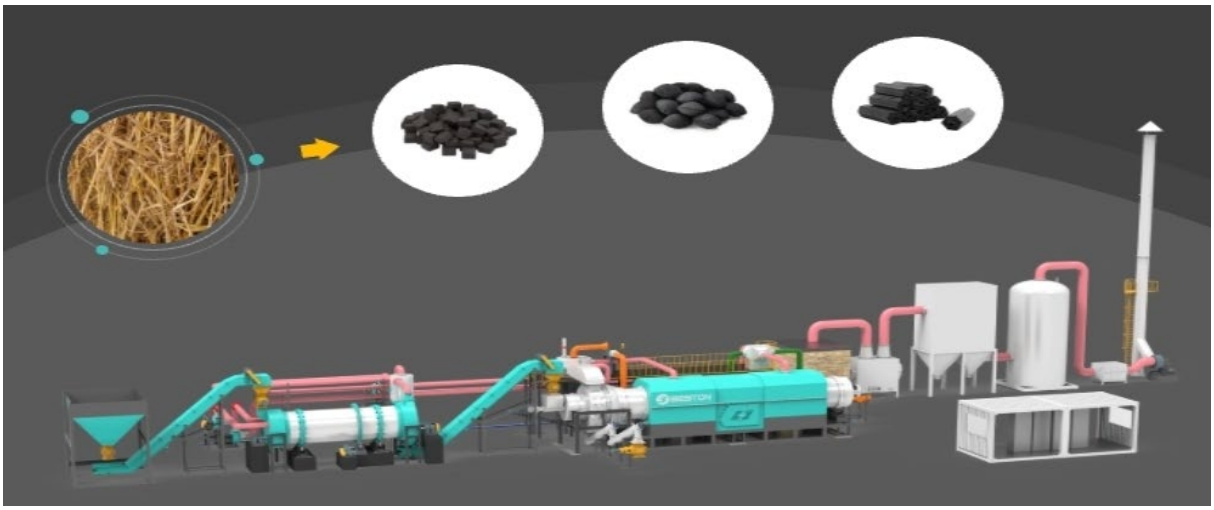

Fig. 5 - Straw biochar production machine
(https://www.bestongroup.com/ro/charcoal-making-machine/straw/amp/)

The straw charcoal production machine is designed to convert agricultural waste, such as straw, into valuable biochar using pyrolysis technology (Fig. 5). This equipment represents an efficient solution for the sustainable management of waste and resource utilization, bringing both economic advantages and environmental benefits. Continue reading to discover the main features of this straw charcoal production machine.

Application Technologies:

Efficient application of biochar to the soil requires the use of adapted equipment to ensure uniform distribution, proper incorporation, and integration into the active soil profile. The choice of the right technology depends on the form of the biochar (granulation, moisture), the type of crop, the soil texture, and the timing of application. In practice, a range of modern agricultural machinery is used, as follows:

1 Solid Fertilizer Distributors: These machines are essential for the uniform distribution of biochar over the land surface. They can be tractor-mounted or self-propelled and are adjustable depending on the desired amount (5–20 t/ha). Modern distributors allow for flow regulation and controlled coverage of areas, reducing losses and ensuring homogeneous application. They are particularly effective in the pre-application phase, before mechanical incorporation.

2 Disc Harrows and Rotary Tillers: After application, biochar must be incorporated into the soil to prevent losses due to wind or leaching. Disc harrows or rotary tillers are used for shallow mixing (10–20 cm), promoting contact with the rhizosphere. Rotary tillers are especially useful in light soils or sensitive crops, where fine and uniform tillage is required.

3 Multifunctional Seeders (Double Reservoir Seeders or "Strip-Till" Systems): In modern agricultural technologies, some seeders are equipped with double reservoirs that allow simultaneous application of seeds and biochar, either in bands (banding) or at row level. This system optimizes space and resources, ensuring localized application closer to the plant's area of interest. These machines are particularly useful in precision farming and conservation systems.

4 Subsoilers and Plows for Deep Tillage: In compacted or poorly developed soils, deep soil preparation is required. Subsoilers allow loosening at depths of 30–40 cm, promoting the penetration of biochar and water, as well as root development across an extended profile. Classic plows (for autumn plowing) ensure the turning of the furrow and are useful for integrating biochar into deeper soil layers, providing good results in traditional agricultural systems.

The choice of application technology should align with the agronomic goal, type of biochar, and pedoclimatic conditions. Integrating these technologies into a sustainable fertilization plan helps maximize the benefits of biochar and increase long-term yield.

RESULTS

The type of raw material used to produce biochar not only influences its physical and chemical characteristics but also its durability, stability, and nutritional composition. Biochar can be produced from a variety of sources, including wood, plant residues, or even organic waste, and each type has its specific advantages and characteristics:

Hardwood Biochar (beech, oak, etc.)

Biochar produced from hardwood is characterized by higher chemical stability and greater durability in the soil. It decomposes much more slowly than biochar derived from more easily biodegradable plant sources, making it ideal for improving soil structure in the long term. Hardwood biochar is nutrient-depleted during production but can be useful in soils that do not require a large amount of additional nutrients, being particularly effective in stabilizing carbon in the soil. This type of biochar is preferred in organic farming, where long-term stability is a priority.

Biochar from Plant Residues (straw, corn residues, grass, etc.)

Unlike hardwood biochar, biochar derived from plant residues is generally richer in nutrients, often being a valuable source of nitrogen, phosphorus, and potassium. This biochar is more biodegradable, with a shorter decomposition time in the soil, and can significantly contribute to nutrient supply for plants, especially in the early growth stages. It is ideal for soils that need additional nutrient supplementation and for applications where rapid replenishment of nutrient reserves is desired. Additionally, plant residue biochar helps improve microbial activity and soil structure, but with lower durability compared to hardwood biochar.

Choosing the Right Biochar Type Based on Soil and Crop Needs

For efficient use of biochar, the selection of raw material type and granulation should be made based on the soil characteristics and the specific requirements of the crop. For example, in soils that require long-term improvement of physical structure and high stability, hardwood biochar with coarse granulation may be the most suitable choice. On the other hand, for soils that benefit from rapid fertilization and quick plant growth, plant residue biochar with fine granulation may be the ideal option.

The use of biochar in agriculture has demonstrated clear benefits for soil fertility and plant development, according to an increasing number of experimental studies. In a study conducted on Luvisol and Fluvisol soils, the application of biochar led to significant increases in the biomass of lettuce plants. It was observed that when biochar was integrated into the soil together with compost, whether pre-composted or not, the effects were clearly positive: biomass increased up to six times in some variants. This development clearly highlights the potential of biochar to support plant productivity (Jeffery et al., 2011), and combinations with other organic amendments can amplify results, without its effectiveness depending solely on additional pre-treatments.

Another consistent result observed in biochar applications is the increase in soil pH values. This effect is particularly valuable in acidic soils, where biochar helps reduce acidity and improve nutrient absorption conditions for plants. Along with this change in soil pH, better mobilization of macro- and

micronutrients, such as phosphorus, potassium, or calcium, has been noted, leading to a more favorable environment for plant growth.

Additionally, the dissolved organic carbon and total nitrogen content increased significantly in soils amended with biochar, indicating an improvement in the natural cycles of organic matter and better biological functioning of the soil. These effects are particularly important in degraded or nutrient-poor soils, where biochar can act as a catalyst for regeneration. By retaining nutrients and providing a stable, porous structure, biochar supports microbial activity and helps form a balanced trophic network in the soil.

Interaction with soil organisms is another crucial aspect. It has been observed that biochar stimulates the activity of microorganisms involved in essential processes such as atmospheric nitrogen fixation, organic matter decomposition, or the formation of stable soil aggregates. By providing a protective and stable physical habitat, biochar supports microbial biodiversity and, implicitly, the efficient functioning of the soil ecosystem.

The results support the idea that biochar, as an organic amendment with unique properties, brings significant improvements to soil structure, chemical composition, and biological activity. These effects are visible both in intensive farming contexts and in ecological restoration systems, especially in soils with low fertility or under stress. Therefore, biochar proves to be a valuable tool for the sustainable increase in agricultural productivity and for restoring the natural capacity of soils to support plant life.

Optimal application dose:

$$D = (K \times (1 + Fs)) / T \quad (1)$$

where:

D = recommended dose (t/ha)

K = amendment coefficient (generally between 10–20)

Fs = soil fertility factor (0 – fertile soil; 1 – poor soil)

T = texture index (1 for sandy, 2 for loamy, 3 for clayey)

For a clearer understanding of how biochar can be applied to soil, two relevant tables are presented below:

Table 1 provides a comparison of the main biochar application methods, highlighting the advantages and disadvantages of each option. Table 2 presents the recommended biochar application rates, depending on crop type and soil texture, in order to maximize its effectiveness.

Table 1

Comparison of biochar application methods

Application Method	Main Advantages	Disadvantages	Estimated Efficiency (%)
Simple Biochar	Easy to apply, stable material	Slow impact, risk of phytotoxicity	40–60%
Mixed with Compost	Easy to apply, nutrient supply	Limited microbial activity	60–80%
Composted Biochar	High biological activity, pH balance	Requires time and space for composting	80–95%

Table 2

Recommended biochar dose based on crop and soil texture

Crop	Soil Texture	Recommended Granulation	Dose (t/ha)	Application Period
Wheat	Loamy	< 2 mm	10–15	Autumn
Corn	Clayey	< 2 mm	15–20	Spring
Grapevine	Loamy-clayey	2–10 mm	5–10	Autumn
Vegetables (various)	Sandy	< 2 mm	10–20	Spring

CONCLUSIONS

The application of biochar to soil represents a promising strategy for sustainable agriculture, especially in the current context of climate change and depletion of natural resources. Its versatility, combined with the proven effectiveness of the composted form, provides a valuable alternative to traditional amendments. To maximize the benefits, it is essential to adapt the application technique to the local specifics: soil texture, crop type, available equipment, and climatic conditions. Additionally, integrating biochar into good agricultural practices, supported by public policies, subsidies, and farmer

training programs, is crucial. Biochar can become a key factor in the transition to a circular, ecological, and resilient agriculture capable of meeting the challenges of the future.

ACKNOWLEDGEMENT

This work was funded by the Ministry of Research, Innovation and Digitalization, within the NUCLEU Program, through Project 9N/ 01.01.2023 "Technology for valorization of plant residues in the form of biochar for improving soil quality" and by the Ministry of Agriculture and Rural Development (MADR), ADER Program - Contract ADER 25.3.1/20.07.2023 "Technology for valorization of poultry manure by obtaining biofertilizers rich in phosphorus".

BIBLIOGRAPHY

[1] Agegnehu, G., Bass, A.M., Nelson, P.N., Bird, M.I., (2016) Benefits of biochar, compost and biochar compost for soil quality, maize yield and greenhouse gas emissions in a tropical agricultural soil, Science of the Total Environment, 543, pp. 295–306, https://doi.org/10.1016/j.scitotenv.2015.11.054

[2] Biederman, L.A., Harpole, W.S., (2013) Biochar and its effects on plant productivity and nutrient cycling: A meta-analysis, GCB Bioenergy, 5(2), pp. 202–214, https://doi.org/10.1111/gcbb.12037

[3] Bruun, E.W., Ambus, P., Egsgaard, H., Hauggaard-Nielsen, H., (2012) Effects of slow and fast pyrolysis biochar on soil C and N turnover dynamics, Soil Biology and Biochemistry, 46, pp. 73–79, https://doi.org/10.1016/j.soilbio.2011.11.019

[4] Chen, X., Zhang, Y., Liu, H., Wang, J., Li, Z., (2024) A global assessment of the long-term effects of biochar application on crop yield, Science of The Total Environment, 902, 170007, https://www.sciencedirect.com/science/article/pii/S2666049024000070

[5] Glaser, B., Lehmann, J., Zech, W., (2002) Ameliorating physical and chemical properties of highly weathered soils in the tropics with charcoal – a review, Biology and Fertility of Soils, 35(4), pp. 219–230, https://doi.org/10.1007/s00374-002-0466-4

[6] Huang, M., Zhang, Y., Thompson, L., Wang, H., (2023) Effect of biochar application on corn and soybean yield in Michigan, Crop, Forage & Turfgrass Management, 9(1), e20245, https://acsess.onlinelibrary.wiley.com/doi/full/10.1002/cft2.20245

[7] Jeffery, S., Verheijen, F.G.A., van der Velde, M., Bastos, A.C., (2011) A quantitative review of the effects of biochar application to soils on crop productivity using meta-analysis, Agriculture, Ecosystems & Environment, 144(1), pp. 175–187, https://doi.org/10.1016/j.agee.2011.08.015

[8] Kumar, A., Ren, W., Tao, H., Tao, B., (2025) Biochar and microbe synergy: A path to climate-smart farming, Phys.org, https://phys.org/news/2025-03-biochar-microbe-synergy-path-climate.html

[9] Li, X., Wu, D., Liu, X., Huang, Y., Cai, A., Xu, H., Ran, J., Xiao, J., Zhang, W., (2024) A global dataset of biochar application effects on crop yield, soil properties, and greenhouse gas emissions, Scientific Data, 11, Article 57, https://doi.org/10.1038/s41597-023-02867-9

[10] Liu, Y., Zhao, W., Wang, X., Chen, J., Li, Q., (2024) Effects of biochar and compost on the abundant and rare microbial communities in soil, Environmental Pollution, 337, 121718, https://www.sciencedirect.com/science/article/abs/pii/S0269749124017184

[11] Schmidt, H.-P., Pandit, B.H., Martinsen, V., Cornelissen, G., Conte, P., Kammann, C.I., Singh, B.P., (2021) Fourfold increase in pumpkin yield in response to biochar–organic nutrient treatment on degraded, sandy soil, Journal of Plant Nutrition and Soil Science, 184(3), pp. 432–441, https://doi.org/10.1002/jpln.202000190

[12] Singh, B.P., Kammann, C.I., Glaser, B., Cowie, A., Lehmann, J., (2023) Advances and prospects of biochar in improving soil fertility, carbon sequestration, and mitigating climate change, Frontiers in Environmental Science, 11, 1114752, https://www.frontiersin.org/articles/10.3389/fenvs.2023.1114752/full

[13] Sohi, S.P., Krull, E., Lopez-Capel, E., Bol, R., (2010) A review of biochar and its use and function in soil, Advances in Agronomy, 105, pp. 47–82, https://doi.org/10.1016/S0065-2113(10)05002-9

[14] Wang, H., Liu, D., Chen, L., Xu, M., Zhang, X., (2024) Biochar-induced changes in soil microbial communities, Environmental Microbiome, 19, Article 31, https://environmentalmicrobiome.biomedcentral.com/articles/10.1186/s40793-024-00631-z

[15] Wijitkosum, S., Rungskunroch, P., Suksawang, T., (2025) Biochar and compost sustain soil fertility and maize yield for five crop cycles, Emerging Science Journal,

https://biochartoday.com/2025/01/29/biochar-and-compost-sustain-soil-fertility-and-maize-yield-for-five-crop-cycles/
[16] Zhang, Y., Zhou, D., Chen, X., Liu, Q., Zhao, Y., (2025) Biochar as a soil amendment: Implications for soil health, carbon sequestration, and sustainable agriculture, Environmental Science and Pollution Research, https://link.springer.com/article/10.1007/s44378-025-00041-8
[17] Zhao, L., Sun, J., Feng, X., Wang, H., Liu, Y., (2025) Enhancing soil fertility through biochar using slaughter-house waste, Scientific Reports, 15, 95558, https://www.nature.com/articles/s41598-025-95558-
[18] *** https://www.bestongroup.com/ro/industry-news/biochar-use-in-agriculture-and-farming/
[19] *** https://bestonmachinery.com/ro/industry-news/use-biochar-in-agriculture/
[20] ***https://www.businessagricol.ro/biocharul-parte-a-economiei-circulare-solutie-ideala-de-transformare-a-deseurilor-organice/
[21] ***https://stratos.ro/blog-biochar-sau-carbunele-vegetal-un-produs-ideal-pentru-practicile-agricole-sustenabile/
[22] *** https://www.bestongroup.com/ro/charcoal-making-machine/rice-husk/
[23] *** https://www.bestongroup.com/ro/charcoal-making-machine/palm-kernel-shell/
[24] *** https://www.bestongroup.com/ro/charcoal-making-machine/bamboo/
[25] *** https://www.bestongroup.com/ro/charcoal-making-machine/straw/amp/
[26] *** https://www.bestongroup.com/ro/biochar-production-equipment/amp/

ANALYSIS OF INTERNATIONAL STANDARDS THAT CERTIFAY THE PRODUCTS QUALITY OF PYROLYSIS PROCESS- REVIEW

/

ANALIZA STANDARDELOR INTERNAȚIONALE CARE CERTIFICA CALITATEA PRODUSELOR OBȚINUTE DIN PROCESUL DE PIROLIZĂ

Alexandra-Liana VIȘAN*, Vasilica ŞTEFAN, Alin HARABAGIU, Radu CIUPERCĂ, Ana ZAICA
National Institute of Research - Development for Machines and Installations Designed to Agriculture and Food Industry - INMA Bucharest / Romania
**Tel: 0724 697 550; *E-mail: alexandrion1982@yahoo.com*

Keywords: *biochar standard, quality, test, certification, capitalization, fertilizer, crop stimulation.*

ABSTRACT

In this paper, are presented some international merchet regulation concerning the bio-char quality certification, so the buyer to have all the necessary information's to apply in safety the pyrolysis products according to: crop type (vegetables, horticulture, pomiculture, etc.); the food category resulted (ecologic, bio, chemical treated, etc.), soil quality, costs, sustainability, conversion, etc. Taking in to consideration, the grate number of pyrolysis technologies on market, the variety of the installations studied in scientific literature that obtain bio-char from a large category of by-products and organic wastes (straw, sawdust, farm manure, food industry waste, etc.), it is necessary that the material obtained to be compliance with quality standards or regulations, so that the buyer/user/reader to have all the correct information's so to be able to adopt the correct technology for the crop and environmental factors and streamline production costs. An important direction in agricultural scientific literature the study of biochar-based fertilizers is known as Slow-Release Fertilizers (SRFs), and is seen as an effective and ecologically approach to advancing sustainable agriculture. Nowadays, experimental fields are established to prove and develop adaptive efficient technology, in accordance with soil and environmental specifications, to improved crop growth and quality.

REZUMAT

În această lucrare se prezintă câteva reglementări ale pieței internaționale privind certificarea bio-cărbunelui de calitate, astfel încât cumpărătorul să aibă toate informațiile necesare pentru a aplica produsele din procesele de piroliză în siguranță și în conformitate cu: tipul culturii (legumicole, floricole, pomicole, etc.); de categoria produselor alimentare rezultate (ecologică, bio, conversie sau tratate chimic) și de calitatea solului, etc. Având în vedere faptul că, există pe piață un număr important de instalațiile de piroliză prezente pe piață, iar în literatura de specialitate sunt studiate variate care produc bio-cărbune din diferite materii secundare sau deșeuri organice (paie, rumeguș, dejecții din ferme, deșeuri din industria alimentară, etc.), este necesar ca materialul obținut să fie în conformitate cu standarde sau reglementări de calitate, pentru ca cumpărătorul/utilizatorul/cititorul să amibe toate datele pentru foi capabil să adopte tehnologia corecta la cultura si al factorii de mediu si sa eficientizeze costurile de producție. O direcție importantă în literatura științifică agricolă o reprezintă fertilizanții bio-cărbune, cunoscuți ca fertilizanți lenți (SRF), care reprezintă o abordare eficienta si ecologica către agricultura sustenabilă. Actualmente, câmpuri experimentale sunt înființate pentru a dovedi și dezvolta tehnologi eficiente si adaptive, la condițiile de sol si de mediu, pentru a crește dezvoltarea si calitatea culturilor.

INTRODUCTION

Scientists from agriculture and soil nutritional improvement, are working to determine some dedicated administration of SRFs technologies to achieve slow release. During research activities it was observed it is a limited available literature on biochar-based SRFs and nano SRFs. More then this the bio-char sample preparation, analysis methodology and test result are made using different devices, measurement equipment's and without mentioning the methodology used.

So, doing so, the results are difficult to replicate and hard to integrate in a dedicated sustainable agriculture technology. For this reason, was needed to implement standards and specific regulations as: Word Certification and International Carbon Standards, European Union (EN), and China standard (GB), have collectively classified these types of fertilizers as SRFs. *(Divyangkumar N., Panwar N.L, 2024).*

The certification system influences the commercial value and utilization of biochar, are set in standards set and guidelines by the European Biochar Certificate Standard (EBC-version 10.5E), World Biochar Certificate (WBC-version 1.1), International Biochar Initiative (IBI), and the Biochar Quality Mandate (BQM) (*Camps-Arbestain, M., Amonette, J.E., Singh, B.,2015, H.-P. Schmidt, 2012)* an intuitive diagram is presented by (*Liu Q., Meki K.,. Zheng H, et. Al, 2022*).

Furthermore, same of the EU patterns, such as: Germany, China, Switzerland, Austria, and Italy, have incorporated biochar into their respective national regulations concerning fertilizers, soil additives, and composts (*Meyer, S., Genesio, L., Vogel, I., et al, 2017*).

Also, Romania has some regulations regarding fertilizer administration but, this documentation must by applied cheerfully in accordance with field agroclimatic specifications and crop needs, so to protect the near fauna and flora, but also to prevent unpredictable environmental damage.

1. ***The International Biochar Initiative (IBI)*** has the main role to established guidelines and standards, in which are define dedicated testing procedures to produce biochar. The aim is to provide stakeholders and commercial entities, a clear framework to identifying biochar's specific qualities and properties. Also, aims to implement the IBI Biochar Certification Program so needed for biochar producers. A large category of byproducts and vegetal /animal waste are considerate feedstocks through diverse thermochemical conversion processes, resulting in various characteristics, only those that have more than 10 % (w%) of organic carbon (C_{org}). These standards classify biochar materials into three main properties: part A - tests for fundamental functional properties (mandatory for all biochar); part B – tests for toxicant evaluation; and part C - test for advanced evaluation and soil improvement properties. The latest version 10.5E of the IBI, include also a part for pyrolysis heat recovery that is suggested to be used to dray the feedstock or as a radiant heating agent in industrial hall of homes in vicinity, that part was necessary to be added in order to improve pyrolysis energetic balance. Another important part is to reintroduce slow pyrolysis generation gases in the reactor, after were extracted the humidity and tar fraction. Consulting the feedstock source table, we so that the poultry litter, is mentioned as a high environmental pollution source, so the handling installations and operators must comply with complex regulation, especially regarding the breading masks.

2. ***The European Biochar Certificate EBC*** are optional industrial standard in Europe and Switzerland however, it is compulsory for the utilization of biochar in agriculture. In this document the Biochar is categorizes into six classes: "Feed", "Agro-Organic", "Agro", "Urban", "Consumer Materials", and "Basic Materials". The EBC guidelines specific that, a biochar must have a C_{org} content of more than 50% (w%). In Annexes are ISO and regional regulation listed methods as: ISO 13909-4 and DIN 51701-3 - for sample preparation; DIN EN ISO 17828- bulk density; DIN ISO 11265- salinity; DIN ISO 10390- pH evaluation; ISO 589 and DIN 51718 - humidity; ISO 1171 and DIN 51719 – ash content 550 °C; ISO 925 and DIN 51726 – carbonate CO_2; ISO 29541 and DIN 51732 – CHN content; ISO 19579 and DIN 51724-3 – Sulphur content; ISO 17247 and DIN 51733 – Oxygen content; DIN EN 17503 – PAH content; EN ISO 12846, DIN 22022-1, DIN 22022-7, DIN EN ISO 17294-2 / DIN EN 1483 - trace metals after microwave-assisted digestion (Pb, Cd, Cu, Ni, Hg, Zn, Cr, B, Mn, As, Ag); ISO 23380, DIN 51729-11, DIN EN ISO 11885 / DIN EN ISO 17294-2 – nutrient content (P, Mg, Ca, K, Na, Fe, Si, S); DIN EN ISO 14238 – water holding capacity; DIN EN 15763- trace metals (As, Pb, Cd, Hg); etc. An important, for our research domain is that poultry litter is not mentioned, and can be integrated in “Animal by-products feedstock” (AB02) or “other animal by-products” (AB03), from the legal point of view in bought categories, the feedstock must have passed an end-point according to Commission Delegated Regulation (EC) 2023/1605.

An older British standard/Dansk Standard/European Standard (DS/EN 13266:2001) which is referring to “Slow-release fertilizers-Determination of the release of the nutrients-Method for coated fertilizer” (2001), was adopted by British Standard (BS confirmed in 2011) - It is focuses on coated SRFs, another technological trend based on the biochar structure and capacity. So, a SRF must comply the next requirements: 1) > 15 % of a nutrient released in 24 h; 2) > 75 % of a nutrient released in 28 days; 3) at least 75 % of a nutrient released at the stated release time. (*Duan, Q., Jiang, S., Chen, F., et all., 2023*)

3. The BS ISO 19670:2017 promulgated the Fertilizer and soil conditioners-Solid urea aldehyde slow-release fertilizer-General requirements." – this document is dedicated solubility urea-based fertilizers, because in bought cases present limited nitrogen nutrients (terms defined: urea aldehyde slow-release fertilizer; cold water insoluble and soluble nitrogen; hot water insoluble and soluble nitrogen). The standard requirements presented in this standard are: (1) visual inspection (shall be in powder, granules, prills, pellets, pastilles, chips, or other solid forms); (2) nitrogen content in the urea-based SRF (total nitrogen > 28% and 36 % formaldehyde/methylene and IBDU/CDU urea fertilizer respectively). The base term was prior defined in ISO 8157:2015, Fertilizers and soil conditioners — Vocabulary. The standard also detail describes the sample preparation and measurement methods. Also, in 2017 was promulgated BS ISO 21263:2017 "Slow-release fertilizers-Determination of the release of the nutrients-Method for coated fertilizers." (*Duan, Q., Jiang, S., Chen, F., et all., 2023*).

4. The Chinese government recently introduced a standard for complex compound fertilizers GB 15063–2001 revised in 2009, and after that supersede by GB/T 15063-2020 Compound fertilizer. As in the other standards here are presented, dedicated terms and complex fertilizers definitions, bulk blending fertilizer, organic-inorganic com-pound fertilizer, primary nutrients, the second element, trace elements, and formula. Requirements of the Standard include: 1 - visual inspection (powder, granules, prills, pellets, pastilles, chips, or other solid forms without any hard particles); 2 - nitrogen content in the urea-based SRF, classified as three grades: high concentration (total nutrients > 40), medium concentration (total nutrients > 30), and low concentration (total nutrients > 25); 3 - particle size is between 1.00 and 4.75 mm; 4- moisture content for high, medium and low concentration samples are < 2.0 %, 2.5 % and 4.0 % respectively. More than this, the Chinese Agricultural Standard promulgated in NY/T 2267–2012, 2016 "Slow-release fertilizers-General Regulation", the terms/definitions and regulations are much more detailed and refers to the most important nutrient release compounds in slow-release fertilizer, as N, P, and K, respectively: percentage; nutrient release ratio (initial and cumulative using GB/T 22923-2008 Determination of nitrogen, phosphorus and potassium for fertilizers by auto analyzer); nutrients release period/point (GB/T 22924-2008 Determination of biuret content for compound fertilizers) complex fertilizers; etc. Also, an important standard is HG/T 2843-1997 named "Chemical fertilizer Products-standard volumetric, standard, reagent and indicator solutions for chemical analysis". The regulations are made only for N, P, and K fertilizers; the raw materials (must meet the safety requirement, including decomposed chemicals after application); the fertilizer content (N > 30% for urea-based, P > 12 % and K >60 % for compound or complex fertilizers); and release ratio (first in 24 hours <15 %, cumulative release in 28 days <60%, and marked total release time for N). Along with this, China has also promulgated Agricultural Standard for evaluation regulations, NY/T 2274–2012 "Slow-Release Fertilizers-Regulations of efficiency experiment and assessment". This regulation has provided detailed requirements and conditions for evaluating the SRFs, like: General chapter in which is described fertilizing amount, method, crop conditions and its growth period (at least 3 months); Experimental design chapter in which all the results are compared with: a) no fertilizer field, b) regular fertilizing, c) equal nutrients as regular fertilizing, and d) 20% less nutrient content than regular fertilizer. Land size parameter is classified as: a) small trial: 20–30 m^2 for high-density crops (wheat and barley, etc.), and 40–50 m^2 for low-density crops (corn, cotton and tobacco, etc.); b) land trial > 3000 m^2 for economic plans and > 10,000 m^2 for agriculture corps. (*Duan, Q., Jiang, S., Chen, F., et all., 2023).*

The synergy between IBC and EBC standards, in this years, it is noted, because were made efforts to unify the holistic overview, and to combine the researchers efforts to set the proper testing and sapling methodology in order to achieve an biochar's classification into five types, based on their soil potential benefits, as: carbon storage; fertilizer value; liming potential; particle-size classes; use in potting mixes and soilless agriculture.

Also the necessity to add the information's regarding the: feedstock source-provenance, production methods-pyrolysis equipment/installation type; quality control based on commune view of testing and presenting the data (IBI, EBC, BQM, or national laws and regulations), was identified in practical research papers published, but also on: biochar technological viability, possibilities for expansion, expenses, long-term carbon storage, verification and monitoring, and the advantages of its application to different carbon reservoirs (*Fawzy, S., Osman, A.I., Mehta, N., et al., 2022*), economic and environmental impact..

Also, the biochar standards treaties subjects such as: biochar quality, limits for organic contaminants; heavy metals in the environment; specifications regarding feedstock manipulation and storage conditions; transit distance, installation energy efficiency, heat recovery system and manufacturing technique. But, in presented international standards/guidelines, are not specify the soil biochar application rules and rates – direction in which are made efforts substantial efforts to make a same models and methodologies.

For example, a specific case study was conducted, on saline soils having high salinity (more than 4 dS/m), respectively high electrical conductivity (EC). This soils typically leads to osmotic plant and microorganisms stress (*Kotula, L., Caparros P.G, Zörb, C., Colmer, et all., 2020).*

The experts, advise to choose biochar with highest nutrient content and a low liming rate (CaCO3-eq < 1%) to minimize the introduction of extra salts while enhancing the primary productivity of the soil. In the case of saline-sodic soil or sodic soil with an exchangeable sodium percentage (ESP) exceeding 15 or a sodium adsorption ratio (SAR) surpassing 13, the presence of high levels of sodium ions and low levels of salt can lead to significant clay dispersion, degradation of aggregate structure, and the reduction of microporosity

MATERIALS AND METHODS

In many research papers wrote on the subject of animal manure biochar showed a higher potential as nutrient source rather than a C sequestration strategy, then the others vegetal biochar fodders (*Conz R.F., Thalita F., Abbruzzini, C.A.A., et al., 2017*).

In order to structure, analyze and deepen the knowledge wort until now, and to structure the future research, conducted by the most prestigious actors in pyrolysis equipment's producers and researchers, temperature and feedstock type are the key parameters that led the biochar properties of biochar, is necessary and almost mandatory to fallow the standards and guidelines drawn in this moment. In this way will obtain international relevant results for better tailored materials that correspond to the expected results while considering its interactions with environmental conditions and soil specification.

For this reason, will be made a case study of two scientific reports published on biochar properties obtained from pyrolysis treatment using several vegetal and animal dejections feedstocks. The experimental research data were conducted differently and lead to others values. Fist case was made in accordance with the International Biochar Initiative Guideline and in second case using their methodology (that is not entirely described in the paper).

From this reports it will be extract some data regarding the poultry litter feedstock that in the bought cases was mixt with sawdust (the mixture ratio is do not mentioned), because in our research project this category of dejections will be capitalized in agriculture as a natural fertilizer.

Case I - Experiment research conducted according the IBI Guidelines

The experiments were conducted, on several types of fodder such as: sugarcane straws, rice husk, poultry litter and sawdust. The poultry is obtained from a sustainable farm, in which the chickens/hens were fed daily with grass. The manure sits on the ground of the facility and it is mixed with sawdust weekly. This mixture is an important factor for biochar production, because poultry litter is mixt with sawdust, so after pyrolysis process will be trace of hemicellulose, lignin and cellulose. In table 1, were centralized the experimental data obtained. (*Conz, R.F., Abbruzzini, T.F., Andrade, C. A., et al., 2017*).

Pre-treatment included several steps: drying at 45 [˚C] during 24 h; grounding at less than 1 [mm] particle size (where used mortar and pestle and sieved to achieve particle size of 150 until 850 *10 $^{-6}$m.); were taken samples send to do a characterization analysis; prior to pyrolysis, the material has been dried at 105 [˚C] until it reaches proximately 13 % moisture (w/w) to improve the reactor efficiency.

The feedstock was pyrolyzed in a 60 L static reactor in N_2 saturated atmosphere with a heating rate of 10 [˚C·min^{-1}], the reactor was heated by six electrical resistances to the temperatures of 350 [˚C], 450 [˚C], 550 [˚C] and 650 [˚C]. The biochar's were removed from the reactor after 12 [h] from reaction time was completed, in this way it can avoid spontaneous combustion.

The mass of all materials contained in the chamber reaction was determined in order to obtain biochar yield. Feedstocks were analyzed accordingly to the biochar methodologies concerning the determinations of: pH, electrical conductivity (EC); cation exchange capacity (CEC); proximate and elemental analysis, presented in Table 1. Additionally, feedstock samples were evaluated in relation to their devolatilization characteristics, through thermogravimetry analysis. Table 2.

Case II- using their experimental and data extraction methodology

This study was conducted to examine how feedstock and pyrolysis temperature affect the final composition of the biochar with respect to the most commonly used analytical protocols to evaluate biochar agronomic value and stability properties using a large set of samples.

Pre-treatment processing: anaerobically digested dairy manure; compressing to extract the liquid fraction via a screw press and mixed in a 1:1 ratio (w/w) with chipped wood waste just prior to pyrolysis to produce composted dairy manure with wood waste biochar: feedstocks was dried at 60 ^{0}C to ca. 10% moisture (w/w) prior to pyrolysis.

Biochar's were produced using the Daisy Reactor, Best Energies Inc.., pyrolyzing the feedstocks in 50 ^{0}C increments from 300 to 600 ^{0}C (Cashton, WI, USA). Approximately 3 kg of feedstock were manually placed into a main chamber, which was purged at N_2 source, while the mixer was running to uniformly heated chamber for 80–90 min. This period includes both raising the temperature from ambient to target at less than 10 ^{0}C per minute, and holding at the target temperature for 15–20 min. The material was released after the equipment was cooled.

Sample preparation methodology. 1. Air-dry biochar's were mortar and pestle ground, sieved prior to analyses to obtain particle size range of 149–850*10^{3}m. Proximate analysis methods were conducted using ASTM D1762-84 Chemical Analysis of Wood Charcoal, this guide was adjusted to fit with biochar reactivity. A low temperature (LT) method was developed to volatiles determination be more relevant to biochar's. All proximate analyses were performed in duplicate. Mode details can be read in (*Enders, A., Hanley, K., Whitman, T., at al., 2012*). The data collected from the graphs were presented in Tabel 1.

In this case were utilized tests developed for the power industry and for soils, to collect data from biochar characterization. One of them it was so-called ''proximate analysis'', conducted according to ASTM D1762-84 to measure the moisture, volatiles, and ash content, with regard to its use as a fuel. The volatile solution content, *(Zimmerman, 2010),* to determine the stability of the material and effects on N availability.

For biochar's the ash ratio is related to metals volatilization at the high temperatures used by ASTM method.

Table 1

Poultry litter biochar properties according the IBI standards & others

Parameter value & M.U	**Pyrolysis temperature (^{0}C)**				**Feed -stock**	**Pyrolysis temperature (^{0}C)**						
	350	**450**	**550**	**650**		300	350	400	450	500	550	600
Yield [%]	59,6	47,1	42,0	40,2	-	78	75	70	68	70	69	70
EC [mS/m]	4,4	3,9	3,5	4,0	11,4	-	-	-	-	-	-	-
pH	8,2	9,8	9,8	9,9	7,3	values 9.5 until 9.9						
CEC [mmol$_c$ /kg]	320	203	106	105	597	-	-	-	-	-	-	-
Volatile matter [%]	60,8	46,9	45,7	42,1	69,7	88	-	92	-	95	-	100
Fixed Carbon [%]	0,0	1	2,8	7,5	0	10	-	8	-	7	-	5
Ash [%]	38,2	51,0	50,3	48,8	29,7	50	-	55	-	56	-	58
P [g/kg]	3,72	2,13	3,51	4,28	-	1	0.8	0.6	0.7	1.3	0.8	1
K [g/kg]	3,13	1,78	2,48	3,05	-	1	0.8	0.6	0.7	1.2	0.8	0.9
Mg [g/kg]	1,16	0,74	1,03	1,28	-	1.5	1.4	1.3	1.2	1.5	1.3	1.4
S [g/kg]	0,76	0,39	0,6	0,65	-	1	0.8	0.6	0.7	1	0.6	0.8
Fe [mg/kg]	0,44	0,34	0,45	0,56	-	-	-	-	-	-	-	-
Mn [mg/kg]	0,05	0,04	0,05	0,06	-	-	-	-	-	-	-	-
Zn [mg/kg]	0,09	0,05	0,08	0,08	-	-	-	-	-	-	-	-
N [%]	-	-	-	-	-	82	65	40	38	39	38	30
C [%]	38.1	29.8	35.3	32.6	30.4	98	86	89	90	78	75	80
O [%]	55.9	68.5	61.5	65.1	62	-	-	-	-	-	-	-
H [%]	3.4	1.7	1.4	0.9	4.5	-	-	-	-	-	-	-
Certified Standard Parameters	Case I (*Conz, R.F., Abbruzzini, T.F., Andrade, C. A., et al., 2017*)					Case II *(Enders, A., Hanley, K., Whitman, T., at al., 2012)*						

Form above results presented numerically in the Table 1, it can be observed that:

- the animal manure derived biochar is shown to accumulate important elements, such as phosphorus, calcium and magnesium. Thus, animal manure derived biochar has higher potential to be used as a nutrient source in agricultural systems, conclusion that was drawn in both cases, (*Azargohar, R., Nanda, S., Kozinski, J.A., et al. 2014*), but with different values,

- macronutrients concentration in biochar increases during the pyrolysis process while volatile matter and water is released from biochar structure. These latter compounds are represented by organic acids, and as pyrolysis temperature increases, the release of such molecules and the accumulation of basic elements such as Ca and Mg are the drivers of high pH in biochar's. These properties support the use of biochar as soil amendment as liming agent and nutrient source, in bought cases, *(Ippolito, J.A., Spokas, K.A., Novak, J.M., at al., 2015).*

- the biochar's derived from manures, accumulates C at different rates by increasing temperature, in bought cases, but this category of feedstock has the property, to lower C quantities in relation to nutrients, *(Ippolito, J.A., Spokas, K.A., Novak, J.M., at.al. 2015).*

- animal manure biochar, presents high ash materials, such as have high inorganic C content bound to carbo-nates, which can decrease the C by 24%, aspect present also in other papers *(Cimo, G., Kucerik, J., Berns, A.E, at al.,2014).*

- the CEC reduction, represents the release of carbonyl and carboxyl organic, fact that represents a decree in intensity. (*Conz R.F., Thalita F., Abbruzzini, C.A.A., et al., 2017*).

- also, was made a FTIR spectroscopy, analyse used to show biochar broadening and flattening with temperature evolution, (*Conz R.F., Thalita F., Abbruzzini, C.A.A., et al., 2017*), fact that indicates loss of: labile aliphatic and toxic compounds (*Kloss, S., Zehetner, F., Dellantonio, A., et al., 2012*); recalcitrant compounds maintenance, such as aromatic chains, specifically, loss of aliphatic C-H bond (*Wu, W., Yang, M., Feng, Q., at all., 2012*); the absence of functional groups represent the pyrolysis of cellulose, hemicellulose and lignin sawdust biochar's, around 1030 cm−1 (*Cantrell, K.B., Hunt, P.G., Uchimiya, M., at all., 2012, Nanda, S., Azargohar, R., Kozinski, J.A. at all., 2014);* the cumulative mass loss was the lowest in poultry manure within the temperature range analyzed (from 25˚C to 600˚C), which was also found by (*Ghani, W.A.K., Ayaz Mohd, A., Silva, G., et al., 2013*).

RESULTS

Many researchers have done experiments on biochar production and administration, but the data where unreliable, because were made in accordance with their needs and feedstock type available: hens or chickens feed with grass or cereals; the poultry litter is mixed with many types of vegetal/ wood subproducts in different concentrations; and the pyrolysis is not always done in the same conditions (installation type, pyrolysis regime, etc.).

So, most of them proposed and sustained the need to unify and agree to draw some guidelines and regulations to obtain from now one reliable results and technologies, in order to elaborate biochar administration mythology properly designed for a sustainable agriculture, poor field, polluted areas or degraded lends, in order to make a safety environment and to reduce air-water-soil pollution.

Based on the above presented results, were drawn important observations, that now have a scientific base applying the IBI guidelines, observations that also are present in scientific paper works published until the publications of guidelines.

In this part will be drawn important concussion recognizing the value of poultry litter biochar and its properties which recommends it to be used in agriculture:

1. Hence poultry litter showed the highest EC values since animal derived feedstock, that usually contain higher nutrient concentration (*Singh, B., Singh, B.P., Cowie, A.L. 2010)*. Particularly for poultry litter biochar's, the decrease in EC and is related with ash increase concentration, and when compared with its feedstock showed much higher values, corroborated with literature. (*Meng, J., Lili Wang L., Liu, X., et al., 2013);*
2. Poultry litter biochar exhibited the highest values of basic salts found in its feedstock, corroborating with the higher concentration. (*Lehmann, J., Rillig M.C., Thies, J., et al.,2011);*

3. The loss of acidic functional groups is due to pyrolysis temperature action was actually observed for poultry litter and sawdust. The CEC was expected to be smaller, in comparison to the respective original biomasses. (*Zhao, L., Cao, X., Masek, O., et all., 2013; Wang, Y., Hu, Y., Zhao, X., at all. 2013);*
4. Poultry litter biochar showed the greatest values for macronutrients especially due to high content of Ca, which explains the higher pH determined for this material *(Kloss, S., Zehetner, F., Dellantonio, A.,et all., 2012)*. The macronutrient content, per total, obtained from animal derived biochar's was higher compared to crop residues and wood derived materials;

5. Contents of P and K found, in case II, were lower than other results found in the literature and also in the IBI guides (case I), due to differences in methodology to elements determine concentration and heterogeneity of poultry litter feedstock. (*Cantrell, K.B., Hunt, P.G., Uchimiya, M., et all., 2012; Song, W. and Guo, M., 2012*);

6. The poultry litter biochar presents significant amounts of mineral analysed elements, compared to other feedstock materials studied, even though the concentrations dropped with temperature increase, justifying its potential use as fertilizer. (*Meng, J., Lili Wang L., Liu, X., et all., 2013*);

7. Poultry litter consist in highest zinc (Zn) concentration, reaching 0.09 ppm, which reflectes the common addition of Zn as a supplement in poultry diet (*Park, S., Birkhold, S., Kubena, L., et all., 2004*). Fact that represents the potential use of biochar's as soil amendment;

8. Rate of ash content is high at poultry litter biochar, which corroborates with literature. Animal derived biochar composition can reach approximately 50% of ash content, and sometimes between 45% and 60% of volatile matter, results similar of those reported by (*Song, W. and Guo, M. 2012), and (Meng, J., Lili Wang L., Liu, X., et all. 2013*);

9. For instance, poultry litter (30% to 40%) showed slightly decreasing content with increasing temperature. High ash materials, have high inorganic C content bound to carbo nates, which can decrease the C by 24% (*Enders, A., Hanley, K., Whitman, T., et all., 2012; Cimo, G., Kucerik, J., Berns, A.E, at all., 2014*).

10. The cumulative mass loss was the lowest in poultry manure and rice hull within the temperature range analysed (from 25˚C to 900˚C), which was also found by (*Azargohar, R., Nanda, S., Kozinski, J.A., et all., 2014; Ghani, W.A.K., Ayaz Mohd, A., Silva, G., et al., 2013*).

11. The higher proportion of volatile matter determined in the poultry litter biochar, indicates higher amount of easily degradable source of C, enabling its use by the microorganisms, which in turn cause soil respiration to spike when comparing to control treatment.

12. It is essential to note that agricultural properties, that support the use of biochar as nutrient source, were improved in manure derived biochar's, while C stability was lower. (*Conz, R.F., Abbruzzini, T.F., Andrade, C. A., et all., 2017).*

CONCLUSIONS

These confirmations are important for scientific research community, in order to recognise the value of the pass experiences and their results, which represent the bases of these regulations.

Aster this case study was identify a need to add and to standardize the thermogravimetric analyses, because could add value and results replicability, also helps to scaleup biochar thermal devolatilization. (*Enders, A., Hanley, K., Whitman, T., et all., 2012*).

Currently the most accessible approach to evaluate recalcitrance is the elemental contents analyse, pH, NPH influence that influence the plant responses.

Higher soil aggregation was also observed for fine-textured soil where wood and animal derived biochar was added (*Wang, D., Fonte, S.J., Parikh, S.J., et all., 2017),* improving soil physical structure, aeration and moisture ratio, consequently an improved environment for root development.

These mechanisms are often related to increased agricultural production; however, results vary due to biochar properties and its interaction with different environmental conditions (*Lorenz, K. and Lal, R., 2014*).

A new trend is now, determination of biochar toxic effects (PAH's, PCDD/Fs, PCB's, As, d, Cr, Cu, Pb, Hg, Ni, Zn), that according to some scientists alters soil physical attributes, toxicity, humidity, if is applied outside the agronomic application rate.

Sometimes, these hazards can be avoided if isn't taken in to consideration all environmental factors, like: clime, soil specifications, vegetal fauna/ crop specifications, rain drops rates, microorganism population and fauna, and in this way the biochar is efficiency used. (*Enders, A., Hanley, K., Whitman, et all., 2017).*

ACKNOWLEDGEMENT

This paper presents the findings from the scientific literature published up on the biochar methodology to assess the obtain from a pyrolysis process financed from ADER 25.3.1 project, named Poultry litter capitalization technology to produce phosphorus reach biofertilizer's.

REFERENCES

[1] Azargohar, R., Nanda, S., Kozinski, J.A., Dalai, A.K. and Sutarto, R. (2014) Effects of Temperature on the Physicochemical Characteristics of Fast Pyrolysis Bio-Chars Derived from Canadian Waste Biomass. Fuel, 125, 90-100. https://doi.org/10.1016/j.fuel.2014.01.083

[2] Camps-Arbestain, M., Amonette, J.E., Singh, B, Wang, T., Schmidt H.P, (2015), A biochar classification system and associated test methods, Biochar for environmental management, 165-193.

[3] Cantrell, K.B., Hunt, P.G., Uchimiya, M., Novak, J.M. and Ro, K.S. (2012) Impact of Pyrolysis Temperature and Manure Source on Physicochemical Characteristics of Biochar. Bioresource Technology, 107, 419-428.https://doi.org/10.1016/j.biortech.2011.11.084.

[4] Cimo, G., Kucerik, J., Berns, A.E, Schaumann, G.E., Alonzo, G., Conte, P., (2014) Effect of Heating Time and Temperature on the Chemical Characteristics of Biochar from Poultry Manure. Journal of Agricultural and Food Chemistry, 62, 1912-1918.https://doi.org/10.1021/jf405549z

[5] Conz, R.F., Abbruzzini, T.F., Andrade, C. A., Milori, D.M., Carlos, B. P., Cerri, E. P., (2017), Effect of Pyrolysis Temperature and Feedstock Type on Agricultural Properties and Stability of Biochars Agricultural Sciences, 8, 914-933. http://www.scirp.org/journal/as

[6] Duan, Q., Jiang, S., Chen, F., Li, Z., Ma, L., Song, Y., Yu, X., Chen, Y., Liu, H., Yu, L., (2023) Ind. Crops Prod. 192, 116075, https://doi.org/10.1016/j.indcrop.2022.116075.

[7] Divyangkumar, N., Panwar, N. L., (2024) Standardization, certification, and development of biochar based fertilizer for sustainable agriculture: An overview, Environmental Pollution and Management, Volume 1, 186-202. https://doi.org/10.1016/j.epm.2024.10.001

[8] Enders, A., Hanley, K., Whitman, T., Joseph, S.D. and Lehmann, J. (2012) Characterization of Biochars to Evaluate Recalcitrance and Agronomic Performance. Bioresource Technology, 114, 644-653.https://doi.org/10.1016/j.biortech.2012.03.022

[9] Fawzy, S., Osman, A.I., Mehta, N., Moran, D., Al-Muhtaseb, A.H., Rooney, D.W., Clean J. (2022). Prod. 371 133660, https://doi.org/10.1016/j.jclepro.2022.133660

[10] Fawzy, S., Osman, A. I., Yang, H., Doran, J., Rooney, D.W., (2021) Industrial biochar systems for atmospheric carbon removal: a review, Environmental Chemistry Letters, Volume 19, pages 3023–3055, https://doi.org/10.1007/s10311-021-01210-1.

[11] Ghani, W.A.K., Ayaz Mohd, A., Silva, G., Bachmann, R. T., Taufiq-Yap, Y. H., Rashid, U., Muhtaseb, A.H.A., (2013), Biochar Production from Waste Rubber-Wood-Sawdust and Its Potential Use in C Sequestration: Chemical and Physical Characterization. Industrial Crops and Products Journal, 44, 18-24.

[12] Ippolito, J.A., Spokas, K.A., Novak, J.M., Lentz, R.D. and Cantrell, K.B. (2015) Biochar Elemental Composition and Factors Influencing Nutrient Retention. In: Lehmann, J. and Joseph, S.D., Eds., Biochar for Environmental Management: Science, Technology and Implementation, Earthscan, 137-162.

[13] Kotula, L., Caparros P.G, Zörb, C., Colmer, T.D., Flowers, T.J., (2020) Plant. Cell Environ. 43 2932–2956, https://doi.org/10.1111/pce.13865.

[14] Kloss, S., Zehetner, F., Dellantonio, A., Hamid, R., Ottner,F., Liedtke, V., Schwanninger, M., Gerzabek, M.H., Soja,G., (2012) Characterization of Slow Pyrolysis Biochars: Effects of Feedstocks and Pyrolysis Temperature on Biochar Properties. Journal of Environmental Quality, 41, 990-1000. DOI: 10.2134/jeq2011.0070.

[15] Lehmann, J., Rillig M.C., Thies, J., Masiello C.A., Hockaday, W.C., Crowley, D., (2011) Biochar Effects on Soil Biota-A Review. Soil Biology and Biochemistry, 43, 1812-1836. https://doi.org/10.1016/j.soilbio.2011.04.022

[16] Liu, Q., Meki, K., Zheng, H., Yuan, Y., Shao, M., Luo, X., Li, X., Jiang, Z., Li, F., Xing, B., Biochar 5 (2023), https://doi.org/10.1007/s42773-023-00244-8.

[17] Lorenz, K., Lal, R., (2014) Biochar Application to Soil for Climate Change Mitigation by Soil Organic Carbon Sequestration. Journal of Plant Nutrition and Soil Science, 177, 651-670. https://doi.org/10.1002/jpln.201400058

[18] Meng, J., Lili Wang L., Liu, X., Wu, J., Philip C., Xu, J., (2013) Physicochemical Properties of Biochar Produced from Aerobically Composted Swine Manure and Its Potential Use as an Environmental Amendment. Bioresource Technology, 142, 641-646.https://doi.org/10.1016/j.biortech.2013.05.086

[19] Meyer, S., Genesio, L., Vogel, I., Schmidt, H.-P., Soja, G., Someus, E., Shackley, S., Verheijen, F.G.A., Glaser, B., Environ, J., (2017) Eng. Landsc. Manag. 25, 175–191, https://doi.org/10.3846/16486897.2016.1254640.

[20] Nanda, S., Azargohar, R., Kozinski, J.A. and Dalai, A.K. (2014) Characteristic Studies on the Pyrolysis Products from Hydrolyzed Canadian Lignocellulosic Feedstocks. Bioenergy Research, 7, 174-191. https://doi.org/10.1007/s12155-013-9359-7.

[21] Park, S., Birkhold, S., Kubena, L., Nisbet, D. and Ricke, S. (2004) Review on the Role of Dietary Zinc in Poultry Nutrition, Immunity, and Reproduction. Biological Trace Element Research, 101, 147-163, https://doi.org/10.1385/BTER:101:2:147

[22] Singh, B., Singh, B.P., Cowie, A.L., (2010) Characterisation and Evaluation of Biochars for Their Application as a Soil Amendment, Australian Journal of Soil Research, 48, 516-525. https://doi.org/10.1071/SR10058.

[23] Schmidt, H.-P., (2012) Uses Biochar Ithaka J, 1, 286–289.

[24] Song, W. and Guo, M. (2012), Quality Variations of Poultry Litter Biochar Generated at Different Pyrolysis Temperatures. Journal of Analytical and Applied Pyrolysis, 94, 138-145. https://doi.org/10.1016/j.jaap.2011.11.018.

[25] Wang, Y., Hu, Y., Zhao, X., Wang, S. and Xing, G. (2013) Comparisons of Biochar Properties from Wood Material and Crop Residues at Different Temperatures and Residence Times. Energy and Fuels, 27, 5890-5899. https://doi.org/10.1021/ef400972z

[26] Wu, W., Yang, M., Feng, Q., McGrouther, K., Wang, H., Lu, H., Chen, Y., (2012), Chemical Characterization of Rice Straw-Derived Biochar for Soil Amendment. Biomass and Bioenergy, 47, 268-276, https://doi.org/10.1016/j.biombioe.2012.09.034

[27] Zhao, L., Cao, X., Masek, O., Zimmerman, A.R., (2013) Heterogeneity of Biochar Properties as a Function of Feedstock Sources and Production Temperatures. Journal of Hazardous Materials, 256-257, 1-9; https://doi.org/10.1016/j.jhazmat.2013.04.015,

[28] Zimmerman, A.R., (2010), Abiotic and microbial oxidation of laboratory-produced black carbon (biochar). Environ. Sci. Technol. 44, 1295–1301.

[29] *** EBC (2012-2025) 'European Biochar Certificate – Guidelines for a Sustainable Production of Biochar.' Carbon Standards International (CSI), Frick, Switzerland. (http://carbon-standards.com/ebc). Version 10.5E from 14th August 2025,

[30] *** EBC 2022, Guidelines for a Sustainable Production of Biochar. Version 10.1 from 10th Jan 2022, 2022
[31] *** WBC (2023): World Biochar Certificate – Guidelines for a Sustainable Production of Biochar and its Certification.' Carbon Standards International, Frick, Switzerland, (http://www.european-biochar.org), version 1.1 from 20th December 2024, https://www.european-biochar.org/media/doc/2/wbc_1_1.pdf
[32] *** Standardized Product Definition and Product Testing Guidelines for Biochar: That Is Used in Soil, n.d. (2015).

CREATING A DATABASE FOR ARTIFICIAL INTELLIGENCE TRAINING / *CREAREA UNEI BAZE DE DATE CU SCOPUL ANTRENARII INTELIGENCEI ARTIFICIALE*

Dorin-Andrei CÎRSTEA*[1)], Robert-Dorin CRISTEA[1)], Mihai Gabriel MATACHE[1)]
[1)]National Institute of Research - Development for Machines and Installations Designed to Agriculture and Food Industry Bucharest / Romania[2)]
E-mail: d_orinel@yahoo.com

Keywords: *dataset, data gathering, artificial intelligence, machine learning*

ABSTRACT
The development of well-structured databases is the first step in the usage of artificial intelligence (AI) systems. This paper presents the methodology and design used in creating a database intended for AI training. Importance is placed on data collection strategies, preprocessing techniques, and quality assurance measures to ensure the accuracy, diversity, and scalability of the dataset. The study focuses on ethical and technical challenges associated with dataset construction, including bias mitigation, and long-term maintainability. The resulting database is evaluated in terms of its applicability to machine learning models and its potential to support future research in AI training.

REZUMAT
Dezvoltarea unor baze de date bine structurate este primul pas în utilizarea sistemelor de inteligență artificială (IA). Această lucrare prezintă metodologia și designul utilizate în crearea unei baze de date destinate instruirii în domeniul IA. Se pune accent pe strategiile de colectare a datelor, tehnicile de preprocesare și măsurile de asigurare a calității pentru a asigura acuratețea, diversitatea și scalabilitatea setului de date. Studiul se concentrează pe provocările etice și tehnice asociate cu construirea setului de date, inclusiv atenuarea erorilor de prejudecată și mentenabilitatea pe termen lung. Baza de date rezultată este evaluată în ceea ce privește aplicabilitatea sa la modelele de învățare automată și potențialul său de a sprijini cercetările viitoare în domeniul instruirii în domeniul IA.

INTRODUCTION

According to (*Gong et al., 2023*), with the rise of big data, the quality of datasets has become a crucial factor affecting the performance of machine learning models. High-quality datasets are essential for the realization of data value. As per (*Hernández López et al., 2022*), the application of machine learning (ML) algorithms to address problems related to model-driven engineering (MDE) is currently hindered by the lack of curated datasets of software models. Training data preprocessing has a great impact on the model's predictive performance, is highly dependent on the modeler's experience, and is not typically reported in engineering-related literature.

The objective of this study was to assess the effects of data preprocessing, hyperparameter selection, and time series size on the model's evaluation metrics, based on a study by (*Aranha et al., 2023*). Supervised learning techniques are ML learning techniques or algorithms that bind previous and current dataset with the help of labeled data to predict future events (L. J. Muhammad et al., 2021) and prevailing data practices tend to abstract away the human labor, subjective judgments and biases, and contingent contexts involved in dataset production (*Paullada et al., 2021*).

It is an undeniable fact that currently information is a pretty significant presence for all companies or organizations (*Yavanoglu et al., 2017*), and that is mainly the reason we chose to create our own. As per (*Eastman et al., 2023*), any machine learning model is only as good as the data it is trained on. (*Mahani et al., 2025*) points out that acquiring a substantial number of data points for training accurate machine learning (ML) models is a big challenge in scientific fields where data collection is resource-intensive. According to (*Gauen et al., 2017*), among all factors that contribute to this development, datasets with labels play crucial roles, which is the reason we chose to focus on creating our own database.

MATERIALS AND METHODS

The datased is composed of around 900 photos (in .PNG format at 1920x1080 resolution), with each photo showing approximately 50-60 different tomoatoes of varied cultivars. The photos included were exclusively gathered locally in the greenhouses of INMA Bucuresti and INCDIBH Ștefănești, taken on varied light conditions: at morning (7:00-11:00) over the course of 2 months, July and August.

The gathering of the photographs also varied in more aspects, such as camera distance from the plant (between 30cm to 1m), or the angle of the camera (between -10° and 40°).

Fig. 1. Different views of the platform and support used for gathering data

As for hardware, the data was gathered using both a ZED i2 camera and a Logitech HD Pro C920, mounted on a support with adjustable distance and height.

The system was moved trough the greenhouses along a path of railways, using a mobile platform. Both the adjustable system and the mobile platform were designed, created and assembled at INMA Bucharest.

Fig. 2. Railways lain between lanes of tomato plants inside greenhouse

As stated by (*Michelini et al., 2021*), a relevant aspect when compiling a large dataset to be used for ML purposes consists of gathering a balanced distribution of data. We have chosen to categorize the individual tomatoes of each photograph using three classes: c_ripe, c_half-ripe and c_green. For labeling we have the LabelStudio software, exporting YOLO.TXT files. Using the software for manually labeling each of the approximately 28 000 instances took around 2 months of work, split among 5 people. This process helps guarantee the high precision for differentiating ripe tomatoes from green or half-ripe tomatoes.

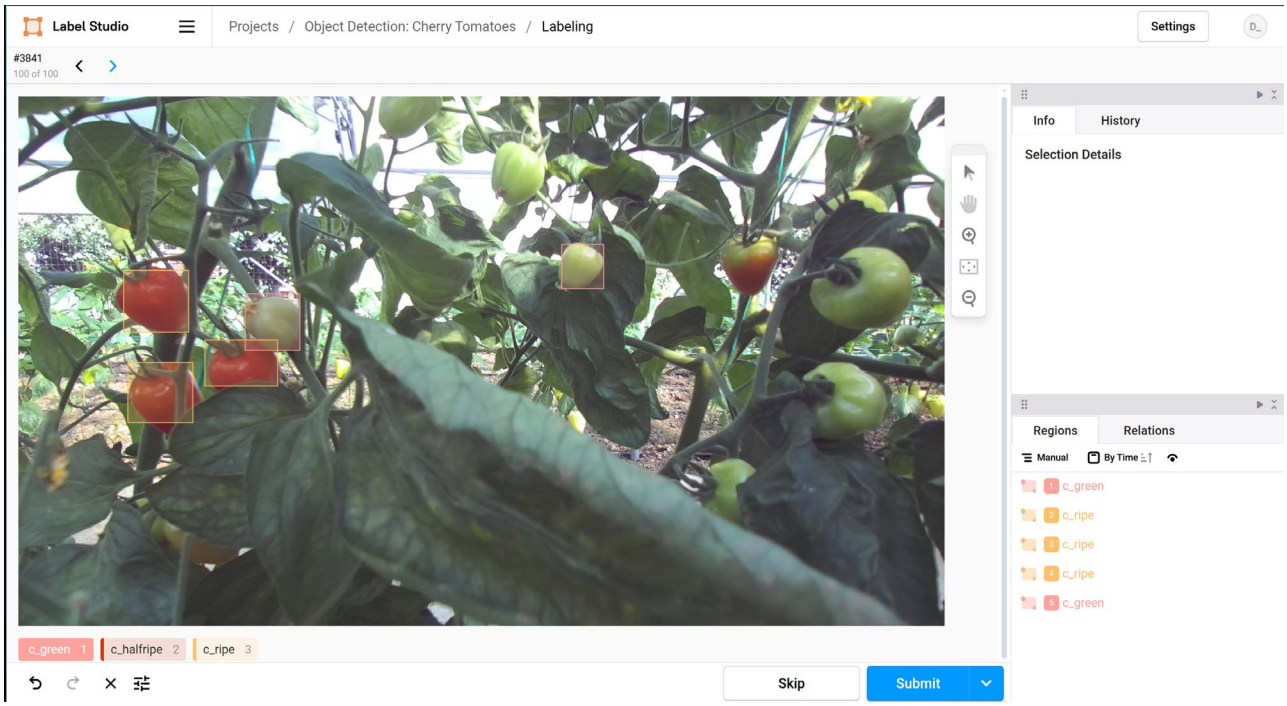

Fig. 3. Process of using the LabelStudio software for processing gathered data

Part of the hardware used for gathering the photographs was Stereolabs ZED 2i stereo depth camera (Stereolabs Inc., San Francisco, USA). The device consists of two 4-megapixel CMOS sensors mounted in a fixed stereo configuration with a 120 mm baseline, enclosed in an IP66-rated aluminum housing suitable for indoor and outdoor use. It provided a field of view of approximately [-10° / 40°]* horizontally.

The ZED 2i records synchronized stereo image pairs at multiple resolutions (up to 2×2208 × 1242 pixels at 15 fps), from which depth maps are computed using Stereolabs' neural stereo engine. The effective depth sensing range is approximately 0.3–20 m with the 2.1 mm lens (up to 35 m with the 4 mm lens).

In addition to stereoscopic imaging, the camera integrates a 9-DoF inertial measurement unit (IMU), magnetometer, and barometer, enabling visual-inertial odometry and improved spatial tracking. Data were transmitted via a USB-C 3.0 interface to a host computer for processing using the ZED SDK.

Simultaneously, a Logitech HD Pro Webcam C920 (Logitech International S.A., Lausanne, Switzerland) was used to capture high-definition data. The device employs a dual-microphone system and a Carl Zeiss® glass lens with autofocus, capable of recording at resolutions up to 1920 × 1080 pixels (Full HD) at 30 frames per second. Still images can be captured at resolutions up to 15 megapixels (software-enhanced).

Fig. 4. Stereolabs ZED 2i stereo depth camera

The webcam connects via a USB 2.0 interface and is compatible with most major operating systems without additional drivers. Automatic light correction and autofocus features allow it to adapt to different illumination conditions, making it suitable for stable, continuous data collection in varied environments.

Fig. 5 – Logitech HD Pro Webcam C920 camera

RESULTS

The collection was organised into a folder unit (photographs and labels), which allowed us to make use of the newly created dataset for directly training and validating AI models. The dataset is built on the standard YOLO format, organised in distinct folders (train, valid and test), which, in turn, contain photographs and label files. Each photograph correlates to an associated .TXT file containing bounding box's coordinates and each individual tomato's class. The connection between photographs and labels is guaranteed by the configuration file .YAML, contained within the dataset.

The roughly 28 000 instances were split between the 3 classes as follows: approximately 19 000 for the c_green class, approximately 6000 for the c_ripe, and approximately 3000 for the c_half_ripe class. Noting the high distribution of instances for the unripe class, this was necessary for having an accurate differentiation between tomatoes (of green color) and the rest of the plant (also green).

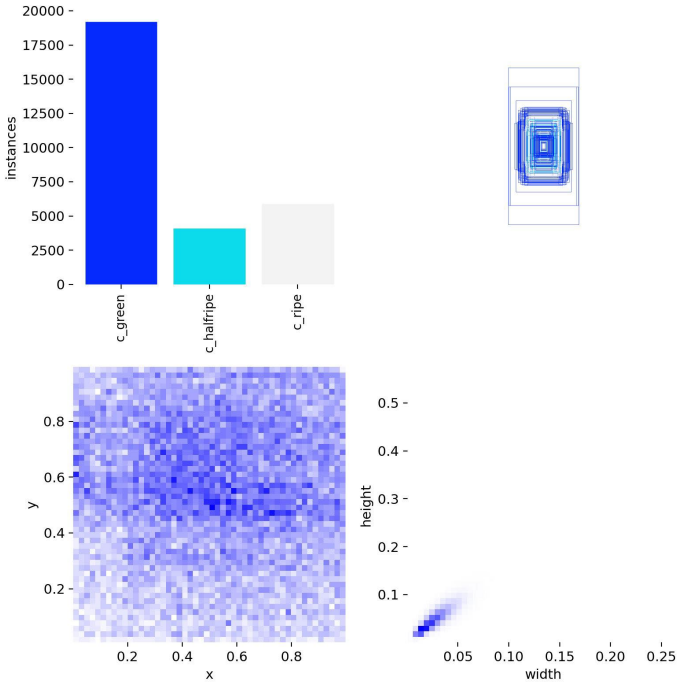

Fig. 6. Visual representation of class distribution

CONCLUSIONS

In this work, we presented the collection of a dedicated image dataset designed to support the development and training of machine learning models for tomato classification. The dataset was curated under varied acquisition conditions and structured into clearly defined classes, which guaranteed the diversity and reliability of the samples. By providing a sufficiently large and well-labeled set of instances, this dataset offers a valuable foundation for advancing automated recognition tasks in agricultural research and practice. Future work will focus on applying and evaluating machine learning techniques on this dataset to assess performance and explore its potential for further deployment.

ACKNOWLEDGEMENT

This work was supported by a grant of the Ministry of Agriculture and Rural Development, contract of sectorial financing, ADER 2023-2026 type, no. 25.1.1, “Technology for robotized harvesting of Solanaceae family vegetables in greenhouses and solariums, using artificial intelligence

REFERENCES

[1] Aranha, A. L., Bernucci, L. L. B., & Vasconcelos, K. L. (2023). Effects of different training datasets on machine learning models for pavement performance prediction. *Transportation Research Record*, *2677*(8), 196–206. https://doi.org/10.1177/03611981231155902

[2] Eastman, P., Behara, P. K., Dotson, D. L., Galvelis, R., Herr, J. E., Horton, J. T., Mao, Y., Chodera, J. D., Pritchard, B. P., Wang, Y., De Fabritiis, G., & Markland, T. E. (2023). SPICE, A dataset of drug-like molecules and peptides for training machine learning potentials. *Scientific Data*, *10*(1), 11. https://doi.org/10.1038/s41597-022-01882-6

[3] Gauen, K., Dailey, R., Laiman, J., Zi, Y., Asokan, N., Lu, Y.-H., Thiruvathukal, G. K., Shyu, M.-L., & Chen, S.-C. (2017). Comparison of visual datasets for machine learning. *2017 IEEE International Conference on Information Reuse and Integration (IRI)*, 346–355.

[4] Gong, Y., Liu, G., Xue, Y., Li, R., & Meng, L. (2023). A survey on dataset quality in machine learning. *Information and Software Technology*, *162*(107268), 107268. https://doi.org/10.1016/j.infsof.2023.107268

[5] Michelini, A., Cianetti, S., Gaviano, S., Giunchi, C., Jozinović, D., & Lauciani, V. (2021). INSTANCE – the Italian seismic dataset for machine learning. *Earth System Science Data*, *13*(12), 5509–5544. https://doi.org/10.5194/essd-13-5509-2021

[6] M R Mahani, Igor A Nechepurenko, Yasmin Rahimof and Andreas Wicht. (2025, July 17). *Optimizing data acquisition: a Bayesian approach for efficient machine learning model training*. Iop.org. https://doi.org/10.1088/2632-2153/ad605f

[7] Muhammad, L. J., Algehyne, E. A., Usman, S. S., Ahmad, A., Chakraborty, C., & Mohammed, I. A. (2021). Supervised machine learning models for prediction of COVID-19 infection using epidemiology dataset. *SN Computer Science*, *2*(1), 11. https://doi.org/10.1007/s42979-020-00394-7

[8] López, J. A. H., Cánovas Izquierdo, J. L., & Cuadrado, J. S. (2022). ModelSet: a dataset for machine learning in model-driven engineering. *Software & Systems Modeling*, *21*(3), 967–986. https://doi.org/10.1007/s10270-021-00929-3

[9] Paullada, A., Raji, I. D., Bender, E. M., Denton, E., & Hanna, A. (2021). Data and its (dis)contents: A survey of dataset development and use in machine learning research. *Patterns (New York, N.Y.)*, *2*(11), 100336. https://doi.org/10.1016/j.patter.2021.100336

[10] Yavanoglu, O., & Aydos, M. (2017). A review on cyber security datasets for machine learning algorithms. *2017 IEEE International Conference on Big Data (Big Data)*, 2186–2193.

ENHANCING SOIL SAMPLING ACCURACY THROUGH IOT INTEGRATION
/
ÎMBUNĂTĂȚIREA PRECIZIEI EȘANTIONĂRII SOLULUI PRIN INTEGRAREA IOT

Alexandru-Cristian CIOACLA*[1)], Iuliana GAGEANU[1)], Robert Dorin CRISTIEA[1)], Mario CRISTEA[1)], Dorin-Andrei CÎRSTEA[1)], Roxana-Georgiana AMARGHIOALEI[2)]
[1)]National Institute of Research – Development for Machines and Installations Designed to Agriculture and Food Industry, Romania; [2)]ARDS Secuieni / Romania
**Tel: 0733537643; E-mail: cioaclacristian@gmail.com*

Keywords:

ABSTRACT
This paper aims to explore and summarize how Internet of Things (IoT) technologies can be integrated into soil sampling systems to enhance precision, efficiency, and automation in agricultural practices. By implementing IoT-based solutions, soil sampling can transition from a manual, time-consuming task to a data-driven, automated process capable of providing continuous and accurate information about soil conditions. Through the collection of detailed soil data—such as moisture levels, temperature, nutrient composition, and pH, farmers can gain a deeper understanding of soil health and stability, which are critical factors in achieving optimal crop growth. The introduction of IoT-enabled soil sampling systems, combined with cloud computing for data storage and processing, offers the potential to fully automate sampling operations using remotely controlled or self-navigating machinery. Such systems can precisely identify sampling points, record their geographic locations using GPS technology, and store the results in real time for immediate or later analysis. This automation not only eliminates the need for manual labor and field driving but also ensures consistency and repeatability in the sampling process.Furthermore, integrating IoT, cloud computing, and artificial intelligence could enable predictive analytics, allowing for early detection of soil nutrient deficiencies or environmental stress factors. As a result, farmers could implement targeted interventions, such as optimized fertilization or irrigation strategies, leading to healthier crops and increased yields. Overall, the adoption of IoT in soil sampling represents a crucial step toward the digital transformation of agriculture, improving productivity, reducing costs, and supporting more sustainable and environmentally responsible farming practices.

REZUMAT
Această lucrare își propune să exploreze și să prezinte modul în care tehnologiile Internet of Things (IoT) pot fi integrate în sistemele de eșantionare a solului pentru a spori precizia, eficiența și automatizarea practicilor agricole. Prin implementarea soluțiilor bazate pe IoT, eșantionarea solului poate trece de la o sarcină manuală, consumatoare de timp, la un proces automatizat, bazat pe date, capabil să ofere informații continue și precise despre condițiile solului. Prin colectarea de date detaliate despre sol cum ar fi nivelurile de umiditate, temperatura, compoziția nutrienților și pH-ul, fermierii pot obține o înțelegere mai profundă a sănătății și stabilității solului, care sunt factori critici în obținerea unei creșteri optime a culturilor. Introducerea sistemelor de eșantionare a solului bazate pe IoT, combinată cu cloud computing pentru stocarea și procesarea datelor, oferă potențialul de a automatiza complet operațiunile de eșantionare utilizând utilaje controlate de la distanță sau cu auto navigare. Astfel de sisteme pot identifica cu precizie punctele de prelevare, pot înregistra locațiile lor geografice folosind tehnologia GPS și pot stoca rezultatele în timp real pentru analiză imediată sau ulterioară. Această automatizare nu numai că elimină necesitatea muncii manuale și a conducerii pe teren, dar asigură și consecvența și repetabilitatea procesului de eșantionare. În plus, integrarea IoT, cloud computing-ului și inteligenței artificiale ar putea permite analiza predictivă, permițând detectarea timpurie a deficiențelor de nutrienți ai solului sau a factorilor de stres din mediu. Prin urmare, fermierii ar putea implementa intervenții specifice, cum ar fi strategii optimizate de fertilizare sau irigare, ceea ce ar duce la culturi mai sănătoase și la randamente sporite. Per total, adoptarea IoT în prelevarea de probe de sol reprezintă un pas crucial către transformarea digitală a agriculturii, îmbunătățind productivitatea, reducând costurile și susținând practici agricole mai sustenabile și mai responsabile din punct de vedere ecologic.

INTRODUCTION

Contemporary agriculture remains predominantly dependent on human labor and manually operated machinery, despite significant technological advancements and concerted efforts to promote automation.

Although automated systems and smart farming technologies are increasingly available, their widespread adoption is constrained in numerous regions by several critical barriers. These include prohibitive implementation costs, a deficit of technical expertise, and insufficient infrastructural support. Consequently, traditional methodologies continue to prevail, underscoring a critical need for more accessible and pragmatically integrated automated solutions to enhance agricultural productivity and operational efficiency. (*Huuskonen and Oksanen, 2018*).

Fig. 1. Hand held soil sampling probe
(*https://www.winfieldunited.com/news-and-insights/spring-soil-sampling-is-no-longer-optional*)

Soil is a mixture of organic matter, minerals, gases, liquids, micro and macroorganisms that together support life. Soil sampling is a fundamental practice in agriculture, environmental monitoring, and land management. Accurate soil sampling allows researchers and farmers to evaluate soil fertility, detect contamination, and make informed decisions about crop management, fertilization, and sustainability strategies. However, traditional soil sampling methods are often manual, labor-intensive, time-consuming, and prone to human error, which can compromise data reliability and reproducibility. Soil testing enables the planning of cultivation and soil management actions as well as providing the basis for a sustainable crop nutrition programme that is accurate, timely and increasingly importantly environmentally responsible (*Abate Gezahagn Goshu, 2024*).

Around the globe agriculture provides for every human the most basic need for food and fiber. The common effort of researchers to introduce new farming techniques in the past century has helped agriculture satisfy the ever-growing population demands for food and agricultural products. However, as the global population continues to grow and income levels rise, the demand for food is expected to increase significantly, placing even greater pressure on already limited natural resources. This situation highlights the urgent need for more sustainable and efficient agricultural practices. With increasing awareness of the environmental consequences of conventional farming such as soil degradation, water scarcity, and greenhouse gas emissions it has become essential to adopt innovative methods that can meet future food requirements while minimizing or even reducing agriculture's ecological footprint. Emerging technologies like geospatial mapping, the Internet of Things (IoT), Big Data analytics, and artificial intelligence (AI) offer powerful tools to address these challenges. By integrating these technologies, farmers and researchers can make more informed and precise management decisions, optimize resource use, and ultimately enhance crop productivity in a sustainable manner (*Sishodia et al., 2020*).

The Internet of Things (IoT) refers to a network of physical objects embedded with sensors, software, processing capabilities, and other technologies that enable them to connect and exchange data with other devices and systems over the internet or through various communication networks. By leveraging IoT technology, agricultural machinery can be remotely operated and monitored, significantly reducing or even eliminating the need for manual field labor. This approach not only minimizes human involvement in repetitive or physically demanding tasks but also enhances the precision, consistency, and overall efficiency of farming operations. As a result, IoT-driven automation allows for better resource management, improved productivity, and more sustainable agricultural practices (*Rajasekaran et al., 2024*).

Cloud computing is a technology that enables the sharing and management of computing resources at a relatively low cost. Service providers offer these cloud-based resources in an affordable and scalable manner, making data storage and processing more accessible for various applications. In agriculture, cloud computing plays a vital role when combined with Internet of Things (IoT) technologies, facilitating the collection, analysis, and storage of large volumes of agricultural data. The integration of artificial intelligence (AI) and cloud computing provides a powerful support system for IoT-based agricultural solutions. This combination allows data gathered from intelligent wireless sensors—such as those mounted on unmanned aerial vehicles (UAVs), satellites, and agricultural machinery—to be processed and analyzed efficiently. Additionally, robotic systems like unmanned ground vehicles (UGVs) equipped with precise positioning tools, including real-time kinematic (RTK) GPS and LiDAR sensors, contribute to high-resolution field monitoring and management. Underpinning these systems is the Wireless Sensor Network (WSN), a network composed of spatially distributed sensor nodes that communicate wirelessly to gather and transmit environmental and operational data for centralized processing in the cloud (*Alahmad et al., 2023*).

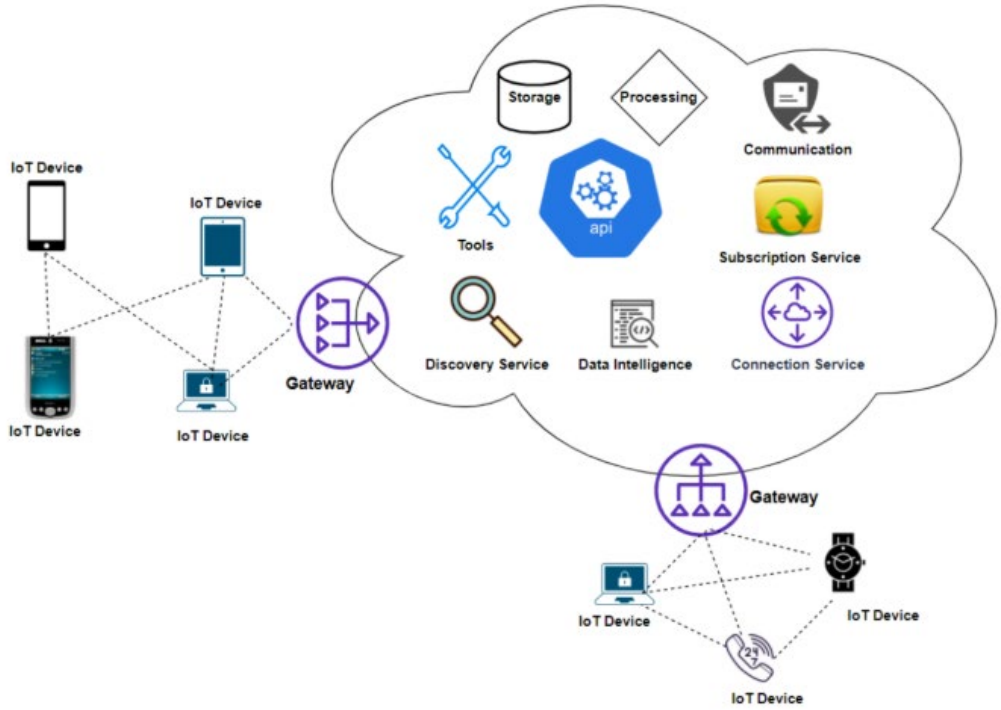

Fig. 2. IoT System Based on Cloud (*Alam T., 2021*)

MATERIALS AND METHODS

2.1 Robot navigation method.

The integration of Global Positioning System (GPS) technology with Internet of Things (IoT)-based sensors establishes a framework for automating and enhancing the precision of soil sampling. A robotic platform equipped with a high-accuracy GPS module can autonomously navigate a field and geotag the precise coordinates of each sampling point. This positional data is augmented by a depth sensor or ultrasonic device that monitors the penetration of the sampling probe, ensuring consistent and reproducible sampling depth across the field. Furthermore, a suite of onboard environmental sensors—capable of measuring parameters such as soil moisture, temperature, and electrical conductivity—can collect supplementary in-situ data. This real-time sensor data provides critical context for interpreting subsequent laboratory analyses and contributes to the generation of high-resolution soil property maps. All sensory data is aggregated and communicated via an IoT network, utilizing wireless protocols (e.g., LoRaWAN, 4G/5G) for real-time transmission to a central base station or cloud platform. This centralized system processes the incoming datastream, visualizes the georeferenced sampling points on a digital field map, and creates a structured database that links each physical sample with its corresponding geographic position and ambient field conditions.

Consequently, this integrated technological synergy enables the accurate identification of spatial nutrient distribution patterns while significantly mitigating the potential for human error intrinsic to manual

sampling methodologies. In summary, the confluence of GPS, IoT communication, and automated sensing facilitates a highly efficient, repeatable, and data-driven paradigm for soil sampling and analysis.

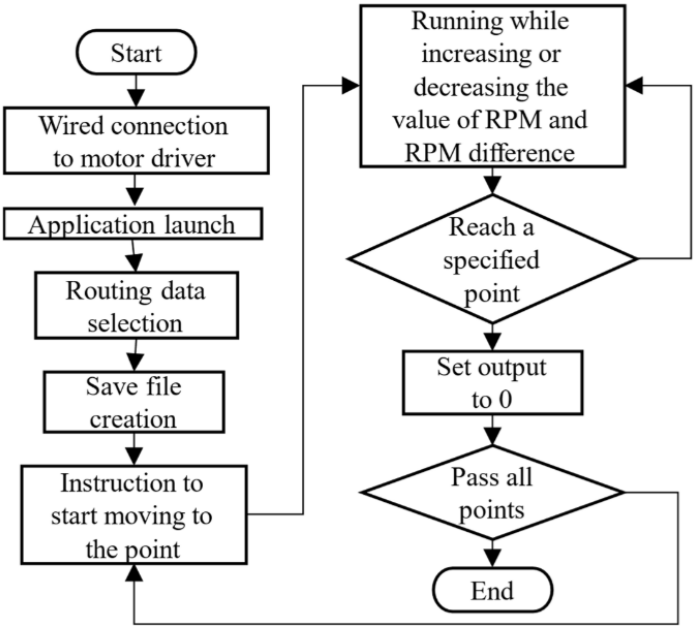

Fig. 3. Automatic driving flowchart of a robot that uses GNSS technology to gather soil samples (*Yang et al., 2025*)

In addition, ultrasonic and infrared sensors are employed to detect obstacles such as rocks, plants, uneven ground, or farming equipment in the robot's path, thereby preventing collisions and potential damage during movement. These sensors constantly emit waves or light signals and measure the time it takes for them to bounce back, enabling the robot to determine the distance to nearby objects with high accuracy. Combined with proximity detection algorithms, they allow the robot to slow down, stop, or reroute in real time when an obstacle is detected. A gyroscope and accelerometer, often integrated as part of an inertial measurement unit (IMU), are used to maintain stability, orientation, and direction, especially when operating on irregular or sloped terrain. This ensures that the sampling mechanism remains steady and that the robot maintains balance throughout its operation.

Additionally, wheel encoders are utilized to measure the distance traveled and the rotational speed of the robot's wheels, which helps correct positioning errors that may occur when GPS signals are weak or temporarily unavailable. By continuously comparing encoder readings with data from the IMU and GPS, the system can estimate the robot's precise location and orientation through sensor fusion techniques. All these navigation sensors communicate with an onboard processing unit, which integrates the incoming data, performs real-time analysis, and dynamically adjusts the robot's trajectory to maintain an optimal and safe path. This intelligent coordination of sensing and control not only guarantees autonomous and collision-free navigation but also enhances operational reliability, efficiency, and adaptability in complex and changing agricultural environments (*Chen et al., 2025*).

At the core of the robot's navigation and control system is a Raspberry Pi, which acts as the central processing unit responsible for coordinating all onboard sensors and actuators. It collects data from the GPS, ultrasonic and infrared sensors, inertial measurement unit (IMU), and wheel encoders, processing this information in real time to determine the robot's position and surroundings. The Raspberry Pi executes navigation algorithms, interprets sensor inputs, and issues control signals to the motors or steering mechanisms to ensure accurate and stable movement. Additionally, it handles wireless communication with the cloud or base station via Wi-Fi, LoRa, or 4G modules, allowing continuous monitoring and data logging. Its versatility, low power consumption, and compatibility with open-source platforms make it ideal for IoT-based agricultural systems. In essence, the Raspberry Pi functions as the robot's "brain," integrating sensing, decision-making, and control functions to enable safe, autonomous, and efficient soil-sampling operations (*Joice et al., 2025*).

2.2 Sampling Method

The robot moves to a predetermined GPS coordinate, where it deploys a mechanical gathering mechanism to extract soil from specific depths. This mechanism usually consists of a vertical drill, auger, or hollow probe that penetrates the ground to collect a core sample. The depth sensor ensures that the gathering device reaches the exact desired depth, maintaining consistency across all sampling points. Once the sample is collected, the system either deposits it into a container or stores it in a labeled compartment, often marked with a QR code or digital ID linked to its GPS location.

Some advanced robots use pneumatic or hydraulic actuators to push and retract the gathering tool smoothly, reducing soil disturbance and ensuring high-quality samples. The soil is then automatically transferred into sealed containers inside the robot's storage unit, preventing contamination. After completing the sampling sequence, the robot navigates to the next point or returns to its base station for unloading. This automated approach significantly improves repeatability, and ensures precise georeferencing of every soil sample collected (*Yang et al., 2025*).

Fig. 4. Automated soil sampling robot designed by Rogo Ag (https://rogoag.com/)

2.3 Automated docking

Upon completion of its pre-defined sampling route, the robotic system will automatically navigate to a base station or a designated collection point for sample processing. This return transit is executed by either retracing the collection path or following a pre-optimized route back to the docking station. At the station, the system initiates an automated sequence for data upload and sample transfer. Each soil sample is housed in an individual cartridge encoded with a unique digital identifier (e.g., a QR code), which is linked to its precise GPS coordinates and sampling depth.

This automated identification eliminates the need for manual sample logging, thereby enhancing traceability and reducing potential human error. The cartridges are subsequently prepared for transport, where they can be manually retrieved or automatically conveyed for laboratory analysis of key chemical and physical properties, including pH, macronutrient content (nitrogen, phosphorus, potassium), and organic matter. Concurrently, the robot's onboard computing system (e.g., a Raspberry Pi) transmits the complete field dataset to a centralized cloud platform using standard wireless protocols such as Wi-Fi, 4G, or LoRa. This dataset encompasses all georeferenced sample locations alongside in-situ sensor readings like soil moisture and temperature.

The cloud infrastructure organizes this information, creating a structured database that is later enriched with the corresponding laboratory results. This integrated dataset is then visualized using geographic information system (GIS) software to generate detailed spatial maps illustrating the variability of soil nutrients and other properties across the field. These maps provide an empirical basis for variable-rate application (VRA) of fertilizers and precision irrigation, enabling data-driven agronomic decisions. Finally, the system concludes its cycle by automatically initiating a recharge cycle at the docking station, ensuring operational readiness for subsequent missions. This closed-loop process—spanning autonomous collection, seamless data integration, and cloud-based analytics—significantly augments the accuracy, efficiency, and scalability of soil management, contributing to more productive and sustainable agricultural systems.

CONCLUSION

The integration of Internet of Things (IoT) technologies into soil sampling represents a significant step toward the automation and modernization of agricultural practices. By combining GPS navigation, environmental sensors, and cloud-based data management, soil-sampling robots can collect highly accurate, georeferenced samples with minimal human intervention. This technological approach not only improves the precision and repeatability of soil data but also saves time, reduces labor costs, and minimizes human error. Once collected, the samples and their associated data can be transmitted to cloud platforms, where they are processed, analyzed, and visualized to generate detailed soil nutrient and condition maps. These insights allow farmers and researchers to make informed decisions regarding fertilizer application, irrigation, and crop rotation, ultimately leading to increased productivity and more sustainable farming practices.

Furthermore, integrating IoT with cloud computing, artificial intelligence, and autonomous navigation lays the groundwork for a fully connected and intelligent agricultural ecosystem. As these technologies continue to advance, the potential for large-scale adoption of automated soil-sampling systems will grow, contributing to the broader vision of precision agriculture - a farming approach that optimizes resource use, enhances crop yields, and supports environmental conservation. In conclusion, IoT-driven soil sampling is not merely a technological improvement but a transformative innovation that bridges automation, data analytics, and sustainability in modern agriculture.

Acknowledgements:

This work was supported by the National Research Authority, through the Project entitled: “An intelligent automated system designed for georeferenced soil sampling.” -- PN 23 04 01 02. Contract no./date 9N/ 01.01.2023.

REFERENCES

[1] Alahmad, T.; Neményi, M.; Nyéki, A. (2023). Applying IoT Sensors and Big Data to Improve Precision Crop Production: A Review. *Agronomy, 13*, 2603. https://doi.org/10.3390/agronomy13102603.

[2] Alam, T. (2021). Cloud-Based IoT Applications and Their Roles in Smart Cities. *Smart Cities, 4,* 1196-1219. https://doi.org/10.3390/smartcities4030064.

[3] Chen Z., Yin J., Farhan S.M., Liu L., Zhang D., Zhou M., Cheng J. (2025). A comprehensive review of obstacle avoidance for autonomous agricultural machinery in multi-operational environment, *Artificial Intelligence in Agriculture*, ISSN 2589-7217, https://doi.org/10.1016/j.aiia.2025.10.001 .

[4] Goshu A.G. (2024). Soil sampling and sample preparation. 10.37532/0970-1907.24.40.6.1-5.

[5] Huuskonen J., Oksanen T. (2018). Soil sampling with drones and augmented reality in precision agriculture,Computers and Electronics in Agriculture,Volume 154,Pages 25-35,ISSN 0168-1699, 10.1016/j.compag.2018.08.039.

[6] Joice, A.; Tufaique, T.; Tazeen, H.; Igathinathane, C.; Zhang, Z.; Whippo, C.; Hendrickson, J.; Archer, D. (2025). Applications of Raspberry Pi for Precision Agriculture—A Systematic Review. *Agriculture 15*, 227. https://doi.org/10.3390/agriculture15030227.

[7] Rajasekaran, C., Jeeva, R., Hariharan, R., Jeevanantham, M., Jayanthi, K.B., Raguvaran K. (2024). An Integrating IoT for Intelligent Soil Analysis and Crop Optimization. 1-4. 10.1109/AIMLA59606.2024.10531447.

[8] Roetman B. (2019). Spring Soil Sampling Is No Longer Optional, https://www.winfieldunited.com/news-and-insights/spring-soil-sampling-is-no-longer-optional.

[9] Sishodia RP, Ray RL, Singh SK. (2020). Applications of Remote Sensing in Precision Agriculture: A Review. Remote Sensing. 12(19):3136. doi.org/10.3390/rs12193136.

[10] Yang, L.; Tomioka, C.; Hoshino, Y.; Kamata, S.; Kikuchi, S. (2025). Research on EV Crawler-Type Soil Sample Robot Using GNSS Information. *Sensors, 25*, 604. https://doi.org/10.3390/s25030604.

[11] https://rogoag.com/